Proceedings of the

Fourteenth American Peptide Symposium

Peptides

Chemistry, Structure and Biology

Pravin T. P. Kaumaya and Robert S. Hodges

Mayflower
Scientific Ltd

Peptides

Chemistry, Structure and Biology

Peptides

Chemistry, Structure and Biology

Proceedings of the Fourteenth American Peptide Symposium
June 18-23, 1995, Columbus, Ohio, USA

Edited by

Pravin T.P. Kaumaya
Departments of Ob/Gyn, Medical Biochemistry and Microbiology and
The Comprehensive Cancer Center
The Ohio State University
Columbus, Ohio 43210, USA

and

Robert S. Hodges
Department of Biochemistry
University of Alberta
Edmonton, Alberta, T6G 2H7, Canada

Mayflower Scientific Ltd. - England - 1996

British Library Cataloguing in Publication Data

Peptides: Chemistry, Structure and Biology: Proceedings of the 14th American Peptide Symposium
1. Peptides
I. Kaumaya, Pravin T.P. II. Hodges, Robert, S.
547.7'56

ISBN 0-9527011-0-3

Publication and distribution enquiries to the publisher:

Mayflower Scientific Ltd.
P.O. Box 13
KINGSWINFORD
West Midlands
England, DY6 0HR, U.K.

Fax:
(U.K.) 01384 294463
(Intnatl.) +44 1384 294463

Printed and bound by Hartnolls Ltd., Bodmin, Cornwall, England, U.K.

Preface

The largest ongoing International gathering in the field of Peptide Science convened on the campus of the Ohio State University, Columbus, Ohio on June 18-23, 1995. The Fourteenth American Peptide Symposium was held under the joint auspices of the American Peptide Society and the hosting institution, the Ohio State University. This meeting attracted 1418 delegates including exhibitor personnel and accompanying guests from 33 countries. It was gratifying to see an increase in the number of students and post-doctoral scientists (30%) at the meeting as well as a sizeable number of newcomers.

The scientific program contained an unprecedented number of lecture presentations (106), comprising a keynote address by Dr. Dan Koshland, the 10th Alan Pierce Award Lecture by John Stewart, 77 plenary lectures, 13 mini-symposium lectures and 16 workshops lectures. Equally impressive was the number of poster communications (670). From the 762 scientific communications, the program committee had the arduous task of selecting speakers for the oral presentations and, even more difficult, the task of selecting approximately 50% of the lecture and poster presentations, some 379 articles, for publication in the proceedings volume. These manuscripts were selected on the basis of originality and scientific significance as judged from abstract submission.

To accommodate this impressive and diverse array of scientific presentations, the program was structured into 15 scientific categories for original contributions, together with 5 workshops and 2 mini-symposia. There were 4 official poster sessions with all posters on display from Sunday through to Thursday. The breakdown of contributions for each scientific category were as follows: Synthetic Methods (144), Peptide Inhibitors/Receptors (80), Peptide Vaccines and Immunology (73), Conformational Analysis (59), Peptide Hormones and Neuropeptides (56), *De Novo* Design (55), Biologically Active Peptides (57), Peptide Mimetics (36), Glyco/Lipo/Phospho/ peptides (34), Peptide Libraries (32), Peptide/Protein Interactions (31), Peptide Delivery/Pharmaceuticals (20), NMR (19) and Signal Transduction (17). There were 31 mini-symposium presentations and 16 lectures in the 5 workshops, titled: Peptide Vaccines (4); Peptides in Membranes (3); Synthetic Peptide Libraries (4); Peptide/ Non-Peptide Mimetics (5) and Finding Biosequence Information on STN international. There were 66 exhibitor booths on display throughout the symposium. It was a formidable task to accommodate the exhibitor displays and intermingled poster display in the Ohio Student Union. The lectures were held in spacious Mershon Auditorium (3062 seating capacity).

One of the highlights of the meeting was the introduction of a Young Investigators Mini-Symposium Program. The goal was to provide opportunities for graduate students, postdoctoral fellows and scientists at an early stage of their scientific career to present a lecture and poster describing their research. We would like to thank the Mini-Symposium Program Committee (Pravin T.P. Kaumaya, James P. Tam, Tomi K. Sawyer, Teresa M. Kubiak and Susan Wang) for reviewing and selecting speakers. Sixteen young scientists presented 15 minute lectures on the Wednesday afternoon. It was especially moving to us (P.T.P.K. and R.S.H.) to see our own graduate students and

others give stellar presentations. It was remarkable to note the level of professionalism in their performance. We sincerely hope that future symposium organizers will continue this successful format as it is important to nurture these young scientists. We continued in the tradition, established at the Thirteenth American Peptide Symposium in Edmonton, of holding workshop sessions. The intention was to enable participants to gain basic knowledge in an area outside their own expertise. The five workshops were held on the last day of the symposium and, to allow maximum participation, only two workshops were held concurrently.

In an unprecedented effort to help students attend the symposium, the American Peptide Society and the Fourteenth American Peptide Symposium organizing committee set aside funds to finance needy participants. Ninety-four students received symposium travel grants totalling $36,000 (awards ranging from $250-$500 per student). We would like to give special thanks to Tomi K. Sawyer (Chair) and his committee members (Garland Marshall, Charles Deber and Henry Mosberg) for their hard work in the selection of the 94 students who received travel grants. The criteria used for these awards were need, field of interest, originality of research and recommendations from their professors.

The Students Affairs Committee (Chairs: John W. Taylor and Jane V. Aldrich, Student Representatives: C. Haskell-Luevano, J. Ho, S. Wang and D.A. Wiegandt) of the American Peptide Society who organized the Job Fair and the Young Investigators Poster Competition must be commended on a great job well done. The Job Fair is an integral activity of the American Peptide Society that support the mutual employment interests of young scientists and potential academic/industrial employers. We provided a free booth to the Student Affairs Committee to conduct their activities.

The Young Investigators poster competition was also a resounding success with 38 entries competing for cash prizes. Only posters accepted by the Fourteenth American Peptide Symposium Program Committee were allowed to compete. A panel of judges selected by the Student Affairs Committee was responsible for reviewing the posters and selecting the winners. The entries were judged by four teams of two judges in a preliminary round. Each team listened to presentations by the investigators and judged a group of nine or ten posters according to the criteria of originality, timeliness/ significance, accuracy of data, analysis and interpretation of results, and effort and workmanship. Three top posters from each group were selected for a final round. In this, the 12 posters selected were judged afresh by four of the judges, without presentations and the scores were tallied direct. The competition result was very close and the standard was very high. The poster competition was deemed to be a valuable approach to recognizing and promoting the efforts of peptide researchers at an early stage of their career. At the awards banquet, held on June 23 at the Hyatt Regency, Columbus, the successful students received prizes and cash awards from Dr. Jean Rivier, the President of the American Peptide Society. Dean Olson from the University of Illinois at the Urbana-Champaign was awarded the first prize ($1000). Two second prize awards ($500) went to Knud Jensen and Hui Shao and finally there were four third prize winners who received $250 each.

The symposium opened with a keynote lecture by the former editor of "Science" magazine, Dr. Daniel E. Koshland, Jr., who spoke on the identity of peptides in signaling

systems. Immediately following his talk was a session on Synthetic Methods. This was dedicated to Dr. Miklos Bodanzsky, a pioneer in the field of peptide chemistry on his 80th birthday. Unfortunately, Dr. Bodanzsky could not attend the symposium and the session in his honour owing to personal reasons. As expected, synthetic aspects of peptide chemistry garnered the largest number of contributions and so required two sessions: Session I: Bodanzsky Session and Session IX: Synthetic Methods II. The Bodanzsky session on Monday morning highlighted the contribution of peptide chemistry to the chemical synthesis of proteins of greater than 50 amino acid residues, synthesis once only in the realm of recombinant DNA methods. Both chemical and enzymatic ligation of peptides figured prominently and demonstrated the power of the technology of using unprotected peptide segments as building blocks. Notwithstanding these major innovative approaches, it is clear that improvements in basic solid phase chemistry continues unabated. Novel methods for anchoring peptides to resins in SPPS, new efficient, rapid-acting coupling reagents for efficient peptide bond formation, improved synthesis and folding of disulfide peptides and development of new linkers and protecting groups figured prominently.

Session II focussed in the delivery of peptides orally, across the blood brain barrier and into living cells. This is an area of the utmost importance if synthetic peptides are to become useful as pharmaceutical drugs. Session III emphasised the continuing and increasing importance that peptides play at the chemistry/biology interface in addressing important biological and chemical problems. Similarly, in Session IV, the study of the complex interactions between peptides and macromolecules can result in the development of unique inhibitors, for example, in the case of HIV protease.

Session V contained the second largest number of presentations and covered the area of Peptide Inhibitors/Receptors. The synthesis of novel inhibitors and antagonists displaying increased potency and duration with highly selective properties for various receptors was described. This area continues to highlight the importance of structure-activity relationships in the rational design of peptide analogs as potential drugs in medicine.

Session VII on Signal Transduction was concerned with phosphonopeptide recognition of SH2 domains and how peptides in general are increasingly being used to decipher the process of signal transduction. Session VIII dealt with synthetic methodologies for O- and N-linked glycopeptides, phosphonopeptides and lipopeptides. Session X, dedicated to Conformational Analysis, emphasised the role of sophisticated biophysical measurements in yielding information concerning peptide bioactive conformation.

Where else could one look for today's state-of-the-art synthetic peptide chemistry and design other than in Session XI entitled *De Novo* Design? In this session, the extent of the peptide chemist's imagination was stretched to the limit. The engineering of novel peptides with pseudo-three-dimensional stuctures and well-defined properties were described.

Session XII dealt with developments in the area of Peptide Hormones/Neuropeptides in which new classes of potent agonists and antagonists are being discovered. The mechanism of action and properties of the various receptors described is leading to the rational design of specific agonists/antagonists of potential therapeutic value. Session

XIII described the continuing progress in the field of peptide mimetics and the ingenuity in the chemistry being developed for the synthesis of various classes of compounds. In Session XIV, high resolution NMR was shown as being increasingly applied to determine peptide conformation. Peptide Vaccines and Immunology, taken together, also gathered one of the largest number of presentations at the symposium with approximately 80 scientific communications (Session XV & XVI). It is clear that the revolutionary new immunological knowledge generated within the last few years is a direct consequence of the use of synthetic peptides. In this session, creative strategies were described for vaccine development and, more importantly, new inroads targeting cancer vaccines/tumor antigens were presented. This is an area still in its infancy and promises to bring exciting new developments in the coming years.

This year's Alan E. Pierce Award Recipient, Dr John M. Stewart, was recognised for his outstanding contributions to the chemistry/biology of peptides, especially to the development of solid phase peptide synthesis. In his memorable lecture, he recounted a four decade retrospective on peptide synthesis and his many contributions in the initial development of solid phase synthesis and the construction of the first synthesizer in the basement shop of his home. John also described his contribution to the area of peptide hormones and neuropeptides, especially bradykinin, angiotensin, GnRH, substance P and ACTH.

As Symposium Chairman, I would like to acknowledge that the success of the symposium was due, in no small measure, to the dedication and hardwork of many individuals. I am indebted to my secretary, Angell Stone for her dedication and patience during the planning and organization of this meeting. She has contributed enormously to the development and execution of the symposium database required to correspond with hundreds of individuals and to keep track of abstract submissions. Her skills at mastering the database made it possible to organize printed materials for the symposium and to access records and participants on the fly. Lastly, in the past year, she has worked entirely on the publication of the proceedings book by converting all diskettes to the appropriate IBM compatible format, implementing editorial corrections to the manuscripts, retyped many of the tables and formatted each single manuscript to the desired style. Special thanks goes to Dan Pierce and John Powell for the financial administration of all symposium transactions, to Mandy Sunassee for the registration database, to Keith Keplinger for his many contributions wherever he was needed, to Susan Conrad for exhibitor/show management, to Bob Hummel for the design of the logo and layout of program and abstract books and to the many volunteers from the Department of Ob/Gyn, including graduate students and postdoctoral associates from my own and other laboratories. I am also indebted to the many individuals associated with the Ohio State University facilities, including the Mershon Auditorium, the Ohio Union, University Housing Services, and University Mail Services, who advised and helped during the planning and execution of the symposium activities. I am thankful to the Greater Columbus Convention & Visitors Bureau, especially Woody King and Barbara Martin for managing the hotel reservations.

We would like to compliment the members of the Program Committee who assisted in organizing the scientific program by evaluating abstracts, both for oral presentation and for publication in the proceedings volume. Special thanks goes to the workshop

leaders and chairmen of the scientific sessions for stimulating discussions and for making sure that the meeting was kept on schedule.

We are especially grateful for the generous financial backing of the Benefactors, Sponsors, Donors and Contributors whose support was critical to maintain the high standards of the meeting. Special thanks goes to Sigma Chemical Company for providing the bulk of funds required for the purchase of the symposium bags and to the Pierce Chemical Company for sponsoring the Pierce Award nominee.

We are grateful also to Roger Epton of Mayflower Scientific Ltd. on many counts. These include the production of a special symposium issue of Biomedical Peptides, Proteins and Nucleic Acids dedicated to Peptide Vaccines. This issue was distributed free to all participants of the Fourteenth American Peptide Symposium. We are indebted for his advice and for his own hard work in the publication of this symposium book.

The Chairman, is personally indebted to the Ohio State University, especially to the Dean, Vice President of the Medical Center, Dr. Manuel Tzagournis, the Department of Ob/Gyn and his Chairman, Dr. Steven G. Gabbe, to the Comprehensive Cancer Center and the Director, Dr. David E. Schuller and to the Vice President of Research, Dr. Edward F. Hayes for their unreserved support of his efforts at all stages of this mammoth enterprise.

Lastly, the Chairman would like to acknowledge his wife, Branka and his daughters, Biljana and Meghan and to express his very special thanks for their understanding and support during a challenging period.

Pravin T.P. Kaumaya
Robert S. Hodges

Fourteenth American Peptide Symposium

The Ohio State University, Columbus, Ohio, USA
June 18-23, 1995

CHAIRMAN - Pravin T.P. Kaumaya, *The Ohio State University*

PROGRAM COMMITTEE

Jean Chmielewski	*Purdue University*
Charles M. Deber	*University of Toronto*
William F. DeGrado	*DuPont Merck Pharmaceutical Co.*
Richard DiMarchi	*Lilly Research Labs*
Olivera J. Finn	*University of Pittsburgh*
Jonathan Greer	*Abbott Laboratories*
Angela Gronenborn	*National Institutes of Health*
Robert S. Hodges	*University of Alberta*
Barbara Imperiali	*California Institute of Technology*
Pravin T.P. Kaumaya	*The Ohio State University*
Vincent H.L. Lee	*University of Southern California*
Maurice Manning	*Medical College of Ohio*
M. Sue O'Dorisio	*Children's Hospital*
	The Ohio State University
Deborah S. Parris	*The Ohio State University*
Terry Reisine	*University of Pennsylvania*
Jeffrey Schlom	*National Cancer Institute*
Steven E. Shoelson	*Harvard Medical School*
Arno F. Spatola	*University of Louisville*
James P. Tam	*Vanderbilt University*
Daniel F. Veber	*Smith Kline Beecham Pharmaceuticals*

THE AMERICAN PEPTIDE SOCIETY

OFFICERS

Jean E. Rivier	President	*The Salk Institute*
Peter W. Schiller	President-Elect	*Clinical Research Inst. of Montreal*
Ruth F. Nutt	Secretary	*Corvas International, Inc.*
John A. Smith	Treasurer	*University of Alabama at Birmingham*

COUNCILLORS

George Barany	*University of Minnesota*
David H. Coy	*Tulane University*
Richard D. DiMarchi	*Eli Lilly and Company*
Bruce W. Erickson	*University of North Carolina*
Arthur M. Felix	*Hoffmann LaRoche, Inc.*
Lila M. Gierasch	*University of Massachusetts*
Robert S. Hodges	*University of Alberta*
Kenneth D. Kopple	*Smith Kline Beecham*
James P. Tam	*Vanderbilt University*
Daniel F. Veber	*Merck Research Laboratories*
Janis D. Young	*Skyline Peptides*

ORGANIZING COMMITTEE - THE OHIO STATE UNIVERSITY

Pravin T.P. Kaumaya	*Chair*
Susan Conrad	*Exhibitor/Show Manager*
Daniel L. Pierce	*Financial Manager*
Keith B. Keplinger	*Operational/Financial Consultant*
Angell R. Stone	*Assistant to the Chair*
Amanda Sunassee	*Assistant to the Chair*
John E. Powell	*Financial Coordinator*
Vernon C. Stevens	*O.S.U. Representative*
David S. Yohn	*O.S.U. Representative*

LOCAL VOLUNTEERS

Charles Brooks
Pia Camacho
Kenneth Chan
Tammy Chan
Chi-Fon Chang
Kimberly Denis
Judy Durilla
Sylvan Frank
Xinyu Gu
Heidi Heffelfinger
Najma Javed
Tiffanie Johnston
Biljana Kaumaya
Michael Lairmore
Mark Maciejewski
Steven Monahan
Susan Olesik
Debbie Parris
Beth Pierce
Elizabeth Shockley
Cindy Smithson
Aimee Stone
Pierre Triozzi
Denise Watts
Yao-Ming Wei
Caroline Whitacre
Donna-Beth Woodbine
Amanda Yee

LOCAL BUSINESS REPRESENTATIVES

Bill Barto	*Mershon Auditorium, The Ohio State University*
Scott Boden	*Conference Housing, The Ohio State University*
Claudia Bonham	*Mershon Auditorium, The Ohio State University*
Darcie Brill	*Variations*
Pam Corte	*Wexner Center Cafe, The Ohio State University*
Katie Dougherty	*Handke's Cuisine*
Mike Doyle	*Motivational Designs*
Kate Garvin	*The Columbus Museum of Art*
Bob Goebel	*Ultimate Tours*
Rob Goebel	*Ultimate Tours*
Tammy Grace	*Fifth Third Bank*
Harmut Handke	*Handke's Cuisine*
Brian Hendrickson	*Conference Housing, The Ohio State University*
Richard Hostrup	*Variations*
Bob Hummel	*BioMedical Communications, Ohio State Univ.*
Molly Leahy	*Ohio Union, The Ohio State University*
Barbara Martin	*Greater Columbus Convention & Visitors Bureau*
Patrick Maughan	*Mershon Auditorium, The Ohio State University*
Joanne Mead	*RoSu Productions*
Theresa Mullins	*Hyatt Regency Catering*
Teri Shary	*The Hyatt on Capitol Square Catering*
Susan Smith	*Hyatt Hotels & Resorts*
Edward Vinson	*Geo. Fern Company*
Bruce Walter	*Geo. Fern Company*
Barbara Zahm	*Chemical Abstracts Service*

Acknowledgments

The Fourteenth American Peptide Symposium Organizing Committee is grateful for the financial and administrative support of the Host Institution:

The Ohio State University
Department of Obstetrics and Gynecology
University Medical Center, College of Medicine
Office of the Vice-President for Research
The Comprehensive Cancer Center

The Fourteenth American Peptide Symposium Organizing Committee also greatly appreciates the support and generous financial assistance of the following organizations:

BENEFACTORS

Advanced ChemTech	*Louisville, KY, USA*
Bachem California	*Torrance, CA, USA*
Eli Lilly and Company,	*Indianapolis, IN, USA*
Perkin-Elmer	*Foster City, CA, USA*
Pierce Chemical Company	*Rockford, IL, USA*
Procter & Gamble	*Cincinnati, OH, USA*
SIGMA Peptides and Amino Acids	*St. Louis, MO, USA*

SPONSORS

Amgen	*Thousand Oaks, CA, USA*
Bachem Feinchemikalien AG	*Bubendorf, Switzerland*
Behrmann Peptide	*Tubingen, Germany*
Hoffmann-La Roche	*Nutley, NJ, USA*
Mallinckrodt Chemical	*Chesterfield, MO, USA*
ProPeptide/Neosystem	*Vert Le Petit, France*
Separations Group	*Hesperia, CA, USA*
Synthetech, Inc.	*Albany, OR, USA*
Zeneca Pharmaceuticals Group	*Wilmington, DE, USA*

DONORS

Biomeasure	*Milford, MA, USA*
Dupont Merck	*Wilmington, DE, USA*

Genzyme Pharmaceuticals and Fine Chemicals	*Cambridge, MA, USA*
Glaxo Research Institute	*Research Triangle Park, NC, USA*
Multiple Peptide Systems	*San Diego, CA, USA*
Peninsula Laboratories, Inc.	*Belmont, CA, USA*
Peptides International, Inc.	*Louisville, KY, USA*
PerSeptive Biosystems	*Cambridge, MA, USA*
Sandoz	*East Hanover, NJ, USA*
The Upjohn Company	*Kalamazoo, MI, USA*
UCB BioProducts	*Braine-L'Alleud, Belgium*

CONTRIBUTORS

Abbott Laboratories	*Columbus, OH, USA*
American Peptide Company	*Sunnyvale, CA, USA*
Biogen, Inc.	*Cambridge, MA, USA*
Bio-Mega	*Laval, Quebec, Canada*
Bristol-Myers Squibb Co.	*Princeton, NJ, USA*
Immunobiology Research Institute	*Annandale, NJ, USA*
Merck Research Labs.	*Rahway, NJ, USA*
ORPEGEN Pharma	*Heidelberg, Germany*
Parke-Davis	*Ann Arbor, MI, 48105*
Pfizer	*Princeton, NJ, USA*
The Peptide Laboratory	*Berkeley, CA, USA*
Smith Kline	*King of Prussia, PA, USA*
Tanabe	*San Diego, CA, USA*
Waters Corp.	*Milford, MA, USA*
Zeneca Pharmaceuticals	*Macclesfield, UK*

Scenes from the Fourteenth American Peptide Symposium

An ice carving of the 14th APS logo of the Santa Maria and the American Peptide Society logo was displayed at the Speakers Dinner held at the Columbus Museum of Art.

Retiring President, Jean E. Rivier, presenting award to Retiring Councillor, John Smith. From far left to right: Peter W. Schiller, Jean E. Rivier, John Smith, Bruce W. Erikson and Arthur M. Felix.

Carl Clark of Pierce Chemical Company presenting the 10th Alan Pierce Award to John Stewart at the Banquet. Standing left to right: Peter W. Schiller, President-elect, Jean E. Rivier, President and Pravin T.P. Kaumaya, Chairman of the 14th APS.

14th APS participants mingling outside the Mershon Auditorium at the Welcome Reception, which was catered by Handke's Cuisine of Columbus.

Jean E. Rivier, presenting awards to students for the poster competition at the banquet.

Speakers Dinner. Standing from left to right: R. Bruce Merrifield, Robert S. Hodges, Jean E. Rivier and Daniel F. Veber. Sitting from left to right: Dr. Steven Gabbe, Chair of the Department of Ob/Gyn at the Ohio State University and wife, Pat Temple, Peter W. Schiller, James P. Tam, Robert Schwyzer and Victor J. Hruby.

Alan E. Pierce Award

(Sponsored by Pierce Chemical Company)

The recipient is an individual who has made outstanding contributions to techniques and methodology in the chemistry of amino acids, peptides and proteins.

1995	**John M. Stewart**	*University of Colorado* Denver, CO
1993	**Victor J. Hruby**	*University of Arizona* Tucson, AR
1991	**Daniel Veber**	*Merck Sharpe and Dohme Research Laboratories,* West Point, PA
1989	**Murray Goodman**	*University of California - San Diego* San Diego, CA
1987	**Choh Hao Li**	*University of California San Francisco* San Francisco, CA
1985	**Robert Schwyzer**	*Swiss Federal Institute of Technology* Zurich, Switzerland
1983	**Ralph Hirschmann**	*Merck Sharpe and Dohme* Rahway, NJ
1981	**Klaus Hofmann**	*University of Pittsburgh School of Medicine,* Pittsburgh, PA
1979	**Bruce Merrifield**	*The Rockefeller University* New York, NY
1977	**Miklos Bodanszky**	*Case Western Reserve University* Cleveland, OH

American Peptide Symposia

Symposium	Chair(s)	Location
First 1968	**Saul Lande** *Yale University, New Haven* **Boris Weinstein** *University of Washington, Seattle*	Yale University New Haven, CT, U.S.A.
Second 1970	**F. Merlin Bumpus** *Cleveland Clinic, Cleveland*	Cleveland Clinic Cleveland, OH, U.S.A.
Third 1972	**Johannes Meienhofer** *Harvard Medical School* *Boston*	Children's Cancer Research Foundation Boston, MA, U.S.A.
Fourth 1975	**Roderich Walter** *University of Illinois* *Medical Center, Chicago*	The Rockefeller University and Barizon Plaza Hotel New York, NY, U.S.A.
Fifth 1977	**Murray Goodman** *University of California-* *San Diego*	University of California - San Diego - San Diego, CA, U.S.A.
Sixth 1979	**Erhard Gross** *National Institutes of Health* *Bethesda*	Georgetown University Washington, DC, U.S.A.
Seventh 1981	**Daniel H. Rich** *University of Wisconsin-Madison*	University of Wisconsin- Madison, Madison, WI, U.S.A.
Eighth 1983	**Victor J. Hruby** *University of Arizona* *Tucson*	University of Arizona Tucson, AZ, U.S.A.
Ninth 1985	**Kenneth D. Kopple** *Illinois Institute of* *Technology, Chicago* **Charles M. Deber** *University of Toronto, Toronto*	University of Toronto Toronto, Ontario, Canada
Tenth 1987	**Garland R. Marshall** *Washington University School of* *School of Medicine, St. Louis*	Washington University St. Louis, MO, U.S.A.

Symposium	Chair(s)	Location
Eleventh 1989	**Jean E. Rivier** *The Salk Institute for Biological Studies, La Jolla*	University of California - San Diego, CA, U.S.A.
Twelfth 1991	**John A. Smith** *Massachusetts General Hospital, Boston*	Massachusetts Institute for Technology Cambridge, MA, U.S.A.
Thirteenth 1993	**Robert S. Hodges** *University of Alberta, Edmonton*	Edmonton Convention Centre Edmonton, Alberta, Canada
Fourteenth 1995	**Pravin T.P. Kaumaya** *The Ohio State University, Columbus*	The Ohio State University Columbus, OH, U.S.A.

American Peptide Society

Honorary Members

Christian Anfinsen (1990)
John Hopkins University

Elkan R. Blout (1991)
Harvard Medical School

Miklos Bodanszky (1990)
Case Western Reserve Univ.

Joseph Fruton (1991)
Yale University

Murray Goodman (1990)
Univ. Cal. San Diego

Roger Guillemin (1990)
The Salk Institute

Ralph Hirschmann (1990)
University of Pennsylvania

Klaus Hofmann (1990)
University of Pittsburgh

Victor J. Hruby (1993)
University of Arizona

R. Bruce Merrifield (1990)
Rockefeller University

Miguel Ondetti (1991)
Bristol-Myers Pharm.

Andrew V. Schally (1990)
Vet. Admin. Medical Center

Robert Schwyzer (1990)
Swiss Fed. Inst. of Technology

John C. Sheehan (1991);
deceased
Mass. Inst. of Technology

John M. Stewart (1995)
University of Colorado

Daniel F. Veber (1991)
Merck Sharp & Dohme

1995 Young Investigator Poster Competition

Awards

First Prize - $1000

Dean L. Olson,	*University of Illinois at Urbana-Champaign*

Second Prize - $500

Knud J. Jenson,	*University of Minnesota*
Hui Shao,	*University of California - San Diego*

Third Prize - $250

Haydn L. Ball,	*Italfarmaco Research Center*
Susanna Borg,	*Uppsala University*
Shun-Cheng Li,	*University of Toronto*
Luckner Ulysse,	*Purdue University*

Honorable Mentions - Certificates

Dyanne Brewer,	*University of Waterloo*
Anne M. Grosset,	*University of Pennsylvania*
Carrie Haskell-Luevano,	*University of Arizona*
Francois Jean,	*Institute de Recherches Cliniques de Montreal*
Maria Kempe,	*University of Minnesota*
Robert Konat,	*Universitat Munchen*
Bih-Show Lou,	*University of Arizona*
T. David Pallin,	*Vanderbilt University*
Chang Rao,	*Vanderbilt University*
Wentao Zhang,	*Rutgers University*

American Peptide Society - 14th APS Symposium
Travel Grant Recipients

	Name	*Institution*, City, COUNTRY
1.	Alsini, Jordi	*U. Barcelona*, Barcelona, SPAIN
2.	Angell, Yvonne	*U. Wisconsin*, Madison, USA
3.	Ban, Annamaria	*Maharishi Int. U.*, Fairfield, USA
4.	Barbar, Elisar	*U. Minnesota*, Minneapolis, USA
5.	Bitan, Gal	*Hebrew U.*, Jerusalem, ISRAEL
6.	Berger-Hoffmann, Renate	*Saarland*, St. Ingbert, GERMANY
7.	Betin, Janis	*Latvian Acad. Sci.* Riga, LATVIA
8.	Bianco, Alberto	*U. Padova*, Padova, ITALY
9.	Bisello, Alessandro	*Beth Israel Hospital*, Boston, USA
10.	Blishchenko, Elena	*Russian Acad. Sci.*, Moscow, RUSSIA
11.	Bouvier, Marlene	*Harvard U.*, Cambridge, USA
12.	Bouzit, Hassiba	*E. Michigan U.*, Ypsilanti, USA
13.	Brewer, Dyanne	*U. Waterloo*, Waterloo, CANADA
14.	Broadridge, Robert	*U. Southampton*, Southampton, UK
15.	Bruins, Robert	*McMaster U.*, Hamilton, CANADA
16.	Buchinska, Todorka	*Bulgarian Acad. Sci.*, Sofia, BULGARIA
17.	Causton, Ashley	*U. British Columbia*, Vancouver,CANADA
18.	Chakravarty, Subrata	*State U. New York*, Stony Brook, USA
19.	Colotte, Adriana	*McMaster U.*, Hamilton, CANADA
20.	Eggleston, Ian	*U. Lausanne*, Lausanne, SWITZERLAND
21.	Englebretsen, Darren	*U. Queensland*, Brisbane, AUSTRALIA
22.	Falcone, Margaret	*U. Maryland*, College Park, USA
23.	Fernandez, Maria	*Louisiana State U.*, Baton Rouge, USA
24.	Ferreira, Paula	*U. Minho*, Braga, PORTUGAL
25.	Geier III, G. Richard	*U. Washington*, Seattle, USA
26.	Goldammer, Carsten	*U. Tubingen*, Tubingen, GERMANY
27.	Guichard, Gilles	*CNRS*, Strasbourge, FRANCE
28.	Grab, Beate	*U. Minnesota*, Minneapolis, USA
29.	Grosset, Anne	*U. Pennsylvania*, Philadelphia, USA
30.	Hari, Siva	*U. California*, Riverside, USA
31.	Harris, Parvez	*U. London*, London, UK
32.	Howl, John	*U. Birmingham*, Birmingham, UK
33.	Hussain, Rohanah	*Birbeck College*, London, UK
34.	Jean, Francois	*Clin. Res. Inst. Montreal*, CANADA
35.	Johnson, Nicole	*U. Nebraska Med. Cntr.*, Omaha, USA
36.	Kaiser, Thomas	*U. Tubingen*, Tubingen, GERMANY

37.	Kaur, Baljit	*Manchester Metro U.*, Manchester, UK
38.	Kempke, Maria	*U. Minnesota*, Minneapolis, USA
39.	Khiat, Abdesslem	U.Quebec, Pointe-Claire, CANADA
40.	Kneller, M. Byron	*U. Washington*, Seattle, USA
41.	Kohn, Wayne	*U. Alberta*, Edmonton, CANADA
42.	Konat, Robert	*Tech. U. Munchen*, Garching, GERMANY
43.	Kowalski, Jennifer	*Purdue U.*, West Lafayette, USA
44.	Kranz, Martin	*Tech. U.* Munchen, Garching, GERMANY
45.	Kulkarni, Sandhya	*Oregon State U.*, Corvallis, USA
46.	L'Archeveque, Benoit	*U. Montreal*, Montreal, CANADA
47.	Lavoire, Annie	*U. Sherbrooke*, Sherbrooke, CANADA
48.	Layden, Selena	*U. Melbourne*, Parkeville, AUSTRALIA
49.	Li, Guigen	*U. Arizona*, Tucson, USA
50.	Li, Shun-Cheng	*Hosp. for Sick Children*, Toronto, CANADA
51.	Liang, Xun	*Nankai U.*, Tianjin, CHINA
52.	Liu, Chuan-Fa	*Vanderbilt U.*, Nashville, USA
53.	Lutz, Karen	*U. Kansas*, Lawrence, USA
54.	Maeda, Dean	*Oregon State U.*, Corvallis, USA
55.	Maletinska, Lenka	*U. Sherbrooke*, Sherbrooke, CANADA
56.	McDonnell, James	*U. London*, London, UK
57.	Mezo, Adam	*U. British Columbia*, Vancouver, CANADA
58.	Moncrieff, Hazel	*Queens U.*, Belfast, N. IRELAND
59.	Murnin, Mark	*Creighton U.*, Omaha, USA
60.	Nishiyama, Yasuhiro	*Kobe-Gakuin U.*, Kobe, JAPAN
61.	Ogrel, Alexei	*Leiden U.*, Leiden, THE NETHERLANDS
62.	Oldziej, Stanislaw	*U. Gdansk*, Gdansk, POLAND
63.	Pallin, T. David	*Vanderbilt U.*, Nashville, USA
64.	Pegoraro, Stefano	*Inst. di Mutagenesi*, Pisa, ITALY
65.	Pellegrini, Maria	*Clark U.*, Worccester, USA
66.	Pluskey, Scott	*Joslin Ctr., Harvard Med. Sch.*, Boston, USA
67.	Rabanal-Anglada, Francesc	*U. Pennsylvania*, Philadelphia, USA
68.	Riche, Estelle	*U. North Carolina*, Chapel Hill, USA
69.	Rinnova, Marketa	*Inst. Org. Chem. Biochem.*, Prague, CZECH
70.	Ripka, Amy	*U. Wisconsin*, Madison, USA
71.	Roberts, Michael	*U. London*, London, ENGLAND
72.	Sabirov, Aydar	*State Res. Ctr.* Koltsova, RUSSIA
73.	Sanchez, Yolanda	*U. Barcelona*, Barcelona, SPAIN
74.	Sanvordekar, Medha	*E. Michigan U.*, Ypsilanti, USA
75.	Schmiedberger, Monika	Max-Plank Inst. Frankfurt, GERMANY
76.	Shao, Hui	*U. California San Diego*, San Diego, USA
77.	Shi, Jishu	*Kansas State U.*, Manhattan, USA
78.	Stockel, Angela	*Martin-Luther U.*, Halle, GERMANY
79.	Sturn, Noel	*U. Arizona*, Tucson, USA
80.	Ulysse, Luckner	*Purdue U.*, West Lafayette, USA
81.	Van Betsbrugge, Jo	*Free U. Brussels*, Brussels, BELGIUM

82.	Videnov, Georgi	*U. Tubingen*, Tubingen, GERMANY
83.	Vlaar, Cornelis	*Louisiana State U.*, Baton Rouge, USA
84.	Vogel, Karen	*Purdue U.*, West Lafayette, USA
85.	Vogen, Shawn	*U. Nebraska Med. Cntr.*, Omaha, USA
86.	Vosekalna, Ilze	*Latvian Inst. Org. Chem.*, Riga, LATVIA
87.	Wade, David	*Rutgers U.*, Piscataway, USA
88.	Wijkmans, Jac	*Leiden U.*, Leiden, THE NETHERLANDS
89.	Wu, Bing	*Rutgers U.*, New Brunswick, USA
90.	Yang, Jenny	*U. Oxford*, Oxford, UK
91.	Ying, Sun	*Chinese Acad. Med. Sci.*, Beijing, CHINA
92.	Zhang, Ruoheng	*Peking U.*, Beijing, CHINA
93.	Zhang, Wentao	*Rutgers U.*, New Brunswick, USA
94.	Zloh, Mire	*U. London*, London, UK

Students Affairs Committee

95.	Haskell-Luevano, Carrie	*U. of Arizona*, Tucson, USA
96.	Ho, Jeff	*U. of Michigan*, Michigan, USA
97.	Wang, Susan	*U. of California*, La Jolla, USA
98.	Wiegandt, De Anna L	*U. of Louisville*, Kentucky, USA

Abbreviations

Abbreviations used in the proceedings volume are defined below

AA, aa	amino acids
AAA	amino acid analysis
Ab	antibody
Abc	4'-(aminomethyl)-2,2'-bipyridine-4-carboxylic acid
ABRF	Association of Biomolecular Resource Facilities
Abu	amino butyric acid
AC	adenylate cyclase
Aca	aminocyclohexyl alanine
ACE	angiotensin-converting enzyme
AChR	acetylcholine receptor
ACN; Acn	acetonitrile
AcOH	acetic acid
AcOZ	acetoxy-benzyloxy-carbonyl group
ACP	acyl carrier protein
ACTH	corticotropin
AD	Alzheimer's disease; asymmetric dihydroxylation
Ada	adamantyl
Adoc	adamantyloxycarbonyl
AFR	autocatalytic fragment religation
Ag	antigen
AGEs	advance glycosylation endproducts
Agl	aminoglycine
Aha	7-aminoheptanoic acid
Ahx	aminohexyl
Aib	α-aminoisobutyric acid
Aic	2-aminoindan-2-carboxylic acid
AIDS	acquired immune deficiency syndrome
AK	adenylate kinase
Amh	amino-mercaptohexanoic acid
AO	antiovulatory
Aoc	1-azabicyclo[3.3.0]-2-carboxylic acid
Apa	6-amino-penicillanic acid
APC	antigen presenting cell
Apo	apolipoprotein
apo A-I	apolipoprotein A-IAPP aminopeptidase P
aPTT	activated partial thromboplastin time
ARP	arginine-rich peptide
Asa	azidosalicylic acid
ASPECT	Augmented Surface PolyEthylene's prepared by or used for Chemical Transformation
AT	antithrombin
Atc	2-aminotetralin-2-carboxylic acid
ATI	ascidian trypsin inhibitor
ATL	adult T-cell leukemia
ATR	attenuated total internal reflection
AUC	area under the curve
AV	arteriovenous
AVP	arginine-8-vasopressin
AZT	3'-azido-3'-deoxy-thymidine zidovudine
b	bovine
Bab	3,5-bis(2-aminoethyl) benzoic acid
Bal	β-alanine
BAL	backbone amide linker
BBB	blood brain barrier

BCECF	bis (carboxyethyl) carboxyfluorescein
BCR	B-cell receptor
BE	B-cell epitopes
BET	Brunauer-Emmett-Teller analysis
BHI	biosynthetic human insulin
BHK	baby hamster kidney cells
b-HLH-zip	basic helix-loop-helix leucine zipper
bhThr	betidehomothreonine
bIle	betideisoleucine
BIV	bovine immuno-deficiency-like virus
BK	bradykinin
Boc	tert butyloxycarbonyl
BOP	benzotriazolyloxy-tris-(dimethylamino) phosphonium hexafluorophosphate
Bpa	benzoylphenylalanine; bipyridylalanine
Bpoc	biphenylpropyloxy-carbonyl
BPTI	basic pancreatic trypsin inhibitor; bovine trypsin inhibitor
BSA	bovine serum albumin
BW	body weight
Bzl	benzyl
cAMP	cyclic adenosyl monophosphate
CAT	chloramphenicol acyl transferase
Cbz, Z	carbobenzoxy; benzyloxycarbonyl
CCK	cholecystokinin
CD	circular dichroism
Cdk	cyclin dependent kinase
cDNA	complementary DNA
CE	capillary electrophoresis
CEA	carcinoembryonic antigen
CF	cystic fibrosis
CFA	complete Freunds adjuvant
CFTR	cystic fibrosis transmembrane conductance regulator
cGMP	cyclic guanosine monophosphate
CGRP	calcitonin gene related peptide
CgTx	conotoxin
Cha	cyclohexylalanine
CHAPS	3-[(3-cholamidopropyl)-dimethyl-ammonio]-1-propane-sulfonate
CHD	cyclohexanedione
CHO	Chinese hamster ovary; aldehyde
Cho	choline
ChTX	charybdotoxin
CJD	Creutzfeldt Jakob disease
CKII	casein kinase II
Cle	cycloleucine (1-amino-1-carboxyl cyclopentane)
ClZ	2-chlorobenzyloxy-carbonyl
CM	chloromethyl; carboxymethyl
CN	cyanopropyl
CNS	central nervous system
ConG	conantokin G
COSY	correlated NMR spectroscopy
Cpa	4-chlorophenylalanine
CPD, CP	carboxypeptidase
CPN	carboxypeptidase N
cpn	chaperonin protein
CPPI	cell-permeable peptide import
CRF	corticotropin releasing factor
CRP	C-reactive protein
CsA	cyclosporin A

CSPPS	convergent solid phase peptide synthesis strategy
CT	charge-transfer
CTL	cytotoxic T-lymphocytes
CVS	cardiovascular system
Cyp	cyclophilin
CyPA	cyclophilin A
CZE	capillary zone electrophoresis
Dab	diaminobutyric acid
DAG	diacylglycerol
DAMGO	[D-Ala^2,*N*-MePhe^4,Gly^5-ol] enkephalin
DBF	dibenzofulvene
DBU	1,8-diazabicyclo [5.4.0]-undec-7-ene
DC	deltorphin C
DCB	1,2-dichlorobenzene
DCCI, DCC	dicyclohexyl carbodiimide
DCCT	diabetes control and complications trial
DCHA	dicyclohexylamine
DCM	dichloromethane
Dcp	dichlorophenyl
DCU	dicyclohexylurea
Dde	*N*-(1-(4,4-dimethyl-2,6-dioxocyclohexylidene) ethyl
DEAE	diethylaminoethanol
Deg	diethylglycine
DG	distance geometry
Dha	dehydroalanine
Dhc	*S*-(2,3-dihydroxy-propyl)cysteine
DIC	*N,N'*-diisopropyl carbodiimide
DIEA	diisopropylethylamine
DIP	4,7-diphenyl phenanthroline
DIPCDI	diisopropylcarbodiimide
DIPEA	diisopropylethylamine
DMA	dimethylacetamide
DMAP	dimethylaminopyridine
DMBA	9,10-dimethyl-1,2-benzathracene
DMF	dimethylformamide
DMPC	dimyristoylphosphatidyl-choline
DMPG	dimyristoylphosphatidyl-glycerol
DMS	dimethyl sulfide
DMSO	dimethyl sulfoxide
DmtOH	2,2-dimethyl-L-thiazolidine-4-carboxylic acid
DNP	dinitrophenyl
Dns	dansyl
DOC	deoxycholate
DOPC	dioleoyl-*sn*-glycero-phosphocholin
DP	dipeptidyl peptidase
Dpa	diphenylalanine
DPCDI	diisopropylcarbodiimide;
DPDPE	cyclo[DPen^{2}-DPen^5] enkephalin
Dpg	dipropylglycine
DPPC	dipalmitoyl phosphatidylcholine
Dpr	2,3-diaminopropionic acid
DQF	double quantum focused
DRE	dermenkephalin
DSIP	delta sleep inducing peptide
DSP	dimethylsulfonium methyl sulfate
DTDP	dithiodipyridine
DTNB	dithiobis(2-nitrobenzoic acid)
DTPA	diethylenetriamine pentaacetic acid
Dts	dithiasuccinoyl
DTT	dithiothreitol
DTX	dendrotoxin
Dyn	dynorphin
EAE	experimental autoimmune encephalomyelitis
ECD	extracellular domain
ECEPP	Empirical Conformational Energy Program for Peptides

ECM	extracellular matrix
ED_{50}	median effective dose
EDT	ethane dithiol
EDTA	ethylenediaminetetraacetic acid
EE	early endosomes
EGF	epidermial growth factor;
EGFR	epidermial growth factor receptor
EIAV	equine infectious anemia virus
ELISA	enzyme-linked immunosorbent assay
EM	electron microscopy; energy minimization
EMIT	enzyme multiplied immunoassay technology
EMSA	electrophoretic mobility shift assay
ER	endoplasmic reticulum
ES	electron spray
ESIMS	electrospray ionization mass spectrometry
ESMS	electrospray mass spectrometry
ESR	electron spin resonance
ET	endothelin
EtA	α-ethylalanine
Etm	ethyloxymethyl
EYPC	egg yolk phosphatidyl-choline
FAA	fatty amino acid
FABMS	fast atom bombardment mass spectrometry
Farn	farnesyl
Fbg	fibrinogen
Fg	fibrinogen
FGF	fibroblast growth factor
FI	feeding inhibition
FITC	fluorescein isothiocyanate
Fm, fm	fluorenylmethyl
FMDV	foot-and-mouth virus
FMOC, Fmoc	9-fluorenylmethoxycarbonyl
Fpa	4-fluorophenylalanine
FPLC	fast protein liquid chromatography
FRE	fibrinogen recognition exosite
G6PdeH	glucose-6-phosphate dehydrogenase
GC	gas chromatography
gCSF	granulocyte colony stimulating factor
GH	growth hormone
GHRH, GRF	growth hormone releasing hormone
GHRP	growth hormone releasing peptide
GITC	2,3,4,6-tetra-*O*-Acb D-glucopyranosyl isothiocyanate
Gla	D-galactopyranosyl; gamma carboxyglutamic acid
Glc	glycosyl
GluDH	glucose dehydrogenase
Gn, Gu	guanidine
GnRH	gonadotropin releasing hormone
GP	glycogen phosphorylase; guinea pig
GPCRs	G-protein coupled receptors
GPGB	guinea pig gallbladder
GPI	guinea pig ileum
GRF, GHRH	growth hormone releasing factor
GRP	gastrin releasing peptide
GSH	reduced glutathione
GST	glutathione *S*-transferase
GT	glutamase
GTP	guanosine triphosphate
h	human
HA	hexosaminidase
HAI	haemagglutination inhibition
HAPyU	*O*-(7-azabenzotriazolyl)-1,1,3,3-bis(tetramethylene) uronium hexafluoro-phosphate

HATU	1-hydroxy-7-azabenzotriazole uronium salt derivative
Hb	hemoglobin
HBsAg	hepatitis B virus surface antigen
HBTU	*O*-benzotriazolyl-*N,N,N',N'*-tetramethyluronium hexafluorophosphate
HBV	hepatitis B virus
HCA, hCA	human carbonic anhydrase
hCG	human chorionic gonadotropin
HDL	high density lipoprotein
HEL	hen egg lysozyme
Hep	heptyl
Hepes	*N*-[2-hydroxyethyl] piperazine-*N'*-2-ethanesulfonic acid]
HF	hydrogen fluoride
HFIAP	hagfish intestinal antimicrobial peptide
HFIP	hexafluoroisopropanol
hGH	human growth hormone
HIV	human immunodeficiency virus
HIVPR	human immunodeficiency virus protease
HLA	human leukocyte antigen
HLE	human leukocyte elastase
HMB, Hmb	hydroxymethylbenzoic acid
HMBA-MBHA	hydroxymethyoxybenzyl alcoholmethylbenzhydrylamine
HNE	human neutrophil elastase
HOAt	1-hydroxy-7-azabenzo triazole
HOBt	*N*-hydroxybenzotriazole
HPLC	high performance liquid chromatography
hPTH	human parathyroid hormone
HR, hr	human recombinant; histamine release
HRG	heregulin
HRT	histamine-releasing toxicity
HS-TP	thiopyridine
HSA	human serum albumin
Hse	homoserine
Hsp	heat shock proteins
HSPS	high speed peptide synthesis
HSV	herpes simplex virus
HTLV	human T-cell leukemia virus
HUVEC	human umbilical vein endothelial cell
Hyp	hydroxyproline
Hz	hertz
i.m.	intramuscular
i.v.	intravenous
IAA	indolizidinone amino acid
IC	inhibitory concentration
ICAM	intracellular adhesion molecule
ICD	intracellular domain
ICE	interleukin convertase
IEC	ion-exchange chromatography
IEF	isoelectric focusing
IFN	interferon
Ig	immunoglobulin
IGF	insulin-like growth factor
IL	interleukin
IN	indolyl-naphthyl
iNOC	isonicotinyl protecting group
IP	inositol phosphate
IR	infrared; insulin receptor
IRMA	immunoradiometric assay
IS-MS	ion spray mass spectroscopy
IU	international units
K-FGF	Kaposi fibroblast growth factor
KLH	keyhole limpet hemocyanin
LCMV	lymphocytic choriomeningitis virus
LCP	lipid-core peptide
LDH	lactate dehydrogenase

LDTOF	laser desorption time-of-flight
LE	late endosomes
LEC	ligand-exchange chromatography
LEP	lysyl endopeptidase
LFA-1	leukocyte function-associated antigen-1
LH	luteinizing hormone; lutropin
LHRH	*see* GnRH
LNC	lymph node cell
LPG	lipophosphoglycan; lysophosphatidyl-glycerol
LpL	lipoprotein lipase
LPS	lipopolysaccharide
LSF	lung surfactant
LUV	large unilamellar vesicle
LYS	lysosomes
m	murine; messenger
MAb, Mab, mAb	monoclonal antibody
MALDI	matrix-assisted laser desorption ionization
MALDI-MS	matrix-assisted laser desorption/ionization mass spectroscopy
MALDI-TOF	matrix-assisted laser desorption/ionization time-of-flight mass spectroscopy
Man	2-mercaptoaniline
MAO-A	monoamine oxidase type A
MAP, MAp	membrane-anchored protein; multiple antigen peptide; mean arterial pressure
MARS	multiple automatic robotic synthesizer
Mba	2-mercaptobenzoic acid
Mbc	4'-methyl-2,2'-bipyridine-4 - carboxylic acid
MBEC	bovine microepithelial cell
Mbh	methoxybenzhydryl
MBHA	methylbenzhydrylamine
MBP	myelin basic protein
McB17	microcin B17
MCPS	multiple constrained peptide synthesis
MD	molecular dynamics
Me	methyl
MeBmt	(4R)-4-[(2'E)-butenyl]-4,*N*-dimethyl-(L)-threonine
MECC	micellar electrokinetic capillary chromatography
MeDOPE	monomethyl dioleoyl-phosphatidylethanol amine
MeOH	methanol
MgTX	margatoxin
MHC	major histocompatibility complex
MIC	minimal inhibitory concentration
MITO	mitochondria
ML	mistletoe lectin
Mls	minor lymphocyte-stimulating gene
MLV	multilamellar vesicle
mMIF	macrophage migration inhibitory factor
MNEI	single-chained monelline
Mot	motilin
MP	mastoparan
Mpa	mercaptopropionyl
Mpg	3-methoxypropyl glycine
Mpr	3-mercaptopropionyl
Mpr	mercaptopropionic acid
mRNA	messenger ribonucleic acid
MS	multiple sclerosis; mass spectrometry
MSCRAMMs	microbial surface components recognizing adhesive matrix molecules
MSH	melanocyte stimulating hormone; melanotropin
Msob	methylsulfinylbenzyl
Msz	methylsulfinylbenzyl oxycarbonyl
MT	metallothionein

mT	middle T antigen of polyoma virus
MTSSL	methane-thio-sulfonate spin label
MuLV	murine leukemia virus
MVD	mouse vas deferens
Mwt	molecular weight
Nal	2-naphthylalanine
Nbb	nitrobenzamidobenzyl
NBD	7-nitrobenz-2-oxa-1,3-diazole
NBS	*N*-bromosuccinimide
NCA	N-carboxyanhydride
NcMT	Neurospora crassa metallothionein
NDF	Neu differentiation factor
Nic	nicotinoyl
NIS	*N*-iodosuccinimide
NK	neurokinin
NLS	nuclear localization sequence
NM	neuromedin
NMB	neuromedin B
NMDA	*N*-methyl-D-aspartate
NMM	*N*-methylmorpholine
NMP	*N*-methyl pyrrolidinone
NMR	nuclear magnetic resonance
NOE	nuclear Overhauser effect
NOESY	nuclear Overhauser enhanced spectroscopy
NPA	nitrophenoxyacetyl
Npp	nitrophenyl pyrazolinone
NPS	*o*-nitrophenylsulfenyl
NPY	neuropeptide Y
Nsc	*N*(α)-2-(4-nitrophenyl) sulfonylethoxycarbonyl
NTHi	nontypeable *Haemophilus influenzae*
NTI	naltrindole
Nva	norvaline
Oic	octa-hydroindole-2-carboxylic acid
OM	otitis media
OMe	methyl ester
OMP	outer membrane protein
ONb	*o*-nitrobenzyl
OPA	*o*-phthaldialdehyde
OSu	*o*-succinimide ester
OT	oxytocin
OVA	ovalbumin
OVLT	organum vasculosum laminate terminalis
Oxa	2-aminomethyloxazole-4-carboxylic acid
OXT	oxytocin
PA	palmitic acid; polyamide
PAb	polyclonal antibodies
PAB	*p*-alkoxybenzyl
PAC, Pac	phenacyl
PAF, Paf	*p*-aminophenylalanine
PAGE	polyacrylamide gel electrophoresis
PAK	*Pseudomonas aeruginosa* strain K
Pal	3-pyridylalanine
PAL	photoaffinity labeling; [5-(4'-aminomethyl-3',5'-dimethoxyphenoxy) valeric acid]
PaO_2	partial arterial oxygen pressure
PBL	peripheral blood lymphocyte
PBS	phosphate-buffered saline; pulsating bubble surfactometer
PC1	prohormone convertase 1
PD-MS	plasma desorption mass spectrometry
PDB	phorbol 12,13-dibutyrate
PDGF	platelet derived growth factor
PE	phosphatidylethanolamine
PEEP	positive end-expiratory pressure
PEG	polyethylene glycol
PEP	prolyl endopeptidase
PG	proteoglycan

PHA	phytohemagglutinin
Phaa	phenylacetic acid
PhAc	phenylacetamido group
PHBT	polymeric hydroxybenzotriazole
Phi	4-iodophenylalanine
Phpa	3-phenylpropanoic acid
PI	phosphatidylinositol; propidium iodode
pI	isoelectric point
Pic	picolinoyl
Pix	S-9-phenylxanthenyl
Piz	piperazic acid
PK	protein kinase
PKC	protein kinase C
PLA_2	phospholipase A_2
PLB	phospholamban
PLC	phospholipase C
PLTX	proteolipid toxin
PM	plasma membrane; portioning mixing method
PMA	phorbol myristate acetate
PMB	polymyxin B
pMH	*p*-methylbenzoyl glycine
PMN	polymorphonuclear leukocyte; neutrophil
pNA	*p*-nitroaniline
PNA's	peptide nucleic acids
PND	principal neutralizing determinant
POPG	palmitoyloleoylphosphatidyl glycerol
PPIase	peptidylprolyl isomerase
PPII	polyproline type II
PPL	porcine pancreatic lipase
Ppt	diphenylphosphinothionyl
PrP	prion protein
PRP	platelet-rich plasma
PS	phosphatidylserine; polystyrene
PS-POE	polystyrene-polyoxyethylene
PS-SCL	positional scanning synthetic combinatorial libraries
PSA	preformed symmetrical anhydride
PT	pertussis toxin
PTB	phosphotyrosine binding
PTC	phenylthiocarbamyl
PTH	phenylthiohydantoin; parathyroid hormone
PTHrP	parathyroid hormone related protein
PTK	protein tyrosine kinase
Ptm	phenyloxymethyl
PTPase	protein-tyrosine phosphatase
PTX	pertussis toxin
PTZ	phenothiazine
PVA	polyvinyl alcohol
PVDF	polyvinylidene fluoride
PyBOP	(benzotriazolyl)-*N*-oxy-pyrrolidinium phosphonium hexafluorophosphate
Pyr	pyrrolidide
PYY	peptide tyrosine tyrosine
R	receptor
r	recombinant
RA	rheumatoid arthritis
RAFT	regioselectively addressable functionalized templates
RDS	respiratory distress syndrome
REDOR	rotational echo double resonance
RET	resonance energy transfer
RGD	Fibrinogen binding sequence
rhEPO	recombinant human erythropoietin
RIA	radioimmunoassay
RIPs	ribosome-inactivating proteins
RLX-2	relaxin 2
RMS, rms	root mean square
RMSD, rmsd	root mean square deviation
RNase	ribonuclease
ROE	rotating frame nuclear Overhauser effect

ROESY	rotating frame nuclear Overhauser enhanced spectroscopy
RP	reversed phase
RPHPLC, RPC	reversed phase high performance liquid chromatography
RPIF	relative positional importance factor
RT	reverse transcriptase
RV	rubella virus
rV-CEA	recombinant vaccinia carcinoembryonic antigen
SAA	serum amyloid A; sugar amino acid
SABR	Structure Activity Bioavailability Relationships
SAP	serum amyloid protein
Sar	sarcosyl; sarcosine
SAR	structure-activity relationships
SCC	short circuit current
SCL	synthetic combinatorial libraries
SCLC	small cell lung carcinoma
SDB	styrene divinylbenzene
SDS	sodium dodecylsulfate
SEC	size exclusion chromatography
SEM	standard error of the mean
SH	sulfhydryl
SIV	simian immunodeficiency virus
SLC	sublethal concentration
SLE	systemic lupus erythematoius
Smc	*S*-methylcysteine
SMPS	simultaneous multiple peptide synthesis
SOC	sequential oligopeptide carrier
SP	substance P; S-protein
SPCL	synthetic peptide combination libraries
SPPS, SPS	solid phase peptide synthesis
SR	sarcoplasmic reticulum
SRIF	somatostatin
ssDNA	single stranded DNA
ST	heat stable enterotoxin
Sta	statin
STI	soybean trypsin inhibitor
Su	succinimide
Suc	succinoyl
TAP	tick anticoagulant peptide
TAR	transactivation response
TASP	template-assembled synthetic protein
Tat	transcriptional activator
TBS	tert butyldimethylsilyl
TBTU	*O*-(benzotriazol-l-yl) *N,N,N′,N′*-tetramethyl-uronium tetrafluoroborate
Tca	trichloroacetamide
TCEP	tris(2-carboxyethyl) phosphine
TCP	trichlorophenyl
TCPP	tris(dimethylamino)chloro-phosphonium perchlorate
TCR	T-Cell receptor
TEA	triethylamine
TETD	tetraethylthiuram disulfide
TFA	trifluoroacetic acid
TFE	trifluoroethanol
TFM	trifluoromethyl
TFMSA	trifluoromethane sulfonic acid
TGF	transforming growth factor
TGN	trans Golgi network
T_h	helper T cell
T_H	hexagonal phase transition temperature
Th	thiazolidines
TH1	T-helper-1 cell
TH2	T-helper-2 cell
THF	tetrahydrofuran

Thia	thiazolidide
THPs	triple-helical polypeptides
THTP	tetrahydrothiophene
Thz	thiazolidine carboxylic acid
TIC, Tic	tetrahydroisoquinoline carboxylic acid
TLC	thin layer chromatography
TM	transmembrane
Tmob	trimethoxybenzyl
TMP	3,4,7,8-tetramethyl phenanthroline
TMS	trimethylsilyl
TMSI	iodotrimethylsilane
TMSOTf	trimethylsilyl trifluoromethanesulfonate
TMVP	tobacco mosaic virus protein
Tn	troponin
TNF	tumor necrosis factor
TOCSY	total correlation spectroscopy
Top	thiopyroglutamic acid
TPA	12-*O*-tetradecanoyphorbol-13-acetate; tissue plasminogen activator
TPTU	1,1,3,3-tetramethyl-2-(2-oxo-1-(2H)-pyridyl)uronium tetrafluoroborate
TRCOSY	transferred rotational correlated NMR spectroscopy
TRH	thyrotropin releasing hormone
Tris	tris(hydroxymethyl)-aminomethane
TRNOE	transferred nuclear Overhauser effect
TSH	thyroid stimulating hormone
T-SS	tachyplesin
TT	thrombin time; tetanus toxoid; tetanus toxin
TxA_2	thromboxane A_2
UK	urokinase
UNCA	urethane protected α–amino acid N-carboxy anhydride
UNCA's	urethane N-carboxyanhydrides
UV	ultraviolet
VIP	vasoactive intestinal peptide
VLDL	very low density lipoprotein
VN	virus neutralization
Vn	vitronectin
VP-1	vasopressin
VSMC	vascular smooth muscle cells
WT	wild type
XAL	5-(9-aminoxanthen-2-oxy)valeric acid
Xan	N-xanthenyl
Z, Cbz	carbobenzoxy; benzyloxycarbonyl

Contents

Session II: Peptide Delivery/Pharmaceutical

Chairs: Jean Rivier and James Samanen

Session III: Biologically Active Peptides

Chairs: Ruth F. Nutt and G.M. Anantharamaiah

Session IV: Peptide-Protein Interactions

Chairs: Y. Shimonishi and Manfred Mutter

Session V: Peptide Libraries

Chairs: Deborah S. Parris and Hossain H. Saneii

Session VI: Peptide Inhibitors/Receptors

Chairs: Daniel F. Veber and Maria-Luisa Maccecchini

Session VII: Signal Transduction

Chairs: Annette M. Doherty and Tom Lobl

Session VIII: Glyco/ Lipo/ Phospho/ Peptides

Chairs: Albert Loffet and Vadim Ivanov

Session X: Conformational Analysis

Chairs: Garland R. Marshall and Claudio Toniolo

Session XI: *De Novo* Design

Chairs: Bruce W. Erickson and Irwin M. Chaiken

Session XII: Peptide Hormones Neuropeptides

Chairs: Arthur M. Felix and Cecilia Unson

Session XIII: Peptide Mimetics

Chairs: Murray Goodman and Waleed Danho

Session XIV: NMR

Chairs: Kenneth D. Kopple and Arnold Satterthwait

Session XV and XVI: Peptide Vaccines & Immunology

Chairs: John A. Smith and Michael D. Lairmore
Conrad Schneider and Helene Grasse-Masse

Mini Symposia I & II

Chairs: Terresa M. Kubaik and Tomi K. Sawyer / John W. Taylor and Susan Wang

Workshop I: Peptide Vaccines

Chairs: Fred Brown and Vernon Stevens

Workshop II: Peptides in Membranes

Chairs: Charles M. Deber and Gerald D. Fasman

Workshop III: Synthetic Peptide/Libraries

Chairs: Derek Hudson and Tom Lobl

Workshop IV: Peptide/Nonpeptide Mimetics

Chairs: Roger M. Freidinger and Arno F. Spatola

Tenth Alan E. Pierce Award Lecture

Dr. John M. Stewart

Chairs: Pravin T.P. Kaumaya and
R. Bruce Merrifield

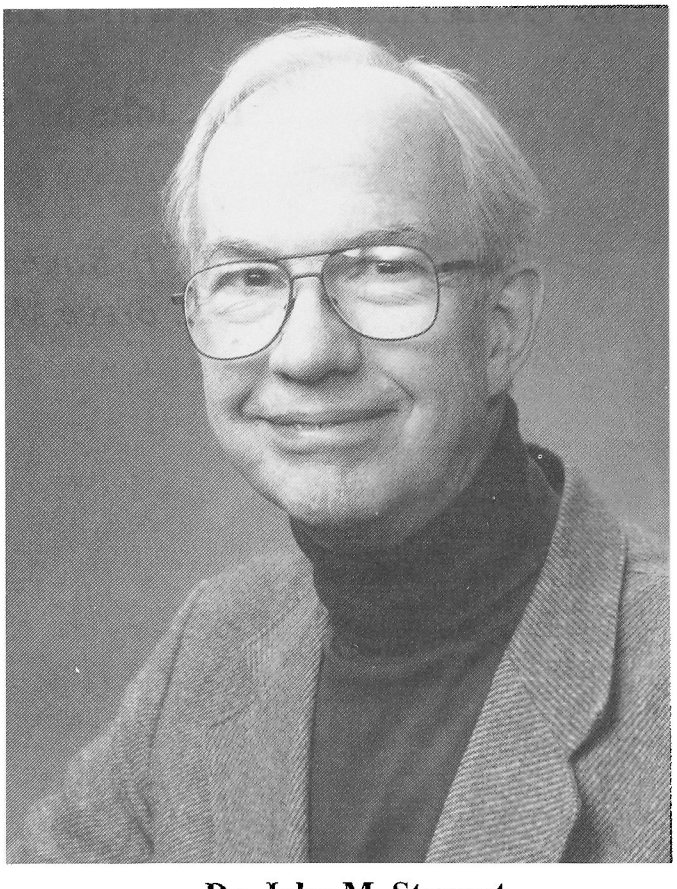

Dr. John M. Stewart

Recipient of the Tenth Alan E. Pierce Award

Peptides: Chemistry, Structure and Biology
Pravin T.P. Kaumaya and Robert S. Hodges (Eds.)
Mayflower Scientific Ltd., 1996

Peptides: Promises, Problems and Practicality Four Decades of Exploration

J.M. Stewart

Department of Biochemistry, Biophysics and Human Genetics, University of Colorado School of Medicine, Denver, CO 80262, USA

Introduction

It is a very great honor and pleasure for me to accept the tenth Alan E. Pierce award of the American Peptide Society. I am particularly pleased that the Pierce Chemical Co. has agreed to transfer the award funds directly to the John M. Stewart Fund for Peptide Research that I have established in the University of Colorado Foundation with the goal of endowing a chair of peptide research at the University of Colorado Medical School.

I am also indebted to Pierce as publisher of the second Edition of "Solid Phase Peptide Synthesis" that Jan Young and I wrote in 1984. It is gratifying that, despite the many advances in peptide chemistry that have come in the last decade, this book is still considered to be useful, and Pierce maintains the book in publication.

Given this opportunity to review some of the events of the last four decades of my work, I am especially happy to acknowledge the dedicated efforts of those persons who have worked with me and have made my achievements possible. I shall mention many of them by name during this review.

These four decades have seen the total transformation of peptide chemistry. At the beginning of these years, two major events had awakened the scientific world to peptides: the determination by Sanger of the amino acid sequence of insulin in 1951 and the synthesis of oxytocin by du Vigneaud in 1953. Those accomplishments, achieved by dedicated, laborious application of methods totally primitive by today's standards, did show, however, that the difficulties of sequence determination and synthesis of peptides could be overcome. These have been exciting years to be active in peptide research and I am pleased to have been able to make some contributions to that excitement.

Contributions to Solid Phase Peptide Synthesis

It was a rare opportunity to have been working in the same laboratory at Rockefeller University where Bruce Merrifield conceived the idea and developed the practice of solid phase peptide synthesis. Bruce and I were both working for D.W. Woolley, who made many contributions to early work on antimetabolites, structural analogs of biologically active molecules that acted as antagonists. He also discovered the neuronal action of serotonin and made important contributions to neurochemistry and the basis of mental diseases. Bruce, working on peptide growth factors with Dr. Woolley, had

isolated Ser-His-Leu-Val-Glu from a partial hydrolysate of insulin, and had so much difficulty synthesizing this peptide by the methods available at that time (1955) that he thought there must be a better way to do peptide synthesis. In 1957 he conceived the idea of assembling the amino acids stepwise while the growing chain was attached to an insoluble support. After many false starts and blind alleys, the solid phase synthesis of the first peptide, Leu-Ala-Gly-Val, was published in 1963.

It is truly remarkable that Bruce, trained as a microbiologist, was able to make a Nobel prize-winning contribution to the methodology of organic synthesis. Since I was trained as an organic chemist, it was logical that he turned to me for help, and I remember many long hours of discussions of organic reactions and organic reaction mechanisms during those years of difficulties. Moreover, I had already been working on peptide synthesis, trying to inhibit racemization during coupling reactions by using mixed anhydrides prepared with an optically active organic acid.

Bradykinin and Solid Phase Synthesis

Bradykinin was discovered in 1946, but it was not until 1960 that its sequence was determined to be Arg-Pro-Pro-Gly-Phe-Ser-Pro-Phe-Arg. Because centrally administered bradykinin was reported to have effects on behavior, Woolley suggested that I try to modify the structure of bradykinin to make an antagonist. In 1962, I began to synthesize analogs of bradykinin, and in order to test the biological activity of the analogs I synthesized, I set up the isolated rat uterus assay, a standard pharmacological assay for bradykinin activity.

Given the peptide chemistry that was available in 1960, bradykinin was a difficult peptide to synthesize, due to the presence of the two arginines. After synthesis of LAGV, Bruce selected bradykinin as the next target for solid phase synthesis. It presented the chemical challenge of the arginine residues, but had the advantage that biological activity of the product could be readily assayed in my laboratory. The successful synthesis of bradykinin, reported in 1964, created great excitement and convinced the peptide world that solid phase synthesis was a reality.

Once Bruce had completed his synthesis of bradykinin, I immediately applied solid phase methodology to my bradykinin work. In a full year of synthesis of bradykinin analogs in solution I had synthesized, purified and assayed three analogs. In the next year, using solid phase synthesis, I synthesized 25 analogs.

Early Chemical Problems

Quite early in the development of solid phase synthesis we had problems with incomplete chain growth, and realized that this might be due to inadequate resin swelling during deprotection of the Boc group. We changed the original deprotection reagent, 1M HCl in glacial acetic acid, which does not swell the resin, to 4M HCl in dioxane, which swells the polystyrene resin highly. Until TFA in DCM was adopted as the reagent for deprotection, preparing dry, peroxide-free dioxane and saturating it with gaseous HCl were major parts of the solid phase mystique. Eventually it was understood that, in order for syntheses to continue without termination, solvents must be used that

swell the resin fully. Simple measurement of polymer swelling in DCM was introduced as a practical measure of usefulness of a given batch of polymer. Measurement of swelling is still a useful practical measure of suitability of a resin for synthesis.

Automatic Solid Phase Synthesis

In his original conception of solid phase synthesis, Bruce had realized that the use of an insoluble support would make the whole process of peptide sythesis amenable to automatic operation. Bruce asked me if I would undertake the design and construction of an automatic instrument, and, after my initial successes with bradykinin analogs, I agreed to do so. Primary control in the automatic synthesizer was by a stepping drum programmer, a commercial instrument that used pegs inserted in holes in a drum to activate microswitches. Fundamental to the success of the instrument was a pair of 12-position rotary Teflon selector valves, designed and built by Nils Jernberg in the Rockefeller instrument shop. Although such valves are commonplace today, they were unique at that time. The first synthesizer used a programmer with a small drum that had positions adequate for only one kind of synthesis chemistry: diimide or active ester coupling. At that time asparagine and glutamine were coupled as nitrophenyl esters, while DCC was used for all others. To change coupling chemistry required stopping the synthesis and changing the programmer drum. The second instrument, built after succesful operation of the first, had a large drum that accommodated program pegs for both coupling chemistries, and switched automatically between them. The first synthesizer is now in the Smithsonian Institution in Washington, DC.

The first two synthesizers were constructed in the basement shop in my home in New Jersey. When I decided to leave Rockefeller and move to Colorado in 1968, I worked with Nils Jernberg on construction of a synthesizer to take to Colorado. This also gave him the information he needed to do any necessary repair work on the two synthesizers remaining in the Merrifield laboratory. The synthesizer I took to Denver underwent several significant improvements over the next few years, and was used continually until 1986. Nils also constructed synthesizers for several other peptide chemists. One of these was in Sao Paulo, Brazil, for Antonio Paiva, who arranged for me to help set up his laboratory for synthesis in 1971 and to teach a laboratory course with students from four Latin American countries. Another synthesizer, purchased by Alejandro Paladini, in Buenos Aires, was set up and operated by Martha Knight, who had come to Denver with me from Rockefeller, and spent two years in Argentina in an exchange with Clara Peña, who, while she was in Denver, synthesized the longest peptide ever synthesized in my laboratory: a 126-residue fragment of human growth hormone. The synthesizer in Sao Paulo is still operating at this time alongside two modern synthesizers.

When Beckman decided to develop the peptide synthesizer, Bruce and I both worked with them on the design. When they marketed the Model 990 synthesizer in the spring of 1972, Bruce received synthesizer serial number one, and I received the serial number two instrument, which is still in routine use in my laboratory in Denver. It has been used for synthesis of literally thousands of peptides.

"The Book"

At the FASEB meeting in 1965 I presented the work on synthesis of bradykinin analogs by solid phase. Jan Young and Eliezar Benjamini heard the talk and invited me to spend the summer at the Kaiser Foundation Research Institute in San Francisco to teach them how to do solid phase synthesis. They also had the specific goal of determining, by synthesis, the epitope in tobacco mosaic virus protein (TMVP) recognized by an anti-serum. Both goals were realized. The TMVP project represented the first precise definition of a protein epitope and stands as a landmark in immunochemistry. Jan had organized the Bay Area Peptide Club, and at their request she wrote a small "cookbook" of solid phase synthesis. At her urging I became involved in the writing, and by 1968 we had finished the manuscript. W.H. Freeman agreed to publish the book and, at our urging, set the price very low ($5.00), so that it would be readily accessible to students. The first edition of 'Solid Phase Peptide Synthesis' was published in 1969.

When the time came for a second edition, Freeman, who had lost money on the book, did not want to publish the second edition. Pierce fortunately published it; and the second edition, published in 1984, is still available from them - although the price is much more than $5! The first edition was translated into Russian in the Soviet Union. We first learned of the translation several years afterward, when a Polish peptide chemist told us about the translation and found copies for us.

Later Improvements in Solid Phase Chemistry

When we began to synthesize analogs of substance P and luteinizing hormone releasing hormone (GnRH), which are amides, we encountered low yields using the benzhydryl-amine resin, which was introduced by Pietta and Marshall. Gary Matsueda, in my laboratory, synthesized the methylbenzhydrylamine resin, in which the peptide-resin link is more labile, and which gives improved yields of most peptide amides.

Although there had been much discussion in the early years about differential solvation of the polystyrene resin and the growing peptide chain, the general use of powerful polar solvents such as DMF minimized most such problems. Then Deber described a truly difficult sequence that was predicted to adopt β-sheet conformation. This very hydrophobic peptide could be expected to aggregate on the resin. At the same time, in work by Eunice York on α-helical peptides, we were surprised by the failure of oligoalanines to grow at about the decapeptide stage. Realizing that secondary structure was a common factor in these two difficult sequences, we examined the incorporation of chaotropic salts in the coupling reaction to break up secondary structure. Wieslaw Klis found that sodium perchlorate and potassium thiocyanate, well-known chaotropic agents, would greatly improve coupling in these difficult sequences. The important common factor was recognition of the role of conformation and structure in these problems.

In another recent chemistry study, the Npys blocking group, introduced by Rei Matsueda, was carefully investigated by Kathie Pugh and Lajos Gera for use as an N-blocking group that can be removed by triphenyl phosphine under neutral conditions, giving an additional level of orthogonal deprotection to solid phase synthesis.

Helical Peptides

In a collaboration with Robert Baldwin, at Stanford, Eunice York has carried out syntheses that defined the rules for formation of α-helices by short peptide sequences. Prior to our work, it was considered that no peptides of modest length (15-20 residues) would show any α-helix in water, even though they were composed of residues with a high helix forming potential. Contrary to this rule was the behavior of the N-terminal peptide (residues 1-13) derived from ribonuclease A by CNBr cleavage (the so-called "C" peptide); it showed partial helix in cold water. This part of RNAse is helical in the intact protein. The key to this behavior was the fact that the CNBr cleavage product is a C-terminal homoserine lactone. Hydrolytic opening of the lactone, yielding the free acid, destroyed the helix.

At that time, Hol had just described the helix induced dipole. Reasoning that this induced charge was inhibiting helix formation, we synthesized the RNAse sequence with the ends blocked: an N-terminal acetyl and a C-terminal amide. Immediately, CD and NMR showed a significant amount of helix in cold water. By choice of appropriate residues, we were able to design peptides of 15-20 residues that are completely helical in cold aqueous solution.

These studies by our group, and later by others, completely redefined the helix-forming tendency (the Zimm-Bragg "s" value) of the normal amino acids. The values determined in these peptides were quite different from the older values derived from "host-guest" studies by Scheraga. In order to define the "s" value of each amino acid, we needed a standard "carrier" or "backbone" peptide in which to insert the residue under study. Oligoalanines would appear to be ideal, due to the high helix-forming tendency of alanine, but acetyl-oligoalanine-amides are about as soluble as sand. In the studies on neutral amino acids, glutamic and lysine residues were used judiciously to give adequate solubility, but for the charged amino acids a neutral carrier was needed to avoid artifacts caused by interaction of the new charged amino acid with the Glu and Lys residues already in the carrier. We designed an oligoalanine containing several glutamine residues to provide water solubility. Being uncharged, these residues did not distort the interpretation of the helix-forming potential of introduced charged residues.

Designed Helix Bundles

Since we knew how to make peptides that would be helical in aqueous solution, it seemed reasonable to try to design a bundle of helical peptides that could serve as a carrier for a group of amino acids having a specific function, as, for example, an enzyme active site. Using the molecular graphics program SYBYL, Karl Hahn designed a molecule consisting of four parallel amphipathic α-helices bearing the "catalytic triad" residues of the chymotrypsin active site on the N-terminus of the bundle. The C-termini of the four helices were tied together covalently to hold the chains in the desired bundle. The Asp-His-Ser residues of the triad were designed to be in the same spatial arrangement as in chymotrypsin, and the hydrophobic core of the bundle would serve to bind the aromatic side chain of the substrate (acetyl tyrosine ethyl ester, a standard chymotrypsin substrate). After much arduous synthetic work by Wieslaw Klis, Kathy

Pugh and Eva Hallakova, we obtained a product that although not homogeneous, did show esterase activity. Subsequent studies by Mike Corey indicated that the catalysis was probably not mediated by a catalytic triad functioning as intended. Although this work stopped for lack of funding, a different approach using attachment to a carrier of preformed peptide chains could perhaps yield better results.

Biologically Active Peptides and their Antagonists

It was always a personal goal to be able to make some contribution that would help people significantly. Once I became involved in peptides and it was apparent that peptides and their antagonists would play important roles in human biology and medicine, I was pleased to be able to work in areas of peptide hormones and of peptides having central nervous system functions, including behavior. Our work on peptide hormones includes bradykinin, angiotensin and GnRH, and on neuropeptides, substance P, opioids and ACTH.

Bradykinin and its Receptors

There are many features in the biology of bradykinin (Arg-Pro-Pro-Gly-Phe-Ser-Pro-Phe-Arg; BK) that make it unique. It is involved in regulation of every major physiological system, and in one system or another it can activate every known second messenger system. In pathophysiology, BK is the most potent agent known for production of pain and hyperalgesia (tenderness). Current evidence suggests that BK is involved in initiation and maintenance of most inflammation.

Bradykinin is produced when trypsin-like enzymes (kallikreins) act on precursor proteins (kininogens) that contain the BK sequence. Venoms of crotalid snakes contain such trypsin-like enzymes. Kallikreins can be activated in many ways. Ischemia causes acidification of the blood and tissues due to accumulation of carbon dioxide and acidic metabolites (lactate). This acidification is sufficient to activate plasma kallikrein and produce BK. BK is produced whenever tissue damage causes blood clotting. Most likely the function of BK in this situation is to stimulate wound repair, since BK has growth factor activity.

Actions of BK are mediated by at least two classes of receptors, B1 and B2, both of which are G-protein coupled receptors. Most physiological functions of BK and also those involved in acute inflammation are mediated by B2 receptors, which are expressed constitutively. The gene for B1 receptors, normally not expressed in most tissues, is induced in chronic inflammation. B2 receptors require the full BK sequence, including both N-terminal and C-terminal arginines, for effective activation, whereas the preferred ligand for B1 receptors is BK-(1-8). B1 receptors were first identified in damaged tissue.

Bradykinin is very rapidly removed from the circulation. Ferreira and Vane showed that BK activity disappeared on passage through the pulmonary circulation. Jim Ryan and Juan Roblero in my laboratory showed that the mechanism of this "disappearance" is enzymatic cleavage. Angiotensin I converting enzyme (ACE), located primarily on the pulmonary capillary walls, inactivates about 99% of the BK in blood on a single

passage through the pulmonary circulation by removing the C-terminal dipeptide, yielding a totally inactive product. The soluble plasma enzyme carboxypeptidase N (CPN) inactivates BK by removing the C-terminal arginine residue. The product of CPN action, BK-(1-8), while inactive at B2 receptors, is a fully active ligand for B1 receptors. One puzzle of chronic inflammation - especially sepsis - is that ACE is lost from the pulmonary capillaries. Most BK is then no longer metabolized by ACE, but by CPN, providing ligands for B1 receptors that aggravate shock by further lowering blood pressure.

Another adventure in BK research involved the BK-potentiating peptides found in *Bothrops jararaca* venom by Ferreira and first sequenced by Lew Greene. Lew and I synthesized the first of these in my laboratory the first year I was in Colorado. These peptides, which inhibit BK degradation, were found by Ferreira and Vane to inhibit ACE. Subsequent research based on these peptides, principally at Squibb, led to development of captopril, the first commercially successful ACE inhibitor.

Bradykinin Antagonists

Bradykinin B1 receptors were first identified by Regoli and coworkers in 1978. They found that replacement of the C-terminal phenylalanine residue in BK-(1-8) by leucine yielded an antagonist for this new class of receptors: [Leu^{8}]-BK-(1-8). Since the B1 antagonist had no effect on any normal BK responses, it generated little interest except to demonstrate that B1 receptors were not involved in most of the actions of BK in physiology or pathophysiology.

After a 22-year search, we found with Ray Vavrek that replacement of the proline residue at position seven of BK by a D-aromatic amino acid, such as D-phenylalanine, yielded a weak partial antagonist for B2 receptors. During the long search for antagonists, our work had shown several ways to increase the potency of BK agonists, both by increasing the affinity of the peptide for receptors, as well as by blocking enzymic degradation. In one attempt to produce antagonists we replaced both phenylalanines with β-(2-thienyl) alanine (Thi). [Thi^{5,8}]-BK was a super-agonist, later found to have extremely high affinity for BK receptors. Reasoning that the weak and partial antagonism shown by [D-Phe ^{7}]-BK might be due to poor receptor affinity, we applied these modifications that had increased the potency of agonists, and were pleased to find that they gave the desired result; D-Arg-[Hyp^{3},Thi^{5,8},D-Phe^{7}]-BK was the first practically useful BK antagonist, used in hundreds of studies by many investigators.

The next major improvement in BK antagonists (the "second generation") came from investigators at Hoechst, who modified our best antagonist by using D-Tic (tetrahydroisoquinoline-3-carboxylic acid) at position seven, and Oic (octahydroindole-2-carboxylic acid) at position eight. This antagonist, known as HOE-140, was the first to have sufficiently high receptor affinity and *in vivo* lifetime to be considered as a drug. Many excellent studies with this antagonist have clearly demonstrated the participation of BK in many normal and abnormal physiological processes. One surprising result was that, in spite its high potency and long duration of action, HOE-140 was not effective in the later stages of chronic inflammation. Addition of B1 antagonists in these studies demonstrated the participation of B1 receptors in sustained inflammation.

Recently, Lajos Gera in my laboratory synthesized α-(2-indanyl)-glycine (Igl) and incorporated the D-isomer at position seven and the L-isomer at positions five and eight into the standard BK antagonist structure. The best of these new analogs, D-arg[Hyp^3, Igl^{5,8},D-Igl^7]-BK, known as B-9430, is the initiator of the "third generation" of BK antagonists. Although this antagonist has the highest potency and longest duration of action *in vivo* of any antagonist, its unique feature, discovered by Eric Whalley at Cortech, is that it is an excellent antagonist for B1 receptors as well as a spectacular performer as a B2 antagonist. It blocks both the early and late stages of inflammation.

Angiotensin Antagonists

The critical structural change in angiotensin II that yielded an antagonist was replacement of the C-terminal phenylalanine by a hydrophobic aliphatic residue. This result implied that the intrinsic activity of Ang-II depends upon a specific aromatic-aromatic interaction with a residue on the receptor. Clara Peña found that replacing the C-terminal Phe residue by N-methylphenylalanine was also a very effective method for producing an antagonist. Thus, changing the conformation of the C-terminal region of Ang-II by adding the methyl group evidently displaces the side chain enough that it prevents the aromatic-aromatic interaction necessary for activation of the receptor.

In another angiotensin project, Antonio and Therezinha Paiva, when they were learning automatic solid phase synthesis in my laboratory, synthesized a family of Ang-II fragments containing the nitrogen mustard alkylating agent chlorambucil at the N-terminus. One of these was found to be a permanent blocker of angiotensin receptors on smooth muscles, implying the presence of a nucleophilic group on the receptor situated so as to interact with the alkylating moiety. Richard Freer applied the same approach to bradykinin, and found not an antagonist, but a permanent potentiator of the guinea pig ileum response to BK. This result suggested that a BK-degrading enzyme was being inactivated by the alkylating agent.

Substance P, Opioids and the Central Nervous System

Substance P (SP) was discovered in the 1930s by von Euler and Gaddum in a "powder" fraction of brain tissue. It was first designated a neuropeptide in 1953 by Lembeck, who found large amounts of it in the dorsal horn of the spinal cord. We now know that its function there is as a neurotransmitter of sensory messages, especially pain inputs. When peripheral tissue injury causes production of BK and stimulation by it of the sensory nociceptors, SP is the neurotransmitter for these messages. Release of SP from these fibers at their first synapse in the dorsal horn of the spinal cord is inhibited by opiates and opioid peptides, and is stimulated by capsaicin, the piquant substance in chili peppers. The structure of SP is Arg-Pro-Lys-Pro-Gln-Gln-Phe-Phe-Gly-Leu-Met-amide. Studies by us and others showed that for its peripheral actions (contraction or relaxation of smooth muscles; lowering blood pressure) the C-terminal pentapeptide is the essential part of the SP molecule. The endopeptidase 3.4.24.11 ("enkephalinase") was soon identified as the principal SP-inactivating enzyme for these functions. Working with William Krivoy, we found that although SP was identified by others as a neuro-

transmitter for pain, when administered centrally it produced antinociception. This discovery was discounted by the established neuroscientists, since SP could obviously not be both a producer and inhibitor of pain. Besides, what did I, a chemist, know about the brain? We soon solved this paradox by showing that SP-(1-7), the product of 3.4.24.11 degradation, was the active antinociceptive (analgesic) agent. Thus the enzyme that destroys SP action in the periphery actually produces a selective, potent agonist for many CNS functions. The other principal SP degrading enzyme, the prolyl endopeptidase that yields SP-(1-4) and SP-(5-11), produces the agonist for classical SP receptors (NKA receptors). Michael Hall in my laboratory found that for a wide range of rodent behaviors the N-terminal [SP-(1-7)] (SP-N) and C-terminal [SP-(5-11)] (SP-C) fragments produce opposite effects. Gaffori and de Wied found that when injected into the nucleus accumbens, SP-N enhances and SP-C destroys learning and memory in rats. Thus these two "SP-degrading" enzymes are actually selective processing enzymes for CNS functions. I have suggsted that SP is the "yin-yang" of behavior.

Mike Hall also showed that SP-(1-7) is evidently the neurotransmitter of the baroreflex, the mechanism by which blood pressure is regulated on a rapid time scale. SP is also the principal stimulus for central dopamine release, and our current evidence suggests that in the nigro-striatal circuit, involved in motor control, the SP- N is the active agent, whereas in the mesolimbic system, involved in interpretation of sensory input, SP-C is active. The major implication of these facts is that drugs to combat Parkinsonism (caused by dopamine deficit in the nigro-striatal system) may be developed that do not cause schizophrenia-like side effects, whereas drugs for schizophrenia (caused by over-functioning of the meso-limbic dopamine system) may be developed that do not produce Parkinson-like side effects. An additional exciting observation is that SP-(1-7) seems to prevent the toxic action in the CNS of the amyloid peptide, strongly implicated as a causative agent in Alzheimer's disease. There is a great need for molecular biologists to clone and sequence the receptor for SP-(1-7) (that we call the "SP-N" receptor) so it may be studied in detail and selective agonists and antagonists may be developed. Structural modification of SP-(1-7) yielded useful antagonists.

When the structures of the enkephalins were announced at the end of 1975, we obtained some support to explore structure-activity relationships in these new peptides. Working with Dan Morris and then Ray Vavrek, we found that the enkephalin sequence could be shortened dramatically, and first synthesized Tyr-D-Ala-3-phenyl-*n*-propyl amide, a potent enkephalin.

Luteinizing Hormone Releasing Hormone (GnRH) and ACTH

Shortly after determination of the sequence of GnRH, the histidine residue at position 2 was identified as essential for its intrinsic activity. Other investigators found that D-amino acid residues were useful at positions 2, 3 and 6 of GnRH antagonists. Working with K.C. Basava, we found that the normal pyroglutamyl residue at the N-terminus could be replaced by an acetyl amino acid, and that D-aromatic residues were also very good at position one of GnRH antagonists. In present potent GnRH antagonists, half of the residues are of the D configuration.

When the alpha-mating factor of *Saccharomyces cerevisiae* was sequenced, it was apparent that it was structurally related to GnRH. We synthesized the α-factor and found it to have GnRH activity. We then conducted a search for related amino acid sequences in other biologically active peptides, and recognized a relationship in the sequence of ACTH. We proposed that DNA coding for three amino acids (one turn of the DNA helix) was excised and reinserted one turn further along the helix; this could be accomplished by offset crossover. With this change, ACTH and GnRH were obviously closely related. At that time, it had just been discovered that ACTH-endorphin (POMC) neurons are present in the brain. Assembling evidence from several fields, using effects on sexual function as a key, I proposed that central ACTH is involved in behavioral effects of acute stress and in REM sleep.

Conclusion

These discoveries and developments have been the source of much pleasure and satisfaction throughout these years of peptide adventures. I hope to continue fruitful explorations in the future.

Session I
Bodanzsky Session
Synthetic Methods I

Chairs: Victor Hruby and R. Bruce Merrifield

&

Session IX
Synthetic Methods II

Chairs: Janis D. Young and Ruth H. Angeletti

Peptides: Chemistry, Structure and Biology
Pravin T.P. Kaumaya and Robert S. Hodges (Eds.)
Mayflower Scientific Ltd., 1996

1
Orthogonal Coupling Method as an Approach to Capture and Acyl Activation in Protein Synthesis

J.P. Tam, C.F. Liu, Y.A. Lu, J. Shao, L. Zhang, C. Rao and Y.S. Shin

Department of Microbiology and Immunology, Vanderbilt University, A5119 MCN, Nashville, TN 37232, USA

Introduction

The use of unprotected peptide segments as building blocks for the synthesis of cyclic, branched and large peptides present significant advantages and exciting challenges [1]. The advantages include aqueous solubility, and accessibility to purification and to characterization by conventional methods. More importantly, large peptide segments can be folded to form ordered structures and offer the possibility of conformational assistance to overcome entropy. These desirable structural features provide significant advantages over the corresponding disordered, protected peptide segments.

The challenge lies in the selectivity of amide bond formation without protecting groups. To achieve a high requirement of regioselectivity in amide bond formation, we have developed orthogonal coupling methods for N^{α}-amine in the presence of other reactive functional groups. The orthogonal coupling method is similar in concept to the chemoselective ligation [1-4] but proceeds independently of amines and other functional moieties to give an amide bond. In this paper, we describe four orthogonal coupling methods which exploit reactions involving thiazolidine, thioester and disulfide.

Results and Discussion

Conceptual approach. The scheme (Figure 1) consists of an orthogonal coupling as a capture step to bring the two segments into close proximity, and acyl activation to give amide bond formation which is effected through a proximity-driven intramolecular acyl transfer [1, 2].

Aldehyde capture. Aldehyde capture was the first orthogonal coupling method to be developed by our laboratory in 1992 [1]. The orthogonality of this reaction exploits the thiazolidine or oxazolidine formation of aldehyde with 1,2-substituted aminothiol or 1,2-aminoethanol. Since only N-terminal amino acid Cys or Thr contains such an arrangement of functional groups, the side chain lysine or other α-amine is excluded from this reaction. The specificity of the aldehyde capture can be demonstrated with a dipeptide library containing 400 dipeptides and N-terminal cysteine which reacts almost immediately with aldehyde to form thiazolidine [3]. We have applied this strategy to the successful synthesis of cyclic, branched, and large peptides including three analogs of HIV-1 protease.

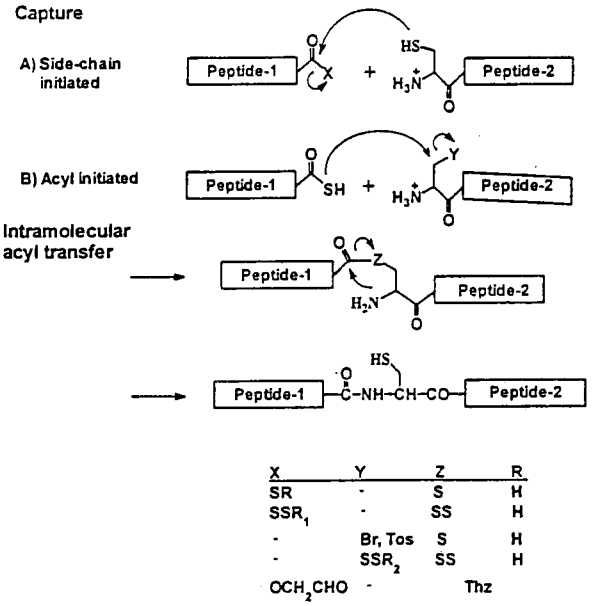

X	Y	Z	R
SR	-	S	H
SSR_1	-	SS	H
-	Br, Tos	S	H
-	SSR_2	SS	H
OCH_2CHO	-	Thz	

Figure 1. *A schematic representation of the orthogonal capture and intramolecular acyl to peptide synthesis of unprotected segments. R_1, R_2 = Npys, Thz = 4-hydroxymethyl thiazolidine.*

Thioester exchange. Another orthogonal coupling method is the thiol-thioester exchange in which the acyl segment containing a thioester exchanges with the amino terminal cysteine to form a covalent thioester [4, 5]. Thioester was relatively stable to aminolysis at acidic or neutral pH, but reacted preferentially with thiols at near neutral pH, as shown in several model peptides containing both an amino terminal cysteine and a lysine. At pH 5.6 to 7.6, the selectivity between the α- and ε-acylation was relatively high with an α/ε ratio of >100:1. Such selectivity was not found in the activated acyl forms such as the succimide ester which reacted with thiol and amine rather nondiscriminately. Although cysteinyl thiols in the internal amino acid sequence would react with thioester, their reaction is nonproductive. Thus, only the N^{α}-terminal with a 1,2-aminothiol would lead to a stable product and thioester. This type of selectivity illustrates the concept of orthogonal coupling where there is a significant difference in the reaction among the N-terminal amino acid (Cys), the side chain, and other α-amine groups.

The reactivity of the sulfhydryl group is both an asset and a problem. Reactivity of the sulfhydryl is necessary for the thiol-thioester exchange, but it gives sixteen other by-products leading to low overall yield, 10-40%. The major side products are α-S-diacylation, disulfide of α-acylated products, and hydrolysis of thioester to carboxylic acid. We have optimized this reaction by activating the thioester while maintaining high orthogonality and keeping the reaction under reducing conditions by using trialkylphosphine and a large excess of reduced thiol.

Because of the strong affinity of trialkylphosphine for sulfur, R_3P reduces disulfides to thiols and thus keeps the thiols in a reducing form and eliminates eleven of the

possible sixteen by-products from being formed. More importantly, it accelerates the thiol-thioester exchange so that the reaction is completed within 17 hr. The excess reduced thiol serves to convert the α-S-diacyl peptide to the desired product and starting material. With this mixture, the yield increased to >90%.

Thioesterification. The covalent thioester was also achieved by direct thioalkylation between a thiocarboxylic acid and bromoalanine. The difference between this method and the previously discussed thioester exchange is that this reaction is initiated by acyl rather than by the thiol side chain. The reaction was performed at pH 4 to 5.5. Under such a condition, the possible side reaction due to β-elimination to give dehydroalanine was not observed. However, the formation of the 3-member ring, aziridine, became significant and was found to be an active intermediate in the reaction pathway.

Disulfide exchange. Finally, disulfide formation was also exploited as an orthogonal coupling method. Mixed disulfides could be achieved between the thiocarboxylic acid and the amino terminal cysteine and is bidirectional, *i.e.*, the capture could be initiated by either thiocarboxylic acid or a cysteinyl side chain. Although this capture method is bidirectional, there are distinctive differences and significant advantages in favoring one direction. In the acyl-initiated mixed-disulfide formation with an acyl disulfide, such as Ellman's reagent, activation of the thiocarboxylic acid with the Ellman's reagent would form a mixed disulfide leading to a reactive species and the advantage of orthogonality including its high reactivity with amines.

To avoid the premature acyl activation and to provide high orthogonality, we found that activation of the side chain of cysteine first by acyl disulfide has significant advantages and will form the desired mixed disulfide with the acyl segment bearing the thiocarboxylic acid. The acyl mixed disulfide would undergo another disulfide exchange to give an acyl-cysteine mixed disulfide [2], subsequently mediated by a six-member ring rather than a five-member ring as in the thioester intermediate. We confirmed this scheme of reaction path by obtaining the final products prior to the reduction step.

To conclude, the development of orthogonal coupling methods allows highly regioselective amide bond formation of the N^{α}-amine and the α-carboxylic acid. We believe that with these approaches, proteins, particularly those proteins >200 amino acids, can be successfully synthesized to usher us into a new era of synthetic protein preparation.

Acknowledgments

This work was supported in part by NIH AI28701, CA36544, and AI35577.

References

1. Liu, C.F. and Tam, J.P., *Proc. Natl. Acad. Sci. USA,* 91 (1993) 6584.
2. Kemp, D.S. and Carey, R.I., *J. Org. Chem.*, 58 (1993) 2216.
3. Tam, J.P., Rao, C., Shao, J. and Liu, C.F., *Int. J. Pept. Prot. Res.*, 45 (1995) 209.
4. Dawson, P.E., Muir, T.W., Clark-Lewis, I. and Kent, S.B.H., *Science*, 266 (1994) 776.
5. Tam, J.P. and Lu, Y.A., *Proc. Natl. Acad. Sci. USA*, 1995, 92 (1995) 12485.

Peptides: Chemistry, Structure and Biology
Pravin T.P. Kaumaya and Robert S. Hodges (Eds.)
Mayflower Scientific Ltd., 1996

2
Chemical Ligation of Proteins and Other Macromolecules

H.F.G. Gaertner[2], R.C. Werlen[1], R.E. Offord[1,2] and K. Rose[1]

[1]Département de Biochimie Médicale, Centre Médical Universitaire, Université de Genève, 1 rue Michel-Servet, 1211 Geneva 4, Switzerland
[2]Gryphon Sciences, 250E Grande Avenue, S. San Francisco, CA 94080, USA

Introduction

If reactivity can be confined to the α groups of a polypeptide chain, we have a method for the controlled joining of unprotected proteins or protein fragments to give defined structures with a contiguous main chain or, alternatively, a means of protein labelling in which one substitution only per molecule will take place and at a determined site.

Our approach to this problem, as far as the α-amino group is concerned, most often involves the generation at the N-terminus of an aldehydic group by very mild periodate oxidation of the 1-amino, 2-ol structure of N-terminal Ser or Thr. For the C-terminus, we most often place a nucleophilic function, such as a hydrazo group, on the α-COOH by reverse proteolysis. These methods have been reviewed elsewhere, both from a general [1] and a practical [2] point of view. The bonds formed when the unprotected fragments are ligated (*e.g.* hydrazone links) are not peptide bonds, but this can often be irrelevant to biological activity and, when one of the structural elements to be incorporated is non-biogenic, the appropriate groups for the formation of such a bond might simply not be present.

As a means of ligating unprotected fragments of proteins, our methods are complementary to those described by Tam and by Wallace elsewhere in this volume, and to the methods described by Kent and colleagues [3]. As a means of ligating together intact proteins, or protein domains, they are efficient, and often highly competitive with recombinant methods even when no non-biogenic structures are to be included. All the methods are very mild, and domains that are folded remain so throughout the process: domains which are not meant to fold up in the presence of one another might fail to do so during the biosynthesis of the construct.

Results and Discussion

We have reported ([4] and references cited therein) the ligation of unprotected fragments of gCSF. The object was the replacement, by various synthetic structures, of a disulphide linked loop thought to be involved in binding to the receptor. We would wish to call attention here to the advantages obtained in this work from using recombinant methods to design the parent protein with the appropriate cleavage sites. As to the effect

of having hydrazone bonds in the main chain, in a gCSF analogue with two unreduced hydrazone bonds the activity relative to the parent native structure was 0.008%; with one of the two bonds reduced, the specific activities were 0.09% and 0.2%, depending on which bond was involved; and with both reduced, the specific activity was 75%. This improvement of activity on reduction is doubtless due to release of the rotation constraint around the N-C bond.

More recently [10], we have used the generation of a reactive carbonyl at the N-terminus to give a unique site on several proteins, to which mono-aminooxy substituted polyethylene glycol (aminooxy-PEG) could be grafted. If so wished, two protein molecules can be joined together through a bisubstituted PEG to give a "dumbell" structure. The oxime bond linking the protein to the PEG chain in all these constructions is very stable under physiological conditions. As hoped, satisfactory prolongations of the first apparent $T_{½}$ of clearance were obtained, and we paid particular attention to Antril (the soluble receptor antagonist of Interleukin-1) and gCSF. Since these PEG-proteins are of very closely defined structure, it is possible to fine-tune their properties by controlled variations in the size and degree of branching of the PEG chains used. For example, two 5kDa PEG chains coupled to the same site *via* a forked linker gave an apparent Stokes radius on gel electrophoresis close to that seen on grafting a single 20kDa PEG chain.

We have proposed the super-mild oxidation of terminal 1-amino, 2-ol structures as a very specific means of protein labelling [5], as has the group of Geoghegan [6]. We are currently using this method to substitute various chemokines with a single fluorophore at the N-terminus [7]. We find this a mild, useful approach. It is easy to make aminooxyacetyl labelling reagents [7] based on such reagents as FITC or NBD chloride (7-chloro-4-nitrobenz-2-oxa-1,3-diazole). Visualization of the receptor and of its internalization with the resulting labelled chemokine derivatives is excellent.

These general techniques have also been used to make chimeric antibodies. Werlen *et al.* [8] describe the removal of the Fc portion of a tumor-directed monoclonal antibody, and its replacement by the dimeric enzyme carboxypeptidase G2, linked through hydrazone bonds. The ligation proved to be an efficient, mild process. The construction had markedly better antigen-binding characteristics than a conjugate prepared by random crosslinking through side chains, and (a desirable property for IgG-enzyme conjugates used for tumour therapy) more rapid clearance from the circulation [8].

Some of the chimeric antibody structures that we have made are closer in concept to the polyoxime constructions described elsewhere in this volume by Rose. As previously described [9], the amino-acid sequence of murine IgG1 is such that reduction of a peptic $F(ab)'_2$ fragment produces a Fab' with three -SH groups, representing inter heavy chain disulphide bridges. The specificity of *Achromobacter* lysine-specific protease permits the further truncation of the heavy chains to leave only one -SH group. This -SH group can then be alkylated with the linker $Br\text{-}CH_2CO\text{-}NHCH_2CH_2NH\text{-}COCH_2\text{-}O\text{-}NH_2$. The resulting $Fab\text{-}O\text{-}NH_2$ can be made to react with a trialdehyde to give a non-reducible $F(ab)'_3$ structure. An $F(ab)'_3$ made by us in this way from a monoclonal directed against carcinoembryonic antigen has been found in preliminary animal studies (Dr. A. Smith, Paul Scherrer Institute, private communication) to have remarkably favourable bio-

distribution properties in terms of specificity of tumour labelling, and therefore shows some promise as a radioimmunoscintigraphic, or even radioimmunotherapeutic agent.

We suggest that the technology mentioned here, and described in full technical detail in the publications we have cited, has shown its robustness, and its applicability to a wide variety of academic and practical problems.

Acknowledgments

We thank Gryphon Sciences, of South San Francisco, for financial support for the general development of this technology.

References

1. Offord, R.E., in Hook, J.B. and Poste, G. (Eds.), 'Protein Design', Plenum, NY, 1990, p. 253.
2. Offord, R.E., in Rees, A. and Sternberg, M. (Eds.), 'Protein Engineering: A Practical Approach', IRL, Oxford, 1992, p. 231.
3. Scholzer, M., and Kent, S.B., *Science,* 256 (1992) 221; and Dawson, P.E., Muir, T.W., Clark-Lewis, I., Kent, S.B., *Science*, 266 (1994) 776.
4. Gaertner, H.F., Offord, R.E., Cotton, R., Timms, D., Camble, R. and Rose, K., *J. Biol. Chem.*, 269 (1994) 7224.
5. Offord, R.E. and Rose, K., in Peeters, H. (Ed.), 'Protides of the Biological Fluids', Pergamon, Oxford, 1986, p. 35.
6. Geoghegan, K.F. and Stroh, J.G., *Bioconjugate. Chem.,* 3 (1992) 138.
7. Alouani, S., Gaertner, H.F., Mermod, J-.J, Power, C.A., Bacon, K.B., Wells, T.N.C. and Proudfoot, A., *Eur. J. Biochem.*, 227 (1995) 328.
8. Werlen, R.C., Lankinen, M., Rose, K., Blakey, D., Shuttleworth, H., Melton, R. and Offord, R.E., *Bioconjugate Chem.*, 5 (1994) 411.
9. Mikolajczyk, S.D., Meyer, D.L., Starling, J.J., Law, K.L., Rose, K., Dufour, B. and Offord, R.E., *Bioconjugate Chem.*, 5 (1994) 636.
10. Gaertner, H.F. and Offord, R.E., *Bioconjugate Chem.*, in press.

Peptides: Chemistry, Structure and Biology
Pravin T.P. Kaumaya and Robert S. Hodges (Eds.)
Mayflower Scientific Ltd., 1996

3

A Synthetic Approach to Study the Structural Biology of Tat Proteins from HIV-1 and EIAV

M. Kraft[1], O. Schuckert[1], J. Wallach[1], M.O. Westendorp[2], P. Bayer[3], P. Roesch[3] and R.W. Frank[1]

[1]Zentrum für Molekulare Biologie, Universität Heidelberg, and
[2]German Cancer Research Center, D-69120 Heidelberg, Germany
[3]Universität Bayreuth, D- 95440 Bayreuth, Germany

Introduction

Primate immunodeficiency viruses and a subset of non primate lentiviruses use a unique machinery to regulate transcription of DNA to viral RNA and efficiently replicate the virus. The viral genomes of the human and simian immunodeficiency viruses (HIV and SIV), equine infectious anaemia virus (EIAV), and bovine immunodificiency-like virus (BIV) encode transcriptional activator (Tat) proteins that bind to the stem loop of the nascent viral mRNA at the transactivation response (TAR) element and promote efficient gene transcription. In addition to its role in virus replication, HIV-1Tat modulates growth, gene expression of unifected cells, and contributes to the cytokine dysregulation and T-cell depletion observed in the course of HIV-1 infection.

Due to the high affinity of Tat proteins for DNA and RNA, efficient purification of recombinant Tat requires denaturation of the protein. However, the extreme lability of the HIV-1 Tat protein, caused by the reactivity of five cysteine residues in its Cys-Loop, makes the purification a tedious task and produces only minute amounts of protein. As a first step to study the structural biology of Tat proteins in more detail, we have undertaken the chemical synthesis of EIAV-Tat and HIV-1 Tat .

The synthesis of the cysteine rich HIV-1 Tat was possible by applying a dedicated deprotection, purification and refolding strategy keeping the cysteine residues protected until after the final purification.

Results and Discussion

The Tat proteins (Table 1) were synthesised on a PS-POE composite resin using Fmoc chemistry. Automated chain assembly was performed on a continuous flow instrument equipped with an on-line monitoring system [1] and a new type of feed-back control. From the profile of the deprotection peak, the relative reaction rates and the amount of Fmoc-groups liberated (coupling yield) are simultaneously quantitated in real time. The value of the relative reaction rate is used to create a feed-back signal controlling deprotection and coupling reactions. In a typical synthesis, Fmoc amino acids (3 equiv.) were automatically dissolved and activated in DMF containing PyBop (3 equiv.) and

NMM (6 equiv.). In order to avoid racemization, Cys was coupled as OPfp-ester with HOBT catalysis. Arg, Asn, Gln, and Ile were routinely double coupled. For all other residues, double coupling was automatically triggered by the feed-back signal when the relative reaction rate dropped below 70% of initial. Simultaneously, the deprotection time was extended to fourfold. During the synthesis of wild type HIV-1 Tat, severe aggregation was observed leading to a breakdown of synthesis efficiency. Due to our on line monitoring we clearly localized the starting point of aggregation at Thr^{40} in the core region. On the basis of a sequence comparison of all known HIV-strains, we replaced Thr^{40} by Lys, a residue with a lower propensity for β-sheet formation. The exchange of only one residue led to much better reaction rates and a product of excellent quality was obtained. The successful synthesis of wild type HIV-1 Tat protein was accomplished by incorporating Leu-Hmb [2] in position 43 to reduce interchain aggregation.

Table 1. *Sequence alignment of EIAV-Tat and HIV-1 Tat. Sequence regions common to Tat-proteins are boxed.*

	N-terminal (acidic)	***Cys-Loop***
EIAV-TAT	LADRRIPGTAEENLQKSSGGVPGQNTGGQEARPN	----------
HIV-TAT	-MDPVDNIEPWNHPGS----------	QPKTA- ***CNRCHCKKCC***

	Core
EIAV-TAT	**YHCQLCFL-RSLGIDY**
HIV-TAT	**YHCQVCFITKGLGISY**
	40 43

	Basic	*Gln*	
EIAV-TAT	LDAS **LRKKNKQRL**	*KAIQQGRQPQYLL*	
HIV-TAT	------- **GRKKRRQRR**	*RPSQGGQTHQDPIPKQPSS*	QPRGDPTGPKE

The extreme lability of the fully deprotected protein provided an additional challenge. Cleavage of the protein from the solid support, and deprotection of side chains was performed in TFA containing 5% triethylsilane and 1% water. Cysteine residues were kept protected by -StBu until after the HPLC purification of the protein. Following deprotection of the cysteine residues by tributylphosphine, the protein was unfolded in 6M urea and renatured by dialysis. Homogeneity and identity of the synthetic product was assessed by automated Edman degradation and laser desorption mass spectrometry.

The synthetic protein was used to generate first time data on the three dimensional structure and molecular dynamics of EIAV Tat and of HIV-1 Tat (Figure 1) by 2D NMR [3, 4]. The synthetic proteins are readily endocytosed and transactivate the viral promoters in low nanomolar concentrations, as measured in cells transfected with a luciferase reporter construct. Binding to TAR-RNA is sequence specific and the binding constant is 5 nM.

Further aspects of Tat function that have been studied are: Tat influence on cytokine activity and expression in non infected cells [5], induction of apoptosis in uninfected

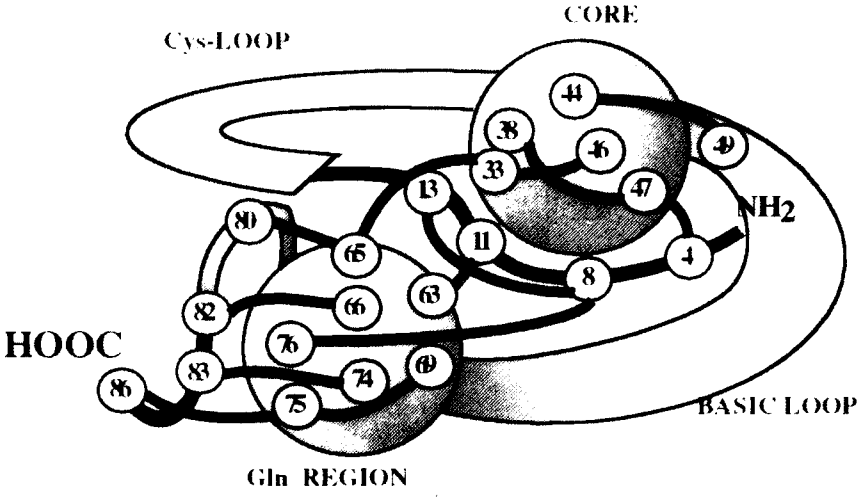

Figure 1. *Cartoon of the general architecture of the HIV-1 Tat protein. The two spheres symbolize rigid substructures. Several long range NOE connectivities are indicated.*

lymphocytes [6], and the mechanism of transactivation of the HIV promoter by Tat. Thus, our results demonstrate that chemical synthesis can be superior to recombinant methods in producing small labile proteins for structural biology investigations.

References

1. Frank, R.W. and Gausepohl, H., in Tschesche, H. (Ed.), 'Modern Methods in Protein Chemistry', de Gruyter, Berlin - New York, Vol. 3, 1988, p.42.
2. Johnson, T., Quibell, M., Owen, D. and Sheppard, R.C., *J. Chem. Soc., Chem. Commun.*, (1993) 369.
3. Willbold, D., Rosin-Arbesfeld, R., Sticht, H., Frank, R.W. and Roesch, P., *Science*, 264 (1994) 1584.
4. Bayer, P., Kraft, M., Ejchart, A., Westendorp, M., Frank, R.W. and Roesch, P., *J. Mol. Biol.*, 247 (1995) 529.
5. Westendorp, M.O., Shatrov, V.A., Schulze-Osthoff, K., Frank, R.W., Kraft, W., Los, W., Krammer, P.H., Dröge, W. and Lehmann, V., *EMBO J.*, 14 (1995) 546.
6. Westendorp, M.O., Frank, R.W., Ochsenbauer, C., Stricker, K., Dhein, J., Walczak, H., Debatin, K-M. and Krammer, P.H., *Nature*, 375 (1995) 497.

Peptides: Chemistry, Structure and Biology
Pravin T.P. Kaumaya and Robert S. Hodges (Eds.)
Mayflower Scientific Ltd., 1996

4

Fragment Condensation Semisynthesis of Protein Analogs is Facilitated by Prior Genetic Manipulation

C.J.A. Wallace[1], A.C. Woods [1] and J.G. Guillemette[2]

[1]Department of Biochemistry, Dalhousie University, Halifax, B3H 4H7, Canada
[2]Department of Microbiology, University of Sherbrooke, Sherbrooke, J1H 5N4, Canada.

Introduction

The construction of proteins by either total synthesis or semisynthesis has been hampered in the past by difficulties inherent in the fragment condensation steps. These difficulties, primarily lack of specificity and inefficiency of coupling methods, appear to have been overcome quite recently with the evolution of several chemoselective and conformationally directed methodologies reviewed [1]. In the chemoselective approach, unique mutually reactive groups are introduced at termini to be joined, forming a linkage that may not necessarily be peptidic. Conformationally-directed methods have been developed and exploited by us in the synthesis of a large number of cytochrome c mutants [2]. This phenomenon, which we call Autocatalytic Fragment Religation (AFR), depends on the common property of large protein fragments to mutally reassociate to give the native backbone fold. Thus, the termini are brought into proximity. If these are reactive, then complex formation both ensures specificity and can catalyse that reaction. The aminolysis of the Ç-terminal homoserine lactone of CNBr fragments is normally slow and uncompetitive with hydrolysis, but when a complex forms between fragments 1-65 and 66-104 of horse cytochrome c, the missing peptide bond spontaneously reforms in 60-80% yield over 24h in neutral phosphate buffer giving a fully functional holoprotein. The apparent advantages of AFR compared to traditional peptide condensation chemistry, the avoidance of side chain protection and conditions harmful to native protein structures, are so great that we would wish to extend the strategy to other sites in cytochrome c and to other proteins.

The problems we face are that methionine residues (target of CNBr cleavage) are rare and not necessarily conveniently located and that in many candidate fragment complexes, lactone aminolysis does not occur and we do not fully understand why. We have addressed these problems by developing other AFR tactics based on serine protease fragments [3]. The seductive simplicity of the CNBr fragment condensation has led us to attempt the synergistic use of site-directed mutagenesis to tailor the protein for semisynthesis. We have demonstrated the feasibility of this idea [4]; our present goal is to try and establish a set of principles to govern the choice of secondary and tertiary structural locales for the introduction of novel cleavage and religation sites.

A supplementary objective is the creation of an efficient semisynthesis strategy for yeast cytochrome c, so that structures of analogs can be determined. Unlike the horse protein, the yeast homolog crystallises easily.

Results and Discussion

We introduced novel methionine residues into a background yeast sequence in which Cys^{102} was replaced by Thr, and Met^{64} by Leu. The gene encoding this protein was incorporated into the pING4 plasmid and mutated, inserted and expressed in yeast by established methods [4]. In order to be a useful site for autocatalytic religation, the local structures must be suitable, but it is also important that the methionine substitution, or the homoserine that replaces it in the ligated product, does not compromise the structure or function of the resulting protein. Sites of mutation were selected with this constraint in mind, as well as the need to explore a variety of structural contexts for suitability. The positions chosen are shown in Table 1. We selected test sites in helices, turns, and Ω-loops either fully or partly buried or surface exposed.

Table 1. *Properties of the mutant cytochromes.*

Cytochrome	Class of mutated residue	HPLC r.t. Fe2+	HPLC r.t. Fe3+	ATP affinity elution t.	pK_{695nm} band loss	E'_M	Bioassay succinate oxidase	Bioassay cytochrome oxidase
Native Yeast		17.6	18.6	47	8.5	279	100%	100%
P25M	Variable	17.8	18.8	46	8.5	288	100%	n.d.
V28M	Variable	17.7	18.7	54	8.1	268	63%	85%
L35M	Conservative	17.6	18.5	54	8.0	276	100%	86%
K55M	Variable	17.3	18.2	41	7.8	284	55%	46%
S65M	Variable	17.6	18.6	49	8.5	270	100%	n.d.
L68M	Invariant	17.5	18.4	52	7.6	268	73%	52%
I75M	Conservative	17.7	18.5	52	8.1	247	48%	92%

Table 1 also sets out the results of physicochemical analyses and biological assays of the mutant gene products, which were all expressed at levels greater than 3 mg of purified protein per liter of culture. Molecular modelling of the mutants did not show significant deviation of their energy-minimized structures from the wild-type fold. These data confirm that some changes resulted in decreased stability of the heme crevice [K55M, L68M and I75M] with a consequent fall in biological activity. Nonetheless, all mutants were sufficiently similar to the parent protein to be useful bases for semi-synthetic routes, and it is of interest that the absolutely conserved Leu^{68} can be changed to Met with limited loss of functionality. In addition to the introduced methionine residue, all cytochromes must contain Met^{80}, which is essential to function as the sixth heme iron ligand. Thus, cleavage can occur at two sites giving, at limiting CNBr concentration, five cleavage products. Generally, cleavage occurs with equal facility at any site, but it was noted that Met^{68} seemed less susceptible than Met^{80}. Mixtures of cleavage products were separated by gel exclusion chromatography. In some mutants, fragments that were coincident in size coeluted. These were resolved by ion-exchange chromatography.

Complexes of purified fragments were prepared in phosphate buffer, pH 7, at sub-millimolar peptide concentrations. These were reduced with sodium dithionite and kept anaerobic at room temperature for 24 h prior to gel-exclusion chromatography. Yields of ligated products were calculated and are shown in Table 2.

Table 2. *Relationship between location of the site and religation efficiency.*

Cytochrome	Location of Cleavage site	CNBr Cleavage Sensitivity	Complex Formation	Coupling yield	Corrected yield	Product Bioactivity
Native yeast [M^{64}]	Hydrophobic face of amphi-pathic helix	Normal	N	0%	0%	n.a.
P25M	Surface-exposed 20s loop extremity	Normal	Y	25%	40%	91%
V28M	Surface-exposed γ-turn	Normal	Y	20%	40%	45%
L35M	Buried residue i of β-turn	Normal	Y	<10%	<20%	17%
K55M	Outer face of short α-helix	Normal	Y	12%	60%	36%
S65M	Hydrophilic face of amphipathic helix	Normal	N	50%	50%	100%
L68M	Interface of amphipathic helix	Low	N	15%	15%	60%
I75M	Partly exposed residue i of β-turn	Normal	N	50%	50%	58%

To conclude: (1) Site-directed mutagenesis can be used with facility to create mutants with shuffled methionine residues. The degree of phylogenetic variability at a potential religation site is not a strict guide to the permissibility of a mutation there. Mutations at the selected sites caused no major disruptions of protein structure or function. (2) Differences in susceptibility to CNBr cleavage of some sites is apparent. Autocatalytic religation can occur at many types of sites, giving functional products. There is a discernible relationship between efficiency and the positions of the peptide bond to be formed, bearing out early indications that buried locations are inhibitory to the reaction. (3) We have developed the ability to predict and to create sites for facile peptide condensation by the Autocatalytic Fragment Religation method. This permits the engineering by semisynthesis of yeast cytochrome c and, potentially, other proteins.

Acknowledgments

We thank Angela Brigley for technical assistance and NSERC of Canada for financial support.

References

1. Wallace, C.J.A., *Curr. Opin. Biotechnol.*, 6 (1995) 403.
2. Wallace, C.J.A., *FASEB. J.*, 7 (1993) 505.
3. Proudfoot, A.E.I., Rose, K. and Wallace, C.J.A., *J. Biol. Chem.*, 264 (1989) 8764.
4. Wallace, C.J.A., Guillemette, J.G., Hibaya, Y. and Smith, M., *J. Biol. Chem.*, 266 (1991) 21355.

Peptides: Chemistry, Structure and Biology
Pravin T.P. Kaumaya and Robert S. Hodges (Eds.)
Mayflower Scientific Ltd., 1996

5
Chemical Synthesis and Purification of Proteins: A Methodology

H. L. Ball and P. Mascagni

Italfarmaco Research Centre, Via Lavoratori, 54, Cinisello B. 20092, Milan, Italy

Introduction

The often poor reliability of classical methodologies for the synthesis and purification of chemically synthesised proteins (>50 residues) can generally be attributed to the generation and subsequent inability to separate closely related sequences from the target protein. Conventional chromatographic techniques, on a semi-preparative scale, are usually not resolving enough when used individually and lead to poor yields when used in combination. We have addressed these apparent limitations by combining (i) the effective coupling reagents HBTU/HOBt, (ii) an efficient capping procedure using N-(2-chlorobenzyloxycarbonyloxy) succinimide [1] and (iii) a reversible probe with enhanced chromatographic properties (*e.g.* lipophilic or affinity label) to aid purification of the target sequence [1-3]. Scheme 1 outlines the general philosophy of an integrated synthetic/purification protocol for protein synthesis.

Results and Discussion

Three chaperonin 10 proteins were synthesised using t-Boc chemistry on a 0.25 mmol scale [3]. Single HBTU/HOBt activated coupling was used throughout except for Arg, Asn and Gln residues which were double coupled. At the end of each synthesis, the N-terminal protecting group of the peptidyl-resin was removed and 4-COR(dodecyl-aminocarbonyl)-Fmoc-OSu (**1**) coupled. The derivatised peptidyl-resins were cleaved using a Low TFMSA/High HF protocol and aliquots of the crude product analysed by RP-HPLC (Figure 1, Panels A, D and G). The addition of probe **1** conferred a greater lipophilic character to the target peptide resulting in a shift in retention time from underivatised impurities, thus facilitating its purification. Peaks labelled 2 (Figure 1) were isolated and the probe removed by a 15 min treatment with 5% aqueous triethylamine. After desalting on RP media, the purified free polypeptides were analysed by RP-HPLC (Figure 1, Panels B,E and H). ESI-MS results for purified Rat cpn10, M.t. cpn10 and Rat - M.t. cpn10 hybrid are shown in Figure 1, Panels C, F and I, respectively. The overall yields for purified Rat cpn10, M.t. cpn10 and Rat - M.t. cpn10 hybrid were 9.8%, 6.2% and 4.6%, respectively. Analytical results reported here as well as more detailed characterisation reported elsewhere [3] clearly show that material with a high degree of purity was obtained. This was confirmed when each purified protein readily adopted its biologically active structure.

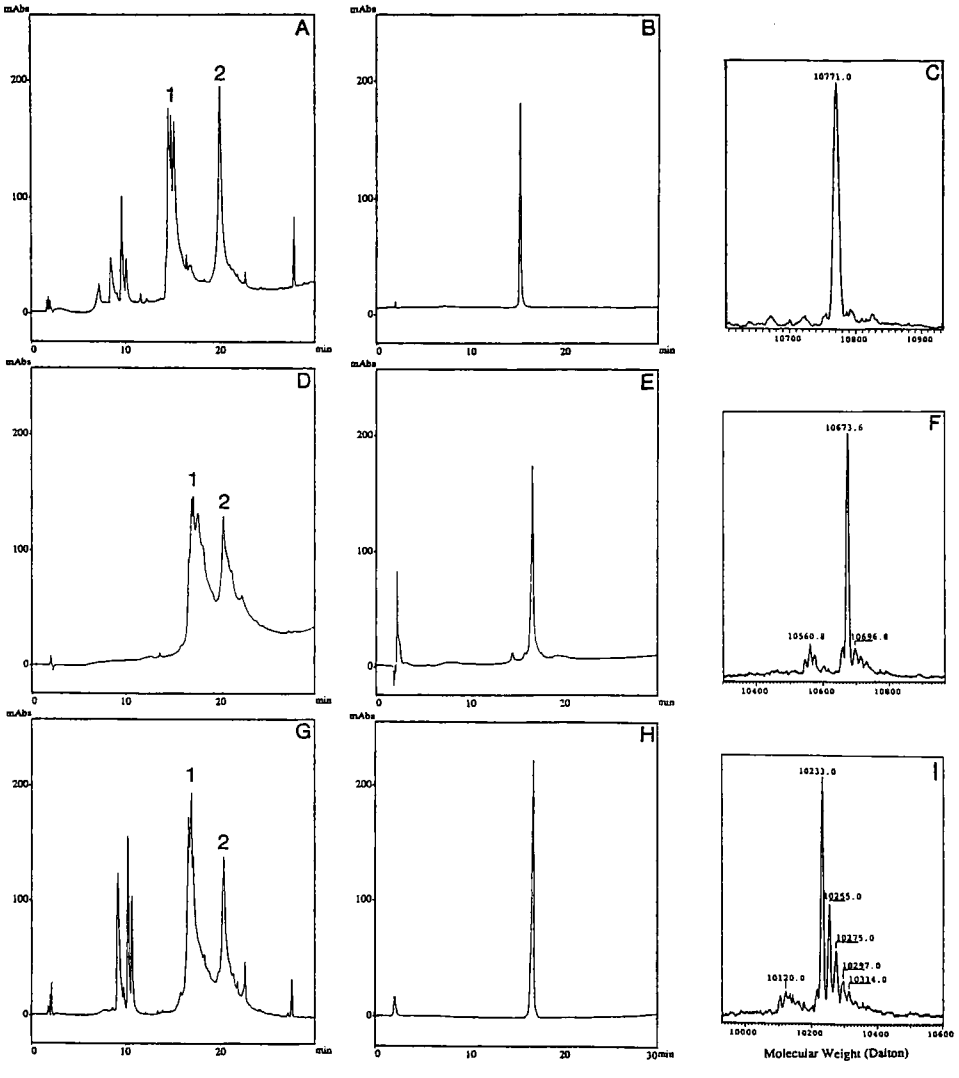

Figure 1. *Analytical data for cpn10 proteins. Panels A-C, D-F and G-I represent crude, purified and ESI-MS analyses for Rat cpn10, M.t. cpn10 and Rat - M.t. cpn10 hybrid, respectively. Peaks labelled 1 are underivatized impurities, while peaks labelled 2 are 'target' protein + 1.*

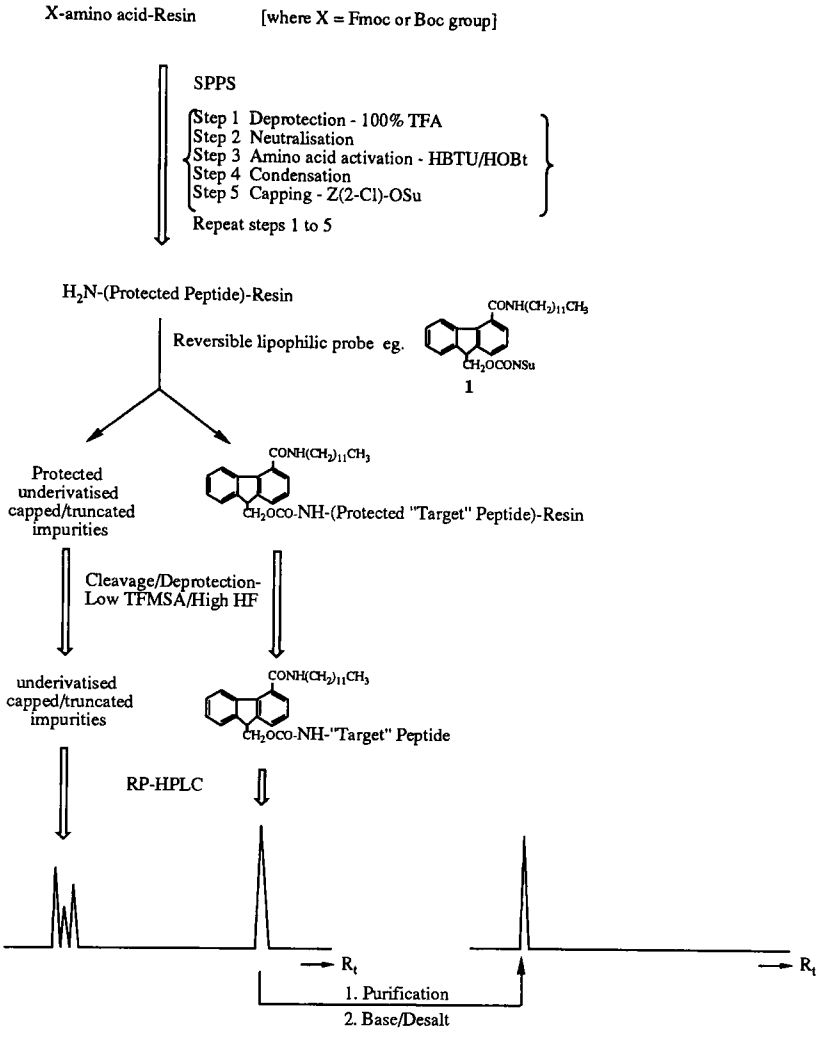

Scheme 1. *General scheme showing application of lipophilic probe 1.*

Acknowledgments

We thank Dr. G. Fossati and Dr. P. Lucietto for the synthesis of M.t. cpn10.

References

1. Ball, H.L., Bertolini, G., Levi, S. and Mascagni, P., *J. Chromatogr. A*, 686 (1994) 73.
2. Ball, H.L. and Mascagni, P., *Int. J. Peptide Protein Res.*, 40 (1992) 370.
3. Ball, H.L. and Mascagni, P., in press.

Peptides: Chemistry, Structure and Biology
Pravin T.P. Kaumaya and Robert S. Hodges (Eds.)
Mayflower Scientific Ltd., 1996

6

A Novel Handle Approach for Solid Phase Peptide Synthesis: Backbone Amide Linker (BAL) Anchoring

K.J. Jensen[1], M.F. Songster[1], J. Vágner[1], J. Alsina[2], F. Albericio[2] and G. Barany[1]

[1]*Department of Chemistry, University of Minnesota, Minneapolis, MN 55455, USA*
[2]*Department of Organic Chemistry, University of Barcelona, 08028 Barcelona, Spain*

Introduction

Most current methods of solid phase peptide synthesis rely on the α-carboxyl function of the eventual C-terminal amino acid residue to achieve anchoring to the support. Attachment of peptides through side-chain functional groups can be desirable, particularly as a strategem to circumvent a variety of problems associated with ester-based linkers (*e.g.*, racemization for sensitive residues, diketopiperazine formation from susceptible dipeptidyl sequences, imide formation with Asn or Gln, *etc.*). Also, side-chain anchoring can be useful for on-resin head-to-tail cyclizations. This approach depends on identifying a trifunctional residue that can serve as a suitable attachment site.

This communication reports on a novel and general concept for anchoring peptides during solid phase synthesis, which involves attachment of a backbone amide nitrogen to an appropriate handle (Figure 1; illustrated for a TFA-cleavable variant). This backbone amide linker (BAL) approach avoids some of the aforementioned problems and allows for the preparation of peptides having a variety of C-terminal functionalities, *e.g.*, not only acids, but also thioacids and thioesters, alcohols, disubstituted amides, and aldehydes, among others. While the concepts of BAL evolve naturally from previous research themes of our laboratories [1, 2], we point out a parallel inspiration from the pioneering work of Weygand [3] and more recently seminal studies by Sheppard and coworkers [4] on protection of α-amide bonds during peptide synthesis. Furthermore, the conceptual similarity of BAL to handles which yield *N*-alkylamide substituted peptides should be stressed.

Results and Discussion

Initial work on BAL adapted the chemistry of the PAL handle [5-(4'-aminomethyl-3',5'-dimethoxyphenoxy)valeric acid], introduced and developed through our earlier efforts [1]. An aldehyde precursor to PAL was coupled through a reductive amination procedure [2] to the α-amine of the prospective C-terminal amino acid, which was protected as a *tert*-butyl, methyl, or allyl ester, or modified to a dimethyl acetal. The resultant intermediates, all secondary amines, were treated with Fmoc-Cl or Fmoc-OSu

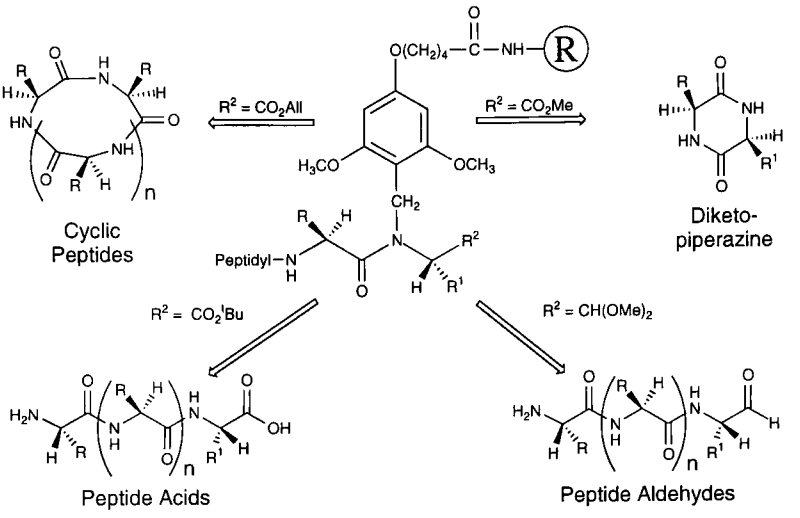

Figure 1. *BAL concept illustrated for a TFA-labile handle.*

to give the corresponding protected amino acid preformed handle derivatives in 40 to 70% yields.

Preformed handles were attached to PEG-PS or PS supports by BOP/HOBt mediated couplings. Alternatively, but less preferred, the PAL aldehyde precursor could be coupled first to the support, followed by on-resin reductive amination [5] (demonstrated for H-Gly-OAl and phenylalaninol, H-Phe-oh). The next step required for stepwise synthesis, *i.e.*, acylation of the α-amino group attached to the handle, was found to be slower than the comparable reactions of unsubstituted primary amines. Commonly applied *in situ* coupling reagents, *e.g.*, HBTU/HOBt, HATU/HOAt, and BOP/HOBt in the presence of NMM or DIEA in DMF, were all inefficient in mediating the acylation of (BAL-PEG-PS)-Phe-O^{t}Bu with Fmoc-amino acids (Gly, Ala, Leu). However, it was possible to acylate the secondary amine in high yield by use of symmetrical anhydrides of Fmoc-amino acids; the optimal solvent was CH_2Cl_2 and no base was needed. A further way to achieve good coupling involved use of the PyAOP reagent in CH_2Cl_2, in the presence of DIEA.

With the C-terminal residue introduced as part of the BAL anchor and the penultimate residue incorporated successfully by the optimized acylation conditions just described, further chain elongation by addition of Fmoc-amino acids proceeded normally under any of a variety of peptide synthesis procedures. An important counter-example was observed with BAL-anchored glycyl *allyl* esters: removal of the Fmoc group at the dipeptidyl level was accompanied by almost quantitative diketopiperazine formation. Such a process is favored by the allyl alcohol leaving group, the sterically unhindered Gly residue, and the BAL secondary amide which allows the required *cis* transition state; diketopiperazine formation was not observed with *tert*-butyl ester protection or with modified end groups. In the cases where diketopiperazine formation did occur, the process was circumvented by: (i) incorporation of the penultimate residue as the

N^{α}-trityl derivative, (ii) selective detritylation with TFA/CH_2Cl_2 (1:99), for 5 min, without cleavage of the BAL anchor, and (iii) incorporation of the third residue as its Fmoc derivative under *in situ* neutralization/coupling conditions mediated by PyAOP plus DIEA in DMF.

Several examples of the BAL concept have been demonstrated: (i) The Fmoc-preformed BAL handle derivative of Gly-OAl was coupled onto PS and extended (including the modified protocol to avoid diketopiperazine formation) to generate the protected peptide-resin Fmoc-Pro-Tyr-Leu-Ala-(BAL-PS)Gly-OAl. Cleavage with TFA/H_2O (19:1) provided the protected peptide Fmoc-Pro-Tyr-Leu-Ala-Gly-OAl in > 85% purity and > 90% yield; correct structure by mass spectrometry. In a preliminary experiment, the allyl ester was removed selectively from the BAL-anchored peptide with Pd(0), the Fmoc group was removed next with piperidine/DMF (1:4), and BOP/HOBt/DIEA-mediated on-resin cyclization gave the expected five-residue head-to-tail cyclic peptide as the major product. (ii) After incorporation of H-Phe-oh (unprotected hydroxyl) onto BAL by on-resin reductive amination, two further residues were introduced smoothly, and cleavage with TFA/H_2O (19:1) provided the protected peptide alcohol Fmoc-Ala-Gly-Phe-oh in > 99% purity and > 97% yield; correct structure by mass spectrometry. (iii) The Fmoc-preformed BAL handle derivative of the dimethyl acetal of glycinal was coupled onto PEG-PS, and extended by six coupling cycles with Fmoc-amino acids. Treatment with TFA/H_2O (19:1) released the peptide from the support with concomitant deprotection of the aldehyde moiety, to give the C-terminal peptide aldehyde H-Ala-Leu-Ala-Lys-Leu-Gly-Gly-H in a purity > 70%. Previous methods to generate peptide aldehydes required post-assembly solution-phase chemistries.

In conclusion, backbone amide linker (BAL) anchoring is promising for solid-phase synthesis of linear peptides with a considerable range of C-terminal modifications, as well as head-to-tail cyclic peptides. Although our studies so far have focused on illustrating the BAL approach by modifications of our previously described PAL chemistry, extensions to other handle principles are readily envisaged.

Acknowledgments

K.J.J. thanks the Alfred Benzon Foundation for a postdoctoral fellowship. This work was supported by NIH grant GM 42722 and CICYT grant PB92-0864.

References

1. Albericio, F., Kneib-Cordonier, N., Biancalana, S., Gera, L., Masada, R.I., Hudson, D. and Barany, G., *J. Org. Chem.*, 55 (1990) 3730.
2. Sharma, S.K., Songster, M.F., Colpitts, T.L., Hegyes, P., Barany, G. and Castellino, F.J., *J. Org. Chem.*, 58 (1993) 4993.
3. Weygand, F., Steglich, W., Bjarnason, J., Akhtar, R. and Khan, N.M., *Tetrahedron Lett.*, (1966) 3483.
4. Johnson, T., Quibell, M. and Sheppard, R.C., *J. Pept. Science*, 1 (1995) 11.
5. Sasaki, Y. and Coy, D.H., *Peptides*, 8 (1987) 119.

Peptides: Chemistry, Structure and Biology
Pravin T.P. Kaumaya and Robert S. Hodges (Eds.)
Mayflower Scientific Ltd., 1996

7
Scope and Limitations of Fmoc Amino Acid Fluorides as Reagents for Peptide Synthesis

H. Wenschuh[1], M. Beyermann[1], M. Bienert[1], A. El-Faham[2], S. Ghassemi[2] and L.A. Carpino[2]

[1]Institut für Molekulare Pharmakologie, Berlin, Germany
[2]Department of Chemistry, University of Massachusetts, Amherst, MA 01003, USA

Introduction

Fmoc amino acid fluorides have been shown to be efficient, rapid-acting coupling reagents. Relative to the analogous acid chlorides, Fmoc-protected amino acid fluorides are unique for several reasons: (i) shelf-stable derivatives can be obtained of amino acids bearing *t*-butyl, Boc, or N-trityl side chain protection, (ii) the formation of the corresponding oxazolones in the presence of tertiary organic bases is very slow [1], (iii) peptide bond formation can be achieved even without any addition of base to combine with the liberated hydrogen fluoride [2], and (iv) their high stability in pure organic solvents, such as DMF, makes them very suitable for multiple peptide synthesis techniques using stock solutions of the activated species [3]. Most interestingly, Fmoc amino acid fluorides have been shown to be particularly well suited for the solid phase assembly of peptides bearing adjacent sterically hindered aminoisobutyric acid residues (Aib) [4]. These favorable properties have made possible highly efficient solid phase syntheses of the Aib-rich peptaibols [5], previously not accessible by SPPS. Such excellent results prompted an investigation of even more hindered residues in order to define the limitations of the acid fluoride technique.

Results and Discussion

With respect to increasing degrees of steric hindrance, couplings of Aib, N-Me-Aib, C(α)-ethylalanine (EtA, or isovaline, Iva), C(α)-diethylglycine (Deg), and C(α)-diphenylglycine (Dpg) to Aib-OMe (0.50 mmoles of Fmoc-aa-F to 0.55 mmoles of Aib-OMe.HCl, 1,05 mmoles of DIEA, 0.5 ml DMF) were studied (Figure 1). While the coupling of Aib and Iva turned out well, in the case of the highly hindered amino acids Deg, Dpg, and N-Me-Aib, the undesired Fmoc-cleavage caused by presence of the base becomes the main reaction as indicated by formation of dibenzofulvene (DBF). In addition, relative to the proteinogenic amino acids, Fmoc amino acid fluorides derived from C(α)-dialkyl amino acids are converted much more rapidly to the corresponding oxazolones. As shown by infrared studies, incubation of Fmoc-Dpg-F in the presence of 1 equiv. of DIEA in DCM results in almost quantitative oxazolone formation within several minutes. On the contrary, in the case of Aib, Iva, and Deg, the acid fluoride is still the main component of such reaction mixtures even after incubation times of 4

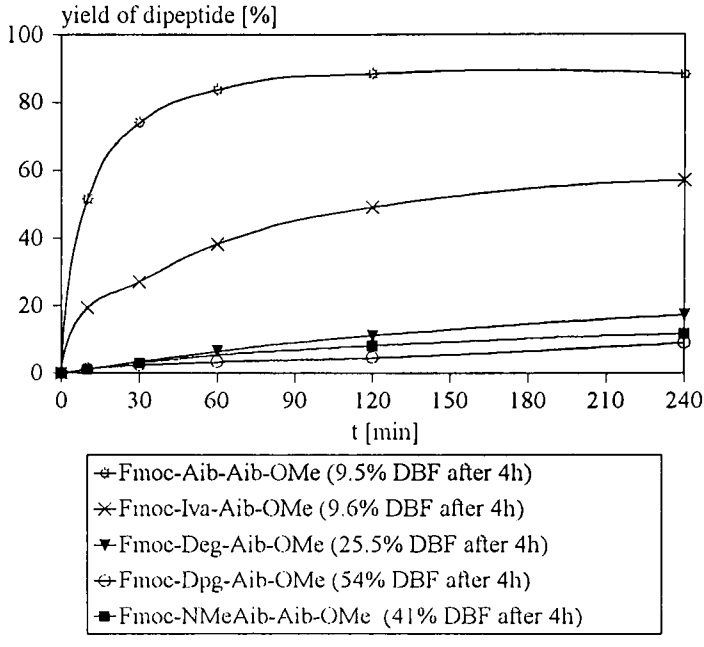

Figure 1. *Coupling of Fmoc C(α)-dialkylamino acid fluorides to Aib-OMe in DMF.*

hours. The very rapid oxazolone formation observed in the case of Fmoc-Dpg-F in the presence of DIEA indicates that the extensive degradation to DBF is caused by the high base lability of the corresponding oxazolone.

The coupling of N^{α}-methylamino acid fluorides to Aib-OMe was also studied under comparable conditions. While the coupling of N-Me-Gly and N-Me-Val turned out well (data not shown), Fmoc-N-Me-Aib-F couples very slowly, and the main reaction was again Fmoc-cleavage. Since both side-reactions, Fmoc-cleavage and oxazolone formation, are base-catalyzed and accelerated by polar solvents, one should avoid such conditions. Consequently, the coupling of Fmoc-NMe-Aib-F to Aib-OMe was carried out in DCM instead of DMF using the hydrogen fluoride salt of Aib-OMe as the amino component. It has been shown that amino acid ester hydrofluorides can be quantitatively coupled in the absence of base. This approach was compared with a similar reaction carried out in the presence of either 1 equiv. of DIEA or 1 equiv. of N,O-bis(trimethylsilyl)-acetamide (N,O-BSA) (Figure 2). The results show that even in the absence of an HF scavenger coupling to Aib-OMe.HF occurs readily, although in the presence of DIEA or N,O-BSA the reaction is significantly accelerated. Most interestingly, in DCM only traces of DBF have been observed indicating that Fmoc-cleavage is very much slower in such non-polar solvents. In contrast to the good results obtained *via* the acid fluoride technique, coupling between the same two amino acids was previously [6] carried out *via* the symmetric anhydride of Z-N-Me-Aib in acetonitrile (72h reflux). Only 17% of the dipeptide was obtained under these conditions.

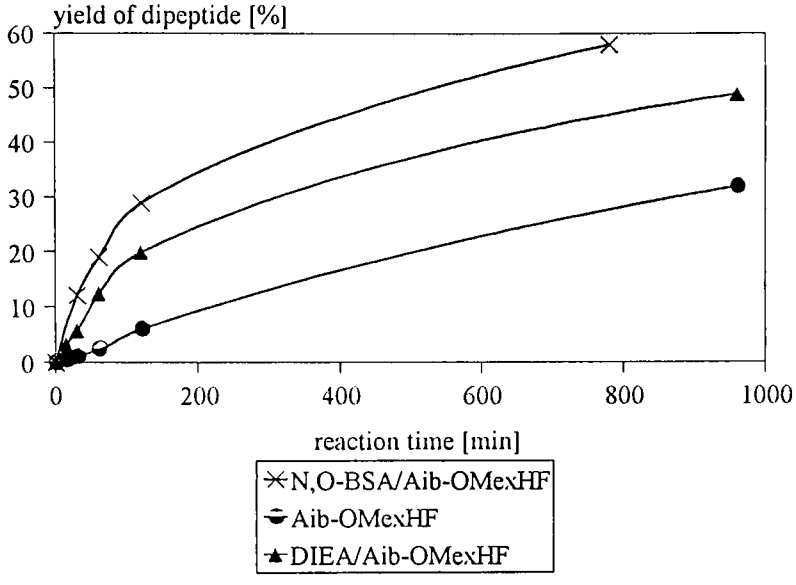

Figure 2. *Coupling of Fmoc-N-Me-Aib-F to Aib-OMe.HF in DCM.*

It is demonstrated that Fmoc amino acid fluorides show high stability as well as high reactivity in non-polar solvents making them well suited for efficient peptide bond formation, especially in the case of sterically very hindered systems.

Acknowledgments

We thank the Deutsche Forschungsgemeinschaft and the Fonds der Chemischen Industrie for financial support of this work in Berlin and the National Science Foundation and the National Institutes of Health for the work at Amherst.

References

1. Carpino, L.A., Sadat-Aalaee, D., Chao, H.-G. and DeSelms, R.H., *J. Am. Chem. Soc.*, 112 (1990) 9651.
2. Wenschuh, H., Beyermann, M., El-Faham, A., Ghassemi, S., Carpino, L.A. and Bienert, M., *J. Chem. Soc., Chem. Commun.*, 1995, 669.
3. Wenschuh, H., Beyermann, M., Rothemund, S., Carpino, L.A. and Bienert, M., *Tetrahedron Lett.*, 36 (1995) 1247.
4. Wenschuh, H., Beyermann, M., Krause, E., Brudel, M., Winter, R., Schümann, M., Carpino, L.A. and Bienert, M., *J. Org. Chem.*, 59 (1994) 3275.
5. Wenschuh, H., Beyermann, M., Haber, H., Seydel, J.K., Krause, E., Bienert, M., Carpino, L.A., El-Faham, A. and Albericio, F., *J. Org. Chem.*, 60 (1995) 405.
6. Moretto, V., Valle, G., Crisma, M., Bonora, G.M. and Toniolo, C., *Int. J. Biol. Macromol.*, 14 (1992) 178.

Peptides: Chemistry, Structure and Biology
Pravin T.P. Kaumaya and Robert S. Hodges (Eds.)
Mayflower Scientific Ltd., 1996

8
Synthetic Strategies for the Preparation of Peptide-based Affinity Labels

J.V. Aldrich[1], L. Leelasvatanakij[1] and D.Y. Maeda[2]

[1]*Department of Pharmaceutical Sciences, School of Pharmacy, University of Maryland at Baltimore, Baltimore, MD 21201, USA*
[2]*College of Pharmacy, Oregon State University, Corvallis, OR 97331, USA*

Introduction

Affinity labels are ligands which bind irreversibly to their targets, and therefore can be useful pharmacological tools to study the structure and function of the target protein. Alkaloid affinity labels such as β-funaltrexamine have been extremely useful tools in the study of opioid receptors [1]. We are interested in preparing opioid peptide analogues containing reactive functionalities as potential affinity labels to study opioid receptors and peptide-receptor interactions. Therefore, we have developed both solution and solid phase synthesis strategies for the incorporation of reactive functionalities into opioid peptide analogues. These synthesis strategies involve the preparation of common precursors into which different electrophilic functionalities, including isothiocyanate and bromoacetamide groups, can then be introduced. These reactive functionalities are attached to the side-chain amine of either a *p*-aminophenylalanine or lysine residue in the sequence.

Results and Discussion

The general synthetic strategy involves preparation of a protected precursor, followed by selective deprotection of the amine side chain, introduction of the reactive functionality, and final deprotection of the peptide. Depending upon the length of the peptide, protected precursors were prepared either in solution or by solid phase synthesis. *t*-Butyl protecting groups were used for semi-permanent protection so that the final deprotection could be performed under mild conditions. An orthogonal protection strategy was used for the side-chain amine where the reactive functionality was to be attached.

The protection of the *p*-amino group of *p*-aminophenylalanine was governed by the reactivity of this functionality. Protecting groups such as Aloc, which could be incorporated *via* the corresponding chloroformate, were readily introduced at the *para* position by selective protection of *p*-aminophenylalanine at pH 4.6 [2]. Because Phe(NHFmoc) was insoluble, an alternative strategy was used to introduce the Fmoc group (see next page).

Two types of small opioid peptide analogues have been prepared in solution. Initially, derivatives of N,N-dialkylated leucine enkephalins [3, 4], which are δ-opioid

receptor antagonists, were prepared. Reactive functionalities were introduced into residue 4 by attachment to *p*-aminophenylalanine to give compounds **1** and **2**.

R_2Tyr-Y-Y-Phe(X)-Leu

1 R = allyl, Y = Aib, X = -N=C=S or -NHCOCH$_2$Br

2 R = benzyl, Y = Gly, X = -N=C=S or -NHCOCH$_2$Br

More recently we have utilized a similar synthetic strategy to prepare potential affinity labels **3** based on the δ-opioid receptor antagonist TIPP (Tyr-Tic-Phe-Phe where Tic = 1,2,3,4-tetrahydroisoquinoline-3-carboxylic acid) [5].

Tyr-Tic-Phe(X)-Phe

3

Fmoc protection was used for the *p*-amino group of *p*-aminophenylalanine. The C-terminal dipeptides were prepared from BocPhe(NO_2)-Leu*O*t*Bu* or BocPhe(NO_2)-Phe*O*t*Bu* by reduction of the nitro group, protection of the resulting *p*-amino group using FmocCl and selective deprotection of the Boc group using trimethylsilyl trifluoromethanesulfonate [6]. The desired protected precursors R_2Tyr(*t*Bu)-Y-Y-Phe(NHFmoc)-Leu*O*t*Bu* for peptides **1** and **2** were prepared by a 3 + 2 segment condensation. The desired protected precursor BocTyr(*t*Bu)-Tic-Phe(NHFmoc)-Phe*O*t*Bu* for the TIPP derivatives **3** was prepared from the C-terminal dipeptide by stepwise synthesis. Following preparation of the protected precursors, the Fmoc protecting group was removed, an isothiocyanate or bromoacetamide group introduced by reaction with thiophosgene or bromoacetyl bromide, respectively, and the *t*-butyl protecting groups removed by treatment with TFA in the presence of anisole.

Analogues of the longer opioid peptide dynorphin A (Dyn A) are being prepared as potential affinity labels for κ opioid receptors. These peptides are being prepared entirely by solid phase synthesis. The synthesis of [Phe(X)^4,D-Pro^{10}]Dyn A-(1-11)NH_2 (**4**) illustrates the synthetic strategy utilized (Figure 1). The protected precursor **5** was synthesized on a PAL polyethylene glycol (PEG)-polystyrene resin using Fmoc-protected amino acids by standard procedures. The Aloc protecting group was then removed by reduction with Pd(0) [7]. The reactive isothiocyanate or bromoacetamide functionalities could then be introduced into the peptide while it was still attached to the resin using thiophosgene or bromoacetyl bromide, respectively. The peptides containing the desired reactive functionalities were then cleaved from the resin using TFA in the presence of scavengers. We have also used this strategy to prepare [Phe(X)^8,D-Pro^{10}]- and [Lys(X)^8,D-Pro^{10}]Dyn A-(1-11)NH_2 containing a reactive functionality in position 8.

The influence of the resin on the solid phase synthesis of peptide-based affinity labels was examined by comparing the preparation of [Phe(X)^4,D-Pro^{10}]Dyn A-(1-11)NH_2 (**4**) on PEG-polystyrene and polystyrene resins. Deprotection of the Aloc group with Pd(PPh_3)$_4$ in 92.5% DCM, 5% AcOH, and 2.5% NMM was much faster on the PEG-polystyrene resin than on the polystyrene resin, requiring 3 hours as opposed to 24 hours for complete reaction. However, the purity of the crude peptides [Phe(N=C=S)^4, D-Pro^{10}]- and [Phe(NHCOCH$_2$Br)^4,D-Pro^{10}]Dyn A-(1-11)NH_2 obtained by synthesis on the polystyrene resin was greater than the purity of peptides synthesized on the PEG-polystyrene resin.

These results illustrate the preparation of peptide derivatives containing reactive functionalities, such as isothiocyanate or bromoacetamide groups, by both solution and solid phase synthesis methods. Peptide-based affinity labels could prove to be valuable tools to explore the interactions between biologically active peptides and their receptors.

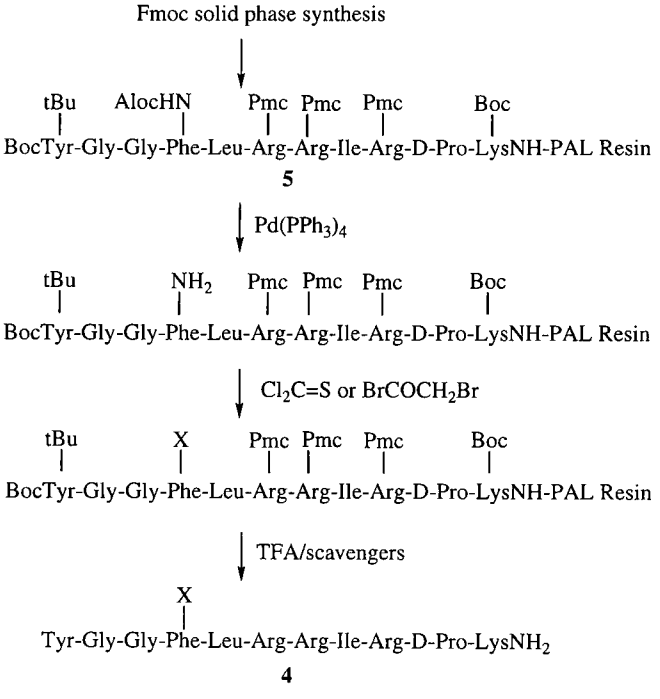

Figure 1. *Solid phase synthesis of [Phe(X)^4,D-Pro^{10}]Dyn A-(1-11)NH$_2$,* ***4***.

Acknowledgments

This research was supported by grants from the National Science Foundation and the American Association of Colleges of Pharmacy.

References

1. Zimmerman, D.M. and Leander, J.D., *J. Med. Chem.*, 33 (1990) 895.
2. Fahrenholz, F. and Thierauch, K.-H., *Int. J. Peptide Protein Res.*, 15 (1980) 323.
3. Cotton, R., Giles, M.G., Miller, L., Shaw, J.S. and Timms, D., *Eur. J. Pharmacol.*, 97 (1984) 331.
4. Aldrich Lovett, J. and Portoghese, P.S., *J. Med. Chem.*, 30 (1987) 1144.
5. Schiller, P.W., Nguyen, T.M.-D., Weltrowska, G., Wilkes, B.C., Marsden, B.J., Lemieux, C. and Chung, N.N., *Proc. Natl. Acad. Sci. USA*, 89 (1992) 11871.
6. Marsmann, H.C. and Horm, H.G., Z. *Naturforsh.*, 27b (1972) 1448.
7. Kates, S.A., Daniels, S.B. and Albericio, F., *Anal. Biochem.*, 212 (1993) 303.

Peptides: Chemistry, Structure and Biology
Pravin T.P. Kaumaya and Robert S. Hodges (Eds.)
Mayflower Scientific Ltd., 1996

9
Chemically Modified Polyolefin Particles for Biomolecule Synthesis, Analysis and Display

R.M. Cook and D. Hudson

Biosearch Technologies, 40 Mark Drive, San Rafael, CA 94903, USA

Introduction

A range of materials are currently employed for biomolecule synthesis, analysis, and display. Polystyrene based materials hold pre-eminent positions in most synthetic and ion-exchange processes, whereas silicas (both controlled pore glass and spherical materials) find optimal application in DNA synthesis, for enzyme immobilization and in HPLC. Crosslinked dextrans and polyamides are useful for low pressure chromatography. The preparation and application is described of unique ASPECT particulate materials (**A**ugmented **S**urface **P**oly**E**thylene's prepared by or used for **C**hemical **T**ransformation).

Results and Discussion

Polyolefin materials have received little attention in these applications; however, plasma aminated polypropylene membranes have recently been used for DNA synthesis [1]. Our investigations started with application of this processing method to powdered polyolefins; very low substitution levels were obtained (Table 1, treatment 2), the method was difficult to perform on powders, and lengthy spacers were necessary to achieve adequate initial coupling yields. In contrast, simple chromic acid oxidation of high molecular polyethylene particles (d = 0.93) gave reasonable substitution levels for DNA synthesis (*ca.* 25 μmol/g), and increasing the severity of the conditions ("superoxidation") gave

Table 1. *Chemical modification of ASPECT 90 micron polyethylene particles.*

Treatment	Group Introduced	Loading (μmol/g)	Surface Area (m^2/g)	Accessibility (%)[a]
1. Repeated CrO_3 oxidation	$-CO_2H$	80-90	13	25-50
2. Plasma processing	$-NH_2$, -OH	<1	0.7	?
3. Oxalyl chloride + Bz_2O_2	-COCl	<1	0.7	>50[c]
4. O_2/O_3 + M^{n+} catalyst[b]	-OH, -C=O, $-CO_2H$	>100	4.5	15
5. 4, then 1	$-CO_2H$	80-90	32	20

[a] Defined as the percent cleavage by chymotrypsin of *t*Boc-Trp-Gly- functionalized material
[b] A variety of transition metal ions are effective; [c] After polyethyleneimine addition

even further improvement (Table 1, treatment 1). Other methods have been developed to functionalize native ASPECT particles (Table 1, treatments 3 to 5). Whereas treatments 2 and 3 result in surface modification only, 1, 4, and 5 produce morphologically modified lower density particles. The nature of the transformations proved difficult to assess. Neither optical microscopy nor scanning white light interferometry showed significant differences. Gas adsorption analyses (BET method) showed a dramatic variation in specific surface area (Table 1), combined with the production of microporosity. Scanning electron microscopy (SEM) shows that the native particles consist of a tightly conglomerated mass of sub-micron spheres (Figure 1a); and that the oxidative functionalization penetrates this mass, augmenting the surface. This process has been termed "chemical invection". ASPECT 4 is finely penetrated, retaining the structural appearance of the parent at low magnification, whereas this has almost been lost from ASPECTs 1 and 5, chemical invection occasionally penetrating the entire particle (Figure 1b).

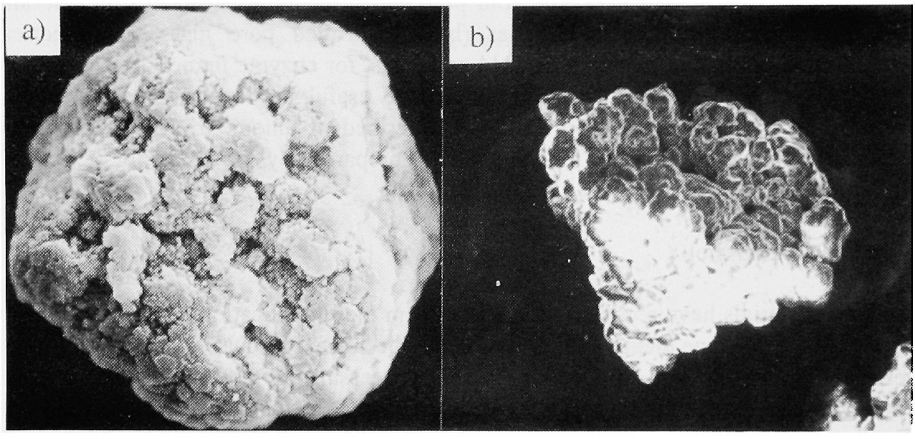

Figure 1. *Scanning electron micrographs of a) unmodified 90 micron Aspect particle, and b) corresponding ASPECT 5.*

ASPECTs 1, 4, 5 have similar synthesis characteristics, are mechanically, chemically and pressure stable, and very much more hydrophilic in nature than the native material. ASPECT 1 can be functionalized for peptide synthesis after BOP mediated addition of 4,7,10-trioxa-1,13-tridecanediamine and $NaBH_4$ reduction of extraneous carbonyl functionalities. Products from procedure 4 are most efficiently functionalized following $LiAlH_4$ reduction. Good quality DNA and peptide products can be assembled on them in purities comparable to those obtained with conventional materials (Figure 2 shows HPLC chromatograms of typical crude peptide products). Remarkably, when YGKAYG was prepared immobilized on ASPECT 1, trypsin rapidly cleaved a high proportion of the pendant peptides. The speed and efficiency of this interaction provides a paradigm for general biorecognition processes mediated on ASPECT particles, especially in affinity chromatography applications, and in bead based library techniques. This observation was studied further by attachment of *t*Boc-Trp-Gly-OH to a variety of materials, and digestion with α-chymotrypsin. Results are depicted as an accessibility

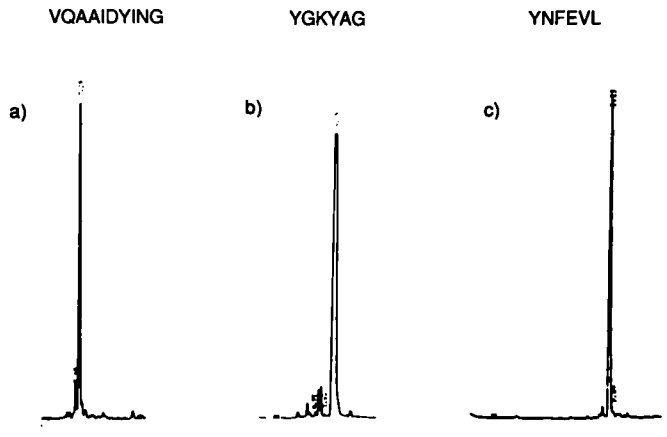

Figure 2. *Reverse phase HPLC analyses of crude products direct from synthesis of a) acyl carrier protein 65-74 VQAAIDYING; b) trypsin test substrate YGKYAG; and c) ribonuclease S protein binding peptide, YNFEVL; Beckman 3 micron ODS column, TFA/CH_3CN system.*

index in Table 1; note with all ASPECTs cleavage efficiency is loading dependent, as is also the case with CPG. Under the conditions employed, <1% cleavage occurs from Tentagel or PEG-PS supports [2]. The method is highly useful in selecting only the most reactive sites in critical applications. A tremendously important observation was that trypsin retained high activity when immobilized to N-hydroxysuccinimide ester carboxyl substituted ASPECT 1.

Numerous chemical transformations, including reductions, reductive alkylations, nitrations, chlorosulfonations, Michael reactions and substitutions have been performed on ASPECT bound groups, showing the inertness of the support and its general usefulness for chemical transformations. Reactions may be monitored spectroscopically, IR being especially useful. Immobilization of chemical reagents (*e.g.* oxidizing and reducing agents) on ASPECT particles is an attractive complementary way of facilitating automated chemical transformations. Additionally, ASPECTs have been shown to be useful in a variety of chromatographic applications, and therefore, promise to be widely useful, in large-scale applications where durability and economy are the primary considerations.

Acknowledgments

Thanks are due to Quantachrome Corp., Boynton Beach, FL for BET analyses, and to the SBIR grant program (NIGMS 1R43 GM50593-01).

References

1. Matson, R.S., Rampal, J.B. and Coassin, P.J., *Anal. Biochem.*, 217 (1994) 306.
2. Vagner, J., Krchnak, V., Sepetov, N.F., Strop, P., Lam, K.S., Barany, G. and Lebl, M., in Epton, R. (Ed.) 'Innovations and Perspectives in Solid Phase Synthesis', Mayflower, Birmingham, UK, 1994, p. 347.

Peptides: Chemistry, Structure and Biology
Pravin T.P. Kaumaya and Robert S. Hodges (Eds.)
Mayflower Scientific Ltd., 1996

10
Formation of Disulfide Bridges in Conotoxin M VII A Oxidative Folding *versus* Selective Bridging: A Comparative Study

J.P. Durieux and R. Nyfeler

BACHEM Feinchemikalien AG, Hauptstrasse 144
CH-4416 Bubendorf, Switzerland

Introduction

For the preparation of peptides having several disulfide bridges, the "one step" oxidative folding of fully reduced precursors seems to be the simplest approach, but no guarantee can be given concerning the correctness of the folding [1]. We have earlier described a selective approach for the synthesis of such sequences [2]. In this paper, we compare the two approaches in the preparation of conotoxin M VII A.

Results and discussion

The syntheses are based on the Fmoc/tBu strategy and follow a convergent approach. The following fragments have been prepared: Fmoc-[1-5]-OH = Fmoc-Cys(R1)-Lys(Boc)-Gly-Lys(Boc)-Gly-OH, Fmoc-[6-18]-OH = Fmoc-Ala-Lys(Boc)-Cys(R2)-Ser(tBu)-Arg(Pmc)-Leu-Met-Tyr(tBu)-Asp(OtBu)-Cys(R3)-Cys(R1)-Thr(tBu)-Gly-OH, and Fmoc-[19-25]-R = Fmoc-Ser(tBu)-Cys(R2)-Arg(Pmc)-Ser(tBu)-Gly-Lys(Boc)-Cys(R3)- Amide resin. The Cys protecting groups are the following: R1 = Mob, R2 = Trt, R3 = Acm for the selective bridging and R1 = R2 = R3 = Trt for the oxidative folding.

Table 1. *Conditions of specific cleavage/ring closure steps.*

Bridge formed	Cleavage/ring closure conditions	Molecular weights	
Cys^{8} - Cys^{20}	air oxidation, pH 8	calcd. found	3025.5 3024.7
Cys^{15} - Cys^{25}	75-fold excess iodine in 80% AcOH	calcd. found	2881.3 2883.0
Cys^{1} - Cys^{16}	a) TFMSA/TFA/p-cresol b) DMSO oxidation	calcd. found	2639.0 2638.4

Table 2. *Oxidative folding - percentage of conotoxin formed*

pH	7.9	6.5	7.7	5.8	7.7	5.8
additive	no	DMSO	Cys 4mM	Cys 4mM	GSSG GSH 2-4mM	GSSG GSH 2-4mM
20hr.	4%	0%	23%	41%	9%	25%
45hr.	4%	0%	34%	45%	9%	30%

Fragments [1-5] and [6-18] are prepared using the super acid labile Sasrin resin and are isolated fully protected after cleavage from the resin. The fragments are combined using TBTU as coupling agent. After detachment from the resin with TFA/EDT/H_2O, the linear precursors are obtained with R1 = Mob, R2 = H, R3 = Acm for the selective bridging and R1 = R2 = R3 = H for the oxidative folding. Both peptides are then prepurified by preparative HPLC on a C18 column, using a 0.1% TFA water/acetonitrile system. In the selective bridging protocol, the disulfide bonds are successively formed using the pathway described in Table 1. The intermediates are purified by preparative HPLC and characterized by PDMS.

For the oxidative folding the linear precursor is solubilized in 0.05M ammonium acetate, at a concentration of $2x10^{-4}$M. The results of different reaction conditions are given in Table 2. The percentage of conotoxin M VII A formed is determined by HPLC.

Our results demonstrate that the oxidative folding is indeed a simple way of preparing peptides with several disulfide bonds. However it is strongly dependent on the reaction conditions. Identifying the correct structure may not always be easy, whereas the selective bridging allows the unambiguous assignment of the disulfide bonds.

References

1. Kubo, S., Chino, N., Watanabe, T.X., Kimura, T., Sakakibara, S., *Peptide Res.* 6(2) (1993) 66
2. Durieux, J.P., Nyfeler, R., in H.L.S. Maia (Ed.), 'Peptides 1994', ESCOM, Leiden, The Netherlands, 1995, p 165.

Peptides: Chemistry, Structure and Biology
Pravin T.P. Kaumaya and Robert S. Hodges (Eds.)
Mayflower Scientific Ltd., 1996

11
Development of a New *ortho*-Nitrobenzyl Photolabile Linker for Solid Phase Synthesis

C.P. Holmes, D.G. Jones, B.T. Frederick and L.-C. Dong

Affymax Research Institute,
4001 Miranda Ave., Palo Alto, CA 94304, USA

Introduction

Photolabile supports have been employed for 20 years in SPPS since the seminal report describing the *ortho*-nitrobenzyl support **1** [1, 2]. Photolytic release of peptides offers a method of orthogonal cleavage which complements the traditional use of TFA or HF, and numerous research groups have capitalized on this concept [3]. Support **1**, however, does suffer from several limitations. Support **1** exhibits unduly slow cleavage kinetics, with typical photolysis times in organic solvents ranging from 12 to 24 h and moreover, workers have been unable to obtain high yields of methionine-containing peptides from **1** without substantial contamination with methionine sulfoxide [3]. While optimizing the photolithographic synthesis of peptides [4] we had occasion to explore the use of a variety of *ortho*-nitrobenzyl compounds as photolabile protecting groups. The most useful among these were the α-methyl-6-nitroveratryl derived protecting groups, which incorporate two additional alkoxy groups onto the benzene ring and a methyl group on the benzylic carbon. Incorporation of these salient features into linker **1** generated a new class of photolabile supports **2**.

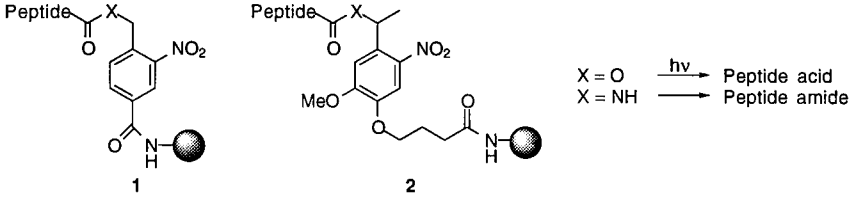

Results and Discussion

Synthesis of a Fmoc-protected amino acid **4** for the synthesis and liberation of peptide amides has been recently described [5]. Attachment of **4** to the support was performed with DIC/HOBt to afford the photolabile resin **5** (Figure 1). Synthesis of the corresponding alcohol **7** from **3** was accomplished in a two pot, three step procedure of nitration, reduction and saponification. Coupling of **7** as before to the resin gave the acid-generating support **8**. We first addressed the TFA stability of the new supports by

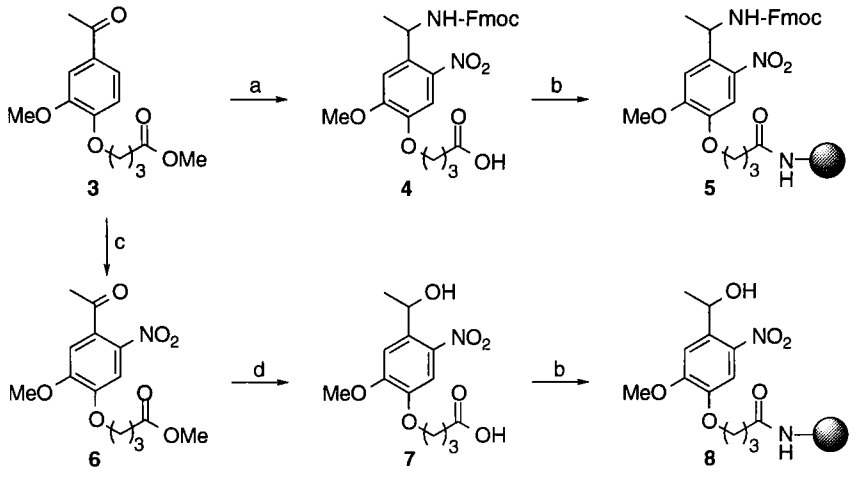

Figure 1. *Synthesis of photolabile supports: (a) ref* [5] *(b) DIC/HOBt, amine-support; (c) HNO_3; (d) $NaBH_4$, then NaOH/MeOH.*

exposing **2** to typical TFA-scavenger cocktails for 2 h; no undesired cleavage was observed. Photolyses were performed with 365 nm UV light from a Hg ARC lamp, which had been previously demonstrated to be compatible with both peptides and small organic molecules [4, 5].

A cholecystokinin peptide (H-Met-Gly-Trp-Met-Asp-Phe-NH_2) was chosen as model peptide to further examine the methionine oxidation phenomena previously noted. After assembly under standard Fmoc-conditions on support **5**, the peptide was found to cleave with 1 hr of irradiation in the presence of hydrazine as scavenger to afford the desired CCK peptide in 87% purity (75% yield). Comparison of the released product with the three possible methionine sulfoxide products independently prepared indicated that less than 4% of oxidized product was present. The rapid release of peptides from **2** now allows one to liberate methionine-containing peptides with minimal oxidation.

The use of various scavengers during cleavage of peptide amides has been found to be beneficial. Basic adjuncts such as hydrazine or ethanolamine afforded greater amounts of peptides during a given photolysis, and the exact origin of this effect is under active investigation. These new supports should find widespread use throughout SPPS and new applications will be reported in due course.

References

1. Rich, D.H. and Gurwara, S.K., *J. Am. Chem. Soc.*, 97 (1975) 1575.
2. Hammer, R.P., Albericio, F., Gera, L. and Barany, G., *Int. J. Peptide Protein Res.*, 36 (1990) 31.
3. Lloyd-Williams, P., Albericio, F., and Giralt, E., *Tetrahedron*, 49 (1993) 11065.
4. Holmes, C.P., Adams, C.L., Kochersperger, L.M., Mortensen, R.B. and Aldwin, L.A., *Biopolymers (Peptide Sci.)*, 37 (1995) 199.
5. Holmes, C.P. and Jones, D.G., *J. Org. Chem.*, 60 (1995) 2318.

Peptides: Chemistry, Structure and Biology
Pravin T.P. Kaumaya and Robert S. Hodges (Eds.)
Mayflower Scientific Ltd., 1996

12
Reversed-phase Chromatography as a Mimic of Ligand-receptor Interactions

C.T. Mant and R.S. Hodges

Department of Biochemistry, and the MRC Group in Protein Structure and Function, University of Alberta, Edmonton, Alberta, T6G 2H7, Canada

Introduction

Since interactions between non-polar residues are the major driving force for protein folding and stability, the hydrophobic environment characteristic of reversed-phase chromatography (RPC) [1] may be a reasonable mimic of such interactions, as well as a good model for ligand-receptor interactions [2, 3]. We have recently described [3] the potential of a simple model ligand-receptor system based on observing the retention behaviour during RPC of *de novo* designed single-stranded amphipathic α-helical peptides representing peptide ligands binding to a complementary receptor (RPC stationary phase). The present study investigates the effect of varying receptor hydrophobicity on the apparent hydrophilicity/ hydrophobicity of polar side-chains buried at the interface between the peptide ligand (model amphipathic α-helical peptides) and the stationary phase (receptor).

Results and Discussion

For the present study, the hydrophobic surface of the receptor, represented by the stationary phase of reversed-phase columns, was varied; whilst the non-variable hydrophobic surface of the ligand was represented by the hydrophobic face of synthetic amphipathic α-helical peptide analogues. We have designed and synthesized an 18-residue amphipathic peptide ligand for our model ligand-receptor model system. The amino acid sequence is Ac-E-L-E-K-L-L-K-E-X-E-K-L-L-K-E-L-E-K-amide, where X (position 9) is substituted by the 20 amino acids found in proteins. Position 9 is in the centre of the hydrophobic face of the helix, surrounded by Leu residues. These peptides exhibit high α-helicity and amphipathicity [3]. The stationary phases representing the protein receptor consisted of silica-based cyanopropyl (CN) and octadecyl (C_{18}) bonded-phase columns, with the C_{18} column considerably more hydrophobic than the CN. From Figure 1, an increase in receptor hydrophobicity (column surface hydrophobicity) enhances hydrophilicity of polar amino acid side-chains on the hydrophobic face of a preferred binding domain of an amphipathic α-helical peptide ligand. This is not observed for ligands lacking a preferred binding domain. The increase in hydrophilicity of the residues on increasing receptor hydrophobicity ranged from a 1.3-fold increase for Lys to a 3.8-fold increase for Ser. In addition, the aqueous

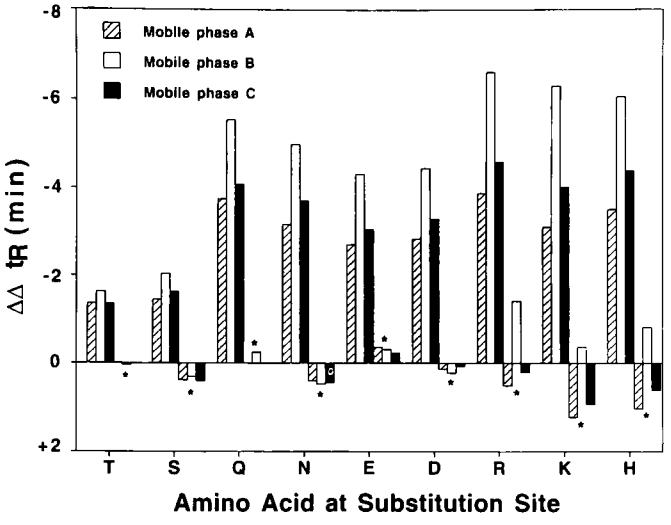

Figure 1. *Effect of varying receptor hydrophobicity on hydrophilicity/ hydrophobicity of polar side-chains substituted in the non-polar face of a model amphipathic α-helical peptide ligand. Conditions: linear gradient of 1% acetonitrile/min and 1 ml/min at room temperature, where Eluent A is 10 mM aq. H_3PO_4 pH 2.2 (A), 10 mM aq. H_3PO_4 pH 2.2, containing 100 mM $NaClO_4$ (B) or 10 mM aq. trifluoroacetic acid (TFA), pH 2.0 (C); Eluent B is 10 mM H_3PO_4 in acetonitrile (A), 10 mM H_3PO_4 in 60% acetonitrile containing 100 mM $NaClO_4$ (B) or 10 mM TFA in acetonitrile (C). For each side-chain, the three histograms on the left are results obtained from the amphipathic α-helical peptide ligand model system (denoted LX peptides) and the three on the right (denoted by a star) are results obtained from the control random coil peptides (denoted Ac-X series). $\Delta\Delta t_R$ = (t_RLX- t_RLG) on the C_{18} column minus (t_RLX-t_RLG) on the CN column for the polar LX analogues; $\Delta\Delta t_R$ = (t_RAc-X - t_RAc-G) on the C_{18} column minus (t_RAc-X-t_RAc-G) on the cyano column for the polar random coil analogues. Thus, $\Delta\Delta t_R$ represents the change in hydrophilicity/hydrophobicity of the polar side-chain in the centre of the hydrophobic face of the peptide ligand (LX peptides) or at the N-terminal end of the random coil peptides effected by the increase in hydrophobicity (CN → C_{18}) of the receptor surface. Note that the hydrophilicity/ hydrophobicity of side-chains have been expressed relative to the Gly analogues (t_RLX- t_RLG and t_RAc-X- t_RAc-G) which represent the case where no side-chain is present at the substituted site.*

environment surrounding the binding site of the receptor and ligand also affects the hydrophilicity/hydrophobicity of amino acids at the binding interface. Thus, the addition of salt (100 mM $NaClO_4$) to the mobile phase enhances interactions between ligand and receptor, and buried hydrophilic side-chains become substantially more hydrophilic when the ligand-receptor is in an aqueous environment of higher ionic strength.

References

1. Mant, C.T. and Hodges, R.S. (Eds.), 'HPLC of Peptides and Proteins: Separation, Analysis and Conformation', CRC Press, Inc., Boca Raton, FL, USA, 1991.
2. Hodges, R.S., Zhu, B.-Y., Zhou, N.E. and Mant, C.T., *J. Chrom.*, 676 (1994) 3.
3. Sereda, T.J., Mant, C.T., Sönnichsen, F.D. and Hodges, R.S., *J. Chrom.*, 676 (1994) 139.

Peptides: Chemistry, Structure and Biology
Pravin T.P. Kaumaya and Robert S. Hodges (Eds.)
Mayflower Scientific Ltd., 1996

13
New Anchor Group for SPPS, and its Use for Peptide Synthesis in Aqueous and Non-aqueous Media

S.V. Kulikov[2], R.S. Selivanov[1] and A.I. Ginak[1]

[1]*St. Petersburg State Institute of Technology, 198013, St. Petersburg, Russia*
[2]*Institute of Highly Pure Biopreparations, 197110, St. Petersburg, Russia*

Introduction

Noncatalytic reduction of nitrobenzyl esters by aqueous sodium dithionite ($Na_2S_2O_4$) at pH 9.5 can be used to obtain both free and blocked amino acids [1]. Building on the nitrobenzyl group (**1**) protection concept, a new 5-hydroxymethyl-2-nitrophenoxyacetyl (2-NPA) (**2**) anchor group has been developed. The possibility of its use for SPPS in aqueous and non-aqueous media is considered.

Results and Discussion

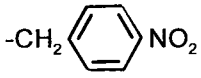

Nitrobenzyl

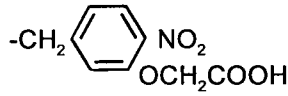

2-NPA

For SPPS in non-aqueous media, the 2-NPA anchor group was attached either to aminomethylated styrene-1% divinylbenzene (SDB) (NH_2 content 0.96 mmol/g), or to polyamide (PA) resin (NH_2 content 0.78 mmol/g). The Gly-2-NPA anchoring bond was stable toward TFA and TEA/DCM. The peptide Val-Gly-Val-Ala-Pro-Gly (**3**) [2] was selected for synthesis, which was carried out by the DCC/HOBt procedure. Completeness of acylation was checked by the Kaiser ninhydrin test [3], and by the TNBS test [4]. On completion of peptide assembly, a part of each Boc-peptidyl resin was deblocked at the N-terminus. Thus Boc-blocked, and unblocked peptidyl-2-NPA SDB resins were obtained. Boc-blocked, unblocked and NO_2Z-blocked peptidyl-2-NPA PA resins were also prepared.

Cleavage of the peptide (**3**) by HF failed. It was detached from H-peptidyl SDB matrix by treatment with sodium dithionite in water-ethanol at 37°C for 4-6 hr. After desalting on Sephadex G-10 or Biogel P-2 in 50 mmol NH_4HCO_3, the peptide (**3**) was obtained with 87% yield and 91% purity. Detachment of the Boc-peptide under these conditions failed.

Boc-blocked, and free peptides were cleaved from the 2-NPA PA matrix by treatment with sodium dithionite (5 equiv. for each group to be reduced) in aqueous

carbonate/bicarbonate buffer, pH 9.0 at 40°C for 4 hr. Purification was achieved either as stated above, or by silica gel chromatography.

SPPS in aqueous media was carried out on a Gly-2-NPA PA resin. This derivative was stable in the pH range 2-10. NPS amino acids were used for the synthesis and were coupled as Nsp esters [5]. Double couplings, each with 2 equivalents of NPS-AA-ONsp at 20°C for 2 hr., were needed for complete acylation. Reaction was carried out as recommended in [5]. The completeness of acylation was checked by TNBS test [4]. The NPS group was cleaved either by 1 M aqueous $Na_2S_2O_3$ [6] or by saturated HCl/AcOEt. In both cases, the NH_2 content generated was the same. However, in the step of NPS dipeptidyl resin deblocking by 1 M $Na_2S_2O_3$, loss of peptide was observed. This occured, most probably, because of deloading *via* diketopiperazine formation. Use of HCl/AcOEt rather than 1 M $Na_2S_2O_3$ led to minimization of this problem.

In the course of deblocking of the NPS group, conversion byproducts appeared in appreciable quantity. This led to deterioration in the hydrodynamic properties of the matrix. To avoid this, washing with AcOEt was introduced. This helped to preserve the matrix swelling, led to increase acylation rate, and to improvement in the quality of the peptide produced. Following this protocol, Gly-Val-Ala-Pro-Gly-2-NPA-PA was prepared. The final valine was introduced as a Boc-Val-ONsp or NO_2Z-Val-ONsp. A part of the Boc-blocked peptidyl-2-NPA PA was deblocked by TFA. Peptides were detached as before.

For the purpose of comparison, the peptide (**3**) was prepared on the Merrifield resin. Synthesis was carried out by DCC/HOBt procedure. The peptide was cleaved by HBr/TFA in 36% yield and in 89% purity.

Thus, it was shown that the suggested anchor group made it possible to obtain the blocked and unblocked peptides in organic and aqueous media by cleavage in very mild reductive conditions.

References

1. Guib-Jempel, E., Wakselman, M., *Synthetic Communications,* 12 (1982) 219.
2. Senior, L.M., Griffin, G.L., Mecham, R.P., Wrenn, D.S., *J. Cell. Biol.*, 99 (1984) 870.
3. Kaiser, E., Colescott, R.L., Bossinger, C.D., Cook, P.I., *Analyt. Biochem.*, 34 (1970) 595.
4. Hancock, W.S., Battersby, J.E., *Analyt.Biochem.*, 71 (1976) 260.
5. Dzubenko, P.S., Medvedkin, V.N., Mitin, Yu.V., *Bioorganitscheskaya Khimiya (Russia)*, 5 (1989) 704.
6. Kessler, V., Iselin, B., *Helv. Chim. Acta,* 43 (1966) 1330.

Peptides: Chemistry, Structure and Biology
Pravin T.P. Kaumaya and Robert S. Hodges (Eds.)
Mayflower Scientific Ltd., 1996

14
A New Approach to Phosphonopeptide Analogs Using Phosphorus (III) α-Amino Acids

M. Fernandez, H. Fan and R.P. Hammer

Department of Chemistry, Louisiana State University, Baton Rouge, LA 70803, USA

Introduction

Phosphonopeptides are important peptide mimics that are effective inhibitors of metallo, aspartyl, and serine proteases [1], and also as haptens in catalytic antibody studies [2]. Currently, phosphonate esters (**1**, X=O, Y=O, Z=O) and phosphonamidates (**1**, X=NR, Y=O, Z=O) are generally formed by first activating a phosphonate monoester to the phosphonochloridate, followed by coupling of the activated species with an alcohol or amine in the presence of base (Figure 1, Path A) [1, 2]. This method usually provides moderate yields, in part due to the slow nucleophilic attack of heteroatom nucleophiles on P(V) centers [3]. We report herein a new method to prepare phosphonates, whereby P(III) compounds (**2**) are used in the key coupling step (Figure 1, Path B). In addition to potentially increasing the yield of **1**, this approach also allows for easy design and preparation of phosphonates with a wide variety of heteroatoms around the phosphorus center (*e.g.*, X=NR, Y=O, Z=S or X=O, Y=S, Z=S), many of which are difficult or impossible to prepare by current methodologies.

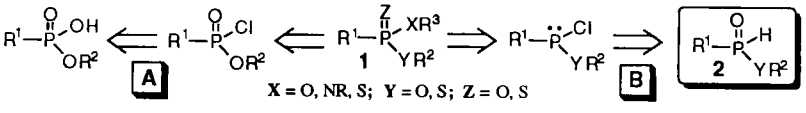

Figure 1. *Synthesis of phosphonate derivatives from P(V) or P(III) derivatives.*

Results and Discussion

We envisaged *H*-phosphinate esters **2** as the ideal precursors for a P(III)-based phosphonate synthesis because of their air stability. We used commercially available dichlorotriphenylphosphorane (DCP) in pyridine to activate **2** (R^1=Ph, Me; R^2=OiPr, OtBu, S*t*Bu) *non-oxidatively* to the phosphonochloridites [$R^1P(YR^2)Cl$]. *In situ* reaction with heteroatom nucleophiles (**R^3XH**; 1 equiv. of alcohol or thiol or 3-4 equiv. of amine) followed by oxidation (4 equiv. anhydrous *t*BuOOH) or sulfurization (1 equiv. S_8) provided phosphonate derivatives in excellent to moderate yields (Table 1). Particularly noteworthy are the good yields for compounds **1g** (70%), **1j** (75%), and **1l** (61%), which all incorporate a very hindered *t*Bu group in the alcohol or amine nucleophile. Such compounds would be difficult to prepare by P(V) approaches because of the sensitivity of these reactions to steric factors [3, 4].

Table 1. *Preparation of phosphonates and phosphonamides from* H-*phosphinates*

Entry	R^1	YR^2	XR^3	Z	Yield of 1	^{31}P (1)
a	Ph	OiPr	OBzl	O	71%	15.9
b	Ph	OiPr	NEt_2	O	61%	18.9
c	Ph	OiPr	OMe	S	85%	85.3
d	Ph	OiPr	OEt	S	70%	83.2
e	Ph	OiPr	OiPr	S	71%	81.4
f	Ph	OiPr	OBzl	S	66%	83.8
g	Ph	OiPr	OtBu	S	70%	74.5
h	Ph	OiPr	NHBzl	S	75%	72.3
i	Ph	OiPr	NEt_2	S	75%	74.6
j	Ph	OiPr	NHtBu	S	75%	68.2
k	Ph	OiPr	SPh	S	83%	88.7
l	CH_3	OtBu	NHtBu	S	61%	69.4
m	CH_3	StBu	OCH_3	S	47%	98.8

The relevance of this method for the preparation of biologically important molecules and its compatibility with sensitive functionality was demonstrated by the synthesis of a phosphonamidopeptide **5** (Figure 2). The N^{α}-Boc-phosphinate amino acid ester **3** was activated with DCP in pyridine to produce phosphonochloridite **4** (^{31}P=170.4 ppm). Reaction of **4** with glycine ethyl ester in the presence of TEA followed by sulfurization produced the novel thiophosphonamide dipeptide **5** as a mixture of diastereomers (^{31}P=73.3, 73.9 ppm) in 50% yield after chromatographic purification. Studies are underway to optimize this chemistry for solution and solid phase synthesis of previously unavailable thio- and dithio-phosphononate peptide analogs, which may be interesting as new classes of protease inhibitors.

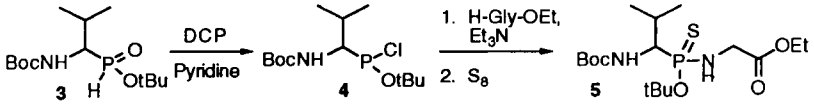

Figure 2. *Use of DCP in the synthesis of a thiophosphonamidopeptide.*

Acknowledgments

We thank the Louisiana State University, the Louisiana Education Quality Support Fund (LEQSF) and the National Science Foundation for financial support.

References

1. Bertenshaw, S.R., Rogers, R.S., Stern, M.K., and Norman, B.H., *J. Med. Chem.*, 55 (1993) 173; Bartlett, P.A., Hanson, J.E. and Giannoussis, P.P., *J. Org. Chem.*, 55 (1990) 6268; Sampson, N.S. and Bartlett, P.A., *Biochemistry*, 30 (1991) 2255.
2. Hirschmann, R., Yager, K.M., Taylor, C.M., Moore, W., Sprengler, P.A., Witherington, J., Phillips, B.W. and Smith III, A.B., *J. Am. Chem. Soc.*, 117 (1995) 6370
3. Letsinger, R.L. and Lunsford, W.B., *J. Am. Chem. Soc.*, 98 (1976) 3655.
4. Campbell, D.A. and Bermak, J.C., *J. Org. Chem.*, 59 (1994) 658.

Peptides: Chemistry, Structure and Biology
Pravin T.P. Kaumaya and Robert S. Hodges (Eds.)
Mayflower Scientific Ltd., 1996

15
Multi-center Study of Post-assembly Problems in Solid Phase Peptide Synthesis

G.B. Fields[1], L. Bibbs[2], L.F. Bonewald[3], J.S. McMurray[4], W.T. Moore[5], A.J. Smith[6], J.T. Stults[7], L.C. Williams[8] and R.H. Angeletti[9]

[1]University of Minnesota, Minneapolis, MN 55455, USA
[2]Research Institute of Scripps Clinic, La Jolla, CA 92037, USA
[3]University of Texas Health Science Center, San Antonio, TX 78284, USA
[4]M.D. Anderson-University of Texas, Houston, TX77030, USA
[5]University of Pennsylvania, Philadelphia, PA 19104, USA
[6]Stanford University, Stanford, CA 94305, USA
[7]Genentech, Inc., South San Francisco, CA94080, USA
[8]USC, Los Angeles, CA 90033, USA
[9]Albert Einstein College of Medicine, Bronx, NY 10461, USA

Introduction

The Peptide Synthesis Research Committee of the Association of Biomolecular Resource Facilities (ABRF) conducts anonymous studies to evaluate the ability of ABRF member laboratories to synthesize and characterize test peptides. Coded samples of peptides synthesized and/or cleaved by these laboratories are analyzed by AAA, HPLC, ESI-MS, MALDI-MS, and Edman sequencing. Cumulative results from the first three studies indicate that the assembly of peptides by solid phase peptide synthesis is no longer a significant problem [1-3]. Therefore, recent studies have focused on post-assembly problems.

Results and Discussion

The 1993 study was initiated to examine potential problems with cleavage procedures. Members of the Peptide Synthesis Committee synthesized large amounts of a peptide by both Boc- and Fmoc-based chemistries [3]. Samples of both peptide-resins were mailed to ABRF members. By standardizing the starting material for cleavage, it was hoped that the committee could identify problems encountered during cleavage procedures. There was no apparent correlation between the cleavage protocol chosen and success in obtaining the desired product.

Based upon these results, the 1994 study sought to identify what parameters in the most popular cleavage procedures were the source of success or failure to obtain the correct peptide product [4]. Participating ABRF laboratories were asked to synthesize H-Val- Lys-Lys-Arg-Cys-Ser-Met-Trp-Ile-Ile-Pro-Thr-Asp-Asp-Glu-Ala-OH, known to

be a nonproblematic synthesis from a previous study, and to remove the peptide from the resin according to one of two detailed cleavage protocols and work-up procedures. Following Fmoc chemistry, participants used either reagent K or reagent B [4]. Those using Boc chemistry chose either a specific HF cleavage procedure or a trimethlsilyl trifluoromethane sulfonate cleavage method. Detailed information on the reagents and laboratory conditions was requested, including: source of reagents, age of reagents, dates when reagents were opened and when used, reagent storage conditions, and type of vacuum system used, if applicable. 93% of the 82 crude samples contained 25% of the desired product. ESI-MS and MALDI-MS estimated that the mean percent desired product was 59%, while RP-HPLC estimated the mean percent desired product as 39%. In contrast to the first study, Fmoc chemistry was used more than Boc chemistry. Dehydration of Asp(O*t*Bu) during Fmoc removal was a significant problem. Overall, there was a lack of correlation between product quality and the choice of cleavage reagents or work-up protocols. Comparison of the detailed protocol sheets submitted with each sample suggested that laboratory technique plays a critically important role in peptide synthesis.

Since cyclized peptides have been shown to be more effective than their linear counterparts in many biological systems, the 1995 study has focused on methods for producing cyclized peptides. ABRF laboratories were asked to synthesize a standard peptide with 2 Cys residues: H-Phe-Cys-Phe-Trp-Lys-Thr-Cys-Thr-NH_2. A choice of 2 protocols each for on-resin and post-cleavage formation of the intrachain disulfide bond would provide the opportunity to test experimental conditions for oxidation of the sulfhydryls, as well as the capabilities of the member laboratories to produce synthetic peptides with intact disulfide bonds. Samples were analyzed by ESI-MS, MALDI-MS, AAA, HPLC, and by spectrophotometric analysis following reaction with Ellman's reagent. A total of 94 samples, 58 of which were cyclized peptides and 36 linear, were received from 40 laboratories. Several laboratories submitted samples using other protocols not suggested by the committee. These included ferricyanide oxidation and use of Ekagen™ resin.

Table 1. *Yields for formation of intrachain disulfide bonds by various protocols.*

Protocol	# samples	≥50% correct product
I (air oxidation with mixing)	25	13
II (oxygen gas)	9	6
III (thallium trifluoroacetate)	10	10
IV (mercuric acetate)	5	0
K Ferricyanide oxidation	5	5
Ekagen resin	3	3

The selected peptide sequence appeared to readily oxidize. This may have caused the unexpectedly high yields of disulfide bonded peptide found in this study (Table 1). Of the 6 protocols used, 5 generally produced an acceptable yield of product. All peptide oxidized by protocol IV, the mercuric acetate on-resin cyclization procedure, showed a strong retention of mercury in the peptide, characterized by a unique mass

spectrum and HPLC retention time. In these cases, only small amounts of the correct cyclized peptide without bound mercury could be detected. Peptides oxidized by protocols I or II, with mixing in the presence of air or oxygen, often produced a good yield of cyclized product. However, variable amounts of the dimeric peptide were detected, up to 60%. Of the samples oxidized by the thallium trifluoracetate on-resin cyclization procedure (protocol III), all produced cyclized product in high yield. Two protocols not in the original study design, ferricyanide oxidation and use of Ekagen™ resin, appeared to produce cyclized product in good yield. However, the sample numbers were very small, particularly since 3 of the ferricyanide samples were derived from one laboratory.

Based upon the data obtained in this study, it appears that producing cyclized peptides with the correct structure can be achieved readily by either on-resin or post-cleavage techniques. The post-cleavage methods are less expensive and provide reasonable yields of the desired product. However, on-resin techniques produce greater yields of the final product, but are more expensive to perform. The mercuric acetate method does not yield the correct peptide product, producing a mercury-peptide adduct which is stable by HPLC and mass spectrometry. In addition, it is best to use a combination of analytical techniques, which complement each other in their ability to detect the correct product and unwanted byproducts.

References

1. Smith, A.J., Young, J.D., Carr, S.A., Marshak, D.R., Williams, L.C. and Williams, K.R., in Angeletti, R.H. (Ed.), 'Techniques in Protein Chemistry III' 1992, pp. 219-229.
2. Fields, G.B., Carr, S.A., Marshak, D.R., Smith, A.J., Stults, J.T., Williams, L.C., Williams, K.R. and Young, J.D., in Angeletti, R.H. (Ed.), 'Techniques in Protein Chemistry IV', 1993, pp. 229-238.
3. Fields, G.B., Angeletti, R.H., Carr, S.A., Smith, A.J., Stults, J.T., Williams, L.C. and Young, J.D., in Crabb, J.W. (Ed.), 'Techniques in Protein Chemistry V', 1994, pp. 501-507.
4. Fields, G.B., Angeletti, R.H., Bonewald, L.F., Moore, W.T., Smith, A.J., Stults, J.T. and Williams, L.C., in Crabb, J.W. (Ed.), 'Techniques in Protein Chemistry VI' 1995, pp. 539-546.

Peptides: Chemistry, Structure and Biology
Pravin T.P. Kaumaya and Robert S. Hodges (Eds.)
Mayflower Scientific Ltd., 1996

16
Fully Enzymatic Synthesis of a Bioactive Peptide

H.L.S. Maia, M.R.J. Rebelo and L.M. Rodrigues

Departamento de Química, Universidade do Minho, Gualtar, P-4710 Braga, Portugal

Introduction

In our laboratory, we have been working on the development of a new approach to the synthesis of the fragment 12-17 of human Gastrin (YGWMDF-NH_2) by fragment condensation using proteases (papain and α-chymotrypsin) in all coupling steps and electrolysis for cleavage of the N-protecting groups.

Results and Discussion

Three peptide fragments were selected as building blocks to construct the required full peptide, *viz.* YG (Fragment A), WM (Fragment B), and DF-NH_2 (Fragment C). The N-terminal dipeptide Bz-Tyr-Gly-OEt (Fragment A) was prepared with α-chymotrypsin in toluene having 0.3% of water by an iterative procedure in a nucleophile pool (70% yield). The benzoyl group was used for N-protection since it is economically advantageous and can be removed by electrolysis.

The synthesis of the middle dipeptide (Fragment B) was initially attempted by using Bz-Trp-OMe as acyl donor and H-Met-OMe as amine donor. The coupling step was investigated under various conditions, but high levels of hydrolysis of the acyl donor were always observed. In view of this result, we changed to papain in combination with -OCH_2CH_2Cl for C-protection of the amine donor (H-Met-OCH_2CH_2Cl), thus increasing the acylating activity of Fragment B. The synthesis of the central dipeptide was then carried out by using toluene with 1% of water in a nucleophile pool (82% yield).

The preparation of the precursor of the C-terminal dipeptide amide (Fragment C) was carried out at room temperature using a 75% ACN medium (pH 9.2) (80% yield). Because the side chain of Asp had to be protected [1], we chose the OBzl group which can be removed by electrolysis. Unfortunately, selective cleavage of Bz with regard to OBzl could not be achieved, possibly because the corresponding peak potentials were too close to each other. In order to circumvent this difficulty, we decided to explore a modification of our previous synthetic scheme by substituting Bz for Bz(4-NO_2) as it shows a less negative cleavage potential (-1.7 V) than OBzl (-2.9 V). Unfortunately, as we could not follow the process by HPLC because of the absence of a good chromophore within the product, we did not obtain direct evidence of its formation. Additionally, we have been experiencing some difficulties with the purification of the electrolysis products since their solubilities were similar to that of the supporting electrolyte. We are presently investigating a new supporting electrolyte (Bu_4NBPhe_4) that has a different solubility behavior.

Trial experiments in the fragment condensation showed that a better yield is obtained with A+B (79% with papain in ACN with 5% of water) as compared to B+C (37% with α-chymotrypsin in toluene with 1% water). The final product (52% yield, (crude) was obtained by coupling AB with C a 52% yield, using α-chymotrypsin in ACN with 5% water. An alternative strategy (A+ BC) is now under a more detailed investigation.

Acknowledgments

We wish to acknowledge the University of Minho and the Junta Nacional de Investigação Científica e Tecnológica for financial support.

Reference

1. Adlercreutz, P., Clapés, P., Mattiasson, B., in Giralt, E. and Andreu, D., (Eds.), 'Peptides 1990', ESCOM, Leiden, The Netherlands, 1991, p. 289.

Peptides: Chemistry, Structure and Biology
Pravin T.P. Kaumaya and Robert S. Hodges (Eds.)
Mayflower Scientific Ltd., 1996

17
Pseudo-prolines (ΨPro) and their Application in Peptide Chemistry

T. Sato, T. Wöhr, F. Wahl, B. Rohwedder and M. Mutter

Institute of Organic Chemistry, University of Lausanne, BCH-Dorigny, CH-1015 Lausanne, Switzerland

Introduction

We have recently shown that pseudo-prolines can be used as a temporary protection for Ser, Thr, or Cys. ΨPro exerts a pronounced effect upon the backbone conformation of polypeptides resulting in a dramatic increase in the solvation of a growing peptide chain in SPPS as well as in the solubility of otherwise sparingly soluble peptides [1-3]. In the present contribution, we demonstrate the use of pseudo-prolines for preparing peptides which have been difficult to access so far by standard SPPS.

Results and Discussion

As a challenging example for the solubilizing power of pseudo-prolines, the SPPS of a transmembrane peptide of pronounced hydrophobic character was investigated.

1 C^{1}-L-A-A-L-L-B-L-L-B-A-L-L-A-X^{15}-L-B-A- L-L-A-NH_2

A Thr-derived ΨPro [X = Thr($\Psi^{H,H}$pro)] was inserted at position 15 of peptide **1** to induce a kink into the otherwise helical structure as observed in natural membrane channel forming peptides (Figure 1). The N-terminal Cys may be used for a subsequent ligation of **1** to a topological template by chemoselective ligation.

For SPPS of **1**, using standard Fmoc chemistry, the incorporation of the pseudo-proline residue is effected *via* the dipeptide Fmoc-Ala-Thr($\Psi^{H,H}$pro)-OH, prepared by acylation of the Thr derived oxazolidine with the corresponding acid fluoride or N-carboxyanhydride [4]. Most significantly, the coupling of the ΨPro containing dipeptide derivative, as well as the following coupling steps, proceeded smoothly to quantitative yields (see HPLC of crude product, Figure 1), pointing to high solvation of the resin bound peptide. This effect was confirmed by the absence of β-sheet formation as seen from the ATR-IR spectrum of the resin bound sequence (Figure 1). The completed sequence was cleaved from the resin with 95% TFA, leaving the oxazolidine system intact. As observed before, the ΨPro containing peptide **1** showed good solubility in a number of organic solvents, thus allowing easy attachment to topological templates according to the TASP approach [5].

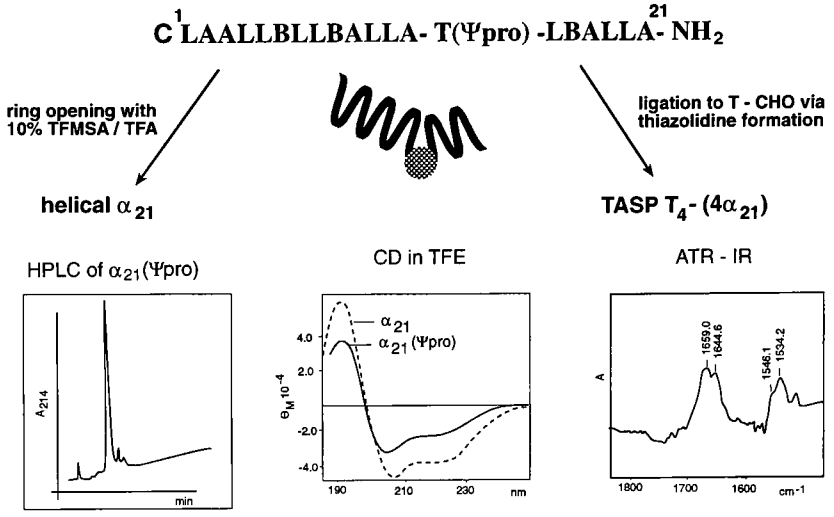

Figure 1. *Synthesis of a ΨPro containing transmembrane helical peptide and its use in TASP design [5].*

In contrast, after ring opening of the ΨPro with strong acid (10% TFMSA in TFA), the peptide showed a significantly lower solubility in organic solvents and in water/TFE mixtures. The CD spectra of the transmembrane peptide clearly reveal the helix-disrupting effect of pseudo-prolines: The observed helicity of the ΨPro peptide (*ca.* 50%) increases significantly by transforming the Thr(ΨPro) building block to a regular Thr by ring opening (*ca.* 90% helicity, Figure 1).

In conclusion, ΨPro residues, used as a temporary protection for Ser, Thr, or Cys, prove to be versatile tools in peptide synthesis and for reversible structural modifications in peptide and protein design.

Acknowledgment

This work was supported by the Swiss National Science Foundation.

References

1. Haack, T. and Mutter, M., *Tetrahedron Lett.*, 33 (1992) 1589.
2. Mutter, M., Nefzi, A., Sato, T., Sun, X., Wahl, F. and Wöhr, T., *Peptide Research,* 8 (1995) 145.
3. Nefzi, A., Schenk, K., and Mutter, M., *Protein and Peptide Lett.*, 1 (1994) 66.
4. Wöhr, T. and Mutter, M., *Tetrahedron Lett.*, 36 (1995) 3847.
5. Cervigni, S., Dumy, P., Kaumaya, P.T.P., Mathieu, M., Nyanguile, O., Peggion, C., Razaname, A., Tuchscherer, G. and Mutter, M., 1995, 1 (1994) 66.

Peptides: Chemistry, Structure and Biology
Pravin T.P. Kaumaya and Robert S. Hodges (Eds.)
Mayflower Scientific Ltd., 1996

18
Enantioselective Synthesis of *H*-phosphinate Amino Acids for Incorporation into Phosphonopeptides

C.P. Vlaar and R.P. Hammer

Department of Chemistry, Louisiana State University, Baton Rouge, LA 70803, USA

Introduction

Phosphonopeptides, which mimic the tetrahedral transition state or intermediate of amide bond hydrolysis, have been successfully employed as powerful protease inhibitors [1]. We are developing a new and general method for the synthesis of phoshonopeptides based on P(III)-compounds whereby protected α-amino-*H*- phosphinates (**1** are used for incorporation into the peptides. A one-pot conversion of *H*-phosphinates to phosphonate derivatives has been achieved by using dichlorotriphenylphosphine in the activating step, which gives access to a wide variety of functionalities around the phosphorus atom [2].

Although there are many racemic preparations, a general approach for enantioselective synthesis of **1** has not been described [3]. We investigated the use of α-metallothio-phosphonamides (**3**, Y = R, A = OR', B = NR_2) as the key intermediates. Amination or bromination (followed by substitution with a nitrogen nucleophile) was expected to give optically active α-substituted aminomethyl- thiophosphonamides **2**. Hydrolysis and reduction with Raney nickel should give the enantioenriched α-aminophosphinates **1**.

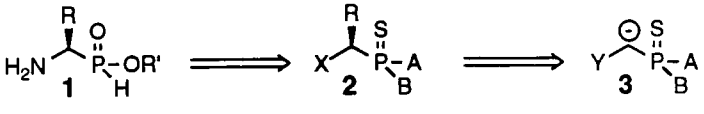

Results and discussion

In Table 1, the results of bromination of the carbanions derived from propyl- and phenylethyl-O-*iso*-propylthiophosphonamides (**3**, R = Et or Bzl, A = OiPr) are presented. The carbanions were generated with *n*-butyl lithium at 0°C or with *n*-butyl-lithium/potassium-*tert*-butoxide at -95°C. 1,2-Dibromo-1,1,2,2-tetrafluoroethane was added after 10 minutes at -70°C and -95°C respectively. The ratio of the two diastereomers of **2** was determined by ^{31}P-NMR.

It can be seen that there is an increase of diastereoselectivity if intramolecular coordination is possible (compare entries 1 and 2 with 3, 4 and 5). Unfortunately, introduction of an extra possible chelating nitrogen group does not lead to much further improvement of the selectivity (entry 6). The hydrazine derivative (entry 7) can provide coordination to the metal atom through a much more favorable 5-membered ring, though

Table 1. *Ratio of diastereomers for bromination of 2 (A = O-i-Pr, Y and B, see table)*

	Y	B	base	ratio
1	$EtCH_3$	$NCH_2CH_2N(CH_3)_2$	BuLi	69:31
2	Bzl	$CH_3NCH_2CH_2N(CH_3)_2$	BuLi	63:37
3	Bzl	$N(CH_3)_2$	BuLi	57:43
4	Bzl	$N(i\text{-}Pr)_2$	BuLi	53:47
5	Bzl	$CH_3NCH_2CH_2CH(CH_3)_2$	BuLi	58:42
6	Bzl	$CH_3N(CH_2)_2N(CH_3)(CH_2)_2N(CH_3)_2$	BuLi	71:29
7	Et	$CH_3NN(CH_3)_2$	BuLi	69:31
8	Et	$CH_3NCH_2CH_2N(CH_3)_2$	BuLi/KOtBu	74:26
9	Et	$CH_3N(CH_2)_2N(CH_3)(CH_2)_2N(CH_3)_2$	BuLi/KOtBu	70:30
10	Et	$CH_3NN(CH_3)_2$	BuLi/KOtBu	90:10

no significant difference in stereoselectivity is observed. If the Schlosser base system BuLi/KO-*t*-Bu is employed, metallation readily takes place at -95°C. For entry 8, there is a slight improvement of stereoselectivity compared to entry 1. For the hydrazine derivative, the change is considerable (compare 7 and 10). This might be due to a temperature effect, but most likely the replacement of lithium with potassium as the counter cation is the predominant factor. Although α-bromothiophosphonamides could now be produced in moderate to reasonable stereoselectivity, their conversion into the corresponding α-aminothiophosphonamides by reaction with NaN_3 or LiN_3 has failed, probably because of competing nucleophilic attack on the phosphorus atom.

This led us to prepare (+)-ephedrine-based thiophosphonamide anions in which a protected α-amino group is already present; **3**, A,B = -$N(CH_3)CH(CH_3)CH(Ph)$**O**-, Y = NLiBoc. Preliminary results for the alkylation of **3** to give the diastereoisomers **2**, X = NHBoc, are given in Table 2. Attempting to improve stereoselectivity, the size of the *N*-alkyl group was increased from Me to iPr. Unfortunately, alkylation experiments with this derivative showed complicated mixtures indicative of decomposition products.

Future work will involve modifications of the amine-protecting group and the chiral auxiliary on the phosphorus and desulfurization to yield the α-amino-*H*-phosphinates.

Table 2. *Alkylation of 3, Y = NLiBoc A,B = -$N(CH_3)CH(CH_3)CH(Ph)$**O**-*

R-X	ratio of diastereoisomers of **2**
H_3CCH_2I	70:30
$H_2C{=}CHCH_2Br$	80:20
$C_6H_5CH_2Br$	85:15

References

1. Sampson, N.S. and Bartlett, P.A., *Biochemistry,* 30 (1991) 2255; Kaplan, A.P. and Bartlett, P.A., *Biochemistry,* 30 (1991) 8165.
2. Fernandez, M.D.F., Fan, H. and Hammer, R.P., this volume.
3. McCleery, P.P. and Tuck, B., *J. Chem. Soc. Perkin Trans. I,* (1989) 1319.

Peptides: Chemistry, Structure and Biology
Pravin T.P. Kaumaya and Robert S. Hodges (Eds.)
Mayflower Scientific Ltd., 1996

19
A Novel Route to Benzodiazepine Diversomers

J. Lutz[1], S. Rudolph-Böhner[1], L. Moroder[1], W. Kolbeck[2], G. Ösapay[3] and M. Goodman[3]

[1]Max-Planck-Institut für Biochemie, 82152 Martinsried, Germany
[2]Collegium Economy Research Technology, 81247 München, Germany
[3]Department of Chemistry and Biochemistry, University of California, San Diego, La Jolla, CA 92093, USA

Introduction

Since benzodiazepines represent important non-peptidic receptor ligands and are most promising molecules for the development of therapeutic agents with good bio-availability, various combinatorial chemistry approaches were recently proposed to generate molecular diversity in this class of compounds [1-3]. Our findings that 2-aminobenzoyl-peptides may serve as precursors of 1,4-benzodiazepine-2,5-diones led us to optimize the conditions for ring closure with concomitant peptide bond cleavage [4] and to elaborate a novel route for the preparation of prodrug libraries and benzodiazepine diversomers.

Results and Discussion

2-Aminobenzoyl (Abz)-amino acids and related esters are readily cyclized under acidic conditions to the corresponding 1,4-benzodiazepine-2,5-diones if the amino acids are N-alkylated, *e.g.* proline, sarcosine and homologs. More surprisingly, even upon extension of the Abz-amino acids to Abz-dipeptides, the cyclization reaction occurs, although only under weakly acidic conditions, thus suggesting a possible anchimeric assistance of the vicinal carboxyl function. This was confirmed by the observation that in the series of peptides H-Abz-Pro-Xxx-Leu-Phe-OH where Xxx = Asp, Lys, Ser, Val, only the Asp-containing peptide at pH 2.0 in aqueous solution leads to [11aS]1,2,3,11a-tetrahydro-5*H*-pyrrolo[2,1]-[1,4]benzodiazepine-5,11(10H)-dione and H-Asp-Leu-Phe-OH by cleavage of the Pro-Asp amide bond ($t_{1/2}$ = 15 h). These findings allowed us to explore a solid phase peptide chemistry approach for the generation of benzodiazepine diversomers. In order to bypass the troublesome diketopiperazine formation of Pro-X dipeptides even when linked to solid supports, peptide spacers with N-terminal Asp were used to link the Abz-Yyy library to the Merrifield resin (Figure 1). H-Asp(OtBu)-Ala-Ala-(P) was built up by conventional Fmoc/tBu SPPS and then extended to the sequences of Boc-Abz-Yyy-Asp(OtBu)-Ala-Ala-(P) by simultaneous incorporation of Pro, Hyp, or azetidine-2-carboxylic acid (Azt). Deprotection of the peptide mixture on the resin by treatment with TFA for 2 h proceeds smoothly without

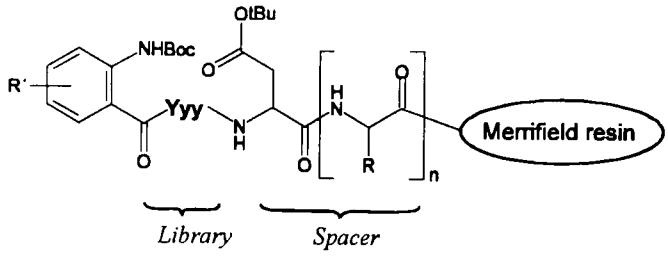

Figure 1. *Synthesis of 1,4-benzodiazepine-2,5-dione diversomers; Yyy = natural and unnatural amino acids; R = H or other amino acid side chains; n = 0,1,2, etc.; R'= substituents.*

releasing of 1,4-benzodiazepine-2,5-diones. Subsequent exposure of the resulting H-Abz-Yyy-Asp-Ala-Ala-(P) to 1% TFA in water/dioxane (1:1) leads to quantitative production of the desired 1,4-benzodiazepine-2,5-diones at a high degree of homogeneity, as assessed by HPLC of the reaction mixture (Figure 2) since potential side products of the synthesis not containing the Abz-Yyy moiety are not released from the resin under these conditions. Mass spectra and a comparison with authentic samples of the three benzodiazepines prepared by acid treatment of the related Boc-Abz-amino acids [4] served to confirm the chemical structures of the reaction products. The $t_{1/2}$ values of the cyclization reactions on the solid support are reported in Figure 2. Following this procedure, libraries of 1,4-benzodiazepine-2,5-ones are readily generated by simultaneous incorporation of diversomers at the Yyy residue or of the Abz moiety or of both of them.

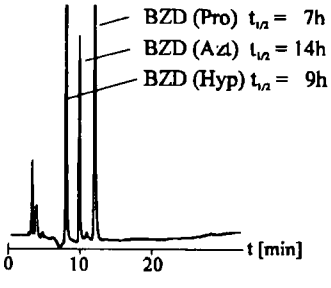

Figure 2. *HPLC elution profile of the reaction mixture of H-Abz-Yyy-Asp-Ala-Ala-(P) with 1% TFA in dioxane/water at 30°C and the related $t_{1/2}$ values of the cyclization reactions.*

References

1. Bunin, B.A. and Ellman, *J.A., J. Am. Chem. Soc.*, 114 (1992) 10997.
2. De Witt, S.H., Kieley, J.S., Stankovic, C.J., Schroeder, M.C., Cody, D.M.R. and Pavia, M.R., *Proc. Natl. Acad. Sci. USA*, 90 (1993) 6909.
3. Plunkett, M.J. and Ellman, J.A., *J. Am. Chem. Soc.*, 117 (1995) 3307.
4. Moroder, L., Lutz, J., Grams, F., Rudolph-Böhner, S., Ösapay, G., Goodman, M., and Kolbeck, W., *Biopolymers.*, submitted.

Peptides: Chemistry, Structure and Biology
Pravin T.P. Kaumaya and Robert S. Hodges (Eds.)
Mayflower Scientific Ltd., 1996

20
New Reagent for the Affinity Purification of Peptides

W.M. Kazmierski and K. Hurley

Glaxo Wellcome Inc., Department of Medicinal Chemistry, Research Triangle Park, NC 27709, USA

Introduction

Stepwise synthesis of hydrophobic peptides frequently results in a complex mixture of deletion peptides, which require laborious purification and product identification. To accelerate the synthesis of pure peptides, we designed and synthesized a new affinity purification reagent **1** (Figure 1), which is used to transiently functionalize the free N-terminus of the peptide (**2**)-resin assembled by a coupling/Ac_2O capping scheme (Figure 2).

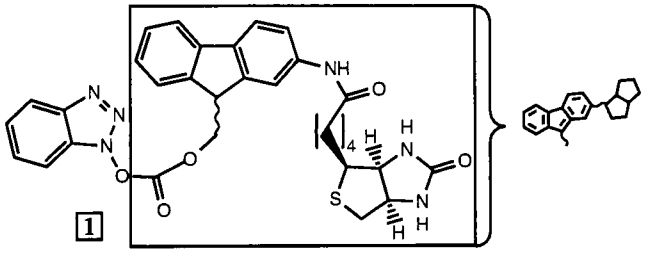

Figure 1. *Structure of the cleavable biotinylation reagent 1.*

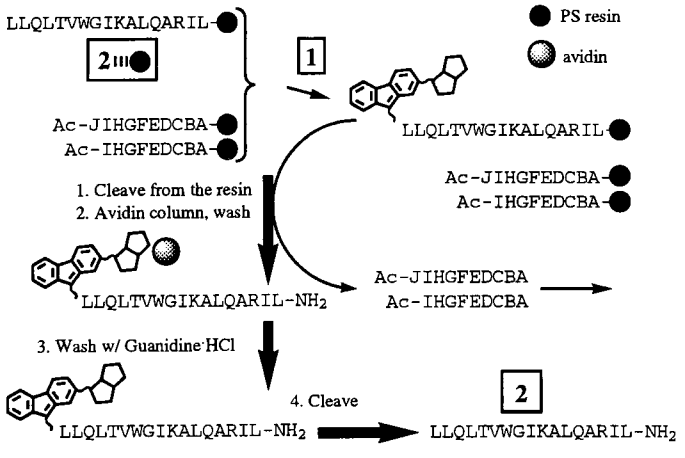

Figure 2. *Affinity purification scheme used to purify peptide 2.*

Results and Discussion

The crude **2** contained a major peak at 13.96 min and several medium to small impurities (Figure 3a). Transient N-biotinylation with **1**, followed by TFA-mediated side-chain deprotection and cleavage from resin, resulted in a mixture which was then dissolved in PBS, absorbed on an avidin-agarose column, and washed with PBS buffer to remove the truncated peptide fragments (Figure 3b). Next, the biotin-peptide conjugate was eluted with 6M guanidine·HCl and treated with piperidine for 10 min (Figure 3c), resulting in **2**.

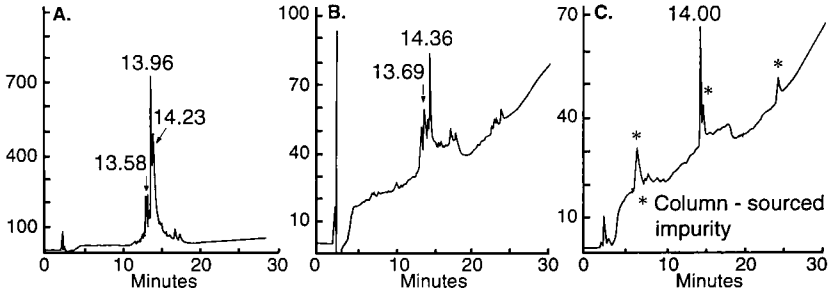

Figure 3. *HPLC traces of (a) crude 2, (b) PBS-eluted fraction, (c) GnHCl-eluted fraction, after piperidine treatment.*

Our method differs from the conventional affinity purification schemes that provide permanently labeled peptides [1]. It yields free N-terminus-peptides, amenable to fragment condensation. Further work will allow us to compare this method with other labile-linker purification schemes [2-4].

References

1. Lobl, T.J., Deibel, M.R. and Yem, A.W., *Anal. Biochem.*, 170 (1988) 502.
2. Ramage, R. and Raphy, G., *Tetrahedron Lett.*, 33 (1992) 385.
3. Sucholeiki, I. and Lansbury, Jr., P.T., *J. Org. Chem.*, 58 (1993) 1317.
4. Funakoshi, S., Fukuda, H. and Fujii, N., *J. Chromatogr.*, 638 (1993) 21.

Peptides: Chemistry, Structure and Biology
Pravin T.P. Kaumaya and Robert S. Hodges (Eds.)
Mayflower Scientific Ltd., 1996

21

N-Protected Aminoacyloxocrotonates: Versatile New Tools in Peptide Synthesis Combining Both Solution and Solid Phase Advantages

C. Birr[1,2], G. Braum[2] and A. Lifferth[2]

[1] Heidelberg University, Faculty of Chemistry, 69120 Heidelberg, Germany
[2] ORPEGEN Pharma, Gesellschaft für Biotechnologische Forschung, Entwicklung und Produktion m.b.H., 69115 Heidelberg, Germany

Introduction

The $Pd^{(0)}$-cleavage of an allylic linker bond in solid phase peptide chemistry is an established technology for a most efficient and entirely non-destructive neutral release of fully protected peptides, glycopeptides, and oligonucleotides from the solid phase [1]. The products have only one single free C-terminal carboxylic function. This is well suited for further chemical transformations, *e.g.*, sequence analog synthesis, amide formation, fragment condensation, cyclization, *etc.*

Because of their orthogonality to all kinds of both N-terminal and side chain protecting groups, we have developed N-urethane protected aminoacyloxocrotonates which have one single carboxylic group free for selective anchoring on any kind of polymer phase [2]. These monomeric allylic linker derivatives render new synthetic strategies possible, combining advantages of both the solid and solution phase technologies, *e.g.*, the use of prefabricated difficult sequences, peptide bridging, rearrangements, and the development of other non-natural structures.

A serious potential problem in SPPS is the occurence of the so-called "difficult sequences", which can result in sudden shrinkage of the expanded gel matrix during synthesis and varying degrees of steric hinderance at the N-terminus. Various attempts have been made to solve this problem using backbone protection, special solvent mixtures, and segment couplings [3].

In preliminary studies on thymic peptides, a difficult sequence was identified in the C-terminus of Thymosin α1. This sequence bears a high content of Val and Glu(O*t*Bu), both known to be associated with difficult sequences [4, 5]. To evaluate the benefits of oxocrotonates in segment coupling, Asp^{28}-Thymosin α1 25-28 (1) and Asp^{28}-Thymosin α1 20-28 [KEVVEEAEN] (2) and were synthesized on Tentagel-resin using the oxo-crotonate linker (Scheme 1). HYCRAM™-resin bound tetrapeptide was elongated both stepwise and by fragment condensation to yield the corresponding nonapeptide. Protected nonapeptide acids (3) were cleaved from the resin and the purity of the crude materials was compared by HPLC (Figure 1).

After stepwise partial deprotection starting from the pentapeptide oxocrotonate (4) to yield (5) and (6), cyclization resulted in the crotonyldepsipeptide (7) (Scheme 2).

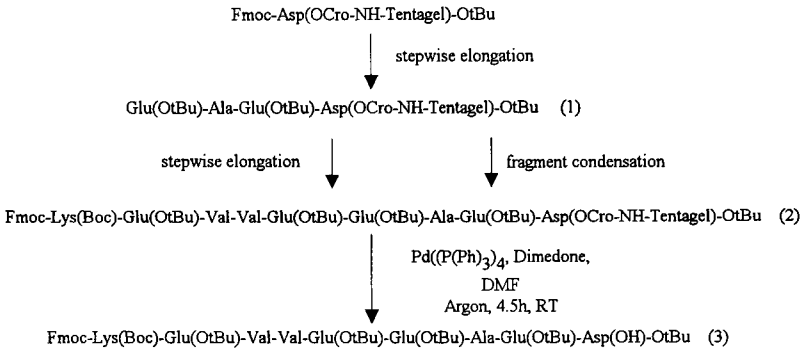

Scheme 1. *Synthesis of Asp[28]- Thymosin α1 20-28 (3).*

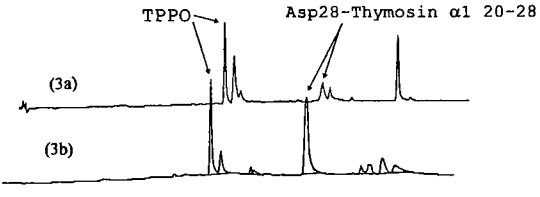

Figure 1. *Comparison of nonapeptide acids (3) by HPLC A: 0.1% TFA in H_2O, B: 0.1% TFA in CH_3CN; Gradient: 0-70% B in 30 min. TPPO: Triphenyl-phosphinoxide. (3a): From stepwise elongation, (3b): From fragment condensation.*

Results and Discussion

SPPS was accomplished on "TentaGel S NH_2" (0,26mmol-NH_2/g) by the Fmoc/Bu^t-strategy. The resin was loaded with Fmoc-Asp(OCro-OH)-OtBu and all couplings were performed with four equivalents of protected amino acid as single couplings by the TBTU-method. Protected Asp[28]-Thymosin α1 20-28 (3) with an unprotected side chain at Asp[28] was obtained after mild $Pd^{(0)}$-cleavage [1] in 90% yield. Coupling of protected Thymosin α1 20-25 pentapeptide acid onto resin bound tetrapeptide (1) was performed as described above, but with an extended reaction time (5hr.). Synthesis of protected Thymosin α1 20-24 (4) was carried out by a solution-phase method using Glu(OtBu)-OCro-OPac as C-terminal residue (Scheme 3). N-terminal Ddz-protection together with Bu^t side chain protection proved to be suitable for quick and efficient chain elongation. However, N-terminal Fmoc-Lys(Boc) was used to assure comparison of protected nonapeptide acids (IIIa,b). Compound (IIIb) was obtained after C-terminal deprotection of (4), fragment condensation, and subsequent cleavage from the resin. Stepwise SPPS of Asp[28]-Thymosin α1 20-28 (2) displayed difficult couplings at Glu[21] and Val[22]. HPLC comparison of the corresponding protected nonapeptide acids (3) shows significantly higher purity for the raw material obtained by fragment condensation (Figure 1).

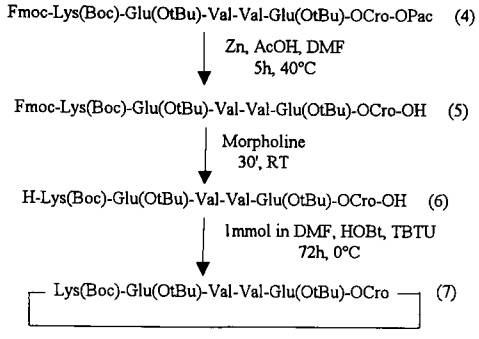

Scheme 2. *Synthesis of protected crotonyldepsipeptide (7).*

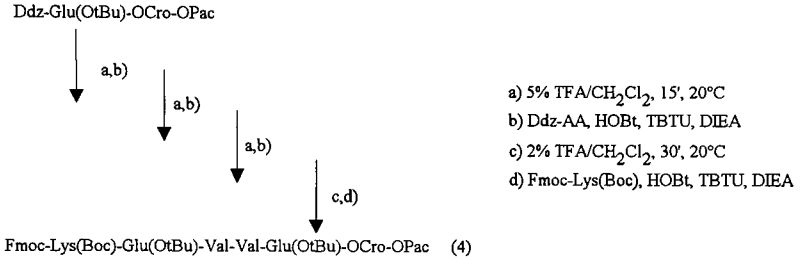

Scheme 3. *Synthesis of protected pentapeptide(4).*

Protected pentapeptide-oxocrotonate (5) was prepared by Zn/AcOH cleavage of the phenacylester (4) in the presence of the acid-sensitive ε-Lys Boc-group with minor amounts of byproduct (Scheme 2). After N-terminal Fmoc-cleavage yielding (6) and cyclization (1mmol/L, 4 equiv. TBTU/HOBt), crotonyldepsipeptide (7) was obtained with a FAB-MS showing the expected mass (881.75 m/e).

References

1. Kunz, H., Dombo, B., *Angew. Chem. Int. Ed. Engl.*, 27 (1988) 711.
2. Birr, Ch., in Epton, R. (Ed.), 'Innovation and Perspectives in Solid Phase Synthesis', Mayflower, Birmingham, UK, 1994, pp. 83-94.
3. Hyde, C., Johnson, T., Owen, D., Quibell, M., Sheppard, R.C., in Epton, R. (Ed.), Innovation and Perspectives in Solid Phase Synthesis', Mayflower, Birmingham, UK, 1994, pp. 29-38.
4. Krchnak, V., Vagner, J., in Epton, R. (Ed), 'Innovation and Perspectives in Solid Phase Synthesis', Mayflower, Birmingham, UK, 1994, pp. 419-424.
5. Otteson, K.M., Noble, R.L., Harrison, J.L. 23rd European Peptide Symposium presentation, 1994.

Peptides: Chemistry, Structure and Biology
Pravin T.P. Kaumaya and Robert S. Hodges (Eds.)
Mayflower Scientific Ltd., 1996

22
Design, Synthesis and Characterization of a Peptide β-Sheet Model

L.H. Kondejewski, D.S. Wishart, B.D. Sykes, C.M. Kay and R.S. Hodges

Department of Biochemistry and the Protein Engineering Network of Centres of Excellence, University of Alberta, Edmonton, Alberta, T6G 2S2, Canada

Introduction

Peptide models of α–helicies have contributed much to our understanding of these elements in protein structure and function. Unfortunately, no simple peptide models for β-sheets exist at this time. A number of models do exist and are based on the use of protein host-guest systems [1, 2], or a peptide model requiring metal-binding to induce β-structure [3]. In the present, study we report on the use of a small cyclic peptide based on the bacterial peptide cyclo(Val-Orn-Leu-D-Phe-Pro)$_2$ (gramicidin S) and its utility as a β-sheet model peptide. This peptide is known to form a two-stranded amphipathic β-sheet containing two type II' β-turns made up by D-Phe and Pro residues [4, 5]. The advantages of this system include: i) its small size, allowing rapid synthesis and characterization by CD and NMR spectroscopy, ii) its water solubility, iii) its amphipathic nature, thereby allowing determination of β-sheet propensities on both hydrophobic and hydrophilic sides, and iv) its amenability to covalent dimerization, allowing investigation of side chain packing and hydrophobic effects within β-sandwiches.

Results and Discussion

In developing a peptide β-sheet model system, we evaluated the effect of strand length on β-sheet stability within the model. Peptides 1 through 7 shown in Table 1 were synthesized by SPPS, purified by RP-HPLC, and cyclized through a head-to-tail amide linkage [6]. Figure 1 shows the CD spectra of a series of cyclic analogs ranging from 6 to 14 residues. Under benign conditions, only the peptides containing either 6 (peptide 1), 10 (peptide 3) or 14 residues (peptide 5) resembled the CD spectrum of gramicidin S and hence contained significant β-sheet. These results indicate that within the cyclic nature of our model system, there is a requirement for an odd number of residues in each strand, likely reflecting the alternating hydrogen bonding pattern found in antiparallel β-sheets.

Comparison of peptides 3, 6 and 7 allowed us to evaluate whether β-sheet propensities could be measured within a 10-residue model system. Table 1 shows that

the β-sheet content as measured, using either α-^{1}H chemical shift indicators [7] or $J_{HNH\alpha}$ coupling constants, decreased slightly with a valine to cysteine substitution, and decreased further with a valine to glycine substitution.

These data indicate that the cyclic β-sheet system used to determine β-sheet propensities should contain an odd number of residues between the two β-turns, and that substitutions can be made within the β-strands to determine relative β-sheet content on either the hydrophobic or hydrophilic face of the molecule.

Table 1. *Sequences and β-sheet content of gramicidin S cyclic peptide analogs.*

Peptide	Length	Sequence[a]	β-Sheet content (%)	
			Chemical shift[b]	Coupling constant[c]
1	6	YPKYPK		
2	8	YPVKYPKL		
3	10	YPVKLYPVKL	84	92
4	12	YPVKLKYPKVKL		
5	14	YPVKLKVYPLKVKL		
6	10	YPGKLYPVKL	38	62
7	10	YPCKLYPVKL	70	68

[a] all sequences use D-tyrosine.

[b] % β-sheet content = (average lysine chemical shift - lysine random coil chemical shift) / (ideal β-sheet chemical shift) x 100. Lysine residues were used as the reference because they are in the center of the β-sheet and are not perturbed by the β-turns.

[c] % β-sheet content = (average lysine coupling constant - average tyrosine coupling constant) / (ideal β-sheet coupling constant - ideal type II' turn coupling constant) x 100.

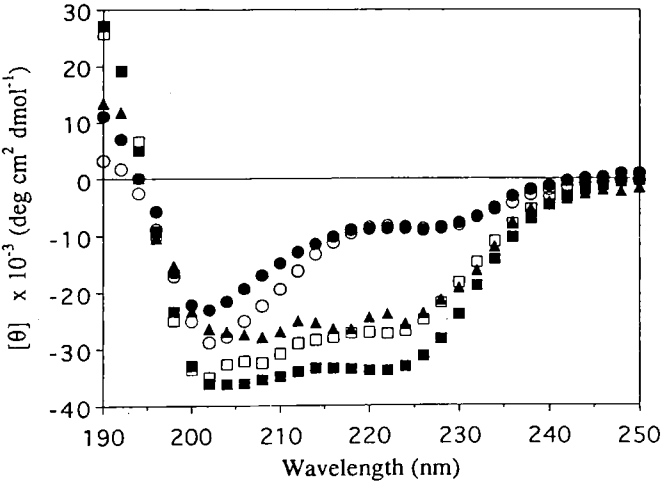

Figure 1. *CD spectra of cyclic analogs varying in strand length. Spectra were recorded in 10mM sodium acetate buffer, pH 5.5 at 20 °C. Peptides contained 6 (open squares), 8 (open circles), 10 (filled squares), 12 (filled circles) or 14 residues (filled triangles), corresponding to peptides 1 to 5 in Table 1.*

References

1. Smith, C.K., Withka, J.M and Regan, L., *Biochemistry,* 33 (1994) 5510.
2. Minor, Jr., D.L. and Kim, P.S., *Nature,* 367 (1994) 660.
3. Kim, C.A. and Berg, J.M., *Nature,* 362 (1993) 267.
4. Hull, S.E., Karlsson, R., Main, P, and Woolfson, M.M., *Nature*, 275 (1978) 206.
5. Nemethy, G. and Scheraga, H.A., *Biochem. Biophys. Res. Comm.*, 118 (1984) 643.
6. Wishart, D.S., Kondejewski, L.H., Semchuk, P.D., Sykes, B.D. and Hodges, R.S., *Protein and Peptide Letters*, submitted.
7. Wishart, D.S. and Sykes, B.D., *Meth. Enzymol.*, 239 (1994) 363.

Peptides: Chemistry, Structure and Biology
Pravin T.P. Kaumaya and Robert S. Hodges (Eds.)
Mayflower Scientific Ltd., 1996

23
Backbone Protection: Synthesis of Difficult Sequences Using N-α-Tmob-protected Amino Acid Derivatives

N. Clausen, C. Goldammer, K. Jauch and E. Bayer

University of Tübingen, Institute of Organic Chemistry, Auf der Morgenstelle 18, D-72076 Tübingen, Germany

Introduction

AA-derivatives used for the purpose of temporary protection of the amide nitrogen of the peptide bond during solid phase synthesis include N-α-2-hydroxy-4-methoxybenzyl-AA (HMB-AA) [1], the preparation of which is laborious and expensive, and Ser- or Thr- derived pseudoprolines [2]. Here we report the use of N-α-Tmob AA derivatives (Tmob = 2,4,6-trimethoxybenzyl) which we have synthesized readily by direct Mannich reaction of an AA or an AA-ester and 1,3,5-trimethoxybenzene in methanol [3]. No significant racemization of the obtained Tmob-protected compounds was found (<0,2%; N-α-Fmoc- N-α-Tmob-AA, N-α-Fmoc-N-α'-Tmob-dipeptides).

Generally, these modifications obviate the development of secondary structures and lead to improved solvation of the resin bound peptide and improved solubility of protected fragments, thus rendering the latter ideally suitable for fragment condensation.

Results and Discussion

A) Structure disrupting potency. To demonstrate the structure disruptive efficiency of Tmob-AA derivatives and the practicability of the dipeptide approach, we chose the synthesis of poly-alanine. This difficult sequence is notorious for strong aggregation from the fifth residue onward, which makes it pointless to continue. An attempted synthesis of Poly-$Ala_{(10)}$ without Tmob-AA derivatives gave an almost insoluble very heterogeneous product with various deletion or termination sequences. In contrast, the synthesis of Poly-$Ala_{(12)}$ with Tmob-protected dipeptides (Ala 4/5 and Ala 8/9) yielded an almost pure product (>90% by HPLC). No difficult deprotection steps during synthesis with Tmob-protected dipeptides were observed. Cleaved as protected peptide, Poly-$Ala_{(12)}Tmob_{(2)}$ is well soluble in the usual solvents and in water. In a first synthesis racemization in the range of 20% D-Ala was observed, probably due to HOBt/DIC activation of dipeptides and to an activation time of 30min. Coupling with HATU/ collidine reduced this level to about 13% [4].

B) Solubilizing effect and suitability for fragment condensation. The powerful solubility enhancing effect of Tmob-backbone protection renders it ideally suitable for fragment condensation strategies. For this purpose, two fragments of HIV-I-protease were synthesised, using N-Fmoc-N-Tmob-Gly-OH in two positions:

1 99-90 H-Leu-Thr(tBu)-Gln(Trt)-Ile-**Gly(Tmob)**-Cys(Acm)-Thr(tBu)-Leu-Asn(Trt)-Phe-OH

2 89-80 H-Thr(tBu)-Pro-Val-Asn(Trt)-Ile-Ile-**Gly(Tmob)**-Arg(Pmc)-Asn(Trt)-Leu-OH

Syntheses were carried out on aminomethylated polystyrene bearing the *p*-carboxy-tritylalcohol linker (TCP-resin) [5]. No difficulties were observed during syntheses, as shown by ABI 433A monitoring. Analysis of Fragment 1 showed a pure crude product by HPLC (>97%) and IS-MS. Due to a work up error after cleavage (HAc/DCM/MeOH/TFE) of Fragment 2, major loss of Asn trityl groups occurred, clearly identifiable by IS-MS and HPLC. However, the synthesis itself proved to be most successful, no deletion sequences being detected. Crude Fragment 2 was easily purified by silica gel column chromatography, yielding a highly pure product (>98% HPLC) of excellent solubility. Thus, 560mg of peptide dissolved easily in <5ml of eluent ($CHCl_3$/MeOH/HOAc), though 1 or 2ml would have sufficed, had the solution not been too viscous for chromatography. A second synthesis of Fragment 2 was carried out and a modified cleavage procedure was applied [6], using DCM/HFIP 4:1 for 15min. After evaporation of the filtrate, crude Fragment 2 was obtained (>98% purity HPLC) in a yield of >96% as a white powder. Using this procedure, no carboxylic acid from the cleavage mixture adheres to the protected fragment and it can be used directly for fragment coupling [6]. Fragment 2 was coupled onto resin-bound Fragment 1. The substitution of Fmoc-deprotected peptide resin was 0.31 mmol/g. The peptide resin was strongly ninhydrin positive. A 5-fold excess of Fragment 2 was used and HATU/collidine was applied as coupling reagent in a solvent system of DMF/DCM 1/2 [4]. After 3hr., the resin gave a completely negative ninhydrin response. HPLC of the fully protected coupling product HIV-I protease (99-80) showed no trace of deprotected Fragment 1. Purity of the coupling product was >96% by HPLC. The correct mass was proved by IS-MS. Racemization of C-terminal Leu of Fragment 2 was about 6.3%.

To conclude, N-α-Tmob protected amino acid derivatives show a strong structure disrupting effect, and enhance resin bound peptide solvation and protected fragment solubility. Thus, they are ideally suitable for fragment condensation strategies. High substitution of the peptide resin did not adversely affect the fragment coupling reaction.

References

1. a) Johnson, T., Owen, D., Quibell, M. and Sheppard, R.C., in Schneider, C.H. and Eberle, A.N. (Eds.), 'Peptides: Chemistry, Structure and Biology', ESCOM, Leiden, The Netherlands, 1993, p.23. b) Johnson, T., Quibell, M. and Sheppard, R.C., *J. Peptide Sci.*, 1 (1995) 11.
2. a) Haack, T., Nefzi, A., Zier, A. and Mutter M., in Schneider, C.H. and Eberle, A.N. (Eds.), 'Peptides: Chemistry, Structure and Biology', ESCOM, Leiden, The Netherlands, 1993, p.595. b) Nefzi, A., Schenk, K., and Mutter, M., *Protein and Peptide Letters*, 1 (1994) 66.
3. Patent application filed on Sept. 3, 1994.
4. Carpino, L.A., El-Faham, A. and Albericio F., *Tetrahedron Letters*, 35 (1994) 15.
5. Bayer, E., Clausen, N., Goldammer, C., Henkel, B., Rapp, W. and Zhang, L., in Hodges, R.S. and Smith, J.A. (Eds.), 'Peptides: Chemistry, Structure and Biology', ESCOM, Leiden, The Netherlands, 1994, p.156. (Resin from PepChem, Im Winkelrain 73, Tubingen)
6. Bollhagen, R., Schmiedberger, M., Barlos, K. and Grell, E., *J. Chem. Soc., Chem. Commun.*, (1994) 2559.

Peptides: Chemistry, Structure and Biology
Pravin T.P. Kaumaya and Robert S. Hodges (Eds.)
Mayflower Scientific Ltd., 1996

24
Preferential Disulfide-bridge Formation for Heterodimers by Derivatization with 2,2'-Dithiodipyridine

P.D. Semchuk, O.D. Monera, L.H. Kondejewski, C. Gannon, L. Daniels, I. Wilson and R.S. Hodges

Department of Biochemistry and the Protein Engineering Network of Centres of Excellence, University of Alberta, Edmonton, Alberta, T6G 2H7, Canada

Introduction

Crosslinking of two different molecules through a disulfide bond is commonly used in synthetic peptide chemistry, protein conjugation, and in protein folding studies. The most common method is air oxidation under slightly alkaline aqueous solutions [1-4], but the use of oxidizing agents is sometimes employed [5-6]. Two problems are often encountered when producing a heterodimer through intermolecular disulfide-bridge formation. These are the presence of undesired homodimers and the need to purify the heterodimer from the homodimers. To address both problems, we have developed a method of exclusively producing the heterodimer, where one of the constituent peptides is derivatized by 2,2'-dithiodipyridine prior to disulfide-bridge formation with the second peptide (Figure 1).

Results and Discussion

As an example, two 35-residue peptides were used to form a 70-residue disulfide-bridged heterodimer. Peptide A-SH was derivatized by dissolving in ethanol (1 mg/ml) and then incubating with a five-fold molar excess of dithiodipyridine (DTDP) at room temperature for about 30 minutes. Ethanol was then removed by rotavaporation and the residue was redissolved in 0.05% aqueous TFA. Excess DTDP and thiopyridine (HS-TP) were extracted three times with equal volumes of diethyl ether and, depending on the desired purity, the aqueous derivatized peptide (A-S-TP) solution can either be used directly with or without prior purification. An equimolar amount of peptide B-SH was dissolved in 0.05% aqueous TFA (1 mg/ml) and then very slowly added into A-S-TP with an equal volume of degassed 50mM phosphate buffer containing 1 mM EDTA at pH 7. The

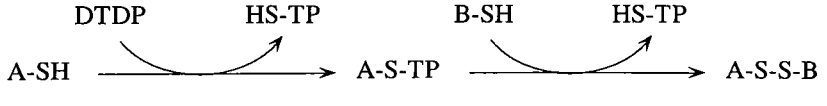

Figure 1. *Reaction scheme of the proposed heterodimeric disulfide-bridge formation. A-SH, reduced peptide A; DTDP, dithiodipyridine; HS-TP, thiopyridine; A-S-TP, thiopyridine-derivatized peptide A; B-SH, reduced peptide B; A-S-S-B, disulfide-bridged AB heterodimer.*

completion of both derivatization and coupling reactions were monitored by reversed-phase HPLC and product identity was confirmed by mass spectrometry.

The reversed-phase HPLC chromatograms of the individual peptides show a narrow range of retention times (Figure 2A). That of the air oxidation without derivatization (Figure 2B) illustrates the two aforementioned problems; (1) decreased yield of the heterodimer from an overabundance of undesired homodimers and (2) similar retention times of the product peaks creating potential purification problems. The use of the derivatization technique yields essentially only the heterodimeric product (Figure 2C-2D) and clearly indicates a significant improvement in yield and ease of purification. The efficiency of the method can be optimized by (1) derivatizing the peptide that oxidizes faster and titrating the peptide derivative with the slow-oxidizing peptide, and/or (2) derivatizing the peptide that has a closer retention time with that of the heterodimer.

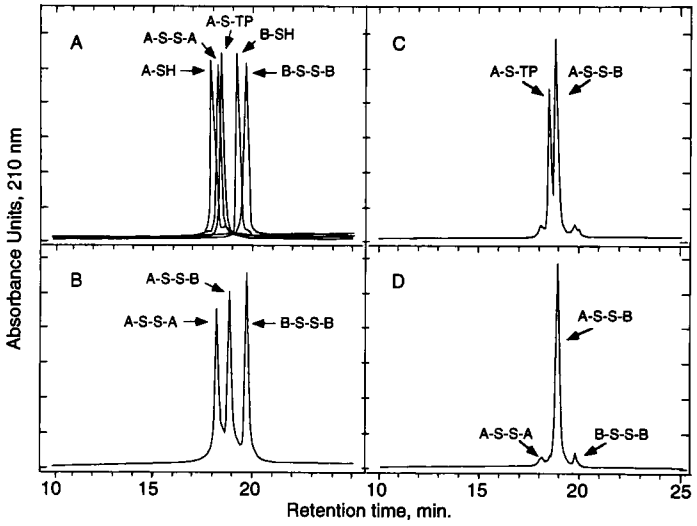

Figure 2. *Reversed-phase HPLC chromatograms of (A) the reduced, oxidized, and A-S-TP peptides, (B) the products of air oxidation, (C) A-S-TP titrated with half-molar equivalent of peptide B, (D) A-S-TP titrated with molar equivalent of peptide B. A-S-S-A and B-S-S-B are the two disulfide-bridged homodimers.*

References

1. Ahmed, A.K., Schaffer, S.W. and Wetlaufer, D.B., *J. Biol. Chem.*, 250 (1975) 8477.
2. Yajima, H. and Fujii, J., *J. Am. Chem. Soc.*, 103 (1981) 5867.
3. Li, C.H., Yamashiro, D., Gospodarowicz, D., Kaplan, S.L. and van Vliet, G., *Proc. Natl. Acad. Sci. USA*, 80 (1983) 2216.
4. Lee, K.K., Black, J.A., and Hodges, R.S., in Mant, C.T. and Hodges, R.S. (Eds.), 'High-performance Liquid Chromatography of Peptides and Proteins: Separation, Analysis, and Conformation', CRC Press, Boca Raton, FL, USA, 1991, p.389
5. Tam, J.P., Wu, C.R., Liu, W. and Zhang, J.W., *J. Am. Chem. Soc.*, 113 (1991) 6657.
6. Hope, D.B., Murti, V.V.S. and Vigneaud, V.D., *J. Biol. Chem.*, 237 (1962) 1563.

Peptides: Chemistry, Structure and Biology
Pravin T.P. Kaumaya and Robert S. Hodges (Eds.)
Mayflower Scientific Ltd., 1996

25

Reversible Peptide Bond Alkylation Improves O-(7-Aza-benzotriazolyl)-1,1,3,3-bis(tetramethylene)uronium Hexafluorophosphate (HAPyU) - mediated Cyclization of All-L-Pentapeptides

A. Ehrlich[1], J. Klose[1], H.-U. Heyne[1], M. Beyermann[1], L.A. Carpino[2] and M. Bienert[1]

[1]*Institute of Molecular Pharmacology, Alfred-Kowalke-Str. 4, D-10315 Berlin, Germany*
[2]*Department of Chemistry, University of Massachusetts, Amherst, MA 01003, USA*

Introduction

In the synthesis of homodetic cyclic peptides, the readiness of an open chain precursor to cyclize depends on the size of the ring to be closed, and usually no difficulties arise for the cyclization of peptides containing seven or more amino acid residues. Although ring closure with hexa- and pentapeptides is more hampered, the ease of cyclization is enhanced by the presence of turn structure-inducing amino acids such as glycine, proline or a D-amino acid [1].

Recently, we demonstrated the superiority of HAPyU for promoting peptide cyclization quickly and with a minimum of racemization [2]. Thymopentin-derived penta- and hexapeptides, which were earlier shown to cyclize with difficulty [3], have now been converted to the corresponding cyclopeptides without extensive stereomutation within 10 min [4]. In addition to yielding the desired cyclomonomers, several linear sequences were found to give large amounts of the corresponding cyclodimers. Therefore, we studied the influence of turn-inducing amino acids on the monomer/dimer ratio and developed a strategy to enhance the probability of obtaining the cyclomonomers by reversible backbone alkylation.

Results and Discussion

In order to investigate the influence of the turn-inducing amino acid proline or of pseudo-prolines [5] on the formation of cyclization-prone conformations of linear peptides, we synthesized the complete proline-replacement set of **1**. Whereas pentapeptide **1** undergoes cyclization to give a mixture of 33% cyclomonomer and 38% cyclodimer, the presence of proline, regardless of its position in the linear sequence, drastically hinders formation of the cyclomonomers (peptides **2, 3**). Similarly for hexapeptides, the cyclization probability was found to be nearly abolished by the presence of proline (peptide **4**). Clearly in such cases, for generation of cyclization-

prone conformations, the assistance of appropriate amino acid residues adjacent to proline is required (*e.g.* -D-Xaa-Pro-, -Pro-Gly-).

In contrast to proline, a single D-amino acid-, glycine- or N-methylamino acid residue (peptides **5, 6, 7**) dramatically increases the formation of cyclomonomers (Table 1). The effect observed in the cyclization of the linear N-methylalanine-containing peptide **7** suggests that reversible modification of peptide bonds, originally introduced in peptide chemistry to reduce β-sheet formation during peptide chain elongation [6], should be useful in promoting the cyclization of peptides devoid of turn-inducing amino acid residues. Indeed the 2-hydroxy-4-methoxybenzyl (Hmb) [6]-substituted peptides **8, 10** and **11** rapidly lead to the formation of the cyclomonomers in high yield, in contrast to the unmodified sequences **1** and **9**.

Table 1. *Influence of turn-inducing amino acids and reversible peptide bond alkylation on cyclomonomer/cyclodimer ratio*[a].

	Peptide	% cyclomonomer	% cyclodimer
1	Arg-Lys(Ac)-Ala-Val-Tyr	33	38
2	Arg-Pro-Ala-Val-Tyr	3	30
3	Arg-Lys(Ac)-Pro-Val-Tyr[b]	9	13
4	Val-Arg-Lys(Ac)-Pro-Val-Tyr[b]	3	41
5	Arg-Lys(Ac)-Ala-Val-DTyr	83	0
6	Arg-Lys(Ac)Gly-Val-Tyr	60	
7	Arg-Lys(Ac)-MeAla-Val-Tyr	60	13
8	Arg-Lys(Ac)-(Hmb)Ala-Val-Tyr	64	8
9	Ala-Ala-Ala-Ala-Ala	43	45
10	Ala-(Hmb)Ala-Ala-Ala-Ala	78	8
11	Ala-Ala-(Hmb)Ala-Ala-Ala	68	23

[a]Cyclization was performed in DMF (peptide concentration 1 mM) using 1.1 eq HAPyU and 3 equiv. DIEA for 10 min at room temperature. [b]Proline in other positions gave similar results.

Acknowledgments

We thank the Deutsche Forschungsgemeinschaft and the Fonds der Chemischen Industrie for financial support of this work in Berlin.

References

1. Kessler, H. and Haase, B., *Int. J. Peptide Protein Res.*, 39 (1992) 36.
2. Ehrlich, A., Rothemund, S., Brudel, M., Beyermann, M., Carpino, L.A. and Bienert M., *Tetrahedron Lett.*, 34 (1993) 4781.
3. Kessler, H. and Kutscher, B., *Liebigs Ann. Chem.*, (1986) 869.
4. Ehrlich, A., Brudel, M., Beyermann, M., Winter, R., Carpino, L.A. and Bienert M., in Maia, H.L.S. (Ed.), 'Peptides 1994' (Proceedings of the 23rd European Peptide Symposium), ESCOM, Leiden, The Netherlands, 1995, p. 167.
5. Haack, T. and Mutter, M., *Tetrahedron Lett.*, 33 (1992) 1589.
6. Johnson, T., Quibell, M. and Sheppard, R.C., *J. Peptide Sci.*, 1 (1995) 11.

Peptides: Chemistry, Structure and Biology
Pravin T.P. Kaumaya and Robert S. Hodges (Eds.)
Mayflower Scientific Ltd., 1996

26
Side Reactions Associated with Acetic Anhydride in Resin-capping, and with Dimethylformamide in Catalytic Hydrogenation

K.H. Hsieh

Department of Veterinary and Comparative Anatomy, Pharmacology and Physiology, Washington State University, Pullman, WA 99164, USA

Introduction

To minimize C-terminal deletion in solid phase synthesis, acetic anhydride (Ac_2O) is often used to acylate reactive nucleophiles on the Boc-amino acid-resin. To reduce additional truncation in the growing peptide chain, acetylimidazole (Ac-Im) has been used to terminate unreacted amine group after the coupling step [1]. For peptide cleavage from the resin, catalytic [2] and transfer [3] hydrogenation are useful alternatives to HF acidolysis, especially when Boc-peptide is desired.

Previous studies of fibrin peptides indicated Arg acetylation during GPR (Aα 17-19) synthesis, and His/Lys formylation of GHRPLDKKREE (Bβ 15-25) during catalytic hydrogenation in DMF. This study demonstrated Ac_2O, but not Ac-Im, modification of Boc-Arg(NO_2) and Boc-Arg(Tos). In addition, DMF, but not its decomposed product of formic acid (HCOOH), was involved in His/Lys modification.

Results and Discussion

Boc-Arg(NO_2) or Boc-Arg(Tos) in DCM was stirred overnight with a 10-fold excess of Ac-Im, Ac_2O, TEA, or the Ac_2O-TEA mixture. The reaction mixtures were analyzed by TLC to separate the modified products from the starting amino acids, and detected by UV and ninhydrin. Boc-Arg(NO_2) remained unchanged upon Ac-Im, Ac_2O, or TEA treatment alone, but gave another UV- and ninhydrin-positive product with Ac_2O-TEA (Table 1). Boc-Arg(Tos) was similarly stable to Ac-Im or TEA, but gave a small amount of a modified product with Ac_2O. However, no Boc-Arg(Tos) remained after overnight treatment with Ac_2O-TEA, suggesting TEA acceleration of the Ac_2O reaction. The results indicate that Ac_2O capping may not be advisable for Arg-containing resin, in spite of the less complex peptide product normally rendered by resin capping.

To determine whether His/Lys formylation was mediated by HCOOH, which can acylate amines [4] and is generated during DMF decomposition, Boc-Arg(NO_2), Boc-His(Bzl), or Boc-Lys(Z) in NMP was subjected to HCOOH- or $HCOONH_4$-mediated transfer hydrogenation with Pd/C. TLC analyses indicated that HCOOH (100-fold) or $HCOONH_4$ (15-fold) treatment completely removed the Z-group in 3 hr to give Boc-Lys with a side-product, but without Boc-Lys(For). On the other hand,

prolonged transfer hydrogenation for 3 days gave primarily unreacted Boc-Arg(NO_2) and Boc-His(Bzl). Similarly, Boc-Lys(Z) was completely reduced by catalytic hydrogention (15 psi H_2, 50°C, 40 hr) with $Pd(OAc)_2$ in DMF or NMP. The former solvent gave some Boc-Lys(For), and the latter gave a side-product identical in R_f values to the side-product from transfer hydrogenation. Catalytic hydrogenation of Boc-Arg(NO_2) in NMP or DMF was not complete under these conditions, but gave Boc-Arg as the only product. Boc-His(Bzl) was completely reduced to Boc-His in NMP, but gave a mixture of Boc-His and Boc-His(For) in DMF. The results suggest that His/Lys-formylation was mediated by DMF, and that catalytic hydrogenation in NMP may be more effective than transfer hydrogenation for Arg- and His-containing peptides. We found that NMP-propionic acid (9:1) replacement for DMF during catalytic hydrogenation of the protected Bβ 15-25-resin increased the peptide yield by one third (29% *vs.* 22%).

Table 1. *Side-chain modification by acetic anhydride and during catalytic hydrogenation in DMF.*

Amino Acid	Treatment	Possible Product	R_f		Detection		
			BAW	BNH_4	UV	Nin	Pauly
Boc-Arg(NO_2)			0.68	0.28	+	+	
	Ac_2O-TEA	Boc-Arg(NO_2)(Ac) deriv.	0.80	0.78	+	+	
Boc-Arg(Tos)			0.72	0.32	+	+	
	Ac_2O	Boc-Arg(Tos)(Ac) deriv.	0.82	0.80	+	+	
Boc-His(Bzl)			0.46	0.28	+	+	-
	H_2/$Pd(OAc)_2$/DMF	Boc-His(For)[a]	0.47	0.29	-	+	+
Boc-Lys(Z)			0.83	0.41	+	+	
	H_2/$Pd(OAc)_2$/DMF	Boc-Lys(For)[b]	0.69	0.22	-	+	

R_f values were determined for silica gel plates developed in the solvent systems of BAW (4:1:5 of *n*-butanol-acetic acid-water, upper phase) and BNH_4 (100:44 of *s*-butanol-3% NH_4OH). [a]Boc-His was the major product, which was UV-negative but ninhydrin- and Pauly-positive, with the respective R_f values of 0.45 and 0.24 in BAW and BNH_4. [b]Boc-Lys was the major product, which was UV-negative but ninhydrin-positive, with the respective R_f values of 0.38 and 0.18 in BAW and BNH_4.

References

1. Markley, L.D. and Doman, L.C., *Tetrahedron Lett.*, 21 (1970) 1787.
2. Schlatter, J.M., Mazur, R.H. and Goodmonson, O., *Tetrahedron Lett.*, 33 (1977) 2851.
3. Anwer, M.K. and Spatola, A.F., *J. Org. Chem.*, 48 (1983) 3503.
4. Fieser, L.F. and Fieser, M., Reagents for Organic Synthesis, Wiley, New York, NY, USA, 1967, p. 404.

Peptides: Chemistry, Structure and Biology
Pravin T.P. Kaumaya and Robert S. Hodges (Eds.)
Mayflower Scientific Ltd., 1996

27
Total Synthesis of *S. solfataricus* RNase

Y. Okada[1], N. Shintomi[1], Y. Kondo[1], Y. Mu[1], Y. Nishiyama[1] and M. Irie[2]

[1]Faculty of Pharmaceutical Sciences, Kobe-Gakuin University, Nishi-ku, Kobe 651-21, Japan
[2]Hoshi College of Pharmacy, 2-4-41, Ebara, Shinagawa-ku, Tokyo 142, Japan

Introduction

Sulfolobus solfataricus RNase consists of 62 amino acid residues and, as shown in Figure 1, does not contain any His residues [1]. In order to study the mechanism of RNase activity of *S. solfataricus* RNase and to study its structure-activity relationships, our studies were directed to the synthesis of *S. solfataricus* RNase and related peptides by employing the newly developed protecting group, 2-adamantyloxycarbonyl (2-Adoc) in order to increase the solubility of protected peptide fragments.

The ε-Amino group of Lys and the hydroxy group of Tyr were protected by a 2-Adoc group to give Lys(2-Adoc) [2] and Tyr(O-2Adoc), respectively.

ATVKFKYKGEEKQV^{15}DISKIKKVWRVGKMI^{30}SFT
Y^{45}DEGGGKTGRGAVSEKDAPKELLQMLE^{60}KQK

Figure 1. *Primary structure of Sulfolobus solfataricus RNase.*

Results and Discussion

For the preparation of large peptides or proteins by the solution method or by the convergent solid phase method, it is very important to develop protecting groups to increase the solubility of peptide intermediates as well as for suppression of side reactions during peptide synthesis. In the present work, we used Asp(O-2-Ada) [3], Lys(2-Adoc) [2] and Tyr(*O*-2-Adoc) derivatives in combination with the N^{α}-Boc protecting group. These side chain protecting groups are stable to TFA and are easily cleaved by 1M TFMSA-thioanisole/TFA or by HF.

Ten peptide fragments were prepared (Figure 2) and, since each peptide fragment was highly soluble in DMF, fragment condensations were carried out in this solvent. Adamantyl derivatives were employed as protecting groups to improve the solubility of a given peptide. In order to dissolve H-(27-62)-OBzl and H-(10-62)-OBzl, a fairly large amount of DMF was required, resulting in slow reaction in fragment coupling.

For studies on structure-activity relationships, besides *S. solfataricus* RNase, the following related protected peptides were prepared: Boc-(57-62)-OBzl, Boc-(52-62)-

OBzl, Boc-(47-62)-OBzl, Boc-(44-62)-OBzl, Boc-(37-62)-OBzl, Boc-(33-62)-OBzl, Boc-(27-62)-Bzl, Boc-(17-62)-Bzl, and finally Boc-(1-62)-OBzl. These were treated with anhydrous HF in the presence of *m*-cresol, thioanisole, ethanedithiol, and dimethylsulfide to give the corresponding deblocked peptide, which was treated with Amberlite IRA-45 (acetate form), followed by the adjustment of pH of the solution to 8 with ammonia. The crude peptide was purified with Sephadex G-15 and G-25 or G-50 and then by HPLC. Each purified peptide exhibited a single peak on the analytical HPLC. Amino acid analysis of an acid hydrolysate of each peptide gave molar ratios in good agreement with the theoretically expected values. Amino acid ratios in an acid hydrolysate of the synthetic RNase was as follows: Asp(3) 3.12; Thr(3) 3.02; Ser(3) 2.46; Glu(9) 9.32; Gly(7) 6.89; Ala(3) 2.87; Val(5) 4.91; Met(2) 1.86; Ile(3) 3.15; Leu(3) 3.00; Tyr(2) 1.97; Phe(2) 2.03; Lys(13) 12.9; Arg(2) 2.04; Pro(1) 0.86 (average recovery 76.3%), Trp was not determined.

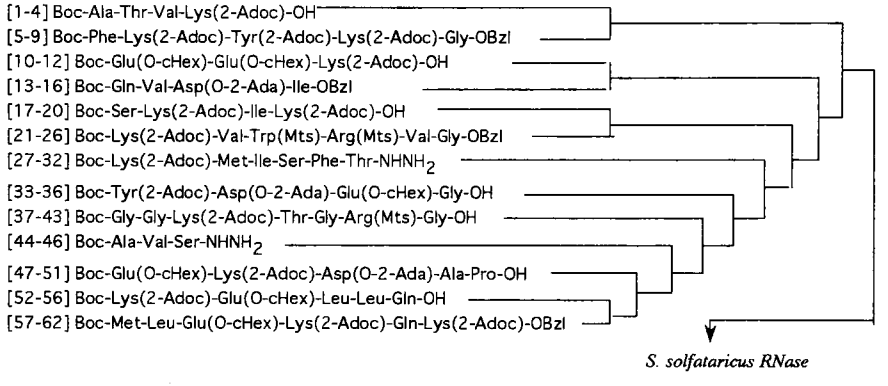

Figure 2. *Synthetic scheme for Sulfolobus solfataricus RNase.*

Acknowledgment

The authors are grateful to Watanabe Chemical Industries for a supply of 2-adamantyl chloroformate.

References

1. Fusi, P., Tedeschi, G., Aliverti, A., Ronchi, S., Tortora, P. and Guerritore, A., *Eur. J. Biochemistry,* 211 (1993) 305.
2 Nishiyama, Y., Shintomi, N., Kondo, Y. and Okada, Y., *J. Chem. Soc., Perkin Trans.,* 1 (1994) 3201.
3. Okada, Y. and Iguchi, S., *J. Chem. Soc., Perkin Trans.,* 1 (1988) 2129.

Peptides: Chemistry, Structure and Biology
Pravin T.P. Kaumaya and Robert S. Hodges (Eds.)
Mayflower Scientific Ltd., 1996

28
Synthetic Proteins and Reversible Chromatographic Probes: Applications

H.L. Ball, G. Bertolini and P. Mascagni

Italfarmaco Research Centre, Via Lavoratori 54, Cinisello B. 20092, Milan, Italy

Introduction

Classical stepwise solid phase peptide synthesis (SPPS) has been used successfully for the synthesis of proteins up to 150 residues in length, although usually with poor yields and homogeneity. The major difficulty relates to the inability of conventional chromatographic techniques to separate closely related impurities (*e.g.* deletion and truncated sequences). To facilitate the isolation of the 'target' peptide, we have developed a one-step purification scheme that is independent of peptide length, amino acid composition, or the strategy (Fmoc or Boc) of synthesis employed [1, 2]. Besides purification, immobilized biotinylated peptides can also be used to isolate ligands from crude cell lysates.

Results and Discussion

The general approach integrates (i) HBTU/HOBt as activating reagents, (ii) an effective capping procedure using N-(2-chlorobenzyloxycarbonyloxy) succinimide, and (iii) the introduction of a probe molecule with enhanced chromatographic properties (*e.g.* lipophilic or affinity group) to the N-terminal amino acid. After acidolytic cleavage and separation of the target sequence from contaminating impurities on appropriate media (*e.g.* RP or immobilised avidin column), the probe is removed with mild base to yield the purified free peptide. We demonstrate the potential of an optimized chemical protocol combined with the use of new simplified probes **1** and **2** for the one-step purification of the 101 residue chaperonin 10 protein from *R. norvegicus* (Rat cpn10).

Rat cpn10 was synthesised using HBTU/HOBt activation, capping and the Boc chemical strategy. Two aliquots of unprotected peptidyl-resin were derivatized with probes **1** and **2**, cleaved using HF, and gave the crude RP-HPLC chromatograms shown in Figure 1A and 1D, respectively. The addition of lipophilic probe **1** resulted in a difference in retention time of about 5 min between derivatized Rat cpn10 and underivatized impurities. One-step purification of the former by RP-HPLC, followed by base treatment gave a highly homogeneous protein (overall yield; 9.6%) as indicated by analytical RP-HPLC (Figure 1B) and capillary zone electrophoresis (CZE) (Figure 1C).

Similarly, affinity purification of crude biotinylated Rat cpn10 (Figure 1D) yielded a relatively pure product (overall yield; 9.4%) after base treatment, as determined by

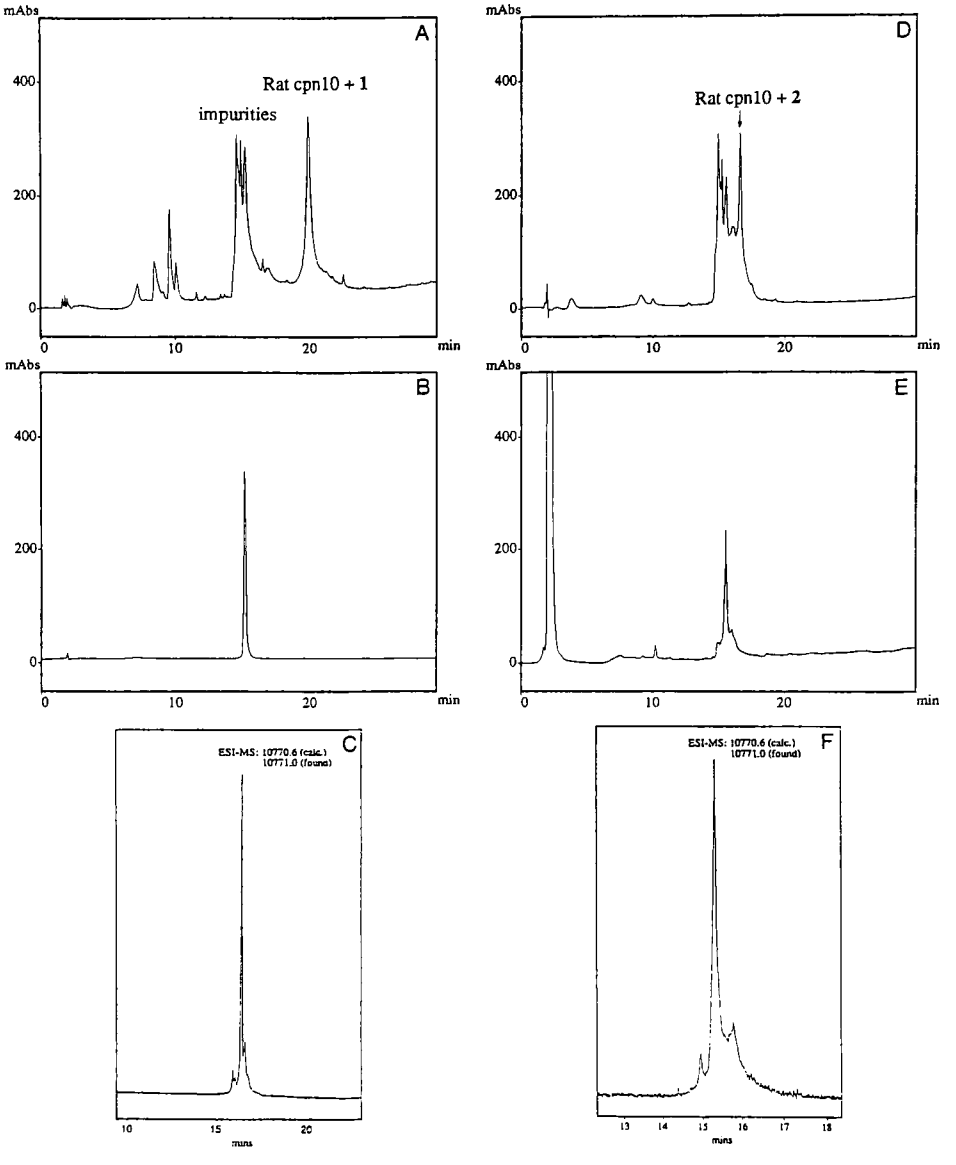

Figure 1. *RP-HPLC of Rat cpn10+1 (A) crude, (B) purified; Rat cpn10+2 (D) crude, (E) purified. CZE and ESI-MS analyses of Rat cpn10 on purification with (C) probe 1; (F) probe 2.*

analytical RP-HPLC (Figure 1E) and CZE (Figure 1F). ESI-MS analysis showed that the correct material had been obtained after purification using both techniques (Figure 1).

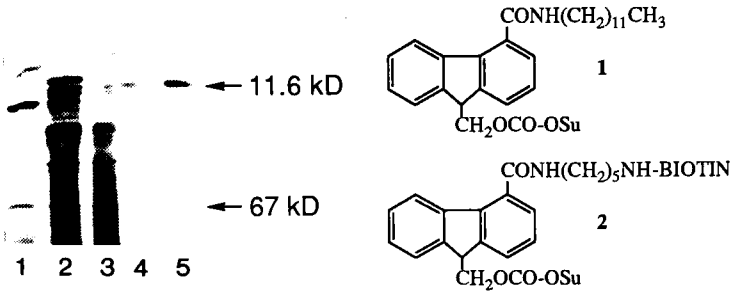

Figure 2. *SDS-PAGE. (1) Recombinant GroEL/GroES, (2) crude lysate, (3) lysate after ultrafiltration, (4) eluted protein, (5) Rat cpn10 + 2.*

To demonstrate the use of **2** for the isolation of ligands from a complex cell lysate mixture, 'trapping' of chaperonin 60 (GroEL) which binds to Rat cpn10 was attempted. Thus, another aliquot of crude biotinylated Rat cpn10 was immobilized on an avidin column and non-binding material eluted off with buffer containing ATP. *E. coli* cells were lysed by sonication, particulates removed by centrifugation, and endogenous ATP removed by ultrafiltration. The supernatant was loaded onto the avidin column and unbound material washed off with buffer. Biotinylated Rat cpn10 together with bound protein was eluted off the column with 0.1M Gly, pH 2.8 and collected.

SDS-PAGE showed that a protein with apparent Mwt of 67kD, corresponding to GroEL had been obtained (Lane 4, Figure 2).

References

1. Ball, H.L. and Mascagni, P., *Int. J. Peptide Protein Res.*, 40 (1992) 370.
2. Ball, H.L., Bertolini, G., Levi, S. and Mascagni, P., *J. Chromatogr. A,* 686 (1994) 73.

Peptides: Chemistry, Structure and Biology
Pravin T.P. Kaumaya and Robert S. Hodges (Eds.)
Mayflower Scientific Ltd., 1996

29

Chemical Synthesis and Heavy Metal-binding Studies of *Neurospora crassa* Metallothionein

Y. Nishiyama[1], Y. Matsuno[1], S. Oka[2], N. Masuyama[2], H. Sakurai[2] and Y. Okada[1]

[1]*Faculty of Pharmaceutical Sciences, Kobe-Gakuin University, Nishi-ku, Kobe 651-21, Japan*
[2]*Department of Analytical and Bioinorganic Chemistry, Kyoto Pharmaceutical University, Yamashina-ku, Kyoto 607, Japan*

Introduction

Metallothioneins (MTs) are a class of low molecular weight, cysteine-rich proteins bound with various heavy metals, including nutritionally essential (Zn and Cu) and toxic (Cd and Hg) metals [1]. It has been suggested that MTs might play important roles in metabolism and detoxification of heavy metals. However, their precise function remains to be solved.

To clarify the relationship between the structure and heavy metal-binding properties, our studies have been directed to the systematic synthesis of various MT-related peptides and examination of their heavy metal-binding properties [2]. We report herein, the chemical synthesis of *Neurospora crassa* MT (NcMT) by solution and solid phase methods and studies on heavy metal-binding properties.

Results and Discussion

NcMT and related peptides shown in Figure 1 were synthesized by the solution method and by Fmoc SPPS. Their heavy metal (Cd^{2+}, Cu^{2+} and Cu^{+}) - binding abilities were examined by measurement of the increase in the absorbance of Cd-mercaptide or Cu-mercaptide at 250 or 265 nm, respectively.

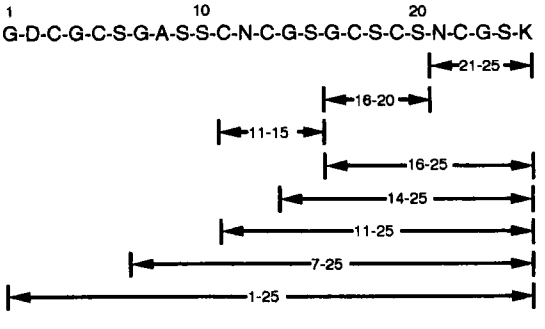

Figure 1. *Amino acid sequences of NcMT and related peptides.*

Cu^{2+}- and Cu^{+}-binding abilities of NcMT-related peptides were as high as those of NcMT, whereas Cd^{2+}-binding abilities of synthetic peptides were fairly structure dependent. These results show that the structure of NcMT is favorable for Cu-binding, and are compatible to our previous reports; MT β-domain and fungal MT-related peptides containing Cys-X-Cys (X = amino acid residue other than Cys) sequence was favorable for Cu-binding, and the MT α-domain-related peptides containing Cys-Cys sequence are favorable for Cd-binding [2].

ESR spectra for Cu-NcMT reconstituted in a vacuumed tube was completely silent as shown in Figure 2 (a). This result indicates that Cu in reconstituted Cu-NcMT is in a reduced Cu(I) state, in good agreement with the finding on naturally isolated NcMT [3]. After short exposure to air, no ESR signal was detected, although the free Cu^{+} ion is highly susceptible to air oxidation. This indicates that Cu^{+} in Cu-NcMT is stabilized to air oxidation in comparison with the free Cu^{+} ion. When H_2O_2 was added to the reconstituted Cu-NcMT solution, a strong ESR signal ($g_{//}$ = 2.415, $A_{//}$ = 12.76 mT) was detected as shown in Figure 2 (b). This result clearly shows that Cu^{+} in Cu-NcMT was oxidized to the Cu(II) state by H_2O_2. ESR parameters suggest that the Cu-binding atom in H_2O_2 oxidized Cu-NcMT is not sulfur.

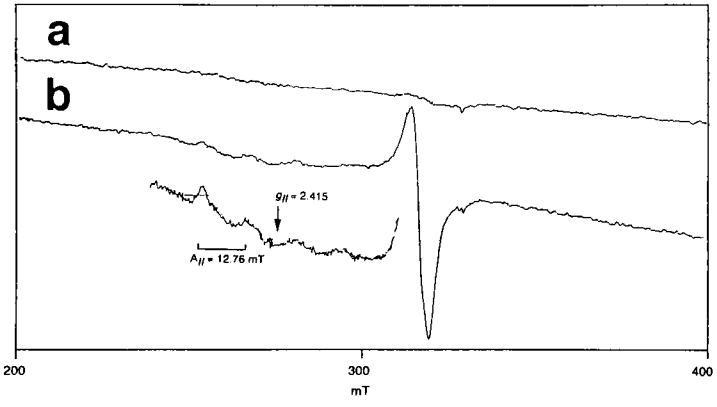

Figure 2. *ESR spectra of reconstituted CuNcMT in the absence (a) and the presence (b) of H_2O_2.*

Acknowledgment

Y. N. is supported by the Research Fellowships of the Japan Society for the Promotion of Science for Young Scientists.

References

1. Käge, J.H.R. and Schäffer, A., *Biochemistry,* 27 (1988) 8509.
2. Matsumoto, S., Nakayama, S., Nishiyama, Y., Okada, Y., Min, K.S., Onosaka, S. and Tanaka, K., *Chem. Pharm. Bull.,* 40 (1992) 2694; Matsumoto, S., Nishiyama, Y., Okada, Y., Min, K.S., Onosaka, S. and Tanaka, K., *Chem. Pharm. Bull.*, 40 (1992) 2701.
3. Lerch, K., *Nature,* 284 (1980) 368.

Peptides: Chemistry, Structure and Biology
Pravin T.P. Kaumaya and Robert S. Hodges (Eds.)
Mayflower Scientific Ltd., 1996

30
Studies with Racemization Resistant Derivatives of L-Cysteine Designed for Practical Use in Peptide Bond Formation

R.I. Carey, O. Bezençon and C.S. Burrell

Department of Chemistry and the Center for Metalloenzyme Studies, University of Georgia, Athens, GA 30602, USA

Introduction

Amide ligations at C-terminal cysteine-bearing peptide fragments are accompanied by anomalously high rates of racemization at the C-terminal cysteine [1-6]. The loading of cysteine derivatives to solid phase synthesis resins is similarly problematic. Stereoelectronic considerations predict that rates of racemization in a base-catalyzed proton abstraction mechanism would progress logically Ser > Cys > Phe > Ala, rather than the observed Cys >> Ser > Phe > Ala. Careful investigation of this subject was carried out by Kovacs and coworkers [2], who, in a series of papers, ruled out β-elimination [3] as the cause of the observed racemization and eventually identified isoracemization [4, 5] (base abstraction in a tight ion pair such that the rate of racemization is significantly less than deuterium incorporation in an exchange experiment) as the probable pathway for the epimerization. Jones [6] and Kemp [7] have reported that active esters of urethane protected thiazolidine carboxylic acids, **4** and **5** do not show the anomalously high rates of racemization that are characteristic of active esters of the structurally analogous Cbz-Cys(SBzl)-OH, **3**.

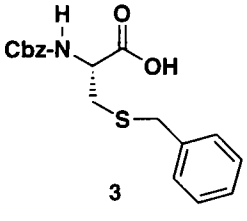

3

Cbz-Cys(Bzl)-OH

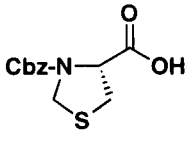

4

Cbz-Thz-OH

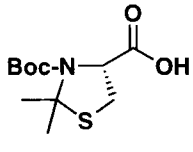

5

Boc-Dmt-OH

Results and Discussion

We report a practical procedure for the racemization-resistant coupling of C-terminal cysteine bearing peptide fragments through the use of the joint N,S-blocked cysteine derivative, 2,2-dimethylthiazolidine-4-carboxylic acid (Dmt). Although the secondary,

neopentyl amine of the Dmt residue is sterically hindered, dipeptides of the type Fmoc-Xxx-Dmt-OH and Boc-Xxx-Dmt-OH have been prepared in high yield through the coupling of H-Dmt-OH with Fmoc-amino acid chlorides or Boc-amino acid fluorides respectively (Xxx = Gly, Ala, Leu, Phe). The hydroxysuccinimide esters, Fmoc-Xxx-Dmt-OSu and Boc-Xxx-Dmt-OSu, have been prepared and found to resist racemization ($k_{rac} < 10^{-8}$ M^{-1} sec^{-1}) in THF in the presence of Et_3N. Under the same conditions, the structurally analogous Boc-Ala-Cys(Bzl)-OSu racemized readily (k_{rac} = 1.3 x 10^{-3} M^{-1} sec^{-1}). These rate constants are comparable to those fournd by Kovacs[2-5], Jones [6], and Kemp [7] in their studies. In the synthesis of the tripeptide Fmoc-Ala-Dmt-Gly-OEt from H-Gly-OH and Fmoc-Ala-Dmt-OH (with BOP, HOBt, and DIEA) less than 0.1% diastereomeric impurity was observed. Treatment of this tripeptide with with Hg^{++} followed by H_2S yields Fmoc-Ala-Cys-Gly-OEt in greater than 90% yield.

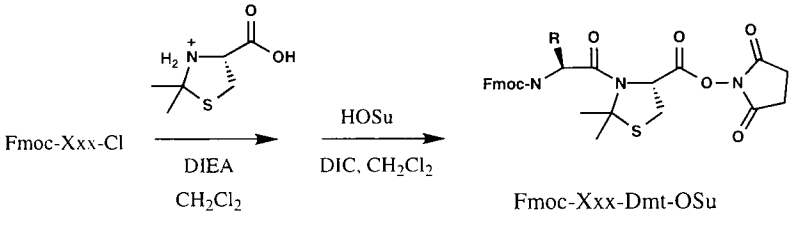

Acknowledgments

The authors gratefully acknowledge support from the University of Georgia Research Foundation.

References

1. Kemp, D.S., in Gross, E. and Meienhofer, J. (Eds.), 'The Peptides, Vol. 1', Academic Press, New York, 1979, p. 315; Kovacs, J., in Gross, E. and Meienhofer, J. (Eds.), 'The Peptides, Vol. 2', Academic Press, New York, 1979, p. 485.
2. Kovacs, J., Mayers, G.L., Johnson, R.H., Cover, R.E., Ghatak, U.R., *J. Org. Chem.*, 35 (1970) 1810.
3. Kovacs, J., Mayers, G.L., Johnson, R.H., Ghatak, U.R., *J. Chem. Soc. Chem. Comm.*, (1968) p. 1066.
4. Kovacs, J., Mayers, G.L., *J. Chem. Soc. Chem. Comm.*, 1970 p.1145; Kovacs, J., Cortegiano, H., Cover, R.E., Mayers, G.L., *J. Am. Chem. Soc.*, 93 (1971) 1541.
5. Kisfaludy, L., Roberts, J., Johnson, R., Mayers, G., Kovacs, J., *J. Org. Chem.*, 35 (1970) 3563.
6. Barber, M., Jones, J.H., in Loffet, A. (Ed.), 'Peptides 1976', Wepion, Belgium, Editions de l'Université de Bruxelles: Bruxelles, 1976. p.109-116.
9. Kemp, D.S., Carey, R.I., *J. Org. Chem.*, 54 (1989) 3640.

Peptides: Chemistry, Structure and Biology
Pravin T.P. Kaumaya and Robert S. Hodges (Eds.)
Mayflower Scientific Ltd., 1996

31
Synthesis of Cyclosporin Peptides by Combined use of Solid-Phase and Solution-Phase Methods

Y.M. Angell, T.L. Thomas and D.H. Rich

School of Pharmacy and Department of Chemistry, University of Wisconsin-Madison, 425 N. Charter Street, Madison, WI 53706, USA

Introduction

The synthesis of Cyclosporin A (CsA, Sandimmune®, **1**) (-MeBmt[1]-Abu[2]-Sar[3]-MeLeu[4]-Val[5]-MeLeu[6]-Ala[7]-(D)-Ala[8]-MeLeu[9]-MeLeu[10]-MeVal[11]-), where MeBmt = (4R)-4-[(2'E)-butenyl]-4,N-dimethyl-(L)-threonine, by solid phase methods is difficult due to the number of sterically hindered and N-methyl amino acids. Our studies of the coupling of N-methylated, sterically hindered amino acids during solid phase peptide synthesis on model tripeptides [1] showed that the novel coupling additives, 1-hydroxy-7-azabenzotriazole (HOAt) [2] and its uronium salt derivative (HATU), gave quantitative couplings in the model tripeptide sequences and facilitated synthesis of the CsA 2-7 sequence [1]. We report here the first solid phase synthesis of a linear undecapeptide precursor of a CsA analog and our attempts to use these methods for the synthesis of CsA itself.

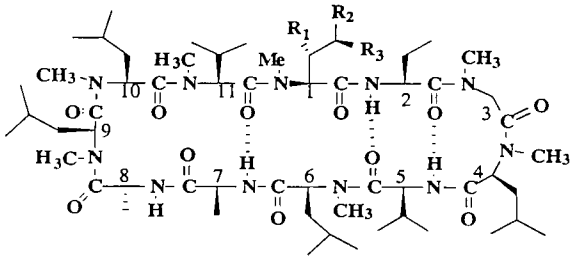

1 CsA: R_1= OH, R_2= $CH_2CH{=}CHCH_3$, R_3 = Me
2 [MeLeu(OH)[1]]-CsA: R_1= OH, R_3,R_2= Me
3 [MeThr[1]]-CsA: R_1= OH, R_2= Me, R_3 = H

Results and Discussion

[MeLeu[1]]CsA, in which MeLeu replaces MeBmt in the 1-position, is synthesized by converting the 2-7 sequence into the linear undecapeptide precursor by adding three sterically hindered, N-methyl amino acids (Fmoc-MeLeu at the 9- and 10-positions, and Fmoc-MeVal at the 11-position). Both HOAt and HATU were effective in coupling hindered amino acids to the hexapeptide. The yields obtained from these couplings are shown in Figure 1. HOAt/DIPCDI gave the highest yields when two 6-hour couplings were used.

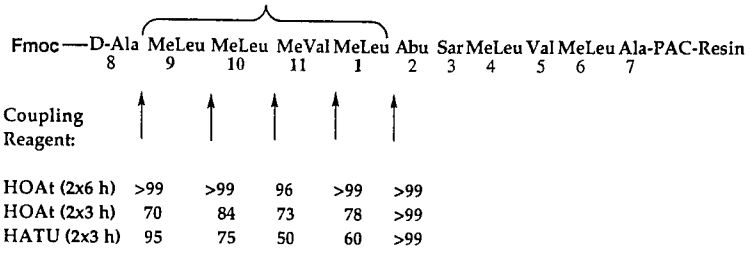

Figure 1. *Solid phase synthesis of [MeLeu^1] CsA.*

The linear undecapeptide was cleaved from the resin (TFA/H_2O (95:5); 3-4 hours) and cyclized in solution according to our usual strategy [3] [0.3 μM in CH_2Cl_2; $(PrPO_2)_3$ (propyl phosphonic anhydride) and DMAP. The cyclized peptide was obtained in 10-15% overall yield, purified by flash column chromatography and RP-HPLC, and characterized by NMR and FABMS (1146.57 calc., 1146.7 found). The NMR spectrum is closely related to that of CsA in chloroform. We also used these methods to synthesize the CsA 8-11 tetrapeptide sequence (H_2N-D-Ala-MeLeu-MeLeu-MeVal-OH).

We have successfully synthesized on solid support the linear undecapeptide precursors for CsA analogs that do not contain a β-hydroxy amino acid in the 1-position as well as heptapeptide fragments representing the CsA 1-7 sequence with β-hydroxy amino acids in the 1-position [β-hydroxy-MeLeu^1, and MeThr(O-Benzyl)^1]. However, the coupling of MeVal^{11} onto the 1-position of precursors to β-hydroxy analogs **2** and **3** is especially difficult when the 1-position contains a β-branched amino acid and low yields (5-40%) were obtained. This could be due either to steric effects or the low solubility of Fmoc-MeVal. Studies investigating different solvent systems are currently in progress, as is investigation of on-resin cyclization techniques yielding CsA analogs *via* side-chain attachment to the resin. Nevertheless, the ability to rapidly synthesize the 8-11 and 1-7 segments of CsA peptides by SPPS should facilitate more rapid synthesis of CsA analogs.

Acknowledgments

Financial support from the National Institutes of Health (AR-32007) and Affymax Research Institute is gratefully acknowledged. We thank Millipore for the generous gifts of HOAt, HATU, and PAC-PEG-PS resin.

References

1. Angell, Y.M., García-Echeverría, C., Rich, D.H., *Tetrahedron Lett.*, 35 (1994) 5981.
2. Carpino, L.A., *J. Am. Chem. Soc.*, 115 (1993) 4397.
3. Colucci, W.J., Tung, R.D., Petri, J.A., Rich, D.H., *J. Org. Chem.*, 55 (1990) 2895.

Peptides: Chemistry, Structure and Biology
Pravin T.P. Kaumaya and Robert S. Hodges (Eds.)
Mayflower Scientific Ltd., 1996

32
An Efficient Synthetic Approach to Aromatic Substituted Unusual Amino Acids

G. Li, W. Haq, T. Maruyama, L. Xiang, R. Hughes, S. Liao, F.-D.T. Lung, G. Han and V.J. Hruby

Department of Chemistry, University of Arizona, Tucson, AZ 85721, USA

Introduction

The aromatic moieties of peptide side-chain groups play important roles in the molecular recognition processes between peptide ligands and specific receptors as well as receptor subtypes. Aromatic ring substituted amino acids can provide valuable tools in developing highly selective peptide ligands with specific structural features [1]. Therefore, it is necessary to develop efficient methods for the enantioselective synthesis of these unusual amino acids. Recently, we have established a new method for the asymmetric synthesis of β-branched α-amino acids in which the Evans-type auxiliary was used as the chiral resolution reagent and resulted in complete stereoselectivity [2]. Here we report our successful synthesis of aromatic substituted unusual amino acids by using this newly developed method for the chiral separation of racemic N^{α}-Boc α-amino acids.

Results and Discussion

The racemic N^{α}-Boc *para*-biphenylalanine was obtained from Synthetec, Inc. The *ortho* and *meta* derivatives were synthesized from Suzuki-type cross coupling reaction [3]. The synthesis started from N^{α}-Boc tyrosine derivatives, which were transferred to tyrosine triflates with triflate anhydride in dichloromethene and pyridine. The resulting tyrosine triflates were then coupled with borophenylic acid to give racemic N^{α}-Boc α-amino acid methyl esters in high yields (Scheme 1).

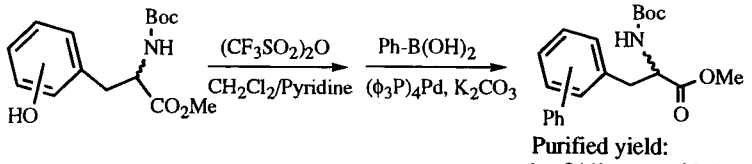

Scheme 1. *Suzuki-type cross coupling reaction.*

The methyl esters were hydrolyzed with potassium hydroxide and this followed by coupling the Evans-type auxiliary to form 4R or 4S 4-phenyl-oxazolidinone derivatives.

The resulting racemic mixture of two isomers were separated by fractional recrystallization or column chromatography to yield two individual isomers, which were then hydrolyzed by using lithium peroxide in THF at 0°C to obtain N^{α}-Boc amino acids (Scheme 2).

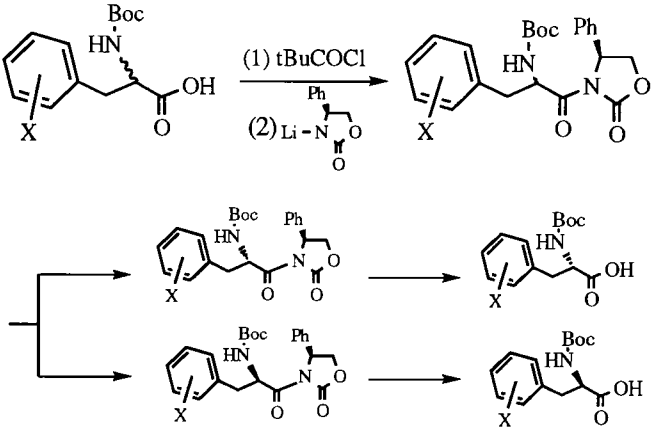

Scheme 2. *The chiral resolution for N^{α}-Boc amino acids. X = Phe, Br, OMe, CN.*

Both D- and L-isomers of *para*-, *ortho*-, and *meta*-biphenylalanines; *para*-bromo, *para*-cyano-, *ortho*-methoxy and *meta*-methoxy phenylalanines have been obtained. Some of these have been used in peptide studies in this laboratory [4]. The scope of this method has been extended for the synthesis of some highly constrained unusual amino acids and α-branched carboxylic acids [4a,5]. The chiral 4-phenyl-oxazolidinone has been used in HPLC and NMR isomeric resolution for α- and β-carboxylic acids and N^{α}-Boc amino acids. It has also been used as a chiral probe in mechanistic studies in which the sharp ^{1}H NMR signals from the oxazolidinone ring protons made identification very clear [6]. Finally, it might also be used as a probe to study biological processes when this motif is incorporated into biologically active molecules.

Acknowledgments

Supported by grants from USPHS, NIDA, University of Arizona Fellowship (G. Li) and DBT of India (W. Haq).

References

1. Hruby, V.J., In Hodges, R.S. and Smith, J.A. (Eds.) 'Peptides: Chemistry, Structure and Biology', ESCOM , Leiden, The Netherlands 1994, pp. 3-17.
2. Li, G., Patel , D., Hruby, V.J. *J. Chem. Soc. Perkin Tran.*, 1 (1994) 3057.
3. Miyaura, N., Yanagi, T., Suzuki, A., *Synth. Commun.*, 11 (1981) 513.
4. (a) Haq, W., Li, G., Hruby, V.J., unpublished results; (b) Li, G. Ph.D. Thesis, University of Arizona, 1995.
5. Xiang, L, Wu, H., Hruby, V.J. *Tetrahedron: Asymmetry*, 1 (1995) 83.
6. Lou, B.-S., Li, G., Lung, T., Hruby, V.J., *J. Org. Chem.*, 60 (1995), 5509.

Peptides: Chemistry, Structure and Biology
Pravin T.P. Kaumaya and Robert S. Hodges (Eds.)
Mayflower Scientific Ltd., 1996

33
CF_3-NO_2-PyBOP: A Powerful Coupling Reagent

J.C.H.M. Wijkmans, F.A.A. Blok, G.A. van der Marel, J.H. van Boom and W. Bloemhoff

Gorlaeus Laboratories, Leiden University, P.O. Box 9502, 2300 RA Leiden, The Netherlands

Introduction

N-methyl amino acids are important constituents of a number of naturally-occurring peptides which exhibit interesting biological functions. It has also been established that the metabolic stability of biologically active peptides can be enhanced by the introduction of N-methylated residues. Unfortunately, incorporation of hindered N-methyl amino acids into peptides under the agency of the standard condensing reagents DCC/HOBt and BOP is not completely satisfactory. Recently [1], it was shown that the efficacy of the latter condensation could be improved substantially by using the halogeno-phosphonium derivatives PyBroP (**1a**) and PyCloP- (**1b**) as the coupling reagents.

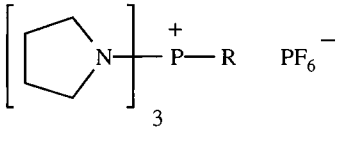

3 PF_6^-

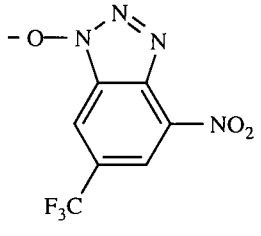

1a: PyBroP: R = Br
b: PyCloP: R = Cl
c: CF_3-NO_2-PyBOP: R = CF_3-NO_2-OBt

CF_3-NO_2-OBt

Here we report the use of the novel reagent CF_3-NO_2-PyBOP (**1c**) in the synthesis of N-methyl amino acid-containing dipeptides.

Results and Discussion

In order to explore the potential usefulness of reagent **1c**, the synthesis of the dipeptides **2a-h** was undertaken. The results of this study are summarized in the Table 1. In addition, yields of the CF_3-NO_2-PyBOP-mediated condensation were compared with those obtained using PyBroP.

It can be seen in Table 1 (entry *1*) that amide bond formation between two 'non-methylated' valines under the agency of PyBroP (**1a**) or CF_3-NO_2-PyBOP (**1c**) is, in both

Table 1. *Relevant data on the synthesis of dipeptides* ***2a-h*** *using PyBroP and CF_3-NO_2-PyBOP as the condensating reagents.*

Entry	Dipeptide		Yield (%)[a]	
			PyBroP	CF_3-NO_2-PyBOP
1	Z-Val-Val-OMe	**2a**	89	98
2	Z-Val-MeVal-OMe	**2b**	49	76
3	Z-Pro-MeVal-OMe	**2c**	43	92
4	Fmoc-Val-MeVal-OMe	**2d**	57	85
5	Boc-Val-MeVal-OMe	**2e**	25	62
6	Boc-MeLeu-MeLeu-OBzl	**2f**	47	87
7	Boc-MeLeu-MeVal-OMe	**2g**	40	76
8	Z-MeVal-MeVal-OMe	**2h**	22	71

[a] Couplings were performed using 1 equiv. N-protected amino acid, 1 equiv. amino acid benzyl or methyl ester hydrochloride, 1 equiv. activating reagent and 3 equiv. DIEA in CH_2Cl_2 (3mL); Yields were determined after 1hr. coupling at room temperature.

cases, a high-yield process. On the other hand, the yields of the CF_3-NO_2-PyBOP-assisted acylations of the more hindered H-MeVal-OMe with either Z-Val-OH (entry *2*) or Z-Pro-OH (entry *3*) were, in comparison with PyBroP, substantially higher. A higher coupling efficiency was also found in the CF_3-NO_2-PyBOP-mediated preparation of the Fmoc-protected dipeptide **2d** (entry *4*). Apart from this, an interesting phenomenon was observed in the condensation of Boc-Val-OH with N-methylated valine (entry *5*). Thus, the PyBroP-mediated peptide bond formation resulted in a low yield of Boc-Val-Val-OMe (**2e**). The poor yield of **2e** may be attributed to the conversion of activated Boc-valine into the corresponding N-carboxyanhydride (NCA) [1]. In contrast, the occurrence of the undesired NCA adduct could not be detected in the CF_3-NO_2-PyBOP-assisted synthesis of dipeptide **2e**. The latter was endorsed by the nearly quantitative formation (yield 92%) within 4 h of the desired Boc-protected dipeptide. The high potency of CF_3-NO_2-PyBOP is demonstrated further in the successful synthesis of di-N-methylated dipeptides **2f,g** (entries *6,7*). Furthermore, it is evident that the rather difficult coupling of two MeVal residues (entry *8*) under the agency of reagent **1c**, instead of **1a**, results in a threefold increase in yield of dipeptide **2h**.

In conclusion, the results presented in this paper clearly indicate that the crystalline reagent CF_3-NO_2-PyBOP shows great promise for the acylation of N-methyl amino acids.

Reference

1. Coste, J., Ferot, E., Jouin, P., *J. Org. Chem.*, 59 (1994) 2437.

Peptides: Chemistry, Structure and Biology
Pravin T.P. Kaumaya and Robert S. Hodges (Eds.)
Mayflower Scientific Ltd., 1996

34
UNCAs in Peptide and Amino Acid Chemistry

J-A. Fehrentz[1], C. Pothion[1], C. Devin[1], P. Chevallet[1], F.Winternitz[1], A. Loffet[2] and J. Martinez[1]

[1]Chimie et Pharmacologie de Molécules d'Intérêt Biologique, URA CNRS 1845, Faculté de Pharmacie, 15 av. C. Flahault, 34060 Montpellier, France
[2]Propeptide, 91710 Vert le Petit, France

Introduction

UNCAs are very reactive amino acid derivatives [1]. They have been used with success in SPPS and we have demonstrated their usefulness in solution peptide synthesis [2]. Furthermore, we have shown that UNCAs can be considered as starting material for the synthesis of various amino acid derivatives.

Results

The chemoselective reduction of UNCAs by sodium borohydride in the presence of water leads in quantitative yield to the corresponding β-amino alcohols [3]. No racemization occurs during the reduction, which is compatible with the common protecting groups. The reaction of UNCAs with Meldrum's acid in the presence of a tertiary amine, followed by the intramolecular cyclization, yields enantiomerically pure tetramic acid derivatives, which are precursors of γ-amino β-hydroxy-acids (statine derivatives); this reaction is very simple, fast and inexpensive [4]. It was performed successfully with various Z, Boc, or Fmoc UNCAs.

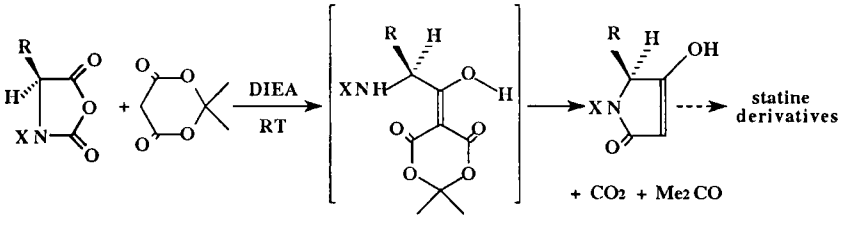

The reduction of UNCAs by the bulky hydrides lithium aluminium tris(tert-butyloxy)-hydride, or lithium aluminium tris[(3-ethyl-3-pentyl)oxy]-hydride yields the corresponding α-amino aldehydes [5].

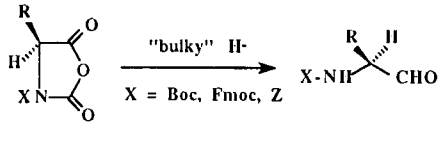

This simple reaction affords a one step procedure for the synthesis of enantiomerically pure α-amino aldehydes from commercial materials in good yields. It is compatible with various protecting groups. UNCAs react smoothly with phosphoranes to produce the corresponding keto phosphoranes in excellent yield [6]. These derivatives can lead to the vicinal tricarbonyl compounds by subsequent oxidation with ozone or with [bis(acetoxy)-iodo-]-benzene. These derivatives are potential inhibitors of serine proteases, or starting materials for the synthesis of various natural compounds.

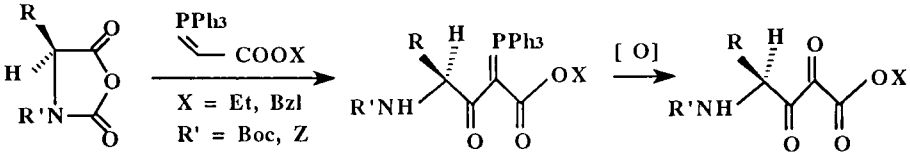

When placed in tert-butanol as solvent, UNCAs (Boc or Z protected) can smoothly lead to the corresponding tert-butyl esters in the presence of potassium bicarbonate and molecular sieves. The yields are about 70% [7]. Dissolved in an anhydrous solvent in the presence of DBU (1,8-Diaza- bicyclo[5.4.0]undec-7-ene), in equimolar or catalytic quantities, UNCAs react promptly giving pyrrolidine-2,4-diones [8]. Currently, we are investigating the absolute configuration of the asymetric carbons by high field NMR.

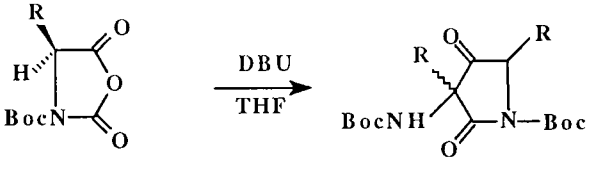

To conclude, UNCAs are useful, not only in peptide synthesis but also for preparing amino acid derivatives of importance in pseudo-peptide or peptoïd chemistry. All these reactions are characterized by their simplicity, efficiency and high yield.

References

1. Fuller, W.D., Cohen, M.P., Shabankareh, M. and Blair, R.K., *J. Am. Chem. Soc.*, 112 (1990) 7414; Xue, C. and Naider, F., *J. Org. Chem.*, 58 (1993) 350.
2. Rodriguez, M., Califano, J.C., Loffet, A., and Martinez, J., in Schneider, R. and Eberle, A. (Eds.), 'Peptides: Chemistry, Structure and Biology', ESCOM, Leiden, The Netherlands, 1993, p. 233.
3. Fehrentz, J.A., Califano, J.C., Amblard, M., Loffet, A., and Martinez, J., *Tetrahedron Letters* 35 (1994) 569.
4. Fehrentz, J.A., Bourdel, E., Califano, J.C., Chaloin, O., Devin, C., Garrouste, P., Lima-Leite, A.C., LLinares, M., Rieunier, F.,Vizavonna, J., Winternitz, F., Loffet, A. and Martinez, J., *Tetrahedron Letters*, 35 (1994) 1557.
5. Fehrentz, J.A., Pothion, C., Califano, J.C., Loffet, A. and Martinez, J., *Tetrahedron Letters*, 35 (1994) 9031.
6. Fehrentz, J.A., Genu-Dellac, C., Amblard, M., Winternitz, F., Loffet, A. and Martinez, J., J. *Peptide Science*, 1 (1995) 124.
7. Fehrentz, J.A., *Letters in Peptide Science*, in press.
8. Fehrentz, J.A., unpublished results.

Peptides: Chemistry, Structure and Biology
Pravin T.P. Kaumaya and Robert S. Hodges (Eds.)
Mayflower Scientific Ltd., 1996

35
Chromatographic Purification of Solid-Phase-Synthesized Peptides Using *n*-Alkyl Probes

C. García-Echeverría

Pharmaceuticals Division, Ciba-Geigy Ltd., CH-4002 Basel, Switzerland

Introduction

We have recently shown that purification difficulties caused by the presence of terminated peptides in crude mixture of solid phase synthesized peptides can be overcome by introducing an *n*-alkyl group into the resin-bound peptide at the last coupling step [1]. This communication reports on an evaluation of the validity of the method, based on the synthesis of a 49-mer peptide:

H-Ala^{58}-Ser-Arg-Ala-Gln-Ile-Leu-Asp-Lys-Ala-Thr-Glu-Tyr-Ile-Gln-Tyr-Met-Arg-Arg-Lys-Asn-Asp-Thr-His-Gln-Gln-Asp-Ile-Asp-Asp-Leu-Lys-Arg-Gln-Asn-Ala-Leu-Leu-Glu-Gln-Gln-Val-Arg-Ala-Leu-Glu-Lys-Ala-Arg^{106}-NH_2

(Max gene product 58-106 [2]; peptide **1**).

Results and Discussion

SPPS of peptide **1** was carried out on a Millipore 9050 Plus automated peptide synthesizer (continuous flow). The required Fmoc-amino acids (3 equiv.; single coupling) were incorporated using their 2,4,5-trichlorophenyl esters with minimum reaction times of 30 min. Double coupling with TPTU was performed for Ile^{85}. The coupling cycle included a capping step with acetic anhydride (5 min) to prevent the formation of deletion sequences. Side chains were protected with the following groups: *tert*-butyl for glutamic acid, aspartic acid, tyrosine, threonine, and serine; 2,2,5,7,8-pentamethyl-chroman-6-sulfonyl for arginine; *tert*-butyloxycarbonyl for lysine; trityl for asparagine, glutamine, and histidine. The hydrophobic probe (**2**; 5 equiv.) was coupled manually to the *N*-terminal residue of the protected peptide resin in the presence of an equimolar amount of HOBt in NMP. After incorporation of the *n*-alkyl probe, the peptide was liberated from the solid support and the side chains deblocked by treatment of the protected peptide resin with TFA/H_2O/EDT(76:4:20 v/v/v) for 3 hr at room temperature. The filtrate from the cleavage reaction was precipitated in diisopropyl

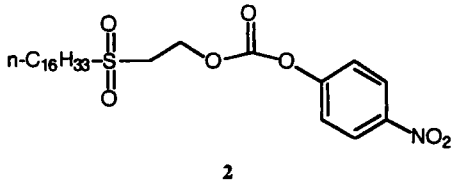

2

ether-petroleum ether (1:1; v/v) at 0°C, and the precipitate was collected by filtration. The crude mixture was treated with a 20% solution of ammonium iodide in water for 5 min at room temperature (reduction of the methionine sulfoxide) and, after precipitation in ether, the precipitate was dissolved in 1 N AcOH and heated at 60°C for 30 min (removal of the *tert*-butyl groups from the sulfonium salts). Figure 1 shows the analytical reversed-phase HPLC chromatograms of the underivatized and derivatized peptides. The lipophilic character of the *n*-alkyl probe substantially changes the chromatographic profile of the target peptide, allowing its separation from closely related terminated peptides by reversed-phase medium-pressure liquid chromatography (Figure 1). The identity of the *N*-terminal alkyl peptide was confirmed by mass spectral (MALDI-TOF) analyses. Complete and clean removal of the *n*-alkyl probe was accomplished by treatment of the derivatized peptide with a 5% solution of NH_4OH in water containing 2% EDT as scavenger. The reaction was followed by reversed-phase analytical HPLC. Complete conversion to the free peptide in its pure form was observed after 6 h at room temperature (Figure 1).

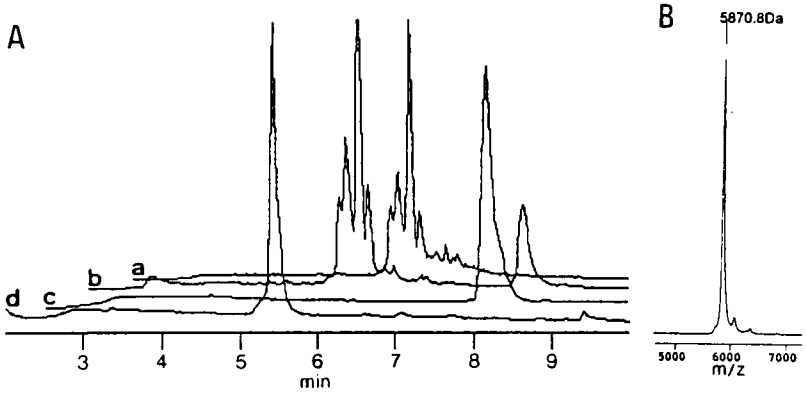

Figure 1. *(A) Analytical reversed-phase HPLC chromatograms of: (a) underivatized Max 58-106 peptide; (b) n-alkyl derivatized Max 58-106 peptide; (c) purified n-alkyl derivatized Max 58-106 peptide; (d) crude Max 58-106 peptide after removal of the n-alkyl group. Linear gradient over 10 min of MeCN-0.09% TFA and H_2O-0.1% TFA from 1:49 to 1:0, flow rate 2 ml min^{-1}, detection at 215 nm. (B) MALDI-TOF mass spectra (positive-ion mode) of the crude free Max 58-106 peptide: Calc. 5870.7 [M + H], found 5870.8. Calcitonin (3417.9) and Synacthen (2933.5) were used as internal standards.*

Acknowledgments

I thank R. Wille for his excellent technical assistance.

References

1. García-Echeverría, C., *J. Chem. Soc., Chem. Commun.*, (1995) 779.
2. Ferre-D'Amare, A.R., Prendergast, G.C., Ziff, E.B., Burley, S.K., *Nature*, 363 (1993) 38.

Peptides: Chemistry, Structure and Biology
Pravin T.P. Kaumaya and Robert S. Hodges (Eds.)
Mayflower Scientific Ltd., 1996

36
Synthesis of Biologically Active Molecules from Enantiopure Amino Acid and Peptide Glyoxals

P.A. Darkins[1], N. McCarthy[1], M.A. McKervey[1], H.M. Moncrieff[1], B. Walker[2] and T. Ye[1]

Schools of [1]Chemistry and [2]Biochemistry, The Queen's University, Belfast, N. Ireland, BT9 5AG, UK

Introduction

A new synthetic route to a wide variety of enantiopure inhibitors of the serine and cysteine classes of protease has been developed using amino acid and peptide α-keto aldehydes (glyoxals) as key intermediates.

Results and Discussion

Glyoxals represent a class of inhibitor in which the C-terminal acid functional group has been replaced by an electrophilic aldehyde moiety. By choosing appropriate amino acids to occupy the P_1 to P_n positions of the inhibitor so as to fulfill the primary and subsite specificity of the individual enzymes, it has been possible to obtain inhibitors which exhibit pronounced selectivity of action. Enantiopure glyoxals can be made from N-protected amino acids and peptides *via* acylation of diazomethane to form diazoketones followed by oxidation using dimethyldioxirane to yield the glyoxals quantitatively in predominately hydrated form (Figure 1) [1].

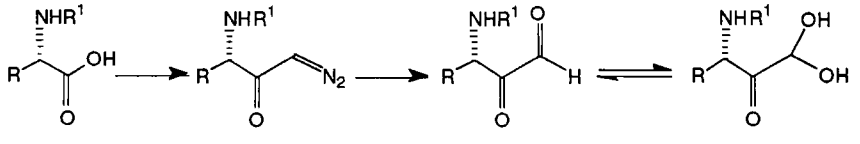

Figure 1. *Preparation of N-protected α-amino glyoxals. R^1 = protecting group.*

A range of dipeptide glyoxals were tested for inhibitory activity against the serine and cysteine proteases [2]. K_i constants in the range of 0.85 μM - 13.0 μM were found for dipeptide sequences targeting chymotrypsin and ~ 80 nM against cathepsin B showing a significant increase in potency for the cysteine class of protease.

Glyoxals are useful synthons, which can undergo Wittig olefination with stabilized yields to give α,β-unsaturated-γ-keto carbonyls (Table 1) in almost quantitative yield. To our knowledge there has been only one report of the inhibition of proteases by peptides bearing an α,β-unsaturated carbonyl group. Hanzlik *et al.* have prepared some

efficient inhibitors of bovine cathepsin B in which the glycine moiety of the dipeptide Z-Phe-Gly-OH has been replaced by -$NHCH_2CH{=}CHCO_2H$ [3]. The synthesis outlined here allows considerable synthetic flexibility without jeopardizing optical integrity. Compounds of this type are potential dipeptide isosteres, which inhibit the enzyme *via* a Michael addition with the active site cysteine residue of the protease. A series of compounds fulfilling the recognition sequences for cathepsin B and α-chymotrypsin were synthesised and tested (Table 1).

Table 1. *Evaluation of α,β-unsaturated-γ-keto carbonyls as inhibitors.*

α, β-unsaturated-γ-keto ester	Inhibition	Enzyme
N-Z-L-Phe-Ala-$CH{=}CHCO_2Me$	2×10^4 M^{-1} min^{-1} (irrev)	Cathepsin B
N-Z-L-Phe-Ala-$CH{=}CHCO_2Et$	0.4×10^4 M^{-1} min^{-1} (irrev)	Cathepsin B
N-Z-L-Phe-Ala-$CH{=}CHCO_2But$	10 M^{-1} min^{-1} (irrev)	Cathepsin B
N-Z-L-Phe-Ala-$CH{=}CHCOCH_3$	none	Cathepsin B
N-Z-L-Phe-Ala-CH=CHCHO	15 μM (slow-binding rev)	Cathepsin B
N-Z-L-Phe-$CH{=}CHCO_2Me$	none	α-Chymotrypsin

A number of points are noteworthy. Firstly, a chymotrypsin targeted sequence failed to inhibit at concentrations of up to and including 150 μM and using incubation periods of up to 30 minutes, indicating that these vinologous ester reagents appear to be selective for cysteine proteases. Secondly, an ester function is indispensable for irreversible inhibition and the nature of this ester grouping has a pronounced effect on inhibitory activity with the methyl ester giving the best inhibition. It should also be noted that an $N^{\alpha}Z$ N^{g}bis Adoc arginine derived α,β-unsaturated-γ-keto ester was found to be a time dependent inactivator of clostripain. We already have preliminary evidence to suggest that these reagents may form the basis of molecular discrimination for targeting individual members of the cysteine protease family [4].

In summary, the methodology described has led to a versatile synthesis of two new classes of enantiopure inhibitors of the serine and cysteine proteases.

Acknowledgments

We thank the Department of Education of Northern Ireland for a postgraduate award to P.D. and the Musgrave Committee for a scholarship to H.M.

References

1. Darkins, P., McCarthy, N., McKervey, M.A., Ye, T., *J. Chem. Soc., Chem. Comm.*, 15 (1993) 1222.
2. Walker, B., McCarthy, N., Healy, A., Ye, T., McKervey, M.A., *J. Biochem*, 293, (1993) 321.
3. Thompson, J.A., Andrews, P.R., Hanzlik, R.P., *J. Med. Chem.*, 29 (1986) 104.
4. McKervey, M.A., Moncrieff, H.M., Walker, B., unpublished data.

Peptides: Chemistry, Structure and Biology
Pravin T.P. Kaumaya and Robert S. Hodges (Eds.)
Mayflower Scientific Ltd., 1996

37

Cysteic- and Homocysteic Acid-S-(2-Aminoethylaminoiminomethyl) Amides and their Derivatives - New Sulfur Containing Unusual Amino Acids Useful in Peptide Synthesis

T.V. Buchinska[1] and S.B. Stoev[2]

[1]Bulgarian Academy of Sciences, Institute of Molecular Biology, Acad. G. Bonchev St., Bl.21, Sofia 1113, Bulgaria
[2]Medical College of Ohio, Department of Biochemistry, C. S. 10008 Toledo, OH 43699, USA

Introduction

The synthesis of new nonproteinogenic α-aminocarboxylic acids is one of the important trends in modern bioorganic chemistry. The newly synthesized aminocarboxylic acids and some of their derivatives could behave as antimetabolites of the natural amino acids in the biological systems. Recently, we synthesized and described the biological activity of some new derivatives of canavanine [2-amino-4-(guanidinoxy)butyric acid], [1, 2], and cysteic acid-s-(aminoiminomethyl)amide [3], which are structural analogues of arginine. Our interest in modified arginines stems from the recent discovery of nitric oxide synthase in vascular tissues, neuronal cells, and macrophages [4-7]. Since L-arginine is utilized as a substrate by all of the known nitric oxide synthase isoenzymes, we hoped to derive modified arginines, which would be selective inhibitors of the nitric oxide synthase isoenzymes.

This study presents the synthesis of two other structural analogues of arginine and its derivatives (Figure 1).

The protecting groups for amino, guanidino and carboxylic functions of substituted amides of cysteic and homocysteic acid were selected with the aim of making the amino acid derivatives synthons for peptide synthesis both in solution and by the solid phase method.

Results and Discussion

The starting compounds **1a,b** were obtained from L(D,L) N^{α}-Z, N^{ε}-Boc cysteic (homocysteic) acid S-(2-aminoethyl) amide benzyl ester [8] by treatment with TFA/DCM as usual. Two methods have been used successfully for the synthesis of **4a,b** (Figure1). Using a method similar to Bernatowicz *et. al.*[9], treatment of **1a,b** with N,N'-bis-Boc protected 1H-pyrazole-1-carboxamidine **(2)** in THF led to formation of **4a,b** (88% yield, mp 132-4°C; 62% yield, mp 141-3°C). A second method utilized the guanilation of **1a,b** in DMF according to a literature procedure [10]. Resolution of the racemates was

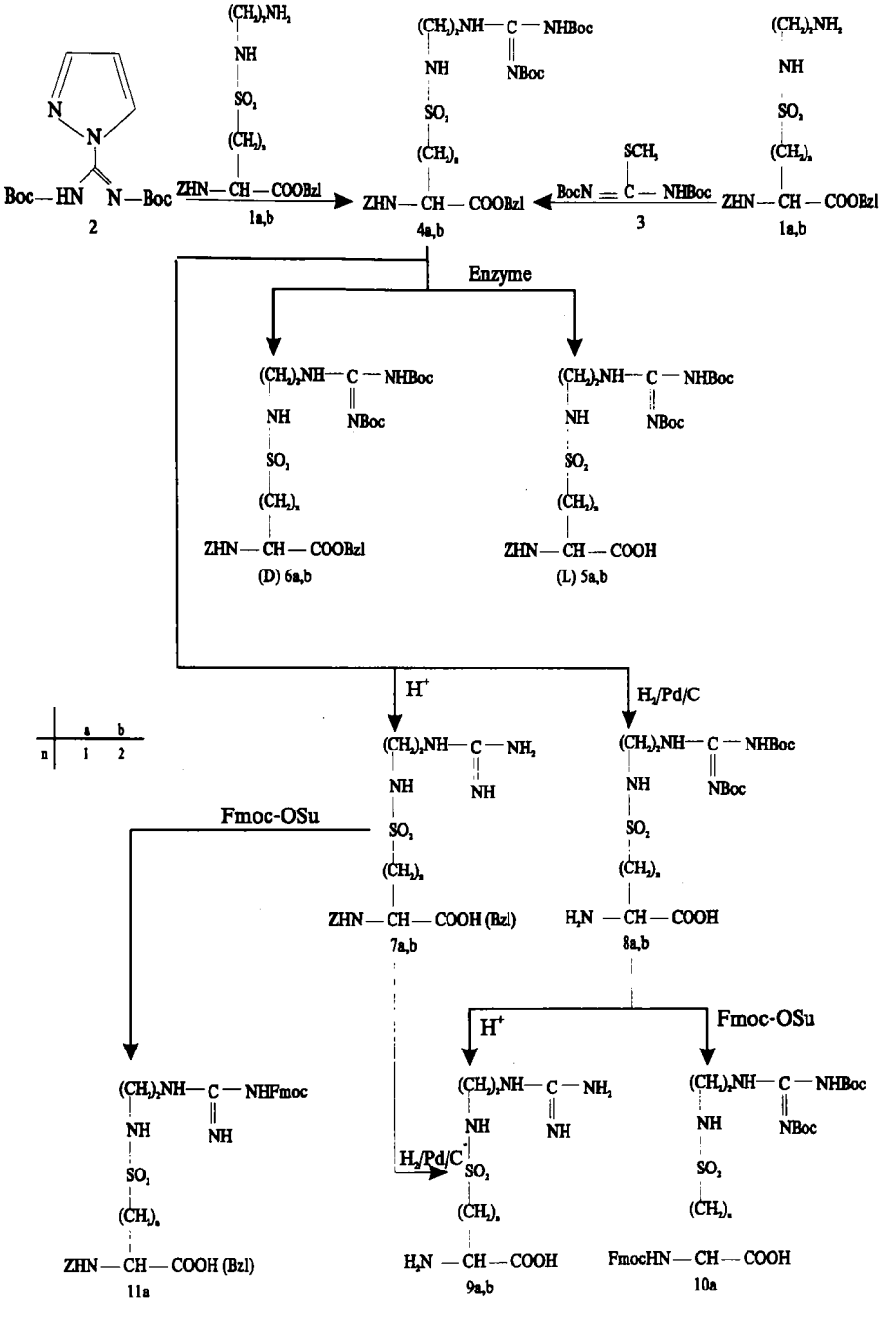

Figure 1. *Synthesis of cysteic- and homocysteic acid-S-(2-aminoethylaminoiminomethyl) amides and their derivatives.*

achieved by an enzymatic procedure [11], using alkaline protease from *Bacillus subtilis* DY strain, in 92% yield. Starting from fully protected **4a** after consecutive hydrogenolysis (H_2,10% Pd on carbon in MeOH or MeOH/DMF, 20-22h, RT) and treatment with Fmoc-OSu [12] we obtained **10a** in 65% yield. The free amino acids **9a,b** were synthesized from N^{α}-,N^{G}- and C-protected **4a,b** by selective deprotection of the Z-, Boc- and OBzl - protecting groups. In all cases, the deprotection of the Z-and OBzl-protecting groups was performed by catalytic hydrogenolysis, and that of the Boc-group by treatment with TFA/DCM (1:1 by volume) in the usual manner. The chemical and optical purities of the final synthetic products were assessed by TLC, optical rotation IR and MS data.

In summary, both cysteic- and homocysteic acid-S-(2-aminoethylaminoiminomethyl) amides have been synthesized by selective deprotection and introduction of various N^{α}-,N^{G}- and C-protecting groups. We have prepared a number of interesting modified arginine derivatives useful in peptide synthesis. The biological tests of deprotected cysteic and homocysteic acid-S-(2-aminoethylaminoiminomethyl) amide as a possible arginine antimetabolites are forthcoming.

References

1. Pajpanova, T., Grantcharov, K., Miersch, J., Tintemann, H, Krauss, G.-J., Stoev, S., Golovinsky, E., *Compt. rend. Acad. Bulg. Sci.*, 45 (1992) 49.
2. Pajpanova, T., Bocheva, A., Stoev, S., Kazakov, L., Golovinsky, *E., Compt. rend. Acad. Bulg. Sci.*, 45 (1992) 45.
3. Buchinska, T. and Stoev, S., Institute of Molecular Biology, Bulgarian Academy of Sciences, Sofia, Bulgaria, unpublished data.
4. Olken, N.M., Marletta, M.A., *J. Med. Chem*, 35 (1992) 1137.
5. Moncada, S., Palmer, R.M.J., Higgs, E.A., *Pharmacol. Rev.*, 43 (1991) 109.
6. Mellion, B.T., Ignarro, L.J., Ohlstein, E.H., Pontecorvo, E.G., Hyman, A.L., Kadowitz, P., *J. Blood,* 77 (1991) 946.
7. Stevens, C.F., *Current Biol.*, 2 (1992) 108.
8. Videnov, G., Aleksiev, B., Stoev, M., Pajpanova, T., Jung, G., *Liebigs Ann. Chem.*, (1993) 941.
9. Bernatowicz, M.S., Wu, Y., and Matsueda G.R., *Tetrahedron Lett.*, 34 (1993) 3389.
10. Verdini, A.S., Lucietto, P., Fossati, G., Giordani, C., in Smith, J.A. and Rivier, J.E. (Eds.), 'Peptides: Chemistry, Structure and Biology', ESCOM, Leiden, The Netherlands, 1992, p.562.
11. Aleksiev, B., Schamlian, P.,Videnov, G., Stoev, S., Zachariev, S., Golovinsky, E., *Hoppe-Seyler's Z. Physiol. Chem.*, 362 (1981) 1323.
12. Chang, C.D., Waki, M., Ahmad, M., Meienhofer, J., Lundell, E., Hang, J.-D., *Int. J. Pept. Protein Res.*, 15 (1980) 59.

Peptides: Chemistry, Structure and Biology
Pravin T.P. Kaumaya and Robert S. Hodges (Eds.)
Mayflower Scientific Ltd., 1996

38

Application of a Swelling-ESR Strategy to Estimate Resin Bead Interior Site-Site Distances: Correlation with the Rate of Coupling Reaction

E.M. Cilli[1], R. Marchetto[2], S. Schreier[3] and C.R. Nakaie[1]

[1]*Department of Biophysics, Universidade Federal de São Paulo, CP 20388, CEP 04044-020, São Paulo, S.P., Brazil*
[2]*Department of Biochemistry, Institute of Chemistry, Universidade Estadual de São Paulo, CP 355, CEP 14800-060, Araraquara, S.P., Brazil*
[3]*Department of Biochemistry, Institute of Chemistry, Universidade Federal de São Paulo, CP 20780, CEP 01498-970, São Paulo, S.P., Brazil*

Introduction

As an alternative to other swelling measurements used to date, we have developed a coupled swelling-ESR strategy. This allows the estimation of the chain-chain distances inside swollen resin beads. In a subsequent step, a possible correlation between this inter-site distance value and the yield of coupling reaction was examined in model peptide-resins.

Results and Discussion

Several differently substituted BHAR batches were spin labeled at their amino-function with our previously introduced paramagnetic amino acid derivative Boc-TOAC [1, 2] and their ESR spectra and swelling degree (microscopic measurements of bead sizes) in DCM and DMF were obtained. By correlating the degree of labeling and the final weight of each resin with the measured swelling values, such as the volume of dry and swollen beads, the volume of solvent absorbed by the bead, *etc.*, it was possible to calculate additional parameters, such as the number of beads/g of resin and the number of sites/bead. By assuming a uniformly distributed cubic lattice of sites within the bead, site-site distance values ranging from 15 Å to a maximum of 170 Å were obtained for these labeled resins in DCM and in DMF. The validity of the swelling approach allowed us to measure the inter-site distance, which was confirmed by the ESR spectral analyses of the TOAC-bound BHARs. The appearance of the well-known spin-spin exchange phenomenon, which induces a significant increase in the line broadening of the ESR spectral resonance peaks, was only detected in those resins with inter-site distance lower than 60 Å. This value is similar to that obtained with the same spin label free in homogeneous solution (DMF), and is in close accordance with the value measured in other heterogeneous systems [3].

An advantage compared to other common swelling parameters is that the inter-site distance value reflects not only the degree of swelling but also the number of sites

solvated per bead. This is, in turn, dependent on the initial substitution degree of each resin. In order to better assess the utility of this parameter and its relationship to the efficiency of the coupling reaction, the comparative yields of coupling obtained in different solvent systems with the aggregating ING (72-74)-ACP and VVLGAAIV sequences bound to low (0.22 mmol/g) and to high (2.62 mmol/g) substituted BHARs are shown in Table 1. The correlation between the site-site distance value and the yield of coupling, whatever the peptide-resin, showed that the larger the distance (and therefore the chain accessibility) the faster the coupling reaction. These preliminary findings demonstrated that the knowledge of unusual parameters such as the inter-site distance, may provide a more appropriate evaluation of the factors which govern the critical coupling step in the SPPS methodology.

Table 1. *Correlation between inter-site distance inside the bead and the yield of Boc-Tyr(2Br-Z) and Boc-Val couplings on ING and VVLGAAIV-resins, respectively.*

Solvent	Inter-site Distance (Å)	Yield of coupling (%)[a]
	ING-BHAR (0.22 mmol/g)	
DCM	37	86[b]
DMF	34	68[b]
DMSO	29	20[b]
	VVLGAAIV-BHAR (0.22 mmol/g)	
DCM	36	51[b]
DMF	35	45[b]
DMSO	31	05[b]
	VVLGAAIV-BHAR (2.62 mmol/g)	
DCM	18	06[c]
DMF	18	02[c]
DMSO	21	25[c]

[a]PSA generated in DCM (0°C, 60 min) and diluted in the appropriate solvent. [b]Yield of coupling after 15 min (at 25°C) in equimolar amounts and in 10^{-3} mol dm^{-3} acylating reagent over the amine component of resin. [c]Yield of coupling after 15 min (at 25°C) with 1.5 molar excess in 2.5 x 10^{-3} mol dm^{-3} acylating reagent over the amine component of resin.

References

1. Nakaie, C.R., Schreier, S. and Paiva, A.C.M., *Biochim. Biophys. Acta,* 742 (1983) 63.
2. Marchetto, R., Schreier, S. and Nakaie, C.R., *J. Am. Chem. Soc.*, 115 (1993) 11042.
3. Sackman, E and Trauble, H., *J. Am. Chem. Soc.*, 94 (1972) 4482.

Peptides: Chemistry, Structure and Biology
Pravin T.P. Kaumaya and Robert S. Hodges (Eds.)
Mayflower Scientific Ltd., 1996

39
4'-(Aminomethyl)-2,2'-bipyridine-4-carboxylic Acid (Abc): Synthesis and Metal Complexation

B.M. Bishop, G.T. Ray, B.H. Mullis, D.G. McCafferty, A. Lim and B.W. Erickson

Department of Chemistry, University of North Carolina at Chapel Hill, Chapel Hill, NC 27599, USA

Introduction

Several research groups have recently used unnatural amino acids to form metal ion-binding sites in synthetic peptides. For example, the metal-ion chelator 2,2'-bipyridine (b) has been incorporated into the side chain of α-amino acids by Imperiali *et al.* [1, 2]. This bidentate ligand has been incorporated into the main chain of a tripeptide analog by Kelly *et al.* [3]. In contrast to this work, we have synthesized the achiral amino acid 4'-(aminomethyl)-2,2'-bipyridine-4-carboxylic acid (Abc), in which the bipyridine ring system is inserted into the main chain of glycine.

Results and Discussion

Starting from 4'-methyl-2,2'-bipyridine-4-carboxylic acid (Mbc), the novel amino acid Abc was synthesized in three steps in 45% isolated yield (Figure 1). Mbc was prepared from 4,4'-dimethyl-2,2'-bipyridine by the method of McCafferty *et al.* [4]. The methyl

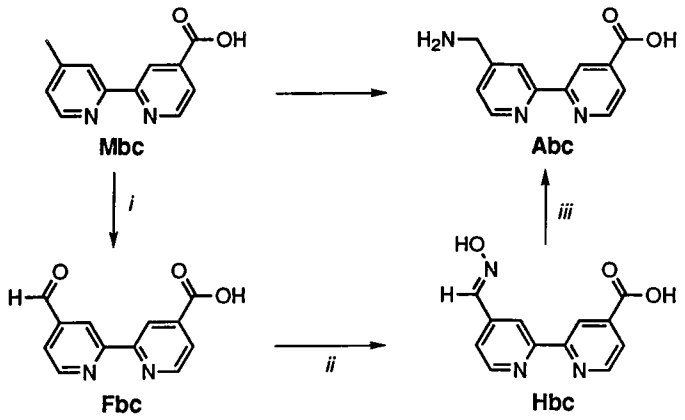

Figure 1. *(i) 5 equiv SeO_2, dioxane, heat, 4 d. (ii) NH_2OH HCl, 1:1 (v/v) pyridine/ethanol, heat, 2 h. (iii) H_2, 10% Pd/C, 0.1M HCl in 1:1 (v/v) ethanol/water, 18 h.*

group of Mbc was selectively oxidized to a formyl group by extended exposure to SeO_2. The formyl group was converted into a hydroximino group by treating Fbc with hydroxylamine.HCl. Finally, the hydroximino group was reduced by catalytic hydrogenation of Hbc in the presence of 10% palladium on carbon to afford Abc, which was purified by silica chromatography.

The *t*-butoxycarbonyl (Boc) derivative of Abc was formed by treating a solution of Abc in 1M NaOH with a dioxane solution of Boc anhydride. Similarly, the 9- fluorenylmethoxycarbonyl (Fmoc) derivative of Abc was produced by treating a partial solution of Abc in 10% Na_2CO_3 with a dioxane solution of Fmoc-OSu. Pure Fmoc-Abc precipitated from solution as it was formed. These N-protected amino acids are suitable for solid-phase synthesis. For example, Boc-Abc was used in a solid-phase synthesis of CH_3CO-Ala-Abc-Ahx-Ahx-Abc-Gly-NH_2, where Ahx is 6-aminohexanoic acid.

The ruthenium(II) complexes Boc-Abc$(Rub_2)^{2+}$ and Fmoc-Abc$(Rub_2)^{2+}$ (Figure 2) were synthesized by heating at reflux overnight a dioxane solution of *cis*-dichlorobis(2,2'-bipyridine)ruthenium(II) and Boc-Abc or Fmoc-Abc and were isolated as their PF_6^- salts. Use of these organometallic amino acids in solid-phase peptide synthesis would avoid the need to introduce the metal ion after assembly of the peptide chain has been completed.

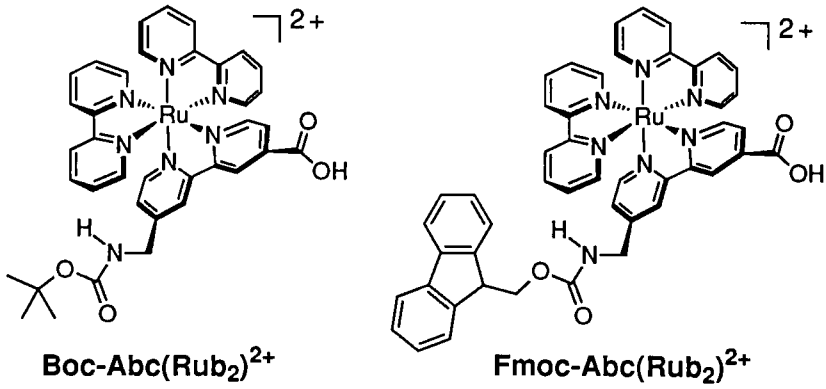

Figure 2. *Bis(2,2'-bipyridine)ruthenium(II) complexes of Boc-Abc and Fmoc-Abc.*

Acknowledgment

This work was supported by NIH research grants GM42031 and HL45100.

References

1. Imperiali, B., Prins, T.J. and Fisher, S.L., *J. Org. Chem.*, 58 (1993) 1613.
2. Wuttke, D.S., Gray, H.B., Fisher, S.L. and Imperiali, B., *J. Am. Chem. Soc.*, 115 (1993) 8455.
3. Schnieder, J.P. and Kelly, J.W., *J. Am. Chem. Soc.*, 117 (1995) 2533.
4. McCafferty, D.G., Bishop, B.M., Wall, C.G., Hughes, S.G., Mecklenberg, S.L., Meyer, T.J. and Erickson, B.W., *Tetrahedron*, 51 (1995) 1093.

Peptides: Chemistry, Structure and Biology
Pravin T.P. Kaumaya and Robert S. Hodges (Eds.)
Mayflower Scientific Ltd., 1996

40
Synthesis of Backbone-modified (N-Farnesyl) Amino Acids and their Incorporation into Peptides

G. Byk and D. Scherman

UMR-133 CNRS/Rhône-Poulenc Rorer, 13 Quai Jules Guesde, B.P. 14, 94403-Vitry Sur Seine, France

Introduction

In order to impart enhanced bioavailability to peptides, we considered the possibility of designing backbone modified peptides targeted by special "backbone side chains". These would be selected for particular cases and would depend on the target to be attained (Figure 1). In order to develop tools for the introduction of "backbone side chains", we propose the novel N-farnesyl amino acids as an initial rational approach for studying peptide bioavailability. Indeed, several cytoplasmic proteins undergo post-translational prenylation or adipoylation on specific cysteine side chains located close to the carboxy terminal. They are then able to penetrate to the cell membrane to bind with their membranal receptor, such as an interacting protein, leading to signal transduction. One of the most investigated prenyl moieties is the farnesyl group, which is involved in the signal transduction of important proteins such as lamin b [1], retinal [2], *ras* [3], and others [4]. Farnesylation of appropriate peptide leads will probably bring about cell membrane localization and/or activity of the peptide.

We report here the synthesis of novel backbone modified amino acids in which the hydrogen of the amino group in the natural amino acid was replaced by a farnesyl "backbone side chain" and was incorporated into a peptide model derived from the tetrapeptide carboxy terminal of *ras* [5].

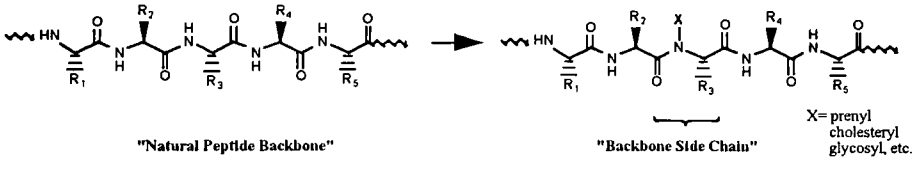

Figure 1. *Introduction of a "backbone side chain" into peptides.*

Results and Discussion

Alkylation of amino acids. We have synthesized (N-farnesyl)amino acids esters by direct alkylation of the corresponding natural amino acid esters with farnesyl bromide. The yield of the mono alkylated products were about 90 % when equivalent quantities of the alkylating agent were employed (Figure 2).

Peptide coupling to (N-farnesyl) amino acids. (N-Farnesyl)amino acids are sterically hindered on the secondary amino group. Coupling reagents such as HBTU, BOP, or PyBrop gave poor results even after 24 h reaction. The desired products were obtained in good yields by mixed anhydride activation with *i*-butyl chloroformate. When the acidic component was Boc-Cys(acm)-Val-Phe the coupling proceeded in similar manner and the final deprotection was carried out using standard conditions (Figure 2)

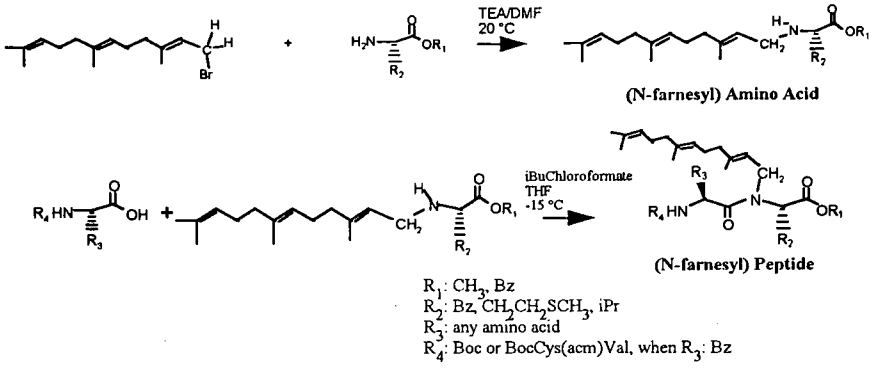

Figure 2. *Synthesis of (N-farnesyl) peptides.*

To conclude, we have described an easy preparation of (N-farnesyl)amino acids and their coupling to protected amino acids or peptides to give backbone farnesylated peptides. We present such amino acid modifications as an initial effort to build up novel tools for directing peptides to different biological/pharmacological targets or for subcellular localisation, such as in membrane vicinity. The so-called "backbone side chain" modification represents a new tool for the development of Structure Activity Bioavailability Relationships studies (SABR). Studies concerning biological and pharmacological behaviour of (N-farnesyl) amino acids and peptides are currently under way.

Acknowledgments

This work was done as part of the "Bioavenir" program supported by Rhône Poulenc, with the participation of the French Ministries of Research and Industry. We thank Martine Danzer, Frederic Herman and colleagues for structural analyses and to Elena Maximova for expert technical assistance.

References

1. Farnsworth, C., Wolda, S., Gelb, M. and Glomset, J.A., *J. Biol. Chem.*, 264 (1989) 20422.
2. Anant, J.S., Ong, O., Xie, H., Clarke, S. and O'Brien, P., *J. Biol. Chem.*, 267 (1992) 687.
3. Clarke, S., Vogel, J., Deschenes, R. and Stock, J., *Proc. Natl. Acad. Sci. USA*, 85 (1988) 4643.
4. Clarke, S., *Annu. Rev. Biochem.*, 61 (1992) 355.
5. Reiss, Y., Goldstein, J.L., Seabra, M.C., Casey, P.J. and Brown, M.S., *Cell*, 62 (1990) 81.

Peptides: Chemistry, Structure and Biology
Pravin T.P. Kaumaya and Robert S. Hodges (Eds.)
Mayflower Scientific Ltd., 1996

41
Preparation of Radiolabeled Peptides Using Iodine Exchange Reactions

M. Breslav[1], A. McKinney[2], J.M. Becker[2] and F. Naider[1]

[1]*Department of Chemistry, College of Staten Island, City University of New York, Staten Island, NY 10314, USA*
[2]*Department of Microbiology, University of Tennessee, Knoxville, TN 37996, USA*

Introduction

Peptides labeled with radioactive ^{125}I can be detected at the extremely low concentrations that are necessary for receptor binding studies and medical applications. Traditional methods of indirect iodination of peptides using Bolton-Hunter reagent or direct oxidative iodination [1] often lead to inactive peptides [2] due to excessive iodination, nonspecific iodination or oxidative damage to the peptide. These disadvantages may be circumvented by labeling ^{127}I containing peptides of a predetermined biological activity using a radioactive ^{125}I exchange reaction.

Results and Discussion.

We recently showed that the biological activity of the *Saccharomyces cerevisiae* α-factor was maintained when Trp^1 was replaced by a hydrophobic residue such as 3,5-diiodo-tyrosine [3]. For the present study, peptides containing ^{127}I were synthesized in solution and by SPPS. The mono and diiodo-Tyr moiety survived HF cleavage and both Boc and Fmoc synthetic protocols. The following peptides were prepared: Tyr(3,5-diiodo)-His-Trp-Leu-Gln-Leu-Arg-Pro-Gly-Gln-Pro-Nle-Tyr, Trp-His-Trp-Leu-Gln-Leu-Lys-Pro-Gly-Gln-Pro-Nle-Tyr(3,5-diiodo), Tyr(3-iodo)-His-Trp-Leu-Gln-Leu-Lys-Pro-Gly-Gln-Pro-Nle-Tyr, Tyr(3,5-diiodo)-Leu, Tyr(3,5-diiodo)-ethionine, Tyr(3-iodo)-Ala-Leu. Peptides were purified by HPLC and had the expected molecular weight as determined by MS.

Peptides for receptor studies were evaluated for their biological potencies and compared to a wild type α-mating factor of *Saccharomyces cerevisiae* [4]. The diiodo-Tyr^1 analog was as active as the α-factor, and the monoiodo-Tyr^1 analog had approximately half of this activity based on the halo assay procedure [5], whereas the diiodo-Tyr^{13} analog was found to be ten times less active.

Radioiodine exchange reaction and radioactive peptide recovery. Tyr(3,5-diiodo)-His-Trp-Leu-Gln-Leu-Arg-Pro-Gly-Gln-Pro-Nle-Tyr (10^{-4} mmol) was dissolved in 50 µl of 0.1M sodium-citrate buffer (pH=3) and 10 µl (350 µCi) of a $Na^{125}I$ solution was added with a syringe. The reaction mixture was held at 99°C in a sand bath for 30 minutes and transferred to a prewashed SepPack Light Cartridge C_{18}. The SepPack was

washed with 0.1% TFA (15 ml) to remove unincorporated iodine and 1 ml fractions were collected until the radioactivity was at background level. Methanol (1 ml) was passed through the cartridge to elute the radioactive peptide. The fractions were monitored for radioactivity, and analyzed by HPLC and TLC. The radioactivity that eluted in the methanol fraction coeluted with the cold diiodo-Tyr^1 analog (Figure 1).

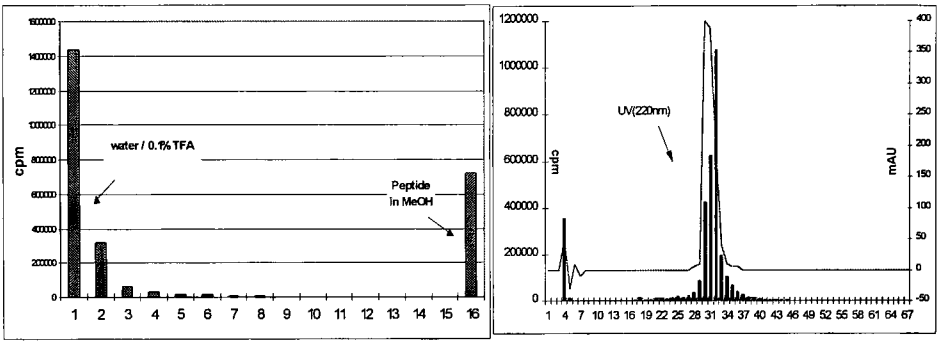

Figure 1. *Radioiodinated Tyr(3,5-diiodo)-His-Trp-Leu-Gln-Leu-Arg-Pro-Gly-Gln-Pro-Nle-Tyr. Left: Radioactivity in 1 ml elution fractions. Right: HPLC analysis of Fraction 16.*

A control with [Nle^{12}]α-factor did not result in meaningful incorporation of radioactivity. Specific activity reached was up to 10 Ci/mmol. Radioactive diiodo-Tyr^1 α-factor was subjected to halo assay evaluation. It showed full biological activity and there was correspondence between growth arrest zones and the incidence of radioactivity on the plate. Similar exchange was obtained with Tyr(3,5-diiodo)-Leu. In contrast, less exchange was obtained with the monoiodo-Tyr analogs.

The results provide evidence that peptides labeled to high specific activity may be obtained by a simple iodine exchange reaction.

Acknowledgments

This work was supported by NIH grants GM22086 & GM22087.

References

1. Bolton, A.E. and Hunter, W.M., *Biochem. J.*, 133 (1973) 529.
2. Schechter, Y., Burstein, Y. and Patchornik, A., *Biochemistry*, 14 (1975) 4497.
3. Jiang, Y., Breslav, M., Khare, R.K., McKinney, A., Becker, J.M. and Naider, F., *Int. J. Pept. Prot. Res.*, 45 (1995) 106.
4. Naider, F. and Becker, J.M., *Crit. Rev. Biochem.*, 21 (1986) 225.
5. Raths, S.K., Naider, F.R. and Becker, J.M., *J. Biol.Chem.*, 263 (1988) 17333.

Peptides: Chemistry, Structure and Biology
Pravin T.P. Kaumaya and Robert S. Hodges (Eds.)
Mayflower Scientific Ltd., 1996

42
One Step Enzymatic Synthesis of Side-chain Protected L-Cysteine Labeled with ^{15}N

B. Deprez[1], N. Palibroda[2], O. Melnyk[1], A. Bouhss[3], A. Tartar[1], K. Soda[4] and O. Barzu[3]

[1]*Bioorganic chemistry, URA CNRS 1309, Institut Pasteur de Lille, 59019 Lille, France*
[2]*Institute of Isotopic and Molecular Technology, 3400 Cluj-Napoca, Romania*
[3]*Biochimie des Régulations Cellulaires, Institut Pasteur, 75724 Paris, France*
[4]*Institute for Chemical Research, Kyoto University, Uji, Kyoto-fu 611, Japan*

Introduction

Chemical synthesis of small proteins offers the posibility of introducing isotopically labelled amino acids into specific positions of the primary sequence, providing unique opportunities to study their tertiary structure. In order to prepare ^{15}N-amino acids, we have used amino acid deshydrogenases NAD(P)-dependent enzymes present in various bacteria and particularly in bacillus species. These catalyze the reversible transformation of α-keto acids to α-amino acids. The equilibrium constant is shifted towards amino acid formation (K_{eq} between 10^{-13} and 10^{-15}). Some of these enzymes exhibit a relatively broad specificity: alanine-, leucine- and phenylalanine- deshydrogenases use alanine, branched-chain or aromatic amino acids as preferred substrates. This property was succesfully used for the synthesis of ^{15}N-amino acids with aliphatic or aromatic side-chains, by introducing the isotope *via* ^{15}N-ammonia and a NAD(P)H regenerating system. These amino acids were succesfully incorporated in several peptides which were used in isotope-edited NMR experiments [1].

Results and discussion

In order to specifically label cysteine residues involved in disulfide bridges, we were interested in the preparation of ^{15}N-cysteine. Using the previously described method proved to be unsuccessful. Moreover, to be used in peptide synthesis, ^{15}N-cysteine ought have required two successive protection steps, one for the thiol group and one for the amino group. In order to circumvent these difficulties and considering the afore-mentioned broad specificity of amino acid deshydrogenases, we have explored the possibility that S-protected derivatives of 3-mercaptopyruvic acid could be used as substrates by amino acid deshydrogenases, leading in one step to the S-protected L-amino acid. Our initial approach was to test the specificity of various enzymes using S-benzyl-L-cysteine **1** (Figure 1).

We discovered that phenylalanine-deshydrogenase isolated from the thermophilic microorganism *Thermoactinomyces intermedius* is able to catalyze the transformation of

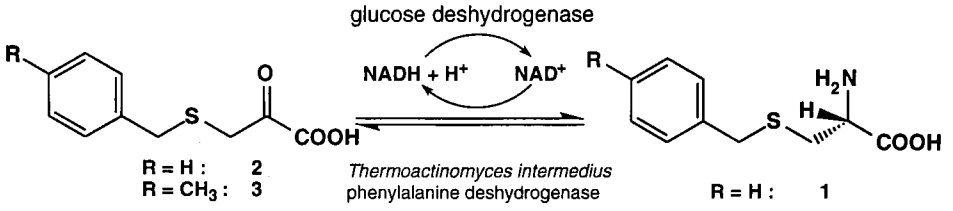

Figure 1. *Interconversion of S-protected 3-mercaptopyruvic acid and S-protected L-cysteine.*

1 with a reaction rate representing approximatively 1% of that with L-phenylalanine. This suggests that, although its aromatic ring is separatated from the α-amino group by an additional thiomethylene linker, **1** could still mimick the natural substrate. The same is true for the corresponding α-keto acid : 3-(benzylthio)pyruvic acid **2** and its homolog, 3-(4-methylbenzylthio)pyruvic acid **3**, which is also a substrate for the enzyme. None of these compounds acted as substrate for alanine-deshydrogenase from *Bacillus cereus* or leucine-deshydrogenase from *Bacillus steraothermophilus*. The kinetic parameters (V_m and K_m) of the purified enzyme are shown in Table 1.

Table 1. *Kinetic parameters of phenylalanine-deshydrogenase with 2 and 3*

α-keto acid	K_m (nM)	Relative V_m
phenylpyruvic acid	0.02	100
2	1.3	3.5
3	0.8	1.7

These parameters, together with the straightforward availability of α-keto-acids **2** and **3** were compatible with the gram-scale syntheses of side-chain protected ^{15}N-amino acids, which are required for their use in peptide synthesis, in a single enzymatic step. In a typical experiment, conditions were as follows: the reaction medium (250 ml) contained 25 mmol of 3-(benzylthio)pyruvic acid **2**, 30 mmol of $^{15}NH_4Cl$ (99% isotopic enrichment), 0.125 mmol of NAD^+, 0.25 mole of glucose, 75 U of phenylalanine-deshydrogenase (corresponding to 50 mg of protein), 250 U of glucose dehydrogenase (GluDH), and the pH was adjusted to 8 by addition of dilute NaOH. The progress of the reaction was monitored by following the disappearence of ammonium ions. After 3 h of incubation at 30°C, *ca.* 25% of **2** was converted to **1**. The reaction was left to proceed for an additional 12 h, then the amino acid, which spontaneously precipitates at pH 8, was collected by filtration. The insoluble material, washed with ethanol and dried afforded **1** in 50% yield. The purity and the ^{15}N content of **1** (between 98 and 99% ^{15}N) was determined by mass spectrometric analysis. **1** was then converted to the N^{α}-Boc protected derivative by reaction with di *t*-butyl dicarbonate.

Reference

1. Munier, H., Blanco, F.J., Precheur, B., Diesis, E., Nieto, J.L., Craescu, C.T., Barzu, O. *J. Biol. Chem.*, 268 (1993) 1695.

Peptides: Chemistry, Structure and Biology
Pravin T.P. Kaumaya and Robert S. Hodges (Eds.)
Mayflower Scientific Ltd., 1996

43

Novel *N*- and *S*-Xanthenyl Protecting Groups for Side-chains of Asparagine, Glutamine and Cysteine and their Applications for Fmoc Solid Phase Peptide Synthesis

N.A. Solé[1,2], Y. Han[1], J. Vágner[1], C.M. Gross[1], J. Tejbrant[1] and G. Barany[1]

[1]*Department of Chemistry, University of Minnesota, Minneapolis, MN 55455, USA*
[2]*PerSeptive Biosystems, Inc., 500 Old Connecticut Path, Framingham, MA 01701, USA*

Introduction

Optimal management of asparagine, glutamine, and cysteine residues remain current concerns of solid phase peptide synthesis by the strategy using the 9-fluorenylmethyloxycarbonyl (Fmoc) group for N^{α}-amino protection. In the cases of asparagine and glutamine, these residues can be incorporated leaving the ω-carboxamides free, but, more recently, applications of acid-labile Fmoc-compatible side-chain protecting groups such as 2,4,6-trimethoxybenzyl (Tmob) or triphenylmethyl (trityl, Trt) have become preferred due to minimization of secondary structure in the growing peptide-resin (hence improving coupling efficiencies) and to lessening the occurrence of a variety of side reactions. Related to this, *S*-Tmob, *S*-Trt, or *S*-Mmt groups have been used to block the β-thiol of cysteine in Fmoc solid-phase synthesis. Selective acidolysis gives the free thiols, whereas oxidative removal conditions provide directly a disulfide bridge. Our present studies exploring *N*- and *S*-xanthenyl (Xan) and corresponding monomethoxy derivatives (2-Moxan, 3-Moxan) for side-chain protection of these residues (Figure 1) were motivated by favorable previous as well as ongoing experiences from our laboratories on xanthenylamide (XAL) anchoring for carboxamides and thiols. The *N*-xanthenyl (Xan) protecting group has been described sporadically in the Boc chemistry literature [1], whereas *S*-9-phenylxanthenyl (Pix) was reported recently [2].

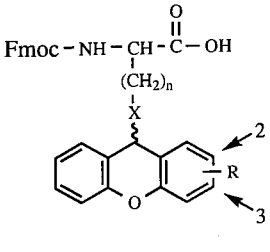

n = 1, X = S,	R=H	Fmoc-Cys(Xan)-OH
n = 1, X = S,	R=OMe at 2	Fmoc-Cys(2-Moxan)-OH
n = 1, X = S,	R=OMe at 3	Fmoc-Cys(3-Moxan)-OH
n = 1, X = (CO)NH,	R=H	Fmoc-Asn(Xan)-OH
n = 1, X = (CO)NH,	R=OMe at 2	Fmoc-Asn(2-Moxan)-OH
n = 1, X = (CO)NH,	R=OMe at 3	Fmoc-Asn(3-Moxan)-OH
n = 2, X = (CO)NH,	R=H	Fmoc-Gln(Xan)-OH
n = 2, X = (CO)NH,	R=OMe at 2	Fmoc-Gln(2-Moxan)-OH
n = 2, X = (CO)NH,	R=OMe at 3	Fmoc-Gln(3-Moxan)-OH

Figure 1. *Structures of protected derivatives of Asn, Gln, and Cys.*

Results and Discussion

Xanthenyl side-chain protection was introduced readily onto the corresponding N^{α}-Fmoc derivatives by acid-catalyzed reactions with the corresponding xanthydrols. Yields and purities were high for the parent Xan and the 2-Moxan derivatives, but problems were encountered with 3-Moxan. The *S*-Xan and *S*-(2-Moxan) groups were removed readily with dilute TFA. In the presence of silanes, 0.1% TFA is sufficient, *e.g.*, TFA/Et_3SiH/CH_2Cl_2 (0.1/0.5/99.4) at 25°C for 1 hr. whereas with thiol scavengers at least 10% TFA is needed, *e.g.*,TFA/β-mercaptoethanol/CH_2C1_2 (2/1/17) at 25°C for 1 hr. N^{ω}-Xan and N^{ω}-(2-Moxan) were removed as well with TFA/scavengers cocktails. Xanthenyl derivatives of Cys can be dissolved readily in CH_2C1_2 and DMF, whereas the various xanthenyl-protected Asn and Gln derivatives have poor solubilities in CH_2Cl_2 (similar to side-chain unprotected Fmoc-Asn-OH and Fmoc-Gln-OH). Solubilities acceptable for peptide synthesis applications (see below) were achieved in DMF, DMA, or NMP.

To better evaluate the usefulness of these derivatives for Fmoc solid phase peptide synthesis, Asn, Gln, and/or Cys-containing peptides were prepared on PAL-PEG-PS supports using the DIC/HOBt, TBTU/HOBt/DIEA or HATU/DIEA coupling protocols. These peptides included Marshall's ACP (65-74) amide [3], Briand's peptide H-Asn-Leu-Ile-Val-Glu-Leu-Lys-Arg-Gly-Thr-NH_2 (problem with *N*-terminal deprotection) [4], a modified Riniker's peptide H-Lys-Gln-His-Asn-Pro-Tyr-Gln-Trp-Asn-Gly-NH_2 [5] and a pentagastrin analogue H-Trp-Met-Asp-Phe-Cys-NH_2 [6] (Trp alkylation side reactions), oxytocin, and several long peptides related to bovine pancreatic trypsin inhibitor (BPTI). Protecting groups were removed concomitant to acidolytic cleavages of the fully assembled protected peptide-resins using Reagent K, TFA/phenol/H_2O/ thioanisole/1,2-ethanedithiol (82.5/5/5/5/2.5), or Reagent R, TFA/thioanisole/1,2-ethanedithiol/anisole (90/5/3/2)] at 25°C in 1 hr. Xan or 2-Moxan protection results were as good, and sometimes better, than those with Tmob or Trt protection. For disulfide-containing peptides, on-resin deprotection/oxidation mediated by I_2 (10 equiv.) in acetic acid or $Tl(tfa)_3$ (1.2 equiv.) in DMF was possible, with results comparable to those reported earlier [6].

Acknowledgment

We are grateful to NIH (GM 42722 and GM 43552) for support of this work.

References

1. Dorman, L.C., Nelson, D.A., and Chow, R.C.L. in 'Progress in Peptide Research, Vol. 2', Gordon and Breach, New York, 1972, p. 65.
2. Echner, H. and Voelter, W. in Epton, R. (Ed.) 'Innovation and Perspectives in Solid Phase Synthesis', Intercept Ltd, Andover, England, 1992, p. 371.
3. Hancock, W.S., Prescott, D.J., Vagelos, P.R. and Marshall, G., *J. Org. Chem.*, 38 (1973) 774.
4. Friede, M., Denery, J., Neimark, J., Kieffer, S., Gausepohl, H. and Briand, J.P., *Peptide Reseach*, 5 (1992) 145.
5. Sieber, P. and Riniker, B., *Tetrahedron Lett.*, 32 (1991) 739.
6. Munson, M.C., García-Echeverría, C., Albericio, F. and Barany, G., *J. Org. Chem.*, 57 (1992) 3013, and references cited therein.

Peptides: Chemistry, Structure and Biology
Pravin T.P. Kaumaya and Robert S. Hodges (Eds.)
Mayflower Scientific Ltd., 1996

44

Recent Developments in Azabenzotriazole-based Coupling Reagents for Use in Solid Phase Peptide Synthesis: PyAOP and HAPyU

S.A. Kates[1], S.A. Triolo[1], E. Diekmann[1], L.A. Carpino[2], A. El-Faham[2], D. Ionescu,[2] and F. Albericio[1]

[1]PerSeptive Biosystems Biosearch Products, 500 Old Connecticut Path, Framingham, MA 01701, USA
[2]Department of Chemistry, University of Massachusetts, Amherst, MA 01003, USA
[3]Department of Organic Chemistry, University of Barcelona, 08028 Barcelona, Spain.

Introduction

Peptide coupling reagents based on 1-hydroxy-7-azabenzotriazole (HOAt) have shown advantages over the corresponding HOBt-based reagents with regard to coupling efficiency and suppression of racemization [1-7]. In this communication, we focus on the practical aspects concerning the use of 7-azabenzotriazol-1-yloxytris(pyrrolidino)-phosphonium hexafluorophosphate (PyAOP) and *O*-(7-azabenzotriazol-1-yl)-1,1,3,3,-bis(tetramethylene)uronium hexafluorophosphate (HAPyU) for solid-phase peptide synthesis.

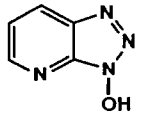
HOAt

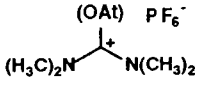
HATU

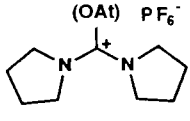
HAPyU

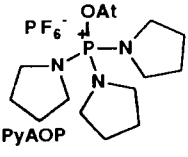
PyAOP

Results and Discussion

In order to determine the compatibility of these reagents with automated peptide synthesizers, the stability of PyAOP and HAPyU in solution and in the solid state was examined *via* HPLC and ^{1}NMR analysis. Both materials are inert as solids and the uronium reagent, when stored in solution (0.5 M in DMF), is stable for 5 days. On the other hand, the phosphonium reagent is not as stable, confirming earlier studies demonstrating its greater reactivity. PyAOP is useful for incorporation of the first Fmoc-amino acid onto a hydroxyl resin. Yields are high and racemization is low especially for His(Trt) and Cys(Trt). The enhanced reactivity of the phosphonium derivative is beneficial for the preparation of cyclic peptides *via* resin-bound reactions.

Fmoc-amino acids are converted to the active esters within 2 min and prolonged preactivation times (>7 min) should be avoided. In order to demonstrate the suitability

of 7-azabenzotriazole-based coupling reagents, several syntheses of the fragment (65-74) (H-VQAAIDYING-NH_2) of the acyl carrier protein were carried out *via* Fmoc/*t*Bu protection (*t*Bu for Tyr and Asp, and Trt for Asn and Gln). The Fmoc-PAL-PEG-PS resin was used along with shortened coupling times and reduced excesses of reagents (Table 1). The addition of HOAt to PyAOP/HAPyU-based couplings is not required except for Fmoc-Asn(Trt)-OH. Although the addition of HOBt to PyAOP-based couplings increases the incorporation of Fmoc-Asn(Trt)-OH, it lowers the coupling efficiency of other amino acids. Side-chain protection of asparagine is required since no incorporation of Fmoc-Asn-OH was detected in 7-azabenzotriazole-based couplings, presumably due to rapid aspartimide formation from Fmoc-Asn-OAt. Hydrated amino acids couple more efficiently with HOAt-based reagents. Finally, it is known that Boc-His(Tos)-OH is unstable upon treatment with HOBt. Similar results were obtained for this amino acid with HAPyU and PyAOP.

For the PerSeptive Biosearch 9050Plus peptide synthesizer, a solution of 0.5 M PyAOP/HAPyU in DMF is recommended. Phosphonium reagents are more sensitive to the base concentration and a 1.0 M solution of DIEA in DMF is preferred. For HAPyU-mediated couplings, 0.5 - 1.0 M solution can be used.

In addition, 7-azabenzotriazole-based coupling reagents are useful also for the preparation of a range of peptides that include those incorporating hindered amino acids, multiple Arg and Trp residues, and short difficult sequences.

Table 1. *Synthesis of ACP(65-74) with 1.5 equiv. of coupling reagent for 1.5 min.*

Coupling Method	ACP	-2Ile	-Ile^{72}	-Ile^{69}	-Val	-Asn
PyBOP	10	22	13	13	3	<1%
PyBOP-HOAt	19	13	12	12	3	2%
PyBOP-HOBt	11	21	14	14	3	<1%
PyAOP	46	3	5	5	2	18
PyAOP-HOAt	60	3	6	7	4	2
PyAOP-HOBt	45	9	12	12	2	2
HAPyU	44	2	5	3	1	33
HAPyU-HOAt	74	0	2	3	2	5
HAPyU-HOBt	52	4	8	8	10	1

References

1. Carpino, L.A., *J. Am. Chem. Soc.*, 115 (1993) 4937.
2. Carpino, L.A., El-Faham, A., Minor, C. and Albericio, F., *J. Chem. Soc., Chem. Commun.*, (1994) 201.
3. Abdelmoty, I., Albericio, F., Carpino, L.A., Foxman, B.M. and Kates, S.A., *Lett. Pept. Sci.*, 1 (1994) 57.
4. Angell, Y.M., García-Echeverría, C. and Rich, D.H., *Tet. Lett.*, 35 (1994) 5981.
5. Erlich, A., Rothemund, S., Brudel, M., Beyermann, M., Carpino, L.A. and Bienert, M., *Tet. Lett.*, 34 (1993) 4781.
6. Carpino, L.A. and El-Faham, A., *J. Org. Chem.*, 59 (1994) 695.
7. Carpino, L.A., El-Faham, A. and Albericio, F., *Tet. Lett.*, 35 (1994) 2279.

Peptides: Chemistry, Structure and Biology
Pravin T.P. Kaumaya and Robert S. Hodges (Eds.)
Mayflower Scientific Ltd., 1996

45
A Continuous Flow Solid Phase Synthesis of Protected Peptide Fragments with Recycling of Trityl Type Support

A.N. Sabirov and V.V. Samukov

State Research Center of Biotechnology and Virology "Vector", Koltsovo, Novosibirsk Region 633159, Russia

Introduction

The synthesis of peptides can be achieved by either solution or solid phase methods or by a combination of both these methods (convergent peptide synthesis [1]): peptide fragments built up on the solid phase are cleaved, purified if necessary, and further used for coupling either in solution or onto a peptide chain attached to a resin support. Protected peptide fragments are, therefore, key building blocks in convergent peptide synthesis. Such fragments are usually synthesized on supports which bear anchoring groups cleavable without alteration of N(α) and side chain protection. In the case of Fmoc methodology, highly acid-sensitive anchoring groups are mainly used for this purpose These include groups of the dialkoxybenzyl, trialkoxydiphenylmethyl and trityl type [2]. Application of trityl type resins is most promising because of the absence of C-terminal amino acid racemization and of diketopiperazine formation.

Results and Discussion

We have developed a method for SPPS of fully protected fragments under low pressure continuous flow conditions with on-line recycling of the polymeric support. For this purpose, an automatic device has been designed on the basis of the Synchrom synthesizer (Figure 1), which consists of microprocessor-controlled membrane pump-valve block, dead volume-free column reactor [3] loaded with 1% DVB-polystyrene resin modified with hydroxy(triphenyl)methyl (hydroxytrityl) groups (1.0 mmol/g), and an array of flow-through cartridges containing dry mixtures of solid reagents; N(α)-2-(4-nitro-phenyl)sulfonylethoxycarbonyl (Nsc) amino acid [4], HOBT and tris(dimethylamino)-chlorophosphonium perchlorate (TCPP).

Activation of the polymer is performed by pumping of 2M HCl/AcOH solution for 15 min, after which a C-terminal Nsc-amino acid is attached to the chlorotrityl polystyrene as its DIEA-salt. The peptide chain is then elongated by successive two-step cycles, each including cleavage of the Nsc-group by treatment with 1% DBU/20% piperidine/DMF (4 min) and coupling of the next amino acid (1.5 eq.) with TCPP/HOBT in DMF/DIEA (50 min). Compared to Fmoc, Nsc-protection is more stable in neutral and weakly basic solutions and allows acylations under more basic conditions, thus providing higher coupling rates and fair stability of the peptide-polymer linkage during

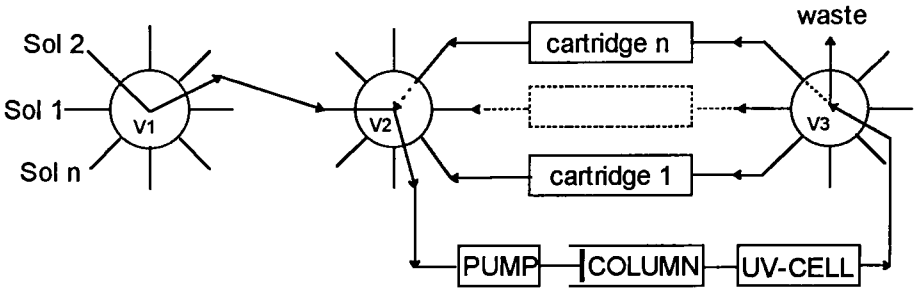

Figure 1. *Flow scheme of the peptide synthesizer.*

the course of the peptide assembly. After completion of the synthesis, protected peptide fragments are cleaved from the support under mild conditions by pumping with 20% AcOH/$CHCl_3$. Hydroxytrityl polymer in the column is then converted into chlorotrityl by HCl/AcOH treatment without any loss of capacity and can be used for assembly of the next peptide sequence .

Synthesis of protected fragments of big endothelin-1 (human) was performed, in the order as shown in Table 1, on the recycled trityl support, on a 0.9 mmol scale, without repacking of the column reactor . After cleavage from the support, the peptides were purified by preparative HPLC on a silica gel column using $CHCl_3$/MeOH/AcOH gradients. All fragments synthesized were of good purity by analytical HPLC (≥95%) and gave a satisfactory amino acid analysis.

Table 1. *Protected fragments of big endothelin-1 (human) synthesized on recycled trityl support.*

Protected fragment	Crude yield	Purified yield
Nsc-Asp(OtBu)-Ile-Ile-Trp-OH	96%	75%
Nsc-Met-Asp(OtBu)-Lys(Boc)-Glu(OtBu)-Cys(Trt)-Val-Tyr(tBu)-OH	70%	53%
Nsc-Lys(Boc)-Cys(Trt)-Val-Tyr(tBu)-OH	96%	79%
Nsc-Glu(OtBu)-His(Trt)-Val-Val-Pro-OH	87%	56%
Nsc-Ser(tBu)-Cys(Acm)-Ser(tBu)-Cys(Trt)-Ser(tBu)-OH	95%	71%

References

1. Pedroso, E., Grandas, A., Saralegui, M.A., Giralt, E., Granier, C. and van Rietschoten, J., *Tetrahedron*, 38 (1982) 1183.
2. Barlos, K., Gatos, D., Kallitsis, J., Papaphotiu, G., Sotiriu, P., Wenqing, Y. and Schafer, W., *Tetrahedron Lett.*, 30 (1989) 3943.
3. Baru, M.B., Ivanov, V.T. and Rodionov, I.L., in Giralt, E. and Andreu, D. (Eds.), 'Peptides 1990', ESCOM, Leiden, The Netherlands, 1990, p.198.
4. Samukov, V.V., Sabirov, A.N. and Pozdnyakov, P.I., *Tetrahedron Lett.*, 42 (1994) 7821.

Peptides: Chemistry, Structure and Biology
Pravin T.P. Kaumaya and Robert S. Hodges (Eds.)
Mayflower Scientific Ltd., 1996

46

Use of Gaseous Ammonia for Detachment of Peptides from Various Carriers - Development of Production Process

M. Flegel[2], M. Rinnová[1], Z. Pánek[2], L. Lepša[2] and I. Bláha[2]

[1]*Institute of Organic Chemistry and Biochemistry, Fleming sq. 2, Prague 6*
[2]*Ferring-Léčiva , Radiová 1 ,10227 Prague 10 , Czech Republic.*

Introduction

The use of gaseous ammonia for the detachment of peptides from solid supports was found to be an efficient method for analytical, preparative and industrial scale. The advantage of this direct ammonolysis method was recently recognized in the multiple synthesis of peptide amides [1]. Vapor phase ammonolytic cleavage under mild conditions can eliminate or reduce the formation peptide-acids, one of the main side reaction products. The results depend on the structure of the peptides, the presence of moisture during ammonolysis, the choice of polymer support and other factors. Both the purity and the yields of amides prepared directly with ammonia vapor were usually betterthan those obtained on ammonolysis carried out in methanol suspension. The gaseous ammonia cleavage process has found application in our production scale preparation of Desmopressin and Terlipressin.

Results and Discussion

During ammonolytic cleavage in methanol, the initial product formed is the peptide-methyl ester. This is then converted to the peptide-amide. However, the conversion from the ester to the amide may not be complete, resulting in a mixture of both compounds. The amount of cleaved peptide, absorbed on the resin depends on solvent used. The peptide should be isolated by extraction of the resin in suitable solvent (*e.g.* DMF). The purity of the extracted peptide is often higher in comparison to the same material obtained from the supernatant.

Table 1. *Influence of solvent on 16 hrs. ammonolysis of [Acm]$_2$-oxytocin. Distribution and purity of peptide-amide (%).*

Solvent	supernatant/HPLC	MeOH /HPLC	DMF/HPLC
chloroform	12/15.4	29/53.1	59/72
iso-butanol	31/9.7	32/33	37/40.3
methanol	68/20.8	10/29.9	22/40.5

The purity of the peptide-amide was superior, if ammonolysis was carried out in solvent ($CHCl_3$), where product solubility was limited. This fact inspired us to use ammonia vapors only. The efficiency of gaseous ammonolysis and the purity of the peptide obtained depends on the hydrophobicity of the carrier. The concentration of water in the reaction centers within the hydrophobic supports was probably very low and the formation of acid was diminished.

Table 2. *Comparison of ammonolysis and acidolysis on various supports.*

Peptide	Support	Yield %	HPLC %
TAIGVGAPG	Tentagel	85	80
PQTAIGVGAPG	Cotton	78	65
VQAAIDYING	Tentagel	89	82
VQAAIDYING	Cotton	88	73
PQTAIGVGAPG*	Cotton	90	87
VQAAIDYING*	Cotton	92	78

* Rink amide linker

In the structure of hydrophilic cotton fibres water is always present and therefore formation of acid was higher. Tentagel was less sensitive and on Merrifield resin hydrolysis was negligible. This type of resin was thus preferred for large scale reactions.

Table 3. *Gaseous ammonolysis in production process.*

Peptide	Peptide-resin (g)	Protected peptide (g)	Yield %	HPLC%
DESMOPRESSIN	683	409	91	91
(**Mpa**YFQNCP**r**G)*	2417	1350	85	86
TERLIPRESSIN	1257	769	96	79
(GGGCYFQNCPKG)	3615	2201	86	70

* Mpa = 3-mercaptopropionic acid r = D-Arg

Reaction was carried out for 3 days in moderate ammonia overpressure (2-3 bar). Peptide-polymer contained in a canvas bag was exposed to ammonia in a stainless steel vessel for three days, after which the solid resin with sorbed cleaved product was dried and then extracted with DMF. Purity and yields of both protected peptides were favorable in comparison to the older methanol-ammonia approach.

Reference

1. Bray, M., Jhingran, A., Valerio, R., Maeji, J., *J. Org. Chem.* 59 (1994) 2197.

Peptides: Chemistry, Structure and Biology
Pravin T.P. Kaumaya and Robert S. Hodges (Eds.)
Mayflower Scientific Ltd., 1996

47
Synthesis of Head-to-tail and Lactam Cyclized Peptide Libraries

D. Tumelty[1], M.C. Needels[1], V.V. Antonenko[2] and P.R. Bovy[1]

Departments of [1]Combinatorial Drug Discovery and [2]Combinatorial Chemistry, Affymax Research Institute, Palo Alto, CA 94304, USA

Introduction

Cyclic peptides have been of interest for many years, both as potential drug leads and as targets for conformational analysis. Several groups have reported solid phase methods for synthesizing "head-to-tail" cyclic peptides using a variety of orthogonal protection strategies. Many involve a side-chain anchored Asp/Glu [1] residue with ring closure *via* a commonly used coupling reagent. Methods which rely on similar strategies for synthesizing N-to-side-chain or side-chain-to-side-chain lactams have also been described. During the development of methods for the synthesis of cyclic peptide libraries, we occasionally observed that the amine functions, involved in the cyclic ring formation, would react with the coupling reagents used to activate the carboxyl group. This led us to develop a protocol which shields the amine functions from potentially adverse side-reactions during the activation process [2]. We wish to report an extension of these methods to include the synthesis of cyclic (side-chain-to-side-chain) lactams.

Results and Discussion

Peptide synthesis was carried out using Fmoc chemistry on either an acid-labile or photolabile [3] linker coupled to a PEG-PS support. Figure 1 shows an example of the general scheme of synthesis, where the peptide sequence has a Glu residue with its γ-carboxyl protected as an allyl ester and a Lys residue with its ε-amino function protected by the 4-methyltrityl group (Mtt) [4]. Chain assembly (where X = Fmoc/tBu protected amino acid residues) was followed by N-terminal acetylation to give the completed peptide resins **1**, with chain lengths up to 11 residues and lactam ring sizes ranging from 15 to 39 atoms.

Removal of the allyl ester with $Pd(PPh_3)_4$ (1 equiv.) and PPh_3 (2 equiv.) in THF (or $CHCl_3$)-morpholine (9:1) over 1 hr. was followed by activation using TFA-OPfp-pyridine in NMP or DMF (2:1:1) for 30 min. [5] to form peptide resins containing a stable active ester **2**. On occasion, TFA-ONp was also used to form the corresponding Np ester. Quantitative activation was demonstrated by derivatizing samples of such activated intermediates with CHA and characterizing the cyclohexylamide products following cleavage from the resin. Selective removal of the Mtt function, in the presence of other tBu-based protecting groups was achieved using a TFA:tri(*iso*-propyl)silane:

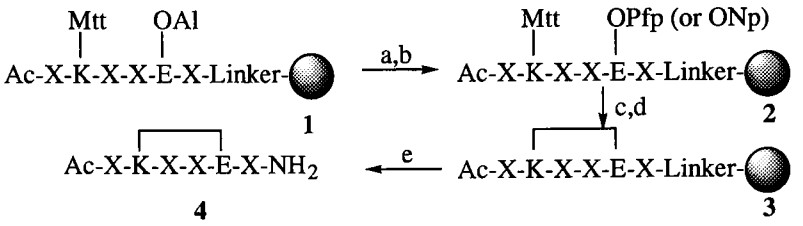

Figure 1. *Generalized solid-phase synthesis of lactam cyclized hexapeptides: (a) allyl ester removal; (b) Pfp (or Np) activation; (c) removal of trityl-based PG (d) neutralization (e) cleavage from solid support.*

DCM (1:5:94) mixture to unmask the ε-amino group of Lys. Neutralization with either DIEA:DMF or DIEA:NMP (1:19), or pyridine:NMP (1:1) for 30-60 min. gave the lactam cyclized peptide resins **3**. Removal of other side-chain protection (if present) was carried out with a TFA:water:phenol:tri(*iso*-propyl)silane (94:3:2:1) mixture for 1 hr. Release of the cyclized peptides from the photolabile linker was performed by photolysis (UV light 365 nm from Hg ARC lamp) in DMSO or DMSO:PBS, pH 7.4 for 1 hr. These conditions enabled biological binding studies for selected peptides to be carried out directly using the photolysis solutions.

Excellent initial purities were obtained for the cyclization products. Quantitative allyl removal and Pfp activation was also demonstrated in each case by analysis of the intermediate linear and CHA-derivatized peptides respectively. With Np-ester activation, release of the yellow *p*-nitrophenolate anion during neutralization enabled a simple visual assessment the end-point in the cyclization. Activated peptide resins **2** were neutralized repeatedly with DIEA/NMP (1:9) for 5 min. periods. The disappearance of the yellow coloration correlated exactly with amine disappearance as judged by Kaiser tests [6], indicating lactam formation *via* aminolysis of the resin-bound active ester.

We investigated the synthesis of a series of twenty-five, eleven-residue lactam cyclized peptides of related sequence with ring sizes ranging from 15 to 39-atoms. Highest yields of the target cyclic peptides were observed with ring sizes of 21-30 atoms and good yields for the smaller ring sizes. However, the largest cyclic lactams were obtained with poor yields of the desired monocyclic peptides, with cyclodimers being the major contaminants.

References

1. McMurray, J.S., *Tetrahedron Lett.*, 33 (1992) 4557.
2. Tumelty, D., Vetter, D. and Antonenko, V.V., *J. Chem. Soc., Chem. Comm.*, (1994), 1067.
3. Holmes, C.P. and Jones, D.G., *J. Org. Chem.*, 60 (1995) 2318.
4. Aletras, A., Barlos, K., Gatos, D., Koutsogianni, S. and Mamos, P., *Int. J. Peptide Protein Res.*, 45 (1995) 488.
5. Vetter, D., Tumelty, D., Singh, S.K. and Gallop, M.A., *Angew. Chem. Int. Ed. Engl.*, 34 (1995) 60.
6. Kaiser, E.T., Colescott, R.L., Bossinger, C.D. and Cook, P.I., *Anal. Biochem.*, 34 (1970) 595.

Peptides: Chemistry, Structure and Biology
Pravin T.P. Kaumaya and Robert S. Hodges (Eds.)
Mayflower Scientific Ltd., 1996

48

N-Dithiasuccinoyl (Dts)-Amines: Novel Sulfurizing Reagents for the Solid Phase Preparation of Thiophosphopeptides and Oligodeoxyribonucleotide Phosphorothioates

Q. Xu[1], K. Musier-Forsyth[1], R.P. Hammer[2] and G. Barany[1]

[1]*Department of Chemistry, University of Minnesota, Minneapolis, MN 55455, USA*
[2]*Department of Chemistry, Louisiana State University, Baton Rouge, LA 70803, USA*

Introduction

Phosphorothioate analogues of the phosphate moiety are of considerable interest in the peptide [1, 2] and nucleic acid [3] fields. Oligonucleotide phosphorothioates are regarded as the first generation of antisense oligonucleotide analogues, which can be used *in vitro* and *in vivo* as inhibitors of gene expression [4]. Site-specific attachment of reporter groups onto DNA and RNA is also facilitated by the incorporation of single phosphorothioate moieties into oligonucleotides [5]. Phosphorothioates have been prepared previously from phosphite triesters by oxidation with sulfurizing reagents, *e.g.*, tetraethylthiuram disulfide (TETD) [6], and 3H-1,2-benzodithiol-3-one 1,1-dioxide (Beaucage reagent) [7]. The present report describes the use of N-dithiasuccinoyl (Dts)-amines as effective sulfurizing reagents for the synthesis of phosphorothioate analogues. The kinetics and mechanisms of these reactions have been elucidated, and practical preparative conditions have been devised.

Results and Discussion

The general scheme for sulfurization of P(III) intermediates is shown in Figure 1. The suitability of Dts-compounds for preparation of oligodeoxyribonucleoside phosphorothioates was evaluated by automated solid phase synthesis using β-cyanoethyl diisopropyl phosphoramidite chemistry. Syntheses of the oligodeoxyribonucleotide d(ATTTp(s)TT) were carried on 0.2 μmol or 1 μmol scales on controlled pore glass supports. Varying concentrations of Dts-compounds were tested, as well as different sulfurizing times. After standard deprotection, cleavage from the solid support, and desalting, the reaction products were analyzed by HPLC and ^{31}P NMR. Good yields and purities were observed, even at low Dts concentrations and with short reaction times. The best results (overall purity > 98%) were obtained using 0.05 M DtsNH in CH_3CN as the sulfurizing reagent with a 1 min reaction-time, or 0.01 M DtsNH in CH_3CN with a 5 min reaction-time.

Dts-amines were also tested for the solid-phase synthesis of thiophosphopeptides. The model peptide H-Gly-Ser-Phe-NH_2, with a phosphorothioate moiety attached to

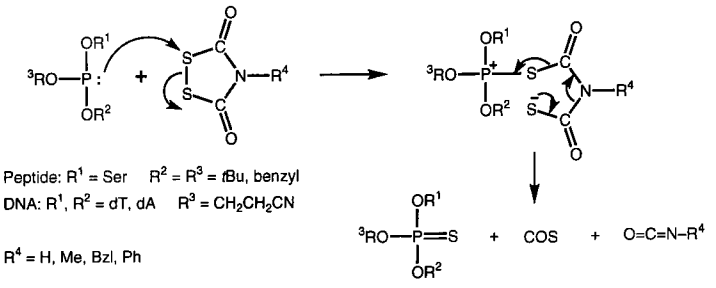

Figure 1. *Mechanism of sulfurization of P^{III} to P^{V}=S, mediated by Dts-amines.*

serine, was synthesized on a 300 μmol scale by a "global" post-assembly phosphorylation strategy [8]. Fmoc-PAL-PEG-PS resin was acylated, in turn, by N^{α} -Fmoc-Phe, N^{α}-Fmoc-Ser, and N^{α}-Boc-Gly, followed by a 15 min sulfurization reaction with 0.05 M $DtsNC_6H_5$ in CH_2Cl_2. The stability of thiophosphoserine peptides to alkylation side reactions upon exposure to typical acid cleavage conditions was also studied. When the phosphate protecting group is *t*-butyl, standard TFA/scavenger cocktails (*e.g.*, reagents K, R) are sufficient to prevent *S*-alkylation. When the phosphate is protected by benzyl groups, then thiophenol, ethanedithiol, and $(CH_3)_3SiBr$ are efficient scavengers that, used together, allow for optimal results. Overall purities directly after cleavage were ~90% by analytical HPLC, and products were characterized further by mass spectra.

Future work will explore applications of Dts-amines to the preparation of phosphorothioate-containing RNA oligonucleotides and thiophosphonopeptide mimics prepared with phosphorus (III) derivatives.

Acknowledgments

This work was supported by NIH grants GM 28934, 42722 and 43552 to GB; GM 49928 to KMF; and grants LEQSF(RF/19931996)-RD-A-42 and NSF CHE-9500992 to RPH.

References

1. de Bont, D.B.A., Moree, W.J., van Boom, J.H. and Liskamp, R.M.J., *J. Org. Chem.*, 58 (1993) 1309.
2. Kitas, E., Kung, E. and Bannwarth, W., *Int. J. Peptide Protein Res.*, 43 (1994) 146.
3. Zon, G. and Stec, W.J., in Eckstein, F. (Ed.), 'Oligonucleotides and Their Analogues: A Practical Approach', IRL, Oxford, 1991, p.87
4. Uhlmann, E. and Peyman, A., *Chem. Rev.*, 90 (1990) 544.
5. Musier-Forsyth, K. and Schimmel, P., *Biochemistry*, 33 (1994) 773.
6. Vu, H. and Hirschbein, B.L., *Tetrahedron Lett.*, 32 (1991) 3005.
7. Iyer, R.P., Phillips, L.R., Egan, W., Regan, J.B. and Beaucage, S.L., *J. Org. Chem.*, 55 (1990) 4693.
8. Andrews, D.M., Kitchin, J. and Seale, P.W., *Int. J. Pept. Protein Res.*, 38 (1991) 469.

Peptides: Chemistry, Structure and Biology
Pravin T.P. Kaumaya and Robert S. Hodges (Eds.)
Mayflower Scientific Ltd., 1996

49

"High Load" Polyethylene Glycol - Polystyrene Graft Supports for Solid Phase Peptide Synthesis

B.F. McGuinness[1], S.A. Kates[1], G.W. Griffin[1], L.W. Herman[1], N.A. Solé[1], J. Vágner[2], F. Albericio[3] and G. Barany[2]

[1]PerSeptive Biosystems Biosearch Products, 500 Old Connecticut Path, Framingham, MA 01701, USA
[2]Department of Chemistry, University of Minnesota, Minneapolis, MN 55455, USA
[3]Department of Organic Chemistry, University of Barcelona, 08028 Barcelona, Spain

Introduction

Ongoing studies from our laboratories have shown potential advantages of polyethylene glycol-polystyrene (PEG-PS) graft supports for both Fmoc/*t*Bu- and Boc/Bzl-based methods, as well as for the construction of peptide nucleic acids (PNA's) [1-3]. PEG-PS resins have been shown to be superior to conventional PS supports for the assembly of hydrophobic peptides, and for peptides that contain post-translational modifications. Furthermore, they are suitable for carrying out allyl-based chemistry and resin-bound cyclization to provide homodetic (lactam) and heterodetic (disulfide) cyclic peptides [4, 5]. Previous work was carried out with resin loadings in the range of 0.15-0.25 mmol/g. This communication focuses on the further extension of beneficial aspects of the PEG-PS concept, as it is applied for resins with higher loadings, *i.e.*, 0.3-0.5 mmol/g.

Results and Discussion

PEG derivatives of various molecular weight were covalently grafted onto PS resins. Resins prepared included MBHA-Nle-PEG2001-NH_2, 0.18 mmol/g; MBHA-Orn(NH_2)-PEG2001-NH_2, 0.44 mmol/g; MBHA-Nle-PEG900-NH_2, 0.25 mmol/g; MBHA-Lys-(PEG900-NH_2)$_2$, 0.29 mmol/g; MBHA-Lys-(PEG600-NH_2)$_2$, 0.53 mmol/g; MBHA-{60% Orn(NH_2)-PEG2001-NH_2}{40% Nle-PEG2001-NH_2}, 0.39 mmol/g; and MBHA-PEG2001-Lys(NH_2)–βAla-NH_2, 0.41 mmol/g. In order to evaluate the suitability of these resins, several syntheses of the challenging model peptide H-(Ala)$_{10}$-Val-NH_2 were carried out. A PAL linker was used and Fmoc-amino acids were added by protocols of 30 min HATU-mediated couplings and 6 min Fmoc removal (piperidine-DMF, 1:4) on a PerSeptive Biosearch 9050Plus continuous-flow peptide synthesizer. The purities of the peptides were determined by reversed-phase HPLC, after cleavage of the peptides from the resins with TFA-H_2O (9:1, 2 h).

An optimal resin in regard to loading, performance, and reproducible structure is formulated on 1% cross-linked PS beads that contain ~ 60-80% ornithine as an "internal

reference" followed by attachment of PEG with a molecular weight of 2001 (Figure 1). The loading of this resin was 0.35-0.5 mmol/g, which is compatible for batch and multiple peptide synthesis, as well as for the construction of peptide and small organic molecule libraries. The PEG content was established readily by elemental analysis, IR, and gel-phase ^{13}C NMR. Scanning electron-microscopic examination of these materials revealed uniform beads. The "high load" PEG-PS resins exhibited excellent swelling properties, comparable to conventional PEG-PS, in a variety of solvents such as H_2O < EtOAc, EtOH < CH_3CN < MeOH < THF < DMF < CH_2Cl_2 (listed in order of increasing swelling). Control experiments indicated that the peptides elongated from either of the ornithine amino groups were of equal quality.

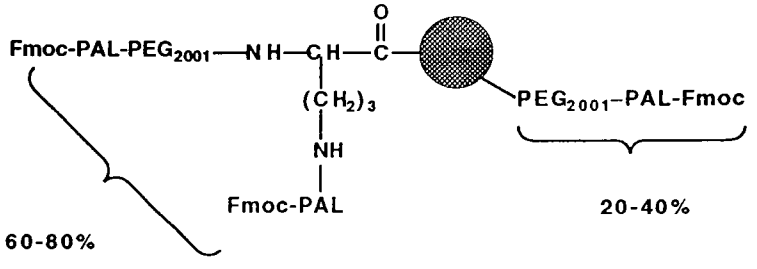

Figure 1. *Optimal formulation of "High Load" PEG-PS.*

In addition to the H-$(Ala)_{10}$-Val-NH_2 model previously described, further continuous-flow peptide syntheses conducted on the optimal "high load" PEG-PS gave excellent results. Reasonably pure peptides of 20-30 residues were assembled with negligible back-pressure. Tachykinin antagonist peptide MEN 10355, *cyclo*(Tyr-Asp-Arg-DTrp-DTrp-Val-DTrp) was prepared in high yield and purity *via* an automated protocol that utilizes allyl removal of side-chain protecting groups with $Pd(PPh_3)_4$ (3 equiv.) in $CHCl_3$/HOAc/NMM (37:2:1) followed by PyAOP-DIEA resin-bound cyclization [6].

References

1. Barany, G., Albericio, F., Solé, N.A., Griffin, G.W., Kates, S.A., and Hudson, D. in Schneider, C.H. and Eberle, A.N. (Eds.), 'Peptides 92', ESCOM, Leiden, The Netherlands, 1993, p. 267.
2. Zalipsky, S., Chang, J.L., Albericio, F., and Barany, G., *React. Polym.* 22 (1994) 243.
3. Albericio, F., Barcardit, J., Barany, G., Coull, J.M., Egholm, M., Giralt, E., Griffin, G.W., Kates, S.A., Nicolás, E., and Solé, N.A. In Maia, H.L.S. (Ed.), 'Peptides 94', ESCOM, Leiden, The Netherlands, 1995, p. 271.
4. Kates, S.A., Solé, N.A., Johnson, C.R., Hudson, D., Barany, G., and Albericio, F., *Tet. Lett.* 34 (1993) 1549.
5. Andreu, D., Albericio, F., Solé, N.A., Munson, M.C., Ferrer, M., and Barany, G. in Pennington, M.W. and Dunn, B.M. (Eds.) 'Methods in Molecular Biology, Vol. 35', Humana Press Inc., Totowa, NJ, 1994, p. 91.
6. Kates, S.A., Daniels, S.B. and Albericio, F., *Anal. Biochem.*, 212 (1993) 303.

Peptides: Chemistry, Structure and Biology
Pravin T.P. Kaumaya and Robert S. Hodges (Eds.)
Mayflower Scientific Ltd., 1996

50

Epimerization of Cys Residues during Fmoc Solid Phase Peptide Synthesis of Peptide Fragments of Mouse Macrophage Migration Inhibitory Factor

T. Kaiser[1], G. Nicholson[2] and W. Voelter[1]

[1]Abtlg. für Physik. Biochemie, Physiologisch-chem. Institut der Universität Tübingen, Hoppe-Seyler-Straße 4, D-72076 Tübingen, Germany
[2]Institut für Organ. Chemie der Universität Tübingen, Auf der Morgenstelle 18, D-72076 Tübingen, Germany

Introduction

Mouse macrophage migration inhibitory factor (mMIF), a 12.5 kDa protein with 115 amino acid residues, is a pituitary-derived multifunctional cytokine with the following primary sequence: MPMFIVNTNVPRASVPEGFLSELTQQLAQATGKPAQYIAVHV VPDQLMTFSGTNDPCALCSLHSIGKIGGAQNRNYSKLLCGLLSDRLHISPDRVYIN YYDMNAANVGWNGSTFA. To study the structure-activity relationships, a total synthesis of mMIF is performed "batch-wise" using the Fmoc convergent solid phase peptide synthesis strategy (CSPPS) *via* protected but C-terminal free fragment condensations on a 2-chlorotrityl resin [1].

Results and Discussion

The protected peptide fragments were synthezised automatically stepwise on a 2-chlorotrityl resin using Fmoc deprotection (2 x 5 and 1 x 20min, 25%Pip/DMF) and TBTU coupling procedures (Fmoc-AA-OH (3equiv., concentration: 0.2mmol/ml DMF), TBTU(3equiv.), HOBt(1equiv.), DIEA(6equiv.), 35 min, RT). For synthesis control, Kaiser tests and TLCs were performed after each deprotection and each coupling step.

During the synthesis of the protected peptide fragment mMIF (70-82), Fmoc-Gly^{70}-Ala-Gln(Trt)-Asn(Trt)-Arg(Pmc)-Asn(Trt)-Tyr(tBu)-Ser(tBu)-Lys(Boc)-Leu-Leu-Cys(Trt)-Gly^{82}-OH, a byproduct, first detected by TLC ($\Delta\Delta R_f$=0.02, $CHCl_3$/MeOH/HAc= 7/2/0,5), was formed after incorporating Fmoc-Lys(Boc)-OH. RP-HPLC work up of the crude resin-cleaved (cleavage: CH_2Cl_2/TFE/HAc=7/2/1, 1h), but otherwise fully protected, as well as deprotected peptides (deprotection: TFA/TA/EDT/Phenol/ H_20=8.4/0.7/0.5/0.2/0.2, 3h), showed identical masses for the two main fractions according to FAB-MS and IS-MS, respectively. Further studies on mMIF (78-82) and mMIF (77-82) peptides (Table 1) indicate that a high degree of racemization occurs during the Fmoc-Cys(Trt)-OH/TBTU/HOBt/DIEA coupling step, which is responsible for the observed side product formed during the mMIF (70-82) synthesis [2]. Numerous variations of the experimental conditions of the base-catalyzed *"in situ"* couplings could

not prevent the epimerization (7-13% D-epimer, RP-HPLC, ASA). Similar degrees of racemization were observed, using Fmoc-D-Cys(Trt)-OH for acylation in the SPPS of the penta- and hexapeptides mMIF (78-82) and mMIF (77-82), enabling the structural proof of the related diastereomers by comparative RP-HPLC and ASA (Table 1).

Applying the neutral preformed symmetrical anhydride (PSA) method for the Cys coupling step reduced the racemization to negligible amounts at the stage of the penta- and hexapeptides (<1%, RP-HPLC). Therefore, the peptide fragment mMIF (70-82) could be synthesized in high purity.

Table 1. *D-amino acid analysis of mMIF(78-82) and mMIF(77-82) peptides*[a].

Peptide	%D-Cys	%D-Leu	%D-Lys	%D-Ser
H-KLLCG-OH[b]	10.30	1.50	0.14	-
H-KLLCG-OH[c]	0.78	0.79	<0.20	-
H-SKLLCG-OH[b]	11.71	1.60	0.21	1.70
H-SKLLCG-OH[c]	1.20	0.59	<0.20	1.80
H-KLL(D-C)G-OH[b]	80.50	0.82	1.60	-
H-KLL(D-C)G-OH[c]	98.30	0.59	0.16	-
H-SKLL(D-C)G-OH[b]	73.70	1.12	<0.50	1.80
H-SKLL(D-C)G-OH[c]	98.80	0.63	0.34	0.55

[a]Determination by GC-MS; conditions: hydrolyses: 6N D_2O/DCl + 1%TGA, 110°C, 24h, vacuum; derivatization: esterification: CH_3OD, 10% DCl, 110°C, 15min; acylation: TFAA, 110°C, 10min; GC-column: Chirasil-Val film (20cm x 0.3mm silica capillary), T= 60°C/3'/ 3,5'/185°C, detection: MS-SIM. [b]Crude deprotected peptides. [c]RP-HPLC-purified peptides.

Epimerization, as an undesired side reaction during DIEA-catalyzed acylation of Fmoc-Cys(Trt)-OH was also observed during other syntheses of Cys-mMIF fragments, indicating that this phenomenon is not caused by the sequence position of Cys. It should be independant of the thiol protecting group [2]. Computer calculation studies (Fa. Schmelz, EDV-Dienstleistungen, Tübingen, Germany) verified the energetic difference of the described peptide diastereomers of mMIF, giving an example for their different chromatographic behavior. Therefore, in general, racemization is a serious problem when Cys peptides are synthesized *via* conventional Fmoc-SPPS, especially if disulfide bonds have to be formed.

References

1. Kaiser, T., Bernhagen, J., Bucala, R., Paulus, G. and Voelter, W., in Maia, H.L.S. (Ed.), 'Peptides 1994', ESCOM, Leiden, The Netherlands 1995, p. 853.
2. Musiol, J.H., Quarzago, D., Scharf, R. and Moroder, L., in Hodges, R.S. and Smith, J.A. (Eds.), 'Peptides: Chemistry, Structure and Biology', ESCOM, Leiden,The Netherlands 1995, p. 62.

Peptides: Chemistry, Structure and Biology
Pravin T.P. Kaumaya and Robert S. Hodges (Eds.)
Mayflower Scientific Ltd., 1996

51
Solid Phase Synthesis of Peptides Containing the Fluorescence Energy Transfer Dabcyl-Edans Couple

J.W. Drijfhout[1], J. Nagel[2], B. Beekman[2], J.M. Te Koppele[2] and W. Bloemhoff [3]

[1]Department of Immunohaematology and Blood Bank, Leiden University Hospital, P.O. Box 9600, 2300 RC Leiden, The Netherlands
[2]Gaubius Laboratory, TNO Prevention and Health, P.O. Box 430, 2300 AK Leiden, The Netherlands
[3]Gorlaeus Laboratories, University Leiden, P.O. Box 9502, 2300 RA Leiden, The Netherlands

Introduction

The activity of proteolytic enzymes can sensitively be monitored with peptide-substrates containing a fluorescence donor and acceptor moiety on either side of the cleavage site. The substrates are non-fluorescent (fluorogenic) because of quenching, *i.e.* the acceptor quenches the fluorescence of the donor due to the fact that the moieties are close in space. Upon cleavage, the fluorescence of the donor becomes detectable as the acceptor is no longer close in space to quench the fluorescence signal. For this application, the Dabcyl-Edans couple [1] seems to be one of the most preferable couples because:

a. There is good spectral overlap between the Edans emission spectrum and the Dabcyl absorption spectrum.
b. The fluorescence efficiency of the Edans moiety is high.
c. The excitation and emission wavelengths involved are so high that interference by amino acid side chains does not play a role and auto-fluorescence is reduced.

Here we report the solid phase synthesis and some properties of peptide substrates which contain an Edans moiety attached to a Glu side chain and a Dabcyl group on the N-terminus.

Results and Discussion

Peptides were synthesized on 10 μmol scale by solid phase strategies on an automated multiple peptide synthesizer (Abimed AMS 422) using tentagel S AC (loading 0.2 μequiv., particle size 90 μm, Rapp), essentially as described before [2]. Repetitive couplings were performed by adding a mixture of 90 μl 0.67 M PyBOP in NMP, 20 μl NMM in NMP 2/1 (v/v), and 100 μl of an 0.60 M solution of the appropriate Fmoc amino acid [3] in NMP (6-fold excess) to each reaction vessel. Coupling time was 45 min. Coupling of Fmoc-Glu(Edans)-OH was performed with a 10-fold excess for 3 hr.

Coupling of the Dabcyl moiety was done with a suspension of 10 equiv. *p*-(*p*-dimethylaminophenylazo)benzoic acid (Sigma), 10 equiv. PyBop and 20 equiv. NMM in 250 µl NMP for 3 hr. Cleavage of the peptide from the resin and removal of the side chain protecting groups was performed by adding 200 µl TFA/water 19/1 (v/v) to the reaction vessel 6 times at 5 min intervals. Three hours after the first TFA addition, the peptides were precipitated from the combined filtrates by addition of 10 ml ether/pentane 1/1 (v/v) and cooling to -20°C, after which the peptides were isolated by centrifugation (-20°C, 2,500g, 10 min). The peptides were analyzed by RP-HPLC (water/CH_3CN/TFA) and by MALDI-TOF MS on a Lasermat (Finnigan MAT). As a typical example, we show here the data of Dabcyl-Gaba-Pro-Gln-Gly-Ile-Ala-Gly-Glu(Edans)-Arg-Glu-Glu-OH (Figure 1).

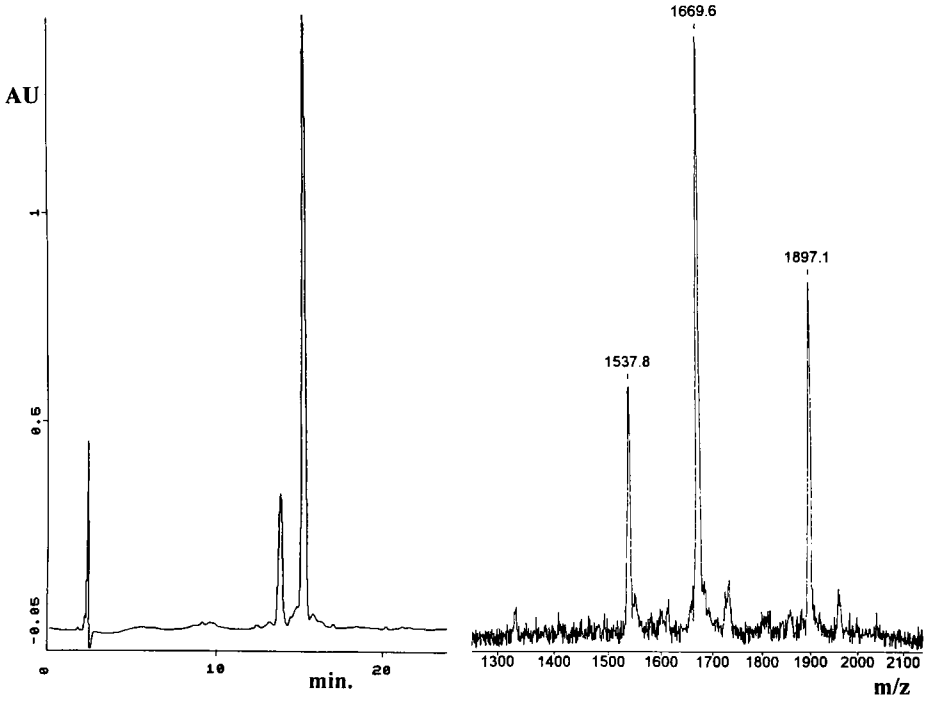

Figure 1. *RP-HPLC of crude Dabcyl-Gaba-Pro-Gln-Gly-Ile-Ala-Gly-Glu(Edans)-Arg-Glu-Glu-OH. MALDI-TOF MS-spectrum (Lasermat, Finnigan MAT) of the purified product (MH^+_{calc}= 1669.8) . The signal at m/z = 1897.1 corresponds to the internal reference peptide. The signal at MH^+ = 1537.8 most likely represents the p-aminobenzoyl derivative of the peptide, which is formed by laser ionization induced cleavage of the azo-bond in the Dabcyl moiety.*

Fmoc-Glu(Edans)-OH was synthesized as follows: To a stirred solution of Fmoc-Glu(OH)-OtBu (1.70 g, 4 mmol, Saxon), Edans (1.07 g, 4 mmol, Sigma) and BOP (1.77 g, 4 mmol, Richelieu) in 10 ml DMF was added at room temperature DIPEA (2 ml, 12 mmol, distilled from CaH_2). After 2 hr., the reaction was complete (TLC, toluene/HOAc, 9/1, v/v). To the reaction mixture, 50 ml CH_2Cl_2 and 50 ml 0.5 M

$KHSO_4$ was added. The organic layer was washed with 0.1 M $KHSO_4$ and water, dried over $MgSO_4$, and evaporated *in vacuo* to yield 2.8 g of an oil. To remove the *t*-butyl group, 10 ml glacial acid and 1 ml 36% hydrochloric acid were added. After 1 hr. of stirring, the solvents were evaporated *in vacuo*. Traces of acetic acid were removed by co-evaporation with DMF (2 x 10 ml). The product was purified, in 45% yield, by RP-HPLC on a Vydac (protein), C18 column (water/CH_3CN). ^{13}C NMR (DMSO-d6): δ23.2 (CH_2), 26.7 (CH_2), 44.2 (CH_2), 46.6 (CH-Fmoc), 53.4 (C_α), 65.7 (CH_2), 67.4 (CH_2), 120.1, 122.6, 122.8, 124.4, 125.2, 125.9, 127.0, 127.6, 128.6 (9 x CH-arom), 123.8, 130.1, 140.6, 143.7, 144.2 (5 x q-arom), 156.1, 171.9, 173.6 (3 x C=O).

Various Dabcyl-Edans peptides were investigated for their quenching properties. Fluorogenic substrates (1.8 μM) were incubated with MMP-9 (5 nM) [5, 6] in 500 μl incubation buffer (50 mM Tris, pH 7.6, 150 mM NaCl, 5 mM $CaCl_2$, 1 μM $ZnCl_2$, 0.01% Brij-35) and, at four time points per incubation, the percentage of substrate hydrolyzed (x, determined by HPLC) and the corresponding fluorescence (Flu(t), Kontron SFM-25) were measured. The percentage quenching was calculated for each time point from the equation:

$$\text{Quenching} = \frac{[100/x] \,.\, [\text{Flu}(t) - \text{Flu}(0)]}{[100/x] \,.\, [\text{Flu}(t)]} \,.\, 100\%$$

The quenching (Q in %) is presented as means of eight observations from two incubations. The number of atoms between aromatic rings of Dabcyl and Edans in the peptides are indicated in brackets below. Peptide 1(33), Q = 98.2 ± 0.18; peptide 2(33), Q = 97.9 ± 0.19; peptide 3(27), Q = 98.7 ± 0.15; peptide 4(27), Q = 98.5 ± 0.07; peptide 5(27), Q = 99.0 ± 0.10.

In conclusion, we have shown that fluorogenic peptides containing a Dabcyl and an Edans moiety can be synthesized by solid phase strategies. For complete incorporation of Fmoc-Glu(Edans)-OH and Dabcyl-OH, extended coupling times can best be applied. The purity of the crude peptide material is satisfactory. The fluorescence quenching of the substrates can be high, even in peptides in which the labels are relatively far apart (about 30 atoms), which makes the peptides very suitable as substrates in systems for sensitive detection of enzyme activity.

References

1. Matayoshi, E.D., Wang, G.T., Krafft, G.A. and Erickson, J., *Science*, 247 (1990) 954.
2. Drijfhout, J.W., Brandt, M.P., D'Amaro, J., Kast, W.M. and Melief, C.J.M., *Human Immunol.*, 43 (1995) 1.
3. Fields, G.B. and Noble, R.L., *Int. J. Peptide Protein Res.*, 35 (1990) 161.
4. Beavis, R.C., Chaudhary, T. and Chait, B.T., *Org. Mass Spectrom.*, 27 (1992) 156.
5. Fosang, A.J., Last, K, Knäuper, V., Neame, P.J., Murphy, G., Hardingham, T.E, Tschesche, H. and Hamilton, J.A., *Biochem. J.*, 295 (1993) 273.
6. Te Koppele, J.M., Beekman, B., Bloemhoff, W. and Drijfhout, J.W., *Acta Orthop. Scand.*, in press.

Peptides: Chemistry, Structure and Biology
Pravin T.P. Kaumaya and Robert S. Hodges (Eds.)
Mayflower Scientific Ltd., 1996

52
Investigation of Racemization in N-to-C Direction (Inverse) Solid Phase Peptide Synthesis

E. Bayer, B. Henkel, G. Nicholson

Institute of Organic Chemistry, University of Tübingen, Auf der Morgenstelle 18, D-72070 Tübingen, Germany

Introduction

Solid phase peptide synthesis is carried out normally in the C-to-N direction. Only a few attempts have been made to couple in the inverse direction in solid phase synthesis [1-6]. We have reported recently on a method of synthesizing peptides in the inverse direction using amino acid-9-fluorenylmethylester HOBt-salts or hydrochlorides [7]. C-terminally modified [Leu^5]enkephalins were synthesized by the solid phase technique using an ABI 431 A synthesizer, the C-terminus being deprotected with 20% piperidine in DMF. The synthesis was performed on a TentaGel-resin bearing the trityl-linker, *p*-(diphenyl-hydroxymethyl) benzoic acid [7]. Few reports have been published as to the extent of racemization and side reactions occuring during N-to-C chain elongation. Two methods for the activation of the C-terminus were investigated; HOBt/DIC and TBTU/NMM. For the exact determination of racemization values, the peptides were hydrolyzed in a mixture of D_2O and DCl and, after derivatization, analysed on a Chirasil-Val capillary by GCMS.

Results and Discussion

Before synthesizing the [Leu^5]enkephalins, the kinetics of the coupling reactions were checked. Coupling with TBTU/NMM was far more rapid, requiring 1 hour for complete reaction, as compared to 18-20 hours with HOBt/DIC. The [Leu^5]enkephalin derivatives (OH, NH_2, OMe) thus synthesized were cleaved from the linker with 20% TFA/10% MeOH/70% DCM.

According to the mass spectra, the crude products synthesized by the TBTU/ NMM method were remarkably pure [7], whereas the peptides synthesized according to the HOBt/DIC method were contaminated with several byproducts. Cyclic peptides were detected. These could result from the attack of a secondary nitrogen at the carbonyl C carrying OBt-ester to form a cyclic amide or from the attack of the OBt-ester by a negatively polarized carbonyl oxygen, analogous to oxazolone formation. In addition, a diketopiperazine formed during cleavage of the peptide from the linker and glycine lost its fluorenylmethylester moiety during the long coupling period resulting in multiple couplings of Gly. The mass spectrum of [Leu^5]enkephalin amide shows the presence of a piperidine amide arising from incomplete neutralization after ester cleavage.

Table 1. *Percentage of D-enantiomers determined by GC-MS, the values for Tyr and Phe were constant irrespective of the C-terminally modified peptide.*

	Tyr	Phe	Leu-OH	Leu-OMe	Leu-NH_2
Amino acid derivative	<0.1	0.94	0.2	0.14	0.11
HOBt/DIC	0.5	8.18	1.13	0.85	1.34
TBTU/NMM	0.08	39.9	0.25	0.2	0.13

The HPLC's of the [Leu^5]enkephalins synthesized according to the HOBt/DIC method display several byproducts. This is in agreement with the results from mass spectrometry. The HPLCs of the 5-mers synthesized according to the TBTU/NMM method show two peaks with similar area, suggesting the presence of diastereomers. The exact rate of racemization of the amino acids was checked by chiral gas chromatography.

It is evident that Phe is the only amino acid with an elevated racemization. The fact that the last amino acid of H-Tyr(DCB)-Gly-Gly-Phe-Leu-OH has not racemized proves that racemization occurs during the activation step. The activated carbonyl C atom is attacked by an oxygen of the former amino acid in the chain to form a ring system (oxazolone). From this oxazolone, a hydrogen could be abstracted, thus forming a delocalized system. In the presence of a base (NMM), racemization occurs very rapidly. The ring systems could be looked upon as an activated C-terminus analogous to an OBt-ester. The reason for the low racemization value of Tyr when using a trityl-type linker is its inability to form a ring system because of steric hindrance.

It has been shown that peptides can be prepared in the inverse direction using two different methods, but that the results are, as yet, unsatisfactory. The HOBt/DIC method led to considerable amounts of by-products as a consequence of the long coupling times required. The TBTU/NMM method gave apparently pure products according to the mass spectra, but the HPLCs, and particularly racemization tests, indicated extensive racemization. It remains to be seen whether new coupling reagents, which are under intensive research at present, can offer a better prospect for the inverse synthesis of peptides.

References

1. Letsinger, R.L., Kornet, M.J., *J. Amer. Chem. Soc.*, 85 (1963) 3045.
2. Letsinger, R.L., Kornet, M.J., Mahadevan, V., Jevina, D.M., *J. Amer. Chem. Soc.*, 86 (1964) 5163.
3. Felix, A.M., Merrifield, R.B., *J. Amer. Chem. Soc.*, 92 (1970) 1385.
4. Mukaiyama, T., Matsueda, R., Suzuki, M., *Tetrahedron Lett.*, (1970) 1901.
5. Sharma, R.P., Jones, D.A., Corina, D.L., Akhtar, M., in Hodges, R.S. and Smith, J.A. (Eds.), Peptides: Chemistry, Structure and Biology, ESCOM, Leiden, The Netherlands 1994, p. 127.
6. Sharma, R.P., Jones, D.A., Broadbridge, R.J., Corna, D.L., Akhtar, M., in Epton, R. (Ed.), Innovation and Perspectives in 'Solid Phase Synthesis: Peptides, Proteins and Nucleic Acids', Mayflower Worldwide Ltd., Birmingham, England, 1994, p.353.
7. Bayer, E., Henkel, B., Zhang, L., Clausen, N., Goldammer, C., Panhaus, G., in Maia, H.L.S. (Ed.), 'Peptides 1994', ESCOM, Leiden, The Netherlands 1995, p. 201.

Peptides: Chemistry, Structure and Biology
Pravin T.P. Kaumaya and Robert S. Hodges (Eds.)
Mayflower Scientific Ltd., 1996

53
Comparative Study on the Large Scale Solid Phase Synthesis of Crystalline Glucagon

R.G. Bizanek, K. Lyons, K. Kiefer, L. Kirchdorfer, N.S. Rangaraju, H.H. Saneii, X. Sun and J. Stone

Advanced ChemTech, Inc., Louisville, KY 40228, USA

Introduction

The increased interest in the application of human glucagon for the treatment of diabetes mellitus prompted us to develop a solid phase synthesis strategy for the rapid and efficient production of large amounts of pharmaceutical grade glucagon and its analogs.

The synthesis of the 29-residue peptide has been reported as quite challenging because of its unusual structure [1]. The first successful synthesis used classical fragment condensation [2], while the second synthesis, accomplished by the Protein Synthesis Group in Shanghai [3], proceeded through a solid phase fragment strategy. The first stepwise solid phase synthesis was reported by Merrifield's group in 1977 [4 - 6] using Bpoc- and Boc-groups as N-protecting groups.

H-His-Ser-Gln-Gly-Thr-Phe-Thr-Ser-Asp-Tyr-Ser-Lys-Tyr-Leu-Asp-
Ser-Arg-Arg-Ala-Gln-Asp-Phe-Val-Gln-Trp-Leu-Met-Asn-Thr-OH

Figure 1. *Sequence of human glucagon.*

Results and Discussion

Initial experiments using our standard protocols did not produce the peptide in high yields. This lead us to undertake a thorough investigation of its solid phase synthesis. Glucagon was synthesized by the Fmoc strategy on Wang resin, Boc strategy on Merrifield and Pam resin, and with a combination of Fmoc and Boc protection on Pam resin. In addition, alternative coupling strategies, reagents and solvent systems were employed, either at the expected difficult couplings or throughout the synthesis. The highest weight gain of 90% was obtained with Fmoc strategy on Wang resin using 1% Tween 20 in DMF/DCM/NMP (1/1/1) [7]. All other synthetic routes gave only 55 to 65% weight gain.

As with most synthetic endeavors in peptide chemistry, construction of the molecule proved not to be the most time-consuming task. Rather it was the purification and isolation of the desired material which took most of the time and effort. A standard purification scheme using reversed phase HPLC on C18 columns gave poor peptide recoveries and was challenged by the required removal of closely related compounds.

Initially, pure material was obtained by ion exchange chromatography followed by purification on reversed phase HPLC in two different buffer systems. This elaborate process did not improve the recoveries of glucagon compared to that of a single pass with the standard system - water/acetonitrile with 0.1% TFA. After extensive optimization of this system with regard to gradient and loading of crude material, the recovery of pure glucagon has been increased from 0.4 to 25%.

Progress to date has resulted in substantial improvements in both the synthesis and purification of human glucagon. However, at this point in time, due to the stringent requirements for production of pharmaceutical grade peptides, several aspects of the work remain under investigation in order to further optimize the overall synthesis yield.

References

1. Schröder, E., in Beyerman, H.C., van de Linde, A. and Massen van den Brink, N. (Eds.), 'Peptides', North-Holland Publishing Co., Amsterdam, The Netherlands, 1967, p. 245.
2. Wünsch, E. and Wendelberger, G., *Chem. Ber.,* 101 (1968) 3659.
3. Protein Synthesis Group, Shanghai Institute of Biochemistry, *Sci. Sin.* 18 (1975) 745.
4. Merrifield, R.B., Barany, G., Cosand, W.L., Engelhard, M. and Mojsov, S., in Goodman, M. and Meienhofer, J. (Eds.), 'Peptides', J. Wiley and Sons, New York, NY, USA, 1977, 488.
5. Mojsov, S. and Merrifield, R.B., *Biochemistry,* 20 (1981) 2950.
6. Mojsov, S. and Merrifield, R.B., *Eur. J. Biochem.,* 145 (1984) 601.
7. Zhang, L., Goldammer, C., Henkel, B., Panhaus, G., Zühl, F., Jung, G. and Bayer, E., in Epton, R. (Ed.), 'Innovation and Perspectives in Solid Phase Synthesis: Peptides, Proteins and Nucleic Acids - Biological and Biomedical Applications', Mayflower Worldwide, Birmingham, UK, p. 711, 1994.

Peptides: Chemistry, Structure and Biology
Pravin T.P. Kaumaya and Robert S. Hodges (Eds.)
Mayflower Scientific Ltd., 1996

54
Advanced Automation for Peptides and Non-peptidic Molecules

H.H. Saneii, M.L. Peterson, H. Anderson, E.T. Healy and R.G. Bizanek

Advanced ChemTech, Inc., Louisville, KY 40228, USA

Introduction

Automation has had a profound impact on the construction of complex biomolecules such as peptides and oligonucleotides, but has been only sporadically employed in more general synthetic applications. However, since it has been estimated that only one out of every 10,000 new chemical entities will eventually become a viable commercial product, it takes an extended period of time for even the most talented team of chemists to manufacture sufficient molecules to discover a single new bioactive substance. Recent emphasis has therefore been placed on the generation of sufficient diversity, either naturally or synthetically, to aid in the search for new bioactive agents. This has created a requirement for the ability to rapidly and efficiently generate a range of chemical structures. Further, once lead compounds are identified, optimization of the molecular architecture to maximize the desired mode of biological action must be accomplished in a reasonable time period. Likewise, processes for the production of these materials need to be improved and optimized. In an effort to address this myriad of needs, initial applications in the above areas are presented using newly developed microprocessor-controlled instrumentation, the ACT Model 496 MOS. The synthesizer allows for accurate control of reaction temperature over a wide range, as well as maintenance of both reactions and reagents under an inert atmosphere. The versatility provided by the Model 496 permits synthetic investigations directed at any type of molecule. Examples as applied to peptides and fullerene derivatives are described herein [1].

Results and Discussion

The ACT Model 496 MOS features a Teflon® reaction block equipped with electrical heating and nitrogen gas cooling systems, capable of attaining -70° to 150°C temperatures. The block used consisted of 96 reaction vessels, each with 2.75 ml capacity and a 1 μ porosity Teflon® frit. All operations are conducted under an inert atmosphere. Reagents are transferred utilizing dual robotic arms with user-controlled selection from four system fluids. The instrument can divert spent reagents and solutions to different waste vessels when safety and chemical reactivity considerations warrant. The entire range of functions, including reagent dispensing, mixing, emptying, washing, temperature control and the cleavage of resin products, is controlled through Windows®-based software and maintained in user-specified ChemFiles.

Recent reports have described the positive effects heating can have on peptide synthesis by improving the efficiency and decreasing the coupling time required for addition of each residue, while also attaining high yield and purity [2, 3]. In order to investigate further this approach and optimize reaction conditions for a particular target, the preparation of LH-RH at elevated temperatures in different solvents has been studied. The following syntheses were conducted starting with 100 mg Rink resin (0.56 mequiv./g) and all manipulations of deprotection, coupling and washing were performed at the indicated temperatures.

A: 25% DMSO/toluene as coupling solvent [2], 40°C temperature, 10 min coupling with two-fold excess of amino acid

B: DMF as coupling solvent, 40°C temperature, 10 min coupling with three-fold excess of amino acid

C: DMF as coupling solvent, 50°C temperature, 10 min coupling with two-fold excess of amino acid

To analyze the results of these experiments, the resins were identically cleaved with a cocktail of TFA/anisole/ethyl methyl sulfide/ethane dithiol (93/3/3/1) for 3 hr. Examination by HPLC analysis of the crude peptide obtained produced the following general conclusions. Long coupling times and large excesses of amino acids are not required when utilizing elevated temperatures. Little difference between the solvent systems was observed. Likewise, the chemistry performed at 40°C and 50°C produced similar results. Indeed, syntheses of other test sequences conducted concurrently in these laboratories at 70°C have resulted in lower relative yields of target peptides than those reported in this study. Therefore, the more traditional DMF solvent system at the more moderate 40-50°C temperature appears sufficient to provide benefits to the chemist in shortened reaction times and lower reagent consumption, while producing high purity and yields of desired peptides.

In contrast to peptide synthesis, the conduct of organic chemistry is performed with a much wider variety of reagents and reaction conditions, essentially all of which are compatible with the automated synthesizer technology. To illustrate this, a series of reactions based on the chemistry of C_{60} (buckminsterfullerene) have been performed [4]. Many derivatives of this fascinating structure possess interesting physical and chemical properties. Among these are adducts formed by the reaction of C_{60} with azomethine ylides from the condensation of carbonyl compounds and amines [5, 6]. These have been studied for optical applications, molecular electronics and the production of superconducting Langmuir-Blodgett thin films. The construction of these and other C_{60}analogs is complicated, however, by the generally low solubility of the fullerene itself, the appearance of multiple addition products and the difficulty in removing unreacted C_{60}. In order to test the applicability of transferring this chemistry to the solid-phase to circumvent these problems and provide additional compounds for study, the reaction of an extensive series of carbonyl compounds with C_{60} and the amino acid substituted BHA resin was performed as shown in Scheme 1. It should be noted that, in contrast to the solution chemistry, toluene was a less effective solvent than 1,2-dichlorobenzene. Automation admirably assisted in determination of the scope of the chemistry, as some of the reactants did not produce the desired target compounds as determined by MS, and demonstrated how rapidly and easily a series of new molecular entities for additional study can be produced, since the synthetic process for two dozen substrates was

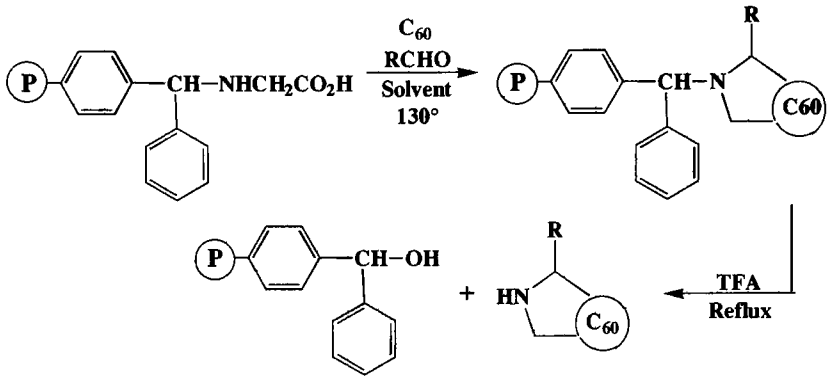

Scheme 1. *Reaction of an extensive series of carbonyl compounds with C_{60} and amino acid substituted BHA resin.*

completed in less than one day. Similar execution manually required about one week of time, although the resins prepared behaved, as would be expected, identically. Further characterization of the reaction products and an investigation of the properties of these materials are still under way.

In addition, Diels-Alder reactions of polymer-bound C_{60} were performed with the results of the automated chemistry consistent with those executed manually [7].

Acknowledgments

The assistance of R. McCorkle in conducting the investigations at 70°C is gratefully acknowledged.

References

1. Christensen, J.W., Peterson, M.L., Saneii, H.H. and Healy, E.T., this volume.
2. Rabinovich, A.K. and Rivier, J.E., *Amer. Biotech. Lab.*, (1994) 48.
3. Lloyd, D.H., Petrie, G.M., Noble, R.L. and Tam, J.P., in Rivier, J.E. and Marshall, G.R. (Eds.), Peptides: Chemistry, Structure and Biology, ESCOM, Leiden The Netherlands 1990, p. 909.
4. Maggini, M., Scorrano, G. and Prato, M., J. Amer. Chem. Soc. 115 (1993) 9798.
6. Maggini, M., Karlsson, A., Pasimeni, L., Scorrano, G., Prato, M. and Valli, L., *Tetrahedron Lett.* 35 (1994) 2985.
7. Guhr, K.I., Greaves, M.D., Rotello, V.M., *J. Amer. Chem. Soc.*, 116 (1994) 5997.

Peptides: Chemistry, Structure and Biology
Pravin T.P. Kaumaya and Robert S. Hodges (Eds.)
Mayflower Scientific Ltd., 1996

55
New Developments in N^{α}-Bpoc and N^{α}-Ddz Solid Phase Peptide Synthesis

R.I. Carey, H. Huang, J.L. Wadsworth, L. Purvis, C.S. Burrell and R.A. Slaughter

Department of Chemistry and Center for Metalloenzyme Studies, University of Georgia, Athens, GA 30602, USA

Introduction

We are currently working on strategies of amide ligation [1-4] for large to medium size peptide fragments that require some solid phase synthesis to be done on a phenyl ester type resin, **1**. For solid phase synthesis on this phenyl ester resin, we have chosen to adopt a strategy using N^{α}-Bpoc amino acids and N^{α}-Ddz amino acids. The repetitive removal of the Bpoc group is compatible with a phenyl ester linkage to the solid phase resin, and the strategy also allows for mild acidolytic deprotection conditions for the removal of the *t*-butyl type side chain protecting groups at the end of the synthesis.

The N^{α}-Bpoc group was introduced for peptide synthesis in 1968 by Sieber and Iselin [5]. Bpoc amino acids were used extensively in the landmark solution phase synthesis of insulin by the Ciba-Geigy group [6] and in the attempted solution phase synthesis of lysozyme by Kenner *et al.* [7]. Although solid phase syntheses using Bpoc-amino acids have been reported [8, 9], the strategy has not gained widespread use, in part because compatible combinations of side-chain protection have not been demonstrated convincingly. Recently, there has been renewed interest in solid phase peptide synthesis with Bpoc amino acids. Kemp and coworkers have reported several syntheses of peptides 25- [1], 29- [3], 34- [10], and 39- [1] amino acid residues in length, as well as reporting practical preparation and deblocking conditions for Bpoc amino acids [11]. Fotouhi and Kemp have addressed the specific problems related to the side-chain protection of N^{α}-Bpoc-tyrosine derivatives [12].

Results and Discussion

We report recent developments in the solid phase synthesis of peptides with N^{α}-Bpoc and N^{α}-Ddz protected amino acid derivatives. Our work has firstly consisted of the preparation of pentafluorophenyl esters of both N^{α}-Bpoc and N^{α}-Ddz protected amino acids. These Pfp esters have been found to be stable, crystalline compounds and effective acylating agents, thus solving the problem of long-term storage and activation problems for Bpoc and Ddz derivatives. Secondly, for Asn, Gln, Lys, Tyr, and His, we have synthesized and characterized new N^{α}-Bpoc and N^{α}-Ddz derivatives [pentafluoro-phenyl esters of Gln(Trt), Asn(Trt), Lys(Alloc), Lys(Tfa), Lys(Adoc), Tyr(Allyl),

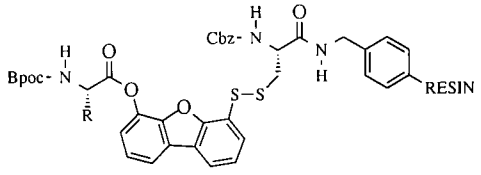

Prior Thiol Capture Method
Solid-Phase Peptide Synthesis
Resin loaded with
4-mercapto-6-hydroxydibenzofuran

1

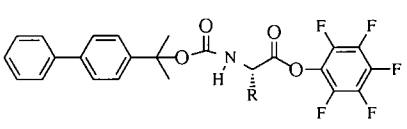

N^{α}-Bpoc amino acid pentafluorophenyl ester

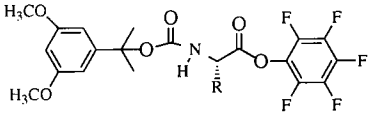

N^{α}-Ddz amino acid pentafluorophenyl ester

His(Trt), His(Bum), His(Pmc)], bearing side-chain protecting groups that are compatible with repetitive Bpoc or Ddz removal and, in the case of Asn and Gln, that are more soluble in coupling reaction mixtures than the derivatives without side-chain protection. Thirdly, these side-chain protected N^{α}-Bpoc and N^{α}-Ddz protected amino acid pentafluorophenyl esters have been used in conjunction with appropriately functionalized polystyrene resins for solid phase peptide synthesis.

Acknowledgments

The authors wish to acknowledge the University of Georgia Research Foundation for support.

References

1. Kemp, D.S., Carey, R.I., *J. Org. Chem.*, 58 (1993) 2216.
2. Kemp, D.S., Carey, R.I., *Tetrahedron Lett.*, 32 (1991) 2845.
3. Fotouhi, N., Galakatos, N.G., Kemp, D.S., *J. Org. Chem.*, 54 (1989) 2803.
4. Kemp, D.S., Carey, R.I., Dewan, J., Galakatos, N.G., Kerkman, D., Leung, S-L., *J. Org. Chem.*, 54 (1989) 1589.
5. Sieber, P., Iselin, B., *Helv. Chim. Acta*, 51 (1968) 614.
6. Kamber, B., Riniker, B., Sieber, P., Rittel, W., *Helv. Chim. Acta*, 59 (1976) 2830.
7. Galpin, I. J., Kenner, G.W., Ohlsen, S.R., Ramage, R., Sheppard, R.C., Tyson, R.G., *Tetrahedron*, 35 (1979) 2785.
8. Colombo, R., *Bioorganic Chem.*, 10 (1981) 219.
9. Wang, S.S., Kulesha, I.D., *J. Org. Chem.*, 40 (1975) 1227.
10. Fotouhi, N., Bowen, B., Kemp, D.S., *Int. J. Peptide, Protein Res.*, 40 (1992) 141.
11. Kemp, D.S., Fotouhi, N., Boyd, J.G., Carey, R.I., Ashton, C.P., Hoare, J., *Int. J. Peptide, Protein Res.*, 31 (1988) 359.
12. Fotouhi, N., Kemp, D.S., *Int. J. Peptide, Protein Res.*, 41 (1993) 153.

Peptides: Chemistry, Structure and Biology
Pravin T.P. Kaumaya and Robert S. Hodges (Eds.)
Mayflower Scientific Ltd., 1996

56
Optimization of the Automated Solid Phase Synthesis of Biphenylalanine and Related Analogs

J.W. Christensen, M.L. Peterson, H.H. Saneii and E.T. Healy

Advanced ChemTech Inc., Louisville, KY 40228, USA

Introduction

Biphenylalanine (Bip) is a component present in several biologically active peptides such as angiotensin II antagonists [1] and the antibiotic WS-43708A [2]. It has also found utility in SAR studies as a substitute for hydrophobic amino acid subunits in peptides such as LH-RH [3]. The synthesis of this unusual amino acid has been reported in the literature using the Pd catalyzed coupling of boronic acids to tyrosine triflate, Tyr(Tf), [4]. It was our wish to extend this synthetic methodology to the solid phase, whereby the Advanced ChemTech Model 496 Multiple Organic Synthesizer could then be employed to allow the concurrent synthesis of a multitude of Bip analogs. Since the ACT Model 496 MOS allows the simultaneous synthesis of up to 96 different moieties, while incorporating the unique advantage of temperature control under an inert atmosphere, both reaction condition optimization as well as reaction scope can be realized with unprecedented efficiency.

Since the literature precedent suggested that heterogeneous conditions were optimal for the Pd catalyzed coupling reaction, it was expected that new reaction conditions were necessary for the successful adaptation of the chemistry to the solid phase. As a result, the study was carried out in two steps. The first was to identify the optimal base/solvent combination and whether other activated Phe derivatives, such as 4-iodo-phenylalanine, Phe(4-I), could be used. The second was to incorporate a host of differentially substituted aryl boronic acids to establish the scope of the reaction. Also included in the second phase was a survey of the efficacy of various catalysts.

Results and Discussion

Step 1. The reported solution phase conditions dictated that K_2CO_3 in toluene was optimal in conversion of Tyr(Tf) to Bip. It was recognized immediately that these conditions would be unlikely to work on the solid phase since this chemistry is essentially heterogeneous itself. As a result, no means of direct proton transfer is possible unless the base is soluble in the reaction medium. To address this concern, as well as determine new optimized reaction conditions, we devised an automated experiment which would test five solvents: DMF, toluene, DMSO, 1,2-dichlorobenzene (DCB), and DMA, against three soluble bases: Et_3N, DMAP, and DIEA, along with solution phase optimal K_2CO_3. We also explored Phe(4-I) as a Tyr(Tf) alternative.

The solid support chosen was HMBA-MBHA resin since the basic conditions needed for cleavage would not compromise the desired Boc protecting group. Tyrosine triflate was generated directly on the instrument using HMBA-MBHA resin loaded with Boc tyrosine under the established solution phase reaction conditions (Tf_2O/Py/DCM/ 0°C, 1h). Boc-Phe(4-I)-HMBA-MBHA resin was prepared and used as the alternative activated Phe analog. Two separate reaction vessels containing the Boc-Tyr and Boc-Phe(4-I) resins were treated only with the appropriate solvents, serving to verify that decomposition did not occur and to determine cleavage yield. A total of 42 separate experiments were performed simultaneously. The scheme below illustrates the sequence of reactions.

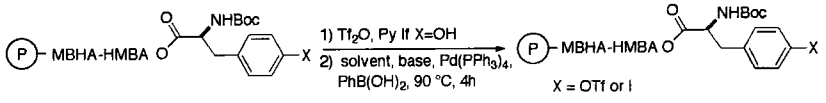

The crucial step in the analysis of the reaction was cleavage of the product from the MBHA-HMBA resin. It was found that freshly prepared $NaOCH_3$ (prepared from sodium metal and methanol) followed by a small amount of water cleanly provided the free acid in 89% of theory. All cleavages were performed directly on the instrument and collected simultaneously using a separate block. Analysis was performed by HPLC using an autoinjector. Suprisingly, in no instance was the conversion of Tyr(Tf) to Bip observed. However, the Phe(4-I) was converted to some degree in every case. Table 1 illustrates the experimental results for the Boc-Phe(4-I) for each base and solvent employed. It was found that the best solvent/base combination was DMF and either Et_3N or DIEA. The control reactions indicated that no decomposition occurred and that the cleaved amino acid derivative could be isolated in the same purity as when loaded.

Table 1. *Effect of base and solvent.*

	DMF	Toluene	DMSO	DCB	DMA
Et_3N	54%	<10%	16%	16%	15%
DMAP	42%	14%	14%	11%	14%
DIEA	53%	49%	43%	46%	44%
K_2CO_3	trace	trace	trace	trace	trace

Step 2. To determine the scope of the reaction, twelve different boronic acids were employed. In addition, six different catalysts were compared under the optimized reaction conditions to provide insight on the necessary nature of the catalyst. Listed in the following tables are the reagents and catalysts used in the study. The reactions were carried out under the optimized conditions from the previous study. However, the number of equivalents of base was increased from 5 to 10, the number of equivalents of catalyst increased from 0.05 to 0.1, and the number of equivalents of $ArB(OH)_2$ increased from 3 to 5. The tables indicate the approximate conversion yield based on HPLC analysis of the crude reaction mixtures. All measurements were made by monitoring at 254 nm and all yields are based on direct integration with respect to starting material. No detector response corrections were made.

Table 2. *Aryl boronic acid substituent effect.*

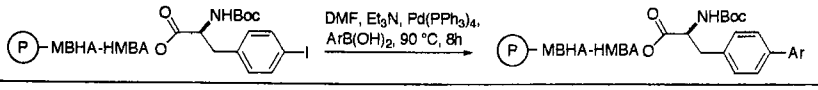

Entry	Substrate	Yield[a]
1	$PhB(OH)_2$	72%
2	2-Thiophene-$B(OH)_2$	65%
3	3-Thiophene-$B(OH)_2$	79%
4	3-NH_2-$PhB(OH)_2$	76%
5	4-CF_3-$PhB(OH)_2$	36%
6	3-CF_3-$PhB(OH)_2$	60%
7	4-CHO-$PhB(OH)_2$	25%
8	4-Cl-$PhB(OH)_2$	59%
9	4-CH_3-$PhB(OH)_2$	67%
10	4-F-$PhB(OH)_2$	69%
11	1-Np$B(OH)_2$	82%
12	2-CHO-$PhB(OH)_2$	74%

Table 3. *Catalyst effect.*

Entry	Catalyst	Yield[a]
13	$Pd(PPh_3)_2(OAc)_2$	25%
14	$Pd(PPh_3)_2Cl_2$	18%
15	$Rh(PPh_3)_3Cl$	18%
16	$Pd(OAc)_2$	24%
17	$Pd_2(PhCH{=}CHCOCH{=}CHPh_3)\cdot CHCl_3$	44%
18	$Pd(PPh_3)_4$	72%

[a] Based on HPLC analysis with respect to unreacted starting material.

In conclusion, we have demonstrated that the Pd catalyzed coupling of activated Phe derivatives can be accomplished on solid phase and that the optimum reaction conditions can vary dramatically from solution to solid phase. We have also shown how simultaneous, systematic, reaction condition optimization using automated synthesis can save weeks of experimentation in the preparation of interesting new organic molecules.

References

1. Hsieh, K., LaHann, T.R. and Speth, R., *J. Med. Chem.*, 32 (1989) 898.
2. Williams, D. and Kannan, R., *J. Org. Chem.*, 52 (1987) 5435.
3. Yabe, Y., Miura, C., Horikoshi, H. and Baba, Y., *Chem. Pharm. Bull.*, 24 (1976) 3149.
4. Shieh, W.C. and Carlson, J.A., *J. Org. Chem.*, 57 (1992) 379.

Peptides: Chemistry, Structure and Biology
Pravin T.P. Kaumaya and Robert S. Hodges (Eds.)
Mayflower Scientific Ltd., 1996

57

The Use of Ion-pairing Reagents Improves the Separation of Hydrophobic Peptides by Capillary Electrophoresis

L.M. Martin

College of Pharmacy, University of Rhode Island, Kingston, RI 02881, USA

Introduction

We have previously synthesized several variable region antibody fragments (68 and 63 amino acids) by solid phase peptide synthesis [1]. C-4 and C-18 RP HPLC analysis under standard conditions of acetonitrile/TFA/water and isopropanol/TFA/water gave poor resolution of these peptides, probably due to aggregation and irreversible binding to the chromatographic support. It is also likely that the synthetic peptides fold in some fashion, and thus several peaks could result from a single, pure sample [2].

Capillary electrophoresis is a relatively new technique for the separation of peptides [3], and it builds upon the principles of both traditional electrophoretic techniques and HPLC separation strategies. Current reviews show it to provide an extremely promising orthogonal separation method [4, 5]. We compared changes in pH, wall coating, and micellar and non-micellar surfactant buffer additives in the CE separation of synthetic antibody fragments VH(1-68) and VL(1-63).

Results and Discussion

CE separations were run at high voltage (30 kV, 72 cm 50 μm i.d.capillary) on several different instruments. Buffer exchange was easily accomplished by vacuum introduction of the buffer into the capillary, and separate capillaries were used for free-solution, coated, and surfactant based separations. Capillaries were conditioned with 1 N NaOH for one hour before washing with the separation buffer. The lyophilized peptide (10% HOAc) was dissolved in either water, or a 1:10 dilution of buffer (1 mg/ml) and 7 nl of a 5-10 μl sample (approx. 1 pmole) was injected by vacuum. Detection was quantitative UV (210 nm). Initial CE runs on uncoated bare silica capillaries gave a saw-toothed broad peak, characteristic of strong adsorption on the wall of the capillary. To prevent the cationic peptides from adhering to the wall of the capillary (pI's>8.5), the pH was increased to pH 9.4. Micellar electrokinetic capillary chromatography (MECC) separations allowed partitioning of the analyte between the aqueous buffer and a micelle. MECC using 100 mM SDS gave excellent separation of our crude synthetic mixture, showing baseline separation of two major components (Figure 1, left).

In the absence of surfactant, the peak shape was still quite broad, due to aggregation of the synthetic peptides. Ion-pairing reagents, such as pentane sulfonic, hexane sulfonic, and octane sulfonic acids, were tested for the ability to prevent aggregation of the

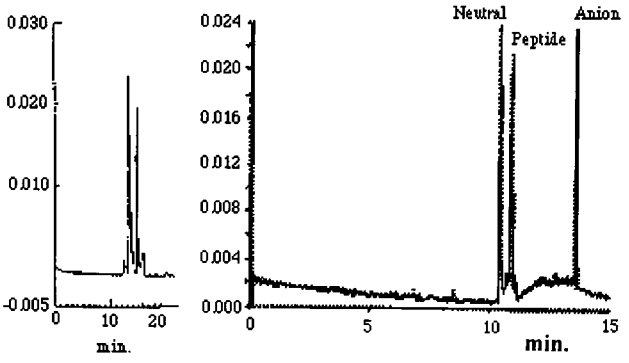

Figure 1. *Left: MECC 100 mM SDS , 25 mM phosphate pH 6.5, Right: 50 mM pentane sulfonic acid , 20 mM borate pH 9.98. VH(1-68) on an uncoated capillary, 417 V/cm².*

synthetic peptides [6]. Pentane sulfonic acid (50 mM) in the CE of VH(1-68) improved peak shape and revealed one main synthetic product with a significant minor component, which is slightly more hydrophobic (Figure 1, right). CE of both peptides with hexane sulfonic and octane sulfonic acids in buffer gave only one peak (inadequate resolution).

C1 coated capillaries (Supelco) also prevented adsorption of the peptides to the wall of the capillary. However, the peak shape was broad, indicating residual aggregation. The aggregation of VH(1-68) and VL(1-63) may be a dynamic process which involves the association between peptides on their exposed hydrophobic faces. This face is buried in the native protein, and aggregation is inhibited by preferential association with the ion-pairing reagent. The dependence of the CE separation on the chain length of the ion-pairing reagent may reflect a complimentarity of the exposed hydrophobic surface with the alkyl chain length.

Acknowledgments

Financial support from the National Institutes of Health (PHS DK01260), and helpful discussions with R.B. Merrifield are gratefully acknowledged.

References

1. Martin, L.M. and Merrifield, R.B., in Smith, J.A. and Rivier, J.E. (Eds.), 'Peptides: Chemistry, Structure and Biology', ESCOM, Leiden, The Netherlands, 1992, p. 849.
2. Cohen, S.A., Benedek, K.P., Dong, S., Tapuhi, Y. and Karger, B.L., *Anal. Chem.*, 56 (1984) 217.
3. Jorgenson, J.W. and Lukacs, K.D., *Science*, 222 (1983) 266.
4. Deyl, Z. and Struzinsky, R., *J. Chromatogr.*, 569 (1991) 63.
5. Landers, J.P. *Bioessays*, 13 (1991) 253.
6. Grossman, P.D., Colburn, J.C., Lauer, H.H., Nielsen, R.G., Riggin, R.M., Sittampalam, G.S. and Rickard, E.C., *Anal. Chem*,. 61 (1989) 1186.
7. Moring, S.E. and Nolan, J.A., in 'Abstracts of the Second International Symposium on High Performance Capillary Electrophoresis, San Francisco' and 'ABI Research News', 1990.

Peptides: Chemistry, Structure and Biology
Pravin T.P. Kaumaya and Robert S. Hodges (Eds.)
Mayflower Scientific Ltd., 1996

58

Formation of N-methyl α-Amino Alcohols and Spiroborates by Borane Reduction of Boc-amino Acids

J.B. Halstrøm and A.F. Spatola

Novo Nordisk A/S, DK2880 Bagsvaerd, Denmark
Department of Chemistry, University of Louisville, Louisville, KY 40292 USA

Introduction

Selective borane reduction of amides has been reported in the presence of a tertiary carbamate [1, 2]. In the reduction of Boc-proline to Boc-prolinol we also find that the tertiary carbamate has excellent stability towards excess borane, even at room temperature. However, when the reduction of other Boc-amino acids is allowed to finish at room temperature with an excess of borane, several over-reduction products are detected by TLC, MS and NMR. These products are reminiscent of those originally reported for the reduction of carbamates with $LiAlH_4$ [3], a far less selective reagent than BH_3 [1, 4].

Results and Discussion

Several Boc amino acids were treated with borane/THF [4, 5] under conditions which had given good yields of Boc-prolinol from Boc-proline (6 mol borane per mol Boc-amino acid, first at 0°C, then at 15-20°C for up to 24 hours). TLC monitoring showed rapid formation of the expected products at 0°C and disappearance of the starting Boc-amino acids. Extended stirring at room temperature, however, caused transformation of the initial products to ninhydrin-positive, more slowly migrating ones. After quenching with water and extraction with ethyl acetate, these secondary products remained in the aqueous phase. Proton NMR of the isolated products confirmed the loss of the Boc group, and revealed the presence of an additional methyl group. Plasma desorption mass spectrometry (PDMS) of the crude products yielded molecular masses indicative of N-methyl amino alcohols dimerization to form the spiroborate (Figure 1) [6] and showed also the presence of the free N-methyl amino acids (Table 1).

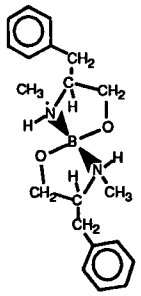

Figure 1. *Spiroborate formed by N-methyl amino alcohol dimerization through a boron atom.*

Table 1. *Analytical data of formed N-methyl amino alcohols.*

N-Me-L-	MW(MS)†	N-Me (dppm)*	MP(°C)	[a]**	Spiroborate MW(MS)†
Ala-ol	n.d.	2.6	n.d.	n.d.	186.2(187.0)
Phe-ol	164.7(165.2)	2.2	69-71	+20.2°	337.9(339.2)
Ser(Bzl)-ol	194.7(195.3)	2.2	41-43	+5.3°	n.d.
Tyr(Cl_2Bzl)-ol	339.4(340.3)	2.6	174-176	+8.1°	688.6(689.4)

†Theory in parenthesis. * ^{1}H NMR in D_2O. ** 589nm/27°C (c 2 in ethanol).

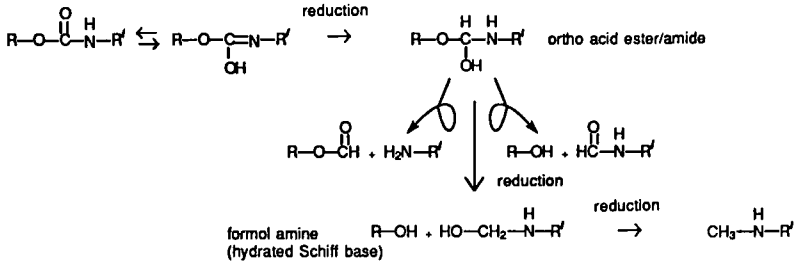

Scheme 1. *Proposed reaction sequence of carbamates (urethanes) with excess borane.*

Traces of the corresponding non-methylated amino alcohols were detected in varying amounts by TLC using reference compounds, or by PDMS. TLC of the ethyl acetate phase showed the presence of some Boc amino alcohol plus an N-acylated, presumably N-formylated amino alcohol. CHN analyses of N-Me-L-Phe-ol and N-Me-L-Ser(Bzl)-ol purified by flash chromatography were in agreement with theory. Yields of purified N-methyl amino alcohols varied from 10-40%. No attempt was made to optimize the yields. N-Me-L-Phe-ol analogously obtained from Z-L-phenylalanine had the same melting point and specific optical rotation as shown in Table 1. Since the Boc group of Boc-prolinol is not reduced, the mechanism probably involves enolization to the isocarbamate (Scheme 1). It is apparent that the yield of any particular product, *e.g.*, the N-Me derivative, may be profoundly influenced by changes in R or R'.

With 3 mol of borane and 1 mol of Boc amino acid reacting over 2 hours at 0°C, the desired Boc-amino alcohols were secured in good yields. Attention is called to an unexpected side reaction in borane reductions involving secondary carbamates. By appropriate choice of R and R', the unexpected side reaction might be exploited to provide N-methyl amines not directly accessible by other routes.

References

1. Brown, H.C. and Heim, P., *J. Org. Chem.*, 38 (1973) 912.
2. Curran, W.V. and Angier, R.B., *J. Org. Chem.*, 31 (1966) 3867.
3. Gaylord, N.G., 'Reduction with Complex Metal Halides', Interscience Publishers, New York, N.Y., 1956, p 636.
4. Yoon, N.M., Pak, C.S., Brown, H.C., Krishnamurthy, S. and Stocky, T.P., *J. Org. Chem.*, 38 (1973) 2786.
5. Stanfield, C.F., Parker, J.E. and Kanellis, P., *J. Org. Chem.*, 46 (1981) 4799.
6. Santiesteban, F., Campos, M.A., Morales, H., Contreras, R. and Wrackmeyer, B., *Polyhedron*, 3 (1984) 589

Session II
Peptide Delivery/Pharmaceutical

Chairs: Jean Rivier and
James Samanen

Peptides: Chemistry, Structure and Biology
Pravin T.P. Kaumaya and Robert S. Hodges (Eds.)
Mayflower Scientific Ltd., 1996

59
Oral Delivery of Peptide-Type Compounds

G.L. Amidon

College of Pharmacy, The University of Michigan, Ann Arbor, MI 48109, USA

Introduction

Oral delivery of peptide-type compounds has been one of the major deterrents to fully exploiting the potency and selectivity of peptide-type drugs. Our recent research has focused on studying the human intestinal membrane permeability and correlations between animal models and humans in order to determine the membrane permeability necessary for good oral absorption. We have also exploited the peptide transport pathway for improving the permeability of polar compounds.

Permeation of the intestinal membrane, including permeation of the mucin and brush-border membrane region of the intestinal membrane, is the first barrier that needs to be overcome in order to achieve a good oral absorption and systemic availability. We are currently measuring human intestinal membrane permeabilities for a variety of compounds including passive and carrier-mediated transport mediated drugs in order to define the essential limiting permeability for good oral absorption [1, 2]. Included in these studies are well absorbed nutrients and a poorly absorbed peptide-type drug, enalaprilate. The range of measured human permeabilities covers approximately a 100-fold range between the permeability of glucose of 1×10^{-3} cm/sec to that of enalaprilate of about 0.1×10^{-5} cm/sec. Other carrier-mediated drugs with relatively high permeabilities include L-dopa and phenylalanine. Based on these results, a permeability of about 1×10^{-4} cm/sec would lead to good oral absorption.

Results and Discussion

A peptide-type drug of particular interest is cyclosporin with a molecular weight of approximately 1200. While estimates of its systemic availability are in the 20-30% range, estimates of its extent of absorption are as high as 70-90% [3]. Based on the molecular weight dependence of oral absorption of polyethylene glycols [4] and assuming that the molecular weight dependence is due to a molecular weight dependence of the diffusion coefficient rather than the partition coefficient, *i.e.*,

$$P_{mem} = \frac{PC_{mem}, D_{mem}}{\delta} \qquad \text{and} \qquad D_{mem} = \alpha M_w^{\beta}$$

we obtain the result shown in Figure 1 where P_{mem}, PC_{mem}, D_{mem} and δ are the membrane permeability, partition coefficient, diffusivity and thickness, respectively, α and β are

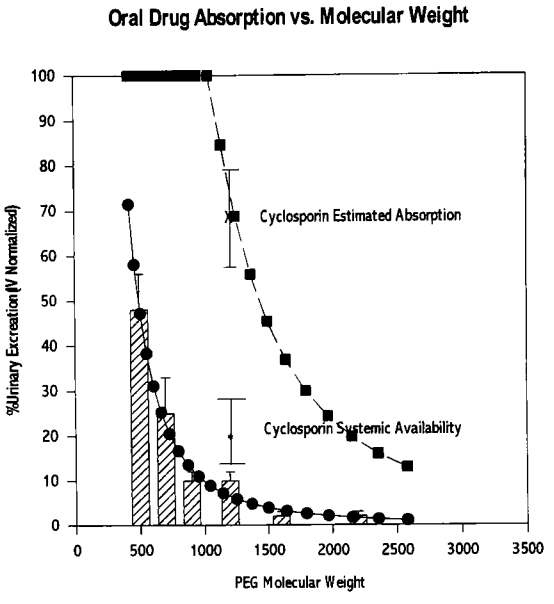

Figure 1. *Percent urinary excretion of PEG in 6 hr in rats as a function of molecular weight.*

fitted parameters. The molecular weight dependence fitted through the polyethylene glycol data when shifted due to PC through the estimated absorption of cyclosporin indicates that good oral absorption may be achieved for molecular weight compounds as high as molecular weight 2000 or more, particularly if they are nonpolar. In a separate set of studies, we have determined the intestinal permeability of cyclosporin in the rat model and estimated its permeability to be about $0.4x10^{-4}$ cm/sec. This is in good agreement with the expected fraction absorbed based on the membrane permeability [2]. However, it remains controversial as to the principal limitation for cyclosporin systemic availability, *i.e.*, solubility or metabolism [3]. However, these results suggest that the limitation may in fact be a permeability limitation due to the relatively high molecular weight. A point of considerable significance based on the cyclosporin results is that the molecular weight limitation for good oral absorption may be considerably higher than it was commonly thought and that there are many potential drugs in the molecular weight range of 500-2000.

For polar compounds, membrane transport is usually facilitated by pores or carriers with pores usually functioning for small ions and carriers functioning for larger molecules such as nutrient and nutrient analogues [5]. In Figure 1, for example, results for phenylalanine and L-dopa indicate relatively high permeability while results for α-methyldopa [6] indicate it has a significantly lower permeability and that its poor oral availability is due to the permeability limitation. Since it is expected that the peptide transporter is less structurally specific for substrates we have made prodrugs of α-methyldopa that would utilize the peptide transporter [7, 8]. In animal studies, the membrane permeability of α-methyldopa was increased by more than 10-fold by the

peptide prodrugs. The results in Table 1 show the increase in systemic availability that was achieved using one of these prodrugs with the systemic availability approaching 100%.

Thus, these results indicate that size up to a molecular weight of 2000 or more is not a fundamental limiting factor in oral absorption and that for polar drugs, specific transport pathways can be utilized to improve the permeability of polar peptide analogues.

Table 1. *Absorption (F) of α-methyldopa and a peptide prodrug* [7, 8].

	α-methyldopa (IV)	α-methyldopa (jejunal)	α-methyldopa from prodrug [a]
C_{max} SEM (ng/ml)		109.0 ± 31.4	235.0 ± 37.4
T_{max} (min)		15.0	60.0
AUC (ng.hr)/ml	380.87 [b]	127.49	358.38
F	1.0	0.33	0.94

[a] Weight equivalent of α-methyldopa
[b] AUC for IV dose was normalized to the jejunal dose

Acknowledgments

The financial support of the National Institutes of Health General Medical Sciences and the Food and Drug Administration is gratefully acknowledged.

References

1. Lennernas, H., Ahrenstedt, O., Hallgren, R., Knutson, L., Ryde, M. and Paalzow, L.K., *Pharm.Res.*, 9 (1992) 1243.
2. Amidon, G.L., Lennernas, H., Shah, V.P. and Crison, J.R., *Pharm. Res.*, 12 (1995) 413.
3. Wacher, V.J., Wu, C.Y. and Benet, L.Z., *Mol. Carcinog.*, (1995), submitted.
4. Donovan, M.D., Flynn, G.L. and Amidon, G.L., *Pharm. Res.*, 7 (1990) 808.
5. Sadee, W., Drubbisch, V. and Amidon, G.L. (1995) in preparation.
6. Merfeld, A.E., Mlodozeniec, A.R., Cortese, M.A., Rhodes, J.B., Dressman, J.B. and Amidon, G.L., *J. Pharm. Pharmacol.*, 38 (1986) 815.
7. Hu, M., Subramanian, P., Mosberg, H.J. and Amidon, G.L., *Pharm.Res.*, 6 (1989) 66.
8. Bai, J.P-F., Hu, M., Subramanian, P., Mosberg, H.I. and Amidon, G.L., *J. Pharm. Sci.*, 81 (1992) 113.

Peptides: Chemistry, Structure and Biology
Pravin T.P. Kaumaya and Robert S. Hodges (Eds.)
Mayflower Scientific Ltd., 1996

60

A Systematic Investigation of Factors that Enhance Penetration of Peptides Across the Blood Brain Barrier

V.J. Hruby[1], T.P. Davis[2], R. Polt[1], H. Bartosz-Bechowski[1], A. Misicka[1], A. Lipkowski[1], S.D. Sharma[1], G. Li[1], G. Bonner[1], J.-P. Meyer[1], D. Patel[1], X. Qian[1], M. Romanowski[1], H.I. Yamamura[2], F. Porreca[2] and D.F. O'Brien[1]

Departments of [1]Chemistry and [2]Pharmacology, University of Arizona, Tucson, AZ 85721, USA

Introduction

The brain possesses hundreds of peptides that act as neurotransmitters and neuromodulators and which control and modulate most bodily functions [1]. The utilization of these ligands as drugs has been limited by their lack of receptor selectivity, their rapid proteolytic degradation, the relative lack of penetration of the BBB (blood brain barrier) by many of the native peptides, and the belief by many that these problems cannot be solved. Considerable effort has been made to overcome these problems [1, 2], but a comprehensive systematic approach that addresses all of them and that works is still lacking. In view of the enormous significance of this problem to human biology and medicine, we have sought to establish a highly systematic approach to investigate these problems and to find solutions. We outline here some of the progress we have made.

Results and Discussion

The systematic approach that we are pursuing includes the following major components: 1) develop highly selective ligands for brain receptor types and subtypes; 2) utilizing conformational constraint and other structural modifications to stabilize peptides against proteolytic degradation; 3) establish structural peptides (consensus sequences) that can be appended to stable, receptor selective ligands at ancillary sites and that can serve as specific sites of cleavage in the brain - prodrug approach; 4) systematically investigate lipophilicity, amphiphilicity, and dynamics as approaches to enhancing penetration of the BBB; 5) evaluate mechanisms for keeping peptides in circulation; 6) evaluate the use of putative carrier-mediated mechanisms such as lipid transporters, glucose transporters, polycation transporters, *etc.* for passage of peptide conjugates through the BBB.

Chemical/biological methods that are used to evaluate progress include: 1) multiple bioassays to establish selectivity; 2) peptide stability studies using serum, brain and other tissue homogenates, and pure enzymes known to be in the brain or at the BBB; 3) development of model membranes for characterization of the thermodynamics and kinetics of peptide-membrane interactions in order to assess peptide interactions with

the BBB; 4) use of the bovine microepithelial cell (BMEC) assay [3] as an *in vitro* screen for BBB penetration; 5) use of *in vivo* assays such as antinoception following peripheral administration with controls to establish BBB penetration.

Table 1. *Peptide prodrugs in vitro conversions in 15% rat brain homogenates.*

Prodrug	Rat Brain Homogenate-$T_{1/2}$(min)
Phe-Tyr-D-Pen-Gly-Phe-D-Pen	3.94
Tyr-D-Pen-Gly-Phe-Cys-Arg-Pro-Ala	9.21
Tyr-D-Pen-Gly-Phe-D-Pen-Phe	109
Tyr-D-Pen-Gly-Phe-Cys-Arg-Gly	40.5

We have made considerable progress in several of these areas. For example, utilizing structural modifications compatible with high receptor potency and selectivity such as cyclization, unusual amino acids, D-amino acids, and pseudopeptides we have developed a variety of peptide ligands that are completely stable to or highly stable against proteolytic degradation. These include the cyclic enkephalin [D-Pen^2,D-Pen^5]-enkephalin, the somatostatin derived μ opioid receptor selective antagonist CTAP (D-Phe-Cys-Tyr-D-Trp-Arg-Thr-Pen-Thr-NH_2), the dynorphin A analogue Tyr-Gly-Gly-Phe-Leu[ΨCH$_2$NH]Arg-Arg-Ile-Arg-Pro-Lys-NH_2, and the cyclic melanotropin Ac-Nle^4-c[Asp^5,D-Phe^7,Lys^{10}] α-MSH(4-10)-NH_2. These stable ligands were used to develop structural vectors that can be appended to them and which are rapidly and specifically cleaved to the bioactive peptide in brain homogenates such as Phe^0-Tyr-c[D-Pen^2, D-Pen^5]Enk, and Tyr-c[D-Pen-Gly-Phe-Cys]-Arg-Pro-Ala (see Table 1). These and other results suggest that specific structural vectors with varying rates of enzymatic cleavage can be developed to serve as prodrugs with a wide variety of brain half lives.

The BMEC assay has been used *in vitro* to quantitatively evaluate peptide passage through the BBB and has worked very well for evaluating peptides that utilize lipophilic, amphipathic or dynamic properties for BBB passage. However, the preparation does not maintain active transporter systems such as the glucose transporters found at the BBB. The method can provide such insights as the observation that *p*-chlorophenylalanine substitution systematically enhances penetration through the BBB (see Table 2). The position of the *p*-Cl Phe in the peptide chain does not appear to be a major factor, nor does the nature of the peptide (linear or cyclic). Comparison of BMEC data with data obtained for brain penetration for the same peptides when given *in vivo* by peripheral administration (i.v. or s.c.) suggests that the BMEC generally correlates well, and thus should serve as an excellent screen for penetration by ligands through the BBB. Model membrane peptidic studies reveal that the transfer of DPDPE type peptides from water to lipid bilayers is entropy driven, and so can be enhanced by more hydrophobic residues. In contrast, the transfer of biphalin type peptides is primarily due to enthalpic differences, and hence penetration can be enhanced by structural changes which favor a folded geometry.

Table 2. *BMEC permeability coefficient for selected peptide analogs.*

Peptide	BMEC Permeability Coefficient ($PCX10^{-4}$)
Tyr-D-Pen-Gly-Phe-D-Pen (DPDPE)	49.2
[Phe(*p*Cl)[4]]DPDPE	82.8
(Tyr-D-Ala-Gly-Phe-NH-)$_2$ (Biphalin)	55.0
[Phe(*p*Cl)[4]] Biphalin	92.0
D-Phe-Cys-Tyr-D-Trp-Arg-Thr-Pen-Thr-NH_2(CTAP)	4.6
[D-Phe(*p*C1)[1]]CTAP	7.6

As for peptides that are peripherally active following systemic administration, biphalin is a good case. Though biphalin is not very potent in classical binding (brain homogenates) or bioassays (MVD & GPI), it is a potent analgesic when given i.p. [4] and has very prolonged activity. Our biophysical studies indicate that it can undergo a conformational change in going from the aqueous to membrane environment, and that this can be important in aiding its penetration through the BBB. Perhaps more interesting is the potent and prolonged acting glycopeptide analogue of enkephalin Tyr-D-Cys-Gly-Phe-D-Cys-Ser(O-D-Glc)-Gly-NH_2 [5]. Though this peptide also is not very potent in classical binding and in vitro bioassays, it has potent and prolonged acting antinociceptive activity when given i.p. Perhaps its high stability and ability to stay in circulation can account to some degree for its activity, but more work will be needed to fully understand its ability to penetrate the BBB.

Though all the problems associated with developing a useful and predictable approach to design of peptide and peptidomimetic analogues that cross the BBB have not been solved, much progress has been made in this important area. Our systematic investigations suggest that a solution to these problems is possible and likely.

Acknowledgments

The financial support of the National Institute of Drug Abuse DA06284 and DA04248 and the Arizona Disease Control Council is gratefully acknowledged.

References

1. Pardridge, W.M., 'Peptide Drug Delivery to the Brain', Raven Press, New York, NY, USA, 1991.
2. Taylor, M.D. and Amidon, G.L. (Eds.), 'Peptide-Based Drug Design: Controlling Transport and Metabolism', ACS, Washington, D.C., 1995.
3. Audus, K.L. and Borchardt, R.T., *Pharmacol. Res.*, 3 (1986) 81.
4. Horan, P.J., Mattia, A., Bilsky, E.J., Weber, S.J., Davis, T.P., Yamamura, H.I., Malatynska, E., Applyard, S.M., Slaninova, J., Misicka, A., Lipkowski, A.W., and Hruby, V.J., *J. Pharmacol. Exp. Ther.*, 265 (1993) 1446.
5. Polt, R., Porreca, F., Szabo, L.Z., Bilsky, E.J., Davis, P., Abbruscato, T.J., Davis, T.P., Horvath, R., Yamamura, H.I., and Hruby, V.J., *Proc. Natl. Acad. Sci. USA.*, 91 (1994) 7114.

Peptides: Chemistry, Structure and Biology
Pravin T.P. Kaumaya and Robert S. Hodges (Eds.)
Mayflower Scientific Ltd., 1996

61
"O→N Intramolecular Acyl Migration"-type Prodrugs of Tripeptide Inhibitors of HIV Protease

Y. Kiso, T. Kimura, J. Ohtake, S. Nakata, H. Enomoto, H. Moriwaki, M. Nakatani and K. Akaji

Department of Medicinal Chemistry, Kyoto Pharmaceutical University, Yamashina-ku, Kyoto 607, Japan

Introduction

The human immunodeficiency virus (HIV), causative agent of AIDS, codes for an aspartic protease essential for retroviral maturation and replication. The HIV protease is a major target for the treatment of AIDS. We have designed and synthesized a series of HIV protease inhibitors containing an unnatural amino acid, allophenylnorstatine [Apns, (2*S*, 3*S*)-3-amino-2-hydroxy-4-phenylbutyric acid] as a transition state mimic. Among them, a tripeptide inhibitor, KNI-272 has excellent characteristics in protease inhibition (K_i=0.0055nM), antiviral activity against a wide spectrum of HIV strains, enzyme selectivity and toxicity. KNI-272 as an oral anti-HIV drug has entered clinical trials [1].

In general, potent inhibitors of aspartic proteases are less hydrophilic and less soluble in water, since the enzymes recognize sequences consisting of hydrophobic amino acids, and some of our inhibitors showed low solubility in phosphate buffered saline (PBS). Solubilization is one of the most important problems for administration of insoluble drugs. In order to overcome this problem, we sought the soluble prodrugs and can report a novel class of "O→N intramolecular acyl migration"-type prodrugs of HIV protease inhibitors for solubilization.

Results and Discussion

Design. The N, O-intramolecular acyl migration is known as a side reaction of Ser- or Thr-containing peptides. The β-hydroxyl groups are acylated by N→O shift under acidic conditions and the resulting O-acyl products can be readily converted to the N-acyl compounds in aqueous buffer (Figure 1). The liberated ammonium ion enhances the solubility of O-acyl products in water. Considering these features, we designed O→N intramolecular acyl migration-type prodrugs of HIV protease inhibitors. Hurley *et al.* reported a study on N, O-acyl migration of renin inhibitor [2].

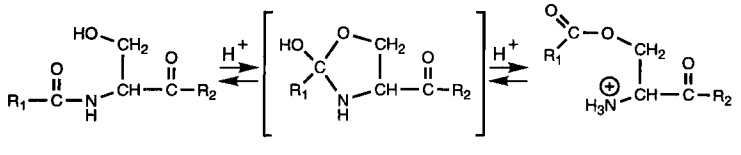

Figure 1. *N,O-Intramolecular acyl migration.*

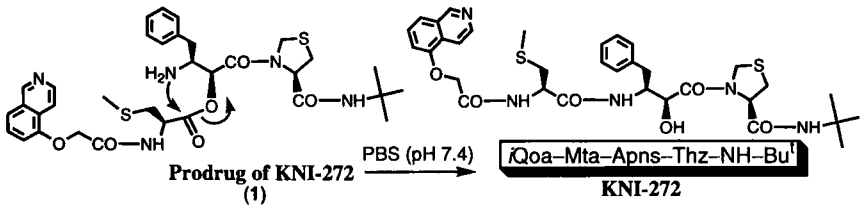

Figure 2. *Conversion of prodrug of KNI-272 into active form by "O →N intramolecular acyl migration".*

Prodrug of KNI-272. The N→O acyl transfer product (**1**) of KNI-272 is regarded as a prodrug because the O-acyl compound can be readily converted to the N-acyl compound in aqueous buffer (Figure 2).

The O-acyl derivative (**1**) of KNI-272 was synthesized as shown in Figure 3. Esterification of the hydroxyl group of **4** with Boc-Mta-OH was achieved in good yield (88%) by the DCC-dimethylaminopyridine (DMAP, 0.1 equiv.) method. *N*-Z protected prodrug (**6**), prepared from **5**, was treated with trifluoroacetic acid (TFA)-anisole (10 equiv.)-dimethylsulfide (10 equiv.) [r.t., 14hr.] to remove the Z group by a "push-pull" mechanism. In the crude sample, 1.2% of byproduct was detected by HPLC-analysis. This was a result of racemization during esterification of Boc-Mta-OH. After purification on a reverse phase-HPLC column, the exchange of counter anion for chloride gave a desired product (**1**) in 78% yield.

The prodrug (**1**) was readily soluble in water and the solubility of this compound was greater than 200mg/ml. The derivatization of KNI-272 into prodrug (**1**) increased its solubility more than 2000-fold. When a solution of prodrug (**1**) of KNI-272 in PBS (pH 7.4) was incubated at 37°C, the prodrug was smoothly converted into KNI-272 by "O→N intramolecular acyl migration" (Figure 4). The half-life period of the prodrug was approximately 1 min. From the analysis by HPLC, the O→N acyl migration proceeded without any side reactions. After *i.d.* administration of the prodrug (**1**), bioavailability of KNI-272 was 35% in rats.

Prodrug of KNI-279. A substitution of Mta, P_2 position of KNI-272, into Val residue gave another inhibitor, KNI-279 (*i*Qoa-Val-Apns-Thz-NHBu^t), which was as potent as KNI-272 [3]. We have also prepared a prodrug (**7**) of KNI-279 by the essentially same manner as synthesis of prodrug of KNI-272. The prodrug of KNI-279 showed good solubility. Conversion of **7** into KNI-279, as in the case of conversion of **1** to KNI-272,

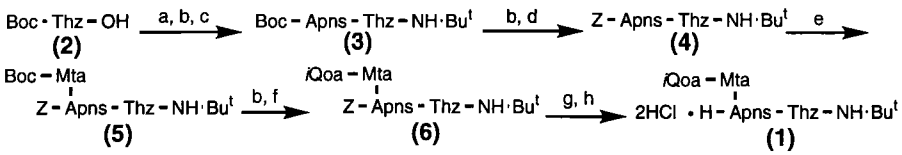

Figure 3. *Synthetic route to prodrug (1) of KNI-272. iQoa = 5-isoquinolyloxyacetyl; Mta = L-methylthioalanine; Thz = L-thiazolidine-4-carboxylic acid. Reagents: a, NH_2Bu^t, DCC, HOBt; b, 4N HCl-DOX; c, Boc-Apns-OH, DCC, HOBt; d, Z-OSu; e, Boc-Mta-OH, DCC, DMAP; f, iQoa-OH, DCC, HOBt; g, TFA, anisole, Me_2S; h, HCl-AcOEt.*

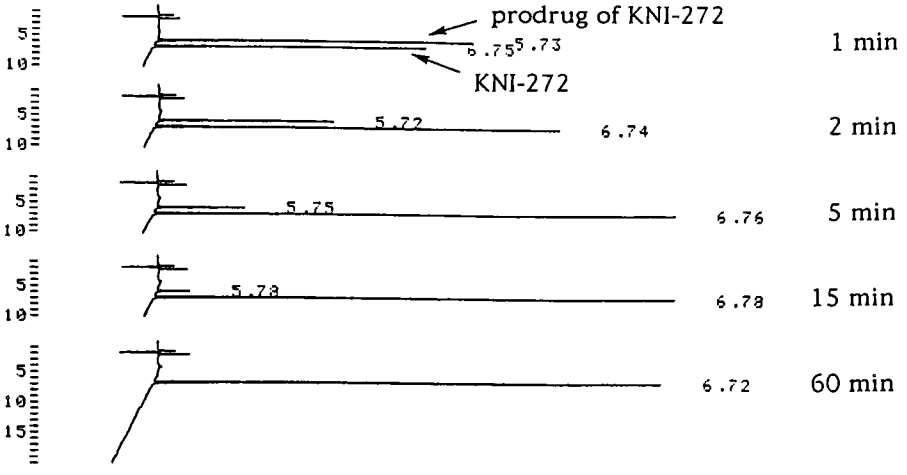

Figure 4. *HPLC patterns of conversion of prodrug (1) to KNI-272 at each reaction time. Column: YMC AM-302(ODS) (4.6x150mm), MeCN 30-80% (20min) in 0.1% TFA, flow rate: 1ml/min, O.D.: 230nm. Retention time; prodrug of KNI-272: 5.72-5.78min, KNI-272: 6.72-6.78min.*

was observed, the half-life period of 7 being 7 min. The conversion rate of 7 was slower than **1**, which may be due to the steric hindrance of the Val residue.

Prodrug containing statine-type backbone. In order to demonstrate the applicability of prodrugs containing the statine-backbone, we prepared a model compound, *i*Qoa-Mta-AHPPA-Thz-NHBu^t [AHPPA = (3*S*, 4*S*)-4-amino-3-hydroxy-5-phenylpentanoic acid], and its prodrug form. The O→N intramolecular acyl migration of the statine-type prodrug was very fast and no starting material was detected in 1min in PBS (pH 7.4). This fast conversion is explained by the lesser steric hindrance of statine in contrast to norstatine-type compounds, owing to the additional methylene.

To conclude, the prodrugs based on "O→N intramolecular acyl migration" had good solubility in water and could be converted into active form in PBS (pH 7.4). These results show that the prodrugs can be administrated by intravenously or orally without special techniques.

References

1. Mimoto, T., Imai, J., Kisanuki, S., Enomoto, H., Hattori, N., Akaji K. and Kiso, Y., *Chem. Pharm. Bull.*, 40 (1992) 2251; Kageyama, S., Mimoto, T., Murakawa, Y., Nomizu, M., Ford, Jr., H., Shirasaka, T., Gulnik, S., Erickson, J., Takada, K., Hayashi, H., Broder, S., Kiso, Y., Mitsuya, H., *Antimicrob. Agent Chemother.*, 37 (1993) 810.
2. Hurley, T.R., Colson, C.E., Hicks G. and Ryan M.J., *J. Med. Chem.*, 36 (1993) 1496.
3. Kisanuki, S., Mimoto, T., Imai, J., Enomoto, H., Hattori, N., Takahashi, O., Katoh, R., Tanaka, S., Sakikawa, H., Kimura, T., Akaji, K. and Kiso, Y., in Yanaihara, N., (Ed.) 'Peptide Chemistry 1992', ESCOM, Leiden, The Netherlands 1993, p. 439.

Peptides: Chemistry, Structure and Biology
Pravin T.P. Kaumaya and Robert S. Hodges (Eds.)
Mayflower Scientific Ltd., 1996

62

A Novel Method for Delivering Synthetic Peptides into Living Cells to Regulate Intracellular Signal Transduction

Y.-Z. Lin, S. Yao, R.A. Veach and J. Hawiger

Department of Microbiology and Immunology, Vanderbilt University School of Medicine, Nashville, TN 37232, USA

Introduction

Delivery of synthetic peptides into living cells is exceedingly difficult because of the poor permeability of most peptides across biological cell membranes. This greatly restricts the use of synthetic peptides in studying and regulating the biological functions of many intracellular proteins and in developing peptide-based therapeutic drugs. We have devised a novel biochemical approach to deliver synthetic peptides into intact cells [1]. We chose as a carrier the hydrophobic region (h-region) of a signal peptide, a segment important for the secretion of intracellular proteins [2]. When such a cell-permeable peptide carried a functional cargo in the form of the nuclear localization sequence (NLS) of the transcription factor NF-κB p50 [3,4], it inhibited subcellular traffic of NF-κB/Rel complexes from the cytoplasm to the nucleus in cultured endothelial and monocytic cells stimulated with agonists [1]. This approach, called Cell-Permeable Peptide Import (CPPI) (1), obviates the need for permeabilization with pore-forming reagents or microinjection of individual cells. Thus, CPPI can be applied to the basic study of intracellular protein-protein interaction and protein trafficking involved in signal transduction and gene transcription.

Results and Discussion

We first designed a 41-residue synthetic peptide (SKP peptide in Figure 1) comprising the h-region of the signal sequence of Kaposi fibroblast growth factor (K-FGF) [5] in its amino-terminal segment. To determine the cellular import of SKP peptide, NIH 3T3 cells were incubated with ^{125}I-labeled SKP peptide and the amount of cell-associated ^{125}I-SKP peptide was measured. In three independent experiments, 4% of the added ^{125}I-SKP peptide was associated with the cells following 30 min incubation. No significant loss of cell-associated radioactivity was observed after extracellular protease treatment (untreated: 21,323 ± 853, pronase-treated: 21,791 ± 1,953, and trypsin-treated: 23,193 ± 310 cpm/1 x 10^6 cells), suggesting the intracellular location of cell-associated ^{125}I-SKP peptide. On average, 20 times more (molar concentration) ^{125}I-SKP peptide was associated with the cells compared to the control ^{125}I-KP peptide lacking a hydrophobic region. This indicates that the h-region of the K-FGF signal sequence mediates the cellular import of SKP peptide.

^{125}I-SKP peptide import into cells was not blocked by adding a 200-fold excess of unlabeled SKP peptide, indicating the lack of receptor-mediated import of ^{125}I-SKP peptide. Inhibitors of endosomal/lysosomal function, ammonium chloride and chloroquine, as well as the protein synthesis inhibitor, cycloheximide, did not affect cellular uptake of ^{125}I-SKP peptide compared to control cells (23,040 ± 2,489, 26,138 ± 5,346, 25,671 ± 522, and 26,089 ± 3,174 cpm/1.6 x 10^6 cells, respectively). Intracellular ATP as a high energy source did not seem to be required for peptide import because ^{125}I-SKP peptide import into cells depleted of ATP was similar to that of control cells (22,266 ± 3,602 *vs.* 20,189 ± 2,109 cpm/1.6 x 10^6 cells).

SKP: ^{1}AAVALLPAVLLALLAPEILLPNNYNAYESYKYPGMFIALSK^{41}

KP: ^{1}EILLPNNYNAYESYKYPGMFIALSK^{25}

N50: ^{1}**VQRKRQKLMP**^{10}

SN50: ^{1}AAVALLPAVLLALLAP**VQRKRQKLMP**^{26}

SM: ^{1}AAVALLPAVLLALLAP*AAADQNQ*LMP^{26}

Figure 1. *Sequences of cell membrane-permeable and control peptides. The membrane-translocating hydrophobic sequence derived from the h-region of the predicted signal peptide sequence of K-FGF is underlined. The peptides without this hydrophobic sequence (KP and N50) were used as comparative controls. The nuclear localization sequence of NF-κB p50 is printed in bold face and the mutated residues in the SM peptide are in italics.*

To test the hypothesis that cell-permeable peptides can carry a functional domain such as the NLS, we synthesized a cell-permeable peptide bearing the NLS of NF-κB p50 subunit (SN50 in Figure 1). Six-step Z-position confocal laser scanning microscopy was employed to verify the import of the SN50 peptide in murine endothelial LE-II cells by analyzing the fluorescent signal of cell sections in an indirect immunofluorescence assay. This import was time-, concentration-, and temperature-dependent. At 4°C, no import of cell-permeable peptide was observed. The maximal fluorescence was observed at 37°C between 30 min and 1 hr in the concentration range of 50 to 100 μg/ml. Within this concentration range, the peptide was not cytotoxic.

The functional effect of the SN50 peptide on nuclear translocation of NF-κB/Rel complexes in cells activated by the proinflammatory agonists, LPS and TNFα, was determined. The NF-κB/Rel complexes translocated from the cytoplasm to the nucleus were analyzed in the nuclear extracts in an electrophoretic mobility shift assay (EMSA) [6]. As shown in Figure 2A, LPS-induced nuclear translocation of the NF-κB in LE-II cells was inhibited by SN50 peptide. In contrast, two control peptides, N50 and SM, were without measurable effect (Figure 2A). N50 peptide lacks a cell-permeable hydrophobic region and contains only the NLS of p50. Cell-permeable SM peptide has mutations in the NLS of SN50 peptide (Figure 1). The inhibition of NF-κB nuclear translocation by SN50 peptide was concentration-dependent, reaching maximum at the extracellular concentration of 50 μg/ml (18 μM) (Figure 2B).

The LPS- or TNF α-induced nuclear translocation of NF-κB was also inhibited in SN50 peptide-treated THP-1 cells. Consistent with the results of the EMSA, the

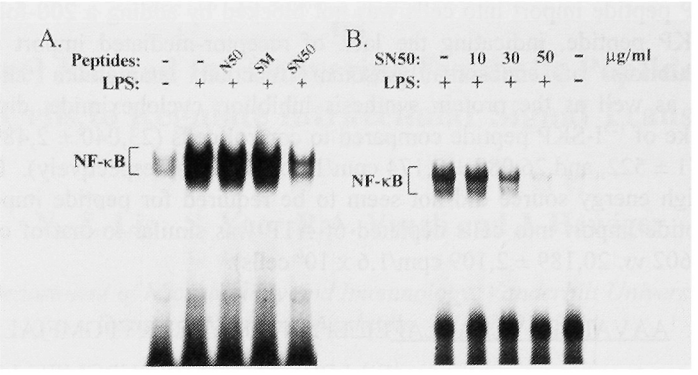

Figure 2. *(A) Cell-permeable SN50 peptide inhibits nuclear translocation of NF-κB induced by LPS in murine endothelial LE-II cell line. Confluent LE-II cells were treated with different peptides (50 μg/ml) for 15 min prior to stimulation with LPS (10 ng/ml) for 2 h. Equivalent amounts of nuclear extracts were prepared and assayed for κB binding activity with [^{32}P]-labeled double-stranded oligonucleotide κB probe using EMSA. (B) Inhibitory effect of SN50 peptide on nuclear translocation of NF-κB in LE-II cells is concentration-dependent.*

immunoblot analysis of the nuclear extracts of LPS- or TNF α-stimulated cells pre-treated with SN50 peptide did not show detectable p50 protein (not shown).

The cell-permeable peptides can be imported into different cell types, such as NIH 3T3 cells, BHK-21 cells, human and murine endothelial cells, human monocytic cells, and T cells. In addition, hydrophobic regions from other signal sequences also endowed peptides with cell membrane permeability. Taken together, our results demonstrate that the cell-permeable peptide method (CPPI) can be used to study intracellular processes involving proteins with functionally distinct domains.

Acknowledgments

This work was supported by NIH grants HL45994, HL30647, GM52500 and by a Mellon Foundation Award for Faculty Development.

References

1. Lin, Y.Z., Yao, S., Veach, R.A., Torgerson, T.R., and Hawiger, J., *J. Biol. Chem.*, 270 (1995) 14255.
2. von Heijne, G., *J. Membrane Biol.*, 115 (1990) 195.
3. Henkel, T., Zabel, K., Zee, K., Muller J., Fanning E., and Baeuerle P., *Cell*, 68 (1992) 1121.
4. Baeuerle, P.A., and Baltimore, D., *Mol. Aspects Cell. Regul.*, 6 (1991) 409.
5. Delli Bovi, P., Curatola, A.M., Kern, F.G., Greco, A., Ittmann, M., and Basilico, C., *Cell*, 50 (1987) 729.
6. Cordle, S.R., Donald, R., Read, M.A., and Hawiger, J., *J. Biol. Chem.*, 268 (1993) 11803.

Peptides: Chemistry, Structure and Biology
Pravin T.P. Kaumaya and Robert S. Hodges (Eds.)
Mayflower Scientific Ltd., 1996

63
A General Method for High Level Recombinant Production of Amidated Peptides in *Eschericia coli*

J.S. Stout, B.E. Partridge, J.M. Couton-Schulte, D.B. Henriksen, I. Singh, S. Premer, B. Holmquist and F.W. Wagner

BioNebraska, Inc., 3820 N.W. 46th St., Lincoln, NE 68524, USA

Introduction

The low natural abundance and prohibitive synthetic cost have limited the pharmaceutical application of bioactive peptides. The peptides of interest are often 20-60 amino acids in length and require C-terminal amidation for full biological activity. Recombinant bacterial production of such peptides is difficult, because the bacteria rapidly degrade small peptides [1] and the glycine monooxygenase and lyase [2] required for C-terminal amidation are not present.

We have developed a generic tripartite fusion protein system to produce peptides, which combines a human carbonic anhydrase II (hCA) carrier protein [3], a cleavable linker, and the peptide of interest with an optional amidation handle added to the C-terminus of the peptide. The amidation handle facilitates the incorporation of an amide group by a post-translational reaction [4].

Results and Discussion

The expression plasmid pBN was constructed by insertion of the T7 expression cassette [5] containing the gene for human carbonic anhydrase II (hCA) into the plasmid pBR322. The transformed *E. coli* BL21 (DE3) cells were resistant to tetracycline and were grown to high cell densities in the presence of this antibiotic.

Both the peptide of interest and the cleavable linker were encoded by a synthetic gene inserted after the hCA gene. The peptide genes were synthesized with optimal codons for *E. coli* . This increased the yield of fusion protein and decreased the amount of degradation products produced. This same general plasmid was used to produce over 20 different peptides.

The selection of the cleavage method was based upon the sequence of the desired peptide and the need for post-translational modification. The selection of a chemical or enzymatic cleavage method compatible with the target peptide occurred early in the design of the cleavable linker and peptide gene. Enterokinase, factor Xa, thrombin, cyanogen bromide, and hydroxylamine cleavable linkers [6] have been used in both soluble and insoluble fusion protein constructs.

The hCA protein constructs were produced in a fed batch *E. coli* fermentation and resulted in 1-2 g/L of protein. The yield was independent of the peptide. However, the

solubility of the product fusion protein was dependent on the nature of the added peptide and cleavable linker. Whether soluble or insoluble, the fusion protein was easily purified. Soluble fusion proteins were rapidly purified by affinity chromatography using immobilized *p*-aminomethylbenzene sulfonamide resin. This resin has a capacity for hCA fusion proteins in excess of 40 g/L. Insoluble fusion proteins were purified as inclusion bodies by differential centrifugation and buffer washes.

Following purification, the fusion protein was dissolved in an appropriate buffer, and the fusion protein cleaved by a reagent which was compatible with both the peptide and the cleavable linker. Carrier protein, hCA, was easily removed from the cleavage reaction by selective precipitation providing relatively pure peptide in solution. The peptide was then purified for subsequent post-translational modifications.

Carbonic anhydrase fusion proteins provide a predictable and reproducible method to produce large quantities of regulatory peptides. Soluble hCA fusion proteins are easily purified by affinity chromatography on immobilized *p*-aminomethylbenzene sulfonamide columns, which are cheap, easy to produce, and have a capacity for hCA-fusion proteins of in excess 40g/L. Insoluble fusion proteins are easily purified by centrifugation and washing of inclusion bodies.

Following cleavage of the fusion protein, the hCA carrier protein is separated from peptide by selective precipitation. This provides 90+% of pure peptides with the use of one or no chromatographic steps. These processing steps are scaleable and allow the production of multigram quantities of peptide.

The peptides produced can be further modified to introduce C-terminal amides or other desired functionalities.

References

1. Goldberg, A.L., and St. John, A.C., *Ann. Rev. Biochem.*, 45 (1976) 747.
2. Ohsuye, K., Kitano, K., Wada, Y., Fuchimura, K., and Tanaka, S., *Biochem. Biophys. Res. Comm.*, 150 (1988) 1275.
3. Van Heeke, G., Stout, J.S., and Wagner, F.W., In Dunn, B.M. and Pennington, M.W. (Eds.), *Methods in Molecular Biology*, Vol. 36: Peptide Analysis Protocols, Humana Press Inc., Totowa, NJ, 1994, p. 245.
4. Henriksen, D.B., Breddam, K., Moller, J., and Buchart, O., *J. Am. Chem. Soc.*, 114 (1992) 1876.
5. Studier, F.W., Rosenberg, A.H., Dunn, J.J., and Dubendorff, J.W., *Methods Enzymol.*, 185 (1990) 60.
6. Carter, P., In Ladisch, M.R., Willson, R.C., Painton, C.C., and Builder, S.E. (Eds.), *Protein Purification: From Molecular Mechanisms to Large Scale Process* (ACS Symposium Series 427), American Chemical Society, Washington, D.C., 1990, p. 181.

Peptides: Chemistry, Structure and Biology
Pravin T.P. Kaumaya and Robert S. Hodges (Eds.)
Mayflower Scientific Ltd., 1996

64
Oral Absortion Studies of Lipidic Conjugates of Thyrotropin Releasing Hormone (TRH) and Luteinizing Hormone Releasing Hormone (LHRH)

N. Flinn[1], S. Coppard[1], W.A. Gibbons[1], A. Shaw[1], P. Artursson[2] and I. Toth[1]

[1]School of Pharmacy, University of London, 29-39 Brunswick Square, London, England, WC1N 1AX, UK
[2]Uppsala University, Biomedicum, Box 580, S-751 23, Uppsala, Sweden

Introduction

The gut epithelium presents a number of physical barriers to oral absorption, including hydrophobic membranes, transport processes across cell junctions, mucus, gastric acidity and peristalsis. Proteolytic activity (from epithelial, pancreatic and bacterial sources) in the GI tract is also a formidable barrier to oral uptake [1].

The thyrotropin releasing hormone (TRH) and luteinizing hormone releasing hormone (LHRH), are rapidly degraded following first-order kinetics, with a half life in humans of approximately 5 min following i.v. administration [2].

Conjugation of lipidic moieties to TRH and LHRH increased the half life of the lipidic conjugates in the presence of degrading enzymes [3]. The peptides were chemically modified by conjugation to a novel class of compounds; the lipoamino acids and their homo-oligomers, the lipopeptides. Here we report the oral absorption studies of these novel lipidic peptide conjugates.

Results and Discussion

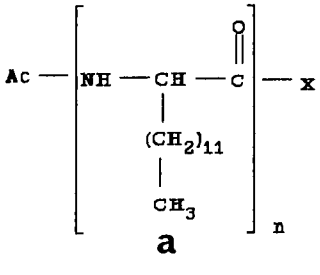

a

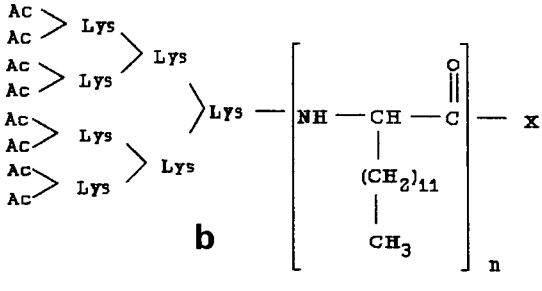

b

Compound	1a	1b	1c	1d	1e	1f	2a	2b
n	0	1	2	0	1	2	2	2
X	TRH	TRH	TRH	LHRH	LHRH	LHRH	TRH	LHRH

The tripeptide TRH and decapeptide LHRH were synthesised (Glu was used instead of PyGlu) and acetylated on the N-terminus resulting in compounds **1a** and **1d**. The TRH and LHRH analogues were extended on the N-terminus with one or two 2-amino-tetradecanoic acids and two 2-amino-tetradecanoic acid and seven lysines, then acetylated with ^{3}H acetic anhydride resulting in compounds **1b, 1c, 1e** and **1f** and polypeptides **2a** and **2b**, respectively. The "monomer" and "dimer" conjugates (conjugation with one or two lipidic amino acids) resulted in a diastereomeric mixture of two and four compounds, which were used without separation, as a diastereomeric mixture.

Caco-2 cell experiments. No major differences in the transport of the TRH-conjugates (**1b**, **1c** and **2a**) as compared to the transport of TRH analogue (**1a**) could be observed in the Caco-2 monolayers. Similarly, no significant differences in [^{14}C]mannitol permeability could be observed after incubation with the TRH-conjugates, for 2 h ($p>0.05$). However, since not all of the initial radioactivity could be accounted for, either in the apical and basal medium or by association with the filter, the cells themselves were examined. Although the transport through the monolayer was low, it was found that almost 60% of **2a** was associated with the cells after 4 hours. Whether the compound is adsorbed onto the surface of the cell or internalised is not yet clear, but in either case this result shows a significant change in the permeability profile of TRH.

Transport of LHRH analogue **1d** was low (25 ng). Conjugation with one lipidic unit (**1e**) increased the amount of transport 8 fold, while there was a 30 fold increase when two lipidic units were added (**1f**) to the LHRH. Lipidic-polylysine conjugation (**2b**) also enhanced the transport of the peptide by 13 times (Figure 1).

The integrity of the cell monolayer was retained throughout the study, thus ruling out the possibility of transport by a paracellular route.

Oral absorption studies. Radiolabelled TRH and LHRH analogues (**1a**, **1d**) and compounds **1b**, **1c**, **1e**, **1f**, **2a** and **2b** were administered orally to rats and the uptake examined. Figure 2 shows the overall uptake of LHRH conjugate indicating 10-15 % oral absorption (blood is not included). Examining the uptake in major organs, the compounds showed different distribution. Compound **1e** had 3-5 % absorption in the

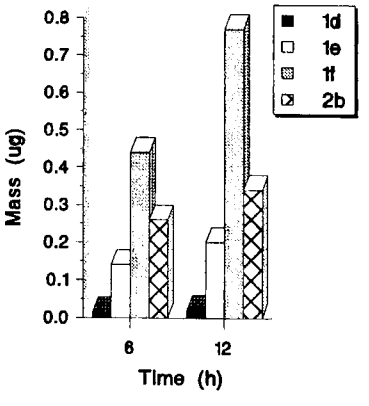

Figure 1. *Mass of LHRH conjugates **1d**, **1e**, **1f**, and **2b** associated with cells and filter after 6 and 12 hours exposure to a 10 μM solution.*

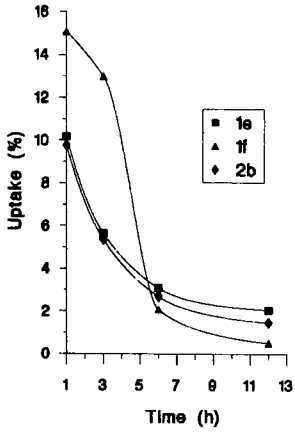

Figure 2. *Oral uptake of LHRH conjugates* ***1e, 1f,*** *and* ***2b*** *observed in stomach, kidney, spleen, liver, small and large intestine.*

stomach, small and large intestine, while compound **1f** had almost 10 % initial uptake in the stomach and also showed 5 % uptake in the small intestine. Compound **2b** showed significant absorption only in the small intestine (9%). The TRH conjugates (**1b**, **1c** and **2b**) showed similar absorption profiles.

Additionally, compounds **1c** and **1f** were extracted out from the blood 3 hours after administration, the extract separated by CE methods and the intact compounds identified by MS. The lipidic conjugation greatly enhanced the biological stability of the peptides.

Addition of lipoamino acids to poorly absorbed peptides is a viable way of increasing oral uptake. The bifunctional nature of the lipidic units allows them to confer hydrophobicity, thus allowing uptake through the gut epithelium. The lipidic moiety also protects the peptide from enzymatic degradation.

References

1. Lee, V., *CRC Crit. Rev. Ther. Drug Car. Sys.* 5 (1988) 69-97.
2. Leppaluoto, J., Virkkunen, P., and Lybek, H., *J. Clin. Endocrinol. Metab.*, 35 (1977) 477-478.
3. Toth, I., Flinn, N., Hillery, A.M., Gibbons, A.M., Artursson, P., *Int. J. Pharm.*, 105 (1994) 241-247.

Peptides: Chemistry, Structure and Biology
Pravin T.P. Kaumaya and Robert S. Hodges (Eds.)
Mayflower Scientific Ltd., 1996

65
Identification of Cadherin Sequences Presumably Responsible for Regulation of Cell-Cell Adhesion in Tight Junctions

K.L. Lutz and T.J. Siahaan

Department of Pharmaceutical Chemistry, University of Kansas, Lawrence, KS 66054, USA

Introduction

Tight junctions present a major obstacle for the delivery of drugs through the blood brain barrier and intestinal epithelium. These tight junctions are regulated in part by cadherins which are calcium dependent cell-cell adhesion molecules [1]. It has previously been shown that resealing tight junctions is inhibited by anti-E-cadherin MAb [2]. Presumably the MAb recognizes the amino acid sequence responsible for homophilic interactions. By scanning the extracelluar domains of N (neural)- and E (epithelial)-cadherin with anti-E-cadherin MAb, we can identify epitopes which may be responsible for cadherin- cadherin interactions. Two ELISAs were established using anti-E-cadherin MAb.

Results and Discussion

The binding of the peptides 1-8 of Table 1 in the regular indirect ELISA is depicted in Figure 1. Both peptides 1 and 2 contain a conserved His-Ala-Val sequence which is the most conserved sequence among cadherins. We also immobilized peptides onto the

Table 1. *The sequences of peptides from the ELISA binding studies in Figure 1. Peptides 4-29 are immobilized on controlled-pore glass with an (amino caproic)$_6$ linker.*

SOLUTION PHASE	**E-CADHERIN EC-1 IMMOBILIZED**	**E-CADHERIN EC-2 IMMOBILIZED**
1. LRA**HAV**DVNG-NH_2	9. PENEKGEFPK	19. FTQEVFEGSV
2. Ac-DRERIATYTLFS**HAV**-SSNGNAVED-NH_2	10. GEFPKNLVQI	20. AEGAVPGTSV
3. QTSVSPSKVI	11. KSNRDKETKV	21. MKVSATDADD
N-CADHERIN EC-1 IMMOBILIZED	12. FYSITGQGAD	22. DVNKTNAAIA
4. PPTGIFIINP	13. KPPVGVFIIE	23. YTIVSQDPEL
5. ISGQLSVTKP	14. RETGQLKVTQ	24. PHKNMFTVNR
6. LDREQIASFH	15. PLDREAIAKY	25. DTGVISVLTS
7. LRA**HAV**DVNG	16. ILYS**HAV**SSN	26. GLDRESYPYY
8. NQVENPIDIV	17. GEAVEDPMEI	27. TLVVQAADLQ
	18. VITVTDQNDN	28. GEGLSTTAKA
		29. VITVKDINDN

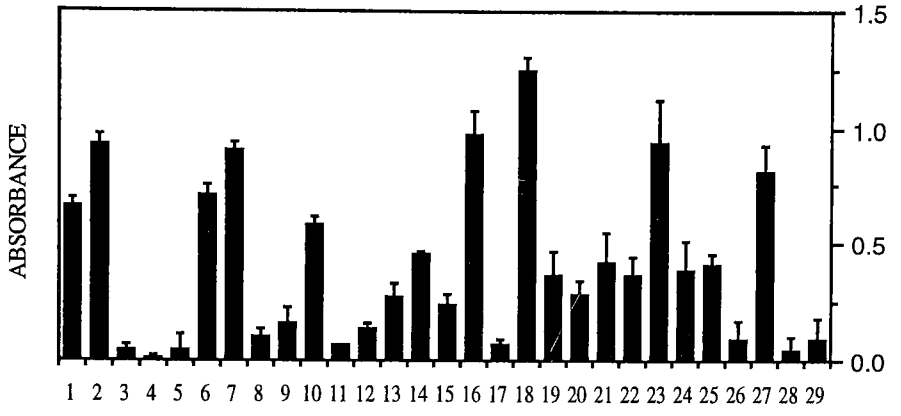

Figure 1. *The binding of the peptides from Table 1 to anti-E-cadherin MAb. Peptides 1, 2, and 3 are solution peptides which were dry coated onto microtiter wells.*

surface of glass beads with a linker of six 6-aminocaproic acid residues. Immobilized peptides 6 and 7 display antigenic reactivity to the anti-E-cadherin MAb whereas 4, 5, and 8 were not recognized. The reactivity of peptide 7, which contains the same sequence as peptide 1, demonstrates the reproducibility of the peptides that are coated on plates *versus* immobilized on glass beads.

Figure 1 also represents the binding of E-cadherin immobilized peptides from the EC-1 and EC-2 domain of E-cadherin. Peptides 16, 18, 23 and 27 display significant antigenic reactivity to the anti-E-cadherin MAb. Peptide 16, also containing the conserved His-Ala-Val sequence, displays significant antigenic reactivity consistent with the previous HAV peptides. Peptide 27, which contains a Gln-Ala-Ala sequence, is the EC-2 domain counterpart of the EC-1 domain HAV sequence. Thus, this region in the various domains appears to be important for cadherin regulation. It has been shown that synthetic LRAHAVDVNG peptide inhibits the compaction of mouse embryos and neurite growth [3]. Our data therefore reconfirms the importance of this HAV region. Peptide 18 is located in one of the proposed calcium binding regions of cadherins. In future studies the following peptide sequences will be used for the regulation of tight junctions and will be tested in an *in vitro* model: (1, 2, 6, 7, 16, 18, 23 and 27) and also active sequences determined from the remaining three extracellular domains.

Acknowledgments

Financial support from the Alzheimer's Association (IIRG-94-097), NSF EPSCoR (EHR92-55223), and the APS Travel Grant committee is gratefully acknowledged.

References

1. Takeichi, M., *Annu. Rev. Biochem.*, 59 (1990) 237.
2. Takeichi, M., *Development*, 102 (1988) 639.
3. Blaschuk, O.W., Sullivan, R., David, S., and Pouliot, Y., *Developmental Biology*, 139 (1990) 227.

Peptides: Chemistry, Structure and Biology
Pravin T.P. Kaumaya and Robert S. Hodges (Eds.)
Mayflower Scientific Ltd., 1996

66
Glutathione-based Anti-cancer Drugs: Animal Efficacy and Bone Marrow Sparing Effects

M.H. Lyttle, A. Satyam, M.D. Hocker, H.C. Hui, C.G. Caldwell, A.S. Morgan, A. Stanboli and L.M. Kauvar

Terrapin Technologies, 750 H Gateway Boulevard, South San Francisco, CA 94080, USA

Introduction

P1-1 Glutathione *S*-transferase (GST) has been shown to be elevated in many major human cancer types, compared to surrounding normal tissue [1]. We have developed a class of glutathione based GST activated cytotoxins which show increased *in vitro* toxicity to cancer cells transfected to overexpress P1-1 GST [2]. A likely activation mechanism is abstraction of a proton α to the sulfone by a basic residue in the GST active site, followed by β-elimination of the cytotoxic species.

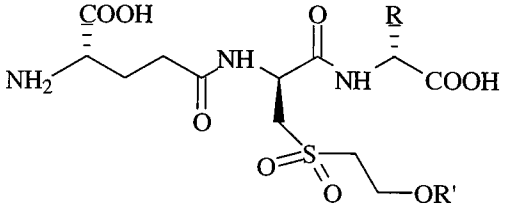

TER 286: R = C_6H_5,
R' = $PO(N(CH_2CH_2Cl)_2)_2$

TER 322: R = H,
R' = $CON(CH_2CH_2Cl)_2$

Results and Discussion

One of these compounds (TER 286) has shown beneficial effects in slowing tumor growth with dose sensitive positive responses in three out of five human xenograft animal tumor models (Figure 1). Unlike cytotoxins of comparable efficacy, the compound does not severely deplete mouse bone marrow granulocyte macrophage (GM) progenitors, which are essential to infection fighting white blood cells. After 5 days of 200 mg/kg/day TER 286, GM progenitor colony forming units extracted from the femurs of mice were only reduced by about 50%, compared to controls.

While TER 286 was activated at equal rates by P1-1 and A1-1 GSTs, another compound, TER 322, showed improved specificity for P1-1 GST (Figure 2). The activation mechanism of this compound is slightly different, involving the generation of a carbamic acid, which loses CO_2 to generate the free amine. This compound adds versa-

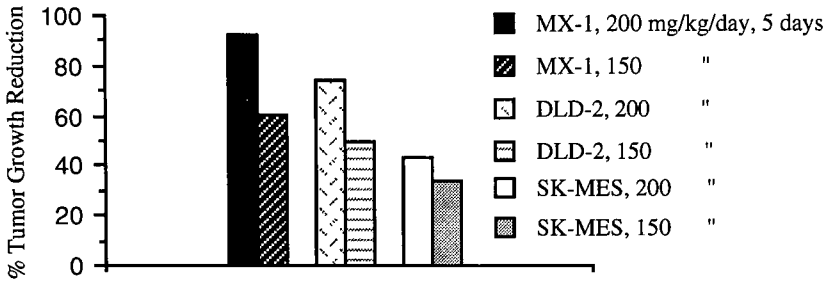

Figure 1. *Reduction of tumor growth rate for three types of human xenografted tumors in the flanks of mice. MX-1 Breast, DLD-2 Colon and SK-MES lung tumors showed positive effects with TER 286, while HT-29 colon and MV-522 lung cancers showed little or no response. Drug dosing regimen was started 10 - 14 days after tumor implantation. Cremophore vehicle was used for I.P. injection with vehicle alone defining 100% tumor growth . The studies were continued until the tumor size in the controls reached 1 - 2 g. Ten mice were in each group.*

tility to the concept, because many drugs are activated by generation of free amines in their structures. TER 322 was not significantly more toxic to MCF-7 cancer cells transfected to overexpress P1-1 GST five fold more than control cells. The diethyl ester of TER 322 did show improved differential toxicity, however, indicating that cell membrane permeation is important in the toxicity of this compound.

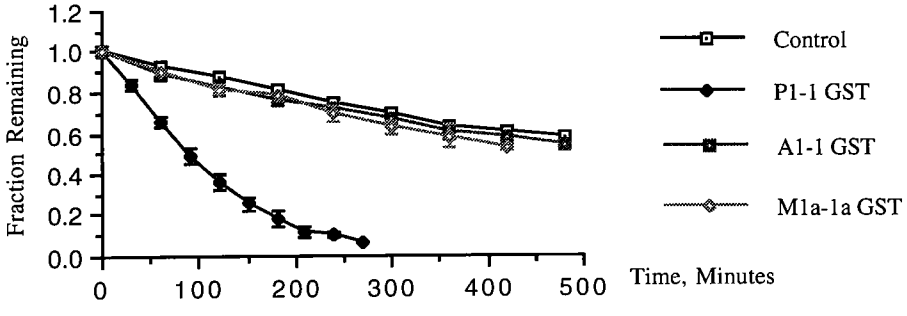

Figure 2. *Decomposition rate of 0.3 mM TER 322 incubated with 3 mM recombinant humanA1-1, M1a-1a or P1-1 GSTs at 37°C in 200 μM phosphate buffer at pH 7.2.*

References

1. Howie, A., Forrester, L., Glancy, M., Schlager, J., Powis, G., Beckett, G., Hayes, J. and Wolf, C., *Carcinogenisis*, 11 (1990) 451.
2. Lyttle, M.H., Satyam, A., Hocker, M.D., Bauer, K.E., Caldwell, C.G., Hui, H.C., Morgan, A.S., Mergia, A. and Kauvar, L.M., *J. Med. Chem.*, 37 (1994) 1501.

Peptides: Chemistry, Structure and Biology
Pravin T.P. Kaumaya and Robert S. Hodges (Eds.)
Mayflower Scientific Ltd., 1996

67

Gamma-glutamyl-neuropeptides Could Be Propeptides in Central Nervous System but Not in Periphery

A. Misicka[1,3], I. Maszczynska[2], A.W. Lipkowski[2,3], D. Stropova[4], H.I. Yamamura[4] and V.J. Hruby[3]

[1]Department of Chemistry, Warsaw University, Warsaw, Poland
[2]Medical Research Centre, Polish Academy of Sciences, Warsaw, Poland
Departments of [3]Chemistry and [4]Pharmacology, University of Arizona, Tucson, AZ 85721, USA

Introduction

Wide distribution of gamma-glutamase (gamma-GT) suggests the possibility of using inactive gamma-glutamyl-peptides as prodrugs which could slowly release the active peptide by interaction with gamma-glutamase [1]. To apply gamma-glutamyl derivatives as propeptides, two major questions had to be answered. The first was whether gamma-glutamyl analogues of longer peptides would be recognized by gamma-GT. The second was whether the rate of the reaction of gamma-GT on gamma-glutamyl-peptides to liberate active peptide would be faster than the rate of reaction of other peptidases which hydrolyzed the active peptide, and thus deactivate the peptide before its liberation.

To answer these questions, the gamma-glutamyl derivative of the opioid peptide dermorphin has been synthesized and its receptor affinities and antinociceptive properties have been tested and compared to the parent dermorphin [2]. Dermorphin has been selected as parent compound for its biological and antinociceptive properties. Dermorphin expresses high affinity to the mu opioid receptor type and potent antinociceptive activity after both systemic (intraperitoneal, i.p.; intravenous, i.v.) and central (intrathecal, i.t.) applications. The systemic antinociceptive activity of dermorphin is lower than opioid alkaloids such as morphine, but significant blood-brain barrier (BBB) permeability is obtained. Therefore, dermorphin is a good leading peptide to check the effect of modification of the parent molecule on activity in both systemic and central systems.

Results and Discussion

The free amino group of the N-terminal tyrosine is a necessary element for interaction with the opioid receptor. Therefore, it is not surprising that gamma-glutamyl-dermorphin did not show affinity to opioid receptors (Table 1). However, when injected i.t., the compound showed antinociceptive activity. The reversible effect of naloxone demonstrated that the observed antinociception is related to interaction of the peptide with opioid receptors. This data strongly suggested transformation of gamma-glutamyl-

Table 1. *Receptor binding and in vivo antinociception of dermorphin and its gamma-Glu-analogue.*

Compound	Receptor Binding IC_{50}(nM)†		*in vivo* Antinociception ($\%MPE_{50}$)†		
	delta*	mu**	i.v. (μM/kg)	i.p. (μM/kg)	i.t. (nM/mouse)
1. Dermorphin (DERM)	396	11.5	0.11	0.36	0.11
2. gamma-Glu-DERM	>80,000	1,840	2.5	>10	0.04

* versus [^{3}H][p-Cl-Phe^4]DPDPE; ** versus [^{3}H]CTOP; † according to methods described in [3].

dermorphin into dermorphin. Interestingly, the gamma-glutamyl analogue produced a significantly prolonged effect, when we compared equipotent doses of dermorphin and analogue (unpublished data). This may be an additional argument that active peptide is liberated from the precursor. The analogue when injected i.p. or i.v. showed an antinociceptive activity more than twenty times less than dermorphin when injected by the same route. This data suggests that the gamma-glutamyl residue in the periphery is more slowly cleaved by gamma-GT, and/or that deactivation of the peptide by other peptidases is more effective. Dermorphin itself when injected i.p. or i.v. showed significant antinociceptive activity as a result of partial permeability of the blood-brain barrier (BBB). Gamma-GT in CNS may transform gamma-glutamyl dermorphin into the active parent compound. The effect of peptidases on the C-terminal part (deactivating metabolism) of dermorphin should be similar as on its gamma-glutamyl analogue. Therefore, the lower antinociceptive activity of the gamma-glutamyl analogue may suggest that permeability of the BBB by the analogue is less than the parent dermorphin.

In conclusion, it has been shown that gamma-glutamyl peptides may be effectively hydrolyzed to the active compound in the CNS. In the periphery, the deactivating effect of other peptidases apparently is much more prevalent to the liberation of active peptide by gamma-GT. In addition, gamma-glutamyl derivatives may be less suitable for BBB permeability. All these observations suggest that gamma-glutamyl peptide analogues could be considered as propeptide drugs for site specific delivery.

Acknowledgments

This work was supported by grants from the Warsaw University, BW 1219/30, the U.S.P.H.S, NS-19972, and N.I.D.A., DA06284.

References

1. Scewczuk, A.. Sobiech, K.A. and Wellman-Bednowski, M., *Arch. Immunol. Ther. Exp.*, 22 (1974) 105-110.
2. Marastoni, M., Salvatori, S., Balboni, G., Borea, P.A., Mazzola, G. and Tomatsis, R., *J. Med. Chem.*, 30 (1978) 1538-1542 and references cited therein.
3. Misicka, A., Lipowski, A.W., Fang, L., Knapp, R.J., Davis, P., Kramer, T., Burks, T.F., Yamamura, H.I., Carr, D.B. and Hruby, V.J., *Biochem. Biophys. Res. Commun.*, 180 (1991) 1290-1297.

Peptides: Chemistry, Structure and Biology
Pravin T.P. Kaumaya and Robert S. Hodges (Eds.)
Mayflower Scientific Ltd., 1996

68
Comparison of Cyclic and Linear Analogs of Vasoactive Intestinal Peptide

D.R. Bolin, J.M. Cottrell, R. Garippa, N. Rinaldi, R. Senda, B. Simko and M. O'Donnell

Roche Research Center, Hoffmann-La Roche, Inc., Nutley, NJ 07110, USA

Introduction

Constraining the conformational flexibility of a linear peptide by cyclization has been shown, in some cases, to impart increased enzymatic stability, enhanced potency and/or receptor selectivity. We and others have reported that side-chain to side-chain cyclic peptides bearing an i→i+4 motif tended to enhance helical secondary structure [1-3]. Since vasoactive intestinal peptide (VIP) has been shown to exhibit helical characteristics between residues 10 and 26, we have prepared i→i+4 cyclic analogs in order to stabilize helical structure and have compared the resultant biological activities with linear analogs.

Results and Discussion

A series of Lys^{i}→Asp^{i+4} cyclic analogs were prepared and assayed as smooth muscle relaxants *in vitro* on guinea pig tracheal tissue. Table 1 shows the bioassay results of cyclic analogs **1-15** relative to the close linear analog, Ac-[Lys^{12},Nle^{17}, Val^{26},Thr^{28}]-VIP. A wide range of potencies was observed. Compounds **1**, **2**, **4**, **5**, **7-9**, **11**, and **14** showed greatly decreased potencies as compared to the linear compound. Compounds **3**, **10**, **12**, and **13** showed potencies nearly equivalent to the linear species. However, compounds **6** and **15**, which are cyclized between Lys^{13}→Asp^{17} and Lys^{23}→Asp^{27}, respectively, displayed enhanced potency. Although all i→i+4 cyclic compounds would have been expected to enhance helical conformations, the observed biological potencies varied significantly with the position of cyclization. The periodicity of potencies aligned well with facial positioning on an amphipathic helix. In those compounds with decreased potencies, the lactam ring might sterically interfere with ligand-receptor interaction.

A second series of 13 pairs of cyclic/linear peptides were synthesized and examined for activity in several bioassays. These cyclic peptides contained a Lys^{21}→Asp^{25} lactam and additional substitutions to enhance potency. *In vitro* on guinea pig tissue, the cyclic analogs generally possessed enhanced potency over the linear counterparts, by about 2- to 35-fold. Four exceptions were noted in which the linear analogs were somewhat more potent than the cyclic compounds. The peptides were assayed for *in vivo* broncho-constriction inhibitory activity. In all but two cases, the cyclic compounds were equal to or more potent than the linear species. Similarly, nearly all of the cyclic compounds

within each pair showed an increased duration of action by up to 5-fold. This may likely be due to an enhanced stability to enzymatic degradation [4]. When tested *in vitro* as smooth muscle relaxants on human bronchial tissue, the cyclic compounds showed a dramatically increased potency over the linear species. The cyclic compounds Ac-[Lys^{12},Nle^{17},Ala^{19},Asp^{25},Leu^{26},$Lys^{27,28}$]-VIPcyclo(21→25), Ac-[Glu^{8},Lys^{12},Nle^{17},Ala^{19}, Asp^{25},Leu^{26},$Lys^{27,28}$]-VIPcyclo(21→25) and Ac-[Ala^{2},Glu^{8},Lys^{12},Nle^{17},Ala^{19},Asp^{25},Leu^{26}, $Lys^{27,28}Ala^{29-31}$]-VIPcyclo(21→25) were 87-, 124-, and 263-fold more potent than their closely related linear analogs, respectively.

Table 1. *Relaxant activity of i→i+4 cyclic analogs on guinea pig tracheal smooth muscle.*

#	Compound	EC_{50} (nM)	Pot.[a]
1	Ac-[Lys^{1}, Asp^{5}, Lys^{12}, Nle^{17}, Val^{26}, Thr^{28}]-VIP cyclo (1→5)	36	0.08
2	Ac-[Lys^{4}, Lys^{12}, Nle^{17}, Val^{26}, Thr^{28}]-VIP cyclo (4→8)	260	0.01
3	Ac-[Lys^{5}, Asp^{9}, Lys^{12}, Nle^{17}, Val^{26}, Thr^{28}]-VIP cyclo (5→9)	3.8	0.71
4	Ac-[Lys^{8}, Asp^{12}, Nle^{17}, Val^{26}, Thr^{28}]-VIP cyclo (8→12)	38	0.07
5	Ac-[Lys^{12}, Glu^{16}, Nle^{17}, Val^{26}, Thr^{28}]-VIP cyclo (12→16)	37	0.07
6	Ac-[Lys^{12}, Lys^{13}, Asp^{17}, Val^{26}, Thr^{28}]-VIP cyclo (13→17)	1.8	1.50
7	Ac-[Lys^{12}, Lys^{14}, Nle^{17}, Asp^{18}, Val^{26}, Thr^{28}]-VIP cyclo (14→18)	27	0.10
8	Ac-[Lys^{12}, Lys^{15}, Nle^{17}, Asp^{19}, Val^{26}, Thr^{28}]-VIP cyclo (15→19)	52	0.05
9	Ac-[Lys^{12}, Lys^{16}, Nle^{17}, Asp^{20}, Val^{26}, Thr^{28}]-VIP cyclo (16→20)	17	0.16
10	Ac-[Lys^{12}, Lys^{17}, Asp^{21}, Val^{26}, Thr^{28}]-VIP cyclo (17→21)	3.0	0.90
11	Ac-[Lys^{12},Nle^{17}, Lys^{19}, Asp^{23}, Val^{26}, Thr^{28}]-VIP cyclo (19→23)	24	0.11
12	Ac-[Lys^{12}, Nle^{17}, Asp^{24}, Val^{26}, Thr^{28}]-VIP cyclo (20→24)	5.3	0.51
13	Ac-[Lys^{12}, Nle^{17}, Asp^{25}, Val^{26}, Thr^{28}]-VIP cyclo (21→25)	3.1	0.87
14	Ac-[Lys^{12}, Nle^{17}, Lys^{22}, Asp^{26}, Thr^{28}]-VIP cyclo (22→26)	41.0	0.07
15	Ac-[Lys^{12}, Nle^{17}, Lys^{23}, Val^{26}, Asp^{27}, Thr^{28}]-VIP cyclo (23→27)	1.4	1.93
16	Ac-[Lys^{12}, Nle^{17}, Lys^{24}, Val^{26}, Asp^{28}]-VIP cyclo (24→28)	2.3	1.17

[a] Potency relative to Ac-[Lys^{12},Nle^{17},Val^{26},Thr^{28}]-VIP, EC_{50} = 2.7 nM (1.0).

References

1. Madison, V.S., Fry, D.C., Greeley, D.N., Toome, V., Wegrzynski, B.B., Heimer, E.P., and Felix, A.M. in Rivier, J.E. and Marshall, G.R. (Eds.), 'Peptides: Chemistry, Structure and Biology', ESCOM, Leiden, The Netherlands 1990, pp. 575-577.
2. Ösapay, G., Gulys, J., Profit, A.A., Gulys, E.S. and Taylor, J.W. in Smith, J.A. and Rivier, J.E. (Eds.), 'Peptides: Chemistry, Structure and Biology', ESCOM, Leiden, The Netherlands, 1992, pp. 239-240.
3. Bolin, D.R., Michalewsky, J., Wasserman, M.A., and O'Donnell, M., *Biopolymer/Peptide Science,* 37 (1995) 57.
4. Bolin, D.R., Cottrell, J., Michalewsky, J., Garippa, R.J., O'Neill, N., Simko, B., and O'Donnell, M., *Biomed. Res.*,13, Suppl. 2 (1992) 25.

Peptides: Chemistry, Structure and Biology
Pravin T.P. Kaumaya and Robert S. Hodges (Eds.)
Mayflower Scientific Ltd., 1996

69

Protection of Re-perfused Canine Ischemic Myocardium by Efegatran Sulfate (LY294468) - A Tripeptide Aldehyde Thrombin Inhibitor

R.T. Shuman, G.F. Smith, B.R. MacDonald, M. Chastain and R.A. Hahn.

The Lilly Research Laboratories, Eli Lilly and Company, Indianapolis, IN 46285, U.S.A.

Introduction

Modern therapy for coronary thrombosis includes thrombolytic agents and angioplasty. Early reperfusion salvages some myocardium at risk of necrosis, but accelerates neutrophil infiltration into ischemic tissue [1]. Recruited neutrophils are thought by many to mediate infarct extension through release of oxidants and proteolytic enzymes [2]. Infarct size and postischemic ventricular dysfunction are major determinants of the prognosis of patients with acute myocardial infarction. Accordingly, cardioprotection in the early stage of myocardial infarction has been the focus of considerable attention. The purpose of this study centers on compound D-MePhe-Pro-Arg-H (LY294468), an inhibitor of thrombin and related serine proteases [3], to assess it's impact on myocardial reperfusion injury. LY294468 was examined in a *non-thrombotic* canine model of myocardial infarction that consists of one hour of mechanical occlusion of the left circumflex coronary artery followed by five hours of reperfusion [4].

Results and Discussion

In the present study, the efficacy of Efegatran (LY294468), a tripeptide aldehyde, was investigated for limiting myocardial infarct size, using a dose regimen known to achieve significant and sustained thrombin inhibition. Dogs were infused i.v. with LY294468 (0.5 mg/kg/hour) during the five hours of reperfusion that followed one hour of regional ischemia, and were compared to dogs that received vehicle. LY294468 infusion produced significant and sustained increments in activated partial thromboplastin and thrombin times without inducing bleeding. LY294468 did not alter arterial pressure, cardiac rate or the myocardial oxygen demand when compared to time related changes observed in control dogs. After reperfusion the heart was excised for infarct quantitation using the standard dualdye staining procedure of Shea *et al.* [5]. LY294468 treatment significantly reduced infarct size (Figure 1) from a control value of 38.4 ± 3.4% of the left ventricle placed at risk of necrosis to 24.1 ± 6.3% ($P<0.05$). Maximal systemic leukocytosis in response to myocardial ischemic injury, and the localization of

neutrophils within ischemic and infarcted myocardium were not altered by LY294468 infusion. These results suggest that LY294468 has cardioprotective activity at an infusion rate that inhibits the coagulant effects of thrombin. Although infarction reduction was associated with thrombin inhibition in this study, the present data do not indicate whether these two pharmacological effects are causally related.

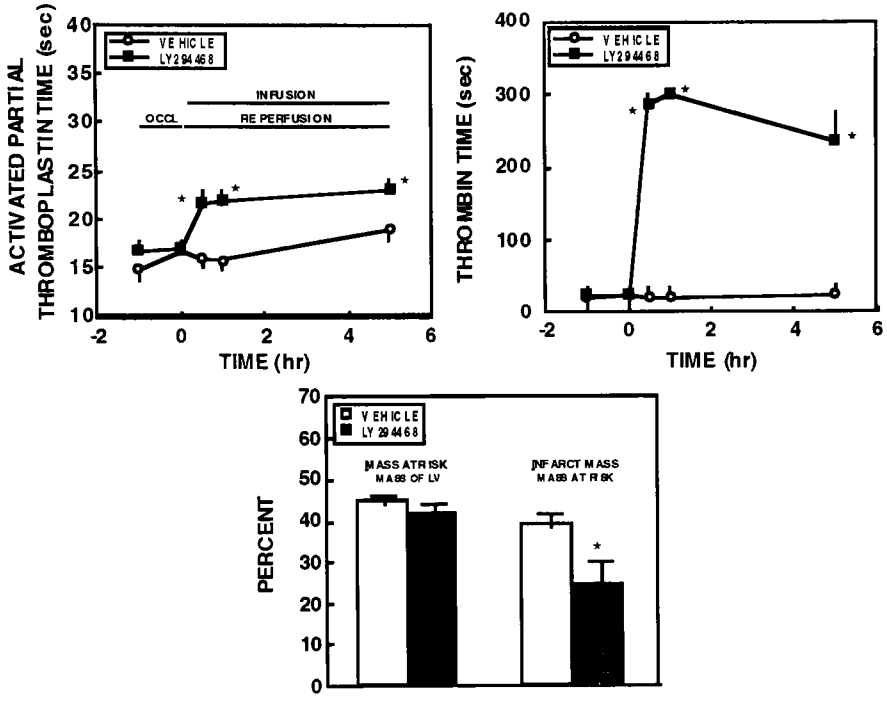

Figure 1. *Effect of LY294468 treatment of blood coagulation parameters (top) and myocardial infarct size (bottom) in anesthetized dogs subjected to coronary artery occlusion and reperfusion. Each value is the mean of 8 dogs, and vertical bars are standard errors. An asterick denotes statistical significance from the respective control value (P<0.05).*

References

1) Lucchesi, B.R., Werns, S.W. and Fantone, J.C., *J. Mol. Cell Cardiol.*, 21 (1989) 1241.
2) Fantone, J.C.and Ward, P.A., *Am. J. Pathol.*, 107 (1982) 397.
3) (a) Bajusz, S., Szell Hasenohrl nee, E., Barabas, and E. Bagdy, D. (1983) U.S. Patent 4,399,065. (b) Bajusz, S., Szell, E., Bagdy, D., Barabas, E., Horvath, G., Dioszegi, M.,Fittler, Z., Szabo, G., Juhasz, A., Tomori, E. and Szilagyi, G., *J. Med. Chem.* , 33 (1990) 1729. (c) Jackson, C.V., Wilson, H.C., Crowe, V.G., Shuman, R.T. and Gesellchen, P.D., *J. Cardiovascular Pharmacol.*, 21 (1993) 587.
4) Hahn, R.A., Macdonald, B.R., Morgan, E., Potts, B.D., Parli, J., Rinkema, L.E., Whitesitt, C.A. and Marshall, W.S., *J. of Pharmacol. and Exp.Ther.*, 260 (1992) 979.
5) Shea, M.J., Murtagh, J.J., Jolly, S.R., Abrams, G.D., Pitt, B., Lucchesi, B.R., *Eur. J. Pharmacol.*, 102 (1984) 63.

Peptides: Chemistry, Structure and Biology
Pravin T.P. Kaumaya and Robert S. Hodges (Eds.)
Mayflower Scientific Ltd., 1996

70

Comparison of Synthetic Amphipathic Peptides with Recombinant Human SP-C in their Ability to Promote the Activity of Artificial Lung Surfactants

W. Voelter[1], H. Echner[1], S. Stoeva[1], T. Kaiser[1], D. Häfner[2], U. Krüger[2] and E. Sturm[2]

[1]Abtlg. für Physik. Biochemie, Physiologisch-chem. Institut der Universität Tübingen, Hoppe-Seyler-Straße 4, D-72076 Tübingen, Germany
[2]Byk Gulden, Postfach 100310, D-78403 Konstanz, Germany

Introduction

The "respiratory distress syndrome" (RDS) is caused by a lack of lung surfactant (LSF), consisting of about 95% phospholipids and 5% proteins, reducing the surface tension at the alveolar air/liquid interphase. This protein mixture is mainly composed of three surfactant-specific components: SP-A, -B and -C [1]. For the development of an artifical LSF, peptides, produced by synthesis or gene technology, are needed having phospholipid(PL)-spreading properties. In this connection, two sequences, KLLLLK-LLLLKLLLLKLLLLK($(KL_4)_4K$) [2] and SucLLEKLLELLK-NH_2(L^8-WMAP10) [3] were synthesized and their biological effects compared with dipalmitoylated recombinant human SP-C (rhSP-C).

Results and Discussion

The syntheses of both peptides were performed by SPS according to the Fmoc/ *t*Bu-strategy using Fmoc amino acids and TBTU as coupling reagent in 3 fold excess. $(KL_4)_4K$ was produced starting with 0.45 g Fmoc-Lys(Boc)-resin of Wang (loading: 0.55 mmol/g). L^8-WMAP10 was synthesised on 5-(4-Fmoc-aminomethyl-3.5-dimethoxy-phenoxy)-valeric acid), attached to an aminomethylpolystyrene support with a loading of 0.8 mmol/g. After removal of the Fmoc group from the polymer with piperidine/DMF, Fmoc-Lys(Boc)-OH was attached to 0.31g resin with TBTU as coupling reagent, and, using a similar protocol as described for $(KL_4)_4K$, the L^8-WMAP10 sequence was synthesized. After removal of the N-terminal Fmoc group, the suc residue was introduced with suc anhydride, dissolved in DMF/DCM. The peptides were cleaved from the resins and simultaneously deprotected (3h; TFA/thioanisole/anisole/water) and precipi- tated with ether yielding 593 mg $(KL_4)_4K$, resp. 350 mg L^8-WMAP10.

For the biological activity assays, mixtures were prepared containing dipalmitoyl-phosphatidylcholine/palmitoyloleoylphosphatidylglycerol (DPPC/POPG) at a ratio of 7:3 plus 2.5% palmitic acid (PA) and 2% of peptide. Surface tension measurements were

Table 1. *Effect of peptides (2%) in LSF perparations (PL matrix: DPPC/POPG (7:3) + 2.5% PA; concentration: 5 mg/ml) on dynamic surface tension measurements.*

Peptide	Surface tension (mN/M)	
	100% bubble area	50% bubble area
PL matrix	60	22
L^8-WMAP10	55	20
$(KL_4)_4K$	36	16
rhSP-C	34	0

performed applying a pulsating bubble surfactometer (PBS); (20 cycles/min), and the values were determined at equilibrium (100% bubble area) and after compression (50% bubble area) (Table 1).

In vivo experiments were also performed with Sprague Dawley rats, subjected to lung lavage (6-8 times), and subsequent intratracheal instillation of the above mentioned LSF mixtures. The rats were artificially ventilated with normal (8 cm H_2O; 2h) resp. reduced (8→0 cm H_2O; 1h) positive end-expiratory pressure (PEEP), and the partial arterial oxygen pressure (PaO_2; [mmHg]) was registered. As the dynamic measurements with the PBS show (Table 1), none of the synthetic peptides in the LSF preparations causes a reduction of the required surface tension to < 5 mN/m under compression conditions, while, in presence of rhSP-C, a value close to zero was observed. In coincidence with these results are the rat lavage model *in vivo* activities found for the LSF preparations. Under constant PEEP conditions, rhSP-C-containing samples prevent most efficiently the reduction of the PaO_2, compared to the synthetic peptide mixtures (decreasing order activities: rhSP-C>$(KL_4)_4K$>L^8-WMAP10). At reduced PEEP conditions (3 cm H_2O), only rhSP-C prevents completely the collapse of the alveoli, $(Kl_4)_4K$ is 30% active and L^8-WMAP10 is completely ineffective.

To conclude, based on these investigations, the synthetic peptides L^8-WMAP10 and $(KL_4)_4K$ as components in artifical LSFs cause only a very weak or partial improvement of respiration, respectively. Neither show the profile observed with human PL mixtures containing the human identical rhSP-C .

References

1. Schröder, C., Günther, A., Seeger, W. and Voelter, W., *Biomed. Peptides,Proteins & Nucleic Acids,* 1 (1994/95) 13.
2. Cochrane, C.G. and Revak, S.D., *Science,* 254 (1991) 566.
3. McLean, L.R., Lewis, J.E., Hagaman, K.A., Owen, T.J. and Matthews, E.R., *J. Pharmacol. and Experimental Therapeutics,* 266 (1993) 551.

Session III
Biologically Active Peptides

Chairs: Ruth F. Nutt and
G.M. Anantharamaiah

Peptides: Chemistry, Structure and Biology
Pravin T.P. Kaumaya and Robert S. Hodges (Eds.)
Mayflower Scientific Ltd., 1996

71
Mechanism of Action of Cecropin A-Melittin Hybrid Peptides on *Leishmania sp.* Parasites

P. Diaz-Achírica[1], J. Ubach[2], A. Guinea[3], D. Andreu[2] and L. Rivas[1]

[1] Centro de Investigaciones Biológicas (C.S.I.C.), Velázquez 144, E-28006 Madrid, Spain
[2]Departament de Química Orgànica, Universitat de Barcelona, Martí i Franquès 1-11, E-08028 Barcelona, Spain
[3]Departamento de Microbiología III, Facultad de Ciencias Biológicas, Universidad Complutense, E-28040 Madrid, Spain

Introduction

The antiprotozoal action of eukaryotic antibiotic peptides has been reviewed recently [1]. We have studied the mechanism of action of synthetic short cecropin A-melittin hybrid peptides on the parasitic protozoa *Leishmania*, the causative agent of leishmaniasis, an important human disease which requires the development of new drugs [2]. These peptides have been reported as good antibacterial agents and also display antimalarial activity [3, 4].

Results and Discussion.

Peptides were synthesized using standard Fmoc-chemistry. Their C-terminus was amidated [3]. Peptide activity on *L. donovani* promastigotes was tested by both MTT reduction and inhibition of parasite proliferation by ^{3}[H]-thymidine incorporation. The antileishmanial activities of the peptides used in this work are summarized in Table 1.

Table 1. *Peptide sequences and their LD_{50} against L. donovani promastigotes.*

Peptide	Sequence	LD_{50} (μM)
CA(1-8)M(1-18)	KWKLFKKIGIGAVLKVLTTGLPALIS-NH_2	2±0.5
CA(1-7)M(4-11)	KWKLFKKAVLKVLTT-NH_2	>20
CA(1-7)M(5-12)	KWKLFKKVLKVLTTG-NH_2	>20
CA(1-7)M(2-9)	KWKLFKKIGAVLKVL-NH_2	>10
(D)-CA(1-80M(1-18)	kwklfkkigigavlkvlttglpalis-NH_2	0.5-1
CA(1-8)	KWKLFKKI-NH_2	>10
cecropin-A	KWKLFKKIEKVGQNIRDGIIKAGPAVAVVGQATQIAK-NH_2	>10
melittin	GIGAVLKVLTTGLPALISWIKRKRQQ-NH_2	0.5

Melittin and CA(1-8)M(1-18) show the highest leishmanicidal activity. This requires both the cationic N-terminal region from cecropin A followed by a hydrophobic region. Its length is quite important; cecropin A and its polar region CA(1-8) are almost

inactive, and the shorter analogs are also less active. D-analog is more effective than the L-analog, quite likely because of its higher resistance to proteinases, extremely abundant in the *Leishmania* promastigote surface.

Assay conditions involved in the interaction between CA(1-8)M(1-18) and *L. donovani* promastigotes were determined. In the standard assay, parasites ($2x10^7$ promastigotes/ml) were incubated with the peptide at 22°C. Binding process is very fast, as the inhibition of parasite proliferation can rise as high as 83% of the final value in the first 5 minutes of incubation. This is in agreement with a killing mechanism based on membrane permeabilization, similar to that described for its antibacterial activity. In our *Leishmania* model, as in membrane-cecropin A interaction [5], there is an initial electrostatic interaction of the peptide with the parasite membrane. Peptide binding to promastigote is strongly inhibited in the presence of polyanionic compounds, such as heparin, but only when this is added previous to the parasite-peptide interaction.

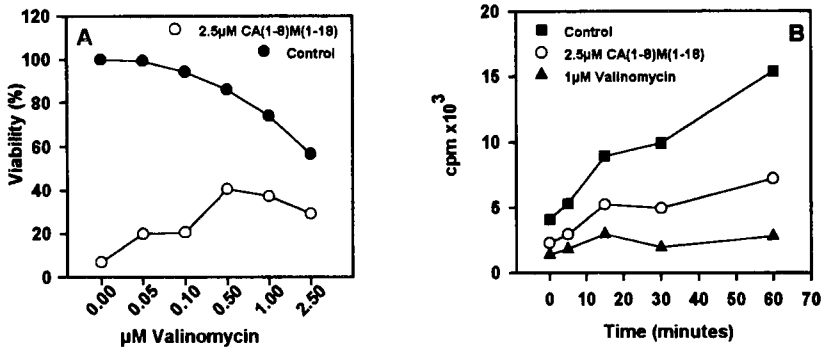

Figure 1. *A) Membrane-potential dependence of CA(1-8)M(1-18) activity. B) ^{3}[H]-proline uptake.*

Membrane potential has been described as an important factor in the permeabilization mechanism, driving the translocation of N-terminal region of cecropin A across the planar lipid membrane, but not required for liposome lysis [6]. Depolarization of *L. donovani* promastigote plasma membrane by valinomycin only protects to some extent (Figure 1A). At the same time, CA(1-8)M(1-18) induces a) dissipation of the proton motive force, utilized for active proline transport by the parasite (Figure 1B), b) decrease in the oxygen consumption rate of the parasites in a dose-dependent manner, and c) equilibration between intracellular and extracellular pHs, measured by fluorescence of parasites loaded with BCECF and resuspended in media with different pHs. Morphological changes, as observed by electron microscopy, include bumps in plasma membrane as well as its detachment from the supellicular microtubule layer.

One of the main components of the promastigote plasma membrane is lipophosphoglycan (LPG), a strongly anionic polysaccharide with pleiotropic functions taking part in parasite invasion of the macrophage and survival (reviewed in [7]). R2D2, a mutant as strain deficient in LPG biosynthesis, is twice as susceptible as compared to the wild strain. Incubation of the peptide with PG (the negatively charged and hydrophilic portion of LPG), prior to the addition of the parasite, inhibits the lethal effect of CA(1-8)M(1-18) (Figure 2B). It is quite speculative to suppose a protective role of

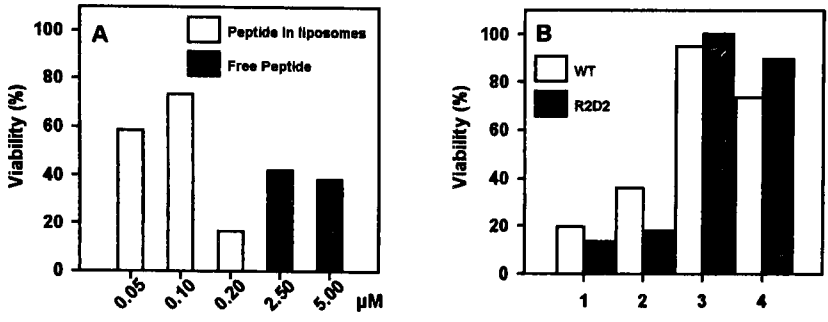

Figure 2. *A) Intracellular amastigotes viability. B) Protection by PG. 1.- Peptide. 2.-Peptide and PG simultaneously added. 3.- Incubation peptide-PG previous to their addition. 4.- Incubation Leishmania-PG previous to the addition of peptide. Concentration of peptide 2.5μM CA(1-8)M(1-18), concentration of PG 62.5 μg/ml.*

antibacterial peptides in the gut of the sandly, the leishmania vector, and the subversion of this defense by parasite LPG, nevertheless this component can protect the pro-mastigote against macrophage antimicrobial peptides during the invasion and survival.

CA(1-8)M(1-18) incorporated in liposomes also acts on the amastigote (the intracellular form of the parasite) on *L. pifanoi* infected peritoneal macrophages (Figure 2A) or *in vivo* as topical application on the ulcer produced by infection of Balb/c mice with *L. major*. However the healing is not as fast as with other reported pharmacological treatments as paranomycyn ointment, or even injection of glucantime. On the other hand, when the parasite inocula is higher than 10^6 parasites, we got only a delay in the onset of the ulcer. Liposomes also reduce the lethal concentration of the peptide.

CA(1-8)M(1-18) has been used as a model to understand peptide interaction with *Leishmania* and to demonstrate a preliminary feasibility of peptide chemotherapy on leishmaniasis. At present, new synthetic peptides with higher and more specific anti-leishmanial action are under study.

Acknowledgments

Financial support for this work has been provided by grants CICyT BIO92- 0936-C02-01 and SAF95-0019 to L.R. and PTR 93-0032 to D.A.

References

1. Boman, H.G., *Ann. Rev. Immunol.*, 13 (1995) 61.
2. Olliaro, P.L. and Bryceson, A.D.M., *Parasitology Today*, 10 (1994) 160.
3. Boman, H.G., Wade, D., Boman, I.A., Wahlin, B. and Merrifield, R.B., *FEBS Lett.*, 259 (1989) 103
4. Andreu, D., Ubach, J., Boman, A., Wahlin, B., Wade, D., Merrifield, R.B. and Boman, H.G. *FEBS Lett.*, 296 (1992) 190.
5. Christensen, B., Fink, J., Merrifield, R.B. and Mauzerall, D., *Proc. Natl. Acad. Sci. USA*, 85 (1988) 5072.
6. Steiner, H., Andreu, D. and Merrifield, R.B., *Biochim. Biophys. Acta*, 939 (1988) 260.
7. Turco, S.J. and Descoteaux, A., *Ann. Rev. Microbiol.*, 46 (1992) 65.

Peptides: Chemistry, Structure and Biology
Pravin T.P. Kaumaya and Robert S. Hodges (Eds.)
Mayflower Scientific Ltd., 1996

72
Binding Site on Human C-reactive Protein (CRP) Recognized by the Leukocyte CRP-receptor

Qin Zen, W. Zhong, X. Han and R.F. Mortensen

Department of Microbiology, Ohio State University, Columbus, OH 43210, USA

Introduction

Tissue damage by either trauma or microbial invasion initiates a cascade of cytokine-driven events that can be amplified into a systemic inflammatory response characterized by an increase in the levels of blood proteins termed acute phase reactants. The increased synthesis of this diverse group is induced at the level of transcription by the inflammatory cytokines IL-1 and IL-6 [1]. C-reactive protein (CRP) is the prototype human acute phase reactant since its level can increase by >1000-fold. CRP is a pentraxin protein composed of five identical, non-covalently-linked subunits arranged in a flat pentameric disk with cyclic symmetry [2, 3]. A single copy gene encodes the 206 amino acid single polypeptide chain composing each protomer subunit [2]. CRP displays Ca^{++}-dependent lectin-like binding reactivity for phosphorylcholine (PC) [3]. The inducible CRP response is conserved among all the vertebrates and suggests an essential role in inducible, nonspecific host-defense.

Two well-defined biological activities ascribed to CRP are opsonization and comple- ment activation. The opsonic activity of CRP is mediated *via* specific leukocyte receptors (CRP-R) for complexes of CRP [4]. A unique property of CRP is that it accumulates at sites of tissue damage where it is degraded by neutrophils into biologically active peptides [1, 5]. To reconcile these two seemingly different activities, we examined CRP synthetic peptides for their ability to interact with the CRP-R. In this study, we identify a cell-binding peptide (CB-Pep) that contains a motif recognized by the CRP-R on the human promonocytic cell line U937 and the human promyelocytic cell line HL-60.

Results and Discussion

To map a site(s) on pentameric CRP that is recognized by the leukocyte CRP-R, a series of synthetic peptides of 10 to 20 residues corresponding to functional regions with a high surface probability on each of the five subunits were tested for their ability to inhibit the binding of labeled CRP. Only 2 of the 7 peptides tested inhibited binding: Pep 27-38, which was previously shown by us to mediate fibroblast attachment *in vitro* and therefore designated CB-Pep [6], and Pep 134-148, a highly conserved segment in all pentraxins that mediates binding of one of the $2Ca^{++}$per subunit [7] (Table 1).

The inhibition by CB-Pep was approximately 50-fold more efficient than Pep 134-148 and therefore both truncated peptides and peptides with single conservative

Table 1. *Effect of synthetic peptides of C-reactive protein (CRP) on the binding of ^{125}I-CRP to U937 cells*[a].

Residues	Designation	% Inhibition of Specific Binding (±SD)
1 - 16	N-terminal	-4.4 (± 5.8)
27 - 38	Cell-Binding	56.1 (± 7.6)
47 - 63	PC-Binding	-8.5 (± 3.1)
134 - 148	Ca^{++}-Binding	48.9 (± 8.2)
152 - 176	Ca^{++}-Binding	8.5 (± 2.2)
174 - 185	Macrophage-Activating	-5.0 (± 6.3)
191 - 206	C-Terminal	5.1 (± 9.4)

[a] A 100-fold molar excess of each peptide was allowed to compete against 2 pmoles of heat modified ^{125}I-CRP per 10^6 U937 human monocytic cells for binding sites.

substitutions within Pep 27-38 were tested for their ability to inhibit CRP binding. Competitive binding between labeled pentameric CRP and a series of synthetic peptides truncated from either the N- or the C-terminus for binding sites on U937 cells revealed that the minimum length recognized by the CRP-R corresponded to residues 31 through 36: **KAFTVC** (Table 2).

Synthetic peptides with a single conservative substitution for each of the amino acids at positions 30 through 37 of the CB-Pep were compared to the CB-Pep itself for their effect on ^{125}I-CRP binding. Residues 32 through 35, **AFTV**, within the CB-peptide were critical (Table 2).

An examination of the effect of the CRP-synthetic peptides of those listed in Table1 on ligand-induced superoxide (O_2^-) production by the HL-60 cells that had been differentiated into granulocytic cells, HL-60(G), revealed that only Pep 27-38 inhibited O_2^- production triggered by the chemotactic peptide, fMLPP (1 μM). A dose-response inhibition of the fMLPP-driven respiratory burst was observed at peptide concentrations of 50 to 16,000 pmoles/ml, with optimal inhibition at ~400 pmoles/ml, the equivalent of 50 μg/ml of CRP. TheCB-Pep by itself did not induce a significant respiratory burst. The truncated CB-Peps were evaluated for inhibition of O_2^- production and the results

Table 2. *Inhibition of specific binding of ^{125}I labelled human C-reactive protein to U937 cells by truncated and sustituted synthetic CB peptides*[a].

Peptide	Sequence	% Inhibition	Peptide	Sequence	% Inhibition
CB28-38	KPLKAFTVCLH	58.6 ± 1.8	CB30I	TKPIKAFTVCLH	68.2 ± 17.1
CB29-38	PLKAFTVCLH	50.6 ± 16.5	CB31R	TKPLRAFTVCL	58.4 ± 11.4
CB30-38	LKAFTVCLH	57.3 ± 15.9	CB32L	TKPLKLFTVCLH	-0.3 ± 2.3
CB31-38	KAFTVCLH	56.6 ± 14.8	CB33Y	TKPLKAYTVCLH	-4.5 ± 3.4
CB32-38	AFTVCLH	3.5 ± 3.0	CB34S	TKPLKAFSVCLH	2.3 ± 1.1
CB33-38	FTVCLH	9.1 ± 4.5	CB35L	TKPLKAFTLCLH	-5.7 ± 2.8
CB27-37	TKPLKAFTVCL	42.3 ± 18.6	CB37I	TKPLKAFTVCIH	60.2 ± 10.2
CB27-36	TKPLKAFTVC	47.5 ± 7.1			
CB27-35	TKPLKAFTV	8.0 ± 3.9			

[a] Peptides are designated by either the number of residues present or the substituted residue.

indicated that the minimum length for significant inhibition is: **KAFTVC**, the same size needed to inhibit binding of CRP to the U937 cells (Table 3). This finding differs somewhat from the minimum length needed to mediate fibroblast cell attachment *in vitro*: **FTVCL** [8]. The hydrophobic residues 32-38 are on a long β-strand in the intact CRP subunit [9]. Based on searches of the gene data bank and the primary literature, we propose that the motif composed of residues 31-36 represents a novel structure recognized by the cells of inflammation.

Table 3. *Effect of truncated CRP cell-binding peptides on fMPLPP-induced superoxide production by HL-60(G) cells.*

Peptide	Sequence	% of Control (±SD)
CB27-38	TKPLKAFTVCLH	72.7 ± 5.5
CB27-37	TKPLKAFTVCL	62.3 ± 6.4
CB27-36	TKPLKAFTVC	63.5 ± 7.1
CB27-35	TKPLKAFTV	95.8 ± 8.5
CB28-38	KPLKAFTVCLH	74.0 ± 6.9
CB29-38	PLKAFTVCLH	83.1 ± 7.1
CB30-38	LKAFTVCLH	86.0 ± 7.7
CB31-38	KAFTVCLH	81.0 ± 7.2
CB37I	TKPLKAFTVCIH	60.2 ± 10.2
CB32-38	AFTVCLH	108.0 ± 9.0
CB33-38	FTVCLH	110.1 ± 8.8

Acknowledgments

Financial support from USPHS NIH grant CA30015. The advice of Dr. P.T.P. Kaumaya on the peptide synthesis strategy is greatly appreciated.

References

1. Kushner, I., *Perspect. Biol. Med.*, 36 (1993) 611.
2. Steel, D.M. and Whitehead, A.S., *Immunol. Today,* 15 (1994) 81.
3. Gewurz, H., Zhang, X.-H. and Lint, T.F., *Curr. Opinion Immunol.*, 7 (1995) 54.
4. Mortensen, R.F., in Zwilling, B.S. and Eisenstein, T.K. (Eds.), Macrophage-Pathogen Interactions, Marcel Dekker, Inc., New York, (1993) p. 143.
5. Robey, F., Ohura, K., Futaki, S., Fujii, N., Yajima, H., Goldman, N., Jones, K. and Wahl, S., *J. Biol. Chem.*, 262 (1987) 7053.
6. Fernandez, M., Mullenix, M., Christner, R. and Mortensen, R., *J. Cell. Bioc.*, 50 (1992) 83.
7. Swanson, S., Mullenix, M. and Mortensen, R., *J. Immunol.*, 147 (1991) 2248.
8. Mullenix, M.C., Kaumaya, P.T.P. and Mortensen, R.F., *J. Cell. Biochem.*, 54 (1994) 343.
9. Srinivasan, N., White, H., Emsley, J., Wood, S., Pepys, M. and Blundell, T., *Structure 2* (1994) 1017.

Peptides: Chemistry, Structure and Biology
Pravin T.P. Kaumaya and Robert S. Hodges (Eds.)
Mayflower Scientific Ltd., 1996

73

New Family of Linear Antimicrobial Peptides from Hagfish Intestine Contains Bromo-tryptophan as Novel Amino Acid

A.E. Shinnar[1], T. Uzzell[1,2], M.N. Rao[1], E. Spooner[3], W.S. Lane[3] and M.A. Zasloff[1]

[1]*Magainin Pharmaceuticals Inc., Plymouth Meeting, PA 19462, USA*
[2]*Department of Ecology, Ethology, and Evolution, University of Illinois, Urbana, IL 61801, USA*
[3]*Harvard Microchemistry Facility, Cambridge, MA 02138, USA*

Introduction

In recent years, the quest for new antibiotics has led to the discovery of a variety of naturally occurring substances, including peptides like the insect cecropins, mammalian defensins, and frog magainins, and squalamine, an aminosterol from dogfish shark [1, 2]. We have continued our search for natural host-defense molecules by examining the Atlantic hagfish, *Myxine glutinosa*. This jawless vertebrate is considered more primitive both phylogenetically and immunologically than jawed vertebrates insofar as it lacks circulating lymphocytes and classical immunoglobulins [3-5]. Intrigued as to how this scavenger fish combats pathogens, we surveyed the major organ tissues for antibiotic substances. We report here on the isolation of a new family of peptides with potent antimicrobial activity.

Results and Discussion

Preliminary screening of hagfish organ systems indicated that intestinal tissue was rich in antimicrobial activity. A family of peptides was extracted from hagfish intestine using organic solvents and purified to homogeneity by size exclusion chromatography, strong cation exchange chromatography, and RP-HPLC. Antimicrobial activity was assayed by detecting a zone of inhibition against a bacterial lawn in an agar plate [6]. Chemical sequencing revealed three closely related cationic peptides, each with two residues that could not be deduced initially by application of conventional AAA and Edman sequencing methods (Figure 1).

The most abundant hagfish intestinal antimicrobial peptide, designated HFIAP-1, was proteolyzed with AspN endopeptidase and then reduced and alkyated. The chemical sequence of these fragments did not contain cysteine, but the fragments revealed UV absorption bands similar to tryptophan, although red-shifted. After trypsinization of HFIAP-1, a tripeptide containing the unknown residue flanked by alanine and arginine

HFIAP		Mass
1	GFFKKAWRKVKHAGRRVLDTAKGVGRHYVNNWLNRYR	4643.3
2	GFFKKAWRKVKHAGRRVLDTAKGVGRHYVNNWLNRYR	4564.0
3	GWFKKAWRKVKNAGRRVL.....KGVG IHYGVGLI	3551.9

Figure 1. *Chemical sequences of hagfish intestinal antimicrobial peptides. After 37 cycles of automated Edman sequencing, HFIAP-1 and HFIAP-2 yielded identical primary structures, although the PTH-residues at positions 7 and 32 were not known. The parent masses, determined by ESI-MS, were consistent with tryptophan at positions 7 and 32, where either both or one residue was substituted with bromine. HFIAP-3 shows 73% homology with HFIAP-1 and HFIAP-2 and appears to be a deletion mutant.*

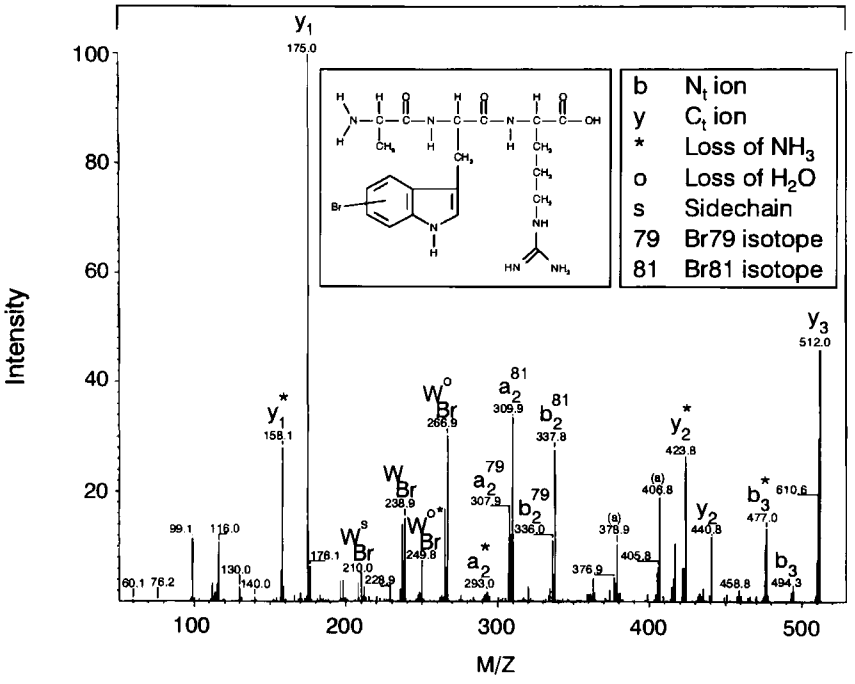

Figure 2. *Tandem ESI mass spectrum of Ala-Trp(Br)-Arg. Mass spectrum of the tripeptide isolated upon trypsinization of HFIAP-1 showed a complete set of N- and C-terminal ions. Each of the b and y ions associated with the unknown residue showed a mass and distinctive isotopic pattern differing by 2 mass units, which is consistent with tryptophan substituted with bromine.*

was isolated and subjected to tandem electrospray ionization mass spectrometry. The unknown residue was identified as bromo-tryptophan, based on mass and on the isotopic distribution (Figure 2). Ala-Trp(5Br)-Arg, prepared by chemical synthesis, exhibited the same fragmentation profile by MS-MS and had a similar UV spectrum.

To complete and to confirm the peptide sequences, cDNA clones were isolated from a library made from hagfish intestinal mRNA. Clones for two distinct genes corresponding to HFIAP-1 and HFIAP-3 were sequenced, revealing homologous signal and spacer regions, but different antibiotic and 3' untranslated regions. Codons for tryptophan were detected at the positions where the Edman sequencing was ambiguous. The presence in both of a glycine codon following the mature sequence suggests that the native peptides are amidated at the carboxy terminus [7]. *In situ* hybridization showed that mRNA is localized in nests of hematopoietic cells in the intestinal submucosa. The abundance of mRNA expressed in the gut tissue suggests that the peptides may have an important host-defense role in this primitive vertebrate.

Chemical synthesis of the sequences containing unmodified tryptophan was achieved by SPPS, using Fmoc chemistry. These peptides were active against gram-positive and gram-negative aerobic and anaerobic bacteria but not against *Candida albicans*. For thirty bacterial isolates, minimum inhibitory concentrations (MICs) for HFIAP-1 ranged from 0.5 to 32 (median 4) μg/ml.

This family of antimicrobial peptides from the hagfish intestine has little primary structure homology with other classes of peptide antibiotics [8, 9]. Secondary structure modeling predicts an Nt amphipathic α-helix from residues 1-22, whereas the Ct domain might be β-strand. Thus, these hagfish peptides are another example of the diversity in peptide antibiotics from animals.

Bromo-tryptophan is a novel residue for vertebrate peptides. Haloperoxidases are responsible for halogenation of ring systems in a wide variety of marine invertebrates [10] but we do not know if hagfish intestine expresses an endogenous bromoperoxidase, or if exogenous bromo-tryptophan might be incorporated by tRNA from the nutrient pool. Our future studies will focus on determining the position of bromine in the native tryptophan ring by NMR, synthesizing these sequences with bromo-tryptophan, and examining the effect of bromo-tryptophan on antimicrobial activity.

References

1. Jacob, L. and Zasloff, M., in 'Antimicrobial Peptides' (Ciba Foundation Symposium 186, 1994), Wiley, Chichester, 1994, p.197.
2. Moore, K.S., Wehrli, S., Roder, H., Rogers, M., Forrest, J.N., McCrimmon, D. and Zasloff, M., *Proc. Natl. Acad. Sci. USA*, 90 (1993) 1354.
3. Forey, P. and Janvier, P., Nature 361 (1991) 129.
4. Varner, J., Neame, P. and Litman, G.W., *Proc. Natl. Acad. Sci. USA*, 88 (1991) 1746.
5. Hanley, P.J., Hook, J.W., Raftos, D.A., Gooley, A.A., Trent, R. and Raison, R.L., *Proc. Natl. Acad. Sci. USA*, 89 (1992) 7910.
6. Moore, K.S., Bevins, C.L., Brasseur, M.M., Tamassini, N., Turner, K., Eck, H. and Zasloff, M., *J. Biol. Chem.*, 266 (1991) 19851.
7. Bradbury, A.F. and Smyth, D.G., *Trends Biochem. Sci.*, 16 (1991) 112.
8. Boman, H.G., *Ann. Rev. Immunol.*, 13 (1995) 61.
9. Maloy, W.L. and Kari, U.P., *Biopolymers (Peptide Science)*, 37 (1995) 105.
10. Butler, A. and Walker, J.V., *Chem. Rev.*, 93 (1993) 1937.

Peptides: Chemistry, Structure and Biology
Pravin T.P. Kaumaya and Robert S. Hodges (Eds.)
Mayflower Scientific Ltd., 1996

74

Identification of Essential Residues in the Potassium Channel Inhibitor ShK Toxin: Analysis of Monosubstituted Analogs

M.W. Pennington[1], W.R. Kem[2], V.M. Mahnir[2], M.E. Byrnes[1], I. Zaydenberg[1], I. Khaytin[1], D.S. Krafte[3] and R. Hill[3]

[1]Bachem Bioscience Inc., 3700 Horizon Dr., King of Prussia, PA 19406, USA
[2]Department of Pharmacology and Therapeutics, University of Florida, Gainesville, FL 32610, USA
[3]Sterling-Winthrop, Box 3000, Collegeville, PA 19426, USA

Introduction

Voltage-gated potassium (Kv) channels regulate a myriad of biological processes. The distribution of different subtypes of Kv channels makes them excellent targets for drug development. A new type of Kv channel-blocking toxin has been isolated from the sea anemone *Stichodactyla helianthus* (ShK toxin) [1]. ShK toxin binds with especially high affinity to Jurkat T-lymphocyte Kv1.3 channels [2], and also high affinity to rat brain Kv1.2 channels [1, 2]. Furthermore, this toxin was found to be nearly twenty-fold more potent in blocking the Jurkat T-lymphocyte Kv1.3 channel than charybdotoxin (ChTX) [2], a potent K-channel blocker isolated from scorpion venom [3]. We have recently synthesized ShK toxin in order to characterize its K-channel blocking selectivity [2]. The disulfide bonds of this 35 residue toxin have recently been determined (see Figure 1) [4]. In the current report, we have synthesized analogs at the highlighted positions of the toxin sequence shown in Figure 1, and then evaluated the biological activity on rat brain Kv1.2 channels and Jurkat T-lymphocyte Kv1.3 channels.

Results and Discussion

Synthetic analogs of ShK toxin were synthesized using an Fmoc/*t*Bu protocol as described in Pennington *et al.* [2]. Following reagent K cleavage [5] for 2 hr, each of the crude peptides was dissolved in 0.1 M NH_4OAc, pH 8.0 and allowed to oxidize in the

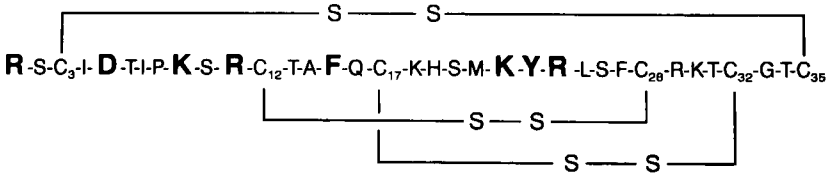

Figure 1. *Structure of ShK toxin with substitution sites in large boldface type.*

presence of air. This protocol afforded peptides having proper disulfide pairings as the major products with good yields (12-22% from starting resin). However, oxidation of the ShK D5N analog resulted in a complex product profile composed of numerous peaks as observed by RP-HPLC. Several peaks were isolated and determined to have the same mass and amino acid composition, indicating the formation of disulfide isomers. The yield for these disulfide isomers was less than 1%. We speculate that the Asp^5 sidechain may be involved in a salt bridge disrupted by replacement with the neutral isostere Asn.

Each of the other synthetic analogs was purified to homogeneity by preparative RP-HPLC and characterized by AAA and FAB-MS. Additionally, folding of each of the purified synthetic products was assessed by CD analysis. Native ShK has a characteristic CD spectra indicative of approximately 30% α-helix. Each of the synthetic analogs showed nearly identical CD profiles except for ShK Y23S. The characteristic minima for α-helix were not observed in this spectrum, indicating that this toxin analog had failed to fold properly.

Biological activity of each analog was measured using radioligand displacement assays with either rat brain Kv1.2 channels using [^{125}I]-dendrotoxin (DTX) or Jurkat T-lymphocyte Kv1.3 channels using [^{125}I]-ChTX as described in Pennington *et al.*, [2]. Analog substitutions were designed to observe the effect of charge neutralization, aromatic sidechain interaction or hydrogen bonding potential at the positions highlighted in Figure 1. Initially, analogs were designed conservatively. However, synthetic problems were observed during some of the analog syntheses (*e.g.* poor coupling efficiencies of difficult residues such as Fmoc-Gln(Trt)). Thus, we changed our strategy to a more conventional Ala scan [6].

As shown in Table 1, the bioactivity data indicates that ShK toxin binding to the Kv1.2 and Kv1.3 channels utilizes different interaction points. In fact, ShK K22A

Table 1. *Ability of ShK toxin analogs to displace binding of [^{125}I]-charybdotoxin to Jurkat T-lymphocytes and [^{125}I]-dendrotoxin to rat brain membranes.*

Toxin Analog	Secondary Structure	IC_{50} (nM) Lymphocyte ^{125}I-ChTX	IC_{50} (nM) Rat Brain ^{125}I-DTX
ShK	Normal	0.04	8
R1S	Normal	0.05	16
D5N	Disordered	N.D.	N.D.
K9Q	Normal	0.31	11
R11Q	Normal	0.64	18
F15A	Normal	0.54	6
F15W	Normal	0.65	6
K22A	Normal	0.30*	300
Y23F	Normal	0.18*	9
Y23S	Disordered	>50*	>5000
R24A	Normal	0.04	10

*Data derived from patchclamp of Jurkat T-lymphocyte Kv1.3 channels. Using this system, native ShK toxin has an IC_{50} of 133 pM [2].

binding is reduced nearly forty fold to rat brain Kv1.2 channels and yet has nearly equivalent affinity for the Jurkat T-lymphocyte Kv1.3 channel. Other differences in the interactive surface were observed at positions 9, 11 and 15. The Tyr^{23} position initially looked essential until CD analysis of the ShK Y23S showed it to be incorrectly folded. Charge neutralization at positions 9 and 11 had a greater effect on the toxin's affinity for the Kv1.3 channel. Similarly, replacement of Phe^{15} with either A or W reduced the affinity for Kv1.3 without affecting affinity for Kv1.2. Substitutions at other positions shown in Table 1 appear to have little effect on binding to these K channels.

In conclusion, the ShK toxin pharmacophore surface requirements for binding to these two Kv channel subtypes is different. Binding to Kv1.3 appears to be more affected by substitutions at positions Lys^{9}, Arg^{11} and Phe^{15}. The Lys^{22} residue appears to be essential for binding to the Kv1.2 channel.

References

1. Karlsson, E., Aneiros, A., Casteneda, O. and Harvey, A.L., in Gopalakrishankone, P. and Tan, C.K., (Eds.), 'Recent Advances in Toxinology Research, Vol. 2', Nat. Univ. Singapore, 1992 p. 378.
2. Pennington, M.W., Byrnes, M.E., Zaydenberg, I., Khaytin, I., de Chastonay, J., Krafte, D., Hill, R., Mahnir, V., Volberg, W.A., Gorczyca, W. and Kem, W.R. *Int. J. Peptide Protein Res.*, 46 (1995) 354-358.
3. Miller, C., Moczydlowski, E., Latorre, R. and Phillips, M., *Nature*, 313 (1985) 316.
4. Pohl, J., Hubalek, F., Byrnes, M.E., Nielsen, K.R., Woods, A. and Pennington, M.W. *Letters in Peptide Sci.*, 1 (1995) 291.
5. King, D.S., Fields, C.G. and Fields, G. *Int. J. Peptide Protein Res.* 36 (1990) 255.
6. de Castiglione, R., Tam, J.P., Liu, J.P., Zhang, J.-W., Galantino, M., Bertolero, F. and Vaghi, F., in Smith, J.A. and Rivier, J.E. (Eds.), 'Peptides: Chemistry and Biology', ESCOM, Leiden, Netherlands 1992, p.402.

Peptides: Chemistry, Structure and Biology
Pravin T.P. Kaumaya and Robert S. Hodges (Eds.)
Mayflower Scientific Ltd., 1996

75
Translocation of Amphiphilic Pore-forming Peptides across Lipid Bilayers

K. Matsuzaki, S. Yoneyama, O. Murase, N. Fujii and K. Miyajima

Faculty of Pharmaceutical Sciences, Kyoto University, Sakyo-ku, Kyoto 606-01, Japan

Introduction

Magainin 2 [1, 2], melittin [3], tachyplesin I (T-SS) and its acyclic analog (T-Acm) [4, 5] kill their target cells by permeabilizing cell membranes. We recently showed [6] that magainin 2 translocates across lipid bilayers by forming a multimeric pore. In this study, we examined the translocation of the other three peptides, to clarify the structual motif required for translocation.

Results and Discussion

Translocation of the peptides has been studied on the basis of resonance energy transfer (RET) from the Trp residues of the peptides to a Dns chromophore incorporated into the membrane (Figure 1a). The addition of Dns-LUVs (large unilamellar vesicles) containing 10% Dns-DPPE at the time indicated by the closed arrow decreased Trp fluorescence at 336 nm (excitation, 280 nm), indicating RET upon membrane binding. The subsequent addition of a large excess of Dns-free LUVs increased Trp fluorescence, because the Dns-free LUVs extracted the peptides which had been bound to the outer leaflets of the Dns-LUVs, relieving Trp from RET. On the other hand, the Trp residues of the peptides which had translocated to the inner leaflets remained quenched. Therefore, the ultimate intensity was different between the two cases, (1) the two kinds of LUVs were added simultaneously (the upper trace in Figure 1a), and (2) the Dns-free LUVs were added after the incubation of the peptide with the Dns-LUVs (the lower traces). This difference (ΔF), a measure of the amount of the translocated peptides, increased with the incubation period.

This experiment clearly demonstrates that the peptide become less exposed in a time dependent manner. In order to confirm the translocation of the peptide, we investigated the pore formation in the inner bilayer of multilamellar vesicles (MLVs). Figure 1b shows that the addition of NBD-labeled MLVs to a sodium dithionite solution decreased NBD fluorescence at 530 nm (excitation, 450 nm), because dithionite reduces NBD to a non-fluorescent compound. Ultimate intensity was about 75% of the initial fluorescence, indicating that this MLV was composed of two lamellas. In contrast, the addition of the NBD-MLVs to a peptide-containing dithionite solution lowered the fluorescence to much

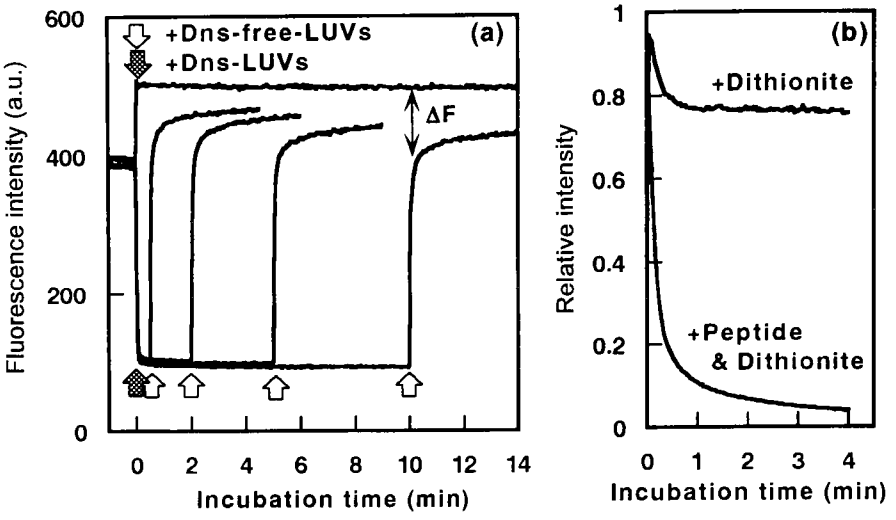

Figure 1. *(a) Detection of translocation by RET. [melittin]=2 μM, [Dns-LUV]=265 μM. (b) Detection of translocation by NBD-fluorescence. [melittin]=2 μM, [NBD-MLV]=99 μM, [$Na_2S_2O_4$]=10 mM.*

less than 25% of the initial intensity, suggesting that the peptide translocates the outmost bilayers and forms pores in the inner ones.

These experiments showed that melittin and T-SS (data not shown) translocated across the lipid bilayer. Moreover, the translocation was coupled to the leakage of a dye, calcein, from the vesicles, as detected previously [1, 4] (data not shown). On the other hand, T-Acm, which forms a β-sheet structure *ca.* 60 Å long, failed to translocate. This peptide was found to cause morphological changes of the vesicles, leading to membrane permeabilization. In conclusion, the prerequisite for membrane translocation is the peptide's ability of forming a membrane spanning amphiphilic conformation *ca.* 30 Å long.

References

1. Matsuzaki, K., Harada, M., Funakoshi, S., Fujii, N. and Miyajima, K., *Biochim. Biophys. Acta*, 1063 (1991) 162.
2. Matsuzaki, K., Murase, O., Tokuda, H., Funakoshi, S., Fujii, N. and Miyajima, K., *Biochemistry*, 33 (1994) 3342.
3. Dempsey, C.E., *Biochim. Biophys. Acta*, 1031 (1990) 143.
4. Matsuzaki, K., Fukui, M., Fujii, N. and Miyajima, K., *Biochim. Biophys. Acta*, 1070 (1991) 259.
5. Matsuzaki, K., Nakayama, M., Fukui, M., Otaka, A., Funakoshi, S., Fujii, N., Bessho, K. and Miyajima, K., *Biochemistry*, 32 (1993) 11704.
6. Matsuzaki, K., Murase, O., Fujii, N. and Miyajima, K., *Biochemistry*, 34 (1995) 6521.

Peptides: Chemistry, Structure and Biology
Pravin T.P. Kaumaya and Robert S. Hodges (Eds.)
Mayflower Scientific Ltd., 1996

76
SAR Studies on Cecropin P1, An Antimicrobial Peptide Isolated from Mammalian Species

M.N. Rao, L.M. Jones, D.L. MacDonald, T.J. Williams, W.L. Maloy and U.P. Kari

Magainin Pharmaceuticals Inc., Plymouth Meeting, PA 19462, USA

Introduction

Cecropin P1, a 31 AA peptide isolated from the pig intestine, was shown to be active against gram negative bacteria [1, 2]. Cecropin P1 has a relatively large hydrophilic N-terminus and a short hydrophobic C-terminus. On association with a lipid membrane, it forms a helical structure and, like other host defense peptides, lyses the bacteria by disrupting the membrane structure. Since the peptide is shown to protect mice against systemic *E. coli* infections, a systematic SAR study to improve its potency and therapeutic index was undertaken.

Results and Discussion

Deletion sequences from the N-terminus, C-terminus and the center were designed to make the compound more amphipathic, based on helical wheel representation. As shown in Table I (compounds 1-8), none of the deletion analogs retained even moderate activity, indicating that the complete length of peptide is needed for full biological activities. Subsequently, analogs were designed to study the effect of modifying the hydrogen bonding pattern along the length of the helix. Substituting Glu with Gln, Asn with Asp (compounds 10-15) led, in general, to retained antibacterial activity but reduced the LD_{50} values. Interestingly, the substitution of Asn with Asp (compound 11), showed staph activity for the first time among cecropins isolated from various species, without any change in toxicity. Inclusion of both the above modifications in a single analog (compound 14, 15), resulted in total loss of activity. Changing Glu to Gln in position 20 appears to be better tolerated than at position 11. Glu at position 20 is known to introduce a kink into the compound; substituting it with Pro retained only *E. coli* activity with no change in toxicity. Substituting Gln for Asn led to retained activity as expected. From the above data, it is evident that the molecule tolerates very few modifications.

Shortened cecropin analogs with C12 fatty acid, attached at the C-terminus, to mimic the hydrophobic tail of the molecule were designed and synthesized as shown in Table 1. Compounds with cecropin 1-14 AA, or 1-21 AA and 12 carbon chain did not show any activity. Introducing a C-terminal acid along with the 12 carbon chain (compounds 18-24) picked up *E. coli* activity, whereas a C8 alkyl chain in the C-terminus retained full biological activities. An octanoyl group at the N-terminus resulted in complete loss of activity.

Table 1. *Biological activity of Cecropin P1 Analogs.*

	Peptide Sequence	MIC (μg/mL) S	E	P	H	LD_{50}
	SWLSKTAKKLENSAKKRISEGIAIAIQGGPR-OH (P1)	257	2	32	1	
1	XXXXXXXXXXXXSAKKRISEGIAIAIQGGPR-OH	257	257	257	1	-
2	XXXXXXXXKLENSAKKRISEGIAIAIQGGPR-OH	257	257	257	1	-
3	XXXSKTAKKLENSAKKRISEGIAIAIQGGPR-OH	257	128	257	1	-
4	SWLAKTAKKLEXXXXXXXXGIAIAIQGGPR-OH	257	257	257	0	-
5	KWLKKTAKKLEXXXXXXXXGIAIAIQGGPR-OH	257	257	257	1	-
6	SWLSKTAKKLENXXXXXISEGIAIAIQGGPR-OH	128	128	257	0	-
7	SWLSKTAKKLENSAKKRISEGXXXXXXXXXX-OH	257	257	257	0	-
8	SWLSKTAKKLQNSAKKRISQGXXXXXXXXXX-NH_2	257	257	257	0	-
9	SWLSKTAKKLENSAKKRISEGIAIAINGGPR-OH	257	2	64	0	150
10	SWLSKTAKKL**Q**NSAKKRIS**Q**GIAIAIQGGPR-OH	257	4	16	15	25
11	SWLSKTAKKLE**D**SAKKRISEGIAIAIQGGPR-OH	64	4	32	5	150
12	SWLSKTAKKL**QD**SAKKRIS**Q**GIAIAIQGGPR-OH	257	128	257	0	-
13	SWLSKTAKKLE**D**SAKKRIS**Q**GIAIAIQGGPR-OH	256	4	256	0	150
14	SWLSKTAKKL**Q**NSAKKRISEGIAIAIQGGPR-OH	256	4	32	0	50-10
15	SWLSKTAKKLDNSAKKRIS**Q**GIAIAIQGGPR-OH	257	4	257	0	-
16	SWLSKTAKKLENSAKKRIS**P**GIAIAIQGGPR-OH	257	4	257		200
17	SWLSKTAKKLE**D**SAKKRIS**A**GIAIAIQGGPR-OH	256	32	128	5	-
18	SWLSKTAKKLENSAK-CO-NH-$(CH_2)_{11}$-CO-NH_2	257	257	257	1	-
19	SWLSKTAKKLENSAK-CO-NH-$(CH_2)_{11}$-CO-R-NH_2	257	257	257	1	-
20	SWLSKTAKKLENSAKKRISEG-CO-NH-$(CH_2)_{11}$-COOH	128	16	256	38	-
21	SWLSKTAKKLENSAKKRISEG-CO-NH-$(CH_2)_{11}$-R-OH	256	8	257	0	-
22	SWLSKTAKKLENSAKKRISEG-CO-NH-$(CH_2)_7$-CH_3	256	4	32	0	-
23	$CH_3(CH_2)_7$-CO-NH-SWLSKTAKKLENSAKKRISEG-OH	257	128	256	0	-
24	$CH_3(CH_2)_7$-CO-NH-KKLENSAKKR-NH_2	257	257	257	0	-
25	**K**WL**K**KTAKKLEN**K**AKKRI**K**EGIAIAIQGGPR-OH	256	4	256	1	-
26	**K**WL**K**KTAKKLENSAKKRISEGIAIAIQGGPR-OH	256	8	64	1	-
27	SWLSKKAKKLEN**K**AKKRIS**A**GIAIAIQGGPR-OH	256	32	256	7	-
28	SWLSKIAK**L**LENA**A**KKL!SQGIAIAIQGGPR-OH	128	32	64	50	-
29	SWLSKTAKKLE**D**SAKKRI**D**EG**K**SIATQGGPR-OH	257	257	257	0	-
30	SWLSKT**A**KALE**K**SAK**G**AI**K**EGIAIAIQGGPR-NH_2	128	32	256	1	-

S - *Staph. aureus*; E - *Escherichia coli*; P - *Pseudomonas aeruginosa*; H - % Hemolysis at 100 μg/mL; 257 - activity at concentration > than 256 μg/mL

References

1. Lee, J.-Y., Boman, A., Sun, C., Anderson, M., Jornall, H., Mutt, V. and Boman, H.G. *Proc. Natl. Acad. Sci. USA*, 86 (1989) 9159-9162.
2. Maloy, W.L. and Kari, U.P., *Peptide Science*, 37 (1995) 105-122.

Peptides: Chemistry, Structure and Biology
Pravin T.P. Kaumaya and Robert S. Hodges (Eds.)
Mayflower Scientific Ltd., 1996

77
Prototype Mystixin Peptides for Pharmacological Investigations

A.A. Kolobov[1], L.V. Olennikova[1], J.N. Tolparov[1], O.A. Kaurov[1], S.A. Ketlinksy[1], N.C. Ling[2], H.A. Thomas[3] and E.T. Wei[3]

[1]*State Institute of Highly Pure Biopreparations, St. Petersburg, Russia 197110*
[2]*Neurocrine Biosciences, Inc. San Diego, CA 92121, USA*
[3]*School of Public Health, University of California, Berkeley, CA 94720, USA*

Introduction

Peptides containing the sequence -Arg-Lys-Leu-(Leu/Met)-X-Ile-(Leu/D-Leu)-NH_2 where X = an anisolylated glutamic derivative (A*) or other aromatic residues were called mystixins [1] because of their mysterious and potent anti-inflammatory effects in models of tissue injury in laboratory animals. For example, D-Leu-Ala-Thr-D-Tyr-Arg-Lys-Leu-Leu-(A*)-Ile-D-Leu-NH_2 **(1)** inhibited heat-induced edema in the anesthetized rat's paw with a median effective intravenous dose (ED_{50}) of 0.05 mg/kg [2]. The non-anisolylated analog, D-Leu-Ala-Thr-D-Tyr-Arg-Lys-Leu-Leu-Glu-Ile-D-Leu-NH_2 **(2),** was relatively inactive with an ED_{50} of 1.9 mg/kg. Some new information on the pharmacological properties of mystixins are presented below as well as data on active analogs that may be obtained by direct synthesis.

Results and Discussion

The undecapeptide mystixin analogs **(1)** and **(2)** were evaluated in standard competitive binding assays against 15 peptide ligands of biological origin in the Nova/NIMH screening program. Each peptide was assayed at 10^{-5}M for % inhibition of binding of reference compounds to membrane receptor preparations. Substances that produced >50% inhibition of binding were considered to yield significant inhibition. **(2)** did not displace binding in ligand-receptor assays for atrial natriuretic factor, angiotensin II, vasopressin (VP-1), gastrin-releasing peptide, peripheral and central cholycystokinin, corticotropin-releasing factor, epidermal growth factor, neurotensin, neuropeptide Y, nerve growth factor, somatostatin, neurokinin A, vasoactive intestinal peptide or substance P. **(1)** inhibited VP-1 binding with an IC_{50} of 1.08 x10^{-7}M and significant inhibition of binding was also observed against gastrin-releasing peptide and neurokin A. Pharmacological analysis with VP-1 and VP-2 receptor antagonists, however, did not reveal any association of the anti-inflammatory activity of **(1)** with activation of VP-1 or VP-2 receptors *in vivo*. In a screening system developed by G.J. Cianciolo (Macronex, Inc., Morrisville, North Carolina) utilizing human white blood cells *in vitro,* **(1)** and **(2)** stimulated interleukin (IL)-1 receptor antagonist formation with an EC_{50} of 0.01 μM and

2.6 μM, respectively. Chemotaxis was affected at 0.4 μM and 6.1 μM, respectively, but no effects were observed on IL-1b, IL-6, IL-8, LTB_4 or PAF production. The activity of mystixins on human neutrophils were confirmed using three assays - the under-agarose method [3], the neutrophil adherence test [4] and the measurement of bipolar shape change [5]. The EC_{50} of mystixins for chemokinetic effects on neutrophils were in the range of 1 to 10 μg/ml and anti-edema and chemokinetic potencies were positively correlated. Shown in Figure 1 is a representative bioassay.

Using standard solid phase methods, a number of undeca-, octa- and hepta- mystixin peptides were synthesized and tested. For Arg-Lys-Leu-(Leu/Met)-X-Ile-D-Leu-NH_2 where X = Ala, His, Leu, Pro, Phe or Tyr, the ED_{50} was > 5 mg/kg i.v. for inhibition of heat-induced edema but the ED_{50} was <1 mg/kg i.v. for X = A* or D-Trp. N-Acetylation enhanced the potency of Arg-Lys-Leu-Leu-D-Trp-Ile-D-Leu-NH_2 from 0.82 mg/kg to 0.084 mg/kg. The deamidated form of the acetylated peptide was less active (ED_{50} 0.60 mg/kg). The solution structures of several prototypes were estimated after using NMR measurements in dimethylsulfoxide and computation of low energy conformers. A tentative bioactive structure was assigned and will serve as a working model for further synthesis.

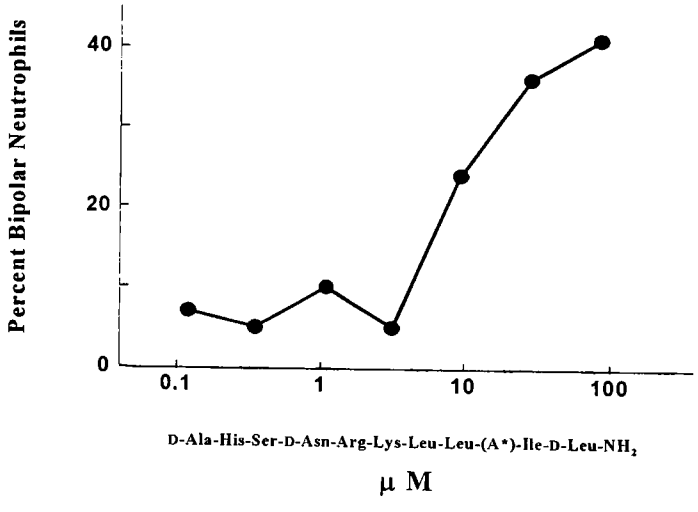

Figure 1. *Human neutrophil shape-changes after exposure to a mystixin analog. The peptide was added to whole blood and incubated at 37°C for 20 min. Cells were stained with Wright Giemsa and evaluated according to reference [5].*

References

1. Wei, E.T. and Thomas, H.A., *Annual. Rev. Pharmacol. Toxicol.*, 33 (1993) 91.
2. Thomas, H.A., Ling, N., Wei, E.T., Berree, F., Cobas, A. and Rapoport, H., *J. Pharmacol. Exp. Ther.*, 267 (1993) 1321.
3. Nelson, R.D., Quie, P.G. and Simmons, R.L., *J. Immunology*, 115 (1975) 1650.
4. Watanabe, K., Kinoshita, S. and Nakagawa, H., *J. Pharmacol. Methods*, 22 (1989) 13.
5. Lord, R.A. and Roath, S., *J. Clin. Pathol.*, 43 (1990) 342.

Peptides: Chemistry, Structure and Biology
Pravin T.P. Kaumaya and Robert S. Hodges (Eds.)
Mayflower Scientific Ltd., 1996

78

Synthesis, Activities and Conformational Analysis of Pheromone Derivatives of *Ustilago maydis*

M. Koppitz[1], R. Haeßner[1], T. Spellig[2], R. Kahmann[2] and H. Kessler[1]

[1]*Institut für Organische Chemie und Biochemie, Technische Universität München, 85747 Garching, Germany*
[2]*Institut für Genetik und Mikrobiologie der Universität München, 80638 München, Germany*

Introduction

The pathogenic form of the fungus *Ustilago maydis* is the causative agent of corn smut disease. The transformation from the non pathogenic haploid form to the pathogenic dikaryon requires pheromones existing in two alleles *a1* and *a2*, which have to bind to their specific receptors located in the membrane. The pheromone sequences are *H*-Gly-Arg-Asp-Asn-Gly-Ser-Pro-Ile-Gly-Tyr-Ser-Ser-**Xaa-*Z*** for *a1* and *H*-Asn-Arg-Gly-Gln-Pro-Gly-Tyr-Tyr-**Xaa-*Z*** for *a2* with **Xaa-*Z*** being an unidentified lipophilic amino acid derivative presumed to be **Cys(farnesyl)-*OMe*** [1,2].

Several lipophilic and hydrophilic C-terminal derivatives of both alleles were synthesized, including the natural compound carrying the postulated farnesyl moiety, and tested for biological activity. Focus of interest were the confirmation of the postulated structure and examination of the requirements on the lipophilic C-terminal residue for biological activity. The structural behaviour of two chosen analogues was examined by NMR measurements in DMSO and SDS/water, simulating the free and membrane bound form of the pheromone analogues [3, 4], and compared with each other.

Results and Discussion

All synthesized pheromone analogues differ in the C-terminal residue containing the same N-terminal peptide fragment a1' = Gly-Arg-Asp-Asn-Gly-Ser-Pro-Ile-Gly-Tyr-Ser-Ser for *a1* analogues and a2' = Asn-Arg-Gly-Gln-Pro-Gly-Tyr-Tyr for *a2* analogues, respectively. Table 1 gives an overview of the synthesized compounds and their biological activities.

The synthesis of compounds **6-9** was performed by condensation of the fully protected fragments of a1' and a2' prepared by Fmoc-strategy with the appropriate methyl ester compound [5, 6] followed by subsequent deprotection with TFA and piperidine. Compounds **1-5** were prepared by condensation of protected a1' and a2' with H-Cys(Trt)-OMe, deprotection with TFA, alkylation with the appropriate alkyl bromide [7] and removal of Fmoc with piperidine. Saponification of the methyl esters was carried out by treatment with NaOH in $MeOH/H_2O$.

Table 1. *Synthesized analogues and biological activities with reference to the activity of the native pheromone.*

Compound	N-terminal Fragment	C-Terminal Residue	Activity
a1, a2	a1', a2'	?	1
1a, 1b	a1', a2'	Cys(farnesyl)-OMe	10^{-2}
2a	a1'	Cys(farnesyl)-OH	10^{-3}
3a, 3b	a1', a2'	Cys(prenyl)-OMe	10^{-4}
4a, 4b	a1', a2'	Cys-OMe	10^{-6}
5a, 5b	a1', a2'	Cys(dodecyl)-OMe	10^{-1}
6a, 6b	a1', a2'	α-aminohexadecanoic acid-OMe	1
7a	a1'	α-aminohexadecanoic acid-OH	10^{-1}
8a, 8b	a1', a2'	α-aminodecanoic acid-OMe	10^{-3}
9a, 9b	a1', a2'	N-hexadecylglycine-OMe	0.5×10^{-1}

Comparison of the activities of the synthetic analogues with *a1* and *a2* reveals that the native pheromones do not contain the presumed Cys(farnesyl)-OMe moiety. Increasing lipophilicity of the C-terminal side chain enhances activity, with alkyl being better than prenyl. While sulfur is not essential for the C-terminal residue and a shift of the lipophilic anchor by one position has only minor influence, replacement of the methyl ester by the free acid decreases binding affinity by one order of magnitude. These results suggest that the lipophilic residue only serves for attachment to the membrane and is not involved in the binding process to the receptor.

Compounds **1** and **6** of both alleles were chosen for structural investigations by NMR in DMSO and SDS/water leading to 8 (2×2×2) different measurements. NMR studies indicate that the lipophilic C-terminal residue has no influence on the structural behaviour of the peptides. Chemical shift and NOE pattern of the short analogue **6b** suggest that its behaviour is similar in DMSO and SDS/water. No evidence is given that the membrane-simulating system SDS/water has a structure-inducing effect on the bound peptide.

References

1. Spellig, T., Bölker, M., Lottspeich, F., Frank, R.W., Kahmann, R., *EMBO*, 13 (1994) 1620.
2. Bölker, M., Urban, M., Kahmann, R., *Cell*, 68 (1992) 441.
3. Schwyzer, R., *Biochemistry*, 25 (1986) 6335.
4. Moroder, L., Romano, R., Guba, W., Mierke, D.F., Kessler, H., Delporte, C., Winand, J., Christophe, J., *Biochemistry*, 32 (1993) 13551.
5. Gibbons, W.A., Hughes, R.A., Charalambous, M., Christodoulou, M., Szeto, A., Aulabaugh, A.E., Mascagni, P., Toth, I., *Liebigs Ann. Chem.*, (1990) 1175.
6. Stewart, F.H.C., *Austr. J. Chem.*, 14 (1961) 654.
7. Yang, C.-C., Marlowe, C.K., Kania, R., *J. Am. Chem. Soc.*, 113 (1991) 3177.

Peptides: Chemistry, Structure and Biology
Pravin T.P. Kaumaya and Robert S. Hodges (Eds.)
Mayflower Scientific Ltd., 1996

79
Light Activated Conformational Switch of Peptides Probed by NMR

L.G. Ulysse and J.A. Chmielewski

Department of Chemistry, Purdue University, West Lafayette, IN 47907, USA

Introduction

The ability to voluntarily control protein and peptides conformation by the use of an internal effector is an area of increasing interest. With the finding that ß-turns are involved in hormone-receptor [1] and protein-protein recognition, several groups have initiated the design and synthesis of ß-turn mimics ranging from constrained cyclic peptides to non-peptidic scaffold. In this paper we describe a strategy to reversibly change the conformation of a cyclic peptide (**1**) from an extended one to one which contains a ß-turn, by incorporating a photoresponsive amino acid within the peptide. The photoresponsive amino acid, an azobenzene containing molecule (**Aza**) can exist in two isomeric *trans* and *cis* forms [2]. The *trans* form was intended to provide an extended conformation to the attached peptide whereas upon isomerization with light to the *cis* form, the peptide would adopt a turn conformation. Two-dimensional NMR was then used to probe the conformation of both isomeric forms.

Results and Discussion

The **Aza** was flanked by four alanine residues, two on each side, to allow flexibility during cyclization, and linked to four residues of ß-turn propensities Gly-Gly-Pro-Asn (Scheme 1) [3].

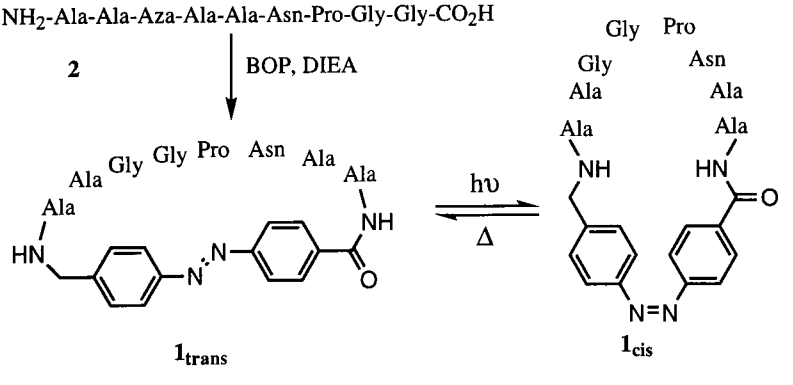

Scheme 1. *Scheme showing cyclization of 2 and isomerization of* 1_{trans}

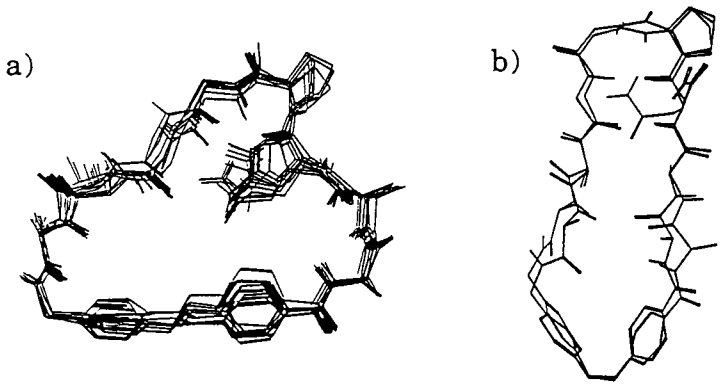

Figure 1. *Structures generated from dynamics simulation for a)* $\mathbf{1}_{trans}$ *b)* $\mathbf{1}_{cis}$.

The linear peptide **2** incorporating **Aza** was synthesized on *p*-alkoxybenzylalcohol resin using Fmoc methodology [4]. Cyclization of **2** in DMSO using BOP (1.1 equiv.) as the activating agent in the presence of DIEA (2 equiv.) provided the cyclic peptide $\mathbf{1}_{trans}$ in greater than 98% purity after HPLC purification.

Peptide $\mathbf{1}_{trans}$ (10 mM) in DMSO was cleanly isomerized to the *cis* form by exposing the solution for 2.5 hr. to a Hg arc lamp that had been filtered from 310 to 410 nm. With both isomeric forms of **1** in hand, structural elucidation was achieved by using two-dimensional NMR. Assignments from DQF COSY [5] and distances obtained from NOESY [6] experiment, were used as restraints in a high temperature (600K) molecular dynamics simulation. Refinement by minimization afforded structures of different conformations for $\mathbf{1}_{trans}$ and $\mathbf{1}_{cis}$ (Figure 1).

The presence of a ß-turn in $\mathbf{1}_{cis}$ comprising the tetrapeptide Gly-Gly-Pro-Asn was a clear indication that Aza served as a ß-turn scaffold when in the *cis* form. The ability to thermally reverse the conformation back to $\mathbf{1}_{trans}$ provides us with a reversible switch to promote the ß-turn conformation when needed. We are pursuing this strategy in biologically active peptides containing ß-turns.

Acknowledgments

We gratefully acknowledge the financial support of the NIH, the NSF and the Monsanto Company.

References

1. Rose, G.D., Gierash, L.M., Smith, J.A., *Adv. Protein Chem.*, 37 (1985) 1-109.
2. Ulysse, L.G., Chmielewski, J.A., *Bioorg. Med. Chem. Lett. 4,* (1994) 2145-2146.
3. Chou, P.Y., Fasman, G.D., *Ann. Rev. Biochem.*, 47 (1978) 251-276.
4. Wang, S.S., *J. Amer. Chem. Soc.*, 95 (1973) 1328-1333.
5. Rance, M., Sorensen, O.W., Bodenhausen, G., Wagner, G., Ernst, R.R., Wuthrich, K., *Biochem. Biophys. Res. Commun.*, 117 (1983) 479-485.
6. Macura, S., Ernst, R.R., *Mol. Phys.*, 41, (1980) 95-117.

Peptides: Chemistry, Structure and Biology
Pravin T.P. Kaumaya and Robert S. Hodges (Eds.)
Mayflower Scientific Ltd., 1996

80
RGD plus X: Structure/Activity Investigations on Cyclic RGD-peptides

R. Haubner[1], R. Gratias[1], S.L. Goodman[2] and H. Kessler[1]

[1]*Department of Organic Chemistry and Biochemistry, Technical University Munich, Lichtenbergstr. 4, 85747 Garching, Germany*
[2]*Merck KGaA Preclinical Research, Frankfurter Str. 250, 64271 Darmstadt, German.*

Introduction

Angiogenesis plays a key role during tumor growth and the formation of metastases. The neovascularization is characterized by invasion, migration and proliferation of endothelial cells [1]. Therefore it seems likely that cell adhesion molecules contribute to the regulation of these processes. It was shown that the $\alpha_v\beta_3$ integrin is abundantly expressed on blood vessels in granulation tissue and is important during neovascularization [2]. Investigations on the structure/activity relationship of cyclic peptides regarding the inhibition of the *in vitro* binding of vitronectin to the isolated $\alpha_v\beta_3$ receptor led to the highly active compounds c(RGDFV) and c(RGDFV) [3]. Recently, it was demonstrated that the latter peptide suppresses tumor-induced angiogenesis on chick chorioallantoic membrane [4]. Based on these peptides, we have investigated the influence of amino acid substitutions in positions four and five concerning their activity and selectivity towards the $\alpha_v\beta_3$ receptor. The resulting peptides can be divided into four distinct classes. Class 1 and 2 differ from 3 and 4 by the position of the structure-inducing D-amino acid. In categories 1 and 2, as in 3 and 4, either position 4 or 5 is screened with a set of hydrophilic and hydrophobic amino acids while the other position is kept unvaried (see Figure 1).

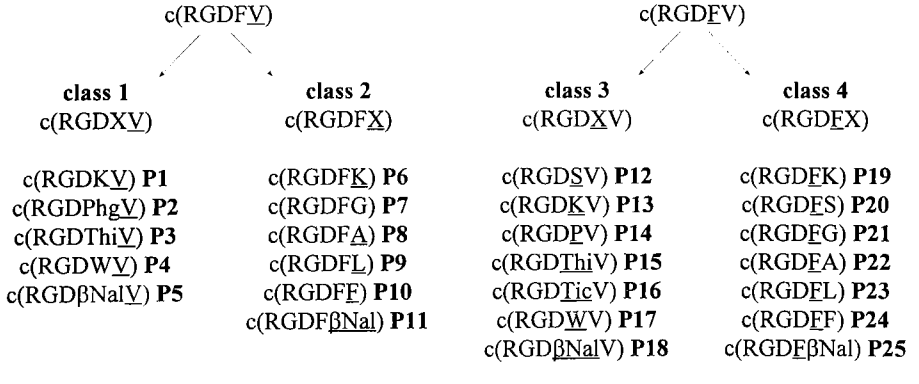

Figure 1. *Classification of the different peptides.*

Results and Discussion

The peptide structures in solution of all four classes are characterized by a βII'/γturn arrangement. The D-amino acid adopts the *i+1* position of the βII'-turn, except for class 2. Here the D-amino acid occupies the *i+1* postion of the γ-turn. Class 3 is divided into two subclasses. Instead of the βII'/γ-turn motif, the peptides **P14 and P16** show a γ/γ-turn arrangement with glycine and the D-amino acid in the *i+1* positions of the two γ-turns. The inhibitory capacities of the cyclic peptides regarding the inhibition of vitronectin (Vn) and fibrinogen (Fbg) binding to the isolated $\alpha_{IIb}\beta_3$ and $\alpha_v\beta_3$ receptors were compared with the linear standard peptide GRGDSPK. In the case of the $\alpha_v\beta_3$ receptor, all peptides except for **P14** reveal an increased activity compared with the standard peptide. The best antagonist **P17** shows a 20,000 fold higher activity. In contrast, the cyclic peptides reveal only weak capacities concerning the inhibition of Fbg binding to the $\alpha_{IIb}\beta_3$ receptor (see Figure 2).

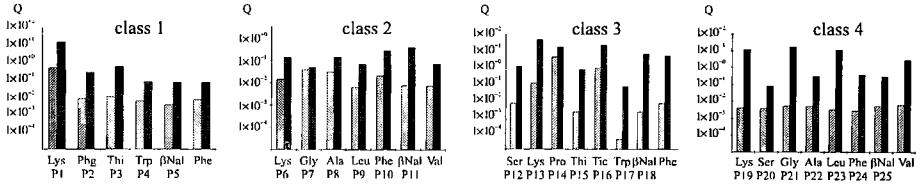

Figure 2. *Diagram showing the activities of the four peptide classes concerning the inhibition of the Fbg binding to the $\alpha_{IIb}\beta_3$ receptor (black) and the Vn binding to the $\alpha_v\beta_3$ receptor (grey). Data given as ratio $Q = IC_{50}$[peptide]/IC_{50}[GRGDSPK].*

The structure/activity investigations show that position 5 of the cyclic peptide is very tolerant towards hydrophobic as well as hydrophilic replacement. In position 4 the introduction of a hydrophobic amino acid increases the activity for both receptors. In contrast, the similarly high activity of **P12** with Ser in position 4 cannot be explained by hydrophobic interactions. We postulate the formation of a hydrogen bond between the side chain hydroxyl group and an acceptor group within the receptor. This could also explain the particularly high activity of **P17**, because the indole system of Trp^4 combines both: the aromatic interaction and a possible hydrogen bond formation *via* the indole NH. The low activity of the peptides **P14** and **P16**, especially for the $\alpha_v\beta_3$ receptor, is explained by the missing hydrogen atom of the amide bond between residue 3 and 4.

References

1. Weinstat-Staslow, D., Steeg, P.S., *FASEB J.*, 8 (1994) 401.
2. Brooks, P.C., Clark, R.A.F., Cheresh, D.A., *Science*, 264 (1994) 569.
3. a) Aumailly, M., Gurrath, M., Müller, G., Calvete, J., Timpl, R., Kessler, H., *FEBS Lett.*, 291 (1991) 50. b) Pfaff, M., Tangemann, K., Müller, B., Gurrath, M., Müller, G., Kessler, H., Timpl, R., Engel, J., *J. Biol. Chem.*, 269 (1994) 20233.
4. Brooks, P.C., Montgomery, A.M.P., Rosenfeld, M., Reisfeld, R.A., Hu, T., Klier, C.D.A., *Cell*, 79 (1994) 1157.

Peptides: Chemistry, Structure and Biology
Pravin T.P. Kaumaya and Robert S. Hodges (Eds.)
Mayflower Scientific Ltd., 1996

81
Development of Peptide Antagonists of the Integrin $\alpha_v\beta_3$

D.G. Mullen, S. Cheng, S. Ahmed, J.M. Blevitt, D. Bonnin, W.S. Craig, R.T. Ingram, C. Mazur, R. Minasyan, J.O. Tolley, J.F. Tschopp and M.D. Pierschbacher

Telios Pharmaceuticals, Inc., 4757 Nexus Centre Drive, San Diego, CA 92121, USA.

Introduction

The integrin $\alpha_v\beta_3$ has been linked to angiogenesis, metastasis, osteoporosis, and restenosis [1]. We report here results from efforts to develop antagonists to this receptor as therapeutics. Two peptide pharmacophores that bind with high affinity to the integrin $\alpha_v\beta_3$ and have unique selectivity profiles are disclosed.

Results and Discussion

To discover lead peptides for our $\alpha_v\beta_3$ antagonist program, a diverse set of peptides from the Telios compound data base was screened in our integrin assays. Peptide **1** (Table 1) proved especially interesting because it exhibited both modest activity and some selectivity, and it contained a unique pharmacophore; the pentapeptide sequence RGDDV.

Next, a high temperature dynamics conformational search of **1** found one structural family of lowest energy. In this conformation, the RGD sequence is found in a β-turn

Table 1. *Activities of RGD peptides in integrin assays, $IC_{50}(\mu m)$.*[a]

#	Sequence[b]	VN/$\alpha_v\beta_3$ ELISA[c]	VN/$\alpha_v\beta_5$ ELISA[c]	FN/$\alpha_5\beta_1$ ELISA[c]	Platelet Aggregation[d]
1	GPenRARGDDVCA	0.026	0.48	0.039	>50
2	RGD(Y-OMe)RE-NH_2	0.0036	10	0.43	0.82
3	RGDDVE-NH2	0.026	0.48	0.039	88
4	(Mpa)RGDDVC-NH_2	0.036	4.8	0.36	77
5	(Mpa)RGDD(t-BuG)C-NH_2	0.006	1.1	0.32	26
6	(Mpa)RGD(tetD)(t-BuG)C-NH_2	0.0017	0.19	0.17	12

a) abbreviations: Pen, penicillamine; Y-OMe, *O*-methyltyrosine; Mpa, 3-mercaptopropionic acid; *t*-BuG, *tert*-butylglycine; tetD, β-tetrazolylalanine; VN, vitronectin; FN, fibronectin. b) residues underlined are either in a disulfide or a lactam ring. c) competitive ELISA, ligand/receptor. d) Platelet aggregation in platelet rich normocalcemic plasma (heparin) induced by ADP (10μm). Platelet aggregation is a cell based assay that measures affinity towards the integrin $\alpha_{IIb}\beta_3$

and the DDV sequence is in a β-strand, which is similar to the active conformation calculated for the RGD(Y-OMe)R pharmacophore in our $\alpha_{IIb}\beta_3$ antagonists [2]. A screen of our $\alpha_{IIb}\beta_3$ antagonists revealed a subclass that bound with high affinity to the integrin $\alpha_v\beta_3$, **2**[d], as well. By substituting the RGDDV sequence into this subclass of peptides, we found that the RGDDV sequence is sufficient for activity and selectivity at the integrin $\alpha_v\beta_3$, **3**, **4**.

A structure-activity relationship has been developed for the RGDDV pharmacophore. Aliphatic, β-branched residues increase potency and selectivity in position 4 [positional assignments in parenthesis as follows:- X_{-1}(-1) -R(0) -G(1) -D(2) -X_3(3) -X_4(4)]; replacing *t*-BuG[a] for Val, **5**, gave a 6-fold increase in potency. Next, changing the carboxyl group of the Asp in position 3 to a tetrazole moiety, **6**, gave another 4-fold increase in activity while maintaining 100-fold selectivity over the other integrins.

In conclusion, we have developed two classes of integrin antagonists active at the nanomolar level. One is selective for the integrin $\alpha_v\beta_3$ and contains the RGDDV pharmacophore; the second selects for integrins that have the β_3 subunit and contains the RGD(Y-OMe)R sequence.

References

1. Cox, D, Aoki, T., Seki, J., Motoyama, Y. and Yoshida, K., *Medic. Res. Rev.*, 14 (1994) 195.
2. a) Craig, W.S., Cheng, S., Mullen, D.G., Blevitt, J. and Pierschbacher, M.D., *Biopolymers Peptide Science*, 37 (1995) 157. b) Cheng, S., Craig, W.S., Mullen, D., Tschopp, J.F., Dixon, D. and Pierschbacher, M.D., *J. Med. Chem.*, 37 (1993) 1.

Peptides: Chemistry, Structure and Biology
Pravin T.P. Kaumaya and Robert S. Hodges (Eds.)
Mayflower Scientific Ltd., 1996

82
Hybrid Cyclic Peptides as Potential Opioid Antagonists

J.E. Burden[1], A.F. Spatola[1], F. Porreca[2] and P. Davis[2]

[1]*Department of Chemistry, University of Louisville, Louisville, KY 40292, USA*
[2]*Department of Pharmacology, University of Arizona, Tucson, AZ 85721, USA*

Introduction

The continuing search for alternative opioid analgesics depends upon the availability of potent, receptor selective compounds for pharmacological evaluations. The cyclic opioid peptide Tyr-c[D-Lys-Phe-Ala], also known as YKFA, was first reported by Darlak *et al.* in 1990 [1]. Although YKFA is one of the most potent opioid peptides known (sub-nanomolar IC_{50}'s at both μ and δ receptors), it is not very selective, with a selectivity ratio, ($IC_{50}(\delta)/IC_{50}(\mu)$ = 4.93). In 1985, Pelton *et al.* [2] reported that a somatostatin analog, D-Phe-c[Cys-Tyr-D-Trp-Lys-Thr-Pen]Thr-NH_2, was a potent and selective μ-antagonist ($IC_{50}(\delta)/IC_{50}(\mu)$ = 271). The potency at opioid receptors of this compound and analogs is surprising in light of the prevailing view that an N-terminal Tyr, as well as an aromatic group at positions 3 or 4, is required for opioid activity. We have synthesized a series of compounds in an effort to modulate the selectivity and agonistic activity of YKFA. Because these compounds are derived from a dermorphin-like sequence (YKFA) and a somatostatin sequence, we have termed them hybrid cyclic peptides.

Results and Discussion

Four small ring dermorphin analogs have been prepared. All retain a backbone to side chain ring structure with 13 atoms in the ring. All four structures can be considered as hybrids of the potent opioid agonist, YKFA, and the potent μ-selective antagonists based on a modified small ring somatostatin.

Results of the *in vitro* bioassays are shown in Table 1. None of the four hybrids appear to have antagonist behavior. Two of the four (2 and 4) are reasonably potent and somewhat μ-selective, with IC_{50} potencies of 30 and 18 nM. The D-Phe[1] analogs are considerably less active. The significant agonist activity is surprising and analogs 2 and 4 are among a small group of opioid peptide analogs that show potent activity without an N-terminal tyramine moiety. Transposition of the Tyr and Phe residues in YKFA results in compounds that retain agonistic activity at the μ receptor. The increase in selectivity for 2 as compared with YKFA is due to a more dramatic decrease in potency at the δ receptor. When the chirality of the Phe[1] residue is changed from L to D, a compound with low activity at both μ and δ receptors is obtained.

Substitution of Ala with Trp results in a more somatostatin-like structure. Replacement of Ala in compound 2 with Trp increased potency at both the μ and δ

Table 1. *In vitro bioassays of hybrid cyclic peptides.*

Compound	GPI IC_{50}(nM)	MVD IC_{50}(nM)	MVD/GPI IC_{50} Ratio
1. H-Tyr-c[D-Lys-Phe-Ala] (YKFA)	0.11 ± 0.013	0.54 ± 0.031	4.93
2. H-Phe-c[D-Lys-Tyr-Ala]	30.38 ± 8.64	367.1 ± 27.1	12.1
3. H-D-Phe-c[D-Lys-Tyr-Ala]	1827 ± 58	9327 ± 2829	5.1
4. H-Phe-c[D-Lys-Tyr-Trp]	17.65 ± 1.91	228 ± 62.3	12.9
5. H-D-Phe-c[D-Lys-Tyr-Trp]	627 ± 123.9	8129 ± 1438	13

receptors without changing the selectivity. The same is true for compound 5. Replacement of Ala in 3 with Trp increases potency better than two-fold for 5, relative to 3. However, the D-Phe substitution again substantially decreases activity at both receptors.

There are a few examples in the literature of potent μ-selective opioid peptides in which Tyr^1 has been replaced with Phe, including the potent somatostatin analog that contain D-Phe in position 1 and Tyr in position 3. However, these compounds proved to be opioid antagonists [2]. Schiller and DiMaio reported some enkephalin analogs containing Phe in position 1 as well as position 4 that retained potency and selectivity [3]. Recently, the combinatorial approach has yielded very potent μ antagonists (acetalins) [4] as well as a μ agonist that consists of all D amino acids [5]. These peptides are acetylated at the N terminus and in both cases the side chain of Arg^1 presumably assumes the role of the protonated N-terminus. In both of these cases, the aromatic amino acids corresponding to the Tyr and Phe in the traditional opioid peptides are Phe and Trp, respectively.

In summary, the compounds reported here leave open the question of the surprising opioid antagonist activity of the somatostatin analogs, but suggest that they may be binding quite differently to the μ receptor than other opioid ligands.

Acknowledgments

This work was supported by NIH GM-33376 and by a GAANN Fellowship.

References

1. Darlak, K., Burks, T.F., Wire, W.S., Spatola, A.F., in Giralt, E. and Andreau, D. (Eds.), 'Peptides, 1990', ESCOM, Leiden, The Netherlands, 1990, p. 401.
2. Pelton, J.T., Gulya, K., Hruby, V.J., Duckles, S.P., Yamamura, H.I., *Proc. Natl. Acad. Sci., USA*, 82 (1985) 236.
3. Schiller, P.W., DiMaio, J., in Hruby, V.J. and Rich, D.H. (Eds.), 'Peptides: Structure and Function', Pierce Chemical Co., Rockford, IL, 1983, 269.
4. Dooley, C.T., Chung, N.N., Schiller, P.W., Houghten, R.A., *Proc. Natl. Acad. Sci., USA*, 90 (1993) 10811.
5. Dooley, C.T., Chung, N.N., Wilkes, B.C., Schiller, P.W., Bidlack, J.M., Pasternak, G.W., Houghten, R.A., *Science*, 266 (1994) 2019.

Peptides: Chemistry, Structure and Biology
Pravin T.P. Kaumaya and Robert S. Hodges (Eds.)
Mayflower Scientific Ltd., 1996

83

Structural Study of the Interaction between the SIV Fusion Peptide and Model Membranes

A. Colotto[1], I. Martin[2], J-M. Ruysschaert[2] and R.M. Epand[1]

[1]*Department of Biochemistry, McMaster University, Health Sciences Centre, Hamilton, ON, L8N 3Z5 Canada*
[2]*Laboratoire de Chimie-Physique des Macromolecules aux Interfaces, Universite Libre de Bruxelles, Brussels, Belgium*

Introduction

It has been shown that a correlation exists between the fusogenecity of synthetic peptides corresponding to the N-terminal segment wild type and mutant forms of Simian Immunodeficiency Virus gp32 (SIV) and their mode of insertion into lipid bilayers [1]. It has been proposed that the orientation of the peptide in the lipid bilayer changes as a consequence of the amino acid sequence which results in a change of the distribution of hydrophobicity around the helix axis, without changing the α-helicity [1, 2]. In this respect, fusogenic activity is only observed when the peptide inserts into the bilayer with an oblique orientation [3]. This corresponds to a situation in which the fusion peptide perturbs the bilayer stability [4]. Since the membrane orientation of the SIV fusion peptide determines its effect on bilayer stability and its ability to promote membrane fusion, it is reasonable to expect bilayer properties such as curvature, bending strength and surface hydration also to play an important role in the process. We use X-ray diffraction to investigate the structural effects of two synthetic peptides on different lipid systems. One peptide corresponds to the wild type sequence (SIV_{wt}), and inserts into the membrane at an oblique angle [1, 2]. The other one has a rearranged sequence ($SIV_{mt\text{-}v}$), and inserts into the membrane along the bilayer normal.

Results and Discussion

For both peptides we observe a disordering effect on lipid structural organization. However, the disorder induced by the SIV_{wt} is relatively higher below T_H (lamellar to hexagonal phase transition temperature), while with $SIV_{mt\text{-}v}$ it is higher above T_H. In both cases, the extent of the disordering effect depends on the lipid system studied. For example, diffractograms taken with the lipid MeDOPE (monomethyl dioleoylphosphatidylethanolamine) alone and in the presence of each of the peptides at relatively high peptide to lipid molar ratios ($R=5x10^{-2}$) are shown. The systems are completely disordered, independent of which peptide is present and at which temperature. However, if the samples are submitted to a fast heating process, which rapidly takes them to a temperature above T_H, it is possible to restore the hexagonal phase to the system containing SIV_{wt} (Figure 1).

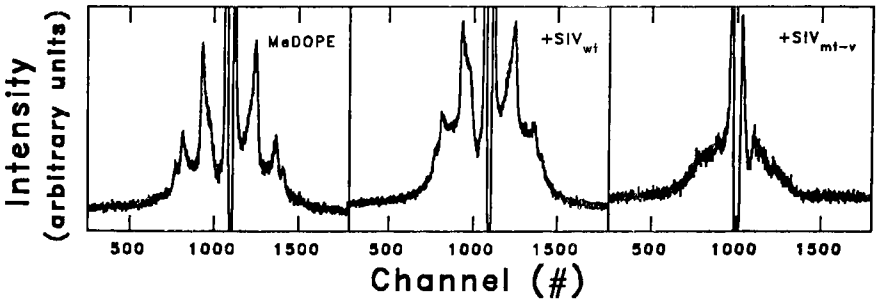

Figure 1. *X-ray diffraction profiles from the MeDOPE lipid system in the absence and in the presence of two different fusion peptides. Diffractograms were taken at 70°C. Samples were heated in one single fast step starting from room temperature. This thermal treatment proved an efficient way of getting more ordered H_{II} structures.*

The differences in the effects of the two peptides with different lipid systems can be understood in terms of the differences in the water/membrane interface and bending energy. These differences between the effects from the two peptides are demonstrated by the bilayer stabilizing action of SIV_{mt-v} as opposed to the bilayer destabilizing action of SIV_{wt}. Effects are weaker for the pure phosphatidylethanolamine system studied, where a large number of interlipid hydrogen bonds accounts for a more stable interface. The effects are stronger for the binary lipid system (ethanolamine/choline mixture 3:1), and even more so for the MeDOPE. For the binary mixture, there might occur partial segregation of the two lipids with the peptide preferentially interacting with certain domains or boundary defects. This segregation might account for part of the disorder observed. For MeDOPE, the peptide has easier access to the membrane/water interface, since the hydrogen bonding is weaker due to the presence of the CH_3 group. Generally, the structural effect of the wild-type peptide is consistent with the finding that it is a bilayer destabilizer [4], whereas that of the SIV_{mut-v} is not consistent with the finding that it is a bilayer stabilizer [4].

References

1. Voneche, V., Potetelle, D., Kettmann, R., Willems, L., Limbach, K., Paoletti, E., Ruysschaert, J.M., Burny, A. and Brasseur, R., *Microbiology*, 89 (1992) 3810.
2 Herth, M., Lambrecht, B., Chuah L., Khim, M., Bex, F., Thiriart, C., Ruysschaert, J.M., Burny, A. and Brasseur, R., *EMBO J.*, 10 (1991) 2747.
3. Martin, I., Defrise-Quertain, F., Mandieau, V., Nielsen, N.M., Saermark, T., Burn, A., Brasseur, R., Ruysschaert, J-M. and Vandenbranden, M., *Biochem Biophys. Res. Comm.*, 175 (1991) 872.
4. Epand, R.F., Martin, I., Ruysschaert, J-M. and Epand R.M., *Biochem Biophys. Res. Comm.* 205 (1994) 1938.

Peptides: Chemistry, Structure and Biology
Pravin T.P. Kaumaya and Robert S. Hodges (Eds.)
Mayflower Scientific Ltd., 1996

84

Constrained Pseudopeptides as Inhibitors of *Ras*-farnesyl Transferase: Structure-activity Relationship Studies

G. Byk[1], C. Burns[2], M. Duchesne[3], F. Parker[3], Y. Lelievre[3], J.D. Guitton[3], F.F. Clerc[3], A. Commerçon[2], B. Tocque[3] and D. Scherman[1]

[1]UMR-133 CNRS/Rhône-Poulenc Rorer and [2]Departments of Chemistry and [3]Biotechnologies Rhône-Poulenc Rorer
13, Quai Jules Guesde B.P. 14, 94403-Vitry Sur Seine, France

Introduction

The *ras* oncogene [1] is found mutated in approximately 25 % of overall human cancers [2]. Many laboratories have recently focused on the mechanism of *ras*-induced cellular transformation in the hope that this mechanism might be useful in the identification of novel anticancer therapeutic approaches [3]. In our laboratory, we are investigating the post-translational modifications of the *ras* gene product, the *ras* protein. The C-terminal CAAX sequence, where C is Cys, A is an aliphatic amino acid and X is any amino acid, is highly conserved in different *ras* proteins. These undergo several post-translational modifications before reaching their site of action in the cell membrane. The first and most important modification is the farnesylation of the thiol group of the cysteine located at the fourth amino acid position of the *ras* C-terminus. *Ras* farnesyl transferase (FTase) catalyses this event. It has been shown [4] that the inhibition of farnesylation of *ras* proteins precludes migration to their site of action in the cell membrane, so preventing their cell transforming activity. Inhibitors of *ras* farnesyl transferase thus represent a new family of potential antitumor agents against the mutated oncogenic *ras*-proteins.

Results and Discussion

Structure activity studies involving backbone modifications of **1** showed that the introduction of a local constraint by replacement of Phe by tetrahydroisoquinoline carboxylic acid (TIC) in **2** and **3** and by replacement of Val by (N-Me)Val in **3** led to peptides with drastically increased inhibitory activity of FTase in isolated enzyme assay, but with inactivity in cell based assays. Backbone modification of **2** by the amino-methylene-pseudopeptide strategy led to **4** in which Cys$\Psi(CH_2NH)$Val replaced Cys-Val. The reduced amide bond isostere clearly disclosed increased inhibitory activity of FTase in isolated enzyme and cell based assays. Additional bond reduction led to **5** which is one of the most potent analogs reported to date in isolated enzyme assay but which displayed lower activity as compared to **4** in cell based assays. Modification of the N-terminal amino acid of **4** by replacement of Cys by a mercaptopropionyl (Mpa) led to **6** and **7** with considerable inhibitory activity in isolated enzyme assay but decreased

activity in cell based assays. Interestingly, introduction of TicΨ(CH_2NH)Met instead of Tic-Met and Mpa instead of Cys led to **8**, which is completely inactive in isolated enzyme and cell based assays. Finally, we have modified **2** by the introduction of a peptoide isostere derived from homocysteine; [N-(HS-CH_2CH_2)]Gly instead of Cys-Val in **9** and a dithio-bridged dimer/methyl ester prodrug in **10**. The products displayed considerable inhibitory activity in isolated enzyme and cell based assays. Moreover, **10** suppressed also the anchorage independent growth of NIH 3T3 cells transformed with oncogenic Ha-*Ras* (IC_{50}= 3 μM) as that of the oncogenic Ki-*Ras* (IC_{50}= 1 μM), but had no effect on growth of NIH 3T3 cells transformed by v-*Raf* oncogene. Inversion of the carboxy-methylene of Gly (CH_2CO) in **9** yielded a "carboxy-retroinverso" peptide bond isostere **11** completely inactive either in isolated enzyme assay or cell based assay.

Table 1. *Inhibition of FTase*[a] *and ras processing*[b] *by pseudopeptides related to Cys-Val-Phe-Met.*

Compound	Formula	IC_{50}	
		in vitro[a] (nM)	cells[b] (μM)
1	CysValPheMet	1,000	-
2	CysValTICMet	10	-
3	Cys[NMe]ValTICMet	5	-
4	CysΨ[CH_2NH]ValTICMet	0.6	100
5	CysΨ[CH_2NH]ValΨ[CH_2N]TICMet	1.2	150
6	MpaΨ[CH_2NH]ValTICMet	0.8	200
7	MpaΨ[CH_2NH]ValΨ[CH_2N]TICMet	2.3	-
8	MpaValTICΨ[CH_2N]Met	$>>10^7$	-
9	[N-($HSCH_2CH_2$]GlyTICMet	100	-
10	-($SCH_2CH_2NHCH_2COTICMet\text{-}OCH_3$)$_2$	145	100
11	$HSCH_2CH_2NHCOCH_2$TICMet	$>>10^7$	-

[a] FTase inhibition was tested on human FTase as previously described [4].
[b] Ras processing inhibition in intact THAC cells was carried out as previously described [5].

We are currently evaluating conformational differences between active and non active compounds by molecular dynamics models and NMR toward the design and synthesis of new generations of non peptidic inhibitors of *ras* FTase.

Acknowledgments

This work was done as part of the "Bioavenir" programe supported by Rhône Poulenc, with the participation of the French Ministries of Research and Industry.

References

1. Barbacid, M., *Annu. Rev. Biochem.*, 56 (1987) 779.
2. Lowy, D. (Ed.), 'Seminars in Cancer Biology', 3 (1992) 167.
3. Brown, M.S., Goldstein, J.L., Paris, K.J., Burnier, J.P. and Masters, J.C., *Proc. Natl. Acad. Sci. USA.*, 89 (1992) 8313.
4. Reiss, Y., Goldstein, J.L., Seabra, M.C., Casey, P.J. and Brown, M.S., *Cell*, 62 (1990) 81.
5. Seuwen, K. and Pouysegur, J., *EMBO J.*, 7 (1988) 161.

Peptides: Chemistry, Structure and Biology
Pravin T.P. Kaumaya and Robert S. Hodges (Eds.)
Mayflower Scientific Ltd., 1996

85
Oral Activity of Tripeptide Aldehyde Thrombin Inhibitors

R.T. Shuman[1], R.B. Rothenberger[1], C.V. Jackson[1], E.W. Roberts[2], B. Singer[3], R.A. Lucas[2] and K.D. Kurz[1]

[1]The Lilly Research Laboratories, Eli Lilly and Company, Indianapolis, IN 46285, USA
[2]The Lilly Research Centre Limited, Eli Lilly and Company, Erl Wood Manor, Windlesham, GU20 6PH, England, UK
[3]Guys Drug Research Unit, London, SE11 YR, England, UK

Introduction

Tripeptide aldehydes, such as D-1-Piq-Pro-Arg-H (**1**) and D-MePhe-Pro-Arg-H [1] (**2**), are small molecular weight direct inhibitors of thrombin that block the enzyme active site and prevent fibrin formation.

Results and Discussion

The ability of compounds **1** and **2** to be effective orally active thrombin inhibitors was determined. The criteria established for the compounds was an acceptable index of bioavailability, antithrombotic efficacy in a rat model of extracorporeal arteriovenous (AV) shunt thrombosis, and to have little or no potential for bleeding liability as measured by a canine template bleeding time. In addition, the compound should have good oral absorption with an acceptable half life in normal human volunteers.

The rat served as the animal model for the estimation of bioavailability because of its small size and ease of study [2]. Due to the lack of an assay for parent drug, absolute bioavailability could not be determined, instead bioactivity, as measured with plasma thrombin time (TT), served as an index of plasma drug concentration to estimate bioavalibility. Plasma TT represents the time between addition of a constant amount of bovine thrombin to a plasma sample and the formation of fibrin. The time course of plasma TT was determined in groups of rats after intravenous bolus and oral administration of the two compounds. The area under the curve (AUC) of the plasma TT time course was determined and adjusted for the different doses. This index of bio-availability, termed "%Relative Activity", was calculated for each compound using the equation %Relative Activity = (AUC po) / (AUC iv) X (Dose iv) / (Dose po) X 100. The estimation of bioavailability using this approach yielded a Relative Activity of approximately 54% for D-1-Piq-Pro-Arg-H and 12% for D-MePhe-Pro-Arg-H.

In the rat AV shunt model, blood was circulated for 15 minutes through a 3-piece shunt of plastic tubing connecting the carotid artery to its contralateral jugular vein. The center section of the tubing contained a thread upon which thrombotic material deposited. The thread was removed and weighed as a measure of thrombosis. The two

compounds were studied at various times after oral administration in this model. Both compounds caused dose-dependent reductions in the weight of the formed thrombus. The results after a single oral dose of 20 mg/kg of compound **1** and **2** in the AV shunt model demonstrated that both compounds reduced thrombus weight in a time-dependent manner. Compound **1** exhibited a significantly greater reduction in thrombus weight after one hours oral dosing and antithrombotic effect persisted longer than compound **2**.

An estimation of bleeding liability was performed using a canine model by measurement of template bleeding times on the gingiva of the left jaw. Both compounds were found to have very little effect on template bleeding time at the doses tested. The doses that caused a significant increase in bleeding time were at 2.0 and 4.0 mg/kg/hr for compound **1** and 4.0 mg/kg/hr for compound **2**.

Both compounds were found be efficacious in the AV-shunt model with compound **1** exhibiting a 5 fold increase in its index of bioavailability. Compound **1** was the more potent antithrombotic after oral administration in this rat model. In addition, both compounds exhibit little effect on potential bleeding liability as measured in a canine template bleeding time. Therefore, these experiments plus many others suggested considerable therapeutic potential for compound **1**. Compound **1** was then evaluated in normal human volunteers in a dose escalating study (Figure 1). The four dose levels of Compound **1** administered to individuals, exhibited a significant dose-dependent oral absorption with an effective half life for the compound of less than two hours. The design of a thrombin inhibitor with a better duration of action remains a major goal.

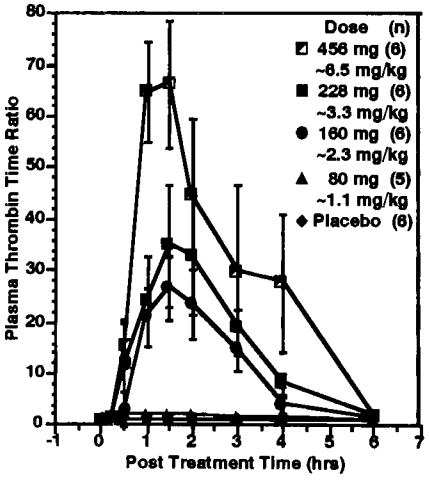

Figure 1. *Time course of plasma thrombin time ratio in normal volunteers.*

References

1. Bajusz, S., Szell, E., Bagdy, D., Barabas, E., Horvath, G., Dioszegi, M., Fittler, Z., Szabo, G., Juhasz, A., Tomori, E. and Szilagyi, G., *J. Med. Chem.*, 33 (1990) 1729.
2. Smith, G.F., Neubauer, B.L., Sundboom, J.L., Best, K.L., Goode, R.L., Tanzer, L.E., Merriman, R.L., Frank, J.D. and Herrmann, R.G., *Thrombosis Research,* 50 (1988) 163.

Peptides: Chemistry, Structure and Biology
Pravin T.P. Kaumaya and Robert S. Hodges (Eds.)
Mayflower Scientific Ltd., 1996

86
A Study of EGF and Heregulin Binding Specificity

E.G. Barbacci, B.C. Guarino, J.G. Stroh, D.H. Singleton, K.J. Rosnack, J.D. Moyer, G.C. Andrews and L. Contillo, Jr.

Pfizer Central Research, Groton, CT 06340, USA

Introduction

The Epidermal Growth Factor Receptor (EGFR) family of tyrosine kinase-linked receptors (EGFR, erbB2/neu, erbB3 and erbB4) are frequently overexpressed in cancer cells and may regulate tumor cell proliferation [1]. A number of peptide growth factors have a demonstrated ability to bind to and modulate these receptors, among them are EGF, and Heregulin (HRG)/Neu differentiation factor (NDF).

The heregulins (HRGs) are a family of proteins that stimulate tyrosine phosphorylation of $p185^{erbB2}$ and have a region of high homology to EGF [2-4]. EGF and HRG bind breast cancer cells with complete specificity to their respective receptors [2, 5]. This binding specificity is obtained despite common structural features in their core domains (Figure 1) [6]. We previously reported the solid phase synthesis of biologically active HRGβ177-226 [7]. Based upon alignment of this core region of HRGβ with EGF, we synthesized a series of fifteen EGF/HRG "chimeras" designed to elucidate sequence components important for receptor selectivity.

Results and Discussion

HRGβ177-226 and EGF1-48 each consist of four intra-cysteine regions and N- and C-terminal tails. Chimeras were synthesized in which these six regions were independently exchanged between EGF and HRG (Figure 1). These chimeric peptides were folded and their structure confirmed by mass spectral analysis and, when possible, by disulfide mapping. These chimeras were evaluated *versus* HRG and EGF controls in 4 distinct breast cancer cell based assays: 1) inhibition of ^{125}I-EGF binding to SKBr3 cells, 2) inhibition of ^{125}I-HRG binding to SKBr3 cells, 3) stimulation of EGFR autophosphorylation in MDA-MB-468 cells, and 4) stimulation of p185 tyrosine phosphorylation in MDA-MB-453 cells.

Substitution of any of the EGF regions into HRG produced chimeras which retained full affinity for the HRG receptor and ability to stimulate p185 phosphorylation in cells. None of these chimeras had affinity for EGFR (Table 1). A chimera of HRG with the EGF N-terminus (not shown) could not be evaluated as it did not produce properly folded material under oxidation conditions successful for all other chimeras. Synthesis of a truncated HRG, minus the N-terminal 5 aa (HRGβ182-226) also did not yield product with proper disulfide bonding.

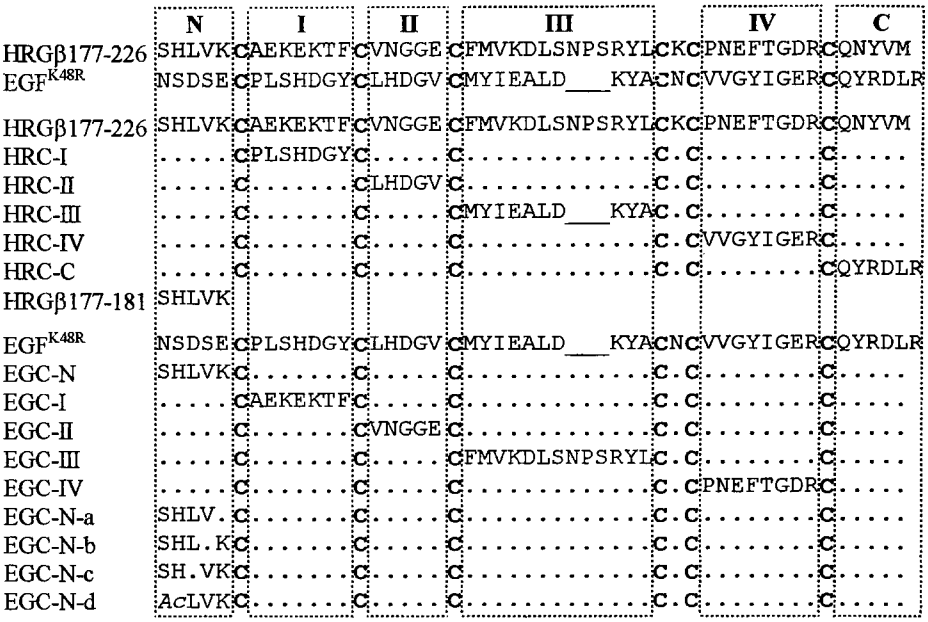

Figure 1. *HRG, EGF, and HRG/EGF chimeras (HRCs) and EGF chimeras (EGCs). Gaps in the aligned sequence are represented by dashes; dots represent sequence identities with the top sequence.*

It is likely that all primary sequence substitutions of EGF into HRG which involve structurally dissimilar residues represent positions in HRG which are unimportant for receptor binding since these non-conservative substitutions do not destroy binding affinity. Inability to fold HRG with a modified N-terminus is consistent with NMR evidence suggesting that this region plays an important role in the generation of tertiary structure [6, 8].

EGC-I, III and IV bound neither receptor with high affinity and did not stimulate phosphorylation of EGFR or p185 (Table 1). EGC-II had moderate affinity for both receptors, but could not stimulate p185 phosphorylation.

Substitution of the HRG N-terminus for the corresponding region of EGF produced a chimera, EGC-N, which bound both receptors with high affinity and was highly active in stimulating EGFR and p185 phosphorylation (Table 1). Further investigation of the N-terminal sequence of EGC-N with chimeras EGC-N-a, EGC-N-b, EGC-N-c showed little effect on affinity for the HRG receptor. Removal of Ser^{177} and His^{178} (EGC-N-d) reduced affinity for the HRG receptor by >10-fold (Table 1) without a corresponding effect for the EGF receptor. The pentapeptide HRGβ177-181 was unable to compete for HRG binding (Table 1).

The N-terminal five amino acids of HRG are, therefore, crucial for generating specific high affinity binding to its receptor, with region II also contributing to specificity in binding. The chimeric EGC-N, a highly potent agonist for both EGF and HRG receptors, represents a first of its kind and is therefore designated "biregulin".

Table 1. *Receptor binding and phosphorylation data.*

	Inhibition of HRG binding IC_{50} (nM)*	Stimulation of p185 phosphorylation	Inhibition of EGF binding IC_{50} (nM)*	Stimulation of EGFR phosphorylation
HRG 177-226	0.16	+	>180	-
HRC-I	0.07	+	>180	-
HRC-II	0.25	+	>200	-
HRC-III	0.19	+	>190	-
HRC-IV	0.18	+	>180	-
HRC-C	0.17	+	>170	-
HRG 177-181	>170000	-	NT	NT
m-EGF	>99	-	0.2	+
EGC-I	>180	-	180	+
EGC-II	46	-	152	+
EGC-III	>170	-	>170	-
EGC-IV	>180	-	>180	-
EGC-N	0.18	+	1	+
EGC-N-a	0.2	NT	NT	NT
EGC-N-b	0.21	NT	NT	NT
EGC-N-c	0.7	NT	NT	NT
EGC-N-d	12	NT	0.8	NT

* Specific binding of ^{125}I-HRGβ177-241 or ^{125}I-EGF to SKBr3 cells [7]; "+" > 2 fold increase in tyrosine phosphorylation relative to untreated control cells; "-" < 10% of the response to positive control (EGF or HRG); "NT" = not tested.

References

1. Prigent, S.A. and Lemoine, N.R., *Progress in Growth Factor Research,* 4 (1992) 1; Aaronson, S.A., *Science*, 254 (1991) 1146.
2. Holmes ,W.E., Sliwkowski, M.X., Akita, R.W., Henzel, W.J., Lee, J., Park, J.W., Yansura, D., Abadi, N., Raab, H., Lewis, G.D., Shepard, H.M., Kuang, W-J., Wood, W.I., Goeddel, D.V. and Vandlen, R.L., *Science*, 256 (1992) 1205; Wen, D., Peles, E., Cupples, R., Suggs, S.V., Bacus, S., Luo, Y., Trail, G., Hu, S., Silbiger, S.M., Ben-Levy, R., Koski, R.A., Lu, H.S. and Yarden, Y., *Cell*, 69 (1992) 559.
3. Lupu, R., and Lippman, M.E., *Breast Cancer. Res. and Treatment*, 27 (1993) 83.
4. Marchionni, M., Goodearl, A.D.J., Chen, M.S., Bermingham-McDonogh, O., Kirk, C., Hendricks, M., Danehy, F., Misunmi, D., Sudhalter, J., Kobayashi, K., Wroblewski, D., Lynch, C., Baldassare, M., Hiles, I., Davis, J.B., Hsuan, J.J., Totty, N.F., Otsu, M., McBurney, R.N., Waterfield, M.D., Stroobant, P., and Gwynne, D., *Nature*, 362 (1993) 312.
5. Peles, E., Bacus, S.S., Koski, R.A., Lu, H.S., Wen, D., Ogden, S.G., Ben-Levy, R. and Yarden, Y., *Cell,* 69 (1992) 205.
6. Nagata, K., Kohda, D., Hatanaka, H., Ichikawa, S., Matsuda, S., Yamamoto, T., Suzuki, A. and Inagaki, F., *EMBO J.*, 13 (1994) 3517.
7. Barbacci, E.G., Guarino, B.C., Moyer, J.D., Andrews, G.C., Singleton, D.H., Rosnack, K.J. and Stroh, J.G., *J. Biol. Chem.*, 270 (1995) 9585.
8. Massefski, W.W., unpublished data.

Peptides: Chemistry, Structure and Biology
Pravin T.P. Kaumaya and Robert S. Hodges (Eds.)
Mayflower Scientific Ltd., 1996

87

Chemical Synthesis of Phospholamban, a Modulator of the Cardiac Sarcoplasmic Reticulum Calcium Pump

V.M. Garsky[1], E.J. Mayer[2], E. McKenna[2], C.J. Burke[2], H. Mach[2], C.R. Middaugh[2], M. Sardana[2], J.S. Smith[2], R.G. Johnson, Jr.[2] and R.M. Freidinger[1]

Departments of [1]Medicinal Chemistry and [2]Pharmacology, Merck Research Laboratories, West Point, PA 19486, USA

Introduction

Phospholamban (PLB) is a 52 amino acid (primarily pentameric) membrane protein (Figure 1) present in stoichiometric amounts with the Ca^{2+} ATPase of cardiac sarcoplasmic reticulum (SR). PLB in its unphosphorylated state attenuates the catalytic activity of Ca^{2+} ATPase by reducing its apparent calcium sensitivity. Phosphorylation of PLB [1], treatment with antibodies directed against PLB [2] or mild trypsin proteolysis of PLB [3] reverses the decreased calcium sensitivity leading to stimulation of Ca^{2+} ATPase activity. Limited quantities of this modulator of the cardiac SR calcium pump from natural sources compounded by its extreme hydrophobic nature have made its isolation difficult and limited its biophysical characterization.

The chemical synthesis of PLB has been reported [4] but a direct comparison with n-PLB was not performed. This report, as well as a more detailed description [5], describes an alternative chemical synthesis and a detailed comparison of n-PLB with s-PLB. A synthetic Cys to Ser analog which does not oligomerize is also described.

Ac-Met-Asp-Lys-Val-Gln-Tyr-Leu-Thr-Arg-Ser-Ala-Ile-Arg-Arg-Ala-Ser-Thr-Ile-Glu-Met-Pro-Gln-Gln-Ala-Arg-Gln-Asn-Leu-Gln-Asn-Leu-Phe-Ile-Asn-Phe-Cys-Leu-Ile-Leu-Ile-Cys-Leu-Leu-Leu-Ile-Cys-Ile-Ile-Val-Met-Leu-Leu-OH

Figure 1. *Primary sequence of phospholamban.*

Results and Discussion

Assembly of the primary structure was achieved on a 0.50 mmole scale using the Applied Biosystems 430A peptide synthesizer [6]. Boc protection for the primary amine along with TFA stable side chain protection was used for all amino acids. A double coupling protocol, as supplied by ABI, was employed at each step using N-methylpyrrolidinone as the reaction solvent. Acetylation of the N-terminal Met was accomplished by coupling acetic acid as described above. The final 52-peptide was cleaved from the resin using the high HF procedure [7] in the presence of *p*-cresol and *p*-thiocresol as scavengers. The

crude product was extensively extracted with 50% acetic acid/H_2O and lyophilized. Due to its extreme insolubility, difficulty was encountered during attempts to purify crude PLB using standard reverse phase (RP) preparative HPLC conditions. Even after solubilization, major product loss was observed on silica based RP supports. However, when a polymer based C-18 support was used (Asahipak® Gel, ODP-200, 20μm) with a formic acid/water/isopropyl alcohol gradient system we were able to efficiently purify 300 mg of crude PLB to yield 27 mg of pure product.

Synthetic and native PLB were shown to be indistinguishable when analyzed by SDS-polyacrylamide gel electrophoresis and both exhibit pentameric complexes which dissociate to monomers upon boiling. Both proteins are phosphorylation substrates for the catalytic subunit of the cAMP-dependent protein kinase. Native and synthetic PLB have identical amino acid analyses which reflect their predicted composition and both yield identical internal PLB sequences following CNBr treatment. Mass spectroscopy results were in agreement with the predicted molecular weight (M = 6123).

A synthetic full-length PLB analog in which the three Cys residues at positions 36, 41 and 46 were replaced with the isosteric amino acid serine was also synthesized. Unlike s-PLB, the Cys to Ser analog does not oligomerize into pentamers as determined by SDS-PAGE and analytical equilibrium centrifugation. The analog was phosphorylated by the catalytic subunit of cAMP-dependent protein kinase, and was recognized by polyclonal antisera. CD spectral analysis of n-PLB and s-PLB indicates about 70% α-helical structure while the Cys to Ser analog shows only 30% α-helical content.

Acknowledgments

Our thanks are expressed to C.F. Homnick and D.G. Kolodin for their technical assistance.

References

1. Tada, M. and Kadoma, M., *BioEssays*, 10 (1989) 157.
2. Suzuki, T. and Wang, J.H., *J. Biol. Chem.*, 261 (1986) 7018.
3. Kirchberger, M.A., Borchman, D. and Kasinathan, C., *Biochemistry*, 25 (1986) 5484.
4. Vorherr, T., Wrzosek, A., Chiesi, M. and Carafoli, E., *Prot. Sci.*, 2 (1993) 339.
5. Mayer, E.J., McKenna, E., Garsky, V.M., Burke, C.J., Mach, H., Middaugh, C.R., Sardana, M., Smith, J.S. and Johnson, Jr., R.G., manuscript in preparation.
6. Kent, S. and Clark-Lewis, I., in Alitalo, K., Partanen, P. and Vaheri, A. (Eds.), 'Synthetic Peptides in Biology and Medicine', Elsevier, Amsterdam, 1985, p. 29.
7. Tam, J.P., Heath, W.F. and Merrifield, R.B., *J. Am. Chem. Soc.*, 105 (1983) 6442.

Peptides: Chemistry, Structure and Biology
Pravin T.P. Kaumaya and Robert S. Hodges (Eds.)
Mayflower Scientific Ltd., 1996

88

Two Different Types of Fibronectin-binding MSCRAMMS from Gram-positive Bacteria

S. Gurusiddappa, D. Joh and M. Höök

Institute of Biosciences and Technology, Center for Extracellular Matrix Biology, Texas A & M University, Houston, TX 77030, USA

Introduction

Bacterial adherence to host tissue is commonly mediated by a member of the adhesin family generally designated MSCRAMMs (Microbial Surface Components Recognizing Adhesive Matrix Molecules). Fibronectin (Fn) binding MSCRAMMs of *S. aureus* (FnbpA), *S. dysgalactiae* (FnbA and FnbB), *S. pyogenes* (Sfb), and *S. equisimilis* (FsE) have been isolated and their respective genes cloned and sequenced. The binding site for Fn on these MSCRAMM molecules is located in a segment consisting of a 30-43 amino acid residues long motif repeated three or four times (Figure 1). Recombinant proteins containing the repeat region and synthetic peptides mimicking the individual repeat units have been shown to bind ^{125}I-labeled Fn. These MSCRAMMs bind Fn by interacting with the 29 kDa amino terminal region of Fn, which is composed of five so-called type I

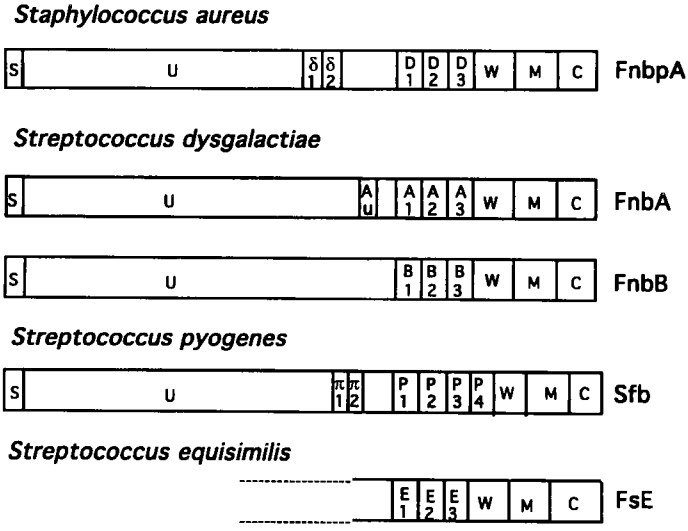

Figure 1. *Domain organization of fibronectin receptors from FnbpA, FnbA, FnbB, Sfb and FsE. Fn binding repeat units are represented by A, B, D, E, and P. The sequence of the N-terminal portion of Fse is not available. S, signal sequences; U, sequence unique to the Fn receptor; W, cell wall-spanning region; M, membrane spanning region; C, intracellular region.*

Table 1. *The ability of synthetic peptides A2 andB3 binding to different finger constructs.*

Peptide	F12	F23	F34	F45
A2	-	+	+	+
B3	+	+	-	-

modules. In the present study, we produced recombinant proteins containing two type I modules (modules 1-2, 2-3, 3-4 and 4-5) and examined their interaction with synthetic peptides mimicking the ligand binding motifs of the Fn binding MSCRAMMs.

Results and Discussion

Type I modules (also called fingers) 1-2, 2-3, 3-4 and 4-5 of Fn were expressed using the maltose binding protein fusion system [1] and purified by amylose-Sepharose chromatography. Purified proteins were separated by SDS-PAGE and blotted onto membrane. Then the membrane was probed with synthetic peptides labeled with biotin (Pierce, Rockford, IL). The results are summarized in Table 1.

The peptides A2 and B3 were able to recognize at least one finger construct in our binding assay. We have earlier reported that synthetic peptides mimicking active motifs in Fn receptors from different Gram-positive bacteria [2] showed a high degree of cross reactivity, *i.e.* (i) motif B3 of *S. dysgalactiae* FnBB, and each of the A motifs of FnbA inhibit binding of both Fn and the N-terminal fragment to cells of *S. aureus*; (ii) each of the A motifs of FnbA inhibit binding of Fn and the N-terminal fragment to *S. dysgalactiae*; and (iii) the A motifs are capable of cross-inhibition of Fn binding to purified FnbB, while B3 inhibits Fn binding to purified FnbA, and the D3 motif from *S. aureus* inhibits binding to both *S. dysgalactiae* receptors. The close observation of A2 repeat sequence reveals that this motif bears a resemblance to the consensus sequence (Figure 2) that conform to Fn binding proteins. This peptide is used to explore binding

```
A1:                      VVEDTQTSQED-IVLGGPGQVIDFTEDSQPGMSGNNSHT
A2:                      ITEDSKPSQEDEVIIGGQGQVIDFTEDTQSGMSGDNSHTDGTV
A3:                      LEEDSKPSQEDEVIIGGQGQVIDFTEDTQSGMSGAGQVESP
P1,3:                  VETEDTKE--P-EVLMGGQSESVEFTKDTQTGMSGQTTPQ
P2:                    VETEDTKE--P-GVLMGGQSESVEFTKDTQTGMSGQTTPQ
P4:                    VETEDTKE--P-GVLMGGQSESVEFTKDTQTGMSG
D1:              QNSGNQSFEEDTEEDKP-KYEQGGNIVDIDFDSVPQIHG
D2:              QNKGNQSFEEDTEKDKP-KYEHGGNIIDIDFDSVPHIHG
D3:              FNKHTEIIEEDTNKDKP-SYQFGGHN-SVDFEEDTLPKV
E1:   EETLPTEQGQSGSTTEVEDT-KV-P-EVMIGGQGEIVEF
E2:   EETLSTEQGQSSSATEVEDT-KG-P-DVLIGGQGEIVEF
B1:   EETLPTEQGQSGSTTEVEDT-KG-P-EVIIGGQGEIVDI
B2:   EENLPTEQGQSGSTTEVEDT-KG-P-EVIIGGQGEVVDI
B3:   EESLPTEQGQSGSTTEVEDS-K--P-KLSIHFDNEWPKED
E3:   EETLPTEHGQSGSTTEVEDS-K--P-KISIHFDNEWPKEE
```

Figure 2. *Aligned sequences of the Fn binding repeat units indicated by A, B, D, E, and P in Figure 1. Sequences of the synthetic peptides used in this study are underlined. The regions of very high similarity are shown in bold type.*

specificity in our present study. However, B3 repeat from FnbB, which lacks the consensus sequence also binds Fn effectively, suggesting there are two types of Fn MSCRAMMS on Gram-positive bacteria.

The results from the Table 1 indicate that the B3 peptide only binds fingers 1-2 and 2-3; whereas the A2 peptide binds fingers 2-3, 3-4 and 4-5. Sequence of the repeat region of FsE is similar to FnbB, suggesting that its Fn-binding mechanism may be similar to that of FnbB. Thus, the Fn binding MSCRAMMs from Gram-positive bacteria can be divided into two types, type I represented by FnbA, FnbpA and Sfb, and type II represented by FnbB and FsE.

Acknowledgments

This work was supported by grants No. AI20624 and HL47313 from the National Institutes of Health.

References

1. Matsuka, Y.V., Medved, L., Brew, S.A. and Ingham, K.C., *J. Biol. Chem.*, 269 (1994) 9539.
2. McGavin, M.J., Gurusiddappa, S., Lindegren, P.-E., Lindberg, M., Raucci, G. and Hook, M., *J. Biol. Chem.*, 268 (1993) 23946.

Peptides: Chemistry, Structure and Biology
Pravin T.P. Kaumaya and Robert S. Hodges (Eds.)
Mayflower Scientific Ltd., 1996

89

NMR Studies in Relation to Biological Effects: Investigations on the Structure-activity Relationship of Human Parathyroid Hormone (hPTH)

W.G. Forssmann[1], U. Marx[2], P. Bayer[2], K. Adermann[1], D. Hock[1] and P. Rösch[2]

[1]The Lower Saxony Institute for Peptide Research (IPF), D-30625 Hannover, Germany
[2]Lehrstuhl für Struktur und Chemie der Biopolymere, Universität Bayreuth, D-95440 Bayreuth, Germany

Introduction

The N-terminal fragment (1-37) of human parathyroid hormone (hPTH) is a bioactive compound that occurs in human blood [1]. The known functional domains of hPTH are located in this N-terminal part of the peptide. Biological effects on bone cells are activation of adenylate cyclase and stimulation of DNA synthesis by a cAMP independent signal pathway. An increase of serum calcium concentration after activation of adenylate cyclase by N-terminal fragments imparts hPTH a high clinical potential, *e.g.* in the treatment of osteoporotic patients [2]. In the present study, we show that cAMP cyclase activity is strongly dependent on the N-terminal structure of hPTH (1-37). The activity correlates with structures of several hPTH fragments obtained from NMR spectroscopy experiments [3, 4].

Results and Discussion

Previous studies have demonstrated that the effect of N-terminal hPTH fragments on calcium concentration in serum *via* cAMP cyclase activation does not depend on the C-terminal structure of peptides. No significant difference in the elevation of calcium levels is observed after application of C-terminal elongated peptides hPTH (1-32) to (1-38) (Table 1). In contrast, the loss of the three N-terminal amino acid residues results in a decrease of calcium concentration in serum. Furthermore, the calcium levels induced by the peptides hPTH (2-37) and hPTH (3-37) differ significantly (Table 1). Parallel investigations on the structures of these hPTH fragments by NMR spectroscopy

Table 1. *Biological activity of N-terminal hPTH fragments in Parsons chicken assay[a][5].*

hPTH fragment	1-34	1-37	2-37	3-37	4-37
relative Ca^{2+} change	100	89	91	8	-4

[a] Change in Ca^{2+} concentration after intravenous injection into chicken relative to PTH (1-34).

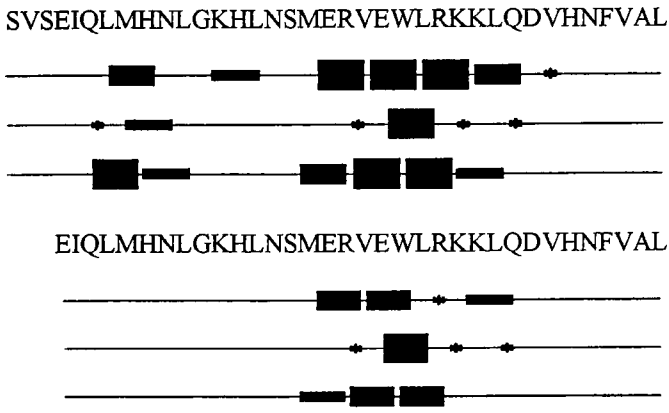

Figure 1. *NOEs vs. sequence. dαβ(i,i+3) NOEs of hPTH-1-37 compared to hPTH (4-37). The thickness of the bars qualitatively indicates the relative strength of NOESY crosspeaks.*

show that deletion of the N-terminus results in a change of structure. Figure 1 shows (i, i+3) NOEs from NMR spectra indicating α-helical regions in hPTH (1-37). The N-terminal helix is not present in the shortened hPTH (4-37). Other parts of hPTH (4-37) are not influenced in their structural behaviour by this modification [3, 4]. The study shows that biological activity of hPTH fragments goes along with these structural properties. However, the role of the N-terminal amino acids with respect to conformational changes during receptor interactions is still unclear.

Acknowledgments

Thanks for support are due to HaemoPep Pharma GmbH, Hannover, and to Boehringer Mannheim GmbH for performing the chicken assay.

References

1. Forssmann, W.G., Schulz-Knappe, P., Meyer, M., Adermann, K., Forssmann, K., Hock, D. and Aoki, A., in Yanaihara, N. (Ed.) 'Peptide Chemistry 1992', ESCOM, Leiden, The Netherlands 1993, p. 553.
2. Finkelstein, J.S., Klibanski, A., Schaefer, E.H., Hornstein, M.D., Schiff, I. and Neer, R.M., *N. Engl. J. Med.*, 331 (1994) 1618.
3. Marx, U.C., Austermann, S., Bayer, P., Adermann, K., Ejchart, A., Sticht, H., Walter, S., Schmid, F.X., Jaenicke, R., Forssmann, W.G. and Rösch, P., *J. Biol. Chem.*, 270 (1995) 15194.
4. Marx, U.C., Bayer, P., Adermann, K., Forssmann, W.G. and Rösch, P., University of Bayreuth, Germany, unpublished data.
6. Parsons, J.A., Reit, B. and Robinson, C.J., *Endocrinology*, 92 (1973) 454.

Peptides: Chemistry, Structure and Biology
Pravin T.P. Kaumaya and Robert S. Hodges (Eds.)
Mayflower Scientific Ltd., 1996

90

Structure-Activity Relationships of a Tripeptide Segment Critical for the Inactivation of Voltage-Gated Sodium Channels

D.M. Leonard[1], C.J. Poulter[1], A.M. Doherty[1], M.F. Rafferty[1], G. Eaholtz[2], C. Taylor[1] and W.A. Catterall[2]

[1]Parke-Davis Pharmaceutical Research, Division of Warner-Lambert Co., 2800 Plymouth Road, Ann Arbor, MI 48105, USA
[2]Department of Pharmacology and Graduate Program in Neurobiology, University of Washington, Seattle, WA 98195, USA

Introduction

Voltage-gated sodium channels are responsible for conducting sodium ions across the cell membrane causing depolarization of the cell and subsequent cellular activation. This event is followed by inactivation of the channel within 1-2 msec [1]. Rapid inactivation is essential for terminating nerve impulses. Research on the molecular basis for the fast sodium channel inactivation has suggested that a positively charged amino acid sequence within the sodium channel may bind to the open channel, causing inactivation [2].

The sodium channel is a single polypeptide chain with four repeating units (I-IV). Each repeat unit contains 6 α-helical transmembrane segments. The short cytoplasmic segment linking domains III and IV ($L_{III/IV}$) of the sodium channel may play a role in the fast inactivation process since deletion or insertion in this region *via* site-directed mutagenesis slow down the inactivation process [3, 4]. The positively charged or paired negatively charged residues in $L_{III/IV}$ were shown not to be essential for fast inactivation of the sodium channel [5]. However, the last ten amino acids at the N-terminus of $L_{III/IV}$ were found to be important for fast inactivation of the sodium channel, through site-directed mutagenesis [5]. In particular, mutations of the three residue cluster: Ile^{1488}-Phe^{1489}-Met^{1490} completely blocked fast sodium channel inactivation [6]. The residue Phe^{1489} is a critical residue since mutation to glutamine caused a 5000-fold decrease in channel inactivation [6].

These results suggest that the tripeptide cluster Ile-Phe-Met may serve as inactivation gate for the sodium channel. Small peptides containing the Ile-Phe-Met sequence (Ac-Lys-Ile-Phe-Met-Lys-NH_2) block sodium channels when applied to cell cytosol *via* microinjection and cause fast inactivation in mutant sodium channels which lack the ability to undergo fast inactivation [7].

Truncation of the pentapeptide was carried out and the tripeptide (Ile-Phe-Met-NH_2) was also found to block the opening of the sodium channel. Therefore, a series of tripeptide analogues were synthesized by solid phase peptide chemistry to evaluate the

structure-activity relationships for the interaction of small peptides with the binding site of the inactivation gate of the sodium channel.

Results and Discussion

The pentapeptide Ac-Lys-Ile-Phe-Met-Lys-NH_2 was found to be effective at causing fast inactivation of the sodium channels (60% block @ 100 mV). The tetrapeptide Lys-Ile-Phe-Met-NH_2 and tripeptide Ile-Phe-Met-NH_2 were also shown to be effective sodium channel blockers (75% and 65% @ 100 mV, respectively). Further truncation to the dipeptides Ile-Phe-NH_2 and Phe-Met-NH_2 or to the amino acid amide Phe-NH_2, gave rise to inactive compounds (20%, 10% and 5% @ 100 mV, respectively). Therefore the tripeptide is the minimum sequence for effective blockade of sodium channels.

Structure-activity relationships were then carried out on the tripeptide Ile-Phe-Met-NH_2. All three mono-Ala substituted analogues were inactive, indicating the importance of each residue. D-amino acid substitution at either the Ile and Met position was tolerated.

Substitution of Met with Nle was tolerated (Ile-Phe-Nle-NH_2, 65% @ 100mV) while substitution with Orn (Ile-Phe-Orn-NH_2) lead to a reduction in potency (30% @ 100 mV). Oxidation of the Met residue (Ile-Phe-Met(O)-NH_2) was not tolerated (10% @ 100 mV), indicating that in the active tripeptide the Met residue is not in the oxidized form.

A tripeptide of similar potency as Ile-Phe-Met-NH_2 was obtained on substitution of Phe by Trp (Ile-Trp-Met-NH_2, 70 % @ 100 mV). Substitution of the Phe residue with Phg (Ile-Phg-Met-NH_2) or diphenylalanine (Ile-Dpa-Met-NH_2) gave rise to less potent sodium channel blockers (both 35% @ 100 mV). Substitution of Phe with the constrained amino acid tetrahydroisoquiniline (Ile-Tic-Met-NH_2) was not tolerated (20% @ 100 mV). *Para*-substitution on the aromatic ring of Phe by an amino group (Ile-*p*(NH_2)Phe-Met-NH_2) did not cause blockade.

In summary, two tripeptides, Ile-Phe-Met-NH_2 and Ile-Trp-Met-NH_2, were found to be the most effective at inactivating voltage-gated sodium channels. These peptides may prove to be useful pharmacological tools to elucidate further the mechanism of inactivation of sodium channels and may enable mimetic design of sodium channel blockers modeled on the residues of the inactivation gate.

References

1. Catterall, W.A., *Trends in Neuroscience*, 16 (1993) 500.
2. Armstrong, C.M. and Bezanilla, F., *J. Gen. Physiol.*, 70 (1977) 567.
3. Stuhner, W., Conti, F., Suzuki, H., Wang, X., Noda, M., Yahagi, N., Kubo, H. and Numa, S., *Nature* (London), 339 (1989) 597.
4. Patton, D.E. and Goldin, A.L., *Neuron*, 7 (1991) 637.
5. Patton, D.E., West, J.W., Catterall, W.A. and Goldin, A.L., *Proc. Natl. Acad. Sci. USA*, 89 (1992) 10905.
6. West, J.W., Patton, D.E., Scheuer, T., Wang, Y., Goldin, A.L. and Catterall, W.A, *Proc. Natl. Acad. Sci. USA*, 89 (1992) 10910.
7. Eaholtz, G., Scheuer, T. and Catterall, W.A., *Neuron*, 12 (1994) 1041.

Peptides: Chemistry, Structure and Biology
Pravin T.P. Kaumaya and Robert S. Hodges (Eds.)
Mayflower Scientific Ltd., 1996

91
A Spectroscopic Investigation of Novel NK1 Tachykinin Receptor Antagonists

B. Pispisa[1], M.Venanzi[1], A. Sisto[2] and P. Lombardi[2]

Dipartimento di [1]Scienze e Tecnologie Chimiche, Universita' di Roma "Tor Vergata", 00133 Roma, Italy
[2]Chimica, Menarini Ricerche Sud, 00040 Pomezia (Roma), Italy

Introduction

Earlier studies on short linear Ala- and Aib-based oligopeptides carrying protoporphyrin IX and naphthalene covalently bound to the ε-amino groups of Lys residues showed that combination of IR, CD and both steady-state and time-resolved fluorescence spectra was productive in determining the structural features of the compounds in methanol or water/ methanol (75/25) solution [1]. We thus proved that they populate helical structures, to an extent depending on chain length, while exhibiting an internal Brownian rotational motion of the side-chains slower than 10 ns. Recently, we have undertaken an optical, chiroptical and fluorescence investigation on novel nonpeptidic NK-1 tachykinin analogs (Figure 1), where S denotes 1,1- or 1,2-disubstituted moieties [2]. The naphthyl (N) and indolyl (I) groups were thought to exhibit a neat π stacking propensity responsible for the biological activity, an idea supported by the spectroscopic results presented here.

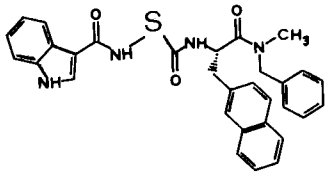

Figure 1. *General formula of nonpeptidic NK-1 tachykinin analogs.*

Results and Discussion

According to absorption and fluorescence spectra in methanol solution, an indolyl-naphthyl (I-N) charge-transfer (CT) complex forms, to an extent depending on the stereochemical features of the compounds, unless the scaffold is so rigid as to prevent the folding of the molecule. This is indeed the case for the blank, where S in Figure 1 is a bicyclo (2.2.1) moiety, exhibiting a biological activity as low as $pK_i = 5.5$, as measured by the cologarithm of the concentration of the antagonist able to displace 50% of substance P bound to the cells [2]. By examining the steady-state fluorescence spectra of the tachykinin analogs, it appears that quenching efficiency ($\lambda_{ex} = 280$, $\lambda_{em} = 340$ nm), as given by $(1-\Phi/\Phi^0)$, where Φ is the quantum yield of the sample and Φ^0 that of the blank,

linearly increases as the biological activity increases. Since only the I and N groups involved in the CT complex undergo the quenching process, it may be concluded that the larger the fraction of CT formed the higher the activity. On the other hand, the charge-separated nature of the I-N stacked complex is revealed by the dependence on the solvent polarity of the weak emission which is observed in the 400-500 nm region [3]. Additionally, absorption spectra indicate that, in all cases, the CT complex has a molar extinction coefficient at 280 nm of $(1.95\pm0.15).10^4$ $M^{-1}cm^{-1}$, implying that the stacking involves always the same moieties, *i.e.* I and N groups.

The CD spectra in methanol solution are fully consistent with the above conclusions. They show common features in the accessible UV region, as shown in Figure 1, but the molar ellipticity of the negative band at around 227 nm is seen to increase (in absolute value) as the pK_i of the molecules increases (Figure 2 insert). This trend suggests that the larger the fraction of the stacked complex the smaller the amount of conformationally mobile chromophores, and hence the higher the ellipticity.

To conclude, irrespective of the type of the disubstitution in the cyclohexane moiety in Figure 1, if the scaffold is flexible enough so as to allow the formation of an I-N stacked complex experiencing partial charge separation, then the molecule stiffens and attains the correct conformation for competing substance P binding to the NK-1 receptor.

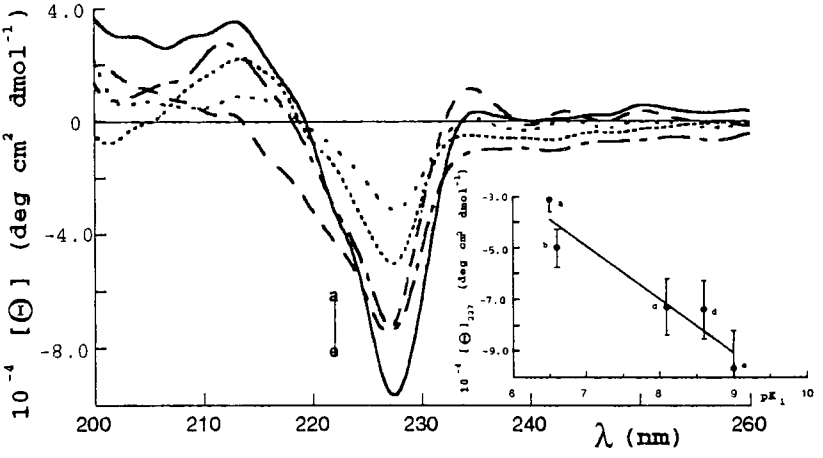

Figure 2. *Typical UV-CD spectra in methanol of 1,1-disubstituted compounds (Figure 1), S representing in this case moieties of different flexibility. Insert: dependence of molar ellipticity at 227 nm on the biological activity, expressed as pK_i (see text). Concentration ≈ 0.5 mM.*

References

1. Pispisa, B., Venanzi, M., Palleschi, A. and Zanotti, G., *Macromolecules*, 27 (1994) 7800; *Biopolymers*, 36 (1995) 497.
2. Sisto, A., Bonelli, F., Centini, F., Fincham, C.I., Potier, E., Monteagudo, E., Lombardi, P., Arcamone, F., Goso, C., Manzini, S., Giolitti, A., Maggi, C.A., Venanzi, M. and Pispisa, B., *Biopolymers*, 36 (1995) 511.
3. Oevering, H., Verhoeven, J.W., Paddon-Row, M.N. and Warman, J.M., *Tetrahedron*, 45 (1989) 4751.

Peptides: Chemistry, Structure and Biology
Pravin T.P. Kaumaya and Robert S. Hodges (Eds.)
Mayflower Scientific Ltd., 1996

92
Structure and Function of VLDL: Perturbation by Class A Amphipathic Helical Peptides

B.H. Chung, M.N. Palgunachari, V.K. Mishra, R. Chang, J.P. Segrest and G.M. Anantharamaiah

Department of Medicine and Biochemistry, University of Alabama at Birmingham, Birmingham, AL 35294, USA

Introduction

The exchangeable apolipoproteins, apo C-I, C-II, C-III and E, in very low density lipoprotein (VLDL) play an important role in regulating the metabolism of VLDL. They can modulate the initial catabolic process of VLDL as well as the removal of remnants from circulating blood [1-3]. It is well established that apo C-II acts as a cofactor for the lipolysis of VLDL triglycerides by lipoprotein lipase (LpL) [1]; apo E and apo C-III act as a specific ligand and an inhibitor, respectively, for binding of VLDL and their remnants to the lipoprotein receptors on hepatic and nonhepatic cells [2, 3]. All of the exchangeable apolipoproteins of VLDL contain amphipathic α-helix as their structural and functional units [4].

Class A amphipathic helices, commonly found in exchangeable apolipoproteins, are characterized by the location of positively charged amino acid residues at the polar-nonpolar interface and negatively charged amino acid residues at the center of the polar face. Synthetic class A peptide analogs have been shown to mimic many properties of native apolipoproteins and thus have been used to study the domains of apolipoproteins responsible for lipid binding, enzyme activation, receptor binding and to probe the structure of lipoproteins [4]. In the present study, we have examined the effect of displacing exchangeable apolipoproteins from human VLDL by class A amphipathic helical peptides with different arrangements of the helical domains on the metabolic and functional properties of VLDL.

Results and Discussion

The three peptide analogs of the class A amphipathic helix used in the present study are: 1) an 18-residue peptide possessing a single helical domain, with the sequence DWLKAFYDKVAEKLKEAF (18A), 2) two 18A molecules separated by a Pro residue (18A-Pro-18A or 37pA), and 3) 18A with the end terminal groups protected to increase helicity (Ac-18A-NH_2). The peptides 37pA and Ac-18A-NH_2 are helical to a similar extent (73% and 72%, respectively) in the presence of 1,2-dimyristoyl-*sn*-glycero-3-phosphatidylcholine [5, 6]. Both of these peptides are able to displace most of the exchangeable apolipoproteins from VLDL, upon incubation with VLDL at a peptide to VLDL (protein) ratio of 1:1 (w/w), without altering the lipid composition and the

morphology of VLDL; under identical conditions 18A has minimal effect. The extent of displacement of exchangeable apolipoproteins by peptides is a function of VLDL to peptide ratio in the incubation mixture. Analysis of the exchangeable apolipoproteins associated with peptide-treated VLDL indicates that the rank order of displaceability of apolipoproteins on VLDL by amphipathic peptides is apo E > apo C-III > apo C-II, indicating that apo E is bound to VLDL with much lower affinity than that of apo C-III, while apo C-II is bound with higher affinity than that of apo C-III. Displacement of apo Cs and/or E by synthetic amphipathic peptides variably affects the function of VLDL to interact with LpL and cultured macrophages; Ac-18A-NH_2 treatment markedly lowered both reactivity of VLDL to purified bovine milk LpL and the ability of VLDL to induce lipid accumulation in cultured macrophages, while 18A and 37pA treatment only minimally lowered these abilities. The loss of reactivity of Ac-18A-NH_2-treated VLDL to LpL was only partially restorable when all of the displaced apolipoproteins were included in the lipolysis mixture. This data suggests that full activation of LpL by apo C-II requires its binding to VLDL. Studies of the interaction of artificial triglyceride emulsion with LpL showed that 37pA, but not Ac-18A-NH_2, can act as an activator of LpL and thus can enhance the hydrolysis of triglycerides in lipid emulsion. The peptide Ac-18A-NH_2 or 37pA had no apparent effect on the hydrolytic activity of another lipolytic enzyme (pancreatic phospholipase) which does not require a cofactor.

The above data indicate that 1) amphipathic helical peptides alter the functional properties of VLDL by dissociating the exchangeable apolipoproteins from VLDL as well as by acting as a functional element following their incorporation into VLDL, and 2) the Pro punctuated dimer of 18A (37pA) exerts significantly different effect on VLDL properties compared to Ac-18A-NH_2, although secondary structures of the two peptides are similar. This observation suggests that, in addition to the secondary structure of many exchangeable apolipoproteins, their arrangement on the VLDL surface modulates VLDL function.

References

1. Havel, R.J., Shore, V.G. and Bier, D.M., *Cir. Res.*, 27 (1970) 595.
2. Windler, E., Chao, Y. and Havel, R.J., *J. Biol. Chem.*, 255 (1980) 5475.
3. Sehajek, E. and Eisenberg, S.J., *J. Biol. Chem.*, 266 (1991) 18259.
4. Segrest, J.P., Jones, M.K., De Loof, H., Brouillette, C.G., Venkatachalapathi, Y.V. and Anantharamaiah, G.M., *J. Lipid Res.*, 33 (1992) 141.
5. Mishra, V.K., Palgunachari, M.N., Lund-Katz, S., Phillips, M.C., Segrest, J.P. and Anantharamaiah, G.M., *J. Biol. Chem.*, 270 (1995) 1602.
6. Mishra, V.K., Palgunachari, M.N., Segrest, J.P. and Anantharamaiah, G.M., *J. Biol. Chem.*, 269 (1994) 7185.

Peptides: Chemistry, Structure and Biology
Pravin T.P. Kaumaya and Robert S. Hodges (Eds.)
Mayflower Scientific Ltd., 1996

93

Synthesis and Study of the Antimicrobial Action of Cecropin and Proline-Arginine-rich Peptides from Pig

S. Vunnam[1], P. Juvvadi[1], H.G. Boman[2] and R.B. Merrifield[1]

[1]The Rockefeller University, 1230 York Ave, New York, NY 10021, USA
[2]Arrhenius Laboratories, Stockholm University, Sweden

Introduction

Two antimicrobial peptides, cecropin P1, with a C-terminal acid [1], and PR-39 with a C-terminal amide, [2] were isolated from the small intestine of the pig and sequenced. Each is active against both Gram positive and Gram negative bacteria, with differences in their mechanism of action [3]. To understand the importance of sequence, direction of amide bond, end group charges, chirality of the amino acids and handedness of the helix, we have synthesized these peptides and several analogs, including the D enantiomers and the retro sequences, each with a free or acetylated amino terminus, and the CP1 amides.

Results and Discussion

The CP1 amide was found to be slightly more active compared to CP1, whereas acetylation of the N^{α}-free amine gave a nearly inactive analog (Table 1). The retro analog of CP1 was less active against all five of the bacteria tested and very interestingly it was hemolytic against sheep red cells. The retro isomer when viewed from the opposite end by rotation in the plane 180°, has the same sequence as the normal analog, but the amide bond direction is opposite [4]. An overall enhancement of the antimicrobial activity was observed with the C-terminal amides in comparison with C-terminal acid derivatives of both normal and retro analogs of CP1. These results show the importance of sequence and indicate that a free amino terminus is essential for the activity. All the peptides were synthesized by a combination of manual and automated (Applied Biosystems 430 A) solid phase techniques [5].

Chirality has no marked effect on the activity of CP1, with the L and D isomers having variable activity against all five test bacteria. Likewise, the enantiomers of PR-39 were not equally active. The ratios of the lethal concentration of L/D isomers were 6.8 and 66 at 12 hr and 60 hr of incubation respectively for *Pseudomonas aeruginosa* and similarly >100 and >1000 for *Staphylococcus aureus*. In the latter case, the lethal concentration for the D isomer was 0.57 μM, whereas this organism was quite resistant to the L-isomer. The other three test organisms, *Escherichia coli, Bacillus subtilis and Streptococcus pyogenes* showed no chiral selectivity.

With a very small inoculum D-PR-39 produced a clear zone of killing *S. aureus* surrounded by a zone of stimulated growth. After prolonged incubation the two zones became one clear zone. PR-39 stops DNA and protein synthesis. Addition of PR-39 to

the wells of a dense plate of growing cells showed a cleared zone after 12 hr for each of the test organisms, indicating that PR-39 lyses the bacteria. PR-peptides appear to stimulate the growth of bacterial colonies instantaneously, followed by slow killing of bacteria. Thus there appears to be a time lag between the interaction of the PR peptide with the bacteria and the killing. In contrast, CP1 causes a very rapid lysis of bacteria.

Sequence appears to be the determining factor for the activity of pig cecropin analogs, though changes in the C-terminal group and blocking of the free N^{α}- amine also alter the activity. There was no marked effect of chirality on the activity of CP1. The activity of all-L and all-D isomers of PR-39 show that chirality has a significant effect on their activity against certain bacteria. These results suggest that different mechanisms may be adopted by the same and also different bacterial strains, and a single mechanism cannot be postulated even for one strain. Finding PR-39 in skin wounds [6] predicts that the peptides assist in maintaining sterility in the wounds and reducing the inflammation.

Table 1. *Lethal and lysis concentrations (μM) for CP1 and PR-39 analogs*[a].

	Peptide	Size	D21	OT 97	Bs 11	Sp 1	Sac 1	SRC
1.	L-CP1-acid	31	0.4	13	10	44	>520	400
2.	D-CP1-acid	31	1.7	>300	3.9	3.2	75	500
3.	Ac-D-CP1-acid	31	16.4	>300	42.4	12.8	>300	190
4.	L-CP1- amide	31	0.3	5.9	6.6	12	>490	>200
5.	Ac-L-CP1- amide	31	0.5	>200	55	28	>500	>300
6.	Retro-L-CP1- amide	31	18	>230	33	15	>300	>400
7.	Ac-Retro-L-CP1- amide	31	18	>280	199	60	>250	>370
8.	Retro-L-CP1- acid	31	61	>350	280	>300	>300	40
9.	Ac-Retro-L-CP1- acid	31	246	>400	290	>300	>300	195

	Peptide	Size	D21	OT 97		Bs 11	Sp 1	Sac1		SRC
				12 hr	60hr			12 hr	60hr	
1.	L-PR-39	39	1.4	9.6	7.3	1.5	2.2	>600	>600	17.4
2.	D-PR-39	39	2.9	1.4	0.11	2.8	3.1	5.6	0.57	>130

[a]Lethal concentrations calculated after 12hr (or 60 hr) from inhibition zones on agarose plates seeded with the respective organisms: D21=*E.coli;* OT97=*P.aeruginosa;* Bs11=*B.subtilis;* Sp1=*S.pyogenes;* Sac1=*S.aureus;* SRC=sheep red cells.

References

1. Lee, J.Y., Boman, A., Chuanxin, S., Andersson, M., Jornvall, H., Mutt, V. and Boman, H.G., *Proc. Natl. Acad. Sci. USA.*, 86 (1989) 9159.
2. Agerberth, B., Lee, J.-Y., Bergman, T., Carlquist, M., Boman, H.G., Mutt, V. and Jornvall, H., *Eur. J. Biochem.*, 202 (1991) 849.
3. Boman, H. G., Agerberth, B. and Boman, A., *Infect. Immun.*, 61 (1993) 2978.
4. Merrifield, R.B., Juvvadi, P., Andreu, D., Ubach, J., Boman, A. and Boman, H.G., *Proc. Natl. Acad. Sci. USA.*, 92 (1995) 3449.
5. Merrifield, R.B., *J. Am. Chem. Soc.*, 85 (1963) 2149.
6. Gallo, R.L., Ono, M., Povsic, T., Page, C., Eriksson, E., Klagsbrun, M. and Bernfield, M., *Proc. Natl. Acad. Sci. USA.*, 91 (1994) 11035.

Peptides: Chemistry, Structure and Biology
Pravin T.P. Kaumaya and Robert S. Hodges (Eds.)
Mayflower Scientific Ltd., 1996

94
Anti-HIV Pentapeptides Containing an N-Alkyl-glycine Residue

M. Wakselman[1], A.M. Mouna[1], G. Née[1], C. Nguyen[1], J.P. Mazaleyrat[1], A. Bousseau[2], Y. Hénin[2] and J.F. Ferron[2]

[1]SIRCOB, Université de Versailles, F78000 Versailles, France
[2]Rhône-Poulenc Rorer, F94403 Vitry-sur-Seine, France

Introduction

N-(2,3-dihalogenopropyl)-glycine containing peptides were previously prepared as potential suicide substrates of the HIV protease or as enzyme-activated prodrugs [1]. Some of them, as well as their synthetic precursor Boc-Ala-Phe-N-(allyl)-Gly-Ile-Val-OMe **I**, showed an activity in counteracting the cytopathic effects of the HIV-1 on CEM cells and decreased the reverse transcriptase activity in cell culture supernatants (antiviral effect). Several modifications of the antiviral compound **I** have now been performed as follows. First, as N-(allyl)-glycine is an irreversible inhibitor of flavine oxidases such as sarcosine oxidase [2], an oxidative bioactivation of compound **I** leading to an epoxide or to a Michael acceptor seemed possible. To probe such an hypothesis, the double bond of molecule **I** was hydrogenated to give a saturated derivative **II** possessing an N-propyl instead of an N-allyl substituent. Second, the N-allyl-glycine and N-propyl-glycine residues, which can be considered as open mimics of proline or as truncated peptoid analogs of isoleucine [3], have been substituted with L- or D-Pro and with N-isopropyl or N-isobutyl-glycine. Third, in order to examine the importance of each amino acid side-chain of molecules **I** and **II** for anti-HIV activity, several substitutions including a series of single point alanine-substituted peptides (alanine scan) were realized.

Results and discussion

The reduced derivative **II** displayed a protective activity against the cytopathic effect induced by the HIV-1 (LAI strain) close to that of the starting molecule, ruling out a possible bioactivation of the allyl group in the case of **I**. Both compounds **I** and **II** were also active on HIV-2 (ROD strain). While reducing the reverse transcriptase activity in cell cultures, infected with HIV-1 or HIV-2, this derivative **II**, like the parent molecule **I**, has no noticeable action both on the HIV-1 protease and on the reverse transcriptase *in vitro*. From the analogous anti-HIV properties of molecule **I** and its reduced form **II**, we can conclude there is no oxidative bioactivation of the allyl group in the case of **I**.

Alanine scan of compounds **I** or **II** showed that Ala substitution in position 4 was tolerated (Table 1). However, replacement of Ile_4 by Phe, Asp(Obzl) or Lys(Z) causes a loss of the antiviral activity.

Table 1. *Alanine scan of the activities of the compounds Boc-Ala-AA_2-AA_3-AA_4-AA_5-OMe against HIV-1 (LAI strain) and HIV-2 (ROD strain) in CEM cell cultures.*

AA_2	AA_3	AA_4	AA_5	EC-50 (HIV-2) μM	CC-50 (HIV-2) μM	SI-50	EC-50 (RT) (HIV-2) μM
Phe	*N*-allyl-Gly	Ile	Val (I)	12.3 (>16.7)	>50.5 (60.7)	4.09	30.3 (#76)
Phe	*N*-allyl-Gly	Ile	Ala	128.2	>158.3	1.23	158.2
Phe	*N*-allyl-Gly	Ala	Val	43.2	>53.9	1.25	32.4
Phe	*N*-allyl-Ala	Ile	Val	118.7 (>297)	>297 (>297)	2.51	89 (NT)
Ala	*N*-allyl-Gly	Ile	Val	>57 (>57)	>57 (>57)		NT

Protective activity against the cytopathic effect induced by HIV was evaluated by MTT assay [4], and inhibition of reverse transcriptase activity in the supernatant of cell cultures was evaluated by RT dosage [5]. EC-50: concentration that reduced by 50% the HIV induced cytopathic effect; CC-50: dose of compound required to reduce the viability of uninfected cells by 50%, SI=IC-50/ EC-50, EC-50 [RT]: dose of compound that reduces reverse transcriptase activity in infected cell supernatant by 50 %; NT: not tested.

N-propyl- and N-allyl-glycines do not behave as open analogs of proline for substitutions with L-Pro or D-Pro and give inactive compounds. Branched alkyl substituents (N-isopropyl- or N-isobutyl-glycine) induce a loss of the antiviral effect. Therefore, the analogy with a truncated peptoid of isoleucine is not valid. Molecules having an unsubstituted glycine or a sarcosine at position 3 are also devoid of activity. The homolog possessing a N-butyl-glycine is active.

Acknowledgment

This work was supported by the ANRS.

References

1. Wakselman, M., Mouna, A.M., Xie, J., Mazaleyrat, J.P., Boulay, R., Lelièvre, Y., Bousseau, A., Nachmansohn, C. and Hénin, Y., *Bioorg. Med. Chem. Letters*, 4 (1994) 2533.
2. Kraus, J.L. and Belleau, B., *Can. J. Chem.*, 53 (1975) 3141.
3. Mouna, A.M., Nguyen, C., Rage, I., Xie, J., Née, G., Mazaleyrat, J.P. and Wakselman, M, *Synthetic. Commun.*, 24 (1994) 2429.
4. Pauwels, R., Balzarini, J., Baba, M., Snoeck, R., Schols, D., Herdewijn, P., Desmyter, J., De Clercq, E., *J. Virol. Methods*, 20 (1988) 309.
5. Schwartz, O., Hénin, Y., Maréchal, V. and Montagnier, L., *Aids Res. Hum. Retroviruses*, 4 (1988) 441.

Peptides: Chemistry, Structure and Biology
Pravin T.P. Kaumaya and Robert S. Hodges (Eds.)
Mayflower Scientific Ltd., 1996

95
Synthesis of Active Microcin B17: A 43-peptide Antibiotic Containing Eight Heteroaromatic Ring Systems

G. Videnov, D. Kaiser, C. Kempter, A. Bayer and G. Jung

Institute of Organic Chemistry, University of Tübingen, Auf der Morgenstelle 18, D-72076 Tübingen, Germany

Introduction

Microcin B17 (McB17) is a ribosomally synthesized peptide antibiotic showing unusual chemical features. We described in 1992 [1, 2] the complete elucidation of McB17, the first known gyrase inhibitor of peptidic nature, which is produced by *Escherichia coli* strain LP17 [3]. The enzymatic backbone modification of the pro-McB17 leads to the formation of 2-aminomethylthiazole-4-carboxylic acid (Thz) and 2-aminomethyloxazole-4-carboxylic acid (Oxa), respectively. Furthermore, two bicyclic modifications were found: 2-[2-aminomethyloxazolyl]-thiazole-4-carboxylic acid (OxaThz) and 2-[2-aminomethylthiazolyl]-oxazole-4-carboxylic acid (ThzOxa) (Figure 1).

The replacement of oxazole by thiazole rings in the recently synthesized all-thiazole microcin B17 resulted in the loss of antibacterial and gyrase inhibitor activity as shown by *in vivo* and *in vitro* assays [4]. Here we report on the first total synthesis of the gyrase inhibitor McB17 with natural sequence [1, 2].

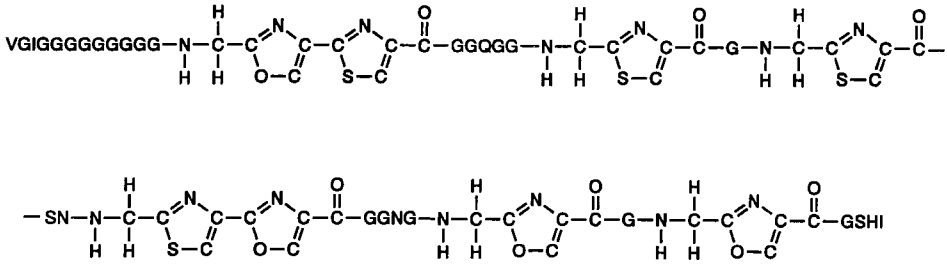

Figure 1. *Structure of the glycine-rich peptide antibiotic microcin B17.*

Results and Discussion

The peptide was synthesized manually on a Wang resin following the Fmoc-strategy and using TBTU/HOBt/DIEA, with control of all coupling steps. The assembled peptide was cleaved from the resin by the mixture DMS/m-cresol/ethane dithiol/TFA (3/3/3/91) and precipitated with ether. The crude synthetic McB17 obtained after cleavage showed a good purity (≈ 40%). The peptide was obtained in high purity (> 95%) by semi-

preparative HPLC (Nucleosil 300 C18 5 μm, 8x250 mm) using a gradient with CH_3CN/ H_2O containing 0.1% TFA. The ion spray mass spectrum of the synthetic microcin B17 shows a double and triple charged molecular ion having the expected molecular mass (Figure 2). The enantiomeric purity of HPLC purified McB17 has been determined by gas chromatography of a derivatized hydrolysate (48 hr.) on Chirasil-Val to be within the usually observed values.

Our results show that we succeeded in the assembly of this unusual and large peptide antibiotic McB17. In addition, the synthesis confirms our previously published structure elucidation [1, 2]. The synthetic McB17 was compared to a sample of the natural McB17 and found to be identical in 2D-NMR experiments and tests for antibacterial activity.

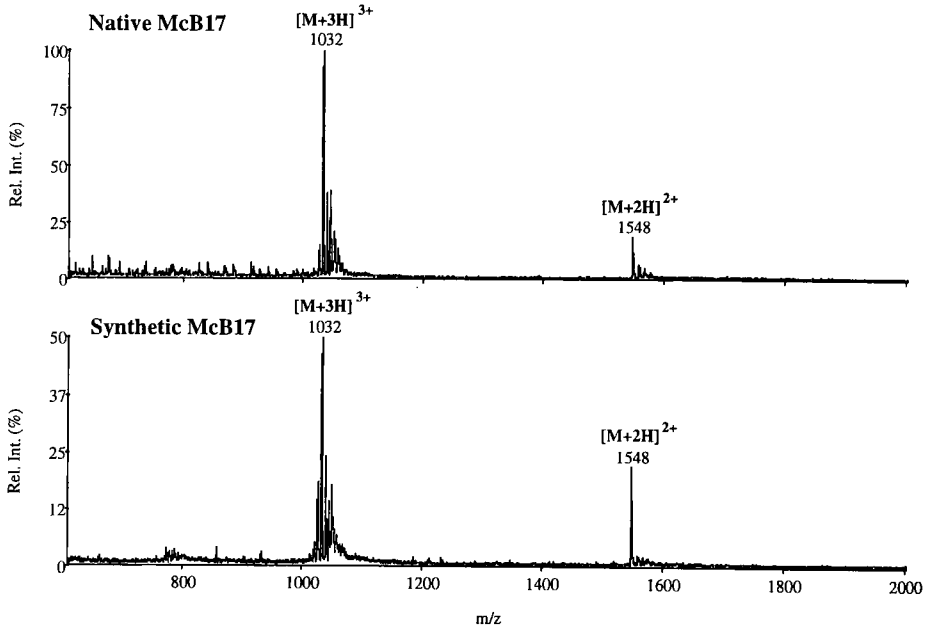

Figure 2. *ESI-MS of purified native and synthetic microcin B17 (RMM det. 3094, RMM calc. 3094 amu).*

References

1. Bayer, A., Stevanovic, S., Freund, S., Metzger, J.M. and Jung, G., in Schneider, C.H. and Eberle, A.N. (Eds), 'Peptides 1992', ESCOM, Leiden, The Netherlands 1993, p. 117.
2. Bayer, A., Freund, S., Nicholson, G. and Jung, G., *Angew. Chem. Int. Ed. Engl.* 32 (1993) 1336.
3. Vizan, J.L., Hernandez-Chico, C., del Castillo, I. and Moreno, F., *EMBO J.*, 10 (1991) 467.
4. Videnov, G., Ihlenfeldt, H.G., Bayer, A. and Jung, G., in Maia, H.L.S (Ed.), 'Peptides 1994', ESCOM, Leiden, The Netherlands 1995, p. 351.

Peptides: Chemistry, Structure and Biology
Pravin T.P. Kaumaya and Robert S. Hodges (Eds.)
Mayflower Scientific Ltd., 1996

96
Antitumor Activity of GnRH Analogs and Their Conjugates with Poly-(N-vinylpyrrolidone-co-maleic acid)

I. Mezö[1], J. Seprödi[1], Zs. Vadász[1], I. Teplán[1], B. Vincze[2], I. Pályi[2], A. Kálnay[2], G. Turi[2], M. Móra[3], J. Pató[3], G. Tóth[4], S. Lovas[5] and R.F. Murphy[5]

[1]1st Institute of Biochemistry, Semmelweis University Medical School, Budapest, Hungary
[2]National Institute of Oncology, Budapest, Hungary
[3]Central Institute for Chemistry, Hungarian Academy of Sciences, Budapest, Hungary
[4]Biological Research Center of the Hungarian Academy of Sciences, Szeged, Hungary
[5]Department of Biomedical Sciences, Creighton University, School of Medicine, 2500 California Plaza, Omaha, NE 68178, USA

Introduction

GnRH-III, pGlu-His-Trp-Ser-His-Asp-Trp-Lys-Pro-Gly-NH_2, [1] has superior direct antitumor activity but no effect on LH release. The compounds in Table 1 were synthesized to examine the area of structural difference, residues 5 to 8, of GnRH and GnRH-III. Effects on antitumor activity of conjugating active analogs were then examined *in vitro* with MCF-7 and MDA-MB-231 and *in vivo* with xenografts of MDA-MB-231 human breast cancer cells in immunosuppressed mice.

Results and Discussion

Data in Table 1 show the importance of a putative salt bridge between Asp^6 and Lys^8 side-chains. A Glu substitution in position 6 (compound 7) decreases inhibition of growth of both breast cancer cell lines. The substitution of Lys for Ser^4 (compound 4) or His^5 (compound 2) diminishes the inhibitory activity. When the sidechains of Asp^6 and Lys^8 are cyclized (compound 3), no interference is observed by Lys in position 5, whereas acetylation prevents interference by the side chain of the Lys^4 (compound 5). Compound 8, when tritiated at Pro^9 can be used as a stable radioligand to show that GnRH-III has 6- and 4-fold higher affinity, than has GnRH and its superagonist, Ovurelin.

Inhibitory activity of peptides was retained following conjugation with copolymer but relative activities did not reflect those of the free compounds. Copolymer was without biological activity. Similar inhibitory effects of free peptides and conjugates obtained with the breast cancer cell lines were observed with PC3 prostate and Ishikawa endometrial cancer cells in culture.

Table 1. *Inhibition of growth of human breast cancer cell lines.*

	% Inhibition of growth					
	Proliferation			Colony formation		
Compounds	Dose (μM)	MCF-7	MDA-MB-231	Dose (μM)	MCF-7	MDA-MD-231
1. GnRH-III	2x30	40	39	50	63	75
2. [Lys^5]GnRH-III	2x30	n.t.	n.t.	50	0	0
3. [Lys^5,cyclo(Asp^5 Lys^5)]GnRH-III	2x30	n.t.	n.t.	50	44	n.t.
4. [Lys^4]GnRH-III	2x30	27	28	50	40	35
5. [Lys4(Ac-ε-N)]	2x30	31	n.t.	50	40	31
6. [Phe^7]GnRH-III	2x30	0	n.t.	50	26	21
7. [Glu^6]GnRH-III	2x30	18	n.t.	50	44	25
8. [$Trp^{3,7}(CHO)_5$ ΔPro^9]GnRH-III	2x30	n.t.	n.t.	50	31	n.t.
9. P-GFLG-1	2x30	10	11	50	15	n.t.
10. P-GFLG-3	2x30	n.t.	n.t.	50	78	82
11. P-GFLG-4	2x30	n.t.	n.t.	50	68	75

Antitumor activity of conjugates *in vivo* was substantially greater than for free peptides as shown with GnRH-III (Figure 1). This may be due to decreased enzymatic degradation of conjugated peptides. The direct inhibitory effect of GnRH-III analogs and conjugates indicates significant therapeutic potential.

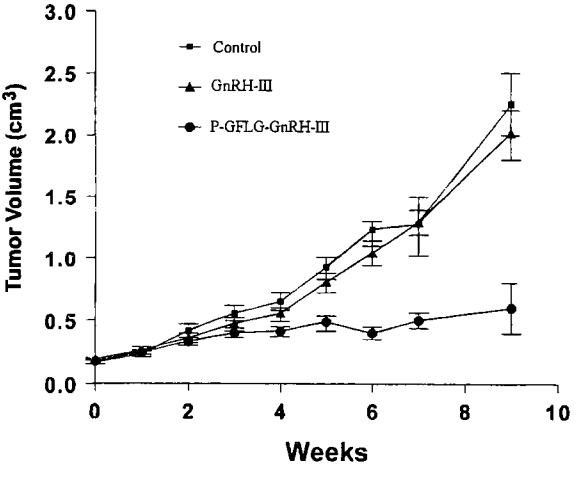

Figure 1. *The effect of GnRH-III and GnRH-III conjugated through GFLG to copolymer on growth of MDA-MB-231 human breast cancer xenografts.*

Reference

1. Sower, S.A., Chiang, Y.-C., Lovas, S. and Conlon, J.M., *Endocrinology*, 132 (1993) 1125.

Peptides: Chemistry, Structure and Biology
Pravin T.P. Kaumaya and Robert S. Hodges (Eds.)
Mayflower Scientific Ltd., 1996

97
Potent Somatostatin Analogs Containing N-terminal Modifications

S.H. Kim[1], J.Z. Dong[1], T.D. Gordon[1], H.L. Kimball[1], S.C. Moreau[1], J.-P. Moreau[1], B.A. Morgan[1], W.A. Murphy[2] and J.E. Taylor[1].

[1]Biomeasure, Inc., Milford, MA 01757, USA
[2]Peptide Research Laboratories, Department of Medicine, Tulane University Medical Center, New Orleans, LA 70112, USA

Introduction

The clinical utility of somatostatin analogs such as Octreotide and Lanreotide is now well established. Recent reports [1-5] on the improved bioavailability of various peptides with certain N- or C-terminal modifications prompted us to investigate the discovery of a second generation of somatostatin analogs with greater potency *in vivo*. Our efforts were focused on N-terminal modification of cyclic octapeptides related to somatostatin. We now report the design, synthesis, and aspects of the *in vitro* and *in vivo* activities of these analogs.

Results and Discussion

The focus of this project was to discover somatostatin analogs with a significant improvement in potency relative to Octreotide (Sandostatin) following parenteral administration. Our initial objective was to identify one or more octapeptide platforms with optimal receptor affinity *in vitro* which were suitable for N-terminal modification. Compounds were evaluated *in vitro* on the AR42J cell SSTR2 receptor from rat pancreas [6]. Analysis of the somatostatin analog database at Biomeasure indicated that, while it was relatively easy to obtain compounds with potencies *in vitro* approximately equal to $SS_{1\text{-}14}$, there were no examples of analogs which were significantly more potent than the parent hormone. Consequently, we concluded that it would be difficult to extract significantly greater potency from the octapeptide pharmacophore, and decided to select platforms for N-terminal modification from our existing compound database. We chose two compounds, BIM-23060, which was approximately equivalent to $SS_{1\text{-}14}$ in potency, and BIM-23023, which was about 2 fold less potent than the tetradecapeptide, but did not contain the unnatural amino acid 2-naphthylalanine.

We next considered desirable characteristics for the nature of the N-terminal modification. Octreotide is a relatively lipophilic peptide. We hypothesized that modification of this parameter should influence pharmacokinetic behavior; consequently, we decided to increase local hydrophilicity in the region of the N-terminus. In addition, we attempted to select substituents which were readily available by synthesis, and were compatible with the conditions used to remove t-butyl based protecting groups.

We describe here two series: the tris series (*e.g.* BIM-23167); and the N-(2-hydroxy-ethyl) piperazine series (*e.g.* BIM-23191). In order to evaluate structures with a greater variety of N-terminal cationic sites, we decided to attach these modifications to the peptide platforms by three linkages: an amide linkage (*e.g.* BIM-23167), an alkane linkage *(e.g.* BIM-23201), and a sulfonamide linkage (*e.g.* BIM-23197). We also decided to compare our modifications with the recently described Amadori derivatives of peptides [3]. Structures and *in vitro* data are listed in Table 1.

Table 1. *Structures and in vitro data on somatostatin analogs.*

compound ref	Sequence										rSSTR2*	inhib GH#
Lanreotide		nal	Cys	Tyr	trp	Lys	Val	Cys	Thr	NH2	0.35	0.40
Octreotide		phe	Cys	Phe	trp	Lys	Thr	Cys	Thr	ol	0.38	0.52
Ilatreotide	Maltose	phe	Cys	Phe	trp	Lys	Thr	Cys	Thr	ol	0.56	0.74
BIM-23060		phe	Cys	Tyr	trp	Lys	Thr	Cys	Nal	NH2	0.10	0.07
BIM-23167	Tris-Suc	phe	Cys	Tyr	trp	Lys	Thr	Cys	Nal	NH2	0.08	0.09
BIM-23179	Tris- Ac	phe	Cys	Tyr	trp	Lys	Thr	Cys	Nal	NH2	0.12	0.14
BIM-23180	Maltose	phe	Cys	Tyr	trp	Lys	Thr	Cys	Nal	NH2	0.45	0.48
BIM-23201	TrisCH2	phe	Cys	Tyr	trp	Lys	Thr	Cys	Nal	NH2	0.14	0.14
BIM-23173	Tris-Suc	phe	Cys	Tyr	trp	Lys	Abu	Cys	Thr	NH2	0.10	0.18
BIM-23182	Tris- Ac	phe	Cys	Tyr	trp	Lys	Abu	Cys	Thr	NH2	0.12	0.21
BIM-23190	HOEt-Pip-Ac	phe	Cys	Tyr	trp	Lys	Abu	Cys	Thr	NH2	0.20	0.24
BIM-23195	TrisCH2	phe	Cys	Tyr	trp	Lys	Abu	Cys	Thr	NH2	0.08	0.21
BIM-23196	Tris-Et-SO2	phe	Cys	Tyr	trp	Lys	Abu	Cys	Thr	NH2	0.09	0.20
BIM-23197	OEt-Pip-Et-SO2	phe	Cys	Tyr	trp	Lys	Abu	Cys	Thr	NH2	0.29	0.23

* = Ki (nM) affinity to rat pancreas AR42J cells. # IC_{50} (nM) inhibition of GRF-induced GH release in male rat anterior pituitary cells in primary culture. Structure of N-terminal derivatives: Maltose = maltose Amadori adduct; Tris = $(HOCH_2)_3CNH$-; Suc = $-COCH_2CH_2CO$-; Ac = $-CH_2CO$-; HOET-Pip = $HOCH_2CH_2$-$N(CH_2CH_2)_2N$- ; Et-SO2 = $-CH_2CH_2SO_2$- .

With the exception of the maltose derivative BIIM-23180, N-substitution had little effect on affinity at the rSSTR2 receptor. The compounds were also evaluated for their ability to block GRF-stimulated GH release in male rat anterior pituitary cells in primary culture. We found that there is an excellent correlation between the affinity at the AR42J receptor, and inhibition of GRF-induced GH release in rat pituitary (correlation coefficient R=0.93). This result adds further weight to the association of the SSTR2 receptor with GH inhibition. However, other than indicating that a reasonable range of substitution is allowed at the N-terminus of somatostatin peptides without compromising either the affinity or efficacy of the parent at SSTR2 receptors, these data provide little basis to assist in the choice of a somatostatin analog with improved potency *in vivo*. We therefore decided to evaluate the compounds in the rat, measuring the inhibition of (D-Ala^2-GRF)- stimulated GH release *in vivo* [7]. From past experience, we initially screened the compounds at a dose of 25 μg/kg s.c., measuring the % inhibition of GH at 2, 4, 6, and 8 hours after the s.c. injection of test peptide. In this test, all analogs gave good inhibition at 2 hours after administration, indicating there was good distribution of drug to the site of action. However, the % inhibition of the BIM-23060 series fell off more rapidly as compared to the BIM-23023 series. Consequently, BIM-23023, 23190,

23195, 23197, and Octreotide were selected for a more detailed study. In this, ED_{50} values for the inhibition of circulating GH were calculated for the compounds of interest at 2, 4, 6 and 8 hours following s.c. administration of test peptide in the ala^2-GRF primed rat. These data are shown in Figure 1. N-terminal modification does appear to have an influence on the potency of the BIM-23023 series, with the most potent analogs (BIM-23190 and BIM-23197) being approximately 3 times better than the parent BIM-23023 at the 8 hour time point. The BIM-23023 series in general are more potent than Octreotide, the most potent compounds, BIM-23190 and BIM-23197, displaying up to 6-times the potency of Octreotide. However, this conclusion can only be confirmed in man by clinical evaluation.

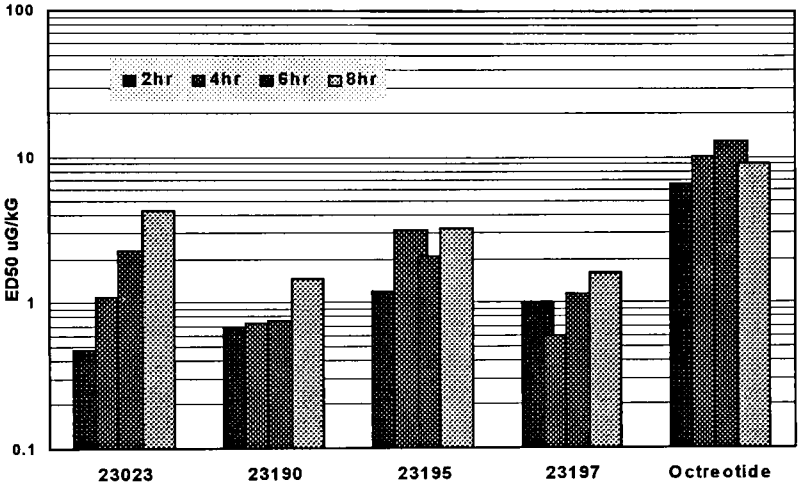

Figure 1. *Inhibition of D-Ala^2-GRF induced GH release in the rat at various times following s.c. administration of test peptide.*

References

1. PCT patent application WO 88/02756 Peptide derivatives.
2. PCT patent application WO 91/09837 Amino acids, peptides or derivatives thereof coupled to fats.
3. Albert, R., Marback, P., Bauer, W., Brinner, U., Fricker, G., Burns, C. and Pless, J., *Life Science*, 53 (1993) 517.
4. Bundy, G.L., Pals, D.T., Lawson, J.A., Couch, S.J., Lipton, S.J., Mauragis, M.A., *J. Med. Chem.*, 33 (1990) 2276.
5. Lu, Y.A. and Felix, A.M., *Peptide Res.*, 6 (1993) 140.
6. Taylor, J.E., Thevenian, M.A., Bashirzadeh, R., Reisine, T. and Eden, P.E., *Peptides*, 15 (1994) 1229.
7. Moreau, S.C., Murphy, W.A. and Coy, D.H., *Drug Devel. Res.*, 22 (1991) 79.

Peptides: Chemistry, Structure and Biology
Pravin T.P. Kaumaya and Robert S. Hodges (Eds.)
Mayflower Scientific Ltd., 1996

98
Biologically Active Peptides Isolated from Brains of Hibernating Ground Squirrel and Cold Adapted Yakutian Horse

R.H. Ziganshin[1], I.I. Mikhaleva[1], V.T. Ivanov[1], Y.M. Kokoz[2], A.E. Alekseev[2], A.F. Korystova[2], D.A. Mavlyutova[2], T.G. Emelyanova[3] and A.K. Akhremenko[4]

[1]*Shemyakin-Ovchinnikov Institute of Bioorganic Chemistry, Russian Academy of Sciences, ul. Miklukho-Maklaya 16/10, Moscow 117871, Russia*
[2]*Institute of Theoretical and Experimental Biophysics, Russian Academy of Sciences, Pushchino, Moscow Region, 142292, Russia*
[3]*Institute of Chemical Physics, Russian Academy of Sciences, Moscow, 117977, Russia*
[4]*Institute of Biology, Russian Academy of Sciences, Yakutsk, 677891, Russia.*

Introduction

Several lines of evidence indicate that brain and peripheral tissues of hibernating and genotypically cold adapted animals may contain biologically active peptides that induce in homoiothermal animals a sharp decrease in metabolism level and in body temperature [1, 2]. It is also known that peptide fractions prepared from these tissues produce alteration in heart rhythm together with other phenomena characteristic of the state of torpidity. In our view, the totality of endogenous regulators responsible for the natural hypobiotic state must include both the inhibitors of various physiological functions as well as their activators providing the restoration of normotropic state. This paper presents some results of our work on isolation of peptides that may be related to regulation of natural hypobiosis in animals.

Results and discussion

Brain extraction and fractionation were effected as described earlier [3, 4]. Subsequent separation of brain extract obtained from the brain of hibernating ground squirrels by ultrafiltration, SEC and various versions of preparative and analytical HPLC resulted in the isolation of several novel peptides capable of regulating inward potential-dependent Ca^{2+} current in cardiac myocytes of rats and ground squirrels.

The separation of the acetic acid extract obtained from the brain of cold adapted Yakutian horse was carried out according to the same scheme. It was shown earlier that the fraction of brain extract retained by the ultrafiltration membrane Amicon UM-2 inhibits protein synthesis in heart and liver mouse cells and decreases body temperature and oxygen consumption in mice after intraperitoneal administration [2]. After SEC separation of this fraction, we obtained three fractions capable of decreasing the body

temperature in rats kept at 4-6°C. The subsequent separation of the most hypothermically active fraction, by various RP-HPLC methods, allowed us to isolate the peptide AVHLPNDFTPAVHASLDK (110-127 fragment of α-chain of horse hemoglobin) that was capable of decreasing body temperature in rats after intraperitoneal administration.

All bioactive peptides were synthesized and investigated in electrophysiological and thermoregulatory assays. The influence of peptides on inward potential-dependent Ca^{2+} current was studied by the perforated patch-clamp technique. Thermoregulatory activity in rats was investigated at low (4-6° C) environmental temperature. Structures of isolated bioactive peptides and some of their biological properties are shown in Table 1.

Table 1. *Structures and biological activity of isolated peptides.*

Structures of peptides	Content of peptides (pmol/g brain tissue)	Results of biological assays	
		Inward Ca^{2+}current in heart cells of rat	Rectal temperature in rat
TSKY	300	inhibiting	increasing
MGRGT	<50	activating	decreasing
YQK	<50	activating	no effect
DY	<50	activating	no effect
AVHLPNDFTPAVHASLDK	1500	inhibiting	decreasing

Acknowledgments

The financial support of the Russian Foundation of Fundamental Investigation (grant 93-04-21784) and of the International Science Foundation (grant RN 1000) are gratefully acknowledged.

References

1. Swan, H., Reinhard, F.G., Caprio, D.L., Schatte, C.L., *Cryobiology*, 18 (1981), p. 598
2. Akhremenko, A.K., Ignatiev, D.A., Zagnoiko, V.I. in 'Biochemical Aspects of Cold Adaptations.' Institute of Cryobiological and Cryomedical Problems, Kharkov, Ukrainian SSR, 1991, p. 21.
3. Vaskovsky, B.V., Ivanov, V.T., Mikhaleva I.I., Kolaeva S.G., Kokoz, Y.M., Svieryaev, V.I., Ziganshin, R.H., Sukhova, G.S., Ignatiev, D.A., in Rivier, J.E. and Marshall, G.R. (Eds.), 'Peptides: Chemistry, Structure and Biology', ESCOM, Leiden, 1990, p. 302.
4. Svieryaev, V.I., Vaskovsky, B.V., Ziganshin, R.H., Mikhaleva, I.I., Ivanov, V.T., Kokoz, Y.M., Povzun, A.A., Alekseev, A.E., Sukhova, G.S., in Giralt, E. and Andreu, D. (Eds.), 'Peptides 1990', ESCOM, Leiden, 1991, p. 751

Session IV
Peptide-Protein Interactions

Chairs: Y. Shimonishi and
Manfred Mutter

Peptides: Chemistry, Structure and Biology
Pravin T.P. Kaumaya and Robert S. Hodges (Eds.)
Mayflower Scientific Ltd., 1996

99
Dissociation of Dimeric HIV-1 Protease: A Novel Means of Enzyme Inhibition

R. Zutshi, P. Bishop, J. Franciskovich and J.A. Chmielewski

Department of Chemistry, Purdue University, West Lafayette, IN 47907, USA

Introduction

Enzyme inhibitors and receptor antagonists have traditionally been targeted to the active site of the enzyme or the ligand binding site on the receptor. A novel approach to designing inhibitors of multiple-subunit enzymes and receptors would be based on the dissociation of enzyme/receptor subunits which ultimately destroys the active/binding site and results in loss of biological activity. To test this mode of inhibition we have targeted the dimeric enzyme HIV-1 protease. The crucial role of this protease in the processing of HIV proteins has made it a prime target for drug design [1].

HIV-1 protease is composed of 99 amino acid residues and self assembles into a homodimeric structure [2]. Dimerization of HIV-1 protease, which is mediated principally by interdigitation of the N- and C-termini into a four-stranded β-sheet (Figure 1), generates the catalytic center of the enzyme and also the substrate binding pocket. By targeting this β-sheet portion of the protease, a region which is highly conserved among HIV-1 isolates, agents may be generated which block the assembly of the homodimer or disrupt the dimeric interface [3].

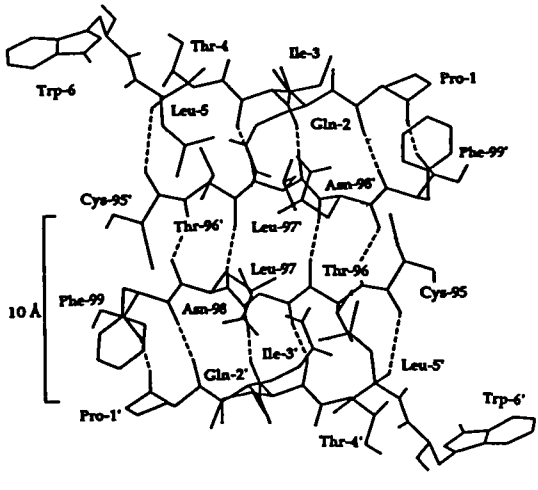

Figure 1. *The four-stranded, β-sheet portion of the HIV-1 protease dimerization interface.*

Results and Discussion

Our preliminary results demonstrated that small peptides corresponding to the N- and C-termini of HIV-1 protease act as inhibitors of protease activity [3a]. The peptides with optimum activity (**1** and **2**) were incorporated into novel structures containing a tether between the two peptide sequences. In the protease, the amino terminal ends of residues Pro(1) and Cys(95) are held at a distance of 10Å (Figure 1). An agent was designed which contained a flexible tether molecule capable of spanning this distance (**3**). Modeling studies suggested that, if both peptides of the inhibitor were to remain incorporated into the β-sheet upon complexation, twelve methylene units were needed in the tether to span the 10Å distance and to minimize interactions with Phe(99) in the protease monomer. The agent designed is unique in that the amino-termini of the protease peptides are covalently crosslinked to yield a compound capable of forming heterodimers with a protease monomer.

Peptides **1** and **2** were synthesized by a solid phase approach on the Wang resin [4] using an Fmoc-based strategy [5]. Agent **3** was synthesized in solution by adding 1 equiv. of di-N-hydroxysuccinimide ester **4** to 1 equiv. each of peptide **1** and peptide **2** (Figure 2), and HPLC purification of the desired products in approximately 10% overall yield. Structures were confirmed by mass spectrometry (FAB) and amino acid analysis.

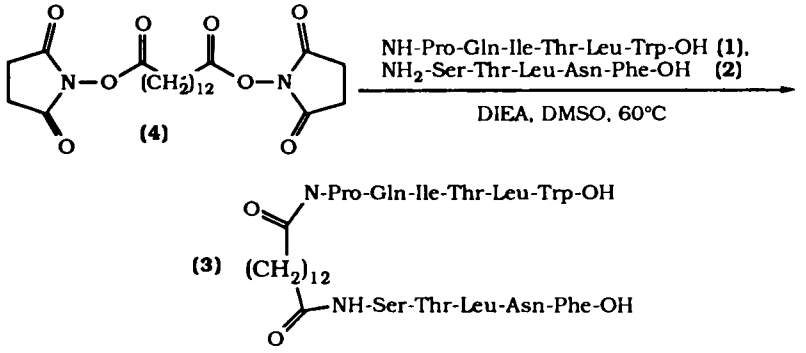

Figure 2. *Synthesis of agent 3.*

The inhibitory effect of compound **3** on HIV-1 protease activity was evaluated using a fluorogenic substrate assay developed by Toth and Marshall [6]. The effect of 60 minute incubation of the agent with HIV-1 protease (100 nM) upon the hydrolysis of substrate was evaluated by monitoring the fluorescence at 430 nm with respect to time. Agent **3** inhibited HIV-1 protease activity with an IC_{50} value of 29.2 μM, which was significantly better than peptides **1** and **2**, either individually or together in the assay solution ($IC_{50} > 200$ μM).

In addition to testing for protease inhibition, an assay was designed to monitor dissociation of HIV-1 protease directly with this agent. Due to the presence of two tryptophan residues within the protease, one which is buried at the interface, we were able to use the fluorescence of HIV protease as a handle for monitoring protease

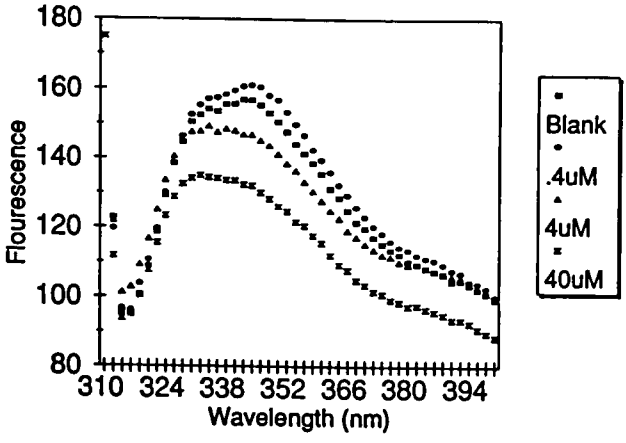

Figure 3. *Fluorescence spectra of HIV-1 protease with agent 3.*

dissociation.[7] Adding increasing amounts of our agents (with Phe replacing Trp in agent **3**) to a constant concentration of protease (300 nM), resulted in a dramatic decrease in the fluorescence of the protease (Figure 3), and little overall effect on the protease fluorescence when a poor inhibitor or an active site inhibitor was used.

In conclusion, we have designed an agent which both inhibits HIV-1 protease activity and decreases the intrinsic fluorescence of the protease with similar conditions and agent concentrations. Additionally, we have shown that active site-targeted agents inhibit the HIV-1 protease activity, but have little effect on the protease fluorescence. This data supports the claim that inhibition with **3** is based on a decrease in the amount of biologically active protease homodimer in solution. Other agents are currently being prepared with modified tethers and peptides.

Acknowledgments

We would like to acknowledge the financial support of the NIH (1 R01 GM52739) and the NSF Young Investigator Award (9457372-CHE).

References

1. Norbeck, D.W., Kempf, D.J., *Annu. Rep. Med. Chem.*, 26 (1991) 141.
2. Wlodawer, A., Miller, A., Jaskolski, M., Sathyanarayana, B., Baldwin, E., Weber, I., Selk, L., Clawson, L., Schneider, J., Kent, S., *Science*, 245 (1989) 616.
3. a) Franciskovich, J, Houseman, K., Mueller, R., Chmielewski J., *Bioorganic and Med. Chem. Lett.*, 3 (1993) 739. b) Zhang, Z., Poorman, R., Maggiora, L., Heinrikson, R., Kezdy, F., *J. Biol. Chem.*, 266 (1991) 15591. c) Schramm, H.J., Nakashima, H., Schramm, W., Wakayama, H., Yamamoto, N., *Biochem. Biophys. Res. Comm.*, 179 (1991) 847. d) Babe, L.M., Rose, J., Craik, C.S., *Protein Science*, 1 (1992) 1244.
4. Wang, S.S., *J. Am. Chem Soc.*, 95 (1973) 1328.
5. Atherton, E., Sheppard, R.C., The Peptides, Academic Press: New York, Vol.9, 1987.
6. Toth, M.V., Marshall, G.R., *Intl. J. Peptide Protein Res.*, 36 (1990) 544.
7. Wetlaufer, D.B., *Adv. Protein Chem.*, 17 (1962) 303.

Peptides: Chemistry, Structure and Biology
Pravin T.P. Kaumaya and Robert S. Hodges (Eds.)
Mayflower Scientific Ltd., 1996

100
Effect of Phosphorylation on Tetramerization of the Tumor Suppressor Protein p53

K. Sakaguchi[1], H. Sakamoto[1], H. Kodama[4], M. Kondo[4], C.W. Anderson[3], M.S. Lewis[2] and E. Appella[1]

[1]Laboratory of Cell Biology, National Cancer Institute, Bethesda, MD 20892, USA
[2]Biomedical Engineering and Instrumentation Program, National Center for Research Resources, Bethesda, MD 20892, USA
[3]Biology Department, Brookhaven Laboratory, Upton, NY 11973, USA
[4]Laboratory of Biochemistry, Faculty of Science and Engineering, Saga University, Saga 840, Japan

Introduction

The tumor suppressor protein p53, a 393 amino acid phosphoprotein, acts as a transcriptional enhancer in its tetrameric form and suppresses cell cycle progression in response to DNA damage [1-3]. The tetramerization domain of p53 is required for efficient site-specific DNA binding and contributes to p53's ability to activate transcription from natural promoters (*e.g.* WAF1/CIP1). Functional inactivation of the protein either by association with viral proteins or, more frequently, by point mutations as found in many human tumors, leads to cellular transformation. Formation of heterotetramers between wild-type and mutant p53 *in vivo* may inactivate wild-type p53 function, thus potentiating tumor development. Wild-type p53 is phosphorylated *in vivo* at several amino-terminal and carboxy-terminal sites [4]. In the carboxy-terminal region, Ser392 in human p53 is phosphorylated *in vivo*, and *in vitro* by casein kinase II (CKII). Serine 315 also is phosphorylated *in vivo*, and this residue can be phosphorylated *in vitro* by the $p34^{cdc2}$ cyclin dependent kinase. Unmodified *E. coli* expressed p53 binds poorly to its consensus recognition sequence, but phosphorylation of Ser392 by CKII or Ser378 by protein kinase C (PKC) enhances sequence-specific DNA binding [5, 6].

To determine whether phosphorylation affects tetramer formation, we synthesized Ser303-Asp393 peptide variants, which contains the core tetramerization domain Asp324-Gly356 [7, 8], by a fragment condensation method [9]. Phosphate was incorporated at Ser315, Ser378, or at Ser392.

Results and Discussion

Seven different 91 amino acid peptides, containing no, one or two phosphorylated serines, were chemically synthesized with high purity by a fragment condensation method using peptide thioesters. Figure 1 shows the scheme of fragment condensation for synthesis of [$Ser(PO_3H_2)^{392}$]p53(303-393). The phosphoserine residues were stable to piperidine treatment during peptide preparation.

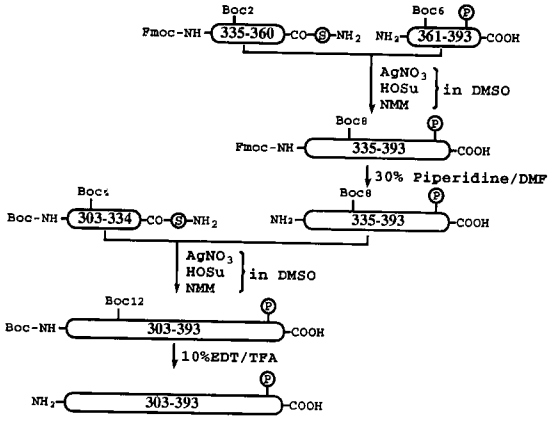

Figure 1. *Synthesis of [Ser(PO_3H_2)^{392}]p53(303-393) by fragment condensation.* ***S*** *and* ***P*** *in circle indicate SCH_2CH_2CO-Ala and phosphate group, respectively.*

Equilibrium ultracentrifugation analysis showed that phosphorylation of Ser392 increased the association constant for tetramer formation by more than ten-fold (Table 1 and Figure 2). Phosphorylation at Ser315 or Ser378 had little effect on tetramer formation. Phosphorylation at both Ser315 and Ser392 resulted in essentially the same association constant as unphosphorylated peptide. Acetylation of five amino groups in the N-terminal region completely eliminated the enhancement of tetramerization by phosphorylation at Ser392 while acetylation itself had minimal effect on the tetramerization of unphosphorylated peptide.

Phosphorylation did not significantly change the secondary structure of the tetramerization domain as determined by circular dichroism. The phosphopeptide at Ser392 in Tris buffer had slightly larger negative ellipticity at 206 nm than the unphosphorylated peptide, and this order was reversed in phosphate buffer.

Table 1. *Standard free energy and dissociation constant for tetramer formation of p53(303-393) variant peptides.*

Peptide	ΔG^o (cal.mol^{-1})[a]	Kd,app (μM)[a,b]	R.A.[c]
SS	-22500	2.61	1.00
SP	-26900	0.202	12.92
PS	-23200	1.74	1.50
378P	-22700	2.25	1.16
PP	-22200	2.92	0.89
AcSS	-22200	3.00	0.87
AcSP	-22000	3.36	0.77

[a]Values at 20°C. [b]The dissociation constant is calculated by Kd, app=$K_{14}^{-1/3}$. [c]Relative affinity with SS=1.

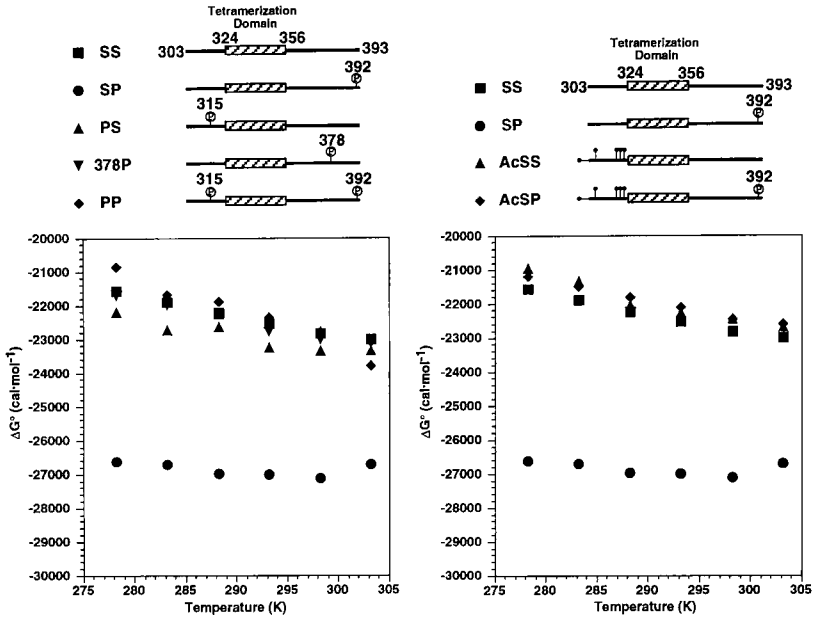

Figure 2. *Free energy for tetramer formation of p53(303-393) variant peptides. The association affinity of the tetramer formation of p53(303-393) variant peptides were analyzed in 50 mM Tris·HCl, 100 mM NaCl, pH 7.5 at various temperatures by analytical ultracentrifuge. Dot (•) and* ***P*** *in circle indicate acetyl and phosphate group, respectively. Positions of phosphoserine residues are indicated. In AcSS and AcSP, α-amino group and four lysine side-chain amino groups at positions 305, 319, 320 and 321 are acetylated.*

These results suggest that phosphorylation at Ser392 may modulate the affinity of tetramers through charge-charge interactions between the carboxy terminus and the positively charged region around Lys319. The enhancement of tetramer formation by Ser392 phosphorylation by CKII may be biologically relevant.

References

1. Levine, A. *J., Annu. Rev. Biochem.*, 62 (1993) 623.
2. Donehower, L.A. and Bradley, A., *Biochem. Biophys. Acta,* 1155 (1993) 181.
3. Ron, D., *Proc. Natl. Acad. Sci., USA*, 91 (1994) 1985.
4. Appella, E., Sakaguchi, K., Sakamoto, H., Lewis, M.S., Omichinski, J.G., Gronenborn, A.M., Clore, G.M. and Anderson, C.W., in Atassi, M.Z. and Appella, E. (Eds), 'Methods in Protein Structure Analysis', New York, Plenum, 1995, p. 407.
5. Hupp, T.R., Meek, D.W., Midgley, C.A. and Lane, D.P., *Cell*, 71 (1992) 875.
6. Takenaka, I., Morin, F., Seizinger, B.R. and Kley, N., *J. Biol. Chem.*, 270 (1995) 5405.
7. Sakamoto, H., Lewis, M.S., Kodama, H., Appella, E. and Sakaguchi , K., *Proc. Natl. Acad. Sci., USA* , 91 (1994) 8974.
8. Clore, G.M., Ernst, J., Clubb, R., Omichinski, J.G., Sakaguchi, K., Appella, E. and Gronenborn, A.M., *Nature Struct. Biol.*, 2 (1995) 321.
9. Hojo, H. and Aimoto, S., *Bull. Chem. Soc. Jpn.*, 65 (1992) 3055.

Peptides: Chemistry, Structure and Biology
Pravin T.P. Kaumaya and Robert S. Hodges (Eds.)
Mayflower Scientific Ltd., 1996

101
Semisynthesis of Chimeric α-Globins: Interspecies Exchange of Segment α_{1-30}

A.S. Acharya, P. Nacharaju and M.J. Rao

Division of Hematology, Department of Medicine, Albert Einstein College of Medicine, Bronx, NY 10461, USA

Introduction

The noncovalent interactions of the complementary segments of proteins play a key role in facilitating the protease catalyzed protein semisynthetic reactions. However, α-Globin semisynthetic reaction, *S. aureus* V8 protease catalyzed splicing of Glu^{30} with Arg^{31} in a mixture of segments α_{1-30} and α_{31-141} [1], is distinct from other semisynthetic reactions. Noncovalent interactions of the splicing fragments is absent in this system. The propensity of the spliced contiguous segment to assume α-helical conformation *in situ* serves as the 'molecular trap' of this splicing reaction [2]. The generation of chimeric α-chains by this approach and the application of chimeric chains to establish the presence of 'crosstalk' between the sequence differences of distinct segments (AB-GH corner) of the mammalian α-chains are presented here.

Results and Discussion

Amino acid sequence of globin chains is encoded in the globin genes by three exons. The exon-intron structure of globin gene is conserved during evolution. Arg^{31} of α-chain is the carboxyl terminal residue of exon 1 product. The exchange of α_{1-30} by the semisynthetic reaction, therefore, represents the exchange of the exon 1 products between α-globins. The residues involved in heme binding and generation of $\alpha_1\beta_2$ interface are in the central exon product, whereas most of the residues of the $\alpha_1\beta_1$ interface, Bohr titration, and effector modulation of O_2 affinity are present in the side exon products [3]. The architecture of the intra- and inter- dimer interfaces is the primary driving force for the assembly of a cooperative tetrameric structure. Though exon intron structure of globin genes are conserved beyond the species boundaries, multiple sequence differences exist between the respective subunits of various mammalian hemoglobins (Hbs). Nonetheless, basic Hb fold and the underlying molecular mechanisms of O_2 transport are conserved during evolution. Thus, either these sequence differences are outside the region dictating the global structure and function of Hb or the sequence differences located in distinct regions of the chain are synchronized with each other. The segregation of the sequence differences of a segment from the rest will facilitate the delineation of the presence of such a 'crosstalk.' Horse, mouse, and swine

α-chains exhibit 18, 19 and 22 sequence differences respectively (Table1). Segment $\alpha_{1\text{-}30}$ of these α-chains (with 3, 8 and 6 sequence differences) have been exchanged [4] with that of human. The reverse exchanges have also been carried out similarly to generate a set of chimeric chains. Chimeric chains assembled with human β-chain and generated cooperative tetramers (Table 1). Crosstalk of the sequence differences of segments $\alpha_{1\text{-}31}$ and $\alpha_{32\text{-}141}$, if present, does not influence tetramer assembly.

However, the situation is distinct in terms of the O_2 affinity. The O_2 affinity of hybrids with either mouse or mouse-human chimeric α-chain is comparable to that of HbA. The tetramer with human-mouse chimeric α-chain exhibited high O_2 affinity (Table 1). The results establish the intrinsic high O_2 affinity inducing potential of mouse $\alpha_{31\text{-}141}$, and its neutralization by the sequence differences of $\alpha_{1\text{-}30}$. AB (residues 18 to 25) and GH corners (residues 110 to 120) of α-chain provide the basic framework for the $\alpha_1\beta_1$ interface. Seven of the 18 sequence differences of the mouse α-chain are located here (Table 1). The formation of chimeric α-chains will have an impact on the noncovalent interactions of the AB-GH corner, as a consequence of the change in its composition. Except for the Leu to His difference of mouse at α_{113}, other differences of the region are conservative. The O_2 affinity of horse α-chain hybrid is also same as that of HbA. The segregation of the sequence differences of horse chain into its $\alpha_{31\text{-}141}$ and $\alpha_{1\text{-}30}$ segment has no influence on the O_2 affinity (Table 1). Of the 4 sequence differences of the AB-GH corner of horse, one is at its AB corner. Its GH corner has 3 differences, two of which are at the same sites as in mouse. Horse has a nonconservative substitution at α_{115}, an Asp residue (Ala in human). The Leu to His substitution of mouse at α_{113} is absent in horse. Accordingly, the intriguing question is whether a correlation exists between the substitution of His at α_{113} and the high O_2 affinity of chimera. The studies with the chimeras of swine and human α-chains support the above concept, namely the conformational aspects of the AB-GH corner of chimeric chain [probably endowed to the region by His at α_{113}] contributes to the high O_2 affinity. AB-GH corner of swine α has seven substitutions. GH corner of swine α has two nonconservative substitutions, His at α_{113} and Asp at α_{115}. AB corner of swine α has 3 nonconservative substitutions; His to Gln at α_{20}, Glu to Ala at α_{23} and a Tyr to His at α_{24}. This is not the case with either horse or mouse; substitutions at AB corner are conservative in both. O_2 affinity of hybrid Hb with swine α is same as that of HbA, and hybrids of horse or mouse. But, the human-swine chimeric α-chain that has His at α_{113} induces high O_2 affinity just as human-mouse chimera.

Accordingly, we speculate that His at α_{113} by itself or along with the other substitutions of the GH corner of mouse or of swine induces high O_2 affinity to the hybrid tetramer. However, the sequence differences of the AB corner of mouse as well as of swine α-chains are synchronized with their respective substitutions at the GH corner to neutralize the high O_2 affinity of the latter. A crosstalk of the sequence differences of the AB and GH corners of the α-chains of swine and mouse is implicated by the studies. The crosstalk determines the O_2 affinity of the tetramer, but such a crosstalk in not critical for either the tetramer assembly or its cooperativity. It is conceivable that a new crosstalk could be established at the AB-GH corner of mouse-swine or swine-mouse

Table 1. *O_2 affinity of hybrids of chimeric α-chains with human β-chains.*

α Component of tetramer	P_{50} pH 7.4	P_{50} pH 6.8	Number of sequence differences Total	AB	GH	Hill Coefficient
α^{H}	4.5	32	-	-	-	2.5
α^{M}	4.5	-	19	3	3	2.4
α^{MH}	4.5	-	8	3	-	2.4
α^{HM}	3.0	-	11	-	3	2.4
α^{Hr}	4.5	-	18	1	3	2.3
α^{HrH}	4.7	-	3	1	-	2.5
α^{HHr}	4.3	-	15	-	3	2.3
α^{P}	-	32	22	4	3	2.4
α^{PH}	-	32	6	4	-	2.4
α^{HP}	-	22	16	-	3	2.4

The O_2 affinity is determined either in 50 mM Bis-Tris acetate, pH 7.4, or in 100 mM phosphate, pH 6.8 at 37°C, using Hem-O-Scan. H, M, Hr, P represent human, mouse, horse and swine, respectively. MH, chimera with 1-30 and 31-141 of mouse and human α-chains; HM chimera with 1-30 and 31-141 of human and mouse α-chain; HHr, chimera with 1-30 and 31 -141 of human and horse α-chains; HrH, chimera with 1-30 and 31-141 of horse and human α-chains; PH, chimera with 1-30 and 31-141 of swine and human α-chains; HP, chimeric α-chain with 1-30 and 31-141 of human and swine α-chains.

chimeric α-chains if these are assembled and such a crosstalk could also neutralize the high O_2 affinity inducing potential of sequence differences of swine $\alpha_{31\text{-}141}$ and mouse $\alpha_{31\text{-}141}$ just as in the parent chains.

Acknowledgments

This work is supported by National Sickle Cell Center Grant HL-38655.

References

1. Roy, R.P. and Acharya, A.S., *Methods Enzymol.*, 231 (1994) 194.
2. Roy, R.P., Khandke, K.M., Manjula, B.N. and Acharya, A.S., *Biochemistry,* 31 (1992) 7249.
3. Eaton, W., *Nature*, 284 (1980) 183.
4. Roy, R.P., Nagel, R.L. and Acharya, A.S., *J. Biol. Chem.*, 268 (1993) 16406.

Peptides: Chemistry, Structure and Biology
Pravin T.P. Kaumaya and Robert S. Hodges (Eds.)
Mayflower Scientific Ltd., 1996

102
Effects of Aspartic Acid Isomerization on Conformation, Antibody Recognition and Serum Stability of Amyloid β-Peptide N-terminal Decapeptide

G.I. Szendrei, K.V. Prammer and L. Otvos, Jr.

The Wistar Institute, Philadelphia, PA 19104, USA

Introduction

The major proteinaceous component of the senile plaques in the brains of Alzheimer's disease patients is the 42-amino acid long Aβ peptide:

DAEFRHDSGYEVHHQKLVFFAEDVGSNKGAIIGLMVGGVVIA (A 1-42)

While C-terminal truncations lead to peptides present in normal body fluids [1], N-terminal [2, 3] and mid-chain mutations [4], as well as mutations around the Aβ domain of the precursor protein [5] modulate, and usually accelerate the deposition of Aβ. Especially noteworthy is the isomerization of Asp^1 and Asp^7 in the parenchyma and leptomeningeal microvasculature in the affected brains [2]. The tendency of the different Aβ isoforms to form aggregates is preferentially characterized by their ability to form fibrils *in vitro* [6] and their ability to form β-pleated sheets [3, 7, 8]. Recently, we have reported how conformational changes following the isomerization of Asp^1 and Asp^7 may help the selective aggregation of Aβ [9]. Although Aβ is not an insoluble peptide *per se* [8], many characteristic properties of the Aβ peptides cannot be studied, due to synthetic difficulties, and to the tendency of Aβ to elute as a broad band from the RP-HPLC column [3, 10] disallowing quantitative determination.

Results and Discussion

The N-terminal decapeptide fragment of Aβ is ideal to study the effects of isomerization of Asp^1 and Asp^7 because: i) it is the helical-turn region of Aβ that was proposed to destabilize the overall β-pleated sheet conformation [9]; ii) it elutes from the C_{18} HPLC column as a sharp peak; and iii) many diagnostic antibodies are directed to the N-terminal third of Aβ. We synthesized four peptides: unmodified Aβ 1-10, $isoAsp^1$, Asp^7 (1iD,7D), Asp^1, $isoAsp^7$ (1D,7iD), and diisoAsp (1,7iD).

Preferred conformations of the peptides were explored by CD analysis and molecular modeling. Unmodified Aβ 1-10 assumes unordered conformation in water, and a loosened α-helix or 3_{10}-helix structure in TFE and TFE-water mixtures containing mostly TFE. This conformation is not influenced by isomerization of Asp^1, but the appearance of the β-aspartic acid bond(s) in peptides 1D,7iD and 1,7iD breaks the helix and results

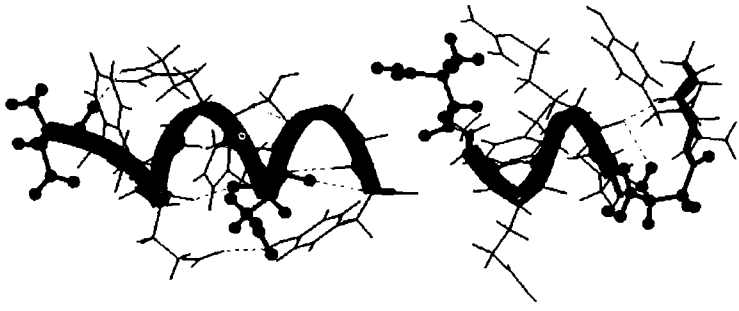

Figure 1. *Low energy conformers of peptide Aβ 1-10 with α-helix between residues 5-9 (left) and 1,7iD with type III β-turn, and Glu at position i+1 (right). Cα traces are indicated by a ribbon and isoaspartic acid residues by a ball and stick plot. [Biosym Inc. software, simulated annealing with a dielectric of 4.5, unconstrained minimization to an RMS difference of 0.005 kcal/A].*

in the formation of reverse-turns that have significant type I (III) character [11]. This conformational change is well-reflected in the energy minimized structures (Figure 1).

Since an increase of isoaspartate bonds was noted in aging proteins [12], we studied how aspartic acid-bond isomerization affects the resistance of the peptide to proteases, as modeled by stability studies in diluted human serum (Figure 2). The diisomerized peptide 1,7iD exhibited significantly increased serum stability compared to the other three analogues, suggesting a possible mechanism for the retention of the isomerized Aβ peptide in the affected brains.

We further investigated how aspartic acid-bond isomerization affects the peptide recognition of MAbs. Diagnostic antibody 6E10 bound to unmodified peptide Aβ 1-10 and to N-terminally isomerized peptide 1iD,7D, but did not bind to 1D,7iD, and 1,7iD peptides that are isomerized in mid-chain position (Figure 3A). The recognition of the small peptides, but not the full size Aβ 1-42, was increased when the peptides were applied to the ELISA plate in TFE, suggesting that MAb 6E10 indeed recognizes the N-terminal helical conformation (Figure 3B). Similar to our earlier findings [13], TFE did not induce MAb binding to peptides that are otherwise unrecognized by the antibody (1D,7iD and 1,7iD).

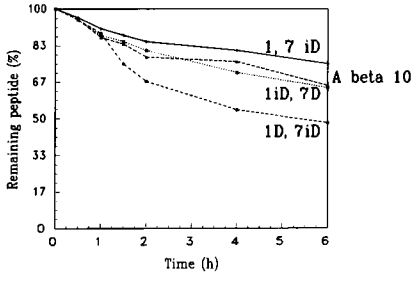

Figure 2. *Stability of the Aβ 1-10 peptide and its isomerized analogues in 12.5% human serum.*

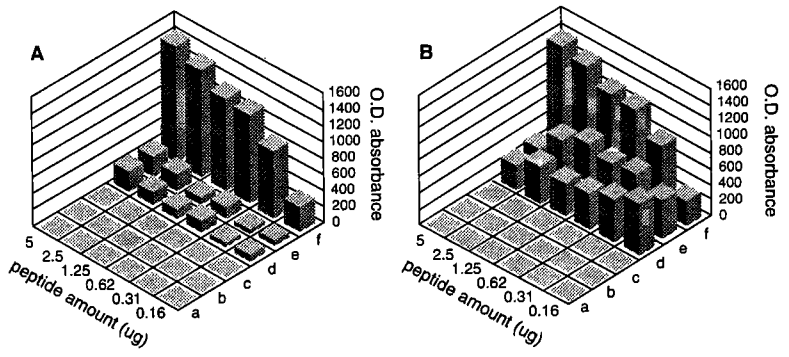

Figure 3. *ELISA of unmodified full size Aβ 1-42 (f), unmodified peptide Aβ 1-10 (e), and its isomerized analogues, Asn7 1-10 (a), 1D,7iD (b), 1,7iD (c), and 1iD,7D (d), by using MAb 6E10.*

Acknowledgments

The authors wish to thank B.D. Greenberg for MAb 6E10 and V.M.-Y. Lee and T.M. Kubiak for helpful discussions. Supported by NIH grant AG 10670.

References

1. Haas, C., Schlossmacher, M.G., Hung, A.Y., Vigo-Pelfrey, C., Mellon, A., Ostaszewski, B.L., Lieberburg, I., Koo, E.H., Schenk, D., Teplow, D.B. and Selkoe, D.J., *Nature*, 359 (1992) 322.
2. Roher, A.E., Lowenson, J.D., Clarke, S., Wolwow, C., Wang, R., Cotter, R.J., Reardon, I.M., Zurcher-Neely, H.A., Heinrikson, R.L., Ball, M.J. and Greenberg, B.D., *J. Biol. Chem.*, 268 (1993) 3072.
3. Otvos, L., Jr., Szendrei, G.I., Lee, V.M.-Y. and Mantsch, H.H., *Eur. J. Biochem.*, 211 (1993) 249.
4. Wisniewski, T., Ghiso, J. and Frangione, B., *Biochem. Biophys. Res. Commun.*, 179 (1991) 1247.
5. Cheung, T.T., Suzuki, N., Cai, X-D., Odaka, A., Otvos, L., Jr., Eckman, C., Golde,T.E. and Younkin, S.G., *Science*, 264 (1994) 1336.
6. Jarrett, J.T., Berger, E.P. and Lansbury, P.T., Jr., *Biochemistry*, 32 (1993) 4694.
7. Hilbich, C., Kisters-Woike, B., Reed, J., Masters, C.L. and Beyreuther, K., *J. Mol. Biol.*, 218 (1991) 149.
8. Barrow, C.J. and Zagorski, M.G., *Science*, 253 (1991) 179.
9. Fabian, H., Szendrei, G.I., Mantsch, H.H., Greenberg, B.D. and Otvos, L., Jr., *Eur. J. Biochem.*, 221 (1994) 959.
10. Yankner, B.A., Duffy, L.K. and Kirschner, D.A., *Science*, 250 (1990) 279.
11. Szendrei, G.I., Fabian, H., Mantsch, H.H., Lovas, S., Nyeki, O., Schon, I. and Otvos, L., Jr., *Eur. J. Biochem.*, 226 (1994) 917.
12. Lowenson, J.D. and Clarke, S., *J. Biol. Chem.*, 267 (1992) 5895.
13. Lang, E., Szendrei, G.I., Lee, M.Y. and Otvos, L., Jr., *J. Immunol. Meth.*, 170 (1994) 103.

Peptides: Chemistry, Structure and Biology
Pravin T.P. Kaumaya and Robert S. Hodges (Eds.)
Mayflower Scientific Ltd., 1996

103
Design, Synthesis and Conformational Analysis of an IL-2/apamin Hybrid: A Peptide with IL-2 Receptor Antagonist Activity

W. Danho, R. Makofske, J. Swistok, J. Hakimi, J.A. Kondas, G. Powers, D. Biondi, T. Varnell, D. Fry, D. Greeley and V. Madison

Roche Research Center, Hoffmann La-Roche Inc., Nutley, NJ 07110, USA

Introduction

Interleukin 2 (IL-2) is the major growth factor for activated T cells, as well as a growth and differentiation factor for natural killer cells, and macrophages. Anti-IL-2 treatment (*e.g.*, antibodies to IL-2 or to the IL-2 receptor) prolongs survival of cardiac allografts in rodents and decreases the severity of disease in collagen induced arthritis in mice. Thus, an orally-active, small-molecule IL-2 antagonist may be efficacious for treatment of immunodisorders. Our goal is to discover compounds that will inhibit the binding of IL-2 to the IL-2Rα subunit. The crystal structure of IL-2 has been determined at 2.0 Å resolution. Using site-specific mutagenesis, four residues (Lys^{35}, Arg^{38}, Phe^{42} ,and Lys^{43}) were implicated in the interaction of IL-2 with the IL-2Rα subunit [1]. Lys^{35}, Arg^{38}, and Phe^{42} are in a short, irregular helical segment and Lys^{43} is in an extended conformation. Our stategy was to incorporate three of the four binding residues into a conformationally restricted helical peptide inhibitory to IL-2 binding, and to use this peptide as a prototype receptor antagonist for further mimetic design. Helical peptides based on the bee venom peptide apamin showed the best competitive binding to the IL-2Rα subunit. Apamin is a conformationally restricted peptide in which a C-terminal helical segment is stabilized *via* a N-terminal loop connected to the helix by two disulfide bonds. Apamin/IL-2 hybrid peptides were designed to retain the N-terminal apamin sequence and disulfide positions, but substitute the IL-2 receptor-binding epitope into the C-terminal segment.

Results and Discussion

The peptides were synthesized by solid phase methodology and purified by preparative HPLC. They were characterized by amino acid analysis (acid hydrolysis), MS, and NMR. The IL-2/apamin hybrids were assayed against IL-2Rα in an ELISA based assay. The apamin/IL-2 hybrid Ro 25-2739 has an IC_{50} of 230 μM with a Hill plot coefficient of 0.98, suggesting that it has 1:1 stoichiometry in displacing IL-2 from the receptor. Apamin has no activity in the assay, nor does Ro25-2379 have activity in the IgE receptor binding assay. Thus, Ro 25-2379 is a specific inhibitor. Substitution of the more hydrophobic residue (2,6-dichlorobenzyl)Tyr for Phe^{42} results in the more potent analog Ro 25-4572 with IC_{50} of 70 μM (Table 1).

Table 1. *Competitive binding of Apamin/IL-2 analogs.*

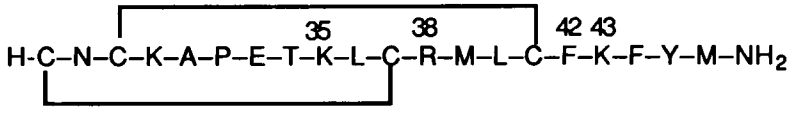

Ro No.	Name	IC_{50}(μm)
23-6721	Apamin	Not active
25-2739	Apamin / IL-2 hybrid	230 ± 90
25-4572	Apamin / IL-2 hybrid [(2,6-DiClBzl)-Tyr^{42}]	70 ± 40
25-5548	Apamin/IL-2 hybrid [Ala^{30}]	40 ± 20
25-5547	Apamin/IL-2 hybrid [Ala^{35}]	Not active
25-5534	Apamin/IL-2 hybrid [(D)Lys^{35}]	50 ± 20

CD and NMR studies of Ro 25-2739 indicate that it has a conformation similar to apamin with a substantial helical segment in aqueous solution. Complete assignments of proton NMR resonances were made in aqueous solution at pH 4.2, 20 °C. Full sets of quantitated NOE's were obtained and converted into interproton distance constraints. Optimization by constrained molecular dynamics and energy minimization showed that the segment from residue 7 (33 in IL-2) to 15 (41 in IL-2) is in a well-ordered α-helix. The helix is frayed at the C-terminus showing considerable flexibility beginning at residue 17 (43 in IL-2). A superposition of the solution conformation of Ro 25-2739 with the binding epitope shows that the corresponding peptide residues overlap Lys^{35}, Arg^{38} and Phe^{42} in IL-2, but not Lys^{43}.

Most of the structure-activity work has been carried out with Ro 25-4572. These studies tend to support a role for each of the four residues which represent the binding epitope. For example, substitution of any of the key residues (Lys^{35}, Arg^{38}, Phe^{42} or Lys^{43}) derived from the IL-2 sequence with Ala results in inactive peptides. As a control, replacement of Lys^{30}, which is derived from the apamin sequence, with Ala had no effect on potency. Binding activity was not sensitive to the stereochemistry of any of these residues except Arg^{38} where stereochemical inversion [(D)-Arg^{38}] led to loss of binding. In an attempt to increase the helicity of the apamin/IL-2 hybrid α-aminoisobutyric acid was substituted for the two C-terminal amino acids. The reduced potency of this analog is consistent with IL-2 crystal structure in which Lys^{43} is seen to be in an extended rather than a helical conformation.

The structure-activity studies with apamin/IL-2 analogs validate the hypothesis that each of the four-residues in the linear epitope identified by site-specific mutagenesis contributes to IL-2/IL-2R binding. These studies suggest that the apamin/IL-2 analogs mimic IL-2 in binding to the IL-2Rα subunit.

Reference

1. Sauve, K., Nachman, M., Spence, C., Bailon, P., Campbell, E., Tsien, W.-H., Kondas, J.A., Hakimi, J. and Ju, G., *Proc. Natl. Acad. Sci. USA*, 88 (1991) 4636.

Peptides: Chemistry, Structure and Biology
Pravin T.P. Kaumaya and Robert S. Hodges (Eds.)
Mayflower Scientific Ltd., 1996

104
Inserting Heavy-atom Labels in Functional Proteins by Solid Phase Peptide Synthesis and Semisynthesis

C.J.A. Wallace[1], I. Clark-Lewis[2], J. Wang[3] and M. Caffrey[3]

[1]*Department of Biochemistry, Dalhousie University, Halifax, NS, B3H 4H7, Canada*
[2]*Department of Biochemistry, University of British Columbia, Vancouver, BC, V6T 1W5, Canada*
[3]*Department of Chemistry, The Ohio State University, Columbus, OH 43210, USA*

Introduction

Protein semisynthesis is a chemical strategy to create interesting mutants for structure-function studies that employs fragments of the natural protein as preformed intermediates in the synthesis [1]. A variety of means can be used to effect the mutation, but the most common is the replacement of one fragment by a totally synthetic substitute in the fragment condensations used to make the holoprotein analog. Thus, semisynthesis can be used in ways that the genetic approach to specific mutants cannot (or cannot easily) be used: to introduce D-amino acids, labels for spectroscopy at specific sites, or other non-coded side chain structures. In the present work, we have used the method to incorporate residues with heavy atoms - here selenium and bromine - into cytochrome *c* for experiments using X-ray standing-waves to visualize protein orientation.

Results and Discussion

X-rays reflected at a shallow angle from a silver mirror set up standing waves. The heights of the field intensity maxima can be tuned by varying the angle. If a monolayer of X-ray fluorescent heavy atom is present above the mirror surface, as when a regular array of labelled macromolecules forms on it, the fluorescence will be at a maximum when a field intensity maximum coincides with the monolayer [2]. The fluorescence is detected and the monolayer's distance from the mirror can be calculated. With two heavy atoms, two distances can be measured and an orientation determined. Since artificial membranes can be layered on the mirror surface, the method is ideally suited to studies of the interaction of membranes and associated proteins or peptide hormones. A variety of heavy atom labels are suitable. We chose selenium and bromine, which have good X-ray fluorescence characteristics and are readily available incorporated in amino acids. Synthetic peptides were prepared by methods previously described [3], purified by preparative HPLC, and checked by analytical HPLC, amino acid analysis, and mass spectrometry. We prepared and used a peptide, residues 66-104 of cytochrome *c*, in which selenomethionine replaces Met^{80} without problems [3, 4]. In making the 3,5-dibromotyrosine^{97} analog of this peptide, and the double mutant, we noted bromine loss by mass spectrometry. Although the product monobromotyrosine appeared stable and

gave useful results, further synthesis employed the stable 4-bromophenylalanine as a substitute for tyrosine at positions 74 and 97. Semisynthesis of protein analogs by condensation of synthetic 66-104 peptides with the native 1-65 fragment followed established procedures [3]. In general, religations occurred with yields of >50% with 1:1 component ratios, though the yield of SeM^{68}, BrF^{74} cytochrome c was only 25%.

Studies of the analogs to validate their suitability as models for the natural cytochrome are tabulated below. Some mutants are less resistant to denaturing conditions, but all indications are that they adopt the native fold; this is reflected in near-full biological activity of all but those containing $SeMet^{80}$. In this case, replacement of sulphur by selenium as the 6th heme iron ligand changes redox potential, and consequently driving force for electron transfer, but leaves the protein otherwise unaffected [3]. Thus, the choice of labels is compatible with the strategy, and semisynthesis provides a simple means to precise and non-invasive labelling.

Table 1. *Properties of the cytochrome analogs.*

Cytochrome	Heme Spectra λmax Fe^{3+}/Fe^{2+}	pK 695nm band loss	$T1_2$ autoxdn.	E'm	HPIEC red	r.t. ox	Bioassay
Native Horse	529,408/549,520,415	9.25	>100h	266mV	13.0 13.6	13.9(a) 14.6(b)	100%
$SeM80^5$	Red shifted	9.20	n.d.	212mV	13.0	13.9(a)	44%
BrY97	minor blue shift	8.85	9h	260mV	13.0	14.0(a)	95±5%
SeM80/BrY97	minor red shift	9.00	<1h	202mV	13.0	14.0(a)	34±5%
SeM68/BrF74	minor blue shift	7.80	8h	254mV	13.6	14.6(b)	90±10%
SeM68/BrF97	minor blue shift	8.75	10h	268mV	13.7	14.7(b)	97±3%
BrF74/SeM80	minor red shift	8.75	1.25h	205mV	13.6	14.6(b)	30±1%

The results obtained with a monolayer of SeM^{80}, BrY^{97} cytochrome c on silver mirrors with and without overlaying lipid suggest that protein orientations on the surface differ in the two cases. That on the lipid film is consistent with that proposed for the biologically productive orientation with the binding surface facing the lipid head groups [5]. A more complete evaluation of these measurements is underway.

Acknowledgments

Thanks are due to Angela Brigley for technical assistance and NSERC and NIH for financial support.

References

1. Wallace, C.J.A., *FASEB J.*, 7 (1993) 505-515.
2. Wang, J., Bedzyk, M.J., Penner, T. and Caffrey, M., *Nature*, 354 (1991) 377-380.
3. Wallace, C.J.A. and Clark-Lewis, I., *J. Biol. Chem.*, 267 (1992) 3852-3861.
4. Wang, J., Wallace, C.J.A., Clark-Lewis, I. and Caffrey, M., *J. Mol. Biol.*, 237 (1994) 1-4.
5. Salemme, R., *Annu. Rev. Biochem.*, 46 (1977) 299-326.

Peptides: Chemistry, Structure and Biology
Pravin T.P. Kaumaya and Robert S. Hodges (Eds.)
Mayflower Scientific Ltd., 1996

105
Specific DNA Recognition by Conformationally Constrained α-Helical Peptides

B.Y. Wu, B.L. Gaffney, R.A. Jones and J.W. Taylor

Department of Chemistry, Rutgers University, Piscataway, NJ 08855, USA

Introduction

During the past decade, design of sequence-specific DNA-binding ligands has focused mainly on small molecules that bind in the DNA minor groove with low specificity and have severe toxic side effects [1]. In contrast, most DNA-binding proteins, which play important roles in gene regulation and gene expression *in vivo*, interact with specific DNA sites *via* various DNA-binding motifs [2]. These DNA-binding motifs use either an α-helix, the "recognition helix", or a β-sheet, to contact the specific DNA site. The "recognition helix" or β-sheet in intact DNA-binding proteins is stabilized by folding into the protein surface to fit into the cognate DNA major groove. If we can make small peptides that are already stable α-helices or β-sheets, with DNA-recognition features, then we could make sequence-specific DNA major groove binders that may compete with the gene regulatory proteins for their critical DNA-binding sites and modulate gene expression. We present our attempts to mimic the DNA-binding features of basic leucine-zipper proteins using conformationally constrained α-helical peptides.

Results and Discussion

Our design of small DNA-binding peptides is based on the basic region (residue 226 to 254) of the bZIP motif of GCN4 protein [3]. The basic region, which is critical for specific DNA-binding, is mostly unstructured in solution, but folds into an α-helix when bound to its recognition DNA site[4, 5]. Our strategy is to stabilize α-helical conformation in the isolated basic region peptide so as to reduce the entropy loss associated with helix formation upon binding. We do this by using intramolecular lactam bridges [6], while retaining DNA recognition features on the α-helical scaffold. We have introduced sidechain to sidechain lactam bridge(s) between Lys(i) and Asp(i+4) at the N- and/or C-terminus, beyond the DNA-contact region of the central sixteen amino acid residues. A set of four GCN4 basic region peptides (Table 1), have been designed and synthesized.

All four peptides show α-helical structure alone in solution. The estimated helix contents of the peptides (Table 1) have the following order GCN4brNC > GCN4brC > GCN4brN > GCN4br. Surprisingly, even the monomeric GCN4 basic region peptide (GCN4br, with a linear structure) binds to the specific DNA site, as demonstrated by the difference CD spectra. All four peptides appear to become much more α-helical in the presence of the symmetric ATF/CREB site (5'GCACA *TGACGTCA*TGTGC3', duplex),

Table 1. *Structure and α-helix contents of the four DNA-binding peptides in 10mM NaH_2PO_4 and 100mM NaCl, pH 7.4, at 25°C.*

Peptide	Peptide Sequence	% Helix
GC N4br	Ac-DPAALKRARNTEAARRSRARKLQRMKQLE-NH_2	44[b]
GCN4brN[a]	Ac-*K*AAA*D*KRARNTEAARRSRARKLQRMKQLE-NH_2	49[b]
GCN4brC[a]	Ac-DPAALKRARNTEAARRSRARKLQR*K*AAA*D*-NH_2	72[b]
GCN4brNC[a]	Ac-*K*AAA*D*KRARNTEAARRSRARKLQR*K*AAA*D*-NH_2	77[b]

[a] Sidechain amide bonds formed between the residues in italics are indicated by bars.
[b] Estimated by fitting the CD spectra to linear combinations of standard peptide spectra [7].

but not the scrambled DNA site (5'GCACTAAGCGCTTAGTGC3', duplex). DNA titration of the GCN4br peptide at 25°C (data not shown) gave a dissociation constant, K_d, of about 5μM for the DNA-peptide binding reaction. Van't Hoff analysis of the concentration dependence of melting temperatures of specific DNA-peptide complexes gives four parallel lines (data not shown), which indicate that peptide affinities for the specific DNA site follow their α-helix contents.

In summary, we have developed a strategy to mimic the DNA-binding features of bZIP proteins using small, conformationally constrained α-helical peptides. We have demonstrated that even the monomeric basic region peptide binds to its specific DNA site with a low-micromolar dissociation constant, in contrast to previous results that dimerization is necessary for specific DNA binding. Introducing lactam-bridge(s) into the basic region peptide stabilizes the α-helix and increases its DNA-binding affinity.

Acknowledgments

The APS Travel Grant to B.Y. Wu is acknowledged. These studies are financially supported by NIH grants GM 31483, GM 38811, and DA 04197.

References

1. Geierstanger, B.H., Mrksich, M., Dervan, P.B. and Wemmer, D.E., *Science*, 266 (1994) 646.
2. Pabo, C.O. and Sauer, R.T., *Ann. Rev. Biochem.*, 61 (1992) 1053.
3. Struhl, K. in Mcknight, S.L. and Yamamoto, K.R. (Eds), 'Transcriptional Regulation', Cold Spring Harbor Laboratory Press, 1992, p.833.
4. Weiss, M.A., Ellenberger, T.E., Wobbe, C.R., Lee, J.P., Harrison, S.C. and Struhl, K., *Nature*, 347 (1990) 575.
5. Talanian, R.V., Mcknight, C.J. and Kim, P.S., *Science*, 249 (1990) 769.
6. (a) Felix, A.M., Wang, C.T., Heimer, E.P. and Fournire, A., *Intl. J. Pept. Protein Res.*, 31 (1988) 231. (b) Ösapay, G. and Taylor, J.W., *J. Am. Chem. Soc.*, 114 (1992) 6966.
7. Perczel, A., Park, K. and Fasman, G.D., *Anal. Biochem.*, 203 (1992), 83.

Peptides: Chemistry, Structure and Biology
Pravin T.P. Kaumaya and Robert S. Hodges (Eds.)
Mayflower Scientific Ltd., 1996

106
Increased Lipid-affinity of a Class A (apolipoprotein) Peptide with a Proline Insertion Between Two Amphipathic Helical Segments

V.K. Mishra[1], M.C. Phillips[2], S. Lund-Katz[2], W.S. Davidson[2], M.N. Palgunachari[1], J.P. Segrest[1] and G.M. Anantharamaiah[1]

[1]*Departments of Medicine and Biochemistry, University of Alabama Medical Center, Birmingham, AL 35294, USA*
[2]*Department of Biochemistry, Medical College of Pennsylvania, and the Hahnemann University, Philadelphia, PA 19129, USA*

Introduction

Human plasma exchangeable apolipoproteins like apolipoprotein A-I (apo A-I), apo A-IV and apo E are postulated to have tandem amphipathic α-helical 22-mer repeats [1]. Many of the tandem 22-mer repeats are punctuated by a Pro residue [2]. To understand the role of Pro residues in lipid-association of these apolipoproteins, we have studied lipid-associating properties of three peptides derived from an 18-residue peptide 18A (DWLKAFYDKVAEKLKEAF). The three peptides studied are 36A (18A-18A), 37aA (18A-Ala-18A), and 37pA (18A-Pro-18A). A helical wheel representation of the peptide sequences indicates that the nonpolar faces of the two amphipathic helical segments are in register in 36A but are twisted out of register by 100° in 37aA and 37pA [3]. We have shown previously that among the three peptides 37pA possesses the strongest and 36A possesses the weakest lipid-associating properties [3]. In the present report, we have further studied the lipid-associating properties of the three peptides using right-angle light scattering measurements and determined the size and morphology of the lipid-peptide complexes by size-exclusion chromatography and electron microscopy (EM).

Results and Discussion

The results of right-angle light scattering measurements are shown in Figure 1. For the three peptides, the rate of micellization of dimyristoylphophatidylcholine (DMPC) and egg yolk phosphatidylcholine (EYPC) mutilamellar vesicles decreases in the following order: 37pA > 37aA > 36A. These data are in agreement with our earlier surface pressure measurements indicating that 37pA has the fastest while 36A has the slowest rate of penetration into an EYPC monolayer [3]. An examination of the peptide-DMPC complexes formed at 1:20 (M/M) ratio by EM revealed that all three peptides formed discoidal complexes. The peptide 37pA formed the smallest particles with the major diameter of the disk being 10.5 ± 1.5 nm; 37aA and 36A formed larger particles with the

major diameters of the disks being 17.6 ± 2.5 nm and 11.3 ± 1.8 nm, respectively. The hydrodynamic diameters of the complexes of 37pA, 37aA, and 36A determined by size-exclusion chromatography were 10.9 ± 1.1 nm, 16.2 ± 1.1 nm, and 11.7 ± 1.1 nm, respectively. Thus, among the three peptides, 37pA forms the smallest size discoidal particles.

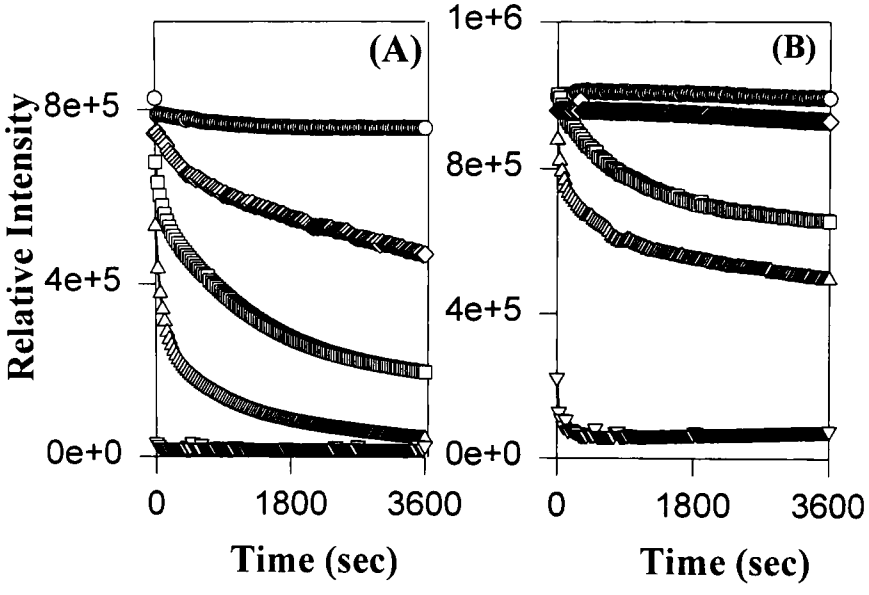

Figure 1. *Decrease in scattered-light intensity at 400 nm from a suspension of (A) DMPC and (B) EYPC multilamellar vesicles after addition of the peptides. Lipid concentration was 0.2 mM and lipid to peptide ratio was 20:1 (M/M). In control experiments, complete dissolution of the lipid vesicles was achieved by adding Triton X-100 at a final concentration of 1 mM. Lipid vesicles alone* (O), *36A* (◇), *37aA* (□), *37pA* (△), *Triton X-100* (▽).

The results of this study suggest that Pro residues in exchangeable apolipoproteins play an important role in lipoprotein assembly, presumably by allowing the apolipoprotein molecules to adopt a flexible structure suitable for rapid binding to the highly curved surface of the lipoprotein particles.

References

1. Segrest, J.P., Jones, M.K., DeLoof, H., Brouillette, C.G. and Anantharamaiah, G.M., *Proteins*, 8 (1990) 103.
2. Segrest, J.P., Garber, D.W., Brouillette, C.G., Harvey, S.C. and Anantharamaiah, G.M., *Adv. Prot. Chem.*, 45 (1994) 303.
3. Mishra, V.K., Palgunachari, M.N., Lund-Katz, S., Phillips, M.C., Segrest, J.P. and Anantharamaiah, G.M., *J. Biol. Chem.*, 270 (1995) 1602.

Peptides: Chemistry, Structure and Biology
Pravin T.P. Kaumaya and Robert S. Hodges (Eds.)
Mayflower Scientific Ltd., 1996

107
Complex-formation Assisted Site-directed Alkylation in Proteins

G. Ösapay[1], K. Ösapay[2] and A. Csiba[3]

[1]Department of Chemistry & Biochemistry, University of California San Diego, La Jolla, CA 92093, USA
[2]Agouron Pharmaceuticals, 3565 General Atomics Court, San Diego, CA 92121, USA
[3]Municipal Hospital Péterfy, H1441, Budapest, Hungary

Introduction

The science of protein structural-functional analysis currently employs powerful techniques such as high-resolution X-ray diffraction analysis, theoretical calculations, recombinant DNA technology and chemical mutagenesis. Beyond the substitution of specific sequential amino acids, the modification of individual residues in a protein frequently provides a starting point for assessing their roles in biological functions. Amino acid side-chain modifications have been achieved *via* synthetic methods. However, reactive compounds non selectively alkylate most of the ε-amino groups of lysine and ring nitrogens of histidine residues in proteins. In order to reduce the number of alkylating points, specific reaction conditions and/or engineered chemical probes must be used. Here we describe methodology developed for studying the factors which have to be considered in the site-directed chemical modification of proteins.

Results and Discussion

Alkylation reactions were studied on human carbonic anhydrase isoenzymes (HCA-I and HCA-II) and thermolysin, each a zinc containing metalloprotein. Computational and experimental techniques were combined to create the following integrated approach to the site-directed alkylations of these enzymes: 1) calculation of pK_A values of ionizable groups in the protein in order to determine relative basicities of potential alkylation targets; 2) use of molecular modeling in selecting alkylating chemical probes with an additional functional group that can coordinate to the metal center of the enzyme while alkylating the target histidine; 3) alkylation reaction, protein purification and analysis; 4) enzymatic activity measurements.

Continuum electrostatic calculations [1] have been performed on structures 1cba, 1hca, and 1hyt from the Brookhaven data bank in order to determine the pK_A values of all titratable groups (His residues are shown in Table 1). We have selected the pH for our reaction where the target histidine is monoprotonated. To obtain high selectivity, the appropriate chain length for a bifunctional chemical probe [N-chloroacetyl/propionyl amino acids (**1**)] was determined by molecular modeling. The probe contains a zinc-coordinating carboxylate group that tethers the alkylating agent to the active site.

Table 1. *Calculated pK_A values of titratable histidines of human carbonic anhydrase isoenzymes I and II and thermolysin.*

HCA-1		HCA-II		Thermolysin	
Residue	pK_A	Residue	pK_A	Residue	pKA
His^{200}	2.79	His^{15}	4.33	His^{88}	5.45
His^{67}	3.57	His^{64}	5.02	His^{216}	5.51
His^{64}	4.67	His^{17}	5.08	His^{250}	6.01
His^{122}	5.19	His^{122}	5.15	His^{74}	7.03
His^{243}	5.96	His^{4}	6.03	His^{231}	7.90
His^{103}	6.30	His^{10}	6.08	His^{105}	8.49
His^{107}	6.31	His^{107}	6.25	-	-
His^{40}	7.00	His^{36}	7.11	-	-

For example, based on the modeling studies, the alkylation reaction of His^{64} in HCA II was performed by using 1.0 equiv. Cl-Ac-Gly-OH at pH 5.2.

Gel electrophoresis with pyrogallol red - molybdate complex staining [2] indicated the homogeneity of the product. The modified HCA species showed suspended esterase activity while their hydratase function became enhanced. These results will be considered in further structure-function studies.

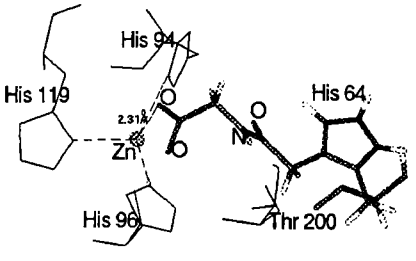

Figure 1. *Computer structure of the active site in the His^{64} modified HCAII isoenzyme. The carboxyl group of the chemical probe -CH_2-Gly-OH coordinates to the zinc ion while it forms a covalent bond to the 3'-nitrogen of His^{64}.*

Compounds (**1**) structurally related to specific anionic inhibitors of the HCA isoenzymes resulted in active-site specific alkylation. Their rapid inhibitory effect on the enzyme function suggests that they form a complex with the zinc ion in the active site which helps to direct the alkylation of a histidine residue in the sterically appropriate position (Figure 1). This hypothesis was supported by the observation that the native conformation of the enzyme was required for a rapid and selective alkylation.

References

1. Bashford, D. and Karplus, M., *Biochemistry*, 29 (1990) 10219.
2. Csiba, A. and Szécsényi-Nagy, L., *Acta Veter. Hung.*, 37 (1989) 191.

Peptides: Chemistry, Structure and Biology
Pravin T.P. Kaumaya and Robert S. Hodges (Eds.)
Mayflower Scientific Ltd., 1996

108
Probing the Channel Structure of the Cystic Fibrosis Transmembrane Conductance Regulator A Peptide Model Approach

N.K. Goto, S.-C. Li, and C.M. Deber

Division of Biochemistry Research, Hospital for Sick Children, Toronto, ON, M5G 1X8, Canada
Department of Biochemistry, University of Toronto, Toronto, ON, M5S1A8, Canada

Introduction

The basic defect behind cystic fibrosis (CF) exists at the molecular level in the form of single site mutations in the gene encoding the cystic fibrosis transmembrane conductance regulator (CFTR) [1]. Although the most frequent CF mutation results in a deletion of phenylalanine at position 508 in the first nucleotide binding fold (ΔF508), mutations associated with CF have been found in all regions of the protein, including the putative channel domain [2].

These mutations may act to affect channel properties by changing the interior surface of the pore or alternatively may exert a deleterious effect on critical helix-helix packing interactions required to stabilize the channel pore. Clearly, structural information regarding the channel domain is required to explain how single amino acid substitutions can sabotage channel function. Unfortunately, a combination of factors including low expression levels and protein hydrophobicity interfere with traditional methods aimed towards large scale production and purification techniques required for structural analysis [3]. For these reasons, an alternative approach involving synthetic peptides was adopted to study the conformational and aggregational behavior of individual transmembrane (TM) segments in the channel domain.

Results and Discussion

Among twelve membrane spanning segments within the hydrophobic domain, the largest number of CF-associated mutations can be localized to the sixth putative TM segment, TM6. This correlates with the high level of homology found in TM6 across species and suggests a pivotal functional role for this segment [4, 5]. Further support is found in patch clamp studies demonstrating that TM6 mutants R347H and R334W exhibit aberrant conductance properties [6]. Similarly, anion selectivity has been shown to reside in the first and sixth putative TM segment through mutations induced at critical arginine residues [7]. This accumulation of data illustrating the importance of TM6 led us to center our approach around this segment.

A series of peptides corresponding to the wild type (WT) and CF-associated mutant sequences of TM6 was constructed as follows:

$$G^{330}\,I\,I\,L\,R^{334}\,K\,I\,F\,T\,T\,I\,S\,F\,C\,I\,V\,L\,R^{347}\,M\,A\,V\,T\,R\,Q^{354}\text{-amide}$$

The numbering corresponds to that of the published CFTR sequence [1]. Mutant peptides were synthesized by solid phase procedures using Fmoc chemistry with substitutions of R347H, R347P, R347L ,and R334W. Due to the presence of a cysteine residue in all five peptides, it was necessary to perform CD studies in the presence of dithiothreitol for direct comparison of peptide secondary structure. Indeed, SDS-PAGE gels of all peptides confirmed that each becomes partially oxidized during the course of purification to produce a mixture of monomers and presumably disulfide-linked dimers. CD analysis of monomeric peptides showed that apart from the proline mutant, all peptides are helical in 100 mM SDS micelles to approximately the same degree. Proline is distinguished by an initial 60% decrease in ellipticity at 222 nm *vs.* WT, suggesting that there is a structural consequence for this mutation. In contrast, this peptide has similar stability to the WT peptide when heated over a range of 25-95°C in SDS. In fact, all the peptides show reversible loss of ellipticity at 222 nm when heated, characteristic of a two-state helix to coil transition [8]. Interestingly, R347H and R334W lost a greater percentage of helicity at higher temperatures compared to WT, R347P, and R347L. His and Trp may not be accommodated into an SDS micelle as easily as Leu or as Arg close to the interface. Also, the fixed Φ angle of Pro may protect against loss of helicity [9].

While the present data are preliminary, work is now underway to expand the library of CFTR peptides. Different combinations of TM segments may reveal an additional level of stability conferred by helix-helix packing interactions. These approaches will hopefully clarify the interactions that mediate channel pore formation and provide an understanding of the possible mechanisms of function disruption.

References

1. Riordan, J.R., Rommens, J.M., Kerem, B.S., Alon, N., Rozmahel, R., Grzelczak, Z., Zielenski, J., Lok, S., Plavsic, N., Chou, J.L., Drumm, M.L., Iannuzzi, M.C., Collins, F.S. and Tsui, L.C., *Science*, 245 (1989) 1066.
2. CF Genetic Analysis Consortium, Dec 1994.
3. Bear, C.E., Li, C., Kartner, N., Bridges, R.J., Jensen, T.J., Ramjeesingh, M. and Riordan, J.R., *Cell*, 68 (1992) 809.
4. Diamond, G., Scanlin, T.F., Zasloff, M.A. and Bevins, C.L., *J. Biol. Chem.*, 266 (1991) 22761.
5. Marshall, J., Martin, K.A., Picciotto, M., Hockfield, S., Nairn, A. and Kaczmarek, L.K., *J. Biol. Chem.*, 266 (1991) 22749.
6. Sheppard, D.N., Rich, D.P., Ostedgaard, L.S., Gregory, R.J., Smith, A.E. and Welsh, M.J., *Nature*, 362 (1993) 160.
7. Anderson, M.P., Gregory, R.J., Thompson, S., Souza, D.W., Sucharita, P., Mulligan, R.C., Smith, A.E. and Welsh, M.J., *Science*, 253 (1991) 202.
8. Park, S.H., Shalongo, W. and Stellwagen, E., *Biochem.*, 32 (1993) 7048.
9. Li, S.C., Goto, N.K., Williams, K.A. and Deber, C.M., (unpublished data).

Session V
Peptide Libraries

Chairs: Deborah S. Parris and Hossain H. Saneii

Peptides: Chemistry, Structure and Biology
Pravin T.P. Kaumaya and Robert S. Hodges (Eds.)
Mayflower Scientific Ltd., 1996

109
Betidamino Acids: Versatile and Constrained Scaffolds for Drug Discovery

J.E. Rivier, G.-C. Jiang, L. Simon, S.C. Koerber, J. Porter, A.G. Craig and C.A. Hoeger

The Clayton Foundation Laboratories for Peptide Biology, The Salk Institute for Biological Studies, 10010 N. Torrey Pines Rd., La Jolla, CA 92037, USA

Introduction

Academic and pharmaceutical research has relied on the characterization of natural extracts (plants, marine organisms or bacterial broths) and on the development of methodologies for generating chemical diversity (organic, peptide or peptidomimetic libraries) for the discovery of new bioactive leads. Similarly, amide bond surrogates and several monomeric building blocks that mimic the peptide backbone have been described. All have advantages and disadvantages when it comes to biocompatibility, biostability and physicochemical properties. Our interest has focused, over the years, on the design of bioactive peptide analogs in an effort to understand the mechanism by which these molecules interact with their receptors. We describe below some exploratory work with a new class of amino acids, the betidamino acids, which are N'-monoacylated aminoglycine (Agl) derivatives where each N'-acyl group may mimic amino acid side chains or introduce novel functionalities. Betides (a contraction of **beta** position and am**ide**) are peptides containing one or more betidamino acids. Betidamino acids have an unlimited number of possible side chains that can be generated by simple acylation *in situ*.

Results and Discussion

We have approached the design of bioactive peptides by investigating ways to constrain backbone as well as side chain conformations while maintaining high affinity for the receptors. We have also investigated ways to increase affinity of these peptides by exploring side chain functionalities and their role in that process. The ω-amino function of ornithine and lysine can be used for the introduction of novel functionalities [1-3], but these are limited in that they can only mimic those amino acids with extended side chains. With the description of the synthesis of differentially substituted/protected α-aminoglycine derivatives, [4-6] and, more recently, of that of racemic α-Fmoc, α'Boc-aminoglycine [Fmoc-Agl(Boc)] by Qasmi *et al.* [7] we recognized that the introduction of an acyl moiety resembling an amino acid side chain on one of the two amino functions would leave the other free to form the peptide backbone thus generating betidamino acids as illustrated in Figure 1. In the cases of betide valine (b-Val), betide isoleucine (b-Ile)

and betidehomothreonine (bh-Thr) we have introduced a N^{β}-methyl group; N^{α}-methylation and C^{α}-methylation (in some cases) are also achievable to generate further constrained scaffolds. It should be recognized that the synthesis of the individual betidamino acids is superfluous as they were shown to be readily available by simple acylation of the adequate scaffolds [Fmoc-Agl(Boc); Boc(Me)-Agl(Fmoc) and Fmoc,Me-Agl(Me,Boc)] on the solid support. We are presently concentrating our efforts on the synthesis of Fmoc,Me-Agl(Me,Boc) and of the corresponding α-aminoalanines. By definition, betidamino acids have an amide bond replacing the β-methylene group.

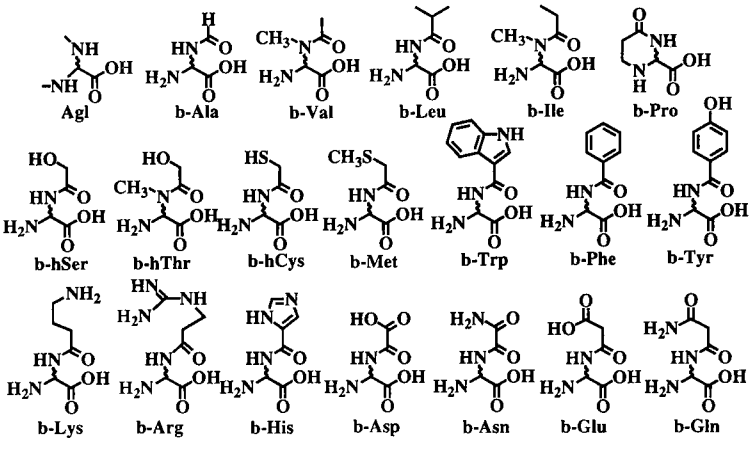

Figure 1. *Proposed structures of the 20 natural betid amino acids.*

Betidamino acids offer several advantages over other amino acids in SAR studies. First, side chain diversity in betidamino acids is virtually unlimited due to the availability of numerous acylating agents. Second, since the N^{β} position can not only be acylated but also derivatized using other reagents (such as sulfonyl chlorides, isocyanates and thioisocyanates), and since one (as in the case of peptoids to generate betoids) or both nitrogens (as well as the C^{α} carbon) can be alkylated as well as alkylated and acylated (such as in the case of α-methyl or β-methyl betidamino acids), a large number of easily accessible amino acid mimetics can be introduced into oligopeptides with the same coupling methodologies used for the amino acid derivatives presently known. The structural constraints introduced by the presence of a betidamino acid were of particular interest to us in the identification of bioactive conformations of peptide hormones and for the design of receptor selective analogs. In particular, this was of interest in studying receptor subtypes of somatostatin, CCK/gastrin, CRF, vasopressin/oxytocin, opioids, kinins and others. When Ramachandran-type plots were calculated for acetylated betidamino acid N'-methylamides together with those of their backbone methylated homologs, we found that the positions of the minima for the non-methylated betide models, N^{α}-methyl, C^{α}-methyl and bis-methylated derivatives were similar to those of the corresponding amino acids, with steeper potential wells which indicated a possible restriction of conformational freedom. In the case of N^{β}-methylation, similar

observations were made. Of particular interest is the fact that N^{α},C^{α}-bismethylation in conjunction with N^{β}-methylation gave unique minima at new, unconventional positions. It remains to be seen whether this scaffold is synthetically accessible as we have encountered difficulties in obtaining differentially protected α-aminoalanine derivatives. Thirdly, we were expecting betides (with an additional amide bond) to be more hydrophilic than the corresponding peptides or beta-methyl amino acid containing peptides. Finally, we have no evidence suggesting that the amide side chain would be any less stable to proteolytic enzymes than backbone amide bonds, except for formyl.

The main limitation to the use of betidamino acids is the difficulty of resolving the scaffolds; therefore, diastereomeric peptides will result from the introduction of such moieties. We have addressed this potential limitation in the accompanying paper where we have used unresolved N^{α}-Boc, $N^{\alpha'}$-Fmoc-Agl and N^{α}-Boc(Me), $N^{\alpha'}$-Fmoc-Agl as the templates for the introduction of betidamino acids in gonadotropin releasing hormone (GnRH) and somatostatin (see Hoeger *et al.*, this volume). Of paramount importance was the realization that the difference in potency between betide diastereomers did not vary significantly (rarely exceeding a factor of 5) and that the potency of the most potent diastereomer equaled that of the parent peptide (unpublished results). This suggested that the conformation assumed by the betidamino acid side chains in their D and L configuration may overlap with that of L or D amino acids in homologous peptides. Preliminary results in the GnRH area suggest that, for reasons unknown to date (increased hydrophilicity or *in vivo* instability), betide analogs will have shorter duration of action. For that reason and the fact that diastereomers will always be formed, we suspect that betides are unlikely drug candidates. However, the versatility of their use should allow rapid identification of optimal side chain functionality (orthogonal scan) at every position of the peptide chain (longitudinal scan) thus giving rise to a new class of combinatorial libraries. This can then be followed up by the synthesis and introduction of the newly defined amino acids or of their corresponding β-substituted homolog in the sequence of the optimized betide to restore duration of action or other desired properties unique to peptides.

Acknowledgments

Supported by NIH grants DK 26741, HD 13527, HL 41910 and the Hearst Foundation.

References

1. Theobald, P., Porter, J., Hoeger, C. and Rivier, J., *J. Am. Chem. Soc.*, 112 (1990) 9624.
2. Theobald, P., Porter, J., Rivier, C., Corrigan, A., Perrin, M., Vale, W. and Rivier, J., *J. Med. Chem.*, 34 (1991) 2395.
3. Rivier, J., Kupryszewski, G., Varga, J., Porter, J., Rivier, C., Perrin, M., Hagler, A., Struthers, S., Corrigan, A. and Vale, W., *J. Med. Chem.*, 31 (1988) 677.
4. Bock, M.G., DiPardo, R.M. and Freidinger, R.M., *J. Org. Chem.*, 51 (1986) 3718.
5. Katritzky, A.R., Urogdi, L. and Mayence, A., *J. Chem. Soc., Chem. Commun.*, (1989) 337.
6. Katritzky, A.R., Urogdi, L. and Mayence, A., *J. Org. Chem.*, 55 (1990) 2206.
7. Qasmi, D., René, L. and Badet, B., *Tetrahedron Lett.*, 34 (1993) 3861.

Peptides: Chemistry, Structure and Biology
Pravin T.P. Kaumaya and Robert S. Hodges (Eds.)
Mayflower Scientific Ltd., 1996

110
The Use of Soluble Polyamine Combinatorial Libraries for the Identification of Potent Opioid Receptor Active Compounds

R.A. Houghten, C.T. Dooley and J.M. Ostresh

Torrey Pines Institute for Molecular Studies
3550 General Atomics Court, San Diego,
CA 92121, USA

Introduction

The development and screening of immense combinatorial libraries of chemically synthesized compounds for basic research and use in the identification of pharmaceutical lead compounds has proceeded at an intense pace. Combinatorial approaches now include organic, peptidomimetic and peptide libraries [1-11]. The ability to systematically generate highly complex, but well-characterized mixtures of peptides by the simultaneous multiple peptide synthesis approach [12] offers the opportunity to prepare individual compounds, as well as organic libraries of equal diversity to those found in combinatorial libraries of peptides, if peptide libraries can be cleanly and reproducibly transformed by chemical means. Peptidomimetic chemistry has long endeavored to enhance the overall activity or properties of individual peptides by modifying side chain functionalities, transforming the peptide backbone, or reducing peptide flexibility through cyclization. In recent work [4], we have shown that modification of the amide backbone by the permethylation of peptide combinatorial libraries yields peptidomimetic diversities having physicochemical properties that are very different from the peptides from which they were obtained (enhanced stability to enzymatic breakdown, ability to cross biological membranes, etc.). We have now developed means for the reproducible chemical transformation of peptide libraries to form polyamine combinatorial libraries through the exhaustive reduction of all of the peptide amide groups. It is anticipated that these soluble polyamine combinatorial libraries will serve as a ready, and quite extraordinarily large, source of polyamines having not only the potential to block the biosynthetic pathways of naturally-occurring polyamines, but also for use as therapeutic agents in a wide range of previously unexplored indications.

Results and Discussion

While we have demonstrated the utility of diborane for the exhaustive reduction of model peptides in earlier studies [5], our interest was in its use for the preparation of a chemical library of functionalized polyamines. Soluble hexapeptide positional scanning synthetic

combinatorial libraries (PS-SCLs) have been shown in a range of earlier studies to permit the rapid identification of specific individual compounds [6-9]. We have now reduced a PS-SCL, consisting of six sublibraries of 20 L-amino acid hexapeptide mixtures, to obtain a positional scanning library of heptamines (from hexapeptide C-terminal amides). As with the starting peptide libraries, each of the resulting polyamine mixtures contained a single defined position with one of the 20 reduced amino acids (represented as O), with the remaining five positions consisting of mixtures of 18 reduced amino acids (represented by X; cysteine and tryptophan were excluded). The six reduced positional sublibraries consist of the same 37,791,360 (20 x 18^5) compounds in approximately equimolar representation, differing only in the location of the defined position. The 120 mixtures making up this polyamine combinatorial library were used to displace ^{3}H-DAMGO from opioid receptor binding sites in crude rat brain homogenates (Figure 1). The most effective amide reduced amino acid functionalities chosen at each of the six positions were: tyrosine for positions 1 and 2, phenylalanine and tyrosine for position 3, phenylalanine and proline for position 4, threonine and tyrosine for position 5, and phenylalanine, methionine, proline, serine, and tyrosine for position 6. Thus, 40 individual heptamines were prepared (1x1x2x2x2x5), with IC_{50} values ranging from 12-309 nM. The two most active heptamines were re(Ac-YYFPTM-NH_2) and re(Ac-YYFPTP-NH_2), with IC_{50} values of 12 and 13 nM, respectively (Table 1). The fifth and sixth positions were found to contribute little to the activities of the compounds. A pentamine [re(Ac-YYFP-NH_2)] was found to have an IC_{50} value of 15 nM.

We have expanded the libraries from libraries concept by combining the alkylation and reduction of combinatorial libraries made up of L-, D- and unnatural amino acids. Along with earlier studies [1-11 and refs. therein], these results serve to further confirm the power of soluble combinatorial libraries [1] and the libraries from libraries concept [4] as unique tools for basic research and drug discovery.

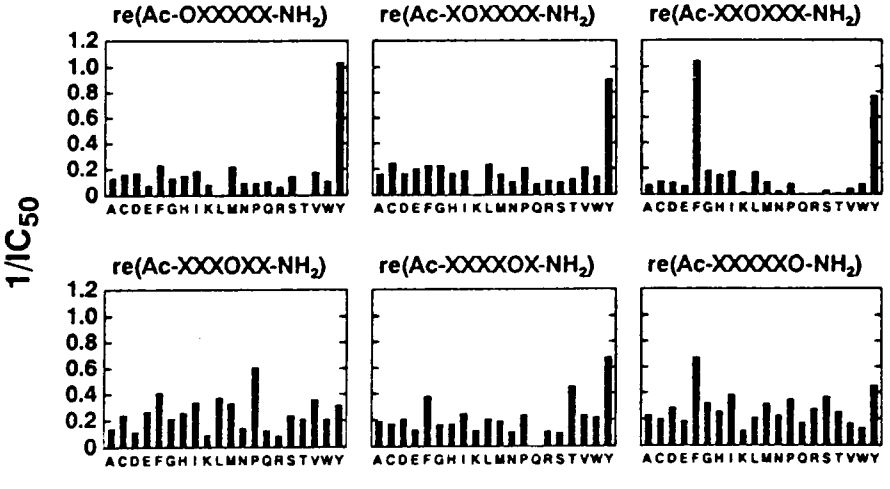

Figure 1. *Polyfunctional heptamine scanning combinatorial library: Inhibition of ^{3}H-DAMGO binding to opioid receptors.*

Table 1. *Individual heptamines identified from a polyfunctional amine scanning combinatorial library.*

Compound	IC_{50} (nM)	Compound	IC_{50} (nM)
re(Ac-YYFPTM-NH_2)	12	re(Ac-YYFPYF-NH_2)	25
red(Ac-YYFPTP-NH_2)	13	re(Ac-YYYPTS-NH_2)	29
re(Ac-YYFPTF-NH_2)	16	re(Ac-YYFPYM-NH_2)	31
re(Ac-YYFPYS-NH_2)	17	re(Ac-YYYPTP-NH_2)	37
re(Ac-YYFPTS-NH_2)	17	red(Ac-YYFFYP-NH_2)	55
re(Ac-YYFPTY-NH_2)	18	re(Ac-YYYPTY-NH_2)	59
re(Ac-YYFPYY-NH_2)	24	re(Ac-YYFFYS-NH_2)	70

Acknowledgment

This work was funded by Houghten Pharmaceuticals, Inc., San Diego, CA.

References

1. Houghten, R.A., Pinilla, C., Blondelle, S.E., Appel, J.R., Dooley, C.T. and Cuervo, J.H., *Nature*, 354 (1991) 84.
2. Pinilla, C., Appel, J., Blondelle, S., Dooley, C., Dörner, B, Eichler, J., Ostresh, J. and Houghten, R.A., *Biopolymers (Pept. Sci.)*, 37 (1995) 221.
3. Dörner, B., Blondelle, S.E., Pinilla, C., Appel, J., Dooley, C.T., Eichler, J., Ostresh, J.M., Pérez-Payá, E. and Houghten, R.A. in Cortese, R. (Ed.), *Molecular Repertoires and Methods of Selection*, Walter de Gruyter & Co., Berlin, 1995, in press.
4. Ostresh, J.M., Husar, G.M., Blondelle, S.E., Dörner, B., Weber, P.A. and Houghten, R.A., *Proc. Natl. Acad. Sci., USA*, 91 (1994) 11138.
5. Cuervo, J.H., Weitl, F., Ostresh, J.M., Hamashin, V.T., Hannah, A.L. and Houghten, R.A. in Maia, H.L.S. (Ed), *Peptides 1994*, ESCOM, Leiden, The Netherlands, 1995, p.465.
6. Pinilla, C., Appel, J.R., Blanc, P. and R.A. Houghten, R.A., *BioTechniques*, 13 (1992) 901.
7. Dooley, C.T. and Houghten, R.A., *Life Sci.*, 52 (1993) 1509.
8. Pinilla, C., Appel, J.R., Blondelle, S.E., Dooley, C.T., Eichler, J., Ostresh, J.M. and Houghten, R.A., *Drug Dev. Res.*, 33 (1994) 133.
9. Eichler, J., Lucka, A.W. and Houghten, R.A., *Pept. Res.*, 7 (1994) 300.
10. Dooley, C.T., Chung, N.N., Schiller, P.W. and Houghten, R.A., *Proc. Natl. Acad. Sci., USA*, 90 (1993) 10811.
11. Dooley, C.T., Chung, N.N., Wilkes, B.C., Schiller, P.W., Bidlack, J.M., Pasternak, G.W. and Houghten, R.A., *Science*, 266 (1994) 2019.
12. Houghten, R.A. , *Proc. Natl. Acad. Sci., USA*, 82 (1985) 5131.

Peptides: Chemistry, Structure and Biology
Pravin T.P. Kaumaya and Robert S. Hodges (Eds.)
Mayflower Scientific Ltd., 1996

111
Cyclic Peptide Libraries

A.F. Spatola, Y. Crozet, P. Romanovskis and E. Valente

Department of Chemistry, University of Louisville, Louisville, KY 40292, USA

Introduction

Cyclic peptides appear to enjoy numerous advantages over linear peptide analogs as stabilized receptor ligands or as lead candidates for further drug development. By introducing additional modifications such as amide bond surrogates (pseudopeptides) or various turn mimics, these leads can be further enhanced with respect to bioavailability, receptor selectivity, and oral activity.

Results and Discussion

We have previously reported that cyclic peptide mixtures can be efficiently synthesized by a side chain attachment strategy involving resin-bound head-to-tail cyclization, provided that the synthesis is optimized for structural and stereochemical integrities. Below we outline additional findings that further improve the quality and utility of the desired cyclic peptide libraries and sublibraries.

Our approach to head-to-tail cyclic peptide mixtures [1, 2] has been further developed by the investigation of new routes for the initial side chain attachment/ resin-bound cyclization strategy. Thus far, our linkages have included Asp, Asn, Glu, Gln, and Lys. Several final deprotective and cleavage conditions have also been used such as anhydrous HF, Yajima's reagent, catalytic transfer hydrogenation, and phase transfer catalysis.

During the course of our synthetic investigations, we observed that the quality of our cyclic library mixtures was affected in predictable fashion by ring size, coupling agents, the absolute configuration of the chiral protected amino acids, and, especially by the presence or absence of turn-inducing residues such as the imino acid proline.

Proline is a constituent of many naturally occurring cyclic peptides. Thus use of proline, other imino acids, amide bond surrogates, or N-methyl amino acids is a reasonable approach both for facilitating macrocyclization as well as for reducing the inherent disadvantages (solvation energies) associated with all-amide structures. This has been cited as a reason why amide structures suffer from limited bioavailability [3].

Accordingly, we have explored the following strategy for the preparation of cyclic peptide mixtures for bioassay: 1) Select one of the possible side chain linkages; 2) Initiate the solid phase synthesis of cyclic peptides of varying ring size (typically 5-8 residues); 3a) Incorporate (serially) a single proline at each position within each cyclic peptide chain (the Pro-scan approach) (as in Table 1); or 3b) Incorporate (serially) a

Table 1. *Examples of cyclic peptide libraries utilizing the Pro-scan approach.*

Ring size	Cyclic peptide sublibrary	No. of Compds.
5	c(Xxx-Xxx-Xxx-Pro-Asp)	216
	c(Xxx-Xxx-Pro-Xxx-Asp)	216
	c(Xxx-Pro-Xxx-Xxx-Asp)	216
	c(Pro-Xxx-Xxx-Xxx-Asp)	216
6	c(Xxx-Xxx-Xxx-Xxx-Pro-Asp)	1,296
	c(Xxx-Xxx-Xxx-Pro-Xxx-Asp)	1,296
	c(Xxx-Xxx-Pro-Xxx-Xxx-Asp)	1,296
	c(Xxx-Pro-Xxx-Xxx-Xxx-Asp)	1,296
	c(Pro-Xxx-Xxx-Xxx-Xxx-Asp)	1,296
7	c(Xxx-Xxx-Xxx-Xxx-Xxx-Pro-Asp)	7,776
	c(Xxx-Xxx-Xxx-Xxx-Pro-Xxx-Asp)	7,776
	c(Xxx-Xxx-Xxx-Pro-Xxx-Xxx-Asp)	7,776
	c(Xxx-Xxx-Pro-Xxx-Xxx-Xxx-Asp)	7,776
	c(Xxx-Pro-Xxx-Xxx-Xxx-Xxx-Asp)	7,776
	c(Pro-Xxx-Xxx-Xxx-Xxx-Xxx-Asp)	7,776

Xxx = glutamic acid, lysine, leucine, tyrosine, serine,and arginine.

flexible pseudopeptide (such as ProΨ[CH_2S]Gly) at each position within each cyclic peptide chain (the Psi-scan approach); 4) Following each synthesis and cleavage, subject the soluble cyclic peptide sublibraries to bioassays to establish the preferred position(s) of the turn-inducing residue; 5) Based on the position selected in step 4, resynthesize a series of cyclic peptides using the positional scan approach [4]; this self-deconvoluting technique is used to identify the preferred residues at each variable position within the cyclic sequence following bioassay.

Thus far we have prepared groups of cyclic peptide analogs totaling over one-half million analogs. Some of these mixtures have been tested in antibiotic screens and also as potential therapeutics in a recently developed National Cancer Institute program for testing libraries against the AIDS virus and in a variety of anticancer screens.

A key concern with the synthesis of cyclic peptides has been the verification of structural and stereochemical integrities of the resulting compounds. By synthesizing mixtures of modest ring size, and by keeping the number and diversity of most sublibraries relatively small, various analytical techniques including NMR analysis, FABMS, electrospray MS, and liquid chromatography-mass spectral analysis can be used to confirm synthetic fidelities. Among our conclusions:

1) The five- and six-membered rings appear to cyclize more easily and reliably than those with seven residues.
2) In a six-residue ring (Table 1), the position of proline accelerates cyclization in the following order ($Pro^1 > Pro^5 > Pro^3 > Pro^4 > Pro^2$), where Asp is defined as Asp^6.
3) In these medium size rings we have seen limited evidence of dimer formation, presumably due to a decreased tendency for β-sheet aggregation among the relatively short linear peptide precursors.

Acknowledgments

We are grateful for mass spectral determinations provided by Phil Andrews and Rachel Loo of the University of Michigan. This work was supported by NIH GM33376, and by the Lilly Company and the Torrey Pines Institute for Molecular Studies.

References

1. Darlak, K., Romanovskis, P. and Spatola, A.F. in Hodges, R.S. and Smith, J.A. (Eds.), 'Peptides: Chemistry, Structure, and Biology', ESCOM, Leiden, the Netherlands, 1994, 981.
2. Spatola, A.F., Chen, J.J., Romanovska, I., Romanovskis, P. and Wen, J.J., in Maia, H.L.S. (Ed.), 'Peptides 1994', ESCOM, Leiden, 1995. p. 96.
3. Conradi, R.A., Hilgers, A.R., Ho, N.F.H. and Burton, P.S., *Pharm. Res.*, 9 (1992) 1453.
4. Pinilla, C., Appel, J.R., Blanc, P. and Houghten, R.A., *Biotechniques*, 13 (1992) 901.

Peptides: Chemistry, Structure and Biology
Pravin T.P. Kaumaya and Robert S. Hodges (Eds.)
Mayflower Scientific Ltd., 1996

112
Design and Structural Validation of a Conformationally-homogeneous Peptide Combinatorial Library

E. Bianchi, A. Folgori, A. Wallace, M. Nicotra, G. Barbato, R. Bazzo, R. Cortese, F. Felici and A. Pessi

Istituto di Ricerche di Biologia Molecolare P. Angeletti (IRBM)
00040 Pomezia (Rome), Italy

Introduction

The combined use of selection methods and combinatorial synthesis is contributing to accelerate the discovery of new drug leads. In fact, it has been proposed that the combinatorial approach will drive a momentous shift in the current paradigm for rational drug design, where the actual design step will be moved from the level of individual molecules (analogs of the initial lead) to the level of selectable populations [1]. The availability of conformationally homogeneous peptide populations, in which all the peptides share a common, predetermined structure, could represent a major step in this direction, since any ligand selected from these libraries would directly yield both the identity and the topography of the pharmacophoric side chains; this is all the information which is required for the design of a first generation peptidomimetic, in which a suitable non-peptidic scaffold will replace the peptide backbone [2]. Key to this process, for which we coined the term selection-driven (peptidomimetic) design, is the design of the conformationally homogeneous libraries: we describe here how a natural protein folding motif, the zinc finger, was successfully used as a template to engineer a large ($>10^6$) population of selectable α-helical peptides.

Results and Discussion

The Cys_2His_2 zinc finger is one of the most common DNA-binding motifs [3, 4] and the specificity resides in the α-helical subdomain [5]. This structure was chosen for several reasons: i) a (limited) natural repertoire of zinc fingers exists which displays structural conservation in the presence of different DNA-binding residues [6-9]; ii) tolerance to sequence variability in all but a few conserved residues was suggested by a minimalist analogue with multiple Ala substitutions, showing the typical zinc finger fold [10]; iii) in all zinc fingers metal coordination and folding are coupled, since in the absence of zinc the peptides show CD spectra typical of a random-coil (Figure 1b). This feature is of utmost importance for the development of a library because metal-dependent binding would represent a built-in control against the selection of structurally undefined sequences.

Using as starting point a consensus 26-amino acid Cys_2His_2 zinc finger peptide (Consensus Peptide-1 or CP-1), H-Pro-Tyr-Lys-Cys-Pro-Glu-Cys-Gly-Lys-Ser-Phe-Ser-Gln-Lys-**Ser**-**Asp**-Leu-**Val**-**Lys**-His-Gln-**Arg**-Thr-His-Thr-Gly-NH_2 [11], we randomized five positions in the α-helical portion (in bold in the sequence). These positions, X^1-X^2-X^3-X^4-X^5 (residues 15,16,18, 19 and 22, respectively), are the most exposed in the helix (side-chain accessibility between 25 and 60%) and cluster on one side of the structure, fully available for interaction with a given receptor; the distance between the C-α carbons of X^1 and X^5 is 12 Å (Figure 1a).

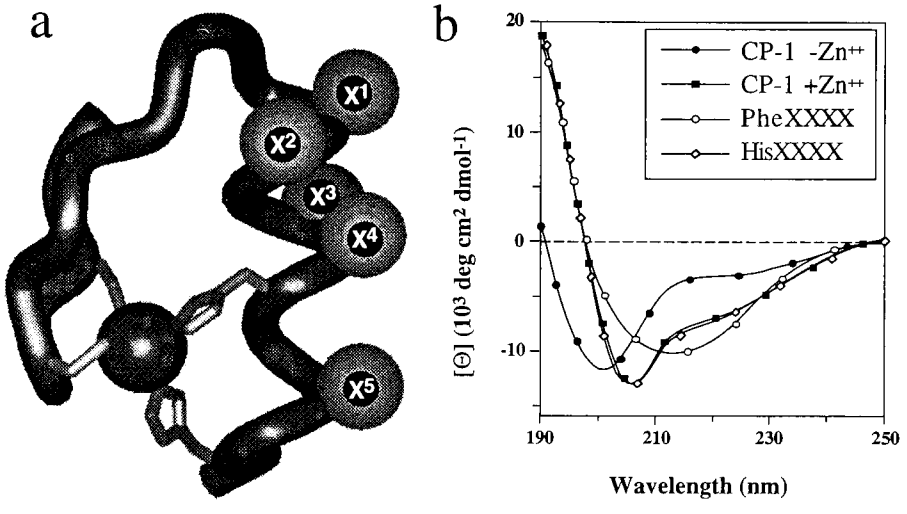

Figure 1. *(a) Structure of the zinc finger library. The randomized residues X^1-X^5 are shown as spheres centred on the side-chain β-carbon. (b) CD spectra of the parent peptide CP-1 in the presence and absence of 2 equiv of $ZnCl_2$, and of two peptide pools representative of type A (Pool HisXXXX) and type B (Pool PheXXXX) spectra, in the presence of 2 equiv of $ZnCl_2$ (see text).*

The tolerance of this naturally evolved fold towards mutations was probed with an expanded set of amino acids, including non-coded residues like 2-aminobutyric acid (Abu), cyclohexylalanine (Cha), norleucine (Nle), norvaline (Nva), ornithine (orn), homophenylalanine (Hph), 4-chlorophenylalanine (Fcl), and 4-nitrophenylalanine (Fno). The library and the individual zinc fingers were synthesized on Polyhype SU-500 by standard Fmoc/t-Bu chemistry, using isokinetic mixtures for the incorporation of the X positions [overall 5-fold excess, concentrations relative to Ala(1): Arg(1), Asn(1), Asp(1), Gln(1), Glu(1), His(1), Ile(2), Leu(1), Lys(1), Met(1), Phe(1.4), Ser(1), Thr(2), Trp(1.4), Tyr(1.4), Val(2), Abu(1), Cha(1), Nle(1), Nva(1), Orn(1), Hph(1.4), Fcl(1.4), Fno(1.4)].

The peptide pools were analysed by CD and Co(II)-complex absorption spectra to establish the homogeneity of the peptide population. Figure 1b shows the two types of CD curves found for the library mixtures: type A spectrum, exemplified by the HisXXXX pool, which is essentially superimposable to that of the canonical zinc finger

indicates structural preservation; type B spectrum, exemplified by the PheXXXX pool, shows a dramatic structural change with an increased content of β-structure. The appearance of type B CD was confined to hydrophobic residues in position X^1, while in positions X^2- X^5 both hydrophilic and hydrophobic residues gave rise to type A spectra, with minor distortions in a few cases. Analogous results were obtained from the Co(II)-complex absorption experiments. Overall, this analysis showed that the zinc finger fold is sufficiently stable to tolerate extensive mutagenesis in the selected positions of the helical subdomain, much beyond the functional needs of the natural repertoire. The exception is represented by the first position in the helix, where hydrophobic amino acids may likely interfere with the packing of the three conserved hydrophobes (Tyr2, Phe11, and Leu17). NMR studies on individual peptides displaying type B spectra are in progress to clarify this point. In the final version of the library, we used the complete 26-aa set in positions X^2- X^5 and a reduced 14-aa set (Ala, Arg, Asn, Asp, Gln, Glu, His, Lys, Met, Ser, Thr, Tyr, Val) in position X^1. All the pools of this library, which collectively included $6.4x10^6$ peptide sequences, showed type A CD spectra.

The zinc finger library was also produced in the form of fusion phage [12], and parallel screening of the phage and synthetic library with a monoclonal IgA yielded its final validation as a source of ligands of pre-determined structure: individual peptides derived from the common consensus sequence showed a very strong, zinc-dependent binding to the mAb, and were shown by CD, Co(II)-complex and NMR to display the expected pharmacophoric structure [13].

References

1. Gordon, E.M., Barret, R.W., Dower, W.J., Fodor, S.P.A. and Gallop, M.A., *J. Med. Chem.*, 36 (1994) 1385.
2. Moore, G.J., *Trends Pharm. Sci.*, 15 (1994) 124.
3. Pellegrino, G.R. and Berg, J.M., *Proc. Natl. Acad. Sci., USA*, 88 (1991) 671.
4. Jacobs, J.H., *EMBO J.*, 11 (1992) 4507.
5. Pavletich, N.P. and Pabo, C.O., *Science*, 241 (1991) 809.
6. Frankel, A.D., Berg, J.M. and Pabo, C.O., *Proc. Natl. Acad. Sci., USA.*, 84 (1987) 4841.
7. Parraga, G., Horvath, S.J., Eisen, A., Taylor, W.E., Hood, L., Young, E.T. and Klevit, R.E., *Science*, 241 (1988) 1489.
8. Lee, M.S., Gippert, G.P., Soman, K.V., Case, D.A. and Wright, P.E, *Science*, 245 (1989) 635.
9. Omichinski, J.G., Clore, G.M., Apella, E., Sakaguchi, K. and Groenborg, A.M., *Biochemistry*, 29 (1990) 9324.
10. Michael, S.F., Kilfoil, V.J., Schmidt, M.H., Amann, B.T. and Berg, J.M., *Proc. Natl. Acad. Sci., USA*, 89 (1992) 4796.
11. Krizek, B.A., Amann, B.T., Kilfoil, V.J., Merckle, D.L., and Berg, J.M. *Proc. Natl. Acad. Sci., USA*, 113 (1991) 4518.
12. Scott, J.K. and Smith, G.P., *Science*, 249 (1990) 386.
13. Bianchi, E., Folgori, A., Wallace, A., Nicotra, M., Acali, S., Phalipon, A., Barbato, G., Bazzo, R., Cortese, R., Felici, F. and Pessi; A., *J. Mol. Biol.*, 247 (1995) 154.

Peptides: Chemistry, Structure and Biology
Pravin T.P. Kaumaya and Robert S. Hodges (Eds.)
Mayflower Scientific Ltd., 1996

113
Identification and Characterization of a Novel Peptide Substrate for P60$^{c\text{-}src}$ Protein Tyrosine Kinase Using a One-bead One-peptide Combinatorial Peptide Library Method

K.S. Lam[1], Q. Lou[1], J. Wu[2], S.E. Salmon[1] and H. Phan[1]

[1]*Arizona Cancer Center and Department of Medicine, University of Arizona, Tucson, AZ 85724, USA*
[2]*Selectide Corporation, 1580 E. Hanley Blvd., Tucson, AZ 85737, USA*

Introduction

Since the introduction of the "one-bead one-peptide" combinatorial peptide library method (or "Selectide" process) four years ago [1, 2], we have successfully applied the method to various biological systems (for recent reviews, see [3] and [4]). These include: monoclonal antibodies that recognize a continuous or a discontinuous epitope, proteases, streptavidin, avidin, MHC-class I molecules, gpIIb/IIIa integrin, and a small organic indigo dye. The biologic screening assays for most of these targets are based on an enzyme-linked colorimetric assay in which the peptide-beads interacting with the macromolecular target changed color. The color beads are then physically isolated for microsequencing. Alternatively, a two-stage solution-phase releasable assay using peptide-beads with orthogonal cleavable linkers has been used (*e.g.* for the gpIIb/IIIa integrin [5]).

Recently, we reported an on-bead functional assay for the elucidation of post-translational modification sites of proteins [6, 7]. We have successfully applied this method for identification of linear peptide substrate motifs for cAMP-dependent protein kinase (a serine/threonine protein kinase) and for p60$^{c\text{-}src}$ protein tyrosine kinase (PTK). In this method, we first incubated the peptide-bead library with [γ-^{32}P]ATP and the protein kinase. After incubation, the beads were washed thoroughly with high salt buffer followed by heating with 1.0 M HCl for 5 minutes to remove all the non-covalent [γ-^{32}P]ATP binding and washed thoroughly again. The beads were then suspended in molten 1.5% (w/v) agarose and plated on a glass plate. The bead-containing gel was then air-dried to form a film and exposed to an X-ray film. Autoradiography was then used to localize the [^{32}P]-labelled beads. The beads corresponding to the autoradiographic spots were removed and suspended in molten agarose solution again for secondary plating. With this dilution, single [^{32}P]-labelled beads could be isolated for microsequencing.

Results and Discussion

Using the above phosphorylation screening method, we rapidly identified the phosphorylation site motif of cAMP-dependent protein kinase as RR_S , which is identical to that reported in the literature, thus validating the technology [7]. When a limited heptapeptide library (500,000 beads) was screened with $p60^{c\text{-}src}$ PTK, a peptide YIYGSFK was identified [8]. Using a solution phase phosphorylation assay with analysis by thin layer chromatography (polyethylene imine cellulose plate), the Km of YIYGSFK was determined to be 53 μM, about 7-fold better than that of the cdc (6-20) peptide, one of the best known peptide substrates for $p60^{c\text{-}src}$. When compared to the cdc(6-20) peptide (15 amino acids long), YIYGSFK (a heptapeptide) was also more specific to the src family PTK.

Using a solid-phase phosphorylation assay, a SAR study was performed on over 70 analogs of YIYGSFK. The peptide analogs were first synthesized on TentaGel S resin with a non-cleavable linker (similar to the synthesis of the bead-library [3]). The peptide-beads were then phosphorylated with $p60^{c\text{-}src}$ PTK, immobilized on a glass plate with agar and the relative amount of phosphorylation per bead quantitated with a PhosphorImager (Molecular Dynamics, Sunnyvale, California). An aromatic residue at positions 1 and 6 (D or L diastereomer) is preferable and a hydrophobic residue (L-diastereomer) at position 2 is essential. An L-tyrosine at position 3 is required as the phosphorylation site. An acidic residue with a primary amine at the side chain (D or L diastereomer) at position 7 is crucial. Table 1 summarizes the result of this study.

Since Tyr^3 is the phosphorylation site, this residue was substituted with various aromatic residues in an attempt to develop a pseudosubstrate-based peptide inhibitor. Preliminary results shown in Table 2 indicate that YI(Nal-2)GSFK is the best inhibitor for $p60^{c\text{-}src}$ with an IC_{50} of approximately 58 μM, very similar to the Km of YIYGSFK.

Work is currently underway in applying the same technology for the identification of substrate motifs and development of potent inhibitors for $p185^{bcr\text{-}abl}$ PTK, an oncogenic protein in chronic myelogenous leukemia.

Table 1. *Phosphorylation scale[a] of YIYGSFK analogues by $p60^{c\text{-}src}$ on solid-phase: Single amino acid substitution.*

Y	I	Y	G	S	F	K
Y=100	I=100	Y=100	G=100	S=100	Y=175	K=100
F=76	L=92	F=7	S=36	T=92	F=100	Dab=86
T=71	V=90	A=4	A=34	A=89	f=31	Orn=82
y=65	Chg=29	y=1	MeG=12	V=48	MeF=30	Dap=77
W=41	A=21		K=7	G=40	W=25	k=56
S=30	i=13		N=6	Y=34	Cha=22	R=26
E=27	Nle=12		a=2	K=33	A=11	A=10
Cha=23	K=7		L=1	N=30	H=7	H=5
A=16	E=6		D=0	s=9		D=1
Orn=15						

[a]Phosphorylation was quantitated by PhosphorImager; YIYGSFK

Table 2. *Pseudosubstrate-based inhibitors (YIXGSFK) for p60 $^{c\text{-}src}$ PTK*

X	IC_{50}, μM
2-naphthalalanine	58
1-naphthalalanine	84
p-chlorophenylalanine	324
p-fluorophenylalanine	558

Acknowledgments

This work is supported by NIH grants CA17094, CA57723, and the Selectide Corporation. Kit S. Lam is a Scholar of the Leukemia Society of America.

References

1. Lam, K.S., Salmon, S.E., Hersh, E.M., Hruby, V.J., Al-Obeidi, F., Kazmierski, W.M. and Knapp, R.J., in Rivier, J.E. and Smith, J.A. (Eds.), 'Peptides: Chemistry, Structure and Biology', ESCOM, Leiden, The Netherlands, 1991, pp 492-495.
2. Lam, K.S., Salmon, S.E., Hersh, E.M., Hruby, V.J., Kazmierski, W.M. and Knapp, R.J., *Nature,* (London), 354 (1991) 82.
3. Lam, K.S. and Lebl, M., *Methods: A Companion to Methods in Enzymology*, 6 (1994) 372.
4. Lebl, M., Krchnak, V., Sepetov, N.F., Seligmann, B., Strop, P., Felder, S., Lam, K.S., *Biopolymers (Peptide Science)*, 37 (1995) 177.
5. Salmon,. S.E., Lam, K.S., Lebl, M., Kandola, A., Khattri, P., Wade, S., Patek, M., Kocis, P. and Krchnak, V., *Proc. Natl. Acad. Sci., USA*, 90 (1993) 11708.
6. Lam, K.S. and Wu, J., *Methods: A Companion to Methods in Enzymology*, 6 (1994) 401.
7. Wu, J., Ma, Q.N., Lam, K.S., *Biochemistry*, 33 (1994) 14825.
8. Lam, K.S., Wu, J.S. and Lou, Q., *Intl. J. Protein Peptide Res.*, 45 (1995) 587.

Peptides: Chemistry, Structure and Biology
Pravin T.P. Kaumaya and Robert S. Hodges (Eds.)
Mayflower Scientific Ltd., 1996

114
The Transformed Group Library Method: A New Library Design and Mixture Decode Strategy

A.M. Bray

Chiron Mimotopes Pty. Ltd., 11 Duerdin Street, Clayton, Victoria 3168, Australia

Introduction

With the objective of maximizing library resolution, whilst minimizing the number of mixtures within a library, a strategy based on group theory arguments has been developed [1]. Library mixtures are organized into sets of binary sublibraries, which are related *via* group transformation operations. Active compounds are deduced from the first screen *via* inter-sublibrary comparison of the screening data [2]. Unlike the iterative library strategy [3, 4], in which each monomer position is elucidated in turn, the transformed group approach allows concurrent elucidation of all monomer positions. Extensive intra-sublibrary comparison enables the relative replaceability of all residue positions to be explored using results from the initial screen. In a working example, a library containing up to 24,137,569 hexapeptides organized into 192 mixtures, identified a group of 324 potential MAb binding peptides in a single screen. This result was confirmed by synthesis and screening of a further 30 mixtures.

Materials and Methods

A support-bound hexapeptide library composed of three 64 mixture sublibraries (A, B and C) was assembled on pins [5] using binary groupings (Table 1). These were devised using the 6 monomer groupings: **a** (Ile, Val, Leu); **b** (homoPhe, Phe, Tyr); **c** (Asp, Glu); **d** (Asn, Gln, Ser); **e** (Ala, Gly, Pro); **f** (Arg, His, Lys). An anti-hemagglutinin MAb 17-09, [6] which binds the native sequence DVPDYA, was screened against the 192 mixtures using a pin ELISA protocol [7]. ELISA data for the top 10 binding peptide mixtures are presented in Table 3. The 30 implied intersection mixtures were prepared using monomer groupings only, and subjected to a second ELISA study with MAb 17-09; Table 4 presents the top 10 binding mixtures from the second round of testing.

Results and Discussion

Each of the related sublibraries (A, B, *etc.*), which comprise a transformed group library, contain the same total peptide set. These are organized so any given mixture in a sublibrary shares a unique set of compounds with any given mixture within a second sublibrary, *e.g.* mixtures A(n) and B(m) have a unique intersection. If A(n) and B(m) were the only mixtures within their respective sublibraries to possess an activity, the inference is that the relatively small intersection mixture contains active compound(s).

Sublibraries are prepared from two mutually exclusive monomer mixtures, called binary groupings and designated 0 and 1 (Table 1), to give mixtures of the general form; ######, where # = 0 or 1. Hence, a given peptide Nmer sublibrary contains 2^N mutually exclusive mixtures (*e.g.* a 6mer sublibrary contains 64 mixtures) - the minimum number that will allow the elucidation each peptide residue position. The monomers used to prepare the library are organized into binary groupings in a two step mixing process. Monomers are combined into an even number of monomer groupings, which are, in turn, combined to give paired binary groupings (Table 1). The process of combining monomer groupings into binary groupings establishes the relationship between the sublibraries; each being definable by a unique group transformation function. Although the number of pairs of binary groupings that can be constructed, hence the number of sublibraries that can be prepared, is given by 0.5n!/(n/2)!2 (n = the number of monomer groupings), far fewer sublibraries are required. Resolution of each residue position is possible provided that no two monomer groupings are paired in all binary groupings. Hence, the minimum number of sublibraries required is $\geq$ log(n)/log(2): 6 monomer groupings implies a minimum of 3 sublibraries. Table 1 presents 3 of 10 possible pairs of binary groupings constructed from the 6 monomer groupings (**a-f**).

Table 1 (left). *Generation of binary groupings for library preparation from 6 monomer Groupings (**a - f**).*

Table 2 (right). *Elucidation of monomer groupings at a given peptide mixture residue by sublibrary comparison. Binary motifs.*

Binary Grouping	Sublibrary A	B	C
0	**[a b c]**	**[a b f]**	**[a e f]**
1	**[d e f]**	**[c d e]**	**[b c d]**

Sub-Library	Monomer Grouping **a**	**b**	**c**	**d**	**e**	**f**
A	0	0	0	1	1	1
B	0	0	1	1	1	0
C	0	1	1	1	0	0

Inter-sublibrary comparison allows the identification of intersection mixtures which may contain active compounds. The intersection between the highest activity mixtures from sublibraries A, B and C (Table 3) (*i.e.*, A(001001)$\cap$B(101101)$\cap$C(110110)) is defined by the string of monomer groupings: **cbecbe** (Table 2). Each residue position is determined by identifying monomer groupings common to each residue position. The string **cbecbe** corresponds to the 324 peptide sequences: (D,E)(Y,F,Z)(A,P,G)(D,E)(Y,F,Z)(A,G,P) (residues present in the native binding sequence are underlined, Z = homoPhe). The 10 top binding mixtures listed in Table 3, however, define 30 intersections. When these implied intersection mixtures were synthesized and screened against MAb 17-09, a clear consensus emerged with 5 of the 6 residue positions being conserved within the limits of the monomer groupings. A binding motif **cbXcbe** was identified (X = replaceable). In a final round of deconvolution, 108 mixtures were prepared and tested. The five defined positions were replaced with individual amino acids, and X was a mixture of monomer groupings **c**, **d** and **e**. Seven strongly binding

sequences were identified in this final study: DZXDYG, EZXDYA, DFXDYG, DYXDYG, DFXDYA, DZXDYA, and DYXDYA.

Data from the first screen can be used to examine replaceability trends by intra-sublibrary comparison. For example, binding data for the active mixture A(001001) can be compared with results obtained for A(101001), A(011001), A(000001), A(001101), A(001011), and A(001000). This analysis demonstrated that position 4 tolerates change, whereas activity was lost if either positions 1 or 5 were altered, hence monomer(s) within binary grouping A(0) were required at these positions. These results are consistent with both the known epitope replaceability properties and the above deconvolution study.

In conclusion, the transformed group library approach allowed a range of potent MAb binding peptides to be identified in three steps, with key properties of all residue positions being established in the initial screen.

Table 3 (left). *Top scoring pin-bound peptide mixtures binding to MAb 17-09.*
Table 4 (right). *Deconvolution by synthesis and screening of 30 implied intersection mixtures. Top scoring mixtures, MAb 17-09.*

Sublibrary	Mixture	ELISA Value
A	001001	611
	000001	494
	000100	307
	000000	285
	100100	206
B	101101	409
	010110	198
C	110110	268
	111111	233
	111110	194

Mixture	ELISA Value	Mixture	ELISA Value
cbXcbe	2827	**cbdcbd**	1573
cbdcbe	2737	**bcbdcb**	1569
cbecbe	2652	**cbccbd**	1365
cbccbe	2457	**bcbccb**	1257

X = mixture of 17 amino acids

References

1. Bray, A.M., U.S. Patent Application, October 14, 1994.
2. A similar concept has been reported; Deprez, B., Willaird, X., Bourel, L., Coste, H. and Tartar, A., in Maia, H.L.S. (Ed.), 'Peptides 1994', ESCOM, Leiden, The Netherlands, 1994, p 455.
3. Geysen, H.M., Rodda, S.J. and Mason, T., *J. Mol. Immunol.*, 23 (1986) 709.
4. Houghten, R.A., Pinilla, C., Blondelle, S.E., Appel, J.R., Dooley, C.T. and Cuervo, J.H., *Nature*, 354 (1991) 84.
5. Fmoc synthesis protocol; Valerio, R.M., Bray, A.M., Campell, R.A., DiPasquale, A., Margellis, C. Rodda, S.J., and Geysen, R.M., *Int. J. Peptide Protein Res.*, 42 (1993), 1.
6. Wilson, I.A., Niman, H.I., Houghten, R.A., Cherenson, A.R., Connelly, M.L. and Lerner, R.A., *Cell*, 37 (1984) 767.
7. Geysen H.M., Rodda, S.J., Mason, T.J., Tribbick, G. and Schoofs, P.G., *J. Immunol. Methods*, 102 (1987) 259.

Peptides: Chemistry, Structure and Biology
Pravin T.P. Kaumaya and Robert S. Hodges (Eds.)
Mayflower Scientific Ltd., 1996

115
Design of Conformationally Defined Combinatorial Libraries Based Upon "Protein-like" Structural Motifs

S.E. Blondelle, B. Forood, R.A. Houghten and E. Pérez-Payá

Torrey Pines Institute for Molecular Studies, 3550 General Atomics Ct, San Diego, CA 92121, USA

Introduction

Synthetic combinatorial libraries (SCLs) have greatly accelerated the potential discovery of new lead compounds [1]. SCL approaches can be used to generate small molecule diversities (*i.e.*, short peptides, peptidomimetics or organic compounds). The generation of such diversities based upon "protein-like" structural motifs is expected to broaden the use of SCLs for those applications that require the occurrence of a well-defined secondary and/or tertiary structure. We have developed an approach for the identification of structurally defined polypeptides by combining the structural characteristics of known peptides with the strength of combinatorial library techniques.

Results and Discussion

In earlier studies, two well defined secondary structural motifs were used as structural units for the construction of conformationally defined libraries: one having an amphipathic α-helix [2], and the other being the linker region between the two α-helical motifs of melittin [3].

Recently, we have designed a 16-residue peptide (Ac-$KA_{14}K$-NH_2, termed KAK) that self-aggregates into an extremely aqueous soluble and stable macromolecular β-sheet structure [4]. The first step in designing a conformationally defined SCL relies on a detailed characterization of the structural motif of interest in order to determine the substitutability and stability of the motif. A set of 25 KAK peptide analogs was designed to study the number of alanine residues necessary to obtain the hydrophobic packing that constitutes the core of the KAK complex. As determined by RP-HPLC and CD, the formation of a β-sheet conformation was observed for the analogs having a minimum of 10 alanine residues (Figure 1A).

In order to study the role of the lysine residues in the complex formation, different substitution and/or insertion analogs at both termini were synthesized and analyzed. The zwitterionic (Ac-$KEA_{13}KE$-NH_2) and negatively charged (Ac-$EA_{13}E$-NH_2) analogs of KAK did not alter the β-sheet complex formation ability, while, on the other hand, no complex was formed with the analog having 2 lysines at each terminus (Ac-$K_2A_{13}K_2$-NH_2) (Figure1B).

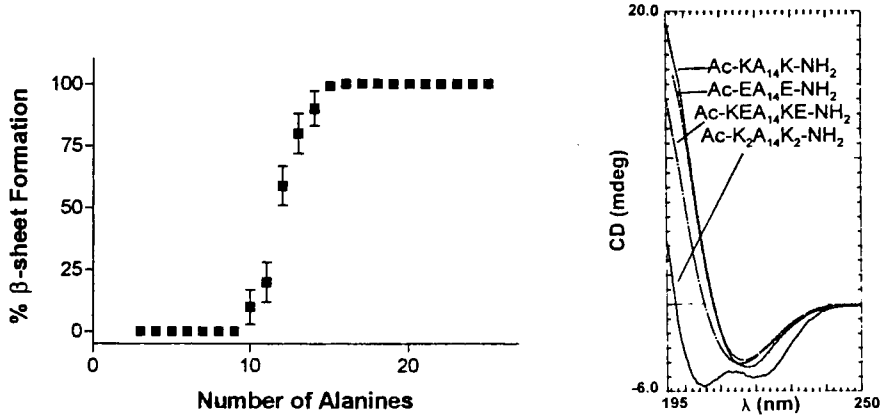

Figure 1. *A. Number of alanine residues necessary for β-sheet complex formation. The % β-sheet was based on RP-HPLC peak area.* ***B.*** *Effect of charged amino acids at both terminus on β-sheet complex formation. The CD spectra were recorded in 5mM MOPS buffer, pH 7, at 25°C.*

Based on these results and on initial binding studies showing that the KAK complex is able to bind to a variety of molecules through electrostatic and hydrophobic interactions, a number of β-sheet SCLs can be envisioned. For instance, mixture positions can be inserted near the termini in order to modulate the compactness of the complex, and hence its binding ability. Furthermore, the β-sheet complex can also be used as a scaffold in order to functionalize it with carboxylic acids, sulfonyl chlorides, isocyanates, and chloroformates, *etc.*, on its hydrophilic surface. We believe that β-sheet SCLs will be useful for the studies of β-sheet formation and to determine the role of hydrophobic cores in naturally occurring proteins, as well as in studies investigating protein/ligand interactions such as protein transport, heme groups binding, and binding-step mimic catalysis.

Acknowledgments

This work was funded in part by National Institutes of Health grant GM 45583 and Houghten Pharmaceuticals Inc., San Diego, CA.

References

1. Pinilla, C., Appel, J., Blondelle, S.E., Dooley, C., Dörner, B., Eichler, J., Ostresh, J. and Houghten, R.A., *Biopolymers (Peptide Science)*, 37 (1995) 221.
2. Blondelle, S.E., Pérez-Payá, E., Dooley, C.T., Pinilla, C. and Houghten, R.A., *Trends Anal. Chem.*, 14 (1995) 83.
3. Blondelle, S.E., Takahashi, E., Houghten, R.A. and Pérez-Payá, E., in Maia, H.L.S. (Ed.), 'Peptides 1994', ESCOM, Leiden, The Netherlands, 1995, p.85.
4. Forood, B., Pérez-Payá, E., Houghten, R.A.and Blondelle, S.E., *Biochem. Biophys. Res. Comm.*, 211 (1995) 7.

Peptides: Chemistry, Structure and Biology
Pravin T.P. Kaumaya and Robert S. Hodges (Eds.)
Mayflower Scientific Ltd., 1996

116
Generation of Consensus Pharmacophore Models from a Library of Constrained Peptides

M. Hassan, A.T. Hagler and R.S. Struthers

Biosym Technologies, Inc. 9685 Scranton Road, San Diego, CA 92121, USA

Introduction

The binding conformation of a biologically active peptide provides a structural basis for design of peptide analogs or peptidomimetics, as well as for screening of organic compound libraries. Strategies to determine the binding conformation have focused on the synthesis and conformational analysis (by molecular modeling and/or NMR spectroscopy) of cyclic or other constrained peptide analogs. Recently, the technique of consensus dynamics has been introduced in which a series of compounds are simulated simultaneously subject to a constraining potential which holds equivalent functional groups together in space [1]. Thus, only regions of the conformational hypersurface which are commonly accessible to the series are visited during the searching procedures. In the ideal case, as the number and diversity of the compounds in the consensus ensemble increases, the number of possible solutions should decrease until a small number of pharmacophore models emerge.

Results and Discussion

We applied the consensus strategy to 23 peptide antagonists of the hypothalamic decapeptide, gonadotrophin-releasing hormone, GnRH. This series of constrained peptides, which includes monocyclic (1-10, 4-10, 5-8, 2-7 and 3-8) and bicyclic (5-8/4-10, 1-5/4-10 and 1-8/4-10) analogs with rings of varying sizes, provides one of the most extensive and diverse ensembles of constrained ligands for a peptide receptor, and so should be ideal for testing the consensus strategy. Starting conformations for the GnRH analogs were obtained by model building. Conformational information from previous studies of some of the analogs [2-5] was also used to build initial conformations. In the consensus simulations, the intermolecular interactions between molecules are turned off, and sets of corresponding equivalent functional groups (which define putative pharmacophore elements) are tethered together by a quadratic function that is added to the force field. Annealed consensus conformations for the ensemble were obtained by taking snapshots from high-temperature molecular dynamics trajectories, each starting from randomized conformations of the individual ensemble members, and quenching them by gradually lowering the temperature to 300K followed by energy minimization.

Homologous functional groups were defined based on selected side chain heavy atoms for residues in positions 1, 2, 3, 5, 6, 7, 8 and 9. Two different sets of consensus restraints were used, differing only in the treatment of the arginine residues. In the first

set, "independent arginines model", arginine residues at positions 5, 6, and 8 were treated as independent groups, *i.e.* a different consensus group was defined for each position. In the second set, "one-site arginines model", arginine residues from the three positions were grouped into only one consensus set, defining a pharmacophore model with a specific site for a guanidinium group. Distance restraints from experimental nmr data [2-5] were also included for four of the molecules in the simulations with the "one-site arginine model" consensus restraints.

Multiple families of pharmacophore models were found that satisfy the consensus restraints. Centroids for each of the pharmacophore groups were defined by calculating the average positions of pseudoatoms that represent each group for all consensus conformations. The resolution of the position of each centroid was calculated as the rms deviation of individual pharmacophore models from the centroid position. The results are illustrated in Table 1, which shows that the resolution in the position of pharmacophore groups ranges between 2 and 6 Å. The definition of one site for the arginine residues and the inclusion of nmr restraints helped improve the resolution of the final models.

Table 1. *Centroid positions and resolution of pharmacophore groups (in angstroms).*

		independent arginines model				one-site arginines model			
residues	position	x	y	z	res.	x	y	z	res.
Δ^3Pro	1	-0.32	5.11	0.28	2.84	-1.35	4.94	-0.76	3.60
D-2Nal	1	-1.37	3.64	-2.87	6.13	-1.46	6.52	-1.73	6.38
D-pClPhe	2	-5.42	5.45	2.78	3.42	-6.47	4.89	2.02	4.04
D-Trp, D-Pal	3	-2.00	1.54	7.00	3.14	-1.93	2.02	4.57	5.40
Tyr	5	-2.47	-6.83	1.59	3.30	-1.68	-3.67	2.32	4.75
D-Trp, D-2Nal	6	0.49	-8.18	-0.38	3.38	1.36	-6.04	1.68	4.12
Leu	7	7.06	-4.83	-0.84	2.60	6.36	-4.92	-2.12	3.66
Pro	9	5.31	1.36	-3.13	2.18	6.01	1.28	-2.98	3.23
Arg	(5, 6, 8)	-0.00	-0.66	-1.81	3.52	-	-	-	-
Arg	5	-	-	-	-	-3.90	-2.17	1.60	4.43
Arg	6	-	-	-	-	0.55	-2.06	0.41	5.41
Arg	8	-	-	-	-	2.52	-0.79	-5.00	4.60

References

1. McDowell R.S., Gadek T.R., Barker, P.L., Burdick, D.J., Chan, K.S., Quan, C.L., Skelton, N., Struble, M., Thorsett, E.D., Tischler, M., Tom, J.Y., Webb, T.R. and Burnier, J.P., *J. Amer. Chem. Soc.*, 116 (1994) 5069.
2. Baniak, E.L., Rivier, J.E., Struthers, R.S., Hagler, A.T., Gierasch, L.M., *Biochemistry*, 26 (1987) 2642.
3. Rizo, J., Koerber, S.C., Bienstock, R.J., Rivier, J.E., Hagler, A.T., Gierasch, L.M., *J. Amer. Chem. Soc.*, 114 (1992) 2852.
4. Rizo, J., Koerber, S.C., Bienstock, R.J., Rivier, J.E., Gierasch, L.M., Hagler, A.T., *J. Amer. Chem. Soc.*, 114 (1992) 2860.
5. Bienstock, R.J., Rizo, J., Koerber, S.C., Rivier, J.E., Hagler, A.T., Gierasch, L.M., *J. Med. Chem.*, 36 (1993) 3265.

Peptides: Chemistry, Structure and Biology
Pravin T.P. Kaumaya and Robert S. Hodges (Eds.)
Mayflower Scientific Ltd., 1996

117
Development of β-Lactam Peptides for Elastase Inhibition in Cystic Fibrosis

A. Lavoie[1], A.M. Cantin[2] and E. Escher[1]

[1]Department of Pharmacology and [2]Department of Medicine, Pulmonary Division, Faculty of Medicine, Universitéde Sherbrooke, Sherbrooke, Québec, J1H 5N4, Canada

Introduction

Human neutrophil elastase (HLE) is a major pathogenic factor in the pulmonary morbidity of cystic fibrosis. Neutrophils are attracted by pulmonary infection and the secreted HLE degrades pulmonary tissue. HLE inhibitors applied by aerosol in combination with antibiotics could become a supportive treatment. Some β-lactam antibiotics are HLE inhibitors and we undertook screening peptide libraries around 6-aminopenicillanic acid (Apa) for potent peptide inhibitors. Libraries are a tool of choice for producing and screening large numbers of potentially active compounds [1]. General screening methods and synthetic procedures exclude, however, the assessment of by-products formed through normally "unwanted" side-reactions and thus, forego many potentially interesting compounds. The present study reveals the presence of highly active HLE inhibitors that were formed not among the regular products but from the normally "unwanted" side-reactions.

Results and Discussion

Library synthesis of the type Aaa_1-Apa-Aaa_3 was carried out by Boc-benzyl strategy. Libraries and individual peptides were HLE assayed [2] after cleavage and lyophilization on the theoretical peptide content for screening purposes. Individual peptides were assembled either by a Fmoc scheme using a trityl-resin link [3] or by classical Boc-benzyl chemistry, using AcTrp as a scavenger during TFA cleavages. Single-well analysis of the Aaa_1-coupled sublibraries single out Val, His, Lys, and revealed Trp as best Aaa_1. Single-well synthesis of Val-Apa-Aaa_3 revealed Trp as the best Aaa_3 and repetition of permutation in Aaa_1 on Aaa_1-Apa-Trp with the four best amino acids revealed highest HLE inhibition for the Trp-Apa-Trp sequence (K_i=2μM). Repetitive C-terminal library extension produced the highest activity for the sequence Trp-Apa-Trp-Trp-Trp (K_i=0,2μM). Bulk synthesis of Trp-Apa-Trp-Trp-Trp by Fmoc procedures produced a crude product with a K_i of only 20 μM in the HLE assay. A parallel bulk synthesis by the Boc-benzyl scheme of the same sequence produced the initially observed K_i of 0.2 μM. Purification of both products followed by FAB-MS analysis of the pure fraction showed that in both synthesis Apa was not incorporated

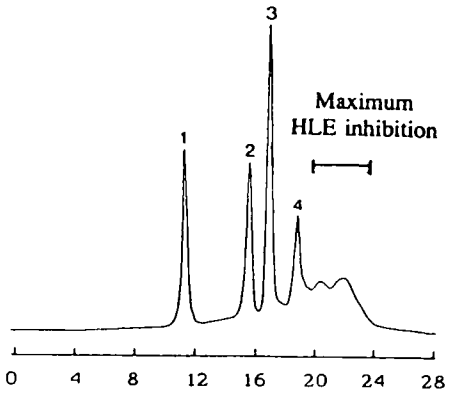

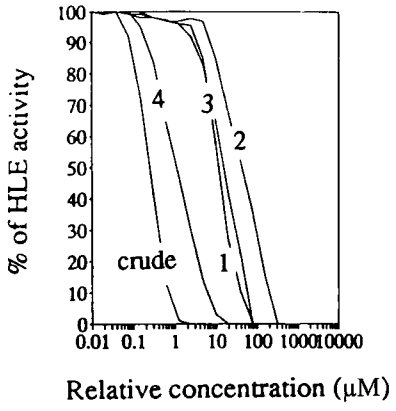

Figure 1 (left). *HPLC elution profile of crude $(Trp)_4$ obtained by Boc/TFA chemistry.*
Figure 2 (right). *HLE inhibition by crude Boc/TFA synthesized $(Trp)_4$ and by 1-4 from Figure 1.*

during the synthesis, although completion of coupling was verified by the ninhydrin test. HLE inhibition after HPLC elution showed the highest activity to be associated to the late fraction (Figure 1). Fraction 3 was Trp-Trp-Trp-Trp (MH^+ 763), fraction 4 was mono (t-butyl)Trp-Trp-Trp-Trp (MH^+ 819), and fraction 1 and 2 are still unidentified with MH^+ as 919 and 857, respectively. The t-butylated fraction had ten-fold higher inhibitory potency than Trp-Trp-Trp-Trp and the two unidentified fractions which are more hydrophilic are still ten-fold lower in activity than the crude product (Figure 2). The bulk of anti HLE activity was, however, associated to later elution times; those products are actually under investigation. It is reasonable to assume that those products are probably multi-butylated peptides and harbour significantly higher anti HLE potency than the already characterized products. In conclusion, we have shown that a reaction condition allowing side-reaction to occur can lead to products of modified peptide structure with much more potential than the unmodified sequence.

Acknowledgments

We thank M. Evans (University of Montreal) for the FAB-MS analysis, G. Bilodeau and M. Martel (University of Sherbrooke) for the HLE analysis and the Canadian Cystic Fibrosis Foundation for financial support.

References

1. Gallop, M.A., Barrett, R.W., Dower, W.J., Fodor, S.P.A., Gordon, E.M., *J. Med. Chem.*, 37 (1994) 1233.
2. Cantin, A.M., Lafrenaye, S., Bégin, R.O., *Pediatr.Pulmonol.*, 11 (1991) 249.
3. Barlos, K., Chatzi, O., Gatos, D. and Stavropoulos, G., *Intl. J. Pept. Protein Res.*, 37 (1991) 513.

Peptides: Chemistry, Structure and Biology
Pravin T.P. Kaumaya and Robert S. Hodges (Eds.)
Mayflower Scientific Ltd., 1996

118
Three Highly Constrained Tricyclic Peptide Libraries Containing Three Disulfide Bonds

C. Rao and J.P. Tam

Department of Microbiology and Immunology
Vanderbilt University, A5119 MCN, Nashville, TN 37232, USA

Introduction

Most structure-function studies of bioactive peptides focus on the development of small constrained peptide or peptide-like structures that have high potency and desirable pharmacokinetic properties. In our studies on peptides of the immune system and growth factors, we designed a series of small peptide templates containing three disulfide bonds for their use in peptide libraries (Figure 1). These peptide templates contain 12 amino acids, six of which are variables and the rest are cysteines for constraining the conformation. A limitation of this approach is the unrealistic number of analogs ($>15\times19^6$) being generated since each peptide analog contains 15 possible disulfide isomers in addition to the 19^6 from the peptide library. In this paper, we describe the methodological development for use in peptide libraries. This will include the strategy of disulfide-formation and the placement of conformation-directing amino acids (Pro and Gly) at key positions to give a manageable library and with high likelihood of obtaining a specific disulfide isomer.

Results and Discussion

Disulfide formation strategy. The strategy to obtain a specific disulfide pairing was studied on a naturally occurring toxin peptide known as Scratch Peptide **4** (SP) which has a sequence motif of template **3** and a disulfide pattern Cys 1-6, 2-4, 3-5 (Figure 1). Our strategy relied on a two-step disulfide formation [1, 2] by protecting two pairs of Cys with MeBzl (in Boc-chemistry) or Trt (in Fmoc-chemistry) and the third pair with Acm. In the first step, the S-MeBzl protecting group was released by HF while a pair of Cys remains protected by Acm. Thus, in the first step oxidation by DMSO [3], only three possible disulfide isomers were obtained during sulfur-sulfur oxidation and the number of disulfide isomers was reduced from 15 to 3. The formation of the third disulfide bond was effected by I_2 under acidic condition to minimize disulfide exchange.

By strategic placing of the Acm, a single disulfide isomer could be obtained. For example, protecting Cys^1 and Cys^{12} with Acm and forming the outermost pair of disulfide in the second step gave a predominant disulfide isomer **5** in 92% yield with Cys pairing of 1-6, 2-4, 3-5. However, by protecting the internal disulfide-pair, Cys^2 and Cys^8 with Acm, a different disulfide isomer in 95% yield corresponding to SP was obtained. Our

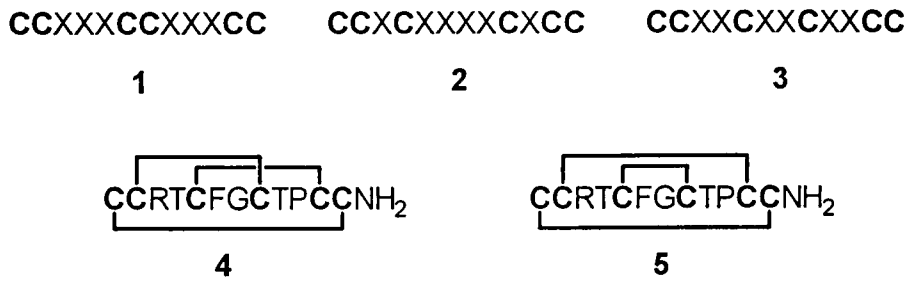

Figure 1. *Templates of small peptides containing six Cys or three disulfide bonds. Peptide 4 is Scratch peptide with Cys pairing 1-6, 2-4, 3-5.*

results suggested that by strategic Cys protection in the two-step disulfide formation, it may be possible to reduce 15 disulfide isomers to a major isomer so that a predominant tricyclic peptide with three disulfide bonds can be generated unambiguously.

Influence of conformational-directing amino acid. With a small tricyclic peptide, conformation-directing amino acids which frequently occur at reverse turns, would greatly influence the disulfide formation. In SP, there are two such amino acids: Gly^7 and Pro^{10}. To evaluate their importance in disulfide formation, we replaced $Gly^7 \rightarrow Ala^7$ in the two-step disulfide formation strategy of placing Acm at position 1 and 12. Our results showed that the major product (75%) from Ala^7 contained a disulfide pattern Cys 1-6, 2-4, 3-5 similar to SP but not the expected product with disulfide pattern Cys 1-6, 2-5, 3-4 of **5**. Two different dimers (25%) were also found.

On replacement of $Pro^{10} \rightarrow Ala^{10}$, the yield of expected disulfide isomer with Cys pairing 1-6, 2-5, 3-4 decreased from 92% to 78%. A minor product (22%) was also obtained. Replacement of Gly^7, $Pro^{10} \rightarrow$Ala resulted in three products with the major disulfide isomer in 56% yield corresponding to the Cys pairing of SP. These results indicate that Gly^7 and Pro^{10} are conformationally important and, in turn, affect the process of disulfide formation. Gly which lies in the interior of disulfide network is particularly sensitive to replacement and may be considered an invariable residue.

In conclusion, the combination of using a two-step disulfide formation scheme and the appropriate placement of Gly or Pro would yield the desired disulfide isomer to create a useful peptide library.

Acknowledgments

This work was in part supported by NIH grant CA35577, AI2870, and CA36544.

References

1. Spetzler, C.J., Rao C. and Tam, J.P., *Intl. J. Peptide Res.*, 43 (1994) 351.
2. Yang, Y., Sweeney, W.V., Chait, B.T. and Tam, J.P., *Protein Res.*, 3 (1994) 1267.
3. Tam, J.P., Wu, C.R., Liu, W. and Zhang J.W., *J. Am. Chem. Soc.*, 113 (1991) 6657.

Peptides: Chemistry, Structure and Biology
Pravin T.P. Kaumaya and Robert S. Hodges (Eds.)
Mayflower Scientific Ltd., 1996

119
Mapping of Antigenic Determinants with Large Random Expression Libraries and Small Random Synthetic Peptide Libraries: A Comparative Study

J.W. Slootstra, W.C. Puijk, G.J. Ligtvoet, J.P.M. Langeveld, W.M.M. Schaaper and R.H. Meloen

Department of Molecular Recognition, Institute for Animal Science and Health (ID-DLO), P.O. Box 65, 8200 AB Lelystad, The Netherlands

Introduction

In recent years, many epitopes have been successfully mapped using immunoscreening of large random peptide libraries composed of millions of different sequences [1]. Here this approach was compared with immunoscreening of small synthetic random peptide libraries containing 4550 random dodecapeptides and 8000 tripeptides, respectively. These small support-bound libraries were synthesized in newly developed 455-well credit-card format microtiter plates. In this way, the antibody reactivity of each of the 4550 dodecapeptides and each of the 8000 tripeptides could be determined. This set of data was used to identify consensus sequences which were compared with the sequences of the respective epitopes and were used to design epitope-mimicking peptides.

Three antibodies were studied; Mab 6A.A6 and Mab 57.9, which bind different epitopes on the spike protein-S of the transmissible gastroenteritis virus, and Mab 32F81 which binds a loop within an EGF-like domain part of the surface protein pfs25 of the malaria parasite *Plasmodium falciparum*. Lead sequences were compared with those from two random expression libraries each of *ca.* 10^7 hexa- and octapeptide sequences. Library construction and immunoscreening were as previously described [2, 3].

Results and Discussion

Lead sequences extracted from the expression libraries show a close resemblance to the linear sequence of the respective epitopes (Table 1). Most of the lead sequences identified using the synthetic peptide libraries contain sequences similar to small parts of the respective epitopes (Table 1). Recognition of sequences such as DKK and DKF by Mab 32F81 suggests that small peptides can also mimic conformational parts of antigenic determinants (see 'Model of 3D-structure of antigenic determinant' in Table 1). Thus, using small synthetic peptide libraries, epitopes can be (partially) mapped. In addition, consensus sequences, determined using the antibody reactivity of all 4550 dodeca-peptides and all 8000 tripeptides, were used to design epitope-mimicking peptides with similar antibody reactivity as lead sequences extracted from the expression libraries or peptides covering the respective antigenic determinants.

Table 1. *Lead sequences extracted from expression- and synthetic peptide libraries using Mabs 6A.A6, 57.9 and 32F81*[a].

Mab	Sequence of antigenic determinants	Expression hexa/octapeptide libraries	Synthetic dodecapeptide library	Synthetic tripeptide library
6A.A6	S R L P P N S D V V L G P I C P S N S E A N C G	S P N S E A * P A H S E A * P I N S E A * P S H S E A * P S N S E A * P S H S D H * G V N S E A *	P N G D P T N G P N N G D W P D P N L V W W K P N S D Q T K P N S C A M E F M S D I A A K D N S D I S N G V N S D I M W L E N S E M M R S D S M	X S D X S E I M W L Y L
57.9	S F F S Y G E I	Q P F S F G S L *	H T E F F S S C E R S F W V M A I K S F G A I A I D Q F Y S T A T M D F V V W S S T E Y M T N F F Q A N F N F P K D G N F N Q L I I W A P F P M M	D F F P F X P Y X F E X A F E X G D
32F81	L D T S N P V K T F D D T D P I K K C I F D D T D C V G K K I P *Model of 3D-structure of antigenic determinant*	S D T S D P T L K C N Y S D P V R K A D G S D P I R K	M K S F D T Y G K M F D T C V L P K F D P P A A I K F E Q S I C F D Y K T G S W D K F G D K I E I V V D K C N H W T D K K D G Y D K V E	X D K X E K X K D X K E K X E F X K

[a]Consensus sequences are boxed. A schematic representation of the putative three-dimensional structure of the loop within the EGF-like domain is shown (bold and boxed). *, taken from [2]; X, different residues allowed.

Acknowledgments

The authors acknowledge the contributions of D. Parohi and D. Kuperus. We thank Dr. A.P. van Nieuwstadt (Lelystad, The Netherlands) for a gift of Mab 57.9.

References

1. Scott, J.K. and Craig, L., *Current Opinion in Biotechnology*, 5 (1994) 40.
2. Lenstra, J.A., Erkens, J.H.F., Langeveld, J.G.A., Posthumus, W.P.A., Meloen, R.H., Gebauer, F., Correa, I., Enjuanes, L. and Stanley, K., *J. Immunol. Methods*, 152 (1992) 149.
3. Geysen, H.M., Meloen, R.H. and Barteling, S.J., *Proc. Natl. Acad. Sci. USA*, 81 (1984) 3998.

Peptides: Chemistry, Structure and Biology
Pravin T.P. Kaumaya and Robert S. Hodges (Eds.)
Mayflower Scientific Ltd., 1996

120
Use of Synthetic Combinatorial Libraries to Identify Peptide Inhibitors of Ca^{2+}-complexed Calmodulin

E. Pérez-Payá[1,2], E. Takahashi[1], I. Mingarro[2], R.A. Houghten[1] and S.E. Blondelle[1]

[1]Torrey Pines Institute for Molecular Studies, 3550 General Atomic Court, San Diego, CA 92121, USA
[2]Departament de Bioquímica i Biologia Molecular, Universitat de València, E-46100 Burjassot, València, Spain

Introduction

Regulation of biological processes by calcium ion involves interactions with high-affinity calcium-binding proteins. One such protein is calmodulin, which has been referred to as an activator and modulator protein [1]. The complex calcium-calmodulin controls the biological activity of more than 30 different proteins, including several enzymes, ion transporters, receptors, motor proteins, and transcription factors in eukaryotic cells. Since calmodulin plays a fundamental role in cell biology, agents that specifically inhibit its action should have important pharmacological impact.

The synthetic combinatorial library (SCL) approach [2] has been used to rapidly identify sequences having the ability to modulate calmodulin activity. We have initiated the search for such calmodulin modulators through the screening of an all D-amino acid peptide library in a positional scanning format (PS-SCL) [3].

Results and Discussion

The PS-SCL used for this study consisted of hexamer peptide mixtures composed entirely of D-amino acids, having an acetylated N-terminus and an amidated C-terminus. This library is composed of six individual positional SCLs represented by the formulae: Ac-$o_1$xxxxx-NH_2, Ac-x$o_2$xxxx-NH_2, Ac-xx$o_3$xxx-NH_2, Ac-xxx$o_4$xx-NH_2, Ac-xxxxo_5x-NH_2, and Ac-xxxxxo_6-NH_2 (o:defined by one of 20 D-amino acids; x:close to equimolar mixture of 19 D-amino acids, cysteine omitted). The entire library is thus composed of 120 (20 x 6) peptide mixtures, each peptide mixture containing 2,476,099 (19^5) individual hexapeptides. Each peptide mixture was initially assayed at a final concentration of 2mg/ml for calmodulin inhibition using a Ca^{2+}-dependent phosphodiesterase assay [4]. Such an assay utilizes the ability of calmodulin to stimulate the activity of phosphodiesterase 3':5'-cyclic nucleotide.

The data derived from each positional SCL yields information about the relative importance of each amino acid at every position which is then used to prepare individual sequences. Thus, D-Leu was selected at position 1, D-Gln and D-Trp at position 2, D-Ile

Table 1. *Calmodulin inhibitors derived from PS-SCL.*

Peptide sequence	IC_{50} (μM)
Ac-lqrihw-NH_2	23
Ac-lqiihw-NH_2	22
Ac-lqihhr-NH_2	21
Ac-lwrilw-NH_2	5
Ac-lqrihr-NH_2	6
Ac-lwrihr-NH_2	8
Ac-lwrhlw-NH_2	7
Ac-lwiilr-NH_2	8
Ac-lwiihw-NH_2	11
Ac-lwihhw-NH_2	21
Commercially available calmodulin inhibitors	
N-(6-aminohexyl)-5-chloro-1-naphthalenesulfonamide (W-7)	58
N-(4-aminobutyl)-5-chloro-2-naphthalenesulfonamide (W-13)	64
Trifluoperazine	8

and D-Arg at position 3, D-His and D-Ile at position 4, D-His and D-Leu at position 5, and D-Arg and D-Trp at position 6. A total of 32 individual peptides, which represent all possible combinations of these selected amino acids (1x2x2x2x2x2=32) were then synthesized, characterized by mass spectral analyses and RP-HPLC, and assayed for calmodulin inhibition (selected sequences shown in Table 1).

We have demonstrated the feasibility of identifying short all D-amino acid peptides from a PS-SCL made up of 52 million D-amino acid peptides that bind to and inhibit the biological properties of Ca^{2+}-complexed calmodulin. Although the possibility that the calmodulin inhibiting peptides identified bind to other proteins or lipids cannot be excluded at this time, our results suggest a potentially useful approach to synthesize non- or slowly hydrolyzable intracellular inhibitors of calmodulin.

Acknowledgments

This work was funded in part by Houghten Pharmaceuticals, Inc., San Diego, California, USA, and by the Spanish Ministry of Science and Education, postdoctoral fellowship to E.P.P. and short-term fellowship to I.M.

References

1. Anderson, S. and Malencik, D. in Cheung, W.Y. (Ed.), 'Calcium and Cell Functions', Academic Press, New York, 1986, Vol. 6, p.1.
2. Houghten, R.A., Pinilla, C., Blondelle, S.E., Appel, J.R., Dooley, C.T. and Cuervo, J.H., *Nature*, 354 (1991) 84.
3. Pinilla, C., Appel, J.R., Blanc, P. and Houghten, R.A., *BioTechniques*, 13 (1992) 901.
4. Sharma, R.K. and Wang, J.H. in Brooker, G., Greengard, P. and Robison G.A. (Eds.), Advances in Cyclic Nucleotide Research, Raven Press, New York, 1979, Vol.10, p.187.

Peptides: Chemistry, Structure and Biology
Pravin T.P. Kaumaya and Robert S. Hodges (Eds.)
Mayflower Scientific Ltd., 1996

121
Synthetic Peptide-, Peptoid- and Oligocarbamate-Libraries Investigated for Binding to MHC I Proteins

K.-H. Wiesmüller[1], B. Teufel[1], R. Brock[1], J. Früchtel[3], R. Warrass[1], G. Jung[1,3] and P. Walden[2]

[1] *NMI, Naturwissenschaftliches und Medizinisches Institut an der Universität Tübingen, D-72762 Reutlingen,Germany*
[2] *Max-Planck-Institut für Biologie, D-72076 Tübingen, Germany*
[3] *Institut für Organische Chemie, Universität Tübingen, D-72076 Tübingen, Germany*

Introduction

Peptide binding is essential for a stable conformation of MHC class I proteins. The synthetic random octapeptide library X_8 and OX_7 sublibraries were prepared in the positional scanning format [1] from L-amino acids and were successfully used to investigate the structural basis for peptide selection by MHC molecules [2]. The qualities of the library preparation were confirmed by electrospray mass spectrometry, pool sequencing, and amino acid analysis [3]. To identify unnatural MHC ligands, sublibraries made from D-amino acids and glycine (ox_7), randomly generated peptoids and oligocarbamates were investigated for MHC binding and induction of target cell lysis by cytotoxic T-cells.

Results and Discussion

Peptide libraries were prepared with a robotic workstation (Syro, MultiSynTech, Bochum, Germany) using Fmoc-D-Pro-2-chlorotrityl resin and 18 Fmoc-D-amino acid-*p*-benzyloxybenzyl alcohol-polystyrene resins and Fmoc-Gly-resin or an equimolar mixture of these 20 resins. Couplings were carried out by DIC/HOBt either with an equimolar mixture of 19 Fmoc-D-aa and Fmoc-Gly equimolar to the resin loading (position mixed), or with a 5-fold excess of Fmoc-aa (position defined). The procedure is characterized by extended coupling times (4.5 h) and initially high content of DCM in the reaction mixture which evaporates during coupling. The peptides were cleaved off the resin (TFA, 5% scavenger) and precipitated from n-heptane:ether (1:1) at -20°C. Close to equimolar representation of individual peptides in the mixtures was found by ES-MS analysis [3].

Automated solid-phase synthesis of oligocarbamates [4] was carried out on Rink-amide-MBHA resin. Fmoc-amino alcohols [5] were prepared from the corresponding Fmoc-amino acid (D,G,H,K,L,N,P,R,S) pentafluorophenyl esters by reduction with $NaBH_4$. Dibenzotriazolylcarbonate [6] and pyridine (5 equiv.) were used for preparing activated carbonates (15 min, 30°C) from these Fmoc-amino alcohols (0.2 M

Table 1. *Octapeptides binding to MHC defined by screening with ox_7 libraries.*

Sequence	mfi (66 μM)	Sequence	mfi (66 μM)
darfaaGs	78	dlrfanGs	25
darGapGs	49	dlrGapGs	23
daraaaas	40	dlrfapGs	19
dcrFaaGs	31	xxxxxxxx	22
dcrGaaGs	23	SIINFEKL	103

mfi: mean fluorescence intensities. The levels of cell surface expression were analyzed by flow cytometry using a FACScan. Linear fluorescence values were averaged.

in DMF). Couplings were carried out in 5-fold excess of activated monomer in DMF for 6 hr. Fmoc deprotection (piperidine/DMF) and cleavage from the resin yielded crude oligocarbamates (purity > 50 %). Peptoids were synthesized according to the sub-monomer method [7]. Couplings of bromoacetic acid on Rink amide resins were performed with DIC. Key side chains for MHC binding were introduced by substitution with benzylamine and isobutylamine to mimic anchor amino acids (F, L) of the natural epitope SIINFEKL.

Oligocarbamates $X_1^cX_2^cF^cX_3^cA$ (X_1^c: S^c, D^c, N^c, F^c; X_2^c: D^c, G^c, K^c, N^c; X_3^c: G^c, K^c, L^c, N^c, R^c, P^c) and peptoids which imitate the natural epitope *(e.g.*, Gly-Nile-Nile-Nabu-Nphe-Nabu-Nleu) were investigated for the stabilization of MHC class I molecules on RMA-S cells. Some of the oligocarbamates showed MHC stabilizing properties in μM concentrations; the best stabilizing ligand was $N^cN^cF^cL^cA$. The peptoids had no biological activity.

All D-aa-peptide sublibraries (ox_7) were used for incubation of RMA-S cells to identify aa which support MHC binding. The stabilizing effects were compared in relation to the corresponding natural ligand SIINFEKL. The amino acid residues (o) of the most prominent MHC stabilizing ox_7 peptide libraries were: d (position 1); a, l, c (P2); r (P3); a, G, f (P4); a (P5); a, p (P6); G (P7); s (P8). Individual peptides were synthesized (Table 1) which represent combinations of amino acids identified with the peptide mixtures. The best stabilizing peptide (darfaaGs) was about 100-fold less active than the natural ligand SIINFEKL.

References

1. Houghten, R.A., *Gene*, 137 (1993) 7.
2. Udaka, K., Wiesmüller, K.-H., Kienle, S., Jung, G., Walden, P., *J. Exp. Med.*, 1995, in press.
3. Metzger, J.W., Stevanovic, S., Brünjes, J., Wiesmüller, K.-H., Jung, G., *Methods*, 6 (1994) 425.
4. Cho, C.Y., Moran, J., Cherry, S.R., Stephans, J.C., Fodor, S.P.A., Adams, C.L., Sundarm, A., Jacobs, J.W., Schultz, P.G., *Science*, 261 (1993) 1303.
5. Kisfaludy, L., Roberts, J.E., Johnson, R.H., Mayers, G.L., Kovacs, J., *J. Org. Chem.*, 35 (1970) 3563.
6. Takeda, L., Ogura, H., *Synth. Commun.*, 12 (1982) 213.
7. Zuckermann, R.N., Kerr, J., Kent, S.B.H., Moos, W., *J. Am. Chem. Soc.*, 114 (1992) 10646.

Peptides: Chemistry, Structure and Biology
Pravin T.P. Kaumaya and Robert S. Hodges (Eds.)
Mayflower Scientific Ltd., 1996

122
Use of Solid Phase Mitsunobu and Wittig Reactions for Construction of Peptide and Non-peptide Libraries

V. Krchňák[1], J. Vágner[2], Z. Flegelová[1], A.S. Weichsel[1], G. Barany[2] and M. Lebl[1]

[1]*Selectide Corporation, 1580 E. Hanley Blvd., Tucson, AZ 85737, USA*
[2]*Department of Chemistry, University of Minnesota, Minneapolis, MN 55455, USA*

Introduction

To increase the structural diversity of combinatorial libraries, we have extended the repertoire of organic reactions that can be performed in the solid phase mode, and used these reactions for the design and synthesis of peptide and non-peptide libraries. Polymer-supported chemistries include formation of ethers by the Mitsunobu reaction [1], and carbon-carbon bond formation by the Wittig reaction [2]. These solid-phase reactions can be used individually or in tandem, and combined with standard reactions for solid phase amide bond formation, to access an array of organic structures.

Results and Discussion

We selected Mitsunobu ether formation as a suitable reaction for combinatorial chemistry based on several criteria: (i) yields and purities of products; (ii) variety of available building blocks; (iii) compatibility with other chemistries; and (iv) "user friendly" reaction conditions. Out of two possible etherification modes we have studied the reaction of polymer-supported phenol with alcohol in solution. Model reactions (Figure 1) were carried out with N-acetylated tyrosine esterified to a graft copolymer, poly(ethylene glycol)-polystyrene-1% divinylbenzene, TentaGel S OH (TG). A typical procedure involved prewash of Ac-Tyr-O-TG with dry THF, followed by slurrying of the resin with a THF solution of PPh_3 and alcohol, chilling the slurry, and initiation of the reaction by addition of diethyl azodicarboxylate (DEAD). Products were cleaved from the resin by alkaline hydrolysis and analyzed by MS, HPLC, and NMR.

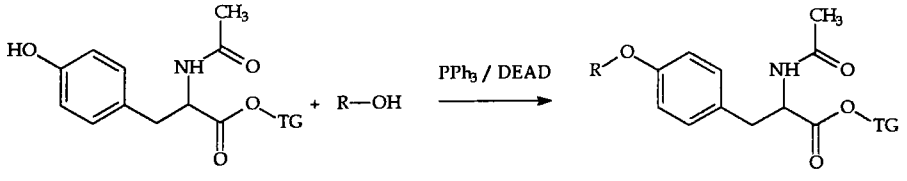

Figure 1. *Reaction scheme for polymer-supported Mitsunobu etherification.*

Figure 2. *Reaction scheme for polymer-supported Wittig reaction.*

Polymer-supported Mitsunobu ether formation can be applied in the design and synthesis of combinatorial libraries in many different ways. We incorporated this reaction into the one-bead-one-compound combinatorial library strategy [3], using the split-mix method for synthesis. Our model library involved three randomization steps: (i) N-protected amino acid attachment to the polymeric support *via* ester linkage, (ii) coupling of aromatic hydroxy acids, and (iii) Mitsunobu ether formation using a set of alcohols.

Polymer-supported carbon-carbon bond formation was performed by the Wittig reaction (Figure 2). We used TentaGel-NH_2 resin functionalized with acidolyzable handles (*e.g.*, PAL) and a chromophoric marker (*e.g.*, *p*-nitro-Phe). Carbonyl functions were introduced in three different ways: (i) oxidation of alcohols; (ii) deprotection of acetals; and (iii) direct coupling of carboxy aldehydes and ketones.

Different carbonyl functionalities were treated with ylides to form alkenes. Stabilized phosphoranes quantitatively transformed aliphatic and aromatic aldehydes to provide E-alkenes, as verified by NMR and HPLC analyses of products released by acidolysis. However, these reactions did not occur when ketone substrates were used in place of aldehydes.

Ylides derived from more reactive phosphonates smoothly transformed aldehydes to alkenes. When triethyl phosphonoacetate was used, E-alkenes formed predominantly. Polymer-supported ketones reacted sluggishly, at first, but conversion was achieved by addition of a strong base: DBU (in the presence of LiBr) or potassium hexamethyl-disilazane. To avoid base-catalyzed side reactions, application of a tertiary amine (*e.g.*, DIEA in the presence of LiBr) represented a good compromise for successful reactions of sensitive substrates.

References

1. Mitsunobu, O., *Synthesis*, (1981) 1.
2. Wittig, G. and Schollkopf, U., *Chem. Ber.*, 87 (1954) 1318; Horner, L., Hoffman, H.G., Wippel, H.G. and Klahre, G., *Chem. Ber.*, 92 (1959) 2499; Wadsworth, W.S. and Emmons, W.D., *J. Am. Chem. Soc.*, 83 (1961) 1733.
3. Lam, K.S., Salmon, S.E., Hersh, E.M., Hruby, V.J., Kazmierski, W.M. and Knapp, R.J., *Nature*, 354 (1991) 82

Peptides: Chemistry, Structure and Biology
Pravin T.P. Kaumaya and Robert S. Hodges (Eds.)
Mayflower Scientific Ltd., 1996

123
Development of a Synthetic Peptide Based Immunoassay for Hepatitis B Surface Antigen

J.M. Carter, K. Mansfield, R. Zizza and V. Lee-Own

Cytogen, 307 College Road East, Princeton, NJ 08540, USA

Introduction

Phage displayed libraries of random peptides are particularly well-suited for discovery of new leads when only functional information is available for a receptor. Their vast complexity, compared to most chemical synthetic libraries, expedites screening. In addition, their replicatable genome facilitates recovery of structural information from the screening assay. Furthermore, their hardiness and intrinsic mass amplification affords their use in panning procedures for sequential enrichment of binding populations [1].

Adequate assays exist, in the form of sandwich ELISAs, for detection of HBsAg in human sera. However, we have used this well-studied antibody-antigen (Ab-Ag) system as a model to analyze our phage libraries and to assess the feasibility of a new type of peptide immunoassay based on enzyme multiplied immunoassay technology (EMIT) [2].

Results and Discussion

We used several libraries of random peptides expressed in M13 bacteriophage. These included peptides of various lengths, some constrained *via* cystine disulfide loops of defined size. Characterization of these libraries indicated high complexity, of the order of 10^8.

From commercial sources, we obtained several antibodies (Ab), both monoclonals (MAb) and polyclonals (PAb), which are reactive with the hepatitis B virus surface antigen (HBsAg). We immobilized these Ab on plastic culture dishes, and then panned for binding phage from our libraries, eluting the phage with acid [3].

The sequence of the peptide displayed by each Ab-binding phage was deduced from its DNA sequence. For each Ab, examination of sequences of binding peptides indicated a clear motif. We prepared synthetic peptides for further study according to these consensus sequences. Because of space limitation, further discussion in this manuscript will be limited to results obtained with one PAb and its epitope.

ELISAs using N-alpha biotinylated peptides as antigens confirmed identity of the epitope and specificity of Ab binding. Furthermore, such immobilized synthetic peptides competed with soluble HBsAg for binding to Ab (Figure 1A). We noted that this epitope comprises a cyclic peptide in the native protein, and we found it only in cyclized form in our libraries. Cyclization was essential for Ab binding in ELISA; linear homologs were inactive. By testing peptides comprising point mutations, we also determined that Asp^6

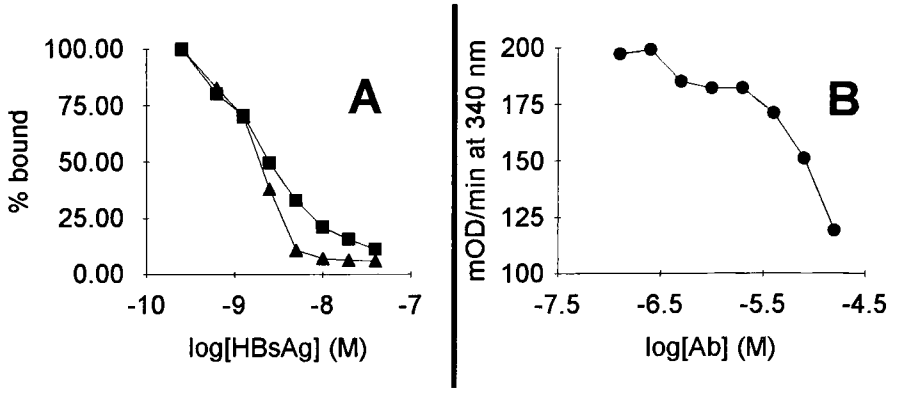

Figure 1. *A: Competition ELISA - soluble HBsAg as competitor with PAb binding to plated Hep1 (triangles) and HBsAg (squares). B: Enzyme inhibition assay - PAb and G6PdeH/Hep1 conjugate (circles). Hep1 = CTKPSDGNC (cyclic disulfide).*

was absolutely necessary for Ab binding, while Lys^3 could be replaced by Arg with no loss in activity.

Conjugation of the enzyme glucose-6-phosphate dehydrogenase (G6PdeH) was performed in the presence of excess NADH and glucose-6-phosphate. In an enzyme assay, the PAb inhibited the activity of this conjugate in a concentration dependent fashion (Figure 1B). However, after extended storage of the conjugate at 4°C, a loss in this specific inhibition was observed. Gel filtration on FPLC indicated almost quantitative release of peptide from the enzyme. Consequently, our latest efforts are directed toward substitution of a more stable chemistry for the peptide-enzyme conjugation.

Acknowledgments

For construction of the phage libraries we very gratefully acknowledge the diligent and skillful efforts of Nils Adey. For DNA sequencing, we acknowledge the technical expertise of Dom Spinella.

References

1. Hoess, R.H., *Current Opin. Struct. Biol.*, 3 (1993) 572.
2. Rubenstein, K.E., Schneider, R.S. and Ullman, E.F., *Biophys. Biochem Res. Comm.*, 47 (1971) 846.
3. Parmley, S.F. and Smith, G.P., *Gene*, 73 (1988) 305.

Peptides: Chemistry, Structure and Biology
Pravin T.P. Kaumaya and Robert S. Hodges (Eds.)
Mayflower Scientific Ltd., 1996

124
Matrix-assisted Laser Desorption Ionization for Rapid Determination of the Sequences of Biologically Active Compounds Isolated from Support-bound Combinatorial Libraries

R.S. Youngquist, G.R. Fuentes, C.M. Miller, G.M. Ridder, M.P. Lacey and T. Keough

The Procter and Gamble Co., Miami Valley Laboratories, P.O. Box 538707, Cincinnati, OH 45253, USA

Introduction

In the study reported here, we have extended our previously reported [1, 2] method for MALDI sequencing of biologically active molecules isolated from support-bound libraries. We have optimized the synthesis and sample handling to facilitate the use of small resin beads (17 μm) and have automated the screening and sorting processes with flow cytometry.

Results and Discussion

Initially, library screening and sorting was done manually, but there were several problems associated with manual sorting. First, the enzymes used for staining require specific conditions (pH = 9) that are different from our screening conditions and this can affect target protein binding. It is also difficult to distinguish varying levels of staining which makes it hard to pick only the darkest beads. Finally, manual isolation of the positive beads is slow and tedious.

To avoid these problems, we automated the screening and sorting process with flow cytometry. As an initial test, a small library containing multiple copies of 128 members was analyzed to see if flow cytometry could successfully isolate the known high affinity ligand (Ac-HPQFx) to streptavidin. The flow cytometry screening and sorting results are given in Figure 1, and several peaks (B,C,D and E) having varying fluorescence intensity are seen in the positive region. The beads associated with the highest fluorescence intensity, peak E, contained the expected recognition sequence. All 10 of the beads that were sequenced from peak E contained Ac-HPQFF. This sequence was not detected in any of the other peaks. The large peak associated with inactive peptides, peak A, showed random sequences having no homology. The observed intensity of peak E, 0.7%, agreed well with the calculated relative abundance of Ac-HPQFF in the small library (0.8%).

Larger libraries consisting of more than a few thousand members will have an extremely low percentage of actives. With these libraries, it is necessary to perform a

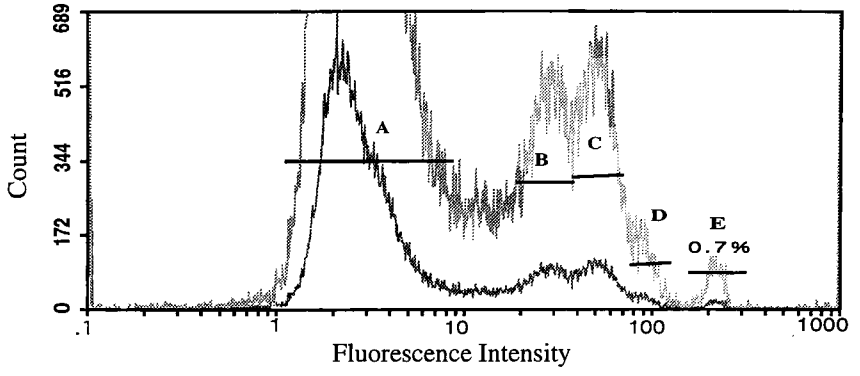

Figure 1. Flow cytometry analysis of high affinity ligand Ac-HPQFx to Streptavidin.

two-pass sort. The first pass sort enriches the sample in positive beads while eliminating negatives. The sorted beads from each library are then run back through the flow cytometer and sorted a second time. The highest fluorescence beads from the target library sorts are then collected for subsequent sequencing with MALDI. With this approach, a library containing over 60,000 members was successfully screened against an anti-gp120 antibody, and the correct high affinity ligands were isolated. We are currently extending automated flow cytometry screening and sorting to libraries containing more than one million members.

Termination synthesis with MALDI sequencing is a very general method. Since it is not degradative, it is compatible with libraries of any compounds that can be prepared in a stepwise synthesis. For instance, it can be used with libraries of poly-*N*-substituted glycines, oligocarbamates, or nucleic acid analogs as well as libraries that combine several different monomers. Even monomers of identical mass, such as geometric or stereoisomers, can be easily distinguished [2]. An example of non-peptide sequencing with termination synthesis/MALDI can be found in our previous study of methylphosphonate oligonucleotides [3].

References

1. Youngquist, R.S., Fuentes, G.R., Lacey, M.P. and Keough, T., *Rapid Commun. Mass Spectrom.*, 8 (1994) 77.
2. Youngquist, R.S., Fuentes, G.R., Lacey, M.P. and Keough, T., *J. Am. Chem. Soc.*, 117 (1995) 3900.
3. Keough, T., Baker, T.R., Dobson, R.L.M., Lacey, M.P., Riley, T.A., Hasselfield J.A. and Hesselberth, P.E., *Rapid Commun. Mass Spectrom.*, 7 (1993) 195.

Peptides: Chemistry, Structure and Biology
Pravin T.P. Kaumaya and Robert S. Hodges (Eds.)
Mayflower Scientific Ltd., 1996

125
Miniaturization in Chemistry: Macrobeads of 600 µm Diameter as Microreactors for Chemical Screening, Peptide Libraries and Combinatorial Chemistry

W. Rapp[1], M. Maier[2], G. Schlotterbeck[2], M. Pirsch[2], K. Albert[2] and E. Bayer[2]

[1]Rapp Polymere GmbH, Ernst Simon Str. 9, D 72072 Tübingen, Germany
[2]Institute of Organic Chemistry, University of Tübingen, Auf der Morgenstelle 18, D 72076 Tübingen, Germany

Introduction

The synthesis of peptide libraries and combinatorial chemistry for the generation of molecular diversity require resins which are compatible with organic reaction conditions as well as the aqueous systems used for biological assays and screening. On standard beads for solid phase synthesis, the maximal loading is in the range of 50-200 pmol per bead. Thus, the yield obtained from one bead by sequential cleavage is not sufficient for both analytical investigations and for application in bioassays. *Inter alia* lysine-branching for higher capacity [1] or tagging with genetic probes [2] have been described to improve the identification of active species. Here, we describe macrobeads as new tools for synthesis, bioassays, and structural characterization of diverse molecules.

Results and Discussion

We have developed TentaGel macrobeads of unusually high particle sizes (400-800 µm). This raises the capacity/bead by a factor of 100 to 1000, to the nanomolar range. Beads used to date have diameters of 90-130 µm and 50-200 pmol capacity. Dependent on particle sizes, capacities of 10-100 nmol/single bead have been confirmed by quantitative Fmoc. The macrobeads are compatible with almost all organic solvents and with aqueous systems. By using high molecular weight cleavage reagents (acids or bases), which cannot penetrate the gelatinous beads, we can differentiate between outer surface and internal reaction space. Some 98-99% of the total capacity is located inside the bead whereas only 1-2% is accessible on the surface. Multifunctional beads are created by attachment of two orthogonal handles inside the bead: acid labile handle AC (4-hydroxymethyl-3-methoxy-phenoxyacetic acid) and base labile *p*-hydroxymethyl-benzoic acid (HMB) are located inside the bead and aminoethyl groups without additional linker are on the outer surface. Synthesis of the histone H1C sublibrary KSGKPKV*XX*A (divide/recombine technique [3, 4]) resulted in a trifunctionalized peptide resin. Acid treatment deprotects the peptides and cleaves off 50% approx. of the peptide so yielding both a soluble and a resin bound peptide library in one synthesis run.

In natural systems, histones interact with the DNA. To screen the interaction of modified histone sequences with oligonucleotides, the polymer-bound peptide library was incubated with a fluorescence labeled oligonucleotide. To differentiate between the strength of the interaction, the beads were washed with different concentrations of aqueous NaCl. Negative beads or beads with reduced intensity were selected. Cleavage of the peptide by base treatment was followed by peptide identification by MS analysis. Phe was found to decrease the interaction, whereas all sequences having Tyr showed strong interaction. Hydrophobic amino acids showed weak to medium interactions.

In combinatorial chemistry, complicated and expensive building blocks are often used. However, for screening and optimization, only small amounts of substance are needed. We have used single beads as micro reactors for the individual synthesis of a set of 9 hydantoins. Reaction conditions include a single bead being treated with 20 µl of a 1 M isocyanate solution, the hydantoins being individually cleaved by treatment with 6M HCL/water, 45 min, 100°C, 4M HCl/THF, 2hr, RT, or by DIPEA/THF, 2h, 100°C. All hydantoins were identified and analyzed by HPLC and LC-MS. For structure information and to control synthesis progress, NMR monitoring of the resin bound intermediate was the method of choice. Recently, Fitch *et al.* have investigated resin bound molecules by CP MAS 1H NMR spectroscopy [5]. We have investigated the hydantoin precursor on a single macro bead by gel phase CP-MAS spectroscopy (Figure 1).

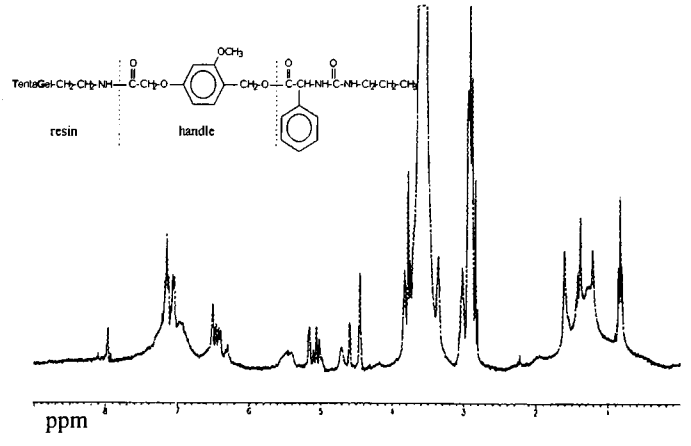

Figure 1. *Gel phase 1H-CP-MAS of one single macro bead, solvent: $CDCl_3$ 2000Hz.*

References

1. Lebl, M., Patek, M., Kocis,P., Krchnak,V., Hruby, V.J., Salmon, S.E. and Lam,K.S., *Intl. J. Protein Res.*, 41 (1993) 201.
2. Brenner, S., Lerner, R.A., *Proc. Natl. Acad. Sci. USA*, 89 (1992) 5381.
3. Furka, A., Sebestyen, F., Asgedom, M. and Dibo, G., *Intl. J. Protein Res.*, 37 (1991) 487.
4. Lam, K.S., Salmon, S.E., Hersh, E.M., Hruby, V.J., Kazmiersky, W.M. and Knapp R.J., *Nature*, 354, 82.
5. Fitch, W.L., Detre, G., Holmes, C.P., *J. Org. Chem.*, (1994) 59.

Peptides: Chemistry, Structure and Biology
Pravin T.P. Kaumaya and Robert S. Hodges (Eds.)
Mayflower Scientific Ltd., 1996

126
Determination of the Binding Conformation of Peptide Epitopes Using Cyclic Peptide Libraries

D. Winkler, R.-D. Stigler, J. Hellwig, B. Hoffmann and J. Schneider-Mergener

Institut für Medizinische Immunologie, Universitätsklinikum Charité, Humboldt-Universität zu Berlin, Schumannstrasse 20-21, 10098 Berlin, Germany

Introduction

Antibody-peptide epitope complexes are well characterized as model systems to study protein-peptide recognition events. Several structures of free and peptide-complexed Fab fragments demonstrate that this recognition event can be best explained by an induced-fit mechanism [1]. In most antibody-peptide complexes, the peptide epitopes bind to the hypervariable regions of their respective antibodies in β-turn conformations [1-3]. However, short linear peptides are unstructured in aqueous solution. Since an *ab-initio* prediction of the binding conformation of the antibody-bound peptide is extremely difficult, if not impossible, we have constructed a cyclic peptide epitope library bound to a continuous cellulose membrane by spot synthesis [4, 5]. This library was designed to obtain hints about the binding conformation of the peptide epitope VSHFND that binds to the antibody Tab2 which recognizes the N-terminal region of transforming growth factor alpha (TGFα) [6].

Results and Discussion

A cyclic peptide epitope library, in which two residues of the starting peptide GVSHFNDG were substituted by two cysteines, was synthesized (Figure 1). This library consists of 28 peptide epitope variants, which were subsequently analyzed for binding Tab2 [5]. Three peptides CCSHFNDG, CVSHFNDC, GCSHFNDC could be detected

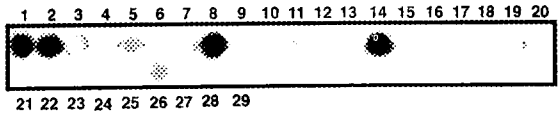

Figure 1. *Binding of the antibody Tab2 to a cyclic peptide epitope library. In peptides 2 to 29, two residues of the starting peptide 1 (GVSHFNDG) were substituted by cysteine residues (CCSHFNDG, CVCHFNDG, CVSCFNDG, GCCHFNDG, etc.). Following synthesis, the deprotected peptides were cyclized on the membrane [5]. Strong binding could be detected for peptides 2 (CCSHFNDG), 8 (CVSHFNDC), and 14 (GCSHFNDC).*

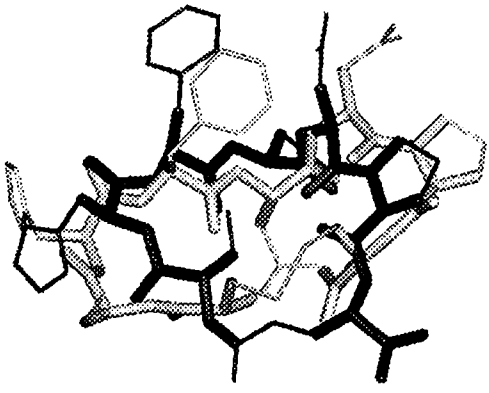

Figure 2. *Overlay of three-dimensional models of the cyclic peptides cyclo(C_1-C_8) CSHFNDPC (grey) and cyclo(Na-E_7)SHFNDPE (black). The backbones are represented by liquorice bonds and were created by using QUANTA/CHARMm (Copyright MSI Inc.).*

that bound Tab2 with similar affinity to the starting peptide (Figure 1). Thus, the loop library not only allowed the detection of high affinity binding cyclic peptides, but also the identification of key residues for binding, which could not be substituted. These results are in good accordance with those from a mutational analysis [7] of this epitope in which each residue of the epitope was substituted by all other 19 amino acids [8].

Figure 2 shows the overlap of the structures of two additional cyclic peptides *cyclo*(C_1-C_8)CSHFNDPC and *cyclo*(Nα-E_7)SHFNDPE, which were identified formerly from combinatorial cyclic peptide libraries [5, 9]. These peptides form a sharp turn including the serine, histidine, and phenylalanine residue.

Interestingly, the serine residue can be substituted by proline without loss of binding [5, 9] supporting the proposed binding conformation.

References

1. Wilson, I.A. and Stanfield, R.B., *Curr. Opinion Struct. Biol.*, 3 (1993) 113.
2. Dysen, H.J. and Wright, P.E., *FASEB J.*, 9 (1995) 37.
3. Stigler, R., Rüker, F., Katinger, D., Elliot, G., Höhne, W., Henklein, P., Ho, J.X., Keeling, K., Carter, D.C., Nugel, E., Kramer, A., Porstmann, T. and Schneider- Mergener, J., *Prot. Eng.*, 8 (1995) 471.
4. Frank, R., *Tetrahedron*, 48 (1992) 9217.
5. Kramer, A., Schuster, A., Reineke, U., Malin, R., Volkmer-Engert, R., Landgraf, C. and Schneider-Mergener, J., *Methods (Comp. Meth. Enzymol.)*, 6 (1994) 388.
6. Hoeprich, P.D., Langton, B.C., Zhang, J.W. and Tam, J.P., *J. Biol. Chem.*, 264 (1989) 19086.
7. Volkmer-Engert, R., Ehrhard, B., Hellwig, J., Kramer, A., Höhne, W. and Schneider-Mergener, J., *Lett. Peptide Sci.*, 1 (1994) 243.
8. Schneider-Mergener, J., Kramer, A., and Reineke, U., in Cortese, R. (Ed.), 'Combinatorial Libraries', Walter de Gruyter, Berlin, Germany,1995, p. 53.
9. Winkler, D., Schuster, A., Hoffmann, B., and Schneider-Mergener, J., in Maia, H.L.S. (Ed.), 'Peptides 1994', ESCOM, Leiden, The Netherlands, 1995, p. 485.

Peptides: Chemistry, Structure and Biology
Pravin T.P. Kaumaya and Robert S. Hodges (Eds.)
Mayflower Scientific Ltd., 1996

127
Applicability of Peptide Omission Libraries in Screening

Á. Furka, E. Câmpian, M.L. Peterson and H.H. Saneii

Advanced ChemTech Inc., Louisville, KY 40228, USA

Introduction

Peptide and non-peptide libraries synthesized by the portioning-mixing (PM) method [1-3] are extensively used in pharmaceutical research to provide a cornucopiae of new compounds. As recently described [4, 5], certain types of partial libraries may play an important role in screening for new bioactive lead compounds.

This paper deals with the potential applicability of another kind of partial library, termed omission libraries. These are defined as those synthesized by intentional omission of a single amino acid in all positions. A complete set of omission libraries (designated as -A through -Y to signify the missing amino acid) is expected to be a useful tool in determining the essential (non-replaceable) amino acid building blocks of the bioactive components of libraries. The number of the amino acid residues can be indicated by an additional figure. A tripeptide alanine omission library, for example, can be symbolized by -A3 .

Results and Discussion

Sets of free tripeptide omission libraries have been synthesized using Fmoc protection strategy and the ACT Model 357 automatic multiple peptide synthesizer [6, 7]. In the synthesis of the first set, different mixtures of 18 L-amino acid Wang resins were used as starting materials to provide tripeptide acids upon cleavage. Similarly, the second set of omission libraries was synthesized on Rink resin to yield the corresponding tripeptide amides. In the first and second coupling position, the same amino acids were used as before. In the third position, pyroglutamic acid was applied as an additional amino acid building block. Cysteine was omitted from all omission libraries.

The full tripeptide amide library (marked All) was tested using an ^{125}I LH-RH radio-immunoassay kit, prepared at Advanced ChemTech Inc., and specific binding was found. Based on this result, 8 omission libraries (marked X3NH_2) were also tested with the same kit.

Figure 1 shows that five omission libraries behave like the full library. Omission of Ala, Pro, or Gly from the library, however, causes a very significant decrease in competitive binding as compared to that of the full and the other libraries. These preliminary data suggest that omission libraries can be effective tools in the identification of new bioactive sequences.

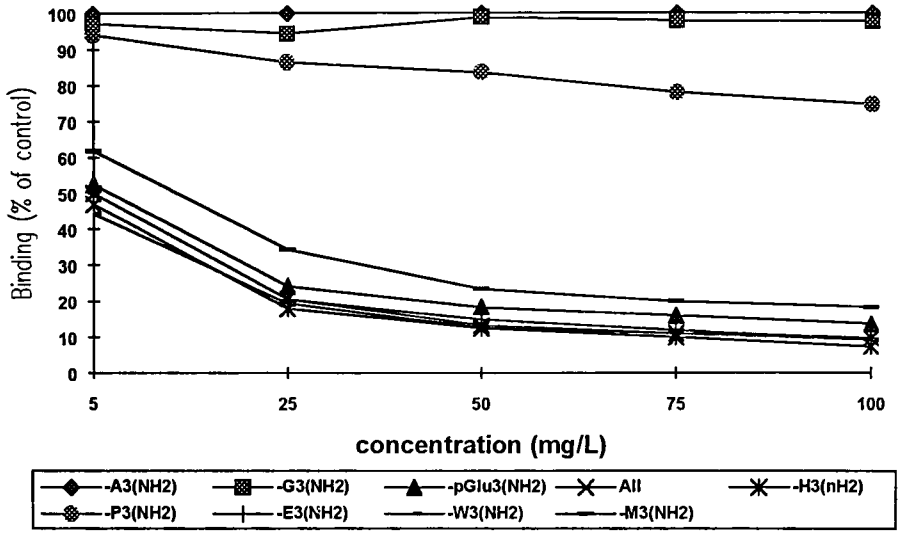

Figure 1. *LH-RH radio-immuno assay of omission and non-omission (All) libraries of tripeptide amides.*

Acknowledgments

One of the authors (Á.F.) thanks the Hungarian Scientific Research Foundation (OTKA, No. T 015718) for financial support and Advanced ChemTech, Inc. for sponsoring his sabbatical. We wish to thank Dr. J. Chou for the RIA results.

References

1. Furka, Á., Sebestyén, F., Asgedom, M., Dibó, G., in 'Abstr. 14th Int Congr Biochem', Prague, Czechoslovakia, 1988, Vol 5, p 47.
2. Furka, Á., Sebestyén, F., Asgedom, M., Dibó, G., in 'Abstr. 10th Int. Symp. Med. Chem.', Budapest, Hungary, 1988, p 288.
3. Furka, Á., Sebestyén, F., Asgedom, M., Dibó, G., *Intl. J. Peptide Protein Res.*, 37 (1991) 487.
4. Furka, Á., Sebestyén, F., PCT application (1993) WO 93/24517.
5. Furka, Á., *Drug Development Research,* 33 (1994) 90
6. Saneii, H.H., Shannon, J.D., Miceli, R.M., Fischer, H.D., Smith, C.W., in Hodges, R.S. and Smith, J.A. (Eds), 'Peptides. Chemistry, Structure and Biology', ESCOM Leiden, The Netherlands, 1994 , p. 1018.
7. Saneii, H.H., Shannon, J.D., Miceli, R.M., Fischer, H.D., Smith, C.W. in Y. Okada (Ed), Peptide Chemistry 1993, Protein Research Foundation, Osaka 1994, p. 117.

Peptides: Chemistry, Structure and Biology
Pravin T.P. Kaumaya and Robert S. Hodges (Eds.)
Mayflower Scientific Ltd., 1996

128
Synthesis of Colored Peptide Libraries

F. Sebestyén[1], K. Kindla[1], W. Rapp[2], E. Câmpian[3] and Á. Furka[3]

[1]Department of Organic Chemistry, Eötvös Loránd University, P.O. Box 32, 1518 Budapest, Hungary
[2]Rapp Polymere, 7400 Tübingen, Germany
[3]Advanced ChemTech, Inc. Louisville, KY 40228, USA

Introduction

Support bound peptide libraries synthesized by the portioning-mixing (PM) method [1-3] can be screened by binding tests using labeled soluble target molecules. Introduction of sub-library kits and the domino strategy [4] as well as application of colored solid supports [5] opens the possibility of using these binding experiments to screen non-peptide libraries, too. In order to facilitate the use of peptide libraries in binding experiments carried out with insoluble receptors and other insoluble target molecules, we suggest the use of soluble peptide libraries carrying colored labels synthesized as described here.

Results and Discussion

Previously described colored resins [5] were prepared by coupling an azo dye to aminomethyl polystyrene resin.

$$\text{Boc-NH-(CH}_2\text{)}_3\text{-N(C}_2\text{H}_5\text{)-C}_6\text{H}_4\text{-N=N-C}_6\text{H}_4\text{-CO-NH-CH}_2\text{-resin}$$

However, in order to prepare soluble libraries carrying colored labels attached to the C-termini of the peptides, a different solid support was required. This was synthesized by coupling the same red dye to a chloromethyl polystyrene resin. On this support, the azo dye was present in a cleavable form.

$$\text{Boc-NH-(CH}_2\text{)}_3\text{-N(C}_2\text{H}_5\text{)-C}_6\text{H}_4\text{-N=N-C}_6\text{H}_4\text{-COO-CH}_2\text{-resin}$$

The labeled peptide libraries synthesized on this support, unfortunately, were practically insoluble in water. Therefore, in addition to the colored label, a solubilizing tag was required as well. To attack this challenge, two kinds of supports were prepared. Resin 1, designed to be used with the Boc technology, contained a pentalysine solubilizing tag and a GABA spacer in addition to the dye.

$$\text{Boc-GABA-NH-(CH}_2\text{)}_3\text{-N(C}_2\text{H}_5\text{)-C}_6\text{H}_4\text{-N=N-C}_6\text{H}_4\text{-CO-[Lys(Z)]}_5\text{-O-CH}_2\text{-resin}$$

Resin 2 was prepared by coupling the above azo dye to the amino group of TentaGel® PAP Resin designed for use with Fmoc protocols. This resin contains a cleavable polyethyleneglycol (PEG) chain that remains attached to the peptide-dye units after cleavage and provides dramatically improved solubility.

In model experiments, the effect of the solubilizing tags was examined by observing the solubility of a labeled hydrophobic pentapeptide synthesized on each of the above-mentioned resins. Labeled Phe-Ala-Val-Leu-Gly was synthesized on Resin 1 with Boc chemistry and on Resin 2 using Fmoc protection. The labeled peptide in both cases proved to be readily soluble in water yielding clear red solutions. These results demonstrate that both the pentalysine and the PEG tags can be applied to solubilize otherwise poorly soluble peptide-dye adducts. Another labeled variant of the same peptide, containing a blue label and a PEG tag attached to the N and C-termini, respectively, also showed good water solubility.

To check the applicability of dual tags in the synthesis of labeled libraries, a pentapeptide library was synthesized on Resin 1 using 19 amino acids in every position (cysteine was omitted). After the last coupling step, the portions were not mixed. The 19 sub-libraries were cleaved and examined separately. All proved to dissolve readily in water.

From the results of these experiments, we conclude that labeled libraries can best be prepared if a solubilizing tag is coupled to the peptides along with the color label. Both Resin 1 and Resin 2 can be applied if libraries labeled at the C-terminus are desired.

Attachment of the solubilizing tags will prove useful, as well, in the synthesis of unlabeled free libraries, since some components of libraries, those containing primarily nonpolar amino acids, are not always readily soluble in water.

Acknowledgments

Financial support by the Hungarian Scientific Research Foundation (OTKA, No. T 015718) is gratefully acknowledged and one of the authors (Á. F.) thanks Advanced ChemTech, Inc. for sponsoring his sabbatical.

References

1. Furka, Á., Sebestyén, F., Asgedom, M., Dibó, G., in Abstr. 14th Int. Congr. Biochem., Prague, Czechoslovakia, 1988, Vol 5, p. 47.
2. Furka, Á., Sebestyén, F., Asgedom, M., Dibó, G., in Abstr. 10th Int. Symp. Med. Chem., Budapest, Hungary 1988, p. 288.
3. Furka, Á., Sebestyén, F., Asgedom, M., Dibó, G., *Intl. J. Peptide Protein Res.*, 37 (1991) 487.
4. Furka, Á., *Drug Development Research*, 33 (1994) 90.
5. Câmpian, E., Sebestyén, F., Major, F., Furka, Á., *Drug Development Research*, 33 (1994) 98.

Peptides: Chemistry, Structure and Biology
Pravin T.P. Kaumaya and Robert S. Hodges (Eds.)
Mayflower Scientific Ltd., 1996

129
Synthesis of Genetic Peptide Libraries

F. Sebestyén[1], A. Kovács[2], W. Rapp[3], E. Câmpian[4], and Á. Furka[4]

[1]Department of Organic Chemistry and [2]Department of General Zoology,
Eötvös Loránd University, P.O. Box 32, 1518 Budapest, Hungary
[3]Rapp Polymere, 7400 Tübingen, Germany
[4]Advanced ChemTech, Inc. Louisville, KY 40228, USA

Introduction

In the course of the synthesis of a pentapeptide library prepared using the portioning mixing (PM) method [1-3], all libraries of shorter peptides are naturally prepared as well. The shorter peptides, however, are built into the C-terminal end of the growing chains. The number and kinds of these peptides at various stages are as follows:

400	dipeptides
8,000	tripeptides
160,000	tetrapeptides

Libraries, including all peptide libraries temporarily formed in the course of the synthesis of a library, are termed: *genetic libraries*. For example, a genetic pentapeptide library, in addition to the pentapeptide library, comprises the libraries of dipeptides, tripeptides, and tetrapeptides, too. The total number of components in tri, tetra, penta, and hexapeptide genetic libraries is the sum of components in di and tri, di and tri and tetra, di and tri and tetra and penta, di and tri and tetra and penta and hexapeptide libraries, respectively.

tripeptide	8,400
tetrapeptide	168,400
pentapeptide	3,368,400
hexapeptide	67,368,400

The libraries of shorter peptides formed in the synthesis of a library of longer ones are also of value. They could be utilized either as separate libraries or in the form of genetic libraries.

Genetic libraries can be prepared by taking samples after each coupling step in the synthesis, then pooling the samples in the proper ratio at the end of the synthesis. It seems possible, however, to apply an even simpler procedure; by adding a sample of the starting resin (or a mixture of amino acid resins if a soluble genetic library is prepared) to the pooled mixture before every new coupling step (quantity, starting before second coupling step: 1/20 then 1/400 then 1/8000 *etc.*).

Results and Discussion

In order to prove the applicability of the second procedure, a very simple tripeptide genetic library was synthesized using three amino acids (E, G, and K) in all positions. (1) Equal amounts (0.1 mmol) of Boc-Gly, Boc-Glu(OBzl), and Boc-Lys(Z) Merrifield resins were swollen and mixed in DCM-DMF (2:1 v/v) then portioned into 4 equal parts. (2) Portions 1 through 3 were each coupled with one of the above-mentioned Boc-amino acids. (3) The three coupled resin samples were combined with the fourth uncoupled one, mixed, then divided into three portions. (4) Each of these portions were then coupled with one of the Boc-amino acids.

The samples after the last coupling step were not mixed to facilitate identification of the formed peptides. After cleavage with TFMSA the three mixtures were submitted to a computer aided two dimensional paper electrophoretic procedure [4]. This allowed identification of the following di and tripeptides:

Mixture I.
Dipeptides EE, EG, EK
Tripeptides EEE, EEG, EEK, EGE, EGG, EGK, EKE, EKG, EKK
Mixture II.
Dipeptides GE, GG, GK
Tripeptides GEE, GEG, GEK, GGE, GGG, GGK, GKE, GKG, GKK
Mixture III.
Dipeptides KE, KG, KK
Tripeptides KEE, KEG. KEK, KGE, KGG, KGK, KKE, KKG, KKK

As can be seen, all the expected peptides were found and this confirms that the simple method outlined above is viable and could also be successfully applied for the synthesis of more complex genetic libraries.

Acknowledgments

Financial support by the Hungarian Scientific Research Foundation (OTKA, No. T 015718) is gratefully acknowledged and one of the authors (Á. F.) thanks Advanced ChemTech, Inc. for sponsoring his sabbatical.

References

1. Furka, Á., Sebestyén, F., Asgedom, M., Dibó, G., in 'Abstr. 14th Int Congr Biochem.', Prague, Czechoslovakia, 1988, Vol 5, p. 47.
2. Furka, Á., Sebestyén, F., Asgedom, M., Dibó, G., in 'Abstr. 10th Int. Symp. Med. Chem.', Budapest, Hungary, 1988, p. 288.
3. Furka, Á., Sebestyén, F., Asgedom, M., Dibó, G., *Intl. J. Peptide Protein Res.*, 37 (1991) 487.
4. Furka Á, Sebestyén F, Gulyás J., in Pick, J. and Vajda, J. (Eds.), 'Proceedings of the 2nd International Conference on Biochemical Separations', Keszthely, Hungary, 1988, p. 35.

Session VI
Peptide Inhibitors/Receptors

Chairs: Daniel F. Veber and
Maria-Luisa Maccecchini

Peptides: Chemistry, Structure and Biology
Pravin T.P. Kaumaya and Robert S. Hodges (Eds.)
Mayflower Scientific Ltd., 1996

130

Design, Synthesis and Structure-activity Relationships of New RGD Peptide Mimetics as Potent Antagonists of GPIIb/IIIa Receptor

I. Ojima[1], S. Chakravarty[1], Q. Dong[1], E. Peerschke[2], S.M. Hwang[3] and A.S. Wong[3]

[1]Department of Chemistry and [2]Department of Pathology, School of Medicine, State University of New York at Stony Brook, Stony Brook, NY 11794, USA
[3]Department of Cellular Biochemistry, SmithKline Beecham Pharmaceuticals, 709 Swedeland Road, P.O. Box 1539, King of Prussia, PA 19406, USA

Introduction

The discovery of RGD sequence-directed cell surface receptors (the integrins) has led to extensive research in the development of small RGD containing peptides and their mimetics as antithrombotic agents which are potential therapeutic drugs for thrombosis related to cardiovascular and cerebrovascular diseases. These agents work by inhibiting platelet aggregation through competitive blocking of fibrinogen to the platelet surface receptor, GPIIb/IIIa. The pharmacophoric nature of the aspartic acid and arginine side chains of the RGD unit has allowed the development of strategies for rational design, largely based on assumed bioactive RGD conformations and lead optimization.

In the course of our study on rational modification of the RGD pharmacophore, we have reported double-strand RGD peptides (**1**) with enhanced antiplatelet activity compared to their single-strand counterparts [1]. This paper describes the simplification of these relatively large peptides into smaller peptide mimetics with very high affinity for GPIIb/IIIa. The receptor specificity as well as some insight into the mode of binding for these highly potent GPIIb/IIIa antagonists will also be discussed.

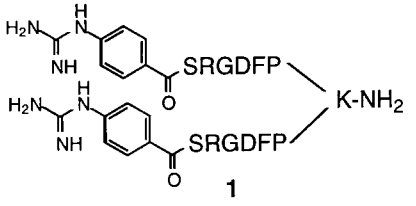

1

Results and Discussion

New RGD peptide mimetics have been designed and synthesized on the basis of a three-point pharmacophoric binding model.

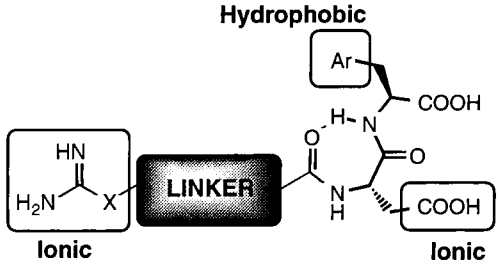

In the previous study, [1] we found that the activities of double-strand RGD peptides were significantly enhanced by N-terminal acylation, with the guanidinobenzoyl group being the most effective acyl moiety (**1**, USB-IPA-090, IC_{50} = 0.087 μM, PRP/ADP) [1].

In an effort to reduce the molecular weight of the inhibitor and make the transition from peptides to peptide mimetics, we studied various fragments of **1** for activity. Our design strategy involved: (1) use of the guanidinobenzoyl moiety to replace the arginine moiety in an RGDF-mimicking sequence; (2) adjustment of the distance between the guanidinobenzoyl moiety and the aspartyl side chain for optimum activity using adequate linkers; (3) use of different C-terminal aromatic groups in order to study a potential *localized* hydrophobic binding site; and (4) modification of the guanidinobenzoyl group.

Our initial lead optimization following the strategy (1)-(3) led to a potent peptide mimetic **2** (USB-IPA-1102, IC_{50} = 0.070 μM). Replacement of the guanidinobenzoyl moiety with an amidinobenzoyl group further improved potency. The guanidinomethyl-benzoyl group was found to be much less effective. Thus, a series of highly potent antagonists **3** (USB-IPA-1300 series, IC_{50} = 0.020-0.047 μM) bearing an amidino-benzoyl group at the N-terminus and a hydrophobic amino acid residue at the C-terminus were obtained. Among these, two most potent antagonists, **3a** (R = 3-indolyl, USB-IPA-1302, IC_{50} = 0.026 μM) and **3b** (R = 4-hydroxyphenyl, USB-IPA-1305, IC_{50} = 0.020 μM) were chosen for further receptor binding studies.

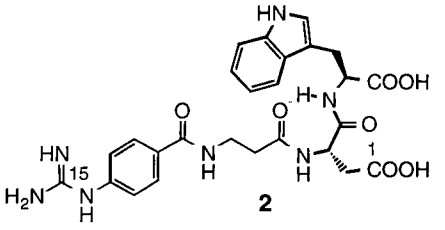

2

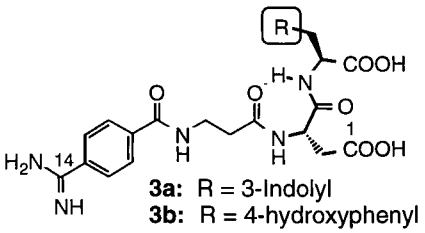

3a: R = 3-Indolyl
3b: R = 4-hydroxyphenyl

Peptide mimetics **3a** and **3b** are found to be not only exceedingly active antagonists of GPIIb/IIIa, but also extremely selective agents to GPIIb/IIIa in comparison with the closely related integrins, vitronectin receptor ($\alpha_v\beta_3$) and fibronectin receptor ($\alpha_5\beta_1$). In a solid phase competitive [^{3}H]-SK&F-107260[2] (***SK***) binding assay to the purified immobilized GPIIb/IIIa ($\alpha_{IIb}\beta_3$) and $\alpha_v\beta_3$ receptors, **3b** showed extremely high affinity to GPIIb/IIIa and a 35,700-fold lowered affinity to $\alpha_v\beta_3$ (K_i = 2.1 ± 0.4 nM, ****SK***-GPIIb/IIIa binding assay; K_i = 75 ± 2.5 μM, ****SK***-$\alpha_v\beta_3$ binding assay). Peptide hybrid **3a** showed a

15,200-fold selectivity to GPIIb/IIIa over $\alpha_v\beta_3$ in the same assay (K_i = 2.3 ± 0.1 nM, ***SK*-GPIIb/IIIa binding assay; K_i = 35 ± 1.5 μM, ***SK*-$\alpha_v\beta_3$ binding assay). Similarly, the competitive ***SK*** binding assay to the purified immobilized GPIIb/IIIa receptor and $\alpha_5\beta_1$ receptor isolated from human placenta disclosed that both **3a** and **3b** did not interact with the $\alpha_5\beta_1$ up to 100 μM concentration. This means that **3a** and **3b** are at least 43,000 times and 47,000 times more selective to the platelet GPIIb/IIIa than to placenta $\alpha_5\beta_1$.

Although the existence of a possible hydrophobic binding site has been alluded to in different systems, [2, 3] no particular investigation has been carried out to establish its precise position in the pharmacophoric model. Our molecular modeling and SAR studies point toward a *localized* hydrophobic binding site. Comparative molecular dynamics simulations indicate that the hydrophobic moiety tends to orients itself on the convex side of the slightly curved backbone. It is suggested that the binding conformations of **3a** or **3b** are stabilized by a γ-turn caused by a hydrogen bonding between the amide hydrogen of the C-terminal residue with the carbonyl oxygen of the β-Ala residue that appears to position the hydrophobic moiety precisely into the binding pocket.

We have also looked at the competitive inhibitory activity of **3a** and **3b** against the fibrinogen fragments, *i.e.,* E-fragments containing $\alpha_{95\text{-}98}$ RGDF sequence and D60-fragment that does not contain any of the known recognition sequences. It has been found that the D60-fragment binding to GPIIb/IIIa is efficiently inhibited by **3a** as well as **3b**, and the addition of EDTA, *i.e.,* abstraction of Ca^{2+} ions, significantly reduces the inhibitory activity of these antagonists. The results indicate that substantial allosteric effects are operative when the inhibitor binds to the receptor, deforming the D60-fragment binding site(s). Also, it is strongly suggested that these antagonists are calcium dependent, which implies the Ca^{2+} ion rich region (GPIIb) being the major binding site of these antagonists. Thus, highly potent antagonists of GPIIb/IIIa provide a powerful tool for characterization of the receptor and investigation into the mechanism of adhesive protein binding.

Acknowledgments

This research was supported by grants from the National Institutes of Health (NIGMS), the Life Science Division of Nippon Steel Corporation, and in part by a grant from the Center of Biotechnology, State University of New York at Stony Brook, sponsored by the New York State Science Foundation. Ms. Lesley Scudder, Ms. Karen Springer and Ms. Joan Hennessey are thanked for excellent technical assistance and Dr. Daniel F. Veber, SmithKline Beecham Pharmaceuticals, is thanked for valuable discussions.

References

1. Ojima, I., Dong, Q., Eguchi, M., Oh, Y.-I., Amann, C.M. and Coller, B.S., *Biomed. Chem. Lett.*, 4 (1994) 1749.
2. Ali, F.E., Bennett, D.B., Calvo, R.R., Elliott, J.D., Hwang, S.-M., Ku, T.W., Lago, M.A., Nichols, A.J., Romoff, T.T., Shah, D.H., Vasko, J.A., Wong, A.S., Yellin, T.O., Yuan, C.-K. and Samanen, J.M., *J. Med. Chem.*, 37 (1994) 769.
3. Ojima, I., Chakravarty, S. and Dong, Q., *Biomed. Chem.*, 3 (1995) 337.

Peptides: Chemistry, Structure and Biology
Pravin T.P. Kaumaya and Robert S. Hodges (Eds.)
Mayflower Scientific Ltd., 1996

131
Inhibition of HIV-1 Replication by Non-immunosuppressive Analogs of Cyclosporin A

D.H. Rich[1], M.-K. Hu[1], S.R. Bartz[2], E. Hohenwalter[2] and M. Malkovsky[2]

[1]School of Pharmacy and Department of Chemistry and [2]Department of Medical Microbiology and Immunology, University of Wisconsin-Madison, 425 North Charter Street, Madison, WI 53706, USA

Introduction

Recently, several investigators have demonstrated that cyclosporin A (CsA, **1**) inhibits replication of the human immunodeficiency virus (HIV) by an unknown mechanism [1]. In addition, HIV-1 gag protein binds to cyclophilins A and B [2], peptidyl prolyl isomerases (PPIase) that are inhibited by CsA . Since we previously synthesized several non-immunosuppressive CsA analogs that are tight-binding inhibitors of cyclophilin, we decided to test if these would inhibit HIV replication. We report here that [L-MeLeu(3-OH)[1], MeAla[4,6]]-CsA (**3**) inhibits HIV and SIV replication at micromolar concentrations and co-stimulates PHA-induced IL-2 production in human lymphocytes.

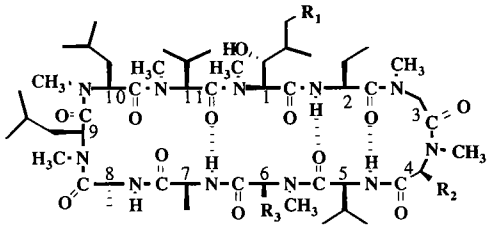

1 CsA: R_1= CH_2CH=CH-CH_3; R_2= R_3 = CH_2 $CH(CH_3)_2$
2 [MeLeu(3-OH)[1]]-CsA: R_1 = H; R_2= R_3 =CH_2 $CH(CH_3)_2$
3 [MeLeu(3-OH)[1], MeAla[4,6]]-CsA: R_1 = H; R_2= R_3 =CH_3

Figure 1. *Structures of cyclosporin A analogs.*

Results and Discussion

[L-MeLeu(3-OH)[1], MeAla[4,6]]-CsA (**3**) was designed by consideration of the structure-activity data for subtle modifications of CsA that diminish immunosuppression [3] and the reported X-ray structure of the cyclophilin-CsA complex [4]. Replacement of

MeBmt by L-N-methyl β-hydroxy leucine [MeLeu(3OH)] in the 1-position of CsA to form [L-MeLeu(3-OH)^{1}]-CsA (**2**) is known to greatly diminish the immunosuppressive activity to less than 0.1% of that of CsA [5]. We determined that this reduced activity is not due to poor binding to cyclophilin since [L-MeLeu(3-OH)^{1}]-CsA (**2**) is a potent inhibitor of the PPIase activity of cyclophilin A (Ki = 11 $\pm$ 3 nM). Similarly, replacement of MeLeu in the 4- and 6-positions by MeAla also diminishes immunosuppressive effects while retaining tight-binding to cyclophilin (*e.g.*, [MeAla^{6}]-CsA, Ki = 16 $\pm$ 2 nM *versus* CsA, Ki = 7 nM; [6]. Incorporation of all three modifications into one analog resulted in the synthesis of [L-MeLeu(3-OH)^{1}, MeAla^{4,6}]-CsA (**3**), which is a tight-binding inhibitor of the PPIase activity of cyclophilin (Ki = 35 $\pm$ 13 nM) and shows no detectable immunosuppressive activity at high concentrations.

To assess if CsA and CsA analogs inhibit replication of HIV, the amounts of HIVp24 in cell-free supernatants from drug-treated or control untreated HIV-infected CEMx174 cultures were assayed by ELISA [6]. In representative experiments, CsA inhibited p24 production by 96% to >99%, [L-MeLeu(3-OH)^{1}]-CsA (**2**) by 96% to 99%, [MeAla^{6}]-CsA by 92% and 97%, and [L-MeLeu(3-OH)^{1}, MeAla^{4,6}]-CsA (**3**) by 95% to 96%, respectively (values for a final drug concentration of 10 mg/ml). Inhibition of replication of HIV did not correlate with immunosuppressive activity. We also found that CsA and the CsA analogs inhibit CPE in newly infected CEMx174 cells. Similar results were obtained with SIV.

Analogs **1-3** were assayed for immunosuppressive activity as measured by inhibition of proliferation of PHA activated human PBMCs and the production of IL-2 [7]. Analogs **2** and **3** produced no immunosuppression but in fact, augmented the PHA-induced DNA synthetic response of human PBMCs at the highest tested concentration (10 mg/ml). Moreover, [L-MeLeu(3-OH)^{1}, MeAla^{4,6}]-CsA (**3**) co-stimulated the PHA-induced IL-2 production in human PBMC, whereas CsA was strongly inhibitory as expected. These data indicate that some CsA derivatives possess an unexpected property of being co-stimulatory for human PBMCs.

Our results establish that non-immunosuppressive analogs of CsA inhibit HIV replication in newly infected cells. Most likely this activity results from binding to cyclophilin that displaces a critical viral protein needed for infection. In contrast, only CsA itself was able to inhibit the production of HIV from the persistently infected HCEM cells, suggesting that a provirus postintegration step in the HIV life cycle can be affected by CsA. Our findings are compatible with the observations of Luban *et al.* [8], who showed that HIV-1 p55^{gag} binds to cyclophilin and that this binding is sensitive to CsA, and Schmidt *et al.* [9], who demonstrated that the binding of NF-kB to the NF-kB site in the HIV-1 LTR is sensitive to CsA. It remains to be seen whether or not these non-immunosuppressive derivatives of CsA would be active in these systems.

The observation of the co-stimulatory and HIV virion infectivity-blocking activities of [L-MeLeu(3-OH)^{1}, MeAla^{4,6}]-CsA (**3**) was quite unexpected. Our preliminary data indicate that HIV particles produced by drug-treated cells contain less cyclophilin A than virions synthesized by untreated cells (Bartz *et al.*, unpublished data). This suggests that the cyclophilin A content in virions may be associated with the level of HIV infectivity. Data supporting this hypothesis have been published recently [8, 9], the latter utilizing another non-immunosuppressive CsA derivative with anti-HIV properties that was

discovered by screening methods [10]. Nevertheless, the potent anti-HIV effect of [L-MeLeu(3-OH)[1], MeAla[4,6]]-CsA (**3**) combined with its immunostimulatory properties may change the fine host-virus balance in favor of the HIV-infected host and result in substantially reduced appearance of virus deleterious effects *in vivo*. The remarkable combination of antiviral and co-stimulatory properties of [L-MeLeu(3-OH)[1], MeAla[4,6]]-CsA (**3**) with no obvious toxicity for proliferating cells *in vitro* makes this molecule a unique lead compound for development of drugs suitable for AIDS treatment.

Acknowledgments

This work was supported by NIH grants RR-00167, AI-33237, AR-32007, and the Tracy, Jamie and Dawn Ruhrup Memorial Fund.

References

1. Karpas, A., Lowdell, N., Jacobson, S. and Hill. F., *Proc. Natl. Acad. Sci. USA*, 89 (1992) 8351-8355.
2. Luban, J., Bossolt, K.L., Franke, E.K., Kalpana, G.V. and Goff, S.P., *Cell*, 73, (1993) 1067-1078.
3. (a) Rich, D.H., Dhaon, M.K., Dunlap, B. and Miller, S.P.F., *J. Med. Chem.*, 29 (1986) 978-984. (b) Durrette, P.L., Boger, J., Dumont, F., Firestone, R., Frankshun, R.A., Koprak, S.L., Lin, C.S., Melino, M.R., Pessolano, A.A., Pisano, J., Schmidt, J.A., Sigal, N.H., Staruch, M.J. and Witzel, B.E., *Transplant. Proc.*, 20 (1988) 51-57.
4. (a) Mikol, V., Kallen, J., Pflugl, G. and Walkinshaw, M.D., *J. Mol. Biol.*, 234 (1993) 1119-1130; (b) Ke, H., Mayrose, D., Belshaw, P.J., Alberg, D.G., Schreiber, S.L., Chang, Z.Y., Etzhorn, F.A., Ho, S. and Walsh, C.T., *Structure*, 2 (1994) 33-44.
5. Kofron, J.L., Kuzmic, P., Kishore, V., Colon-Bonilla, E. and Rich, D.H., *Biochemistry*, 30 (1991) 6127-6134.
6. Hoxie, J.A., Haggarty, B.S., Bonser, S.E., Rackowski, J.L., Shan, H. and Kanki, P.J., *J. Virol.*, 62 (1988) 2557-2568.
7. Malkovsky, M., Asherson, G.L., Stockinger, B., Watkins, M.C., *Nature (London)*, 300 (1982) 652-655.
8. Franke, K.E., Yuan, H.E.H., and Luban, J., *Nature (London)*, 372 (1994) 359-362.
9. Thali, M., Bukovsky, A., Kondo, E., Rosenwirth, B., Walsh, C.T., Sodroski, J. and Gottlinger, H.G., *Nature (London)*, 372 (1994) 363-365.
10. Rosenwirth, B., Billich, A., Datema, R., Donatsch, P., Hammerschmid, F., Harrison, R., Hiestand, P., Jaksche, H., Mayer, P., Peichl, P., Quesniaux, V., Schatz, F., Schuurman, H.-J., Traber, R., Wenger, R., Wolff, B., Zenke, G. and Zurini, M., *Antimicrobial Agents and Chemotherapy*, 38 (1994) 1763-1772.

Peptides: Chemistry, Structure and Biology
Pravin T.P. Kaumaya and Robert S. Hodges (Eds.)
Mayflower Scientific Ltd., 1996

132

Development of Highly Potent and Selective α-Keto Carbonyl Thrombin Inhibitors with Novel P_1 Side Chains: Synthesis and Biological Profile of L-370,518

S.F. Brady[1], S.D. Lewis[2], C.D. Colton[1], K.J. Stauffer[1], J.T. Sisko[1], A.S. Ng[2], C.F. Homnick[1], M.J. Bogusky[1], J.A. Shafer[2], D.F. Veber[1] and R.F. Nutt[1]

[1]Departments of Medicinal Chemistry and [2]Biological Chemistry, Merck Research Laboratories, West Point, PA 19486, USA

Introduction

Inhibitors of the enzyme thrombin, a key mediator in the blood coagulation system, have been shown to be efficacious in animal models of thrombosis and offer the promise of improved treatment of a number of thrombogenic states [1]. Several small peptidic inhibitors of thrombin which act *via* reversible binding of an electrophilic carbonyl moiety to the active-site Ser-195 residue exhibit high potencies [2]. Studies in these laboratories of the natural product cyclotheonamide-A [3] suggested that peptidomimetic structures containing a basic P_1 α-keto carbonyl moiety might constitute more potent and selective inhibitors of thrombin. A prototype series of analogs derived from lysine [4], specifically H-N-Me-D-Phe-Pro-Lys-α-keto amides, exhibited dissociation constants (Ki) $\leq$ 1 nM, but failed to show significant selectivity for thrombin over trypsin. In the present work we report the analog derived from *trans*-4-aminocyclohexyl glycine (*t*-Acg), L-370,518, which shows enhanced potency and exceptional selectivity for thrombin over a number of other serine proteases, including trypsin.

Results and Discussion

Early studies in the somatostatin area [6] had demonstrated that basic residues having side-chain constraint, in particular *trans*-4-aminocyclohexyl alanine (*t*-Aca), are effective replacements for lysine in peptide analogs. In the present effort, we assessed a number of such residues in place of arginine (**X**) in substrate-based carboxamides, H-D-Phe-Pro -**X**-NH_2, as a guide to attaining enhanced thrombin binding selectivity in the corresponding α-keto amides. The most potent (Ki = 5 μM) and selective (up to 160-fold) compounds of this group were tripeptides wherein **X** constitutes *t*-Acg or *t*-Aca.

As summarized in Table 1, the corresponding α-keto carbonyl inhibitors were synthesized in this series, which culminated in the highly potent and selective α-keto amide L-370,518. The α-keto acid ***2*** corresponding to L-370,518, though equipotent *vs.* thrombin, shows ten-fold less selectivity *vs.* trypsin. The analogs derived from *t*-Aca ***(1,3)*** are seen to be considerably less potent and selective.

Table 1. *Potencies and selectivities of α-keto carbonyl analogs with novel P_1. Enzyme assay run in Tris buffer at pH 7.4 [5a, 5b].*

No.	Structure	Ki (nM) Thrombin	Trypsin	Ratio
1	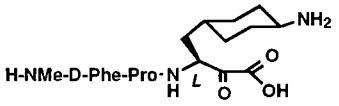	9.4	420	45
2	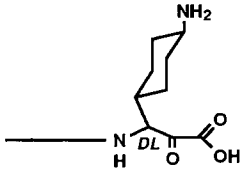	0.05	51	1000
3	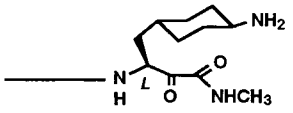	52	1440	28
4	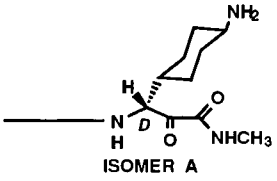	3.3	7000	2100
370,518	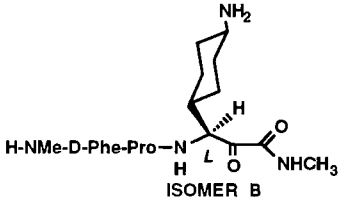	0.09	1151	12800

The synthesis of L-370,518 (Figure 1) is representative of our generally applied methodology for this class of structures. The requisite precursor, protected *t*-Acg ***5*** was obtained racemic at the α-carbon from 4-acetamidobenzaldehyde *via* a modified Strecker procedure leading to 4-aminophenylglycine, followed by selective Boc protection and hydrogenation of the aromatic ring. Although the desired *trans* isomer was the *minor* product of the reduction, it proved readily separable from the *cis* component by column chromatography [6]. Homologation of ***5*** through four steps *via* aldehyde ***6*** yielded the pivotal α-hydroxy ester intermediate *7*. N-terminal addition of the N-Me-D-Phe-Pro-segment by standard means, followed by saponification, led to α-hydroxy acid ***8***, poised for the final steps of amide formation, oxidation, and blocking group cleavage. The separability of the diastereoisomeric constituents by preparative HPLC (**A** earlier, **B** later) enabled the assignment of configuration through X-ray crystallography of isomer **B**

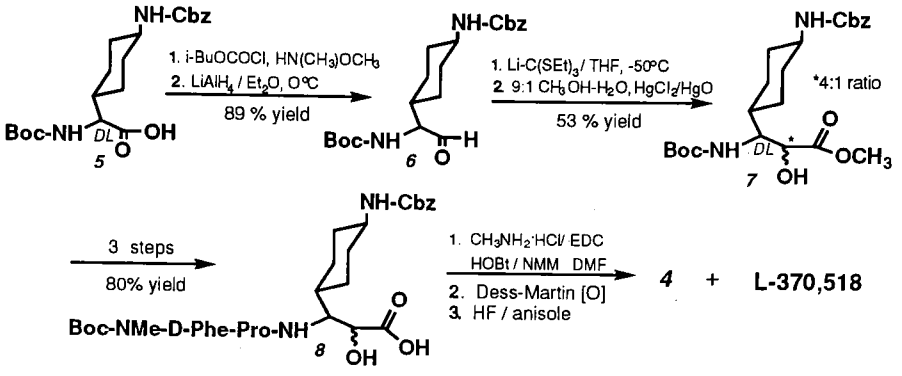

Figure 1. *Synthesis of L-370,518 from protected trans-4-aminocyclohexyl glycine.*

[7]. The C-terminal acids *1* and *2* and the *t*-Aca α-keto amide *3* were synthesized by analogous chemistry.

In summary, we have prepared the novel and highly potent thrombin inhibitor L-370,518, which is $>10^4$ selective *vs.* trypsin and several other serine proteases [5b]. As with cyclotheonamide A and similar synthetic inhibitors [3-5a, 5b], L-370,518 exhibits slow-binding kinetics. Despite the need for a relatively high dose to affect *ex vivo* clotting time (2XAPTT = 2.0 μM), L-370,518 shows efficacy comparable to that of hirudin in a rat model of arterial thrombosis [5b, 8]. This compound has proven useful for our studies of the biochemistry and therapeutic potential of thrombin inhibition.

Acknowledgment

We thank Jean F. Kaysen for preparation of the manuscript.

References

1. Tapparelli, C., Metternich, R., Ehrhardt, C. and Cook, N.S., *Trends Pharm. Sci.*, 14 (1993) 366.
2. Lyle, T.A., *Perspect. Drug Discovery Design*, 1 (1994) 453.
3. Lewis, S.D., Ng, A.S., Baldwin, J.J., Fusetani, N., Naylor, A.M. and Shafer, J.A., *Thromb. Res.*, 70 (1993) 173.
4. Iwanowicz, E.J., Lin, J., Roberts, D.G.M., Michel, I.M. and Seiler, S.M., *Bioorg. Med. Chem. Lett.*, 2 (1992) 1607.
5. (a) Brady, S.F., Sisko, J.T., Stauffer, K.J, Colton, C.D., Qiu, H., Lewis, S.D., Ng, A.S., Shafer, J.A., Bogusky, M.J., Veber, D.F. and Nutt, R.F., *Bioorg. Med. Chem.*, 3 (1995) 1063. (b) Lewis, S.D., Ng, A.S., Lyle, E.A., Mellott, M.J., Appleby, S.D., Brady, S.F., Stauffer, K.J., Sisko, J.T., Mao, S.-S., Veber, D.F., Nutt, R.F., Lynch, J.J., Cook, J.J., Gardell, S.J. and Shafer, J.A., *Thrombosis and Haemostasis*, 74 (1995) 1107.
6. Nutt, R.F., Curley, P.E., Pitzenberger, S.M., Freidinger, R.M., Saperstein, R. and Veber, D.F., in Deber, C., Hruby, V. and Kopple, K. (Eds.) 'Peptides, Structure and Function', Pierce Chemical Co., Rockford, IL 1985. p.441.
7. Mulichak, A.M. and Chen, Z.-G., Merck Research Laboratories, unpublished results.
8. Lyle, E.A., Lynch, J.J. and Cook, J.J., Merck Research Laboratories, unpublished results.

Peptides: Chemistry, Structure and Biology
Pravin T.P. Kaumaya and Robert S. Hodges (Eds.)
Mayflower Scientific Ltd., 1996

133
SAR of Margatoxin, a Potent and Selective Inhibitor of Voltage-activated Potassium Channel (Kv1.3) in Human T-cell Lymphocytes

M.A. Bednarek[1], B.A. Johnson[2], S.P. Stevens[3], R.M. Bugianesi[3], J.P. Felix[3], R.J. Leonard[3], R.S. Slaughter[3], G.J. Kaczorowski[3] and J.M. Williamson[3]

Departments of [1]Medicinal Chemistry, [2]Biophysical Chemistry and [3]Membrane Biochemistry and Biophysics, Merck Research Laboratories, P.O. Box 2000, Rahway, NJ 07065, USA

Introduction

Margatoxin (MgTX), a 39-amino acid scorpion toxin, is a potent and specific inhibitor of a voltage-gated K channel in human T lymphocytes (Kv1.3) [1].

Thr-Ile-Ile-Asn-Val-Lys-Cys-Thr-Ser-Pro-Lys-Gln-Cys-Leu-Pro-Pro-Cys-Lys-Ala-Gln-Phe-Gly-Gln-Ser-Ala-Gly-Ala-Lys-Cys-Met-Asn-Gly-Lys-Cys-Lys-Cys-Tyr-Pro-His

The toxin blocks proliferative response and production of lymphokines in T cells activated by pathways that induce a rise in $[Ca^{+2}]_i$, [2, 3]. The *in vitro* immunosuppressive properties of MgTX are similar to those of FK-506 and cyclosporine but the sites of actions are different. Development of potent and selective inhibitors of Kv1.3, which mimic the action of MgTX, might yield novel immunosuppressants useful for prevention of transplant rejection and for treatment of autoimmune disorders. An understanding of which residues of MgTX are directly involved in peptide-channel recognition should facilitate the design of small molecule mimetics of MgTX. This study describes identification of four residues, Lys28, Met30, Asn31 and Tyr37 in MgTX, involved in binding to the Kv1.3 channel.

Results and Discussion

Modifications of margatoxin were prepared either by solid phase synthesis or by recombinant techniques. The toxins were air oxidized, purified by RP HPLC [1, 4] and tested *in vitro*, in a Jurkat plasma membrane binding assay (competition against ^{125}I-MgTX binding) and a $^{86}Rb^+$ flux assay using a CHO cell line stably transfected with the human Kv1.3 channel.

Analogs of MgTX modified at the N-terminal amino (acetylation, biotinylation) and/or at C-terminal carboxyl (amidation) group were only slightly less potent than the wild type toxin, suggesting that neither N-terminal amino group nor C-terminal carboxyl group of the toxin is intimately involved in the channel recognition [4]. A series of toxins with single or multiple amino acid deletions is presented in Table 1.

Table 1. *Single and multi amino acid deletions in MgTX (activities relative to MgTX).*

Toxin															Binding Assay	Flux Assay
1				5			8		35		37		39			
Thr	Ile	Ile	Asn	Val	Lys	Cys	Thr	...	Lys	Cys	Tyr	Pro	His		1	1
-	-	-	-	-	-	-	-	...	-	-	Tyr	Pro	His		20,000	>200
-	-	-	-	-	-	-	-	...	-	-	-	Pro	His		300	47
-	-	-	-	-	-	-	-	...	-	-	-	-	His		45	44
-	-	-	-	-	-	-	-	...	-	-		Pro	-		20	20
-	-	-	-	-	-	-	-	...	-	-	Tyr	-	-		5,000	650
Thr	Ile	Ile	Asn	Val	Lys	-	-	...	-	-	Tyr	Pro	His		7,500	>400

Removal of the last three residues of MgTX, Tyr-Pro-His, drastically reduced potency of the truncated toxin (7,500-fold), implying that the three residues, or perhaps some of them, are essential for binding of MgTX to Kv1.3. Analysis of toxins with single amino acid deletion, at position 37 (Tyr) or 38 (Pro) or 39 (His), proved that Tyr37 is the most critical, of these three, for toxin-channel recognition (5,000-fold drop in binding potency). Omission of Pro38 or His39 alone destabilized toxin binding only 20-40 fold.

The sequence of MgTX was also scanned with single, conservative and non-conservative, amino acid replacements. The largest changes in potency of the modified toxins were observed for mutations in the C-terminal portion of MgTX, Table 2.

Table 2. *Single amino acid mutations of C-terminal end of MgTX (activities relative to MgTX).*

Toxin															Binding Assay	Flux Assay
	28		30		32			35			37		39			
...	Ala	- Lys	- Cys	- Met	- Asn	- Gly	- Lys	- Cys	- Lys	- Cys	- Tyr	- Pro	- His		1	1
...	-	-	-	-	-	-	-	-	-	-	-	-	Asn		25	13
...	-	-	-	-	-	-	-	-	-	-	-	-	Lys		4	14
...	-	-	-	-	-	-	-	-	-	-	-	-	Phe		30	32
...	-	-	-	-	-	-	-	-	-	-	-	Asn	-		5	5
...	-	-	-	-	-	-	-	-	-	-	Phe	-	-		1	3
...	-	-	-	-	-	-	-	-	-	-	Trp	-	-		20	114
...	-	-	-	-	-	-	-	-	-	-	Gln	-	-		300	55
...	-	-	-	-	-	-	-	-	Gln	-	-	-	-		11	9
...	-	-	-	-	-	Lys	-	-	-	-	-	-	-		0.1	1
...	-	-	-	-	Gly	-	-	-	-	-	-	-	-		1200	327
...	-	-	-	Ile	-	-	-	-	-	-	-	-	-		45	7
...	-	-	-	Gln	-	-	-	-	-	-	-	-	-		50	2
...	-	Gln	-	-	-	-	-	-	-	-	-	-	-		1750	445

Non-conservative changes at position 37 (Tyr) significantly destabilized binding of the mutants to Kv1.3, Table 2. Equally large changes in potency were observed for modifications at Asn31 and Lys28. Substitutions at Met30, however, only moderately

affected potency of the analogs. Mutations at other positions of the toxin yielded compounds with activities similar to an unmodified MgTX. It appears that the spatially separated Lys28, Asn31, Tyr37 are the crucial anchoring residues of MgTX, and Met30 is an auxiliary residue, vital for an efficient binding of the toxin to Kv1.3. Probably, upon binding, they are in a direct contact with the pore region of Kv1.3. These residues are chemically distinct, from a positively charged Lys28 to a hydrophobic Met30 or Tyr37, suggesting that the high affinity of MgTX for Kv1.3 derives both from the electrostatic and hydrophobic interactions. Previously, Miller *et al.* noticed similar effects of C-terminal mutants of charybdotoxin (ChTX) analyzed for interaction with either Shaker or Maxi K channels [5, 6]. These workers identified Lys27, Met29, Asn30, Arg34 and Tyr36 of ChTX as critical residues for efficient binding of the toxin to the Shaker channel and Ser10, Trp14, Arg25, Lys27, Met29, Asn30, Arg34 and Tyr36 for interaction with the Maxi K channel.

NMR structure of MgTX has shown that, in solution, the C-terminal part of MgTX forms two strands of an antiparallel β-sheet, on which the four essential residues are located [7]. Similarly, as for ChTX-Shaker channel (or Maxi K channel) interactions, the β-sheet of MgTX appears to form the contact surface of the toxin with Kv1.3. In solution, the antiparallel strands of MgTX are maintained rigid by three disulfide bridges. A cyclic peptide, cyclo(Cys-Gly-Ala-Lys-Ala-Met-Asn-Gly-Lys-Ala-Lys-Ala-Tyr-Cys), which encompasses these strands but lacks the disulfide scaffold, has no detectable inhibitory activity. Apparently, the high conformational flexibility of the cyclic peptide effectively disrupts the intimate contacts of the critical residues with a vestibule of the channel's pore and precludes efficient binding of the peptide.

Not surprisingly, also, a MgTX with all Cys residues replaced by Ala residues and short, linear, overlapping peptides spanning the entire sequence of MgTX, did not show any activity even at 10 μM peptide concentration. Only the N-terminal peptide, 1-11 fragment of MgTX, demonstrated some ability to block Kv1.3 but this peptide was 25,000-fold less efficient than MgTX.

References

1. Garcia-Calvo, M., Leonard, R.J., Novick, J., Stevens, S.P., Schmalhofer, W., Kaczorowski, G.J. and Garcia, M.L., *J.Biol.Chem.*, 268 (1993) 18866.
2. Lin, C.S., Boltz, R.C., Blake, J.T., Nguyen, M., Talento, A., Fischer, P.A., Springer, M.S., Sigal, N.H., Slaughter, R.S., Garcia, M.L., Kaczorowski, G.J. and Koo, G.C., *J. Exp. Med.*, 177 (1993) 637.
3. Leonard, R.J., Garcia, M.L., Slaughter, R.S. and Reuben, J.P., *Proc. Natl. Acad. Sci. USA*, 89 (1992) 10094.
4. Bednarek, M.A., Bugianesi, R.M., Leonard, R.J. and Felix, J.P., *Biochem. Biophy. Res. Commun.*, 198 (1994) 619.
5. Stempe, P., Kolmakova-Patensky, L. and Miller, C., *Biochemistry*, 33 (1994) 443.
6. Goldstein, S.A.N., Pheasant, D.J. and Miller, C., *Neuron*, 12 (1994) 1377.
7. Johnson, B.A., Stevens, S.P. and Williamson, J.M., *Biochemistry*, 33 (1994) 15061.

Peptides: Chemistry, Structure and Biology
Pravin T.P. Kaumaya and Robert S. Hodges (Eds.)
Mayflower Scientific Ltd., 1996

134
Small Molecule Inhibitors of the Leukocyte Integrin VLA-4

T. Arrhenius, A. Chiem, M. Elices, Y.-B. He, L. Jia, A. Maewal, D. Müller and F. Gaeta

Cytel Corporation, San Diego, CA, 92121, USA

Introduction

The integrin VLA-4 (also known as $\alpha 4\beta 1$ and CD49d/CD29) is a cell adhesion molecule which has been implicated in the process of leukocyte trafficking at sites of inflammation [1, 2]. This trafficking is mediated by the interaction of VLA-4 with its ligands, alternatively spliced fibronectin (CS-1 fibronectin) [3, 4] and the vascular cell adhesion molecule VCAM-1 [5-7]. VLA-4 is generally expressed on T-cells, B-cells, eosinophils and monocytes, precisely those cells which are involved in chronic inflammatory responses. The blockade of VLA-4 mediated cell adhesion would, therefore, appear to be an attractive therapeutic approach to the treatment of chronic inflammatory diseases. Such blockade could be accomplished by small molecule mimics of VLA-4 ligands. In the present study, small, high affinity VLA-4 binding molecules are developed, their ability to competitively inhibit VLA-4 mediated cell adhesion is examined, and efficacy in animal models of disease is assessed.

Results and Discussion

Alternatively spliced forms of fibronectin, containing the CS-1 fragment (Figure 1) bind to VLA-4. The VLA-4 binding motif is contained within the C-terminal 10 amino acid portion of this molecule [3, 4]. This peptide sequence served as a convenient starting point for the discovery of small molecule CS-1 mimics.

DELPQLVTLPHPNLHGPEILDVPST

Figure 1. *CS-1 fragment of fibronectin.*

To precisely define the location of the VLA-4 recognition site, truncation analysis of CS-1 derived peptides was performed. The core binding region of CS-1 was thus determined to be the pentapeptide ILDVP (Table 1).

Having identified the minimal CS-1 derived peptide, capable of inhibiting VLA-4 mediated cell adhesion, the influence of single amino acid substitutions on inhibitory potency was examined. It was found that, with the exception of aspartic acid, each of the residues in the pentapeptide ILDVP could be substituted by a variety of amino acids without significantly decreasing the VLA-4 binding affinities. In some instances, these

Table 1. *Inhibitory potency of truncated CS-1 peptides.*

Sequence	IC_{50}(μM)
GPEILDVPST	150
ILDV	> 10,000
LDVP	> 10,000
ILDVP	250

IC_{50} for the inhibition of binding of VLA-4 expressing cells to CS-1.

substitutions resulted in enhanced binding affinity. By combining the most favorable amino acid substitutions in a single peptide, FLDFp (IC_{50} = 25 μM, p designates D-proline amide), a 10 fold improvement in VLA-4 binding affinity could be achieved.

In order to further enhance the VLA-4 binding affinities of these peptides and to protect them from exopeptidase degradation, the replacement of the carboxy and amino terminal residues by non-amino acid moieties was examined. As shown in Tables 2, molecules with much improved inhibitory potencies were synthesized.

Table 2. *Modifications at termini.*

Modification	IC_{50} (μM)
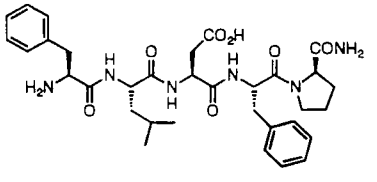	8.9
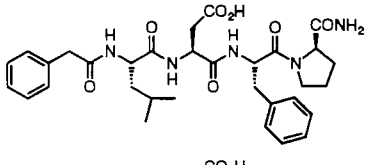 (compound 1)	0.5
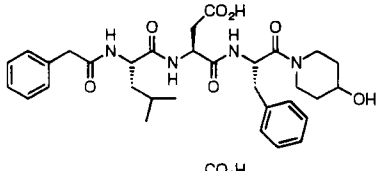	0.3
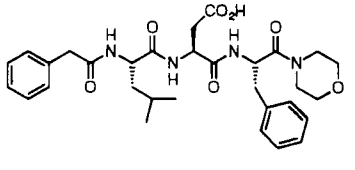	0.2

IC_{50} for the inhibition of binding of VLA-4 expressing cells to CS-1

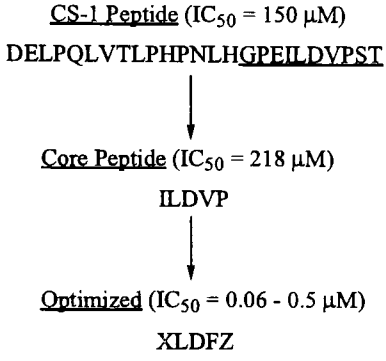

Figure 2. *Optimization summary.*

At an early stage in our discovery program, compound **1** (Table 2) was chosen for testing in animal models of disease. Efficacy was demonstrated in several different animal models, including delayed-type hypersensitivity in mice, asthma in rabbit and sheep, and arteriopathy in rabbit.

In conclusion, using CS-1 fibronectin as a starting point for our drug discovery effort, we have developed a series of high affinity VLA-4 antagonists (Figure 2). These compounds show efficacy in several animal models of disease.

Acknowledgments

We are indebted to Dr. C. Chen, P. Pushpavanam,, S. Tamaraz, Dr. J. Metzger, Dr. W. Abraham, Dr. S. Molossi, Dr. M. Rabinovitch, Dr. J. Paulson, and D. Strahl for their invaluble contributions to this project.

References

1. Hemler, M.E., *Ann. Rev. Immunol.*, 8 (1990) 365.
2. Hemler, M.E., Elices, M.J., Parker, C. and Takada, Y., *Immunol. Rev.*, 114 (1990) 45.
3. Wayner, E.A., Garcia-Pardo, A., Humphries, M.J., McDonald, J.A. and Carter, W.G., *J. Cell Biol.*, 109 (1989) 1321.
4. Guan, J.L. and Hynes, R.O., Cell, 60 (1990) 53.
5. Elices, M.J., Osborn, L., Takada, Y., Crouse, C., Luhowskyj, S., Hemler, M.E. and Lobb, R.R., *Cell,* 60 (1990) 577.
6. Rice, G.E., Munro, J.M. and Bevilacqua, M.P., *J. Exp. Med.*, 171 (1990) 1369.
7. Schwartz, B.R., Wayner, E.A., Carlos, T.M., Ochs, H.D. and Harlan, J.M., *J. Clin. Invest.*, 85 (1990) 2019.

Peptides: Chemistry, Structure and Biology
Pravin T.P. Kaumaya and Robert S. Hodges (Eds.)
Mayflower Scientific Ltd., 1996

135

Conantokin G Mimetics as Modulators of the NMDA Receptor: Localization of the Regions and Conformations Responsible for Agonist, Partial Agonist, and Antagonist Activity

M.-L. Maccecchini[1], L.-M. Zhou[1,2], P. Skolnick[2], G.I. Szendrei[3], K. Valentine[4], S.J. Opella[4] and L. Otvos, Jr.[1,3]

[1]Symphony Pharmaceuticals, Malvern, PA 19355, USA
[2]Laboratory of Neuroscience, National Institutes of Health, Bethesda, MD 20892, USA
[3]The Wistar Institute and [4]Department of Chemistry, University of Pennsylvania, Philadelphia, PA 19104, USA

Introduction

Conantokin G (ConG) is a heptadekapeptide that acts as N-methyl D-aspartate (NMDA) antagonist [1]. Neurochemical studies indicate ConG to be a non-competitive inhibitor of the positive modulatory effects of polyamines at NMDA receptors [2]. The presence of five carboxyglutamic acid residues and the unusual high level of helicity in aqueous solution [3] render this peptide ideal for structure- and conformation-activity analyses. In the current study, ConG analogs were synthesized with Ala, Ser, and Ser(P) substituted for Gla in order to assess the contribution of individual Gla residues to biological activity and secondary structure of:

H-Gly-Glu-*Gla*-*Gla*-Leu-Gln-*Gla*-Asn-Gln-*Gla*-Leu-Ile-Arg-*Gla*-Lys-Ser-Asn-NH_2.

Results and Discussion

The conformation of ConG and its analogs was characterized by two-dimensional NMR and CD experiments in aqueous solution and several model membrane environments. A three-dimensional structure resulted from a simulated annealing protocol based on 196 NOEs and 6 dihedral constraints measured in two-dimensional experiments. According to the NMR data, the structure of ConG consists of a loose helix near the amino terminus and a well-formed helix at residues 6 though 15 with the two C-terminal residues in a loose helix. The model membrane environments of 50% TFE and dodecylphosphocholine micelles had little effect on the peptide structure. In contrast, the calculated helix content of ConG and its analogues is markedly increased in 50% TFE, as determined by the CD ellipticity values (Table 1) at 208 nm. The aqueous CD spectra of ConG and its analogues are characterized with a positive band at 188 nm, and with negative bands at

204 and 224 nm, reminiscent to type C CD spectra, and type I (III) β-turns or 3_{10} helices as the dominant conformation. Ala substitutions were made to stabilize the hypothetical α-helical structure, Ser substitutions to stabilize the non-α-helical conformation, and phosphoSer substitutions to reveal the effects of the above-average negative charge of Gla. As Table 1 shows, the synthetic ConG analogs exhibited a wide spectrum of NMDA modulatory properties ranging from increased antagonism through partial agonism to inactivity. Gla^{10} and Gla^{14} residues could be replaced without a major alteration of the biological activity. While substitution of Gla in position 3 resulted in peptide analogues with partial agonist actions, substitutions in position 4 resulted in inactive peptides. The Ala^7 derivative of ConG was approximately four times more potent than the parent peptide, both as an inhibitor of spermine-enhanced [^{3}H]MK-801 binding (IC_{50} = 45 nM) and of NMDA-stimulated increases in cyclic GMP levels (IC_{50} = 77 nM) in cerebellar granule cells. Electrophysiological studies show that ConG is specific for the NR1/NR2B subtype of the NMDA receptors and has no effect on the NR1/NR2A or NR1/NR2C combinations [4]. Our findings permit us to "dial in" the desired level of agonist or antagonist activity and design modified peptides and mimetic molecules that preserve the affinity, activity, and receptor subtype selectivity of the original peptide.

Table 1. *Effects of ConG and its derivatives on spermine-enhanced [^{3}H]MK-801 binding and comparison with α-helical content in water*[a].

Peptide	Inhibition	Efficacy	Helix content in	
	% $Spermine_{max}$	% $Spermine_{max}$	H_2O	50% TFE
CongG	100	0	31	77
Ala^3-ConG	100	0	34	69
Ser^3-ConG	23	62	48	93
phosphoSer^3-ConG	34	68	56	90
Ala^4-ConG	0	0	45	68
Ser^4-ConG	0	0	51	68
phosphoSer^4-ConG	0	0	27	72
Ala^7-ConG	100	0	41	88

[a]The rest of the 7- as well as all of the 10- and 14-substituted analogues exhibited NMDA inhibitory activity very similar to that of unmodified ConG.

References

1. Haack, J., Rivier, J., Parks, T., Mena, E., Cruz, L.J. and Olivera, B.M., *J. Biol. Chem.*, 265 (1990) 6025.
2. Chandler, P., Pennington, M., Maccecchini, M.-L., Nashed, N.T. and Skolnick, P., *J. Biol. Chem.*, 268 (1993) 17173.
3. Myers, R.A., McIntosh, J.M., Imperial, J., Williams, R.W., Oas, T., Haack, J.A., Hernandez, J.-F., Rivier, J., Cruz, L.J. and Olivera, B.M., *J. Toxicol. Toxin Rev.*, 9 (1990) 179.
4. Williams, K., University of Pennsylvania, unpublished data.

Peptides: Chemistry, Structure and Biology
Pravin T.P. Kaumaya and Robert S. Hodges (Eds.)
Mayflower Scientific Ltd., 1996

136

Core Domain of *Hirudinaria Manillensis* Hirudin: Chemical Synthesis, Purification and Characterization of Trp-3 Analog of Fragment 1-47

V. De Filippis, A. Vindigni, L. Altichieri and A. Fontana

CRIBI Biotechnology Centre, University of Padua, Via Trieste 75, 35121 Padua, Italy

Introduction

Leech hirudins are the most potent and specific inhibitors of thrombin so reported, with an inhibition constant (K_I) as low as 22 fM [1]. NMR studies conducted on hirudin HV1 from *Hirudo medicinalis* [2] revealed that it is composed of a compact N-terminal region (core) domain, crosslinked by three disulfide bridges, and a flexible C-terminal tail. A novel hirudin (variant HM2) has been recently isolated from *Hirudinaria manillensis* and efficiently expressed in *E. coli*. Hirudin HM2 shows 75% sequence identity with the HV1 variant and similarly high thrombin inhibitory activity (K_I = 0.78 pM) [1]. We have previously shown that the N-terminal proteolytic fragment 1-47 of hirudin HM2 maintains anti-thrombin activity [1]. Here we report the solid phase chemical synthesis of an analog of fragment 1-47 bearing a $Tyr^3 \rightarrow Trp$ exchange (Y3W analog) (Figure 1).

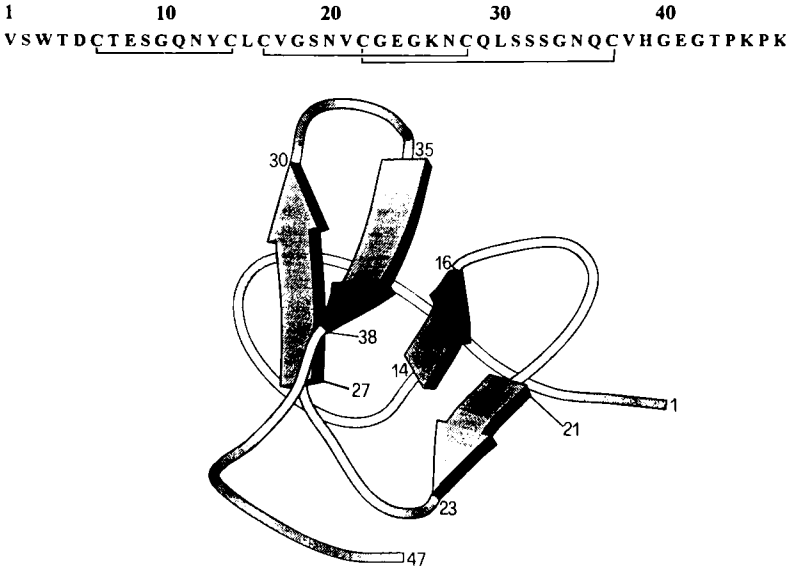

Figure 1. *(Top) Amino acid sequence of the Y3W analog of the N-terminal fragment 1-47 of hirudin HM2[1]. (Bottom) Schematic representation of the 3D structure of natural fragment 1-47.*

Results and Discussion

The crude, reduced peptide was purified by RP-HPLC and subjected to oxidative folding to the disulfide crosslinked species (Figure 2). The folding process of the Y3W analog was highly efficient (~90%). The overall final yield of the synthetic product was ~35% and its identity and homogeneity established by a number of analytical techniques (RP-HPLC, HPCE, MS). The unique alignment of the three disulfide bridges of the Y3W analog was established by enzymatic peptide mapping and shown to be identical to that of the natural fragment.

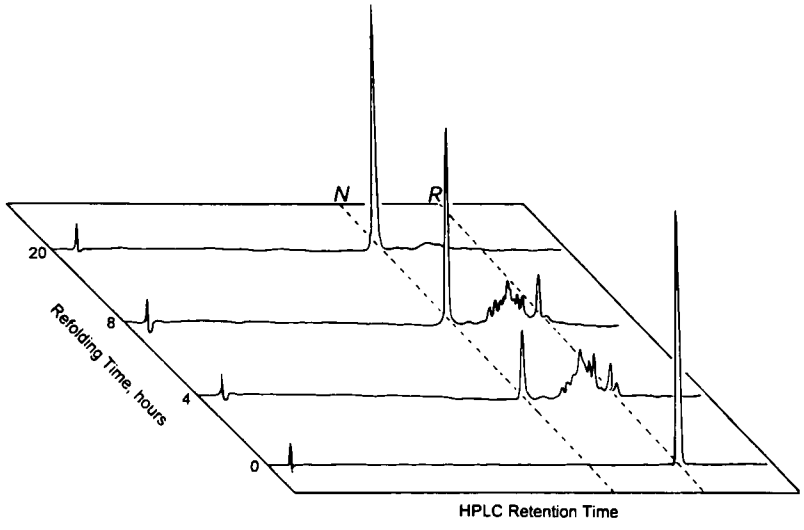

Figure 2. *Oxidative folding of synthetic Y3W analog. Native (N) and reduced (R) peptide species.*

The Y3W analog essentially retains the conformational and stability properties of the natural species and is approximately five-fold more active (K_I = 30 ± 5 nM) than the natural fragment 1-47 (K_I = 150 ± 20 nM) in inhibiting thrombin. Of interest, the difference in the free energy of binding to thrombin at 37°C, $\Delta\Delta G_b$, between the Y3W analog and natural species (4.2 $kJ.mol^{-1}$) was that expected for the difference in hydrophobicity between the two polypeptides resulting from the Tyr→Trp exchange. The results of this study indicate that solid-phase chemical synthesis represents a convenient and high-yield procedure to prepare analogs of the biologically active, N-terminal core domain of hirudin with improved functional properties.

References

1. Vindigni, A., De Filippis, V., Zanotti, G., Visco, C., Orsini, G. and Fontana, A., *Eur. J. Biochem.*, 226 (1994) 323.
2. Folkers, P.J.M., Clore, G.M., Driscoll, P.C., Dodt, J., Kohler, S. and Gronenborn, A.M., *Biochemistry*, 28 (1992) 2601.

Peptides: Chemistry, Structure and Biology
Pravin T.P. Kaumaya and Robert S. Hodges (Eds.)
Mayflower Scientific Ltd., 1996

137
Somatostatin-based Neuromedin B Receptor Antagonists: Dissociation of Neuromedin B and Somatostatin Receptor Binding

D.H. Coy[1], N-Y. Jiang[1] and J.E. Taylor[2]

[1]Peptide Research Laboratories, Department of Medicine, Tulane University Medical Center, New Orleans, LA 70112, USA
[2]Biomeasure, Inc., Milford, MA 01757, USA

Introduction

Neuromedin B (NMB), *G-N-L-W-A-T-G-H-F-M-*NH_2, is a bombesin/gastrin releasing peptide-related peptide possessing unique receptors with different tissue distributions and biological actions relative to the latter [1]. None of the many extremely potent types of competitive receptor antagonists developed for the bombesin/GRP [2] receptor have retained much affinity for NMB receptors. However, large scale screening of a family of cyclic somatostatin (SRIF) analogs recently revealed [3, 4] several with appreciable affinity for NMB receptors present both in transfected cells and rat olfactory bulb tissue. The most potent of these was *D-Nal-Cys-Tyr-D-Trp-Lys-Val-Cys-Nal-*NH_2, which binds with a Ki of 47 nM, inhibits NMB-induced IP production (IC_{50} 32 nM) and effectively blocks some behavioral actions of NMB [5]. However, this peptide retains much higher affinity (Ki 0.84 nM) for SSTR2 receptors on pancreatic AR42J cells where it functions as a full agonist, thus complicating its use in basic physiological studies. Additional analog studies have now been undertaken in an effort to reduce or eliminate affinity for SRIF receptors. The most successful of these involved modifications to the Lys side-chain in the recognized active site sequenceof the cyclic octapeptide SRIFs, -D-Trp-Lys-.

Results and Discussion

Several of the cyclic SRIF octapeptides have previously been found to have high affinity for μ-opiate receptors [5]. It was possible [6] to completely dissociate these properties from traditional SRIF effects, in particular by modifications to Lys in position 5. In the present study, replacement of Lys by Orn (side-chain shortened by 1 CH_2 group) resulted in good retention of NMB receptor affinity (Table 1) but in more than a 50-fold loss of SRIF receptor affinity. Further side-chain shortening by another CH_2 using a α,γ-diaminobutyric acid (Dab) substitution was even more succesful in dissociating affinities since SRIF receptor affinity decreased by more than 1000-fold. The continued necessity for a basic group on the side-chain group was, however, apparent from the loss

of affinity with an Ala substituted analog but continued retention of binding with an Arg substitution. In addition, all active peptides were able to block NMB-stimulated inositol phosphate production with IC_{50} values in agreement with the binding data (Table 1) and all had little affinity for the bombesin/GRP receptor.

Table 1. *Affinities of new cyclic somatostatin analogs for NMB and GRP receptors on transfected cells and SSTR2 receptors on pancreatic AR42J cells. Binding data for SRIF, NMB and GRP are shown for comparison.*

Peptide Ki	NMB IC_{50} (nmole)	IP_3 Ki	GRP Ki	SRIF
SRIF	>1000	-	>10000	0.86
NMB	1.1[a]	-	19	>10000
GRP	297[a]	-	1.8	>10000
DNalCysTyrDTrpLysValCysNalNH$_2$	46.8	31.7	2867	0.84
DNalCysTyrDTrpOrnValCysNalNH$_2$	65.0	60.2	>10000	54.2
DNalCysTyrDTrpDabValCysNalNH$_2$	43.8	39.1	2921	1032
DNalCysTyrDTrpArgValCysNalNH$_2$	80.3	45.0	2632	407
DNalCysTyrDTrpAlaValCysNalNH$_2$	>1000	-	>1000	>1000

[a]Data from rat olfactory bulb tissue binding.

In view of the demonstrated effectiveness of the Orn analog to block some of the well-known effects of NMB [5] on appetite in the rat, it is expected that the new Dab analog will be an even more useful tool for investigating physiological functions of NMB since possible side-effects due to interaction with SRIF receptors should be largely eliminated.

Acknowledgment

This research was supported in part by NIH grant CA-45153.

References

1. Wada, E., Way, J., Shapira, H., Kusano, K., Lebacq-Verhayden, A.M., Coy, D.H., Jensen, R.T and Battey, J., *Neuron,* 6 (1991) 421.
2. Jensen, R.T. and Coy, D.H., *Trends Pharm. Sci.*, 12 (1991) 13.
3. Orbuch, M. J.E. Taylor, J.E., Coy, D.H., Mrozinski, J.E., Mantey, S., Battey, J.F., Moreau, J-P. and Jensen, R.T., *Mol. Pharmacol.*, 44 (1993) 841.
4. Coy, D.H., Taylor, J., Moreau, J-P., Jiang, N-Y.,Orbuch, M., Mrozinsky, J., Mantey, S. and Jensen, R.T. in Hodges, R.S. and Smith, J.A. (Eds.) 'Peptides: Chemistry, Structure and Biology', ESCOM, Leiden, The Netherlands, 1994, p. 496.
5. Ladenheim, E.E. , Taylor, J.E. Coy, D.H. and Moran, T.H., *Eur. J. Pharmacol.*, 271 (1994) R7.
6. Walker, J.M., Bowen, W.D., Akins, S.T., Hemstreet, M.K. and Coy, D.H., *Peptides,* 8 (1987) 869.

Peptides: Chemistry, Structure and Biology
Pravin T.P. Kaumaya and Robert S. Hodges (Eds.)
Mayflower Scientific Ltd., 1996

138
Conformational Re-addressing of Peptides towards Interactions with Other Specific Receptors

G.V. Nikiforovich[1], S.A. Kolodziej[2], W.-J. Zhang[2], B. Nock[3], N. Bernad[4], J. Martinez[4] and G.R. Marshall[1,2]

[1]Center for Molecular Design and Departments of [2]Pharmacology and [3]Psychiatry, Washington University, St. Louis, MO 63130, USA
[4]Chimie et Pharmacologie de Molécules d'Intérêt Biologique, Faculté de Pharmacie, 34060 Montpellier, France

Introduction

To induce potent and selective peptide-receptor interactions, "message" functional groups of a ligand should be spatially arranged to satisfy a specific 3D "address" of receptor. In this way, almost any peptide containing corresponding "message" elements could be modified to bind a receptor with known 3D "address". To demonstrate this, conformationally constrained analogs were designed starting from the sequences of cholecystokinin and angiotensin fragments (CCK-8,Asp-**Tyr**-Met-Gly-**Trp**-Met-Asp-Phe-NH_2 and AT 4-8, **Tyr**-Val-His-Pro-**Phe**). The aim was to target δ-opioid receptor ("message" elements are shown in bold).

Results and Discussion

The basic idea for the design was to find conformational constraints which would force functional groups constituting the "message", to adopt the "address" spatial arrangement. The amino acid sequence of CCK-8 resembles the sequence of DPDPE in that the "message" residues in both sequences are separated by a Xxx-Gly dipeptide fragment. Accordingly, it was relatively easy to design the **Tyr**-*cyclo*(D-Pen-Gly-**Trp**-L/D-3-*trans*-mercaptoproline)-Asp-Phe-NH_2 sequences (compounds **1a** and **1b**, respectively), using 3-mercaptoproline, which is a "chimeric" residue combining features of penicilamine and proline. In the AT sequence, however, the "message" residues are separated by the tripeptide fragment. There is no way to "squeeze" the backbone of the pentapeptide AT 4-8 fragment to accommodate the template conformation of the **Tyr**-D-Pen-Gly-**Phe** tetrapeptide backbone. It was possible, however, to constrain the Tyr^4 and Phe^8 side chains of a modified AT 4-8 fragment into the required spatial positions by re-directing the peptide backbone of AT 5-8 not along the "backbone", but along the "disulfide" side of DPDPE cyclic moiety. In this way, after several unsuccessful attempts, sequences of the **Tyr**-*cyclo*(D-Cys-Xxx-4-*cis*-mercaptoproline)-D-**Phe** type (Xxx = Gly, D-Ala, D-His, compounds **2a**, **2b** and **2c**, respectively) were designed using 4-mercaptoproline, which is a "chimeric" residue combining features of homocysteine and proline. After extensive energy calculation studies, each of the

low-energy conformers for compounds **1a**, **1b** and **2a** was compared with the models of the δ-receptor-bound conformation of DPDPE [1] by overlapping the nitrogen atom of α-amino group; the C^{γ} and C^{ζ} atoms of the Tyr and Phe aromatic rings; and the C^{α} atom of the residue in position 2. Low-energy 3D structures, which were compatible with the model in question, were found for each compound.

All compounds were tested for their binding to μ-, δ- and κ-types opioid receptors (Table 1). Except in one instance(compound **2c**), the designed compounds are able to bind to δ-opioid receptors with affinity and selectivity comparable to DPDPE. The loss of affinity for compound **2c** could be attributed to the presence of an extra aromatic ring (the imidazole moiety of the D-His residue), which might compete for the same receptor binding sites with the Tyr/Phe side chains, not bearing the same "message" information.

Table 1. *Results of binding assays for different types of opioid receptors.*

Compound *		K_i (nM)		
		Receptor Type		
		δ	μ	κ
	Tyr-*cyclo*(D-Pen-Gly-**Phe**-D-Pen)(DPDPE)	1.7	576	>5,000
(1a)	**Tyr**-*cyclo*(D-Pen-Gly-**Trp**-L-3-Mpt)-Asp-Phe-NH_2	4.5	>5,000	>5,000
(1b)	**Tyr**-*cyclo*(D-Pen-Gly-**Trp**-D-3-Mpt)-Asp-Phe-NH_2	19.0	226	>5,000
(2a)	**Tyr**-*cyclo*(D-Cys-Gly-L-4-Mpc)-D-**Phe**	11.6	>100**	>1000**
(2b)	**Tyr**-*cyclo*(D-Cys-D-Ala-L-4-Mpc)-D-**Phe**	42.0	>100**	>1000**
(2c)	**Tyr**-*cyclo*(D-Cys-D-His-L-4-Mpc)-D-**Phe**	>100*	>100**	>1000**

* Mpt and Mpc are *trans*- and *cis*-mercaptoprolines, respectively.

** No competition with standard labeled compounds at that concentration.

The results are consistent with the concept that the "message" information is associated with particular functional groups of the peptide molecule, and the "address" with their relative three-dimensional arrangement. The study confirms the validity of the three-dimensional δ-opioid pharmacophore model proposed earlier [1], emphasising the importance of using reliable pharmacophore models as templates for rational design. In our case, we have demonstrated that conformational constraints compatible with the proper three-dimensional template ensure highly potent and selective interaction with δ-opioid receptors for virtually any peptide sequence of the Tyr-$(Xxx)_n$-Phe... type, where n = 1, 2, 3. Opioid peptides with n = 3 have not been described previously. Finally, our results open the way to peptidomimetics for δ-opioid (and other) receptors. Indeed, there is no need to mount the "message" groups on scaffolds of peptidic nature. Almost any other scaffold would suffice, provided it stabilizes the "message" groups in the correct "address" spatial arrangement. This approach would yield "true" peptidomimetics, competing with the parent bioactive peptides for the same receptor sites.

Reference

1. Nikiforovich, G.V., Hruby, V.J., Prakash, O. and Gehrig, C.A., *Biopolymers,* 31 (1991) 941.

Peptides: Chemistry, Structure and Biology
Pravin T.P. Kaumaya and Robert S. Hodges (Eds.)
Mayflower Scientific Ltd., 1996

139
New Bradykinin Antagonists Having High Potency at Both B1 and B2 Receptors

L. Gera[1], J.M. Stewart[1], E. Whalley[2], W. Hanson[2] and R. McCullough[2]

[1]Department of Biochemistry, Biophysics and Human Genetics
University of Colorado School of Medicine, Denver, CO 80262, USA
[2]Cortech, Inc., Denver, CO 80221, USA

Introduction

Biological actions of bradykinin (Arg-Pro-Pro-Gly-Phe-Ser-Pro-Phe-Arg; BK) are mediated by at least two classes of receptors, B1 and B2, both of which are G-protein coupled receptors. Most physiological functions of BK and also those involved in acute inflammation are mediated by B2 receptors, which are expressed constitutively. The gene for B1 receptors, normally not expressed in most tissues, is induced in chronic inflammation. B2 receptors require the full BK sequence, including both N-terminal and C-terminal arginines, for effective activation, whereas the preferred ligand for B1 receptors is BK-(1-8). B1 receptors were first identified in damaged tissue. B1 antagonists, for example [Leu^8]-BK-(1-8), are characterized by having an aliphatic residue in position 8. The "first generation" B2 antagonists, for example D-Arg-[Hyp^3,Thi^{5,8}, D-Phe^7]-BK, had low potency and short action *in vivo* [1]. The "second generation" antagonists came from investigators at Hoechst, who modified our best antagonist by using D-Tic (tetrahydroisoquinoline-3-carboxylic acid) at position seven, and Oic (octahydroindole-2-carboxylic acid) at position eight. This antagonist, known as HOE-140, was the first to have sufficiently high receptor affinity and *in vivo* lifetime to be investigated as a drug. Many studies with this antagonist have demonstrated the participation of BK in many normal and abnormal physiological processes [2]. One surprising result was that, in spite its high potency and long duration of action, HOE-140 was not effective in the later stages of chronic inflammation. Addition of B1 antagonists in these studies demonstrated the participation of B1 receptors in sustained inflammation.

Recently we have synthesized α-(2-indanyl)-glycine (Igl) and N-(2-indanyl)-glycine and incorporated them into several positions of our standard BK antagonist structure. The best of these new antagonists, D-Arg-[Hyp^3,Igl^5,D-Igl^7,Oic^8]-BK, known as B9430, is a representative of the new "third generation" of BK antagonists. Although this antagonist has the highest potency and longest duration of action *in vivo* against B2 receptors of any known antagonist, its unique feature is that it is an excellent antagonist for B1 receptors as well. It blocks both the early and late stages of inflammation in animal models. Examples of these new antagonists are given in Table 1.

Table 1. *Structures and activities of selected bradykinin antagonists.*

Number	Structure	Biological Activities		
		RUT	GPI	RA
B9430	DArg-Arg-Pro-Hyp-Gly-Igl-Ser-DIgl-Oic-Arg	10.0	8.6	6.5
B9340	DArg-Arg-Pro-Hyp-Gly-Thi-Ser-DIgl-Oic-Arg	8.9	8.6	6.9
B9464	DArg-Arg-Pro-Hyp-Gly-DThi-Ser-DIgl-Oic-Arg	8.5	6.0	0.0
B9456	DArg-Arg-Pro-Hyp-Gly-DIgl-Ser-DIgl-Oic-Arg	8.6	8.0	0.0
B9616	DArg-Arg-Pro-Hyp-Gly-Igl-Thr-DIgl-Oic-Arg	8.0	7.0	---
B9588	DArg-Arg-Pro-Hyp-Gly-Igl-Lys-DIgl-Oic-Arg	7.8	7.6	---
B9686	Arg-Arg-Pro-Hyp-Gly-Igl-Ser-DIgl-Oic-Arg	8.0	7.5	---
B9480	DArg-Arg-Pro-Hyp-Gly-Igl-Ser-DIgl-Cpg-Arg	7.8	6.8	---
B9330	DArg-Arg-Pro-Hyp-Gly-Thi-Ser-DTic-Nig-Arg	8.3	7.2	0.0
B8974	DArg-Arg-Pro-Hyp-Gly-Cpg-Ser-DCpg-Igl-Arg	7.4	7.2	6.4
B9226	DArg-Arg-Pro-Hyp-Gly-Phe-Ser-DIgl-Oic-Arg	7.8	7.6	6.8
B9228	Aca-DArg-Arg-Pro-Hyp-Gly-Phe-Ser-DIgl-Oic-Arg	8.7	7.4	5.9
B9224	Aca-DArg-Arg-Pro-Hyp-Gly-Thi-Ser-DIgl-Oic-Arg	8.7	8.6	6.6
B9256	Aaa-DArg-Arg-Pro-Hyp-Gly-Thi-Ser-DIgl-Oic-Arg	8.2	7.8	6.2
B9324	Dhq-DArg-Arg-Pro-Hyp-Gly-Thi-Ser-DIgl-Oic-Arg	8.1	7.2	---
B9334	Sin-DArg-Arg-Pro-Hyp-Gly-Thi-Ser-DIgl-Oic-Arg	8.3	7.3	---

Cpg -α-Cyclopentylglycine; Igl -α-(2-Indanyl)-glycine; Nig - N-(2-indanyl)-glycine; Oic - Octahydroindole-2-carboxylic acid; Thi - β-2-Thienyl-alanine; Tic - 1,2,3,4-Tetrahydroisoquinoline-3-carboxylic acid; Aaa - Adamantaneacetyl-; Aca - Adamantane carboxyl-; Dhq - 2-Dehydroquinuclidine-3-carboxyl-; Sin - Sinapinyl-(3,5-dimethoxy-4-hydroxycinnamyl-). RUT - isolated rat uterus (B2); GPI - isolated guinea pig ileum (B2); RA - isolated rabbit aorta (B1). Potencies are given as the pA_2.

These BK antagonists show very long duration of action *in vivo*; the effect of B9430 lasts more than four hours in the rat and dog. They appear to be indefinitely stable on exposure to human plasma and tissue homogenates. They show very high affinity for human B1 and B2 BK receptors.

These are the first B1 antagonists having an intact C-terminal arginine. The reason for the B1 potency of these antagonists is not known. Because of their combined B2 - B1 activity, these antagonists represent a new generation of BK antagonists having the broadest known spectrum of activity.

Acknowledgments

This work was aided by NIH grant HL-26284. We thank Robin Reed and Paul A. Bury for assistance with chemistry, and Frances Shepperdson for the assays.

References

1. Stewart, J.M. and Vavrek, R.J., in Burch, R.M. (Ed.), in 'Bradykinin Antagonists', Pergamon, Oxford, UK,, 1991, p 51.
2. Bhoola. K., Figueroa, C.D. and Worthy, K., *Pharmacol. Rev.*, 44 (1992) 1.

Peptides: Chemistry, Structure and Biology
Pravin T.P. Kaumaya and Robert S. Hodges (Eds.)
Mayflower Scientific Ltd., 1996

140
Modeling of the δ-Opioid Receptor Transmembrane α-Bundle

I.D. Pogozheva, A.L. Lomize and H.I. Mosberg

College of Pharmacy, University of Michigan, Ann Arbor, MI 48109, USA

Introduction

The δ-opioid receptor belongs to the large family of G-protein coupled receptors (GPCRs), transmembrane proteins which transduce external signals to the activation of G-proteins. All members of the rhodopsin-like GPCR family share the common spatial structure of the transmembrane 7-α-bundle, which represents the most evolutionarily conserved part of these receptors.

A new approach for GPCR structure modeling originates from the observation that the content of hydrophilic residues in the GPCR family is unusually high for membrane proteins. It is known that polar groups buried from water in the protein interior have a strong tendency to form hydrogen bonds with each other. The pairs of buried hydrogen-bonded polar residues that appear and disappear in a correlated manner in amino acid sequences can be identified from analysis of multisequence alignments. Hydrogen bonds thus obtained can be used as distance constraints for the packing of the transmembrane α-helices using a distance geometry algorithm.

Results and Discussion

The computational procedure includes several iterative refinement steps of the initial receptor model, constructed from the 7 α-helical fragments packed in accordance with the electron microscopy map of rhodopsin [1] and helix assignment, proposed by Baldwin [2]. The initial model was used to select spatially proximate correlated residues from multisequence alignments of 370 GPCRs by our programs ALIGN and ADJUST and to produce a list of H-bond distance constraints between correlated polar residues. To maximize the number of interhelical distance constraints the sequence of the "average" receptor was designed, containing H-bonds from different GPCRs. The structure of this "average" receptor was calculated by a distance geometry algorithm using the set of ~250 distance and ~600 angle constraints (sidechain-sidechain H-bonds together with α-helix mainchain and sidechain angles and H-bonds). C^{β}-C^{β} distances between pairs of conservative residues, taken from the "average" receptor structure, and two different sets of interhelical H-bonds were used to obtain the sets of structures (r.m.s.d.<1.5 Å) for "active" and "inactive" conformations of the δ-opioid receptor. The final receptor structures were minimized with the δ-selective peptide agonist,

trans-3-(4'-hydroxy)-phenylproline-c[D-Cys-Phe-D-Pen]OH ([Hpp^1]JOM-13) and the alkaloid antagonist, naltrindole (NTI).

In the "inactive" and "active" conformations of the δ-opioid receptor, sidechains of 30 polar residues form networks of 24 and 25 H-bonds respectively, and Asp^{128}, Tyr^{129}, Lys^{214} and His^{278} form H-bonds with ligands (N^+, second and third peptide group carbonyls, and tyrosine O^η of [Hpp^1]JOM-13, respectively). The two receptor conformations differ in H-bond networks due to rotation of the sidechains of residues: Asn^{131}, Asp^{145}, Arg^{146}, Tyr^{308}.

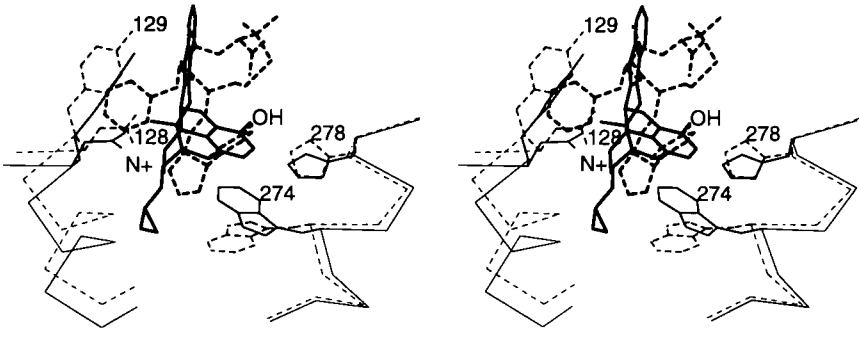

Figure 1. *Stereoview of "inactive" receptor state with antagonist NTI (solid line) and "active" state with agonist [Hpp^1]JOM-13 (dashed line). Several C^α-atoms of fragments of helix III (right) and helix VI (left) and the important residues for ligand binding are shown.*

[Hpp^1]JOM-13 and NTI are complementary to the ligand binding sites in "active" and "inactive" receptor conformations, respectively. The residues Asp^{128}, Tyr^{129}, Asn^{131}, Met^{132}, Phe^{133}, Ile^{183}, Lys^{214}, Leu^{215}, Phe^{218}, Trp^{274}, Ile^{277}, His^{278}, Val^{281}, Val^{296}, Val^{297}, Leu^{300}, Cys^{303}, Ile^{304} and Tyr^{308} form the ligand binding pocket. Agonist and antagonist are bound to the same receptor site and their important N^+ and OH groups interact with residues Asp^{128} and His^{278}, but the orientations of the tyramine aromatic rings are different (Figure 1), thus the agonist and antagonist stabilize conformations of the receptor with different orientations of the Trp^{274} sidechains.

Acknowledgments

Financial support from the NIH (DA03910 and DA00118) and from a University of Michigan, College of Pharmacy Upjohn Research Award are gratefully acknowledged.

References

1. Unger, V.M. and Schertler, G.F.X., *Biophys. J.*, 68 (1995) 1776.
2. Baldwin, J.M., *EMBO J.*, 12 (1993) 1693.

Peptides: Chemistry, Structure and Biology
Pravin T.P. Kaumaya and Robert S. Hodges (Eds.)
Mayflower Scientific Ltd., 1996

141

Mapping the Adhesintope of the Pilin Proteins of *Pseudomonas aeruginosa* Strains PAK and KB7

W.Y. Wong[1,4], W. Paranchych[2], R.S. Hodges[3,4] and R.T. Irvin[1,4]

Departments of [1]Medical Microbiology and Infectious Diseases, [2]Biological Sciences, [3]Biochemistry, and [4]the Protein Engineering Network of Centres of Excellence, University of Alberta, Edmonton, Alberta, T6G 2H7, Canada

Introduction

Pseudomonas aeruginosa utilizes the pilus adhesin to initialize attachment to epithelial cells [1]. The adherence process is mediated through the C-terminal region of the pilin protein [2]. Although the sequence of this region is only semi-conserved among different *P. aeruginosa* strains, there exists a common receptor [3]. In order to examine how the pilus adhesins from different strains recognize and bind to the same receptor, single-alanine substituted peptide analogs corresponding to the C-terminal 17-residue region of the pilin proteins from *P. aeruginosa* strains PAK and KB7 were synthesized. The ability of these peptide analogs to inhibit the binding of the biotinylated PAK pili to A549 human pneumocyte cell line was determined. The results were used to investigate the contribution of specific residues for adhesin function and map the receptor binding residues or adhesintope on the pilin proteins.

Results and Discussion

In this study, a single alanine substituted peptide analog that has an I_{50} value (*i.e.* amount of peptide that cause 50% inhibition of the binding of biotinylated PAK pili to A549 cells) greater than 3 fold of that of the native peptide will be considered as an indicator of an important residue for receptor binding. Our current data showed that the interactions between the C-terminal peptide of the PAK pilin and the A549 cells require a conformational adhesintope, which contains six amino acid residues Ser^{131}, Gln^{136}, Ile^{138}, Pro^{139}, Gly^{141}, Lys^{144} and the disulfide bridge (Table 1). Furthermore, two structural requirements, such as a *cis* conformation and the presence of type I and type II ß-turn, are proposed from recent NMR structure information [4, 5]. These structural elements require the presence of an intrachain disulfide bridge between Cys^{129} and Cys^{142}, and the residues Pro^{139} and Gly^{141}. Other residues, such as Ser^{131} and Gln^{136}, may contribute to hydrogen bond formation, whereas Ile^{138} may be involved in hydrophobic interaction and Lys^{144} may provide a positive charge for receptor interaction. Similarly, nine residues were found to be important for the KB7 pilin peptide binding to A549 cells, they are Ala^{130}, Thr^{131}, Thr^{132},Val^{133}, Asp^{134}, Ala^{135}, Lys^{136}, Arg^{138}, and Pro^{139} (Table 1). These residues can also be classified into four categories such as polar (Thr^{131},Thr^{132}), hydrophobic (Ala^{130},Val^{133},Ala^{135}), ionic (Asp^{134},Lys^{136},Arg^{138}), and conformational

control (Pro^{139}). When these residues are compared with those found in the PAK adhesintope, it seems likely that compensatory mutations could occur to give rise to the KB7 sequence, in which different mutations work together to maintain the functionality of the adherence binding domain. That is, multiple mutations such as Thr^{130}→Ala, Ser^{131}→Thr, Asp^{132}→Thr, Gln^{133}→Val, Glu^{135}→Ala, Gln^{136}→Lys, and Ile^{138}→Arg are required in order for the KB7 pilin to maintain the side-chain and structural requirements for receptor interactions. Interestingly, the major hydrophobic interaction between the receptor and the pilus adhesin involves Ile^{138} in PAK and Val^{133} in KB7 but not Phe^{137}, which is a conserved residue found in many *P. aeruginosa* strains. These results suggest that sequence homology is not necessarily a predictor of the adhesintope.

Table 1. *Comparison of the adhesintope sequences found on the C-terminal 17-residue region of the pilin proteins from P. aeruginosa strains PAK and KB7.*

Sequence	128	129	130	131	132	133	134	135	136	137	138	139	140	141	142	143	144
PAK*	Lys	Cys	Thr	**Ser**	Asp	Gln	Asp	Glu	**Gln**	Phe	**Ile**	**Pro**	Lys	**Gly**	Cys	Ser	**Lys**
KB7*	Ser	Cys	**Ala**	**Thr**	**Thr**	**Val**	**Asp**	**Ala**	**Lys**	Phe	**Arg**	**Pro**	Asn	Gly	Cys	Thr	Asp

*Amino acid residues that are important for binding to A549 cells are underlined and printed in bold (see text).

In conclusion, the amino acid residues required for both PAK and KB7 pilin binding to A549 cell were elucidated. This information sheds light on how the pilus adhesin interacts with the epithelial cell receptors, and is of importance for the design and development of therapeutics that prevent *P. aeruginosa* infections.

Acknowledgments

This work was supported by grants from the Protein Engineering Network of Centres of Excellence, Canadian Cystic Fibrosis Foundation, and Canadian Bacterial Diseases Network.

References

1. Pier, G.B., *J. Infect. Dis.*, 151 (1985) 575.
2. Irvin, R.T., Doig, P., Lee, K.K., Sastry, P.A., Paranchych, W., Todd, T. and Hodges, R.S., *Infect. Immun.*, 57 (1989) 3720.
3. Sheth, H.B., Lee, K.K., Wong, W.Y., Srivastava, G., Hindsgaul, O., Hodges, R.S., Paranchych, W. and Irvin, R.T., *Mol. Microbiol.*, 11 (1994) 715.
4. McInnes, C., Sönnichsen, F.D., Kay, C.M., Hodges, R.S. and Sykes, B.D., *Biochemistry*, 32 (1993) 13432.
5. McInnes, C., Kay, C.M., Hodges, R.S. and Sykes, B.D., *Biopolymers*, 34 (1994) 1221.

Peptides: Chemistry, Structure and Biology
Pravin T.P. Kaumaya and Robert S. Hodges (Eds.)
Mayflower Scientific Ltd., 1996

142
β-Turn Nomenclature: A Topographical Classification System

G.T. Bourne, J.H. McKie, P.J. Cassidy, M.L. Smythe, P.F. Alewood and P.R. Andrews

Center for Drug Design and Development.
University of Queensland, Brisbane, Queensland 4072, Australia

Introduction

Molecular recognition, in biological processes is widely accepted as a surface phenomenon. This is particularly true for proteins, where it has often been shown that surface loops are responsible for recognition events [1]. A majority of all categorized protein surface loops consist of β-turns [2], which are consequently a well-studied structural motif. Unlike other structural motifs such as the α-helix and the β-sheet, the backbone conformation of the β-turn is highly variable. This variability has led to many definitions and subcategories based upon the backbone conformations [3], but these classification procedures have provided little information on side chain orientations.

Here we report a novel β-turn classification protocol based upon the Cα to Cβ vectors of the reverse turn (Figure 1). Since the Cα to Cβ atoms direct these side chains (the informational units), we were led to compare the vector orientations of this initial bond. As a result, an alternative description for the β-turn has been developed.

Results and Discussion

A program was written that automates the collection and analysis of β-turns from a set of randomly selected proteins from those in the Brookhaven protein database with a

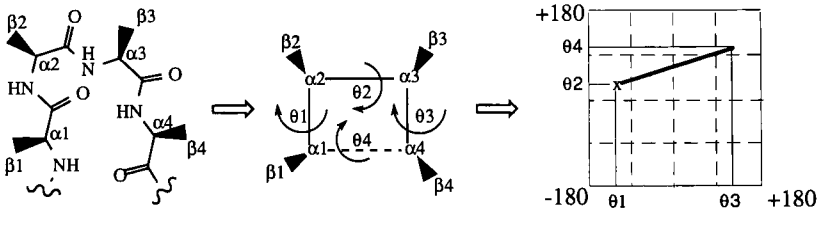

Figure 1. *As a visual guide towards the grouping of β-turns collected, a mapping of the dihedral angles θ (1 to 4) defined as Cβ(i)-Cα(i)-Cα(i+1)-Cβ(i+1) for i = 1 to 3 and Cβ(i+3)-Cα(i+3)-Cα(i)-Cβ(i) was used. The four dihedral angles θ1 to θ4 of each turn were plotted on a 2-dimensional dihedral graph. Each individual line corresponds to a β-turn.*

resolution of less than 2Å. The set of β-turns collected were then clustered [4] using rms comparisons of the Cα and Cβ atoms. This resulted in 7 different families consisting of ~30% of the whole dataset (r = 0.950).

The novelty of this method is that the β-turn is described using all four amino acid residues. This is in contrast to previous classification systems which grouped on the basis of the *"i+1"* and *"i+2"* residues [3]. We believe that this classification system will help in the design of β-turn mimetics and will yield valuable information on the conformation of biologically active protein surfaces.

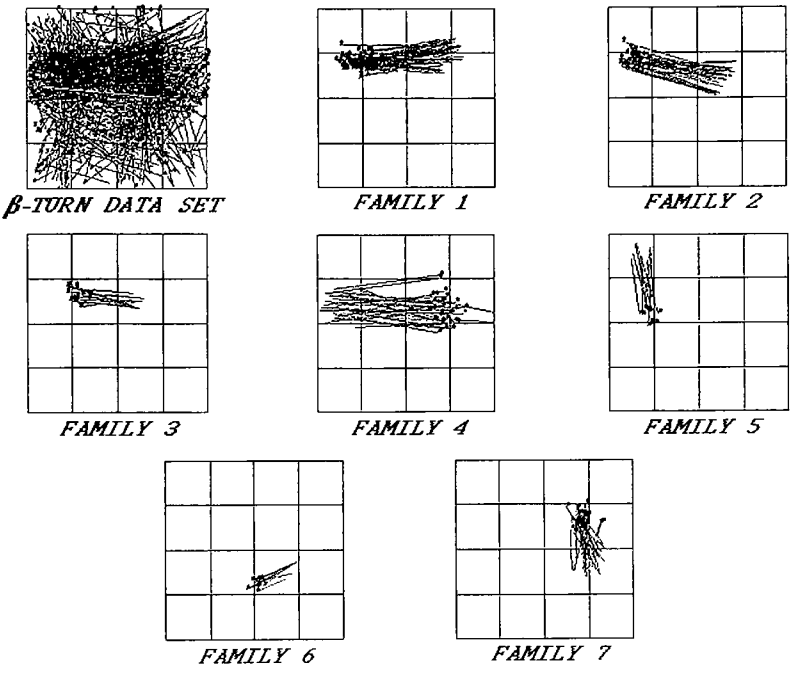

Figure 2. *Plot of side-chain orientations of the β-turns collected within the dataset and the identification of 7 distinct families at a rms 0.950.*

Acknowledgments

We would like to thank Wellcome (Australia) for their financial support.

References

1. Ptitsyn, O.B., *FEBS Lett.*, 131 (1981) 197.
2. Sibanda, B.L., Blundell T.L., Thorton, J.M., *J. Mol. Biol.*, 206 (1989) 759.
3. Wilmot, C.M., Thorton, J.M., *Protein Eng.*, 3 (1990) 479.
4. Sokol, R.R., in Ryzin, J.V. (Ed.), 'Classification and Clustering', Academic Press, New York, USA, 1977, p.1.

Peptides: Chemistry, Structure and Biology
Pravin T.P. Kaumaya and Robert S. Hodges (Eds.)
Mayflower Scientific Ltd., 1996

143
Arginyl Methylketones in the Design of Highly Potent Bivalent Thrombin Inhibitors

T. Steinmetzer[1], P. Rehse[1], B.Y. Zhu[2], B.F. Gibbs[1], J. Lefebvre[1], M. Cygler[1] and Y. Konishi[1]

[1]Biotechnology Research Institute, National Research Council of Canada, 6100 Royalmount Ave., Montreal, Quebec, H4P 2R2, Canada
[2]BioChem Therapeutic Inc., 275 Armand-Frappier Blvd., Laval, Quebec, H7V 4A7, Canada

Introduction

The potent and selective inhibition of thrombin may overcome various thrombotic disorders. The natural polypeptide hirudin from the leech *Hirudo medicinalis* binds simultaneously to both the active site and fibrinogen recognition exosite (FRE) of thrombin with the highest affinity of 20 fM. Synthetic inhibitors, which mimic the binding mode of hirudin have been developed [1]. They are composed of an active site inhibitor segment, a FRE inhibitor segment and a linker connecting these parts. Arginyl methylketone derivatives were incorporated in the P_1-P_1' region of the active site inhibitor segment and enhanced the binding affinity of the inhibitors. The synthesis and inhibitory potency of new bivalent thrombin inhibitors is presented.

Results and Discussion

Boc-Arg(Z_2)-chloromethylketone **1** is the starting material for the building units **2** - **4**, which were used in SPPS (Figure 1).

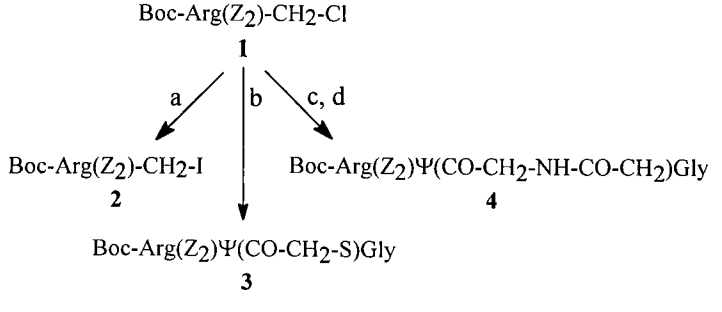

Figure 1. *Synthesis of the building units. a) NaI in DMF, 24 h, 35°C, b) HS-CH_2-COOH in THF, RT, 24 h, c) NH_3 in methanol/THF, d) succinic anhydride in THF.*

The P_1'-linker and the FRE inhibitor segment of the inhibitors listed in Table 1 were synthesized by conventional SPPS. The building unit **2** was used in the synthesis of the inhibitors **5 - 10** through alkylation of the corresponding P_1' residue, while the side chains of the linker and FRE inhibitor segment on Pam resin were still protected. The synthesis was completed by coupling of the corresponding P_3-P_2 dipeptide to the N-terminal Arg residue. Similarly, the building units **3** and **4** were used in the synthesis of the inhibitors **11** and **12**, respectively.

Table 1. *Inhibition constants of thrombin catalyzed hydrolysis of the fluorogenic substrate Tos-Gly-Pro-Arg-AMC by the synthesized inhibitors.*

No.	Sequence	K_i (pM)
5	DPhe-P-ArgΨ(CO-CH_2-NH)Gly-GGGG-DFEEIPEEYLQ	83 ± 15
6	DPhe-P-ArgΨ(CO-CH_2-NCH_3)Gly-GGGG-DFEEIPEEYLQ	83 ± 8
7	DCha-P-ArgΨ(CO-CH_2-NAc)Gly-GGGG-DYEPIPEEY-Cha-D	1.7 ± 0.3
8	DCha-P-ArgΨ(CO-CH_2-NCH_3)Gly-GGGG-DYEPIPEEY-Cha-D	2.0 ± 0.3
9	DCha-P-ArgΨ(CO-CH_2-NCH_3)Gly-GGGGNG-DYEPIPEEA-Cha-DGlu	0.87 ± 0.03
10	DCha-P-ArgΨ(CO-CH_2-$N^+C_5H_4$)Gly-GGGG-DYEPIPEEA-Cha-DGlu	0.045 ± 0.01
11	DPhe-P-ArgΨ(CO-CH_2-S)Gly-GGGG-DFEEIPEEYLQ	9.4 ± 1.2
12	DPhe-P-ArgΨ(CO-CH_2-NH-CO-CH_2)Gly-GGGG-DFEEIPEEYLQ	7290 ± 390

The inhibitors **5**, **6**, **8** and **9** have an ionizable secondary or tertiary amine in the P_1' residue. Its protonated form may pull out the electron from the carbonyl carbon of Arg and form a transition state analog in their bound state, resulting in an enhanced binding affinity. However, no enhanced affinity was induced in the inhibitor **8** compared to the inhibitor **7**, in which the acetylated amine is not protonatable. On the contrary, the introduction of a permanently charged pyridinium ketone in the inhibitor **10** improved the affinity ~ 50-fold compared to compounds **7** or **8**. The crystal structure of the inhibitor **10**/thrombin complex demonstrated the formation of a transition state analog hemiketal. Thus, the electron withdrawing effect of the secondary or tertiary amine seems to be insufficient to induce a tetrahedral intermediate and a permanently charged pyridinium group is required for this induction. An incorporation of sulfur in the P_1' residue (inhibitor **11**) also improved the affinity ~ 10-fold compared to the corresponding inhibitors **5** and **6**.

The inhibitor **11** has another advantage of a high yield in the synthesis (~75 % after HF cleavage). Surprisingly, reversing the NH-CH_2 of the P_1' residue (Gly to CH_2-NH-CO in inhibitor **12**) drastically reduced the affinity of the inhibitor (~90-fold). The arginyl methylketone derivatives not only remove the scissile peptide bond but also improve the affinity of the thrombin inhibitors up to the level of natural hirudin.

Reference

1. Maraganore, J.M., Bourdon, P., Jablonski, J., Ramachandran, K.L., Fenton II, J.W., *Biochemistry*, 29 (1990) 7095.

Peptides: Chemistry, Structure and Biology
Pravin T.P. Kaumaya and Robert S. Hodges (Eds.)
Mayflower Scientific Ltd., 1996

144
Recognition of a Hormone Binding Site of the Insulin Receptor by Anti-peptide Antibodies

R. Scherbaum[1], M. Casaretto[1], M. Fabry[1], J. Tenelsen[1], H. Hoecker[1], H. Stieve[2] and D. Brandenburg[1]

[1]Deutsches Wollforschungsinstitut, Veltmanplatz 8, D-52062 Aachen, Germany
[2]Institut fuer Biologie 2, RWTH Aachen, Kopernikusstrasse 16, D-52074 Aachen, Germany

Introduction

The detailed analysis of ligand binding sites of peptide hormone receptors is important for understanding mechanisms of action and as a basis for therapeutic progress. We have previously identified regions 20-121 and 390-470 of the insulin receptor as insulin binding sites by photoaffinity labelling [1]. Since both domains are relatively large, further refinements are required in order to define the hormone binding region as precisely as possible. To this end, the application of anti-peptide antibodies appeared promising.

Results and Discussion

Based on the antigenic index algorithm [2] we have selected and synthesized four receptor sequences, two from each binding domain, with an N-terminal Cys extension:

IRP1 (11-25)	C-M-D-I-R-N-N-L-T-R-L-H-E-L-E-N
IRP2 (66-81)	C-V-Y-G-L-E-S-L-K-D-L-F-P-N-L-T-V
IRP3 (405-419)	C-N-Q-N-L-R-Q-L-W-D-W-S-K-H-N-L
IRP4 (451-465)	C-R-Q-E-R-N-D-I-A-L-K-T-N-G-D-K

Fmoc SPPS was used to assemble the peptides on an alkoxybenzylalcohol resin using TBTU or DIC/HOBt as coupling reagent. After medium pressure liquid chromato- graphy, the peptides were obtained in 97-99% purity according to HPLC. Amino acid analyses showed the correct composition. The purified peptides were linked to keyhole limpet hemocyanine *via* 3-(2-pyridyldithio) propionic acid. Two rabbits were immunized (4-5x) with each conjugate in complete Freund's adjuvant to produce 8 antisera (AS1- AS8), which were ELISA positive with titers ranging from 1/100 to 1/1000,000 against the corresponding peptide.

Soluble insulin receptor ectodomain, which contains both complete α-subunits and the extracellular part of both β-subunits [3], was recognized by all 8 antisera in a dot immunoassay on nitrocellulose with undiluted sera, and some after dilution 1/10. All

presera were negative. The antisera were tested with respect to their ability to compete with ^{125}I-labelled insulin for receptor sites on IM-9 cells. Antisera against peptides 66-81 and 451-465 did not interfere with binding of labelled insulin. However, AS2, directed against peptide 11-25, and antisera AS5 and AS6, directed against the sequence 405-419, inhibited insulin binding to the extent of 25-30% at maximal concentration.

Based on the results reported above, we have reached the following conclusions:

1. The receptor sequences 66-81 and 491-465 appear to contain continuous epitopes, since they are recognized by the anti-peptide antibodies. However, they are neither directly nor indirectly involved in insulin binding.
2. In contrast, the receptor sequence 405-419 may be part of the hormone binding site within the large C-terminal receptor domain 390-470 [1]. Its surface accessibility, flexibility and hydrophobic/hydrophilic amino acid sequence make it a good candidate for this role.
3. In the N-terminal domain 20-121, the amino end 20-25 seems to be most important.
4. While steric hindrance or a negative allosteric effect of antibodies on receptor confor- mation cannot presently be excluded, we hypothesize that these antibodies compete directly for the insulin binding site.

Acknowledgments

We dedicate this paper to the memory of Ms. Margot Leithaeuser. Our sincere thanks are due to Drs. L. Ellis and E. Schaefer for the insulin ectodomain, and Drs. J.-C. and F. Sodoyez for labelled insulin.

References

1. Fabry, M., Schaefer, E., Ellis, L., Kojro, E., Fahrenholz, F. and Brandenburg, D., *J. Biol. Chem.*, 267 (1992) 8950 .
2. Jameson, B.A. and Wolf, H., *CABIOS,* 4 (1988) 181.
3. Schaefer, E.M., Siddle, K., and Ellis, L., *J. Biol. Chem.* 265 (1990) 13248.

Peptides: Chemistry, Structure and Biology
Pravin T.P. Kaumaya and Robert S. Hodges (Eds.)
Mayflower Scientific Ltd., 1996

145
Interaction of the Glucagon Receptor and a D64K Mutant with Position 12, 17, and 18 Replacement Analogs of Glucagon

C.G. Unson, C.P. Cheung, C.-R. Wu, and R.B. Merrifield

The Rockefeller University, New York, NY 10021, USA

Introduction

Recently, Carruthers *et al.* synthesized and expressed a gene for the rat glucagon receptor [1]. COS-1 cells expressing the synthetic receptor bound glucagon with affinity and peptide hormone specificity similar to native receptors on liver cells. The transfected COS cells also increased levels of intracellular cAMP when stimulated with glucagon. In initial mutagenesis studies, the functional role of Asp^{64} in the extracellular N-terminal domain of the receptor was tested. A mutation at this site in the related growth hormone releasing factor receptor, was shown to be responsible for a genetic defect that results in mice of small size with hypoplastic pituitary glands [2]. Replacement of Asp^{64} resulted in a mutant receptor that did not bind glucagon and indicated that Asp^{64} played an important role in glucagon receptor binding [1]. This work was conducted to find the corresponding positively charged residue in the peptide hormone, which presumably could be involved with Asp^{64} of the receptor in an electrostatic interaction.

Results and Discussion

The hormone contains basic residues Lys^{12}, Arg^{17} and Arg^{18}, aside from His^{1} which are protonated at the physiological pH. We have previously shown that the amino terminal histidine contributes a determinant for both receptor recognition and the subsequent transduction of the hormone signal [3]. Nine glucagon analogs containing amino acid replacements at positions 12, 17, and 18 were synthesized by the solid phase method and tested for binding to receptors on liver membranes, and for the ability to stimulate adenylate cyclase. (Table 1).

Replacement of lysine at position 12 with a neutral alanine residue (analog #1) resulted in 83% loss in binding affinity for the glucagon receptor. Deletion of position 1 histidine (analog #2) reduced it further to less than 1%. Neutralization of the charge at Lys^{12} by acetylation in the analog ε-acetyl lysine glucagon amide (analog #3), resulted in about 50% loss in binding. Reversal of the charge at position 12, in the analogs Asp^{12} (analog #4), Glu^{12} (analog #5) and des-$His^{1}Glu^{12}$ (analog #6), resulted in 99% loss in binding. Interestingly, residual binding affinity in analogs # 1-6 was still sufficient to

Table 1. *Replacement analogs of positively charged residues in glucagon.*

Analog of glucagon amide	% Binding affinity	Cyclase activation	
		% Max. activity	% Rel. Potency
glucagon amide	100	100	15
1. Ala^{12}	17	60	17
2. des-$His^{1}Ala^{12}$	0.92	12	0.15
3. $AcLys^{12}$	47	90	32
4. Asp^{12}	0.6	78	10
5. Glu^{12}	1	80	50
6. des-$His^{1}Glu^{12}$	0.11	28	0.28
7. Ala^{17}	38	29	0.013
8. des-$His^{1}Ala^{17}$	2.3	29	0.28
9. Ala^{18}	13	94	71

transduce the signal, since all of these peptides were able to stimulate adenylate cyclase with relative potencies ranging from 10-50% with reduced activity for each of the *des*-His^{1} derivatives. Replacement of Arg^{17} with a neutral alanine (analog #7) resulted in an analog that retained 38% binding but whose relative potency in the cyclase assay was reduced to 0.013%. In contrast, replacement of Arg^{18} with alanine (analog #9) affected binding with a loss of 87% affinity but had only a slight effect on adenylate cyclase activity. At position 12 and 18, the positive charge appears to be important for binding only. However, at position 17, the positive charge influences both receptor recognition and activation.

The D64K mutant of the glucagon receptor was synthesized by replacement in the synthetic gene of a 74-bp *Bsi*WI-*Kpn*I restriction fragment with a duplex containing the desired codon alteration. COS-1 cells expressed the mutant receptor gene at normal levels, but failed to bind glucagon. However, upon incubation with Asp^{12} or Glu^{12} glucagon amide, cells expressing D64K caused a 32% and 43% increase in intracellular cAMP levels compared to cells expressing wild-type receptor when challenged with glucagon. This result might suggest that the opposite but complementary substitutions on both ligand and receptor restored some of the binding affinity, enough to partially allow transduction of the signal. Not one particular residue but all four positive residues in glucagon may contribute to binding affinity and interaction with Asp^{64} of the glucagon receptor. This study was supported by USPHS grant DK24039.

References

1. Carruthers, C.J.L., Unson, C.G., Kim, H.N. and Sakmar, T.P., *J. Biol. Chem.*, 269 (1994) 29321.
2. Lin, S.-C., Lin, C.R., Gukovsky, I., Lusis, A.J., Sawchenko, P.E. and Rosenfeld, M.G., *Nature*, 364 (1993) 208.
3. Unson, C.G., Macdonald, D. and Merrifield, R.B., *Arch. Biochem. Biophys.*, 300 (1993) 747.

Peptides: Chemistry, Structure and Biology
Pravin T.P. Kaumaya and Robert S. Hodges (Eds.)
Mayflower Scientific Ltd., 1996

146
Conformationally-constrained Macrocyclic Norstatine-based Inhibitors of HIV Protease

R.A. Smith[1], J.J. Chen[2], P.J. Coles[3] and A. Krantz[4]

[1]Bayer Research Center, West Haven, CT 06516, USA
[2]Roche Bioscience, Palo Alto, CA 94304, USA
[3]Glaxo Canada Inc., Mississauga, Ontario, L5N 6L4, Canada
[4]RedCell Inc., San Francisco, CA 94104, USA

Introduction

A great number of inhibitors have been developed for HIV protease [1]. Norstatine-based inhibitors of this enzyme, which bear a key hydroxyamide functionality, have been investigated in our laboratories [2], as well as in other research groups [3]. We recently described the design, synthesis, and activity of conformationally-constrained macrocyclic peptide-based inhibitors of HIV protease which incorporate a hydroxyethylamine functionality as the transition-state mimetic group [4]. Another example of a macrocyclic HIV protease inhibitor, based on a linear peptidyl difluorostatone inhibitor, has been described by Podlogar *et al.* [5]. We now report the incorporation of the hydroxyamide (norstatine) transition-state analog group into our macrocyclic peptide template structure.

Results and Discussion

We decided to first assemble the P_3-P_1 macrocycle, then generate the hydroxyamide functionality, and finally incorporate the P_1' group. The synthesis of the macrocycle template was achieved efficiently in four steps; unfortunately, conversion of this macrocyclic methyl ester to the required α-hydroxy ester was problematic, and the route which was successful in providing both diastereomers of product only proceeded in low yield. However, pure samples of both the (*S*)-CHOH- (**1**) and (*R*)-CHOH- (**2**) diastereomers of final hydroxyamide product could be obtained.

Protease inhibition (BRU/IIIB) and HIV-antiviral activity (MT-2 cells, HTLV-1 RF virus) were determined [4] to be for **1**: IC_{50} 19 nM, antiviral EC_{50} 76 nM; and for **2**: IC_{50} 3,800 nM. Similar to our previous studies [4], the macrocyclic hydroxyamide diastereomer with preferred chirality at -CHOH- (**1**, designated *S* in the hydroxyamide series) provides ~200-fold greater HIV protease inhibition than the *R*-diastereomer **2**. The hydroxyamides **1** and **2** are ~20 times more potent than the macrocyclic hydroxyethylamine analogs which lack only the carbonyl functionality at the transition-state mimetic group [4]. Although **1** provides ~17-fold less HIV protease inhibition than a

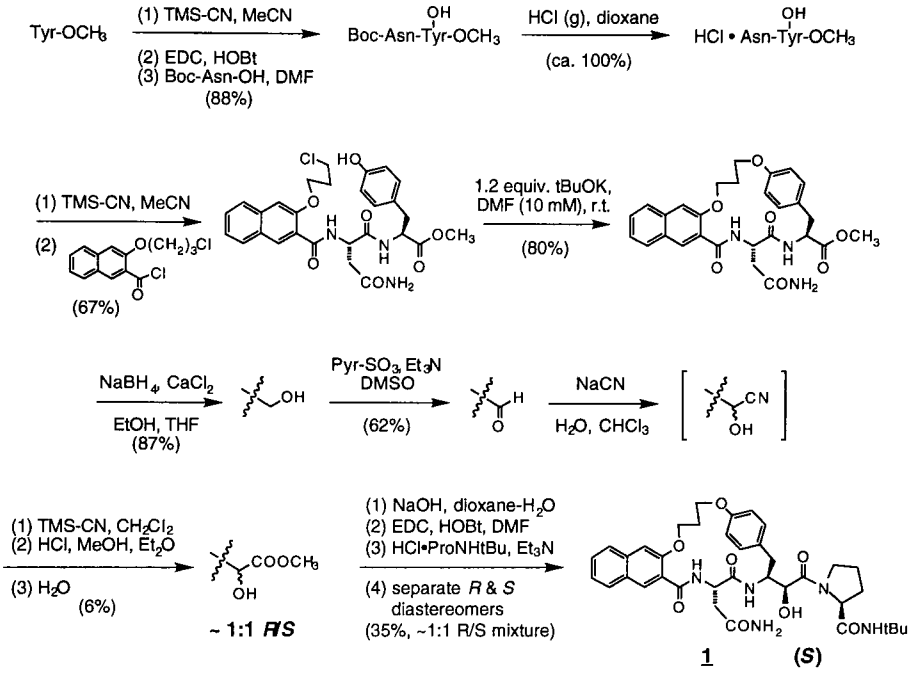

related acyclic hydroxyamide analog with quinolin-2-ylcarbonyl at P_3 [2], *it is 2-fold more effective than this acyclic analog in the HIV cell assay.* The ratio of inhibitory activities in the cell assay *vs.* enzyme assay (*i.e.*, EC_{50}/IC_{50}) was also generally superior for the macrocyclic inhibitors, as compared to the ratio observed for acyclic analogs, in our previous study [4]. This observation suggests that our macrocyclic inhibitors may have improved cell permeability and/or resistance to cellular enzymes, relative to their acyclic counterparts.

References

1. (a) Meek, T.D., *J. Enzyme Inhibition*, 6 (1992) 65. (b) Huff, J.R., *J. Med. Chem.*, 34 (1991) 2305.
2. Tam, T.F., Carrière, J., MacDonald, I.D., Castelhano, A.L., Pliura, D.H., Dewdney, N.J., Thomas, E.M., Bach, C., Barnett, J., Chan, H. and Krantz, A., *J. Med. Chem.*, 35 (1992) 1318.
3. (a) Mimoto, T., Imai, J., Kisnauki, S., Enomoto, H., Hattori, N., Akaji, K. and Kiso, Y., *Chem. Pharm. Bull.*, 40 (1992) 2251. (b) Raju, B. and Deshpande, M.S., *Biochem. Biophys. Res. Commun.*, 180 (1991) 181. (c) Sakurai, M., Higashida, S., Sugano, M., Komai, T., Yagi, R., Ozawa, Y., Handa, H., Nishigaki, T. and Yabe, Y., *Bioorg. Med. Chem.*, 2 (1994) 807.
4. Smith, R.A., Coles, P.J., Chen, J.J., Robinson, V.J., MacDonald, I.D., Carrière, J. and Krantz, A., *Bioorg. Med. Chem. Lett.*, 4 (1994) 2217.
5. Podlogar, B.L., Farr, R.A., Friedrich, D., Tarnus, C., Huber, E.W., Cregge, R.J. and Schirlin, D., *J. Med. Chem.*, 37 (1994) 3684.

Peptides: Chemistry, Structure and Biology
Pravin T.P. Kaumaya and Robert S. Hodges (Eds.)
Mayflower Scientific Ltd., 1996

147
A Highly Potent Cyclic α-MSH Antagonist Containing Naphthylalanine

V.J. Hruby[1], S.D. Sharma[1], S. Lim[1], D. Lu[2], R.A. Kesterson[2], M.E. Hadley[3] and R.D. Cone[2]

Departments of [1]Chemistry and [2]Anatomy, University of Arizona, Tucson, AZ 85721, USA
[3]Vollum Institute for Advanced Biomedical Research, Oregon Health Sciences Center, L-474, Portland, OR 97201, USA

Introduction

α-MSH is a linear tridecapeptide (Ac-Ser[1]-Tyr-Ser-Met-Glu[5]-His-Phe-Arg-Trp-Gly[10]-Lys-Pro-Val-NH_2) which is involved in many important biological activities including skin pigmentation and a variety of proposed CNS-related activities [1]. α-MSH has been the subject of extensive structure-activity studies primarily related to its pigmentation effects [2]. Recent cloning of 5 melanocortin receptor types [3], two of which are found primarily in the brain, has greatly raised interest in this peptide. There is a great need to develop potent and selective agonists and antagonists for each receptor. In previous studies, we and others have obtained only a few weak antagonists (pA_2 values 5-8), and they did not provide structurally specific insights as to why they behaved as antagonists rather than agonists. One of the best of these, with a pA_2 value of 8.4, was obtained by substitution of His^6 and Arg^8 with Trp^6 and Nle^8, respectively, in an analogue of the superagonist [Nle^4,D-Phe^7]α-MSH to give a potent antagonist. However, the same substitution followed by lactam cyclization between the Asp^5 and Lys^{10} side chains gave an agonist [4]. This has led us to explore the effect of substituting position 7 which has been a critical residue.

A series of *p*-substituted unusual aromatic D-amino acid residues were substituted into the 7 position of the superagonist cyclic lactam α-MSH analogue N-Ac-Nle^4-c[Asp^5,D-Phe^7,Lys^{10}]α-MSH(4-10)-NH_2 [5]. Some of the analogues examined are shown in Table 1. Several important results have been obtained. For the first time, highly potent antagonist analogues for the classical frog skin receptor has been obtained. The D-Phe(pI)[7] and D-Nal(2')[7] analogues **4** and **5**, with pA_2 values of 10.3 and 10.5, respectively, are subnamolar antagonists at the classic receptor. Furthermore, both compounds, but especially the latter compound, are potent antagonists at the human MC4 receptor, and also are selective for this receptor over the human MC3 receptor (not shown) [6]. Interestingly, though they are structurally analogous to antagonists **4** and **5**, compounds **2**, **3** and **6** are all potent agonists. Even more unexpectedly, all of the new analogues **2-6** are agonists at the cloned mouse MC1 receptor and human MC1 receptors.

Table 1. *Bioactivities of D-amino acid 7-substituted analogues of a super potent cyclic lactam α-melanotropin.*

Compound[a] (Amino Acid in Position 7)	Biological Activities - EC_{50} (nM)			
	Frog Skin[b]	mMC1-R[c]	hMC1-R[c]	hMC4-R[c]
1 α-MSH	0.10	1.3	0.091	0.210
2 D-Phe(*p*F)	0.10	0.026	0.016	0.019
3 D-Phe(*p*Cl)	2.0	0.0095	0.005	0.018
4 D-Phe(*p*I)	Antagonist (pA_2=10.3)	0.19	0.055	Partial agonist (pA_2=9.7)
5 D-NaI(2')	Antagonist ($pA_2 \geq 10.5$)	0.039	0.036	Antagonist (pA_2=9.3)
6 D-NaI(1')	0.50	N.D.	Agonist	Agonist

[a] Analogues of Ac-Nle[4]-Asp-His-D-Phe[7]-Arg-Trp-Lys[10]-NH_2.
[b] Rana pipien skins; [c] c AMP dependent β-galactosidase activity of cloned receptors.

Presumably this will be the case *in vivo.* Knowledge of the structural differences between frog skin, mouse and human receptors might provide important insights into the differential structural requirements of these receptors for interactions with agonists and antagonists.

Acknowledgments

Support by grants from the USPHS DK-17420 (VJH), DK 44239 and HD 30236 (RDC).

References

1. Hadley, M.E. (Ed.), 'The Melanotropic Peptides', Vols. I, II and III, CRC Press, Boca Raton, FL., 1988
2. Hruby, V.J., Sharma, S.D., Toth, K., Jaw, J.Y., Al-Obeidi, F.A., Sawyer, T.K. and Hadley, M.E., *Ann. N.Y. Acad. Sci.*, 680 (1993) 51.
3. Cone, R.D., Mountjoy, K.G., Robbins, L.S., Nadeau, J.H., Johnson, K.R., Roselli-Rehfuss, L. and Mortrud, M.T., *Ann. N.Y. Acad. Sci.*, 680 (1993) 342.
4. Al-Obeidi, F., Hruby, V.J., Hadley, M.E., Sawyer, T.K. and Castrucci, A.M., *Int. J. Peptide Protein Res.*, 35 (1990) 228.
5. Al-Obeidi, F.A., Hadley, M.E., Pettitt, B.M. and Hruby, V.J., *J. Am. Chem. Soc.*,111, 3413.
6. Hruby,V.J., Lu, D., Sharma, S.D., de L. Castrucci, A., Kesterson, R.A., Al-Obeidi, F., Hadley, M.E. and Cone, R.D., *J. Med. Chem.*, 38 (1995) 3454.

Peptides: Chemistry, Structure and Biology
Pravin T.P. Kaumaya and Robert S. Hodges (Eds.)
Mayflower Scientific Ltd., 1996

148
Discriminatory Affinity-labeling of μ- and δ-Opioid Receptor Subtypes by Disulfide Bridging with Enkephalin Analogs

T. Yasunaga[1], Y. Shimohigashi[2], S. Motoyama[2], A. Tatsui[2], H. Kodama[3], M. Kondo[3] and M. Ohno[2]

[1]*Manufacturing Process Development Division, Otsuka Pharmaceutical Co., Ltd., Saga Factory, Saga 842-01, Japan*
[2]*Laboratory of Biochemistry, Department of Chemistry, Faculty of Science, Kyushu University, Fukuoka 812-81, Japan*
[3]*Department of Chemistry, Faculty of Science and Engineering, Saga University, Saga 840, Japan*

Introduction

The presence of free mercapto group(s) in the ligand binding site of opioid receptors has been suggested for smooth muscle preparations from both the guinea pig ileum (GPI) and mouse vas deference (MVD). We have shown that [D-Ala^2,Leu(CH_2S-Npys)^5]-enkephalin (**1**) binds covalently to μ receptors in GPI and MVD, and [D-Ala^2,Leu^5]-enkephalyl-Cys(Npys)^6 (**2**) binds exclusively to δ receptors in MVD [1, 2]. These *S*-Npys (3-nitro-2-pyridinesulfenyl)-containing enkephalin analogs were expected to bind first to the ligand binding site of the receptors and then to cross-link the receptor mercapto group by the thiol-disulfide exchange reaction. Affinity-labeled receptors exhibited continuing activities. In the present study, in order to evaluate whether or not similar affinity-labelings are feasible for δ and μ receptors in the central nervous system, we carried out the receptor binding assays using rat brain membranes.

Tyr-D-Ala-Gly-Phe-Leu(CH_2S-Npys) (1)
Tyr-D-Ala-Gly-Phe-Leu-Cys(Npys) (2)

Figure 1. *Amino acid sequences of S-Npys-containing enkephalin analogs.*

Results and Discussion

Synthesis of enkephalin analogs were carried out by the conventional solution method as reported previously [1, 2]. The ordinary radio-labeled receptor binding assays using rat brain membrane preparations were carried out essentially as described previously [3]. Radio-ligands employed were [^{3}H]-[D-Ala^2,MePhe^4,Gly-ol^5]enkephalin (^{3}H-DAGO) for μ receptors and [^{3}H]-[D-Ser^2,Leu^5]enkephalyl-Thr^6 (^{3}H-DSLET) for δ receptors. The

Table 1. *IC_{50} and EC_{50} values of S-Npys-enkephalin analogs.*

	IC_{50} (nM)		EC_{50} (μM)		
	^{3}H-DAGO	^{3}H-DSLET	^{3}H-DAGO	^{3}H-DSLET	Selectivity
1	1.74	2.56	0.051	5.0	μ/δ=98
2	42.7	8.01	5.1	0.034	δ/μ=1.50

DAGO; [D-Ala^2,MePhe^4,Gly-ol^5]enkephalin
DSLET; [D-Ser^2,Leu^5]enkephalyl-Thr^6

results were analyzed by the computer program ALLFIT [4] and the IC_{50} values are shown in Table 1. Compound **1** is highly potent for both μ and δ receptors, while **2** is slightly δ-selective with a moderate binding affinity.

To evaluate the possible affinity-labeling, rat brain membranes were first incubated with **1** or **2** for 30 min at 25°C. The concentrations of peptides were 1.0, 10, 100 nM, 1.0 and 10 μM. After four consecutive washings of membranes by centrifugation, they were further incubated with radio-labeled ligands of ^{3}H-DSLET to assess the number of δ receptors remaining and ^{3}H-DAGO for μ receptors. With increasing concentration of peptides **1** and **2**, the receptor population available for these hot ligands decreased sharply. This is a clear indication to demonstrate that **1** and **2** can bind covalently to the receptors. From the curves showing the relationships of the labeled receptor population (%) versus the concentration of **1** or **2** utilized, the effective concentration (EC_{50}) of *S*-Npys-containing enkephalins to label 50% of the receptors were calculated and are summarized in Table 1.

It should be noted that **1** labeled the μ receptors about 100 times more effectively than δ receptors. Since compound **1** showed no binding selectivity for δ and μ receptors in the ordinary binding assays, this high selectivity for μ receptor in affinity-labeling may imply that the *S*-Npys group of **1** is in close proximity to the thiol group of μ receptors, but not of δ receptors. On the other hand, *S*-Npys-enkephalin **2** was found to label the δ receptors about 150 times more effectively than μ receptors. This receptor selectivity in affinity labeling is also much higher than that in binding affinity.

These results indicated that the opioid receptor subtypes in the central nervous system also possess the free mercapto group in their ligand binding sites. The present study showed that properly designed Npys-containing enkephalins can affinity-label these thiols discriminatively.

References

1. Kodama, H., Shimohigashi, Y., Ogasawara, T., Koshizaka, T., Kurono, M., Matsueda, R., Soejima, K., Kondo, M. and Yagi, K., *Biochem. Int.*, 19 (1989) 1159.
2. Matsueda, R., Yasunaga, T., Kodama, H., Kondo, M., Costa, T. and Shimohigashi, Y., *Chem. Lett.*, (1992) 1259.
3. Shimohigashi, Y., English, M.L., Stammer, C.H. and Costa, T., *Biochem. Biophys. Res. Commun.*, 104 (1982) 583.
4. Lean, A.De., Munson, P.J. and Rodbard, D., *Am. J. Physiol.*, 235 (1978) E97.

Peptides: Chemistry, Structure and Biology
Pravin T.P. Kaumaya and Robert S. Hodges (Eds.)
Mayflower Scientific Ltd., 1996

149
Analysis of Integins that Mediate Cell Adhesion to α1(IV) 531-543 in Collagen

A.J. Miles[1,2], J.R. Knutson[2], A.P.N. Skubitz[1,2], J.B. McCarthy[1,2], L.T. Furcht[1,2] and G.B. Fields[1,2,3]

[1]Biomedical Engineering Center, and Departments of [2]Laboratory Medicine and Pathology, and [3]Biochemistry, University of Minnesota, Minneapolis, MN 55455, USA

Introduction

Various sequences within human type IV collagen have been identified as cellular recognition sites. The region α1(IV)531-543 was initially identified as the third heparin binding site in basement membrane collagen [1], and was thus designated Hep-III. Hep III and its D-enantiomer (D-Hep III) incorporating this sequence (Gly-Glu-Phe-Tyr-Phe-Asp-Leu-Arg-Leu-Lys-Gly-Asp-Lys-Tyr) were subsequently shown to promote equivalent adhesion of melanoma and ovarian carcinoma cell lines (A375SM and SKOV3, respectively) [2]. The integrins α1β1, α2β1, and α3β1 have been shown to participate in cellular adhesion to type IV collagen [3].

Results and Discussion

We have used monoclonal antibodies (mAb) against the integrin subunits β1, α1, α2, α3, and α5 to inhibit the adhesion of melanoma and ovarian carcinoma cells to Hep III or D-Hep III. ^{35}S-labeled cells were incubated with each of the mAbs at various concentrations (between 0.0005 to 5 μg/ml) for 1 hour, using normal mouse IgG as a control. This was followed by an incubation of 1 hour on plates coated with 5.71 μM Hep III or D-Hep III. The β1, α2, and α3 mAbs were effective at inhibiting the adhesion of the melanoma and ovarian carcinoma cells to both Hep III or D-Hep III (Figure 1). Normal mouse IgG and mAbs against α1 and α5 were ineffective.

Affinity chromatography was used to isolate the cell surface receptors that bind to Hep III. ^{125}I-labeled extracts from the melanoma and ovarian carcinoma cells were passed over a column of Hep III covalently bound to CH-Sepharose beads. The column was first eluted with 20 mM EDTA, to elute integrins, and then with 1 M NaCl, to elute the remaining components bound to the column. Immunoprecipitation of the eluate with mAbs against β1, α1, α2, α3, and α5 was performed to identify specific integrin subunits involved in the adhesion of the cells to Hep III. The results were analyzed by SDS-PAGE, followed by autoradiography.

Two components of 120 and 150 kD were immunoprecipitated when the β1 or α3 mAbs were used, corresponding to the size of non-reduced β1 and α3 integrin subunits,

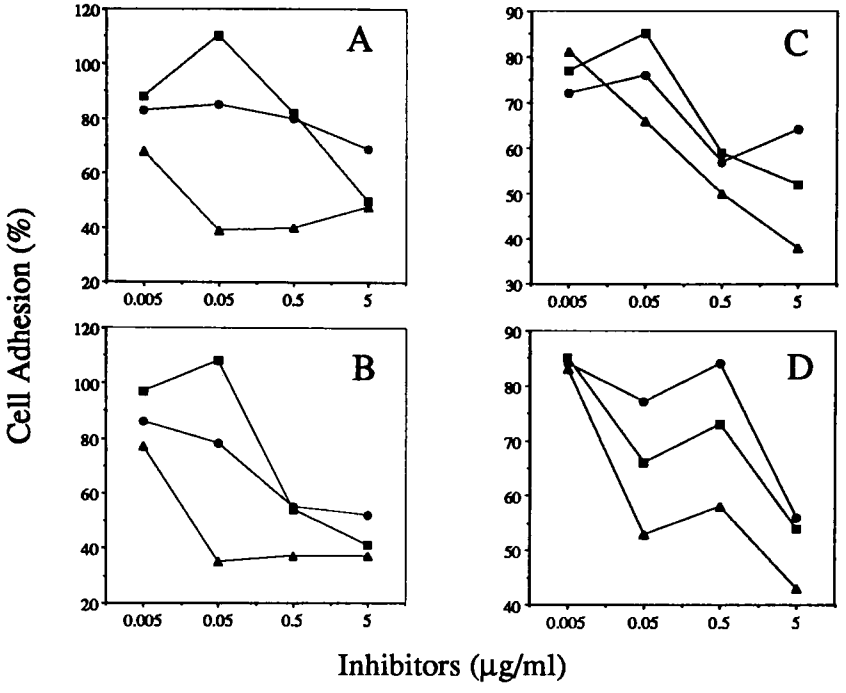

Figure 1. *Inhibition of ovarian and melanoma cell adhesion to 5.71 μM of Hep III or D-Hep III with the mAbs β1 (square), α2 (circle), and α3 (triangle). A and C are with Hep III, B and D are with D-Hep III. The melanoma cells are A and B, while the ovarian cells are C and D.*

respectively. Each mAb immunoprecipitated the same two components for both the melanoma and ovarian carcinoma cells. The α1, α2, and α5 subunits were not detected.

The inhibition studies with mAbs against the integrin subunits β1, α2, and α3 indicate that they may be involved in mediating adhesion of the ovarian and melanoma carcinoma cells to Hep III or D-Hep III. The immunoprecipitation studies suggest that the α3 and β1 subunits are associated with and bind to α1(IV) 531-543 in collagen.

Acknowledgments

This work was supported by NIH grants KD 44494 and AR 01929 (G.B.F.), CA 21463, CA 29995, and EY 09065 (L.T.F.), and CA 60658 (A.P.N.S.) and by the American Cancer Society and a McKnight-Land Grant Professorship (G.B.F.).

References

1. Koliakos, G.G., Kouzi-Koliakos, K., Furcht, L.T., Reger, L.A. and Tsilibary, E.C., *J. Biol. Chem.*, 264 (1989) 2313.
2. Miles, A.J., Skubitz, A.P.N., Furcht, L.T. and Fields, G.B., *J. Biol. Chem.*, 269 (1994) 30939.
3. Hynes, R.O., *Cell*, 69 (1992) 11.

Peptides: Chemistry, Structure and Biology
Pravin T.P. Kaumaya and Robert S. Hodges (Eds.)
Mayflower Scientific Ltd., 1996

150
Conformational Mapping of p21$^{Waf1/Cip1}$ Protein, and Cyclin Dependent Kinase-modulating Effect of its Peptide Fragments

M. Akamatsu[1], I-T. Chen[2], A.J. Fornace, Jr.[2], P.M. O'Connor[2] and P.P. Roller[1]

Laboratories of [1]Medicinal Chemistry and [2]Molecular Pharmacology, Developmental Therapeutics Program, Division of Cancer Treatment, National Cancer Institute, NIH, Bethesda, MD 20892, USA

Introduction

Cells responding to genotoxic damage caused by UV or X-ray radiation or toxic agents, for example, normally undergo a halting of their periodic cell division in order to allow time for repair of damaged DNA [1]. For this purpose the cell's growth signal is modulated by the p53 tumor suppressor protein, which activates the growth suppressor *WAF1/CIP1* [2, 3]. This gene encodes an inhibitor of cyclin dependent kinases (Cdk). This inhibitor protein, called p21$^{Waf1/Cip1}$ (called Waf1 hereafter) accumulates following DNA damage and is associated with cell cycle arrest in G1 phase. The sequence of this 164 aa long protein is conserved among several species. However, its conformation and its mode of Cdk inhibitory action are not known. For structural and bioactivity studies, we have synthesized the whole protein in peptide segments, determined their conformation and identified the regions of protein most likely responsible for its biological function.

Results and Discussion

The complete human-Waf1 protein was synthesized in ten 20-26 aa long peptide segments with 4 aa overlaps and with free N- and C-terminals. tBoc chemistry-based SPPS was used on a Biosearch Model 9600 synthesizer. Cys protecting group was 4-methoxybenzyl. Merrifield resin cleavage was achieved with HF in presence of anisole and DMS. Cys containing peptides were reduced after HF cleavage with DTT in 6 M Gn/0.1 M Tris.HCl, pH 8. Peptides were purified on a Sephadex G-25 column with 1 N aq. acetic acid, followed by RPLC.

Conformation of the 10 peptides was measured with circular dichroism (CD) spectroscopy in buffer, and α-helical propensities were estimated by measurements in 1/1 TFE/buffer. Conformational components were calculated using Woody's Self Consistent Variable Selection Method [4]. Peptides in buffer showed very low conformational order, with some α-helical content in peptide **2** (Table 1) and in Peptide(106-125). Large increase in helical content was only observed in peptides **2**

Table 1. *Relevant peptide segments of Waf1 protein.*

Peptide **1**(15-40)	SKACRRLFGPVDSEQLSRDCDALMAG
Peptide **2**(21-45)	LFGPVDSEQLSRDCDALMAGCIQEA
Peptide **3**(58-77)	PLEGDFAWERVRGLGLPKLY
Peptide **4**(139-194)	GRKRRQTSMTDFYHSKRRLIFSKRKP

(34% α-helix) and **4** (41% α-helix) in the lipophilic TFE solvent (Figure 1), suggesting that these regions are either in the interior of the protein or function in interchain or intermolecular lipophilic interactions.

Using the ten peptides, three biologically active regions were discovered here termed regions A, B and C. It was found that the more N-terminal α-helical region juxtaposes two Cdk2 interacting segments in the protein: region A in peptide **1** blocked Waf1 binding, and also the inhibition of cyclin E/Cdk2 kinase by Waf1; region B in peptide **3**, on the opposite side of the same helical region also, antagonized Waf1 activity, but this peptide did not affect the ability of Waf1 to interact with cyclinE/Cdk2. The C-terminal α-helical segment **4**, termed region C, was found to suppress Waf1 - PCNA interactions. Identification of active site segments of Waf1 may prove useful in generating small molecule regulators of cell cycle checkpoints for antitumor therapy.

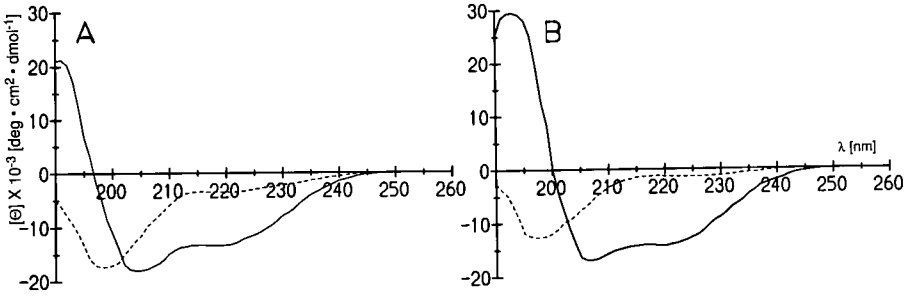

Figure 1. *CD spectra of peptide segments **2** (Panel A) and **4** (Panel B) of Waf1 protein that show induction of α-helical conformation in TFE. Dotted line, samples in buffer, 50 mM PO_4 pH 7.2; solid line, samples in 1:1 buffer:TFE. Note: Chou-Fasman prediction estimates high α-helical content in aa region 36-51.*

References

1. Hartwell, L.H. and Kastan, M.B., *Science*, 266 (1994) 1821.
2. El-Deiry, W.S., Tokino, T., Valculescu, V.E., Levy, D.B., Parsons, R., Trent, J.M., Lin, D., Mercer, W.E., Kinzler, K.W. and Vogelstein, B., *Cell*, 75 (1993) 817.
3. Harper, J.W., Adami, G.R., Wei, N., Keyomarsi, K. and Elledge, S.J., *Cell*, 266 (1993) 805.
4. Sreerama, N. and Woody, R.W., *Anal. Biochem.*, 209 (1993) 32.

Peptides: Chemistry, Structure and Biology
Pravin T.P. Kaumaya and Robert S. Hodges (Eds.)
Mayflower Scientific Ltd., 1996

151
Position 3 Modified AVP Antagonists: Surprising Findings

W.A. Klis[1], L.-L. Cheng[1], S. Stoev[1], N.C. Wo[2], W.Y. Chan[2] and M. Manning[1]

[1]Department of Biochemistry and Molecular Biology, Medical College of Ohio, Toledo, OH 43699, USA
[2]Department of Pharmacology, Cornell University Medical College, New York, NY 10021, USA

Introduction

Position 3 in vasopressin has long been considered very intolerant of change. Introduction of tetrahydro-isoquinoline-3-carboxylic acid (Tic) at position 3 in the potent, non-selective VP antagonist d(CH_2)$_5$-D-Tyr(Et)-VAVP (A, Table 1) gave diminished V_{1a} and OT antagonism but surprisingly led to full retention of V_2 antagonism (B, Table 1) [1]. We now present an exploration of this lead with other conformational probes; 2-aminotetralin-2-carboxylic acid [(+)Atc], [(-)Atc], HO-Tic and other aromatic amino acids (Trp, Tyr, Table 1). Furthermore, we present an examination of Tic[3] substitutions in some of our selective antagonists (C, D and E, Table 2).

Table 1. *Pharmacological properties of position 3 modified AVP V_{1a}/V_2/OT antagonists d(CH_2)$_5$-[D-Tyr(Et)^2,X^3]VAVP.*

No.	X^3	Anti-V_2 pA_2[a]	Anti-V_{1a} pA_2	Anti-OT (*in vitro*) pA_2 (No Mg^{2+})
A	Phe[b]	7.81 ± 0.07	8.22 ± 0.12	8.32 ± 0.10
B	Tic[b]	7.69 ± 0.05	6.95 ± 0.03	7.54 ± 0.05
1	HO-Tic	7.20 ± 0.05	7.27 ± 0.05	7.67 ± 0.05
2	(+)Atc	6.86 ± 0.02	7.45 ± 0.04	7.44 ± 0.04
3	(-)Atc	5.66 ± 0.09	5.62 ± 0.03	~ 6.2 (agonist ~ 0.15)
4	Tyr	7.58 ± 0.05	7.45 ± 0.05	7.53 ± 0.04
5	Trp	7.61 ± 0.08	7.64 ± 0.01	7.63 ± 0.04
6	Tic[c]	7.52 ± 0.06	6.61 ± 0.08	7.39 ± 0.07
7	Tic[d]	7.57 ± 0.01	6.53 ± 0.04	7.61 ± 0.03

[a]Estimated *in vivo* pA_2 values represent the negative logarithms of the dose (in nmoles/kg) (the "effective dose") that reduced the response seen with 2x units of agonist to equal the response seen with x units of agonist administered in absence of the antagonist divided by the estimated volume of distribution (67 ml/kg); [b]Data from ref. 1; [c]Peptide 6 is modified at position 6 by D-Cys; [d]Peptide 7 is modified at position 9 by Tyr-NH_2.

Table 2. *Pharmacological properties of position 3 modified selective AVP V_2 antagonists.*

No.	Peptide	Anti-V_2 pA_2[a]	Anti-V_{1a} pA_2	Anti-OT (*in vitro*) pA_2 (No Mg^{2+})
C	$d(CH_2)_5$[D-Ile^2,Ile^4,Ala-NH_2^9]AVP[b]	8.16 ± 0.03	6.25 ± 0.02	
8	$d(CH_2)_5$[D-Ile^2,Tic^3,Ile^4, Ala-NH_2^9]AVP	6.67 ± 0.10	5.35 ± 0.04	7.28 ± 0.38
9	$d(CH_2)_5$[D-Ile^2,Tyr^3,Ile^4, Ala-NH_2^9]AVP	6.59 ± 0.03	(agonist 0.01 U/mg)	6.92 ± 0.03
D	$d(CH_2)_5$[D-Ile^2,Ile^4,Tyr-NH_2^9]AVP[b]	7.85 ± 0.03	6.43 ± 0.11	
10	$d(CH_2)_5$[D-Ile^2,Tic^3,Ile^4, Tyr-NH_2^9]AVP	6.71 ± 0.07	< 5.0	7.08 ± 0.02
E	Aaa-D-Tyr(Et)-Phe-Val-Asn-Abu-Pro-Arg-Arg-NH_2[c]	8.11 ± 0.07	7.75 ± 0.07	
11	Aaa-D-Tyr(Et)-Tic-Val-Asn-Abu-Pro-Arg-Arg-NH_2	7.15 ± 0.07	5.51 ± 0.05	7.25 ± 0.04

[a]See footnote Table 1; [b]data from ref. 2; [c]Data from ref. 3.

Results and Discussion

With the exception of the (-)Atc^3 analog (No. 3, Table 1) which exhibits drastic reductions in V_2, V_{1a} and OT antagonistic potencies and the (+)Atc^3 analog (No. 2) which retains about 10% of the V_2 antagonism of A, all of the remaining position 3 analogs in Table 1 exhibit potent V_2 antagonism. The two new Tic^3 analogs (Nos. 6 and 7) exhibit enhanced anti-V_2/anti-V_{1a} selectivity similar to B. Tic^3 substitution in two of our selective V_2 antagonists (peptides C and D, Table 2) led to large losses of antagonistic potencies. However, peptides 8-10 preserve the V_2 selectivities of the parent peptides. Most surprisingly, Tyr^3 substitution in (C) resulted in a complete loss of anti-V_{1a} potency. Peptide 9 exhibits infinite anti-V_2/V_{1a} selectivity. These studies demonstrate that position 3 in AVP V_2/V_{1a} antagonists can be modified with good retention of V_2 antagonistic potencies, and/or V_2/V_{1a} selectivities.

Acknowledgments

We thank Ms. Ann Chlebowski for her expert help in the preparation of this manuscript and NIH grants GM-25280 and DK-01940.

References

1. Manning, M., Cheng, L.-L., Stoev, S., Bankowski, K., Przybylski, J.P., Klis, W.A., Sawyer,W.H., Wo, N.C. and Chan, W.Y., *J. Peptide Sci.*, 1 (1995) 66.
2. Sawyer, W.H., Bankowski, K., Misicka, A., Nawrocka, E., Kruszynski, M., Stoev, S., Klis, W.A., Przybylski, J.P. and Manning, M., *Peptides*, 9 (1988) 157.
3. Manning, M., Klis, W.A., Kruszynski, M., Przybylski, J.P., Olma, A., Wo, N.C., Pelton, G.H. and Sawyer, W.H., *Int. J. Peptide Protein Res.*, 32 (1988) 455.

Peptides: Chemistry, Structure and Biology
Pravin T.P. Kaumaya and Robert S. Hodges (Eds.)
Mayflower Scientific Ltd., 1996

152
Rational Design of Enzymatically Resistant, Peptide Based, Multi-site Directed, α-Thrombin Inhibitors

A. Lombardi[1], F. Nastri[1], S. Galdiero[1], R. Della Morte[2], N. Staiano[2], C. Pedone[1] and V. Pavone[1]

[1]Centro Interdipartimentale di Ricerca su Peptidi Bioattivi, University of Naples "Federico II", via Mezzocannone 4, 80134 Napoli, Italy
[2]Dip. di Biochimica e Biotecnologie Mediche, University of Naples, via Pansini 5; 80100 Napoli, Italy

Introduction

Hirudin, a small protein of 65 amino acids from the leech *Hirudo medicinalis*, is the most potent natural thrombin inhibitor known to date [1]. It binds specifically to thrombin and thereby inhibits the cleavage of fibrinogen and fibrin clotting.

The recent elucidation of the three-dimensional structure of recombinant hirudin/ human thrombin complex [2], and the comparative analysis of the biological activities of several hirudin analogues and fragments [3, 4], have led us to rationally design more potent, enzymatically resistant, peptide analogues. These may find therapeutic use in various clinical disorders, such as vascular diseases and inflammatory response [5].

The main structural features of hirudin human thrombin interactions are: i) the hirudin N-terminal segment is located near the thrombin active site. It is positioned in a non-natural mode because the peptide chain aligns parallel to the α-thrombin residues Ser^{214}-Gly^{216}, whereas the natural mode of substrate interaction corresponds to an antiparallel alignment; ii) the hirudin C-terminal 3_{10} helical segment (Pro^{60}-Gln^{65}) interacts with the thrombin anion binding exosite; iii) the hirudin segment Pro^{48}-Ile^{59} is in an extended conformation; iv) the hirudin core Cys^{6}-Lys^{47} interacts with the thrombin surface at only a few points. Synthetic analogues [3,4,6] have been developed with the aim of obtaining lower molecular weight compounds capable of reproducing the natural hirudin mechanism of action. These analogues contain a catalytic site directed moiety, an anion binding exosite, and a spacer linking these segments. They all bind to thrombin in a manner that is slightly different from hirudin. They penetrate the active site the same way a substrate does, thus causing a scissile peptide bond to undergo catalytic cleavage. The insertion of peptide bond surrogates and of extra-methylene groups is required to improve potency.

We have designed a series of low molecular weight hirudin analogues (named Hirunorms) that bind to thrombin analogues to hirudin, but different to other hirudin-like molecules. Our analogues act as multi-site directed thrombin inhibitors which penetrate the thrombin active site in a non-natural mode (parallel mode) and bind to the anion binding exosite.

Results and Discussion

Our most active compound is hirunorm V: (H-Chg-Val-2-Nal-Thr-Asp-ala-Gly-βAla-Pro-Glu-Ser-His-h-Phe-Gly-Gly-Asp-Tyr-Glu-Glu-Ile-Pro-Aib-Aib-Tyr-Cha-glu-OH).

The synthesis of hirunorms was performed using the standard Boc strategy solid phase method. The peptide chains were assembled on the PAM resin. Deprotection and cleavage from the resin was obtained by treatment with anhydrous HF. The extracted crude materials were purified to homogeneity by preparative RP-HPLC with a water/acetonitrile (0.1% TFA) linear gradient. Fab-Mass spectra gave the expected molecular ion peak values. The yields were satisfactory for all peptides.

Hirunorms are potent thrombin inhibitors: i) Hirunorm V inhibits thrombin-catalyzed hydrolysis of a chromogenic substrate (Chromozym) with an apparent inhibition constant Ki'=0.2nM; ii) Inhibitor concentration to double Thrombin Time (TT) in human plasma in *in vitro* experiments is 70nM, whereas to double activated Partial Thromboplastin Time (aPTT) it is 425nM; iii) Hirunorm V inhibits thrombin induced platelet aggregation with an IC_{50}=50nM. Hirunorms are also highly selective, being unable to inhibit plasmin, t-PA and trypsin up to 10 μM concentration and, interestingly, Hirunorm V is stable to the amidolytic action of thrombin for at least 2 h and is stable in human plasma for more than 2 h.

Preliminary experiments indicate that Hirunorm V inhibits stasis-induced venous thrombosis and arterial thrombosis in anaesthetized rats at 0.20 mg/kg i.v. and 1 mg/kg after 15 min drug infusion, respectively. Furthermore, Hirunorm V shows a surprising safety profile (personal communication from M. Criscuoli).

Hirunorms represent a new class of multi-site directed human α-thrombin inhibitors. They were rationally designed to interact through their N-terminal end with the thrombin active site in a non substrate mode, and to specifically bind the anion binding exosite. An appropriate spacer that is able to properly position the N-terminal end in the active site was also selected. The peculiar structure of these molecules makes them stable to the amidolytic action of thrombin without the introduction of any peptide bond modification. Furthermore, the molecules display long lasting activity in human plasma, due to the presence of several unnatural amino acids in susceptible positions. Hirunorms are potential candidates for injectable anticoagulants, due to their potency, specificity of action, long lasting activity and safety profiles.

References

1. Stone, S.R. and Hofsteenge, J., *Biochemistry*, 25 (1986) 4622.
2. Rydel, T.J., Ravichandran, K.G., Tulinsky, A., Bode, W., Huber, R., Roitsch, C. and Fenton II, J.W., *Science*, 249 (1990) 277.
3. Skrzypczak-Jankun, E., Carperos, V.E., Ravichandran, K.G., Tulinsky, A., Westbrook, M. and Maraganore, J.M., *J. Mol. Biol.*, 221 (1991) 1379.
4. Zdanov, A., Wu, S., DiMaio, J., Konishi, Y., Li, Y., Wu, X., Edwards, B.F.P., Martin, P.D., Cygler, M., *Proteins: Structure, Function, and Genetics*, 17 (1993) 252.
5. Bichler, J. and Fritz, H., *Hematology*, 63 (1991) 67.
6. Tsuda, Y., Cygler, M., Gibbs, B.F., Pedyczak, A., Féthière, J., Yue, S.Y. and Konishi,Y., *Biochemistry*, 33 (1994) 14443.

Peptides: Chemistry, Structure and Biology
Pravin T.P. Kaumaya and Robert S. Hodges (Eds.)
Mayflower Scientific Ltd., 1996

153
Inhibition of Human Renin by Statine Alkylamide-containing Peptides with Varying Alkyl Sidechain Structures

M.K. Guha, Y. Luo and K. Misono

Department of Molecular Cardiology, and Protein Chemistry Core Facility, Research Institute, The Cleveland Clinic Foundation, Cleveland, OH 44195, USA

Introduction

Renin catalyzes cleavage of decapeptide angiotensin I from its protein substrate angiotensinogen. This is the first and rate-limiting step in a series of reactions leading to formation of a potent hypertensive peptide factor angiotensin II. Hence, renin inhibitors are potential therapeutic agents against hypertension and other cardiovascular diseases. Inhibitor peptides containing a statine (Sta) residue as a transition-state mimetic have previously been prepared [1-3]. The Sta residue provides an isobutyl side chain that corresponds to the Leu residue at P_1 position and a hydroxymethylene group that mimics the tetrahedral transition-state in renin catalysis. In such inhibitors, the Sta residue is followed generally by a P1' amino acid residue. However, the Sta residue inserts two extra C-C bonds in the peptide backbone, causing misalignment of sidechains in P1', P2' and P3' sites. We have synthesized a series of peptide derivatives of general structure, Ac-His-Pro-Phe-His-Sta-CO-NH-R, in which the amide alkyl group, R, was varied to mimic the substrate sidechains in P1' and P2' positions. These compounds represent a new group of renin inhibitors that do not require natural amino acids at P' positions.

Results and Discussion

Inhibitor compounds with a general structure, Ac-His-Pro-Phe-His-Sta-CO-NH-R, were synthesized as follows: Ac-His-Pro-Phe-His-Sta-OH, with His- and Sta- sidechains protected, was synthesized on chlorotrityl-resin by the solid-phase Fmoc synthesis. The C-terminal carboxyl of the protected peptide was activated to *N*-hydroxysuccinimide ester using dicyclohexylcarbodiimide. The peptide alkylamide was formed by addition of a respective amine. The peptide was then deprotected and purified by reverse-phase HPLC. Inhibition of recombinant human renin by the peptide amides was determined using tetradecapeptide renin substrate. Angiotensin I formation was measured by radioimmunoassay.

Our approach to the design of renin inhibitor was to grow an alkyl sidechain, R, after the Sta residue to fill P1' and P2' positions. The synthesized inhibitors and their IC_{50} values are shown in Table 1. Compounds **2** and **3** with one and two methyl groups on the amide nitrogen, respectively, mimicking the Val sidechain at P1, were several fold more

potent than **1** with a free carboxyl group. The piperidine ring in **4** caused a 5-fold increase in inhibitory potency over **3**, suggesting that the constrained structure contributed to tighter binding. The cyclohexylamide moiety in **5** showed a similar but slightly lower potentiating effect. The isopropylamide moiety in **6** may extend beyond P1' but does not reach P2' site, possibly causing lower potency than **3**. Further extension of the alkyl residue by one and two methylene groups in **7** and **8** gave 4- and 10-fold increase, respectively, in the inhibitory potency over **6**. These results suggest that alkyl groups in **7** and **8** reach P2' position. Addition of a hydroxyl group in P1' position in **9** and **10** did not improve the inhibitory activity. The significant difference in IC_{50} between the diastereomers **9** and **10** reflects a stereochemical preference in P1' site. Our data suggest that P1' and P2' positions are equally important in binding of inhibitors to renin and that P1' site is more flexible and accommodates a larger group.

Table 1. *Inhibition of human renin by statine alkylamide containing peptides.*

No.	Structure of the Inhibitor Compounds	IC_{50} (nm)
	P_5 P_4 P_3 P_2 P_1 - P_1' P_2'	
1	Ac-His-Pro-Phe-His-Sta-CO-OH	1,500
2	Ac-His-Pro-Phe-His-Sta-CO-NH-CH_3	400
3	Ac-His-Pro-Phe-His-Sta-CO-N$(CH_3)_2$	300
4	Ac-His-Pro-Phe-His-Sta-CO-NH(piperidine)	50
5	Ac-His-Pro-Phe-His-Sta-CO-NH(cyclohexylamine)	90
6	Ac-His-Pro-Phe-His-Sta-CO-NH-CH$(CH_3)_2$	320
7	Ac-His-Pro-Phe-His-Sta-CO-NH-CH_2-CH$(CH_3)_2$	90
8	Ac-His-Pro-Phe-His-Sta-CO-NH-CH_2-CH_2-CH$(CH_3)_2$	30
9[a]	Ac-His-Pro-Phe-His-Sta-CO-NH-C*H(CH_2OH)-CH$(CH_3)_2$	60
10[a]	Ac-His-Pro-Phe-His-Sta-CO-NH-C*H(CH_2OH)-CH$(CH_3)_2$	180

[a]Compounds **9** and **10** are diastereomers. The asterisk indicates asymmetric carbons.

Acknowledgments

This work was supported by grants HL37399 and HL33713. We thank Dr. Stephen T. Rapundalo of Parke-Davis for kindly providing us with recombinant human renin. We thank Robin Lewis for her assistance in preparing the manuscript.

References

1. Hui, K.Y., Carlson, W.D., Bernatowicz, M.S. and Haeber, E., *J. Med. Chem.*, 30 (1987) 1287.
2. Boger, J., in Lambert, R.W. (Ed.), 'Proceedings of the 3rd SCI-RSC Medicinal Chemistry Symposium', Royal Society of Chemistry, London, 1986. p. 271.
3. Boger, J., Lohr, N.S., Ulm, E.H., Poe, M., Blaine, E.H., Faneli, G.M., Lin, T.Y., Payne, P.S., Schorn, T.W., La Mont, B.I., Vassil, T.C., Stabilito, I.I., Veber, D.F., Rich, D.H. and Bopari, A.S., *Nature*, 303 (1983) 81.

Peptides: Chemistry, Structure and Biology
Pravin T.P. Kaumaya and Robert S. Hodges (Eds.)
Mayflower Scientific Ltd., 1996

154
Molecular Model of the G-Protein Coupled Melanocortin Receptor, hMC1R: Possible Interactions with α-MSH Peptides

C. Haskell-Luevano[1], T.K. Sawyer[2] and V.J. Hruby[1]

[1]Department of Chemistry, University of Arizona, Tucson, AZ 85721, USA
[2]Department of Chemistry, Parke-Davis Pharmaceutical Research Division, The Warner-Lambert Company, Ann Arbor, MI 48109, USA

Introduction

α-Melanotropin (α-MSH, Ac-Ser-Tyr-Ser-Met-Glu-His-Phe-Arg-Trp-Gly-Lys-Pro-Val-NH_2) is recognized for its role in skin darkening and has been the target of extensive structure-function studies for several decades. Isolation of the human melanocortin receptor, hMC1R [1, 2], has allowed us to prepare a 3-dimensional molecular model of this receptor. The model was developed based on homology modeling using the bacteriorhodopsin [3] template. The superpotent peptides Ac-[Nle^4, DPhe^7]α-MSH (NDP-MSH, MT-I) [4, 5] and cyclo(Asp^5, Lys^{10}) Ac-Nle^4-Asp^5-His^6-DPhe^7-Arg^8-Trp^9-Lys^{10}-NH_2 (MT-II) [5, 6] have been docked into this model. These studies were performed to gain molecular insight into probable peptide-receptor interactions.

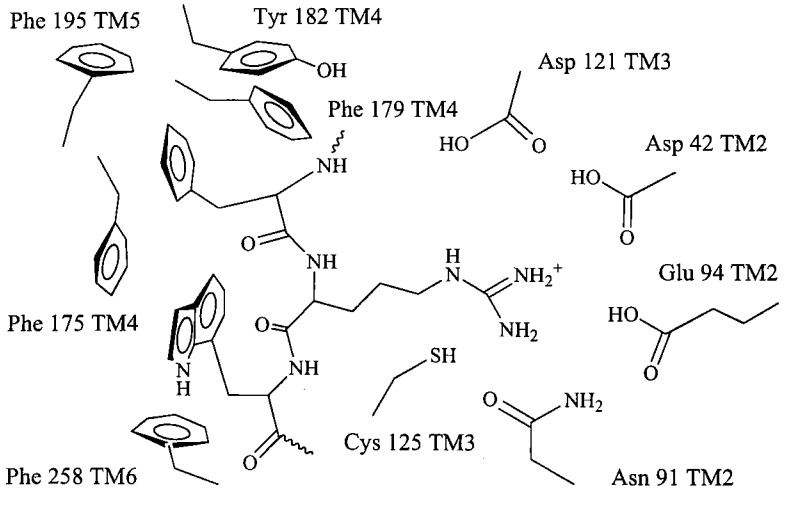

Figure 1. *The pharmacophore residues (DPhe-Arg-Trp) of MT-I and specific receptor interactions proposed in the modeled receptor binding pocket.*

Results and Discussion

We have developed a 3D molecular model of the peripheral melanocortin receptor, hMC1R, believed to be involved in skin pigmentation. Superpotent agonists MT-I and MT-II were docked into the proposed binding pocket to identify probable ligand-receptor interactions involved in physiological response. Figures 1 and 2, of MT-I and MT-II respectively, illustrate the peptide pharmacophore residues, DPhe-Arg-Trp, interacting with specific receptor residues in the modeled binding pocket . Alternative binding locations for the Trp residue in the linear and cyclic peptides have been identified. This observation is supported by functional differences observed between binding efficacy, cAMP generation, and dissociation studies. Since little receptor mutagenesis data has been published to date, alternative peptide-receptor interactions (not shown) have been identified by manipulation of the transmembrane spanning α-helical regions to try to maximize identification of possible specific and chemical interactions occuring between the peptides and this receptor. This work was supported by a grant from the USPHS.

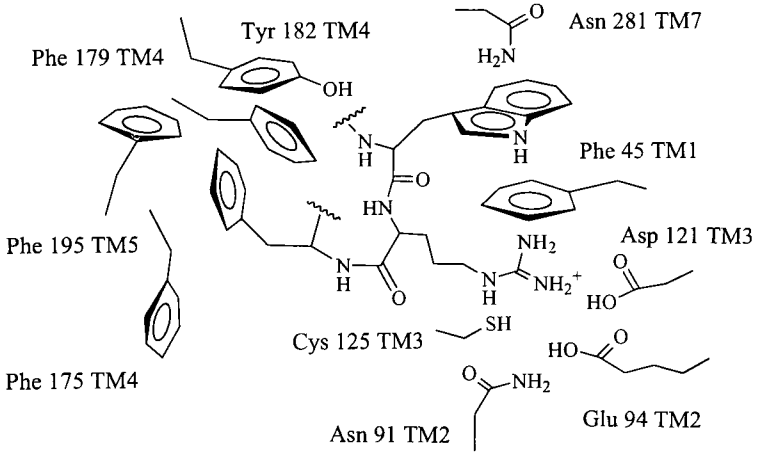

Figure 2. *The pharmacophore residues (DPhe-Arg-Trp) of MT-II and specific receptor interactions proposed in the modeled receptor binding pocket.*

References

1. Mountjoy, K.G., Robbins, L.S., Mortrud, M.T. and Cone, R.D., *Science*, 257 (1992) 1248.
2. Chhajlani, V. and Wikberg, J.E.S., *FEBS Lett.*, 309 (1992) 417.
3. Henderson, R., Baldwin, J.M., Ceska, T.A., Zemlin, F., Beckmann, E. and Downing, K.H., *J. Mol. Biol.*, 213 (1990) 899.
4. Sawyer, T.K., Sanfillippo, P.J., Hruby, V.J., Engel, M.H., Heward, C.B., Burnett, J.B. and Hadley, M.E., *Proc. Natl. Acad. Sci. USA*, 77 (1980) 5754.
5. Haskell-Luevano, C., Miwa, H., Dickinson, C., Hruby, V.J., Yamada, T. and Gantz, I., *Biochem. Biophys. Res. Commun.*, 204 (1994) 1137.
6. Al-Obeidi, F., Hadley, M.E., Pettitt, B.M. and Hruby, V.J., *J. Am. Chem. Soc.*, 111 (1989) 3413

Peptides: Chemistry, Structure and Biology
Pravin T.P. Kaumaya and Robert S. Hodges (Eds.)
Mayflower Scientific Ltd., 1996

155
Position 5 Modifications of Vasopressin and Oxytocin Antagonists Enhance OT Receptor Selectivity

L.-L. Cheng[1], A. Olma[1], W.A. Klis[1], M. Manning[1], W.H. Sawyer[3], N.C. Wo[2] and W.Y. Chan[2]

[1]Department of Biochemistry and Molecular Biology, Medical College of Ohio, Toledo, OH 43699, USA,
[2]Department of Pharmacology, Cornell University Medical College, New York, NY 10021, USA
[3]Department of Pharmacology, College of Physicians and Surgeons, Columbia Univ., New York, NY, 10032, USA

Introduction

Position 5 in OT agonists has long been known to be essential for agonistic activity [1]. Remarkably, the replacement of the Asn^5 residue by Thr^5 and Asp^5 in the OT antagonist [Pen^1,D-Phe^2,Thr^4]OVT led to good retention of *in vitro* anti-OT potencies [2]. We now present data (Manning, M., Olma, A., Klis, W.A. and Sawyer, W.H., unpublished) on the effects of some position 5 changes in the potent non-selective VP antagonist $d(CH_2)_5$[D-Phe^2]VAVP (A, Table 1). We also present OT antagonists B-E, (Table 2) isosterically modified at position 5 to give the five analogs 6-10 (Table 2).

Table 1. *Analogs of the VP antagonist $d(CH_2)_5$[D-Phe^2]VAVP modified at position 5.*

				Anti-OT (*in vitro*)	
No.	X^5	Anti-V_2 pA_2[a]	Anti-V_{1a} pA_2[a]	pA_2 (no Mg^{2+})	pA_2 (0.5 mM Mg^{2+})
A	Asn[b]	8.07 ± 0.09	8.06 ± 0.03	7.74 ± 0.06	8.29 ± 0.05
1	Ser[c]	6.21 ± 0.08	7.71 ± 0.09	7.67 ± 0.06	7.20 ± 0.09
2	Gln[c]	~ 5.6	6.55 ± 0.08	7.25 ± 0.07	6.81 ± 0.09
3	Phe[c]	~ 5.7	~ 5.7	Agonist (3.4 ± 0.3)[d]	Agonist (1.2 ± 0.2)[d]
4	Val[c]	~ 6	6.48 ± 0.01	7.36 ± 0.10	7.00 ± 0.08
5	Thr[c]	~ 6.4	7.29 ± 0.07	8.01 ± 0.07	7.43 ± 0.05

[a]Estimated *in vivo* pA_2 values represent the negative logarithms of the dose (in nmoles/kg) (the "effective dose") that reduced the response seen with 2x units of agonist to equal the response seen with x units of agonist administered in absence of the antagonist divided by the estimated volume of distribution (67 ml/kg); [b]Data from Manning, M., Klis, W.A., Olma, A., Seto, J. and Sawyer, W.H.; J. Med. Chem., 25 (1982) 414; [c]This publication; [d]U/mg.

Table 2. *OT antagonists with isosteric modifications at position 5.*

No.	Peptide	Anti-OT pA_2[a,b]	Anti-V_{1a} pA_2[a]	Antidiuretic (U/mg)
B	$d(CH_2)_5$[Tyr(Me)^2,Thr^4,Tyr- NH_2^9]OVT[c]	7.63 ± 0.07	7.02 ± 0.07	0.015 ± 0.006
6	Dap^5 Analog of B[d]	7.56 ± 0.06	5.35 ±0.04	< 0.001
7	Dab^5 Analog of B[d]	7.29 ± 0.05	< 5.0	< 0.001
C	desGly-NH_2d$(CH_2)_5$[D-Tyr^2, Thr^4]OVT[c]	7.77 ± 0.04	5.39 ± 0.04	antagonist pA_2 < 5.5
8	Dap^5 Analog of C[d]	6.67 ± 0.02	ND	< 0.0005
D	desGly-NH_2d$(CH_2)_5$[D-Phe^2, Thr^4]OVT[c]	7.90 ± 0.06	5.30 ± 0.04	< 0.008
9	Dap^5 Analog of D[d]	7.11 ± 0.03	ND	< 0.0005
E	desGly-NH_2d$(CH_2)_5$[D-Trp^2, Thr^4]OVT[c]	8.02 ± 0.03	5.43 ± 0.04	< 0.010
10	Dap^5 Analog of E[d]	7.47 ± 0.25	ND	< 0.005

[a]See footnote Table 1; [b]*in vitro* (no Mg^{2+}); [c]Data from ref. 3; [d]This publication; [e]Data from ref. 4; Dap = Diaminopropionic acid; Dab = Diaminobutyric acid; ND = non-detectable.

Results and Discussion

With the exception of the Phe^5 analog (which exhibits OT agonism), the remaining four position 5 analogs (Table 1) retain good *in vitro* OT antagonism and much reduced V_2 and V_{1a} antagonism.

The Dap^5/Asn^5 interchange in B-E led to good retention of *in vitro* OT antagonism in all four resulting analogs 6, 8-10. This interchange totally abolished V_{1a} antagonism in 8-10 (Table 2). Analogs 8-10 are the first reported totally selective OT antagonists.

Acknowledgments

We thank Ms. Mary Schmidbauer and Ms. Ann Chlebowski for expert help in the preparation of this manuscript and NIH grants GM-25280 and DK-01940.

References

1. du Vigneaud, V., Denning, G.S., Drabarek, S. and Chan, W.Y., *J. Biol. Chem.*, 238 (1963) PC 1560.
2. Hill, P.S., Chan, W.Y., and Hruby, V.H., *Int. J. Pep. Prot. Res.*, 28 (1991) 32.
3. Manning, M., Kruszynski, M., Bankowski, K., Olma, A., Lammek, B., Cheng, L.L., Klis, W.A., Seto, J., Haldar, J. and Sawyer, W.H., *J. Med. Chem.* 32 (1989) 382.
4. Manning, M., Miteva, K., Pancheva, S., Stoev, S., Wo, N.C. and Chan, W.Y., *Int. J. Peptide Protein Res.*, 46 (1995) 244.

Peptides: Chemistry, Structure and Biology
Pravin T.P. Kaumaya and Robert S. Hodges (Eds.)
Mayflower Scientific Ltd., 1996

156

Design of Potent Lipophilic Peptide Inhibitors of Human Neutrophil Elastase: *In Vitro* and *In Vivo* Studies

I. Toth[1], M. Christodoulou[1], K. Bankowsky[1], N. Flinn[1], W.A. Gibbons[2], G. Godeau[2], E. Moczar[2] and W. Hornebeck[2]

[1]*The School of Pharmacy, University of London, 29-39 Brunswick Square, London, WC1N-1AX, UK*
[2]*Faculte Chirurgie Dentaire - University R. Descantes, 1 rue M. Arnoux, Montrouge, France*

Introduction

Human neutrophil elastase (HNE; EC 3.4.21,37) plays physiological functions in host defense against bacterial infections and extracellular matrix (ECM) remodelling following tissue injury [1]. Ala-Ala-Pro-Val sequence fits the P_4-P_1 sub-sites of elastase and inhibits HNE competitively with K_i approx.10^{-4}M. The covalent coupling of lipophilic moieties as long chain *cis* unsaturated fatty acids was found to considerably increase the inhibitory capacity of the substance, in keeping with the presence of an unusual hydrophobic binding site in HNE located near its active center [2-4]. In order to get a better insight of the size of this hydrophobic pocket, a series of lipopeptides of increasing lipophilic character were synthesized keeping constant the peptide moiety (Ala-Ala-Pro-Val) and analyzed for their HNE inhibitory capacities. In the present investigations, we also evaluated *in vivo* the bifunctionality of one such lipopeptide using elastin as the target macromolecule and quantified our data by automated image analysis.

Results and Discussion

In vitro inhibition of HNE amidolytic activity towards $Suc(Ala)_3NA$ by lipopeptides **1b**, **1c**, **1d** and **1e** increased with increased lipophilicity of the substances; all compounds were more potent HNE inhibitors than N-oleoyl-$(Ala)_2$Pro-Val-OH (**1a**). Compound **1d** inhibited HNE with IC_{50} = $1.8x10^{-10}$ M as compared with IC_{50}=10^{-4} M [2] for the peptidic moiety above. Such difference indicated, in keeping withthe size of the lipidic part of the molecule, that the extended hydrophobic subsites of HNE could accommodate large hydrophobic molecules. Modifying the end carboxylic group of the lipopeptide to an ester (**1e**) led to decreased inhibitory capacity of the compound. This substantiates earlier studies suggesting a primordial site in ionic interactions between ARG^{217} in HNE and the free carboxylate of the enzyme.

X-L-Ala-L-Ala-L-Pro-L-Val-Y

1a	$X=CH_3(CH_2)_7CH=CH(CH_2)_7CO$	**Y**=OH
1b	$X=(CH_3)_3COCO$-D,L-$NH[CH(CH_2)_{11}CH_3]$	**Y**=OH
1c	$X=(CH_3)_3COCO\{D,L\text{-}NH[CH(CH_2)_{11}CH_3]CO\}_2$	**Y**=OH
1d	$X=(CH_3)_3COCO\{D,L\text{-}NH[CH(CH_2)_{11}CH_3]CO\}_3$	**Y**=OH
1e	$X=(CH_3)_3COCO\{D,L\text{-}NH[CH(CH_2)_{11}CH_3]CO\}_3$	**Y**=OCH_3

The *in vivo* HNE inhibitory capacity of **1d** as well as its protective functions against elastolysis by elastin was further investigated (Figure 1 $p>0.0001$). Intradermal injections of lipopeptide **1d** did not modify A_λ% of rabbit skin elastic fibres, as compared to animals where only PBS was administered. HNE administrations, in similar conditions, resulted in a significant reductions of dermal elastic fibres levels. When **1d** was administered prior (15 min), with or after HNE, it could protect elastic fibre degradations induced by the enzyme. Such results extend previous studies demonstrating the *in vitro*, *ex vivo* and *in vivo* bi-functionality of lipopeptides acting as potent elastase inhibitors and elastic fibre protectors against elastolysis.

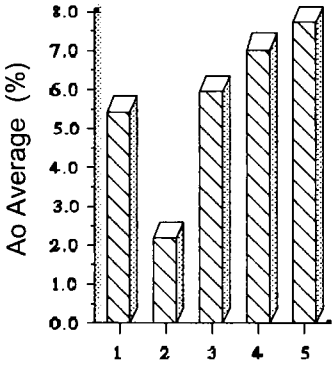

Figure 1. *In vivo HLE activity of compound* ***1d****. 1. Two hundred µL of phosphate buffered saline (PBS) pH 7.4, 2. 7.6 µM HNE in 200 µL PBS, 3. Two hundred and fifty µg of* ***1d*** *dissolved in 1:1 (v/v) EtOH/PBS followed 15 minutes later by administration at the same site of 7.6 µM of HNE (100 µL solution in PBS), 4. 7.6 µM HNE (100 µL solution in PBS) followed 15 minutes later by local administration of 250 µg of* ***1d*** *dissolved in EtOH/PBS 1:1 (v/v). 5. 7.6 µM HNE with 250 µg of* ***1d*** *injected simultaneously.*

References

1. Takahashi, L.H., Radhakrishnan, R., Rosenfield, Jnr., R.E., Meyer, Jnr, E.F. and Trainor, D.A., *J. Am. Chem. Soc.*, 111 (1989) 3368.
2. Hornebeck, W., Moczar, E., Szecsi, J. and Robert, L., *Biochem. Pharmacol.*, 34 (1985) 3315.
3. Lafuma, C., Frisdal, E., Robert, L., Moczar, E., Lefrancier, P., Hornebeck, W., in Aubry, A., Marraud, M., Vitoux, b., (Eds.), 'Second Forum on Peptides', Colloque INSERM/John Libbey Eurotext Ltd., 184 (1989) 321-324.
4. Boduier, C., Godeau, G., Hornebeck, W., Robert, L., Bieth, J.G., *Am. J. Respir. Cell Mol. Biol.*, 4 (1991) 497-503.
5. Toth, I., Flinn, N., Hillery, A., Gibbons, W.A., Artursson, P., *Int. J. Pharm.* 105 (1994) 241.

Peptides: Chemistry, Structure and Biology
Pravin T.P. Kaumaya and Robert S. Hodges (Eds.)
Mayflower Scientific Ltd., 1996

157
Asymmetric Synthesis of an Extended Dipeptide Mimic Suitable for Incorporation into Polypeptides

L. Chen, R.V. Trilles and J.W. Tilley

Roche Research Center, Hoffmann-La Roche Inc., Nutley, NJ 07110, USA

Introduction

Antibodies against the IL-2Rα chain have proven clinically effective as immunosuppressant agents [1] and thus we have sought small molecules capable of blocking the IL-2-IL-2Rα interaction as potential orally active successors to the antibody drugs. A combination of X-ray crystallographic studies of IL-2 [2] and site directed mutagenesis [3] identified a linear region comprising Lys^{35}, Arg^{38}, Phe^{42} and Lys^{43} as critical for the binding of IL-2 to IL-2Rα. Modeling experiments suggested that the pentapeptide Lys-Arg-Gly-Phe-Lys in an extended conformation with Gly serving as a spacer could span the region from Lys^{35} to Lys^{43} and achieve good overlap of its side chains with the corresponding key residues of IL-2.

While such peptides are only weak IL-2 antagonists, incorporation of elements which promote the bioactive conformation would be expected to improve potency. In keeping with recent interest in such constrained spacers, we perceived that phenylogous amino acids mimic the geometry of extended dipeptide as illustrated in Figure 1.

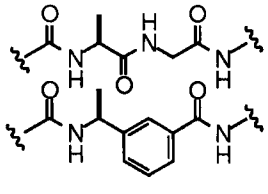

Figure 1. *Comparison of extended conformation of Ala-Gly with corresponding dipeptide mimic.*

We outline in Figure 2 the synthesis of the phenologous Arg-Gly mimic which is suitably protected for insertion into polypeptides. The key step in the synthesis of this compound involved the addition of allyl magnesium bromide to the chiral Schiff's base **1** in the presence of $CeCl_3$ at -50°C. [5, 6]. The reaction proceeded in 85-90% yield to give the allyl amine **2** which was shown to be essentially diastereomerically pure by ^1H NMR. Hydroboration and oxidative cleavage of the chiral auxiliary using lead tetraacetate to afforded the amine **3** in 40% yield for the two steps. The absolute stereochemistry of **3** was confirmed by X-ray crystallographic analysis. The amine was protected as the Boc derivative prior to palladium catalyzed carboalkoxylation [7].

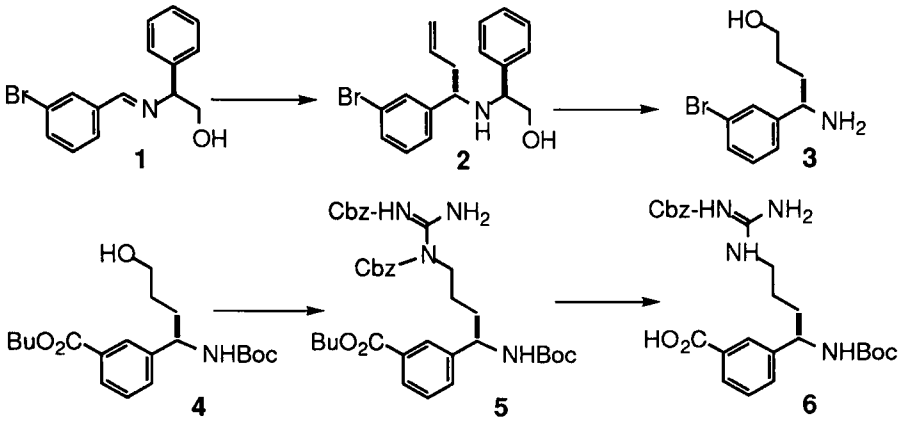

Figure 2. *Synthesis of phenylogous Arg-Gly mimic suitable for insertion into polypeptides.*

Investigation of the conditions for this step led to the selection of $Pd(Ph_3P)_2Cl_2$ in a mixture of n-butanol, DMF and Et_3N (4/3/3 by volume) at 80°C under 40 psi of carbon monoxide. This reliably gave 85-95% yields of carboxylate from aryl bromide. To complete the synthesis, the carboalkoxylation product **4** was treated with N,N-bis-Cbz-guanidine under Mitsunobu conditions resulting in the orthogonally protected Arg-Gly mimic **5**. Treatment with lithium hydroxide in aqueous THF effected cleavage of the ester and one of the Cbz groups to give the target Arg-Gly mimic **6** in 72% yield for the final two steps.

The Arg-Gly mimic **6** was readily inserted into IL-2 related peptides by the use of conventional solution phase chemistry. However, this did not lead to an enhancement of potency for the resulting binding epitope analogs. Nevertheless, the general methods described should be useful for preparation of other extended Xaa-Gly dipeptide mimics, either derived directly from **4** or from **1** utilizing the broad array of organometallic reagents available for the stereoselective introduction of the Xaa side chain.

References

1. Waldmann, T.A., *Immunology Today,* 14 (1993) 264.
2. Hatada, M., Surgenor, A., Weber, D., Madison, V., unpublished results.
3. Sauvé, K., Nachman, M., Spence, C., Bailon, P., Campbell, E., Tsien, W.-H., Kondas J.A., Hakimi, J. and Ju, G., *Proc. Nat. Acad. Sci. USA*, 88 (1991) 4636.
4. Giannis, A. and Kolter, T., *Angew. Chem. Int. Engl.*, 32 (1993) 1244; Olson, G.L., Bolin, D.R., Bonner, M.P., Bös, M., Cook, C.M., Fry, D.C., Graves, B.B.J.; Hatada, M., Hill, D.E., Kahn, M., Madison, V.S., Rusiecki, V.K., Sarabu, R., Sepinwall, J., Vincent, G.P. and Voss, M., *J. Med. Chem.*, 36 (1993) 3039.
5. For a recent review on the application of allylic organometallic compounds in stereoselective synthesis, see Yamamoto, Y and Asao, N., *Chem. Rev,*. 93 (1993) 2207.
6. Wu, M.-J. and Pridgen, L.N., *J. Org. Chem.*, 56 (1991) 1340.
7. Schoenberg, A. and Heck, R.F., *J. Org. Chem.*, 3318; ibid, 39 (1974) 3327; Davies, S. and Pyatt, D., *Heterocycles,* 28 (1989) 163.

Peptides: Chemistry, Structure and Biology
Pravin T.P. Kaumaya and Robert S. Hodges (Eds.)
Mayflower Scientific Ltd., 1996

158

Elucidation of an Antagonist Binding Site on the Human B2 Bradykinin Receptor Using Chimeric Receptors

N. Nash[1], M.A. Connolly[2], T.M. Stormann[3] and D.J. Kyle[4]

[1]Department of Neurology, Emory University School of Medicine, Atlanta, GA 30322, USA
[2]Guilford Pharmaceuticals, 6200 Freeport Center, Baltimore, MD 21224, USA
[3]NPS Pharmaceuticals, 420 Chipeta Way, Suite 240, Salt Lake City, UT 84108, USA
[4]Scios Nova Inc., 820 W. Maude Ave., Sunnyvale, CA 94086, USA

Introduction

There have been a variety of single alanine point mutations experimentally introduced into both rat and human bradykinin B2 receptors. These have been shown to decrease the affinity for bradykinin [1-3]. In contrast, there have been no mutations reported which adversely affect the ability of any peptide antagonists to bind to the receptor. The ultimate identification of the amino acid residues which make up this antagonist site would be another valuable asset toward the goal of structure-based design of novel non-peptide antagonists.

Results and Discussion

We previously reported that characterizations of the bradykinin B2 receptors from rat and human using NPC 17410 revealed different pharmacologies [3]. Specifically, it showed a higher affinity for the human B2 receptor than it did for the rat B2 (human IC_{50}=0.95 nM , rat IC_{50} = 48.0 nM). This ligand "tool" provided a means for evaluating a series of bradykinin rat/human B2 receptor chimeras. The chimeras used are depicted schematically in Figure 1, together with the IC_{50} values determined for NPC 17410. Chimeras I through III sample the N- and C-terminal sections of the receptor for any contributions to an antagonist binding site. The remaining chimeras sample the core transmembrane domains of the receptor. Each chimera was shown to respond to bradykinin in a fashion similar to wild type when expressed in *Xenopus* oocytes. For each NPC 17410 assay, [^{3}H]-NPC 17731 was used as the radioligand.

From this systematic approach, specific groups of residues within the receptor were identified as possible contributors to an antagonist binding site. NPC 17410 binding to Chimeras III, IV, V and VIII showed rat-like pharmacology (low NPC 17410 affinity). NPC 17410 binding to chimeras I, II, VI, and VII showed human-like NPC 17410 pharmacology (high receptor affinity). Comparisons of rat and human receptor sequences in the regions sampled by the chimeras reveals that only two clusters of residues differ between rat and human B2 receptors. Specifically, TM3 has a cluster of 3

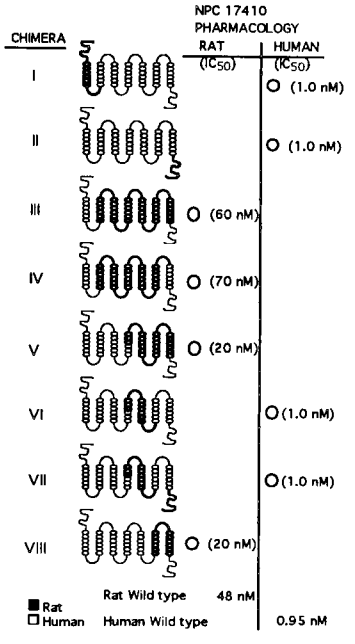

Figure 1. *Receptor binding curves for the binding of NPC 17410 and NPC 17643 to B2 receptors from the guinea pig ileum and cloned rat and human B2 receptors.*

residues which differ, and TM6 has a cluster of 5 residues which differ in rat and human receptors. These represent important targets for follow-up point (and cluster) mutation experiments. Our current thinking is that the largest effects on NPC 17410 pharmacology, if any, might be derived from the TM3 mutants since between rat and human, these are quite diverse. However, it is also possible that the cluster of residues identified in TM6, while not radically dissimilar may, as a group, create different hydrophobic environments between these species homologues. The most significant individual difference within the TM6 zone is the Phe^{259}(rat)→Leu^{257}(human) swap and might therefore be most significant in this regard. Currently, we have prepared these mutant receptors, but at this time binding to NPC 17410 remains unfinished.

References

1. Freedman, R. and Jarnagin, K., in Fritz, H., Müller-Esterl, W., Jochum, M., Roscher, A. and Luppertz, K. (Eds.) 'Recent Progress on Kinins', Birkhauser Verlag, Basel, Switzerland, 1992, p. 487.
2. Burch, R.M., Kyle, D.J. and Stormann, T.M., 'Molecular Biology and Pharmacology of Bradykinin Receptors', R.G. Landes Company, Austin, TX, USA, 1993, p. 1.
3. Kyle, D.J., Chakravarty, S., Sinsko, J.A. and Stormann, T.M., *J. Med. Chem.*, 37 (1994) 1347.

Session VII
Signal Transduction

Chairs: Annette M. Doherty and Tom Lobl

Peptides: Chemistry, Structure and Biology
Pravin T.P. Kaumaya and Robert S. Hodges (Eds.)
Mayflower Scientific Ltd., 1996

159
Distinct Mechanisms for Phosphopeptide Recognition by Modular PTB *versus* SH2 Domains

S.E. Shoelson, G. Wolf, E. Ottinger, A. Lynch, L. Groninga, M. Miyazaki, J. Lee, and T. Trüb.

Research Division, Joslin Diabetes Center and Department of Medicine, Harvard Medical School, Boston, MA 02215, USA

Introduction

Many cell surface receptors initiate their effects on cellular growth, metabolism, and differentiation by catalyzing tyrosine phosphorylations within their own sequences and additional cellular substrates. Insulin, PDGF, EGF and related receptors have intrinsic kinase activity, whereas lymphocyte, cytokine and related receptors associate non-covalently with cytoplasmic tyrosine kinases to initiate their signaling events. Phosphorylated tyrosines frequently act, in turn, as docking sites for proteins Src homology 2 (SH2) domains. SH2 domains are phosphotyrosine-binding modules associated with a variety of cytoplasmic proteins participating in intracellular signal propagation [1, 2].

Recently, a second type of phosphotyrosyl recognition domain having no sequence homology with SH2 domains has been described in the amino-terminus of the kinase substrate Shc [3-5]. Shc is phosphorylated upon activation of many cell surface receptors and acts as a docking protein for Grb2 which, in complex with another protein called Sos, regulates Ras. The Shc phosphotyrosine binding (PTB) domain binds directly with activated kinases or associated proteins, including insulin, EGF, and NGF receptors, erbB2, erbB4, and the polyoma virus middle T antigen (mT) *via* NPXpY peptide motifs [6-8]. IRS-1 is phosphorylated more selectively in cells following insulin stimulation and may contain a related PTB domain [9, 11]. We have expressed protein segments from human Shc and IRS-1 and compared the capacity of these proteins *versus* multiple SH2 domains to bind with intact phosphoproteins and corresponding synthetic phosphopeptides.

Results and Discussion

For comparative analyses of binding specificity, Shc and IRS-1 PTB domains expressed as glutathione S-transferase (GST) fusion proteins were combined with radiolabeled and unlabeled phosphopeptides as described previously for SH2 domain competition assays 6, 10]. For example, the Shc PTB domain binds a mT peptide with highest affinity and IL4 and insulin receptor sequences with lower affinities (Figure 1). In contrast, the IRS-1 PTB domain binds the IL4 receptor sequence with highest affinity, the insulin receptor sequence with intermediate affinity, and not at all with the mT-derived sequence

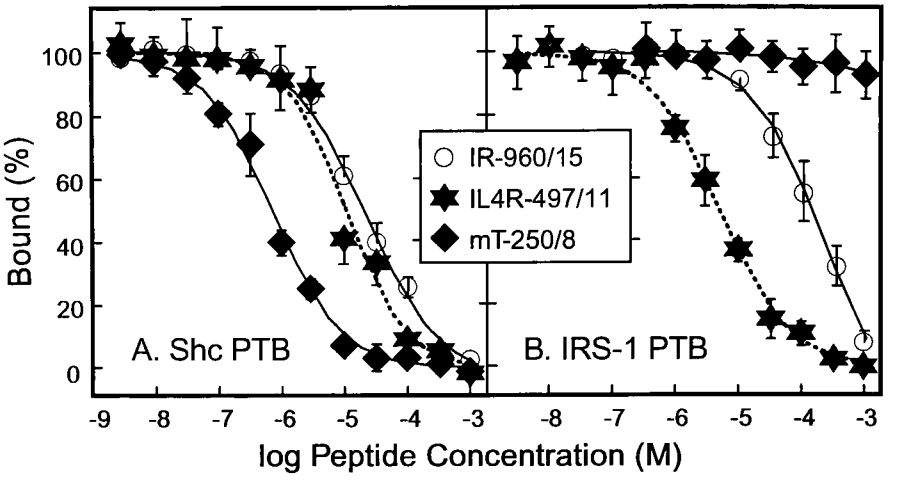

Figure 1. *Differential specificities of Shc and IRS-1 PTB domains. Competition curves for binding of A. Shc or B. IRS-1 PTB domains with peptides derived from polyoma virus mT antigen (LSNPTpYSV), insulin receptor (LYASSNPEpYLSASDV), and IL4 receptor (LVIAGNPApYRS) are displayed.*

to demonstrate significant differences in binding specificities between PTB domains. Studies with unphosphorylated and scrambled sequences show that phosphorylation and peptide sequence are critical for high affinity and specificity [6]. Additional analyses with over 50 native and substituted sequences, including those presented in Table I, provide a basis for summarizing PTB domain specificities.

The Shc PTB domain binds with highest affinity with peptides having the consensus sequence $\Psi XN\beta_1\beta_2pY$ derived from mT, TrkA, Erb4 and IL2 or EGF receptors (Ψ= hydrophobic, β_1=P,Q,L; β_2=T>A>E). The IRS-1 PTB domain does not bind with this

Table 1. *Specificity of Shc and IRS-1 PTB domains demonstrated by relative phosphopeptide affinities. Peptide names denote protein source, site of phosphorylated tyrosine and peptide length (note the common NPXpY motif).*

Peptide Source	Sequence	Shc PTB ID_{50}± SEM (μM)	IRS-1 PTB ID_{50}± SEM (μM)
mT-250/9	LLSNPTpYSV	0.6 ± 0.1	>300
mT-250/7	SNPTpYSV	>300	>300
mT-250/6	LSNPTpY-NH_2	2.6 ± 0.3	>300
IL2R-364/10	SCFTNQGpYFF	0.8 ± 0.05	>300
TrkA-490/8	IENPQpYFS	6.3 ± 0.5	>300
ErbB4-1242	AKKAFDNPDpYWN	1.4 ± 0.2	>300
IR-960/15	LYASSNPEpYLSASDV	30 ± 5.3	170 ± 53
IR-960/A-1	LYASSNPApYLSASDV	12 ± 1.3	5.4 ± 0.7
IL4R497/11	LVIAGNPApYRS	19 ± 2.4	4.2 ± 0.6
IL4R497/10	VIAGNPApYRS	31 ± 3.9	114 ± 38
IL4R497/9	IAGNPApYRS	>300	>300

motif. Whereas both the Shc and IRS-1 PTB domains bind $\Psi XXXN\beta_1\beta_2 pY$ sequences derived from insulin or IL4 receptors, specificities vary in detail. 1D and 2D ^1H NMR studies show that these peptides form stable β-turns in solution [6], although configurations of PTB domain-bound peptides are unknown.

Binding interactions mediated by PTB domains of Shc and IRS-1 are closely related to analogous SH2 domain interactions in that binding affinities are similar, phosphorylation serves as the on-off switch, and the surrounding sequence provides specificity. However, the PTB domains show a direct reversal in orientation of required peptide interactions compared to SH2 domains, since residues amino but not carboxyl terminal to pTyr determine specificity. Unlike SH2 domains that recognize peptides in an extended conformation, PTB domains recognize β-turn forming sequences. Since Shc interacts with and is phosphorylated by many receptor types including TrkA, TrkB, ErbB2, ErbB3, ErbB4, the insulin, IL2 and EGF receptors, and the polyoma virus mT antigen, while IRS-1 interacts selectively with the insulin and related IGF-1 receptors (IRS-2/4PS interacts with the IL4 receptor in hematologic cells), biological specificity is faithfully recapitulated by the PTB domains of these proteins. The apparent promiscuity of Shc as a substrate of many receptor-linked tyrosine kinases and fidelity of IRS-1 as a selective substrate of insulin receptors may be accounted for by the inherent specificities of their PTB domains.

References

1. Pawson, T., *Nature*, 373 (1995) 573.
2. Cohen, G.B., Ren, R., and Baltimore, D., *Cell*, 80 (1995) 237.
3. Kavanaugh, W.M. and Williams, L.T., *Science*, 266 (1994) 1862.
4. Blaikie, P., Immanuel, D., Wu, J., Li, N., Yajnik, V. and Margolis, B., *J. Biol. Chem.*, 269 (1994) 32031.
5. van der Geer, P., Wiley, S., Lai, V.K.-M., Olivier, J.P., Gish, G.D., Stephens, R., Kaplan, D., Shoelson, S.E., and Pawson, T., *Curr. Biol.*, 5 (1995) 404.
6. Trüb, T., Choi, W., Wolf, G., Ottinger, E., Chen, Y., Weiss, M.A. and Shoelson, S.E., *J. Biol. Chem.*, 270 (1995) 18205.
7. Songyang, Z., Margolis, B., Chaudhuri, M., Shoelson, S.E. and Cantley, L.C., *J. Biol. Chem.*, 270 (1995) 14863.
8. Kavanaugh, W.M., Turck, C.W., and Williams, L.T. *Science*, 268 (1995) 1177.
9. Gustafson, T.A., He, W., Craparo, A., Schaub, C.D. and O'Neill, T.J., *Mol. Cell. Biol.* 15 (1995) 2500.
10. Case, R.D., Piccione, E., Wolf, G., Bennett, A.M., Lechleider, R.J., Neel, B.G. and Shoelson, S.E., *J. Biol. Chem.*, 269 (1994) 20467.

Peptides: Chemistry, Structure and Biology
Pravin T.P. Kaumaya and Robert S. Hodges (Eds.)
Mayflower Scientific Ltd., 1996

160
Novel Phosphotyrosine and Hydrophobic D-Amino Acid Replacements in the Design of Peptide Ligands for pp60^{src} SH2 Domain

A. Shahripour[1], M.S. Plummer[1], E.A. Lunney[1], J.V.N. Vara Prasad[1], J. Singh[1], K.S. Para[1], C.J. Stankovic[1], S.R. Eaton[1], J.R. Rubin[1], A.G. Pavlovsky[1], C. Humblet[1], J.H. Fergus[2], J.S. Marks[2], S.J. Decker[3], R. Herrera[3], S. Hubbell[3], A.R. Saltiel[3] and T.K. Sawyer[1]

Departments of [1]Chemistry, [2]Biochemistry, and [3]Signal Transduction, Parke-Davis Pharmaceutical Research, Division of Warner-Lambert Company, Ann Arbor, MI 48105, USA

Introduction

pp60^{src} is a nonreceptor tyrosine kinase which is known to interact with several key signalling proteins *via* sequence specific phosphotyrosine (pTyr) mediated binding with its SH2 domain [1]. A structure of the v-Src SH2 domain complexed with **1** (see below) has been determined by X-ray crystallography at 2.7 Å resolution [2].

H-Glu-Pro-Gln-pTyr-Glu-Glu-Ile-Pro-Ile-Tyr-Leu-OH **1**
P_{-1} P P_{+1} P_{+2} P_{+3} P_{+4}
Binding site nomenclature

The design of prototype peptidomimetics has been derived from the above X-ray crystallographic structure of phosphopeptide **1** complexed with Src SH2 domain. Such structure-based drug design efforts have led to the discovery of potent, specific, and stable series of peptide ligands which have novel pTyr and hydrophobic D-amino acid replacements.

Results and Discussion

Based on the 3D-structure of the Src SH2 complex [2], two series of compounds were designed as analogs of **2**, [3] and **9** which showed low μM affinity for the Src SH2 domain (Table 1). Relative to the parent pentapeptide **2**, removal of the N-terminal acetamide group results in about a 5-fold decrease in binding affinity for **3**. The α-methyl substituted analog **4** is less potent than the parent analog **2**, however it was discovered that α-phenyl substitution at the pTyr moiety did provide high affinity in a stereochemically selective manner. The α-carboxymethyl analog **7** was the most potent of this series. Finally, the D-pTyr analog **8** was 5-fold less potent than the parent

Table 1. *Binding affinities of phosphopeptides to Src SH2.*

Compound	Peptide	$IC_{50}\mu M$
2	Ac-pTyr-Glu-Glu-Ile-Glu	0.48
3	pHpp-Glu-Glu-Ile-Glu	3.40
4	pHpp(α-CH_3)-Glu-Glu-Ile-Glu	20.00
5	pHpp(α-C_6H_5)-Glu-Glu-Ile-Glu	1.90 (isomer 1)
6	pHpp(α-C_6H_5)-Glu-Glu-Ile-Glu	9.3 (isomer 2)
7	pHpp(α-CH_2CO_2H)-Glu-Glu-Ile-Glu	0.35
8	Ac-D-pTyr-Glu-Glu-Ile-Glu	2.85
9	Ac-pTyr-Glu-D-Hph-NH_2	7.80
10	Ac-pTyr-Glu-D-Trp-NH_2	4.20
11	Ac-pTyr-Glu-D/L-Trp(α-CH_3)-NH_2	4.00
12	Ac-pTyr-Glu-D-Nle-NH_2	10.40
13	Ac-pTyr-Glu-D-Ser(Bn)-NH_2	5.10
14	Ac-pTyr-Glu-D-Phg-NH_2	8.30
15	Ac-pTyr-Glu-D-Hcy-NH_2	2.10
16	Ac-pTyr-Glu-D/L-MeTrp-NH_2	11.50
17	Ac-pTyr-Glu-D-MePhe-NH_2	2.10
18	Ac-pTyr-Glu-D-MeCha-NH_2	0.96
19	pHpp-Glu-D-Trp-NH_2	21.00
20	pHpp(α-CH_3)-Glu-D-Trp-NH_2	14.00
21	pHpp(α-C_6H_5)-Glu-D-Trp-NH_2	28.0
22	Ac-F_2Pmp-Glu-Glu-Ile-Glu	1.10
23	Ac-F_2Pmp-Glu-D-Hcy-NH_2	4.90

Abbreviations: **Hpp**, 3-(4-hydroxy-phenyl)-propionic acid; **Phg**, phenylglycine; **Hcy**, homo-cyclohexylalanine; **Hph**, homophenylalanine; **MeTrp**, N^{α}-methyl-tryptophan; **MePhe**, N^{α}-methyl-phenylalanine; MeCha, N^{α}-methyl-cyclohexylalanine.

phosphopeptide. Relative to the parent tripeptide **9**, a 30-fold range of binding affinity to Src SH2 was observed for a series of P_{+2} D-amino acid modification (*e.g.*, **10**-**21**). Specifically, replacement of the D-Hph of **9** by a more hydrophobic, constrained amino acid D-Trp (**10**) or D/L-Trp(α-methyl) (**11**) resulted in about 2-fold increased binding activity. Replacing the P_{+2} aromatic amino acid by D-Nle (**12**) resulted in 2-fold lowered binding affinity. Homologation of the alkyl side chain of **9** to give compound **13**, effected a slight increase in binding affinity. Interestingly, when D-Phg (**13**) is substituted for D-Hph the binding affinity remains essentially the same. Increasing the lipophilicity of the D-Hph was accomplished by reducing the aromatic ring to a cyclohexane ring **15** which led to a 4-fold increase in affinity. Finally, several N-methyl-D-amino acid substituted analogs (**16**-**18**) led to identification of a compound which was nearly 10-fold more potent than the parent tripeptide.

Modification of the N-terminal acetyl group in **10** was accomplished by employing a phosphorylated 3-(4-hydroxyphenyl)-propionic acid for compound **19**, 2-(R)-methyl-3-(4-hydroxyphenyl)-propionic acid for compound **20**, and a 2-(R/S)-phenyl-3-(4-hydroxyphenyl)-propionic acid for compound **21**. These substituted pTyr modifications provide a 2-4 fold reduction in affinity when compared with **10**, which underscores the

likely contribution of a hydrogen bond between the amino-terminal acetamide and Arg-155. Similar to such replacements in a pentapeptide series (*vide supra*) a significant decrease in binding was found, (compounds **3**-**5**).

Finally, we examined a replacement for the labile phosphate group of the above pTyr-substituted peptides. A nonhydrolyzable mimetic of the phosphate was prepared by replacement of the phosphate ester oxygen with an α,α-difluoromethylene moiety. Phosphonates of this type have proven to be useful in a number of biological studies [4], since α,α-difluoro-phosphonomethyl phenylalanine (F_2Pmp) is a nonhydrolyzable mimetic of pTyr. Two compounds, **22** and **23**, were synthesized employing F_2Pmp, and were found to be 2-3 fold less potent than the parent pTyr containing peptides. The loss of activity may be partially attributed to a lower pK_{a2} of the F_2Pmp-phosphonate relative to that of the pTyr phosphate (pK_{a2} 6.22 *versus* 7.72 respectively) [4] or to the incompatibility of the larger difluoromethylene unit relative to the oxygen atom.

References

1. Margolis, B., *Cell Growth & Differ.*, 3 (1992) 73.
2. Waksman, G., Shoelson, S.E., Pant, N., Cowburn, D., and Kuriyan, *J., Cell*, 72 (1993) 779.
3. Gilmer, T., Rodriguez, M., Jordon, S., Crosby, R., Alligood, K., Green, M., Kimery, M., Wagner, C., Kinder, D., Charifson, P., Hassell, A.M., Willard, D., Luther, M., Rusnak, D., Sternback, D.D., Mehrotra, M., Peel, M., Shampine, L., Davis, R., Robins, J., Patel, I.R., Kassel, D., Burkhart, W., Moyer, M., Bradshaw, T. and Berman, J., *J. Biol. Chem.*, 269 (1994) 31711.
4. Smyth, M.S., Ford, H. and Burke, T.R., Jr., *Tetrahedron Lett.*, 33 (1992) 4137.

Peptides: Chemistry, Structure and Biology
Pravin T.P. Kaumaya and Robert S. Hodges (Eds.)
Mayflower Scientific Ltd., 1996

161
Enzymatic Synthesis of Peptide Conjugates - Tools for the Study of Signal Transduction Processes

H. Waldmann, E. Nägele, M. Schelhaas and D. Sebastian

Institut für Organische Chemie, Universität Karlsruhe, Richard-Willstätter-Allee 2, 07128 Karlsruhe, Germany

Introduction

Lipo-, phospho-, nucleo-, and glycoproteins are critically involved in the transduction of signals from the extracellular space into the cell and ultimately to the cell nucleus. A recent spectacular example which highlights their biological importance is the elucidation of the *Ras* pathway of signal transduction which is central to growth control in mammals and other organisms [1]. For the study of such signal transduction pathways structurally well-defined lipo-, phospho-, nucleo-, and glycopeptides carrying the characteristic structural elements of the parent proteins, are required. The synthesis of such peptide conjugates, however, is complicated by their multifunctionality and chemical lability. Numerous orthogonally stable protecting groups have to be applied, which all must be removable under the mildest, preferably neutral, conditions.

We have developed enzymatic protecting group techniques which fulfill these criteria [2] as efficient tools for the synthesis of peptide conjugates.

Results and Discussion

For the C-terminal enzymatic deprotection of peptides and peptide conjugates, we have used the heptyl (Hep) esters, and the choline (Cho) esters (Scheme 1).

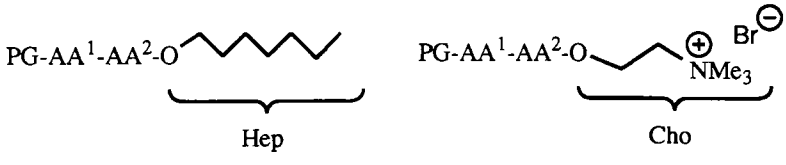

Deprotection conditions:
Lipase from *Rhizopus niveus*,
pH 7, 37°C,
50-96%

Deprotection conditions:
Butyrylcholine esterase,
pH 6.5, 25°C,
70-90%

PG = Z, Boc, Aloc,

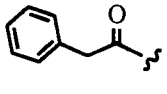

Scheme 1.

The Hep esters are readily removed from simple peptides [3] and complex glycopeptides [4] by means of lipase-mediated saponification of the ester group under mildest conditions. Peptide choline esters can be selectively deprotected under similarly mild conditions by employing butyryl choline esterase from horse serum as biocatalyst [5]. In contrast to the heptyl esters the choline esters display pronounced solubility-enhancing properties and render the peptidic substrates for the enzymes highly soluble in aqueous solutions, thereby guaranteeing that the enzymatic transformations proceed smoothly.

For the N-terminal enzymatic deprotection of peptides and peptide conjugates the phenylacetamido (PhAc) group and the *p*-acetoxy-benzyloxycarbonyl (AcOZ) group were employed. The PhAc amide can be cleaved from peptides under mildest conditions by means of the enzyme penicillin G acylase from *E. coli* [6] (Scheme 2). However, it has the drawback that, as a non-urethane blocking function, it leads to 3-5% racemization of the N-terminal amino acid during peptide coupling. The AcOZ group represents the first enzymatically removable protecting function for peptide chemistry by which this problem is overcome. It is cleaved at pH 6-7 *via* hydrolysis of the phenolic acetate by the enzyme acetyl esterase and subsequent spontaneous fragmentation of the phenol generated thereby to liberate the desired peptide or peptide conjugate [7] (Scheme 2).

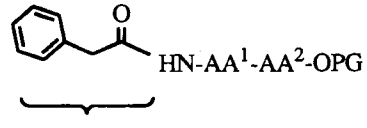

Deprotection conditions:
Penicillin G acylase from *E. coli*
pH 7-8, 25°C,
65-95%

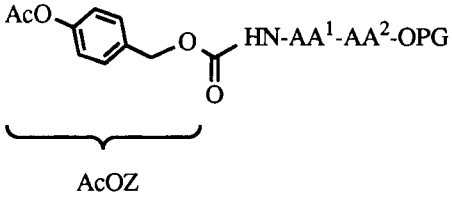

Deprotection conditions:
Acetyl esterase,
pH 7, 45°C,
57-70%

PG = Me, t-Bu, Bzl, All

Scheme 2.

The advantageous properties of these enzyme-labile blocking functions allowed for a successful synthesis of characteristic structural elements of different peptide conjugates. For instance, a glycopeptide which represents a characterisitic partial sequence of a glycoprotein found on the surface of human breast cancer cells was built up by employing the lipase-mediated hydrolysis of the heptyl esters as protecting group technique [4]. In particular, the use of the choline ester as enzyme-labile C-terminal protecting function and of the AcOZ-urethane as enzymatically removable N-terminal

blocking group allowed for the first synthesis of the characteristic C-terminal lipohexapeptide of the human N-*Ras* protein (Scheme 3). This peptide carries a very base-labile palmitic acid thioester as well as an acid-sensitive farnesyl thioether, so that protecting groups which are removed by means of acids or bases like the Boc- and the Fmoc group cannot be employed in its construction.

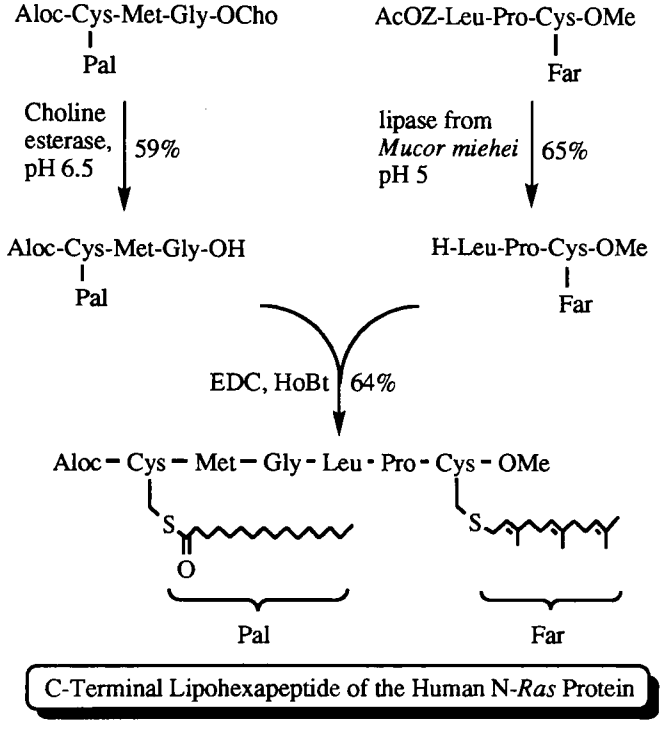

Scheme 3.

Acknowledgments

This research was supported by the Deutsche Forschungsgemeinschaft and the Fonds der Chemischen Industrie.

References

1. McCormick, F., *Nature,* 366 (1993) 643.
2. Waldmann, H. and Sebastian, D., *Chem. Rev.,* 94 (1994) 911.
3. Braun, P., Waldmann, H., Vogt, W. and Kunz, H., *Liebigs Ann. Chem.,* (1991) 165.
4. Braun, P., Waldmann, H. and Kunz, H., *Bioorg. Med. Chem.,* 1 (1993) 197.
5. Schelhaas, M., Glomsda, S., Hansler, H., Jakubke, H.-D., and Waldmann, H., *Angew. Chem.,* 108 (1996) 82.
6. Waldmann, H., *Liebigs Ann. Chem.,* (1988) 1175.
7. Waldmann, H. and Nägele, E., *Angew. Chem.,* 107 (1995) 2425.

Peptides: Chemistry, Structure and Biology
Pravin T.P. Kaumaya and Robert S. Hodges (Eds.)
Mayflower Scientific Ltd., 1996

162
Direct Interaction of Ligands with Extracellular Domains of Neurohypophysial Hormone Receptors

J. Howl and M. Wheatley

School of Biochemistry, University of Birmingham, Edgbaston, Birmingham B15 2TT, UK

Introduction

The structurally homologous mammalian neurohypophysial peptide hormones [arginine^8]vasopressin (AVP) and oxytocin (OT) have distinct physiological roles. In common with other hormones and neurotransmitters, subtypes of vasopressin receptor (VPR) have been distinguished by pharmacological criteria [1]. Analysis of the amino acid sequence of cloned AVP and OT receptor proteins identifies two highly conserved domains in the first and second extracellular loops which are hypothesized to provide a ligand recognition site [2]. This investigation was designed to determine whether molecular recognition occurs between the extracellular domains of neurohypophysial hormone receptors and peptide/non-peptide ligands. Our data also endorse the application of mimetic peptides to delineate functional receptor domains.

Results and Discussion

We used a ligand binding protocol [3] in which the interaction between a labelled ligand and a receptor mimetic peptide reduced ligand occupancy of the rat V_{1a} vasopressin receptor ($rV_{1a}R$, Figure 1). Mimetics inhibited the binding of [^{3}H]AVP, [^{3}H][d(CH_2)$_5$-Tyr(Me)^2]AVP (a V_{1a}-selective antagonist, [4]) and [^{3}H]SR 49059 (a nonpeptide V_{1a}-selective antagonist, [5]) in a concentration-dependent manner (Figure 1). Comparative pK_i values of mimetic peptides corresponding to the extracellular surface of the $rV_{1a}R$ (Table 1) indicate that the first extracellular loop (ECII) contains a major binding-site determinant with further contributions provided by the N-terminal (ECI) and second loop (ECIII). The pharmacological properties of the $rV_{1a}R$-, and human oxytocin receptor (hOTR-)-, derived ECII mimetic peptides were very similar, binding all three classes of ligand investigated with comparable pK_i values. In contrast, molecular recognition by the rat V_2 VPR (rV_2R) ECII mimetic peptide DATDRFHGPDAL was restricted to the natural agonist [^{3}H]AVP (Table 1). These data indicate that the ECII domain of neurohypophysial hormone receptors play a major role in ligand recognition and determining V_1/V_2 selectivity. The binding of [^{3}H]SR 49059 to the $rV_{1a}R$ was inhibited with comparable affinity by both $rV_{1a}R$-, and hOTR-, derived ECII mimetic peptides (Table 1) even though this ligand binds with very low affinity to native OTRs. These findings indicate that additional binding-site epitopes are presented by native receptors which determine the pharmacological specificity of non-peptide vasopressin antagonists.

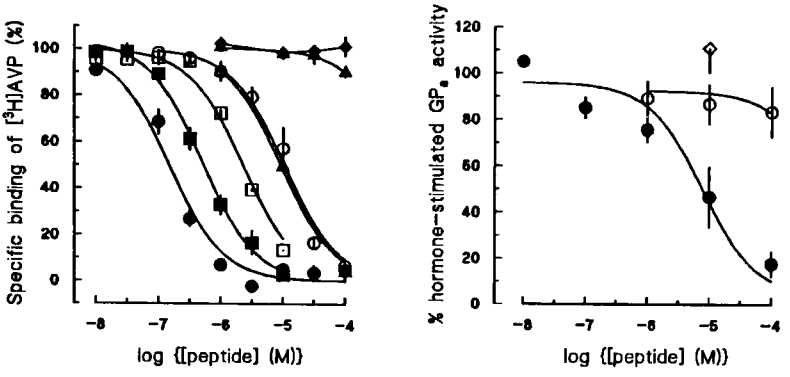

Figure 1. *Left, dose-dependent inhibition of specific [^{3}H]AVP binding (0.42-0.62nM) to the rat liver V_{1a} VPR by receptor mimetic peptides. All curves are representative of 3-5 independent determinations of the apparent K_i:* (●) *DITYRFRGPDWL $rV_{1a}R^{102-113}$,* (■) *DITFRFYGPDLL $hOTR^{100-111}$,* (▲) *DATDRFHGPDAL $rV_2R^{100-111}$,* (○) *TYRFRGPD $rV_{1a}R^{104-111}$,* (□) *QDCWATFIQP $rV_{1a}R^{193-203}$,* (△) *DRSVGNSSPWWPLTTE $rV_{1a}R^{9-24}$,* (♦) *(rD)peptide) LWDPGRFRYTID $rV_{1a}R^{113-102}$. Right, inhibition of hormone-stimulated GP_a [3] in isolated rat hepatocytes. Data are mean ± SEM (n = 3-6):* (●) *DITYRFRGPDWL + AVP (0.5nM),* (○) *TYRFRGPD + AVP,* (◊) *DITYRF RGPDWL + angiotensin II (10nM).*

Table 1. *Comparative inhibition constants of receptor mimetic peptides.*

Peptide	radioligand	Apparent pK_i		
		AVP	$[d(CH_2)_5Tyr(Me)^2]$	SR 4905
ECI				
DRSVGNSSPWWPLTTE	$rV_{1a}R^{9-24}$	4.94	5.13	5.13
EGSNGSQEAARLGEGD	$rV_{1a}R^{24-39}$	<2	<2	<2
DSPLGDVRNEELAK	$rV_{1a}R^{39-52}$	<2	<2	<2
ECII				
DITYRFRGPDWL	$rV_{1a}R^{102-113}$	6.75	6.57	6.73
TYRFRGPD	$rV_{1a}R^{104-111}$	4.71	4.56	4.70
DITFRFYGPDLL	$hOTR^{100-111}$	6.25	6.43	6.76
DATDRFHGPDAL	$rV_2R^{100-111}$	3.1	<2	<2
LWDPGRFRYTID (*rD*peptide)	$rV_{1a}R^{113-102}$	<2	<2	<2
ECIII				
EVNNGTKTQDCWAT	$rV_{1a}R^{185-198}$	4.55	4.61	3.89
EVNNGTKTQD	$rV_{1a}R^{185-194}$	<2	<2	<2
QDCWATFIQP	$rV_{1a}R^{193-202}$	5.70	5.54	5.46
WATFIQPWGT	$rV_{1a}R^{196-205}$	4.65	4.49	4.60
ECIV				
DENFIWTDSEN	$rV_{1a}R^{313-323}$	<3	<3	<3

Carboxy-amidated peptides were purified and characterized as previously described [3]. Values are arithmetic means from at least three independent determinations of K_i. Peptides are grouped according to position on the extracellular surface (ECI-ECIV). The rDpeptide LWDPGRFRYTID is a retroinverso homologue synthesized from D aa.

None of the peptide mimetics used in this study inhibited [^{3}H]angiotensin II binding to the rat liver AT_1 receptor. Clearly, peptide mimetics of the extracellular domains of neurohypophysial hormone receptors display ligand selectivity as they can distinguish AVP/OT analogues from other peptide ligands of a similar size. Moreover, the $rV_{1a}R$ ECII reverse D-mimetic peptide (LWDPGRFRYTID) was not able to "recognize" any vasopressin receptor ligand (Table 1), indicating that backbone atoms of the ECII domain of the $rV_{1a}R$ contribute to ligand recognition [6].

We predicted that potent binding site mimetics would concomitantly reduce receptor occupancy and inhibit AVP-induced effects. The peptide DITYRFRGPDWL did indeed inhibit AVP-stimulated hepatic glycogen phosphorylase$_a$ (GP_a) in a dose-dependent manner (Figure 1). This effect was specific for AVP, as the ECII mimetic did not inhibit angiotensin II-stimulated GP_a activity (Figure 1). The truncated $rV_{1a}R$ ECII mimetic TYRFRGPD, which has c.100-fold lower affinity for AVP (Table 1), was far less potent at inhibiting AVP-stimulated GP_a activity (Figure 1).

In summary, our data provide direct evidence that peptide and non-peptide ligands specifically interact with common/overlapping binding-site determinants contained within the extracellular loops of the $rV_{1a}R$. Recent studies [7,8] have also emphasized a critical role of the ECII domain in determining agonist specificity for vasopressin receptors. We suggest that this selective molecular recognition process achieves the initial "capture" of the ligand. Additional hydrophobic interactions probably determine the final "docked" position of ligands within the binding site. This "capture and docking" model allows peptide and non-peptide ligands to interact differently with sites within the receptor protein when in their "docked" position.

Acknowledgments

We gratefully acknowledge the British Heart Foundation, the Royal Society, Wellcome Trust and the AFRC for financial support and thank R. Parslow for technical assistance.

References

1. Howl, J. and Wheatley, M., *Gen. Pharmacol.*, in press.
2. Wheatley, M., Howl, J., Morel, A. and Davies A.R.L., *Biochem. J.*, 296 (1993) 519.
3. Howl, J. and Wheatley, M., *Meth. Neurosci.*, 13 (1993) 281.
4. Kruszynski, M., Lammek, B., Manning, M., Seto, J., Haldar, J., and Sawyer, W.H., *J. Med. Chem.*, 23 (1980) 364.
5. Serradeil-Le Gal, C., Wagnon, J., Garcia, C., Lacour, C., Guiraudou, P., Christophe B., Villanova, G., Nisato, D., Maffrand, J.P., Le Fur, G., Guillon, G., Cantau, B., Barberis, C., Trueba, M., Ala, Y., and Jard, S., J. *Clin. Invest.*, 92 (1993) 224.
6. Jameson, B.A., McDonnell, J.M., Marini, J.C. and Korngold, R., *Nature*, 368 (1994) 744.
7. Ufer, E., Postina, R., Gorbulev, V. and Fahrenholz, F., *FEBS Lett.*, 362 (1995) 19.
8. Chini, B., Mouillac, B., Ala, Y., Balestre, M-N., Trumpp-Kallmeyer, S., Hoflack, J., Elands, J., Hibert, M., Manning, M., Jard, S, and Barberis, C., *EMBO J.*, 14 (1995) 2176.

Peptides: Chemistry, Structure and Biology
Pravin T.P. Kaumaya and Robert S. Hodges (Eds.)
Mayflower Scientific Ltd., 1996

163
The Regulation of GTP-Binding Regulatory Proteins by Substance P, Mastoparan and their Derivatives

H. Mukai[1,2], T. Higashijima[2], Y. Suzuki[1] and E. Munekata[1]

[1]*Institute of Applied Biochemistry, University of Tsukuba, Tsukuba, Ibaraki 305, Japan*
[2]*Department of Pharmacology, University of Texas Southwestern Medical Center, Dallas TX 75235, USA*

Introduction

Cells are regulated by many chemical mediators. Most of such mediators bind to plasma membrane receptors and induce cell response. GTP-binding regulatory proteins (G proteins) are the molecules which convey signals from plasma membrane receptors to cytoplasmic effectors such as adenylyl cyclase, phospholipase C, and ion channels [1]. Receptors for various peptidergic hormones and neurotransmitters are known to couple with G proteins [1, 2]. Mastoparan (MP), a tetradecapeptide isolated from wasp venom, stimulates exocytosis from various cells such as histamine secretion from peritoneal mast cells [3]. Recently, MP has been shown to directly activate some G proteins such as G_i protein which involves in the inhibition of adenylyl cyclase and the activation of phospholipase C [4, 5]. MP catalyzes nucleotide exchange on G proteins in a manner similar to that of plasma membrane receptors in the reconstituted phospholipid vesicles of G_i. The activation of G_i protein is prevented by the ADP-ribosylation of it by the treatment of pertussis toxin (PTX). Following these findings, a similar mechanism of G protein regulation has been proposed for substance P (SP), a neuropeptide isolated from mammals [5]. These results let us hypothesize that these amphiphilic compounds can directly activate G proteins even in cell systems. If MP and SP cause exocytosis from mast cells as a result of the direct activation of G proteins, there would be a relationship between the structural requirements of them for the stimulation of exocytosis and its activation of G proteins. Moreover, there would be a difference between the exocytotic mechanisms stimulated by them and those induced by the stimulants of receptors.

Here, the mechanisms of MP- and SP-induced exocytotic secretion from rat peritoneal mast cells, which may cause direct activation of G proteins, were investigated. To elucidate whether MP and SP can directly activate G proteins in peritoneal mast cells, the structure-activity relationships of them with exocytosis from those cells and with the activation of G proteins were studied. β-hexosaminidase (β-HA) release was measured to assess exocytotic secretion, because this enzyme is found in secretory vesicles. The leakage of lactate dehydrogenase (LDH) was monitored to assess the cytotoxicity of peptides. The GTP hydrolysis of G_i protein purified from rabbit liver, which demonstrate the existence in peritoneal mast cells [6], in the reconstituted phospholipid vesicles of G_i was also measured to clarify G protein activation.

Results and Discussion

Mechanisms of exocytosis. MP and SP induced non-lytic β-HA release from mast cells in concentration dependent manner (Figure 1 for MP, the data by SP were not shown). First, time course of the enzyme secretion stimulated by MP at various temperatures was measured. MP stimulated β-HA release at 20°C and 37°C, but not at 0°C (data not shown). The enzyme was released after MP stimulation with a lag time of 10 sec at 20° although the release was initiated less than 3 sec after MP stimulation at 37°C. The percentage of released β-HA compared with the total content of it in mast cells was also

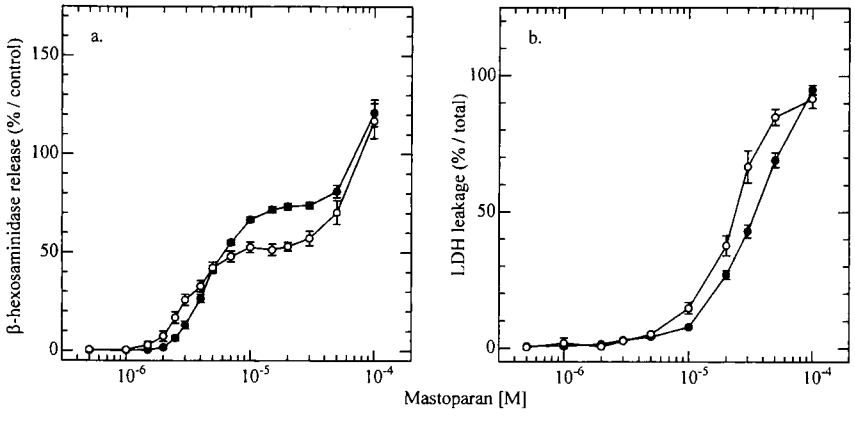

Figure 1. *Effects of extracellular Ca^{2+} on β-HA release (a) and LDH leakage (b) induced by mastoparan: (●) in the presence of 0.9 mM extracellular Ca^{2+}; (○) in the absence of extracellular Ca^{2+}. Each point represents the mean ± SEM of separate experiments.*

Table 1. *The activities of MP and its analogs on β-HA and LDH release, and GTP hydrolysis of G_i stimulated by them.*

Peptides	EC_{50}(μM)		GTPase activity (min^{-1})	
	β-HA	LDH	10 μM	100 μM
mastoparin (MP)	7.1	90	0.12	0.21
[Leu^{13}]MP	3.7	100 <	0.1	0.17
[Leu^{13},Ala^{14}]MP	17.4	100 <	0.05	0.19
[Ala^{13}]MP	27.3	-	0.04	0.12
[Ala^{12},Leu^{13}]MP	3.8	30	0.27	0.70
[Ala^{11},Leu^{13}]MP	7.9	50	0.09	0.23
[Lys^{10},Leu^{13}]MP	0.5	-	0.02	0.12
[Ala^{9},Leu^{13}]MP	30 <	100 <	0.05	0.11
[Ala^{6},Leu^{13}]MP	21.5	-	0.04	0.13
[Ala^{4},Leu^{13}]MP	4.2	50	0.06	0.16
[Ala^{3},Leu^{13}]MP	16.2	-	0.04	0.14
[$Gln^{4,11}$,Ala^{12},Leu^{13}]MP	-	100 <	0.02	0.08

affected by temperature; 20 μM MP induced about 62 % enzyme release at 37°C, but about 22 % at 20°C.

We examined effect of extracellular free Ca^{2+} on the time course of enzyme release caused by MP. In the presence of 0.9 mM extracellular Ca^{2+}, the enzyme release was initiated within 3 sec, and the t/2 was about 5 sec in the presence of 20 μM MP. In the absence of extracellular Ca^{2+}, the enzyme was also secreted, but the t/2 was 30 sec after stimulation with 20 μM of MP. As shown in Figure 1, the concentration dependence and maximal secretion of the enzyme were also affected by extracellular Ca^{2+}. These results demonstrated that extracellular Ca^{2+} was not essential for MP-induced secretion, but it increased the kinetics. In addition, removing extracellular Ca^{2+} increased the sensitivity to MP. The same characteristics were observed in the stimulation of exocytosis from mast cells induced by SP.

The β-HA release and the GTP hydrolysis of G_i stimulated by the various analogs of MP were measured to determine the structure requirements of MP to stimulate exocytosis from peritoneal mast cells and to activate G_i protein in reconstituted phospholipid vesicles of it. As shown in Table 1, the structure-activity relationships of MP and its analogs on the stimulation of exocytosis from mast cells and on the activation of G_i correlated well in the study of hydrophobic and hydrophilic amino acid replacements. Both the stimulation of β-HA release and the activation of G_i by MP and its analogs were prevented by the treatment of PTX. [Lys^{10},Leu^{13}]MP was the most potent stimulator of β-HA release without causing cell lysis. However, this peptide only slightly activated G_i. Therefore, further studies are required to understand how G protein is directly activated by amphiphilic compounds, that is, the translocation of these compounds across the cell membrane.

Acknowledgments

We thank Drs. E. M. Ross and. K. Wakamatsu for their kind suggestions. This work was supported by research grants from United States Public Health Service (No. GM40676), the Ministry of Education, Japan (No. 06680605), the program of Special Research Project on Circulation Biosystems, University of Tsukuba, and the Naito Research Foundation.

References

1. Gilman, A.G., *Ann. Rev. Biochem.*, 56 (1987) 615.
2. Ross, E.M., *Neuron*, 3 (1989) 141.
3. Hirai, Y., Yasuhara, T., Yoshida, H., Nakajima, T., Fujino, M. and Kitada, C., *Chem. Pharm. Bull.*, 27 (1979) 1942.
4. Higashijima, T., Uzu, S., Nakajima, T. and Ross, E.M., *J. Biol. Chem.*, 263 (1988) 6491.
5. Higashijima, T., Burnier, J. and Ross, E.M., *J. Biol. Chem.*, 265 (1990) 14176.
6. Aridor, M., Rajmilevich,G., Beaven, M.A. and Sagi-Eisenberg, R., *Science*, 262 (1993) 1569.

Peptides: Chemistry, Structure and Biology
Pravin T.P. Kaumaya and Robert S. Hodges (Eds.)
Mayflower Scientific Ltd., 1996

164
Allosteric Regulation of an SH2 Domain Enzyme by Simultaneous Occupancy of both SH2 Domains

S. Pluskey, T. Trüb, and S.E. Shoelson

Research Division, Joslin Diabetes Center and Department of Medicine, Harvard Medical School, Boston, MA 02215, USA

Introduction

Cell surface receptors with tyrosine kinase activity initiate cellular effects by catalyzing tyrosine phosphorylations within their own sequences and additional cellular substrates. Proteins (enzymes) with SH2 domains bind these phosphorylation sites to propagate the signals to intracellular destinations. While the role of SH2 domains as binding modules participating in the formation of signaling complexes has been well publicized, SH2 domains can also act as allosteric regulators of enzymatic activity. We have screened many SH2 domains and found a particularly high level of regulation for SH-PTP2. Therefore, we have used SH-PTP2 as a model for detailed analyses of the mechanism of allosteric regulation by SH2 domain occupancy.

Results and Discussion

We mapped the specificities of the two SH2 domains of SH-PTP2 to find that monophosphoryl peptides 1172 (SLNpYIDLDLVK) and 1222 (LSTpYASINFQK) corresponding to IRS-1 sequences bind with highest affinity to the N- and C-terminal domains, respectively [1]. We also showed that monophosphoryl peptide occupancy of either domain stimulates catalysis [2], while simultaneous occupancy of both domains has a greater stimulatory effect at much lower ligand concentrations (Figure 1A) [3]. Additional studies investigate potential mechanisms of activation.

In the original study we linked the 1172 and 1222 peptides with 4 tandem amino-hexanoic acid (Ahx) moieties (1172Ahx$_4$1222), based on spacer distances between phosphorylation sites in the PDGF receptor and ζ chains of T cell receptors. Since the peptides bind selectively with alternative SH2 domains, we tested the effect of reversed orientation on activation. When aligned tail-to-head (1222Ahx$_4$1172) rather than head-to-tail, the mode of activation was distinctly different than 1172Ahx$_4$1222 and resembled that of a monophosphoryl peptide (Figure 1B). The effect of tether length was tested, as well. When the number of tandem Ahx spacers was reduced, less activation was observed and higher peptide concentrations were required for the effect (Figure 1C). Presumably, this was because binding motifs were being brought too close together. Levels of activation similarly dropped off with increasing spacer length, in this case perhaps due to an entropic penalty for increased flexibility.

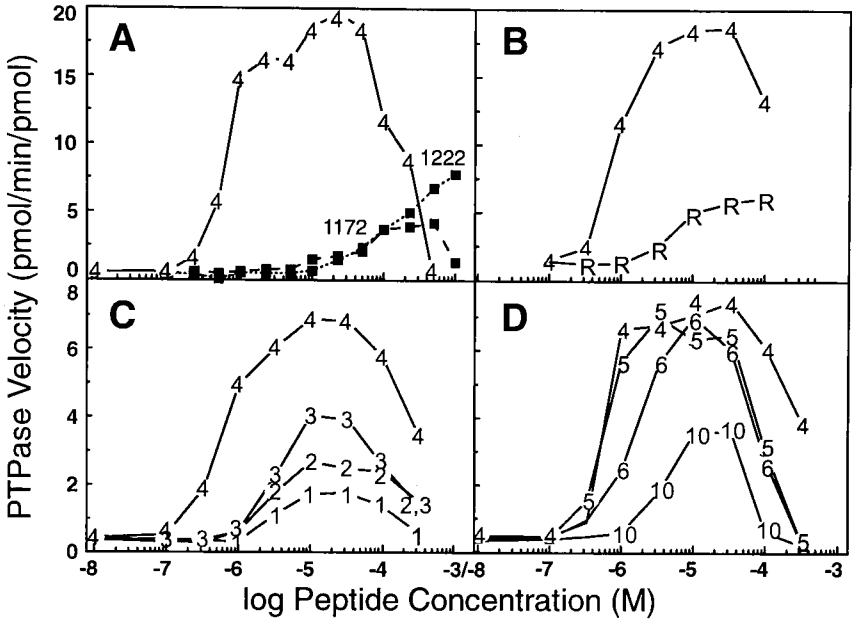

Figure 1. *PTPase activation by SH2 domain occupancy: A. Monophosphoryl peptides 1172 and 1222 activate at high peptide concentrations, while the tethered bisphosphoryl peptide (1172Ahx$_4$ 1222, labeled 4) stimulates to higher levels at lower peptide concentrations; B. Reversing the peptide order (1222Ahx$_4$1172; labeled R) gives levels of activation similar to the monophosphoryl peptides; C and D. Effects of tether length. The number (n) of Ahx spacers within the bisphosphoryl peptide (1172Ahx$_n$1222) was varied between 1 and 10 as shown.*

Thus, the originally designed bisphosphoryl ligand (1172Ahx$_4$1222) is most effective. SH-PTP2 is potently activated by bisphosphoryl peptide ligation of its SH2 domains, suggesting coordinate regulation by the two SH2 domains. The distance between SH2 domains can be mapped by varying bisphosphoryl peptide spacer lengths; a distance of ≈ 72 Å between phosphotyrosines is optimal. However, reversing the linker orientation is not tolerated, suggesting selective modes of binding. These findings agree with a recently solved crystal structure of the tandem SH2 domains of SH-PTP2 [4].

References

1. Case, R.D., Piccione, E., Wolf, G., Bennett, A.M., Lechleider, R.J., Neel, B.G. and Shoelson, S.E., *J. Biol. Chem.*, 269 (1994) 10467.
2. Sugimoto, S., Wandless, T., Shoelson, S.E., Neel, B.G. and Walsh, C.T., *J. Biol. Chem.*, 269 (1994) 13614.
3. Pluskey, S., Wandless, T., Walsh, C.T. and Shoelson, S.E., *J. Biol. Chem.*, 270 (1995) 2897.
4. Eck, M.J., Pluskey, S., Trüb, T., Harrison, S.C. and Shoelson, S.B., *Nature*, in press.

Peptides: Chemistry, Structure and Biology
Pravin T.P. Kaumaya and Robert S. Hodges (Eds.)
Mayflower Scientific Ltd., 1996

165
Correlated Mutation Analysis of G Protein α-Chains to Search for Residues Linked to Binding

L. Oliveira[1], A.C.M. Paiva[1] and G. Vriend[2]

[1]Department of Biophysics, Escola Paulista de Medicina, 04023-062 São Paulo, SP, Brazil
[2]BIOcomputing, EMBL, Postfach 10-2209, D-6900 Heidelberg, Germany

Introduction

The 3D structures of several G protein α-chains have been solved [1-3] but this has not yet led to a full understanding of their structure-function relationships. The extreme C-terminal sequence of Gα chains were shown to be crucial for receptor binding [4]. However, other results point to a different picture [5-7] suggesting that G protein coupling to receptors should involve other regions of Gα chains. Here we try to find these regions using the correlated mutation analysis [8] of multiple aligned sequences of G protein α-chains.

Results and Discussion

Table 1 shows the most important network of positions obtained by correlation analysis of Gα chain sequences, which discriminates three main classes of chains. Five out of thirteen positions in this network (188, 190, 333, 336 and 340) form a nest of correlated residues at apposing regions of the β2-β3 loop and the central part of helix α5 in the C-terminal segment of G proteins. For each Gα chain class, different residues can occupy these five positions. Residue 190 is always hydrophobic but different charged, polar and non-polar residues are found in the other positions. Figure 1 schematically indicates these correlated mutated residues and the conserved Asp 337 in the transducin structure.

Table 1. *Networks of correlated mutated residue positions obtained from multiple aligned sequences of Gα chains*[a]

Gα chains	Residue Positions												
	50	76	145	176	188	190	250	258	314	333	336	340	348
Gi group	K	S	N	K	K	L	C	T(I)	E	D	T	I	G
Gs group	R	A	I	L	D	V	W	I	Y	N(D)	R	Q	E
Gq group	R	A	S(E)	P	Q(E)	V(I,T)	I	S	I(V)	A	K	L	N

[a]Residue position number as in the transducin structure.

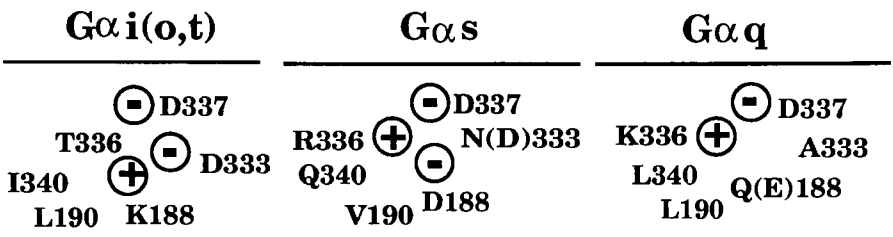

Figure 1. *Schematic organization of the clustered correlated residues 188 and 190 (β2-β3 loop) and 333, 336 and 340 (helix α5). Residue Asp337 is conserved for all Gα chains.*

The position of charged side chains is different in different Gα chains, but the presence of at least one negative charge and one positive charge, and one uncharged but polar group is maintained throughout all Gα chains. Thus, a conserved polar locus at the surface of Gα chains is a common feature of these proteins. The C-terminal segment containing the correlated mutated residues 333, 336, and 340 was not yet described as being involved in receptor binding despite the fact that it is placed between two protein segments, 311-328 and 340-350, which were found to be crucial for receptor coupling [4]. However, receptor binding experiments leading to these results were performed with C-terminal peptides rather than with complete G protein molecules. Future research should envisage the possibility that the polar locus formed by the C-terminal helix α5 and the β2-β3 loop might be important in receptor-Gα chain coupling.

References

1. Noel, J.P., Hamm, H.E. and Sigler, P.B., *Nature,* 366 (1993) 654.
2. Sondek, J., Lambright, D.G., Noel, J.P., Hamm, H.E. and Sigler, P.B., *Nature,* 372 (1994) 276.
3. Coleman, D.E., Berghuis, A.M., Lee, E., Linder, M.E., Gilman, A.G. and Sprang, S.R., *Science,* 265 (1994) 1405.
4. Hamm, H.E, Deretic, D., Arendt, A., Hargrave, P.A., Koenig, B. and Hoffman, K.P., *Science,* 241 (1988) 832.
5. Kosugi, S., Okajima, F., Ban, T., Hidaka, A., Shenker, A. and Kohn, L.D., *J. Biol. Chem.,* 267 (1992) 24153.
6. Kleuss, C., Hescheler, J., Ewel, C., Rosenthal, W., Schultz, G. and Wittig, B., *Nature,* 353 (1991) 43.
7. Cerione, R.A., Staniszewski, C., Benovic, J.L., Lefkowitz, R.J., Caron, M.G., Gierschik, P., Somers, R., Spiegel, A.M., Codina, J. and Birnbaumer, L., *J. Biol. Chem.*, 260 (1985) 1493.
8. Oliveira, L., Paiva, A.C.M. and Vriend, G., in Maia, H.L.S., (Ed.), 'Peptides, 1994', ESCOM, Leiden, The Netherlands, 1995, p. 797.

Peptides: Chemistry, Structure and Biology
Pravin T.P. Kaumaya and Robert S. Hodges (Eds.)
Mayflower Scientific Ltd., 1996

166
Intracellular Signal Transduction Involved in Neurokinin Receptors

S. Fukuhara, H. Mukai, M. Shimizu and E. Munekata

Institute of Applied Biochemistry, University of Tsukuba, Tsukuba, Ibaraki 305, Japan

Introduction

The neurokinin peptides, substance P (SP), neurokinin A (NKA), and neurokinin B (NKB), regulate various physiological processes [1]. These actions are thought to be mediated by three pharmacologically distinct cell-surface receptors classified as NK-1, 2, and 3. The preferred endogenous ligand appears to be SP for NK-1, NKA for NK-2, and NKB for NK-3 [1]. Recently, we showed that murine neuroblastoma C1300 cells expressed neurokinin receptors [2]. In this study, we investigated neurokinin-related signaling in this cell line and an AR42J rat pancreatic acinar cell line, which also has neurokinin receptors [3], to probe intracellular signal transduction caused by each neurokinin receptor subtype.

Results and Discussion

Neurokinins induced elevation of intracellular free calcium ($[Ca^{2+}]_i$) concentration in a concentration-dependent manner (Figure 1). To identify the subtype(s) of neurokinin receptors expressed in C1300 and AR42J cells, we performed RNA blot hybridization using each specific probe for NK-1,2, and 3, and examined the inhibitory effects of selective antagonists on neurokinin-induced Ca^{2+} mobilization. In C1300 cells, both NK-2 and NK-3 mRNAs were detectable, and NKA- and NKB-evoked Ca^{2+} mobilization was inhibited by SR48968 and MEN10,376 (NK-2 antagonists), but [βAla^8]NKA(4-10) (a NK-2 agonist) did not induce the elevation of $[Ca^{2+}]_i$ (Figure 1-A). The response to NKA and NKB was not inhibited by CP-96,345 and [Trp^7,βAla^8]NKA(4-10) (NK-1 and 3 antagonists, respectively). In AR42J cells, only NK-1 mRNA was detectable, and SP-evoked Ca^{2+} mobilization was inhibited by CP-96,345. These results suggested that C1300 cells expessed, at least, NK-2 receptors having features different from known NK-2 receptors, and AR42J cells have only NK-1 receptors.

The mechanisms of Ca^{2+} mobilization in response to neurokinins were examined to elucidate the neurokinin-related signaling. In both cell lines, neurokinins stimulated the elevation of $[Ca^{2+}]_i$ even in the absence of extracellular Ca^{2+}, but the maximal increase was attenuated. The response to neurokinins was also reduced in the presence of nickel or cobalt (inorganic Ca^{2+} influx blockers). These findings indicated that the elevation of $[Ca^{2+}]_i$ by neurokinins was dependent on both mobilization of internal Ca^{2+} and influx of extracellular Ca^{2+} in both cell lines. Furthermore, nifedipine and ω-conotoxin, blockers of L- and N-type voltage-dependent Ca^{2+} channels, respectively, had no effect on NKA-

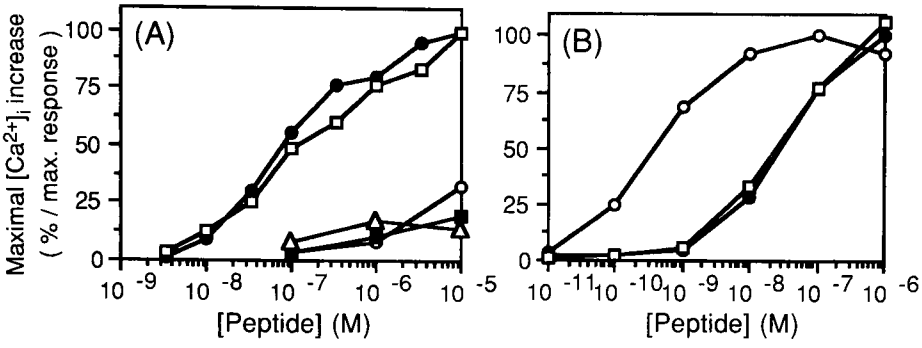

Figure 1. *Concentration-response curves of the $[Ca^{2+}]_i$ increase in C1300 (A) and AR42J (B) cells induced by neurokinins and related peptides. Cells were stimulated by the indicated concentration of SP* (○), *NKA* (●), *NKB* (□), *[Ala^8]NKA(4-10)* (■) *and senktide* (Δ).

and NKB-evoked Ca^{2+} mobilization in C1300 cells, and the depolarization by 60 mM K^+ did not affect the $[Ca^{2+}]_i$. This suggests the influx of extracellular Ca^{2+} occurs *via* voltage-independent Ca^{2+} channels in C1300 cells. The inhibitory effect of U73122, a putative phospholipase C (PLC) inhibitor, was examined to determine whether PLC activation was essential for neurokinin-induced Ca^{2+} mobilization. Neurokinins response in both cell lines was inhibited by U73122. In addition, SP stimulated the formation of inositol trisphospate in AR42J cells. In various cell systems, inositol 1,4,5-trisphosphate ($Ins(1,4,5)P_3$), which is produced by PLC, interacts with its receptors on a Ca^{2+}-storing intracellular organelle, and induces the release of Ca^{2+}. These and the present findings suggest that the neurokinins-evoked mobilization of internal Ca^{2+} in these cell lines may be caused by $Ins(1,4,5)P_3$, generated by the activation of PLC. To investigate whether neurokinin receptors in the cell lines couple to adenylate cyclase, neurokinins stimulated cyclic AMP accumulation was measured. Although forskolin, an activator of adenylate cyclase, stimulated the accumulation of cAMP, neurokinins did not in either cell line.

In conclusion, it was suggested that C1300 and AR42J cells expressed endogenous NK-2 and NK-1, respectively, and that neurokinins activated PLC to evoke Ca^{2+} mobilization, but not adenylate cyclase through these receptors.

Acknowledgments

We thank Dr. S. Nakanishi for providing cDNAs of neurokinin receptors, Dr. A. Nagahisa for CP-96,345 and Dr. X. Emonds-Alt for SR48968. This study was supported by a research grant from the Special Research Project on Circulation Biosystems, University of Tsukuba, the Naito Foundation, and a Grant-in Aid for Scientific Research from the Ministry of Education, Japan (No. 06680605).

References

1. Munekata, E., *Comp. Biochem. Physiol.*, 98C (1991) 171.
2. Fukuhara, S., Mukai, H. and Munekata, E., *Peptides*, 16 (1995) 211.
3. Christophe, J., *Am. J. Physiol.*, 266 (1994) G963.

Peptides: Chemistry, Structure and Biology
Pravin T.P. Kaumaya and Robert S. Hodges (Eds.)
Mayflower Scientific Ltd., 1996

167
Elastin Peptides Induce Monocyte Chemotaxis by Increasing the Level of Cyclic GMP, an Intracellular Second Messenger

Y. Uemura[1], S. Kamisato[1], K. Arima[1], N. Takami[2] and K. Okamoto[1]

[1]Department of Biochemical Engineering and Science, Kyushu Institute of Technology, Iizuka-shi, Fukuoka 820, Japan
[2]Radioisotope Center, Fukuoka University School of Medicine, Jonan-ku, Fukuoka 814-01, Japan

Introduction

Elastin, the core protein of extracellular elastic fiber, is chemotactic in its proteolytic fragments for monocytes [1]. Monocytes participate in the pathogenesis of atherosclerosis and in the development of pulmonary emphysema: elastin fragments generated at diseased sites are chemoattractants for monocytes. Several repeating peptides are included in the hydrophobic regions of elastin. Among these repeating peptides, the repeating hexapeptide Val-Gly-Val-Ala-Pro-Gly (VGVAPG) is known to be chemotactic for human monocytes [2, 3], but its intracellular mechanism is not yet clarified. The aim of this study is to assess the chemotactic potency of repeating elastin peptides and α-elastin (chemically treated fragments of elastin), and to clarify the mechanism of signal transduction pathway.

Results and Discussion

In Figure 1, the positive migration of monocytes in response to a concentration gradient ranging from 10^{-4} to 10^{4} showed that maximal activities were at 0.1 μg/ml and 1 μg/ml for α-elastin and the high polymer of hexapeptide repeat, (VGVAPG)n, respectively. The checkerboard assays established that these elastin peptides stimulated direct (chemotaxis) rather than random (chemokinesis) migration of monocytes [4]. In contrast, the high polymer of pentapeptide repeat, (VPGVG)n, was not chemotactic for monocytes (Figure 1). However, among the repeating peptides in elastin, the cross-linked high polymer of pentapeptide repeat has been known to be the only elastomer [5]. The fact that these repeating peptide sequences exhibit distinct properties is of interest for understanding the functions of elastin.

Uemura *et al.* [4], observed that the cyclic GMP (cGMP) level in monocytes is elevated by two chemoattractants, α-elastin and (VGVAPG)n, but not by the non-chemoattractant, (VPGVG)n, and that the cyclic AMP level in monocytes is not changed

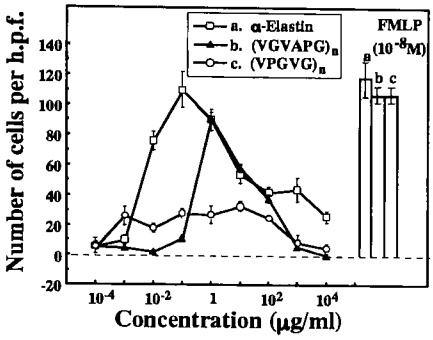

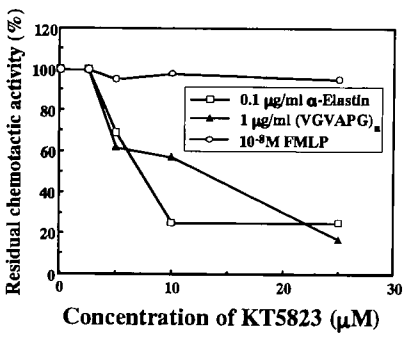

Figure 1 (left). *Monocyte migration in response to α-elastin, (VGVAPG) n and FMLP. Mean and standard error are shown, n=9. Background migration (buffer alone) was 43, 28 and 28 cells per high power field (h.p.f.), respectively.*
Figure 2 (right). *Effect of PKG inhibitor(KT5823) on monocyte chemotactic response to α-elastin, (VGVAPG) n and FMLP. Ordinate shows the residual chemotactic activity as percent of control stimulated migration in the absence of the inhibitor.*

by α-elastin,(VGVAPG)n or (VPGVG)n. This observation suggests that the chemotactic activity of elastin peptides is correlated with the enhanced level of cGMP. Therefore, in order to examine the effect of cGMP dependent kinase (PKG), monocytes were preincubated with an inhibitor specific for PKG (KT5823) at 37°C for 10 min, and then tested for their migration to α-elastin, (VGVAPG)n and FMLP at optimal concentrations (0.1 μg/ml, 1 μg/ml and 10^{-8}M, respectively) in the presence of inhibitor. KT5823 inhibited monocyte migration to α-elastin and (VGVAPG)n in a dose-dependent manner (Figure 2). A 50% inhibition of α-elastin-induced monocyte migration was observed at 7 μM KT5823, its inhibitory effect being higher than that for (VGVAPG)n-induced monocyte migration. However, KT5823 had no inhibitory effect toward FMLP-induced monocyte migration. Another inhibitor specific for protein kinase C (Chelerythrine) was tested, and the results exhibited that FMLP-induced migration was markedly inhibited by this inhibitor, but α-elastin- and (VGVAPG)n-induced migrations were not [4]. These results suggest that elastin peptides such α-elastin and (VGVAPG)n induce monocyte chemotaxis by increasing the level of cGMP through a signal transduction pathway distinct from that of FMLP, which is known to induce cell migration by a complex pathway of phosphoinositide cascade through the receptor.

References

1. Senior, R.M., Griffin, G.L. and Mecham, R.P., *J. Clin. Invest.*, 66 (1980) 859.
2. Senior, R.M., Griffin, G.L., Mecham, R.P., Wrenn, D.S., Prasad, K.U., and Urry, D.W., *J. Cell Biol.*, 99 (1984) 870.
3. Uemura, Y., Okamoto, K., Fan, J. and Watanabe, T., in Yanaihara, N. (Ed.), 'Peptide Chemistry 1992', ESCOM, Leiden, 1993, p. 396.
4. Uemura, Y., Takami, N. and Okamoto, K., Kyushu Institute of Technology, Iizuka, Fukuoka, Japan, unpublished data.

Peptides: Chemistry, Structure and Biology
Pravin T.P. Kaumaya and Robert S. Hodges (Eds.)
Mayflower Scientific Ltd., 1996

168
Structure-Activity Relationships of Peptides That Block the Association of PDGF β-Receptor with Phosphatidylinositol 3-Kinase

S.R. Eaton[1], K. Ramalingam[1], W.L. Cody[1], D.R. Holland[1], R.L. Panek[2], G.H. Lu[2], and A.M. Doherty[1]

Departments of [1]Chemistry and [2]Cardiovascular Therapeutics, Parke-Davis Pharmaceutical Research, Division of Warner-Lambert Company, 2800 Plymouth Road, Ann Arbor, MI 48105, USA

Introduction

A significant number of patients (20-45%) that have undergone percutaneous transluminal coronary angioplasty (PTCA) suffer from reocclusion of the arteries, also known as restenosis [1]. There is compelling evidence that growth factors such as platelet derived growth factor (PDGF) and/or fibroblast growth factors (FGFs) are partially responsible for this proliferation and migration of vascular smooth muscle cells. Therefore, strategies to block the signalling pathways initiated by the binding of PDGF to its receptor have become interesting therapeutic targets. The association of PDGF β-receptor with intracellular signal-transducing proteins that contain Src-homology 2 (SH2) domains such as phosphatidylinositol (PI) 3-kinase can be blocked by specific phosphorylated pentapeptides [2, 3]. In particular, we have studied the pentapeptide, Tyr(PO_3H_2)-Val-Pro-Met-Leu, from the kinase insert region of the PDGF β-receptor that corresponds to tyrosine 751 [2]. This compound (**1**) blocks the association of PDGF β-receptor and the C-terminal SH2 domain of the p85 subunit of PI 3-kinase with an IC_{50} of 0.67 μM [4]. In order to further elucidate the structure-activity relationships (SAR) of this peptide, we synthesized several analogues to evaluate the importance of the amine and carboxy terminus. In addition, we have prepared analogues that are stabilized against intracellular phosphotases.

Results and Discussion

Compound **1**, Tyr(PO_3H_2)^{751}-Val-Pro-Met-Leu, has an IC_{50} of 0.67 μM in blocking the association of PDGF β-receptor and the C-terminal SH2 domain of the p85 subunit of PI 3-kinase (Table 1). N-terminal acetylation and C-terminal amidation (compounds **2-4**) enhanced the ability of the phosphorylated pentapeptide to inhibit this interaction. In particular, the acetylated and amidated analogue (compound **4**) had an IC_{50} of 0.16 μM. However, truncation of the peptide by deletion of Leu (compound **5**) resulted in a ten-fold loss of activity. Interestingly, the corresponding tetrapeptide carboxamide (compound **6**) showed a six-fold enhancement of activity. Likewise, as in the penta-

peptide series, the N-acetylated and C-amidated tetrapeptide analogue (compound **7**) possessed submicromolar affinity with an IC_{50} of 0.24 μM. Molecular modeling of the C-terminal SH2 domain of the PI 3-kinase p85 subunit complexed with compound **7** supports the high affinity binding observed, suggesting several important interactions [5].

In order to further evaluate the potential therapeutic utility of this series of phosphorylated peptides, demonstration of cellular activity is critical. It has been shown that phosphorylated tyrosines are rapidly metabolized by cellular phosphotases. Substitution of the corresponding methylene phosphonate derivative [Pmp (4-phosphono-methylphenylalanine), compound **8**] resulted in 10-fold loss of affinity. The di-fluorinated derivative [CF_2Pmp, 4-phosphono(difluoromethyl)phenylalanine)] has been reported to be a substitution that maintains high binding affinity while imparting cellular stability [6]. Substitution of the CF_2Pmp into the pentapeptide (compound **9**) and the tetrapeptide (compound **10**) resulted in analogues with 1-2 μM affinity. These stabilized analogues are undergoing further evaluation in a cell based assay to access cell membrane permeability as well as their effects on inhibiting the association of PDGF β-receptor with PI 3-kinase and on DNA synthesis.

Table. *Analogues of Tyr(PO_3H_2)^{751}-Val-Pro-Met-Leu (compound 1).*

Cmpd.	Sequence						IC_{50}(μM)	n[a]
1		Tyr(PO_3H_2)-	Val-	Pro-	Met-	Leu	0.67	38
2	Ac-	Tyr(PO_3H_2)-	Val-	Pro-	Met-	Leu	0.18	2
3		Tyr(PO_3H_2)-	Val-	Pro-	Met-	Leu-NH_2	0.40	2
4	Ac-	Tyr(PO_3H_2)-	Val-	Pro-	Met-	Leu-NH_2	0.16	2
5		Tyr(PO_3H_2)-	Val-	Pro-	Met		7.9	3
6		Tyr(PO_3H_2)-	Val-	Pro-	Met-NH_2		1.3	2
7	Ac-	Tyr(PO_3H_2)-	Val-	Pro-	Met-NH_2		0.24	28
8		Pmp-	Val-	Pro-	Met-	Leu	8.7	2
9		CF_2Pmp-	Val-	Pro-	Met-	Leu	1.2	2
10		CF_2Pmp-	Val-	Pro-	Met-NH_2		1.7	7

[a]number of determinations.

References

1. Herrman, J.R., Hermans, W.R.M., Vos, J. and Serruys, P.W., *Drugs,* 46 (1993) 18.
2. Fantl, W.J., Escobedo, J.A., Martin, G.A., Turck, C.W., del Rosario, M., McCormick, F. and Williams, L.T., *Cell,* 69 (1992) 413.
3. Waksman, G., Shoelson, S.E., Pant, N., Cowburn, D. and Kuriyan, J., *Cell,* 72 (1993) 779.
4. Ramalingam, K., Eaton, S.R., Cody, W.L., Lu, G.H., Panek, R.L., Waite, L.A., Decker, S.J., Keiser, J.A. and Doherty, A.M., *Bioorg. Med. Chem.*, 3 (1995) 1263.
5. Holland, D.R., Parke-Davis Pharmaceutical Research, Division of the Warner-Lambert Company, Ann Arbor, Michigan, USA, personal communication, 1995.
6. Burke, T.R., Smyth, M.S., Otaka, A., Nomizu, M., Roller, P.P., Wolf, G., Case, R. and Shoelson, S.E., *Biochem.*, 33 (1994) 6490.

Peptides: Chemistry, Structure and Biology
Pravin T.P. Kaumaya and Robert S. Hodges (Eds.)
Mayflower Scientific Ltd., 1996

169
Structural Model for Binding of SOS-derived Peptides to SH3 Domains of Grb2

C. Mapelli, M. Wittekind, V.G. Lee, V. Goldfarb, L. Mueller and C.A. Meyers

Bristol-Myers Squibb Pharmaceutical Research Institute, Princeton, NJ 08543, USA

Introduction

SH3 domains are small protein modules found in numerous signal transduction and cytoskeletal proteins. The triple-domain growth factor receptor-bound protein 2 (Grb2) utilizes its SH2 domain to bind to Tyr-phosphorylated intracellular domains of activated tyrosine kinase receptors and its two SH3 domains to bind to the proline-rich C-terminal domain of the guanine nucleotide exchange factor son of sevenless (Sos). This is a key step in the Ras signaling pathway.

Results and Discussion

In earlier studies [1] we showed that the mouse C-terminal Sos2-derived peptide SPLLPKLPPKTYKRE (Sos-A) binds to the N-terminal SH3 domain (N-SH3) of Grb2 in an orientation opposite to that observed for the library-selected peptide RKLPPRPSK (RLP1) bound to the SH3 domain of phosphatidylinositol 3-kinase (PI3K) [2]. We have now determined the refined solution structure of the Grb2 N-SH3 domain complexed with the tighter binding peptide VPPPVPPRRR (Sos-E) derived from the mouse Sos1 sequence (Figure 1). The structure is very well-defined due to assignment of all ^{1}H, ^{15}N, and ^{13}C NMR resonances of the complex and unambiguous identification of 117 inter-molecular NOE restraints, allowing for determination of a higher resolution structure than those previously published [3, 4]. The structure of the N-SH3 shows two hydrophobic peptide-binding sub-sites: a shallow S1 sub-site that contacts the peptide Pro_2 and Pro_3 residues and a deeper sub-site S2 contacting the peptide Val_5 and Pro_6 residues. Adjacent to S2 is a third negatively charged sub-site S3, characterized by a dynamically averaged set of peptide and N-SH3 sidechain conformations. We have observed partial ordering of the sidechain of the peptide Arg_8 residue due to a set of weak NOEs to the N-SH3 Trp_{36} indole ring protons. The periodicity of peptide side chain intercalation into the sub-sites S1, S2, and S3 of the N-SH3 is consistent with the adoption of a nearly ideal polyproline type II (PPII) helix by much of the peptide backbone. As expected, the binding orientation of the Sos-E peptide is the same ("minus" [5]) as that of the Sos-A peptide.

An intriguing feature of the pseudo-symmetric nature of the PPII helix is the possibility of ligands binding to the same SH3 domain in two opposite orientations [6].

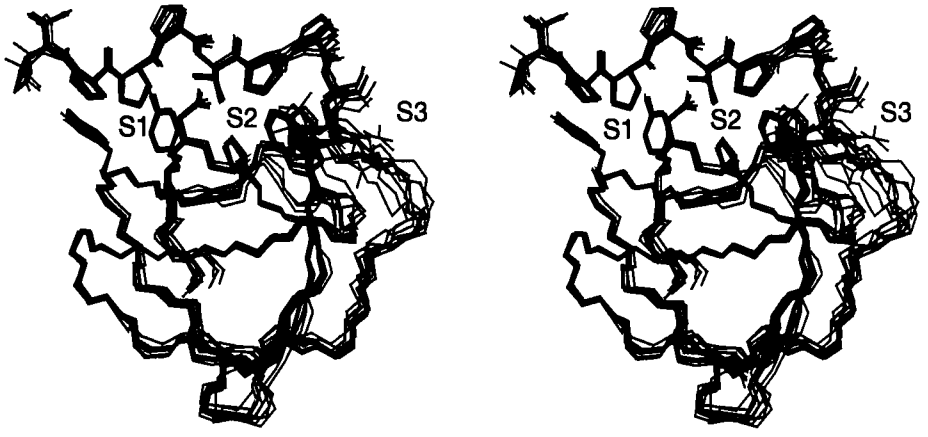

Figure 1. *Stereo views of the superposition of the final refined structures of the Sos-E-Grb2 N-SH3 complex.*

Simple reversal of the amide backbone directionality of Sos-E yields a ligand (RRRPPVPPPV, retro Sos-E) which can still bind to Grb2 N-SH3, albeit with ten-fold reduced affinity. Substitution of the Val_6 with Pro in retro Sos-E restored binding to a high degree. This is because in the "plus" binding orientation most likely adopted by the retro analog, the Val_6 sidechain points away from the S2 hydrophobic pocket instead of intercalating into the S2 subsite like the corresponding Val_5 side chain does in the Sos-E peptide (Figure 1). The packing defect left by Val_6 in the plus orientation can be obviated by proline, because of its N-alkyl substitution [5]. Thus, peptide binding affinities can be modulated by subtle changes in the molecular packing against the N-SH3 surface.

In contrast, the all D-amino acid retroinverso analog of the Sos-E peptide (rrrppvpppv) showed no binding affinity for NSH3, suggesting that in the context of the chiral left-handed PPII helix the retro-inverso modification abolishes the overall topological equivalence to the parent peptide.

References

1. Wittekind, M., Mapelli, C., Farmer, B.T., Suen, K.L., Goldfarb, V., Tsao, J., Lavoie, T., Barbacid, M., Meyers, C.A. and Mueller, L., *Biochemistry,* 33 (1994) 13531.
2. Yu, H. Chen, J.K., Feng, S., Dalgarno, D.C., Brauer, A. W. and Schreiber, S. L., *Cell,* 76 (1994), 933.
3. Goudreau, N., Cornille, F., Duchesne, M., Parker, F., Tocque, B. , Garbay, C. and Roques, B.P., *Nature Struct. Biol.*, 1 (1994) 898.
4. Terasawa, H., Kohda, D., Hatanaka, H. Tsuchiya, S., Ogura, K., Nagata, K., Ishii, S., Mandiyan, V., Ullrich, A., Sclessinger, J. and Inagaki, F., *Nature Struct. Biol.*, 1 (1994) 891.
5. Lim, W. A., Richards, F.M. and Fox, R.O., *Nature*, 372 (1994) 375.
6. Feng, S., Chen, J.K., Yu, H., Simon, J. A. and Schreiber, S. L., *Science,* 266 (1994) 1241.

Session VIII
Glyco/Lipo/Phospho/ Peptides

Chairs: Albert Loffet and
Vadim Ivanov

Peptides: Chemistry, Structure and Biology
Pravin T.P. Kaumaya and Robert S. Hodges (Eds.)
Mayflower Scientific Ltd., 1996

170
Application of New Synthetic Methods in Studies of Immunology and Enzymology of O-linked Cytosol- and Mucin-glycopeptides

M. Meldal[1], E. Meinjohanns[1], K. Frische[1], K. Bock[1] and H. Paulsen[2]

[1]Department of Chemistry, Carlsberg Laboratory, Gamle Carlsberg Vej 10, DK-2500 Valby, Denmark
[2]Department of Organic Chemistry, Martin-Luther-King-Platz 6, D-20146 Hamburg, Germany

Introduction

The mucous parts of intestinal tracts are covered with mucin glycoproteins [1, 2] carrying a large variety of glycosylation, which serve the purpose of lubricating and protecting the vulnerable epithelia from physical, chemical and biological damage. In case of malignant tissue, *e.g.* colon cancer, the structures present in the mucins are shifted towards fucosylated and sialylated core 1 structures, whereas core 2, 3 and 4 structures are reduced by down regulation of the glycosyl transferases involved in their synthesis [3]. In order to study these processes it is important to have access to glycopeptides as substrates and reference compounds for the study of enzymatic reactions and the recognition by the immune system. We recently reported the use of the Dts group for amino sugar protection in the synthesis of cytosol O-GlcNAc glycopeptides [4-6]. In the present work, we describe the application of the Dts group in the synthesis of more complex building blocks from mucin core 2, 3 and 4 for use in glycopeptide synthesis.

Results and Discussion

The introduction of the Dts group for amine protection in D-glucosamine proceeds as follows [5]. Glucosamine hydrochloride was reacted with S-carboxymethyl O-ethyl dithiocarbonate followed by O-acetylation and reaction with chlorocarbonyl sulfenyl chloride. This gave an acceptable yield of Ac_4-D-GlcNDts, which could be converted quantitatively into the β-bromide. This bromide was hydrolysed and converted into the β-trichloroacetimidate **1**, which was used in the 1,2-*trans* glycosylation of Fmoc-Ser/ Thr-OPfp. These building blocks were subsequently used for synthesis of glycopeptides containing up to three GlcNAc residues [6].

The glycosyl donor **1** is very valuable in the selective synthesis of complex oligosaccharides containing β-linked GlcNAc residues. The exclusive formation of β-linked product may be ascribed to the bulky character and the participation of the Dts group in the glycosylation reaction. Furthermore, the Dts-group can be converted into different *N*-acyl groups under extremely mild conditions allowing labile orthogonal

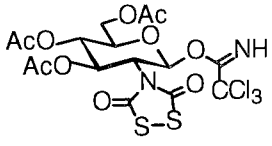

1

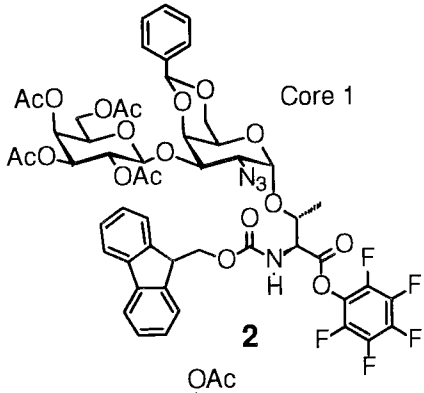

2

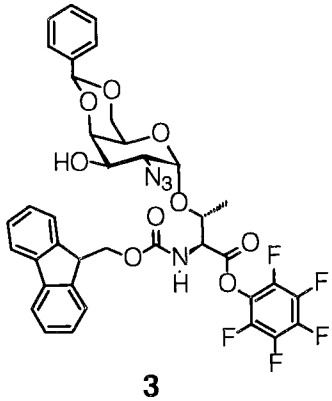

3

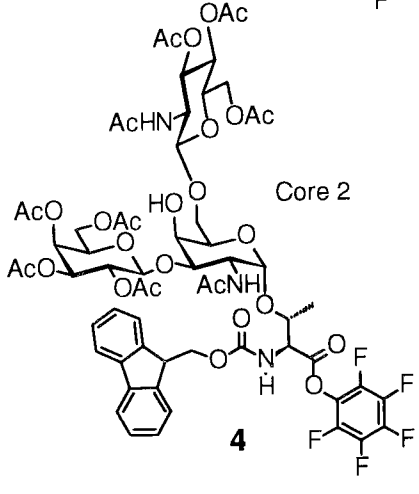

4

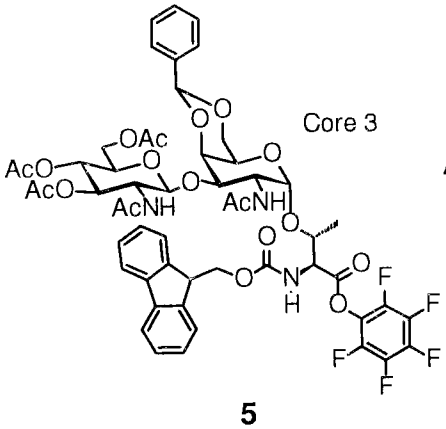

5

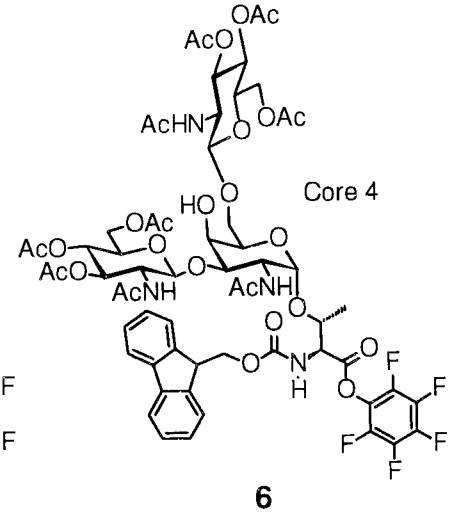

6

protection schemes. Thus, the reduction of the Dts group with a few equivalents of dithiothreitol (DTT) affords the free amine, which can subsequently be acylated. Alternatively, the Dts groups can be converted directly into N-acetates by reduction with zinc in the presence of acetic anhydride in THF, similarly to the reported conversion of allyloxycarbonyl groups into N-acetates[7]. In this way, the reaction of, for example, Pfp ester with the amine can be avoided. With DTT or zinc the simultaneous reduction of azido groups can be achieved, whereas reduction with sodium boron hydride is selective and only reduces the Dts-group. Utilizing the flexibility of the Dts-group building blocks corresponding to mucin core 2, core 3 and core 4 were synthesized and analyzed by ^{1}H NMR spectroscopy. Hydrolysis of the benzylidene group in compound **2** [8] followed by selective TMSOTf catalysed glycosylation at the 6-position with **1** gave 67% of trisaccharide, which could be converted into the core 2 building block **4** by zinc (activated with $CuSO_4$ solution) in THF, Ac_2O and AcOH (3/2/1). Similarly, compound **3** was glycosylated at the 3-position with **1** in the presence of TMSOTf to yield 95% glycosylation product, which could be converted in 68% yield to the core 3 building block **5** with zinc, THF, Ac_2O and AcOH. Alternatively, the benzylidene group in the above glycosylation product could be removed with aqueous acetic acid and the 6-position selectively glycosylated with **1** promoted by TMSOTf in an overall yield of 65%. This trisaccharide amino acid product containing two Dts groups, an azido group, a Pfp ester and an Fmoc group was finally converted by the zinc reduction into the core 4 building block **6** in 61% yield. Glycopeptides recognized by carbohydrate specific T-cells have been synthesized using core 1 building block **2** and a similar study is in progress with compounds **4 - 6**.

References

1. Allen, H.J. and Kisailus, E.C. (Eds), Glycoconjugates, Marcel Dekker, Inc., New York, 1992, p. 263.
2. Podolsky, D.K., *J. Biol. Chem.*, 260 (1985) 8262.
3. Yang, J.-M., Byrd, J.C., Siddiki, B.B., Chung, Y.-S., Okuno, M., Sowa, M., Kim, Y.S., Matta, K.L. and Brockhausen, I., *Glycobiology*, 4 (1995) 873.
4. Meinjohanns, E., Meldal, M. and Bock, K., Abstr. XVII'th International Carbohydrate Symposium, Ottawa, 1994. p. 260.
5. Meinjohanns, E., Meldal, M., Paulsen, H. and Bock, K., *J. Chem. Soc. Perkin Trans.*, 1 (1995) 405.
6. Meinjohanns, E., Vargas-Berenguel, A., Meldal, M. and Bock, K., *J. Chem. Soc. Perkin Trans.*, 1995, 2165.
7. Vargas-Berenguel, A., Meldal, M., Paulsen, H. and Bock, K., *J. Chem. Soc. Perkin Trans.*, 1 (1994) 2615.
8. Frische,K., Jensen, T., Galli-Stampino, L., Mouritsen, S., Werdelin, O. and Meldal, M. in Schneider, C.H. (Ed), 'Proc. Symp. Pept. Immunol.', John Wiley and Sons, Ltd., in press.

Peptides: Chemistry, Structure and Biology
Pravin T.P. Kaumaya and Robert S. Hodges (Eds.)
Mayflower Scientific Ltd., 1996

171
Synthetic Approaches for the Structural Characterization of a Novel Family of Proteolipid Spider Toxins

W.D. Branton[1], Y. Zhou[1], C.G. Fields[2,3] and G.B. Fields[2,3]

Departments of [1]Physiology, [2]Lab Medicine and Pathology, and [3]The Biomedical Engineering Center, University of Minnesota, Minneapolis, MN 55455, USA

Introduction

Potent biological toxins have been essential to our emerging understanding of voltage dependent ion channels. Members of a family of proteolipid toxins from the venom of *Plectreurys tristes* (PLTX's) were among the first presynaptic calcium channel blockers to be purified from spider venom [1]. Structural characterization of this family of toxins presents unique challenges due the presence of fatty-acyl modifications of the peptide backbone. We have used RP-HPLC, Edman degradation sequence analysis, and electro-spray mass spectrometry (ESMS) in combination with Fmoc solid phase synthesis to determine the structures of two representative members of the PLTX family. We have shown that complete synthesis of such toxins, including the fatty-acyl moiety, is feasible by Fmoc chemistry.

Results and Discussion

Toxins from *Plectreurys* venom can be isolated in high purity by application of size exclusion chromatography followed by RP-HPLC [1, 2]. We have fully characterized two representative members of the fatty-acyl PLTX family. PLTX II, an inhibitory calcium channel blocker, was the first characterized [1]. Recently, we have also characterized a structurally homologous, excitatory calcium channel blocker, PLTX VI. PLTX II has a hydrophilic peptide backbone containing 44 amino acid residues, including 10 Cys residues that are apparently involved in 5 disulfide bonds. The primary structure of PLTX II was determined by Edman degradation analysis of reduced and S-pyridinethylated toxin. Treatment of PLTX II with base resulted in release of a very hydrophobic moiety from the C-terminal region. Loss of the hydrophobic component apparently results in complete loss of biological activity. Chromatographic analysis and ESMS suggested that the hydrophobic component was palmitic acid. A combination of sequence and mass spectrometric analysis of a C-terminal fragment of PLTX II suggested a novel structure that included a C-terminal carboxyamidated, O-palmitoylated Thr residue (Figure 1).

We undertook the chemical synthesis of the proposed O-palmitoylated, C-terminal peptide fragment of PLTX-II to (i) confirm the natural toxin structure, and (ii) provide

the means for synthesis of the entire peptide toxin, since the quantity that can be isolated from the natural source is limited. Post-translational modifications such as glycosylation, phosphorylation, or sulfation have been approached by one of two general chemical methods in solid-phase synthesis. The first is an on-resin reaction, where a desired sequence is assembled and then chemically treated to modify a specific residue or residues. The second is the solution-phase synthesis of a modified amino acid residue, followed by incorporation of the modified residue into the desired sequence. Both methods provided the desired fragment Cys(Pye)-Asp-Thr(Pal)-NH_2, as determined by collision-induced dissociation mass spectra. For the synthesis utilizing Fmoc-Thr(Pal), the Pal group underwent a partial O→N acyl shift upon base (piperidine) treatment, resulting in some O-branched peptide. The C-terminal O-acylation of the native toxin was confirmed by comparison to the chemically synthesized material [3].

A structural analysis of PLTX VI, similar to that performed upon PLTX II, showed that PLTX VI is homologous to PLTX II. Mass spectrometry and sequence analysis indicated that PLTX VI contains 40 amino acids, including 10 Cys residues that are apparently involved in 5 disulfide bonds (Figure 1). PLTX VI, however, contains a carboxyamidated, O-palmitoylated Ser residue in place of the identically modified Thr residue found in PLTX II. The C-terminal structure of PLTX VI was also proven by comparison to a chemically synthesized C-terminal fragment.

Ala-Asp-Cys-Ser-Ala-Thr-Gly-Asp-Thr-Cys-Asp-His-Thr-Lys-Lys-Cys-Cys-
Asp-Asp-Cys-Tyr-Thr-Cys-Arg-Cys-Gly-Thr-Pro-Trp-Gly-Ala-Asn-Cys-Arg-
Cys-Asp-Tyr-Tyr-Lys-Ala-Arg-Cys-Asp-Thr(Pal)-NH_2

Ile-Gly-Glu-Cys-Ala-Gly-Trp-Asn-Asp-Asn-Cys-Asp-Lys-Arg-Ser-Cys-
Cys-Asp-Gln-Cys-His-Gln-Cys-Arg-Cys-Lys-Phe-Gly-Ser-Asn-Cys-
Arg-Cys-Thr-Gly-Thr-Lys-Pro-Cys-Ser(Pal)-NH_2

Figure 1. *Primary structures of PLTX-II (top) and PLTX-VI (bottom).*

The entire PLTX-VI was also assembled using Fmoc chemistry. Ser was loaded onto Rink amide resin [4] without side-chain protection, followed by coupling of Fmoc-Cys(Acm). The side-chain of Ser was then acylated with palmitic acid. The remaining sequence was assembled, and the peptide cleaved and side-chain deprotected with water/TFA (5/95). [Cys(Acm)]-PLTX-VI was purified by RP-HPLC and then characterized by RP-HPLC and ESMS (Figure 2). The protected toxin could be obtained by Fmoc chemistry with the palmitoyl group intact. The use of Acm protection allowed for the purification of the desired sequence from deletion and/or truncation sequences without interference from disulfide crosslinked peptide oligomers. Folding studies of PLTX-VI are currently underway.

The post-translational, O-palmitoylation at a C-terminal Thr or Ser is unique to the *Plectreurys tristes* family of toxins. The presence of the palmitoyl residue is required for biological activity. We have demonstrated that Fmoc chemistry is a feasible approach for synthesis of small [3] and large O-palmitoyl peptides.

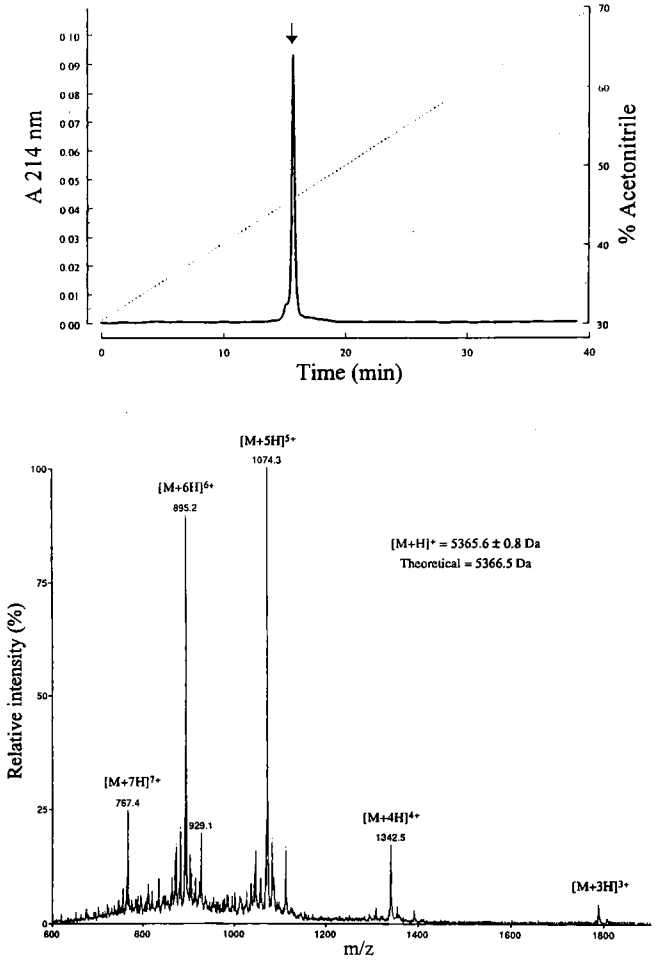

Figure 2. *RP-HPLC and ESMS analysis of purified synthetic [Cys(Acm)]-PLTX-VI.*

Acknowledgments

This work was supported by the NIH (GM42829 to WDB and DK44494 to GBF) and a McKnight-Land Grant Professorship to GBF.

References

1. Branton, W.D., Kolton, L., Jan, Y.N. and Jan, L.Y., *J. Neurosci.*, 7 (1987) 4195.
2. Branton, W.D., Rudnick, M.S., Zhou, Y., Eccleston, E.D., Fields, G.B. and Bowers, L.D., *Nature*, 365 (1993) 496.
3. Branton, W.D., Fields, C.G., VanDrisse, V.L. and Fields, G.B., *Tetrahedron Lett.*, 34 (1993) 4885.
4. Rink, H., *Tetrahedron Lett.*, 28 (1987) 3787.

Peptides: Chemistry, Structure and Biology
Pravin T.P. Kaumaya and Robert S. Hodges (Eds.)
Mayflower Scientific Ltd., 1996

172
Inherent Microheterogeneity of Recombinant Human Erythropoietin: "How Pure is Pure" with this Recombinant Glycoprotein Pharmaceutical?

C. Birr[1,2], M. Singhofer-Wowra[2], V. Ehemann[2], A. Hofmann[2] and M. Scharf[2]

[1]Heidelberg University, Faculty of Chemistry, 69120 Heidelberg, Germany
[2]ORPEGEN Pharma Gesellschaft für biotechnologische Forschung, Entwicklung und Produktion m.b.H., 69115 Heidelberg, Germany

Introduction

Among recombinant human growth factors and cytokines currently on the market or under pharmaceutical development, the major group are glycoproteins. They represent a most complex combination of biomolecular recognition elements, *e.g.* protein conformation and polyfunctional branched oligosaccharide antennuarities. This molecular complexity, undoubtedly, never could be synthesized by chemical means. For glycoproteins, biological production *via* recombinant mammalian cell culture techniques is the only way to make these molecules available for drug developments. While the glycoprotein sequence is defined by the recombinant nature of the engineered DNA , the post-translational disulfide formation and glycosylation is dependent on the biochemical machinery of the cell line utilized, *e.g.* from rodents like chinese hamster ovary cells (CHO), and baby hamster kidney cells (BHK), or from primates like monkey kidney cells (COS). Recombinant human erythropoietin (rhEPO), with its pharmaceutical potential, is one of the most challenging glycoproteins to manufacture [1-3]. In nature, EPO expressed in the kidney appears in the circulation for the generation of erythrocytes from pre-committed bone marrow stem cells. For the pharmaceutical development of rhEPO, a recombinant rodent kidney cell line was studied regarding the expression system, the glycosylation pattern and the cell culturing conditions including downstream processing.

Results and Discussion

From post-translational biological folding and processing, monkey as well as human EPO do contain small disulfide ring bridging at the positions 29-33. The mouse (rodent) glycoprotein does not contain this disulfide. Instead, mouse as well as monkey EPO present a mercapto function in position 139, competing for disulfide bonding at the small ring. All these EPO structures, however, contain a large second disulfide loop crosslinking position 161 and 7. It is essential to note that human and monkey EPO but not the rodent protein present an O-glycosylation site at position 126 (serine). These structural features have to be considered crucial in addition to the question on

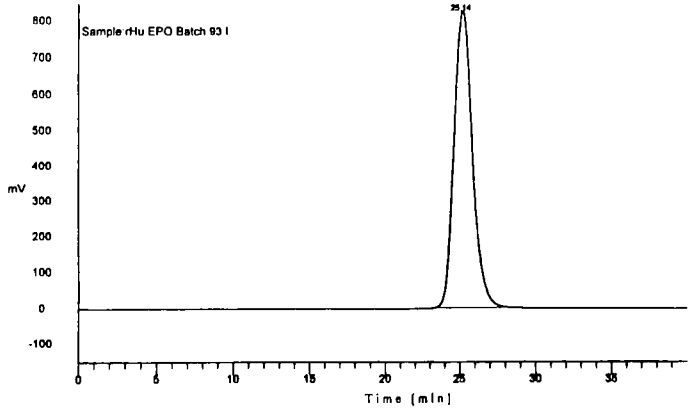

Figure 1. *Size exclusion gel chromatography profile of rhEPO as described in [5].*

species-specific glycosylation patterns when an appropriate mammalian expression system is chosen. The rhEPO glycoprotein obtained from our studies showed a symmetrical peak on size exclusion gel chromatography, typical for its molecular volume at a molecular mass of about 34-39 kD (Figure 1). On PAGE, a diffuse banding behaviour can be visualized which by Western blotting shows complete identity with rhEPO standard. This polyanionic nature of the recombinant product can be further elucidated by narrow range isoelectric focussing experiments resulting in 6 distinct bands of precisely discriminated isoelectric pI values. By 2D laser scanning the proportions within this IEF pattern have been quantified on validated grounds for the demonstration of the batch-to-batch consistency of the bioproduct, though microheterogeneous. Obviously, the complex oligosaccharide antennuarity is of key importance for the complete description of recombinant glycoproteins. In collaboration with Conradt *et al.*, [4], the IEF bands were analyzed individually by HPAE PAD chromatography and alligned with increasing contents of sialic acid moieties in the branched oligosaccharides as shown in Figure 2. By a combination of enzymic digests and acidic hydrolyses followed by HPLC/MS comparisons with synthetic sugar standards, Conradt elucidated the entire antennuarity of the rhEPO expressed and isolated by us [5].

Obviously, recombinant glycoproteins when harvested from mammalian cell culture occur in microheterogeneous form. This results not only from natural deviations in the oligosaccharide branching but also from biotechnological invasion into the post-translational processing cascade consisting of at least 15 distinct enzymatic transformations. This way the glycoprotein is finally trimmed with respect to its disulfide formation, protein folding and enzymatic oligosaccharide rearrangements. With human erythropoietin the terminal degree of sialoylation is of particular importance in this respect. There remains the question, what kind of oligosaccharide antennuarity comes closest with the human EPO glycolsylation pattern [6]? Obviously, different cell lines glycolsylate differently [7]. The comparative basis, *e.g.* human urinary EPO, can only be described to a limited degree of accuracy due to metabolic degradations of the product varying with the individual patients studied. This then results in another kind of

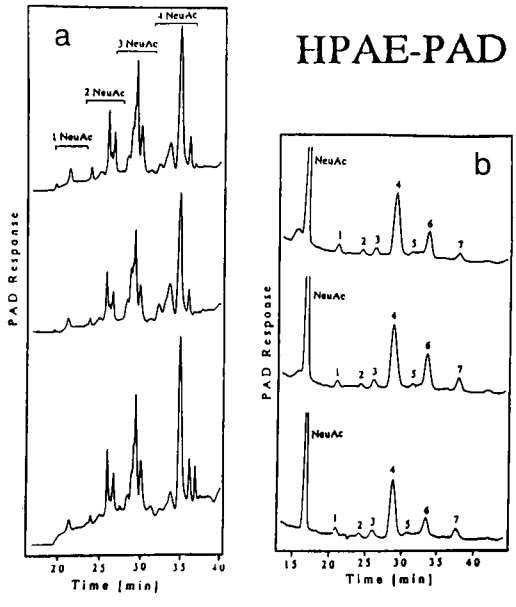

HPAE-PAD chromatograms, (a) of the native branched oligosaccharides and (b) after their digestion on treatment with sialidase for the cleavage of sialinic acid (NeuAc). Comparison of 3 batches of rhEPO from BHK cells (ORPEGEN, Heidelberg). The peak numbering correlates with the according reference oligosaccharides.

Figure 2. *HPAE-PAD chromatography profiles on both the sialoylation pattern of rhEPO and of the oligosaccharide composition on consecutive harvests to demonstrate the batch-to-batch consistency achieved by ORPEGEN Medizinisch-Molekularbiologische Forschungsgesellschaft m.b.H., Heidelberg.*

inherent microheterogeneity which one has to live with when natural glycoproteins are concerned and are to be reproduced by recombinant techniques. Details on "how pure is pure" with the rhEPO expressed and isolated by us have been published elsewhere [5].

References

1. Lin, F.-K., Suggs, S., Lin, C.-H., Browne, J.K., Smalling, R., Egrie, J.C., Chen, K.K., Fox, G.M., Martin, F., Stabinsky, Z., Badrawi, S.M., Lai, P. and Goldwasser, E., *Proc. Natl. Acad. Sci. USA*, 82 (1985) 7580.
2. Powell, J.S., Berkner, K.L., Lebo, R.V. and Adamson, J.W., *Proc. Natl. Acad. Sci. USA*, 83 (1986) 6465.
3. Jacobs, K., Shoemaker, C., Rudersdorf, R., Neill, S.,D., Kaufmann, R.J., Mufson, A., Seehra, J., Jones, S.S., Hewick, R., Fritsch, E.F. Kawakita, M., Shimizu, T., Miyake, T., *Nature*, 313 (1985) 806.
4. Conradt, H.S., 'GBF Jahresbericht 1990', Braunschweig, Germany, 1990, p. 115.
5. Nimitz, M., Martin, W., Wray, V., Klöppel, K.-D., Augustin, J. and Conradt, H.S., *Eur. J. Biochem.*, 213 (1993) 39.
6. Miyake, T., Kung, C., K.-H. and Goldwasser, E., *J. Biol. Chem.*, 252 (1977) 5558.
7. Tsuda, E., Goto, M., Murakami, A., Akai, K., Ueda, M., Kawauishi, G., Takahashi, N., Sasaki, R., Chiba, H., Ishihara, H., Mori, M., Tejima, S., Endo, S. and Arata, Y., *Biochemistry*, 27 (1988) 5646.

Peptides: Chemistry, Structure and Biology
Pravin T.P. Kaumaya and Robert S. Hodges (Eds.)
Mayflower Scientific Ltd., 1996

173
Peptide-Oligonucleotide Conjugates: Synthesis, Intracellular Localization and Anti-HIV Activity

K. Arar[1], C. Pichon[1], A-M. Aubertin[2], L. Gazzolo[3], A-C. Roche[1], M. Monsigny[1] and R. Mayer[1]

[1]Centre de Biophysique Moléculaire, C.N.R.S., F-45071 Orléans Cedex 02, France
[2]Laboratoire de Virologie, INSERM U74, F-67000 Strasbourg, France
[3]Faculté de Médecine, F-69372 Lyon Cedex 8, France

Introduction

Antisense oligonucleotides are putative therapeutic agents for selective inhibition of gene expression. With the aim to target oligonucleotides to specific compartments within the cell, we investigated the possibility of coupling them to a Lys-Asp-Glu-Leu (KDEL) signal peptide [1]. This C-terminal sequence should be able to convey oligonucleotides to the endoplasmic reticulum (ER) and from there to the cytosol and the nucleus where their targets (mRNAs) are located.

As a step towards this goal, we synthesized peptide-oligonucleotide conjugates. The one-step solid phase synthesis of such hybrids appears unsatisfactory due to side reactions during the coupling and the cleavage steps because of the lack of "universal" protecting groups suitable for such a strategy. Alternatively, such hybrids may be prepared by conjugation of separately synthesized peptide and oligonucleotide moieties, each one being adequately functionalized [2].

Here we describe an alternative post-synthesis conjugation by linking, in a single step, through a thioether bond, an oligonucleotide bearing a thiol group to a N-bromo-acylated peptide, and the influence of the KDEL signal peptide on the intracellular traffic and on the antiviral activity of the conjugate.

Results and Discussion

Several peptide-oligonucleotide conjugates made of phosphodiester oligodeoxy-nucleotide linked to a peptide with a KDEL sequence at its C-terminal end, were synthesized. The phosphodiester oligonucleotides used were either the nonadecamer ($^{5'}$GGCTCCATTTCTTGCTCTC) or the pentacosamer ($^{5'}$CTCTCGCACCCATCT-CTCTCCTTCT), specific for tat_{HIV} and gag_{HIV} genes, respectively. They were substituted at the 3' end by an amino group and at the 5' end by thiol group protected by a thiopyridyl moiety. The use of tris (carboxyethyl) phosphine (TCEP) to reduce the disulfide bond leads to an intermediate oligonucleotide mercaptan and, without any purification step, to the peptide-oligonucleotide conjugate avoiding oligonucleotide dimerization.

The peptide GEEDTSEKDEL, corresponding to the C-terminal sequence of the ER resident luminal protein GRP 78 was synthesized on solid support by Fmoc strategy. It was either N^{α}-substituted by a Cys(Npys) residue or a bromoacetyl-tyrosine residue to get, upon reaction with the oligonucleotide, a conjugate containing a disulfide bridge or a thioether bond, respectively.

The conjugate with a thioether bond was obtained, under nitrogen, by adding the N^{α}-bromoacetyl peptide (5 μmol) to a solution of the oligonucleotide mercaptan (1 μmol) in 1 ml of 0.1 M phosphate buffer pH 7.0, 2 M NaCl. The reaction was complete within 6 h at 40°C. The conjugate with a disulfide bridge was obtained by adding the N^{α}-Cys(Npys)-peptide (2 μmol) into a solution of the oligonucleotide mercaptan (1 μmol) under the same experimental conditions. This compound was used as a control; the disulfide bridge being easily reduced inside the cell. Peptide-oligonucleotide conjugates were characterized by reversed-phase chromatography, amino acid analysis and electrospray mass spectrometry.

The conjugates were labelled with a fluorescent tag, and their uptake and intracellular localization were investigated by confocal microscopy. Both conjugates and peptide-free oligonucleotides enter the cells and were mainly concentrated in vesicles, but their fate was different. By co-incubation experiments at 37°C, the fluorescein-labelled peptide-free oligonucleotide and the rhodamine-labelled peptidyl-oligonucleotide conjugate adopted a different intracellular routing, as they were localized in distinct vesicles. When the incubation temperature was lowered to 15°C, in order to slow down the vesicular trafficking, only the conjugate is co-localized with a fluorescent antibody specific of a protein marker of the intermediate compartment between the ER and the Golgi (ERGIC-53). The presence of oligonucleotide-peptidyl-KDEL conjugates in the ER domain suggests that the KDEL signal sequence is involved in their retrieval from distal Golgi stacks and in their retention in the endoplasmic reticulum.

The antiviral activity of peptide-oligonucleotide conjugates directed against HIV gag gene was assessed on human peripheral blood mononuclear cells infected with HIV-1 and on chronically infected THP-1 cells. The anti-gag conjugate with a thioether bond (IC_{50} = 0.6 μM) was three times more efficient than the corresponding peptide-free oligonucleotide and ten times more efficient than the same conjugate made with a disulfide bridge (IC_{50} > 5 μM). The conjugates did not elicit any toxicity at 10 μM, the highest concentration used.

Acknowledgments

The financial support of the Agence Nationale de Recherche sur le Sida is gratefully acknowledged.

References

1. Munro, S. and Pelham, H.R.B., *Cell*, 48 (1987) 899.
2. Arar, K., Monsigny, M. and Mayer, R., *Tetrahedron Lett.*, 34 (1993) 8087.

Peptides: Chemistry, Structure and Biology
Pravin T.P. Kaumaya and Robert S. Hodges (Eds.)
Mayflower Scientific Ltd., 1996

174
Lipogastrins as Potent Inhibitors of Viral Fusion

R.F. Epand[1], L. Moroder[2], J. Lutz[2], T.D. Flanagan[3], S. Nir[4] and R.M. Epand[1]

[1]*Department of Biochemistry, McMaster University, Hamilton, Ontario L8N 3Z5, Canada*
[2]*Max Plank Institut fur Biochemie, Martinsried, Germany*
[3]*Department of Microbiology, School of Medicine and Biomedical Sciences, State University of New York at Buffalo, Buffalo, NY 14214, USA*
[4]*The Seagram Centre for Soil and Water Sciences, Faculty of Agriculture, The Hebrew University of Jerusalem, Rehovot 76100, Israel*

Introduction

Enveloped viruses must fuse with the plasma membrane for infectivity. A strategy to inhibit the infectivity of these viruses is to block membrane fusion by altering the surface properties of target membranes. Placing hydrophilic groups at the membrane surface, with the use of a natural product lipophosphoglycan, has proven to be an effective strategy for greatly reducing the viral fusion rate constant [1]. The current investigation explores the use of lipopeptides for this purpose.

The lipopeptide we have chosen to study is lipogastrin. The peptide was covalently linked to a diacyl-lipid moiety to form a lipopeptide as has previously been described [2]. The sequence of gastrin-(2-17) is: Gly-Pro-Trp-Leu-Glu-Glu-Glu-Glu-Glu-Ala-Tyr-Gly-Trp-Nle-Asp-Phe-NH_2.

Results and Discussion

We have studied the fusion of Sendai virus to large unilamellar vesicles made of egg phosphatidylethanolamine (PE) with 5 mol %, G_{D1a} with or without the addition of 1.8 mol % of a lipogastrin. The octadecylrhodamine lipid dilution assay [3] was used to monitor the kinetics of viral fusion. The DP-gastrin-(2-17) (DP-g) greatly reduced the rate of fusion. The fusion kinetics were analyzed to separate the rate constants of association and dissociation of the virus with the target membrane, as well as the rate constant for membrane fusion. Addition of 1.8 mol% DP-g reduces the fusion rate constant 3.5-fold without affecting the reversible binding of the virus to the target liposome. There is also a 2-fold decrease in the final extent of fusion, a measure of the fraction of virus that is bound in a manner that can proceed to fusion [4].

We have begun to evaluate the factors contributing to the inhibitory action of DP-g.Lowering of the final extent of fusion is a common feature of anionic amphiphiles [5], of which this lipopeptide is an example. However, negative charge is not the only

factor reducing the extent of Sendai fusion to these liposomes. A lipopeptide with the same lipid anchor but with $(Glu)_5$ replacing the gastrin-(2-17), had no effect on the rate or extent of membrane fusion. This $(Glu)_5$-containing lipopeptide lowers the T_H of dipalmitoleoyl PE. This is in contrast to the DP-g which markedly raises this transition temperature. This stabilization of the lamellar phase by DP-g is a property common to several inhibitors of viral fusion [1, 5, 6]. We have also studied the free gastrin peptide as well as the lipid anchor itself. Neither of these components of DP-g had any viral inhibitory activity. In addition, forms of lipogastrin truncated from the amino terminus had either lower or no inhibitory activity. The truncated gastrins, the free peptide and the lipid anchor, all had weaker effects compared with DP-g in raising T_H. We have also considered the role of steric interference. The greatest steric interference should occur with DP-g. However, we have calculated that the maximal protrusion of this lipopeptide from the membrane surface is only 50 Å, less than half of the 120 Å that the F-protein protrudes from the membrane. Alternatively if the peptide covered the surface of the liposome the cross-sectional surface area of the peptide would be sufficient to cover all of the lipid. However, we believe this arrangement to be unlikely since fluorescence and CD measurements show the DP-g to be devoid of secondary structure and are exposed to an aqueous environment [7]. In addition, the Pro residue and the sequence of five Glu residues would be expected to cause the peptide to protrude more from the membrane surface. Thus lipogastrins provide novel inhibitors of viral fusion whose mechanism is to prevent the membrane bilayer from forming highly curved structures required as intermediates in membrane fusion.

Acknowledgments

The support of the Medical Research Council of Canada is acknowledged.

References

1. Miao, L., Stafford, A., Nir, S., Turco, S.J., Flanagan, T.D. and Epand, R.M., *Biochemistry*, 34 (1995) 4676.
2. Romano, R., Musiol, H.-J., Weyher, E., Dufresne, M. and Moroder, L., *Biopolymers*, 32 (1992) 1545.
3. Hoekstra, D., de Boer, T., Klappe, K. and Wilshut, J., *Biochemistry*, 23 (1984) 5675.
4. Nir, S., Duzgunes, N., Pedroso De Lima, M.C. and Hoekstra, D., *Cell Biophysics*, 17 (1990) 181.
5. Cheetham, J.J., Nir, S., Johnson, E., Flanagan, T.D. and Epand, R.M., *J. Biol. Chem.*, 269 (1994) 5467.
6. Epand, R.M., in Aloia, R.C. and Curtain, C.C. (Eds.), 'Membrane Interactions of HIV: Implications for Pathogenesis and Therapy in AIDS', Wiley-Liss Inc., New York, N.Y., 1992, p.99.
7. Romano, R., Dufrensne, M., Prost, M.-C., Bali, J.-P., Bayerl, T.M. and Moroder, L., *Biochim. Biophys. Acta,* 1145 (1993) 235.

Peptides: Chemistry, Structure and Biology
Pravin T.P. Kaumaya and Robert S. Hodges (Eds.)
Mayflower Scientific Ltd., 1996

175

α-O- or β-N-linked Glycosylation Influences the Conformation and MHC-binding Potency of T-helper Cell Epitopes in a Significantly Different Manner

L. Otvos, Jr., G.I. Szendrei, K.V. Prammer, I. Varga and H.C.J. Ertl

The Wistar Institute, Philadelphia, PA 19104, USA

Introduction

The improved chemical and biological properties of synthetic glycopeptides over unmodified peptides suggest their use as T cell agonists or antagonists [1, 2]. A pre-requisite for both agonist and antagonist activity is that the molecules bind to the MHC proteins and exhibit a longer duration of action than the original antigens. Glycopeptides have been used as immunogens [3, 4]. While class I restricted glycopeptide epitopes appear to retain their ability to bind to the MHC independent of the anomeric configuration of the attached sugars [4], β-N-glycosylated class II epitopes usually lose their MHC-binding ability in an asparagine host location-dependent manner [5-7]. In the current study, we investigated the MHC-binding and T cell-stimulatory activities as well as the conformation of internally α-O- or β-N-glycosylated analogues of two class II restricted rabies virus peptides, VVEDEGCTNLSGF (VF13) and AVYTRIMMNGGR-LKR (31D).

Results and Discussion

In contrast to β-N-glycosylation, coupling of α-linked GalNAc or Gal-GalNAc moieties to the serine or to the threonines present in the two peptides or replacing the Asn residue in the VF13 sequence (this is a natural point mutation in the glycoprotein of some rabies-related viral strains) resulted in epitopes that lowered rather than abolished the MHC-binding and T cell-stimulatory activities (Table 1). α-O-glycosylation was more efficient than β-N-glycosylation in breaking the helical conformation of the peptides resulting in the formation of reverse-turns or unordered structure (Table 1).

We studied the MHC: peptide interactions by molecular modeling, and obtained structural support for the anomeric specificity of MHC binding. While α-O-linked glycopeptides can bind to HLA-DR1 and I-E^k without major alterations in the spatial arrangements and hydrogen bonding pattern of class II: peptide binding, the binding of β-N-linked glycopeptides is considerably less favorable due to steric and columbic conflicts [8]. The strength of the interaction of the MHC:peptide complexes with the T cell receptor depends upon the length and location of the saccharide along the peptide sequence. Application of this approach to other antigenic stimuli offers a good model to

Table 1. *In vitro T cell-stimulatory/MHC-binding ability and conformation of glycosylated class II rabies epitopes.*

Peptide	Amino acid host	Sugar	Anomeric configuration	T cell stimulation/ MHC binding	Structure by CD
31D		-		+++	α-helix
	Asn	GlcNAc or Glc-Glc	β	-	turns
	Thr	Gal-GalNAc	α	++	multiple
VF13		-		+++	loose helix
	Asn	GlcNAc	β	-	turns
	Thr	Gal-GalNAc	α	+	loose turns
	Ser	GalNac	α	++	NA
	Asn→Thr	-	α	++	helix-turn
	Asn→Thr	Gal-GalNAc	α	++	unordered

"dial in" necessary sugar identity, length, and anomeric configuration, and promising amino acid hosts for the successful design of T cell agonist or antagonist glycopeptides.

The ability of some MHC proteins to discriminate between α- and β-linked carbohydrates on epitopes they bind may support two earlier theories. It was proposed that both the MHC proteins [9] and the T cell receptor [10] originated from the glycosyltransferases and may have retained some glycosyltransferase activity. Critical comparisons will be possible when the number of published transferase sequences approaches the number of MHC sequences.

Acknowledgments

This work was supported by NIH grants GM 45011 and AI 27435.

References

1. Otvos, L., Jr., Urge, L., Xiang, Z.Q., Krivulka, G.R., Nagy, L., Szendrei, G.I. and Ertl, H.C.J., *Biochim. Biophys. Acta*, 1224 (1994) 68.
2. Otvos, L., Jr., Krivulka, G.R., Urge, L., Szendrei, G.I., Nagy, L., Xiang, Z.Q. and Ertl, H.C.J., *Biochim. Biophys. Acta*, 1267 (1995) 55.
3. Harding, C.V., Kihlberg, J., Eloffson, M., Magnusson, G. and Unanue, E.R., *J. Immunol.*, 151 (1993) 2419.
4. Haurum, J.S., Arsequell, G., Lellouch, A.C., Wong, S.Y.C., Dwek, R.A., McMichael, A.J. and Elliot, T., *J. Exp. Med.*, 180 (1994) 739.
5. Mouritsen, S., Meldal, M., Christiansen-Brams, I., Elsner, H. and Werdelin, O., *Eur. J. Immunol.*, 24 (1994) 1066.
6. Ishioka, G.Y., Lamont, A.G., Thomson, D., Bulbow, N., Gaeta, F.C.A., Sette, A. and Grey, H.M., *J. Immunol.*, 148 (1992) 2446.
7. Jackson, D.C., Drummer, H.E., Urge, L., Otvos, L., Jr. and Brown, L.E., *Virology*, 199 (1994) 422.
8. Prammer, K.V., Ertl, H.C.J. and Otvos, L., Jr., *Biomed. Pept. Prot. Nucl. Acids*, 1 (1995) 163.
9. Roth, S.Q., *Rev. Biol.*, 60 (1985) 143.
10. Blanden, R.V., Hapel, J. and Jackson, D.C., *Immunochemistry*, 13 (1976) 179.

Peptides: Chemistry, Structure and Biology
Pravin T.P. Kaumaya and Robert S. Hodges (Eds.)
Mayflower Scientific Ltd., 1996

176

Amphipathic Peptide Helices: Structure of a Trichogin A IV Analog Containing Serine, Octanoyl-Aib-Ser-Leu-Aib-Ser-Ser-Leu-Aib-Ser-Ile-LeuOMe

X. Shui[1], D. S. Eggleston[1], V. Monaco[2], F. Formaggio[2], M. Crisma[2] and C. Toniolo[2]

[1]SmithKline Beecham Pharmaceuticals, P.O. Box 1539, UW 2950, King of Prussia, PA 19406, USA
[2]Biopolymer Research Center, C.N.R., Department of Organic Chemistry, University of Padova, 35131 Padova, Italy

Introduction

Trichogin A IV (**1**), one of several linear lipopeptaibol isolated from *Trichoderma* strains [1], is a blocked and modified decapeptide (N-terminus acylated by an octanoyl group; leucinol C-terminus). Members of this peptide class contain a high proportion of glycine residues and display membrane modifying properties. Previous structural studies [1, 2] determined a unique "amphipathic" helical structure with Gly residues on the hydrophilic side. Dimer formation is thought to be resposible for its biological activity. To further examine the helical propensity and to explore biological activity associated with the substitution of glycine residues, we synthesized, crystallized and determined the structure of Trichogin A IV analog (**2**) in which serine replaces all glycine residues.

Results and Discussion

The right-handed, amphipathic helical structure (Figure 1) initiates with two Type III β-turns then transition into an α-helix through Aib 8. An intramolecular hydrogen bond between C=O of Ser 6 and the OH of Ser 9 forms the last 13-membered "alpha" helical ring. Subsequently, the conformation changes into a C_{10} structure which resembles an irregular Type I turn at Aib 8/Ser 9. The molecular conformation finishes in a coiled shape. All peptide bonds are trans; ω values are within ± 8° of 180°. The backbones of **1** and **2** overlay very well in the corresponding α-helical region (torsion angle for both listed in Table 1). Significant differences between the conformation of **2** and of the L-isomer of **1** occur at the beginning two C_{10} structures, where the Type I turns for **1** provide a different twist to the first three residues, in the orientation of the Leu 7 side chain, and along the backbone at the C-terminal Leu-OMe. Molecules are linked head-to-tail through intermolecular hydrogen bonds to form infinite chains parallel to the **b**-axis. Hydrogen bonds with solvent molecules also link the parallel chains. This structure presents a rare view of a truly amphipathic helix to form a hydrophilic channel.

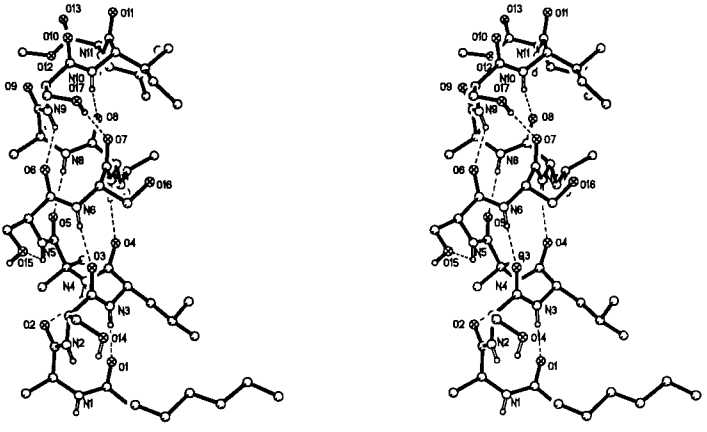

Figure 1. *A stereoview of 2. Only heteroatoms are labeled and, for clarity, only amide hydrogen atoms have been included. Intramolecular hydrogen bonds are illustrated with dashed lines.*

Channels are defined by the juxtaposition of four chains of head-to-tail pairs generated by the crystallographic 2-fold screw along the **b**-axis and translation along the **a**-axis. The Ser residues and the solvent molecules are aligned inside of these channels. This predominantly helical scaffold, which is maintained even in the presence of Gly or Ser will be useful for further modifications designed to probe membrane permeability.

Table 1. *ϕ/ψ and $\chi 1$ torsion angles in the structures of 1 and 2.*

Residue	2	1	
		Molecule A*	Molecule B*
	$\phi/\psi/\chi^{1\dagger}$	$\phi/\psi/\chi^{1\dagger}$	$\phi/\psi/\chi^{1\dagger}$
Aib 1	-54.1/-37.5	-53.2/-36.0	-53.3/-35.8
Ser 2‡	-68.1/-11.2/56.3	-70.3/-7.2	-63.1/11.5
Leu 3	-69.9/-36.4/-58.5	-92.2/-13.9/-68.0	-99.4/-8.5/-60.7
Aib 4	-57.5/-49.4	-53.5/-45.7	-56.0/-48.0
Ser 5‡	-74.8/-35.5/50.1	-69.2/-32.9	-67.2/-33.0
Ser 6‡	-58.0/-47.8/-175.0	-62.0/-46.5	-57.1/-43.5
Leu 7	-58.4/-48.2/-179.2	-65.7/-46.1/-70.4	-65.1/-48.4/-69.9
Aib 8	-57.5/-33.1	-54.3/-43.2	-53.3/-40.5
Ser 9‡	-78.0/-13.3/82.4	-76.0/-25.0	-73.8/-17.9
Ile 10	-94.7/-51.1/-60.0	-90.6/-32.1/72.8	-96.6/-39.6/-67.3
LeuOMe§,¶	-95.7/-41.4/-59.6	-107.0/45.1/-56.3	-100.3/68.1/-58.4

* Values given are for the molecule containing L-residues; †Estimated standard deviations are less than 1.0°; ‡ Gly for **1** ; § Leuol for **1**; ¶ For **2** ϕ is C'-N-Cα-C' and ψ is N-Cα-C'-O while for **1** ϕ is C'-N-Cα-CH_2 and ψ is N-Cα-CH_2-O.

References

1. Auvin-Guette, C., Rebuffat, S., Prigent, Y. and Bodo, B., *J. Am. Chem. Soc.*, 114 (1992) 2170.
2. Toniolo, C., Peggion, C., Crisma, M., Formaggio, F., Shui, X. Q. and Eggleston, D.S., *Nature Struct. Biol.*, 1 (1994) 908.

Peptides: Chemistry, Structure and Biology
Pravin T.P. Kaumaya and Robert S. Hodges (Eds.)
Mayflower Scientific Ltd., 1996

177

The Conformational Properties of Glycopeptide Enkephalin Analogues in Solution Determined by NMR and Molecular Modeling

B. Lou, L. Szabó, M.D. Shenderovich, R. Polt and V.J. Hruby

Department of Chemistry, University of Arizona, Tucson, AZ 85721, USA

Introduction

High resolution NMR methods can yield peptide conformational information for peptides that may be applied to rational drug design [1]. Conformational analysis requires the availability of NMR parameters such as chemical shifts, coupling constants, nuclear Overhauser enhancements (NOEs), and temperature dependency of amide proton chemical shifts. Of particular interest is the glycopeptide enkephalin analogue (LSZ 1025) sequence:

Tyr-D-Cys-Gly-Phe-D-Cys-Ser(-β-O-Glucp)-Gly-NH_2

This produces long acting analgesia following intraperitoneal administration in mice, and shows evidence for penetration of the blood-brain barrier [2]. Its solution conformation was examined by a combined approach including NMR measurements (TOCSY and ROESY) in DMSO, molecular modeling, and molecular dynamic (MD) simulations.

Results and Discussion

NOEs between the NH of Phe^4 and D-Cys^5, $^3J_{N\alpha}$ coupling constant for Phe^4, and low temperature coefficients (<1 ppb/K) for the amide proton of D-Cys^5 indicate that a β turn is formed around residues D-Cys^2-Gly^3-Phe^4-D-Cys^5. Rotamer populations calculated from $J_{\alpha\beta}$ coupling constants shows that the side chain of Phe^4 strongly prefers the *gauche(-)* rotamer, while the side chains of D-Cys^4 and Ser^6 favor the *gauche(+)* rotamer. A total of 9 restraints deduced from NOE and coupling constants were incorporated into molecular modeling studies. A sample of 20 energy-minimized MD structures (Figure 1) shows that the Tyr^1 and Phe^4 aromatic rings and the one sugar group are pointed in three different directions. In addition, the variations of ϕ,ψ dihedral angles observed during the MD simulations reveal that the peptide backbone of residues from D-Cys^2 to Phe^4 is well constrained, while the C-terminal residues from D-Cys^5 to Gly^7 are quite flexible. Distributions of ϕ,ψ angles in the Ramanchandran plots (Figure 2) confirm that most of the MD conformers of the glycopeptide contain a Type II' β-turn, with (ϕ,ψ) dihedral angles for the i+1 position (Gly^3) around (60, -120) and for the i+2 position (Phe^4) around (-80, 0).

Figure 1. *Superimposed of 20 structures of LSZ1025 from 100 ps MD simulations.*

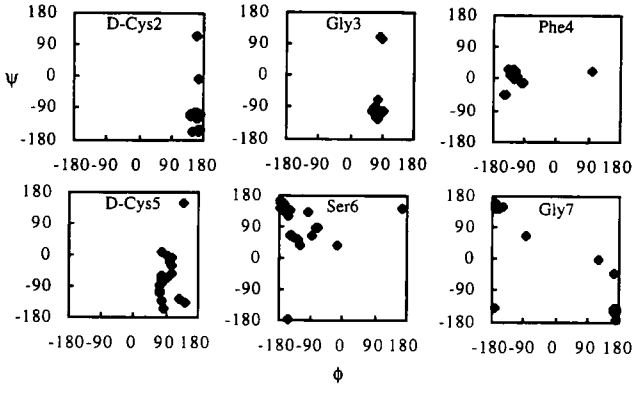

Figure 2. *Ramanchandran plot (ϕ, ψ) of LSZ1025 obtained from 100 ps MD simulations.*

The conformation of the 14-membered ring of the glycopeptide generally is similar to that found in the crystal structure of DPDPE (RMS of 0.4 Å for the lowest-energy conformation). The studies of glycopeptides with different sugar groups indicate strong similarity among conformations of their peptide moieties. Our study suggests that the sugar moiety does not influence the binding conformation of cyclic enkephalin glycopeptide analogues. This is shown by receptor binding and bioassay data on a series of the glycopeptides. The effect *in vivo* are different, however, which may be explained by differences in transport rates, stability, and clearance rates.

Acknowledgments

We thank the National Institute on Drug Abuse (DA06284), the National Science Foundation (CHE-9201112), and the Arizona Disease Control Research Commission for support of this work.

References

1. Fesik, S.W., *J. Med. Chem.*, 34 (1991) 2937.
2. Polt, R., Porreca, F., Szabo, L., Bilsky, E.J., Davis, P., Abbruscato, T.J., Davis, T.P., Horvath,R., Yamamura, H.I. and Hruby, V.J., *Proc. Nat. Acad. Sci. USA*, 91 (1994) 7114.

Peptides: Chemistry, Structure and Biology
Pravin T.P. Kaumaya and Robert S. Hodges (Eds.)
Mayflower Scientific Ltd., 1996

178
Development of a Direct Quantitative Method for N^G-Phosphoarginine Determination in Proteins

H. Kodama[1], K. Owaki[1], M. Kondo[1], F. Yokoi[2] and A. Kumon[2]

[1]Department of Chemistry, Faculty of Science and Engineering, Saga University, Saga 840, Japan
[2]Department of Biochemistry, Saga Medical School, Saga 849, Japan

Introduction

The function of O-phosphorylation on Ser, Thr and Tyr residues play an important role in intracellular signaling systems [1]. On the other hand, though the presence of controlling enzymes is known, the role of intracellular N-phosphorylation in signaling processes is not yet clear. Among the N-phosphorylated amino acids, phosphoarginine (P-Arg, Figure 1) has been considered to possess important functions. Recently, the phosphatase of P-Arg has been identified [2-4]. It has been shown that phosphorylating and dephosphorylating actions of basic amino acids also participate in the functional adjustment of enzymes *in vivo*. Therefore, developing a method for determination of P-Arg has been required. Until now, inorganic phosphate determination (malachite green method) [5] has been used for the detection of P-Arg. However, confusion due to the presence of other phosphorylated amino acids could limit the use of this method, as it is not able to specifically distinguish different kinds of phosphoamino acids contained in proteins. In the present study, we attempted to develop a method that can selectively determine the phosphorylated arginine residues.

Results and Discussion

Our method proceeds through modification of the dephosphorylated free arginine for the purpose of direct determination of its phosphorylated form. A way to do this is to use a modification reagent that is specific for the guanidino group of the arginine side-chain. An essential condition for modification reagents in the present method is that because the N-P bond of arginine side-chain is labile under acidic conditions, the modification reaction must be carried out in neutral or alkaline environments where the N-P bond is stable. Moreover, it is required for the modification to be irreversible, and arginine should not be regenerated under the procedures that follow. As a result, the use of 1,2-cyclohexanedione (CHD) [6], which satisfies these restrictions, is recommended.

When a protein, containing both the phosphorylated arginine (P-Arg) and free arginine (Arg) residues, is reacted with CHD, Arg residues are converted to N^7,N^8-(1,2-dihydroxycyclohex-1,2-ylene)-arginine (DHCH-Arg, Figure 1). Furthermore, the addition of boric acid to the mixture forms a stable complex of DHCH-Arg-borate in this procedure.

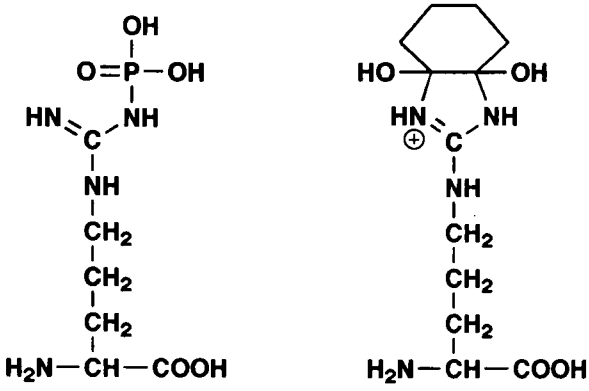

Figure 1. *Structures of phosphoarginine and DHCH-Arg.*

Under the above-mentioned conditions, phosphorylated Arg is not modified by the reagent or converted to any other compounds. The mixtures are then hydrolyzed under acidic conditions. In this treatment, P-Arg residues are converted to free Arg. However, the DHCH-Arg-borate complex results in unknown products [6]. In this manner, the Arg derived from P-Arg hydrolysis was allowed to react with phenylisothiocyanate, and determined by phenylthiocarbamyl (PTC) amino acid analysis [7]. The amount of P-Arg in the protein is determined as the detected PTC-Arg peak. P-Arg content of the analyzed samples showed a reasonable agreement with the calculated values.

Furthermore, we applied this quantitative method to model peptides containing P-Arg and O-phosphothreonine (P-Thr) residues. These peptides were treated with alkaline phosphatase [4], which hydrolyzes both O-P and N-P bonds. The P-Arg content was selectively determined by the above-mentioned method, and the decrease of phosphoarginine was observed in a time-course manner. The presence of P-Thr did not affect the analysis of P-Arg. As a result, an effective method for the selective quantitation of phosphorylated-Arg has been developed.

In conclusion, in the present study, it was confirmed that the specific determination of P-Arg by using CHD-PTC method was useful for investigation of enzymes participating in the functional adjustment *in vivo*.

References

1. Krebs, E.G., *Angew. Chem. Int. Ed. Engl.*, 32 (1993) 1122.
2. Kuba, M., Ohmori, H. and Kumon, A., *Eur. J. Biochem.*, 208 (1992) 747.
3. Yokoyama, K., Ohmori, H. and Kumon, A., *J. Biochem.*, 113 (1993) 236.
4. Nishino, M., Tsujima, S., Kuba, M. and Kumon, A., *Archiv. Biochem. Biophys.*, 312 (1994) 101.
5. Lanzetta, P. A., Alvarez, L. J., Reinach, P. S. and Candia, O. A., *Anal. Biochem.*, 100 (1979) 95; Kallner, A., *Clin. Chim. Acta*, 59 (1975) 35.
6. Patthy, L. and Smith, E.L., *J. Biol. Chem.*, 250 (1975) 557.
7. Bidlingmeyer, B.A., Cohen, S.A. and Tarvin, T.L., *J. Chromatography*, 336 (1984) 93.

Peptides: Chemistry, Structure and Biology
Pravin T.P. Kaumaya and Robert S. Hodges (Eds.)
Mayflower Scientific Ltd., 1996

179

Development of a Practical Synthetic Methodology Using Dimethylphosphono Amino Acid for Phosphopeptides

A. Otaka[1], K. Miyoshi[1], H. Tamamura[1], P.P. Roller[2], T.R. Burke Jr.[2] and Nobutaka Fujii[1]

[1]*Faculty of Pharmaceutical Sciences, Kyoto University, Sakyo-ku, Kyoto 606, Japan*
[2]*Laboratory of Medicinal Chemistry, NCI, NIH, Bethesda, MD 20892, USA*

Introduction

Phosphopeptides have received much attention as important biochemical tools to elucidate signal transduction pathways [1] and have been the object of intense synthetic activity [2]. Disadvantages of methods reported to date include lack of general applicability, the need for complicated manipulations and side reactions owing to harsh acid deprotection. Our recent studies on nonhydrolyzable phosphopeptide mimetics [3], have stimulated us to develop a practical synthetic method for the preparation of biologically important phosphopeptides. This involves a combination of dimethyl-protected phosphoamino acids **1-3** and a two step deprotection protocol.

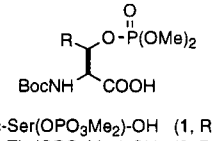

Boc-Ser(OPO_3Me_2)-OH (**1**, R = H)
Boc-Thr(OPO_3Me_2)-OH (**2**, R = Me)

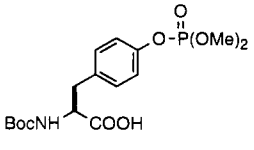

Boc-Tyr(OPO_3Me_2)-OH (**3**)

Results and Discussion

To evaluate acidic reagent systems for the final deprotection of dimethyl-protected phosphoamino acid-containing peptide resins, three model peptide resins [Boc-Arg(Mts)-Arg(Mts)-Val-Ser(OPO_3Me_2)-Val-Ala-Ala-Glu(OBzl)-Merrifield resin **4**, Boc-Lys(ClZ)-Arg(Mts)-Thr(OPO_3Me_2)-Leu-Arg(Mts)-Arg(Mts)-Leu-Leu-PAM resin **5** and Boc-Thr(Bzl)-Glu(OBzl)-Pro-Gln-Tyr(OPO_3Me_2)-Gln-Pro-Gly-Glu(OBzl)-Merrifield resin **6**] were used. Previously, we reported that the Me groups on a pSer residue were efficiently removed by two-step deprotection consisting of high acidic and low acidic treatments [4]. Thus, we first established the reaction conditions of the first-deprotection step [1 M trimethylsilyl trifluoromethanesulfonate (TMSOTf)-thioanisole in TFA, *m*-cresol, ethane dithiol (EDT)] needed to cleave the peptides from the resins (**4**, **5** and **6**) with concomitant removal of the Mts, ClZ and Bzl groups. After treating **4**, **5** and **6** with the first-step reagent, composite additives [dimethyl sulfide (DMS) + TMSOTf] were added in different ratios and deprotection monitored by HPLC-analyses of the crude deprotected

peptides. Optimized deprotection conditions for dimethyl-protected phosphoamino acid-containing peptide resins were established to be a combination of the first-step reagent [1 M TMSOTf-thioanisole in TFA (100), *m*-cresol (5), EDT (5), (v/v)] and the second-step reagent [First-step reagent (110) + DMS/TMSOTf (30:20 ~ 40:10), (v/v)]. Using this methodology, we achieved the synthesis of a 19-residue MAP-kinase peptide possessing two phosphoamino acid (pThr and pTyr) and also Met and Trp (Figure 1).

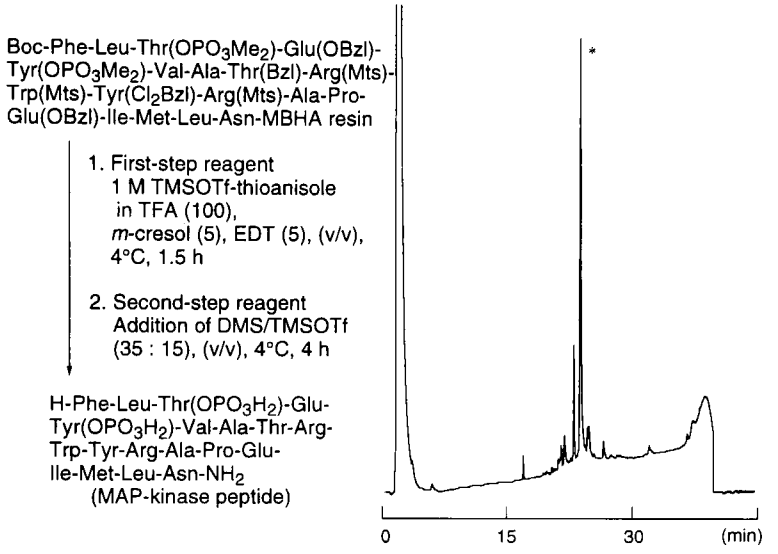

Figure 1. *Two-step deprotection for the synthesis of MAP-kinase peptide (* desired peptide).*

The use of dimethyl-protected phosphoamino acid derivatives in conjunction with two-step deprotection protocols involving the combination of high acidic and low acidic deprotection provides an efficient general procedure for phosphopeptides synthesis. The method uses commercially available dimethylphosphono amino acid derivatives, compatible with standard Boc-based solid-phase techniques, and one-pot deprotection with an appropriately modified TMSOTf deprotection system. It enables the synthesis of phosphopeptides in a manner similar to that used for non-modified peptides.

References

1. Johnson, G.L. and Vaillancourt, R.R., *Curr. Opin. Cell Biol.*, 6 (1994) 230.
2. Shapiro, G., Swoboda, R. and Stauss, U., *Tetrahedron Lett.*, 35 (1994) 869; Kitas, E.A., Perich, J.W., Tregear, G.W. and Johns, R.B., *J. Org. Chem.*, 55 (1990) 4181; Lee. E-.S. and Cushman, M., *J. Org. Chem.*, 59 (1994) 2086.
3. Burke, T.R. Jr., Smyth, M.S., Otaka, A. and Roller, P.P., *Tetrahedron Lett.*, 34 (1993) 4125; Otaka, A., Miyoshi, K., Burke, T.R. Jr., Roller, P.P., Kubota, H., Tamamura, H. and Fujii, N., *Tetrahedron Lett.*, 36 (1995) 927.
4. Otaka, A., Miyoshi, K., Roller, P.P., Burke, T.R. Jr., Tamamura, H. and Fujii, N., *J. Chem. Soc., Chem. Commun.*, (1995) 387.

Peptides: Chemistry, Structure and Biology
Pravin T.P. Kaumaya and Robert S. Hodges (Eds.)
Mayflower Scientific Ltd., 1996

180
Mapping Distances Between SH2 Domains of PI3-Kinase *via* Peptide Binding

D.H. Singleton[1], G.C. Andrews[1], L.G. Contillo[1], J.P. Gardner[1], E.M. Gibbs[1] and J.J. Herbst[2]

[1]Pfizer Central Research, Groton, CT 06340, USA
[2]Dartmouth Medical School, Hanover, NH 03755, USA

Introduction

The β subunit of the PDGF receptor associates with and activates PI3-Kinase through the 85 kDa (p85) subunit's two src-homology (SH2) domains when Tyr^{740} and Tyr^{751} are phosphorylated (Y*) [1,2]. Peptides with two tethered phosphotyrosines bind with high affinity (1nm) and activate PI3-K at similar concentrations [1].

This study defines distances between the two SH2 domains of p85 by exploiting a 500 fold difference in mono *versus* bidentate binding affinities as measured by surface plasmon resonance analysis.

Results and Discussion

Synthetic peptides were constructed with the basic p85 SH2 binding probe using Y*ZPZ, where Z = norleucine. Based on the spacing between Tyr^{740} and Tyr^{741} of the PDGF-r, a series of peptides with gly-ser linkers separating the Y*ZPZ motifs were synthesized (1-5). The sequence containing 12 amino acids between phosphotyrosine residues (5) is shown to bind to and stimulate PI3-K at 5nm. Removal of intradomain serine-glycine pairs by shortening the sequence to six or five intervening amino acids (3, 4) afforded a slight increase in PI3-K binding. This peptide (3), was of optimal separation revealing a minimum distance for bidentate phosphotyrosine binding. Truncation by an additional residue (2) resulted in affinity between that of mono and bidentate. Decreasing the spacing with the two Y*ZPZ motifs juxtaposed (1) hinders binding.

The systematic truncation and replacement by glycines attempted a determination of a minimum required distance between phosphorylated tyrosines. Although the loss of binding energies of the +1, +2 and +3 amino acids gave intermediary levels of binding (6), this exceeded monodenate binding by allowing the amino-terminal phosphotyrosine to reach its binding pocket. By deletion of amino acids (7-10) intermediate binding is maintained with a sub-optimal fit of the second phosphotyrosine, until a minimum spacing of one amino acid was reached. This peptide (11) no longer allows the amino-terminal phosphotyrosine to occupy the second binding site affording mono-dentate binding.

The relative contribution to binding of amino or carboxy Y*ZPZ motifs was elucidated. Peptide 5, in a singly phosphorylated version (15, 16) bound with equivalent ED 50 of 10,000nm. Clearly, neither phosphotyrosine contributes more binding energy than the other. Peptide 3 was modified in positions +1, +2 and +3 to the phospho tyrosines with glycine substitution (6,13). These data suggest the carboxy-terminal ZPZ motif contributes 10 fold more binding energy than does the amino-terminal counterpart.

The interdomain distance between the +3 position and the phosphotyrosine is indicated to be 6A, as displayed by peptide 3. The distance between phosphotyrosine binding pockets is 16 A. It remains unclear as to which peptide Y*ZPZ motif binds to which protein SH2 domain binding pocket. The possibility exists that the peptide carboxy-terminal Y*ZPZ motif emulates Tyr^{751} (not Tyr^{740}) of the PDGF receptor.

Table 1.

Cpd	Sequence	ED50 (nm)	MW(calc)	MW(obs)
1	Ac-Y*ZPZY*ZPZS-CONH2	2,000	1,279.3	1,279.6
2	Ac-Y*ZPZSY*ZPZS-CONH2	120	1,366.4	1,366.1
3	Ac-Y*ZPZSSY*ZPZS-CONH2	1	1,453.5	1,453.2
4	Ac-Y*ZPZSGSY*ZPZS-CONH2	2	1,510.6	1,510.2
5	Ac-Y*ZPZS$(GS)_4$Y*ZPZS-CONH2	5	1,942.9	1,942.6
6	Ac-Y*$(G)_5$Y*ZPZS-CONH2	140	1,241.2	1242.3(MH+)
7	Ac-Y*$(G)_4$Y*ZPZS-CONH2	400	1,184.1	1,184
8	Ac-Y*GPGGY*ZPZS-CONH2	160	1,224.2	1,223.7
9	Ac-Y*GGGY*ZPZS-CONH2	170	1,127.1	1,127
10	Ac-Y*GGY*ZPZS-CONH2	200	1,070	1071.3(MH+)
11	Ac-Y*GY*ZPZS-CONH2	800	1,013	1014.2(MH+)
12	Ac-Y*ZPZSY*GGGG-CONH2	5,000	1,184.1	1185.0(MH+)
13	Ac-Y*ZPZSSY*GGGG-CONH2	1,100	1,271.2	1,271
14	Ac-Y*ZPZS-CONH2	1,200	710.7	710.8
15	Ac-Y*ZPZS$(GS)_4$YZPZS-CONH2	10,000	1,862.9	1,862.5
16	Ac-YZPZS$(GS)_4$Y*ZPZS-CONH2	10,000	1,862.9	1863.6(MH+)

Acknowledgments

The authors thank Dr. Justin Stroh and Mr. Kenneth Rosnack for Electrospray Mass Spectrometry molecular weight determinations.

References

1. Kashishian, A., Kazlauskas, A., Cooper, J.A., *EMBO J.*, 11 (1992) 1373.
2. Rordorf-Kikolic, T.R., Van Horn, D.J., Chen, D., White, M.F., Backer, J.M., *J. Biol. Chem.*, 270, (1995) 3662.

Peptides: Chemistry, Structure and Biology
Pravin T.P. Kaumaya and Robert S. Hodges (Eds.)
Mayflower Scientific Ltd., 1996

181
Positional and Sequence-dependent Problems in the Synthesis of Biotinylated Phosphotyrosine Peptides

S.F. Conrad[4] and P.T.P. Kaumaya[1,2,3,4]

Departments of [1]Obstetrics and Gynecology, [2]Microbiology and [3]Medical Biochemistry and the [4]Comprehensive Cancer Center,
The Ohio State University, Columbus, OH 43210, USA

Introduction

The synthesis of phosphotyrosine-containing peptides is problematic, particularly if the peptides are large or contain multiple phosphotyrosine residues. Several procedures have been used for the synthesis of peptides containing phosphotyrosine. First, the phosphotyrosine residue may be incorporated as a protected phosphate ester, such as the dimethyl or dibenzyl phosphate derivative. However, during Fmoc synthesis, monodemethylation and monodebenzylation occurs during Fmoc blocking group removal by piperidine. Significant loss of the phosphate group during the synthesis and/or cleavage reactions occurs when Fmoc-TyrP(dibenzyl) is used [1]. The alternate use of Fmoc-TyrP(di-*t*-butyl) [2] is precluded because of the difficulty in its synthesis [3]. Fmoc-TyrP(dimethylphenylsilyl) ethyl, which is stable to piperidine treatment [4], is readily removed by TFA, thus making this derivative attractive for synthesis of phosphotyrosine-containing peptides. An alternative strategy is the "post-assembly" approach, where tyrosine is incorporated as the unprotected side-chain derivative which can then be phosphorylated post-synthesis.

In this report, we opted to use a third synthetic approach that involves incorporation of phosphotyrosine by use of unprotected Fmoc-TyrP derivative to synthesize a series of four synthetic peptides (Figure 1). A 27 residue sequence from a tyrosine kinase receptor was selected for two reasons: 1) to investigate the positional and sequential dependent problems in the synthesis of phosphotyrosine peptides, and 2) for use as an affinity ligand for purification and analysis of protein kinases.

Results and Discussion

Using the BOP/HOBt/NMM protocol synthetic peptides P1-P4 (Figure 1) were synthesized and the products after HPLC purification were analyzed by capillary electrophoresis and mass spectrometry. The synthesis of P1 (no phosphotyrosine) was straightforward and the major product (MW 3169) was obtained in high yield. On the other hand, the synthesis of P2 with a single phosphotyrosine (MW 3249) near the amino terminus resulted in low yield (10%) after HPLC purification with the major product being a deletion peptide lacking the TyrP (MW 3005). Similarly, P3 with a single phosphotyrosine near the carboxy terminus was obtained in low yield (MW 3248) with

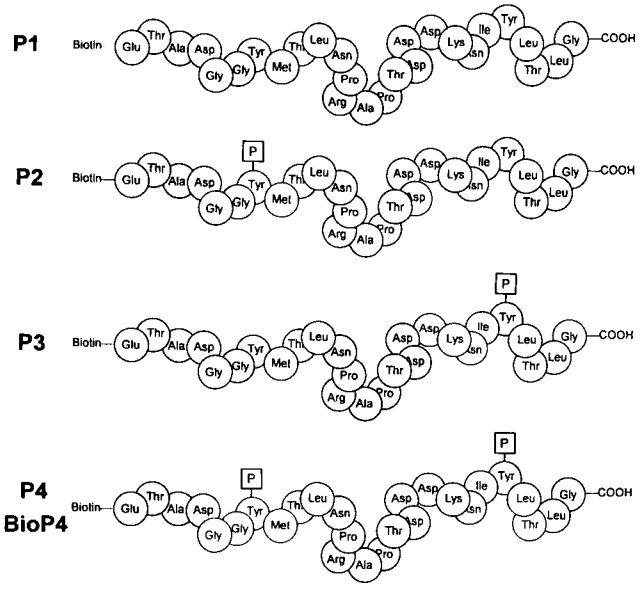

Figure 1. *Schematic representation of the P1, P2, P3, P4 and BioP4 peptide constructs.*

the major product (MW 3005) being the TyrP deletion and no measurable product was obtained after HPLC purification. The synthesis of P4 (2 phosphotyrosine) resulted in a complex mixture of all possible combinations. HPLC purification and mass spectral determination of the mixtures indicated that incorporation of the carboxyl-terminal Fmoc Tyr P was exceptionally low.

Using the BOP/HOBt/DIEA protocol, extensive monitoring of individual steps and repeated couplings of certain residues, we were able to synthesize the correct peptide in a reasonable yield. Mass spectral data depending on the number of phosphotyrosine in the peptide indicate that in every case an adduct consisting of either the MW + 135 or MW + 270. We hypothesize that this stable adduct is an addition of HOBT. Further studies are underway to clarify this problem.

References

1. Kitas, E.A., Wade, J.D., Johns, R.B., Perich, J.W. and Tregear, G.W., *J. Chem. Soc., Chem. Commun.*, (1991) 338.
2. Perich, J.W., Ruzzene, M., Pinna, L.A. and Reynolds, E.C., *Intl. J. Peptide Protein Res.*, 43 (1994) 39.
3. Perich, J.W. and Reynolds, E.C., *Intl. J. Peptide Protein Res.*, 37 (1991) 572.
4. Chao, H.G., Bernatowicz, M.S., Reiss and P.D., Matsueda, G.R., *J. Org. Chem.* 59 (1994) 6687.

Peptides: Chemistry, Structure and Biology
Pravin T.P. Kaumaya and Robert S. Hodges (Eds.)
Mayflower Scientific Ltd., 1996

182
Effects of Glycosylation of a Peptide Epitope from HTLV-1 gp46 on Structure and Immunogenicity

S.F. Conrad[1], I.L. Byeon[4], A.M. DiGeorge[2], M.D. Lairmore[1,3], M.Tsai[4] and P.T.P. Kaumaya[1,2]

[1]Comprehensive Cancer Center, [2]Department of Obstetrics and Gynecology, [3]Department of Pathobiology and [4]Department of Chemistry, The Ohio State University,Columbus, OH 43210, USA

Introduction

The env gene product of the human retrovirus HTLV-1 plays an important role in infection and is involved in the production of neutralizing antibodies. The 68 kD precursor glycoprotein contains N-linked glycosyl moieties at five sites, four of which are found in the gp46 and one in gp21 products. A requirement for the presence of carbohydrate in group-specific neutralization has been demonstrated for several retroviral systems. It has been shown that removal of glycosylation sites directly affects syncytium formation. Thus, N-glycosylation may be involved in modulating neutralizing antibody responses by directing the immune response towards selected epitopes.

The effects of N-glycosylation on stabilization of peptide structure and in modulating antibody responses remain to be fully elucidated. However, recent studies indicate that addition of glycosyl moieties to Asn residues tends to promote β-turn formation and stabilization [1]. As part of our ongoing studies of stabilization of peptide epitopes into immunogenic constructs, we investigated the 233-253 sequence of HTLV-1 gp46 which contains a carbohydrate moiety at Asn244. Epitope 242-257, of gp46 is recognized by sera from HTLV-1$^+$ individuals, and harbors a conformational determinant. Antibodies to 242-257 recognized native gp46 but did not inhibit syncytium formation and did not protect rabbits against infection with the HTLV-1 virus. The goals of this study were: 1) to synthesize and to characterize the 233-253 peptide with and without a sugar residue at the Asn 244 site. 2) To determine the solution conformation of the peptide and glycopeptide using two-dimensional NMR and 3) To investigate the antibody response to both the peptide and glycopeptide.

Results and Discussion

Peptide and Glycopeptide Engineering and Characterization. The 233-253 sequence was selected to incorporate a single glycosyslated residue (244), with one β-turn structure near the middle of the peptide. A "promiscuous" T cell epitope from measles virus (MVF) was incorporated into the SC1MVF and SC2MVF immunogens for raising antibodies.

The CD spectra of SC1 and SC2 indicate the presence of β-turn conformation as shown by the weak minima ($[\theta]_{M,\lambda}$ approximately -800·deg cm^2/dmol) at 200 nm. The CD spectra of SC1MVF and SC2MVF in aqueous solution are similar to the SC1 and SC2 constructs. Complete ^{1}H NMR assignments of SC1 and SC2 were obtained using standard two-dimensional methods. There are significant changes in the chemical shifts of protons in the β-turn region, residues 9-13, between the glycosylated and the non-glycosylated construct. The GLcNAc residue on Asn12 caused the most perturbation in the amide proton of the adjacent Val13 residue. Sequential and medium-range NOEs observed for SC1 and SC2 indicate that both peptides exist in extended chain conformations with a β-turn configuration around Asn12. A small ensemble of peptides may be adopting a helical or turn structure in the Thr4-Val7 segment.

Immune Response to the Various Constructs. Human sera from HTLV-I infected individuals reacted to a slightly greater extent with SC2MVF than SC1MVF but there was no significant difference between reactivity with SC1 *vs.* SC2. Reactivity towards the chimeras was substantially higher than to the individual epitopes, indicating stabilization of the peptide conformation within the chimeric construct.

Table 1. *Summary of immune responses in rabbits to SC1MVF and SC2MVF.*

Assay	SC1MVF Immunogen		SC2MVF Immunogen	
Titer	Rabbit 1	Rabbit 2	Rabbit 1	Rabbit 2
vs. SC1MVF	>128,000	64,000	128,000	128,000
vs. SC2MVF	>128,000	64,000	64,000	64,000
vs. SC1	>128,000	64,000	64,000	64,000
vs. SC2	>128,000	64,000	64,000	128,000
RIPA	negative	positive	positive	positive
whole virus ELISA	0.20	1.34	0.85	0.85

Titers are for secondary + two week sera and are expressed as the antibody dilution at which the absorbance reading is 0.2 units above background. Results for the whole virus ELISA for 1:40 dilution of antisera and are adjusted for background absorbances for pre-immune sera. Positive reaction in the radioimmunoprecipitation assay (RIPA) indicates binding of antiserum to gp46 of viral lysate (labeled with [^{35}S]methionine) as determined by autoradiography of SDS-PAGE gels.

Antibodies in rabbits against each chimera showed significant titers as early as primary + three weeks, with very high titers exhibited in the tertiary response (Table 1). The anti-SC1MVF antibodies recognized SC1MVF, SC1 and the SC2-containing peptides, but not the MVF sequence. Likewise, the anti-SC2MVF antibodies cross-reacted with the SC1-containing constructs. Rabbits immunized with SC1MVF and SC2MVF rabbit sera exhibited strong response in whole virus ELISA and RIPA in this assay (Table 1).

References

1. I. Laczko, M. Hollosi, L. Urge, K.E. Ugen, D.B. Weiner, H.H. Mantsch, J. Thurin, L. Otvos, Jr., *Biochemistry*, 31 (1992) 4282.
2. A. Perczel, E. Kollat, M. Hollosi, G.D. Fasman, *Biopolymers*, 33 (1993) 665.

Peptides: Chemistry, Structure and Biology
Pravin T.P. Kaumaya and Robert S. Hodges (Eds.)
Mayflower Scientific Ltd., 1996

183
Intramolecular Crosslinking by Pentosidine: Model Studies of the Maillard Reaction of Arg-Lys with D-Glucose, D-Fructose or D-Ribose

Y. Al-Abed and R. Bucala

The Picower Institute for Medical Research, 350 Community Dr., Manhasset, NY 11030, USA

Introduction

Advanced glycosylation endproducts (AGEs) have been linked to the development of many of the long-term complications of diabetes, renal insufficiency, and normal aging [1, 2]. The formation of these products follows many of the principles of the Maillard reaction and begins with the non-enzymatic addition of reducing sugars such as glucose to the primary amino groups of macromolecules [3]. These "early" Schiff base and Amadori adducts then slowly undergo a series of rearrangement, dehydration, and oxidation-reduction reactions to produce the "late" products termed AGEs. AGEs crosslink amino groups and are sufficiently stable to persist for the life of the affected macromolecule [2, 3]. Although the structures of the most abundant AGEs which occur *in vivo* are unknown, Monnier *et al.* recently isolated the fluorescent crosslink pentosidine from human dura collagen [4]. Pentosidine appears to form as the condensation product of lysine, arginine, and a reducing sugar precursor. *In vitro*, pentosidine may be readily produced upon incubation of Nα-protected derivatives of arginine, lysine, and sugars such as ribose, glucose, fructose, ascorbate and dehydroascorbate [5].

Results and Discussion

Measurements of pentosidine content in a variety of biological specimens have revealed that this bi-functional condensation product accounts for only a small percentage (<1%) of potential glucose-derived crosslinks [6]. Furthermore, when bovine serum albumin (BSA), which contains 59 lysine and 23 arginine residues, is incubated with D-glucose in phosphate buffer, pentosidine forms in a yield of only 1 mmol/mol protein. It also has been noted that while many proteins such as ovalbumin and BSA can undergo a high degree of modification or "impairment" of lysine and arginine residues during advanced glycosylation, protein oligomerization rarely ensues. These observations prompted us to examine the contribution of intra molecular crosslinking to the formation of pentosidine in model systems *in vitro*. We noted that the amino acid sequence of BSA contains an arg-lys (RK) sequence at positions 411 and 412 which, on the basis of kinetic considerations, might serve as a highly reactive site for intramolecular pentosidine formation.

We first incubated the dipeptide arg-lys (RK) at 70°C with two equivalents of D-ribose, D-glucose or D-fructose in phosphate buffer for 48 h. HPLC analysis with UV (λ_{max} 320 nm) detection revealed, in each case, a major peak with an identical elution time. The characteristic UV spectrum (λ_{max} 320 nm) of pentosidine was evident. MS spectra (m/z 361) and ^{1}H-NMR spectra confirmed the structure of a pentosidine-RK condensation product. Other peaks present in low concentrations were assigned the structure of a pentosidine moiety linking two RK molecules (intermolecular crosslinks).

In a second model study, the α-amino group of RK was protected in order to study the reactivity of the R and K side chains in a domain more closely resembling that of a native protein. The incubation of Nα-CBZ-RK with two equivalents of D-ribose in 0.2 M phosphate buffer (pH 7.4) for three weeks at 37 °C yielded pentosidine as a major fluorescent compound in 4.5% yield. Separation and purification of this compound was carried out by reversed phase HPLC. The ^{1}H-NMR spectrum of the compound revealed, beside the protons of the starting material, three protons which resonate as an ABX system at δ = 7.85 (d, J = 6.4 Hz), 7.67 (d, J = 7.4 Hz) and 7.15 (bdd, J = 7.2, 6.9 Hz), and which are consistent with the pentosidine structure. The electron spray (ES) mass spectrum showed a molecular ion at 495 (M) which is consistent with the molecular formular $C_{25}H_{31}N_6O_5$ (hrFAB 495.2482, calc. 495.2356) and the stucture shown below.

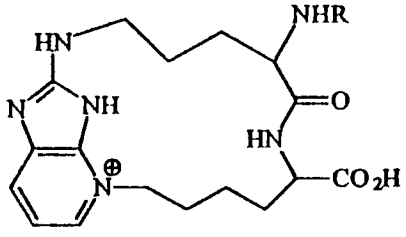

R = H or CBZ

A similar mechanism may account for the formation of pentosidine from D-glucose, which first undergoes oxidative cleavage in the Maillard reaction to arabinose. As expected, incubation of RK with glucose under antioxidative condition (EDTA, N_2) failed to show any pentosidine formation even after 4 weeks incubation at 37°C.

These model studies support the high reactivity of dibasic amino acid systems toward Maillard reactants and suggest a potentially active competition between intra- and intermolecular crosslink formation *in vivo*. These data also may account for the low frequency of pentosidine formation in certain protein substrates.

References

1. Bucala, R., Cerami, A., *Adv. Pharmacol.*, 23 (1992) 1.
2. Njoroge, F.G., Monnier, V.M., *Prog. Clin. Biol. Res.*, 304 (1989) 85.
3. Ledl, F., Schleicher, E., *Angew. Chem. Int. Ed. Engl.*, 29 (1990) 565.
4. Sell, D.R. and Monnier, V.M., *J. Biol. Chem.*, 264 (1989) 21597.
5. Grandhee, S.K. and Monnier, V.M., *J. Biol. Chem.*, 266 (1991) 11649.
6. Bailey, A.J., Sims, T.J., Avery, N.C., Miles, C.A., *Biochem. J.*, 296 (1993) 489.

Peptides: Chemistry, Structure and Biology
Pravin T.P. Kaumaya and Robert S. Hodges (Eds.)
Mayflower Scientific Ltd., 1996

184
Compounds Derived from an Adjuvant Muramylpeptide GMDP and Tuftsin: A Structure-activity Study

V.M. Titov, E.A. Meshcheryakova, L.G. Alekseeva, T.M. Andronova and V.T. Ivanov

Shemyakin-Ovchinnikov Institute of Bioorganic Chemistry, Miklukho-Maklaya ul.16/10, 117871, Moscow, Russia

Introduction

The muramylpeptide GMDP (N-acetylglucosaminyl-(β1→4)-N-acetylmuramyl-L-alanyl-D-isoglutamine) (see below), a potent immunostimulator, has been extensively studied by us [1]. Recently, we found that combination by mixing or by chemical conjugation of GMDP with tuftsin (Thr-Lys-Pro-Arg) [2], a known stimulator phagocytosis by macrophages *in vivo*, leads to mutual enhancement of their immunostimulating activities [3]. Here we describe structural analogs of the GMDP-tuftsin conjugates.

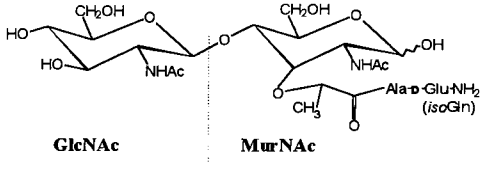

GMDP

Results and Discussion

All compounds were synthesized in solution and characterized by TLC, RP-HPLC, FAB-MS and, in several cases, ^{1}H-NMR. The activities in the adjuvancity and phagocytosis stimulation tests were determined as described [3] (Table 1).

The immunostimulating properties of muramyl peptides can be enhanced by incorporation of a lipophilic substituent. We synthesized a series of stearoyl derivatives of the conjugates and tuftsin. We found that lipophilization of tuftsin enhanced its activity. In the case of the conjugates, lipophilization reasonably improved the less active one, but not the more active (**L1** and **L2**, respectively). We prepared a lipophilic analog of GMDP-TKPR with intact N-terminus of tuftsin (**L3**) that was active but not better than **L1** in which this position was occupied.

Evaluating whether the presence of the complete structure of tuftsin is required for activity, we conjugated GMDP with a tuftsin antagonist, Lys-Pro-Arg [4]. The conjugates were slightly more active than GMDP but less active than GMDP-TKPR; lipophilization potentiated the activity. GMDP was also potentiated when mixed with the

Table 1. *Structures and activities of the analogs of GMDP-tuftsin conjugates and related compounds. (Gmdp- = GlcNAc-MurNAc-Ala-D-*isoGln*-, Ste=stearoyl).*

Compound	Structure	Adjuvant activity		Phagocytosis stimul.
		Optimal dose, μM/mouse	Stimulation index vs. GMDP	Stimulation index vs. tuftsin
GMDP	Gmdp-OH	$1.44*10^{-1}$	n.a.	1.5
Tuftsin	TKPR	$1.44*10^{-1}$	0.2	n.a.
GMDP-TKPR [3]	Gmdp TPR	$1.44*10^{-2}$	1.6	1.8
L1	Gmdp-TK(Ste)PR	$1.44*10^{-1}$	2.3	1.8
L2	Gmdp Ste-TKPR	$1.44*10^{-1}$	0.4	1.2
L3	Gmdp-K(Ste) TKPR	10^{-2}	1.3	1.7
Ste-TKPR(1)	Ste-TKPR	10^{-1}	0.9	2.3
Ste-TKPR(2)	TK(Ste)PR	10^{-1}	0.6	3.9
KPR	KPR	10^{-1}	0.5	0.8
GMDP+KPR	equimolar mixture	10^{-1}	2.0	1.2
GMDP-KPR(1)	Gmdp-KPR	10^{-1}	1.4	1.4
GMDP-KPR(2)	Gmdp KPR	10^{-1}	0.3	1.3
GMDP-Ste-KPR	Gmdp-K(Ste)PR	n.d.	n.d.	1.7
GMDP-dA-TKPR	Gmdp-D-Ala TKPR	10^{-1}	0.1	1.8
GMDP-Aca-TKPR	Gmdp-Aca TKPR	10^{-3}	0.5	1.9

peptide. These results confirm our hypothesis [3] that tuftsin receptors may be involved in the mechanism of the conjugate's action.

Attempts to improve the GMDP-TKPR conjugate by incorporating spacers (D-Ala and 6-aminocaproyl, Aca) between GMDP and the tuftsin moieties produced only weakly active conjugates. Thus, direct binding of GMDP to tuftsin seems to be important.

Acknowledgments

Financial support from Peptech (UK) Ltd. the ISF (USA-Russia) and spectral work of Dr.A.Sulima (FAB-MS) and Dr.V.Bushuev (NMR) are gratefully acknowledged.

References

1. Andranova, T. and Ivanov, V., *Soy. Medical Rev. D. Immun.*, 4 (1991) 1.
2. Fridkin, M. and Najjar, V.A., *Crit. Rev. Biochem. Mol. Biol.*, 24 (1989) 1.
3. Titov, V.M., Mescheryakova, E.A., Balashova, T.A., Andronova, T.M. and Ivanov, V.T., *Int. J. Peptide Protein Res.*, 45 (1995) 348.
4. Siemion, I.Z. and Konopinska, D., *Mol. Cell Biochem.*, 41 (1981) 99.

Peptides: Chemistry, Structure and Biology
Pravin T.P. Kaumaya and Robert S. Hodges (Eds.)
Mayflower Scientific Ltd., 1996

185
Methodological Improvements in the Solid Phase Synthesis of Glycopeptides

L. Urge and L. Otvos, Jr.

The Wistar Institute, Philadelphia, PA 19104, USA

Introduction

Glycopeptides, similar to phosphopeptides and sulfopeptides, can be prepared by solid-phase synthesis using two alternative methods. The first is the building block method, in which glycosylated amino acids are used as monomers to introduce sugars into peptides [1-3]; and the second is the "global" glycosylation, in which suitably protected resin-bound oligopeptides with a free side-chain hydroxyl [4] or carboxylic acid [5] function are glycosylated after the peptide chain assembly is completed. Both strategies tend to be difficult when a series of extended or complex sugars are used because: i) the preparation of many individual Fmoc-Asn(sugar)-OH compounds is tedious, and ii) the activated aspartic acid side-chain is prone to intramolecular aspartimide formation.

Results and Discussion

We attempted to overcome the first difficulty by aminating a commercially available mixture of 4-11 glucose unit-containing malto-oligosaccharide analogues and coupling the 1-amino-sugar mixture to Fmoc-Asp-O^{t}Bu. As with other glycoamino acids [6], the glycosylated asparagine "synthons" can be separated by in one RP-HPLC step (Figure 1).

To eliminate the undesired aspartimide formation during the "global" glycosylation procedure, we blocked the amide NH group C-terminal to the aspartate using secondary amino acids. An allyl group was used to protect and Pd to deprotect the side chain of the aspartic acid residue to be glycosylated. Two types of backbone protecting groups were employed: the non-removable methyl group to avoid any possible steric hindrance, and the TFA cleavable Hmb group to enable the preparation of true glycopeptides. Both backbone-protecting groups could be used to improve N-glycosylation efficiency of with a monosaccharide, GlcNAc [7]. While the methyl group was also effective in improving heptasaccharide incorporation, acylation of the same 1-amino-maltoheptose remained troublesome with the Hmb protected peptide due to steric hindrance [7]. This strategy can be generally used to avoid undesired ring formation in aspartyl peptide synthesis.

As a third line of investigation, we compared three different deacetylation methods of O-glycopeptides that contain Thr residues carrying acetylated disaccharide moieties. The most frequently used sugar hydroxyl-protecting group is the acetyl group, which is removed principally by nucleophilic substitutions. Although the proposed β-elimination during the acetyl removal [8] can be avoided only by using 2 M NH_3/MeOH and not by

using 0.1 M NaOMe or 0.1-0.001 M NaOH, the targeted ester hydrolysis proceeds much faster than the unwanted side reactions even using the latter reagents. This finding is in agreement with recent reports that the concern of β-elimination in glycopeptides has been exaggerated [9, 10].

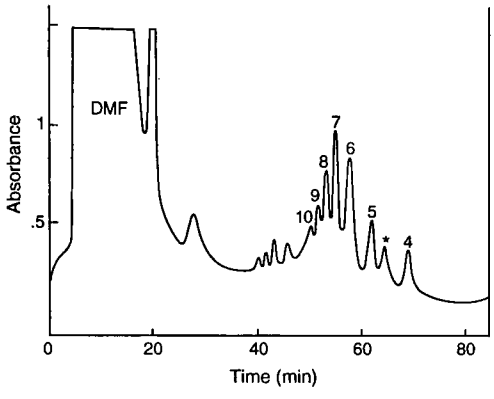

Figure 1. *Preparative scale separation of Fmoc-Asn(maltooligosaccharide)-O'Bu derivatives on RP-HPLC. Chromatographic conditions: Column: C_{18} 150x25 mm. Solvent A: H_2O/0.1% TFA; Solvent B: CH_3CN/0.1% TFA. Gradient in the Fmoc-Asn(sugar)-O'Bu range: 0.1% B/min with 9 ml/min flow rate. Detection: 214 nm. The peaks were identified by MS by using a LaserTec Benchtop 2 laser-desorption time of flight instrument. The numbers indicate the number of glucose units. The asterisk indicates an unidentified peak.*

Acknowledgments

This work was supported by NIH grant GM 45011.

References

1. Otvos, L., Jr., Wroblewski, K., Kollat, E., Perczel, A., Hollosi, M., Fasman, G.D., Ertl, H.C.J. and Thurin, J., *Pept. Res.*, 2 (1989) 362.
2. Meldal, M. and Bock, K., *Tetrahedron Lett.*, 31 (1990) 6987.
3. Filira, F., Biondi, L., Cavaggion, F., Scolaro, B. and Rocchi, R., *Int. J. Pept. Protein Res.*, 36 (1990) 86.
4. Andrews, D.M. and Seale, P.W., *Int. J. Pept. Protein Res.*, 42 (1993) 165.
5. Anisfeld, S.T. and Lansbury, P.T., Jr., *J. Org. Chem.*, 55 (1990) 5560.
6. Otvos, L., Jr., Urge, L. and Thurin, J., *J. Chromatogr.*, 599 (1992) 43.
7. Urge, L. and Otvos, L., Jr., *Lett. Pept. Sci.*, 1 (1995) 207.
8. Szabo, L. and Polt, R., *Carbohydr. Res.*, 258 (1994) 293.
9. Meldal, M., Bielfeldt, T., Peters, S., Jensen, K.J., Paulsen, H. and Bock, K., *Int. J. Pept. Protein Res.*, 43 (1994) 529.
10. Kihlberg, J. and Vuljanic, T., *Tetrahedron Lett.*, 34 (1993) 6135.

Peptides: Chemistry, Structure and Biology
Pravin T.P. Kaumaya and Robert S. Hodges (Eds.)
Mayflower Scientific Ltd., 1996

186
Scope and Limitations of the Phosphoramidite Approach for Multiple Syntheses of Phosphopeptides

R. Hoffmann[1], D. Stoll[2], T. Hoffmann[1], A. Tholey[1], K.-H. Wiesmueller[2], C. Kempter[3] and G. Jung[3]

[1] Biochemie, Universitaet des Saarlandes, D-66123 Saarbruecken, Germany
[2]NMI Naturwissenschaftliches und Medizinisches Institut, D-72762 Reutlingen, Germany
[3] Institut fuer Organische Chemie, Universitaet Tuebingen, D-72076 Tuebingen, Germany

Introduction

Because of the acid and base instability of phosphoserine and phosphothreonine [1, 2], the typical approach to synthesize phosphopeptides on solid phase containing these amino acids is the introduction of the hydroxy-unprotected amino acids. After peptide synthesis, the free hydroxyl functions are phosphitilated (phosphoramidite, tetrazole) and oxidized (*m*-chloroperbenzoic acid, I_2, tBuOOH). In contrast, phosphotyrosine can be incorporated as a building block [Fmoc-Tyr(PO_3R_2)-OH; R = Me, Et, Bzl].

We present the data of a multiple synthesis of more than 40 peptides (0.02 mmol) followed by multiple phosphitilation [0.75 mmol 1H-tetrazole, 0.36 mmol $(tBuO)_2$-$PNEt_2$], oxidation (0.2 mmol *m*-chloroperbenzoic acid) and cleavage (82.5% TFA, 5% water, 5% thioanisol, 5% phenol, 2.5% EDT). The methyl groups of phosphotyrosine were cleaved by TMSBr [3]. All the crude peptides, phosphorylated or not, were characterized by electrospray-MS.

Results and Discussion

After synthesis on solid phase and TFA-cleavage of the unphosphorylated peptides, we obtained the expected molecular masses for most of the peptides. For some peptide sequences we detected higher masses, which most probably are O-acylated peptides. In the case of GGXA (X = S, T), we only detected different higher masses probably due to O-acylation.

After phosphorylation, we identified the phosphopeptides and furthermore three by-products by MS. These by-products seemed to be typical for the phosphoramidite approach used.

As expected, the phosphorylation on solid phase was not quantitative, as indicated by variable contents of the unphosphorylated peptides: 53% (20 of 36) of the phosphorylated peptides contained this by-product in low amounts (up to 20%), but in 8% (3 of 38) it was the main product.

The oxidation of the phosphitilated peptides was not quantitative, resulting in H-phosphonopeptides. The content of this common by-product depends on both the

phosphitilated amino acid (S, T) (Table 1) and the sequence and possibility of steric hindrance. The H-phosphonopeptides were obtained in 95% (36 of 38 peptides) of the phospho- rylated peptides. In one of these peptides it was the main component.

In 34% (13 of 38) of the phosphorylated peptides, we detected peptides bridged *via* a phosphodiester linkage. Recently, we described this by-product for the model peptides GGSA and GGTA [3]. This by-product was obtained after phosphorylation mostly on threonine- but also on serine-residues (Table 1). The typical content was in the range of 10 to 20%. Only for one sequence, phosphorylated at threonine, was this bridged peptide the main product.

Table 1. *Content of crude peptide and by-products after phosphorylation of threonine (14 peptides) and serine (19 peptides).*

aa	free	$X(PO_3H_2)$	$X(PO_2H_2)$	bridged
T	71% 10/14	100% 14/14	100% 14/14	71% 10/14
S	63% 12/19	100% 19/19	89% 17/19	11% 2/19

To circumvent O-acylation for sequences described above, we checked selectively cleavable O-protecting groups [trityl, tert.-butyl dimethyl silyl (tbdms)]. After the peptide synthesis, these protecting groups were cleaved (1% TFA, 5% triisopropyl silane in DCM for trityl; 1.5 equiv. Bu_4NF for tbdms). The deprotected hydroxyl group was phosphorylated as described above. This procedure allowed us to synthesize both the unmodified and the phosphorylated peptides in high yields and purities [80% for $GGS(PO_3H_2)A$ and 50% for $GGT(PO_3H_2)A$].

References

1. Lacombe, J.M., Andriamanampisoa, F. and Pavia, A.A., *Int. J. Pept. Prot. Res.*, 36 (1990) 275.
2. Perich, J.W., Terzi, E., Carnazzi, E., Seyer, R. and Trifilieff, E., *Int. J. Pept. Prot. Res.*, 44 (1994) 305.
3. Hoffmann, R., Wachs, W.O., Berger, R.G., Kalbitzer, H.R., Waidelich, D., Bayer, E., Wagner-Redeker, W. and Zeppezauer, M., *Int. J. Pept. Prot. Res.*, 45 (1995) 26.

Peptides: Chemistry, Structure and Biology
Pravin T.P. Kaumaya and Robert S. Hodges (Eds.)
Mayflower Scientific Ltd., 1996

187
Partial Amino Acid Sequence of the B Chain of the Mistletoe Lectin I

M. Huguet[1], S. Stoeva[1], C. Decker[2], S. Wilhelm[2], T. Stiefel[2], G. Paulus[3] and W. Voelter[1]

[1]Abteilung für Physikalische Biochemie des Physiologisch-chemischen Instituts der Universität Tübingen, Hoppe-Seyler-Str. 4, D-72076 Tübingen, Germany
[2]Biosyn Arzneimittel GmbH, Schorndorfer-Str. 32, D-70734 Fellbach, Germany
[3]Shimadzu Europe GmbH, Albert-Hahn-Str. 6-10, D-47269 Duisburg, Germany

Introduction

Mistletoe lectin I (ML I), the ß-galactoside-specific lectin from *Viscum Album L.*, is a component of a commercially available mistletoe extract which has federal approval for clinical application in human cancer treatment. Regular injections of optimal doses of ML I yield an enhancement of several cellular parameters which are generally believed to be involved in antitumor immunity [1]. ML I consists of two different subunits, both N-glycosylated and linked by a disulphide bond. The A chain (29 kDa) is cytotoxic, whereas the immunomodulatory potency are attributed to the B chain (34 kDa).

After previous determination of the primary structure of the toxic subunit [2], we present the partial amino acid sequence of the B chain of ML I. Sequence information was obtained from the analysis of two sets of peptides generated by endoproteinase Asp-N and trypsin, respectively. After digestion, the peptides were purified by RP-HPLC and characterized by laser desorption mass spectometry (Kratos MALDI III equipment, Shimadzu, Europe) and Edman degradation sequence analysis.

Results and Discussion

Sequence alignment of the characterized peptides originating from cleavage of the B chain of ML I was made by comparison with the cDNA-deduced B chain amino acid sequences of abrin-a [3] and ricin-D [4] (Figure 1) which are toxic lectins structurally related to ML I [5]. These proteins are collectively known as ribosome-inactivating proteins (type II RIPs) and share the same mechanism of action [6]. After binding to eukariotic cells by interacting with cell-surface galactosides they enter the cytosol *via* endocytic uptake, irreversibly inhibiting protein synthesis and promoting cell death.

The sequence comparison of the primary structure of the B chain of ML I with those of abrin-a and ricin-D shows a significant degree of similarity, whereby terminal regions appear as the most conserved parts of the molecule. In the N-terminal segment (44 residues) 52% and 67% of the amino acid residues overlap with the abrin-a respectively ricin-D sequence,while for the C-terminus (34 residues) an identity of 50% (abrin-a),

respectively, 42% (ricin-D) is observed. All Trp residues distributed along the sequence remain invariant as well. Undeterminable residues indicated by X at positions 155, 168, 194 and 212 are presumably Cys residues, which probably build two internal disulfide bridges.

Further examinations of the reported results show that residues which are involved in the active galactose-binding sites in the B chain of the ricin molecule are also conserved in the amino acid sequence of the B chain of ML I. These are Asp23, Gln36 and Trp38 (subdomain 1α) and Asp239, Tyr253, Asn260 and Gln261 (subdomain 2γ) [7]. It has been proven that these galactose-receptors are responsible for surface binding of ricin and for the translocation of its toxic subunit into the cytosol [8]. Based on these results and on the reported homology between primary structures of both proteins, it can be postulated that ML I may recognize specifically glycosylated lectin ligands present on the surface of lymphocytes and monocytes through its galactose-binding sites. This lectin-carbohydrate interaction is supposed to be responsible for the immunostimulating properties of ML I.

```
Abrin-a   IVEKSKICSSRYEPTVRIGGRDGMCVDVYDNGYHNGNRIIMWKCKDRLEENQLWTLKSDK  60
Ricin-D      ADVCMD-PEPIVRIVGRNGLCVDVRDGRFHNGNAIQLWPCKSNTDANQLWTLKRDN  55
ML I         DDVTSSASEPTVRIVGRNGMRVDVRDDDFHDGNQIQLWPSKSNN              44

Abrin-a   TIRSNGKCLTTYGYAPGSYVMIYDCTSAVAEATYWEIWDNGTIINPKSALVLSAESSSMG 120
Ricin-D   TIRSNGKCLTTYGYSPGVYVMIYDCNTAATDATRWQIWDNGTIINPRSSLVLAATSGNSG 115
ML I                                    EATIWQIWG                     116

Abrin-a   GTLTVQTNEYLMRQGWRTGNNTSPFVTSIS--G-YS-DLCMQAQGSNVWLADCDSN--KK 174
Ricin-D   TTLTVQTNIYAVSQGWLPTNNTQPFVTTIV--G-LY-GLCLQANSGQVWIEDCSSE--KA 169
ML I           TLDYTLGQGWLAR    VF-INEGAIGVLSRDLXMESNGGSVWVETXNSNLQKP 175

Abrin-a   EQQWALYTDGSIRSVQNTNNCLTS-K-DHKQGSPILLMG-CSNGWAS-QRWLFKNDGSIY 230
Ricin-D   EQQWALYADGSIRPQQNRDNCLTS--DSNIRETVVKILS-CGPASSG-QRWMFKNDGTIL 225
ML I      --QWALYGDGSIRPKQNNDQXLTSGRQSN-AGDPV-QLSAXSPGVVQVGRWGFR-DGSIR 230

Abrin-a   SLYDDMVMDVKGSDPSLKQIILWPYTGKPNQIWLTLF                        267
Ricin-D   NLYSGLVLDVRRSDPSLKQIILYPLHGDPNQIWLPLF                        257
ML I         DDDFRDVAQANPKLRRIIIYPATGKPNQMWLPLFL                       268
```

Figure 1. *Comparison of the determined B chain sequence of ML I with the of cDNA-deduced ones of abrin-a and ricin-D. Conserved amino acids are underlined. So far undetermined residues are indicated by X.*

References

1. Hajto, T., Hostanska, K. and Gabius, H.-J., *Cancer Research,* 49 (1989) 4803.
2. Maia, H.L.S., Peptides 1994, ESCOM, Leiden, The Netherlands, 1995, p. 737.
3. Hung, Ch.-H., Lee, M.-Ch., Lee T.-Ch. and Lin, J.-Y., *J. Mol. Biol.,* 229 (1993) 263.
4. Halling, H.C., Halling, A.C., Murray, E.E., Ladin, B.F., Houston, L.L. and Weaver, R.F., *Nucl. Acids Res.,* 13 (1985) 8019.
5. Franz, H., Ziska, P. and Kindt, A., 'Lectins - Biology, Biochemistry, Clinical Biochemistry, Vol. II', Walter de Gruyer and Co., Berlin-New York 1982, p. 771.
6. Endo, Y., Mitsui, K., Motizuki, M. and Tsurugi, K., *J. Biol. Chem.,* 262 (1987) 5908.
7. Lord, J.M., Roberts, L.M. and Robertus, J.D., *FASEB J.,* 8 (1994) 201.
8. Youle, R.J. and Neville, D.M., *J. Biol. Chem.*, 257 (1982) 1598.

Peptides: Chemistry, Structure and Biology
Pravin T.P. Kaumaya and Robert S. Hodges (Eds.)
Mayflower Scientific Ltd., 1996

188
Synthesis of Phosphotyrosine-containing T-cell Receptor ζ-Subunit Peptides: Conformational and Immunological Studies

G.K. Tóth[1], I. Laczkó[2], Z. Hegedűs[2], E. Vass[3], M. Hollósi[3], T. Janáky[1], G. Váradi[1], B. Penke[1] and É. Monostori[2]

[1]*Department of Medical Chemistry, A. Szent-Györgyi Medical University,Hungary*
[2]*Institute of Genetics and Biophysics, Biological Research Center, Szeged, Hungary*
[3]*Department of Organic Chemistry, Eötvös University, Budapest, Hungary*

Introduction

The ζ-chain of the TCR/CD3 complex plays a central role in cell signalling *via* the TCR [1, 2]. On receptor stimulation, the ζ-chain is phosphorylated on tyrosine residues in the intracellular region of this molecule. It has not yet been revealed which of the seven tyrosines present in the ζ-polypeptide are phosphorylated nor which kinase is involved in this event [3, 4]. Dephosphorylation of the protein is necessary for the downregulation of T-cell activation, but the phosphatases participating in dephosphorylation have not yet been identified [5]. Different peptide fragments and the corresponding phosphorylated derivatives of the ζ-subunit were synthesized in order to investigate the roles of the individual phosphotyrosine residues in the biochemical process of T-cell activation. The phosphorylated ζ-peptides were also applied to establish whether any of them are substrates for CD45, a lymphocyte-specific transmembrane tyrosine phosphatase.

Results and Discussion

Both the synthon approach and the global method were applied in the synthesis of seven short phosphorylated (and non-phosphorylated) fragments of the TCR, CD3 ζ-chain. Of the separation methods applied for the purity control MECC seemed best. Preliminary experiments revealed that six short ζ-related peptides, corresponding to the conservative sequences of the ζ-polypeptide are substrates for the src kinases, and one of the seven peptides (PPAYQQG), which lies outside the conservative motifs, is not a target for *in vitro* phosphorylation by the src kinases used (lck and fyn) [6]. CD45, a lymphocyte surface protein, which has tyrosine phosphatase activity, seems to be responsible for the dephosphorylation of the ζ-chain. It has been demonstrated that CD45 dephosphorylates

PPAY(*P*)QQG, 61P; NQLY(*P*)NEL, 69P; REEY(*P*)DVL, 80P; QEGLY(*P*)NEL, 106P; AEAY(*P*)SEIG, 119P; DGLY(*P*)QGL, 138P; KDTY(*P*)DAL, 149P

Figure 1. *The structures of the synthesized peptides.*

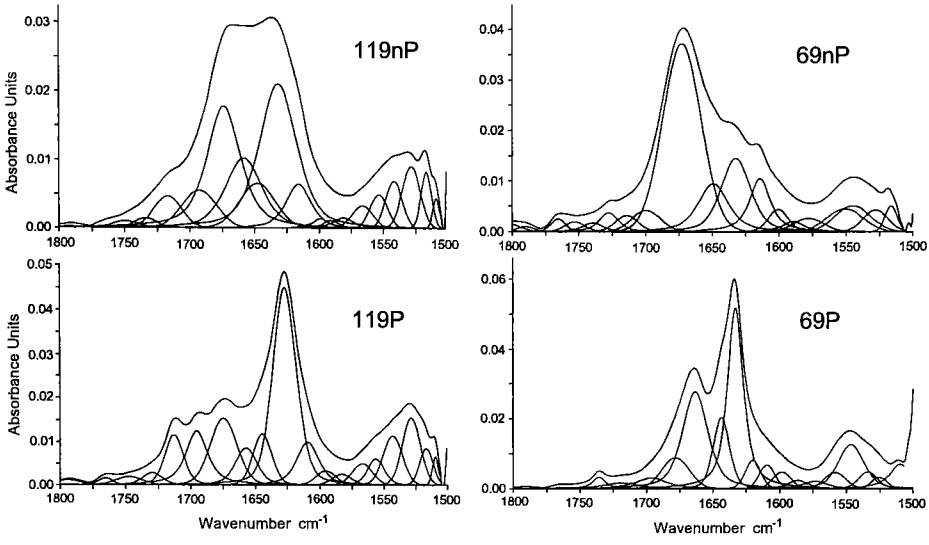

Figure 2. *The FT-IR spectra of several peptides. Band at 1633 cm^{-1} indicates ß-sheet formation.*

phosphorylated ζ- oligopeptides, indicating that this tyrosine phosphatase may play a role in the downregulation of T-cell activation. In water, both the non-phosphorylated (nP) and phosphorylated (P) peptides give CD spectra characteristic of a predominantly random conformation (strong negative band below 200 nm). In TFE solution, the peptides exist as mixtures of conformers, and the CD spectra reflect more than one prevailing secondary structure. The conformational investigations of these phospho-peptides by means of CD and FTIR spectroscopy supported the idea that the phosphorylation event can change the conformations of the parent peptides, mostly leading to an increase in the ß-sheet conformation.

Acknowledgments

This work was supported by the following grants: OTKA T 016156 and ETT T03/523 to GKT, OTKA T 005159 to TJ and OTKA T 005257 to EM.

References

1. June, C.H., Fletcher, M.C., Ledbetter, J.A., Schieven, G.L., Siegel, A.F., Phillips, A.F. and Samelson, L.E., *Proc. Natl. Acad. Sci. USA,* 87 (1990) 7722.
2. Irving, B.A. and Weiss, A., *Cell,* 64 (1991) 891.
3. Barber, E.K., Dasgupta, J.D., Schlossman, S.F., Trevillyan, J.M. and Rudd, C.E., *Proc. Natl. Acad. Sci. USA,* 86 (1989) 3277.
4. Samelson, L.E. and Klausner, R.D., *J. Biol. Chem.*, 267 (1992) 24913.
5. Isakov, N., *Mol. Immunol.*, 30 (1993) 197.
6. Hegedüs, Z., Andó, I., Tóth, G.K., Váradi, G. and Monostori, É., *BioTechniques,* 18 (1995) 632.

Session X
Conformational Analysis

Chairs: Garland R. Marshall and Claudio Toniolo

Peptides: Chemistry, Structure and Biology
Pravin T.P. Kaumaya and Robert S. Hodges (Eds.)
Mayflower Scientific Ltd., 1996

189
The Role of Homology Modeling and Design

J. Greer, C.W. Hutchins, C. Abad-Zapatero, K. Stewart and K.J. Puttlitz

Department of Structural Biology, Abbott Laboratories, Abbott Park, IL 60064, USA

Introduction

Homology modeling has been useful for the rapid construction of three-dimensional model structures of proteins for over twenty years [1]. The rapid growth in the number of available protein sequences due to genome projects has made the ability to rapidly develop good quality model structures much more important. We have used homology modeling to develop structures of a wide range of proteins including members of the serine protease [2], aspartic proteinase [3] and anaphylatoxin [4] families. These models have been used to help understand enzyme specificity [5] and site-specific mutations [6], as well as for drug design [3, 7, 8].

During the course of these studies, we have developed a number of model structures whose experimental structure has been determined subsequently, either by crystallography or NMR. To properly evaluate the utility of homology modeling, we initiated a detailed comparison of each model with its respective crystal structure. In this work, we describe studies on the aspartic proteinase family (Table 1).

Table 1. *Comparison of available model and experimental structures in the aspartic proteinase family.*

Protein	Model	Ref.	Experiment	Ref.
Renin	1983-1991	[3]	1991-1992	[9-11]
Cathepsin D	1991		1993	[12]
Candida protease	1993		1994	[13]

Results and Discussion

The secondary structure of the experimental structures were assigned by the Kabsch and Sander algorithm in PROCHECK [14]. The RMSD of the α-carbons of the residues for each of the α helices and β strands were compared. The α-carbon positions of the secondary structure were then evaluated by domain and for the entire protein. In this manner, successively larger pieces of the protein were analyzed. Random coil and turns were compared separately. These regions have larger RMSD values than the conserved secondary structure since these may be highly flexible loops often affected by crystal

contacts. The active sites, those residues within 6Å of an inhibitor, were also compared. Since many of these models were intended to be used for the design of novel inhibitors, it is the similarity of the active site of the model to the experimental structure that is of greatest interest. Other geometrical details, such as the position and conformation of the side chains, were also examined. Methods, such as the PROCHECK suite of programs and the Profiles methodology [15], were used to assess the models.

The crystal structures of the complex of porcine pepsin with A-62095 [16] and chymosin [17] were used as the basis for the development of models of human renin [3] and human cathepsin D. A model of a secreted aspartyl protease from *Candida albicans* was developed using the crystal structure of bound rhizopuspepsin as the core. This model was compared to the recent crystal structure of the complex of A-70450 in the Candida SAP2 enzyme [13].

The overall structure of the models compared to the crystal structures was generally good, Table 2 (RMSD for secondary structure of the protein ranged between 1.58 and 2.72Å). The active sites of the proteins also compared well (RMSD ranged from 1.08 to 2.16Å). In the *Candida albicans* proteinase, the insertion of 9 residues near the first disulfide bridge (residues 45-50) was properly placed and the deletion of the helix at residues 110-116 of the other aspartic proteinases was correctly modeled.

Table 2. *RMSD Values (in Å) for comparison of the secondary structure of the model and experimental structures (number of residues compared).*

Protein	N-Term	C-Term	Active Site	Total
Renin				
REN [9]	1.70 (120)	1.40 (91)	1.08 (41)	1.58 (211)
REN [10]	1.74 (120)	1.20 (91)	1.21 (41)	1.88 (211)
BBS [11]	1.71 (120)	1.19 (91)	1.26 (41)	1.70 (211)
Cathepsin	3.76 (94)	1.18 (117)	1.56 (43)	2.72 (211)
Candida	2.37 (73)	2.33 (90)	2.16 (41)	2.45 (163)

However, the conformations of the external loops were, in many cases, significantly different between the models and the respective crystal structures. In renin, the 240 and the 280 loops are involved in crystal contacts in two crystal structures which causes a twisted conformation rather than the more classical β strand-turn-β strand seen in pepsin. This leads to a large RMSD of the alpha carbon positions of these loops. In the third renin crystal structure, these loops are not involved in crystal contacts, but are exposed to solvent and are disordered.

Occasionally, an error occurs over a short stretch of the model where decisions on the alignment of the protein sequences and the resultant placement of residues in the model were made incorrectly based on the then available crystal structures of homologous proteins. For example, in renin, residues 98-110 of the model are one residue off from the crystal structure, which differs in this region from the other aspartic proteinases. The misalignment could be detected using the Profiles-3D software, which was not available at the time the model was built. However, it is not obvious from a modeling perspective how to build the structure correctly.

Using the *Candida* crystal structure, homology models were constructed for the six related *Candida* proteinases which are reported to be virulence factors. Additions and deletions near the active site suggested a common specificity for these *Candida* enzymes, especially in the vicinity of the S3 binding pocket [13]. Compounds are currently being designed to fit the unusual requirements of the *Candida* enzyme active site as potential antifungal agents.

In summary, homology modeling permits rapid construction of reasonable models for new proteins. The core of the model structure, the defined secondary structure, compares favorably with the crystal structure. The flexible loops and the insertions and deletions display significant variation from the experimental structure. Fortunately, most of these loop deviations are not in the active site, but some are close enough to affect ligand specificity. Computational tools are emerging that may allow us to recognize residues or regions of the model structure that are wrong, but the correct solution is often not obvious. Nature still surprises us with novel structures.

References

1. Browne, W.J., North, A.C.T., Phillips, D.C., Brew, K., Vanaman, T.C. and Hill, R.L., *J. Mol. Biol.*, 42 (1969) 65.
2. Greer, J., *Proteins*, 7 (1990) 317.
3. Hutchins, C. and Greer, J., *Crit. Rev. Biochem. Mol. Biol.*, 26 (1991) 77.
4. Greer, J., *Science*, 228 (1985) 1055.
5. Greer, J., *J. Mol. Biol.*, 153 (1981) 1043.
6. Davidow, L.S., Dumais, D.R., Smyth, A.P., Greer, J. and Moir, D.T., *Protein Eng*, 4 (1991) 923.
7. Sham, H.L., Bolis, G., Stein, H.H., Fesik, S.W., Marcotte, P.A., Plattner, J.J., Rempel, C.A. and Greer, J., *J. Med. Chem.*, 31 (1988) 284.
8. Yang, H., Henkin, J., Kim, K.H. and Greer, J., *J. Med. Chem.*, 33 (1990) 2956.
9. Sielecki, A.R., Hayakawa, K., Fujinaga, M., Murphy, M.E., Fraser, M., Muir, A.K., Carilli, C.T., Lewicki, J.A., Baxter, J.D. and James, M.N., *Science*, 243 (1989) 1346.
10. Rahuel, J., Priestle, J.P. and Grutter, M.G., *J. Struct. Biol.*, 107 (1991) 227.
11. Dhanaraj, V., Dealwis, C.G., Frazao, C., Badasso, M., Sibanda, B.L., Tickle, I.J., Cooper, J.B., Driessen, H.P., Newman, M., Aguilar, C., Wood, S.P., Blundell, T.L., Hobart, P.M., Geoghegan, K.F., Ammirati, M.J., Danley, D.E., O'Connor, B.A. and Hoover, D.J., *Nature*, 357 (1992) 466.
12. Baldwin, E.T., Bhat, T.N., Gulnik, S., Hosur, M.V., Sowder, R.C., Cachau, R.E., Collins, J., Silva, A.M. and Erickson, J.W., *Proc. Natl. Acad. Sci. USA*, 90 (1993) 6796.
13. Abad-Zapatero, C., Goldman, R., Muchmore, S.W., Hutchins, C., Stewart, K., Navaza, J. and Ray, T.L., 1995, *Protein Science,* in press.
14. Laskowski, R.A., MacArthur, M.W., Moss, D.S. and Thornton, J.M., *J. Appl. Crys.*, 26 (1993) 283.
15. Luthy, R., Bowie, J.U. and Eisenberg, D.A., *Nature*, 356 (1992) 83.
16. Chen, L., Erickson, J.W., Rydel, T.J., Park, C.H., Neidhart, D., Luly, J. and Abad-Zapatero, C., *Acta Cryst. B*, 48 (1992) 476.
17. Gilliland, G.L., Winborne, E.L., Nachman, J. and Wlodawer, A., *Proteins*, 8 (1990) 82.

Peptides: Chemistry, Structure and Biology
Pravin T.P. Kaumaya and Robert S. Hodges (Eds.)
Mayflower Scientific Ltd., 1996

190

Synthetic Peptides Model α-Helix-β-Sheet Conformational Changes in the Prion Protein

M.A. Baldwin[1], H. Zhang[1,2], T. Bekker[1], S. Zhou[1], J. Nguyen[1], A.C. Kolbert[5], J. Heller[5,6], T.L. James[2], D.E. Wemmer[5,6], A. Pines[5,7], F.E. Cohen[2,3,4] and S.B. Prusiner[1,3]

Departments of [1]Neurology, [2]Pharmaceutical Chemistry, [3]Biochemistry and Biophysics, and [4]Medicine, University of California, San Francisco, CA 94143, USA
[5]Department of Chemistry and [6]Graduate Group in Biophysics, University of California, Berkeley, CA 94720, USA
[7]Material Sciences Division and Structural Biology Division, Lawrence Berkeley Laboratory, Berkley, CA 94720, USA

Introduction

The prion protein (PrP) plays a central role in the development of fatal neurodegenerative diseases that can occur in sporadic, inherited and infectious forms [1]. Although the function of the normal, cellular protein (PrP^C) is unknown, mice in which the PrP gene is ablated, are resistant to infection with prions. The only known component of the infectious prion particle is an abnormal isoform designated PrP^{Sc}, which is formed by an unknown posttranslational process. There are no known covalent differences between the two isoforms, but PrP^C is α-helical whereas PrP^{Sc} is rich in β-sheet [2]. Limited proteolysis of PrP^{Sc} causes N-terminal truncation to give PrP 27-30 which polymerizes into amyloid rods. Sequence homology allowed secondary structure predictions that identified four regions of 13-17 residues likely to be structured, although there was ambiguity between different algorithms as to whether α-helices or β-sheets would be favored [3]. Three of four synthetic peptides H1-H4 preferentially adopted β-sheet structure, both in the solid state and in aqueous solution, from which amyloid fibrils precipitated [4]. They could also form α-helices in certain solvents, thus the ambiguities of the structural predictions were reflected in the behavior of the peptides. This led to the hypothesis that conversion of PrP^C to PrP^{Sc} involves a conformational transition of one or more of the putative helices [5]. For the reasons below, H1 (MKHMAGAAAAGAVV, residues 109-122) is believed to play a major role in this conformational change.

- Peptide H1 displays both α-helix and β-sheet character [4] and can induce β-sheet structure in other PrP peptides [6].
- H1 is in the most highly conserved region of PrP, even showing high homology between mammalian and avian forms.

- It is in a region bordered by the N-terminus of infectious PrP 27-30 (residue 90) and an amber mutation in a patient who died from a prion disease (residue 145).
- It is in a region identified in PrP plaques (residues 58-150).
- It is in a region in which sequence variations have the greatest influence on the barriers to transmission of disease between species (residues 90-130).

Results and Discussion

Solvent-induced transitions of H1 and related peptides were monitored by CD and correlated with ultrastructure seen by electron microscopy (EM). α-Helices were promoted in H1 by 50% aqueous hexafluoroisopropanol (HFIP) whereas aqueous media induced β-sheet. The more hydrophilic 104H1 (KPKTN-H1, residues 104-122) showed three separate conformations; α-helix in 50% HFIP, coil in aqueous media and β-sheet in 50% acetonitrile (AcN). Peptide AGAAAAGA (residues 113-120), conserved across all species, retained its β-sheet structure under almost all conditions. In both H1 and 104H1, helix formation was independent of concentration, indicating the helical species to be monomeric, whereas the transition from the α-helix or coil to β-sheet was concentration dependent. EM showed aggregation of both helical and sheet structures, the former giving large ribbons several microns in length and up to 100 nm wide, unlike the β-sheet fibrils which were similar in morphology, dimensions and Congo red binding to the amyloid fibrils of Alzheimer's Aβ peptides.

The lifetime of hydrogen/deuterium exchange for hydrogens protected from rapid exchange by hydrogen bonding due to secondary structure is suited to monitoring by mass spectrometry. This revealed that for H1 and 104HI, the 7-8 residues involved in the slowly exchanging β-sheets were identical for both peptides, whereas peptide H2 (MLGSAMSRPMMHF, residues 129-141) showed a reduced half-life consistent with this peptide being predominantly coiled.

The conformations of peptides in the solid state can be studied by infrared spectroscopy. For unstructured regions of a peptide or protein, the frequencies of the carbonyl bond vibrations that contribute 90% of the amide I absorption are 1645-1650 cm^{-1}. Dipole-dipole interactions in anti-parallel β-sheets cause a splitting of the FTIR absorption into high (~1690 cm^{-1}) and low (~1625 cm^{-1}) frequency components, the latter being the strongest. Dipole-dipole interactions in the β-sheet are disrupted by introducing ^{13}C at individual carbonyls, reducing the frequency of the vibration by ~35-40 cm^{-1}. Disruption of the transition-dipole coupling caused splitting of the low frequency peak for H1 when isotope labels were incorporated in residues Gly^{114}-Val^{121}, thus the β-sheet extends over the 8-residue region GAAAAGAV.

Solid state ^{13}C-NMR chemical shifts also characterize peptide conformations. Cross-polarization magic angle spinning NMR of ^{13}C-H1 analogs confirmed the existence of β-sheet in the same region as identified by FTIR. Upon lyophilization from HFIP, ~70% of the signal shifted to values indicative of α-helix. The helical conformation showed only limited stability and spontaneously reverted to the β-sheet form, particularly in moist air. Double ^{13}C-labeled H1 analogs are being studied by rotational resonance to measure internuclear distances of up to 8 Å, to obtain a 3-D

structure of the β-sheet. Preliminary data indicate the presence of a β-turn. H1 and longer peptides linking H1 and H2 were analyzed by high resolution proton NMR in solution in micelles of perdeutero-SDS. The chemical shifts for residues 112-122 of peptide H1 were upfield relative to random coil values, indicating α-helical characteristics that were confirmed by NOE's. The chemical shift of His^{111} was downfield, thus this was not involved in the α-helix. Thus residues 112-122 in peptide H1 (109-122) formed an α-helix when dispersed in SDS. Peptide H2 showed no tendency to form α-helix, whereas longer peptides (residues 109-141 and 90-145) embracing both H1 and H2 showed enhanced secondary structure with both regions being helical [7]. Thus helix H1 stabilizes H2, consistent with the 4-helix bundle model for PrP^C in which H1 and H2 interact through hydrophobic patch sites [3].

Due to insolubility and the difficulty of obtaining sufficient pure protein, no high resolution structures have yet been obtained by crystallography or NMR for either isoform of PrP. Peptides are particularly valuable to help substantiate aspects of theoretical models of these structures. Peptide H1 can be stable either as an α-helix or a β-sheet under a wide variety of conditions. The region of the amino acid sequence corresponding to residues 113/114-121/122, (A)GAAAAGAV(V), appears to be the most highly structured, irrespective of the conformation of the peptide (α-helix or β-sheet), its physical state (solid or solution) or the nature of any solvent. These findings further support the probable importance of region H1 and may aid the understanding of the molecular basis of the transition from PrP^C to PrP^{Sc}.

Acknowledgments

This research was supported by NIH (NS14069, AG08967, AG02132, NS22786), the American Health Assistance Foundation, the Department of Energy, the Sherman Fairchild Foundation and the Bernard Osher Foundation.

References

1. Prusiner, S.B., *Science*, 252 (1991) 1515.
2. Pan, K.M., Baldwin, M.A., Nguyen, J., Gasset, M., Serban, A. Groth, D., Mehlhorn, I., Huang, Z., Fletterick, R.J., Cohen, F.E. and Prusiner, S.B., *Proc. Natl. Acad. Sci. USA* , 90 (1993) 10962.
3. Huang, Z., Gabriel, J.M., Baldwin, M.A., Fletterick, R.J., Prusiner, S.B. and Cohen, F.E., *Proc. Natl. Acad. Sci. USA*, 91 (1994) 7139.
4. Gasset, M., Baldwin, M.A., Lloyd, D., Gabriel, J.M., Holtzman, D., Cohen, F.E., Fletterick, R. and Prusiner, S.B., *Proc. Natl. Acad. Sci. USA,*, 89 (1992) 10940.
5. Cohen, F.E., Pan, K.M., Huang, Z., Baldwin, M.A., Fletterick, R.J. and Prusiner, S.B., *Science*, 264 (1994) 530.
6. Nguyen, J., Baldwin, M.A., Cohen, F.E. and Prusiner, S.B., *Biochemistry*, 34 (1995) 4186.
7. Zhang, H, Kaneko, K., Nguyen, J.T., Livshits, T.L., Baldwin, M.A., Cohen, F.E., James T.L. and Prusiner, S.B., *J. Mol. Biol.*, 250 (1995) 514.

Peptides: Chemistry, Structure and Biology
Pravin T.P. Kaumaya and Robert S. Hodges (Eds.)
Mayflower Scientific Ltd., 1996

191
Proline: α-Helix Breaker or β-Sheet Breaker?

S.-C. Li[1,2] and C.M. Deber[1,2]

[1]*Biochemistry Research Division, Research Institute, Hospital for Sick Children, Toronto, M5G 1X8, Canada*
[2]*Department of Biochemistry, University of Toronto, Toronto, Ontario, M5S 1A8, Canada*

Introduction

Proline is known as a classic breaker of both the α-helical and β-sheet structures in water-soluble proteins and peptides. However, the Pro residue is widely distributed in the putative transmembrane (TM) domains of many protein transporters and channels, regions believed to be α-helical [1]. To address the structural features of this interesting residue as a function of molecular environment, we have studied the conformations of a series of Pro-containing model peptides in various solvents such as aqueous buffer, organic solutions, and lipid micelles. These studies reveal that proline can be a helix former in helix-promoting media, whereas its character as a β-sheet breaker is retained in both aqueous and membranous environments.

Results and Discussion

We have designed peptides of generic sequence H_2N-(Ser-Lys)$_2$-Ala-Leu-Z-Ala-Leu-Z-Trp-Ala-Leu-Z-(Lys-Ser)$_3$-OH, where Z = Ala or Pro. Peptides with 0, 1, 2, or 3 Pro residues in their corresponding hydrophobic core (underlined) are indicated ALA [2], 1P, 2P, and 3P, respectively (Table 1). Variation of Pro contents was made to examine the influence of Pro residues on peptide conformation individually as well as collectively.

Table 1. *Amino acid sequences of Pro-containing model peptides.*

Name	Pro No.	Amino Acid Sequence[a]
ALA	0	SKSK-ALA-ALA-W-ALA-KSKSKS
1P	1	SKSK-ALA-AL**P**-W-ALA-KSKSKS
2P	2	SKSK-AL**P**-AL**P**-W-ALA-KSKSKS
3P	3	SKSK-AL**P**-AL**P**-W-AL**P**-KSKSKS

[a]Peptide termini are unblocked. Single letter codes of amino acids are used.

Peptide conformations in aqueous buffer, pH 11.3, were first examined by circular dichroism (CD) spectroscopy. As shown in Figure 1a, peptide ALA, containing no prolines in its hydrophobic core, is partially α-helical at low temperatures. Introduction of proline(s) into the peptide sequence results in a complete loss of α-helicity for the

corresponding peptides 1P, 2P and 3P (Figure 1b and 1c). Moreover, peptide ALA was observed to undergo a transition from α-helix to β-sheet when the temperature is increased to *ca.* 40°C (Figure 1a). Interestingly, none of the Pro-containing peptides was able to form β-structures at elevated temperatures (Figure 1b and 1c). These results show proline to be an effective breaker of both α-helical and β-sheet structures in water.

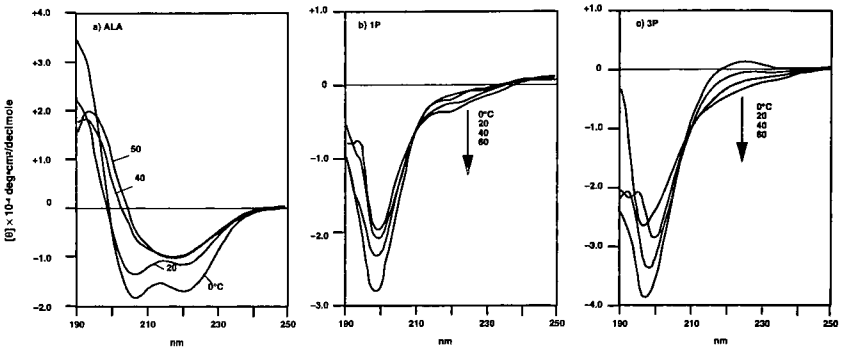

Figure 1. *Temperature dependence of peptide conformation in aqueous buffer, pH 11.3. CD spectra are shown for peptides a) ALA, b) 1P and c) 3P. Curves are as labeled. CD spectra were recorded on a Jasco-720 spectropolarimeter. Peptide concentration: 60 μM.*

The peptides were then analyzed in the membrane-mimetic environments of sodium dodecylsulfate (SDS) and lyso-phosphatidylglycerol (LPG) micelles at either pH 7.0 or 11.3 to examine the impact of the positive charges of Lys residues on peptide-lipid interactions and peptide conformation. Peptides ALA and 1P displayed significant contents of α-helicity in both micellar systems regardless of pH (Figure 2). However, peptides 2P and 3P were largely random under these conditions. These results suggest that proline can be tolerated in an α-helix, yet it is still destabilizing to the α-helical conformation in membrane environments and this destabilizing effect is additive.

Unlike lipid micelles, organic solvents provide a homogeneous, low dielectric environment which can facilitate secondary structure formation in peptides. As shown in Figure 3a, CD spectra recorded for the peptide series in 90% methanol are qualitatively similar to those in lipid systems, suggesting peptides in the latter media are likely situated at the water-micellar interface due to the short length of the hydrophobic core. Addition of salt (NaCl) into the medium of 90% methanol has minimal effect on peptide conformation except for peptide 1P, which undergoes a transition from partial α-helix to β-structure (Figure 3b). As Pro is known to promote β-turns in proteins, this transition may be mediated by the single Pro residue at the middle position of peptide 1P primary sequence such that a β-turn-β strand structure motif is formed. By this rationale, the Pro residue in peptide 1P is more likely in a β-turn conformation rather than being within the β-strands. In support of this notion is the observation that neither of peptides 2P and 3P forms β-sheets under the same conditions (Figure 3b). It is tempting to propose that the extra Pro residue(s) in the latter peptides actually participate in destabilization of the β-sheet conformation.

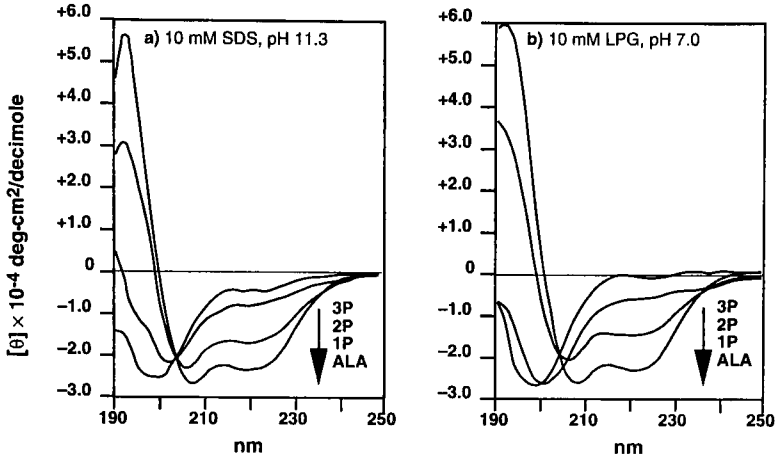

Figure 2. *CD spectra (25°C) of peptides ALA, 1P, 2P, and 3P in a) 10 mM SDS, pH 11.3, and b) 10 mM LPG, pH 7.0. Peptide concentration: 30 μM.*

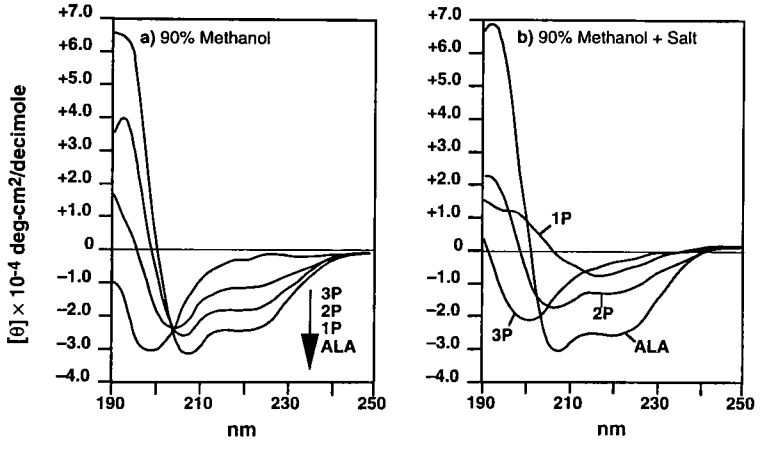

Figure 3. *CD spectra of peptides ALA, 1P, 2P, and 3P at 25°C in a) 90% methanol, and b) 90% methanol with 10 mM NaCl. Peptide concentration: 30 μM. The pH's of the solutions were ca. 4.5. Curves are as labeled on the diagram.*

The overall results suggest that proline is a prototypical β-sheet breaker in both aqueous and membrane environments, but it is not, in essence, an α-helix breaker in membranes. These characteristics of Pro may impart specific structural and functional properties to transmembrane segments of membrane proteins.

References

1. Brandl, C.J. and Deber, C.M., *Proc. Natl. Acad. Sci. USA*, 83 (1986) 917.
2. Li, S-C. and Deber, C.M., *Nature Struct. Biol.*, 1 (1994) 368.

Peptides: Chemistry, Structure and Biology
Pravin T.P. Kaumaya and Robert S. Hodges (Eds.)
Mayflower Scientific Ltd., 1996

192
Thermodynamic Model of α-Helix in Aqueous Solution and Micelle-bound State

A.L. Lomize and H.I. Mosberg

College of Pharmacy, University of Michigan, Ann Arbor, MI 48109, USA

Introduction

The theoretical model of α-helix formation presented here is the first part of a more general approach to calculation of the lowest free energy partition of peptides and proteins into elements of regular secondary structure and coil under different experimental conditions. Estimations of secondary structure stability in the method are based on unfolding free energies measured in peptide substitution and protein engineering experiments and on transfer free energies of model compounds. In the simplest case of linear peptides, considered here, when there is no intra- and intermolecular aggregation of α-helices, the lowest energy partition of peptide into helices and coil can be calculated using the dynamic programming algorithm. However, for flexible peptides, the situation is complicated by averaging of many helix-coil partitions. Recent ^{1}H NMR studies of more than a hundred peptides in aqueous solution and complexes with micelles are used here to verify the model.

Results and Discussion

The thermodynamic model of α-helix formation is based on consideration of different helix-coil partitions of a peptide molecule as conformational states for which free energies, ΔG_l, relative to the coil in aqueous solution are given by

$$\Delta G_l = G_l \sum_{i=1}^{N} \Delta G_i^{\alpha}$$

where ΔG_i^{α} is the helix-coil free energy difference for helix i from the l-th partition. The additivity of helix energies works as long as the helices do not interact with each other.

The energy expression for the α-helix in aqueous solution, ΔG_i^{α}, is a sum of mainchain enthalpy and entropy per residue contributions for the "host" polyAla peptide (ΔH and ΔS), the $\Delta\Delta G_{Ala \to X}$ free energy differences for individual residues in middle helix, N-cap, N-turn, and C-turn positions, and contributions of electrostatic, hydrogen-bonding and hydrophobic interactions between sidechains. Most of the sidechain parameters were taken or estimated from published protein engineering and peptide substitution data. Hydrophobic interactions between side chains were estimated based on decrease of their accessible surfaces.

For a micelle bound peptide, relative free energies of helix-coil partitions, can be approximately given by

$$\Delta G_l = \sum_i \Delta G_i^{\alpha} + \sum_j \Delta G_j^{coil}$$

where the energy of every micelle bound helix, ΔG_i^{α} , is the sum of the helix-coil free energy difference in aqueous solution plus an additional term describing transfer of the helix from aqueous solution to the micelle interior:

$$\Delta G_{lip} + \min_{k,n,\varphi,\omega}\{ \sum_{\substack{j=k \\ j \in A(\varphi,\omega)}}^{n} \Delta G_{tr,j}^{sch}\}$$

where ΔG_{lip} is the "detergent perturbation energy" due to embedding of the helix into a micelle, ΔG_{tr}^{sch} are water-cyclohexane transfer energies of sidechain analogs, corrected for their burial in the helix, A(φ,ω) is the set of buried residues from the helix arc whose position and size are defined by the angles φ and ω, and the residue numbers *k* and *n* define the fragment of the helix *i* which is immersed into the micelle. The immersed fragment of the helix *i* and its equilibrium rotational orientation at the water-micelle interface are calculated by optimization of the total transfer energy with respect to the *k*, *n*, φ, and ω variables. The size of the helix arc, ω, and the length of the micelle-incorporated helix fragment are related by the geometrical hydrophobic matching condition.

The energy expression for bound coil, ΔG_j^{coil}, was based on consideration of different coil configurations with buried or solution exposed side chains which reflect the tendency of all hydrophobic side chains in the coil to be buried in the micelle, but in which "anchoring" of the hydrophilic mainchain at the water-micelle interface does not allow burial of more than two sequential side chains.

After calculation of helix-coil free energy differences (ΔG^{α}) and energy of bound coil (ΔG^{coil}) for every fragment of peptide chain, occupancies P_i of every helix turn from residue *i* to *i+2* were calculated using two averaging models: (1) Boltzman averaging of all partitions containing one and two helices; (2) two state equilibrium of the lowest energy partition and coil. The fragments of peptide molecule with occupancy P_i exceeding a detectability cutoff P_d were considered as helical and compared with helices identified by ^{1}H NMR spectroscopy by the presence of medium range i/i+3,4 NOEs (next page).

The following parameters of the model provide the best fit of calculated and NMR spectroscopy detected helices: for peptides in aqueous solution, ΔH = -1.1 kcal/mol, ΔS = 3.8 cal/mol/K, P_d = 0.25; for peptides in complexes with micelles, ΔH = -1.15 kcal/mol, ΔS = 3.95 cal/mol/K, ΔG_{lip} = 1.2 kcal/mol; P_d = 0.30. Parameters of bound coil indicate that coil fragments do not compete significantly with helices for binding with micelles.

The calculated (bold) and experimentally detected (underlined) helices for peptides in complexes with micelles are shown below.

Annexin -AQWD **ADELRAAMKGL** GTD **EDTLIEILASR** TNK
Mitochondrial presequence ML S **LRQSIRFF** KPATRTLCSSRYLL
Mitochondrial ALDH signal peptide M **LRA ALSTARRLSRLLSY** A-
Mellitin G **IGAVLKVLTTGLPALISWIKRK** RQQ-
Glucagon HSQGTFTSDYSKYLDS RR **AQDFVQWLMN** T
Histocompatibility complex derived peptide GN **EQSFRV DLRTLLR** Y A
Glucagon-like peptide HAEGTFT SNVSSYL **EGQ AAKEFIAWLVK** G R-
Calcitonin CSNLS **TCVLGKLSQELHKLQ** TY PRTNTGSGTP-
M13 Coat protein
AEGD**DPAKAAFNSLQASA**TE YIG**YAWAMVVVIVGATIGIKLFKKF**TSKAS
T4 lysozyme 1-13 M **NIFEMLRID** EGL
Bombolitin III IK I **MDILAKLGKVLAH** V
Dynorphin A (1-17) YG **G FLRRIR PKLK** WDNQ
L6L8 OmpA peptide MKK **TALALAVALAGFATVAQA A** PKD
des-8 OmpA peptide MKKT **AIAAVALAGFATVAQAA** PKD
des-6-9 OmpA peptide MKK **TAVALAGFATVAQAA** PKD
β-endorphin (12-26) T **PL VTLFKNAI** IKNA
bacteriorhodopsin 34-65 VSDPDAK **KFYAITTLVPAIAFTMYLSMLL** GYG
1-35 -QAQITGR **PEWIWLALGTALMGLGTLYFLV** KG MGVSD
hGRF fragment 15-32 GQL **S ARKLLQDILSR** QQG-
Uteroglobin (18-47) PSSYETSLKEFEPD **DTMKDAGMQMKK V** LDS
Eledoisin -EPS **KD AFI** GLM- Substance P RPK **PQQFFGLM**-
Lysozyme 59-81 TKDE **AEKLF** N **QDVDAAVRGILR** N
Thiolase 1-21 M **ALLRGVFIVAAKR** TPFGAYG
Met-Enkephalin YGGFM Bradykinin RPPGFSPFR
Retro-Bombolitin I V **H ALVKGLKALMTTIK** I-
Antihemophilic factor peptide TR **YLRI** H **PQSWVHQIALRM E** VL

For the total of 77 peptides in aqueous solution (34 NMR detected helices) and 28 peptides in complex with micelles (31 NMR detected helices), the thermodynamic model correctly predicts 91% and 88%, respectively, of the helix or coil states if Boltzmann averaging is used. For the two state model, correctly predicted states are 87% and 83% for peptides in aqueous solution and in complex with micelles, respectively. A number of unstable helices in aqueous solution were not detected with the two state model because corresponding experimentally observed NOEs arise from averaging of different helix-coil partitions with similar energies.

Acknowledgments

Financial support from NIH grants DA03910 and DA00118 is gratefully acknowledged.

Peptides: Chemistry, Structure and Biology
Pravin T.P. Kaumaya and Robert S. Hodges (Eds.)
Mayflower Scientific Ltd., 1996

193
Tilted and Twisted Peptide Structures

M. Goodman, H. Shao, X. Jiang and P. Gantzel

Department of Chemistry and Biochemistry University of California, San Diego, La Jolla, CA 92093, USA

Introduction

The amide bond, the fundamental linkage of peptides and proteins, can adopt *cis* or *trans* conformations by a partial π-electron delocalization between carbonyl and amide units to maintain a coplanar and rigid linkage among the four adjacent bonded atoms. The *cis-trans* isomerization of amide bonds involves a high energy barrier (16~22 kcal/mol) and it is important in many processes that require alternation to protein structures. It has been proposed that the *cis-trans* isomerization involves an unstable transition state in which the planar arrangement present in the ground state is distorted by twisting or tilting. The unstable nature of this transition state has made it difficult to study. In order to investigate the complicated biophysical mechanism of amide rotation in peptides, we designed linear peptidomimetics that contain stable tilted or twisted amides to obtain accurate information on their structures [1].

Results and Discussion

We have synthesized a series of aziridine-containing model amino acid and dipeptide derivatives using the published methods (Figure 1). The presence of the aziridine ring was expected to induce specific conformational preferences in peptide backbones. Based on the Brown's definition of tilt and twist angles of an amide [4], the constrained aziridine structure forces the pyramidation and rehybrization of the nitrogen from sp^2 toward sp^3-like geometry. The N-pyramidization generates a net tilt angle of the lone pair away from the normal perpendicular position to the plane of carbonyl and nitrogen atoms. Along with this tilt, a rotation of the lone pair from the parallel position to the π-electron pair of the carbonyl group can occur to produce a twist angle.

In the X-ray diffraction studies of **1** and **2** (see the aziridine central part of the crystal structures, Figure 2), structure **1** adopts a tilt angle of 37° and twist angle of 7° in the urethane group. In the crystal structure of **2**, the amide bond to the aziridine ring generates tilt angle of 38° and a twist angle of 15°. These amide distortions were also maintained in solution as shown by ^{13}C-NMR experiments [2, 3]. The characteristic chemical shifts of carbonyl groups of amides in peptides fall between 175ppm and 167ppm. As a consequence of the tilt and twist angles, the carbonyl group attached to the aziridine nitrogen is more ketone-like, which is revealed in the ^{13}C-NMR spectra by a down field chemical shift. It is believed that the tripeptide **3** adopts the similar distorted amide form in the aziridine region.

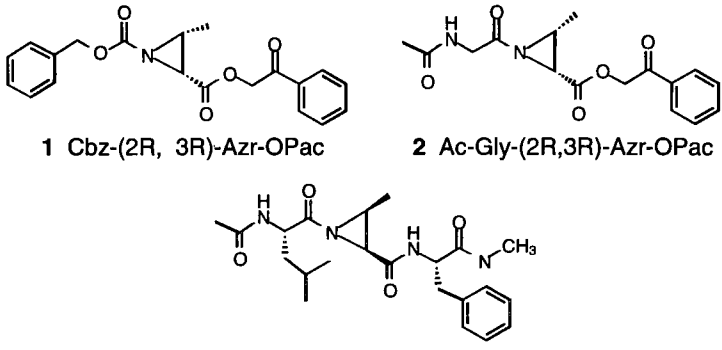

Figure 1. *The representative aziridine-containing amino acid and peptide derivatives.*

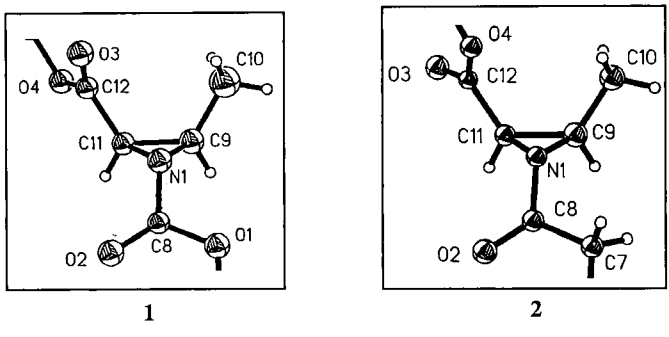

Figure 2. *The X-ray structures of the tilted and twisted amide bonds in the aziridine central part of compound 1 and 2.*

We have shown that the quite stable tilted and twisted amides based on an aziridine structure can be synthesized. Currently, we are working on the binding assay of some aziridine-containing model compounds for peptidyl-prolyl rotamase activities.

References

1. Shao, H., Jiang, X., Gantzel, P. and Goodman, M., *Chem. and Biol.*, 1 (1994) 231.
2. Kuyl-Yeheskiely, E., Lodder, M.,Vandermarel, G.A. and Vanboom, J.H., *Tetrahedron Lett.*, 33 (1992) 3013.
3. Korn, A. Rudolphbohner, S. and Moroder, L., *Tetrahedron Lett.*, 50 (1994) 1717.
4. Bennet, A.J., Wang, Q.P., Slebockatilk, H., Somayaji, V. and Brown, R.S., *J. Am. Chem.Soc.*, 112 (1990) 6383.

Peptides: Chemistry, Structure and Biology
Pravin T.P. Kaumaya and Robert S. Hodges (Eds.)
Mayflower Scientific Ltd., 1996

194

An $Ala^2 \rightarrow Thr^2$ Modification in Bovine GRF Leads to a More Rigid N-terminus: Possible Correlation with Decreased *in vitro* GH-releasing Activity

T.M. Kubiak, D.A. Kloosterman, T.A. Scahill, W.C. Krueger, M.D. Prairie and R.A. Martin

The Upjohn Company, Kalamazoo, MI 49001, USA

Introduction

An $Ala^2 \rightarrow Thr^2$ modification in GRF displays a dual effect: (i) provides resistance to proteolytic cleavage by dipeptidylpeptidase-IV, the main plasma enzyme degrading Ala^2-containing GRFs from various species, and (ii) leads to a greatly reduced *in vitro* GH-releasing activity [1]. An additional replacement of Gly^{15} with Ala^{15} in the Thr^2-format was only marginally effective in improving the *in vitro* GH-releasing activity [1] even though the Ala^{15}-modification itself led to a significant potency enhancement [1, 2]. We decided to examine solution conformations of [Leu^{27}]bGRF(1-29)NH_2 (parent peptide, **1**, its Ala^{15} counterpart **2** as well as Thr^2- **3** and Thr^2,Ala^{15}- **4** modified analogs of **1** with the hope of finding some structural differences which could explain the greatly reduced *in vitro* activity resulting from the Thr^2 substitution.

Results and Discussion

CD studies indicated that the Thr^2 for Ala^2 substitution did not affect the overall α-helix forming potential. More α-helix was induced in the Ala^{15}-modified GRF analogs **2** and **4** as compared with their respective Gly^{15}-containing counterparts in the presence of 0-40% methanol (Table 1). ^1H NMR studies in 35% TFE in sodium phosphate buffer pH 4

Table 1. *CD analysis of GRF analogs in 10 mM sodium phosphate buffer pH 7.4 in the presence of various methanol concentrations.*

Analog	% α-Helix[a]				
	0% MeOH	20% MeOH	40% MeOH	60% MeOH	80% MeOH
1	12 ± 3	38 ± 4	70 ± 5	85 ± 6	114 ± 12
2	25 ± 3	62 ± 4	80 ± 5	86 ± 6	90 ± 12
3	14 ± 3	38 ± 4	70 ± 5	85 ± 6	119 ± 12
4	25 ± 3	60 ± 4	75 ± 5	83 ± 6	106 ± 12

[a] % α-Helix was calculated by the method of Chen *et al.* [4].

revealed a highly helical secondary structure of **4** which was generally similar to that of **1** [3] but differed by (i) an increased stability of the α-helix in the region of residues 9-29 due to the Ala^{15} substitution, and (ii) stabilization of a non-random irregular secondary structure in the N-terminal region (residues 1-8) due to the presence of Thr^2, rendering this part of the molecule more rigid. This is in contrast to the parent peptide whose N-terminus seemed to be more flexible. A greater degree of α-helical structure for **4** relative to **1**, most likely due to the Ala^{15} substitution, was also seen by NMR for the region of residues 4-9, as evidenced by $C\alpha H_i$ - NH_{i+3} NOE crosspeaks in the NOESY spectrum of **4**. However, significantly higher $\Delta\delta/\Delta T$ values for Ile^5NH (11.2 *vs.* 6.0 ppb/°C) and Asn^8NH (14.0 *vs.* 8.5 ppb/°C) for **4** *vs.* **1** suggest that these NHs are more solvent exposed in **4** than in **1**. This is the opposite of that expected for a pure equilibrium between helical and random conformers in **4** for which the degree of helicity was found to be enhanced. We infer that non-helical, non-random N-terminal (residues 1-8) conformer populations in **4** are present which are due to the Thr^2 substitution rather than to Ala^{15}. Other ^1H NMR data pointing to a greater rigidity (*i.e.* less degree of random structure) for the N-terminus of **4** which might be attributed to the Thr^2 substitution include: (i) a medium strength Asp^3NH - Ala^4NH NOE in **4** *vs.* none in **1**, and medium *vs.* strong $Asp^3\alpha H$ - Ala^4NH NOEs in **4** *vs.* **1**, (ii) the significantly smaller $\Delta\delta/\Delta T$ of 6.0 ppb/°C for Thr^2NH *vs.* 14.5 ppb/°C for Ala^2NH, and (iii) a $^3J_{NH\text{-}\alpha}$ of 8.0 Hz for Thr^2NH *vs.* 6.0 Hz for Ala^2NH. Since the Ala^{15} for Gly^{15} modification has been shown to improve inherent GH-releasing activity of GRF [1, 2], it is hypothesized that the observed structural effects of Thr^2 might negatively affect the way the Thr^2-substituted GRF peptides interact with the receptor and this could be responsible for the analogs' decreased inherent GH-releasing activity.

References

1. Kubiak. T.M., Friedman, A.R., Martin, R.A., Ichhpurani, A.K., Alaniz, G.R., Claflin, W.H., Goodwin, M.C., Cleary, D.L., Hillman, R.M., Kelly, C.R., Downs, T.R., Frohman, L.A. and Moseley, W.M., *J. Med. Chem.*, 36 (1993) 888.
2. Felix, A.M., Wang, C.T., Heimer, E., Fournier, A., Bolin, D., Ahmad, M., Lambros, T., Mowles, T. and Miller, L., in Marshall, G.R. (Ed), 'Peptides: Chemistry and Biology', ESCOM, Leiden, The Netherlands, 1988, p. 465.
3. Kloosterman, D.A., Scahill, T.A., Brown, D.M., Hillman, R.M., Cleary, D.L. and Kubiak, T.M., *Peptide Research*, 4 (1991) 72.
4. Chen, Y.-T., Yang, J.T and Martinez, H.M., *Biochemistry*, 11 (1972) 4120.

Peptides: Chemistry, Structure and Biology
Pravin T.P. Kaumaya and Robert S. Hodges (Eds.)
Mayflower Scientific Ltd., 1996

195
Secondary Structure Stabilization of Peptides Using Metal Complexation

H. Yamamoto, T. Nishina, T. Obata, N. Yumoto, T. Taguchi, Y. Tatsu and S. Yoshikawa

Department of Organic Materials, Osaka National Research Institute
Agency of Industrial and Technology, Ministry of International Trade and Industry
Midorigaoka, Ikeda, Osaka 563, Japan

Introduction

Although peptides have prominent possibility as versatile functional molecules, *de novo* designs of the peptides with stable secondary structure are still problematic. Here we present a possible structure controlling method by metal complexation using bipyridyl alanine as a metal binding site.

Results and Discussion

Metal binding amino acid, S-2-amino-3-(2,2'-bipyridin-5-yl) propanoic acid (Bpa), was obtained by the published method [1-3]. To evaluate the effect on secondary structure stabilization, model peptides having two Bpa residues were synthesized by solid phase synthesis using Fmoc strategy. The amino acid sequences of the model peptides are shown in Table 1. Except for the Thr residue in BPA4, all residues other than Bpa have only an alkyl side chain to restrict the metal coordination sites to the bipyridyl groups.

Table 1. *The amino acid sequences of the model peptides containing two Bpa residues.*

Code	Sequence
BPA0	Ala-Bpa-Bpa-Ala
BPA1	Ala-Bpa-Ala-Bpa-Ala
BPA2	Ala-Bpa-Ala-Ala-Bpa-Ala
BPA3	Ala-Bpa-Ala-Leu-Ala-Bpa-Ala
BPA4	Ala-Bpa-Ala-Leu-Thr-Ala-Bpa-Ala

We have previously demonstrated that these model peptides having two Bpa residues form stable complexes with various metal ions [1, 4]. Circular dichroism studies of these peptide-complexes with metal cations indicated the possibility of controlling the secondary structure, *i.e.*, the direction of elipticity at around 310 nm (attributed to the bipyridyl groups coordinated to the metal ion) changes alternatively with increasing number of residues between the two Bpa residues [4, 5]. This spectroscopic evidence

indicates that complexation of metal ion induces the formation of chiral complexes involving both bipyridyl groups in the peptides. Thus, we tried to determine the exact structures of these peptide complexes with metal ion.

To elucidate the molecular structures of the peptide-metal complexes, 2D-NMR studies of zinc complexes were carried out. During the analyses of NOESY experiments, many long-range NOEs were observed between the residues near the N- and C-terminus. The existence of such type of NOEs clearly indicates that the peptidic chain has a turn-like structure. Although we failed to find any information about the bipyridyl groups because of the large quadrupole moment of the Zn^{2+} cation, we were able to get enough distance constraints for restrained molecular mechanics calculations. The molecular structures were determined by restrained molecular mechanics using CHARMm and QUANTA. As shown in Figure 1, the chirality around the metal center was systematicaly changed according to the number of residues between two Bpas. This result is quite consistent with the results from CD experiments.

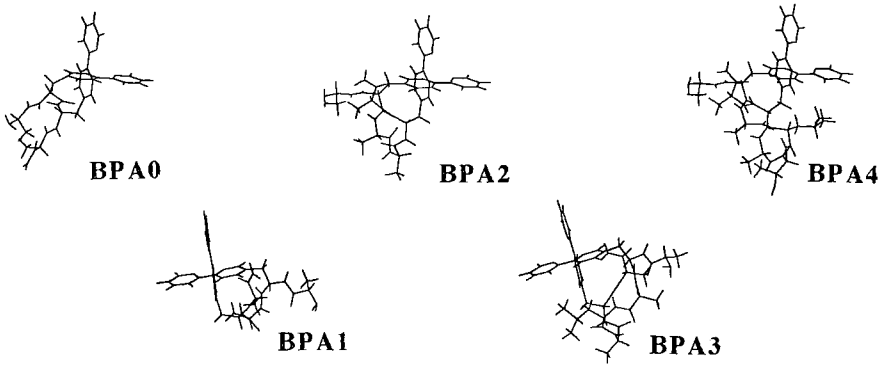

Figure 1. *Molecular structures of Zn^{2+} complexes of the model peptides.*

In conclusion, incorporation of two Bpa residues into a peptide framework has been proved to be useful in designing the three dimensional structure and various functions of *de novo* peptides, since the Bpa residue combines the wide scope of coordination chemistry with a versatile peptide chemistry.

References

1. Yamamoto, H., Nishina, T., Yumoto, N., Tatsu, Y., Taguchi, T. and Yoshikawa, S., *Peptide Chemistry*, (1993) 41.
2. Imperiali, B., Prins, T.J., Fisher, S.L., *J. Org. Chem.*, 58 (1993) 1613.
3. Imperiali, B. and Fisher, S.L., *J. Am. Chem. Soc.*, 113 (1991) 8527.
4. Yamamoto, H., Nishina, T., Ando, T., Obata, T., Yumoto, N., Taguchi, T., Tatsu, Y. and Yoshikawa, S., *Peptide Chemistry*, (1994) 461.
5. Yamamoto, H., Nishina, T., Yumoto, N. Taguchi, T., Tatsu, Y. and Yoshikawa, S., in Maia, H.L.S. (Ed.), 'Peptides 1994', ESCOM, Leiden, The Netherlands, 1994, p.541.

Peptides: Chemistry, Structure and Biology
Pravin T.P. Kaumaya and Robert S. Hodges (Eds.)
Mayflower Scientific Ltd., 1996

196
^{1}H NMR Study of the 77-100 Actin Peptide and Its Interaction with Cardiac Myosin Subfragment-1: Use of Selective ^{13}C Labeling

A. Aumelas[1], P. Eldin[2], D. Le-Nguyen[3], A.M. Cathiard[2], M. Le Cunff[2], J. Léger[2] and D. Mornet[2]

[1]*Centre de Biochimie Structurale INSERM U414, France*
[2]*INSERM U300, Faculté de Pharmacie, 15 Avenue Ch. Flahault, 34060 Montpellier, France*
[3]*INSERM U376, CHU A. de Villeneuve, 371 rue du doyen G. Giraud, 34295 Montpellier, France*

Introduction

The actomyosin interface is involved in the conversion of chemical energy in muscle contraction reviewed in [1]. The three-dimensional structure of globular and filamentous actins has been resolved [2]. Domains 3 and 4 of actin are involved in filament building whereas domains 1 and 2, located on the surface of the molecule, are able to interact with myosin. Given the involvement of the residues Arg^{95} [3], Glu^{99} and Glu^{100} [4] in actin-myosin interaction, three peptides belonging to region 77-100 of actin (TNWDDM EKIWHHTFYNELRVAPEE) have been synthesized. Their structures in solution and their interaction with cardiac myosin subfragment-1 (S1) were studied by ^{1}H NMR.

Results and Discussion

Because Ac-77-95-NH_2 aggregated in water at pH 3.2, the NMR experiments were carried out in the presence of 10% TFE. NMR data were in agreement with those obtained by CD and indicated the ability of this peptide to display a helical structure with increasing amounts of TFE. The solution structure of Ac-91-100-NH_2 and Ac-77-100-NH_2 actin peptides was examined by two-dimensional ^{1}H NMR at 600 MHz at pH 3.2 and pH 8.0 in water. Based on NMR-derived interproton distances, the structures of Ac-77-100-NH_2 were calculated and then compared with that of the corresponding fragment observed in the crystallographic structure of actin [2]. We found that three helix turns spanning 79-89 residues out of four were conserved in solution; the first one appeared loosened. In addition, the *trans* conformation of the Ala^{97}-Pro^{98} amide bond remained unchanged. These results clearly showed that the helical structure was conserved in solution.

The interaction of these three peptides with a 0.15 mM S1 solution (pH 8.0) was studied at 10°C by observing the chemical shift and line width of the aromatic signals of these peptides. In preliminary experiments, we observed a new low field Ala^{97} methyl

signal in the presence of S1. However, the increase in intensity of this signal with time was not in agreement with peptide-S1 interaction. Consequently, [methyl-^{13}C]Ala^{97} labeled Ac-91-100-NH_2 and Ac-77-100-NH_2 were synthesized to better identify this chemical shift variation by using both direct ^{1}H and ^{1}H-^{13}C-edited spectra. The ^{1}H-^{13}C-edited spectra only display the methyl signal of Ala^{97} and clearly showed that this new signal was significantly thinner than the initial one. The fact that the same behavior was observed with Ac-77-100-NH_2 and Ac-91-100-NH_2 suggested that the Arg^{95}-Val^{96} amide bond was cleaved by a trypsin-like enzyme co-purified with S1. After addition of trypsin to the peptide solutions, similar spectra were obtained and the new signal was identified as being that of the VAPEE-NH_2 pentapeptide.

In the presence of EETI II, a trypsin inhibitor, the ^{1}H-^{13}C-edited spectra showed that this cleavage was indeed reduced (Figure 1). From the line width of the peptide aromatic signals in the presence of S1, we observed that aromatic signals of Ac-91-100-NH_2 were not affected and that those of Ac-77-100-NH_2 were broader than the signals of Ac-77-95-NH_2; these data suggest a stronger interaction between S1 and Ac-77-100-NH_2.

These results allow us to conclude that the 77-92 helical part of the peptide along with Glu^{99} and Glu^{100} residues are involved in actin-myosin interaction. Using recombinant myosin fragments, we will attempt to identify the myosin residues involved in this actin-myosin interaction site.

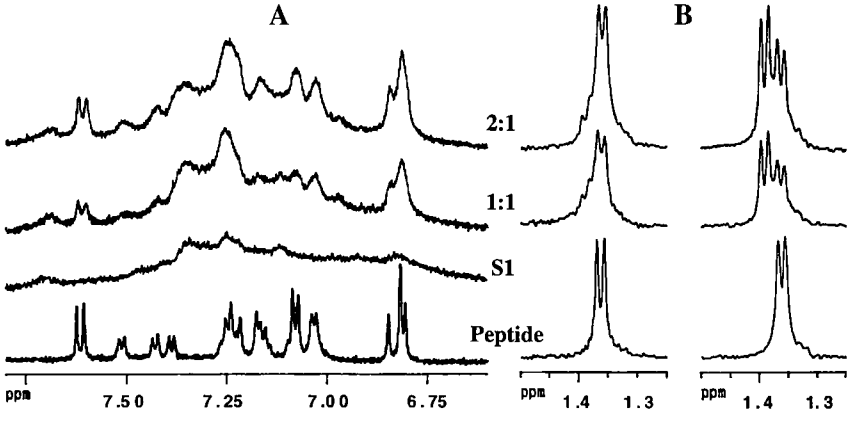

Figure 1. *^{1}H and ^{1}H-^{13}C edited spectra of the [methyl-^{13}C]Ala97 Ac-77-100-NH_2 peptide with and without cardiac myosin S1 (0.15 mM, pH 8.0, and at 10°C). Part A, low field spectra in the presence of EETI II: peptide, S1, peptide and S1 in a 1:1 and a 2:1 ratio. Part B, ^{1}H-^{13}C edited spectra of the Ala^{97} methyl signal with (left) and without EETI II (right).*

References

1. Dos Remedios, C., and Moens, P.D.J., *Biochim. Biophys. Acta*, 1228 (1995) 99.
2. Kabsch, W., Mannherz, H.G., Suck, D., Pai, E.F., Holmes, K.C., *Nature*, 247 (1990) 37.
3. Bonafé, N., Chaussepied, P., Capony, J.P., Derancourt, J., and Kassab, R., *Eur. J. Biochem.*, 213 (1993) 1243.
4. Johara, M., Toyoshima, Y.Y., Ishijima, A., Kojima, H., Yanagida, T., and Sutoh, K., *Proc. Natl. Acad. Sci. USA*, 90 (1993) 2127.

Peptides: Chemistry, Structure and Biology
Pravin T.P. Kaumaya and Robert S. Hodges (Eds.)
Mayflower Scientific Ltd., 1996

197
Conformational Studies of Irreversible HIV-1 Protease Inhibitors Containing a *cis*-Epoxide as an Amide Isostere

S. Ro, S.G. Baek, B. Lee, S.C. Kim, H. Yoon and J. Ok

Biotech Research Institute, LG Chemical Ltd. / Research Park, P.O. Box 61 Yu Sung, Science Town, Taejeon 305-380, Korea

Introduction

Our laboratories have designed and synthesized irreversible HIV-1 protease inhibitors containing a *cis*-epoxide (*i.e.* Qc-Asn-Phe [(1S,2R)-*cis*-epoxide]Gly-NH-CH(isopropyl)(X) where Qc stands for 2-quinaldic acid; X = C(O)NH(OMe), LB71097; benzyl, LB71112; isopropyl, LB71116; phenyl, LB71119) [1]. The irreversible inhibitory action of these compounds is caused by the formation of a covalent bond between HIV-1 protease and these inhibitors resulting in ring opening of the epoxide [2]. Although the epoxide ring of these inhibitors is opened in HIV-1 protease, it remains in solution where the inhibitors are recognized by the enzyme. Thus, understanding the conformational preferences of these inhibitors in solution is important for designing new target compounds in this series. In this report, we describe NMR and molecular modelling studies of these inhibitors.

Results and Discussion

The proton resonances of the inhibitors were assigned employing DQF-COSY. Vicinal coupling constants and NOE intensities were measured from 1D-spectra and ROESY experiments, respectively. The observed NMR data of the inhibitors are almost identical, indicating that conformational preferences of these compounds are similar to each other. For example, strong-medium NOEs were observed between Phe(cep) NH and the C^1H of the epoxide from the ROESY spectra of all four analogs [where Phe(cep) is the N-terminal side residue generated by the replacement of the Phe-Gly peptide bond with a *cis*-epoxide]. In addition, there is no NOE between Phe(cep) $C^{\alpha}H$ and the C^1H of the epoxide. These results indicate that the Ψ angles of Phe(cep) prefer to adopt about 140° in all of the four analogs.

Probable conformations of LB71116 were obtained from quenched molecular dynamics using DISCOVER. Starting conformations of these calculations were obtained from the MOPAC minimization of the structures which were generated from INSIGHT II or intuitively constructed on the basis of NMR data.

Among the probable conformations of LB71116, the structures complied with NMR data were selected as preferred conformations in solution. The three preferred

conformations were obtained (Figure 1). Free molecular dynamics started from each of the three preferred conformation were carried out to prove that the three conformations are in a conformational equilibrium.

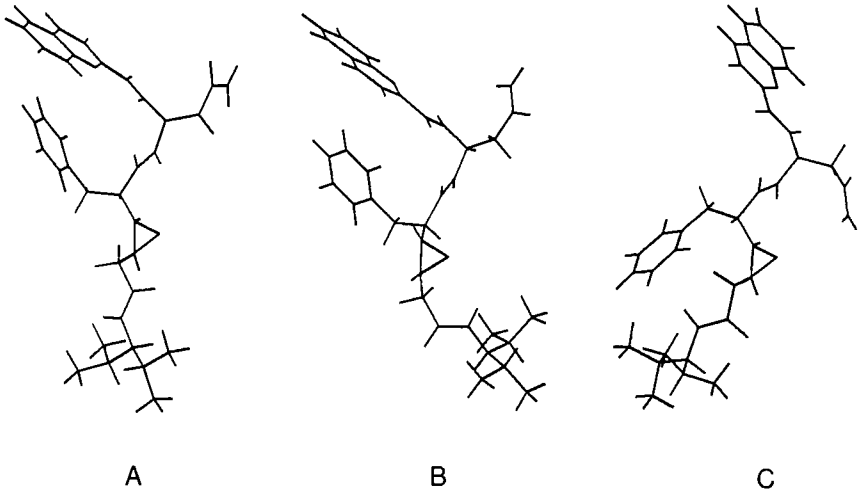

Figure 1. *Preferred conformations of LB71116.*

As seen in Figure 1, the preferred conformations of LB71116 in solution contain extended structures similar to β-sheet.

In stabilizing these conformations, the epoxide has important roles. To avoid steric hindrance with the epoxide ring, the Ψ of Phe(cep) is maintained about 140°. As mentioned, these results are supported by NMR data.

The three preferred conformations were compared with the binding conformation of LB71116 observed in the X-ray studies of LB71116/HIV-1 protease complex [2]. Although the epoxide ring is opened in this complex, the orientations of sidechains and distances among pharmacophoric groups are similar to those of the conformation A, which is energetically the most favorable among these preferred conformations. We believe that such similarity can explain high activities and selectivities of these inhibitors to the HIV-1 protease.

References

1. Kim, S.C., Choy, N., Lee, C.S., Son, Y.C., Choi, H., Koh, J.S., Yoon, H., Park, C.H., Kim, S., Patent Number EP 601486; Kim, S.C., Choy, N., Lee, C.S, Son, Y.C., Choi, H., Koh, J.S., Yoon, H., Park, C.H., Kim, S., in '10th International Conference of AIDS / International Conference of STD', Yokohama, Japan, 1994.
2. S. Kim *et al.*, unpublished data.

Peptides: Chemistry, Structure and Biology
Pravin T.P. Kaumaya and Robert S. Hodges (Eds.)
Mayflower Scientific Ltd., 1996

198
Assembly and Stability of Double- and Triple-stranded α-Helical Coiled-coil Structures of Laminin Peptides

M. Nomizu[1], A. Utani[1], A. Otaka[2], P.P. Roller[2] and Y. Yamada[1]

[1]Laboratory of Developmental Biology, National Institute of Dental Research and
[2]Laboratory of Medicinal Chemistry, DTP/DCT, NCI, National Institutes of Health, Bethesda, MD 20892, USA

Introduction

Laminins are large heterotrimeric glycoproteins specifically located in basement membranes. Several laminin isoforms have been identified with at least eight genetically distinct subunits [1]. They serve diverse biological functions including promotion of cell adhesion, growth, migration and differentiation, and influence on the metastatic potential of tumor cells [2]. Laminin-1 consists of three chains designated α1, β1 and γ1, which are held together in a triple-stranded α-helical coiled-coil structure in the long arm region and form a cruciform shaped molecule [2]. Recently, we have demonstrated that a short sequence from the carboxy-terminus of the long arm of each chain is required to initiate assembly of the laminin chains [3, 4]. Site-directed mutagenesis studies suggested that charged amino acid residues within these short sequences were important for the specific formation of double- and triple-stranded coiled-coil structures [3, 4]. Synthetic peptides, **B1** and **B2** (51-mers from the mouse laminin β1 and γ1 chains, respectively), and **M** (55-mer from the laminin α2 chain), containing these sites were found to assemble into double- and triple-stranded coiled-coil structures in a chain specific manner. The heterotrimer of the synthetic peptides showed a high thermal stability (Tm = 62°C) similar to those of the recombinant trimers (approximately 200 amino acids long for each chain) [5]. Furthermore, the hydrophobic residues, such as isoleucine in the laminin α2 and γ1 chains, were found to be crucial for stabilizing the heterotrimeric coiled-coil structure [5]. Here we focus on the mechanism of laminin assembly and examine the peptide conformation and stability under various conditions using CD spectroscopy.

Results and Discussion

The synthetic peptides, **B1**: SKLQLLEDLERKYEDNQKYLEDKAQELVRLEGEVRSL LKDISEKVAVYSTC (mouse laminin β1 chain position 1735-1785), **B2**: KASDLDRK VSDLESEARKQEAAIXDYNRDIAEIIKDIHNLEDIKKTLPTGC (mouse laminin γ1 chain position 1548-1598. Met (position 1571) was replaced with norleucine (X) and **M**: VRNLEQEADRLIDKLKPIKELEDNLKKNISEIKELINQARKQANSIKVSVS SGGD (mouse laminin α2 chain position 2095-2149) were synthesized by Boc based SPPS methodology utilizing the two-step deprotection method [6, 7].

CD spectra of the synthetic peptides **B1-B2** dimer (5 mM) and **B1-B2/M** trimer (3.3 mM) were recorded at 190 nm to 250 nm in 50 mM sodium phosphate solutions at different pH (2, 7.4 and 10) at 20°C. The **B1-B2** dimer at basic and neutral conditions (pH 7.4 and 10) showed similar CD spectra (55% and 56% α-helix, respectively), while at pH 2 the α-helicity of **B1-B2** (66%) was significantly increased. These results indicate that there are intra- and/or interchain repulsions by acidic amino acids in the **B1-B2** dimer, and these repulsions partially destroy its α-helical conformation. At acidic conditions, α-helicity of the **B1-B2/M** (50%) was lower than those of the trimer at neutral and basic conditions (69% and 67% α-helix, respectively). The CD spectrum of **B1-B2/M** was comparable to the sum of the CD spectra of **B1-B2** and **M** at pH 2. These results suggest that **B1-B2/M** is dissociated into **B1-B2** and **M** at these acidic conditions.

Next, we determined the pH dependence of the thermal stabilities of **B1-B2** and **B1-B2/M** by monitoring changes in the CD spectra (222 nm) at various temperatures. At pH 7.4, the Tm values of **B1-B2** and **B1-B2/M** were 43°C and 62°C, respectively. The thermal stabilities of the dimer and the trimer were increased at low pH. **B1-B2** and **B1-B2/M** showed the highest Tm values at pH 2 (71°C and 72°C, respectively). This suggests that **B1-B2/M** is dissociated to the dimer and monomer, and that the melting curve of **B1-B2/M** at pH 2 is primarily dependent on conformational change of the **B1-B2** dimer. While at higher pH, the Tm values for the dimer and the trimer were decreased slightly, the Tm values for **B1-B2** and **B1-B2/M**, were 39°C and 56°C at pH 10, respectively. This suggests that there are intra- and/or interchain repulsions by acidic amino acids in **B1-B2** chains. These repulsions could create a less stable double-stranded coiled-coil structure of **B1-B2** at neutral and basic conditions. At acidic conditions, the repulsions are minimized by side chain protonation of aspartic acid or glutamic acid, and the dimer is stabilized largely by hydrophobic interactions.

These findings suggest that ionic interactions between **B1-B2** dimer and **M** are critical for the formation of the triple-stranded coiled-coil structure. The intra- and/or interchain repulsions in the **B1-B2** dimer by acidic residues seem to be compensated by heterotrimeric assembly with the **M** peptide to form the triple-stranded coiled-coil structure, in which interchain ionic interactions are highly contributory.

References

1. Burgeson, R.E., Chiquet, M., Deutzmann, R., Ekblom, P., Engel, J., Kleinman, H.K., Martin, G.R., Meneguzzi, G., Paulsson, M., Sanes, J.R., Timpl, R., Tryggvason, K., Yamada, Y. and Yurchenco, P.D., *Matrix Biol.*, 14 (1994) 209.
2. Beck, K., Hunter, I. and Engel, J., *FASEB J.*, 4 (1990) 148.
3. Utani, A., Nomizu, M., Timpl, R., Roller, P.P. and Yamada, Y., *J. Biol. Chem.*, 269 (1994) 19167.
4. Utani, A., Nomizu, M., Sugiyama, S., Miyamoto, S., Roller, P.P. and Yamada, Y., *J. Biol. Chem.*, 270 (1995) 3292.
5. Nomizu, M., Otaka, A., Utani, A., Roller, P.P. and Yamada, Y., *J. Biol. Chem.*, 269 (1994) 30386.
6. Nomizu, M., Inagaki, Y., Yamashita, T., Ohkubo, A., Otaka, A., Fujii, N., Roller, P.P. and Yajima, H., *Int. J. Peptide Protein Res.*, 37 (1991) 145.
7. Nomizu, M., Utani, A., Shiraishi, N., Yamada, Y. and Roller, P.P., *Int. J. Peptide Protein Res.*, 40 (1992) 72.

Peptides: Chemistry, Structure and Biology
Pravin T.P. Kaumaya and Robert S. Hodges (Eds.)
Mayflower Scientific Ltd., 1996

199
Restrained Molecular Dynamics of RGD-containing Cyclic Peptides Using Time-averaged NOEs

A.C. Bach, II[1], S.X. Tang[1], J.R. Espina[1], P.F.W. Stouten[1], W.F. DeGrado[1], J. Fennen[2], A.E. Torda[2], A.P. Nanzer[2] and W.F. van Gunsteren[2]

[1]*The DuPont Merck Pharmaceutical Company, Experimental Station, Wilmington, DE 19880, USA*
[2]*Department of Physical Chemistry, Swiss Federal Institute of Technology Zürich, 8092 Zürich, Switzerland*

Introduction

We have previously analyzed NMR data with a computational protocol which combines distance geometry and energy minimization (DG/EM) to examine the solution conformations of several novel RGD-containing cyclic peptides which are active as $GP^{IIb/IIIa}$ receptor antagonists [1]. We are now extending this work using time-averaged molecular dynamics (MD) calculations where the NOE constraints are satisfied over an average time period rather than in a static manner. Here, we present our first results from time-averaged MD studies on *cyclo* (D-Ala-Arg-Tyr-Asp-Mamb) **1** (Mamb, *m*-amino methyl benzoic acid). Although similar in composition to the tightly binding *cyclo*(D-Abu-N-Me-Arg-Gly-Asp-Mamb) **2**, **1** is not active in the $GP^{IIb/IIIa}$ receptor binding assay [2]. The lack of activity could either be caused by the steric bulk of the Tyr residue or **1** may fail to adopt a backbone conformation consistent with binding. We wanted to investigate whether **1** could adopt the active backbone conformation found in **2** using both the DG/EM and time-averaged NOE methods.

Results and Discussion

NMR analysis of **1** in DMSO-d6 at 25°C produced 20 useful NOEs which were used as calculated upper and lower bounds. 500 DG conformations were generated using this set of NOEs. After two energy minimization steps and a $J_{NH\alpha}$ coupling constant check, 28 conformations remained which clustered into two families. Neither conformation was similar to the solution conformation of **2**.

The centroid conformations of the two DG/EM families were used as the starting conformations for two time-averaged MD calculations. Each started with 10 ps of equilibration time-averaged MD, followed by 220 ps of time-averaged MD, both steps using the GROMOS suite of programs [3]. NOE upper and lower bounds were not used in this calculation, the distance derived from each NOE was used as constraints. A united atom approach was used for all methylenes which reduced the number of

constraints to 16 [3]. Analysis of the distance violations at 2 ps intervals over the time course of the calculations showed that both reached a reasonable level of convergence after 50 ps. The final 60 conformations (120 ps) were used for analysis from each calculation.

Cluster analysis of 28 final DG/EM conformations combined with the last 60 conformations from both MD trajectories (148 total conformations) yielded four conformational families. Cluster 1 contains a mixture of DG/EM and MD run 1 conformations. Its centroid conformation contains γ-turns centered on the Asp and Arg residues. Cluster 2 contains a mixture of DG/EM and MD run 2 conformations. Its centroid conformation contains a type II' β-turn centered at D-Ala-Arg and a γ-turn centered at Asp. This conformation is very similar to that found for **2** in both its NMR and crystal structures (see Table 1) [1]. Cluster 3 only contains conformations from MD run 2. Its centroid conformation contains a γ-turn centered on Arg and an inverse γ-turn centered at Asp. The latter is the only difference between cluster 3 and cluster 1 and may be artificially caused by not running the MD calculation long enough. Cluster 4 only contains DG/EM conformations. The members of this cluster all exhibit a very different backbone conformation which contain very few observable regular secondary structures.

Table 1. *ϕ and Ψ angles from the centroid conformations of 1 and 2.*

Centroid	D-Ala/D-Abu		Arg		Tyr/Gly		Asp	
conformation	ϕ	Ψ	ϕ	Ψ	ϕ	Ψ	ϕ	Ψ
1 c1	130	-111	-88	40	-140	55	37	-60
1 c2	58	-137	-95	77	173	156	-75	99
1 c3	127	-100	-84	-42	-54	132	-49	74
1 c4	159	-71	-150	40	-164	-72	-145	-80
2 NMR	52	-112	-117	55	-143	-161	-74	94
2 x-ray	55	-113	-107	36	-118	-144	-94	93

In conclusion, cluster 2 shows that **1** can adopt a backbone conformation similar to that of **2**. This backbone conformation was only observed using time-averaged MD calculations. The time-averaged MD failed to find conformations similar to cluster 4. These preliminary results suggest the DG/EM approach may be generating unrealistic virtual conformations. The lack of biological activity for **1** thus appears related to steric restrictions imposed by $GP^{IIb/IIIa}$ rather than an inactive backbone conformation.

References

1. Bach, II, A.C. , Eyermann, C.J., Gross, J.D., Bower, M.J., Harlow, R.L., Weber, P.C. and DeGrado, W.F., *J. Amer. Chem. Soc.*, 116 (1994) 3207.
2. Jackson, S., Degrado, W., Dwivedi, A., Parthasarathy A., Higley, A., Krywko, J., Rockwell, A., Markwalder, J., Wells, G., Wexler, R., Mousa, S. and Harlow, R., *J. Amer. Chem. Soc.*, 116 (1994) 3220.
3. van Gunsteren, W. F. and Berendsen, H.J.C., 'Groningen Molecular Simulaton (GROMOS)', Biomos, Groningen, The Netherlands, 1987.

Peptides: Chemistry, Structure and Biology
Pravin T.P. Kaumaya and Robert S. Hodges (Eds.)
Mayflower Scientific Ltd., 1996

200

Biophysical Studies of the Combined ET_A/ET_B Endothelin Receptor Antagonist Ac-DBhg[16]-Leu-Asp-Ile-NMeIle-Trp[21] (PD 156252) Suggest Structural Features Relevant to the Increased Metabolic Stability

W.L. Cody[1], M.D. Reily[1], J.X. He[1], B.H. Stewart[2], E.E. Reynolds[3] and A.M. Doherty[1]

Departments of [1]Chemistry, [2]Pharmacokinetics and Drug Metabolism and [3]Cardiovascular Therapeutics, Parke-Davis Pharmaceutical Research, Division of Warner-Lambert Company, 2800 Plymouth Road, Ann Arbor, MI, 48105, USA

Introduction

The endothelins (ETs) are potent constrictors of vascular smooth muscle. The ETs possess a hydrophobic C-terminal hexapeptide that has been utilized to develop potent antagonists, such as PD 142893 (Ac-DDip[16]-Leu-Asp-Ile-Ile-Trp[21], Dip = 3,3-diphenyl-alanine) [1] and PD 145065 (Ac-DBhg[16]-Leu-Asp-Ile-Ile-Trp[21], Bhg = 10,11-dihydro-5H-dibenzo [a,d] cycloheptene glycine) [2]. Both of these compounds exhibited low nanomolar affinity for the ET_A (40 and 3.5 nM, respectively) and for the ET_B receptor (60 and 15 nM, respectively) and antagonized ET-stimulated vasoconstriction *in vitro*. Unfortunately, PD 142893 and PD 145065 have relatively short half-lives (18.1 and 10.6 min., respectively), in rat intestinal perfusate [3]. We have shown that incorporation of NMeIle in position 20 results in analogues that maintain high affinity for the ET receptors and have enhanced metabolic stability. In particular, Ac-DBhg[16]-Leu-Asp-Ile-NMeIle-Trp[21] (PD 156252) has low nanomolar affinity for both ET receptors (ET_A; 1.0 nM/ ET_B; 40 nM) and exhibits greatly enhanced stability (538 +/- 52 min) in rat intestinal perfusate. Interestingly, proton NMR and molecular modeling studies of the disodium salt of PD 156252 reveals that in an aqueous environment the molecule exists in a fully extended conformation while in DMSO it adopts a strikingly different conformation. The NOE patterns indicate that a geometric isomerization about the Ile[19]-NMeIle[20] imide bond takes place upon changing from a hydrophilic to a hydrophobic medium.

Results and Discussion

The proton NMR spectra of PD 156252.2Na differs dramatically dependent upon the solvent. In particular, in water the spectrum is characterized by a large degree of dispersion in the methyl region with the γ-methyl protons of Ile[19] at exceptionally high field (0.18 ppm), while in DMSO the dispersion collapses in the methyl region and is replaced by significant dispersion in the amide region. In fact, NOE measurements have

shown that these spectral changes can be attributed to geometric isomerization around the Ile^{19}-$NMeIle^{20}$ peptide bond. Thus, in water this imide bond is *trans* and the peptide takes on an extended conformation, while in DMSO this bond is completely *cis* and the peptide prefers a more compact structure (Figure 1).

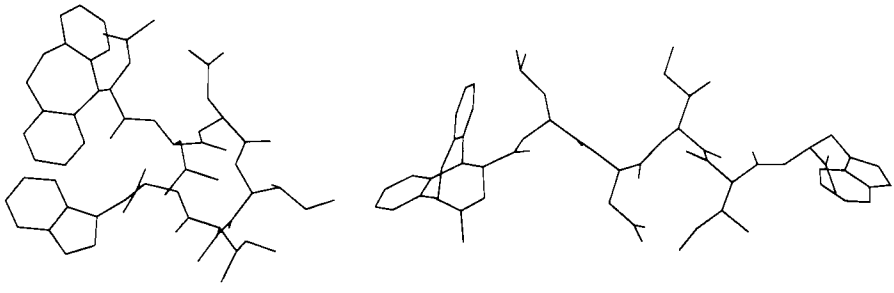

Figure 1. *Calculated structure of PD 156252.2Na in DMSO (right) and a hypothetical extended structure of PD 156252.2Na in water (left).*

These observations may have implications on the increased half-life of PD 156252 observed in rat intestinal perfusate. It has been shown that the major metabolite of PD 145065 is Ac-DBhg-Leu-Asp-Ile-Ile, probably as a result of carboxypeptidase activity [4]. In fact, carboxypeptidase inhibitors have been shown to increase the half-life of PD 145065 by 75% in rat intestinal perfusate [5]. Currently, the structure of PD 156252 under physiological conditions is not known. However, since the barrier of *cis/trans* interconversion is demonstrably lower for PD 156252 it may be hypothesized that this "alternative conformation" would render the C-terminus less accessible to carboxypeptidase activity, thus accounting for the enhanced metabolic stability while maintaining high receptor affinity. Likewise, it is also possible that methylating the p-1 amino acid of a substrate leads to an analogue that does not fit properly into the enzyme, either sterically or by disruption of a critical hydrogen bonding interaction. These observations may provide a unique strategy for the preparation and delivery of metabolically stabilized peptides.

References

1. Cody, W.L., Doherty, A.M., He, J.X., DePue, P.L., Rapundalo, S.T., Hingorani, G.A., Major, T.C., Panek, R.L., Dudley, D.T., Haleen, S.J., LaDouceur, D., Hill, K.E., Flynn, M.A. and Reynolds, E.E., *J. Med. Chem.*, 35 (1992) 3301.
2. Cody, W.L., Doherty, A.M., He, J.X., DePue, P.L., Waite, L.A., Topliss, J.G., Haleen, S.J., LaDouceur, D., Flynn, M.A., Hill, K.E. and Reynolds, E.E., *Med. Chem. Res.*, 3 (1993) 154.
3. Cody, W.L., He, J.X., Doherty, A.M., DePue, P.L., Kaltenbronn, J.S., Reisdorph, B.R., Walker, D.M., Welch, K.M., Haleen, S.J., Reynolds, E.E., Tse, E., Reyner, E.L. and Stewart, B.H., in Maia, H.L.S. (Ed.), Peptides 1994, ESCOM, Leiden, The Netherlands, 1995, p. 38.
4. Stewart, B.H., Reyner, E.L., Tse, E., Hayes, R.N., Cody, W.L. and Doherty, A.M., *Pharm. Res.*, 11 (1994) S-257.
5. Stewart, B.H. and Reyner, E.L., personal communication, 1995.

Peptides: Chemistry, Structure and Biology
Pravin T.P. Kaumaya and Robert S. Hodges (Eds.)
Mayflower Scientific Ltd., 1996

201
Conformational Analysis of Lactam-containing Analogs of the *Saccharomyces cerevisiae* α-factor

W. Yang[1], O. Antohi[1], H.R. Marepalli[1], J.M. Becker[2] and F. Naider[1]

[1]*Department of Chemistry, The College of Staten Island, The City University of New York, Staten Island, NY 10314, USA*
[2]*Department of Microbiology, University of Tennessee, Knoxville, TN 37996, USA*

Introduction

The *Saccharomyces cerevisiae* peptide pheromone, α-factor(WHWLQLKPGQPMY), has been suggested to assume a bent form as its biologically active structure [1, 2]. Constrained analogs of α-factor containing a covalent bond that force the middle of this pheromone into a turn, such as *cyclo*^{7,10}[Lys^7, Glu^{10}, Nle^{12}]α-factor (**C42**) and *cyclo*^{7,10}[Orn^7, Glu^{10}, Nle^{12}]α-factor (**C32**) manifested very different bioactivities. Specifically, **C42** was 20 times more potent than **C32** in the growth arrest assay against strain *RC629* [3]. In order to discern whether these different biological potencies were related to the conformation of the lactam ring in the center of these pheromones, we analyzed these peptides using NMR and CD techniques and modeled their structures using Boltzmann searches and AMBER minimization. For comparison, similar investigations were also carried out on two model tetrapeptides *cyclo*^{1,4}[Ac-Lys-Pro-Gly-Glu-NH_2] (Tetra **42**) and *cyclo*^{1,4}[Ac-Orn-Pro-Gly-Glu-NH_2] (Tetra **32**).

Results and Discussion

The conformations of *cyclo*^{7,10}[Lys^7, Glu^{10}, Nle^{12}]α-factor (**C42**) and *cyclo*^{7,10}[Orn^7, Glu^{10}, Nle^{12}]α-factor (**C32**) were studied in DMSO-d_6 using NMR spectroscopy. The assignment of all observed resonances was based on the combined use of COSY, TOCSY, NOESY or ROESY experiments. The temperature coefficients (dδ/dT) of the amide protons for the Glu^{10} αNH of **C32** (-0.06 ppb/K) and the Glu^4 αNH of Tetra **32** (-0.9 ppb/K) indicated that both protons were involved in a strong intramolecular hydrogen bond. In the Lys-containing peptides (**C42** and Tetra **42**), a strong intramolecular hydrogen bond was not detected. However, the relatively small dδ/dT values observed for the Gly NH of **C42** and Tetra **42** (-3.1 ppb/K) were consistent with weak but significant hydrogen bonding for this proton.

Models of the studied peptides were built with the BIOPOLYMER module of the SYBYL software package, and searched using an iterative constrained annealing procedure based on the measured NOE restraints. The resulting models were minimized

with the AMBER force field and the conformers best fitting the experimental data were identified. The analysis of these structures reveals the following: 1) The turn regions in the two 13mers adopt conformations similar to those of the corresponding tetramer cyclic compounds. 2) The proline dihedral angles in the **42** compounds seem to accommodate a seven membered ring comprising the Gly NH hydrogen bonded to the carbonyl of Lys, very similar to that encountered in the center of a γ' turn. This is consistent with the fact that the Gly NH has the lowest temperature coefficient of all amide protons in these molecules. 3) Another feature of the **42** molecules is that the Gly residue is less bent. Consequently, the NH of Glu points to the outside of the ring. This is consistent with the high temperature coefficient observed for this proton. 4) In the models of the **32** compounds the Glu NH appears to form a bifurcated hydrogen bond to both the Pro carbonyl (forming a γ-turn like seven membered ring) and to the Lys carbonyl (forming a type II β-turn like 10 membered ring). Both the quantitative NMR data and the ensuing computational analysis support the fact that the conformation realized in the 13mer is closer to a β-turn, while that in the tetramer is closer to a γ-turn like ring. 5) A notable difference between the **32** and **42** compounds is the orientation of the side chain amide group. In the **32** molecules the side chain carbonyl points towards the same side of the ring as the Pro carbonyl, and in the **42** molecules the side chain carbonyl points toward the opposite direction.

Since this γ-carbonyl has been previously shown to be a critical element for the α-factor activities [3], it is significant that the Glu γ-carbonyl in the less active analog (**C32**) has a very different orientation from that in the more active analog (**C42**). The data suggests that **C32** may be less active because the γ-carbonyl of Glu in this molecule is in a position that differs from that present in the biologically active conformation. These results help to refine our understanding of the stereochemical requirement for the central region of the pheromone.

Acknowledgments

This study was supported by grants from the National Institutes of Health (GM 22086 and GM 22087).

References

1. Xue, C.-B., Eriotou-Bargiota, E., Miller, D., Becker, J.M. and Naider, F., *J. Biol.Chem.*, 264 (1989) 19161.
2. Gounarides, J.S., Xue, C.-B., Becker, J.M. and Naider, F., *Biopolymers*, 34 (1994) 709.
3. Yang, W., McKinney, A., Becker, J.M. and Naider, F., *Biochemistry*, 34 (1995) 1308.
4. Stroup, A.N., Rockwell, A.L., Gierasch, L.M., *Biopolymers*, 32 (1992) 1713.

Peptides: Chemistry, Structure and Biology
Pravin T.P. Kaumaya and Robert S. Hodges (Eds.)
Mayflower Scientific Ltd., 1996

202
Reverse Micelles as Membrane Mimicking Environment in Conformational Studies

D. Quarzago and L. Moroder

Max-Planck-Institut für Biochemie, 82152 Martinsried, Germany

Introduction

In order to mimic cell membrane environments, conformational analysis of bioactive peptides is generally performed in TFE or surfactant micelles. The use of phospholipid bilayers as more proper mimicry is severely limited by poor solubility of the lipids, particularly if higher concentrations of peptides are required for spectroscopic experiments. The search for an alternative two-phase system led us to reverse micelles which are frequently used in protein chemistry [1], but which have rarely been employed in conformational studies. For comparative analysis of the various membrane mimetic environments, the gastrointestinal hormone secretin was used as model peptide [2].

Results and Discussion

Secretin was shown to interact with the zwitterionic DMPC vesicles (lipid/peptide molar ratio = 90) by microcalorimetric measurements as the pretransition of the ripple phase is lowered by 2°C and a shoulder appears in the hs-DSC endotherm above the T_c of the DMPC. This peptide lipid interaction was further confirmed by AT-FT-IR spectra where the decreased intensities of the CH_3 and CH_2 bands reflect the disordering effect of secretin on the lipid packing of the DMPC bilayer. Nevertheless the CD spectra of secretin in presence of DMPC vesicles (lipid/peptide molar ratio = 100) indicate only a marginal increase in α-helical content which is, however, significantly enhanced in the presence of negatively charged DMPG vesicles (Table 1). Despite the higher solubility of DMPG *vs.* DMPC which allowed characterization of the conformational state of secretin in the presence of DMPG vesicles even by IR spectroscopy (Figure 1), a maximal lipid/peptide molar ratio of merely 37:1 could be achieved. As about 2000-3000 phospholipid monomers are needed to form a single vesicle, the numerical ratio of vesicle-to-peptide is very low. We have therefore analyzed the conformational properties of secretin in reverse micelles. The water pool entrapped in the hydrophobic core of reverse micells is known to show properties different from those of bulk water and to resemble the water at lipid/water interphases [1]. In fact, in reverse micelles of bis (2-ethylhexyl) sulfosuccinate (AOT)/isooctane/water secretin entrapped in water pool is folded into ordered conformations consisting of α-helix and β-turns similarly to what is observed in presence of DMPG bilayers as well documented by the CD (Table 1) and IR spectra (Figure 1). Both the DMPG vesicles and AOT reverse micelles are characterized by a negatively charged interphase. Natural cell membranes, although mainly built up by

Table 1. *CD spectroscopy data of secretin in various systems; % α-helical content was determined using* $[\theta]_{222} = 36100$ *deg cm*^{2} *dmol*$^{-1}$ *for 100% α-helix.*

System	$[\theta]_{222}$	% helix	System	$[\theta]_{222}$	% helix
phosphate buffer	9300	26	90% TFE	27800	77
DMPG vesicles	15600	43	SDS micelles	17200	48
DMPC vesicles	12400	34	AOT reverse micelles	14700	41

the zwitterionic phosphatidylcholine lipids, also contain clusters of negative headgroups. Thus, both systems are related to natural membrane environments. The ability of reverse micelles to properly mimic phospholipid bilayers is further substantiated by the comparison of the structuring effect of AOT and DMPC reverse micelles with that of normal SDS micelles or TFE (Table 1) (Figure 1). From NMR analysis of secretin, it is known that this peptide hormone may fold into a rod-like α-helical structure or into helical stretches interrupted by more or less pronounced β-bends depending upon the α-helix inducing effect of the solvent used [3, 4]. The present data confirm the too strong α-helix inducing effect of TFE and clearly indicate the reverse micelle system as well suited for conformational analysis in membrane mimetic conditions, particularly in view of its full optical transparency even at high reverse micelle-to-peptide ratios which are readily obtained because of the low surfactant aggregation number.

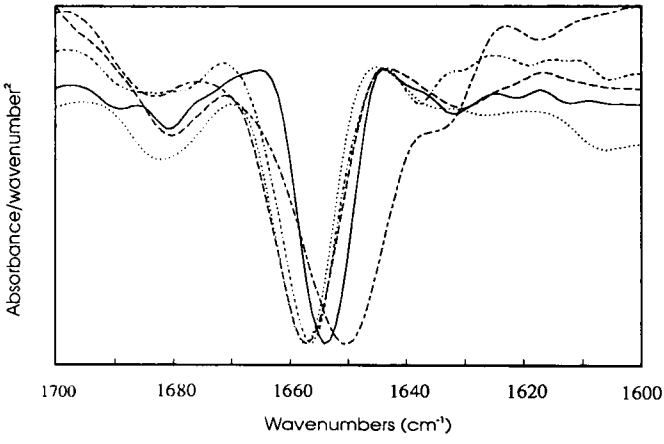

Figure 1. *FTIR spectra of secretin in aqueous solution (– – –), 90% TFE (····), DMPG vesicles (- - - - ·), DMPC reverse micelles (——) and AOT reverse micelles* (w_o*=10) (- - -); all systems in 5mM phosphate buffer (pH=5.4), 20°C.*

References

1. Luisi, P.L. and Steinmann-Hofmann, B., *Meth. Enzymol.*, 136 (1987) 188.
2. Quarzago, D. and Moroder, L., *LIPS*, 1 (1995) 171.
3. Gronenborn, A.M., Bovermann, G. and Clore, G.M., *FEBS Lett.*, 215 (1987) 88.
4. Clore, G.M., Nilges, M., Brünger, A. and Gronenborn, A.M., *Eur. J. Biochem.*, 171 (1988) 479.

Peptides: Chemistry, Structure and Biology
Pravin T.P. Kaumaya and Robert S. Hodges (Eds.)
Mayflower Scientific Ltd., 1996

203
Conformation of New Cyclopentapeptide Neurokinin Antagonists in Solution

M. Pinori[1], S. Cappelletti[1], G. Di Gregorio[1], M. Porcelli[2], G. Murgia[3] and P. Mascagni[1]

[1]Italfarmaco Research Centre, Chemistry Department via dei Lavoratori, 54 I-20092 Cinisello B. (Milan), Italy
[2]University of Cagliari, Chemistry Department and [3]CRS4 srl, I-09124 Cagliari, Italy

Introduction

Cyclopentapeptides of chiral composition (-D-L-D-D-L-) have well defined preferences for a γ/βII conformation when at least one of the L residues is proline [1]. Recently, cyclopeptides of this type have been described as selective endothelin antagonists (*i.e.* BQ-123; cyclo-[DVal-Leu-DTrp-DAsp-Pro-]) [2] and their conformations, studied in solution, revealed the typical γ/βII preference, with the γ turn centred at the fifth (Pro) residue [3].

As both endothelin and neurokinin receptors belong to the G-Protein Coupled Receptors (G-PCR), family they may be presumed to posses topologically similar binding sites for small size antagonists; if this were the case, these conformationally rigid cyclopentapeptides may be expected to represent a template of general utility in obtaining G-PCR's antagonists.

We used sequences from known linear neurokinin antagonists (*i.e.* Spantide) [4] to synthesize two new cyclopeptides (**ITF-1544** cyclo-[-DTrp-Phe-DTrp-DLys-Pro-] and **ITF-1565** cyclo-[-DTrp-Pro-DLys-DTrp-Phe-]) which showed good NK1 and/or NK2 antagonistic properties.

Results and Discussion

Both ITF-1544 and ITF-1565 were prepared in solution and cyclized using a procedure already described by Spatola [5]. The HPLC profiles (220 nm) showed purity of more than 97% and FAB-MS and AAA gave the expected results.

Effects of ITF 1544 and ITF 1565 were measured on i) contraction induced by substance P (SP) in rabbit caval vein, ii) neurokinin A (NKA) in rabbit pulmonary artery and iii) endothelin (ET) in rat aorta. The results showed that both the peptides are weak antagonists for the NK2 receptor, while only ITF-1565 is a potent and competitive antagonist for NK1 receptor (pA_2=6.93).

1D and 2D ^{1}H-NMR spectra of both ITF 1544 and ITF 1565 (6 mg/ml in 80% CD_3CN + 20% H_2O) were recorded at 30°C on a VARIAN VXR spectrometer operating at the nominal proton frequency of 300 MHz. The NMR pulse sequences used for the

proton resonance assignments included COSY, TOCSY, and ROESY. The temperature dependence of the NH chemical shift was studied in the range 5 to 40°C. Initial random structures were produced by means of distance geometry algorithms implemented in the program DGEOM [6]. Both structure optimizations and molecular dynamic calculations were carried out using the program DINAMICA [7]. From the NMR experiments and the molecular modelling studies, evidences were obtained that both ITF 1544 and ITF 1565 are quite rigid molecules which prefer the typical γ/βII conformation. The γ turn appears to be centered at residue 5 (Pro in ITF 1544 and Phe in ITF 1565) in both peptides, confirming the prevailing role of the D-L-D-D-L configuration in determining the backbone conformation of cyclopentapeptides [1].

As a consequence, the presumed pharmacophore DTrp-Phe-DTrp would occupy either positions *i* to *i+2* of a reverse γ-turn (ITF 1565) or positions *i* to *i+2* of a βII-turn (ITF 1544).

In conclusion, we have demonstrated that it is possible to use cyclo-pentapeptides of D-L-D-D-L configuration as a rigid template to obtain antagonists of different G-protein coupled receptors. The possibility of determining the 3D requirements for antagonistic effects will be of great value in the design of new non-peptide peptidomimetics.

Acknowledgments

We are grateful to Mr A. Biffi (Italfarmaco) for skillful technical assistance and Dr J. Mizrahi, head of Pharmacology (Italfarmaco), for critical suggestions and biological testing of the peptides.

References

1. Stradley, S.J., Rizo, J., Bruch, M.D., Stroup, A.N. and Gierasch, L.M., *Biopolymers*, 29 (1990) 263.
2. Ishikawa, K., Fukami, T., Nagase, T., Fujita, K., Hayama, T., Niiyama, K., Mase, T., Ihara, M. and Yano, M., *J. Med. Chem.*, 35 (1992) 2139.
3. Bean, J.W., Peishoff, C.E. and Kopple, K.D., *Int. J. Peptide Protein Res.*, 44 (1994) 223.
4. Regoli, D., Boudon A. and Fauchere, J., *Pharm. Rev.*, 46, (1994) 551.
5. Spatola, A.F., Anwer, M.K., Rockwell A.L. and Gierasch, L.M., *J. Am. Chem. Soc.*, 108 (1986) 825.
6. Blaney, J.M., Crippen, G.M., Dearing, A. and Dixon, J.S., DGEOM, Quantum Chemistry Exchange Program n° 590, in QCPE Bulletin, QCPE Eds., Indiana University, 1990.
7. Corongiu, G. and Martorana, V., in Clementi, E. (Ed.) in 'Methods and Techniques in Computational Chemistry, Vol C', STEF, Cagliari, 1993, p. 81.

Peptides: Chemistry, Structure and Biology
Pravin T.P. Kaumaya and Robert S. Hodges (Eds.)
Mayflower Scientific Ltd., 1996

204
Conformational Analysis of Potent Bicyclic Antagonists of Oxytocin: NMR, CD and Molecular Dynamics Study

M.D. Shenderovich[1], K.E. Kövér[1], S. Wilke[1], M. Romanowski[1], A. Liwo[2], L. Lankiewicz[2], E. Gwizdala[2], J. Ciarkowski[2] and V.J. Hruby[1]

[1]Department of Chemistry, University of Arizona, Tucson, AZ 85721, USA
[2]Faculty of Chemistry, University of Gdansk, Sobieskiego 18, 80952 Gdansk, Poland

Introduction

A novel class of conformationally constrained bicyclic antagonists of oxytocin (OT-BC) with the amino acid sequences

$$Xxx^1\text{-}Tyr^2\text{-}Ile^3\text{-}Glu^4\text{-}Asn^5\text{-}Cys^6\text{-}Pro^7\text{-}Lys^8\text{-}Gly^9\text{-}NH_2,$$

where Xxx are β'-mercaptopropionic acid (Mpa) or (β'-mercapto-β,β-dimethyl)-propionic acid (dPen) [1, 2], presents a unique opportunity to reveal conformational features responsible for the uterine receptor binding of oxytocin antagonists. Here we report results of extensive conformational studies of the two OT-BC analogs.

Results and Discussion

^1H and ^{13}C NMR spectra indicate presence of one predominant isomer for both OT-BC analogs in DMSO at 300 K. ^{13}C chemical shifts of C^α and C^β carbons of Pro^7 (31.8 and 21.7 ppm, respectively, for [Mpa^1]OT-BC), as well as NOE cross-peaks between $C^\alpha H$ protons of Cys^6 and Pro^7 definitely prove a *cis* conformation for the Cys^6-Pro^7 peptide bond in both bicyclic analogs. Strong NOEs between amide protons of residues 2 to 4 and low temperature coefficients observed for NH of Ile^3 and Glu^4 are indicative of a type I or III β-turn located at the residues Tyr^2-Ile^3.

The conformational features revealed by NMR were consistent with one of three models of 3D structure of OT-BC suggested by an independent conformational search [3, 4]. This model was tested by distance-restrained, φ-torsion-restrained and free molecular dynamics (MD) simulations at 300 K performed for both OT-BC using the AMBER force field with $\varepsilon = 45$ characteristic of DMSO. The distance and φ angle restraints were derived from NOEs and $^3J_{N\alpha}$ coupling constants, respectively. Average interproton distances obtained from MD trajectories were in good agreement with NOE data. MD simulations at 500 K revealed conformational transitions in the lactam bridge moiety, which were consistent with $^3J_{\alpha\beta}$ coupling constants for Glu^4 and Lys^8. Applying torsion

angle constraints gradually shifted with 20° steps either to the C^{β}-S-S-C^{β} angle or to the $\chi 1$ angle of Cys^6, we found transitions between left-handed conformers of the disulfide bridge with a *gauche (-)* rotamer of Cys^6 and right-handed conformers of the disulfide bridge with a *gauche (+)* rotamer of Cys^6, suggested by $^3J_{\alpha\beta}$ coupling constants and NOEs observed for $C^{\beta}H_2$ protons of Cys^6.

Based on the NMR data and results of MD simulations, we propose a dynamic model for the solution structure of OT-BC with a stable backbone conformation containing a type III β-turn at Tyr^2-Ile^3 and a *cis* peptide bond Cys^6-Pro^7, and with relatively flexible disulfide and lactam bridge moieties. This conclusion is confirmed by CD spectroscopy. The two OT-BC analogs in aqueous solution have identical CD bands in the far UV region which reflect their similar backbone structure. In contrast, the CD bands at 245 nm, which may be assigned to the disulfide chromophore, are different for the two OT-BC and sensitive to the type of solvent.

Supported by the U.S. Public Health Service, Grant No. DK-17420, and by Polish Scientific Research Committee (KBN), Grant No. DS/8145-4-0094-5.

Figure 1. *A dynamic model of solution structure of [Mpa^1]OT-BC: superposition of low-energy conformers with different conformations of the disulfide and lactam bridges.*

References

1. Hill, P.S., Smith, D.D., Slaninova, J. and Hruby, V.J., *J. Am. Chem. Soc.*, 112 (1990) 3110.
2. Smith, D.D., Slaninova, J. and Hruby, V.J., *J. Med. Chem.*, 35 (1992) 1558.
3. Shenderovich, M., Balodis, J., Mishlyakova, N., Liwo, A., Kasprzykowski, F., Kasprzykowska, R., Tarnowska, M. and Ciarkowski, J., in Schneider, C.H. and Eberle, A.N. (Eds.), 'Peptides 1992', ESCOM, Leiden, The Netherlands 1993, p. 535.
4. Shenderovich, M., Wilke, S., Kövér, K., Collins, N., Hruby, V., Liwo, A. and Ciarkowski, J., *Polish J. Chem.*, 68 (1994) 921.

Peptides: Chemistry, Structure and Biology
Pravin T.P. Kaumaya and Robert S. Hodges (Eds.)
Mayflower Scientific Ltd., 1996

205
Conformational Study of a Nuclear Targeting Peptide

L. Chaloin[1], J. Méry[1], N. Lamb[1], A. Heitz[2], R. Bennes[1] and F. Heitz[1]

[1]CRBM-CNRS and U 249-INSERM, Route de Mende, BP 5051, F-34033 Montpellier Cédex, France
[2] CBS-CNRS, INSERM, Faculté de Pharmacie, F-34060 Montpellier Cédex, France

Introduction

In an accompanying note [1] we have shown that a peptide built of a signal sequence associated with a nuclear localization (NLS) leading to the sequence Ac-M-G-L-G-L-H-L-L-V-L-A-A-A-L-Q-G-A-W-S-Q-P-K-K-K-R-K-V-Cya is able to facilitate the transport of fluorescent probes toward cellular nuclei, these probes being covalently linked to the peptide through the mercaptoamide or Cya moiety. However, it must be noticed that the efficiency of this type of peptide is strongly reduced when the incubation is made in presence of proteases. In order to enhance their resistance toward proteolysis by substitution of some residues by non natural amino acids without altering the overall properties of the peptides, it was of major importance to elucidate its conformation(s). This was achieved mainly by means of CD, FTIR and NMR.

Results and Discussion

By CD measurement, this peptide, when dissolved in water, is in a random coil conformation while the addition of TFE induces, as usual, formation of an α helical structure [2]. However, such a random coil → α transition is not the sole conformational transition which can be induced for this peptide. Indeed, an increase in the ionic strength of the medium leads to a CD spectrum characterized by a minimum centered at 215 nm which is indicative of the formation of β structures [3]. The same trend is observed when lipid vesicles (DOPC or DOPG) are added to the medium. The tendency for this peptide to form β structures is confirmed by an infrared spectroscopy study in the solid state. Indeed, the spectrum of a film cast from a solution containing TFE shows an amide I band centered at 1656 cm^{-1} (Figure 1) [4] which is characteristic of a fully α helical structure, while an incubation with water or lipids such as DOPG leads to a complex spectrum with two major components at 1656 and 1625 cm^{-1} (Figure 1). The presence of this latter band, which is characteristic of the presence of β structures [4], confirms that the nature of the medium from which the peptide is recovered may strongly influence its conformational state. As the aim of this work is the precise determination of the conformation responsible for the translocation process of fluorescent probes, we undertook an NMR study of this peptide. Up to now, only the α helical structure could be observed by NMR investigations made in a water/TFE (70/30) mixture. Several

NOEs of dNN, $d_{\alpha}N(i,i+3)$ and $d_{\alpha\beta}(i,i+3)$ type can be detected from residue 1 throughout residue 20. The finding of these NOEs is consistent with the presence of an α helix [5] which ends at the Pro21 residue. The C-terminal part of the peptide is in a non ordered form as no typical NOE corresponding to structured forms can be detected in this part of the peptide sequence.

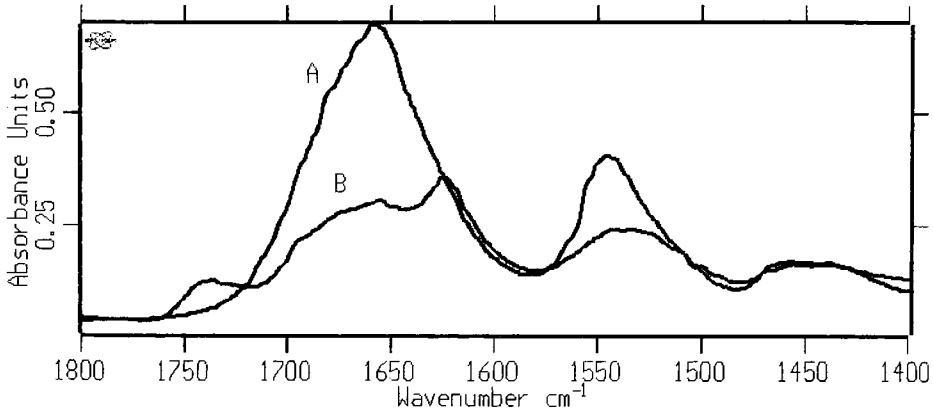

Figure 1. *Solid state FTIR spectrum of the peptide. Spectrum A: peptide recovered after evaporation of TFE. Spectrum B: peptide film leading to spectrum A and then incubated with DOPG vesicles.*

At the present stage, owing to the strong conformational versatility of the peptide, it would be premature to propose a mechanism which accounts for the transfer properties of the peptide. Additionally, we do not know whether the whole peptide is translocated and which conformation is involved, although our results suggest that the β structures could play a major role. Further investigations dealing with the identification of the conformational state and also with the positioning of the peptide with respect to lipid bilayers are under way.

Acknowledgments

This work was supported by the GDR 1153, 'Peptides et protéines amphipathiques', from the CNRS.

References

1. Chaloin, L., Méry, J., Lamb, N., Heitz, A., Bennes, R. and Heitz, F., this volume.
2. Jasanoff, A. and Fersht, A.R., *Biochemistry*, 33 (1994) 2129.
3. Perczel, A., Hollósi, M., Tusnady, G. and Fasman, G.D., *Protein Eng.*, 4 (1991) 669.
4. Miyazawa, T., in Fasman, G.D., (Ed.), Poly-α-Amino Acids, Dekker, Inc., New York, 1967, p. 69.
5. Wüthrich, K., 'NMR of Proteins and Nucleic Acids', John Wiley and Sons, 1986, p.1.

Peptides: Chemistry, Structure and Biology
Pravin T.P. Kaumaya and Robert S. Hodges (Eds.)
Mayflower Scientific Ltd., 1996

206
Conformational Requirements for Potent Decapeptide Agonists of Human C5a Anaphylatoxin

S.M. Vogen[1], O. Prakash[2], L. Kirnarsky[1], S.A. Sherman[1], J. Ember[3], A.M. Finch[4], S.M. Taylor[4] and S.D. Sanderson[1]

[1]*Eppley Institute, University of Nebraska Medical Center, Omaha, NE 68198, USA*
[2] *Department of Biochemistry, Kansas State University, Manhattan, KS 66506, USA*
[3]*Department of Immunology, Scripps Research Institute, La Jolla, CA 92137, USA*
[4]*Department of Pharmacology, University of Queensland, St. Lucia 4072, Australia*

Introduction

Human C5a is a 74 residue glucopolypeptide generated by the enzymatic cleavage of the fifth component of the complement cascade and is generally recognized as a principle mediator of local and systemic inflammation. Due to its pro-inflammatory activities, C5a has been implicated as a pathogenic factor in a number of inflammatory and autoimmune disorders. Consequently, there is considerable interest in understanding the structural features associated with C5a receptor binding and signal transduction.

Human C5a has a highly ordered N-terminal region consisting of a tightly packed, 4-helix bundle which is primarily associated with receptor recognition and binding [1]. Protruding from the ordered domain is the flexible C-terminal region (residues 65-74), which is primarily responsible for signal transduction. Thus, a peptide synthesized with sequence homology to the C-terminal ($C5a_{65-74}$ or ISHKDMQLGR) behaves as a full agonist relative to the parent polypeptide, but at a markedly reduced potency (*ca.* 0.001% of C5a) [2, 3]. As part of an ongoing structure-function study, we recently synthesized a panel of $C5a_{65-74}$Y65,F67 analogues in which conformational flexibility in the C-terminal end was restricted [4]. One of these analogues, YSFKDMPLaR, expressed about 5% of full C5a activity. In this study, we use NMR and conformational analyses to identify the structural features of this analogue responsible for the increase in potency.

Results and Discussion

A panel of C5a agonist peptides based on the sequence of $C5a_{65-74}$ Y65, F67, (YSFKDMQLGR) was used in a structure-function analysis of the likely conformational features responsible for biological activity. Different methods were used to restrict flexibility and bias certain features of backbone conformation in the C-terminal region (residues 71-74) [4]. These conformationally constrained peptides were tested in two different assay systems: (1) spasmogenic activities (smooth muscle contraction of human fetal artery and guinea pig platelet aggregation); and (2) human neutrophil (PMN) activities (PMN polarization and β-glucuronidase release). A structure-function analysis of these conformationally restricted peptides led to the identification of an analogue,

YSFKDMPLaR, that expressed approximately 5% of the activity of natural C5a. A detailed conformational analysis led to the prediction of a helix-like conformation for residues 65-69 and an extended backbone conformation for residues 70-71. The C-terminal residues, (71)72-74, correlated with a β-turn of either type II or V for the expression of spasmogenic and platelet aggregatory activities [4], while a β-turn of type V appeared to be favored in the PMN polarization and enzyme release activities [5].

To further identify the specific type of β-turn associated with the increased biological activity, α-amino-isobutyric acid, (Aib) was substituted for D-Ala at position 73 [YSFKDMPL(Aib)R]. The presence of Aib in position 73 locks a β-turn turn of type II into the C-terminal region of the peptide (residues 71-74). In smooth muscle contraction, this peptide expressed only 0.003% of C5a activity, supporting the notion that a type II β-turn is probably not a preferred conformation for this response.

Sequence specific proton resonance assignments for the potent peptide YSFKDMPLaR were obtained using DQF-COSY, TOCSY, and NOESY 2D NMR experiments. The NMR results suggest that residues 65-69 have α-helical character due to the presence of medium NOE between the proton of Ser66 and amide of Asp69, $d_{\alpha N}(i, i+3)$, and NOE cross peaks, $d_{NN}(i, i+1)$, between the amide protons of Ser66 and Phe67 as well as between Lys68 and Asp69. The absence of NOEs consistent with well defined secondary structural features in the region comprised by residues 70-71, suggest that this is a region of extended backbone conformation. In the C-terminal, four residues (-PLaR), the NMR data indicated that the structural feature associated with the increase in biological activity appears to be a β-turn of type V [6]. This observation is based on the following NOE cross peaks: (1) a weak NOE cross peak $d_{NN}(i+2, i+3)$ [D-Ala73, Arg74]; (2) a weak NOE cross peak $d_{\alpha N}(i+2, i+3)$ [D-Ala73, Arg74]; and (3) a medium NOE cross peak $d_{\beta N}(i+2, i+3)$ [D-Ala73, Arg74]. Thus, it appears that the three important structural features responsible for increased biological activity in the agonist peptide YSFKDMPLaR, include helix-like conformation (residues 65-69), extended backbone conformation (residues 70-71), and a type V β-turn (residues 71/72-74).

References

1. Mollison, K.W., Mandeki, W., Zuiderweg, E.R.P., Fayer, L., Fey, T.A., Krause, R.A., Conway, R.G., Miller, L., Edalji, R.P., Shallcross, M.A., Lane, B., Fox, J.L., Greer, J. and Carter, G.W., *Proc. Natl. Acad. Sci. USA*, 86 (1989) 292.
2. Ember, J.A., Sanderson, S.D., Taylor, S.M., Kawahara, M. and Hugli, T.E., *J. Immunol.*, 148 (1992) 3165.
3. Morgan, E.L., Sanderson, S.D., Scholz, W., Noonan, D.J., Weigle, W.O. and Hugli, T.E., *J. Immunol.*, 148 (1992) 3937.
4. Sanderson, S.D., Kirnarsky, L., Sherman, S.A., Ember, J.A., Finch, A.M. and Taylor, S.M., *J. Med. Chem.*, 37 (1994) 3171.
5. Sanderson, S.D., Kirnarsky, L., Sherman, S.A., Vogen, S.M., Ember, J.A., Finch, A.M. and Taylor, S.M., submitted.
6. Sherman, S.A., Andrianov, A.M. and Akhrem, A.A., 'Science and Technique', Minsk, USSR, pp. 1-240.

Peptides: Chemistry, Structure and Biology
Pravin T.P. Kaumaya and Robert S. Hodges (Eds.)
Mayflower Scientific Ltd., 1996

207
Theoretical Conformational Analysis of Conformationally Restricted Cyclic β-Casomorphin Analogs

B.C. Wilkes, R. Schmidt and P.W. Schiller

Laboratory of Chemical Biology and Peptide Research,
Clinical Research Institute of Montreal, Montreal, Quebec, H2W 1R7, Canada

Introduction

The cyclic β-casomorphin analog H-Tyr-c[-D-Orn-2-Nal-D-Pro-Gly-] (Nal = naphthylalanine) represents the first known cyclic opioid peptide having mixed μ agonist/δ antagonist properties [1]. In an effort to improve the activity profile of this compound, 5-position analogs represented by the formula H-Tyr-c[-D-Orn-2-Nal-D-Pro-Xxx-] (Xxx = Ala, D-Ala, Aib, Sar, NMeAla, D-NMeAla, and NMeAib) were prepared [2]. All analogs were potent μ-agonists and also were potent δ-antagonists (Xxx = D-Ala, Aib, Sar), or weak δ-antagonists (Xxx = Ala, NMeAib), or partial δ-agonists (Xxx = NMeAla, D-NMeAla) [2]. In the present paper we describe low energy conformers of these compounds resulting from a molecular mechanics study.

Results and Discussion

The "bare" ring structure for each of these compounds was studied using a systematic grid search procedure [3]. For the Gly^5 parent peptide, 32 low energy ring structures (< 3 kcal/mol above the minimum) were obtained. This ring structure is moderately flexible, with local constraints imposed only by the $D\text{-}Pro^4$ residue. In the case of the Ala^5-, $D\text{-}Ala^5$- and Aib^5-analogs, 24-30 low energy structures were found. Analysis of the Sar^5-peptide resulted in 16 low energy ring conformations and the remaining analogs containing an N-methylated Xxx^5 residue had the most rigid ring structures (9-13 low energy conformers).

An analysis of the complete peptides was performed for the $D\text{-}Ala^5$-, Sar^5-, and $NMeAla^5$-containing analogs. The Tyr^1 residue and the $2\text{-}Nal^3$ side chain were attached to the low energy ring structures, and a systematic search and energy minimization was performed. Representative low energy conformations are shown in Figure 1. The $D\text{-}Ala^5$-analog was the only peptide found to contain hydrogen bonds. The three hydrogen bonds consistently observed were: D-Ala-NH to D-Orn-CO (type II β-turn); 2-Nal-NH to Tyr-CO (inverse γ-turn); D-Orn-ε-NH to 2-Nal-CO (type I β-turn). The Sar^5-analog was unique in that it was the only peptide with *cis* peptide bonds. Although the lowest energy structures had no *cis* peptide bonds, conformations 2 kcal/mol above the lowest energy conformation contained two *cis* peptide bonds, one between 2-Nal and D-Pro, and one between D-Pro and Sar.

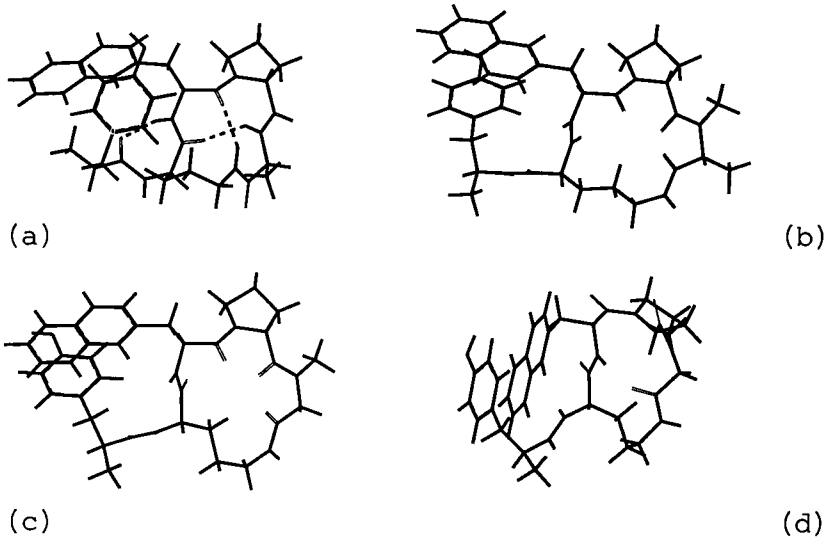

Figure 1. *Representative low energy conformations of H-Tyr-c[-D-Orn-2-Nal-D-Pro-Xxx-] where Xxx = D-Ala (a); NMeAla (b); Sar (c); and Sar with cis peptide bonds (d). Hydrogen bonds are represented with dashed lines.*

These conformations were found to be in good agreement with structural parameters determined by NMR spectroscopy [4]. Despite the fact that each compound showed different backbone preferences, low energy conformers characterized by a tilted stacking arrangement of the two aromatic rings were found for all three of them, in good agreement with a proposed model of the receptor-bound conformation of cyclic dermorphin analogs that are μ-agonists [3]. Low energy conformations of the D-Ala^5- and Sar^5-analogs, but not of the NMe-Ala^5-peptide, showed good spatial overlap of their two aromatic rings and terminal amino group with the corresponding moieties of the non-peptide δ antagonist naltrindole. These results provide a structural explanation of the mixed μ agonist/ δ antagonist profile of the D-Ala^5- and Sar^5-analogs.

Acknowledgments

Supported by the Medical Research Council of Canada (grant MT-10131).

References

1. Schmidt, R., Vogel, D., Mrestani-Klaus, C., Brandt, W., Neubert, K., Chung, N.N., Lemieux, C. and Schiller, P.W., *J. Med. Chem.*, 37 (1994) 1136.
2. Schmidt, R., Chung, N.N., Lemieux, C. and Schiller, P.W., this volume.
3. Wilkes, B.C. and Schiller, P.W., *Biopolymers*, 29 (1990) 89.
4. Carpenter, K.A., Schmidt, R. and Schiller, P.W., this volume.

Peptides: Chemistry, Structure and Biology
Pravin T.P. Kaumaya and Robert S. Hodges (Eds.)
Mayflower Scientific Ltd., 1996

208

Calculation of Peptide Orientation at a Lipophilic Surface: A Useful Tool for "Conformation-Function" Analysis

S.G. Galaktionov[1], V.M. Tseytin[2], I. Vakser[1] and G.R. Marshall[1]

[1]Center for Molecular Design, Washington University, St. Louis, MO, 63130, USA,
[2]Institute of Microbiological Industry, 220600 Minsk, Belarus

Introduction

Many biologically active peptides have been shown to interact with their specific receptors mainly due to hydrophobic forces. The hypothesis suggesting that the receptor-bound conformation of a peptide is close to that at the lipid-water interface seems to be endorsed, though indirectly, by a number of independent experimental results [1]. These findings offer several new elements for analysis of "conformation-function" relationships and conformationally directed computer design of peptide bio- regulators based on the predictions of the peptide ligand orientation with respect to the receptor surface. We have extended the tools of molecular mechanics to adapt them to the calculation of stable molecular conformations at a phase boundary, the "water - lipophilic phase" [2, 3]. Here we discuss some applications of this approach in peptide drug design.

Results and Discussion

The phase boundary is the surface dividing two compartments, which possess the solvation properties of water and octanol. The ECEPP force field and rigid valence geometry were used for calculation of intramolecular interaction energy; the solvation energy was calculated according to the Hopfinger-Scheraga approach. For each starting conformation, the program successively carried out the energy minimization for the sum of intramolecular and solvation energies with respect to dihedral angles, the depth of molecule immersion into the lipophilic phase, and the macrorotation angles which determine the orientation of the molecule at the phase boundary. The energy of transfer from water to the phase boundary may be estimated as the difference between the energies of those conformers which are most stable at the phase boundary and in water.

This offers several new elements for the analysis of "conformation-function" relationships of peptide bioregulators. The conformer stability at the phase boundary rather than in vacuum can be used for selection of the set of preferred structures for elucidation of the receptor-bound structure. Further, one may reduce the set of conformations eligible as "biologically active" by rejecting those conformations not common in the sets of boundary-stable conformers of all active compounds. Assuming that the orientation of the peptide molecule with respect to the phase boundary mimics its orientation in the receptor-bound state, we may suggest that any conformers having one or more of functionally important groups definitively exposed into water, so that it is

impossible for any contact with the lipophilic phase seem unlikely to be the "biologically active" ones. The introduction of additional bulky groups on the receptor-adjacent side of the peptide molecule should result in loss of activity. Activity of such modified analogs implies that the added bulky groups are not oriented toward the receptor surface in receptor-bound conformation. Therefore, conformers having these bulky groups deeply immersed into the lipophilic should be also eliminated from the set of tentative "biologically active" conformers. Finally, it is reasonable to assume that the receptor-bound structures of two active analogs would possess similar orientations at the phase boundary. This provides another criterion for the restriction of the set of candidates for "biologically active" conformer.

This approach is exemplified in brief by examination of the set of tentative receptor-bound conformations proposed for δ-opioid peptides dermenkephalin (DRE) and the cyclic analog DPDPE ([4], Table IX and VII, respectively). Of the 6 candidate conformers of DRE, conformer, #2 is significantly more stable at the phase boundary (6.1 kcal/mole less than second stable conformer #6).

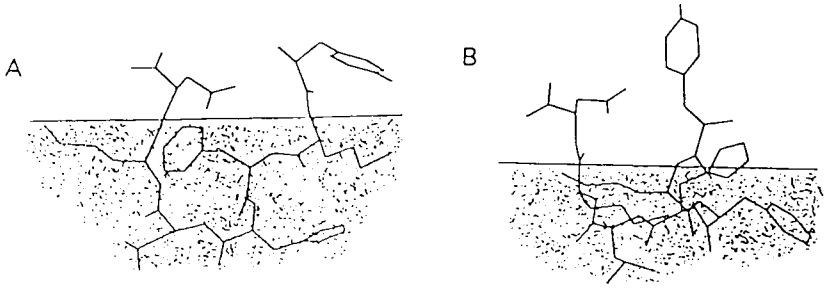

Figure 1. *DRE conformers #2 (A) and #6 (B) at phase boundary (lipophilic phase at the bottom).*

This conformer also has the most favorable orientation of its functionally important groups (sidechains of Phe and Tyr, and the amino group) with respect to lipid phase; all of them located close to the phase boundary (Figure 1A). The structures with the Tyr sidechain conformers $\chi_1 \approx \pm 60°$ are bound at the lipid surface such that this residue protrudes far into the aqueous phase (Figure 1B). Of the three candidate DPDPE conformers, structures #1 and #2 are significantly more stable at the boundary. Conformers #1 and #2 of DPDPE were found structurally close to conformers #2 and #4 of DRE[4], respectively. Conformer #1 of DPDPE has an arrangement of functionally important groups at the phase boundary very similar to that of conformer #2 of DRE; in the case of the second pair of structures, their orientations are completely different. These observations serve to favor the first pair of structures as candidates for the receptor-bound conformers.

References

1. Schwyzer, R., *Chemtracts Bioch. Mol. Biol.*, 3 (1992) 347.
2. Galaktionov, S.G., Tseytin, V.M. and Vakser, I.A., *Biophysics*, 33 (1988) 595.
3. Galaktionov, S.G. and Marshall, G.R., *Biophys. J.*, 65 (1993) 608.
4. Nikiforovich, G.V., Hruby, V.J., Prakash, O. and Gehrig, C.A., *Biopolym.*, 31 (1991) 941.

Peptides: Chemistry, Structure and Biology
Pravin T.P. Kaumaya and Robert S. Hodges (Eds.)
Mayflower Scientific Ltd., 1996

209

Structural Distinctions Among 1-Aminocylcoalkane-1-carboxylic Acid Substituted Deltorphins Determined Using Molecular Dynamics Simulations

S.D. Bryant[1], S. Salvadori[2], R. Guerrini[2], M. Attila[3] and L.H. Lazarus[1]

[1] *Peptide Neurochemistry, Laboratory of Environmental Neuroscience, National Institute of Environmental Health Sciences, Research Triangle Park, NC 27709, USA*
[2] *Department of Pharmaceutical Sciences, University of Ferrara, I-44100 Ferrara, Italy*
[3] *Department of Pharmacology and Toxicology, Division of Pharmacy, University of Finland, SF-00014, Helsinki, Finland*

Introduction

The deltorphins consist of naturally occurring peptides isolated from amphibian skin and contain a D-amino acid at position 2 [1-3]. These peptides exhibit both higher affinity and selectivity for the δ opioid receptor than do enkephalins or their derivatives [1, 2]. Deltorphin A [Tyr-D-Met-Phe-His-Leu-Met-Asp-NH_2] [2, 3] and deltorphin C [Tyr-D-Ala-Phe-Asp-Val-Val-Gly-NH_2] [2,3] associate with the δ_1 receptor subtype [4], while deltorphin B [Tyr-D-Ala-Phe-Glu-Val-Val-Gly-NH_2] [2, 3] prefers the second receptor subtype δ_2 [5]. The existence of multiple binding sites and receptor subtypes suggests that there are differences in either the receptor binding site or in the conformation of the peptide [6]. Molecular dynamics simulations of the deltorphins [6] offered low energy conformations with extended and compact features. These topographies could be utilized to predict multi-site binding [6]. Substitution of 1-aminocycloalkane-1-carboxylic acid residues for either D-Ala, Phe, or Asp in deltorphin C (DC) is a method for characterizing δ opioid receptor properties and evaluating multiple receptor binding sites. Molecular dynamics simulations of DC and these analogues provide a method for estimating structural motifs of small molecules that interact with δ opioid receptors.

Results and Discussion

Synthesis and purification of the deltorphins [7] and deltorphin C analogues were performed by solid phase methods and radioreceptor assays used synaptosomal membranes according to published procedures [7]. Statistical analyses incorporated graded concentrations of each analogue in competition assays and assessed the data for one- and two-site binding with the non-linear regression analysis of InPlot™ (GraphPad). Only the combination of the following criteria validated the heterogeneous binding sites: $\eta < 0.850$, 95% confidence levels for η not < -0.900 and $P < 0.0001$ in the F-test

comparing fits to one- and two-site binding models [8]. AMBER dynamics (v. 3.0, rev. A) and simulated annealing using MacroModel (v. 4.0) were performed on a Silicon Graphics Indigo^2 computer system and graphics visualization of AMBER output utilized Multi (v. 3.0.0).

Alteration of DC by substitution of 1-aminocyclohexane (Ahx), pentane (Apn), and propane (Apr) at positions 2, 3 or 4 characterized δ receptor properties. Ahx at positions 2 and 3 displayed about a 10-fold loss of in δ affinity but higher δ selectivity (K_i^{μ}/K_i^{δ} = 1,254 and 1,666, respectively) than DC (K_i^{δ} = 0.15 nM, K_i^{μ}/K_i^{δ} = 980). Apn and Apr substituted at position 3 exhibited moderate δ affinities (K_i^{δ} = 10.1 nM and 17.5 nM, respectively) and selectivities (443 and 535). However, Apn substitution at position 4 exhibited high δ and μ affinities (K_i^{δ} = 0.054 nM, K_i^{μ} = 0.58) with minimal δ selectivity. Substitutions at Phe^3 resulted in a loss of δ and μ affinities indicating that this residue is not essential *per se*; however the aromaticity of Phe^3 enhanced δ affinities. Loss of chirality at position 2 by the substitution of [Ahx^2] for D-Ala only resulted in a moderate loss of δ affinity indicating that the D-isomer may not be required depending on the replacement residue. Loss of the charged residue at position 4 enhanced δ and μ affinities suggesting that an anionic residue is not necessary for δ binding and inhibits μ binding. DC, [Apr^3], and [Apn^4] fitted one-site δ binding models while [Ahx^2], [Ahx^3] and [Apn^3] fitted two-site δ binding models.

Molecular dynamics simulations indicated that these peptides adopt distinct conformations in solution. β-Turns in the N-terminal regions and extended C-terminal regions seem to be a conformational motif linked with binding at the δ receptor; furthermore, structures containing β-turns exhibited lower energies than extended conformations. Higher energy conformers offered correlations between the extended structures and one-site δ binding models and peptide analogues with turns fitted two-site δ binding models.

References

1. Balboni, G., Marastoni, M., Picone, D., Salvadori, S., Tancredi, T., Temussi, P.A. and Tomatis, R., *Biochem. Biophys. Res. Commun,* 169 (1990) 617.
2. Erspamer, V., Melchiorri, P., Flaconieri Erspamer, G., Negri, L., Corsi, R., Severini, C., Barra, D., Simmaco, M. and Kreil, G., *Proc. Natl. Acad. Sci. USA*, 86 (1989) 5188.
3. Lazarus, L.H. and Attila, M., *Prog. Neurobiol.*, 41 (1993) 473.
4. Improta, G. and Broccardo, M., *Peptides,* 13 (1992) 1123.
5. Xu, H., Partilla, J.S., de Costa, B.R., Rice, K.C. and Rothman, R.B., *Peptides,* 13 (1991) 1207.
6. Bryant, S.D., Salvadori, S., Attila, M. and Lazarus, L.H., *J. Am. Chem. Soc.,* 115 (1993) 8503.
7. Lazarus, L.H., Salvadori, S., Santagada, V., Tomatis, T. and Wilson, W.E., *J. Med. Chem.,* 34 (1991) 1350.
8. Bryant, S.D., Attila, M., Salvadori, S., Guerrini, R. and Lazarus, L.H., *Pept. Res.*, 7 (1994) 175.

Peptides: Chemistry, Structure and Biology
Pravin T.P. Kaumaya and Robert S. Hodges (Eds.)
Mayflower Scientific Ltd., 1996

210
The Helix-Loop-Helix Motif of Calmodulin: Influence of the Helical Regions on the Affinity of the Calcium Binding Loops

Y. Sharma[1], D. Balasubramanian[1] and T. Fairwell[2]

[1]*Centre for Cellular and Molecular Biology, Hyderabad - 500 007, India*
[2]*National Heart, Lung, and Blood Institute, Bethesda, MD 20892, USA*

Introduction

Each calcium binding site in calmodulin has the characteristic EF-hand motif, also called the helix-loop-helix motif conformation [1, 2]. The calcium binding ability of these sites varies over a wide range, and since the actual binding of calcium occurs in the 12 residue loop region, most of the studies have concentrated on varying the sequence of this region [3, 4]. In order to study the effect of the E and F helices on the binding affinities of the loop region, we have synthesized two sets of peptides corresponding to the sites 1 and 4 of calmodulin. Spectroscopic methods involving calcium ion mimics are primarily used for studying the affinities of small peptides, since direct assay methods are difficult. The cationic dye "Stains-All" generates specific absorption peaks and induced circular dichroism (CD) peaks when it binds to calcium binding peptides and proteins [5-7]. Upon binding to rod-like or helical regions of a peptide, the Γ-band, occurring at around 500 nm of the dye is activated while binding to globular or unordered region of the peptide activates the J-band at around 610 nm. Thus, "Stains-All" can provide information on the conformational status of the calcium binding region.

Results and Discussion

We have synthesized and studied two sets of EF-hand peptides corresponding to the weak site 1 and the strong site 4 of calmodulin by monitoring the induced ellipticities of the dye "Stains-All." In the first set of peptides the E and F helices from site 4 were used and the binding loops were changed. In the second set, the helices from site 1 were used while changing the binding loops from 1 to 4 (Table 1). The length of the F helix in site

Table 1. *Calmodulin peptides with helices from sites I and IV.*

Peptides	Amino acid sequence
111	FKEAFSLF**DKDGDGTITTKE**LGTVMRSL
141	FKEAFSLF**DIDGDGQVNYEE**LGTVMRSL
414	VDEMIREA**DKDGDGTITTKE**FVQMMTAK
444	VDEMIREA**DIDGDGQVNYEE**FVQMMTAK

4 was only eight amino acids from the end of the binding loop. Hence, in order that an appropriate comparison of the effects of these helices on the calcium binding loop be made, we decided to keep the helix length to eight residues to either end of the binding loop. As a result, all the peptides used for this study are 28 residues in length. Exchange of the helices in both cases is seen to lead to a significant change in the affinity of peptides to "Stains-All."

When the E and F helices flanking site 1 is replaced with those of site 4 (*i.e.* modifying peptide 111 to 414), it leads to a 35-fold increase in the affinity to "Stains-All" in the J-band region. Likewise, 414 effects a 70-fold increase in the ellipticity of the Γ-band of the dye. (Table 2). Similarly, the inducibility of dye bands by peptide 141 is greatly reduced in relation to peptide 444. Peptide 444 induces a 20-fold increase in ellipticity of the J band of "Stains-All" compared to peptide 141. In the Γ-band region, the ability of peptide 141 to induce ellipticity is decreased by 3-fold (Table 2).

Table 2. *Normalized relative ellipticities induced by the various peptides in "Stains-All".*

Peptides	J-band	Γ-band
111	154	182
414	5780	12860
141	28210	112850
444	642900	382600

These results suggest that the role of the E and F helices sandwiching the ion-binding loop can be significant. In addition to the composition and sequence of the loop, those of the helices are also important to the calcium binding process, a point that would be of importance when chemically designing peptides such as the calcium binding motifs of calmodulin and related calcium binding proteins.

Acknowledgments

This work was made possible through the NIH-CCMB collaborative program.

References

1. Krestinger, R.H. and Nockolds, C.E., *J. Biol. Chem.*, 248 (1973) 3313.
2. Krestinger, R.H., *CRC Crit. Rev. Biochem.*, 8 (1980) 119.
3. Marsden, B.J., Hodges, R.S. and Sykes, B.D., *Biochemistry*, 28 (1989) 8839.
4. Reid, R.E., *J. Biol. Chem.*, 265 (1990) 5971.
5. Caday, C.G. and Steiner, R.F., *J. Biol. Chem.*, 260 (1985) 5985.
6. Sharma, Y., Rao, C.M., Rao, S., Gopalakrishna, A., Somasundaram, T. and Balasubramanian, D., *J. Biol. Chem.*, 264 (1989) 20923.
7. Sharma, Y., Gopalakrishna, A., Balasubramanian, D., Fairwell, T. and Krishna, G., *FEBS Lett.*, 326 (1993) 59.

Peptides: Chemistry, Structure and Biology
Pravin T.P. Kaumaya and Robert S. Hodges (Eds.)
Mayflower Scientific Ltd., 1996

211

Synthesis of a Heterotrimeric Triple Helical "Mini-collagen" with a C-terminal Disulfide Knot for Induction of the Correct Register

R. Battistutta, L. Moroder and K. Kühn

Max-Planck-Institut für Biochemie, D-82152 Martinsried bei München, Germany

Introduction

Collagen-like polypeptides based on the Gly-Pro-Hyp repetitive motif are known to form homotrimeric triple helical structures in solution. In order to stabilize the triple helix *via* covalent links, homotrimeric "mini-collagens" have been constructed using di-lysine as template [1]. In nature, both homo- and heterotrimeric collagens are found, whereby the exact registration of the three chains is essential for a correct folding. In type III collagen, the folding of the three α1 chains from the C-terminal end is initiated by a nucleus stabilized by interchain disulfide bonds. We have used this cystine-knot principle for the synthesis of a heterotrimeric mini-collagen molecule containing Gly-Pro-Hyp repeating units and the α1β1-integrin recognition site of the basement membrane collagen $[\alpha1(IV)]_2\alpha2(IV)$ [2]. Unlike nature, that uses three disulfide bridges to tighten the assembly of the three chains, our synthetic approach foresees two disulfide bridges and two different cysteine protecting groups that allow for selective disulfide pairings. The four cysteines (one in each α1(IV)-mimetic chain and two in the α2(IV)-mimetic chain) were positioned at the C-termini by modelling the triple helix in the correct register according to the Fraser model of the collagen triple helix (Figure 1).

Results and Discussion

The single peptide chains related to the sequences 457-469 of the α1 and α2 chains of the human basement membrane type IV collagen [2] and extended with Gly-Pro-Hyp repeats to 31mers and 32mers were synthesized by standard SPPS procedures on a Wang-resin following the Fmoc/tBu strategy. HBTU/HOBt was used as coupling reagent except for the cysteines that were coupled *via* the Pfp esters/HOBt. As shown in Figure 1, the cysteines were protected as S-StBu and S-Acm derivatives; both are stable

(α1): H-$(GPO)_3$-GPO-GDQ-GPO-GIO-$(GPO)_2$-GC(StBu)-G-G-OH
(α2): H-$(GPO)_3$-GAK-GRA-GFO-GLO-$(GPO)_2$-GC(Acm)C(StBu)-GG-OH
(α1'): H-$(GPO)_3$-GPO-GDQ-GPO-GIO-GYO-GPO-GPC(Acm)-GG-OH

Figure 1. *Sequences of the peptide chains used for the construction of a heterotrimeric mini-collagen molecule with a cystine-knot (O = Hyp).*

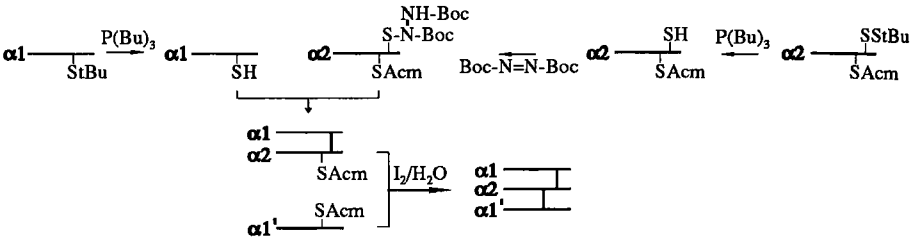

Figure 2. *Scheme of disulfide bridging of the three collagen-type peptide chains.*

to the acid treatment of the resin-cleavage step. Amino acid analysis, HPLC and MS, were used to characterize the three S-protected peptides. Assembly of the three peptide chains is shown in Figure 2. In the first step, the α1- and α2-peptide were deprotected at the S-StBu function with tributylphosphine. Then, the α2-peptide was activated at the thiol function with azodicarboxylic acid di-tert-butyl ester [3] and reacted with the free thiol group of the α1-peptide. After heterodimer purification by size-exclusion chromatography and its characterization by MS, the final interchain disulfide bridging with the α1′-peptide was carried out in water in a potential coil-dependent selective manner assuming a partition of the monomer between the homo- and heterotrimer, but in favor of the latter aggregate. After size exclusion chromatography at RT and at 60°C, amino acid analysis indicated the correct assembly of the three chains into the expected heterotrimer. Such heterotrimer exhibited the characteristic collagen-type CD spectrum and a sharp melting curve with a melting temperature of 54°C (Figure 3), 28°C higher than that of the α1′- peptide-homotrimer; this confirmed our working assumption for the last oxidation step in water. The protection scheme used should also allow for a second selective disulfide formation, *e.g. via* $CH_3OCOSCl$, under denaturating conditions.

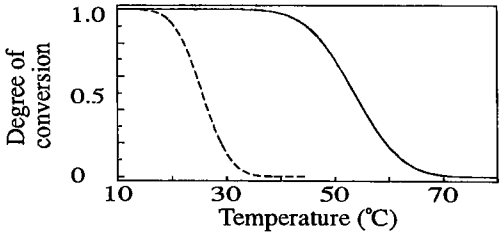

Figure 3. *Thermal denaturation curves of the α1′ monomer (– –) and of the synthetic heterotrimeric mini-collagen (——) in 0.1 M phosphate buffer pH 7.4.*

References

1. Fields, C.G., Michelson, D.J., Drake, S.L., McCarthy, J.B. and Fields, G.B., *J. Biol. Chem.*, 268 (1993) 14153.
2. Eble, J.A., Golbik, R., Mann, K. and Kühn, K., *EMBO J.*, 12 (1993) 4795.
3. Wünsch, E., Romani, S. and Moroder, L., in Blaha, K. and Malon, P. (Eds.), 'Peptides 1982', Walter de Gruyter, Berlin, 1983, p.183.

Peptides: Chemistry, Structure and Biology
Pravin T.P. Kaumaya and Robert S. Hodges (Eds.)
Mayflower Scientific Ltd., 1996

212
Study of Triple-helical Structure Using Peptide-amphiphiles

Y.C. Yu[1], P. Berndt[1,3], M. Tirrell[1,3] and G.B. Fields[1,2]

[1]Biomedical Engineering Center, and Departments of [2]Laboratory Medicine and Pathology, and [3]Chemical Engineering and Material Sciences, University of Minnesota, Minneapolis, MN 55455, USA

Introduction

Self-assembling molecules incorporating functional groups have potential biomedical applications such as drug delivery and biointerface modification. We have developed self-assembling amphiphiles with peptide head groups for directly measuring and manipulating the structures and intermolecular forces in model membranes. Several sequences from collagens which are responsible for cell adhesion and migration have been reported. In many cases, triple helical conformation is essential for receptor recognition. We have synthesized amphiphiles containing the α1(IV)1263-1277 collagen sequence Gly-Val-Lys-Gly-Asp-Lys-Gly-Asn-Pro-Gly-Trp-Pro-Gly-Ala-Pro *([IV-H1])*, which binds K1735 M4 mouse melanoma cells [1]. In the present study, we show that these peptide amphiphiles self assemble into triple helical structure and have increased thermal stability as compared with the peptide alone.

Results and Discussion

The structure of the compounds used in our study are shown below. Peptides are covalently coupled to the dialkyl ester of Glu with a C_2 spacer using Fmoc solid-phase synthesis and purified by reversed-phase HPLC [2]. All investigated peptide amphiphiles form stable monolayers at the air water interface. Surface pressure is detectable at molecular areas <2.5 nm^2/molecule. The layer can be compressed to a molecular area of 0.6 nm^2/molecule. This indicates a fully stretched out structure of the peptide in the headgroup.

At 25°C both $(Gly\text{-}Pro\text{-}Hyp)_4$-*[IV-H1]*-$(Gly\text{-}Pro\text{-}Hyp)_4$ and the peptide-amphiphile exhibit CD spectra with a maximal ellipticity near λ=225 nm, characteristic of triple helical structure (Figure 1). In contrast, at 25°C peptide *[IV-H1]*-$(Gly\text{-}Pro\text{-}Hyp)_4$ does not show positive ellipticity at this wavelength. When the solution is heated, peptide $(Gly\text{-}Pro\text{-}Hyp)_4$-*[IV-H1]*-$(Gly\text{-}Pro\text{-}Hyp)_4$ gives a typical sigmoidal transition associated with the transformation of triple-helical to single-stranded structure (T_m=36°C). On the other hand, the peptide-amphiphile shows a gradual transition starting at 40°C to 80°C. NMR spectra of the peptide and the peptide-amphiphile show the same trend of change with increasing temperature. These observations are indicative of greatly enhanced thermal stability of the triple-helical structure incorporated into amphiphile headgroups.

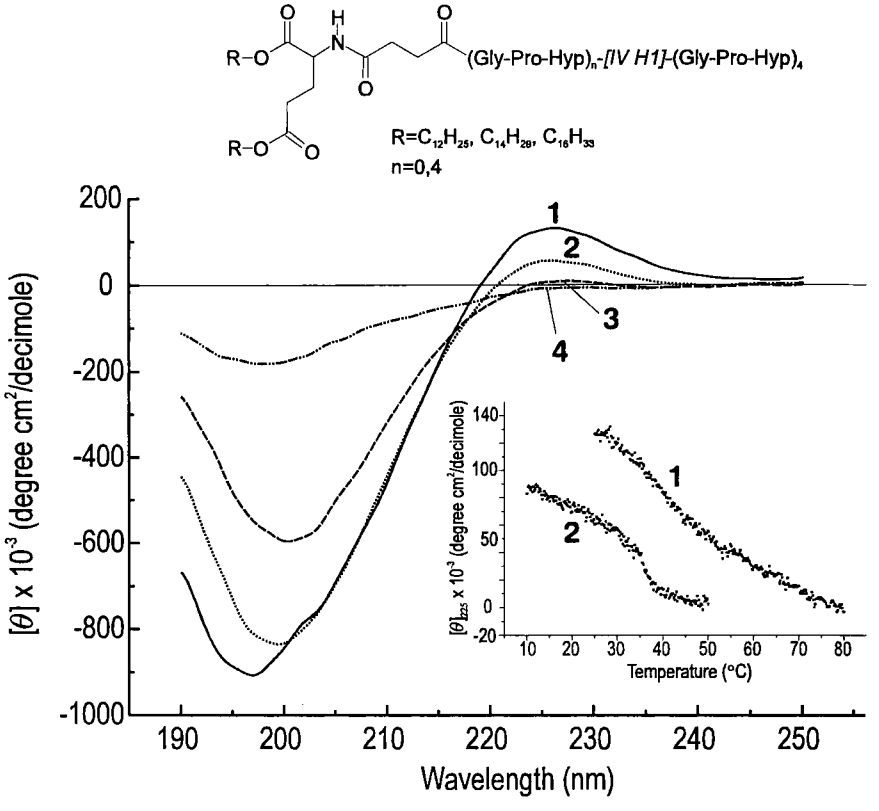

Figure 1. *Circular dichroism study of:* ***1*** *$(C_{12})_2$-Glu-C_2-[IV-H1]-(Gly-Pro-Hyp)$_4$,* ***2*** *(Gly-Pro-Hyp)$_4$-[IV-H1]-(Gly-Pro-Hyp)$_4$,* ***3*** *[IV-H1]-(Gly-Pro-Hyp)$_4$, and* ***4*** *IV-H1 (25°C). The inset shows the melting curve for:* ***1*** *$(C_{12})_2$-Glu-C_2-[IV-H1]-(Gly-Pro-Hyp)$_4$, and* ***2*** *(Gly-Pro-Hyp)$_4$-[IV-H1]-(Gly-Pro-Hyp)$_4$.*

Acknowledgments

This work was supported by the NIH grants AR 01929 and KD 44494, McKnight Land Grant Professorship, Earl E. Bakken Professorship, and BIE program of the Center for Interfacial Engineering.

References

1. Chelberg, M.K., McCarthy, J.B., Skubitz, A.P.N., Furcht, L.T. and Tsilibary, E.C., *J. Cell Biol.*, 111 (1990) 261.
2. Berndt P., Fields G.B., Tirrell M., *J. Am. Chem. Soc.* submitted.

Peptides: Chemistry, Structure and Biology
Pravin T.P. Kaumaya and Robert S. Hodges (Eds.)
Mayflower Scientific Ltd., 1996

213
A Conformational Study in Solution of Prosomatostatin Fragments by NMR and Computational Methods

L. Paolillo[1], G. D'Auria[1], L. Falcigno[1], F. Fraternali[1], D.M. Manduca[1], M. Simonetti[2] and C. Di Bello[2]

[1]*Department of Chemistry, University of Naples, Naples 80134, Italy*
[2]*Institut of Industrial Chemistry, University of Padua, Padua 35131, Italy*

Introduction

The elucidation of the conformational features of linear peptides in solution is a hard task to achieve in particular with small and medium size compounds. Moreover, in the case of molecules of biological interest, the experimental conditions in which they are active are not easy to simulate in the laboratory.

We have recently studied some peptide fragments related to the hormone precursors of oxytocin and somatostatin [1]. The interest for such peptides arises from the lack of knowledge about the exact mechanism leading to the maturation of the inactive pro-forms. The proteolytic enzymes involved in the bioactivation process act at the level of pairs or singlets of basic residues such as arginine and lysine in the pro-forms. It was proposed that the basic residues, constituting the active site, are located in flexible structural segments close to β-turns and/or loops [2].

To characterize such structural parameters, which are thought to play a key role in the enzyme-substrate recognition, and to verify if these features represent a general motif, also shared by different pro-hormones [3], we have undertaken a conformational study on a series of peptides reproducing the sequence around the proteolytic dibasic site of Pro-somatostatin:

H-Pro-Ala-Met-Ala-**Pro**-Arg-Glu-Arg-Lys- Ala-Gly-Ala-Lys-Asn-NH_2	SomWT
H-Pro-Ala-Met-Ala-**Ala**-Arg-Glu-Arg-Lys-Ala-Gly-Ala-Lys-Asn-NH_2	SomI
H-Pro-Ala-Met-Ala-**Gly**-Arg-Glu-Arg-Lys-Ala-Gly-Ala-Lys-Asn-NH_2	SomII
H-Pro-Ala-Met-Ala-**Ser-Ser-Asn-Arg**-Lys Ala-Gly-Ala-Lys-Asn-NH_2	SomIII

These peptide analogues represent a useful system to evaluate specific structural requirements necessary for the recognition mechanism. The conformational analysis was carried out in different solvents by a combination of spectroscopic techniques such as CD, IR [4], NMR and computational methods. The NMR data have been used as conformational constraints in a series of conformational searches and energy minimizations in order to build-up realistic models in solution. The results appear to indicate the existence of folded conformation that is characterized by a β-turn architecture.

Results and Discussion

For each peptide a set of consecutive dαN(i,i+1) and dNN(i,i+1) were identified in the NOESY or in the ROESY spectra and other NOEs and ROEs involving sidechain consecutive residues. In some cases, resonance overlaps lead to some ambiguities in the attribution of NOE or ROE contacts. It should be noted that a common pattern of NOE effects has been observed for each peptide in the proximity of the active site. The same pattern of NOE effects have been evaluated both in DMSO and DMSO/H_2O.

For peptides SomWT, SomII and SomIII, all recognized as substrates by the enzyme [4], NOE data indicate the occurence of a β-turn in the 4-7 and 11-14 regions of the polypeptide chain, respectively on the left and right sides of the dibasic site (Arg^8-Lys^9). On the other hand, for peptide SomI, not recognized by the endoprotease, the NOE contacts suggest a β-turn between Ala^5-Arg^8 and Gly^{11}-Asn^{14}. It should be noted that, in this case, the first β-turn is shifted by one amino acid involving the first residue (Arg^8) of the cleavage site. Such observation could justify the lack of recognition from the enzyme.

The structural NMR informations have been confirmed by a series of energy minimizations. Experimental NMR data are generally consistent with the minimizations carried out. In the final structures, the turns in the regions 4-7 and 11-14 are found to be stable, even though modest deviations from the canonical β-turns are observed.

In conclusion, our study indicates the occurrence of folded segments close to the dibasic site in the C-terminal fragments of prosomatostatin. By considering previous work [5-7] on model peptides representing prohormone sequences around the active site, these structural features seem to indicate a general motif in these proforms.

References

1. Paolillo, L., D'Auria, G., Falcigno, L., Fraternali F., Saviano, M., Simonetti, M. and Di Bello, C., in 'Current Topics in Peptide and Protein Science, Res.Trends Publ.', Trivandrum, India, 1 (1994) 193.
2. Rholam, M., Nicolas, P. and Cohen, P., *FEBS Lett.*, 207 (1986) 1.
3. Paolillo, L., Simonetti, M., D'Auria, G., Falcigno, L., Saviano, M., Carlomagno, T., Scatturin, A., DiBello, C. and Cohen P., in Hodges, R.S. and Smith, J.A. (Eds.), 'Peptides: Chemistry, Structure and Biology', ESCOM, Leiden, 1994, p. 808.
4. Brakch, N., Boileau, G., Simonetti, M., Nault, C., Joseph-Bravo, P., Rholam, M. and Cohen, P., *Eur. J. Biochem.*, 216 (1993) 39.
5. Aumelas, A., Andousset-Puech, M.P., Heitz, A., Bataille D. and Martinez, J., *Int. J. Pept. Protein Res.*, 34 (1989) 268.
6. Rholam, M., Cohen, P., Brakch, N., Scatturin, A., Paolillo, L. and Di Bello, C., *Biochem. Biophys. Res. Commun.*, 168 (1990) 1066.
7. Paolillo, L., Simonetti, M., Brakch, N., D'Auria, G., Saviano, M., Dettin, M., Rholam, M., Scatturin, A., Di Bello, C. and Cohen, P., *EMBO J.*, 7 (1992) 2399.

Peptides: Chemistry, Structure and Biology
Pravin T.P. Kaumaya and Robert S. Hodges (Eds.)
Mayflower Scientific Ltd., 1996

214

Evaluation of Structural Changes for Synthetic Alzheimer β-Peptide Solutions on Coordination with Al(III) Ions: A Low Field ^{27}Al NMR and UV/CD Study

S.B. Vyas[1] and L.K. Duffy[2]

[1]College of Pharmacy, University of Michigan, Ann Arbor, MI 48109, USA
[2]Department of Chemistry and Biochemistry, and Institute of Arctic Biology, University of Alaska Fairbanks, Fairbanks, AK 99775, USA

Introduction

The pathological features of postmortem brain afflicted with Alzheimer's disease (AD) include amyloid deposition in the senile plaques and cerebral blood vessels, and the neurofibrillary tangles [1]. One major proteinaceous component of amyloid deposits is a 40 amino acid protein, ß1-40, which also circulates freely in skeletal tissues and cerebrospinal fluid in a soluble form [2]. Aluminum salts have been reported to promote synthetic ß1-40 aggregation in solution [3, 4], and significantly affects the solution conformation of ß1-40 and derived analogs [5, 6]. In this study, the number of aluminum ions involved and their binding sites on the synthetic ß1-40:

Asp[1]-Ala-Glu-Phe-Arg-His-Asp-Ser-Gly-Tyr-Glu-Val-His-His-Gln-Lys-Leu-Val-Phe-Phe-Ala-Glu-Asp-Val-Gly-Ser-Asn-Lys-Gly-Ala-Ile-Ile-Gly-Leu-Met-Val-Gly-Gly-Val-Val[40]

were determined using complementary data from ^{27}Al NMR and UV/CD spectroscopy.

Results and Discussion

The low field ^{27}Al NMR spectra of Al(III) solution in the presence of increasing amounts of ß1-40 show a distinct signal near 15 ppm (Figure 1) and was attributed to the generation of a Al(III)-complexed ß1-40 species. The intersection of the titration curves from the plot of intensity of this novel signal relative to the reference hexaaquo ion signal at 0 ppm (Figure 1B) suggests the stoichiometry of the observed species. If it is assumed that all the detectable ^{27}Al species were observed, then within these limits there are between 4 and 6 Al(III) complexed with each ß1-40 molecule.

The CD spectrum of a ß1-40 solution in the presence of Al(III) is shown in Figure 2. On addition of equimolar EDTA, in terms of Al(III), the Al(III)-induced conformational change is all but abolished. Aluminum titrations of the CD spectra show a pseudo-sigmoidal behavior suggesting cooperativity, and the corresponding Hill plot gives the average association constant of 150 μM, with an intercept of 1.67. Earlier, it has been shown that there are at least 3 amino acid modifications in ß1-40 [7]. Taken together with the ^{27}Al NMR data and the poor signal/noise ratios for the CD could account for the disagreement between the two spectroscopic determinations in this report.

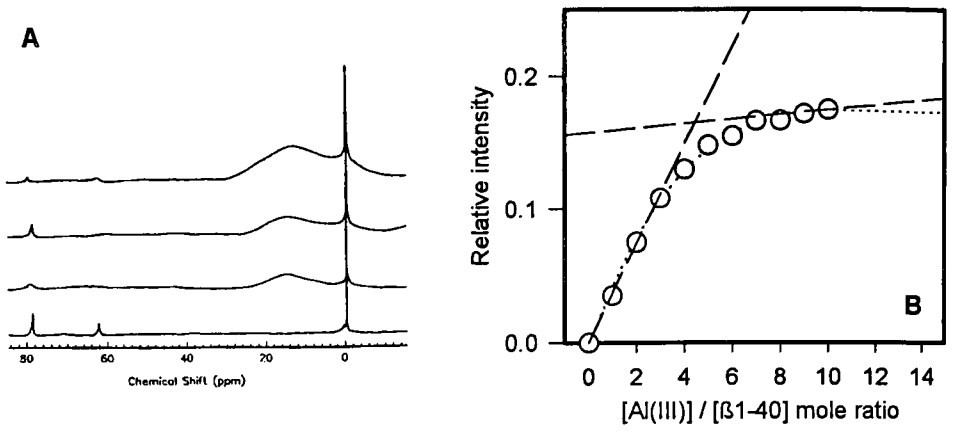

Figure 1. *(A) The 23.30 MHz ^{27}Al NMR spectra of Al(III) binding to ß1-40 at pH 4.5. (B) The relative intensity of the Al(III)-ß1-40 signal near 15 ppm as a function of Al(III):ß1-40 mole ratio.*

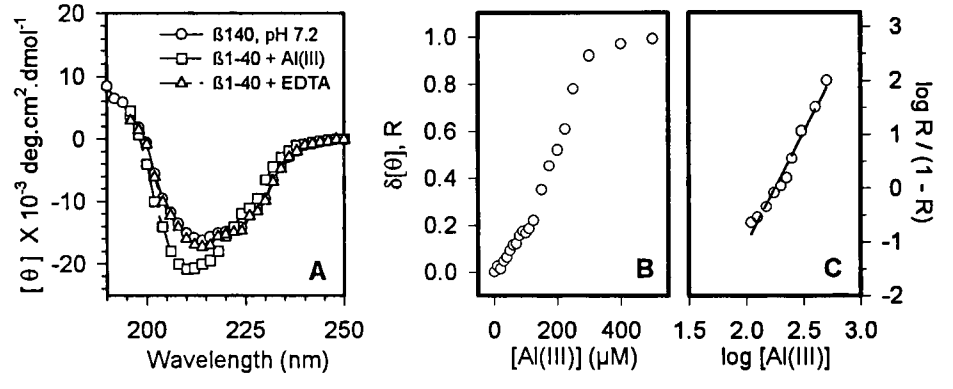

Figure 2. *CD spectra of 0.25 mM ß1-40 solution in presence of 0.5 mM Al(III) and EDTA (A). Panel B gives the fractional change in ellipticity at 215 nm. The Hill plot of CD data near midpoint of fractional ellipticity transition is given in C.*

References

1. Selkoe, D.J., *Annu. Rev. Neurosci.*, 12 (1989) 463.
2. Shoji, M., Golde, T.E., Ghiso, J., Cheung, T.T., Estus, S., Shaffer, L.M., Cai, X.-D., McKay, D.M., Tintner, R., Frangione, B. and Younkin, S.G., *Science*, 258 (1992) 126.
3. Mantyh, P.W., Ghilardi, J.R., Rogers, S., DeMaster, E., Allen, C.J., Stimson, E.R. and Maggio, J.E., *J. Neurochem.*, 61 (1993) 1171.
4. Kawahara, M., Muromato, K., Kobayashi, K., Mori, H. and Kuroda, Y., *Biochem. Biophys. Res. Commun.*, 198 (1994) 531.
5. Exley, C., Price, N.C., Kelly, S.M. and Birchall, J.D., FEBS Lett., 324 (1993) 293.
6. Vyas, S.B. and Duffy, L.K., *Biochem. Biophys. Res. Commun.*,206 (1995) 718.
7. Vyas, S.B. and Duffy, L.K., *J. Prot. Chem.*, in press.

Peptides: Chemistry, Structure and Biology
Pravin T.P. Kaumaya and Robert S. Hodges (Eds.)
Mayflower Scientific Ltd., 1996

215
Conformational Studies of Emerimicin 1-9 by Independent Experimental and Computational Approaches

D.D. Beusen, R.D. Head and G.V. Nikiforovich

Center for Molecular Design, Washington University, St. Louis, MO 63130, USA

Introduction

The emerimicins are members of the peptaibol family of antibiotics which act as voltage-gated ion channels. As an aid in understanding their mechanism of action, we have been studying their conformations by experimental and computational methods. Previous structural studies of the N-terminal fragment of emerimicin (Ac-Phe-Aib-Aib-Aib-Val-Gly-Leu-Aib-Aib-OBzl, EM 1-9) have shown it to be α-helical in the crystalline state [1] and mixed $\alpha/3_{10}$-helical in DMSO [2]. Here, we compared these experimental results with theoretical studies of conformations of the 1-9 fragment of emerimicin.

Results and Discussion

A relaxation-rate matrix approach within the program Macrosearch [3] was used to extract distance restraints from solution NMR data of EM 1-9 in DMSO [2]. These restraints, along with torsion angle restraints and explicit H-bond restraints, were used in systematic conformational searches to identify conformations consistent with the NMR data. All 32 possible H-bonding patterns were considered for the five residues which are solvent-shielded. This analysis confirmed previous studies suggesting that the peptide is a mixed $\alpha/3_{10}$ helix, and several of these mixed forms were consistent with the NMR data. In an independent study, energy calculations were performed employing the ECEPP force field and the build-up calculation protocol [4] in which the solvent was represented by a constant dielectric, $\varepsilon = 45$. Several tens of low-energy backbone conformers ($E - E_{min} < 10$ kcal/mol) were found for EM 1-9. The family containing the lowest energy conformer was found to be helical. The lowest energy conformer was in agreement with the α-helical X-ray structure obtained previously for EM 1-9 (Table 1). To study local flexibility of this low-energy helical conformer, Monte Carlo simulations were performed as described previously [4]. When the 35,000 conformations generated in the vicinity of the local minimum were averaged, the resulting structure was found to compare favorably to the X-ray structure. The torsion angle ranges sampled during the Monte Carlo analysis were very similar to those allowed in the Macrosearch analyses of the NMR data. The interproton distances predicted by the Monte Carlo simulations largely reproduced the interproton distances measured by NMR. In the Monte Carlo data, 48% of the conformations had six *i - i+4* hydrogen bonds, which is the predicted number for an α-helical EM 1-9 structure. Many conformations possessed one, two or three hydrogen bonds of the *i - i+3* or 3_{10}type. No pure 3_{10}-helical structure was found.

The experimental and computational results in this study are consistent with each other and with other studies suggesting that the energy barrier between α- and 3_{10}-helical forms is small, and that the transition between them is not concerted but instead involves mixed $\alpha/3_{10}$ states [5].

Table 1. *EM 1-9 conformers determined by experimental and computational methods.*

Residue	Angle	NMR+ Macrosearch	Lowest energy	Monte Carlo $\bar{x}$	Monte Carlo σ	X-ray [1]
Phe	φ	-60 to -50	-56	-71	15	-61.9
	ψ	-50 to -20	-44	-38	10	-43.4
Aib	φ	-70 to -40	-54	-56	4	-50.7
	ψ	-40 to -10	-53	-48	7	-57.4
Aib	φ	-90 to -50	-61	-60	4	-58.1
	ψ	-60 to -10	-42	-40	5	-49.9
Aib	φ	-90 to -40	-55	-56	4	-55.0
	ψ	-50 to -10	-43	-42	7	-52.4
Val	φ	-110 to -60	-71	-74	7	-76.3
	ψ	-40 to -10	-40	-37	6	-27.6
Gly	φ	-90 to -60	-58	-59	6	-59.7
	ψ	-60 to -40	-40	-41	8	-32.6
Leu	φ	-60	-76	-76	9	-82.1
	ψ	-60 to -30	-47	-44	7	-32.4
Aib	φ	-80	-57	-54	5	-53.7
	ψ	-30 to -10	-31	-38	8	-38.1
Aib	φ	40 to 80; 150 to -160 -90 to -70; -50 to -30	56	55	5	55.1
	ψ	-180 to +180	64	61	15	47.7

Acknowledgments

This work was supported in part by NIH grant GM 24483. Emerimicin 1-9 was provided by J. Zabrocki and M.T. Leplawy.

References

1. Marshall, G.R., Hodgkin, E.E., Langs, D.A., Smith, G.D., Zabrocki, J. and Leplawy, M.T., *Proc. Natl. Acad. Sci. USA.*, 87 (1990) 487.
2. Beusen, D.D., Hutton, W.C., Kotyk, J.J., Zabrocki, J., Leplawy, M.T. and Marshall, G.R., in Giralt, E., and Andreu, D. (Eds.), Peptides 1990, ESCOM, Leiden, The Netherlands, 1991, p. 545.
3. Beusen, D.D., Head, R.D., Clark, J.D., Hutton, W.C., Slomczynska, U., Zabrocki, J., Leplawy, M.T. and Marshall., G.R., in Schneider, C.H. (Ed.), Peptides 1992, ESCOM, Leiden, The Netherlands, 1993, p. 79.
4. Nikiforovich, G.V., Prakash, O., Gehrig, C.A. and Hruby, V.J., *J. Am. Chem. Soc.*, 115 (1993) 3399.
5. Smythe, M.L., Huston, S.E. and Marshall, G.R., *J. Am. Chem. Soc.*, 117 (1995) 5445.

Peptides: Chemistry, Structure and Biology
Pravin T.P. Kaumaya and Robert S. Hodges (Eds.)
Mayflower Scientific Ltd., 1996

216
Design and Conformational Studies of DPMPT, a Novel Highly Potent δ-Opioid Peptide

G.V. Nikiforovich[1], K.E. Kövér[2], S.A. Kolodziej[3], B. Nock[4] C. George[5], J.L. Flippen-Anderson[5] and G.R. Marshall[1,3]

[1]Center for Molecular Design, Departments of [3]Pharmacology and [4]Psychiatry, Washington University, St. Louis, MO 63130, USA
[2]L. Kossuth University, H-4010 Debrecen, Hungary
[5]Laboratory for the Structure of Matter, Naval Research Laboratory, Washington, DC 20375, USA

Introduction

The problem of opioid analgesics interacting with δ-receptors is very urgent in modern molecular pharmacology. In this respect, studies of δ-selective peptides are especially valuable, since known non-peptide opioids possess just a moderate δ-selectivity. We have previously developed a model for δ-receptor pharmacophore based on energy calculations [1], which was strongly confirmed by synthesis and biological testing of several conformationally constrained analogs of opioid peptides with distinct selectivity, as well as with the X-ray data for DPDPE [Tyr[1]-cyclo(D-Pen[2]-Gly[3]-Phe[4]-D-Pen[5])] [2]. Here we report the use of the model as a template for computational design of novel rigidified analogs of DPDPE with high potency of binding and δ-selectivity, using 3-mercaptoproline, a "chimeric" residue combining features of penicilamine and proline.

Results and Discussion

Employing energy calculations, we have designed two compounds, Tyr[1]-*cyclo* (D-Pen[2]-Gly[3]-Phe[4]-L-3-Mpt[5]) (DPMPT) and Tyr[1]-*cyclo*(D-Pen[2]-Gly[3]-Phe[4]-D-3-Mpt[5]) (DPDMPT). Each of low-energy conformers of DPMPT and DPDMPT was compared with the models for the δ-receptor-bound conformation of DPDPE [1] by overlapping the nitrogen atom of α-amino group, the C^{γ} and C^{ζ} atoms of the Tyr and Phe aromatic rings, and the C^{α} atom of the D-Pen residue. Results of comparison showed that some low-energy 3D structures of DPMPT and DPDMPT are compatible with the model for the δ-receptor-bound conformation of DPDPE (Table 1).

DPMPT and DPDMPT were tested for their binding to δ-, μ- and κ-opioid receptors. The corresponding K_i values were 3.5, 68, and >5,000 nM for DPMPT, and 103.7, >5,000, and >5,000 nM for DPDMPT, respectively. Independent studies by homo- and heteronuclear 2DNMR spectroscopy and energy calculations showed that DPMPT exists in DMSO solution in conformational equilibrium between several backbone conforma-

tions with the same type of 3D structure for the cyclic moiety, but with somewhat different conformers of the acyclic part of the molecule and two types of rotamers for the D-Pen side chain, namely **t** and **g**$^-$. For DPDMPT, energy calculations combined with the experimental data suggest that any one out of four low-energy conformers belonging to the same type of the backbone of cyclic moiety may be a possible candidate for DPDMPT conformer in DMSO. DPDMPT structure revealed by the X-ray crystallography showed remarkable similarity to DPDMPT solution conformations (Table 1).

Table 1. *Description of low-energy conformers of DPMPT and DPDMPT.*

Residue	Tyr		D-Pen[2]		Gly		Phe			3-Mpt/D-Pen[5]	
Angle	ψ	χ1	ϕ	ψ	ϕ	ψ	ϕ	ψ	χ1	ω	ϕ
Models of δ-receptor-bound conformers											
DPMPT	141	180	79	21	-86	-25	-140	73	-60	167	-75
DPDMPT	140	180	78	35	-94	-33	-141	73	-60	15	75
DPDPE	142	180	80	-145	66	27	-157	-57	-75	179	126
Low-energy conformers of DPMPT backbone interconverting in DMSO solution											
I	140	-	76	-146	80	-73	-136	74	-	-178	-75
II	140	-	140	-149	80	-72	-136	75	-	-178	-75
III	140	-	73	-147	81	-72	-138	73	-	-177	-75
IV	140	-	140	-149	80	-72	-136	75	-	-178	-75
Possible low-energy conformers of DPDMPT backbone in DMSO and in crystals											
I	138	-	141	-151	123	-124	-153	67	-	14	75
II	140	-	73	-146	123	-125	-153	66	-	13	75
III	80	-	142	-151	127	-121	-155	66	-	13	75
IV	80	-	73	-146	123	-125	-153	66	-	12	75
X-ray	124	-	127	-140	114	-126	-127	69	-	6	86

The determined solution conformations of both compounds were compared to their suggested δ-receptor-bound conformers, using the same six atomic centers (rotamers of the side chains of the Tyr and Phe residues were assumed to be **t** and **g**$^-$, respectively). Results showed that all four possible solution conformations of DPDMPT are non-similar to DPDMPT δ-receptor-bound conformation, whereas two possible solution conformations of DPMPT are compatible to the suggested δ-receptor-bound conformation of DPMPT with **rms** = 0.83 Å. This can explain the difference in binding of DPMPT and DPDMPT to δ-receptors by a suggestion that the δ-receptor-bound conformation of DPMPT pre-exists in solution, whereas solution conformations of DPDMPT should be more significantly distorted to match the δ-receptor-bound conformation of DPDMPT.

References

1. Nikiforovich, G.V., Hruby, V.J., Prakash, O. and Gehrig, C.A., *Biopolymers*, 31 (1991) 941.
2. Flippen-Anderson, J.L., Hruby, V.J., Collins, N., George, C. and Cudney, B., *J. Am. Chem. Soc.*, 116 (1994) 7523.

Peptides: Chemistry, Structure and Biology
Pravin T.P. Kaumaya and Robert S. Hodges (Eds.)
Mayflower Scientific Ltd., 1996

217
Conformational Studies of Analogs of Parathyroid Hormone Related Protein (PTHrP) Containing Lactam-bridged Side-chains

M. Chorev[1], A. Bisello[1], V. Behar[1], C. Nakamoto[1], M. Rosenblatt[1], S. Maretto[2], S. Mammi[2] and E. Peggion[2]

[1]Beth Israel Hospital, Harvard Medical School, Boston, MA 02215, USA
[2]University of Padova, Department of Organic Chemistry, Biopolymers Research Center, Via Marzolo 1, I-35131 Padova, Italy

Introduction

We have recently studied the conformational properties of two highly potent PTH/PTHrP receptor antagonists, *i.e.*, [Leu^{11}, D-Trp^{12}]PTHrP(7-34)NH_2 and [Ahx^{8,18}, D-Trp^{12}, Tyr^{34}]PTH(7-34)NH_2 using CD, 2D-NMR and computer simulations [1]. In 1:1 TFE-water, both analogs adopt a helical structure comprising the sequence 15-32. In an attempt to identify the relevant elements of bioactive conformation, we synthesized by solid phase methodology the following structurally constrained analogs of PTHrP in which i-to-(i+4) side-chain to side-chain cyclization through a lactam bridge was introduced:

[Lys^{13}, Asp^{17}]PTHrP(7-34)NH_2 (1) **[Lys^{26}, Asp^{30}]PTHrP(1-34)NH_2 (2)**

Analog **1** is a potent PTH/PTHrP antagonist, while analog **2** is a potent agonist.

Results and Discussion

In aqueous solution, both analogs exhibit CD properties typical of a random structure with a small amount (~15%) of helix. Thus, the constraint imposed by the lactam bridge is insufficient to stabilize the helical conformation in water. Upon addition of TFE, a sharp increase of the helical content occurs in both analogs between 0 and 20% (v/v) (Figure 1). Saturation conditions are reached practically at 30% TFE, with two overlapping CD spectra corresponding to a helical content of 75%. The profile of the conformational change as a function of the solvent composition is different from that of the linear peptides PTHrP(1-34) and PTH(1-34) for which a folded structure was assigned [2, 3]. In those cases, the conformational change occurs at higher TFE concentration and an initial folding of an α-helical domain in the C-terminal portion of the sequence at low TFE concentration was suggested, followed by folding of a second, N-terminal helical domain at higher TFE concentration [3]. In analogs **1** and **2**, the lactam constraints were introduced in the PTH/PTHrP receptor binding domain [4]. Our

results seem to indicate that these constraints facilitate the propagation of the α-helical structure upon addition of TFE. The relevant elements of secondary structure of both analogs in TFE/water (1:1) were assessed by 2D-NMR. From the NOE pattern of analog **1** it is possible to identify a helical segment extending from residue 13 to 34. Thus, with respect to previous results on PTHrP(7-34) [4], the lactam bridge contributes to stabilize the helical structure and to extend it toward the N-terminal portion of the sequence. In line with previous work on PTH(1-34) [3], the NOE pattern of analog **2** indicates the presence of two helical stretches, from residue 5 to residue 12 and from residue 14 to residue 34. In this case, the lactam bridge is positioned within the principal binding domain (sequence 25-34), where the linear peptide has already a high propensity to fold into the helical conformation. Further stabilization of the helix of the principal binding domain enhances the binding properties of this analog which maintains full agonistic activity because of the presence of the functionally important activation domain at the N-terminus. Studies on more constrained cyclic analogs of PTHrP are underway in an attempt to obtain more information on the bioactive conformation of PTH/PTHrP.

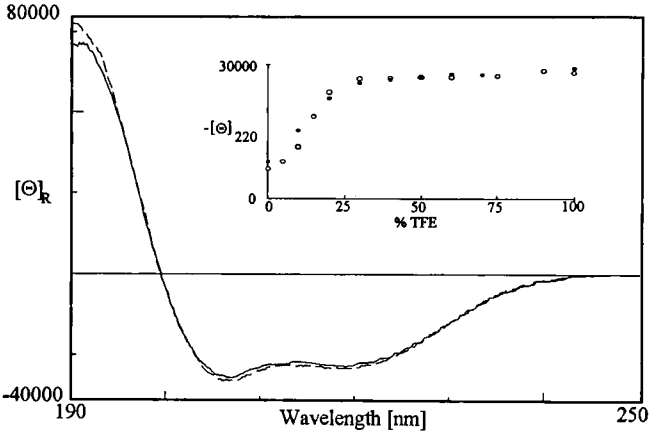

Figure 1. *CD spectra of analogs 1 (——) and 2 (– – –) in TFE. In the insert, the molar ellipticity at 220 nm as a function of TFE content for analogs 1 (○) and 2 (●) is reported.*

References

1. Chorev, M., Behar, V., Yang, Q., Rosenblatt, M., Mammi, S., Maretto, S., Pellegrini, M. and Peggion, E., *Biopolymers*, 36 (1995) 485.
2. Cohen, F.E., Strewler, G.J., Bradley, M.S., Carlquist, M., Nilsson, M., Ericsson, M., Ciardelli, T.L. and Nissenson, R.A., *J. Biol. Chem.*, 266 (1991) 1997.
3. Neugebauer, W., Surewicz, W.K., Gordon, H.L., Somorjai, R.L., Sung, W. and Willick, G.E., *Biochemistry*, 31 (1992) 2056.
4. Chorev, M., and Rosenblatt, M., in Bilezikian, J.P., Levine, M.A. and Marcus, R., (Eds.), 'The Parathyroids', Raven Press, New York, 1994, p.139.

Peptides: Chemistry, Structure and Biology
Pravin T.P. Kaumaya and Robert S. Hodges (Eds.)
Mayflower Scientific Ltd., 1996

218
Solid-state NMR Analysis of the Conformation of an Inhibitor Bound to Thermolysin

D.D. Beusen[1], U. Slomczynska[2], L.M. McDowell[3] and J. Schaefer[3]

[1]Center for Molecular Design and Departments of [2]Pharmacology and [3]Chemistry
Washington University, One Brookings Drive, St. Louis, MO 63130, USA

Introduction

A number of experimental methods are used to determine the receptor-bound conformation of peptides as part of the process of rational drug design, including X-ray diffraction and solution-NMR methods such as transferred- and isotope-edited NOESY. Many receptor/ligand systems are not amenable to these types of analyses due to dynamic properties incompatible with solution-NMR analysis or difficulties in preparing crystalline samples. In these cases, solid-state NMR can provide structural information that would otherwise not be available. Rotational-echo double resonance (REDOR) NMR is a solid-state, magic-angle spinning experiment that measures heteronuclear dipolar coupling between pairs of labeled nuclei and allows interatomic separation to be determined based on the r^{-3} distance dependence of dipolar coupling [1]. Thermolysin was the first metalloproteinase to be characterized in atomic detail [2], and has provided insights into the mechanism and specificity of other zinc proteases. In this study, we compare REDOR measurements of internuclear distances in bound Cbz-Gly^{P}-[1-^{13}C]Leu-[^{15}N,2-^{13}C]Ala (ZG^{P}LA), a phosphonamidate transition-state analog inhibitor of thermolysin [3], to the corresponding crystallographically determined distances.

Results and Discussion

Specifically labeled ZG^{P}LA was synthesized [3] and infused into thermolysin crystals [2] which were then recovered by centrifugation for analyses. The ^{31}P chemical shifts of the bound, free, and hydrolyzed forms of the inhibitor in the solid-state were the same as seen previously in solution spectra of this inhibitor complexed to thermolysin [4].

In a solid with ^{31}P-^{15}N dipolar coupling, the ^{31}P rotational spin echoes which form each rotor period can be prevented from reaching full intensity by rotor-synchronized ^{15}N π pulses. The difference (ΔS) between the ^{31}P NMR spectrum obtained under these conditions (S) and one obtained with no ^{15}N π pulses (S_o) depends on the strength of the dipolar coupling (D), the number of rotor cycles over which dephasing occurs (N_c) and the rotor period (T_r). From the ratio ΔS/S determined at several values of N_c, an average ^{31}P-^{15}N distance of 3.89±0.10 Å was determined for ZG^{P}LA bound to thermolysin.

A ^{13}C-observed, ^{31}P-dephased REDOR experiment analogous to the experiments described above could, in principle, yield the desired ^{13}C-^{31}P distances. However,

natural-abundance ^{13}C contribution to the full-echo signal is a potential source of error. This can be circumvented by incorporating a nearby ^{15}N and using it to select the ^{13}C signals of interest [1]. In these measurements, two REDOR experiments were performed successively. The first experiment used ^{15}N π pulses to dephase the ^{13}C signal. Because the ^{15}N-^{13}C pair are directly bonded, their interaction dominates the ^{15}N-^{13}C dipolar coupling in the sample and $\Delta S/S_0$ maximizes in a number of rotor cycles of dephasing at which background ^{13}C contributions to ΔS are negligible [1]. In the second REDOR experiment, ^{31}P dephasing pulses result in a difference signal, ΔS, from which the ^{13}C-^{31}P dipolar interaction can be calculated using S_0 for the specifically labeled ^{13}C atoms as determined from the first ^{15}N-^{13}C experiment. Using this double-REDOR approach, ^{31}P-$^{13}C'$ and ^{31}P-$^{13}C\alpha$ distances in the enzyme/inhibitor complex were found to be 3.61±0.10 and 5.37±0.13 Å, respectively.

Although no X-ray coordinates have been reported for ZG^{P}LA bound to thermolysin, there are four published complexes of phosphorous-based, transition-state analog inhibitors having all or most of the atoms involved in these REDOR studies: ZF^{P}LA and ZG^{P}LL [5], and P-Leu-NH_2 and phosphoramidon [6]. All are similar to ZG^{P}LA in having Leu at the R_1' position, and are nearly superimposable with respect to the atoms in this REDOR study. The average P-N, P-C', and P-Cα distances in these complexes are 3.91±0.13, 3.58±0.04, and 5.17±0.18 Å, respectively. These distances are consistent with our solid-state NMR measurements, demonstrating that REDOR NMR has the ability to provide information on the receptor-bound conformation of a ligand equivalent to that obtainable by solution NMR and X-ray methods.

Acknowledgments

This work was supported by NIH grants GM-40634 and GM-24483.

References

1. Holl, S.M., Marshall, G.R., Beusen, D.D., Kociolek, K., Redlinski, A.S., Leplawy, M.T., McKay, R.A., Vega, S. and Schaefer, J., *J. Am. Chem. Soc.*, 114 (1992) 4830.
2. Matthews, B.W., Jansonius, J.N., Colman, P.M., Schoenborn, B.P. and Dupourque, D., *Nature New Biol.*, 238 (1972) 37.
3. Bartlett, P.A. and Marlowe, C.K., *Biochem.*, 22 (1983) 4618.
4. Copie, V., Kolbert, A.C., Drewry, D.H., Bartlett, P.A., Oas, T.G. and Griffin, R.G., *Biochem.*, 29 (1990) 9176.
5. Holden, H.M., Tronrud, D.E., Monzingo, A.F., Weaver, L.H. and Matthews, B.W., *Biochem.*, 26 (1987) 8542.
6. Tronrud, D.E., Monzingo, A.F. and Matthews, B.W., *Eur. J. Biochem.*, 157 (1986) 261.

Peptides: Chemistry, Structure and Biology
Pravin T.P. Kaumaya and Robert S. Hodges (Eds.)
Mayflower Scientific Ltd., 1996

219
Conformational Analysis of YSPTSPSY-DNA Interactions

A. Khiat and Y. Boulanger

INRS-Santé, Université du Québec, Pointe-Claire, Québec H9R 1G6, Canada

Introduction

Experimental evidence [1] shows that YSPTSPSY (peptide 1) binds to DNA by intercalation of tyrosine residues. In the model proposed previously [1], both sequences SPTS and SPSY form a type I β-turn. As demonstrated by NMR [2], there is a good evidence for the presence of type I and II β-turns in the first sequence SPTS, but the second sequence SPSY is less structured. In this study, strategies based on random search energy minimizations have been applied to generate populations of conformers characterizing peptide 1. Subsequent analysis based on statistical methods and clustering allowed to determine the existence of four families of conformers containing β- and/or γ-turns. Employing a Monte-Carlo based docking procedure, peptide 1 was docked in a DNA double helical fragment with the sequence $[d(GACGTC)]_2$. The peptide binds on the minor groove stacking the CG base pairs. Upon binding, the structure of SPSY is modified into a type I β-turn. Five intermolecular hydrogen bonds are observed but the van der Waals interactions constitute the major stabilization factor for the complex.

Results and Discussion

Conformational domains of YSPTSPSY: The most stable conformers are distributed into four major families respectively 1,2,3,4:

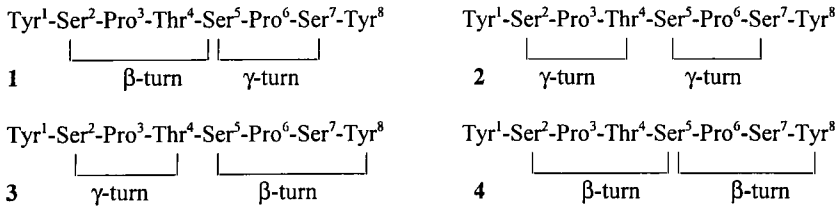

The largest number and the most stable conformers belong to family 1. Conformers with two β-turns (family 4) are the least stable and the least abundant. The results indicate that the second sequence SPSY is less structured than the first sequence SPTS. The majority of turns founds are type III, in agreement with the NMR results [2]. In most conformers, the aromatic rings are positioned on the same side of the peptide 1 with Tyr^1-Tyr^8 distances suitable for intercalation into DNA.

Structure of the YSPTSPSY-DNA complex: The major stabilizing factor is due to van der Waals contacts. Additional stabilization is provided by aromatic ring stacking.

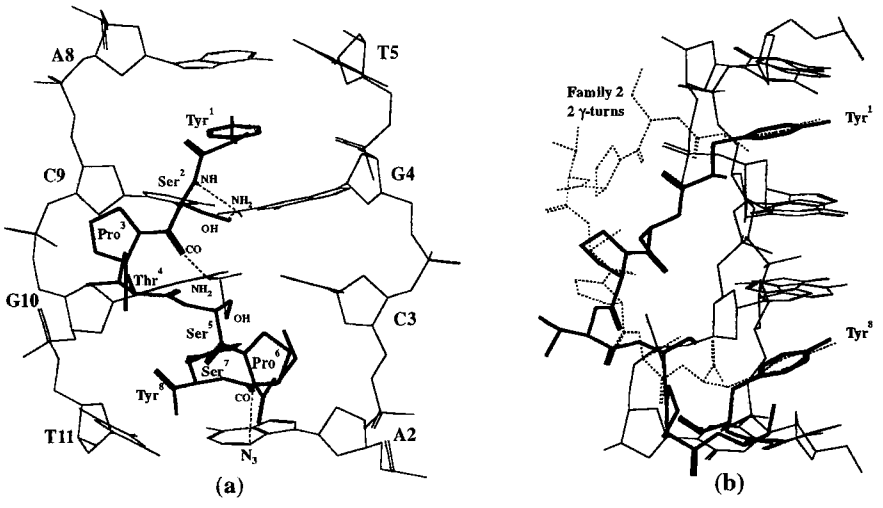

Figure 1. *Peptide 1-$[d(GACGTC)]_2$ complex (a) front view in the major groove showing intermolecular hydrogen bonds (dotted lines) and (b) side view showing the difference between a family 2 conformer (dotted lines) and a docked conformer (full lines).*

In addition to van der Waals interactions between Ser^2 or Ser^5 and the central CG base pairs, four intermolecular hydrogen bonds are observed (Figure 1a). This suggests that Ser^2 and Ser^5 are the key residues for the binding of peptide 1 to DNA.

Comparison of peptide 1-DNA and triostin A-DNA complexes: In both complexes, strong van der Waals contacts and four hydrogen bonds between the central CG base pairs and the serine or alanine residues are found for peptide 1 or triostin A, respectively. The pattern of stacking interactions between the base pair rings and the aromatic rings of peptide 1 or triostin A are similar. Strong conformational similarities are observed between peptide 1 and triostin A.

Conformation of YSPTSPSY in the complex: The lowest energy conformation of peptide 1, of family 1 has been docked into the DNA fragment. The docking results indicate the major stabilization factor to be the interaction between the N-terminal part of peptide 1 and the CG base pairs. Interaction is only possible if the N-terminal segment is folded to form a β-turn. It is evident from Figure 1b that conformers of family 2 or family 3 cannot bind to DNA, even though their tyrosine rings intercalate. Atoms from the N-terminal end remain far from the CG base pairs and so interactions essential to complex formation cannot occur. Following docking and energy minimization of the complex, the docked conformer rearranges and the ψ angle of Thr^4 deviates by 40° from the ideal value of a type I β-turn. The C-terminal segment changes from a γ-turn to a type I β-turn. This new geometry is similar to the structure proposed previously [1]. The conformation of free peptide 1 is therefore modified as a result of bisintercalation.

References

1. Suzuki, M., *Nature,* 344 (1990) 562.
2. Harding, M.M., *J. Med. Chem.*, 35 (1992) 4658.

Peptides: Chemistry, Structure and Biology
Pravin T.P. Kaumaya and Robert S. Hodges (Eds.)
Mayflower Scientific Ltd., 1996

220
Effects of N-Methyl Isosteres on Helix Stability

C.-F. Chang[1] and M.H. Zehfus[2]

[1]Biophysics Program and [2]Division of Medicinal Chemistry, The Ohio State University, Columbus, OH 43210, USA

Introduction

Isosteres are linkages that replace peptide bonds but preserve the C_α-C_α distance between amino acids. The effects of isosteres on protein secondary structure is not known. Here we focus on inserting the N-methyl isostere into a model peptide to study its effect on secondary structure. This isostere should have two major effects. It will remove the ability of the NH group to act as a proton donor in a hydrogen bond and it replaces a hydrogen atom with a bulky methyl group. The effects of the N-methyl isostere on α-helix formation were measured by CD and analyzed using helix-coil transition theory. This allowed us to quantitate the change in total energy associated with the replacement of the peptide bond with the isostere.

Results and Discussion

Melting curves for the control peptide of sequence Ac-WGG$(EAAAR)_4$A-Amide and similar peptides with the N-methyl isostere at positions 5, 11, 16, 21 and D-Ala at position 11 have been obtained. If we assume that the helix coil transition is a simple two-state model, C⇌H, then the pseudo-equilibrium constant can be expressed as K=Helix/Coil= $([\theta]-[\theta]_C)/([\theta]_H-[\theta])$; where $[\theta]$ is the observed ellipticity, $[\theta]_H$ is the ellipicity of the helix, and $[\theta]_C$ is the ellipicity of the coiled state. The thermodynamic properties are described by the van't Hoff relationship, $\ln K=-\Delta H°/R(1/T-1/T_m)$. The parameters T_m and H° are derived by finding the best fit of these parameters to the experimental melting curves. At any particular temperature ΔG and ΔS can be obtained, and all modified peptides are compared to the control peptide to obtain ΔΔH, ΔΔG, and ΔΔS for the change of a peptide bond to the isostere linkage (Table 1).

However, helix formation by small peptides in aqueous solution is not a simple two-state transition. At a given temperature, we do not have a simple equilibrium between a fully helical and a fully coiled state; instead we have a population of conformations where helix and coil residues are distributed heterogeneously throughout the peptide. Therefore, we use Lifson-Roig (LR) theory [1] to model this conformation population. The LR model describes the state of each amino acid in a sequence using statistical weights for helix elongation (w), helix nucleation (v), and coil probabilities (u). These weights are then combined to form a partition function that describes the system. The mathematics of the system are expressed in matrix form and may be easily manipulated using the mathematical software package MAPLE [2].

In the uniform helix model, we assumed that u=1, v=0.048, and <w> is a constant for all amino acids. <w> was adjusted to match experimental data for the control peptide, while w' and v' were altered to fit the experimental data for the modified peptides, and $\Delta\Delta G$=-RTln(w'/<w>). In the full helix model, we keep u=1, v=0.048, but each amino acid has it's own w factor [3], and the partition function is expressed as a series of 4x4 matrices [4]. Factors for salt bridges, temperature dependence, and end capping are also included. In this full helix model $\Delta\Delta G$=-RTln(w'/w_{Ala}).

Table 1. *$\Delta\Delta G$ (kcal/mole), $\Delta\Delta H$(kcal/mole), $\Delta\Delta S$(eu) values for #05 and d11 at 0°C.*

	Two-state model			Uniform helix model			Full helix model		
	$\Delta\Delta G$	$\Delta\Delta H$	$\Delta\Delta S$	$\Delta\Delta G$	$\Delta\Delta H$	$\Delta\Delta S$	$\Delta\Delta G$	$\Delta\Delta H$	$\Delta\Delta S$
#05[a]	+0.28	+0.51	+0.88	+1.25	+1.14	+0.40	+1.25	+2.68	+5.20
d11[b]	+0.67	+0.75	+0.40	+2.75	+11.80	+33.00	+1.83	+3.14	+4.80

[a]N-methyl isostere at position 5, [b]D-Ala at position 11; data for other isosteres could not be analyzed because w' is negative.

The numbers derived from the simple two-state model are much lower than those derived from the more detailed LR analysis (Table 1). We believe that the LR model fits this system better, but have found that frequently the w' parameter of a single amino acid becomes negative. A negative w' term means that the isostere has disrupted more than one single residue in the helix. This can be done in two ways. First, the isostere may disrupt adjacent hydrogen bonds. This effect is readily seen with computer models. Second, when the isostere disrupts the helix, it should also disrupt the salt bridge holding that part of the helix together. The charged groups that made up the salt bridge are then free to interact with the charged groups of adjacent salt bridges to disrupt additional salt bridges. While we do not see this effect in our modeling studies, it can be removed by changing our model helix to one that does not depend on salt bridges for stabilization.

Further work is needed to differentiate between these two possibilities. If salt bridges are the problem, then a new model peptide will eliminate this factor from the analysis. If disruption of adjacent residues is the problem, then the LR theory must be modified to mimic the actual system more closely. We are currently expanding this approach to include other isosteres like $COCH_2$ (ketomethylene) and CH_2NH_2 (reduced ketone). These isosteres remove the ability of the peptide backbone to hydrogen bond without introducing additional bulky groups. By comparing the differences between different isosteres, it should be possible to determine the strength of the α-helix hydrogen bond as well as quantitate other backbone-backbone interactions.

References

1. Lifson, S. and Roig, A., *J. Chem. Phys.*, 34 (1961) 1963.
2. Abell, M.L. and Braselton, J.P., 'The Maple V Handbook', AP Professional, 1994.
3. Chakrabartty, A., Kortemme, T. and Baldwin, R.L., *Protein Science*, 3 (1994) 843.
4. Doig, A.J., Chakrabartty, A., Klingler, T.M. and Baldwin, R.L., *Biochemistry*, 33 (1994) 3396.

Peptides: Chemistry, Structure and Biology
Pravin T.P. Kaumaya and Robert S. Hodges (Eds.)
Mayflower Scientific Ltd., 1996

221

Can we "TOAC" Peptides? The Incorporation and Characterization of a New Fmoc Nitroxide Spin Label Amino Acid into Peptides

M.P. Hanson[1], G.V. Martinez[1], G.L. Millhauser[1], F. Formaggio[2], M. Crisma[2], C. Toniolo[2] and C. Vita[3]

[1]*Department of Chemistry and Biochemistry, University of California at Santa Cruz, Santa Cruz, CA 95064, USA*
[2] *Biopolymer Research Center, CNR, Department of Organic Chemistry, University of Padova, 35131 Padova, Italy*
[3]*Département d'Ingénierie et d'Etudes des Proteins, CE Saclay, Gif-sur-Yvette, France*

Introduction

Helical peptides may serve as models for probing the secondary and higher order structure of proteins. Electron spin resonance (ESR) of peptides doubly spin labeled with the methane-thio-sulfonate spin label (MTSSL) has provided several new insights regarding helical structure [1-3]. To further explore these observations, doubly labeled peptides of varying length, incorporating the modified amino acid TOAC [4], were made such that a full turn of the helix could be examined. The TOAC label is unique in that the nitroxide moiety is rigidly attached to the peptide backbone and, as such, may be capable of reporting subtle local changes to the conformation of the peptide.

Results and Discussion

Two processes are at work in the spectra obtained from the spin labeled peptides (see Figure 1). The first process, dipole-dipole coupling, appears exclusively in the longer sixteen and twenty residue peptides because the molecular tumbling is not sufficiently rapid to average the dipole tensor to zero. Dipole-dipole interactions are inversely dependent upon the cube root of the distance between the labels [5]. The second process is through-space J-coupling and is observed in all the peptides. Through space coupling arises from overlap of the nitroxide wave functions which, in turn, is exponentially dependent on the distance between the labels [8]. These distance-dependent interactions provide the cornerstone to interpreting the ESR spectra of the biradicals.

In hexameric peptides, the labels provided spectroscopic evidence that reported structural changes resulting from modifications to the primary sequence. For example, we explored the influence of Aib, a strong helix-favoring amino acid, upon the structure of the peptide. Analysis of the resulting biradical spectrum revealed increased through-space coupling indicating the helical structure of the hexamer had been stabilized by the Aib. Comparison of the spectra from a hexamer and pentamer peptide

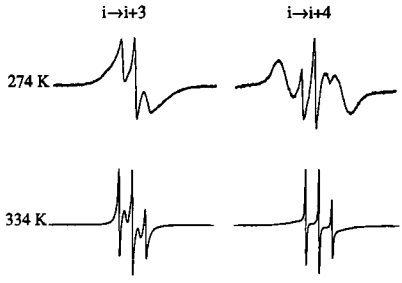

Figure 1. *ESR spectra (200 gauss scan width, 0.2 gauss Mod. Amp.) of the 20 residue, alanine based peptides in water (5 mM MOPS, pH 7.1).*

revealed the increased helicity that occurs with increasing peptide length [6, 7]. Also, changes in the N^{α}- blocking groups lead to observable changes in the EPR spectrum offering insight into how the varying electronic properties of such groups control helicity.

In conjunction with the spectra from the hexamer, longer sixteen and twenty residue peptides revealed a length dependent transition from 3_{10}- to α-helix observed previously by both ESR and crystallographic experiments [1, 6, 7]. The doubly TOAC labeled peptides also provided spectroscopic evidence unique to the two helical conformations, α and 3_{10}-helix. From the distance dependence of the dipole-dipole interaction at 274K, the distance ranking for the labels is $D_{i\rightarrow i+4} < D_{i\rightarrow i+3}$, characteristic of an α-helical conformation. As the temperature increases, the rotational correlation time decreases leading to an averaging of the dipole-dipole tensor to zero. However, at 334K the spectra show a motionally narrowed through space J-coupling component (i→1+3) and a dipole-dipole interaction (i→i+4) to be present. From the $1/r^3$ distance dependence of the dipole-dipole interaction, we conclude that these 20 residue Ala-based peptides remain mostly α-helical at higher temperatures. In the motionally narrowed component, the presence of a strong J-coupling in the i→1+3 peptide and lack a strong J-coupling in the i→1+4 peptidesuggests the formation of 3_{10}-helix.

In summary, increased structural resolution obtained from the TOAC label provides new insights into helical peptides. With two unique spectral components observable, the question of relative proportions of 3_{10} and α-helix becomes a tractable problem.

References

1. Fiori, W.R., Miick, S.M., Millhauser, G.L., *Biochemistry*, 32 (1993) 11957.
2. Fiori, W.R., Lundberg, K.M., Millhauser, G.L., *Nature Structural Biology*, 1 (1994) 374.
3. Miick, S.M., Martinez, G.V., Fiori, W.R., Todd, A.P., Millhauser, G.L., *Nature*, 359 (1992) 653.
4. Marchetto, R., Schreier, S., Nakaie, C.R., *J. Am. Chem. Soc.*, 115 (1993) 11042.
5. Luckhurst, G.R., in Berliner, J. (Ed.), 'Biradicals as Spin Probes', Academic Press, New York, 1976.
6. Pavone, V., Benedetti, E., Diblasio, B., Pedone, C., Santini, A., Bavaso, A.,Toniolo, C., Crisma, M. and Sartore, L., *J. Biomol. Struct. Dyn.*, 7 (1990) 1321.
7. Karle, I.L., Flippen-Anderson, J., Gurunath, R., Balaram, P., *Protein Science*, 3 (1994) 1547.
8. Closs, G.L., Forbes, M.D.E., Piotrowiak, P., *J. Am. Chem. Soc.*, 114 (1992) 3285.

Peptides: Chemistry, Structure and Biology
Pravin T.P. Kaumaya and Robert S. Hodges (Eds.)
Mayflower Scientific Ltd., 1996

222
Structural Analysis of [Aib^3]deltorphin I in Terms of Conformational Mixtures

O. Crescenzi[1], P. Amodeo[3], D. Picone[1], P.A. Temussi[1], S. Salvadori[2], R. Tomatis[2] and T. Tancredi[3]

[1]*Dipartimento di Chimica, Università di Napoli Federico II, via Mezzocannone 4, I-80134 Napoli, Italy*
[2]*Dipartimento di Scienze Farmaceutiche, Università di Ferrara, I-44100 Ferrara, Italy*
[3]*Istituto Chimica MIB del CNR, via Toiano 6, I-80072 Arco Felice, Napoli, Italy*

Introduction

As we have recently reported [1], introduction of Aib in the third position of deltorphin I (*i.e.*, in lieu of the, supposedly, necessary Phe^3 of the message domain) yields a peptide that not only retains a fairly high opioid agonism but has a δ/μ selectivity substantially higher than the parent peptide. This observation can be interpreted in two ways: either i) by admitting that the "message" is constituted by the tyramine moiety alone (and selectivity is entirely due to the address domain) or ii) by hypothesizing that the "message domain" can not be defined purely in terms of constitution (*i.e.* sequence) but mainly in terms of (outer) surface features. In order to answer these questions, we have performed a detailed conformational analysis of [Ac$_6$c^3]- and [Aib^3]deltorphin I.

Results and Discussion

[Aib^3]- and [Ac$_6$c^3]deltorphin I were examined by NMR spectroscopy in DMSO at room temperature and in a DMSO/water cryomixture at low temperature. The peptides are highly structured in both solvents, as indicated by the exceptional finding of a nearly zero temperature coefficient for the Val^5 NH resonance. NMR data cannot be explained on the basis of a single structure, as apparent from the presence of self-contradictory backbone NOEs, but it was possible to interpret all NMR data on the basis of a few structural families. The conformational averaging was analyzed by means of an original procedure: in practice, a starting set of base conformers is generated by conformational searches and energy minimization, each one of them being compatible with the requirements of a solvent-shielded Val^5 NH and with the experimental absent NOEs (anti-NOEs). The base conformers can enter in a generic conformational ensemble with individual mole fractions x_i. A penalty function is associated to each conformational ensemble (*i.e.*, to each vector $\{x_i\}$, i = 1... N_{conf}, $\Sigma_i x_i = 1$), which measures the weighted mean square difference of calculated and experimental NOEs and J coupling constants, and the relative minima of this function are searched by an algebric procedure, the mole fraction normalization costraint being accounted for by a Lagrange multiplier.

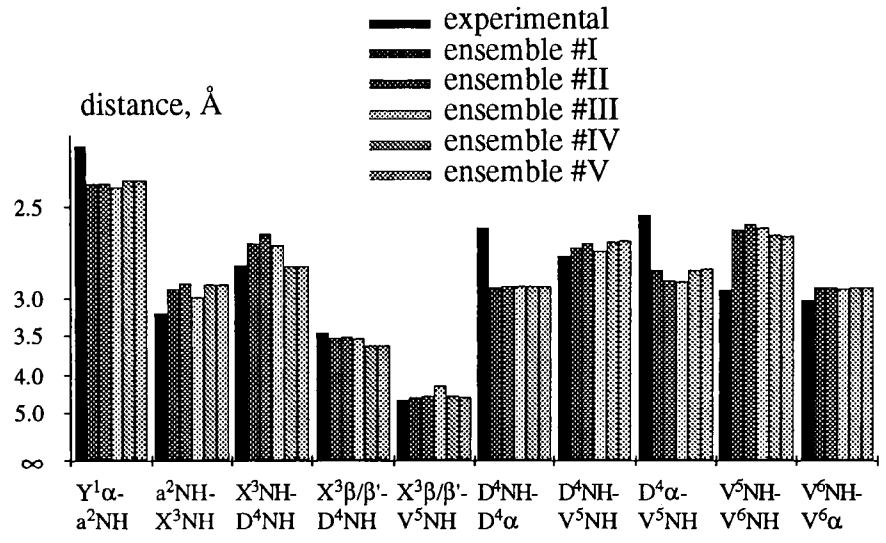

Figure 1. *Experimental vs. calculated backbone NOEs for the best conformational ensembles.*

Figure 1 shows the excellent agreement of experimental and calculated backbone NOEs for the ensembles corresponding to the first 5 minima of the global penalty function. Analysis of the corresponding ensembles shows that there is no single prevailing conformer, nor even a prevailing mixture: while confirming our hypothesis of a conformational averaging, this result points to the possibility that each one of the structures represented in the ensembles be regarded as a putative bioactive conformation. Accordingly, the shapes of all base conformers entering in the selected ensembles were compared with rigid δ-selective opiate agonists, *e.g.* SIOM [2]. Surprisingly, we found that the best overlay was realized by conformers which place in the region of space occupied by the second aromatic residue of non peptidic agonists the side chains of Val^5 and Val^6, *i.e.* two residues normally attributed to the address domain [3]. These facts may be interpreted as a strong indication that a rigid subdivision between message and address domains is generally difficult or impossible. It is important to recall that the domain concept [4], as imported from the protein field, is inextricably linked to global shape rather than constitution of a portion of the peptide sequence. The intrinsic structural stability of most proteins makes the two definitions nearly coincident in most cases, but this may be far from true in short-sequence peptides.

References

1. Picone, D., Amodeo, P., Crescenzi, O., Temussi, P.A., Salvadori, S., Cavicchioni, G., Lazarus, L.H. and Tancredi, T., in Maia H.L.S. (Ed.), 'Peptides 1994', Escom, Leiden, 1995, p.630.
2. Portoghese, P.S., Moe, S.T. and Takemori, A.E., *J. Med. Chem.*, 36 (1993) 2572.
3. Amodeo, P., Motta, A., Tancredi, T. ,Salvadori, S., Tomatis, R., Picone, D., Saviano, G., Temussi, P.A., *Peptide Research*, 4 (1992) 48.
4. Schwyzer, R., *Biochemistry*, 25 (1986) 6335.

Peptides: Chemistry, Structure and Biology
Pravin T.P. Kaumaya and Robert S. Hodges (Eds.)
Mayflower Scientific Ltd., 1996

223
Stability and Dynamics of Human Growth Hormone [6-13] Peptide Analogues at Hydrophobic Surfaces

T.-H. Lee, P.E. Thompson, M.T.W. Hearn and M.-I. Aguilar

Department of Biochemistry & Molecular Biology and Centre for Bioprocess Technology, Monash University, Clayton, Vic. 3168, Australia

Introduction

A type II' β-turn has been previously proposed as a critical component in mediating the insulin-potentiating activity of human growth hormone (hGH) [6-13] related peptide analogues [1]. In order to enhance the biological potency of hGH [6-13] peptides, the metabolic stability of this peptide has been increased through the synthesis of several non-homologous sequences and non-peptidic mimetics [1]. As the conformational flexibility of these peptides during their interaction with biological surfaces is a critical factor in their biological action, we have studied the surface-mediated conformational and dynamic properties of these hGH [6-13] peptide analogues using reversed phase high performance liquid chromatography (RP-HPLC).

Results and Discussion

Parameters related to the hydrophobic interactive contact area (S-value) and binding affinity (log k_0 value) of each peptide for the stationary phase ligands [2, 3] were determined for the peptide analogues listed in Table 1 over a range of temperatures between 5 and 85°C. The S and log k_0 values were determined from log κ *versus* φ plots as previously described [2]. The dependence of S and log k_0 values on temperature for the α-aminosuccinimide, the β-aspartyl and the D-Ala^{11}Pro^{12} analogues chromatographed on a C18 silica sorbent are shown in Figure 1. Peptide 1 is the active form of the parent hGH [6-13] with a cyclization at the Asp^{11}-Asn^{12} linkage which allows a putative type II' β-turn to be adopted [2]. The β-aspartyl analogue (peptide 2) is a linear rearranged product of the α-amino-succinimide peptide and cannot adopt a type II' β-turn [2]. The

Table 1. *Physical characterisitics of peptides used in this study.*

No	Peptide	Sequence	Active[1]	β-turn[2]
1	α-aminosuccinimide	H_2N-LSRLFDNA-$CONH_2$	Yes	Yes
2	β-aspartyl	H_2N-LSRLFDNA-$CONH_2$	No	No
3	D-Ala^{11}-Pro^{12}	H_2N-LSRLFaPA-$CONH_2$	Yes	Yes

[1] Insulin potentiating activity from reference [1].
[2] Determined from NMR and molecular dynamics studies.

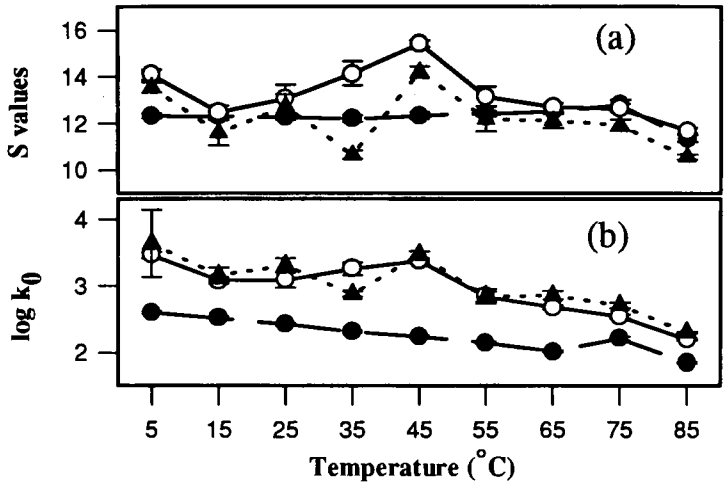

Figure 1. *Dependence of S and log k_0 on temperature for peptides 1(○), 2 (●) and 3(▲) separated on a C18 sorbent.*

D-Ala[11]- Pro[12] analogue contains a proline residue at postion 11 and also adopts a β-turn conformation [2]. It can be seen in Figure 1 that there is very little change in the S and log k_0 values for the linear peptide 2 over the temperature range 5-85°C, behaviour which is indicative of a peptide which does not adopt any significant stabilized secondary structure [3, 4]. In contrast, the corresponding cyclized α-amino-succinimide peptide 1 exhibited significant variation in S and log k_0 values over the same temperature range. In particular, there was a decrease in both parameters between 5-15°C, which corresponds to a decrease in the interactive contact area and associated affinity. Between 15-45°C there was an increase in S and log k_0 followed by a decrease up to 85°C. These results are consistent with large changes in the conformation of the peptide with increasing temperature which alters the number of interactive residues. The decrease in S and log k_0 values at higher temperature suggest that the highly flexible structure which exists at high temperatures interacts with the immobilized ligands through a much smaller proportion of its molecular surface and with reduced affinity. The dependence of S and log k_0 on temperature for the proline containing analogue also exhibited large variations compared to the linear analogue. In addition, there was a large decrease in these parameters at 35°C which was not observed for the imide analogue. The results demonstrate that relatively small differences in peptide conformation can be detected by RP-HPLC.

Peak bandbroadening can also be used to provide information on peptide conformational changes in interactive systems. Significant changes in the molecular contact region which occur within the time scale of the separation are manifested as large changes in experimental bandwidths [4]. The dependence of experimental bandwidths on temperature and column residence time for the linear peptide is shown in Figure 2(a). The data reveal a small increase in bandwidth at longer residence times which again is consistent with a peptide that does not adopt any secondary structure. In contrast, the

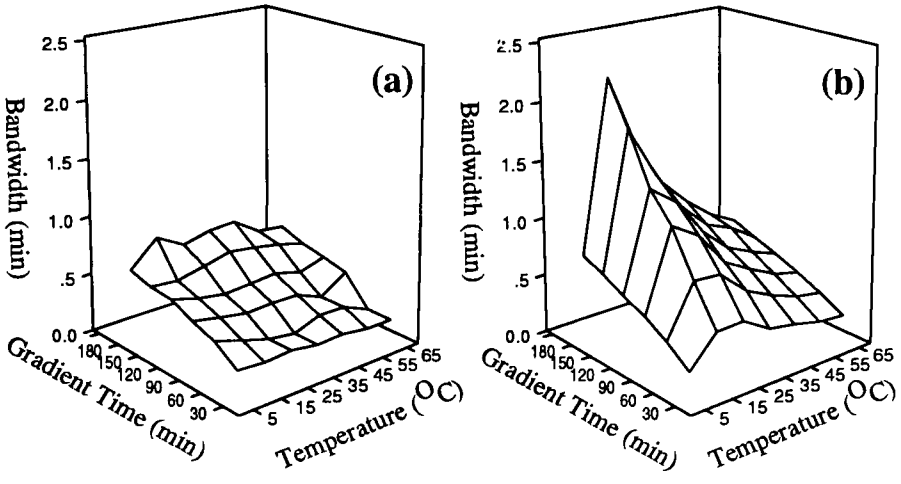

Figure 2. *Dependence of bandwidth on temperature and gradient time for (a) peptide 2 and (b) peptide 3 separated on a C18 sorbent.*

corresponding 3D mesh plot for the proline containing analogue (peptide 3) is shown in Figure 2(b) and demonstrates a large rise in the bandwidths between 15-45°C at longer gradient times. This temperature range also corresponds to the temperatures at which large changes occurred in the S and log k_0 values and indicates that the conformational changes associated with the change in retention parameters occurred at a much slower rate than the changes associated with the unfolding of the α-aminosuccinimide analogue. Overall, these results have further illustrated the potential of RP-HPLC for monitoring subtle changes in peptide structure.

Acknowledgments

The financial support of the Australian Research Council is gratefully acknowledged.

References

1. Thompson, P.E., Lim, N., Ede, N.J., Ng, F.M., Rae, I.D. and Hearn, M.T.W., *Drug Design and Discovery*, 13 (1995) 55.
2. Higgins, K., Thompson, P.E. and Hearn, M.T.W, *Int. J. Pept. Prot. Res,* in press.
3. Purcell, A.W., Aguilar, M.I. and Hearn, M.T.W., *J. Chromatogr.*, 593 (1992) 103.
4. Aguilar, M.I., Richards, K.L., Round, A.J. and Hearn, M.T.W., *Pept. Res.*, 7 (1994) 207.
5. Purcell, A.W., Aguilar, M.I. and Hearn, M.T.W., *Anal. Chem.*, 65 (1993) 3038.
6. Purcell, A.W., Aguilar, M.I., Wettenhall, R.E.H. and Hearn, M.T.W., *Pept. Res.*, 8 (1995) 160.

Session XI
De Novo Design

Chairs: Bruce W. Erickson and
Irwin M. Chaiken

Peptides: Chemistry, Structure and Biology
Pravin T.P. Kaumaya and Robert S. Hodges (Eds.)
Mayflower Scientific Ltd., 1996

224
Helix-promoters, Non-natural Residues, Retro-peptides and Non-peptidic Inserts

I.L. Karle

Laboratory for the Structure of Matter, Naval Research Laboratory, Code 6030, Washington, DC 20375, USA

Introduction

X-ray crystallography of single crystals has been a major tool for establishing the folding of peptides, properties of the molecular surface, precise hydrogen bonding, and motifs for aggregation. The latter are particularly important for ion channel formation. Two categories of peptides will be addressed; helical peptides (in collaboration with P. Balaram, Indian Institute of Science) and retropeptides with a variety of core inserts (in collaboration with D. Ranganathan, CSIR, Trivandrum, India).

Results and Discussion

The presence of one or more Aib residues in a sequence results in a helical backbone almost without exception; a 3_{10}-helix for a small number of residues and an α-helix for a larger number (greater than 8 or 9) [1]. Facile transition between 3_{10}- and α-helices in heteropeptides as a function of length has been demonstrated [2]. More recent analyses with one Dxg residue (dipropyl or dibutyl glycine) show good α-helix formations for decapeptides, without any spatial problems arising from the extra bulky side-chain on the α,α-disubstituted residue, Figure 1 [3]. The position of the Dxg residue in the sequence does not seem to matter. Placing the Dxg residue near the N terminus or in the middle of a peptide sequence does not appear to affect the helix forming propensity.

The successful design and assembly of predictable helix modules suggested the possibility of combining helices with linkers to obtain 2-helix bundles, and eventually 4-helix bundles. A helix-linker combination, Boc-Val-Ala-Leu-Aib-Val-Ala-Leu-*Acp*-OMe (Acp ε-aminocaproic acid), results in an α-helix with an extension of the Acp at a right angle to the helical backbone. In the next step, the helix-linker-helix combination, Boc-Val-Ala-Leu-Aib-Val-Ala-Leu-*Acp*-Val-Ala-Leu-Aib-Val-Ala-Leu-OMe, has an identical conformation for the helix-linker portion; however, the second helix is attached at 180° to the desired conformation. That is, the axes of the two helices are offset but they continue in the same direction [4] rather than in an antiparallel U shape. A different, although related, approach is to attach the linker at the N-terminal rather than the C-terminal. In Boc-Gly-Dpg-Gly-Val-Ala-Leu-Aib-Val-Ala-Leu-OMe, the Boc-Gly segment is extended away from the α-helix formed by the remaining residues in the molecule [5]. The plan is to attach a helix at the Boc moiety.

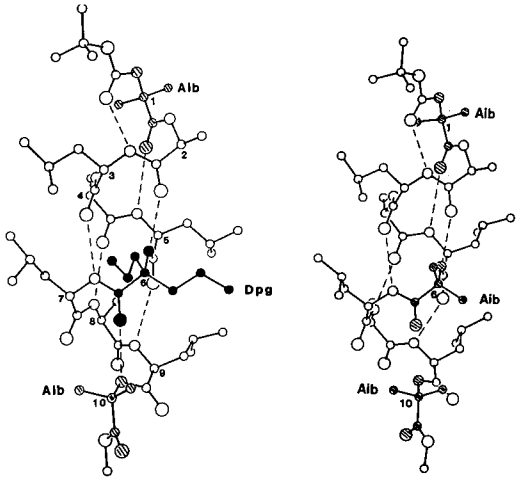

Figure 1. *The isomorphous structures of Boc-Aib-Ala-Leu-Ala-Leu-Dpg-Leu-Ala-Leu-Aib-OMe and Boc-Aib-Ala-Leu-Ala-Leu-Aib-Leu-Ala-Leu-Ala-Leu-Aib-OMe where Dpg[5] (left) replaces Aib[6] (right).*

The Pro or Hyp residues are frequent helix breakers, but appear to be necessary for severely bending the helices that form funnel-shaped ion channels. The ion transport peptide Leu-zervamicin and its synthetic apolar analog have an almost identical backbone conformation with a severely curved helix [6]. Thus, the curvature of the

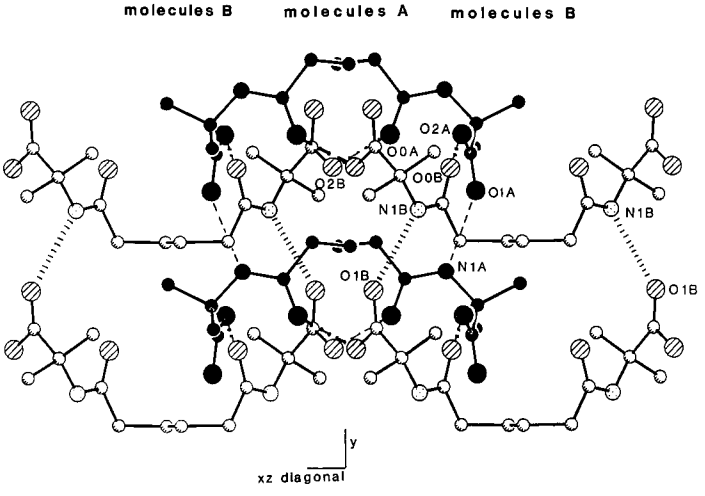

Figure 2. *Independent molecules A (black) and B (white) of (HOOC-Aib-CO-CH_2-CH_2-)$_2$ each having 2-fold rotation symmetry. Molecules A are joined into ribbons by pairs of N1A...O1A hydrogen bonds. Molecules B are joined into a separate, similar ribbon by pairs of N1B...O1B hydrogen bonds. The A and B ribbons, extending along the vertical direction (y axis), are components of an extensive β-network that is formed by hydrogen bonds O2B...O0A and O2A...O0B.*

backbone has not been affected by the removal of all polar moieties from the amphiphilic Leu-zervamicin. The apolar analog still retains some weak ion transport properties [7], probably due to backbone carbonyls that are extended away from the curved backbone in the vicinity of the Pro residues.

Nonpeptidic inserts into the central core of peptides and bis retropeptides can play the role of stiffeners, spacers, or templates for the control of molecular orientation and subsequent self-assembly in a supramolecular sense. In a family of Aib retro bispeptide dicarboxylic acids, inserts of oxalyl, fumaryl, and adipoyl, making use of the same two types of hydrogen bonds, yield three different self-assembly patterns [8]: a two-dimensional β-network, β-networks combined into a three-dimensional γ-network [9] and interdigitating ribbon assemblies, respectively. The interdigitating ribbon patterns created by the adipoyl insert are shown in Figure 2 [8]. Oxalo inserts in a variety of bis retropeptide diesters produce extended sheets, or helix assemblies, or ribbons by extensive hydrogen bonding in a supramolecular assembly.

Acknowledgments

The major contributions of Prof. P. Balaram, Bangalore, India and Dr. Darshan Ranganathan, Trivandrum, India, as well as the support from NIH grant GM30902 and the Office of Naval Research are gratefully acknowledged.

References

1. Karle, I.L. and Balaram, P., *Biochemistry*, 29 (1990) 6747.
2. Karle, I.L., Flippen-Anderson, J.L., Gurunath, R., and Balaram, P., *Protein Science*, 3 (1994) 1547.
3. Karle, I.L., Balaji Rao, R., Prasad, S., Kaul, R. and Balaram, P., *J. Amer. Chem. Soc.*, 116 (1994) 10355.
4. Karle, I.L., Flippen-Anderson, J.L., Sukumar, M., Uma, K. and Balaram, P., *J. Amer. Chem. Soc.*, 113 (1991) 3952.
5. Karle, I.L., Balaji Rao, R., Kaul, R., Prasad, S. and Balaram, P., unpublished data.
6. Karle, I.L., Flippen-Anderson, J.L., Sukumar, M. and Balaram, P., *Proc. Natl. Acad. Sci.*, 84 (1987) 5087.
7. Balaram, P., Krishna, K., Sukumar, M., Mellor, I.R. and Sansom, M.S.P., *Eur. Biophys. J.*, 21 (1992) 117.
8. Karle, I.L. and Ranganathan, D., *Biopolymers*, 36 (1995) 323.
9. Chang, Y.L., West, M.A., Fowler, F.W., and Lauher, J.W., *J. Amer. Chem. Soc.*, 115 (1993) 5991.

Peptides: Chemistry, Structure and Biology
Pravin T.P. Kaumaya and Robert S. Hodges (Eds.)
Mayflower Scientific Ltd., 1996

225
Peptidyl Models for Coenzyme Catalysis

B. Imperiali, R. Sinharoy and L. Wang

Division of Chemistry and Chemical Engineering, California Institute of Technology, Pasadena, CA 91125, USA

Introduction

The coenzymes constitute a powerful class of catalytically competent biomolecules. We have recently reported the development of coenzyme-amino acid chimeras, which allow exploitation of this catalytic potential within synthetic polypeptides [1]. Towards this end, α-amino acids with the core functionality of the coenzymes pyridoxal phosphate and thiamin diphosphate have been synthesized and incorporated into diverse peptidyl constructs. Here we report on the utility of these residues in functional protein design.

Results and Discussion

The pyridoxal chimera (Pal, **1**) was incorporated into peptides as a pyridoxol precursor (Pol, **2**) and obtained from the latter *via* a post-synthesis oxidation [2]. The thiazole-amino acid (Thz, **4**) was synthesized from L-Asp [3]. The Thz residue was transformed to the thiazolium species (Taz, **3**) by alkylation of the protected peptide. Peptides were synthesized using solid phase Fmoc methodology, purified by RPHPLC, and characterized by mass spectrometry.

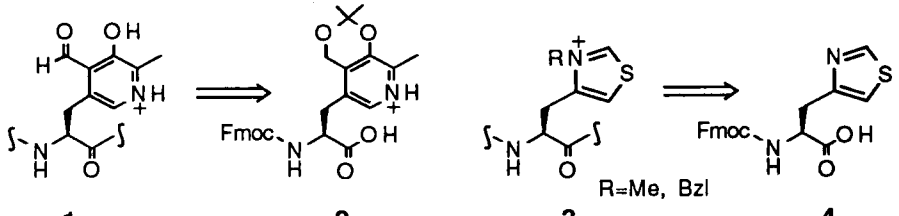

1 **2** **3** **4**

Pyridoxal phosphate catalyzes many transformations involving amino acid substrates. We initially focused on the ability of the Pal-peptides to mediate the trans-amination of an α-amino acid (L-Ala) to the corresponding keto acid (pyruvate) in the presence of Cu(II). Modest rate enhancements (compared to 5'-deoxypyridoxal) were obtained with "hairpin" hexapeptides **P2** and **P3** [2]. In these peptides, Pal- mediated transamination was amenable to catalysis by a general base (His, **P2**; 3-(3-pyridyl)alanine (Pyr), **P3**) situated across a heterochiral type-II reverse turn [4]. Consequently, the transaminase activity of these peptides paralleled the acidity of the residue at this position (Table 1). The importance of secondary structure in delivering the general base was highlighted by the poor reactivity of peptide **P4**, which lacks the reverse turn.

Table 1. *Transamination kinetics for the model Pal hexapeptides. Assay conditions: [L-Ala]= 1M, [Pal peptide]=0.1 mM, [$CuCl_2$]=0.1 mM, pH 4.0, μ = 0.29 (KCl).*

	Coenzyme System	$k_{obs}x10^5$ (min^{-1})	$t_{1/2}$ (h)
P1	Ac-T-V-P-DA-Pal-G-NH_2	165	7.0
P2	Ac-T-H-P-DA-Pal-G-NH_2	225	5.1
P2	Ac-T-Pyr-P-DA-Pal-G-NH_2	278	4.1
P2	Ac-T-H-P-G-Pal-G-NH_2	62	18.7
Control	5'-deoxypyridoxal	59	19.6

At a higher level of structural complexity, the coenzyme-amino acid chimeras offer convenient access to peptidyl models for coenzyme catalysis. Underscoring this point is our semisyntheses of RNase-S derivatives incorporating the Pal residue [1]. The S-$peptide_{1-14}$ fragment serves as a convenient vehicle for the introduction of unnatural amino acids into the RNase-S complex. The optimized Pal-RNase complex (**C1-SP**) is able to mediate the transamination reaction in the absence of metal ions (Table 2). Apparently, a steric "lock" on the Schiff base intermediate in this species is sufficient for activation. In contrast, Cu(II) was essential for the activity of complex **C3-SP** in which few steric constraints operate on the Pal^7 chimera. The poor activity of complex **C2-SP** resulted from occlusion of the coenzyme moiety by Nle^7. Together, these RNase-S complexes demonstrated the ability to modulate coenzyme reactivity within existing protein templates.

Table 2. *Transamination kinetics for the RNase-S derivatives incorporating the Pal residue. See Table 1 for assay conditions. Sufficient S-Protein (SP) was added for 90% complex formation with the Pal peptides.*

RNase-S Complex: S-$peptide_{1-14}$ sequence	$k_{obs}x10^5$ (min^{-1})		k_{rel}
	+Cu(II)	-Cu(II)	[-Cu(II)]
C1-SP: Ac-Nle-E-T-A-A-A-Gly-Pal-E-R-Q-H-Nle-D-NH_2	510	1288	16.7
C2-SP: Ac-Nle-E-T-A-A-A-Nle-Pal-E-R-Q-H-Nle-D-NH_2	198	107	1.4
C3-SP: Ac-Nle-E-T-A-A-A-Pal-Phe-E-R-Q-H-Nle-D-NH_2	427	77	1.0

In addition to protein semisynthesis, we are actively exploring the *de novo* design of functional biomolecules utilizing the Taz chimera. The reactivity of the thiazolium heterocycle in thiamin-dependent processes is due to facile ionization of the C2-methine promoted by a hydrophobic environment, which stabilizes the zwitterionic intermediate [5]. We have replicated this phenomenon by positioning the Thz residue at the hydrophobic interface of an amphiphilic helix bundle patterned after the $\alpha 1\beta$ motif by DeGrado [6]. An N-terminal "helix capping" SALEE sequence [7] was included for enhanced helicity. Activation of the Thz residue to the Taz heterocycle was accomplished by a post-synthesis alkylation (Figure 1).

Methyl (MetTaz) and benzyl (BzTaz) derivatives of Thz-helices were synthesized and analyzed by CD. The Thz-peptide is 55% helix. Methylation erodes the structure

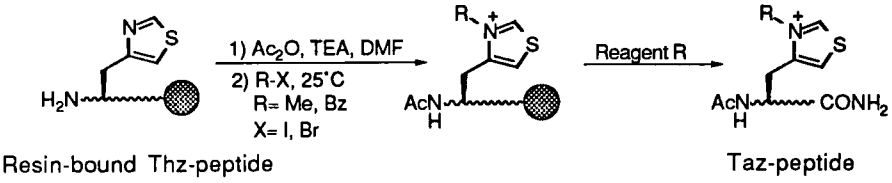

Figure 1. *Post-synthesis alkylation strategy for the Thz-peptides.*

probably due to adverse electrostatics, which affect helix packing. Interestingly, the benzylated analog exhibits increased helicity, indicative of favorable hydrophobic interactions at the helix interface. Hydrogen/deuterium (H/D) exchange rates were measured to evaluate the effects of peptide architecture and N-3 substituent on the acidity of the C-2 methine. Thiazolium salts (Table 3, entries 1 and 2) were used as controls. The benzylated derivatives consistently showed faster exchange rates reflecting the increased hydrophobic environment of the thiazolium moiety. As predicted by the CD analyses, optimum exchange rates were observed with BzTaz-Helix (Table 3, entry 4). This motif is therefore well suited to the future construction of functional Taz-peptides.

Table 3. *H/D exchange kinetics at 27°C (pH 5.1, 50 mM NaOAc/D_2O, 150 mM NaCl).*

No.	Substrate	% helix	$t_{½}$(min)	k_{obs}(min^{-1})
1	3,4-dimethylthiazolium bromide	-	>50	0.014
2	3-benzyl-4-methylthiazolium bromide	-	11.3	0.061
3	Ac-S-A-L-E-E-MetTaz-L-K-L-L-A-E-L-L-K-NH_2	27	3.2	0.22
4	Ac-S-A-L-E-E-BzTaz-L-K-L-L-A-E-L-L-K-NH_2	63	~0.5	1.38

Acknowledgments

The financial support of the Office of Naval Research and the Beckman Foundation is gratefully acknowledged.

References

1. Imperiali, B. and Sinha Roy, R., *J. Am. Chem. Soc.*, 116 (1994) 12083.
2. Imperiali, B. and Sinha Roy, R., *J. Org. Chem.*, 60 (1995) 1891.
3. Hsiao, C.N., Leanna, M.R., Bhagavatula, L., De Lara, E., Zydowsky, T.M., Horrom, B.W. and Morton, H.E., *Synth. Commun.*, 20 (1990) 3507.
4. Imperiali, B., Fisher, S.L., Moats, R.A. and Prins, T.J., *J. Am. Chem. Soc.*, 114 (1992) 3128.
5. Breslow, R., *J. Am. Chem. Soc.*, 80 (1958) 3719.
6. Osterhout Jr., J.J., Handel, T., Na, G., Toumadje, A., Long, R.C., Connolly, P.J., Hoch, J.C., Johnson Jr., W.C., Live, D. and DeGrado, W.F., *J. Am. Chem. Soc.*, 114 (1992) 331.
7. Harper, E.T. and Rose, G.D., *Biochemistry*, 32 (1993) 7605.

Peptides: Chemistry, Structure and Biology
Pravin T.P. Kaumaya and Robert S. Hodges (Eds.)
Mayflower Scientific Ltd., 1996

226
Lactam Bridge Stabilization of α-Helices and Enhancement of Dimerization

M.E. Houston, Jr., C.M. Kay and R.S. Hodges

Department of Biochemistry, the Protein Engineering Network of Centres of Excellence, University of Alberta, Edmonton, Alberta T2G 2H7, Canada

Introduction

The formation of a lactam bridges between the side chains of lysine and acidic residues has proven a useful tool in inducing helical structure in peptides of biological [1] and synthetic origin [2, 3]. The focus of this study was to determine the effect of spacing and orientation of lactam bridges formed between the side chains of glutamic acid or aspartic acid and lysine. All peptides are 14 residues in length and have the general structure;

Ac-EI(X)ALK(Z)EI(X)ALK(Z)-NH_2

where X = Glu, Asp, or Lys and Z = Glu or Lys.

Two lactam bridges were incorporated at the N- and C-termini of the cyclized peptides. In addition, the hydrophobic residues are arranged in a 3,4 repeat common to coiled-coils in order to facilitate peptide dimerization and increase the helical content [4]. In order to determine the effect of hydrophobicity in the dimer interface to peptide helicity, Ile^2 and Ile^9 were substituted by Val in both the lactam bridged and linear peptides.

Results and Discussion

The peptides listed in Table 1 were prepared by solid-phase peptide synthesis as described previously [3]. Where sequence changes were made to study different orientations of the lactam bridge, the linear homolog was synthesized as a control. Peptide 2EKI (*i*, *i*+4) is essentially 100% helical in benign conditions and only a slight increase in molar ellipticity at 222 nm is observed in 50% TFE. The peptide is characterized by minima at 222 and 208 nm and a maxima at 192 nm typical of α-helices. Reversing the orientation of the (*i*, *i*+4) lactam bridge to Lys-Glu surprisingly decreases the helical content relative to the EK peptide. Peptide 2KEI (*i*, *i*+4) has 27% helical content under benign conditions but readily adopts a helical conformation in the presence of TFE. Although 2KEI (*i*, *i*+4) is substantially less helical than 2EKI (*i*, *i*+4) and Linear EKI, there is a marked increase in helical content relative to its own linear counterpart Linear KEI. The low helical content of the linear peptide may be attributed to a destabilizing interaction between the charged groups of the side-chains and the partial charges arising from the helix dipole [5]. This interaction is removed upon lactam formation and therefore cannot account for the discrepancy in helical content between

EK and KE oriented lactams. Modeling studies suggest that the carbonyl oxygen of KE lactams may closely approach the carbonyl oxygen of the i[th] peptide bond (Lys-Ala). In order to alleviate this disruptive interaction, the peptide adopts a random structure.

Decreasing the size of the (*i*, *i*+4) lactam by incorporating Asp in place of Glu (DKI (*i*, *i*+4)) results in a peptide with only 22% helical structure under benign conditions and 34% in 50% TFE. The peptide is less helical than its linear counterpart in benign conditions (22% *vs.* 27%) and very much less in 50% TFE (34% *vs.* 83%). These results contradict work by Felix and coworkers [7] in which DK (*i*, *i*+4) lactams increased the proportion of helix in [Ala[15]]-GRF(1-29) peptides. In our model system, our results clearly indicate that DK (*i*, *i*+4) lactams result in peptides with destabilized helices.

Table 1. *Circular dichroism result of lactam bridged and linear peptides. Peptide concentrations 750 mM +/- 30 mM.*

		$[\theta]_{222}$[a]		Helix Content[b]	
Sequence	Peptide Name	Benign	50% TFE	Benign	50% TFE
Ac-EIEALKKEIEALKK-am	Linear EKI	-18600	-30000	61	98
Ac-EIEALKKEIEALKK-am	2EKI(*i*,*i*+4)	-30350	-32150	99	105
Ac-EIKALKEEIKALKE-am	Linear KEI	-2900	-14000	10	45
Ac-EIKALKEEIKALKE-am	2KEI (*i*,*i*+4)	-8600	-29100	27	95
Ac-EIDALKKEIDALKK-am	Linear DKI	-8200	-25500	27	83
Ac-EIDALKKEIDALKK-am	2DKI (*i*,*i*+4)	-6700	-10300	22	34

[a] calculated molar ellipticity of the peptide at 222 nm (deg.cm^2.dmol^{-1})

[b] The % helical content was calculated from the ratio of the observed $[\theta]_{222}$ divided by the predicted molar ellipticity (-30700) as determined for a peptide of 14 residues [6].

The helical content associated with Peptides 2EKI (*i*, *i*+4) and Linear EKI is dependent upon peptide concentration indicative of the existence of a monomer/dimer equilibrium. In order to determine the effect of hydrophobicity on dimerization and helical content, the hydrophobicity was decreased by substituting residues Ile[2] and Ile[9] with Val. From Table 2, it is apparent that this substitution reduces the helical content of the lactam bridged and linear peptide as compared to the EKI peptides. However, the decrease in helicity is significantly less for 2EKV (*i*, *i*+4). In addition, concentration dependence studies indicate this peptide associates as a dimer whereas its linear homolog does not suggesting these lactams enhance dimerization. Moreover, the amount of helical stabilization that can be attributed to lactam bridges (Table 2, Linear - lactam) is similar in magnitude to the amount of helicity induced in the linear sequences in 50% TFE (Benign- TFE), indicating the efficacy of these lactam bridges in imparting helical structure.

Table 2. *Circular dichroism results of lactam bridges and linear peptides.*

Peptide	$[\theta]_{222}$[a]		$\Delta[\theta]_{222}$[b]	$\Delta[\theta]_{222}$[b]	Helix Content (%)[c]	
	Benign	50% TFE	(Benign-TFE)	Linear-Lactam Benign	Benign	50%TFE
Linear EKI	-18600	-30000	11400	---	61	98
2EKI (*i*, *i*+4)	-30350	-32150	1800	11750	99	105
Linear EKV	-7550	-27500	19950	---	25	90
2EKV (*i*, *i*+4)	-24500	-31100	6600	16950	80	101

[a] calculated molar ellipticity of the peptide at 222 nm ($deg.cm^2.dmol^{-1}$).

[b] $\Delta[\theta]_{222}$ is the difference between the ellipticity at 222 nm in benign buffer and in 50% TFE for the linear peptide and lactam peptide of the same sequence.

[c] The % helical content was calculated from the ratio of observed $[\theta]_{222}$ divided by the predicted molar ellipticity (-30700) as determined for a peptide of 14 residues [6].

In summary, our study of lactam bridged peptides clearly shows the importance of lactam orientation in inducing and stabilizing helical content in small amphipathic peptides. In addition, this study reaffirms the value of lactam bridges as a method of stabilizing α-helices and enhancement of dimerization.

Acknowledgments

This research was supported by the Government of Canada through the Protein Engineering Networks of Centres of Excellence (PENCE).

References

1. Felix, A.M., Heimer, E.P., Wang, C.-T., Lambros, T.J., Fournier, A., Mowles, T.F., Maines, S., Campbell, R.M., Wegrzynski, B.B., Toome, V., Fry, D.C. and Madison, V.S., *Int. J. Pept. Protein Res.*, 32 (1988) 441.
2. Osapay, G. and Taylor, J.W., *J. Am. Chem. Soc.*, 112 (1990) 6046.
3. Houston, Jr., M.E., Gannon, C.L., Kay, C.M. and Hodges, R.S., *J. Pept. Sci.*, 1 (1995) 274.
4. Zhou, N.E., Zhu, B.-Y., Kay, C.M. and Hodges, R.S., *Biopolymers*, 32 (1992) 419.
5. Shoemaker, K.R., Kim, P.S., York, E.J., Stewart, J.M. and Baldwin, R.L., *Nature*, 326 (1987) 563.
6. Chen, Y.-H, Yang, J.T. and Chau, H.M., *Biochemistry*, 11 (1974) 3350.
7. Felix, A.M., Wang, C.-T., Campbell, R.M., Toome, V., Fry, D.C. and Madison V.S., in Smith, J. A. and Rivier, J. E. (Eds.), 'Peptides: Chemistry and Biology', ESCOM, Leiden, The Netherlands, 1992, p. 77.

Peptides: Chemistry, Structure and Biology
Pravin T.P. Kaumaya and Robert S. Hodges (Eds.)
Mayflower Scientific Ltd., 1996

227

De Novo Design of Peptide Models of Cytochromes: Towards the Synthesis of a Photosynthetic Reaction Center Maquette

F. Rabanal[1], W.F. DeGrado[1,2] and P.L. Dutton[1]

[1]The Johnson Research Foundation, Department of Biochemistry and Biophysics, University of Pennsylvania, Philadelphia, PA 19104, USA
[2]The Du Pont Merck Pharmaceutical Co., Department of Chemical and Physical Sciences, Experimental Station, Wilmington, DE 19880, USA

Introduction

De Novo design is a challenging endeavor that critically tests our understanding of protein folding and structure while also laying the groundwork for the design of novel biomimetic polymers and molecular devises. We are interested in designing novel mimics of redox-active proteins, that are far simpler than their natural counterparts, but that nevertheless contain the minimal requirements for function [1]. We refer to these mimetics as maquettes because they resemble the simplified scale models employed by architects and artists to appreciate various aspects of their full-scale designs. We recently demonstrated the feasibility of this approach through the design of helix-link-helix peptides, designated α_2, that dimerize to form four-helix bundles capable of binding one, two or four hemes. In each case, the heme-binding site consisted of two His residues which ligate the heme iron, and hydrophobic residues, which interact favorably with the porphyrin macrocycle. The multiheme proteins displayed many of the remarkable properties of natural multiheme cytochromes including electrochemical and spectroscopic non-equivalence between various bound hemes, as well as redox co-operativity arising from interheme charge interactions. Encouraged by this success ,we endeavored to introduce a closely associated porphyrin dimer as a mimic of the special pair in the reaction center.

Results and Discussion

The RC is a 95 kd protein whose membrane spanning portion includes 11 transmembrane α-helices. The cofactors which include four chlorophylls b, two pheophytins b, and two quinones, are arranged with nearly perfect two-fold symmetry. Two of the chlorophylls are closely associated (*ca* 7 Å) and form the so-called special pair which is central to the primary events of light activated electron transfer. In the present work, we modeled the reaction center by using $[\alpha_2]_2$ as a scaffold to effect the cofacial dimerization of two hemes in a manner reminiscent of the special pair of chlorophylls [2]. Coproporphyrin I (CP), which contains four equivalent propionates, was coupled to the N-terminus

of α (whose sequence is CGGGELWKLHEELLKKFEELLKLHEERLKKL-$CONH_2$) to render **CP**-α and heterodimerized with the 5-nitro-2-pyridinesulphenyl (pNpys) derivative of Ac-α to finally yield **CP**-α_2 [3]. This covalent dimer further dimerizes by noncovalent forces to form a four-helix bundle, 124 residue protein [**CP**-α_2]$_2$.

The UV-Vis spectrum of [**CP**-α_2]$_2$ reveals that the CP chromophore is in a dimeric form (Soret at λ=372 nm) above 10^{-8} M, its limit of detection [4]. Since the K_D of CP in the same conditions is *ca* 2 x 10^{-5} M, it is inferred that the dimeric structure of [**CP**-α_2]$_2$ lowers the dimerization constant of the prophyrin by at least a factor of 10^3. In addition, the covalently attached **CP** serves as a probe of the topology of the bundle; the spectral results proves that [**CP**-α_2]$_2$ is an all-parallel bundle of helices, because only this orientation allows the cofacial dimerization of the probe.

The dimer-monomer equilibrium can also be shifted to higher values of K_D by addition of trifluoroethanol (TFE). TFE disrupts the hydrophobic interactions that stabilize the quaternary and tertiary structure of proteins, while simultaneously maintaining the helicity of monomeric α-helices [5, 6]. Titration of [**CP**-α_2]$_2$ in aqueous milieu with TFE gave a neat transition from dimer to monomer spectrum between 10% and 32 % TFE, consistent with the dissociation of [**CP**-α_2]$_2$ to yield monomeric **CP**-α_2. These spectral changes are parallel to those found in a simple concentration experiment with free **CP** in the same aqueous buffer conditions. These dimer-monomer transitions are characterized by a red-shift of the Soret band (372 to 394 nm, isosbestic point at 378 nm) with concomitant blue-shift of the Q_x-Q_y bands (500-600nm region) and general hyperchromicity (Figure 1).

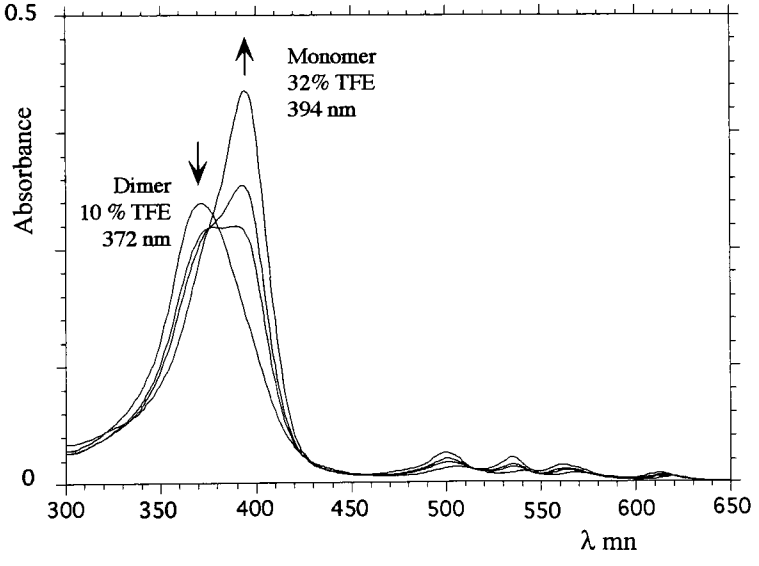

Figure 1. *UV-Vis monitoring of the dissociation of [CP-α_2]$_2$ into CP-α_2 monomers by addition of TFE (4.5 μM) concentration of peptide in 50 mM Tris buffer, 100mM NaCl at pH 8.5). Traces recorded are (in % TFE): 10, 19, 24 and 32.*

In conclusion, we have succeeded in preparing a protein that self-associates two porphyrins in a cofacial manner. This same protein is capable of binding four additional iron protoporphyrin IX molecules (data not shown), resulting in a structure with a total of six prosthetic groups. Ongoing work is aimed at arranging the hemes in a geometry that will give rise to high-yield electron transfer as in the reaction center.

Acknowledgments

F.R. acknowledges the receipt of a postdoctoral fellowship from the European Molecular Biology Organization (EMBO). This work was funded with grants GM 41048 and GM 48130.

References

1. Robertson, D.E., Farid, R.S., Moser, C.C., Urbauer, J.F., Mulholland, S.E., Pidikiti, R., Lear, J.D., Wand, A.J., DeGrado, W.F. and Dutton, P.L., *Nature*, 368 (1994) 425.; Choma, C.T., Lear, J.D., Nelson, M.J., Dutton, P.L., Robertson, D.E. and DeGrado, W.F., *J. Am. Chem. Soc.*, 116 (1994) 856.
2. Norris, J.R., Uphaus, R.A., Crespi, H.L. and Katz, J.J., *Proc. Natl. Acad. Sci USA*, , 68 (1971) 625; Deisenhofer, J., Epp, O., Mikki, K., Huber, R. and Michel, H., *Nature*, 318 (1985) 618.
3. Rabanal, F., DeGrado, W.F. and Dutton, P.L., *J. Am. Chem. Soc.*, 118 (1996) 473; Rabanal, F., DeGrado, W.F. and Dutton, P.L., *Tetrahedron Lett.*, in press.
4. Karns, G.A., Gallagher, W.A. and Elliot, W.B., *Bioorg. Chem.*, 8 (1979) 69; Brown, S.B., Shillcock, M., and Jones, P. *Biochem. J.* , 153 (1976) 279.
5. Dill, K.A., Bromberg, S., Yue, K., Fiebig, K.M., Yee, K.P., Thomas, P.D. and Chan, H.S., *Protein Sci.*, 4 (1995) 561.
6. Zhou, N.E., Kay, C.M. and Hodges, R.S., *J. Biol. Chem.*, 267 (1992) 2664.

Peptides: Chemistry, Structure and Biology
Pravin T.P. Kaumaya and Robert S. Hodges (Eds.)
Mayflower Scientific Ltd., 1996

228
Template-assisted Protein Design: Chimeric TASP by Chemoselective Ligation

S.E. Cervigni[1], P. Dumy[1], P.T.P. Kaumaya[2], M. Mathieu[1], O. Nyanguile[1], C. Peggion[1], A. Razaname[1], G. Tuchscherer[1] and M. Mutter[1]

[1]*Institute of Organic Chemistry, University of Lausanne, BCH - Dorigny, CH -1015 Lausanne, Switzerland*
[2]*The Ohio State University, Comprehensive Cancer Center,Columbus, OH 43210, USA*

Introduction

Recent progress in chemoselective ligation, orthogonal protection techniques, and solubilization of peptide fragments have increased our potential for constructing protein-like molecules. In particular, the ligation of unprotected peptides to Regioselectively Addressable Functionalized Templates (RAFT) allows for the design of Template Assembled Synthetic Proteins (TASP) exhibiting complex structural and functional properties. In the present contribution, we report on recent progress in template-assisted protein *de novo* design [1-3].

Results and Discussion

A number of recently proposed chemoselective ligation methods [4-6] have been evaluated for use in TASP design. To this end, the orthogonally protected topological template **1** [Y_1=Boc, Y_2=Aloc, Y_3=1-(4,4-dimethyl-2,6-dioxo-cyclohexylidene)ethyl

1

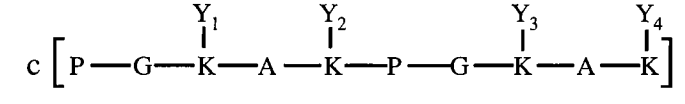

(Dde), Y_4= Fmoc] has been transformed into a multifunctional RAFT molecule suitable for the chemoselective ligation of unprotected peptide blocks - a means for overcoming the poor solubility of fully protected peptide derivatives in TASP synthesis [7]. Special attention was given to the orthogonally protected aminooxy group needed for oxime bond formation. This transformation is achieved by selective deprotection of Y_i and subsequent reaction with the corresponding Y_i-aminooxyacetyl derivative in the order as given for **1**. A prototype of a RAFT molecule giving access to a combination of different chemoselective ligation procedures such as oxime, thioether, and thiazolidine formation is shown in Figure 1. Starting from the orthogonally protected template **1**, the chemo-selectively addressable sites on the template are introduced according to the following strategy: (i) removal of Fmoc (position 4, Figure 1) with piperidine/DMF and attachment

of a COOH - containing maleimide derivative, (ii) removal of Dde (position 3, Figure 1) by hydrazine and coupling of N^{α}-Fmoc-Ser, (iii) removal of Boc (position 1, Figure 1) by 50% TFA and coupling of Boc-aminooxy acetic acid, (iv) removal of Aloc (position 2, Figure 1) by palladium / tributyltinhydride and coupling of N^{α}-Aloc-Ser.

For fixing up to four different peptide blocks to this RAFT molecule, the following strategy has been explored: (i) thioether formation at position 4, (ii) removal of the N^{α}-Fmoc group of Ser at position 3 and oxidation to the aldehyde [5] the subsequent ligation with a peptide containing N-terminal Cys results in a thiazolidine ring system [6, 8], (iii) removal of the Boc group in position 1 and ligation with a peptide containing an aldehyde group [9] to give oxime 1, (iv) removal of the N^{α}-Aloc group of Ser at position 2 and oxidation to the aldehyde as in ligation step (ii), ligation with a peptide containing a N-terminal aminooxy group results in oxime 2.

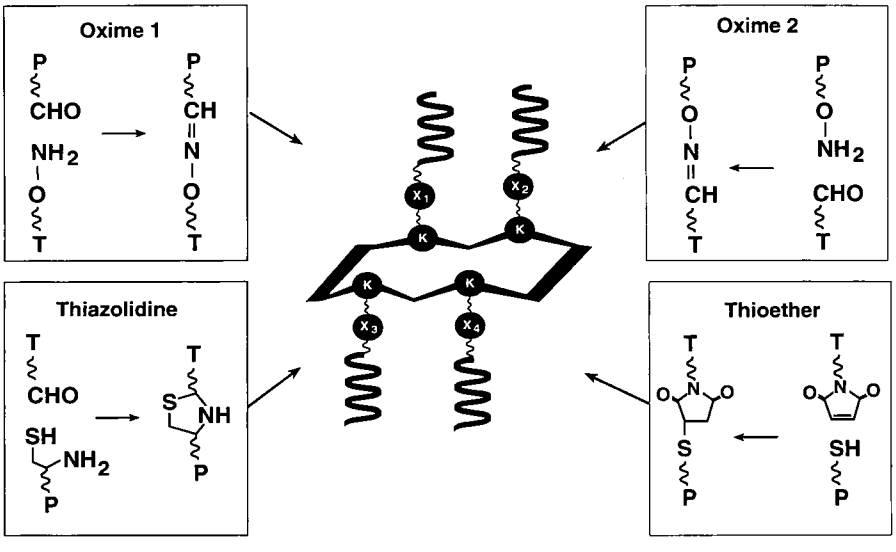

Figure 1. *Regioselectively Addressable Functionalized Template (RAFT) for the construction of TASP molecules by chemoselective ligation procedures (see text).*

These procedures are currently used to construct chimeric TASP molecules mimicking antigenic, binding, and catalytic sites of proteins. Applying analogous procedures, two-domain TASP molecules exhibiting independent folding topologies have been prepared as depicted in Figure 2. The combination of B-cell (P_1) and T-cell (P_2) epitopes may result in TASP of immunological relevance. Two-domain TASP of the type P_1 = ion channel forming 4α-helix bundle, P_2 = receptor ligand, may be used as versatile biosensor systems.

Nonpeptidic molecules (P_2) have been attached to the opposite face of the template in order to modulate the physicochemical and pharmacokinetic properties of peptide hormones (P_1). The preparation of a two-domain TASP with somatostatin analog RC-160 as P_1 and fructose as P_2 illustrates the synthetic approach depicted in Figure 2 as

follows: (1) deprotection of the Aloc group and coupling with D-*arabino*-hexos-2-ulose by reductive amination [10], (2) Boc removal followed by the attachment of RC-160 *via* chemoselective ligation.

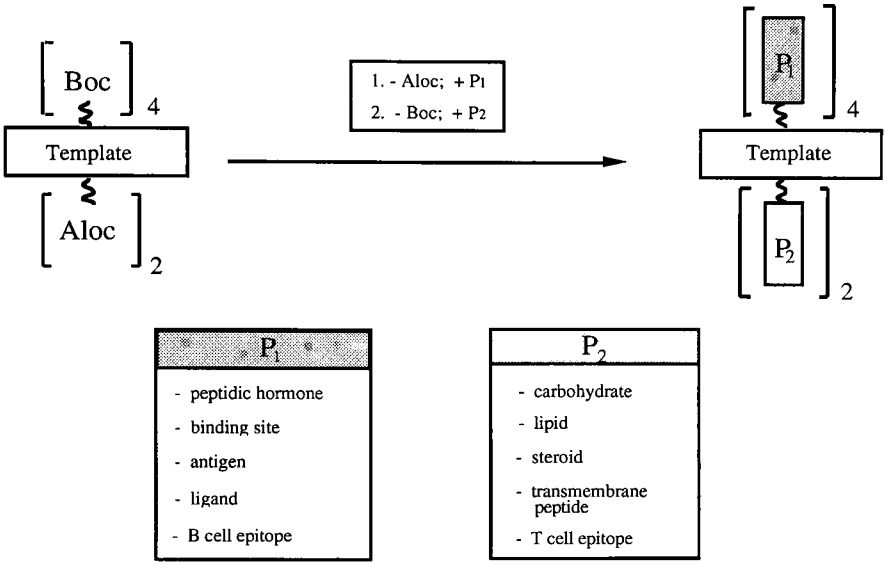

Figure 2. *Chimeric two domain TASP for the construction of template-assembled bioactive molecules (P1) with modulated physicochemical properties (P2) (see text).*

Acknowledgments

This work was supported by the Swiss National Science Foundation.

References

1. Mutter, M., in Marschall, G.R. (Ed.), 'Peptides: Chemistry, Structure and Biology', ESCOM, Leiden, The Netherlands, 1988, p.349.
2. Pawlak, M., Meseth, U., Dhanapal, B., Mutter, M. and Vogel, H., *Protein Sci.*, 3 (1994) 1788.
3. Tuchscherer, G. and Mutter, M., *J. Peptide Science*, 1 (1995) 3.
4. Dawson, P.E. and Kent, S.B.H., *J. Am. Chem. Soc.*, 115 (1993) 7263.
5. Vilaseca, L.A., Rose, K., Werlen, R., Meunier, A., Offord, C.L., Nichols, C.L. and Scott, W.L., *Bioconjugate Chem.*, 4 (1993) 515.
6. Shao, J. and Tam, J.P., *J. Am. Chem. Soc.*, 117 (1995) 3893.
7. Dumy, P., Eggleston, I.M., Cervigni, S., Sila, U., Sun, X. and Mutter, M., *Tetrahedron Lett.*, 36 (1995) 1255.
8. Sato, T., Wöhr, T., Wahl, F., Rohwedder, B. and Mutter, M., this volume.
9. Tuchscherer, G., *Tetrahedron Lett.*, 34 (1993) 8419.
10. Walton, D.J., Hvidt, T. and Szarek, W.A., *Carbohydrate Res.*, 167 (1987) 123.

Peptides: Chemistry, Structure and Biology
Pravin T.P. Kaumaya and Robert S. Hodges (Eds.)
Mayflower Scientific Ltd., 1996

229

Is the Topological Equivalence Between Retro-enantiomers a General Concept?

Y.M. Sánchez[1], T. Haack[1], M.J. González[1], D. Ludevid[2] and E. Giralt[1]

[1]Departament de Química Orgànica, Universitat de Barcelona, Martí i Franqués 1-11, E-08028 Barcelona, Spain
[2]Departament de Genètica Molecular, CID-CSIC, Jordi Girona 18-26, E-08034 Barcelona, Spain

Introduction

The retro-enantio concept [1-3] derives from the first ideas of Prelog and Gerlach [4] on the topology of cyclic peptides, continued by Shemyakin *et al.* [5], but especially developed and extended to linear peptides for nearly two decades by Goodman *et al.* [6, 7]. If the chirality of all the stereogenic centers of the parent peptide are inverted, the enantio peptide is obtained and the side chains adopt the topology of the mirror image of the parent peptide. If the sequence is reversed and the peptide rotated 180° in plane, the retro peptide obtained again has the mirror image side chain topology. However, most interesting is that the parent side chain topology is obtained if both changes are performed, that is, in the retro-enantio peptide. Nevertheless, the extrapolation of the retro-enantio concept from small rather flexible peptides to large peptides or proteins with fixed secondary or tertiary structure is, in our opinion, not so straightforward, especially in those cases where a chiral backbone is present, such as the α-helix.

Results and Discussion

The N terminal part of Staphylococcal protein A (SpA), a cell wall constituent of *Staphylococcus aureus*, consists of five highly homologous Fc-binding domains designated as E, D, A, B, and C. Each 60 aa domain is known to bind the Fc region of IgG molecules of various mammalian species. The 3-D structure of the B domain has been studied both in solution using NMR spectroscopy [8] and, in a complex with an Fc fragment of human Ig antibodies, by X-ray crystallography [9], from which it has been deduced that the B domain is composed of a bundle of three α-helices. We have studied the C terminal α-helix (helix III) of this bundle to explore the validity of the retro-enantio concept in systems with a high helical content. We have prepared the four versions of helix III, normal (**1**), retro (**2**), enantio (**3**), and retro-enantio (**4**), and the complete B domain with and without three additional residues in the N terminal part, **5a** and **5b** respectively, and also some variations of **5a**, referred to as **6** and **7**.

Ac-D-P-S-Q-S-A-N-L-L-A-E-A-K-K-L-N-D-A-Q-A-P-K-NH_2 **1**
Ac-K-P-A-Q-A-D-N-L-K-K-A-E-A-L-L-N-A-S-Q-S-P-D-NH_2 **2**

Ac-*D-P-S-Q-S-A-N-L-L-A-E-A-K-K-L-N-D-A-Q-A-P-K*-NH_2 **3**

Ac-*K-P-A-Q-A-D-N-L-K-K-A-E-A-L-L-N-A-S-Q-S-P-D*-NH_2 **4**

Ac-A-P-K-A-D-N-K-F-N-K-E-Q-Q-N-A-F-Y-E-I-L-H-L-P-N-L-N-E-E-Q-R-N-G-F-I-Q-S-L-K-D-D-P-S-Q-S-A-N-L-L-A-E-A-K-K-L-N-D-A-Q-A-P-K-NH_2 **5a**

Ac-A-D-N-K-F-N-K-E-Q-Q-N-A-F-Y-E-I-L-H-L-P-N-L-N-E-E-Q-R-N-G-F-I-Q-S-L-K-D-D-P-S-Q-S-A-N-L-L-A-E-A-K-K-L-N-D-A-Q-A-P-K-NH_2 **5b**

Ac-A-P-K-A-D-N-K-F-N-K-E-Q-Q-N-A-F-Y-E-I-L-H-L-P-N-L-N-E-E-Q-R-N-G-F-I-Q-S-L-K-D-K-P-A-Q-A-D-N-L-K-K-A-E-A-L-L-N-A-S-Q-S-P-D-NH_2 **6**

Ac-A-P-K-A-D-N-K-F-N-K-E-Q-Q-N-A-F-Y-E-I-L-H-L-P-N-L-N-E-E-Q-R-N-G-F-I-Q-S-L-K-D-*K-P-A-Q-A-D-N-L-K-K-A-E-A-L-L-N-A-S-Q-S-P-D*-NH_2 **7**

The four 22-residue peptides (**1-4**) were synthesized on a *p*-methylbenzydrylamine resin using the Boc/Bzl strategy. After HF cleavage they were purified by MPLC and analyzed by amino acid analysis, HPLC, HPCE, and ES-MS. The CD spectra of the four peptides in water show, in all cases, a very small tendency to adopt helical structures; the spectra of **1** and **2** are the mirror images of **3** and **4**. Nevertheless, the addition of TFE or hexafluoroisopropanol (HFIP) increases the helix content considerably. This behavior is parallel to that observed by 500 MHz NMR. In water, peptides **1** and **2** have weak N_iN_{i+1} NOESY peaks, while in d_3-TFE or d_2-HFIP both peptides show a higher degree of helical structure. The n.O.e. pattern and the δ_α values point to a continuous distribution of the tendency to adopt helical structure along the sequence.

Peptides **5a**, **5b**, **6**, and 7 were synthesized, purified, and analyzed in the same way as described above. The CD spectrum of **5a** in water shows, in contrast to the spectra of peptides **1-4**, a high degree of helicity that is increased slightly by addition of TFE or HFIP. Our design of peptide **5a** includes three extra residues from the preceding domain (APK) at the N terminal part. The aim of this modification was to confirm the helix promoting effect of the proline. The comparison of the CD spectra of **5a** and **5b** and the 500 MHz NMR spectrum of **5a** in water clearly confirms this characteristic. The 1D-NMR spectrum shows a large chemical shift dispersion at the NH region and the presence of several anomalous methyl group chemical shifts above δ 0.8. TOCSY, DQF-COSY, and NOESY experiments provided a more detailed description of the molecule. Altogether, our results point towards a structured molecule with a high α-helix content. When helix III of the **5a** peptide was substituted by the retro or retro-enantio peptide (**6** or 7), the properties of the molecule changed dramatically. The comparison of CD spectra of peptide **5a, 6,** and 7 in water (Figure 1), suggests a considerable loss of tertiary structure in peptide **6**, with an almost complete loss of structure in peptide 7. This agrees with the NMR spectra of **6** and 7. Addition of TFE or HFIP gave an increase in helicity. A preliminary ELISA with anti-mouse IgG conjugated with peroxidase showed a serious loss of IgG binding ability of peptides **6** and 7 when compared with **5a**.

In conclusion, all of our results indicate that it is difficult to retain the side-chain topology in highly helical compounds synthesized using D-aa. Nevertheless, we have not explored all the possibilities of our system. In particular we have not synthesized peptides in which helix III is rotated through 180° which is crucial in the retro-enantio concept. Our results represent the first example of extensive use of D-aa in a complete secondary structure element of a protein or a protein domain, keeping an all-L

configuration for the rest of the molecule. We propose the term diastereo-proteins for this type of situation. We think that diastereo-proteins will play an increasing role in rational design of artificial proteins with new foldings and/or improved properties.

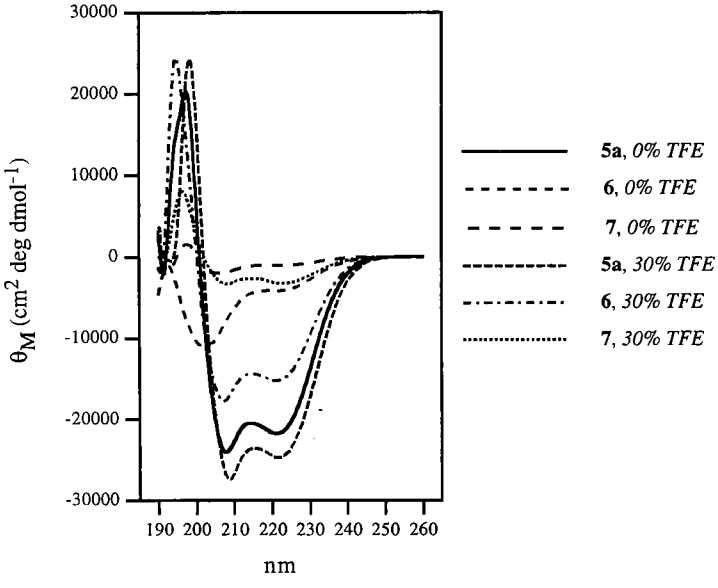

Figure 1. *CD spectrum of the **5a**, **6** and 7 peptide in 0% and 30% TFE/3mM potassium phosphate.*

Acknowledgments

Research supported by CICYT (Grant PB920864) and Generalitat de Catalunya (Centre de Referència en Biotecnologia).

References

1. Jameson, B., McDonnell, J., Marini, J. and Korngold, R., *Nature*, 368 (1994) 744.
2. Guichard, G., Benkirane, N., ZederLutz, G., Van Regenmortel, M.H.V., Briand, J.P. and Muller, S., *Proc. Natl. Acad. Sci. USA*, 91 (1994) 9765.
3. Merrifield, R.B., Juvvadi, P., Andreu, D., Ubach, J., Boman, A. and Boman, H.G., *Proc. Natl. Acad. Sci. USA*, 92 (1995) 3449.
4. Prelog, V. and Gerlach, V., *Helv. Chim. Acta*, 47 (1964) 2288.
5. Schemyakin, M.M., Ovchinnikov, Y.A. and Ivanov, V.T., *Angew. Chem. Int. Ed. Engl.*, 8 (1968) 492.
6 Goodman, M. and Chorev, M., *Acc. Chem. Res.*, 12 (1979) 1.
7. Chorev, M. and Goodman, M., *Acc. Chem. Res.*, 26 (1993) 266.
8. Gouda, H., Torigoe, H., Saito, A., Sato, M., Arata, Y. and Shimada, I., *Biochemistry*, 31 (1992) 9665.
9. Deisenhofer, J., *Biochemistry*, 20 (1981) 2361.

Peptides: Chemistry, Structure and Biology
Pravin T.P. Kaumaya and Robert S. Hodges (Eds.)
Mayflower Scientific Ltd., 1996

230
Synthetic Vehicles for Non-viral Somatic Gene Therapy

J.T. Sparrow[1], S.L.C. Woo[2], S. Gottschalk[2], J. Duguid[3], C. Li[3] and L.C. Smith[1,2]

Departments of [1]Medicine and [2]Cell Biology, Baylor College of Medicine, One Baylor Plaza, Houston, TX 77030, USA
[3]GeneMedicine, Inc., 8301 New Trails Drive, The Woodlands, TX 77381, USA

Introduction

For a completely synthetic vehicle for gene therapy, we believe that we will need the following: a DNA condensing agent, an endosomal lysis agent, a cellular receptor ligand, and a nuclear localization signal. To test this hypothesis, we have designed a series of synthetic peptides to serve these various functions. The DNA condensing peptides were based on polylysine, a known DNA condensing agent [1], and contain from six to twelve lysine residues with the sequence, $YKAK_nWK$, (K*n*). Since we desired endosomal lysis where the pH is acidic, a hydrophobic amphipathic helical peptide [2] of twenty amino acids composed primarily of glutamic acid and leucine residues was designed, GLFEALLELLESLWELLLEA, (JTS-1). The nuclear localization signal was chosen from the large T antigen of SV40 [3] and the receptor ligand was from apolipoprotein E [4]. Here, we present results using the first two components of this hypothetical system to prepare a purely synthetic gene delivery complex.

Results and Discussion

The peptides were synthesized by solid phase peptide synthesis techniques [5] using fast Boc chemistry [6] as implemented in our laboratories, cleaved with HF containing 10% anisole and 1% ethanedithiol (60 ml/g resin), and purified by reversed phase HPLC [7, 8]. The DNA condensing peptides were purified on a Vydac C_{18} column using a gradient of 0.1% TFA and 5% 2-propanol. The acidic amphipathic helical endosomal lysis peptides were purified on a Vydac C4 column in 0.01M ammonium phosphate/2-propanol at pH 6.7. Purity was determined by analytical reversed phase HPLC, amino acid analysis, FAB (lytic peptides) or electrospray (condensing peptides) mass spectroscopy.

Since polylysines are known to be cytotoxic [9], the condensing peptides were tested for cytotoxicity on HepG2 cells. After 24 hrs, 100% of the cells were viable at 100 μM of the K8 peptide while all cells were killed by 0.1 μM polylysine. When the condensing peptides were added to a CMV-β-galactosidase DNA vector [10], stable particles of 50 to 300 nm, as determined by dynamic laser light scattering [11], were formed. The complexes were stable from 20 to 140 hrs. Particle size and stability were dependent on the number of lysine residues in the peptide and the peptide to DNA molar ratio.

The α-helicity of the lytic peptide, JTS-1, was determined by CD spectroscopy to be 95% even in 6M GnHCl suggesting a highly aggregated peptide. Indeed, size exclusion chromatography on Superose 75 in phosphate buffered saline (PBS) at pH 7.4 gave a molecular weight of 44 kDa. A molecular weight of 13.5 kDa was found in 3M GnHCl indicating formation of a very stable hexamer. The introduction of Pro at position 13 resulted in a reduction of the helicity to 75%. The molecular weight of this analog was determined to be 13 kDa in PBS and 2.3 kDa in 3 M GnHCl. The endosomal lytic agents were tested for their effects on liposomes and erythrocytes at pH 7.5 and 5.5. As expected, these peptides were capable of lysing liposomes and erythrocytes efficiently at pH 5.5 but not at pH 7.5.

When combined to form ionic complexes with the DNA/Kn peptide complex and added to cells in culture, we found that a variety of cell types could be transfected. Using CMV-β-Gal as the DNA vector, K8 as the condensing peptide, and JTS-1 as the lytic peptide, we found the following percentage of blue cells when these cell lines were stained with X-gal [12]: 3T3, 25%; 9L, 15%; C6, 5%; sol8, 30%; MCA-26, 30%; HCT-116, 25%; ML3, 5%; HepG2, 25%; SKOV3, 1% , and 293, 40%. The transduction efficiency was dependent on the amino acid sequence of the condensing and lytic peptides as reflected in the complex particle size, stability and charge. We conclude that these peptide/DNA complexes can be used as vehicles for very efficient gene delivery *in vitro* and show great promise for *in vivo* studies.

Acknowledgments

The authors wish to thank Joseph Walter and Andrea Tran for expert technical assistance. Financial support was provided by HL-50422, HL-51754 and contracts from GeneMedicine, Inc. (JTS, LCS). S. Gottschalk was a recipient of a Deutsche Forschungsgemeinschaft training fellowship. S.L.C. Woo is an Investigator of the Howard Hughes Medical Institute.

References

1. Shapiro, J.T., Leng, M. and Felsenfeld, G., *Biochemistry,* 8 (1969) 3219.
2. Sparrow, J.T. and Gotto, A.M., *J. Crit. Rev. Biochem.,* 13 (1982) 87.
3. Lanford, R.E., Kanda, P. and Kennedy, R.C., *Cell,* 46 (1986) 575.
4. Mims, M.M., Darnule, A.T., Tovar, R.W., Pownall, H.J., Sparrow, D.A., Sparrow, J.T., Via, D.P. and Smith, L.C., *J. Biol. Chem.,* 269 (1994) 20539.
5. Barany, G. and Merrifield, R.B., in Gross, E. and Meienhofer, J. (Eds.), 'The Peptides: Analysis, Synthesis, Biology', Academic Press, NY, 1980, p.3.
6. Reid, G.E. and Simpson, R.J., *Anal. Biochem.*, 200 (1992) 301.
7. Hancock, W.S. and Sparrow, J.T., *J. Chromatogr.*, 206 (1981) 71.
8. Hancock, W.S. and Sparrow, J.T., 'HPLC Analysis of Biological Compounds, Chromatographic Science Series', Volume 26, Marcel Dekker, Inc., NY, 1984.
9. Morgan, D.M., Larvin, V.L. and Pearson, J.D., *J. Cell Sci.*, 94 (1989) 553.
10. MacGregor, G.R. and Caskey, C.T., *Nuc Acids Res.*, 17 (1989) 2365.
11. Arscott, P.G., Li, A.Z. and Bloomfield, V.A., *Biopolymers,* 30 (1990) 619.
12. MacGregor, G.R., Mogg, A.E., Burke, J.R. and Caskey, C.T., *Somat. Cell Mol. Genet.*, 13 (1987) 253.

Peptides: Chemistry, Structure and Biology
Pravin T.P. Kaumaya and Robert S. Hodges (Eds.)
Mayflower Scientific Ltd., 1996

231
Engineering of Betabellins 15D and 12/15: Two Beta Proteins that Bind Divalent Metal Ions

M. Kroll, Y. Yan, A. Lim, J.C. Kearney, K.E. Dukes, M.J. Saderholm and B.W. Erickson

Department of Chemistry, University of North Carolina at Chapel Hill, Chapel Hill, NC 27599, USA

Introduction

The betabellin target structure is a β-sandwich protein consisting of two 32-residue β sheets packed against one another by hydrophobic interactions [1-3]. Thus, betabellin 12D [4, 5], betabellin 14D [5, 6], and betadoublet [7], a 66-residue β sandwich, are covalent homodimers having a single disulfide bridge between the β sheets. However, betabellin 12S is a noncovalent homodimer that folds into a β sandwich even though it lacks a disulfide bridge between the β sheets [4, 5].

Results and Discussion

We have designed, synthesized, and characterized two 64-residue β-sheet proteins that bind divalent metal ions (Figure 1). Betabellin 15D is a homodimer containing two disulfide-bridged betabellin-15 chains, whereas betabellin 12/15 is a heterodimer having a betabellin-15 chain disulfide-bridged to a betabellin-12 chain. Each chain contains three pairs of D-amino acids (pd, ph, or pk) to promote the formation of inverse-common (type-I') β turns [8]. If their β sheets were folded as in Figure 2, betabellin 15D would contain six imidazole ligands at one edge of the β sandwich, and betabellin 12/15 would have four. Both of these 64-residue nongenetic proteins were assembled by the solid-phase method, purified by RP-HPLC, and found to bind divalent metal ions by circular dichroic (CD) spectroscopy. Betabellin 15D formed more stable complexes with Co^{II} and Cu^{II} but betabellin 12/15 bound only Mn^{II}.

Betabellin 15D:

HSLTAKIpkLTFSIAphTYTCAVpkYTAKVSH
|
HSLTAKIpkLTFSIAphTYTCAVpkYTAKVSH

Betabellin 12/15:

HTLTASIpdLTYSINpdTATCKVpdFTLSIGA
|
HSLTAKIpkLTFSIAphTYTCAVpkYTAKVSH

Figure 1. *Structures of betabellins 15D and 12/15. Lower-case letters are D-amino acids.*

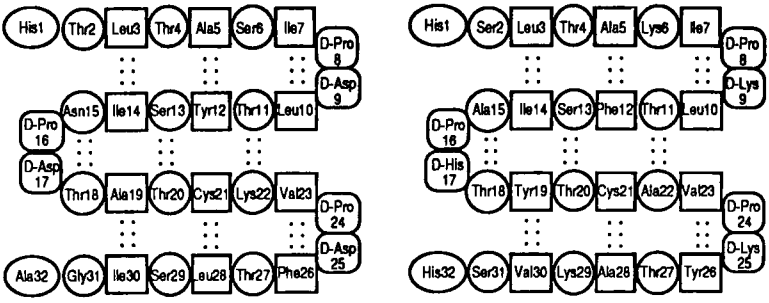

Figure 2. *β-Sheet structures of betabellin-12 chain (left) and betabellin-15 chain (right) looking down on nonpolar face. Note the 18 β-sheet hydrogen bonds (...) between 3 pairs of polar residues (circled, side chains back) and 6 pairs of nonpolar residues (boxed, side chains forward).*

Unlike the betabellin-12 chain, the betabellin-15 chain did not fold in buffer to form a noncovalent dimer. Hydrophobic interaction of the nonpolar faces of two betabellin-15 sheets did not induce folding as a β sandwich. But betabellins15D and 12/15 each folded into a β-sheet structure in 50mM NaCl/50mM K phosphate (strong negative CD band at 218nm). The extent of β structure varied with the temperature, pH, and ionic strength. Betabellin 12/15 was very soluble in water (15mg/mL) and thermally stable (T_m=69°C , H_m=39kcal/mol, pH6.5). Betabellin 15D was also stable (T_m=72°C , H_m=38kcal/mol, pH6.4) and very soluble in water (30mg/mL). The β structure of betabellin 15D nearly doubled when it bound Cu^{II} but its T_m decreased to 55°C when it bound Mn^{II}. In electron paramagnetic resonance studies, the Cu^{II} site of Cu^{II} Co^{II} betabellin 15D was reduced to Cu^{I} inefficiently by H_2O_2 and efficiently by $K_4Fe(CN)_6$. Betabellins 15D and 12/15 are the first β-sandwich proteins engineered *de novo* to bind metal ions.

Acknowledgments

This work was supported by NIH research grant GM42031.

References

1. Richardson, J.S. and Richardson, D.C., in Oxender, D.L. and Fox, C.F. (Eds.), 'Protein Engineering', Liss, New York, 1987, p.149.
2. Erickson, B.W., Daniels, S.B., Reddy, P.A., Higgins, M.L., Richardson, J.S. and Richardson, D.C., *ICSU Short Rep.*, 8 (1988) 4.
3. Hecht, M.H., *Proc. Natl. Acad. Sci. USA*, 91 (1994) 8729.
4. McClain, R.D., Yan, Y., Williams, R.W., Donlan, M.E. and Erickson, B.W., in Smith, J.A. and Rivier, J.E. (Eds.), 'Peptides: Chemistry and Biology', ESCOM, Leiden, 1992, p.364.
5. Wagner, D.S., Melton, L.G., Yan, Y., Erickson, B.W. and Anderegg, R.J., *Protein Sci.*, 3 (1994) 1305.
6. Yan, Y. and Erickson, B.W., *Protein Sci.*, 3 (1994) 1069.
7. Quinn, T.P., Tweedy, N.B., Williams, R.W., Richardson, J.S. and Richardson, D.C., *Proc. Natl. Acad. Sci., USA*, 91 (1994) 8747.
8. Yan, Y., Tropsha, A., Hermans, J. and Erickson, B.W., *Proc. Natl. Acad. Sci. USA*, 90 (1993) 7898.

Peptides: Chemistry, Structure and Biology
Pravin T.P. Kaumaya and Robert S. Hodges (Eds.)
Mayflower Scientific Ltd., 1996

232
De Novo Design and Immunogenicity of a Conformational Dependent HTLV-I gp46 Epitope

Y. Wei[2], S.F. Conrad[1], M.D. Lairmore[1,2] and P.T.P. Kaumaya[1,2]

[1]Comprehensive Cancer Center, [2]Department of Obstetrics and Gynecology, and [3]Department of Veterinary Biosciences, College of Veterinary Medicine, The Ohio State University, Columbus, OH 43210, USA

Introduction

Human T-cell leukemia virus type 1(HTLV-I) is the etiologic agent of adult T-cell leukemia (ATL). An immunodominant domain located in the central region of envelope protein gp46 (SP4a, aa190-209) as well as a major T-cell epitope (gp46 194-210) have been identified with synthetic peptides [1, 2]. In previous studies, we have engineered the SP4a epitope as a chimeric construct incorporating a promiscuous T cell epitope. This peptide vaccine can induce high-titered antibodies specific for the native viral envelope protein [3]. However, the neutralizing efficacy is low, suggesting that the sp4a epitope encompasses a conformational epitope that is poorly duplicated by 190-209 sequence. In this study, we re-engineered the epitope by extending the sequence to aa 175-209 (designated SP4ex) in order to obtain a reactive mimic. SP4ex and SP4exMVF (a peptide construct incorporating sp4ex and a promiscuous T cell epitope MVF) were synthesized. These constructs were compared for immunogenicity in both mice and rabbits. In addition, we evaluated the ability of sera from HTLV-I infected persons to recognize the peptide constructs. SP4ex elicited high titered antibodies in animals which recognized both immunogens as well as native form of gp46. The majority of sero-positive human sera reacted with SP4ex in ELISA.

Results and Discussion

A panel of 12 specimens of HTLV-I infected patient serum were acquired and their reactivity against SP4ex was evaluated by ELISA. Ten of HTLV-I patient sera tested positive, indicating SP4ex is a major immunogenic domain, and as such, a promising candidate for a peptide-based vaccine. Both SP4ex and SP4exMVF were used to immunize 10 ICR outbred mice. Antibodies elicited by either peptides recognized both immunogens and sp4ex-containing recombinant proteins. However, SP4exMVF was a more effective immunogen than sp4ex and was capable of inducing higher-titered antibodies in a greater percentage of mice. This is likely due to the stimulatory nature of MVF to enhance immunogenicity of peptides.

The chimeric construct SP4exMVF was also used to immunize three New Zealand white rabbits as described in ref [3]. All three rabbits generated high-titered antibodies

as shown by direct ELISA. The rabbit sera were also studied by competitive ELISA (Figure 1). Both SP4ex and SP4exMVF were good inhibitors of antibody binding to the recombinant protein RE-3 and MTA-1, suggesting the peptides were mimicking the structure of the corresponding domain in the native protein, gp46. Thus, by engineering the new sequence SP4ex, we were able to demonstrate further the importance of conformation in the design of peptide vaccines able to elicit high affinity antibodies specific for native protein.

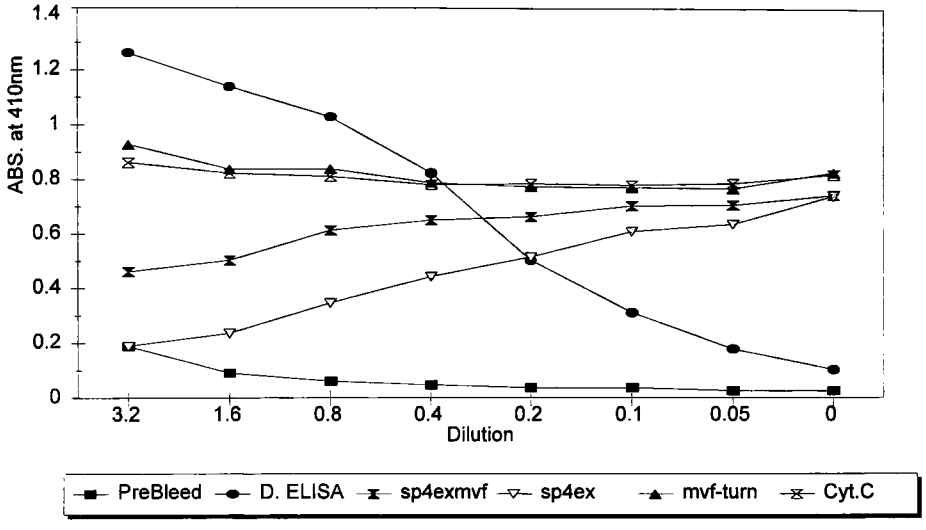

Figure 1. *Competitive ELISA with pooled rabbit anti-sera collected three weeks after tertiary immunization. Direct ELISA starts with 800 fold dilution of sera. The dilution of sera used for competitive ELISA is 1600 fold. MVF-turn is a portion of SP4exMVF without the SP 4ex. The control peptide Cyt.C is a 40-residue peptide corresponding to a sequence in Cytochrome c.*

To conclude, the engineered conformational synthetic HTLV-I peptide epitope was highly immunogenic in mice and rabbits. Antibodies raised to the epitope were highly specific for the native protein. The protective effect of the immunogen is being evaluated by syncytia inhibition assay and by monitoring virus status of rabbits challenged with HTLV-I-infected cells. This work was supported by Grant CA16058 to PTPK and MDL.

References

1. Palker, T., Tanner, M., Scearce, R., Streilein, R., Clark, M., and Haynes, B., *J. Immunol.*, 142 (1989) 971.
2. Baba, E., Nakamura, M., Tanaka, Y., Kuroki, M., Itoyama, Y., Nakano, S., and Niho, Y., *J. Immunol.*, 151 (1993) 1013.
3. Lairmore, M.D., DiGeorge, A.M., Conrad, S.F., Trevino, A.V., Lal, R.B., and Kaumaya, P.T.P., *J. Virol.*, 69(10) (1995) 6077.

Peptides: Chemistry, Structure and Biology
Pravin T.P. Kaumaya and Robert S. Hodges (Eds.)
Mayflower Scientific Ltd., 1996

233
A Nuclear Targeting Peptide: Its Design and Properties

L. Chaloin[1], J. Méry[1], N. Lamb[1], A. Heitz[2], R. Bennes[1] and F. Heitz[1]

[1]CRBM-CNRS and U 249-INSERM, Route de Mende, BP 5051, F-34033 Montpellier Cédex, France
[2] CBS-CNRS, INSERM, Faculté de Pharmacie, F-34060 Montpellier Cédex, France

Introduction

In spite of numerous investigations and proposals of *de novo* designed peptide facilitating the transport of drugs toward intracellular domains, the efficiency of such vehicles is still rather poor, especially with regard to their selectivity[1-3]. In order to improve these points, we developed a new type of carrier in order to get a better insight of the mechanisms involved in the various translocation processes, namely the crossing of the various barriers encountered on going from the external medium to cellular nuclei. Here we describe the basis of the design of a peptide which is able to carry fluorescent probes, its synthesis and the nuclear localization of the probes induced by the peptide.

Results and Discussion

The design of the peptide was based on simple principles: it must contain *i)* a hydrophobic sequence to facilitate membrane anchoring, and *ii)* a sequence which gives the target address. In addition, the synthesized peptide must be available for further chemical modifications such as the addition of the fluorescent probe. This can be achieved by the conventional Fmoc-method [4, 5] and by use of C-terminus mercapto-amide peptides which can be easily obtained after removal of disulfide linked peptide-resin. To satisfy the above criteria, a sequence corresponding to a nuclear localization signal (NLS) [6] and a signal peptide [7] having a hydrophobic sequence was selected. The choice for the signal peptide sequence was *camian crocodylus* Ig (v) light chain because it has a low valine content, thus facilitating synthesis of the assembly, which is associated through a proline containing linker to the NLS sequence of the SV40 large T antigen. The latter was chosen because it is a small fragment. The following sequence has been synthesized: Ac-M-G-L-G-L-H-L-L-V-L-A-A-A-L-Q-G-A-W-S-Q-P-K-K-K-R-K-V-Cya, where Ac corresponds to an acetyl group and Cya to the mercaptoamide or cysteamide function.

After synthesis, the peptide was further modified by coupling to either lucifer yellow iodoacetamide or fluorescein maleimide. The peptides were incubated for 3 min. with fibroblast cells which were then examined by confocal microscopy. As fluorescein alone has a spontaneous nuclear localization it appears that the most significant result is obtained with the lucifer yellow derivative.

The localization of lucifer yellow is shown in plate 1 which reveals a nuclear localization of the fluorescent chromophore when in the conjugate form while it is perinuclear in its free form.

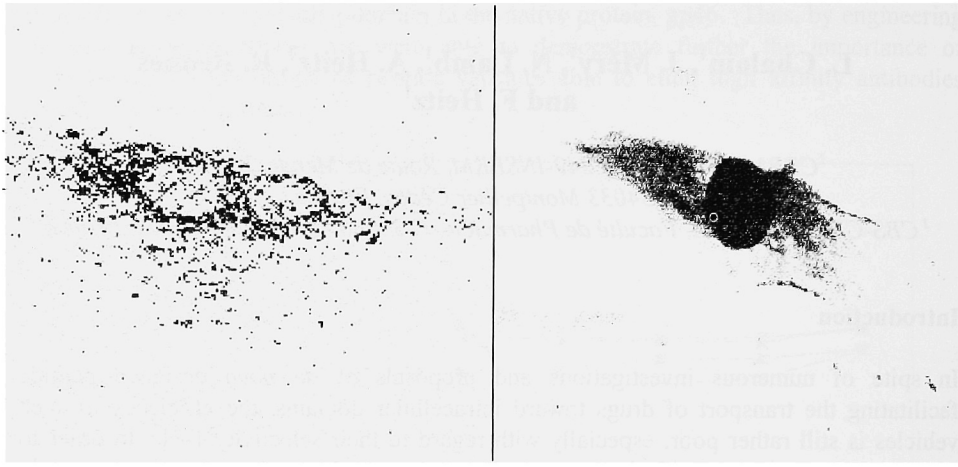

Figure 1. *Confocal microscopy localization of lucifer yellow in fibroblast cells. Left panel: free form showing the perinuclear localization. Right panel: conjugate form with nuclear localization.*

In conclusion, it appears that peptides built of a hydrophobic sequence, such as that of a signal peptide sequence associated with a nuclear localization sequence, are able to facilitate the transport of material toward nuclei of cells. Peptide conformation which can lead to these properties are discussed in an accompanying report [8].

Acknowledgments

This work was supported by the GDR 1153 'Peptides et protéines amphipathiques' from the CNRS.

References

1. Derossi, D., Joliot, A.H., Chassaing, G. and Prochiantz, A., *J. Biol. Chem.*, 269 (1994) 10444.
2. Sheldon, K., Liu, D., Ferguson, J. and Gariépy, J., *Proc. Natl. Acad. Sci. USA*, 92 (1995) 2056.
3. Bongartz, J-P., Aubertin, A-M., Milhaud, P.G. and Lebleu, B., *Nucleic Acids Res.*, 22 (1994) 4681.
4. Méry, J., Brugidou, J. and Derancourt, J., *Pept. Res.*, 5 (1992) 233.
5. Méry, J., Granier, C., Juin, M. and Brugidou, J., *Int. J. Pept. Protein Res.*, 42 (1993) 44.
6. Kalderon, D., Richardson, W.D., Markham, A.F. and Smith, A.E., *Nature* (London), 311 (1984) 33.
7. Briggs, M.S. and Gierasch, L.M., *Advances in Protein Chemistry*, 38 (1986) 109.
8. Chaloin, L., Méry, J., Lamb., Heitz, A., Bennes, R. and Heitz, F., this volume.

Peptides: Chemistry, Structure and Biology
Pravin T.P. Kaumaya and Robert S. Hodges (Eds.)
Mayflower Scientific Ltd., 1996

234
Structure-function Studies of *De Novo* Lytic Peptides

M.L. McLaughlin[1], M. Javadpour[1], S.M. Bishop[1], S.M. Cowell[1], C.L. Becker[1], J. Lo[2], M.M. Juban[3] and K.M. Morden[3]

Departments of [1]Chemistry, [2]Veterinary Pathology, and [3]Biochemistry, Louisiana State University, Baton Rouge, LA 70803, USA

Introduction

Cecropins and magainins inhibit bacteria at concentrations that are harmless to mammalian cells [1]. These peptides have amphipathic α-helical domains that are probably necessary for their function. Using the amphipathic α-helix as a minimalist starting point, this paper describes our efforts to synthesize peptides that retain or enhance the selectivity of natural lytic peptides. The peptides have triad/heptad repeats and can be summarized as follows: $(PN_1N_2PPN_1N_2)_n$ or $(PN_1N_2PN_1N_2P)_n$ where P = lysine, N_1 = leucine or phenylalanine, N_2 = alanine or glycine, and n = 1-3. The peptides were assayed for minimum inhibitory concentration (MIC) against bacteria and sublethal concentration (SLC) against cultured mammalian fibroblasts (3T3 cells). Circular dichroism (CD) spectra were used to determine peptide secondary structure in SDS micelles. These data show that peptide helicity in model membranes correlates with biological selectivity. Peptides with reduced helicity have greater biological selectivity than even magainin 2, which is considered to be a selective peptide antibiotic.

Results and Discussion

The sequences of peptides synthesized, the MIC against *E. coli* and *S. aureus,* and the SLC against 3T3 cells are summarized in Table 1. The 7-mer peptides are not lytic, whereas the 14- and 21-mers are quite potent against both bacterial strains. The 14-mer peptides and $(KLGKKLG)_3$ are more selective than the natural lytic peptide, magainin 2. Comparable concentrations of these peptides and magainin 2 are needed to inhibit bacterial growth and much higher concentrations of the peptides are required for lysis of mammalian cells. The other 21-mers tested are comparable in selectivity to the peptide toxin, melittin. Melittin inhibits bacteria and lyses mammalian cells at about the same peptide concentrations [2].

CD spectra of several of these peptides in SDS micelles have been obtained and the % helicity has been calculated. The helicity of the peptides correlates with cytotoxicity against 3T3 cells (Table 1). Highly helical peptides are highly cytotoxic. Magainin is moderately helical and cytotoxic, and the 14-mers and $(KLGKKLG)_3$ have low helicity and cytotoxicity.

Table 1. *Peptide MIC* [a] *(bacteria) and SLC* [b] *(3T3 cells) in μM and % Helicity in SDS Micelles.*

Peptide[c]	*E. coli*	*S. aureus*	3T3	% Helicity[d]
(KLAKKLA)	>100	>100	Not lytic	None
(KLAKLAK)	>95	>95	Not lytic	None
$(KLAKKLA)_2$	6.0	6.0	>272	24
$(KLAKLAK)_2$	5.8	5.8	>517	37
$(KFAKKFA)_2$	4.8	4.8	>294	---
$(KLGKKLG)_2$	8.2	16.4	Not lytic	None
$(KLAKKLA)_3$	4.2	4.2	11	79
$(KLAKLAK)_3$	3.7	3.7	9	79
$(KALKALK)_3$	3.9	7.8	11	---
$(KFAKKFA)_3$	1.8	2.7	5	---
$(KFAKFAK)_3$	3.0	2.8	11	---
$(KLGKKLG)_3$	3.4	3.4	>393	33
Magainin 2	9.4	18.8	60	46
Melittin	3.0	3.0	1	93

[a]MICs were determined against *E. coli* ATCC 25922 and *S. aureus* ATCC 25723.
[b]SLCs were determined using 2:1 serial dilutions with minimal essential media (MEM) and applied to a 1-day old monolayer of 3T3 cells (~ 1 x 10^4 cells per well). The supernatant was removed and the cells were treated with 0.2% trypan blue stain. Inclusion of trypan blue dye within a cell is indicative of cell death. Sublethal dose is defined as the highest dilution in which at least one adherent cell is not stained.
[c]Peptide concentrations were determined by quantitative amino acid analysis.
[d]Based on $[\theta]_{222}$ in 25 mM SDS micelles and 10 mM sodium phosphate buffer pH=7.4; % α-helix = $-100\ ([\theta]_{222} + 3000)/33000$.

Idealized amphipathic α-helical peptides have been synthesized with greater *in vitro* bacterial inhibition than magainin 2 and with lower cytotoxicity against a mammalian cell line. The low helicity of these peptides in SDS micelles correlates with this selective biological activity.

Acknowledgments

The financial support of the National Science Foundation *via* NSF/EPSCoR Grant [(RII/EPSCoR)LEQSF(1992-96)-ADP] is gratefully acknowledged. Also we thank Professor M. D. Barkley, F. Enright, and R. Hammer for their expert assistance.

References

1. Boman, H.G., Hultmark, D., *Ann. Rev. Microbiol.*, 41 (1987) 103; Bevins, C.L., Zasloff, M., *Ann. Rev. Biochem*, 59 (1990) 395.
2. Habermann, E., Jentsch, J., *Hoppe-Seylers Z. Physiol. Chem.*, 348 (1967) 34.

Peptides: Chemistry, Structure and Biology
Pravin T.P. Kaumaya and Robert S. Hodges (Eds.)
Mayflower Scientific Ltd., 1996

235
Design of Metal Ion Nests in an α-Helix Bundle Structure

N. Nishino[1], T. Kato[1], H. Hasegawa[1], H. Nakayama[1], T. Arai[1], T. Fujimoto[1] and S. Yoshikawa[2]

[1]*Faculty of Engineering, Kyushu Institute of Technology, Tobata 804, Japan*
[2]*Osaka National Research Institute, AIST, Ikeda, Osaka 563, Japan*

Introduction

In *de novo* design of artificial proteins, metal ion complexes have been employed to combine α-helical peptide segments for the bundle structure [1-3]. They are placed at the end of the peptide chains, which are usually exposed to hydrophilic environments. Since the metal ion complex moieties are hydrophilic, there has not been an attempt to place them at the hydrophobic inside of the α-helix bundle structure. In designing metalloprotein models for artificial functions, the use of various ligand groups is required to build metal ion nests.

Results and Discussion

We designed a 3 α-helix bundle structure on a cyclic pseudopeptide template [4, 5] as illustrated in Figure 1. Two cyclohexylalanines (Cha) were introduced in the amphiphilic 13-peptide segment to enhance it's hydrophobicity. The hydrophobic residues (Cha and

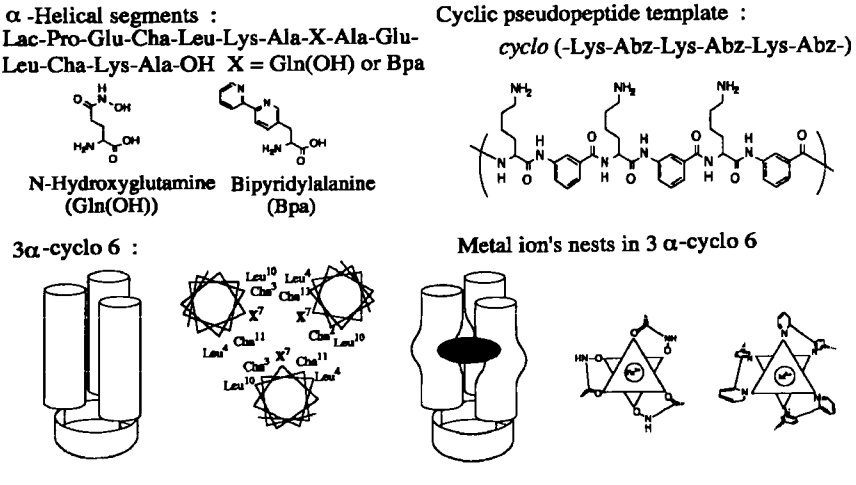

Figure 1. *Design of 3α-helix bundle structure with hydroxamates and bipyridines.*

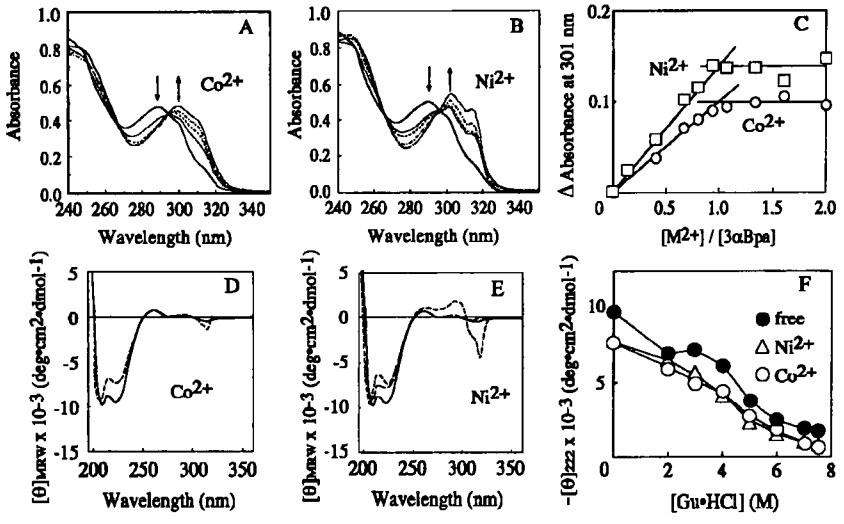

Figure 2. *Spectral analyses of the complex formation of 3αBpa with Co^{2+} and Ni^{2+}.*

Leu) are expected to form a tight hydrophobic core to surround the hydrophilic metal ion nest, for which N-hydroxy glutamine (Gln(OH)) and 5-bipyridylalanine (Bpa) are employed [6, 7]. Three similar segments were combined in parallel to cyclo(L-Lys-*m*-Abz)$_3$ (Abz = aminobenzoyl).

The binding of Fe^{3+} to the hydroxamate nest was monitored by an increasing absorption band at 420 nm. The pseudoprotein was saturated by equimolar amount of $Fe(NO_3)_3$. The binding of Co^{2+} and Ni^{2+} to the trisbipyridine nest was also monitored by absorption spectral changes with the addition of these ions. In both cases, a band at 288 nm decreased, when metal ions were added while new bands at 300 and 301 nm for Co^{2+} and Ni^{2+}, increased with isosbestic points (Figures 2A,B). From the titration curves (Figure 2C), the pseudoprotein, 3αBpa formed a 1:1 complex with these ions. The α-helicity decreased slightly on formation of metal ion complexes (Figures 2D,E). The CD absorption band was significantly increased upon the addition of Co^{2+} and Ni^{2+}. As shown in Figure 2F, the 3αBpa·M^{2+} are fairly stable during the denaturation with guanidine hydrochloride. These results demonstrate that it is possible to form metal ion complexes in an hydrophobic environment.

References

1. Lieberman, M. and Sasaki, T., *J. Am. Chem. Soc.*, 113 (1991) 1470.
2. Gahdiri, M.R., Soares, C. and Choi, C., *J. Am. Chem. Soc.*, 114 (1992) 825.
3. Gahdiri, M.R. and Case, M.A., *Angew. Chem. Int. Ed. Engl.*, 32 (1993) 1594.
4. Mutter, M., Vuilleumier, S., *Angew. Chem. Int. Ed. Engl.*, 28 (1989) 535.
5. Arai, T., Ide, Y., Tanaka, Y., Fujimoto, T., Nishino, N., *Chem. Lett.*, (1995) 381.
6. Imperiali, B., Prins, T.J. and Fisher, S.L., *J. Org. Chem.*, 58 (1993) 1613.
7. Nishino, N., Arai, T., Hayashida, J., Ogawa, H.I., Yamamoto, H. and Yoshikawa, S., *Chem. Lett.*, (1994) 2435.

Peptides: Chemistry, Structure and Biology
Pravin T.P. Kaumaya and Robert S. Hodges (Eds.)
Mayflower Scientific Ltd., 1996

236
Effect of a Single Residue Change on Assembly of Homodimeric Four-α-Helical Bundle Hemopeptides

A.M. Grosset, F. Rabanal, R.S. Farid, D.E. Robertson, D.L. Pilloud, W. F. DeGrado and P.L. Dutton

Johnson Research Foundation, Department of Biochemistry and Biophysics, University of Pennsylvania, Philadelphia, PA 19104, USA

Introduction

Synthetic hemopeptides derived from *de novo* design principles are being used as molecular maquettes of redox proteins to study structure and function. In previous work, a 31-amino acid α-helical peptide (α, *Ac*-CGGGELWKLHEELLKKFEELLKLAEER-LKKL*CONH*$_2$) with a heme-binding histidine at position 10 was synthesized and linked *via* the disulfide to form homo-α-dihelix structures (α_2), which in turn assembled to form $(\alpha_2)_2$, a four helix homodimer. The α-helices of $(\alpha_2)_2$ were deduced to be parallel because of charge coupling between hemes in the 10 position [1]. We have sought to confirm the all-parallel association of (α_2) to form the $(\alpha_2)_2$ structure and to explore the possibility to form an antiparallel $(\alpha_2)_2$ by altering the amino acid composition of the α building block. Here we provide further evidence that the original $(\alpha_2)_2$ is all-parallel and have located a single point in the sequence, alanine-24, that if changed to serine-24, apparently leads to an antiparallel $(\alpha_2)_2$ assembly.

Results and Discussion

The methods used to elucidate the α-helical $(\alpha_2)_2$ hemopeptide structure include the following: electrostatic interactions between hemes, ligated by histidine pairs in the 10 position; measurement of free thiols by reaction of Ellman's Reagent with self-assembled monolayers; and attachment of fluorescent pyrene probes to each (α_2) dihelix structure.

In a parallel configuration electrostatic interactions would bring interacting hemes into van der Waals contact with an Fe-to-Fe distance of 13 Å. This could be expected to give charge interaction through the interior of a water-soluble protein in the range of 100 mV. However, an antiparallel assembly with hemes at the 10 position would have an Fe-to-Fe distance of 26 Å along the axis of the molecule where the high aqueous dielectric dominates over and diminishes the charge interactions to <5 mV. Redox titration revealed two potentials in the alanine-24 $(\alpha_2)_2$ peptide ($E_{midpoint}$ = -215 mV, -100 mV), suggesting a heme interaction between peptides in the parallel position, while the serine-24 $(\alpha_2)_2$ peptide exhibited only one potential ($E_{midpoint}$ = -200 mV). Such a result could derive from separation of the helices and subsequent loss of charge coupling, or

from an alteration in the alignment/orientation of the dihelix dimers. These results are consistent with the conclusion that the change resulted in the transformation of a parallel assembly in the alanine-containing $(\alpha_2)_2$ hemopeptide to an antiparallel assembly in the serine-containing $(\alpha_2)_2$ hemopeptide. Self-assembled monolayer films confirmed this effect: cyclic voltammetry demonstrated one versus two potentials and Ellman's reagent indicated the presence of free thiol groups in the serine-24 $(\alpha_2)_2$ hemopeptide, though not in the alanine-24 $(\alpha_2)_2$ hemopeptide.

A second method to identify the parallel or antiparallel nature of the original $(\alpha_2)_2$ and its derivatives used pyrene. 1-Pyrenebutyric acid was coupled to the N-terminus of both peptides [2-4], one pyrene molecule per (α_2) dihelix structure. When excited at 350 nm, both the alanine-24 and serine-24 $(\alpha_2)_2$ peptides in aqueous solution show some pyrene monomer fluorescence at 380 and 400 nm, while only the alanine-24$(\alpha_2)_2$ peptide shows a clear pyrene excimer peak at 480 nm indicating that the pyrenes are in close proximity, as would occur in a parallel arrangement. The H10 peptides both contain tryptophan at the 7 position and pyrene-tryptophan interactions by exciplex formation might be responsible for the weak fluorescence observed between 450 and 500 nm [5-7]. Through the observation of heme interactions and attached fluorescent probes, this study revealed that substituting a single critical residue appears to significantly alter the $(\alpha_2)_2$ peptide assembly.

Acknowledgments

We are grateful for the valuable assistance of Dr. Christopher Moser for computer graphics. This work was funded by grants GM 41048 and GM 48130.

References

1. Robertson, D.E., Farid, R.S., Moser, C.C., Urbauer, J.F., Mulholland, S.E., Pidikiti, R., Lear, J.D., Wand, A.J., DeGrado, W.F. and Dutton, P.L., *Nature*, 368 (1994) 425.
2. Rabanal, F., DeGrado, W.F. and Dutton, P.L., Philadelphia, PA, submitted for publication.
3. García-Echeverria, C., *J. Am. Chem. Soc.*, 116 (1994) 6031.
4. Turro, N.J., 'Modern Molecular Photochemistry', University Science Books, Mill Valley, CA 1991, p. 141.
5. Engelke, M., Behmann, T., Ojeda, F. and Diehl, H.A., *Chem. and Phys. of Lipids*, 72 (1994) 35.
6. Helsen, N. Viaene, L., Van der Auweraer, M. and De Schruyver, F.C., *J. Phys. Chem.*, 98 (1994) 1532.
7. Castanheira, E.M.S. and Martinho, J.M.G., *J. Photochem. Photobio. A: Chem.*, 80 (1994) 151.

Peptides: Chemistry, Structure and Biology
Pravin T.P. Kaumaya and Robert S. Hodges (Eds.)
Mayflower Scientific Ltd., 1996

237

The Role of a Strain Free Disulfide Bridge in Stabilizing β-Sheet Structures in Short Peptides

S. Janardhanam, D. Balachari, D.T. Corson and K.P. Nambiar

Department of Chemistry, University of California, Davis, CA 95616, USA

Introduction

Designing water soluble β-sheet peptides remains a challenging problem in bioorganic chemistry. Progress in this area include use of alternating hydrophobic and hydrophilic residues [1-5], use of planar hydrogen bonding templates [6] and use of benzofuran derivatives to anchor two peptide chains at a suitable distance from each other [7], and use of cystine disulfide linkages to hold two strands together [8-10]. In order to systematically study the effect of disulfide bridge length on β-sheet conformation, we synthesized short peptides containing cysteine, homocysteine, and (S)-α-amino-ε-mercaptohexanoic acid (Amh) and oxidized them to yield the disulfide bridged dimers. Peptides with a strain free disulfide bridge show more pronounced β-sheet character as compared to cystine peptides.

Results and Discussion

In an earlier report, we had shown that, while short peptides containing S-protected thiol amino acids adopt random coil structures, their disulfide bridged dimers fold into β-sheet structures [10]. Cystine disulfide bridges do not possess the correct geometry to hold two peptide chains in perfect β-sheet conformation [11]. We had observed that replacing a cystine disulfide bridge between two adjacent peptide strands with a strain free disulfide bridge formed between the side chains of Amh residues located at staggered positions on adjacent peptide strands results in a dramatic increase in the β-sheet character of the peptide [10]. In the present studies, we have synthesized three disulfide bridged peptide dimers, each containing a different thiol amino acid to determine the effect of disulfide bridge length on β-sheet stability. The secondary structure was determined using CD spectroscopy on 5 μM solution of the peptides in water containing 100 μM SDS at room temperature. Peptide **1** containing a cystine disulfide bridge shows only modest β-sheet character while peptides **2** and **3** containing strain free disulfide bridges, formed between the side chains of homocysteine and Amh respectiely, show much more pronounced β-sheet character (Figure 2). The results clearly show that a longer, strain free disulfide bridge between two peptide strands is much more efficient in stabilizing the β-sheet structure of the peptide dimer as compared to a cystine disulfide bridge.

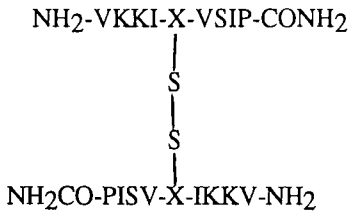

Peptide	X
1	Cysteine
2	Homocysteine
3	Amh

Figure 1. *Sequence of peptides* ***1-3***

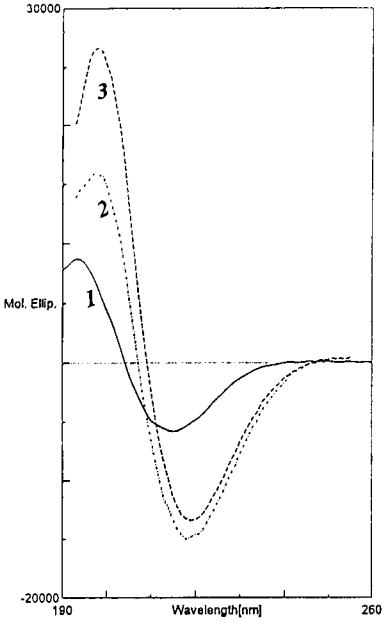

Figure 2. *CD spectra of 5μM solutions of peptides* ***1-3*** *in aqueous solution containing 100 μM SDS at RT.*

Acknowledgments

This research was supported by NIH grant GM 39822.

References

1. Brack, A. and Orgel, L.E., *Nature*, 256 (1975) 383.
2. Brack, A. and Caille, A., *Int. J. Peptide Protein Res.*, 11 (1978) 128.
3. Osterman, D., Mora, R., Kezdy, F.J., Kaiser, E.T. and Meredith, S. C., *J. Am. Chem. Soc.*, 106 (1984) 6845.
4. Altman, K.H., Florsheimer, A. and Mutter, M., *Int. J. Peptide Protein Res.*, 27 (1986) 314.
5. Zhang, S., Holmes, T., Lockshin, C., and Rich, A. *Proc. Natl. Acad. Sci. USA*, 90 (1993) 3334.
6. Kemp, D.S., Blanchard, D.E. and Muendel, C.C., in Smith, J.A. and Rivier, J.E (Eds.), 'Peptides: Chemistry and Biology', ESCOM, Leiden, The Netherlands, 1992, p. 319.
7. Diaz, H., Tsang, K.Y., Choo, D. and Kelly, W.J., *Tetrahedron*, 49 (1993) 3533.
8. Balaram, H., Uma, K. and Balaram, P., *Int. J. Pept. Prot. Res.*, 35 (1990) 495.
9. RuizGayo, M., Royo, M., Fernandez, I., Alberico, F., Giralt, E. and Pons, M., *J. Org. Chem.*, 58 (1993) 6319.
10. Aberle, A.M., Reddy, H.R., Heeb, N.V. and Nambiar, K.P., *Biochem. Biophys. Res. Commun.*, 200 (1994) 102.
11. Richardson, J.S., *Adv. in Protein Chem.*, 34 (1981) 167.

Peptides: Chemistry, Structure and Biology
Pravin T.P. Kaumaya and Robert S. Hodges (Eds.)
Mayflower Scientific Ltd., 1996

238

The Design of pH-dependent Amphipathic α-Helices to Trigger Cytoplasmic Delivery of Liposome Encapsulated Molecules.

K.M. Vogel, S. Wang, P.S. Low and J.A. Chmielewski

Department of Chemistry, Purdue University, West Lafayette, IN 47907, USA

Introduction

The development of liposomes as agents of cytoplasmic drug delivery has received much attention. Recently, a method to efficiently transport liposomes into cells through the pathway of receptor-mediated endocytosis was developed and found to enhance drug delivery through the presence of a folate-PEG-PE lipid conjugate [1]. Although drugs may be delivered to cells *via* liposomes, the drugs remain trapped within the endosomal compartments. This has led to the development of pH sensitive liposomes, recently reviewed by Chu and Szoka [2]. We have developed a new pH sensitive cell target specific liposome preparation that does not contain lipid components that have been shown to have pH sensitive characteristics, *i.e.* CHEMS, DOPE, or oleic acid [2]. Our liposomes, containing PC and PE, have been shown to enhance the stability of the liposome preparation, while achieving pH sensitive content delivery due to the presence of a helix forming peptide. The peptide (EALA), having the sequence AALAEALAE ALAEALAEALAEALAAAAGGC(Acm), was designed to enhance the favorable aspects of Szoka's GALA peptide [3] while making it available for covalent modification. EALA was predicted to cause cytoplasmic leakage of endocytosed liposomes due to its ability to form an amphipathic α-helix under mildly acidic conditions, and consequently interact with and disrupt membrane bilayers.

Results and Discussion

Studies using peptides to induce membrane fusion relied on the introduction of peptides both non-covalently and external to the liposome [3]. Our strategy involved the encapsulation of EALA into the aqueous interior of liposomes and the covalent attachment of EALA to a maleimide derivative of PE to achieve irreversible membrane anchoring of this peptide. To quantitate the extent of cytoplasmic delivery of liposomal contents, a new methodology was developed that exploits the dramatic increase in quantum yield of propidium iodode (PI) upon binding DNA [4].

EALA was synthesized using solid phase methodology [5] on PAB resin [6] using Fmoc strategy [7]. Purification and characterization of the peptide was achieved using HPLC and FAB-MS. pH dependent CD experiments confirmed the ability of EALA to adopt an enhanced α-helical conformation under acidic conditions [4]. The covalent

attachment of EALA to maleimido phosphatidyl ethanolamine (EALA-PE) was achieved by Acm deprotection of C-terminal Cys [8] followed by DTT reduction of the resulting methyl mercaptan derivative. Liposomes were prepared by the extrusion method [9], and contained 10:1 egg PC:folate-PEG-PE encapsulating 5 μM PI and either co-encapsulated 10 μM EALA or containing an additional 5% of EALA-PE lipid component.

To study the kinetics of release of encapsulated PI following endocytosis by KB cells, the fluorescence of the cell suspension was measured (λ_{ex}=540nm and λ_{em}=615nm) and compared to the maximum PI release achieved by sonication of the same cell sample. Introduction of EALA into the liposome interior caused impressive cytoplasmic delivery of encapsulated PI, ~20%. An additional rate enhancement of the release was observed with covalently lipid-linked EALA [4].

Table 1. *The stability of Folate-PEG-PE liposomes.*

	Percent Efflux of PI	
Liposome Type	4°C in PBS, 1 week	37°C in Serum, 4 hours
PE/PC	0	4
PE/PC EALA[a]	0	3
PE/PC/EALA-PE[b]	0	40
CHEMS/DOPE	11	56
CHEMS/DOPE EALA[a]	11	58

[a]Liposomes encapsulating EALA peptide; [b]Liposomes containing covalently lipid-linked EALA peptide.

The ability of liposomes to retain their vesicle contents is important if they are to be modified for the purpose of drug delivery. The results of the stability of these liposomes, versus those preparations containing pH sensitive lipid components, upon storage and serum treatment are presented in Table 1. We believe the stability of these liposomes coupled with their cell type specificity and intracellular delivery characteristics will make them a desirable vehicle of cell-specific drug delivery.

References

1. a) Lee, R.J. and Low, P.S., *J. Biol. Chem.*, 269 (1994) 3198, b) Lee, R.J. and Low, P.S., *Biophys. Acta*, 233 (1995) 134.
2. Chu, C.J. and Szoka, F.C., *J. Liposome Res.*, 4 (1994) 361.
3. Subbarao, N.K., Parente, R.A., Szoka, F.C., Nadasdi, L. and Pongracz, K., *Biochemistry*, 26 (1987) 2964.
4. Vogel, K., Wang, S., Lee, R.J., Chmielewski, J. and Low, P.S. submitted for publication.
5. Merrifield, R.B., *J. Am. Chem. Soc.*, 85 (1963) 2149.
6. Wang, S.S., *J. Am. Chem. Soc.*, 95 (1973) 1328.
7. Atherton, E. and Sheppard, R.C., in Gross, E. and Meienhofer, J. (Eds.), 'The Peptides', Academic Press, New York, 1987, p. 1.
8. Bishop, P., Jones, C. and Chmielewski, J., *Tetrahedron Letters*, 34 (1993) 4469.
9. Hope, M.J., Bally, M.B., Webb, G. and Cullis, P.R., *Biochim. Biophys. Acta*, 812 (1985) 55.

Peptides: Chemistry, Structure and Biology
Pravin T.P. Kaumaya and Robert S. Hodges (Eds.)
Mayflower Scientific Ltd., 1996

239
Peptide-unit Assembling: New Approaches for Construction of α-Helical Protein Models

S. Futaki[1], T. Ishikawa[1], M. Aoki[1], F. Kondo[1], M. Niwa[1], K. Kitagawa[2] and T. Yagami[3]

[1]Faculty of Pharmaceutical Sciences, The University of Tokushima, Tokushima 770, Japan
[2]Niigata College of Pharmacy, Niigata 950-21, Japan
[3]National Institute for Health Sciences, Tokyo 158, Japan

Introduction

Recently, three-dimensionally designed peptides have been successfully employed to elucidate protein function. Montal *et al.*, applied Mutter's template-assembled synthetic protein (TASP) approach to the construction of Ca channel models and obtained insight into the roles of S3 segments. Such peptide-based approaches seem promising to obtain a different kind of information on protein function from that obtained through gene-manipulation. We report here new approaches to construct four-helix-bundle protein models, the main feature of which is the feasibility to construct protein models composed of four α-helices with different amino acid sequences. Using one of these approaches, a model of voltage sensor region (S4) of Na channel was constructed.

Results and Discussion

We have developed three approaches. In the first, peptide-units were assembled through disulfide cross-linking by activation of a cysteine through pyridinesulfenylation. In the second, assembly was accomplished through cross-linking using nucleophilic attack of sulfhydryl group on a bromoacetyl moiety. These two approaches were used to obtain antiparallel four-helix-bundle proteins (Figure 1). The third approach involved chloroacetylated peptide units being introduced onto a modified Mutter template [4-Cys-template (CyT) : H-Cys(Acm)-Lys-Cys(SH)-Pro-Gly-Cys(MBzl)-Glu-Cys(Ada)-Gly-OH (MBzl: *p*-methoxybenzyl)]. Stepwise protecting group removal from the three cysteines should allow successive introduction of four peptide units to yield parallel four-helix-bundle proteins. To see if a protein model with four α-helices was constructible with this approach, a model of the voltage sensor region (S4) of Na channel was constructed.

α-Helical peptide-units were designed as shown in Figure 2. Peptide-units named [NaI], [NaII], [NaIII], [NaIV] correspond to the S4 region of *Electrophorus electricus* Na channel, which region was assumed to work as the voltage sensor region of the channel. On the N-terminus of the sequences, chloroacetyl-GABA was placed as a linker. Incorporation of [NaII] onto CyT was conducted by reacting free SH group of the

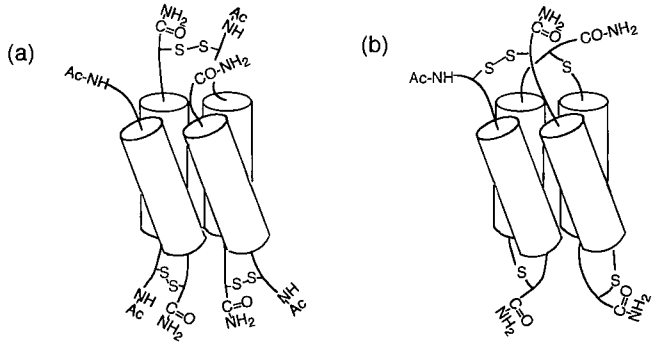

Figure 1. *Four helix-bundle proteins constructed by peptide-unit assembling using (a) selective disulfide formation and (b) selective S-alkylation.*

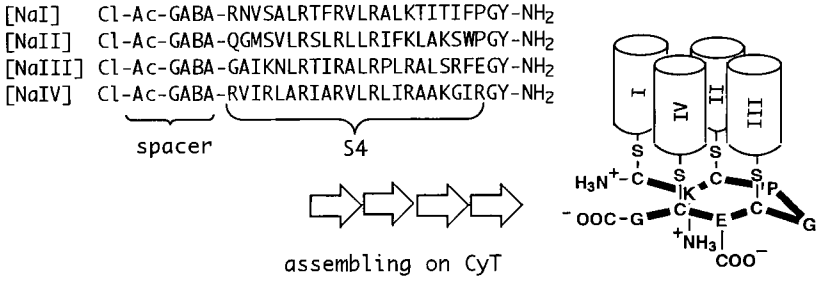

Figure 2. *Construction of a model of the voltage sensor region (S4) of Na channel using CyT.*

template with chloroacetyl moiety of the [NaII] in 6M GnHCl-0.1M Tris (pH 8.0) (room temperature, 16h). The product was treated with 1M TMSBr-thioanisole / TFA (0°C, 2h) to remove MBzl group. After introduction of [NaIII], the obtained peptide was treated with 1M TFMSA- thioanisole / TFA (0°C, 1.5h) to remove Ada group. Then, [NaIV] was introduced and Acm group removed by AgOTf / TFA treatment (0°C, 1.5h). Finally, introduction of [NaI] afforded the desired protein. The sample was examined on HPLC and found to be highly pure. The estimated molecular weight (13,000) from SDS-PAGE and the amino acid compositions after 6N HCl hydrolysis were in good agreement with the theoretical values. Thus, fidelity of the structure of the model was confirmed. The CD spectrum of the protein in MeOH was suggestive that the protein has α-helical structure in the membrane $[\theta]_{222}$: -13,100 deg cm^2/dmol (14μM protein/ MeOH)]. A preliminary experiment showed the protein to have ion channel activity in a lipid membrane. Further characterization of the channel activity is under way.

Acknowledgment

The authors are grateful to Professor Y. Nakaya, Faculty of Medicine, the University of Tokushima for his kind help on measuring the channel activity.

Peptides: Chemistry, Structure and Biology
Pravin T.P. Kaumaya and Robert S. Hodges (Eds.)
Mayflower Scientific Ltd., 1996

240
Rational Design of Irreversible, *Pseudo*-C_2-Symmetric Inhibitors of HIV-1 Proteinase

C. Park, J.S. Koh, H. Choi, N. Choy, Y.C. Son, C.S. Lee, K.Y. Moon, W.H. Jung, E. Kim, M. Yun, S. Kim, S.C. Kim and H. Yoon

Biotech Research Institute, LG Chemical Ltd/Research Park, Box 61 Yu Sung, Science Town, Taejon 305-380, Korea

Introduction

The human immunodeficiency virus encodes a proteinase which is responsible for the processing of polyprotein products of the *gag* and *pol* genes into their mature forms [1]. The enzyme is an aspartyl proteinase comprising a highly conserved domain. Asp-Thr-Gly are at the active site and functions as a C_2-symmetric homodimer [2]. As the native enzyme can adopt a conformation in which a two-fold symmetry axis extends through the active site, it might also be desirable to include the C_2 symmetry through the center of the inhibitors. With this in mind, another important factor was taken into account for the design of inhibitors; that is, irreversibility. Although many transition state analogues have been developed with success so far [3], their inherent reversible characters made us question their long term efficacy *in vivo*. In an effort to develop epoxide-containing irreversible inhibitors with high potency, we utilized the concept of symmetry for the design of novel inhibitor structures.

Results and Discussion

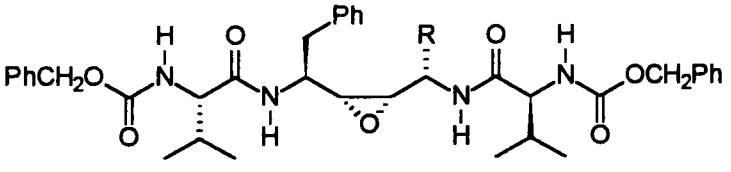

1 R : CH_2Ph
2 H_2

Compound **1** worked as a reversible inhibitor on the enzyme with K_i of 75nM, which was 300-fold less potent than Abbott's C_2-symmetric compound A75925. If the catalytic water molecule attacks the epoxide ring, **1** should be converted to A75925 after a long period of time and observed K_i value of **1** should be same as that of A75925. After preincubation of **1** with HIV-1 protease, however, new species such as A75925 have not been detected and K_i value of **1** was 300-fold higher than that of A75925. The lower potency of **1** compared to A75925 could be interpreted as the rigidity of the epoxide ring. Compared with the diol isostere, the epoxide ring in compound **1** was so rigid that the

overall conformation of **1** should be totally different from the active conformation of A75925, which suggested that P1', P2' and P3' in **1** would be in a different orientation from that of A75925. Also, the absence of hydrogen bonding of the epoxide ring with the two aspartyl groups in contrast to the hydroxyl groups in A75925 could be another reason for the lower potency of **1** compared to A75925. To overcome this problem, the phenylalanine was replaced for glycine at P1' for two reasons. First, computer modeling based on the X-ray structure of enzyme-A75925 complex suggests that the removal of P1' benzyl side chain make **1** in the arrangement that the epoxide ring could make a direct contact with the two active site aspartates. If that is the case, a new designed compound would exhibit irreversible character. Second, the greater importance of the P region than the P' region was previously observed for the binding of renin inhibitors and a similar observation was noted for the asymmetric peptidomimetic inhibitor complexes of HIV protease [4].

As expected, the resulting compound **2** displayed rapid, time-dependent inactivation of HIV-1 protease following pre-incubation of various concentrations of **2** with the enzyme at different time intervals. The calculated bimolecular rate constant for the formation of HIV-1 protease-**2** complex (k_{ina}/K_i) was 1.5x108 $M^{-1}min^{-1}$ and the active site titration studies using 0.1-1 molar equivalent of **2** over the concentration of the protease indicated 1:1 stoichiometric binding ratio of inhibitors to the protease. In addition, X-ray crystallographic structure of HIV-1 protease-2 analogue complex showed that Asp25 of the enzyme attacked the epoxide ring and made a covalent bond with **2**. Therefore, inactivation of HIV-1 protease by **2** involves enzyme-catalyzed alkylation of the unprotonated active site aspartyl residue, in analogy to the inactivation of simian immunodeficiency virus by EPNP. The 50% inhibition constant (IC_{50}) of 2 was 30 nM against HIV-1 in H9 and Sup T1 cell lines as assessed by syncytium formation and reverse transcriptase assay.

In conclusion, the design of **2** was successful in that it produced an inhibitor with high affinity and irreversibility. Studies of X-ray crystallographic structure of HIV-1 protease-**2** complex suggested that the inactivation of HIV-1 protease by **2** was due to covalent modification of an active-site residue.

References

1. Kay, J. and Dunn, B.M., *Biochim.Biophys.Acta.*, 1048 (1990) 1.
2. Navia, M.A., Fitzgerald, P.M.D., McKeever, B.M., Leu, C.-T., Heimbach, J.C., Herber, W.K., Sigal, I.S, Darke, P.L. and Springer, J.P., *Nature,* 337 (1989) 615.
3. Meek, T.D., Lambert, D.M., Metcalf, B.W., Petteway Jr., S.R. and Dreyer, G.B. in E. DeClercq (Ed.), 'Design of anti-AIDS drugs', Elsevier, Amsterdam, 1990, pp225.
4. Erickson, J. *Perspect. Drug Discovery Design*, 1 (1993) 109.

Peptides: Chemistry, Structure and Biology
Pravin T.P. Kaumaya and Robert S. Hodges (Eds.)
Mayflower Scientific Ltd., 1996

241
Evaluation of GrowMol: A Novel Structure Generation Program; Generation of Known Pepsin Inhibitors and Identification of Novel Potential Inhibitors

A.S. Ripka[1], R.S. Bohacek[2] and D.H. Rich[1]

[1]The School of Pharmacy and the Department of Chemistry, University of Wisconsin at Madison, Madison, WI 53706, USA
[2]Pharmaceuticals Division, CIBA Corporation, Summit, NJ 07901, USA

Introduction

GrowMol [1] is a unique structure generating program that grows potential inhibitors in the enzyme active site atom by atom. A three dimensional coordinate is entered as the growth point and inhibitor construction begins by calculation of rotational isomeric states for that atom and selection of one of these for the new atom. This atom is then given a complementarity score based on how well it interacts with nearby active site atoms. A hydrogen bond donor near a hydrogen bond acceptor would receive a high score whereas a hydrophobic atom in a hydrophilic pocket would receive a low score. After the desired number of atoms for a molecule has been generated, the molecules are minimized inside and outside the active site. This gives the inhibitor a strain energy that is related to the free energy difference between the bound and unbound states. An evaluation program is then used to rank the inhibitors based on their complementarity scores.

Results and Discussion

The search focused on generating known cyclic aspartic protease inhibitors of pepsin such as Szewczuk's alkyl bridging di-cysteinyl pepstatin analogs [2].

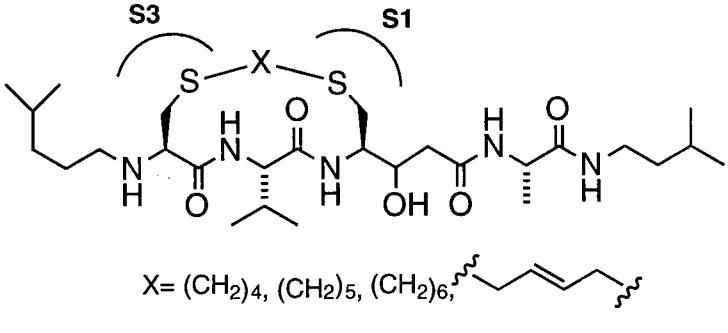

Growth began at the beta carbon of the P3 side chain. After the initial run did not discover Szewczuk's compounds, the atom selector table was modified. This table allows the user to change the probability that a given atom will be chosen for attachment to the new growth point. The preference for amide bond formation was lowered and the probability for heteroatoms and carbon were set equal; this gave a better result as to the atom that best fit in the active site. After this modification, two compounds identical to Szewczuk's (x=$(CH_2)_4$ and $(CH_2)_6$) were generated by GrowMol. Several other related compounds surfaced from multiple GrowMol trial runs. Some of these novel synthetic targets are currently being synthesized in our labs.

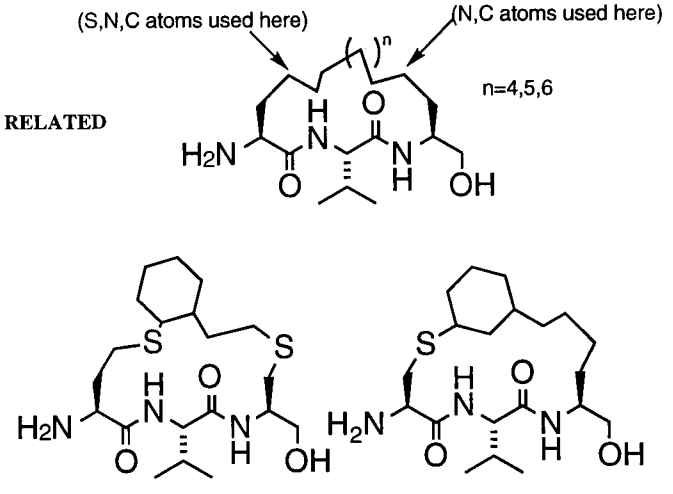

GrowMol has demonstrated the capability of reproducing known potent inhibitors for *R. chinensis* pepsin. This suggests that similar novel structures generated by the program will also be active.

Acknowledgments

Financial support form the National Institutes of Health is gratefully acknowledged. We also thank Dr. Ken Satyshur for assistance with Sybyl calculations and graphics printing.

References

1. Bohacek, R.S. and McMartin, C., *J. Amer. Chem. Soc.*, 116 (1994) 5560.
2. Szewczuk, Z., Rebholtz, K.L., and Rich, D.H., *Int. J. Peptide Protein Res.*, 40 (1992) 233.

Peptides: Chemistry, Structure and Biology
Pravin T.P. Kaumaya and Robert S. Hodges (Eds.)
Mayflower Scientific Ltd., 1996

242
Synthesis and Characterization of a *De Novo* Four-helix Bundle

B.C. Gibb, A.R. Mezo and J.C. Sherman

Department of Chemistry, University of British Columbia, Vancouver, British Columbia, V6T 1Z1, Canada

Introduction

The use of templates to assist in the organization of peptides to form three-dimensional protein-like structures has emerged as a useful technique in studying the protein folding problem [1]. We are interested in linking peptide strands to cavitands (rigid organic macrocycles that contain enforced cavities [2]) to form a new family of Template Assembled Synthetic Proteins (TASPs), which we have named *caviteins* (*cavi*tand + pro*tein*). Here we briefly describe the design, synthesis, and characterization of a four-helix bundle cavitein.

Results and Discussion

We have recently synthesized tetrathiol cavitand **1** in our laboratory and have linked it to various activated L-phenylalanine derivatives [3]. This demonstrated the synthetic utility of tetrathiol **1** as a building block to synthesize caviteins. The rigid tetrathiol **1** is particularly attractive as a template because its thiol functionalities are spaced about 7 Å apart, nearly ideal for a four-helix bundle [4]. Furthermore, its enforced hydrophobic cavity may act as a binding site for various substrates in future caviteins.

We designed the peptide sequence, **2** (Figure 1B), to be an amphiphilic α-helix such that the hydrophobic faces can self-assemble to form the core of a four-helix bundle. Incorporated into the design are intrastrand salt bridges and an amidated C-terminal glycine [5], both of which are known to stabilize α-helical structures.

Peptide **2** was synthesized by standard methods using Fmoc chemistry and an amidating resin [6]. The last step involved coupling of the free N-terminus with chloroacetyl chloride followed by cleavage from the resin with TFA. The crude peptide was then reacted with tetrathiol **1** with DIEA in DMA overnight at room temperature (Figure 1A). Purification of cavitein **3** was carried out with RP-HPLC to afford a white solid. The purified cavitein was characterized by electrospray mass spectrometry and CD. Preliminary CD spectra (Figure 2) for cavitein **3** show minima at 208 and 220 nm and a maximum at 195 nm which are typical for α-helices.

A.

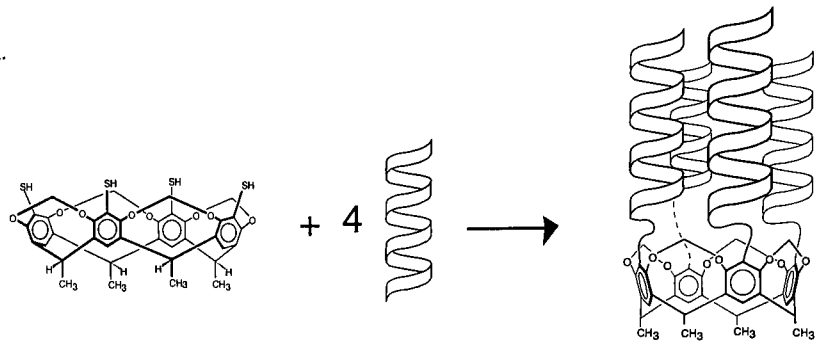

1 2 3

B. 2: Cl-CH_2-CO-Glu-Glu-Leu-Leu-Lys-Lys-Leu-Glu-Glu-Leu-Leu-Lys-Lys-Gly-NH_2

Figure 1. *A. Schematic representation of the synthesis of cavitein 3 where the linkage between tetrathiol 1 and the peptide is [-SCH_2CO-] B. Amino acid sequence of peptide 2.*

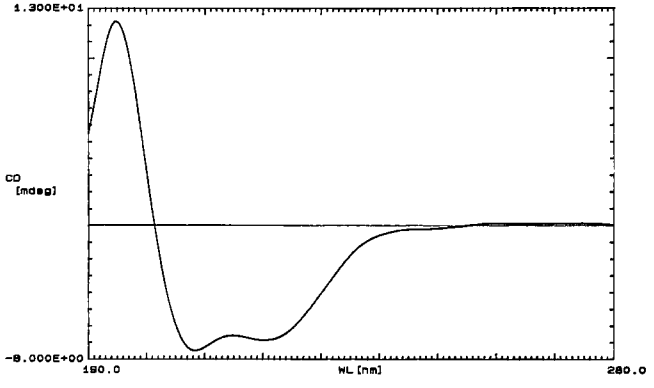

Figure 2. *CD spectrum of cavitein 3 at 25°C in 10 mM borate buffer at pH 7.5.*

In conclusion, we have designed and synthesized the first cavitein with significant α-helical structure. Studies on the stability of this cavitein and caviteins containing more flexible linkers are underway.

References

1. Mutter, M. and Vuilleumier, S., *Agnew. Chem., Int. Ed. Engl.*, 28 (1989) 535.
2. Moran, J.R., Karbach, S. and Cram, D.J., *J. Am. Chem. Soc.*, 104 (1982) 5826.
3. Gibb, B.C., Mezo, A.R., Causton, A.S., Fraser, J.R., Tsai, F.C.S. and Sherman, J.C., *Tetrahedron*, 51 (1995) 8719.
4. Reddy, B.V.B. and Blundell, T.L., *J. Mol. Biol.*, 233 (1993) 464.
5. Forood, B., Reddy, H.K. and Nambiar, K.P., *J. Am. Chem, Soc.*, 116 (1994) 6935.
6. Rink, H., *Tetrahedron Lett.*, 28 (1987) 3787.

Peptides: Chemistry, Structure and Biology
Pravin T.P. Kaumaya and Robert S. Hodges (Eds.)
Mayflower Scientific Ltd., 1996

243
β-Sheets: Template Assembly Using an Organic Macrocycle

A.S. Causton and J.C. Sherman

Department of Chemistry, University of British Columbia, Vancouver, British Columbia, V6T 1Z1, Canada

Introduction

Insight into some of the forces involved in protein folding can be gained through studying models of protein substructure. We are modeling β-sheet structure using "template assembled synthetic proteins" (TASP's) [1]. We call our family of TASP's "caviteins" [2], as they involve rigid organic macrocycles covalently linked to peptide strands. Through careful design, we hope to overcome the two major problems associated with modeling β-sheets: low water solubility and uncontrollable aggregation. Here we describe the design and synthesis of a cavitein that can form an eight-stranded antiparallel β-sheet.

Results and Discussion

We have recently reported the synthesis of a cavitein using a tetrathiol cavitand [2]. The β-sheet cavitein **1** was synthesized using the same method. This cavitein has interstrand distances that promote dimerization (*via* complementary interstrand hydrogen bonds) to form an eight stranded antiparallel β-sheet TASP **2** (Figure 1A). With each peptide strand hydrogen bonded to its two neighbors, a "closed surface" is formed. The peptide strands are designed to have both a hydrophobic and a hydrophilic face. The hydrophobic side chains will be directed into the core of this "closed surface" TASP, and the hydrophilic side chains will be exposed to the solvent, thus imparting water solubility.

The properties of cavitein **1** were compared to those of a single stranded "control" compound **3** (Figure 1B). Preliminary CD studies at pH 7.5 indicate that **1** shows β-sheet structure at 200μM, but is mostly random coil at low concentrations. Control **3** shows only random coil structure up to 1000μM. This result is consistent with template-promoted β-sheet structure. We are currently investigating the stability of cavitein **1** and confirming the proposed dimeric structure.

A.

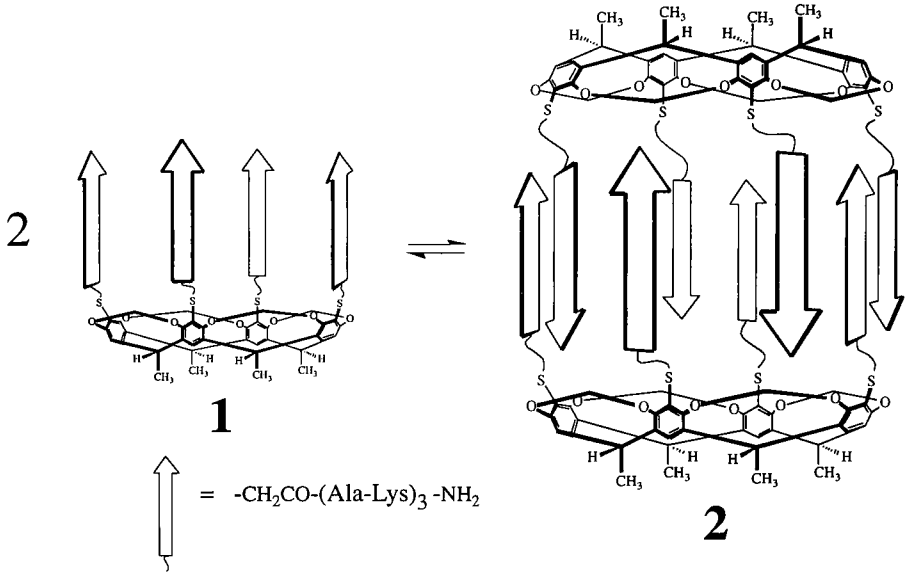

B.

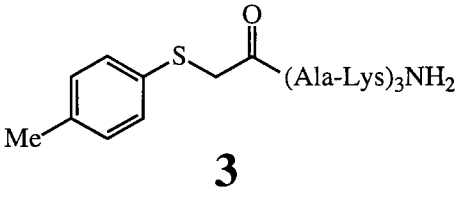

3

Figure 1. *A. Proposed dimerization of 1 to form an eight-stranded antiparallel β-sheet 2. B. "Control" compound for CD studies.*

Acknowledgments

We would like to thank the Natural Sciences and Engineering Research Council (NSERC) of Canada for financial support. A.S.C. thanks Park-Davis for a travel grant.

References

1. Mutter, M., Tuchscherer, G.G., Altmann, E., Altmann, K.H., Hersperger, R., Koziej, P., Nebel, K., Vuilleumier, S. and Gremlich, H.U., *Helv. Chim. Acta.*, 71 (1988) 835.
2. Gibb, B.C., Mezo, A.R., Causton, A.S., Fraser, J.R., Tsai, F.C.S. and Sherman, J.C., *Tetrahedron*, 51 (1995) 8719.

Peptides: Chemistry, Structure and Biology
Pravin T.P. Kaumaya and Robert S. Hodges (Eds.)
Mayflower Scientific Ltd., 1996

244
Structure/Function Studies of the "Flaps" Region of HIV-1 Protease by Total Chemical Synthesis

D.R. Englebretsen, D.A. Bergman, B.G. Garnham, R.I. Brinkworth, D.P. Fairlie and P.F. Alewood

Centre for Drug Design and Development, The University of Queensland, Brisbane 4072, Australia

Introduction

Hydrogen bonds contributed by the residues in the 'flaps' region ($I^{47}GGIGG^{52}$) of HIV-1 protease (HIV-1 PR) are crucially important for proteolytic activity. We envisaged that selected replacement of a Gly-Gly sequence by a thioether or thioester [1] isostere would allow some insight into enzyme-inhibitor recognition. We therefore synthesized, *via* chemoselective ligation, two pairs of HIV-1 PR analogues in which the $Gly^{48,49}$ or $Gly^{51,52}$ residues were replaced with thioester or thioether isosteres. α-Aminobutyric acid (Aba) was used as an isosteric replacement for Cys^{67} and Cys^{95}. Synthesis of thioether ligated HIV-1 PR is shown in Figure 1.

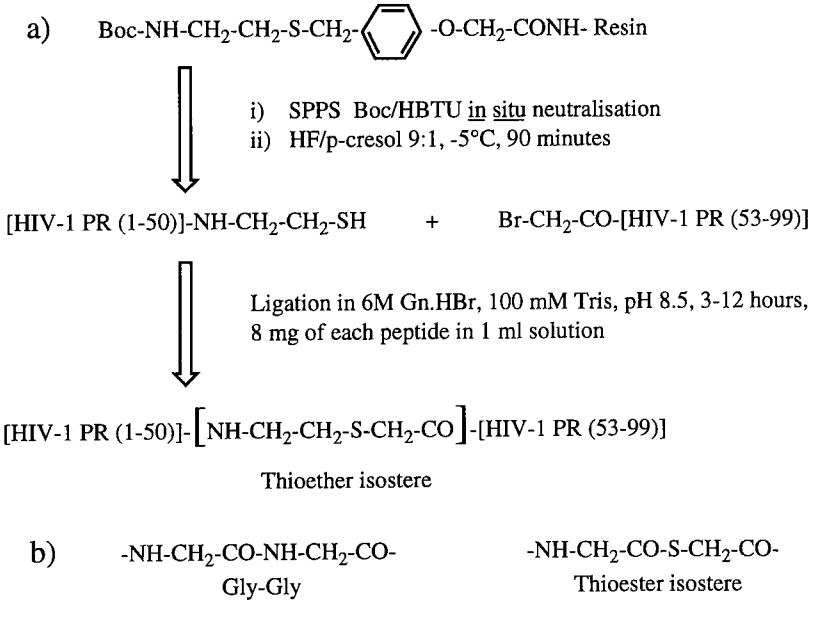

Figure 1. *a) Synthesis and ligation of HIV-1 PR with $Gly^{51,52}$ replaced by a thioether isostere; b) Gly-Gly and Thioester isostere structures for comparison with the Thioether isostere.*

Results and Discussion

HPLC purified chemoselectively ligated HIV-1 PR analogues gave mass spectra consistent with the expected structure. Tryptic digest of $[NHCH_2CH_2SCH_2CO]^{51\text{-}52}$ HIV-1 PR gave fragments of the expected masses as determined by LC-MS analysis. Using a modification of the method described in [2] (pH 6.5, I = 0.1M, 37°C), kinetic parameters and inhibition constants for the inhibitors JG365 [3] and DMP323 [4] were determined for the HIV-1 PR analogues (Table 1).

Table 1. *Kinetic parameters and inhibition constants of HIV-1 PR and analogues.*

HIV-1 protease	Km (μM)	k_{cat} (sec^{-1})	JG365 K_i (nM)	DMP323 K_i (nM)
Recombinant (HXB2 isolate)	45	10.6	4	1.6
$[NH\text{-}CH_2\text{-}CH_2\text{-}S\text{-}CH_2\text{-}CO]^{49\text{-}49}$	200	0.011	200,000	17
$[NH\text{-}CH_2\text{-}CH_2\text{-}S\text{-}CH_2\text{-}CO]^{51\text{-}52}$	80	1.2	1,900	9
$[NH\text{-}CH_2\text{-}CO\text{-}S\text{-}CH_2\text{-}CO]^{49\text{-}49}$	250	0.3	30,000	30
$[NH\text{-}CH_2\text{-}CO\text{-}S\text{-}CH_2\text{-}CO]^{51\text{-}52}$	8	4.6	40	0.8
1-99 Synthetic (SF2 isolate)	21	8	1.8	1.0

Comparison of both $Gly^{48,49}$ isosteric HIV-1 PR analogues with X-ray structures of apo (5) and inhibited (3) HIV-1 PR suggest that the decrease of activity of these analogues was due to changes in both H-bonding within the secondary structure of the flaps, and changes in H-bonding to inhibitor (and presumably substrate). The lower activity of the $Gly^{51,52}$ thioether analogue may be due to differences in stereochemistry within the structure of the flaps of this analogue. This study highlights the sensitivity of HIV-1 PR to subtle changes in the flaps region.

References

1. Schnolzer, M. and Kent, S.B.H., *Science*, 256 (1992) 221.
2. Toth, M.V. and Marshall, G.R., *Int. J. Peptide and Protein Res.*, 36 (1990) 544.
3. Swain, A.L., Miller, M.M., Green, J., Rich, D.H., Schneider, J., Kent, S.B.H. and Wlodawer, A., *Proc. Natl. Acad. USA*, 87 (1990) 8805.
4. Otto, M.J., Reid, C.D., Garber, S., Lam, P.Y.-S., Scarnati, H., Bacheler, L.T., Rayner, M.M. and Winslow, D.L., *Anitmicrob. Agents Chemother.*, 37 (1993) 2606.
5. Wlodawer, A., Miller, M., Jaskolski, M., Sathyanarayana, B.K., Baldwin, E., Weber, I.T., Selk, L.M., Clawson,L., Schneider, J. and Kent, S.B.H., *Science*, 245 (1989) 616.

Peptides: Chemistry, Structure and Biology
Pravin T.P. Kaumaya and Robert S. Hodges (Eds.)
Mayflower Scientific Ltd., 1996

245
The Design and Synthesis of a Metalloporphyrin-peptide Hybrid Artificial Protein

G.R. Geier III and T. Sasaki

Department of Chemistry, University of Washington, Seattle, WA 98195, USA

Introduction

The design and synthesis of artificial proteins have become an increasingly popular approach for studying protein folding, for understanding the behavior of native proteins, and for developing novel catalysts. In this study, we report the design and synthesis of an Fe(III)porphyrin-peptide hybrid artificial protein (Figure 1).

In many artificial proteins, a templating molecule is used to organize short peptide chains into secondary and tertiary structures. In our hybrid, the porphyrin ring acts as a template by crosslinking the peptide. The Fe(III)porphyrin plays a second role as a possible catalytic site. Metalloporphyrins are well known prosthetic groups in many oxygen binding proteins. In monooxygenases, such as the cytochrome P450 family, the porphyrin delivers a single oxygen atom to an alkane or alkene substrate.

Like the porphyrin, the peptide performs a pair of functions. First, it enhances the water solubility of the porphyrin. Second, it determines the environment directly surrounding the metal center of the porphyrin. By varying the amino acid sequence, one could produce a family of artificial proteins each with a unique binding site.

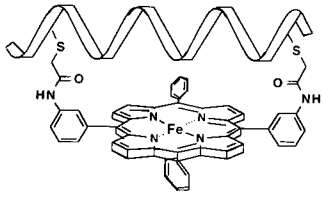

Figure 1. *Schematic drawing of the Fe(III)porphyrin-peptide hybrid artificial protein.*

Results and Discussion

The Fe(III)porphyrin-peptide hybrid was designed to approximate the active site of native cytochrome P450 [1, 2]. This required tethering an amphiphilic alpha helix in reasonable proximity to the porphyrin ring. The peptide sequence was selected to adopt an alpha helical structure [3, 4] with hydrophilic residues projecting away from the porphyrin ring to enhance the water solubility of the hybrid, and non-polar residues projecting toward the porphyrin ring to produce a hydrophobic binding site. Two cysteine residues at i and i+11 positions were included for coupling to the porphyrin.

The porphyrin ring selected provides two linking groups for coupling to the peptide, spaced the distance of three turns of an alpha helix. In addition, the linking arms position the peptide reasonably close to the porphyrin. The porphyrin fragment was synthesized *via* a phenyl-dipyrrylmethane intermediate [5-7]. The peptide chain (Ac-Ala-Cys-Glu-Gln-Leu-Leu-Lys-Glu-Leu-Leu-Gln-Lys-Cys-Ala-NH_2) was synthesized on an Applied Biosystems 430A peptide synthesizer. N-terminal Fmoc protection, DCC/HOBt coupling, and Rink resin were used. The hybrid was prepared from the porphyrin and peptide fragments [8], and metallated with Fe(II) acetate [9]. CD spectra of both the metal free and Fe(III) hybrids support our design. The hybrids are very helical with helicity independent of concentration ($2x10^{-5}$M to $2x10^{-6}$M) and percent TFE added. The independence of helicity with concentration suggests that the peptide is non-aggregating. The constant helicity with increasing TFE suggests high initial helicity. Solubility behavior of the hybrids is consistent with the amphiphilic nature of the peptide. The porphyrin alone is insoluble in aqueous media, but the hybrids are readily soluble in water with only a small amount of TFE added (10%-20%).

Comparison of the NMR spectra of the peptide fragment and metal free hybrid also is in agreement with the intended structure. Protons on residues predicted to be close to the porphyrin ring are shifted up field owing to the aromatic ring current. Finally, CD spectra recorded at low TFE show a large induced CD band in the Soret region (400-450 nm). Also, the λ_{max} of the Soret band in the UV/Vis spectrum shifts and broadens with decreasing TFE. This suggests the formation of a face to face dimer. At low TFE, the open hydrophobic face of the porphyrin appears to prefer aggregation with a second porphyrin over contact with water.

This study demonstrates an effective design and synthesis of a metalloporphyrin-peptide hybrid. Studies examining the catalytic behavior of the hybrid, and the production of related molecules with different amino acid sequences are forthcoming.

Acknowledgments

GRG has been supported by a research training grant in biotechnology from the NIH and by scholarships from the ARCS Foundation and the NCAA. GRG thanks the APS for the travel award.

References

1. Poulos, T.L., Finzel, B.C., Gunsalus, I.C., Wagner, G.C. and Kraut, J., *J. Biol. Chem.*, 260 (1985) 16122.
2. Ravichandran, K.G., Boddupalli, S.S., Hasemann, C.A., Peterson, J.A. and Deisenhofer, J., *Science*, 261 (1993) 731.
3. Chou, P.Y. and Fasman, G.D., *Biochemistry*, 2 (1974) 211.
4. Kaiser, E.T., *Protein Engineering*, (1987) 193.
5. Hammel, D., Erk, Schuler, B., Heinze, J. and Mullen, K., *Adv. Mater.*, 4 (1992) 737.
6. Lindsey, J.S., Schreiman, I.C., Hsu, H.C., Kearney, P.C. and Marguerettaz, A.M., *J. Org. Chem.*, 52 (1987) 827.
7. Sun, Y., Martell, A.E. and Tsutsui, M., *J. Heterocyclic Chem.*, 23 (1986) 561.
8. Dawson, P.E. and Kent, S.B.H., *J. Am. Chem. Soc.*, 115 (1993) 7263.
9. Sasaki, T. and Kaiser, E.T., *J. Am. Chem. Soc.*, 111 (1989) 380.

Peptides: Chemistry, Structure and Biology
Pravin T.P. Kaumaya and Robert S. Hodges (Eds.)
Mayflower Scientific Ltd., 1996

246
Synthesis of a Covalently Linked Spermine-Peptide Conjugate Displaying Enhanced Helicity

M.B. Kneller, J.K. Porter and T. Sasaki

Department of Chemistry, University of Washington, Seattle, WA 98195, USA

Introduction

Polyamines are ubiquitous biomolecules and play crucial roles in many cellular events [1], but the mechanisms by which they do what they do are largely unknown. The di- and polyamines putrescine, spermidine, and spermine have been found as mono- and di- γ-glutamyl derivatives in rat liver homogenates [1]. This finding suggests that these molecules may influence the structure and function of proteins and peptides as a result of covalent attachment *via* glutamyl side chains. It is also known that in a peptide α-helix, amino acid side chains at positions *i*, *i+4*, *i+7*, and *i+11* project from the same face of the helix. A helix may thus be stabilized if these side chains can be crosslinked, either covalently or noncovalently [3]. The distances between side chains in such an arrangement are approximately 5.5 Å, the per-turn translation distance of the α-helix.

The polyamine spermine contains four amino groups, protonated at physiological pH, that are separated by three, four ,and three carbons respectively. The distances between these positive charges are 4.6, 6.0, and 4.6 Å, and could conceivably form ion pairs with negatively charged side chains in the *i*, *i+4*, *i+7*, and *i+11* positions.

In fact, spermine associates non-covalently with a synthetic peptide, SBP (Ac-YEQA AEQQEAAQEA-$CONH_2$), increasing its α-helicity from 19 to 38% [4]. This peptide contains glutamates in the requisite positions for ionic interaction with spermine amino groups. In the present paper, we present evidence that another synthetic peptide, SBPII (Ac-YQAAAEAAEAA AEA-$CONH_2$), can be covalently modified with spermine at the glutamyl side chain using guinea pig liver transglutaminase (GPLT). The covalently bound spermine is then in a position to form ion pairs with glutamates in the *i+4*, *i+7*, and *i+11* positions of the helix. The effect on the helicity is even more dramatic than that caused by the non-covalent attachment.

Results and Discussion

SBPII was synthesized using standard Fmoc/DCC/HOBt chemistry. When spermine was added to SBPII, in the presence of GPLT, Ca^{+2}, and DTT in pH 8 buffer at 37°C, a new compound formed in near-quantitative yield over 24 hours [4]. This compound was identified as SBPII-spermine by electrospray-ionization mass spectrometry [(ESI-MS): 781.9 $(M+2H)^{2+}$; and AAA (found/expected): Tyr (1/1), 4 Glx (4/4) Ala (9/9).

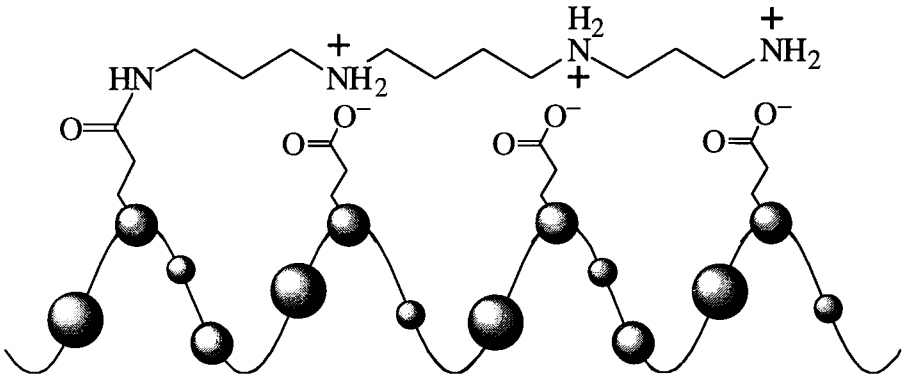

Figure 1. *Schematic of spermine attached to SBPII via Gln [2]. Proposed ionic interactions between positively charged amines of spermine and Glu[6], Glu[9], and Glu[13] are shown.*

SBPII-spermine is significantly more helical (60% helical) than SBPII (30% helical) (at pH 7, in the presence of 20% TFE) as determined by the molar ellipticity per residue at 222 nm. At pH 7, the side chains of the Glu residues are largely deprotonated, and the amino groups of spermine are largely protonated, leading to efficient ion pair formation. These interactions are decreased at other pH values, as either the Glu side chains become protonated and neutral, or the spermine amino groups become deprotonated and likewise neutral. In fact, SBPII-spermine shows similar helicity to SBPII at pH 5, 6, 8, and 9.

The helical stabilization gained by covalently attaching spermine to a peptide appears to be much greater than that gained by non-covalent spermine-peptide association. Work is currently underway to synthesize a peptide covalently cross-linked by spermine through the *i* and *i+11* positions.

References

1. Coffino, P. and Poznancki, A., *J. Cell. Biochem.*, 45 (1991) 54.
2. Beninati, S., Piacentini, M., Argento-Cerù, M.P., Russio-Caia, S. and Autuori, F., *Biochem. Biophys. Acta*, 841 (1983) 120.
3. Ruan, F., Chen, Y., Hopkins, P.B., *J. Amer Chem. Soc.*, 112 (1990) 9633.
4. Tabet, M., Labroo, V., Sheppard, P. and Sasaki, T., *J. Amer Chem. Soc.*, 115 (1993) 3866.
5. Persico, P., Calignano, A., Mancuso, F., Marino, G., Pucci, P., Esposito, C., Mariniello, L. and Porta, R., *Peptides*, 13 (1992) 151.

Peptides: Chemistry, Structure and Biology
Pravin T.P. Kaumaya and Robert S. Hodges (Eds.)
Mayflower Scientific Ltd., 1996

247
Homo-oligomeric and Hetero-oligomeric Multifunctional Peptide Analogs

D.L. Wiegandt Long, W. Ma and A.F. Spatola

Department of Chemistry, University of Louisville, Louisville, KY 40292, USA

Introduction

A common consequence of peptide hormone interactions is receptor aggregation. Little is known concerning the cause, mechanism, or function of this event. Dimeric and heterodimeric compounds have been shown to affect multiple biological properties [1] and even to convert a hormone antagonist into an agonist [2]. We have explored new synthetic routes designed to lead to homo-oligomeric and hetero-oligomeric peptide analog structures based on modifications of the Tam MAP (multiple antigenic peptide) [3] approach, and have characterized both linear and cyclic [4] ligands.

Oligomeric peptide analogs have intriguing prospects for probing the nature of biochemical molecular recognition. Here we report the synthesis and characterization of homo-oligomeric and hetero-oligomeric peptide analogs using two bioactive pharmacophores as shown in Figure 1.

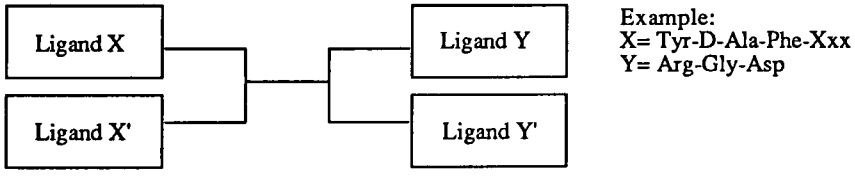

Figure 1. *Representative structures of homo-oligomeric (X=X'=Y=Y') and hetero-oligomeric (X=X' and Y=Y') or (X=Y and X'=Y') peptide analogs.*

Results and Discussion

The expected products (Table 1) were obtained based on amino acid analysis, mass spectrometry and, in some cases, proton NMR. All showed dramatic decreases from the predicted opioid activities. Most are based on deltorphin-like sequences, (Tyr-D-Ala-Phe-Xxx-), which are known to be highly potent and usually δ selective. Enkephalin dimers have been previously shown by several groups to furnish analogs with good potency [5]. It is likely that the MAP core hinders effective receptor binding. We are now modifying the core structure and we hope that utilizing appropriate spacer functions will overcome this apparent limitation. In the case of a dimeric peptide library (compound IV), this non-opioid derivative nevertheless shows modest (micromolar)

Table 1. *Properties of oligomeric peptide analogs.*

Compound	MS		IC_{50}	
	calc.	found	GPI	MVD
(Y-d-A-F-E)$_2$-K-Aca-A	1351.5	1351	1.9% at 10 μM	21.7% at 10 μM
(Y−a−F)$_2$−K−G−K−A (R−G−D)$_2$−K−G−	2007.3	2007.2	4561 ±1105	59.1% at 10 μM
Y−a−F α K−G−K−A−OH R−G−D ε Y−a−F α K−G− R−G−D ε	2007.3	2007.9	25.9% at 10 μM	3.2% at 10 μM
C-Gly-B-Gly-A-Gly Lys—Gly C'-Gly-B'-Gly-A'-Gly A, B, C and A', B', C' = Glu, Tyr, Arg	1320.5-1524.8	1320-1524	5545 ± 931 nM	2086 ± 946 nM

activity in both the mu and delta assays. The additional "spacer" elements (glycine introns) may help overcome the MAP deficiencies cited above. Efforts are underway to deconvolute this library (27 x 27 analogs) to identify the most potent analog(s).

We conclude that the preparation of these interesting peptide hybrids is synthetically feasible and can represent a useful starting point for new types of combinatorial sequences for drug discovery.

Acknowledgments

We gratefully acknowledge Dr. Frank Porreca and Peg Davis (University of Arizona Pharmacology Department) for the opioid bioassays. Mass spectral determinations were performed at the University of Michigan and Nebraska. This work was supported by NIH GM33376 and by a GAANN fellowship.

References

1. Cheronis, J.C., Whalley, E.T., Nguyen, K.T., Eubanks, S.R., Allen, L.G., Duggan, M.J., Loy, S.D., Bonham, K.A., Blodgett, J.K., *J. Med. Chem.*, 35 (1992) 1563.
2. Conn, P.M., Rogers, D.C., Stewart, J.M., Niedel, J., Sheffield, T., *Nature*, 296 (1982) 653.
3. Tam, J.P., *Proc. Natl. Acad. Sci. USA* , 85 (1988) 5409.
4. Picard, I.L., Wiegandt, D.L., Spatola, A.F., in Hodges, R.S. and Smith, J.A. (Eds.), 'Peptides: Chemistry, Structure and Biology', ESCOM, Leiden, The Netherlands, 1994, p.104.
5. Shimohigashi, Y, Ogasawara, T., Koshizaka, T., Waki, M., Kato,T., Izumiya, N., Kurono, M., Yagi, K., *Biochem. Biophys. Res. Commun.*, 146 (1987) 1109.

Peptides: Chemistry, Structure and Biology
Pravin T.P. Kaumaya and Robert S. Hodges (Eds.)
Mayflower Scientific Ltd., 1996

248
Analysis of Complex Synthetic Polypeptides: Confirming the Identity and Purity of Synthetic 'Mini-collagens'

C.G. Fields, B. Grab and G.B. Fields

Biomedical Engineering Center and Department of Laboratory Medicine and Pathology, University of Minnesota, Minneapolis, MN 55455, USA

Introduction

Collagens are composed of three α chains that intertwine to form a right-handed super-helix. To fully understand the subtleties of collagen structure, we developed a branching protocol for solid-phase synthesis that ensures proper alignment of three peptide strands in triple-helical conformation [1, 2]. The resulting triple-helical polypeptides (THPs), or "mini-collagens", are composed of 79-124 amino acids [1-3]. Following chemical synthesis of small proteins in the ~80-125 residue range, reversed-phase (RP) HPLC is typically the purification method of choice as well as one of the analytical techniques used to verify product purity. We have studied the chromatographic behavior of three homo- trimeric THPs (see below), one of 124 residues and two of 106 residues, with the goal of developing conditions that optimize THP resolution and separation of impurities.

THP-5: $[(GPP^{*})_{8}GVKGDKGNPGFPGAP(Aha)]_{3}(K,K)YG$
THP-6: $[(GPP^{*})_{6}GVKGDKGNPGWPGAP(Aha)]_{3}(K,K)YG$
THP-7: $[(GPP^{*})_{6}GPQGIAGQRGVVGLP^{*}(Aha)]_{3}(K,K)YG$

Results and Discussion

Seven different RP-HPLC columns were used in this study (Table 1). All three THPs were purified in two steps, first using preparative column 1 followed by semi-preparative column 2. Analytical RP-HPLC was initially used on a fraction of THP-5 eluting from column 1. This fraction, which contained the desired THP-5 by Edman degradation analysis, eluted as a very broad peak on large-pore columns 3 and 4. Substituting IPA for ACN, increasing column temperature to 60°C, or replacing TFA with either HFBA or sulfate/phosphate buffer, did not improve peak broadening. Switching to small-pore column 5 improved peak sharpness considerably. Sharpness was further improved on diphenyl column 6, but resolution was still poor. Finally, non-porous C_{18} column 7 produced a well-resolved chromatogram. Following the second step purification with column 2, columns 6 and 7 eluted THP-5 as the sharpest and most well-resolved peaks.

THP-6 was analyzed following two-step RP-HPLC purification. Sequencing showed that one purified fraction contained the desired THP-6. As was the case for THP-5, the sharpest peaks from this fraction were eluted by columns 6 and 7.

Following two-step purification, THP-7 RP-HPLC analysis was performed on fractions eluting at 31.0-32.0 min (fraction 1) and 36.5-39.0 min (fraction 2). These two fractions eluted from columns 6 and 7 as sharp, single peaks, having unique retention times. Sequence analysis indicated that fraction 1 was a deletion peptide while fraction 2 was the desired THP-7. The apparent purity and difference in retention time of the two fractions demonstrated the effectiveness of the two-step purification to isolate the desired synthetic product from our crude mixture.

Table 1. *RP-HPLC column descriptions.*

Column	Vendor	Support	Particle size (μm)	Pore size (Å)	Column size (mm)
1	Vydac	C_{18}	15-20	300	250 x 22
2	Vydac	diphenyl	5	300	250 x 10
3	Dynamax	C_{18}	12	300	250 x 4.6
4	Dynamax	C_4	5	300	250 x 4.6
5	Hypersil	C_{18}	5	120	200 x 2.1
6	Vydac	diphenyl	5	300	250 x 4.6
7	Tosohaas	C_{18}	2.5	non porous	35 x 4.6

We found that THPs can be best resolved from synthetic impurities by diphenyl or non-porous C_{18} RP-HPLC. The present and prior studies [1, 2] indicate that the homogeneities and compositions of THPs can be confirmed by a combination of Edman degradation sequence analysis, MS, AAA, HI-HPLC, SE-HPLC, and diphenyl and non-porous C_{18} RP-HPLC. While RP-HPLC is an indispensable tool for the purification of THPs, critical analysis of these biomolecules should be based on techniques that minimize or are not affected by triple-helical structural perturbations.

Acknowledgments

We gratefully acknowledge support of this work by the NIH (KD 44494 and AR 01929) and a McKnight-Land Grant Professorship.

References

1. Fields, C.G., Mickelson, D.J., Drake, S.L., McCarthy, J.B. and Fields, G.B., *J. Biol. Chem.*, 268 (1993) 14153.
2. Fields, C.G., Lovdahl, C.M., Miles, A.J., Matthias Hagen, V.L. and Fields, G.B., *Biopolymers*, 33 (1993) 1695.
3. Miles, A.J., Skubitz, A.P.N., Furcht, L.T. and Fields, G.B., *J. Biol. Chem.*, 269 (1994) 30939.

Peptides: Chemistry, Structure and Biology
Pravin T.P. Kaumaya and Robert S. Hodges (Eds.)
Mayflower Scientific Ltd., 1996

249
Evaluation of GrowMol: Synthesis and Inhibition Kinetics of Unsymmetrical Peptidyl Ureas

N.A. Dales[1], R.S. Bohacek[2] and D.H. Rich[1]

[1]*Department of Chemistry, University of Wisconsin-Madison, Madison, WI 53706, USA*
[2]*Pharmaceuticals Division CIBA Corporation, Summit, NJ 07901, USA*

Introduction

GrowMol [1] is a computational method for the *de novo* generation of novel structures complementary to the active site of a target enzyme. GrowMol is useful for discovering novel inhibitors of metalloproteases [1] and rediscovering known inhibitors [2]. The method has been successfully applied to the aspartic acid protease pepsin. Here, we discuss the discovery of a new class of pepsin inhibitors, unsymmetrical peptidyl ureas.

Results and Discussion

Application of GrowMol to the pepsin-Abbott renin inhibitor (A66702) [3] complex (inhibitor removed) created approximately 25,000 potential inhibitors. Many, highly diverse, unsymmetrical peptidyl ureas were generated. The majority of these potential inhibitors were comprised of two hydrophobic moieties connected by a urea linkage. The GrowMol-generated structure **1** was simplified to the unsymmetrical peptidyl urea **2**, to provide the initial synthetic target (Scheme 1). The procedure [4] for the preparation

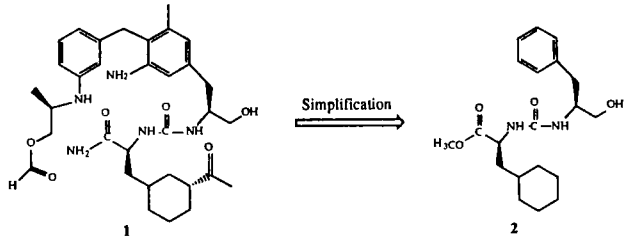

Scheme 1.

of unsymmetrical ureas is shown for the initial target **2** (Scheme 2). In the presence of diisopropylethylamine (DIEA), ß-cyclohexylalanine methyl ester **3** was added slowly to triphosgene solution at 0°C. A solution of phenylalaninol **4** and DIEA was then added, in one portion, at room temperature to afford the unsymmetrical peptidyl urea **2** (82%).

Pepsin inhibition assays were conducted under standard conditions [5]. Methyl ester **2** and the benzylphenyl analog **5** moderately inhibited pepsin, Ki = 68 ± 7 μM and Ki = 35 ± 10 μM, respectively (Table 1). Incorporation of a statine moiety (**6**) increased

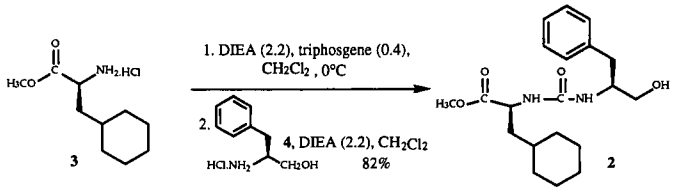

Scheme 2.

pepsin inhibition (Ki = 20 ± 2 μM). The terminal amide analog **7** did not inhibit pepsin at its solubility limit (100 μM) and the benzyl ether control **8** was inactive. The dipeptide control **9** was a moderate pepsin inhibitor, Ki = 83 ± 6 μM.

Table 1. *Inhibition constants for the simplified GrowMol target and several analogs.*

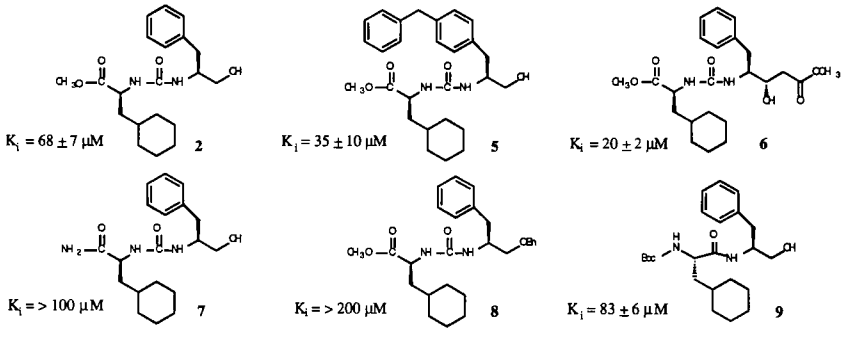

GrowMol was used to discover a new class of pepsin inhibitors, unsymmetrical peptidyl ureas. A series of unsymmetrical ureas was synthesized and shown to display moderate inhibition. This work demonstrates that GrowMol successfully predicts novel biologically active enzyme inhibitors.

Acknowledgments

Support from the NIH (GM50113) and the use of KineTic version 1.3 are appreciated. Special thanks are given to Dr. P. Kuzmic, Dr. G.R. Flenke, and J.J. Glinski.

References

1. Bohacek, R.S., McMartin, C., *J. Am. Chem. Soc.*, 116 (1994) 5560.
2. Ripka, A.S, Bohacek, R.S., Rich, D.H., this volume.
3. Chen, L., Erickson, J.W., Rydel, T.J., Park, C.H., Neidhart, D., Luly J., Abad-Zapatero, C., *Acta Cryst.*, B48 (1992) 476.
4. Majer, P., Randad, R.S., *J. Org. Chem.*, 59 (1994) 1937.
5. Dunn, B.M., Kammermann, B., McCurry, K.R., *Anal. Biochem.*, 138 (1984) 68.

Peptides: Chemistry, Structure and Biology
Pravin T.P. Kaumaya and Robert S. Hodges (Eds.)
Mayflower Scientific Ltd., 1996

250
Voltage-dependence of a Designed Ion Channel

G.A. Woolley, A.S.I. Jaikaran, Z. Zhang and S. Peng

Department of Chemistry, University of Toronto, Toronto M5S 1A1, Canada

Introduction

A key component in the design of artificial ion channels is the design of regulatory elements. As a first step in this direction, we have synthesized a derivative of the peptide ion channel, gramicidin, with an extension designed to act as a gate at the entrance (and exit) of the channel. A conformational change of the gate (*cis-trans* isomerization of a carbamate group) moves a charged amino group relative to the mouth of the channel and regulates cation flux. This process results in conductance steps in single-channel recordings of these derivatives [1]. Since modelling indicates that the charged amino group may actually enter the mouth of the channel, and may therefore experience some of the voltage-drop across the membrane, we were interested in testing for a voltage dependence of the conformational behaviour of these channels.

Results and Discussion

Figure 1 shows single channel recordings of gramicidin-1,3-propane diamine in glycerol-monooleate/hexadecane membranes. In this derivative, $OC(O)NH(CH_2)_3^+$ has replaced the C-terminal hydroxyl group of the parent molecule. The derivative was synthesized and purified as described previously [1]. The steps to and from the baseline correspond to dimerization and dissociation of gramicidin channels, respectively. The steps to different current levels which occur during the lifetime of the dimer are a result of cis-trans isomerization of the two carbmate linkages in the channel [1] (one linkage on each monomer). As the applied voltage increases, the two upper current levels and the two lower current levels merge. We have shown previously, using channels with only one end modified, that at 200mV it is isomerization of the carbamate group at the entrance of the channel which is responsible for the largest current steps [1]. Clearly, at lower voltages, the conformational state of the carbamate group at the channel exit can also have a significant effect on the observed current (Figure 1). For each voltage, we measured the total time spent in each state over a time period long enough so that each state was well-sampled. The fraction of time the channel had a cis-carbamate at the entrance was 14% of the total at 50 mV and increased to 25% at 300 mV. This finding indicates a clear linkage between applied voltage and conformation. The magnitude of the effect is modest, and we suggest that it might be due to a stabilizing effect of voltage on a subset of *cis*-state conformers which place the charged terminal amino group partially within the channel itself.

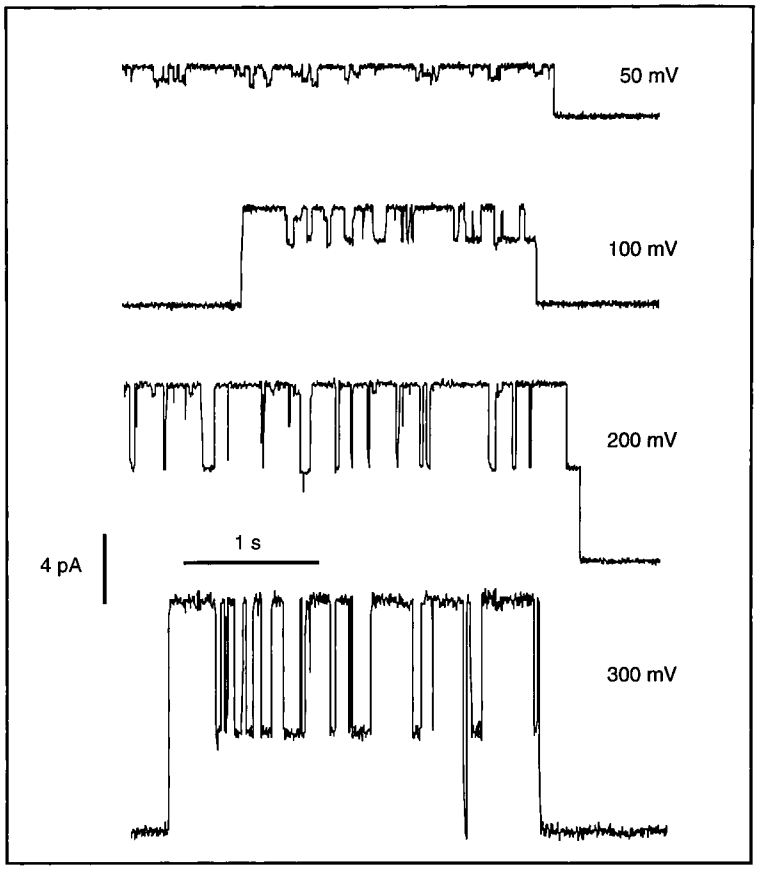

Figure 1. *Single-channel recordings of gramicidin-1,3-diaminopropane at different voltages.*

Acknowledgments

Financial support of NSERC and the CCFF is gratefully acknowledged.

References

1. Woolley, G.A., Jaikaran, A.S.I, Zhang, Z. and Peng, S., *J. Am. Chem. Soc.*, 117 (1995) 4448.

Peptides: Chemistry, Structure and Biology
Pravin T.P. Kaumaya and Robert S. Hodges (Eds.)
Mayflower Scientific Ltd., 1996

251
Structure-activity Studies of Collagen: Chemical Synthesis and Cellular Interaction of Collagen Type I Related Sequences

B. Grab, L.T. Furcht and G.B. Fields

Department of Laboratory Medicine and Pathology and The Biomedical Engineering Center, University of Minnesota, Minneapolis, MN 55455, USA

Introduction

Collagen type I serves as a structural protein and is an important recognition element in the interaction of cells with molecules of the extracellular matrix. Type I collagen is the most abundant of the collagens and has a heterotrimeric structure consisting of two α1(I) chains and one α2(I) chain. Several regions of the α1(I) chain have been identified as binding sites for cell receptors. One of these sites, the sequence α1(I) 757-791 within the cyanogen bromide fragment 7 [α1(I)CB7], inhibits the fibronectin-mediated adhesion of Chinese hamster ovarian cells to type I collagen [1]. Applying solid-phase methodology developed to synthesize branched triple-helical collagen-model peptides (THPs) allows the study of the significance of the triple-helical conformation in biological processes [2].

Results and Discussion

A collagen-model polypeptide incorporating residues 772-786 from the collagen α1(I)-chain (Gly-Pro-Gln-Gly-Ile-Ala-Gly-Gln-Arg-Gly-Val-Val-Gly-Leu-Hyp) with a triple-helical conformation was synthesized. The α1(I)772-786 THP was purified on a preparative C_{18}-reversed-phase HPLC and a second purification was performed on a semi-preparative reversed-phase diphenyl column [3]. The molecule was characterized by Edman degradation sequence analysis, analytical HPLC and LD-MS. Edman degradation sequence analysis indicated that the crude THPs contained at least 50% of the desired product. From the purification, a small fraction of a peptide was isolated which by Edman degradation was characterized to contain the deletion sequence 772-783, missing the first three amino acids close to the branch. In conformation analysis by CD, the α1(I)772-786 THP exhibited typical features of a collagen-like conformation such as a large negative mean residue ellipticity $[\Theta]_m$ at 200 nm and a positive $[\Theta]_m$ at 225 nm. On recording the ellipticity as a function of temperature, α1(I)772-786 THP exhibits a temperature dependent melt with a melting temperature of *ca.* 43°C.

Cellular responses were studied by adhesion of normal human dermal fibroblasts (NHDF) to the triple-helical peptides α1(I)772-786 THP, α1(I)772-783 THP, the linear

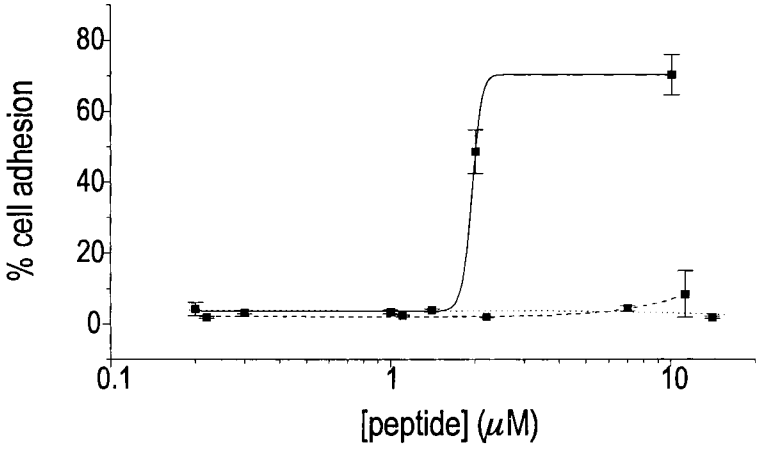

Figure 1. *Adhesion of fibroblasts as a function of α1(I)772-786 THP (solid line), α1(I)772-783 THP (dashed line), or α1(I)772-786 SSP (dotted line) concentration.*

single stranded peptide α1(I)772-786 SSP and the triple-helical peptide GPP* containing only the structural motif through 8 repeats of Gly-Pro-Hyp.

No adhesion could be observed for the linear peptide at a concentration below 70 μM. The NHDF showed a profound preference for adhesion to the triple-helical peptide α1(I)772-786 THP with a 50% cell adhesion at 2 μM peptide concentration. Fibroblasts showed a considerably lower adhesion activity towards the shorter α1(I)772-783 THP. No adhesion activity could be seen with the generic triple-helical peptide GPP*. These results demonstrate the importance of amino acid residues 784-786 in cellular recognition and the significance of the triple-helical conformation for cell adhesion to this specific collagen recognition site.

Acknowledgments

This work was supported by NIH grant AR 01929 and also a McKnight-Land Grant Professorship. B.G. was supported by an APS Travel Grant Award.

References

1. Kleinman, H.K., McGoodwin, E.B., Martin, G.R., Klebe, R.J., Fietzek, P.P., Woolley, D.E., *J. Biol. Chem.*, 253 (1978) 5642.
2. Fields, C.G., Lovdahl, C.M., Miles, A.J., Matthias Hagen, V.L. and Fields G.B., *Biopolymers*, 33 (1993) 1695.
3. Fields, C.G., Grab, B. and Fields, G.B., this volume.

Peptides: Chemistry, Structure and Biology
Pravin T.P. Kaumaya and Robert S. Hodges (Eds.)
Mayflower Scientific Ltd., 1996

252
Conformational Studies of RAFT Molecules for Protein Design

P. Dumy[1], I.M. Eggleston[1], G. Esposito[2], S. Nicula[1] and M. Mutter[1]

[1]Institute of Organic Chemistry, University of Lausanne, BCH Dorigny, CH 1015 Lausanne, Switzerland
[2]Dipartimento di Scienze e Tecnologie Biomediche, Università di Udine, 33100 Udine, Italy

Introduction

Regioselectively addressable functionalized templates (RAFT) [1] are valuable topological scaffolds for use in protein *de novo* design according to the TASP concept (Template Assembled Synthetic Proteins) [2]. In this context, we have performed the first detailed conformational investigation of such molecules using a combination of NMR, restrained molecular dynamics, and CD spectroscopy.

Results and Discussion

RAFT molecules are typically orthogonally protected lysine-containing cyclic decapeptides. In this study, three prototype RAFT were examined which contain up to four selectively addressable sites (**1**, **2**) or have selectively addressable faces (**3**). They may be represented by the general formula:

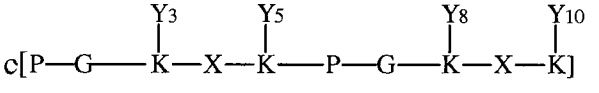

1-3

(For X = A; **1** has Y^8 = Dde[3], Y^{10} = Boc, Y^3 = Aloc, Y^5 = Fmoc; **2** has Y^8, Y^3 = Aloc, Y^5, Y^{10} = Boc. For X = K; **3** has Y^3, Y^5, Y^8, Y^{10} = Boc, Y^4 = Y^9 = Aloc)

Templates of this type with only one kind of protecting group cannot be studied readily by NMR, owing to the inherent residue redundancy and consequent loss of information. In **1-3** however, the removal of symmetry by differential protection permitted a full characterization by 600MHz COSY, TOCSY, and NOESY experiments. The progressive change in the symmetry of these systems was particularly evident on comparison of the NOESY spectrum of **1** with those of **2** and **3**, where in the former case, all four lysine spin systems could be identified. NOE experiments also demonstrated that all the peptide bonds in the templates are trans; in the case of proline this was shown by an NOE between H^{α}-$Lys^{5/10}$ and H^{δ}-$Pro^{6/1}$.

Based on additional data from amide thermal coefficient analysis and selective (soft-COSY) experiments, a type II β-turn was predicted about the Pro-Gly units. This was supported by CD spectra in several different solvents, which for all three RAFT resemble the so-called Class B spectrum [4], indicative of such turns (Figure 1.)

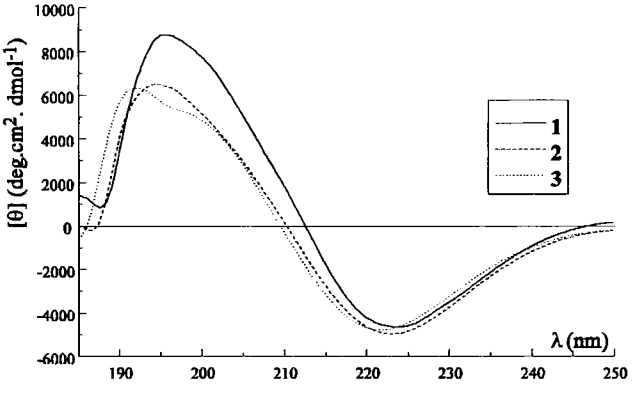

Figure 1. *CD spectra of* ***1-3*** *in H_2O-MeOH (50/50, v/v); concentration 0.5mg/ml.*

For restrained molecular dynamics simulations of **1**, the starting structure deduced from the NMR results was based on two type II β-turns, linked by two tripeptide motifs in an extended conformation with all lysines on one face of the template. In the course of 100ps simulations at 600K and 900K, no significant violations of the NMR-derived constraints were observed, and no structures in which lysines were oriented on both faces of the template were generated. The averaged (Φ, Ψ) values obtained for the $Pro^{1/6}$ and $Gly^{2/7}$ residues were still close to those expected for a slightly distorted type II β-turn [5].

In summary, we have demonstrated that RAFT **1-3** have stable well-defined conformations. This knowledge should prove very useful in applications of RAFT that use their ability to present functional groups in fixed spatial orientations.

Acknowledgments

This work was supported by the Swiss National Science Foundation. I.M.E. thanks the American Peptide Society for a Travel Award.

References

1. Dumy, P., Eggleston, I.M., Cervigni, S., Sila, U., Sun, X. and Mutter, M., *Tetrahedron Lett.*, 36 (1995) 1255.
2. Mutter, M. and Vuilleumier, S., *Angew. Chem. Int. Ed. Engl.*, 28 (1989) 535.
3. Bycroft, B.W., Chan, W.C., Chhabra, S.R., Hone, N.D., *J. Chem. Soc. Chem. Commun.*, (1993) 778.
4. Woody, R.W., in Hruby, V.J. (Ed.), 'The Peptides Vol. 7: Conformation in Biology and Drug Design', Academic Press Inc., New York, USA, 1985, p.15.
5. Dumy, P., Eggleston, I.M., Esposito, G., Nicula, S. and Mutter, M., *Biopolymers*, in press.

Session XII
Peptide Hormones/Neuropeptides

Chairs: Arthur M. Felix and
Cecilia Unson

Peptides: Chemistry, Structure and Biology
Pravin T.P. Kaumaya and Robert S. Hodges (Eds.)
Mayflower Scientific Ltd., 1996

253
Structure-agonist/antagonist Activity Relationships of TIPP Analogs

P.W. Schiller[1], G. Weltrowska[1], T.M.-D. Nguyen[1], C. Lemieux[1], N.N. Chung[1], B. Zelent[2], B.C. Wilkes[1] and K.A. Carpenter[1]

[1]Laboratory of Chemical Biology and Peptide Research, Clinical Research Institute of Montreal, 110 Pine Avenue West, Montreal, Quebec, H2W 1R7, Canada
[2]Department of Biochemistry and Biophysics, University of Pennsylvania, Philadelphia, PA 19104, USA

Introduction

Recently, we reported the discovery of a new class of opioid peptide-derived δ antagonists that contain a tetrahydroisoquinoline-3-carboxylic acid (Tic) residue in the 2-position of the peptide sequence [1]. The two prototype antagonists were the tetrapeptide H-Tyr-Tic-Phe-Phe-OH (TIPP) and the tripeptide H-Tyr-Tic-Phe-OH (TIP). The pseudopeptide analog H-Tyr-TicΨ[CH_2-NH]Phe-Phe-OH (TIPP[Ψ]) showed high δ antagonist potency, extraordinary δ selectivity and stability against enzymatic degradation [2]. Subsequently, the Ala^3-analog of TIP was shown to retain moderate δ antagonist potency [3]. Surprisingly, iodination at the 3'-position of the Tyr^1 phenol ring converted the antagonist into an agonist in the case of TIPP, but not in the case of TIP and TIPP[Ψ] [4]. Here we describe TIPP analogs containing an aliphatic amino acid residue in the 3-position of the peptide sequence that are highly potent and selective δ antagonists. We present the opioid activity profiles of Trp^3-analogs of TIP(P) and an analysis of their tryptophan fluorescence decay in dilute aqueous solution, in an effort to examine the possibility of differences in aromatic ring clustering.

Results and Discussion

Replacement of Phe^3 in TIPP with Leu, Ile or norvaline (Nva) resulted in compounds that retained potent δ antagonist activity in the mouse vas deferens (MVD) assay and showed high δ selectivity in the opioid receptor binding assays (Table 1). Obviously, an aromatic residue in the 3-position of the peptide sequence is not absolutely required for high δ antagonist potency. Most interestingly, saturation of the Phe^3 aromatic ring in TIPP, as achieved through substitution of cyclohexylalanine (Cha), led to a compound (H-Tyr-Tic-Cha-Phe-OH [TICP]) with substantially increased δ antagonist potency and higher δ selectivity than the parent peptide. The corresponding pseudopeptide H-Tyr-TicΨ[CH_2-NH]Cha-Phe-OH (TICP[Ψ]) showed a further improvement in δ antagonist activity.

Table 1. *In vitro opioid activities of TIPP analogs.*

Compound	MVD assay	Opioid receptor binding[b]		
	K_e [nM][a]	K_i^{μ} [nM]	K_i^{δ} [nM]	K_i^{μ}/K_i^{δ}
H-Tyr-Tic-Phe-Phe-OH	4.80	1720	1.22	1410
H-Tyr-TicΨ[CH_2-NH]Phe-Phe-OH	2.89	3230	0.308	10500
H-Tyr-Tic-Leu-Phe-OH	8.59	904	2.84	318
H-Tyr-Tic-Ile-Phe-OH	13.1	6460	4.37	1480
H-Tyr-Tic-Nva-Phe-OH	8.17	6900	2.62	2630
H-Tyr-Tic-Cha-Phe-OH	0.438	3600	0.611	5890
H-Tyr-TicΨ[CH_2-NH]Cha-Phe-OH	0.219	1050	0.259	4050
H-Tyr(3'-I)-Tic-Cha-Phe-OH	12.7	4010	3.33	1200
H-Tyr-Tic-Trp-Phe-OH	2.56	1790	0.301	5950
H-Tyr-Tic-Trp-OH	6.23	5000	7.55	662
H-Tyr(3'-I)-Tic-Trp-Phe-OH	19.8 (IC40)[c]	1630	2.20	741

[a]Determined against DPDPE. [b]Displacement of [^{3}H]DAMGO (μ-selective) and [^{3}H]DSLET (δ-selective) from rat brain membrane binding sites. [c]Partial agonist (maximal inhibition of electrically evoked contractions = 80%).

In comparison with H-Dmt-Tic-Phe-Phe-OH (Dmt = 2',6'-dimethyltyrosine) [4], TICP[Ψ] shows the same extraordinarily high δ antagonist potency but is seven times more δ-selective. It is a 13 times more potent δ antagonist than TIPP[Ψ] and, due to the presence of the reduced peptide bond, can be expected to be equally stable against enzymatic degradation [2]. Thus, TICP[Ψ] represents a superior new δ antagonist. Interestingly, the analog H-Tyr(3'-I)-Tic-Cha-Phe-OH was an antagonist in the MVD assay with a potency about 30 times lower than that of TICP. Thus, unlike in the case of TIPP, introduction of an iodine substituent at the 3'-position of Tyr^1 in TICP did not produce a δ agonist. This result demonstrates again how a relatively subtle structural modification, such as the saturation of an aromatic ring, can have a determinant effect on agonist *versus* antagonist behavior.

TIP(P) peptides are very hydrophobic and structurally flexible molecules that may undergo a so-called "hydrophobic collapse" [5] in an aqueous environment. It is possible that subtle structural modifications, such as introduction of an iodine substituent at the 3'-position of Tyr^1 or saturation of the Phe^3 aromatic ring may produce different patterns of aromatic ring clustering that may result in either δ agonist or δ antagonist activity, as described above. To examine this possibility, we prepared and characterized Trp^3-analogs of TIP(P) peptides. H-Tyr-Tic-Trp-Phe-OH (TITP) and H-Tyr-Tic-Trp-OH (TIT) were found to be very selective δ antagonists with activity profiles similar to those of their respective parent peptides (TIPP and TIP) (Table 1). On the other hand, H-Tyr(3'-I)-Tic-Trp-Phe-OH showed a nearly full δ agonist effect in the MVD assay, in parallel to the δ agonist behavior observed with its iodinated parent H-Tyr(3'-I)-Tic-Phe-Phe-OH [4]. Tryptophan fluorescence decay measurements were performed in aqueous buffer (pH 7.5, 20°C) at low concentration (5×10^{-5} M). Analysis of the fluorescence decay of N-acetyltryptophanamide resulted in a single fluorescence lifetime (τ = 3.04 ns) which reflects the aqueous environment of this reference compound (Table 2). In the

Table 2. *Tryptophan fluorescence decay analysis of TIPP-related peptides.*

Compound	τ_i [ns]	α_i
H-Tyr-Tic-Trp-Phe-OH	2.645	0.415
	1.463	0.536
	0.323	0.049
H-Tyr-Tic-Trp -OH	2.610	0.484
	1.340	0.470
	0.317	0.046
H-Tyr(3'-I)-Tic-Trp-Phe-OH	5.087	0.231
	1.590	0.680
	0.253	0.089
N-acetyltryptophanamide	3.040	1.0

case of the peptides a three-component analysis produced the best fit with the fluorescence decay curves. The longest fluorescence lifetime determined for TITP and TIT was about 2.6 ns, indicating that the indole moiety in these peptides is exposed to the aqueous environment. On the other hand, the iodinated Trp^3-analog showed a longest-lived component of 5.1 ns with an amplitude factor (α) of 0.23, suggesting that in a significant proportion of conformers the Trp side chain is somewhat shielded from the solvent and located in a more hydrophobic environment provided by the other aromatic rings present in the molecule. It thus appears that iodination at the 3'-position of Tyr produced a change in the pattern of aromatic ring clustering which may be related to the observed conversion of an antagonist into an agonist.

Acknowledgments

Supported by grants from the MRCC (UI-12356) and NIDA (DA-04443).

References

1. Schiller, P.W., Nguyen, T.M.-D., Weltrowska, G., Wilkes, B.C., Marsden, B.J., Lemieux, C. and Chung, N.N., *Proc. Natl. Acad. Sci. USA,* 89 (1992) 11871.
2. Schiller, P.W., Weltrowska, G., Wilkes, B.C., Chung, N.N. and Lemieux, C., *J. Med. Chem.*, 36 (1993) 3182.
3. Temussi, P.A., Salvadori, S., Amodeo, P., Bianchi, C., Guerrini, R., Tomatis, R., Lazarus, L.H., Picone, D. and Tancredi, T., *Biochem. Biophys. Res. Commun.*, 198 (1994) 933.
4. Schiller, P.W., Nguyen, T.M.-D., Weltrowska, G., Wilkes, B.C., Marsden, B.J., Schmidt, R., Lemieux, C. and Chung, N.N., in Hodges, R.S. and Smith, J.A. (Eds.), 'Peptides: Chemistry, Structure and Biology', ESCOM, Leiden, The Netherlands, 1994, p. 483.
5. Wiley, R.A. and Rich, D.H., *Med. Res. Rev.*, 13 (1993) 327.

Peptides: Chemistry, Structure and Biology
Pravin T.P. Kaumaya and Robert S. Hodges (Eds.)
Mayflower Scientific Ltd., 1996

254

Design of (a) *in vivo* Antagonists of Oxytocin More Potent and More Selective than Atosiban and of (b) Novel Radioiodinatable Ligands for the Human Oxytocin Receptor

M. Manning[1], S. Pancheva[1], K. Miteva[1], S. Stoev[1], L.-L. Cheng[1], C. Barberis[2], N.C. Wo[3] and W.Y. Chan[3]

[1]Department of Biochemistry and Molecular Biology, Medical College of Ohio, Toledo, OH 43699, USA
[2]Inserm U. 401, CCIPE, Montpellier, France
[3]Department of Pharmacology, Cornell University Medical College, New York, NY 10021, USA

Introduction

Oxytocin (OT) antagonists are of potential therapeutic value for the prevention of pre-term labor and as pharmacological tools for studies on the physiological actions of OT [1]. A radioiodinated OT antagonist from these laboratories [^{125}I] d(CH_2)$_5$[Tyr(Me)^2, Thr^4,Tyr-NH_2^9]OVT [2] has found widespread use for studies on OT receptor localization and characterization [1-3]. Here we present a series of OT antagonists based on modifications of our lead OT antagonist desGly-NH_2, d(CH_2)$_5$[Tyr(Me)^2,Thr^4]OVT (A) [4] modified at position two (Table 1) [5], which are more potent and more selective than Atosiban (d[D-Tyr(Et)^2,Thr^4]OVT [6], the sole OT antagonist currently in clinical trial for the prevention of premature labor [7]. We also present a new series of radioiodinatable OT antagonists (Table 2). These were designed by incorporating a variety of iodinatable substituents at the C-terminal of A *via* an Eda (ethylene diamine) linker.

Results and Discussion

Replacement of the Tyr(Me)^2 residue in A [4] Table 1 by D-Tyr(Me)^2, Tyr^2, D-Tyr^2, D-Phe^2 and D-Trp^2 led to the series of OT antagonists 1-5 (Table 1) [5] which, with the exception of No. 2, are all more potent than Atosiban [5, 6]. More significantly, four of these new peptides (Nos. 2-5) exhibit substantial reductions in anti-V_{1a} potencies relative to Atosiban. Thus all are as potent or more potent than Atosiban and all are more selective than Atosiban. They are thus promising candidates for development as potential tocolytic agents for the prevention of pre-term labor. The four new retromodified radioiodinated OT antagonists (Nos. 2 to 5, Table 2) possess very similar pharmacological properties to those of No. 1, Table 2 [2]. These retromodified OT

Table 1. *Oxytocin antagonists based on desGly-NH_2,d$(CH_2)_5$[X^2,Thr^4]OVT which are more potent and more selective in vivo than Atosiban.*

No.	X^2	Anti-OT ED[a]	Anti-V_{1a} ED[a]	ED Ratio[f]	Potency *vs* Atosiban[g]	Selectivity *vs* Atosiban[h]
	Atosiban[b,c]	5.95	48.5	8	1	1
A	Tyr(Me)[4] (A)[d]	1.3	23	17	5	2
1	D-Tyr(Me)[e]	1.09	38	35	5.5	4.4
2	Tyr[e]	5.87	420	72	1	9
3	D-Tyr[e]	2.85	272	95	2.1	12
4	D-Phe[e]	3.86	338	88	1.5	11
5	D-Trp[e]	3.08	248	80	1.9	10

[a]The effective dose (ED) is defined as the dose *in vivo* (in nanomoles/kilogram) of antagonist that reduces the response to 2 x units of agonist to the response with x units of agonist administered in the absence of antagonist; [b]Atosiban is d[D-Tyr(Et)^2,Thr^4]OVT [6]. Originally reported in ref. 6 as a V_{1a} agonist; [c]Data from a repeat synthesis reported in ref. 5; [d]Data from ref. 4; [e]This publication and ref. 5. [f]ED Ratio = anti-V_{1a} ED/anti-OT ED. [g]Anti-OT potencies relative to the ED of Atosiban. [h]ED Ratios relative to ED Ratio of Atosiban.

Table 2. *Retromodified radioiodinatable OT antagonists.*

No.	Peptide	Anti-OT pA_2[a,c]	K_i, nM[d]	Anti-V_{1a} pA_2[b,c]	Anti-V_2 pA_2[b,c]
1	d$(CH_2)_5$[Tyr(Me)^2,Thr^4,Tyr-NH_2^{9}]OVT[e]	7.83 ± 0.04	0.17	7.02 ± 0.07	~ 5.2
2	d$(CH_2)_5$[Tyr(Me)^2,Thr^4,Eda^9← Tyr^{10}]OVT[f]	7.50 ± 0.04	2.40	7.07 ± 0.09	~ 6.0
3	d$(CH_2)_5$[Tyr(Me)^2,Thr^4,Eda^9← D-Tyr^{10}]OVT[f]	7.66 ± 0.06	1.50	6.96 ± 0.04	~ 5.8
4	d$(CH_2)_5$[Tyr(Me)^2,Thr^4,Eda^9← HO-Phaa^{10}]OVT[f]	7.55 ± 0.03	0.27	6.98 ± 0.06	~ 5.5
5	d$(CH_2)_5$[Tyr(Me)^2,Thr^4,Eda^9← HO-Phpa^{10}]OVT[f]	7.53 ± 0.03	0.47	6.86 ± 0.03	~ 5.5
Scatchard analysis using radioiodinated antagonists:			K_d, nM[g]		
6	[^{125}I]-d$(CH_2)_5$[Tyr(Me)^2,Thr^4, Tyr-NH_2^{9}]OVT[f,h]		0.095		
7	[^{125}I]-d$(CH_2)_5$[Tyr(Me)^2,Thr^4, Eda^9 ←HO-Phaa^{10}]OVT[f]		0.076		

[a]*In vitro* pA_2 values represent the negative logarithm to the base 10 of the average molar concentration of antagonist which reduces the response to 2 x units of agonist to the response with x units of agonist; [b]Estimated *in vivo* pA_2 values represent the negative logarithms of the "effective dose" (see footnote a Table 1) divided by the estimated volume of distribution (67 ml/kg); [c]Anti-OT, anti-V_{1a} and anti-V_2 pA_2 values have been estimated for the rat receptors; [d]K_i values have been estimated for the human OT receptor except for analogue 1, where it was the rat OT receptor; [e]Original synthesis and pharmacological data reported in ref. 2; [f]This publication; [g]K_d values have been estimated for the human OT receptor; [h]Data from ref. 3.

antagonists exhibit high affinities for the human OT receptor. They can be radioiodinated in good yield. The [^{125}I] OT antagonist (No. 7) is an excellent radioligand. It has a very good affinity and a low non-specific binding. At 80 pM, a concentration not far from the K_d value, the non specific binding is only 7.5% of the total binding. Another attractive property of these molecules should be their resistance to proteolytic degradation. This could make these antagonists suitable for *in vivo* studies (*e.g.* intracerebroventricular administration for behavioral studies or intravenous administration for other functional studies). These retromodified OT antagonists could also be promising new candidates for use in the treatment of pre-term labor.

We have presented in Tables 1 and 2 a series of new OT antagonists which are more potent *in vivo* than Atosiban [5, 6]. Those in Table 1 are also much more selective with respect to V_{1a} receptor antagonism than Atosiban. The new potent and selective *in vivo* OT antagonists in Table 1 appear to offer advantages over Atosiban for development as tocolytics for the prevention of pre-term labor. We have also presented in Table 2 a series of new retromodified radioiodinatable OT antagonists which have high affinity for the human OT receptor. The [^{125}I] derivative (No.7) is a potentially useful new tool for studies on OT receptor localization and characterization.

Acknowledgments

We thank Ms. Ann Chlebowski for her expert help in the preparation of this manuscript and NIH grant GM-25280.

References

1. Manning, M., Cheng, L.-L., Klis, W.A., Stoev, S., Przybylski, J., Bankowski, K., Sawyer, W.H., Barberis, C. and Chan, W.Y., in Ivell, R. and Russel, J. (Eds.), 'Oxytocin - Cellular and Molecular Approaches in Medicine and Research', Plenum Press, NY, in press.
2. Elands, J., Barberis, C., Jards, S., Tribollet, E., Dreifuss, J.J., Bankowski, K., Manning, M. and Sawyer, W.H., *Eur. J. Pharmacol.*, 147 (1988) 197.
3. Chini, B., Mouillac, B., Ala, Y., Balestre, M.-N., Trumpp-Kallmeyer, S., Hoflack, J., Elands, J., Hibert, M., Manning, M., Jard, S. and Barberis, C., *EMBO Journal*, in press.
4. Manning, M., Kruszynski, M., Bankowski, K., Olma, A., Lammek, B., Cheng, L.-L., Klis, W.A., Seto, J., Haldar, J. and Sawyer, W.H., *J. Med. Chem.*, 32 (1989) 382.
5. Manning, M., Miteva, K., Pancheva, S., Stoev, S., Wo, N.C. and Chan, W.Y., *Int. J. Peptide and Prot. Res.*, in press.
6. Melin, P., Trojnar, J., Johansson, B., Vilhardt, H. and Akerlund, M., *J. Endocrinol.*, 111 (1986) 125.
7. Goodwin, T.M., Paul, R., Silver, H., Spellacy, W., Parsons, M., Chez, R., Hayashi, R., Valenzuela, G., Creasy, G.W. and Merriman, R., *Amer. J. Obstet. & Gynecol.*, 170 (1994) 475.

Peptides: Chemistry, Structure and Biology
Pravin T.P. Kaumaya and Robert S. Hodges (Eds.)
Mayflower Scientific Ltd., 1996

255
Vasopressin and Oxytocin Receptors: From Pharmacology to Molecular Biology

C. Barberis, B. Mouillac, E. Mahé, Y. Ala, M.N. Balestre, T. Durroux, R. Seyer, B. Chini and S. Jard

INSERM U 401, CCIPE, rue de la Cardonille, 34094 Montpellier Cedex 5, France

Introduction

The nonapeptide [Arg^8] vasopressin (AVP) and oxytocin (OT) are two closely related members of a hormone family that differ by only two amino-acids. They apparently derive from the same ancestral gene and both are secreted from the posterior pituitary of male and female mammals. These hormones exert their biological effects on a large variety of cell types, including nerve cells, by receptors which are members of the opsin superfamily and which have the typical architecture of seven transmembrane domains. Within this superfamily, the four known AVP and OT receptors constitute a subclass.

Results and Discussion

Mammals have three types of vasopressin receptors (V1a, V1b and V2) and at least one type of oxytocin receptors [1]. Complementary DNAs encoding each of these have been isolated [2]. The primary structures of the V1a, V1b, V2 and OT receptors of several species including lower vertebrates as fish and snail are now available. Their relatedness resides predominantly in the transmembrane domains and the extracellular loops 1 and 2. The gene encoding for the human V2 receptor has been localized to the distal region of the long arm on the X chromosome at the level of q28-qter locus, a region identified as the locus for congenital nephrogenic diabetes insipidus [3]. The gene encoding for the human OT receptor has been localized on chromosome 3p26.2, an area not associated with known genetic disorders [4]. Both genes contain introns [3-5].

A huge amount of pharmacological data on the biological actions of AVP and OT and on their receptors have been published [6]. They have led to the design of AVP and OT analogues that are potent and selective agonists and antagonists of the antidiuretic (V2-mediated) and vasopressor (V1-mediated) responses to vasopressin and of the uterotonic response to oxytocin. Pharmaceutical companies have also developed nonpeptide antagonists for V1a, V2 and OT receptors. It should be noted that there are marked differences among mammalian species in the ligand selectivity and distribution of AVP and OT receptors [2]. Transposition of pharmacological data obtained in the rat to other mammalian species may be hazardous and lead to erroneous interpretations.

In collaboration with M. Manning and his group, we have developed a series of radioiodinated antagonists having a high affinity and a high selectivity for the V1a and

OT receptors. These ligands are very useful for identification, pharmacological characterization and localization of AVP and OT receptors, particularly in the central nervous system. They have been essential to reveal the plasticity of AVP and OT receptors as well as the potential role of AVP receptors in nerve cell regeneration [7]. Equally worth mentioning is the design of a series of photoactivatable and iodinatable vasopressin linear antagonists that should be suitable to identify the antagonist binding domain of the receptor using a biochemical approach.

While the primary structures of many receptors are now known, their conformations are not. However, a three dimensional model of the vasopressin V1a receptor has been proposed [8], based on the model of bacteriorhodopsin and refined according to the experimental projections map of bovine opsin. The model predicts that AVP, which is characterized by a cyclic structure could be completely buried into a 15-20Å deep cleft defined by the transmembrane helices of the receptor and interact with amino-acids located within this region. Some of these amino-acids involved in agonist binding have been selected for site-directed mutagenesis. In addition, this model is proposed for all the members of this receptor family. The agonist binding cleft of this receptor family would be situated in a position equivalent to that described for the cationic neurotransmitters.

Using our three dimensional model [8], and data obtained after labelling the renal V2 receptor with a photoreactive vasopressin [9], a single residue, located on the first extracellular loop of the receptor, has been shown to be crucial not only for agonist high affinity binding but also for receptor selectivity [10]. One hopes that a better understanding of the structure-function relationships will help to determine the molecular basis of the pharmacological properties of these receptors and lead to a rational design of specific agonists and/or antagonists.

References

1. Jard, S., Elands, J., Schmidt, A. and Barberis, C., in Imura, H. and Shizume, K., (Eds.), 'Vasopressin and oxytocin receptors: An overview', in 'Progress in Endocrinology', Elsevier, Amsterdam, (1988) 1183.
2. Burbach, J.P.H., Adan, R.A.H., Lolait, S.J., Van Leeuwen, F.W., Mezey, E., Palkovitz, M. and Barberis, C., 'Molecular neurobiology and pharmacology of the vasopressin/oxytocin receptor family', in press.
3. Seibold, A., Brabet, P., Rosenthal, W. and Birnbaumer, M., *Am. J. Hum. Genet.*, 51, (1992) 1078.
4. Inoue, T., Kimura, T. Azuma, C., Inazawa, J., Takemura, M., Kikuchi, T., Kubota, Y., Ogita, K. and Saji, P., *J. Biol. Chem.*, 269, (1994) 32451.
5. Rozen, F., Russo, C., Banville, D. and Zingg, H.H., *Proc. Natl. Acad. Sci. USA*, 92, (1995) 200.
6. Manning, M. and Sawyer, W.H., *J. Recept. Res.*, 13, (1993) 195.
7. Tribollet, E., Arsenijevic, Y., Barberis, C., Marguerat, A. and Dreifuss, J.J., *Proc. Natl. Acad. Sci. USA*, 91, (1994) 9636.
8. Mouillac, B., Chini, B., Balestre, M.N., Elands, J., TrumppKallmeyer, S., Hoflack, J., Hibert, M., Jard, S. and Barberis, C., *J. Biol. Chem.*, 270 (1995) 25771.
9. Kojro, E., Eich, P., Gimpl, G. and Fahrenholz, F., *Biochemistry*, 32 (1993) 13537.
10. Chini, B., Mouillac, B., Ala, Y., Balestre, M.N., Trumpp-Kallmeyer, S., Hoflack, J., Elands, J., Hibert, M., Jard, S. and Barberis, C., *EMBO J.*, 14, 2176.

Peptides: Chemistry, Structure and Biology
Pravin T.P. Kaumaya and Robert S. Hodges (Eds.)
Mayflower Scientific Ltd., 1996

256
Design of an Optimal Mealtime Insulin (Lys-Pro) and its Assessment in Phase III Clinical Studies

J.H. Anderson, Jr., R.E. Chance, L.J. Slieker, L. Vignati and R.D. DiMarchi

Lilly Research Laboratories, Indianapolis, IN 46285, USA

Introduction

Diabetes is a systemic disease most readily characterized by hyperglycemia. Insulin has proven to be a highly effective drug in the management of elevated blood glucose and thus sustained life for millions of diabetics. However, it is extremely difficult to normalize blood glucose with conventional insulin therapy. The Diabetes Control and Complications Trial (DCCT) was a multicenter study that examined the influence of intensive glucose management over the course of the last decade [1]. The results clearly confirmed the reduction of diabetic microvascular complications in those persons with diabetes capable of maintaining a more normal glucose profile. The most disconcerting features to the intensively insulinized patients were an increase in severe hypoglycemic events and the rigid lifestyle imposed by multiple dose insulin regimens.

Insulin analogs that provide a more precise time of action have been postulated as a means to improved and safer glucose control. Current insulin formulations are poor surrogates for normal physiology where insulin release from the pancreas is closely matched to increases in glucose concentrations. Subcutaneous injection of a mealtime insulin, such as soluble regular insulin (currently the most rapid acting commercial formulation), provides insulin in a protracted fashion for an excessively extended duration [2]. The absorption of insulin is influenced by several molecular and physiological factors. The inherent ability of insulin to self-associate to higher molecular forms, most notably the hexamer, is an apparent rate limiting step in achieving a biological response since insulin must dissociate to a primarily monomeric form to enter the circulation. Consequently, there is significant interest in understanding the physical and chemical aspects that govern insulin self-association and recognition by the insulin receptor [3].

The foundation of our approach to the structural improvement of human insulin was grounded in the thinking that only the slightest of change should be introduced. Lys(B28), Pro(B29) human insulin (Lys-Pro) is an analog where the naturally occurring amino acid sequence of insulin at positions B28 and B29 is reversed [4]. The design of this particular analog was inspired by the natural sequence of Lys-Pro at the homologous position in Insulin Like Growth Factor I [5]. Lys-Pro insulin is equipotent to human insulin and yet absorbed more quickly from subcutaneous injection sites [6]. This renders the insulin more suitable for mealtime glucose control where administration is

timed nearly simultaneous to a meal and the duration of action appears nearly identical to the extent of the glucose excursion. Physicochemical studies suggest that this more desirable time action is due primarily to a weakend propensity to self-association relative to human insulin [7].

Results and Discussion

In this report, we present results from one year clinical studies in 631 patients with diabetes mellitus that were designed to compare the mealtime efficacy of Lys-Pro insulin to human regular insulin in regimens of intensive insulin management. Patients with diabetes were randomized to subgroups using either Lys-Pro or regular as a pre-meal insulin with no change in the basal insulin. The glycemic treatment goals were a fasting glucose of 140 mg/dL without hypoglycemia and maintenance of 2 hour post-meal glucose concentrations below 180 mg/dL. Patients administered regular insulin 30-45 min before or Lys-Pro 0-15 min before each meal. The recommended injection-meal intervals were used to avoid biasing the studies in favor of the more rapid acting Lys-Pro [8, 9]. All injections were advised to be given subcutaneously in the abdominal area only. Hypoglycemia was defined as a patient experiencing any sign or symptom normally associated with hypoglycemia (regardless of serum glucose), or a serum glucose value below 36 mg/dL.

In insulin-dependent patients with diabetes the mean postprandial rise in serum glucose concentration was 92% lower at two hours in Lys-Pro treated patients than those using regular insulin. At study completion, the mean HbA_{1c} level was slightly but significantly lower in the Lys-Pro group compared to the regular insulin group (8.1% *vs.* 8.4%, p=.03). There was no difference in the overall rate of hypoglycemic episodes between Lys-Pro and human regular insulin treated patients. However, there was evidence of reduced risk of hypoglycemia in Lys-Pro treated patients experiencing improved glucose control. Among all patients with hemoglobin A_1c values of < 7%, treatment with Lys-Pro resulted in a 33% reduction in the number of patients experiencing more than 2 episodes of hypoglycemia each 30 days compared to regular insulin. There was no evidence of a significant Lys-Pro specific immunogenic response or an increased crossreactive insulin antibody titer. The magnitude of slight weight gain was comparable in both groups and there were no differences in the frequency or types of adverse events between the two study groups.

In summary, the inversion of the B28 and B29 residues of human insulin to yield Lys-Pro insulin results in an analog with the same amino acid composition and isoelectric properties as human insulin. Large scale clinical studies have proven Lys-Pro insulin to be an efficacious, safe, and convenient mealtime insulin agonist.

References

1. DCCT Research Group, *New England Journal of Medicine,* 329 (1993) 977.
2. Berger, M., Cuppers, H.J., Hegner, H., Jorgens, V. and Berchtold, P., *Diabetes Care,* 5 (1982) 77.
3. Slieker, L.J., Brooke, G.S., Chance, R.E., Fan, L., Hoffmann, J.A., Howey, D.C., Long, H.B., Mayer. J., Shields, J.E., Sundell, K.L. and DiMarchi, R.D., in LeRoith, D. and Raizada, M.K.

(Eds.), 'Current Directions in Insulin-like Growth Factor Research', Plenum Press, New York and London, 1993, p.25.

4. DiMarchi, R.D., Mayer, J.P., Fan, L., Brems, D.N., Frank, B.H., Green, L.K., Hoffmann, J.A., Howey, D.C., Long, H.B., Shaw, W.N., Shields, J.E., Slieker, L.J., Su, K.S., Sundell, K. and Chance, R.E., in Smith, J.A. and Rivier, J.E. (Eds.), 'Peptides: Chemistry and Biology', ESCOM, Leiden, The Netherlands, 1992, p. 26.
5. DiMarchi, R.D., Chance, R.E., Long, H.B., Shields, J.E. and Slieker, L.J., *Horm. Res.*, 2 (1994), 93.
6. Howey, D.C., Bowsher, R.R., Brunelle, R., Woodworth, J.R., *Diabetes,* 43 (1994) 396.
7. Brems, D.N., Alter, L.A., Beckage, M.J., Chance, R.E., DiMarchi, R.D., Green, L.K., Long, H.B., Pekar, A.H., Shields, J.E. and Frank, B.H., *Protein Engineering,* 5 (1992) 527.
8. American Diabetes Association, *Diabetes Care,* 1 (1995) 29.
9. Howey, D.C., Rowe, H., Brunelle, R., Downing-Shelton, J., *Diabetes,* 1 (1993) 80A.

Peptides: Chemistry, Structure and Biology
Pravin T.P. Kaumaya and Robert S. Hodges (Eds.)
Mayflower Scientific Ltd., 1996

257

Design of Receptor Selective Peptides that Antagonize the Actions of Amylin *In Vivo*

K.S. Prickett, E. Albrecht, C.J. Soares, R.H. Lumpkin, L.S.L. Gaeta, C.X. Moore, A.A. Young, N.R.A. Beeley and K. Beaumont

Amylin Pharmaceuticals, Inc., 9373 Towne Centre Drive, San Diego, CA 92121, USA

Introduction

Amylin is a 37 residue, disulfide-bridged, C-terminally amidated peptide hormone that shows some amino acid sequence homology with CGRP and calcitonin. It is co-secreted with insulin from pancreatic β-cells in response to nutrients and is believed to act as a partner to insulin in regulating blood glucose. The biological actions of amylin have recently been reviewed [1, 2] and appear to be the result of activation of high affinity amylin receptors first identified in the nucleus accumbens region of rat brain [3]. In juvenile-onset (Type I) and late stage maturity-onset (Type II) diabetes amylin is deficient. However, amylin levels appear to be elevated in insulin resistant obese people, including many with hypertension, and in those with the so-called "syndrome X". It has been proposed that excess amylin action contributes to the metabolic and cardiovascular disorder of "syndrome X" and that amylin blockade is a novel therapeutic approach to this apparently pre-diabetic (Type II) state. Herein, we describe the identification of potent and selective peptide amylin antagonists, two of which have been investigated preclinically and in Phase I clinical studies.

Results and Discussion

All peptides were synthesized using standard solid phase Boc or Fmoc strategies, purified by HPLC and tested for inhibition of ^{125}I-rat amylin binding to nucleus accumbens membranes [3]. In previous studies with CGRP, truncated analogs lacking the disulfide bridge were reported to be full CGRP receptor antagonists [4]. We initially tested the following truncated peptides for binding to the amylin receptor: rat amylin 8-37, hCGRP 8-37 and salmon calcitonin 8-32 (Ia). Surprisingly, we found that the shorter peptide, salmon calcitonin 8-32 (Ia) was the most potent amylin inhibitor. A series of analogs of (Ia) was designed and synthesized in an effort to specifically enhance binding and selectivity to the amylin receptor. The results are shown in Table 1. In the first series of peptides (Ib-Ih) several positions in (Ia) were chosen for replacement (underlined) by the corresponding amylin amino acids. The effects of peptide length and acetylation were also explored. The most potent peptide of this series, (Ig) (AC253) (Ki = 0.06 ± 0.01 nM), was also tested for inhibition of ^{125}I-hCGRP binding to the CGRP

Table 1. *Inhibition of radioligand binding by peptide antagonists.*

Peptide	Amino Acid Sequence[a]	Ki (nM)[b]
rAmylin 8-37	ATQRLANFLVRSSNNLGPVLPPTNVGSNTY -NH_2	289 ± 82
hCGRP 8-37	VTHRLAGLLSRSGGVVKNNFVPTNVGSKAF- NH_2	8.4 ± 4.0
Ia	VLGKLSQELHKL----------QTYPRTNTGSGTP-NH_2	1.22 ± 0.24
Ib	Ac-VLGKLSQELHKL----------QTYPRTNTGSGTP-NH_2	0.22 ± 0.02
Ic	Ac-VLGKLSQELHKL----------QTYPRTNTGSNTY-NH_2	0.34 ± 0.09
Id	Ac-LGKLSQELHKL----------QTYPRTNTGSNTY-NH_2	0.70 ± 0.07
Ie	Ac-LGKLSQELHRL----------QTYPRTNTGSNTY-NH_2	0.07 ± 0.02
If	Ac-LGRLSQELHKL----------QTYPRTNTGSNTY-NH_2	0.18 ± 0.01
Ig (AC253)	Ac-LGRLSQELHRL----------QTYPRTNTGSNTY-NH_2	0.06 ± 0.01
Ih	Ac-GRLSQELHRL----------QTYPRTNTGSNTY-NH_2	17.6 ± 3.2
IIa	Ac-ATQRLANFLVRS---------PVLPPTNVGSNTY-NH_2	63 ± 24
IIb	Ac-ATQRLANFLVRS---------QTYPRTNVGSNTY-NH_2	0.5 ± 0.1
IIc	Ac-ATQRLANFLVRL---------QTYPRTNVGANTY-NH_2	0.04 ± 0.01
IId	Ac-TQRLANFLVRL--------QTYPRTNVGANTY-NH_2	0.10 ± 0.02
IIe (AC625)	Ac-ATQRLANELVRL---------QTYPRTNVGSNTY-NH_2	0.64 ± 0.13
IIf	Ac-ATQRLANQLVRL---------QTYPRTNVGSNTY-NH_2	0.13 ± 0.05
IIg	Ac-ATQLLANELVRL---------QTYPRTNVGSNTY-NH_2	1.71 ± 0.02
IIh	Ac-ATQQLANELVRL---------QTYPRTNVGSNTY-NH_2	2.7 ± 0.4
IIi	Ac-ATQLLANQLVRL---------QTYPRTNVGSNTY-NH_2	0.46 ± 0.08

[a] The dashes in the sequences have been introduced to allow the alignment of the peptides with the sequence of rat amylin 8-37 and CGRP 8-37.

[b] Results are Ki's (mean ± SEM, n ≥ 2) for inhibition of ^{125}I-rat amylin binding to nucleus accumbens membranes.

receptor in SK-N-MC cell membranes [5] and for inhibition of ^{125}I-human calcitonin (^{125}I-hCT) binding to the calcitonin receptor in C1a-6 cell membranes [6]. The Ki's at these receptors were 13.5 ± 2.4 nM and 0.4 ± 0.05 nM, respectively. This peptide was selected for further evaluation (*vide infra*).

In the second series of peptides we incorporated selected features of sequence (Ia) into amylin 8-37. Based upon a homology alignment with (Ia), five amino acids in the middle of rat amylin 8-37 were deleted resulting in (IIa) which had increased potency. Subsequent modifications (underlined) to this peptide were done to incorporate residues thought to be important for potency in series (Ia-Ih) as well as other residues to explore different properties. Although (IIe) (AC625) was not the most potent amylin inhibitor (Ki = 0.64 ± 0.13 nM) *in vitro* from series II, comparative *in vivo* data resulted in its selection for further evaluation. Ki's for (IIe) as an inhibitor of ^{125}I-hCGRP binding to the CGRP receptor in SK-N-MC cell membranes and of ^{125}I-hCT binding to the calcitonin receptor in C1a-6 cell membranes were 6.1 ± 0.4 nM and 2.6 ± 0.4 nM, respectively.

To test for the ability of (Ig) (AC253) and (IIe) (AC625) to antagonize the effects of pharmacologic doses of amylin *in vivo* [7] each peptide was administered to fasted, anesthetized rats as a bolus injection of 1.5mg followed by a continuous infusion at

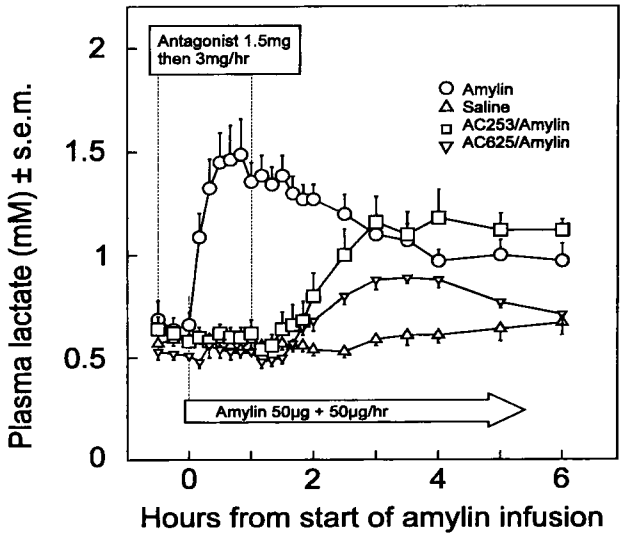

Figure 1. *Prevention of amylin-induced increase in plasma lactate by preinfusion with amylin antagonist in anesthetized rats [7].*

3mg/hr for 1.5 hr. Thirty minutes after the start of antagonist infusion a 50 µg bolus of rat amylin was injected, followed by a continuous infusion of rat amylin at 50 µg/hr for a further 6 hours. The results, shown in Figure 1, illustrate the ability of (Ig) (AC253) and (IIe) (AC625) to inhibit amylin-induced hyperlactemia.

In summary, we have identified two series of peptides, (Ia-Ih) and (IIa-IIi), which inhibit binding of amylin to its receptor in nucleus accumbens membranes and are effective *in vivo* in antagonizing metabolic actions of amylin. Two of these peptides, (Ig) (AC253) and (IIe) (AC625), have been further evaluated preclinically and in Phase I clinical studies.

References

1. Young, A.A., Pittner, R., Gedulin, B., Vine, W. and Rink, T.J., *Biochem. Soc. Trans.*, 23 (1995) 323.
2. Cooper, G.J.S., *Endocrine Rev.*, 15 (1994) 163.
3. Beaumont, K., Kenney, M.A., Young, A.A. and Rink, T.J., *Mol. Pharmacol.*, 44 (1993) 493.
4. Dennis,T., Fournier, A., Cadieux, A., Pomerleau, F., Jolicoeur, F.B., St-Pierre, S. and Quirion, R., *J. Pharmocol. Exp. Ther.*, 254 (1990) 123.
5. van Valen, F., Piechot, G. and Jurgens, H., *Neurosci. Lett.*, 119 (1990) 195.
6. Beaumont, K., unpublished data.
7. Young, A.A., Rink, T.J. and Wang, M-W., *Life Sci.*, 52 (1992) 1717.

Peptides: Chemistry, Structure and Biology
Pravin T.P. Kaumaya and Robert S. Hodges (Eds.)
Mayflower Scientific Ltd., 1996

258

Identification of Mu-selective Tetrapeptides Using a Positional Scanning Combinatorial Library Containing L-, D- and Unnatural Amino Acids

C.T. Dooley, A.N. Bower and R.A. Houghten

Torrey Pines Institute for Molecular Studies, San Diego, CA 92121, USA

Introduction

Individual compounds can be identified from soluble synthetic combinatorial libraries by either of two methods, the iterative strategy [1] or the positional scanning strategy [2, 3]. In the positional scanning approach, a single defined position (O) is walked through all positions along the peptide length, *e.g.* OZZZ-NH_2, ZOZZ-NH_2, ZZOZ-NH_2, and ZZZO-NH_2. The most active amino acids can be determined for each position in a single screening. Individual peptides representing all possible combinations of the most active amino acids are then synthesized and tested for activity. Thus, using this method only a single synthesis is required to obtain individual peptides following screening. During synthesis of a mixture position (Z) in a positional scanning library, all amino acids are coupled simultaneously. Due to the different coupling rates of the amino acids, the amino acid mixture used for coupling must contain amino acid ratios which will yield an approximately equimolar coupling of all amino acids present in the mixture. Such ratios have been determined for a series of L-, D- and unnatural amino acids. A positional scanning tetrapeptide library has now been prepared containing 16 L-, 14 D-, and 20 unnatural amino acids. This library was screened in a radioreceptor assay selective for the μ opioid receptor and used to rapidly identify potent new μ-selective peptides.

Results and Discussion

Each of the mixtures making up the tetrapeptide positional scanning library was screened for its ability to inhibit binding of [^{3}H]-DAMGO to rat brain membranes. The mixtures were initially screened at a fixed concentration (0.008 mg/ml). IC_{50} values were subsequently calculated for those mixtures which inhibited >90% of [^{3}H]-DAMGO binding for positions 1-4. The most active mixtures found were: position 1, YZZZ-NH_2 (IC_{50} = 500 nM); position 2, Z(D-Nve)ZZ-NH_2 (IC_{50} = 690 nM), and Z(D-Nle)ZZ-NH_2 (IC_{50} = 1112 nM); position 3, ZZFZ-NH_2 (IC_{50} = 824 nM), ZZGZ-NH_2 (IC_{50} = 1119 nM) and ZZWZ-NH_2 (IC_{50} = 1227 nM); and position 4, ZZZ(L-Nap)-NH_2 (IC_{50} = 279 nM) and ZZZW-NH_2 (IC_{50} = 850 nM). Thus, amino acids chosen for inclusion in the synthesis of individual peptides were as follows: position 1-Tyr, position 2- D-Nve and D-Nle, position 3 - Phe, Trp and Gly, position 4- L-Nap and Trp. Twelve combinations of these amino acids were synthesized as individual peptides. IC_{50} values obtained for

Table 1. *IC_{50} values for individual peptides in assays selective for μ, δ, and κ receptors.*

	μ	δ	κ	Ratio	
Peptide	IC_{50} (nM)	IC_{50} (nM)	IC_{50} (nM)	δ/μ	κ/μ
Y-(D-Nve)-G-Nal-NH_2	0.2	28	203	140	1015
Y-(D-Nle)-G-Nal-NH_2	1	27	816	27	816
Y-(D-Nve)-G-W-NH_2	3	90	1701	30	567
Y-(D-Nle)-G-W-NH_2	5	107	2250	21	450
Y-(D-Nve)-F-W-NH_2	5	92	228	18	46
Y-(D-Nve)-W-Nal-NH_2	5	201	214	40	43
Y-(D-Nve)-W-W-NH_2	5	257	752	51	150
Y-(D-Nve)-F-Nal-NH_2	7	219	1221	31	174
Y-(D-Nle)-F-W-NH_2	15	178	1178	12	79
Y-(D-Nle)-W-W-NH_2	17	816	2045	48	120
Y-(D-Nle)-F-Nal-NH_2	30	223	1859	7	62
Y-(D-Nle)-W-Nal-NH_2	32	164	1226	5	38

these peptides in assays selective for the μ, δ and κ receptors are given in Table 1. The screening of this library of 6.3 million tetrapeptides (50^4) and testing of the twelve individual peptides identified was accomplished in two weeks. This study illustrates the power of the positional scanning concept for the rapid identification of new receptor ligands.

Acknowledgments

This work was funded by Houghten Pharmaceuticals Inc., San Diego, CA.

References

1. Houghten, R.A., Pinilla, C., Blondelle, S.E., Appel, J.R., Dooley, C.T. and Cuervo, J.H., *Nature*, 354 (1991) 84.
2. Pinilla, C., Appel, J.R., Blanc, P. and Houghten, R.A., *Biotechniques*, 13 (1992) 901.
3. Dooley, C.T. and Houghten, R.A., *Life Science*, 52 (1993) 1509.

Peptides: Chemistry, Structure and Biology
Pravin T.P. Kaumaya and Robert S. Hodges (Eds.)
Mayflower Scientific Ltd., 1996

259

Synthesis and Biological Activities of Enzymatically Stable and Selective Dyn A(1-11)-NH_2 Analogs

J.P. Meyer[1], F.D. Lung[1], P. Davis[2], I. DeLeon[2], T. Gillespie[2], T.P. Davis[2], F. Porreca[2], H.I. Yamamura[2] and V.J. Hruby[1]

Departments of [1]Chemistry and [2]Pharmacology, University of Arizona, Tucson, AZ 85721, USA

Introduction

Dynorphin A is the putative endogenous ligand for the κ opioid receptor and is highly potent at all three of the commonly accepted opioid receptors. This characteristic is shared by Dyn A(1-11)-NH_2 (**1**), which was used as a template in this study (Table 1). The *in vivo* use of Dyn A-like peptides is hindered by at least two problems: i) a lack of selectivity for the κ receptor; and ii) a high sensitivity of several peptide bonds of Dyn A analogs to enzymatic degradation. We recently reported that alkylation of the tyrosine residue in position 1 and replacement of the glycine residue in position 3 with L- and D-alanine (**2-5**) lead to peptides with μ vs κ selectivity ratios ranging from 57 to 350 [1, 2]. Synthesis and testing for *in vitro* stability in mouse brain homogenates of a series of analogs of **1** with one reduced bond showed that the Leu^5-Arg^6 bond was the most susceptible to enzymatic degradation, though this bond modification lead to a non-selective peptide **6** [3, 4]. In an attempt to increase both selectivity and enzymatic stability, we have synthesized analogs containing two or three of the above mentioned modifications.

Results and Discussion

Replacing the Arg^6 by its D counterpart lead to a stable analog, as the $t_{1/2}$ for **7** was > 500 min, compared to 42 min for **1**. As for **6**, that also displayed a $t_{1/2}$ > 500 min, though high potency was retained, the κ vs μ selectivity was very poor. Stable analogs **8** and **9** with a D-alanine residue in position 3 displayed a slight increase in κ selectivity and complete resistance to enzymatic degradation. Unfortunately, this increase was only small when compared to the one obtained for peptides **1**, **4** and **5**, so apparently the changes are not additive. Also, it seems that modifications at the 3 and 6 positions are mutually exclusive, as shown by the loss in affinity for **9**. Adding a propyl chain onto the tyrosine residue (**10**) only decreased further the affinity at all three receptors. **10** and **11** were synthesized and tested to see if the two modifications that increase drastically the selectivity for the κ receptor with no loss of affinity were additive. Results were not as good as expected, as these analogs showed about a 4 to 7 fold loss in affinity for the κ

Table 1. *Binding affinities, selectivities and enzymatic stabilities of various Dyn A analogs*[a].

		IC_{50}(nM)[a]			Selectivity		Stability
	Peptide[b]	κ	μ	δ	μ/κ	δ/κ	$t_{1/2}$(min)
1	Dyn A(1-11)-NH_2	0.58	9.9	26	17	44	42
2	[Propyl-Tyr^1]	1.02	192	637	188	625	60
3	[Butyl-Tyr^1]	2.15	123	319	57	148	55
4	[D-Ala^3]	0.76	260	1,000	350	1300	82
5	[Ala^3]	1.10	210	730	190	660	--
6	[$(CH_2$-NH)$^{5-6}$]	0.61	0.64	32	1	52	>500
7	[D-Arg^6]	0.90	3.1	45	3	50	>500
8	[D-Ala^3, $(CH_2$-NH)$^{5-6}$	2.8	13	3,600	5	1286	>500
9	[D-Ala^3,D-Arg^6]	15	268	5,680	18	379	>500
10	[Propyl-Tyr^1,D-Ala^3,D-Arg^6]	56	939	14,210	17	254	>500
11	[Propyl-Tyr^1,D-Ala^3]	5.2	1437	3,879	276	679	--

[a] Binding affinities and enzymatic stabilities were determined as described in [3, 4].
[b] All peptides, except **1**, are Dyn A(1-11)-NH_2 analogs.

receptor. Nevertheless, the κ *vs* μ and δ selectivities were conserved or even improved in **10** which contained a N-propyl tyrosine residue in position 1. The κ *vs* μ selectivities slightly decreased, when compared to **4**. Overall, results indicated that the best selectivities were obtained with the combination of the N-propyl Tyr^1 and D-Ala^3 modifications.

We have been able to design peptides that were stable to enzymatic degradation, but that displayed no or very poor κ *vs* μ selectivity. This feature was improved by the incorporation in the message segment of these peptides of modifications that we had previously found to yield highly selective Dyn A analogs. Finally, the combination of both message modifications lead to peptides which displayed no increase in selectivity when compared to their parent compounds. It therefore seems that the two modifications were not additive.

Acknowledgments

This work was supported by a grant from NIDA (DA 04248).

References

1. Meyer, J.P., Porreca, F., Yamamura, H.I.and Hruby, V.J., *J. Med. Chem.*, to be submitted.
2. Lung, F.D., Meyer, J.P., Li, G., Lou, B.S., Stropova, D., Davis, P., Yamamura, H.I., Porreca, F., Davis, T. and Hruby, V.J., *J. Med. Chem.*, 38 (1995), 585.
3. Meyer, J.P., Gillespie, T.J., Hom, S., Hruby, V.J. and Davis, T.P., *Peptides*, 16 (1995) 1215.
4. Meyer, J.P., Davis, P., Lee, K.B., Porreca, F. and Hruby, V.J., *J. Med. Chem.*, 38 (1995) 3462.

Peptides: Chemistry, Structure and Biology
Pravin T.P. Kaumaya and Robert S. Hodges (Eds.)
Mayflower Scientific Ltd., 1996

260
Isolation and Characterization of Porcine Prorelaxin Processing Enzymes

S.S. Layden and G.W. Tregear

Howard Florey Institute of Experimental Physiology and Medicine.
University of Melbourne, Parkville, Victoria 3052, Australia

Introduction

Relaxin is a two chain peptide hormone made by the corpus luteum of the ovary during pregnancy [1]. Relaxin's best known action is to remodel smooth muscle and connective tissue of the reproductive tract in preparation for parturition [2], and newly detected sites of production and action suggest it has a wider physiological role. Relaxin is found in male prostate tissue and seminal plasma, and high affinity receptors for the hormone have been detected in rat heart [3] and brain tissue [4].

Relaxin is member of the insulin family of peptide hormones [5] and is produced by processing of a larger precursor, prorelaxin, which consists of the B chain linked to the A chain by a connecting C peptide of around 100 residues. During processing, the C peptide is excised and the A and B chains trimmed to their mature lengths. Structures of the stored and secreted forms of relaxin are known and the processing sites have been postulated [6]. Cleavage occurs between a Leu and Ser at the B chain - C peptide border and after the tetrabasic sequence between the C peptide and A chain. The enzymes that process prorelaxin have not been elucidated.

A simple test was designed to detect prorelaxin processing activity. It was applied to fractionated porcine ovary extracts and cleavage at prorelaxin processing sites detected. Active material was isolated, characterized and found to be a member of the prohormone convertase (PC) [7] family of processing enzymes.

Results and Discussion

A rapid and convenient test was established to detect prorelaxin processing activity in porcine ovary extracts. Unmodified peptide substrates were chemically synthesized which represent the two prorelaxin processing sites. Cleavage of these peptides was detected using reversed phase high performance liquid chromatography (RP-HPLC) and capillary electrophoresis (CE) and resulting fragments were identified by their retention times compared to synthetic standards.

Secretory granules were purified from the granulosa cells of pregnant pigs and the contents of the granules were fractionated. After ammonium sulfate precipitation, the proteins were separated by affinity-, anion exchange-, then hydrophobic interaction chromatography. Fractions from each step were tested for ability to cleave the synthetic substrates at the prorelaxin processing sites.

The fractions were also tested for immunoreactivity with polyclonal antisera raised against synthetic peptides that represent sequences from prohormone processing enzymes. Fractions that were active in both tests were further purified by microbore RP-HPLC and analyzed by immunoblotting and Edman sequencing.

A 67kD enzyme was purified which was immunoreactive with the polyclonal antisera. The enzyme cleaved the C peptide - A chain spanning peptide after the tetrabasic sequence Arg Lys Lys Arg and did not cleave the peptides at any other sites. The enzyme was Ca^{2+}dependent, with optimal activity in the peptide cleavage test at a Ca^{2+} concentration of 10mM and at pH 5.5-6.5. The inhibition profile of the enzyme suggested it was a serine protease. Sequence analysis identified the enzyme as the porcine form of the processing enzyme prohormone convertase 1 (PC1).

The PCs are a family of proprotein processing enzymes which have varied tissue distributions. PC1 and PC2 are found mainly in endocrine tissues and have been shown to correctly process a number of prohormones including proinsulin. This is the first time PC1 has been detected in the pig. It is also the first time the enzyme has been described in the ovary.

A candidate prorelaxin processing enzyme has been isolated from the corpora lutea of pregnant pigs. Characterization of this enzyme demonstrates that it is the porcine form of prohormone convertase 1. Colocation of the enzyme with relaxin and prorelaxin in the luteal cell secretory granules suggests porcine PC1 is a potential prorelaxin processing enzyme.

Acknowledgments

The authors thank Mr. M. Petrovski and Ms. M. John for excellent technical assistance. This work is supported by an Institute Block Grant from the NH & MRC of Australia.

References

1. Sherwood, O.D. in Knobil, E. and Neill, J., (Eds.), 'The Physiology of Reproduction', Raven Press, New York, USA, 1994, p.861.
2. Downing, S.J. and Sherwood, O.D., *Endocrinology*, 116 (1985) 1215.
3. Osheroff, P.L. and Phillips, H.S., *Proc. Natl. Acad. Sci. USA*, 88 (1991) 6413.
4. Osheroff, P.L., Ling, V.T., Vandlen, R.L., Cronin, M.J. and Lofgren, J.A., *J. Biol. Chem.*, 265 (1990) 9396.
5. Blundell, T.L. and Humbel, R.E., *Nature*, 287 (1980) 781.
6. Haley, J., Hudson, P., Scanlon, D., John, M., Cronk, M., Shine, J., Tregear, G. and Niall, H., *DNA*, 1 (1982) 155.
7. Halban, P.A. and Irminger, J-C., *Biochem. J.*, 299 (1994) 1.

Peptides: Chemistry, Structure and Biology
Pravin T.P. Kaumaya and Robert S. Hodges (Eds.)
Mayflower Scientific Ltd., 1996

261
Cyclic Opioid Peptide Analogs Containing the Essential Tyrosine Residue Within the Ring Structure

P.W. Schiller, T.M.-D. Nguyen, B.C. Wilkes, N.N. Chung and C. Lemieux

Laboratory of Chemical Biology and Peptide Research, Clinical Research Institute of Montreal, Montreal, Quebec, H2W 1R7, Canada

Introduction

All cyclic opioid peptide analogs with high potency and high selectivity for either μ or δ receptors that have been reported to date contain the essential tyrosine residue at the N-terminal position outside the ring structure [1]. Addition of a lysine residue to the N-terminus of various linear opioid peptides was reported to result in compounds retaining considerable μ agonist potency [2]. In an effort to obtain cyclic opioid peptides containing the tyrosine residue as part of the ring structure, we prepared a series of peptides corresponding to the N-terminal tetrapeptide segment of deltorphin I or II that were N-terminally extended with L- or D-lysine and were cyclized between the ε-amino group of Lys^0 and the ω-carboxylate function of Asp or Glu in the C-terminal position of the peptide sequence.

Results and Discussion

The cyclic parent pentapeptide H-**Lys**-Tyr-D-Ala-Phe-**Asp**-NH_2 was a fairly potent μ agonist in the μ receptor-representative guinea pig ileum (GPI) assay and a weak agonist in the mouse vas deferens (MVD) assay (δ receptor-representative) (Table 1). The D-Lys^1-analog of this peptide was a weak antagonist (K_e = 2.63 μM) against the μ-selective agonist H-Tyr-D-Ala-Phe-Phe-NH_2 (TAPP) in the GPI assay. Diastereomers with a D-configured Asp^5 residue or with D-configuration at both the 1- and the 5-position residue showed weak activity in both assays. Expansion of the peptide ring structure through replacement of Asp^5 with Glu resulted in a compound, H-**Lys**-Tyr-D-Ala-Phe-**Glu**-NH_2, with an unchanged activity profile. Surprisingly, reduction of the Tyr^2 - $D\text{-}Ala^3$ peptide bond produced a drastic decrease in both μ and δ agonist potency. The Gly^3-analog H-**Lys**-Tyr-Gly-Phe-**Asp**-NH_2 also turned out to be a weak μ agonist, whereas the corresponding Glu^5 analog showed weak μ antagonist activity (K_e = 2.66 μM). It thus appears that increased structural flexibility in the central part of the peptide sequence is detrimental to high μ agonist potency. Replacement of Tyr^2 in the parent peptide with 2',6'-dimethyltyrosine (Dmt) led to a compound, H-**Lys**-Dmt-D-Ala-Phe-**Asp**-NH_2, that showed a very potent μ agonist effect in the GPI assay (IC50 = 25.4 nM).

Table 1. *In vitro opioid activities and receptor affinities of cyclic peptide analogs.*

	GPI assay	MVD assay	Receptor binding assays[a]	
Compound	IC50 [nM]	IC50 [nM]	K_i^{μ} [nM]	K_i^{δ} [nM]
H-**Lys**-Tyr-D-Ala-Phe-**Asp**-NH_2	508	9580	624	>700000
H-**D-Lys**-Tyr-D-Ala-Phe-**Asp**-NH_2	2630 (K_e)[b]	966	11600	>14500
H-**Lys**-Tyr-D-Ala-Phe-**D-Asp**-NH_2	4650	4070	>10000	41700
H-**D-Lys**-Tyr-D-Ala-Phe-**D-Asp**-NH_2	>10000	>10000	18600	>360000
H-**Lys**-Tyr-D-Ala-Phe-**Glu**-NH_2	409	63300	4030	6870
H-**Lys**-TyrΨ[CH_2NH]D-Ala-Phe-**Asp**-NH_2	>10000	>10000	3020	7050
H-**Lys**-Tyr-Gly-Phe-**Asp**-NH_2	5430	8640	>18900	275000
H-**Lys**-Tyr-Gly-Phe-**Glu**-NH_2	2660 (K_e)[b]	>10000	>50000	>100000
H-**Lys**-Dmt-D-Ala-Phe-**Asp**-NH_2	25.4	part. agonist[c]	391	135
H-**Lys**-D-Dmt-D-Ala-Phe-**Asp**-NH_2	490	54.0 (K_e)[d]	3720	408
[Leu^5]enkephalin	246	11.4	9.43	2.53

[a]Displacement of [^{3}H]DAMGO (μ-selective) and [^{3}H]DSLET (δ-selective) from rat brain membrane binding sites. [b]Antagonist (K_e determined against TAPP). [c]Partial agonist (maximal inhibition of electrically evoked contractions = 30%). [d]Antagonist (K_e determined against DPDPE).

The effect was μ receptor-mediated, since it was reversed by low concentrations of naloxone (K_e = 2.16 nM). This compound represents the first example of a cyclic opioid peptide that contains the essential Tyr (Dmt) residue within the ring structure and still retains high μ agonist potency. Its high μ agonist activity observed in the GPI assay was in contrast to its low μ receptor affinity determined in the binding assay. This discrepancy may reflect either a species difference or a difference in the structural requirements between central and peripheral μ receptors. Therefore, this peptide may turn out to be a valuable tool in further studies of μ receptor heterogeneity. The diastereomeric peptide H-**Lys**-D-Dmt-D-Ala-Phe-**Asp**-NH_2 was a moderately potent μ agonist in the GPI assay and a fairly potent δ antagonist against [D-Pen^2,D-Pen^5] enkephalin (DPDPE) in the MVD assay, thus representing another prototype of a mixed μ agonist/δ antagonist.

Acknowledgments

Supported by grants from the FMCQ and MRCC (UI-12356).

References

1. Schiller, P.W., in Ellis, G.P. and West, G.B. (Eds.), 'Progress in Medicinal Chemistry', Vol. 28, Elsevier, Amsterdam, The Netherlands, 1991, p. 301.
2. Vavrek, R.J., Cui, R.-L., York, E.J., Stewart, J.M., Paterson, S. and Kosterlitz, H.W., *Life Sci.*, 33 (1983) 451.

Peptides: Chemistry, Structure and Biology
Pravin T.P. Kaumaya and Robert S. Hodges (Eds.)
Mayflower Scientific Ltd., 1996

262
p-Methylhippuric Acid is a Novel N-terminal Tyr Replacement for Growth Hormone-releasing Hormone (GHRH)

D.L. Smiley, R.D. DiMarchi, P.L. Surface, G.C. Harris and M.L. Heiman

Lilly Research Laboratories, Eli Lilly and Co. Indianapolis, IN 46285, USA

Introduction

GHRH is a 44 residue hypothalamic peptide that stimulates both synthesis and release of pituitary GH [1]. The biological activity of GHRH resides in the N-terminus and hGHRH(1-29)NH_2 is the shortest fragment that retains full bioactivity [2]. GHRH, however, is cleaved by dipeptidyl peptidase IV (DAP-IV) that circulates in the plasma of most species to yield an inactive GHRH(3-44) [3]. Thus, most analogs have been designed to resist DAP-IV activity. Some success in producing longer acting analogs has been achieved by introducing modified tyrosines for Tyr^1, substituting D-amino acid surrogates for Tyr^1 or Ala^2, and substituting beta- branched Val or Thr for Ala^2. We surmised that a relatively simple modification could be made at the N-terminus that would maintain activity and impart resistance to DAP-IV activity.

We chose to explore analogs of Leu^{27}GHRH(1-29)NH_2 where Tyr^1 was replaced by acyl glycines because of their ease of synthesis, high coupling efficiency, and lack of potential for racemization. N-acetylGly^1 and *p*-methylbenzoylGly^1 (pMH) analogs were prepared by SPPS and compared with native Tyr^1 and des-NH_2Tyr^1 for their ability to stimulate GH secretion in cultured rat pituitary cells and resist DPP-IV activity.

Results and Discussion

The results of *in vitro* GH release are shown in Table 1. Both the des-NH_2Tyr^1 and N-acetylGly^1 analogs were significantly ($p<0.05$) less potent stimulators of GH secretion than were either native hGHRH(1-29)NH_2 or the corresponding Leu^{27} reference peptide. The pMH^1 analog, however, was surprisingly only slightly less active than native hGHRH(1-29)NH_2 and twice as potent as the Leu^{27} parent.

The resistance to DAP-IV was assessed by measuring the degradation of 30 μg each of Leu^{27} hGHRH and the pMH^1 analog exposed to 1ml of porcine plasma at 37°C during a 2 hour incubation period. A linear regression of parent peptide remaining in solution [log absorbance (214nm) peak area] was used to calculate an apparent half-life of 12.2min for Leu^{27}(1-29)NH_2 and 121.5min. for the pMH^1 analog. Further, no peak corresponding to hGHRH (3-29)NH_2 was observed at any time point for the pMH^1 analog.

Table 1. *Potency of GHRH(129)NH_2 and its analogs to release GH from rat primary pituitary cells*[*].

Analog	N	EC_{50} (nM)
hGHRH(1-29)NH_2	6	0.09±0.01
L^{27},hGHRH(1-29)NH_2	5	0.30±0.07
des-NH_2Tyr^1,L^{27},hGHRH(1-29)NH_2	3	1.44±0.60
N-AcGly^1,L^{27},hGHRH(1-29)NH_2	6	2.12±0.43
pMH^1,L^{27},hGHRH(1-29)NH_2	6	0.14±0.06

[*]Pituitary cells were exposed to doses of each peptide ranging from 0nM to 20nM. GH secreted into the medium was measured by RIA [4]. Data obtained for each dose was analyzed by ALLFIT to obtain the median effective concentration for stimulating GH release (EC50). Values represent the mean±SEM for 36 determinations.

Previous studies have shown that the aromatic character and hydrogen bonding capability of Tyr^1 is critical for activity and replacement of Tyr^1 with most other residues has resulted in significant loss of receptor-ligand interaction [5]. We have shown that the use of a glycine linker to attach aromatic moieties to the N-terminus of hGHRH restores the activity that would normally be lost to a Gly^1 substitution. We believe the pMH^1 N-terminus could be integrated into the final stages of a recombinant synthesis to provide a potent, long-acting GHRH analog. In the course of this study, we found that *p*-methylbenzoyl Gly^1 (pMH) substituted GHRH provides a new analog with therapeutic potential for conditions of GH deficiency and insufficiency.

References

1. Fukata, J., Diamond, D., and Martin, J., *Endocrinology*, 117 (1985) 457.
2. Lance, V., Murphy, W., Sueiras-Diaz, I. and Coy, D., *Biochem. Biophys. Res. Comm.*, 119 (1984) 265.
3. Frohman, L., Downs, T., Williams, T., Heimer E., Pan, Y. and Felix, A., *J. Clin. Invest.*, 78 (1986) 906.
4. Heiman, M, Nekola, M., Murphy, W, Lance, V. and Coy, D., *Endocrin*, 116 (1985) 410.
5. Ling, N., Baird, A., Wehrenberg, W., Ueno, N., Munegumi, T., Chiang, T., Regno, M. and Brazeau, P., *Biochem. Biophys.Res.Comm.*, 122 (1984) 304.

Peptides: Chemistry, Structure and Biology
Pravin T.P. Kaumaya and Robert S. Hodges (Eds.)
Mayflower Scientific Ltd., 1996

263

The Design and Synthesis of Glucagon Antagonists by Modifications at Asp^{9}, Ser^{11}, Ser^{16}, Arg^{17,18} and Asp^{21}

N.S. Sturm, A.M. Hutzler, C.S. David, B.A. Van Tine, B.Y. Azizeh, D. Trivedi and V.J. Hruby

Department of Chemistry, University of Arizona, Tucson, AZ 85721, USA

Introduction

Diabetes mellitus is a widespread, degenerative disease that can be divided into two major categories: type I, or insulin dependent diabetes; and type II or non-insulin dependent diabetes. Type I diabetes is characterized by lack of suitable production of insulin by the beta cells of the pancreas, while in type II diabetes insulin levels are near normal, but increased gluconeogenesis and glycogenolysis are observed. According to Unger and Orci's [1, 2] bihormonal hypothesis of diabetes mellitus, insulin abnormality causes impairment of glucose utilization, and glucagon might be a primary mediator of the overproduction of glucose and ketone bodies in diabetes. Glucagon is a 29 residue polypeptide (MW=3,482) which interacts with hepatic receptors to stimulate glucose production and release during a hypoglycemic state (Figure 1).

```
1                5                  10                  15
H-His-Ser-Gln-Gly-Thr-Phe-Thr-Ser-Asp-Tyr-Ser-Lys-Tyr-Leu-Asp-Ser-Arg-Arg-Ala-
                      20                  25                  29
                      Gln-Asp-Phe-Val-Gln-Trp-Leu-Met-Asn-Thr-OH
```

Figure 1. *Primary sequence of glucagon.*

In order to obtain a complete understanding of the mechanism of action of glucagon and its involvement in the diabetic state, new insights into glucagon structure-activity relationships are needed. Synthetic glucagon analogues can be used as specific biochemical probes that might enhance and identify those molecular features essential for receptor recognition (the binding message) and those necessary for transduction of message and corresponding physiological response (the activity message).

Results and Discussion

Previous results from the Hruby [3] and Merrifield [4] laboratories were considered in conjunction with incorporation of neutral, hydrophobic amino acid residues in positions 9, 11 and 16 of the glucagon molecule. Six different glucagon analogues were designed, synthesized, characterized and evaluated for binding affinity and adenylate cyclase stimulation (Table 1).

Table 1. *Biological activities of synthetic glucagon analogues.*

	Binding		Adenylate Cyclase		
Compound	IC_{50}(nM)	Relative Binding Potency (%)	EC_{50}(nM)	Maximum % Stimulation	pA_2
Glucagon	1.5	100	8	100	
1-[desHis^1,Val^9, Ile^{11},Ile^{16}]-NH_2	6.0	25	ia @ 10μM	0	6.15
2-[desHis^1,Val^9, Val^{11},Val^{16}]-NH_2	6.0	25	ia @ 10μM	0	6.20
3-[desHis^1,Val^9, Leu^{11},Leu^{16}]-NH_2	11.0	14	ia @ 10μM	0	6.30
4-[desHis^1,Val^9, Leu^{11},Leu^{16},Lys^{17}, Lys^{18},Glu^{21}]- NH_2	6.5	23	ia @ 10μM	0	6.25
5-[desHis^1,Nle^9, Leu^{11},Leu^{16},Lys^{17}, Lys^{18},Glu^{21}]-NH_2	7.0	21	ia @ 10μM	0	7.25
6-[desHis^1,Nle^9, Ile^{11},Ile^{16}]-NH_2	9.0	17	ia @ 10μM	0	7.25

Compared to glucagon (IC_{50}=1.5nM), analogues **1-6** were found to have IC_{50} values of 6.0nM, 6.0nM, 11.0nM, 6.5nM, 7.0nM and 9.0nM, respectively. When these compounds were tested for their ability to block adenylate cyclase (AC) activity, they were found to be antagonists having no stimulation of AC and pA_2 values of 6.15, 6.20, 6.30, 6.25, 7.25 and 7.25, respectively. This suggests that replacing Asp^9, Ser^{11} and Ser^{16} with more hydrophobic residues, produces little loss in binding potency, while inhibiting adenylate cyclase activation. From a kinetic point of view, there is an interesting lack of correlation between glucagon antagonist binding and pA_2 values. This may be due, in part, to a difference in agonist *versus* antagonist binding which leads to varying dissociation rates.

Acknowledgments

This work was supported in part by a research grant from U.S. Public Health Service Grant DK-21085 and by HHMI 71109-52130.

References

1. Unger, R.H., *Metabolism*, 27 (1978) 1691.
2. Unger, R.H. and Orci, L., *Lancet*, 1 (1975) 14.
3. Krstenansky, J.L., Trivedi, D., Hruby, V.J., *Biochemistry*, 25 (1986) 3833.
4. Unson, C.G., Andreu, D., Gurzenda, E.M., Merrifield, R.B., *Proc. Natl. Acad. Sci.*, 84 (1987) 4083.

Peptides: Chemistry, Structure and Biology
Pravin T.P. Kaumaya and Robert S. Hodges (Eds.)
Mayflower Scientific Ltd., 1996

264
Betide Based Strategy for the Design of GnRH and Receptor Selective Somatostatin Analogs

C.A. Hoeger[1], G.-C. Jiang[1], S.C. Koerber[1], T. Reisine[2], G. Liapakis[2] and J.E. Rivier[1]

[1]The Clayton Foundation Laboratories for Peptide Biology, The Salk Institute for Biological Studies, La Jolla, CA 92037 USA
[2]Department of Pharmacology, University of Pennsylvania, Philadelphia, PA 19104, USA

Introduction

We have recently described the introduction of racemic α-Fmoc, α'-Boc-aminoglycine [Fmoc-D/L-Agl(Boc)] [1] and Fmoc-D/L-Agl(Me, Boc) into peptides as scaffolds for SAR studies (see J. Rivier, *et al.* this volume, p. 275). Acylation/alkylation of the side chain amino function of a newly incorporated Agl readily mimics the side chains of most amino acids by simply varying the acylating/alkylating agent employed. The use of these racemic betidamino acids for SAR, however, is predicated on the working hypothesis that aminoglycine and its alkylated and acylated derivatives are compatible with biological systems. We herein report on (i) the introduction of betidamino acids into a bioactive gonadotropin releasing hormone (GnRH) antagonist and (ii) their utilization in the identification and design of new receptor-specific somatostatin (SRIF) analogs.

Results and Discussion

Peptides were synthesized by SPPS using a Boc/benzyl strategy employing standard protocols [2]. After incorporation of either racemic Fmoc-Agl(Boc) or Fmoc-Agl(Me, Boc), removal of the Boc protection and acylation of the newly unmasked amino side chain using an appropriate acyl halide or carboxylic acid, the Fmoc group was cleaved and the synthesis completed. The SRIF analogs were oxidized (following HF cleavage) using I_2 in AcOH. The crude, diastereomeric peptide mixtures were purified by preparative RP-HPLC using two solvent systems [3]. A nomenclature scheme based on elution position in 0.1% TFA/CH_3CN has been adopted with the hydrophilic diastereomeric peptide being arbitrarily labeled as containing L or D-Agl(acyl) and the hydrophobic one as containing D or L-Agl(acyl). Peptides obtained were characterized by HPLC, CZE and LSIMS and shown to have purities in excess of 95%.

To investigate biocompatability of the betide scaffold, we prepared Agl(acyl)-substituted analogs of the GnRH antagonist Acyline [Ac-D2Nal-D4Cpa-D3Pal-Ser-4Aph(Ac)-D4Aph(Ac)-Leu-ILys-Pro-DAla-NH_2] (4Aph is 4-aminophenylalanine, Ilys is N^{ε}-isopropyllysine) [4]. Acyline is fully active in an antiovulatory assay at 2.5 μg/rat

and is long acting; replacement of D-2Nal with L-2Nal decreases the potency by a factor of ten (full inhibition at 25 μg/rat). Using the corresponding betidamino derivative D/L-Agl(2-naphthoyl) [b2Nal], one diastereomer ([Ac-L- or D-b2Nal^1]Acyline) obtained was equipotent to Acyline and the other one ([Ac-D- or L-b2Nal^1]Acyline) was less potent by only a factor of two . Replacing the D3Pal at position 3 with D/L-Agl(3-nicotinoyl) [b3Pal] gave diasteromeric peptides equipotent to the parent Acyline. These results (and others) lead to the conclusion that acylated Agl substitutions are compatible with biological systems and that D- and L-betidamino acid containing peptides (most of the time) only differ in potency by a factor of 1 to 5 (*versus* 5-1000 fold difference for the corresponding D- and L-amino acid substitutions in most peptides), suggesting that peptides with D- and L-betidamino acid substitutions may assume similar conformations.

Using this betidamino strategy, we have begun to probe the structural requirements of the five known membrane-associated SRIF receptor subtypes (SSTR1-5), as only few receptor-specific SRIF ligands have been identified [5]. We report the biological effect of Agl-based substitutions at position 8 of des-AA^{1,2,4,5,12,13}[DTrp^8]SRIF, (Cys^3-Phe^6-Phe^7-DTrp^8-Lys^9-Thr^{10}-Phe^{11}-Cys^{14}), an analog with good affinity at all five cloned SRIF receptors. Both des-AA^{1,2,4,5,12,13}[D- and L-b2Nal^8]SRIF had IC_{50} > 1000 nM at SSTR1-5. Using Fmoc-D/LAgl(Me, Boc) provided des-AA^{1,2,4,5,12,13}[L- or D-bβMe2Nal^8]SRIF which showed marked selectivity for SSTR1 and SSTR3 (IC_{50} 600 and 200 nM resp.). The other diastereomeric peptide, des-AA^{1,2,4,5,12,13}[D- or L-bβMe2Nal^8]SRIF, had high selectivity and good potency for SSTR3 only (IC_{50} = 62 nM and IC_{50} > 1000 nM for SSTR1, 2, 4 and 5). Presumably, the introduction of the methyl group on the side chain of the betidamino acid influenced the available range of accessible conformational space, increasing the specificity of the ligand toward one receptor while concomitantly decreasing specificity toward the others. The conformational basis of these results is being investigated spectroscopically and computationally. Longitudinal scans (each amino acid in a sequence is substituted by the corresponding alkylated and non-alkylated betidamino acids) and orthogonal betide scans (libraries where Agl is reacted with a large number of acylating agents) will play a major role in peptide drug discovery.

Acknowledgments

This work was supported by NIH grants DK 26741, HD 13527, MH 45533, MH 48518 and the Hearst Foundation. We are indebted to W. Low, P. Arballo, T. Goedken, D. Pantoja, Dr. A. G. Craig and C. Miller for their expert assistance in the synthesis, purification and chemical characterization of the GnRH and SRIF analogs.

References

1. Qasmi, D., René, L. and Badet, B., *Tetrahedron Lett.*, 34 (1993) 3861.
2. Stewart, J.M. and Young, J.D. (Eds.), 'Solid Phase Peptide Synthesis', Pierce Chemical Co., Rockford, IL, 1984.
3. Hoeger, C., Galyean, R., Boublik, J., McClintock, R. and Rivier, J., *Biochrom.*, 2 (1987) 134.
4. Rivier, J.E., Jiang, G., Porter, J., Hoeger, C., Craig, A.G., Corrigan, A., Vale, W. and Rivier, C.L., *J. Med. Chem.* 38 (1995) 2649.
5. Bell, G.I. and Reisine, T., *Trends in Neu. Sci.*, 16 (1993) 34.

Peptides: Chemistry, Structure and Biology
Pravin T.P. Kaumaya and Robert S. Hodges (Eds.)
Mayflower Scientific Ltd., 1996

265

An Enzymatic-Chemical Synthesis of Insulins with Non-proteinogenic Amino Acid Residues *via* Chain Condensation and Subsequent Disulfide Folding

V.J. Lenz, M. Leithäuser, M. Casaretto, H.G. Gattner, D. Brandenburg and H. Höcker

Deutsches Wollforschungsinstitut an der TH Aachen e.V., Veltmanplatz 8, D-52062 Aachen, Germany

Introduction

The production of proteins containing non-proteinogenic amino acid residues by recombinant techniques is methodically limited. In order to obtain insulins with non-proteinogenic amino acid residues a convenient enzymatic-chemical approach was pursued, which circumvents the oxidative combination of the separate A- and B-chain. The approach is based on the enzymatic condensation of both chains with subsequent oxidative folding of the monocatenate species. In this study, the practicability of the method for preparing insulins with non-proteinogenic amino acid residues is illustrated by the synthesis of [Tyr$(NO_2)^{A14}$,Abz^{B1}]des-B30-single-chain insulin containing 2-amino- benzoic acid (Abz) and 3-nitrotyrosine. This donor/acceptor pair can be used for distance dependent resonance-energy transfer measurements [1].

Results and Discussion

[Tyr$(NO_2)^{A14}$,Abz^{B1}]des-B30-single-chain insulin **1** was synthesized to investigate the distance dependent intramolecular resonance-energy transfer between Abz^{B1} and Tyr$(NO_2)^{A14}$ [2], which should allow the monitoring of the formation of tertiary stucture by fluorescence emission measurements made during oxidative folding.

[Tyr$(NO_2)^{A14}$]insulin-(A1-A21)-peptide **2** was prepared by SPPS on Wang-resin using the Fmoc/TBTU protocol whereas N^{B1}-Boc[Abz^{B1}]insulin-(B1-B29)-peptide **3** was obtained by semisynthesis from native insulin. For the synthesis of **1**, Lys^{B29} of **2** and Gly^{A1} **3** were condensed using lysyl endopeptidase (LEP) catalysis. After Boc deprotection, reduction with mercaptoethanol and removal of the reducing agent, oxidation in air yielded the disulfide-folded product **1** (RP-HPLC purity 93%). In Figure 1A, RP-HPLC tracings of acid trapped folding intermediates and products at different times of air oxidation are shown. Fluorescence emission spectra recorded at different reaction times (Figure 1B) reveal that the oxidative folding and formation of tertiary structure are accompanied by an increase of energy transfer from the donor to the acceptor (decrease of fluorescence quantum yield) and demonstrate that distance dependent processes during oxidative folding can be followed by the method.

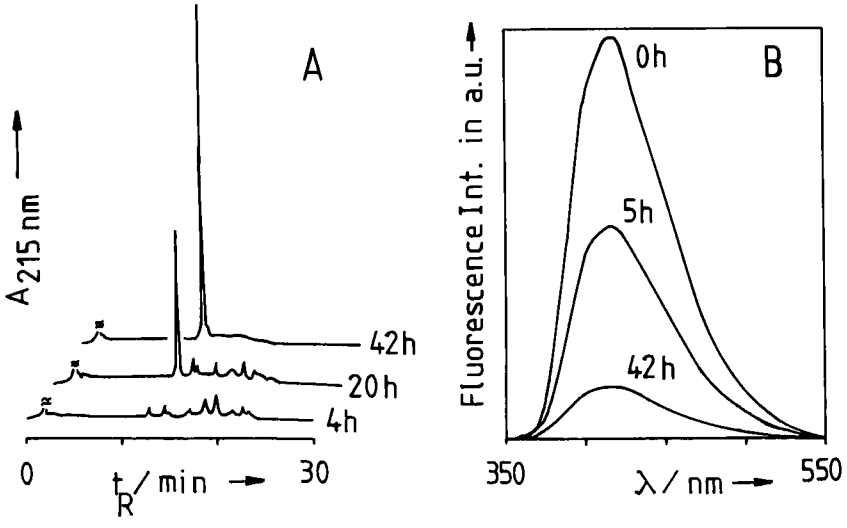

Figure 1. *(A) RP-HPLC diagrams of acid trapped samples during the oxidative folding of [Tyr(NO$_2$)^{A14},Abz^{B1}]des-B30-single-chain insulin* ***1****. The hexathiol form was oxidized under air in aqueous 0.1 M glycine/NaOH buffer at pH 10.6, c(protein) = 0.5 mg / ml. (B) Fluorescence emission spectra at different times of the oxidative folding of* ***1****. Excitation wavelength: 350 nm.*

After isolation of the folded product **1**, it was proteolyzed by LEP to yield the dicatenate des-(B30)-insulin derivative. A LEP catalyzed transpeptidation carried out according to the procedure described in the literature [3] leads to the full-chain insulin analogue. The enzymatic-chemical approach described in this study allows us to prepare efficiently single-chain insulins as well as dichenar insulins starting from native and/or synthetic chains.

Acknowledgments

Insulin and LEP were generous gifts of Dr. R. Obermeier, Hoechst AG, Frankfurt/M. (Germany). This work was supported by a grant of the DFG.

References

1. Carmel, A., Kessler, E. and Yaron, A., *Eur. J. Biochem.*, 7 (1977) 617.
2. Lenz, V.J., Gattner, H.-G., Leithäuser, M., Brandenburg, D., Wollmer, A. and Höcker, H., *Anal. Biochem.*, 221 (1994) 85.
3. Morihara, K. and Ueno, Y., *Biotechn. Bioeng.*, 37 (1991) 693.

Peptides: Chemistry, Structure and Biology
Pravin T.P. Kaumaya and Robert S. Hodges (Eds.)
Mayflower Scientific Ltd., 1996

266

The Development of Non-peptide NK_3 Receptor Antagonists: The Application of a Dipeptide Chemical Library to Drug Design

P. Boden, J.M. Eden, J. Hodgson, D.C. Horwell, W. Howson, K. Meecham, N. Suman-Chauhan, M.C. Pritchard and J. Raphy

Parke-Davis Neuroscience Research Centre, Addenbrookes Hospital Site, Hills Road, Cambridge, CB2 2QB, England, UK

Introduction

We have previously reported the development of NK_1 and NK_2 tachykinin receptor antagonists by the application of a "peptoid" design strategy [1, 2]. This paper describes how a synthetic dipeptide library [3] has been implemented in the development of nanomolar dipeptide [4] and subsequently non-peptide [5] NK_3 receptor selective antagonists.

Results and Discussion

From the screening of our dipeptide chemical library through a cloned human NK_3 receptor binding assay, Boc(S)Phe(S)PheNH_2 (IC_{50}=1550nM) was identified as an initial lead compound. Conformational constraint was first introduced into this dipeptide by alpha-methylation at the C-terminal phenylalanine residue to give Boc(S)Phe(RS) αMePheNH_2, (IC_{50}=1520nM). Examination of the C-terminal SAR of this dipeptide led to a series of modified dipeptides exemplified by PD 157672 Boc(S)Phe(R)αMePhe $NH(CH_2)_7NHCONH_2$, (IC_{50}=16nM). This compound is selective for the NK_3 receptor over the NK_1 and NK_2 receptors and acts as a competitive NK_3 receptor antagonist in human and guinea pig functional assays [4].

Our next consideration was to reduce the peptidic nature of this ligand and hence the replacement of the N-terminal Boc(S)Phe moiety was investigated. The αMeTrp derivative (RS)isopropylbenzyloxycarbonyl(RS)αMeTrp(Sαmethylbenzylamine was prepared as part of our NK_1 receptor program. As this compound was found to have micromolar affinity for the NK_3 receptor (IC_{50}=1200nM), the N-terminal isopropylbenzyloxycarbonyl moiety was identified as a possible replacement for the N-terminal BocPhe moiety in our dipeptide ligands. Replacement of the N-terminal BocPhe moiety in PD157672 with (S)isopropylbenzyloxycarbonyl resulted in a non-peptide ligand with an IC_{50} value of 43nM for the NK_3 receptor.

Optimization of the phenyl ring of the αMePhe residue led to identification of PD 161182 (Figure 1) which binds selectively to the NK_3 receptor with an IC_{50} value of 7nM.

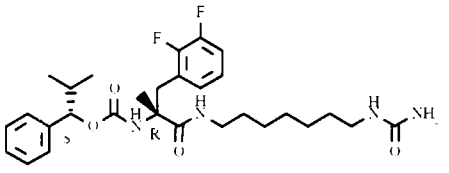

Figure 1. *PD 161182.*

In vitro functional assays in human and guinea pig paradigms indicate that PD 161182 is a competitive NK_3 receptor antagonist (Table 1).

Table 1. *In vitro functional data for PD 161182.*

In vitro functional assays, (Ke, nM)		Binding affinities (IC_{50}, nM)	
CHO cells[a]	GP[b] habenula	CHO cells[c]	GP[d]
0.9(0.5-1.5)	6(4-7)	7(6-10)	4(1-6)

a,b,c,d see reference [4].

We have described how a micromolar lead obtained from a dipeptide library has been developed into a high affinity non-peptide NK_3 receptor selective antagonist. To our knowledge this represents the first example of the development of high affinity non-peptide antagonists for a membrane bound peptide receptor based on the screening of a synthetic peptide library.

References

1. Boyle, S., Guard, S., Higginbottom, M., Horwell, D.C., Howson, W., McKnight, A.T., Martin, K., Pritchard, M.C., O'Toole, J., Raphy, J., Rees, D.C., Roberts, E., Watling, K.J., Woodruff, G.N. and Hughes, J., *Bioorg. Med. Chem.*, 2 (1994) 357.
2. Boyle, S., Guard, S., Hodgson, J., Horwell, D.C., Howson, W., Hughes, J., McKnight, A.T., Martin, K., Pritchard, M.C., Watling, K.J. and Woodruff, G.N., *Bioorg. Med. Chem.*, 2 (1994) 101.
3. Horwell, D.C., Howson, W., Ratcliffe, G.S. and Rees, D.C., *Bioorg. Med. Chem. Lett.*, 13 (1993) 799.
4. Boden, P., Eden, J.M., Hodgson, J., Horwell, D.C., Howson, W., Hughes, J., McKnight, A.T., Meecham, K., Pritchard, M.C., Raphy, J., Ratcliffe, G.S., Suman-Chauhan, N. and Woodruff, G.N., *Bioorg. Med. Chem. Lett.*, 4 (1994) 1679.
5. Boden, P., Eden, J.M., Hodgson, J., Horwell, D.C., Pritchard, M. C., Raphy, J. and Suman-Chauhan, N., *Bioorg. Med. Chem. Lett.*, in press.

Peptides: Chemistry, Structure and Biology
Pravin T.P. Kaumaya and Robert S. Hodges (Eds.)
Mayflower Scientific Ltd., 1996

267

Amino-methylene, ψ(CH_2NH) Substitution of Amide Bonds in the C-terminal Portion of the Insulin B Chain

M. Zhao and R.D. DiMarchi

Division of Endocrine Research, Lilly Research Laboratories, Indianapolis, IN 46285, USA

Introduction

This paper describes our continuing effort to develop insulin analogs with optimized pharmacodynamics for improved control of blood glucose and to evaluate the importance of the insulin C-terminal B chain region in insulin self-association. Our current approach is based on the introduction of cationic charge repulsion in the insulin dimer interface through substitution of the naturally occurring amide bond with an amino-methylene, ψ[CH_2NH] moiety.

Results and Discussion

A sequential series of ψ[CH_2NH] human insulin analogs in the B24-29 region were prepared by a combination of chemical methodologies including solid-phase, solution-phase and semisynthetic techniques.

All new peptides were studied, *in vitro*, by assaying for their ability to interact with both insulin and IGF-1 receptors on human placental membranes [1] and to stimulate glucose transport in isolated rat adipocytes [2]. As shown in Table 1, whereas most analogs retain considerable biological activity, the replacement of the peptide amide bonds in both Phe^{B24} and Phe^{B25} results in analogs with severely decreased biological potency. To examine the causes for the extremely low biological potencies observed in these Pheψ[CH_2NH] analogs, we further explored four additional analogs bearing both the ψ[CH_2NH] and a single D-amino acid substitution at position B24, B25 or B26 (Table 1). However, these substitutions afforded only inactive insulin analogs.

The effects of introducing the ψ[CH_2NH] unit in the C-terminal B chain region on insulin self-association was examined using equilibrium ultracentrifugation (Figure 1) [3]. All of the analogs examined were shown to self-associate to a considerably lesser extent than native human insulin. In particular, the replacement of the amide bond with the ψ[CH_2NH] unit within the aromatic B24-B26 region led to even less aggregated analogs than [Lys^{B28}, Pro^{B29}]-insulin, LysPro. It is known from analysis of the 2 Zn X-ray structure of insulin that the Phe^{B24}, Phe^{B25} and Tyr^{B26} residues play a critical role in the formation of an anti-parallel β-sheet within the dimer [4]. Therefore, the introduction of cationic charge repulsion in the aromatic β-sheet forming region effectively weakened the insulin dimer association.

Table 1. *Relative receptor binding affinity and biological activity in the isolated rat adipocyte assay.*

Peptides	Receptor binding potency		Biological
	Insulin	IGF-1	potency
Human insulin	1.00	1.00	1.00
IGF-1	0.03±0.003	402.45±92.31	---
[Phe^{B24}ψ(CH$_2$NH)]-HI	0.03±0.003	0.14±0.07	0.01
[Phe^{B25}ψ(CH$_2$NH)]-HI	0.02±0.003	0.23±0.15	0.01
[Try^{B26}ψ(CH$_2$NH)]-HI	1.25±0.19	2.06±0.76	0.76
[Thr^{B27}ψ(CH$_2$NH)]-HI	0.47±0.06	0.52±0.21	0.53
[Pro^{B28}ψ(CH$_2$NH)]-HI	1.09±0.10	1.65±0.47	0.90
[Lys^{B29}ψ(CH$_2$NH)]-HI	1.05±0.17	1.19±0.22	0.94
[D-Phe^{B24}ψ(CH$_2$NH)]-HI	<0.01		
[D-Phe^{B25}ψ(CH$_2$NH)]-HI	<0.001		
[D-Phe^{B24},Phe^{B25}ψ(CH$_2$NH)]-HI	<0.01		
[D-Tyr^{B26},Phe^{B25}ψ(CH$_2$NH)]-HI	<0.001		

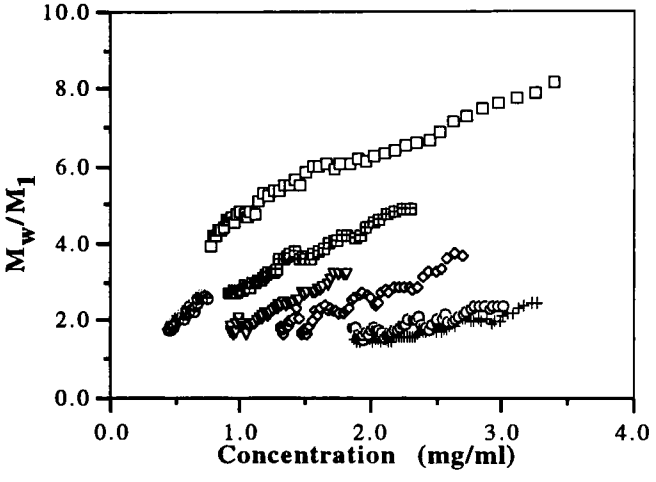

Figure 1. *Equilibrium ultracentrifugation of human insulin and analogs in the absence of Zn. Human insulin (□); LysPro (◊); Phe^{B24}ψ(CH$_2$NH)-insulin (○); Tyr^{B26}ψ(CH$_2$NH)-insulin (+); Thr^{B27}ψ(CH$_2$NH)-insulin (△); Pro^{B28}ψ(CH$_2$NH)-insulin (▽);Lys^{B29} (CH$_2$NH)-insulin (⊕).*

References

1. De Meyts, P., in Blecker, M. (Ed.), 'Methods in Receptor Research' (in Laskin, A.I. and Last, J.A., (Eds.), Mol. Biology, vol. 9, part 1), Dekker, New York, 1976, p. 301.
2. Moody, A., Stan, M.A., Stan, M. and Gliemann, J., *Horm. Metab. Res.*, 6 (1974) 12.
3. Brems, D.N., Alter, L.A., Beckage, M.J., Chance, R.E., DiMarchi, R.D., Green, L.K., Long, H.B., Pekar, A.H., Shields, J.E. and Franks, B.H., *Protein Eng.*, 5 (1992) 527.
4. Baker, E.N., Blundell, T.L., Cutfield, J.F., Cutfield, S.M., Dodson, E.J., Dodson, G.G., Hodgkin, D.M.C., Hubbard, R.E., Isaacs, N.W., Reynolds, C.D., Sakabe, K., Sakabe, N. and Vijayan, N.M., *Philos. Trans. R. Soc. London (Biol.)*, 319 (1988) 369.

Peptides: Chemistry, Structure and Biology
Pravin T.P. Kaumaya and Robert S. Hodges (Eds.)
Mayflower Scientific Ltd., 1996

268
Sequential Replacement of the C-terminal Residues of the Human Insulin B Chain with Alanine

M. Zhao, L. Fan, H.B. Long, A.H. Pekar, L.J. Slieker, R.E. Chance and R.D. DiMarchi

Division of Endocrine Research, Lilly Research Laboratories, Indianapolis, IN 46285, USA

Introduction

In the view of their importance in insulin self-association and biological activity, the C-terminal residues (B24-B30) of the human insulin B chain have been the subject of numerous physicochemical and biological activity studies. Previous studies indicated that the absence of the terminal pentapeptide, Tyr-Thr-Pro-Lys-Thr, is of only modest biological consequence, and yet its presence is required for proper insulin self-association. Here we report our attempt to examine the effect of each amino acid residue in the C-terminal B chain pentapeptide on insulin self-association through the sequential substitution of each naturally occurring amino acid residue with L-alanine.

Results and Discussion

The human insulin analogs were prepared either by conventional solid-phase and trypsin-catalyzed semisynthetic methods, or by chain combination using a synthetic B chain analog and an *E. coli*-expressed A chain. Each analog was assayed both for its affinities to the human placental insulin and IGF-1 receptors (Table 1) and its propensity to self-associate (Figure 1). Our results demonstrate that sequential alanine substitutions in this region of insulin have only modest changes in biological effects relative to human insulin, which is consistent with the previous structure-function analysis in this region. In equilibrium sedimentation experiments, each analog presented a diminished propensity to self-associate when compared to the native human insulin. The largest disruption to association was observed in [Ala^{B26}]-insulin. The 2 Zn insulin X-ray crystal structure revealed that both of the Tyr^{B26} residues in the insulin dimer are involved in the formation of hydrogen bonds and hydrophobic interactions within the anti-parallel β-sheet of the C-terminal region of the B chains [1]. Consequently, it was expected that the alanine replacement for Tyr^{B26} would result in an analog with the weakest self-association in the series. The fact that [Ala^{B27}]- and [Ala^{B29}]-insulin analogs showed a similar reduced capacity for self-aggregation indicates that a nonpolar amino acid residue, such as alanine, at either B27 or B29 positions can also significantly alter insulin aggregation. This also suggests that the native Thr^{B27} and Lys^{B29} play a role in stabilizing the insulin dimer. An unexpected result is observed in the study of [Ala^{B28}]-insulin. Its

Table 1. *Receptor binding assays.*

Peptides	Relative receptor binding affinity	
	Insulin	IGF-1
Human insulin	1.00	1.00
IGF-1	0.017 ± 0.001	456.84 ± 158.41
[Ala^{B26}]-Human insulin	0.87 ± 0.04	0.64 ± 0.05
[Ala^{B27}]-Human insulin	0.95 ± 0.05	1.28 ± 0.04
[Ala^{B28}]-Human insulin	0.37 ± 0.06	0.43 ± 0.03
[Ala^{B29}]-Human insulin	0.62 ± 0.02	0.43 ± 0.07
[Ala^{B30}]-Human insulin	1.01 ± 0.09	0.87 ± 0.04

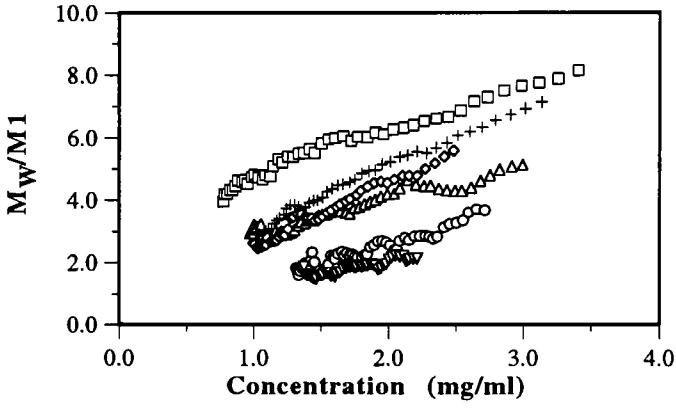

Figure 1. *Equilibrium ultracentrifugation of human insulin and analogs in the absence of Zn. Ala^{B26}-insulin (▽); Ala^{B27}-insulin (◊); Ala^{B28}-insulin (+); Ala^{B29}insulin (△); LysPro (○).; Human insulin (□).*

aggregation profile shows that it self-associates slightly better than the other analogs in this series. The importance of the Pro^{B28} residue in insulin self-association is recognized. Our findings surprisingly demonstrate that modification of Pro^{B28} can yield an insulin analog with high-affinity self association. Furthermore, [Ala^{B28}]-insulin showed a relatively low bioactivity *in vitro* but was fully active *in vivo* (unpublished data). In conclusion, our study demonstrates a clear structural basis for optimal insulin self-association.

References

1. Baker, E.N., Blundell, T.L., Cutfield, J.F., Cutfield, S.M., Dodson, E.J., Dodson, G.G., Hodgkin, D.M.C.,Hubbard, R.E., Isaacs, N.W., Reynolds, C.D., Sakabe, K., Sakabe, N. and Vijayan, N.M., *Philos. Trans. R. Soc. London (Biol.)*, 319 (1988) 369.

Peptides: Chemistry, Structure and Biology
Pravin T.P. Kaumaya and Robert S. Hodges (Eds.)
Mayflower Scientific Ltd., 1996

269

Development of Cyclic Casomorphin Analogs with Potent δ Antagonist and Balanced Mixed μ Agonist/ δ Antagonist Properties

R. Schmidt, N.N. Chung, C. Lemieux and P.W. Schiller

Laboratory of Chemical Biology and Peptide Research, Clinical Research Institute of Montreal, Montreal, Quebec, H2W 1R7, Canada

Introduction

Recently, the cyclic casomorphin analog H-Tyr-c[-D-Orn-2-Nal-D-Pro-Gly-] (**1**) has been shown to be an opioid peptide with mixed μ agonist/δ antagonist properties [1]. Compounds with this activity profile are thought to have potential as analgesics that may not produce tolerance and dependence [2]. Structure-activity studies of this class of opioid peptides revealed that the 2-Nal[3] residue could be replaced by aromatic amino acid residues containing a second aromatic ring without compromising δ antagonism. However, these modifications resulted in an almost complete loss of μ activity [3]. Therefore, in the present study, the 2-Nal[3] residue was maintained and parent peptide **1** was modified in position 1 by substitution of Tyr with N-MeTyr (**2**) or 2',6'-dimethyl-tyrosine (Dmt)(**3**) and in the 5-position by replacement of Gly with α-aminoisobutyric acid (Aib)(**4**), N-methylaminoisobutyric acid (MeAib)(**5**), β-Ala (**6**), D- or L-Ala (**7**,**8**), sarcosine (Sar)(**9**) or D- or L-N-methylalanine (MeAla)(**10**,**11**).

Results and Discussion

The cyclic ß-casomorphin analogs were synthesized by conventional solution synthesis (**1-5**) or manual solid-phase peptide synthesis on Sasrin resin (**6-11**). The opioid activity profiles of the peptides were determined using the GPI- and MVD bioassays and receptor binding assays based on displacement of [^{3}H]DAMGO (μ-selective) and [^{3}H]DSLET (δ-selective) from rat brain membrane binding sites.

N-Methylation of the Tyr[1] residue of **1** resulted in a compound (**2**) with 4 times higher potency in the GPI assay and almost 10-fold increased δ antagonist potency in the MVD assay (Table 1). The Dmt[1]-analog (**3**) bound to both μ and δ receptors with affinities in the subnanomolar range (~0.5 nM), was a potent μ-agonist (IC_{50} = 7.88 nM), and showed 100 fold increased δ antagonist potency as compared to analog **1**. Thus, this compound is a highly potent and balanced mixed μ agonist/δ antagonist.

Table 1. *Opioid activities and receptor affinities of cyclic β-casomorphin-5 analogs.*

no.	GPI	MVD			Binding assay		
	IC_{50}, nM	IC_{50}, nM	K_e, nM		K_i^{μ} nM	K_i^{δ}, nM	K_i^{μ}/K_i^{δ}
			Deltorphin I	DPDPE			
1	384		202	233	5.89	17.2	0.342
2	92.5		38.8	45.9	1.70	1.30	1.31
3	7.88		3.37	2.13	0.460	0.457	1.01
4	477		55.8	31.6	22.6	4.53	5.00
5	288		480	370	29.2	9.04	3.23
6	609	1000(25%)[a]			67.4	66.7	1.01
7	600		5.99	5.35	72.0	0.755	95.4
8	108		950	1290	16.4	107	0.153
9	159		7.81	11.2	14.8	2.41	6.14
10	355	1000(30%)[a]			10.8	66.9	0.161
11	35.3	3000(25%)[a]			14.5	282	0.0514

[a] Partial agonist; value in parentheses indicates maximal inhibition of the electrically evoked contractions.

Compounds **6**, **10** and **11** were partial δ agonists, whereas compounds **5** and **8** showed weaker δ antagonism than parent peptide **1**. Analogs **4**, **7** and **9** turned out to be mixed μ agonist/δ antagonists, displaying 5-40 fold enhanced δ antagonist potency in the MVD assay and similar μ agonist activity in the GPI assay in comparison with compound **1**. Interestingly, the D-Ala^5 containing analog **7** showed subnanomolar affinity for the δ receptor, but low μ receptor affinity representing the most δ selective β-casomorphin-5 analog reported to date. The δ binding affinities of the antagonists are in good correlation with the δ antagonist potencies determined in the MVD assay ($r = 0.945$).

Acknowledgment

Supported by grants from the MRCC (MT-5655) and NIDA (DA-04443).

References

1. Schmidt, R., Vogel, D., Mrestani-Klaus, C., Brandt, W., Neubert, K., Chung, N.N, Lemieux, C. and Schiller, P.W., *J. Med. Chem.*, 37 (1994) 1136.
2. Abdelhamid, E.E., Sultana, M., Portoghese, P.S. and Takemori, A.E., *J. Pharmacol. Exp. Ther.*, 258 (1991) 299.
3. Schmidt, R., Chung, N.N., Lemieux, C., Wilkes, B.C. and Schiller, P.W., In Maia, H.L.S. (Ed.), 'Peptides 1994', ESCOM, Leiden, The Netherlands 1995, p. 605.

Peptides: Chemistry, Structure and Biology
Pravin T.P. Kaumaya and Robert S. Hodges (Eds.)
Mayflower Scientific Ltd., 1996

270
Galanin: Structure-Function Study

K. Yamabe[1], H. Kakuyama[2], N. Takatsuka[2], T. Mochizuki[2], N. Kurokawa[3], C. Yanaihara[3] and N. Yanaihara[4]

[1]Nihon PerSeptive Ltd, Osaka 532, Japan
[2]University of Shizuoka, Shizuoka 422, Japan
[3]Osaka University School of Medicine, Suita, Osaka 565, Japan
[4]Yanaihara Institute Inc., Fujinomiya, Shizuoka 418, Japan

Introduction

Galanin, a 29- amino acid peptide, was originally isolated from porcine intestine [1] and subsequently reported to be widely distributed in the peripheral and central nervous systems [2, 3]. Using synthetic galanin fragments and analogs, we have been able to demonstrate that the receptor binding site of galanin resides in the N-terminal portion of the peptide [4-7]. Recently, we have demonstrated that galanin(1-15) analog, such as [D-Thr^6, D-Trp^{8,9}]-galanin(1-15)-ol, acts as an antagonist for the inhibitory effect of galanin on glucose-induced insulin release *in vitro* [6]. In this study, we have examined the structural requirement of galanin for occupancy of rat hippocampal and human small cell lung carcinoma (SCLC) cell membranes, and the effects of galanin-related peptides on $[Ca^{2+}]_i$ mobilization in human SCLC (SBC-3A) and glucose-induced insulin release from the isolated rat pancreas were compared.

Results and Discussion

Binding study: Table 1 shows comparison of the ability of galanin-related peptides to inhibit the binding of ^{125}I-rat galanin and ^{125}I-human galanin in rat hippocampal and human SBC-3A cell membranes, respectively. Human and rat galanin and galanin(1-15) were found to be nearly equipotent in displacing the tracer on human SBC-3A cell membranes, whereas the C-terminal fragments such as human galanin(9-30) and galanin(16-30) did not displace ^{125}I-human or -rat galanin even at concentration up to 10^6M (data not shown). Among the analogs examined, [D-Trp^8]-galanin(1-15)-ol showed significantly higher affinity than those of human and rat galanins on both rat hippocampal and human SBC-3A cell membranes, suggesting the importance of D-Trp at postion 8 for the binding.

Effect of galanin-related peptides on $[Ca^{2+}]i$ mobilization: Galanin(1-15)-ol and [D-Trp^8]-galanin(1-15)ol as well as human and rat galanins increased $[Ca^{2+}]_i$ mobilization significantly in human SBC-3A cells (Table 1), while galanin(1-11) and human galanin(9-30) and (16-30) did not show any effect on $[Ca^{2+}]_i$ (data not shown). These results indicate strongly that the active site of galanin resides in the N-terminal 1-15 sequence. For binding assays with rat hippocampal membranes, ^{125}I-rat galanin was used

Table 1. *Relative potencies of galanin-related peptides in binding ability and their effects on $[Ca^{2+}]i$ mobilization.*

	Relative potency (%)		$[Ca^{2+}]_i$ mobilization
	Rat hippocampus	SBC-3A cell	in SBC-3A cell
Human galanin	105.8	100	+
Rat galanin	100	144.0	+
Tuna galanin	12.6	4.2	not tested
Galanin (1-15)	11.4	92.4	+
[D-Trp^8]-galanin (1-15)-ol	175.0	549.0	+

as radiolabeled ligand, while ^{125}I-human galanin was used for assays with human SBC-3A membranes. Potencies relative to that of galanin are calculated as [IC_{50}: human galanin/IC_{50}: galanin related peptide] x 100.

Effects of galanin analogs on glucose-induced insulin release: Synthetic tuna galanin with Ala at position 6 showed binding affinity to both the hippocampal and SBC3A membranes, although the potency was lower than those of mammalian galanins. However, synthetic tuna galanin peptide at 10^{-8}M did not cause any inhibition against glucose-induced insulin release. Synthetic [Ala^6, D-Trp8]-galanin(1-15)-ol at 10^{-8}M did not show any significant effect on glucose-induced insulin release. However, synthetic [Ala^6, D-Trp^8]-galanin(1-15)-ol as well as [D-Thr^6, D-Trp^{8,9}]galanin(1-15)-ol at 10^{-7}M were found to abolish the inhibitory effect of 10^{-9}M rat galanin on glucose-induced insulin release in the isolated perfused rat pancreas.

The present study revealed clearly the importance of the N-terminal 1-15 sequence of galanin for receptor binding and $[Ca^{2+}]_i$ mobilization in human SBC-3A cells. In addition, the present results suggests that both [D-Trp^8]-galanin(1-15)-ol and [Ala^6, D-Trp^8]-galanin(1-15)-ol may be a key compound for development of galanin super-agonist or antagonist.

References

1. Tatemoto, K., Rökaeus, Å., Jörnvall, H., McDonald, T.J. and Mutt., V., *FEBS Lett.*, 164 (1983) 124.
2. Rökaeus, Å., Melander, T., Hökfelt, T., Lundberg, J.M., Tatemoto, K., Carlquist, M. and Mutt., V., *Neurosci.Lett.*, 47 (1984) 161.
3. Ching, J.L., Christofides, N.D., Anand, P., Gibson, S.J., Allen, Y.S., Su, H.C., Tatemoto, K., Morrison, J.F., Polak, J.M. and Bloom, S.R., *Neuroscience*, 16 (1985) 343.
4. Kuwahara, A., Ozaki, T. and Yanaihara, N., *Regul.Pept*, 29 (1990) 23.
5. Yanaihara, N., Mochizuki, T., Iguchi, K., Hoshino, M., Nagashima, T., Takatsuka, N., Ishikawa, J., Greeley Jr., G.H., Yanaihara, C. and Kuwahara, A, in Hokfelt, T., Bartfai, T., Jacobowitz D., and Ottoson, D., Eds.), 'Galanin', Macmillan Education Ltd, (1991) pp. 185.
6. Yanaihara, N., Mochizuki, T., Takatsuka, N., Iguchi, K., Sato, K., Kakuyama, H., Li, M. and Yanaihara, C., *Regul.Pept.*, 46 (1993) 93.
7. Hedlund, P.B., Yanaihara, N. and Fuxe K., *Eur. J. of Pharmac.*, 224 (1992) 203.
8. Habu, A., Ohishi, T., Mihara, S., Ohkubo, R., Hong, Y.-M., Mochizuki, T. and Yanaihara, N., *Biomed.Res.*, 15 (1994) 357 .

Peptides: Chemistry, Structure and Biology
Pravin T.P. Kaumaya and Robert S. Hodges (Eds.)
Mayflower Scientific Ltd., 1996

271
Synthesis and Biological Activities of Glycopeptides of Tachykinin NK_2 Receptor Antagonists

D. Pinzani[1], A.M. Papini[1], M.E. Vallecchi[1], M. Chelli[1], M. Ginanneschi[1], C.A. Maggi[2], R. Patacchini[2], M. Astolfi[2], L. Quartara[2], F.M. Arcamone[2] and G. Rapi[1]

[1]*Dipartimento di Chimica Organica "Ugo Schiff" and Centro di Studio sulla Chimica e la Struttura dei Composti Eterociclici e loro Applicazioni, Università di Firenze, Via Gino Capponi 9, I-50121 Firenze, Italy*
[2]*Dipartimento di Chimica e Farmacologia, A. Menarini Industrie Farmaceutiche Riunite, Via Sette Santi 3, I-50131 Firenze, Italy*

Introduction

The oligosaccharide moieties of glycoproteins and other glycoconjugates of the biological membranes play a key role in cell-cell recognition. This fact may be due to the strongly hydrophilic chains, normally located at the outer surface of the molecules in aqueous environments, which render them available for the interaction with other molecules. Glycosylation may also affect the conformation and the stability of proteins [1]. Relevant effects of glycosylation have been proved also on small peptides. For example, the introduction of sugar moieties on small hydrophobic peptides can produce the formation of compact, turn folded conformations in aqueous solvents [2]. Among the peptides of the tachykinin family, SP, NKA and NKB play a transmitter role in mammals. These peptides act as the preferred, yet not exclusive, endogenous ligands at either peripheral or central level for three distinct receptors termed NK_1, NK_2 and NK_3 respectively, which mediate the actions encoded by the common C-terminal sequence of tachykinins. In particular, the NK_2 receptor mediates the spasmogenic effect of tachykinins on human smooth muscle; therefore the development of NK_2 tachykinin receptor selective antagonists is of great interest. The introduction of D-Trp residues in the sequence of NKA(4-10) led to the development of a family of potent and selective tachykinin NK_2 receptor antagonists [3].

Results and Discussion

We have investigated the influence of glycosylation on the structure-activity relationship of the antagonist heptapeptide MEN 10376 (H-Asp-Tyr-D-Trp-Val-D-Trp-D-Trp-Lys-NH_2) and of its minimal active fragment, *i.e.* the pentapeptide MEN 10414 (H-Asp-Tyr-D-Trp-Val-D-Trp-NH_2). Glycosylated Tyr, Ser and Asn were introduced in the antagonists in the N-terminal position or in the place of the corresponding unmodified amino acid. The syntheses were performed by the SPPS following the Fmoc/tBu strategy, using glycosylated building-blocks as Pfp esters in a standard synthetic protocol [4] using the NovaSyn Gem continuous-flow synthesizer on TentaGel S RAM resin. All the compounds were purified by

RP-HPLC and characterized by FABMS and amino acid analysis. N^{α}-Fmoc-N^{γ}-(2,3,4,6-tetra-O-acetyl-β-D-glucopyranosyl)-Asn-OPfp [5], N^{α}-Fmoc-O-(2,3,4,6-tetra-O-acetyl-β-D-glucopyranosyl)-Tyr-OPfp [6], N^{α}-Fmoc-O-(2,3,4,6-tetra-O-benzoyl-β-D-glucopyranosyl)-Ser-OPfp [7] were at this purpose synthesized following the procedure previously described. In fact, this is the most versatile and general approach presently available for the preparation of a large variety of N-, phenolic O- and aliphatic O-linked glycopeptides with well defined and predetermined structure [8]. We synthesized the following glycosylated analogs of the two NK_2 antagonists MEN 10376 and MEN 10414: MEN 11038 [H-Asn(Glc)-Asp-Tyr-D-Trp-Val-D-Trp-D-Trp-Lys-NH_2], MEN 10871 [Asp-Tyr(Glc)-D-Trp-Val-D-Trp-NH_2], MEN 11201 [H-Asp-Tyr(Glc)-D-Trp-Val-D-Trp-D-Trp-Lys-NH_2], MEN 11202 [H-Tyr(Glc)-Asp-Tyr-D-Trp-Val-D-Trp-D-Trp-Lys-NH_2], MEN 11258 [H-Ser(Glc)-Asp-Tyr-D-Trp-Val-D-Trp-D-Trp-Lys-NH_2] and MEN 11259 [H-Ser(Glc)-Asp-Tyr-D-Trp-Val-D-Trp-NH_2].

The antagonist activity of the described glycopeptides at the NK_2 receptor of the rabbit pulmonary artery bioassay, expressed as pA_2 values resulted of 7.2 for MEN 11202, 7.3 for MEN 11258, 6.7 for MEN 11038, 6.2 for MEN 11201, < 5 for MEN 10871 and < 6 for MEN 11259. These results indicate that the antagonist activity is preserved, as compared to MEN 10376 (pA_2 = 8.1), when the glycosylated amino acids were added to the entire sequence, while the introduction of the glycosyl moiety (Glc) on the side-chain of Tyr induced a dramatic decrease in affinity.

The general decrease of activity produced by the addition of the glycosyl moiety might be attributed to the steric hindrance of Glc. For the active analogs MEN 11202 and MEN 11258 *in vivo* investigations will show whether the presence of Glc is a consequence in terms of absorption and distribution of the glycosylated drugs in the animal.

References

1. Haro, I., Busquets, M.A., Torres, J.L., Valencia, G., Garcia-Anton, J.M. and Reig, F., *J. Pharm. Sci.*, 79 (1990) 74.
2. Imperiali, B. and Rickert, K.W., *Proc. Natl. Acad. Sci. USA*, 92 (1995) 97.
3. Rovero, P., Pestellini, V., Maggi, C.A., Patacchini, R., Regoli, D. and Giachetti, A., *Eur. J. Pharmacol.*, 175 (1990) 113.
4. Kunz, H., *Pure & Appl. Chem.*, 65 (1993) 1223.
5. Christiansen-Brams, I., Meldal M. and Bock, K., *J. Chem. Soc., Perkin Trans. 1*, (1993) 1461.
6. Jensen, K.J., Meldal, M. and Bock, K., *J. Chem. Soc., Perkin Trans. 1*, (1993) 2119.
7. Reimer, K.B., Meldal, M., Kusumoto, S., Fukase, K. and Bock, K., *J. Chem. Soc., Perkin Trans. 1*, (1993) 925.
8. Meldal, M. and Bock, K., *Glycoconjugate J.*, 11 (1994) 59.
9. Maggi, C.A., Giuliani, S., Ballati, L., Lecci, A., Manzini, S., Patacchini, R., Renzetti, A.R., Rovero, P., Quartara, L. and Giachetti, A., *J. Pharmacol. Exp. Ther.*, 257 (1991) 1172.
10. Quartara, L., Patacchini, R., Giuliani, S., Renzetti, A.R., Rovero, P. and Maggi, C.A., *Life Sci.*, 51 (1992) 1929.

Peptides: Chemistry, Structure and Biology
Pravin T.P. Kaumaya and Robert S. Hodges (Eds.)
Mayflower Scientific Ltd., 1996

272

Production of Recombinant Growth Hormone Releasing Factor *via* Post-translational C-Terminal α-Amidation

D.B. Henriksen, J.S. Stout, B.E. Partridge, B. Holmquist and F.W. Wagner

BioNebraska, Inc., Lincoln, NE 68524, USA

Introduction

Many secretory peptide hormones and growth factors carry an amide group at their carboxyl terminus which is essential for full biological activity. The natural form of Growth Hormone Releasing Factor (GRF(1-44)-NH_2), a potential therapeutic agent for osteoporosis and other growth related disorders [1], is a member of this family. Two major hurdles in the production of peptides using recombinant technology are adventitious proteolysis and C-terminal α-amidation. These have been overcome using a process involving 3 enzymatic steps and a 2-stage HPLC purification, to enable us to prepare multi-gram amounts of injectable grade GRF(1-44)-NH_2. GRF(1-44) containing a C-terminal Ala extension has been expressed in *E. coli* as a fusion protein linked to human carbonic anhydrase (HCA) through an interlinking peptide containing recognition sites for thrombin and enterokinase.

Since prokaryotic expression systems lack the specific enzymes involved in the C-terminal α-amidation, the Ala extension provides an enzymatic recognition site for post-translational α-amidation. Incorporation of the peptide onto HCA affords protection against proteolytic degradation [2].

Results and Discussion

Fusion protein from fermentations is readily isolated in the form of inclusion bodies by differential centrifugation. Dissolution followed by proteolysis with thrombin provides the Ala extended LNK-GRF(1-44) precursor peptide, where LNK is part of the linking peptide containing an enterokinase recognition site.

The conversion to the natural C-terminal α-amidated peptide utilizes a unique process involving a photolabile amidating agent, *o*-nitrophenylglycine amide (ONPGA), *via* a carboxypeptidase-Y catalyzed transpeptidation [3]. After transpeptidation, the solution is desalted, purged with argon and the resulting LNK-GRF(1-44)-ONPGA adduct is irradiated at $\lambda > 320$ nm for 2 hours to give LNK-GRF-NH_2 in high yields (~95%). This solution is diluted 5 fold with 50 mM succinic acid and pH is adjusted to 5.5. GRF(1-44)-NH_2 is obtained by hydrolysis with enterokinase followed by a two-step HPLC purification involving ion exchange (IE) and C_8 chromatography (Scheme 1).

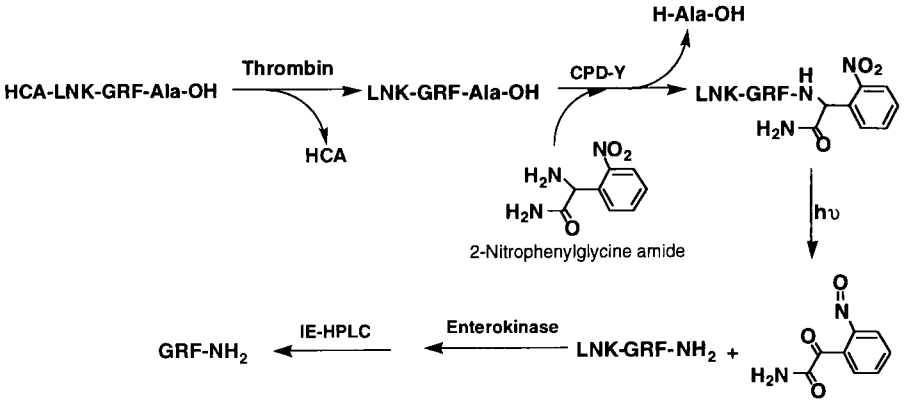

Scheme 1.

Homogeneity and purity are established by HPLC using a C_8 reverse phase column, HPLC using a Polysulfoethyl Aspartamide column and capillary electrophoresis, all calibrated with authentic GRF(1-44)-NH_2. The identity of GRF(1-44)-NH_2 is further established by amino acid residue composition and sequence, MALDI and FAB mass spectroscopy. All analyses are in agreement with the theoretical values expected based on the peptide sequence.

Since the apparent sequence and amino acid compositions of GRF(1-44)-OH and GRF(1-44)-NH_2(Met^{27}SO), potential side products of the process, are identical to GRF(1-44)-NH_2, it was necessary to demonstrate that these peptides can be separated chromatographically. GRF(1-44)-NH_2 is completely separated from GRF(1-44)-OH and GRF(1-44)-NH_2(Met^{27}SO) with the use of the Polysulfoethyl Aspartamide column.

The drug product, prepared for an IND study, has been characterized completely as to structure, composition, and biological activity and is considerably more homogeneous than material synthesized by solid phase chemical methods. A pilot study on the effectiveness of recombinant GRF(1-44)-NH_2 in the treatment of osteoporosis is in progress.

References

1. Gelato, M.C., *The Endocrinologist,* 4 (1994) 64.
2. Goldberg, A.L. and John, A.C.S., *Ann. Rev. Biochem.*, 45 (1976) 747.
3. Henriksen, D.B., Breddam, K. and Buchardt, O., *Int. J. Pep. Prot. Res.*, 41 (1993) 169.

Peptides: Chemistry, Structure and Biology
Pravin T.P. Kaumaya and Robert S. Hodges (Eds.)
Mayflower Scientific Ltd., 1996

273
Novel Substitutions of Position 6 of LHRH Antagonist to Improve Potency and Safety

R.E. Swenson[1], F. Haviv[1], N.A. Mort[1], Y.S. Or[1], E.N. Bush[1], G.J. Diaz[1], G.F. Bammert[1], N.S. Rhutasel[1], A Nguyen[1], J.A. Leal[1], V.A. Cybulski[1], J. Knittle[2] and J. Greer[1]

[1]*Pharmaceutical Products Division, Abbott Laboratories,*
[2]*TAP Pharmaceuticals Inc., Abbott Park, IL 60064, USA*

Introduction

LHRH agonists are currently used to treat a variety of sex hormone dependent diseases such as prostate cancer, endometriosis, uterine fibroids and precocious puberty[1]. However, because of their mechanism of action, LHRH agonists may occasionally cause an initial flare of the disease. This provided the impetus for the major research effort devoted to the discovery of a LHRH antagonist, but progress was slow due to inadequate potency and safety [2]. We have previously reported a variety of substitutions at positions 7, 8 and 9 of the antagonist NAcD2Nal-D4ClPhe-D3Pal-Ser-NMeTyr-DCit-Leu-Arg-Pro-DAla-NH_2 (**1**)[3]. We next focussed on position 6 to improve the potency and safety of our compounds, particularly we substituted various ureas at the N-epsilon amine of DLys[6].

Results and Discussion

To expedite the synthesis of our compounds, we developed a method for making ureas by SPPS. By this method the decapeptide was prepared with MBHA resin using standard protocols [4] with BocDLys(N-ε-Fmoc) at position 6. After removal of the Fmoc group the peptide-resin was treated first with 1,1'-carbonyldiimide and then with an appropriate amine. When a diamine was reacted with DLys(N-ε-imidazole-carbonyl), the resulting free amine was further coupled to various acids. The decapeptides were cleaved from the resin with HF and then purified by HPLC. These novel LHRH antagonists were then tested for *in vitro* LH suppression (pA_2), for histamine release (HR) (ED_{50}) in rat peritoneal mast cells (Table 1), and for LH suppression *in vivo* in castrate rats at 30μg/Kg (Figure 1) [4].

The pA_2 values for most of the compounds prepared was above 11.0. However, all of the compounds had HR ED_{50}'s ≤ 3. Three antagonists containing DLys(shikimyl-1,3-diaminopropylcarbonyl)[6] (**2**), DLys(Shikimyl-1,2-diaminoethyl carbonyl)[6] (**3**), or DLys-(hydroxyethylpiperazinocarbonyl)[6] (**5**), when tested in the castrate rat, suppressed LH with a duration of action longer than (**1**) (Figure 1). This new method of preparing ureas allowed rapid production of novel LHRH antagonists that had improved *in vivo* activity.

Table 1. *In vitro activities of LHRH antagonists.*

NAcD2Nal[1]-D4C1Phe[2]-D3Pal[3]-Ser[4]-NMeTyr[5]-X[6]-Leu[7]-Arg[8]-Pro[9]-DAla[10]-NH_2

Compound	X	pA_2[a]	ED_{50}[b]
1	DCit	10.87±0.34	1.65±0.37
2	DLys(Shikimyl-1,2-diaminoethylcarbonyl)	11.55±0.52	3.68±0.90
3	DLys(Shikimyl-1,3-diaminopropylcarbonyl)	10.59±0.01	2.87±0.17
4	DLys(2-Furanoyl-1,2-diaminoethylcarbonyl)	10.90±0.07	<3
5	DLys(Hydroxyethylpiperazinocarbonyl)	10.74±0.20	3.26±1.93
6	DLys(Hydroxyethylaminocarbonyl)	11.00±0.05	<3
7	DLys(Morpholinoethylaminocarbonyl)	11.00±0.10	<3
8	DLys(Cyclohexylaminocarbonyl)	11.30±0.30	<3
9	DLys(Morpholinocarbonyl)	11.30±0.10	3.33±0.50
10	DLys(Methylpiperazinocarbonyl)	11.50±0.20	<3
11	DLys(Histaminecarbonyl)	11.56±0.16	<3

[a]pA_2=the negative logarithm of the concentration of antagonist that requires 2-fold higher concentration of agonist to release LH from rat pituitary cells. [b]ED_{50}=the effective dose of antagonist that gives 50% of maximal release of histamine from rat peritoneal mast cells.

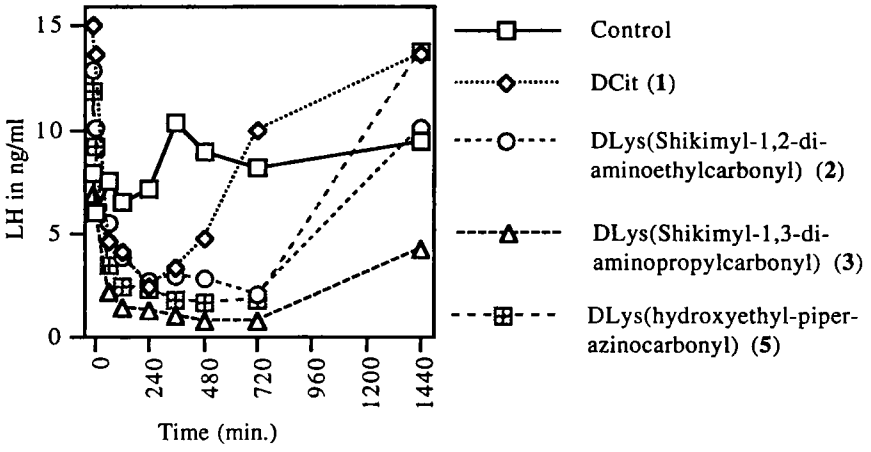

Figure 1. *Suppresion of LH in the castrated rat following sc injection of 30 μg/Kg.*

References

1. Conn, P.M., Crowley, Jr., W.F., *Annu. Rev. Med.* 45 (1994) 391.
2. Karten, M.J., Rivier, J.E., *Edocr. Rev.* 7 (1986) 43.
3. Swenson, R.E., Mort, N.A., Haviv, F., Bush, E.N., Diaz, G., Bammert, G., Rhutasel, N., Nguyen, A., Leal, J., Cybulski, V., Knittle, J., Greer, J., in Hodges, R.S. and Smith, J.A. (Eds.), 'Peptides: Chemistry, Structure and Biology', Escom, Leiden, The Netherlands, 1994, p. 452.
4. Haviv, F., Palabrica, C.A., Bush, E.N., Diaz, G., Johnson, E.S., Love, S., Greer, J., *J. Med. Chem.*, 32 (1989) 2340.

Peptides: Chemistry, Structure and Biology
Pravin T.P. Kaumaya and Robert S. Hodges (Eds.)
Mayflower Scientific Ltd., 1996

274

The Use of the Message-Address Concept in the Design of Potential Antagonists Based on Dynorphin A

S.N. Kulkarni[1], H. Choi[1], T.F. Murray[1], G.E. DeLander[1] and J.V. Aldrich[2]

[1]College of Pharmacy, Oregon State University, Corvallis, OR 97331, USA
[2]Department of Pharmaceutical Sciences, School of Pharmacy, University of Maryland at Baltimore, Baltimore, MD 21201, USA

Introduction

The opioid peptide dynorphin A (Dyn A) shares a common N-terminal sequence, referred to as the message sequence [1], with other mammalian opioid peptides and has a unique C-terminal address sequence which imparts high affinity for kappa opioid receptors. We used this message-address concept to design Dyn A analogues as potential opioid receptor antagonists by combining the message sequence from novel peptides reported to have δ and μ antagonist activity with the C-terminal address sequence of Dyn A-(1-11). We synthesized [Tic^2,Phe^3,D-Pro^{10}]Dyn A-(1-11), **1**, and "extracet" (AcRFMWMRR-(D-A)-RPKNH$_2$), **6**, along with selected analogues, using the reported δ antagonist TIPP (Tyr-Tic-Phe-Phe, where Tic = 1,2,3,4-tetrahydroisoquinoline-3-carboxylic acid) [2], and the μ antagonist [Arg^6]acetalin (AcArg-Phe-Met-Trp-Met- ArgNH$_2$) [3], respectively, as the "message sequence".

Results and Discussion

The Dyn A analogues were synthesized by solid phase peptide synthesis using Fmoc-protected amino acids. In the case of **1** and its analogues, HATU plus HOAt improved the efficiency of couplings involving the hindered amino acid and significantly improved the yield and purity of the desired peptide.

The affinities of the synthesized peptides for κ, δ, and μ opioid receptors were evaluated in radioligand binding assays using [^{3}H]diprenorphine, [^{3}H]DPDPE, and [^{3}H]DAMGO, respectively, and cloned opioid receptors stably expressed in Chinese hamster ovary cells. (Table 1). [Tic^2,Phe^3,D-Pro^{10}]Dyn A-(1-11), **1**, exhibited modest affinity for κ-receptors, but preferentially interacted with δ opioid receptors, a finding also reported recently by Schiller and coworkers for [Tic^2,Phe^3,D-Pro^{10}]Dyn A-(1-11)NH$_2$ [4]. Replacement of Tic^2 by other conformationally restricted amino acids, Pip (pipecolic acid) or N-MePhe, had little effect on κ receptor affinity, but δ and μ receptor affinity varied over a 10 to 20-fold range. [NMePhe^2,Phe^3,D-Pro^{10}]Dyn A-(1-11), **3**, exhibited the best κ vs δ receptor selectivity within this series, but only had a small preference for κ over μ receptors. Replacement of Tic^2 by Phe, **4**, substantially

Table 1. *Opioid Receptor Binding Affinities of Selected Dyn A-(1-11) Analogues.*

	Peptide	Kappa_K_i (nM)	K_i Ratio (κ/δ/μ)
1	[Tic^2,Phe^3,D-Pro^{10}]	18.4±1.5	1/0.32/3.7
2	[Pip^2,Phe^3,D-Pro^{10}]	13.8±1.6	1/0.83/0.55
3	[NMePhe^2,Phe^3,D-Pro^{10}]	15.9±3.7	1/7.9/1.6
4	[Phe^2,Phe^3,D-Pro^{10}]	80.7±4.7	1/8.5/3.7
5	[Tic^2,Gly^3,D-Pro^{10}]	35.2±0.4	1/1.9
6	Extracet	6.6±2.5	1/22/0.17

decreased affinity for all three opioid receptors types, indicating that the conformational restriction in position 2 enhanced receptor affinity. Replacement of Phe^3 by Gly, **5**, had a small effect on κ receptor affinity, but decreased δ receptor affinity greatly. Combination of the μ receptor antagonist [Arg^6]acetalin with the "address" sequence of Dyn A to give extracet, **6**, markedly enhanced κ receptor affinity, (65-fold) compared to [Arg^6]acetalin (K_i=1.6 nM). N-terminal acetate group removal of extracet decreased the κ receptor affinity 6-fold (data not shown).

Opioid activity was evaluated in the electrically stimulated guinea pig ileum (GPI). [Tic^2,Phe^3,D-Pro^{10}]Dyn A-(1-11) and its analogues generally exhibited weak agonist activity (30-60 % inhibition of the muscle twitch at 1 μM). [Tic^2,Gly^3,D-Pro^{10}]Dyn A-(1-11), **5**, however, did not exhibit significant agonist activity at doses up to 3 μM. The [Arg^6]acetalin "message" sequence decreased efficacy at opioid receptors, resulting in potent partial agonists (maximum response 30-60% for "extracet" and [Arg^6]acetalin).

These results suggest that incorporation of a modified "message" sequence into Dyn A analogues can affect opioid activity and that the C-terminal address sequence of Dyn A can be used to significantly enhance κ opioid receptor affinity. These initial peptides thus represent interesting lead compounds which can be used in the further development of opioid antagonists based on the structure of Dyn A.

Acknowledgments

This research was supported by a NIDA grant (R01 DA05195).

References

1. Chavkin, C. and Goldstein, A., *Proc. Natl. Acad. Sci. USA*, 78 (1981) 6543.
2. Schiller, P.W., Nguyen, Thi M.-D., Weltrowska, G., Wilkes, B.C., Marsden, B.J. Lemieux, C. and Chung, N.N., *Proc. Natl. Acad. Sci. USA*, 89 (1992) 11971.
3. Dooley, C.T., Chung, N.N., Schiller, P.W. and Houghten, R.A., *Proc. Natl. Acad. Sci. USA*, 90 (1993) 10811.
4. Schmidt, R., Chung, N.N., Lemieux, C.W., *Regulatrory Peptides*, 54 (1994) 259.

Peptides: Chemistry, Structure and Biology
Pravin T.P. Kaumaya and Robert S. Hodges (Eds.)
Mayflower Scientific Ltd., 1996

275
Synthesis and Binding Properties of PYY(22-36) Analogs: Development of a Potent Proabsorptive Peptide

A. Balasubramaniam[1], Z. Tao[1], W. Zhai[1], M. Stein[1], J.E. Fischer[1], J.E. Taylor[2], P. Eden[2], T. Voisin[3], M. Laburthe[3], C.D. Liu[4] and D.W. McFadden[4]

[1]Department of Surgery, University of Cincinnati Medical Center, Cincinatti, OH 45267, USA
[2]Biomeasure, Inc., Milford, MA 01757, USA
[3]Institut National de la Sante et de la Recherche Medicale U410, 75018 Paris,France
[4]Department of Surgery, UCLA Center for Health Sciences, Los Angeles, CA 90024, USA

Introduction

Peptide YY (PYY), a 36-residue peptide amide mainly localized in the endocrine cells of colon, inhibits intestinal blood flow, motility, and secretion in rats. The antisecretory effect has also been demonstrated in humans [1]. PYY which is released in response to nutrient stimuli also enhances basal and postprandial absorption [2], and promotes intestinal growth [3]. These actions of PYY are mediated by intestinal PYY-preferring receptors which has different structural requirements for interaction than those mediating the peripheral cardiovascular effects of PYY and its homologue, neuropeptide Y [1, 4]. PYY(22-36) has been identified as the active site for interaction with intestinal PYY receptors, and inhibiting short circuit current (SCC) in the intestine [4]. To improve the binding and selectivity, a number of PYY(22-36) analogs were synthesized, and their affinities for Y-1 (SK-N-MC), Y-2 (SK-N-BE2) and intestinal PYY receptors were investigated.

Results and Discussion

Since preliminary studies revealed that substitution of Tyr^{27} dramatically altered the SCC potency [4], a series of N-α-Ac-PYY(22-36) analogs with various aromatic residues at position 27 were synthesized. These exhibited the following order of intestinal receptor affinities: Dip < Pcp < Nal < Bth ~ Tic ~ Trp < Bip ~ Phe < Thi < intact PYY. However, investigation of their effects on SCC in rat jejunal preparations revealed that N-α-Ac-[Trp^{27}]PYY(22-36) to be the most potent, exhibiting even higher potency [EC_{50} = 0.005 nM] than intact PYY [1.0 nM] [5]. Therefore, the effects of N-α-Ac-[Trp^{27}] PYY(22-36) on intestinal absorption were investigated in awake dogs with jejunal, ileal

Table 1. *Peak Probsoptive effects of 200 and 300 pmol/kg/hr N-α-Ac-[Trp^{27}]PYY(22-36) in canine ileum and colon, respectively.*

	Ileum		Colon	
	Basal	Peak*	Basal	Peak*
H_2O (μl/min)	437±92	725±98	204±25	503±49
Na^+ (μEq/min)	68±13	120±14	41±5	78±9
Cl^- (μEq/min)	63±9	101±13	45±5	77±8

* $p < 0.05$ *vs.* basal by ANOVA; peak absorptions were observed 30 and 90 min after starting intraluminal infusion in ileum and colon, respectively.

and/or colonic Thiry-Vella-Fistulas [2]. Intraluminal (Table 1) and intravenous (not shown) administration of this analog significantly increased the colonic and ileal H_2O, Na^+ and Cl^- absorptions.

Further SAR studies revealed that substitution of Leu residues in N-α-Ac-PYY(22-36) with Trp at 28 or 30 (0.6 nM) increased the receptor affinity while that at 24 reduced it. N-α-Ac-[Nle^{24,28,30}, Nva^{31}]PYY(22-36) with Nle→Leu and Nva→Ile, exhibited good affinity (0.59 nM). This analog may have increased proteolytic stability, especially at Asn^{29}-Leu^{30} which is known to be susceptible to endopeptidase-24.11. Although N-α-Ac-[Phe^{27}]PYY(25-36) exhibited comparable affinity (3.2 nM), PYY (27-36) analogs bound poorly. All the 22-36 and 25-36 analogs interacted poorly with Y-1 cells, but with a few exceptions, bound to Y-2 cells and hippocampus with a potency comparable to that of intestinal receptors.

In summary, we have synthesized high affinity Y-2 receptor selective ligands, and shown for the first time that a PYY peptide can stimulate absorption both during IV and intraluminal infusions. These analogs may prove useful in treating malabsorption problems in patients undergoing intestinal surgery and those with AIDS.

Acknowledgments

This work was supported in part by grants from PHS (GM 47122) and NATO 890094.

References

1. Laburthe, M., *Trends Endocrionol. Metab.* 1 (1989) 168.
2. Bilchik, A.J., Hines, O.J., Adrian, T.E., McFadden, D.W., Berger, J.J., Zinner, M.L. and Ashley, S.W. *Gasteroenterology,* 105 (1993) 1441.
3. Gomez, G., Zhang, T., Rajaraman, S., Thakore, K., Yanaihara, N., Townsend, C.M., Thompson, J.C. and Greeley, G.H., *Am. J. Physiol.*, 268 (1995) G71.
4. Balasubramaniam, A., Cox, H.M., Servin, A.L., Voisin, T., Labuthe, M. and Fischer, J.E., *Peptides,* 14 (1993) 1011.
5. Eto, B., Boisset, M., Eden, P., Balasubramaniam, A. and Desjeux, J.F. unpublished data.

Peptides: Chemistry, Structure and Biology
Pravin T.P. Kaumaya and Robert S. Hodges (Eds.)
Mayflower Scientific Ltd., 1996

276
Substitution of Pro^3 in [Leu^{13}]Motilin Affords Antagonists to the GI Motilin Receptor

M.J. Macielag[1], I. Depoortere[2], J.R. Florance[1], T.L. Peeters[2], R. Dharanipragada[1], J. Kim-Dettelback[1], M.S. Marvin[1] and A. Galdes[1]

[1]*Ohmeda PPD, New Providence, NJ 07974, USA*
[2]*Gut Hormone Laboratory, Gasthuisberg O & N, B-3000, Leuven, Belgium*

Introduction

Motilin (Mot), a linear polypeptide of 22 amino acid residues (H-Phe-Val-Pro-Ile-Phe^5-Thr-Tyr-Gly-Glu-Leu^{10}-Gln-Arg-Met-Gln-Glu^{15}-Lys-Glu-Arg-Asn-Lys^{20}-Gly-Gln-OH), is found in the duodenojejunal mucosa of several species, including man. The peptide appears to be involved in stimulating peristaltic contractile activity of the upper gut during fasting [1]. In addition, recent *in vitro* experiments have demonstrated that motilin induces an endothelium-dependent relaxation of coronary strips, suggestive of a role in the regulation of vascular tone [2]. Definitive evidence for the involvement of motilin in these physiological processes has been lacking due to the paucity of specific motilin receptor antagonists. Recently, we described the *in vitro* pharmacological properties of two high affinity motilin antagonists that resulted from replacement of Pro^3 with phenylalanine in both [Leu^{13}]Mot and its truncated analog, [Leu^{13}]Mot-(1-14) [3, 4]. In the present study, we have systematically modified the residue in position 3 of [Leu^{13}]Mot-(1-14) in order to elucidate the physicochemical and conformational factors leading to motilin agonism and antagonism.

Results and Discussion

Peptides were synthesized by SPPS on PEG-PS resins using Fmoc continuous flow techniques. Receptor binding affinity (pK_d) was determined by the displacement of [(^{125}I)Nle^{13}]-motilin bound to rabbit antral smooth muscle membranes. Contractility (pEC_{50}) was measured in a tissue bath assay employing rabbit duodenal segments.

Replacement of Pro^3 in [Leu^{13}]Mot-(1-14) (**1**) with Gly^3 (**2**) or Asn^3 (**3**) produced analogs that behaved as full agonists in the tissue bath assay (Table 1). In contrast, the incorporation of charged residues (**4, 5**) was incompatible with high affinity binding, affording extremely weak agonists. This result is in accord with previous SAR studies of motilin which had indicated that the sequence H-Phe^1-Val^2-Pro^3-Ile^4 bound to a generous hydrophobic pocket within the receptor protein.

Substitution of Pro^3 with hydrophobic aromatic or alicyclic amino acids (**6-8**) produced high affinity motilin antagonists. Inversion of configuration maintained

Table 1. *Comparison of receptor affinities and contractile activities of Pro[3] substituted [Leu[13]]motilin-(1-14) analogs.*

H-Phe-Val-Pro[3]-Ile-Phe-Thr-Tyr-Gly-Glu-Leu-Gln-Arg-Leu-Gln-OH

#	Analog	pEC_{50}	pK_d	% Inhibition[b]	pA_2
1	[Leu[13]]Mot-(1-14)	7.55	8.36		
	Postion 3 modifications:				
2	Gly	7.17	8.23		
3	Asn	6.33	7.13		
4	Glu	5.77	5.97		
5	Lys	4.03	4.96		
6	Phe	Ant	8.16		7.03
7	2-Nal[a]	Ant	7.56	12	
8	Cha[a]	Ant	7.68	98	
9	D-Phe	Ant	8.09	74	
10	h-Phe	6.29	8.06		
11	Tic[a]	5.29	7.75		
12	D-Tic	4.71	6.67		
13	N-MePhe	Ant	8.79	86[c]	

[a]3-cyclohexylalanine, Cha; 1,2,3,4-tetrahydroisoquinoline-3-carboxylic acid, Tic; 3-(2-naphthyl)-alanine, 2-Nal. [b]Inhibitory effect of 10^{-5} M antagonist on the maximum contractile effect of 10^{-7} M motilin. [c]$10^{-4.5}$ M antagonist was used.

antagonist activity (**9**). However, introduction of the conformationally mobile phenethyl side chain of h-Phe[3] gave an analog (**10**) that behaved as a full agonist at high concentrations. In light of the latter result, we investigated the effect of constrained analogs of Phe[3] on bioactivity. Surprisingly, restricting the χ_1 and χ_2 torsion angles of phenylalanine through $N\text{-}C^{\delta}$ cyclization, as in Tic[3] (**11**) and D-Tic[3] (**12**), also led to significant residual agonism. The agonistic properties of **11** and **12**, however, are not due to substitution of the N^{α}-H of Phe[3], as evidenced by the superior antagonistic activity of the N-MePhe[3] analog (**13**).

References

1. Peeters, T.L., Vantrappen, G. and Janssens, J., *Gastroenterology,* 79 (1980) 716.
2. Higuchi, Y., Nishimura, J. and Kanaide, H., *Biochem. Biophys. Res. Comm.,* 202 (1994) 346.
3. Depoortere, I., Peeters, T.L., Macielag, M.J., Dharanipragada, R., Florance, J.R. and Galdes, A., *Eur. J. Pharmacol.,* 286 (1995) 241.
4. Peeters, T.L., Depoortere, I., Macielag, M.J., Dharanipragada, R., Marvin, M.S., Florance, J.R. and Galdes, A., *Biochem. Biophys. Res. Comm.,* 198 (1994) 411.

Peptides: Chemistry, Structure and Biology
Pravin T.P. Kaumaya and Robert S. Hodges (Eds.)
Mayflower Scientific Ltd., 1996

277
Alanine and D-Amino Acid Scan of Human Parathyroid Hormone

F.O. Gombert, R. Gamse, J.H.M. Feyen and F. Cardinaux

Sandoz Pharma Ltd., Preclinical Research, CH-4002 Basle, Switzerland

Introduction

Parathyroid hormone (PTH), a linear peptide of 84 amino acid residues, maintains calcium homeostasis through its effects on kidney and bone. Full biological activity and potency are located in its N-terminal segment, residues 1 to 34 or larger. We have substituted systematically each amino acid of the human hormone, hPTH-(1-36)-NH2, by either by L-alanine or by the corresponding D-amino acid. All analogs were tested for binding to the PTH-receptor and for receptor activation in bone-derived cells.

The aim of this study was to gain, in a short time, an overview on structure-activity-relationships of this 36-mer peptide by the use of multiple peptide synthesis and of standardized, crude preparations in cellular assays for bioactivity. Results obtained in this way were validated by re-testing a number of the purified analogs.

Results and Discussion

A comparison of the binding and cAMP data of the Ala substitution series is shown in Figure 1.

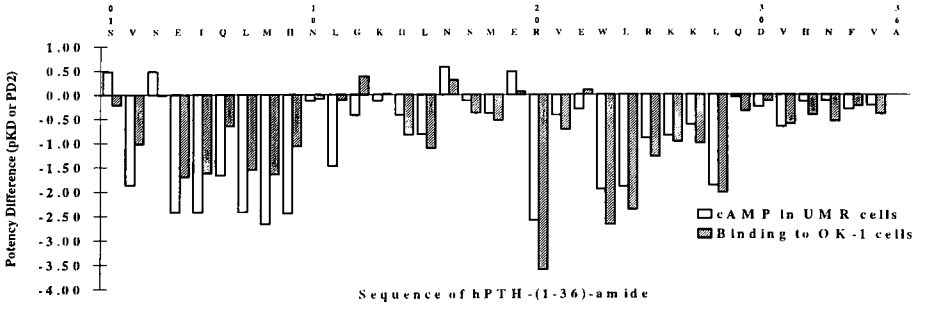

Figure 1. *Binding of [Ala^n] hPTH-(1-36)-NH$_2$ analogs to oppossum kidney cells (OK-1) [1] and production of cAMP in rat osteosarcoma cells (UMR-106-06) [2]. Binding constants (pK$_D$) and activity constants (pD$_2$) shown relative to hPTH-(1-36)-NH$_2$. Peptides were synthesized by Fmoc/tBu tactics on a multiple peptide synthesizer, model SMPS 350 by Zinsser Analytic (Frankfurt, Germany), and the crude preparations standardized by HPLC using hPTH-(1-36)-NH$_2$ as an external standard and ES-MS for identification.*

The effects of Ala substitution on binding clearly showed a regional difference: strong effects in the (2-8) and (20-28) segment; weak effects in the (9-19) and (29-36) segment. There was no significant increase in potency by Ala substitution with mostly a decrease in potency being observed. The strongest effects were seen in the (20-28) segment, notably for substitution of R^{20}, W^{23}, L^{24} and L^{28}. The effects of Ala substitution on cAMP response were similar to the ones on binding with the strongest (negative) effects seen in the (2-8) segment. There was a weak increase upon Ala substitution for K^{13}, N^{16}, and E^{19}. There was good agreement between the crude, standardized preparations and several purified analogs (data not shown).

The effects of D-aa substitution on binding and cAMP response were very similar (Figure 2). Epimerization at any aa-residue caused a significant decrease in potency for both, binding and receptor activation. A segmentation was much less evident than was observed with the Ala scan. D-aa substitutions were relatively best tolerated at the C-terminal (32-36). The most pronounced negative effects on potency in either series were observed for substitutions in those regions which are known to adopt an amphiphilic, helical conformation [3].

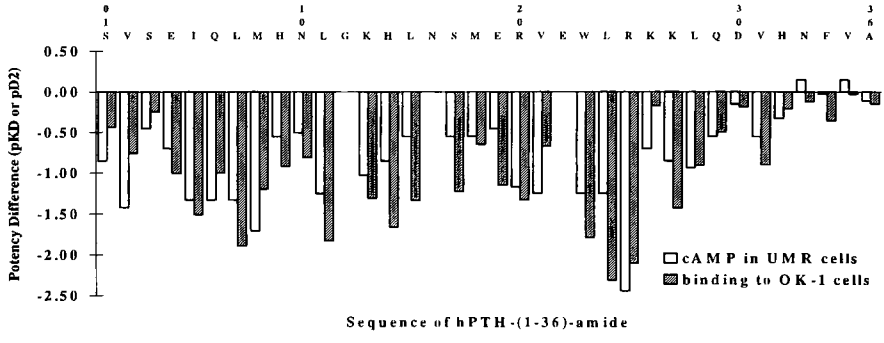

Figure 2. *Binding and cAMP production of [D-aa^n] hPTH-(1-36)-NH$_2$ analogs. Conditions for assays and peptide synthesis as for Figure 1. Purity (by HPLC) ranged from 16 % to 70 % for the crude preparations.*

Multiple peptide synthesis was applied successfully to the synthesis of a large series of 36-mer peptides. The use of standardized, crude preparations for bioassay provided a quite reliable overview on the structure-activity-relationship in about six weeks time per series including testing. The effect of Ala and D-aa substitution in most positions of hPTH was to decrease affinity to and activation of the PTH receptor. The information is useful for the design of further analogs of PTH.

References

1. Schneider, H., Feyen, J.H.M., Seuwen, K. and Movva, A.R., *Europ. J. Pharmacol.*, 246 (1993) 149.
2. Salomon, Y., in Greengard, P. and Robinson, G.A. (Eds.), 'Advances in Cyclic Nucleotide Research', Vol. 10, Raven Press, New York, NY, USA, 1979, p.35.
3. Barden, J.A., Kemp, B.E., *Biochem.*, 32 (1993) 7126.

Peptides: Chemistry, Structure and Biology
Pravin T.P. Kaumaya and Robert S. Hodges (Eds.)
Mayflower Scientific Ltd., 1996

278
LHRH Antagonists Conformationally Restricted at the N-terminus

R.E. Swenson[1], N.A. Mort[1], F. Haviv[1], C.J. Nichols[1], E.N. Bush[1], G.J. Diaz[1], G.F. Bammert[1], N.S. Rhutasel[1], A Nguyen[1], J.A. Leal[1], V.A. Cybulski[1], J. Knittle[2] and J. Greer[1]

[1]*Pharmaceutical Products Division, Abbott Laboratories,*
[2]*TAP Pharmaceuticals Inc., Abbott Park, IL 60064, USA*

Introduction

The development of an effective and safe LHRH antagonist is a long term goal for the treatment of prostrate cancer, endometriosis and other sex steroid dependent diseases. We previously reported that N-methylation of position 5 of several LHRH antagonists maintained activity, either *in vitro* or *in vivo*, and improved water solubility [1]. In an effort to improve the duration of action and the safety of LHRH antagonists we examined conformational restrictions of the N-terminus of the known decapeptide antagonist NAcD2Nal-D4ClPhe-D3Pal-Ser-NMeTyr-DCit-Leu-Arg-Pro-DAla-NH_2 (**1**)[1].

Results and Discussion

Initially we substituted N-α-methyl at position 1 of compound (**1**) to prepare NAcN-MeD2Nal[1] analog (**2**). This antagonist was as potent as (**1**) *in vitro*, and had increased duration of action *in vivo* as determined by LH suppression in the castrate rat at 30 μg/kg (Figure 1) [2]. In the histamine release (HR) assay from rat peritoneal mast cells [3],

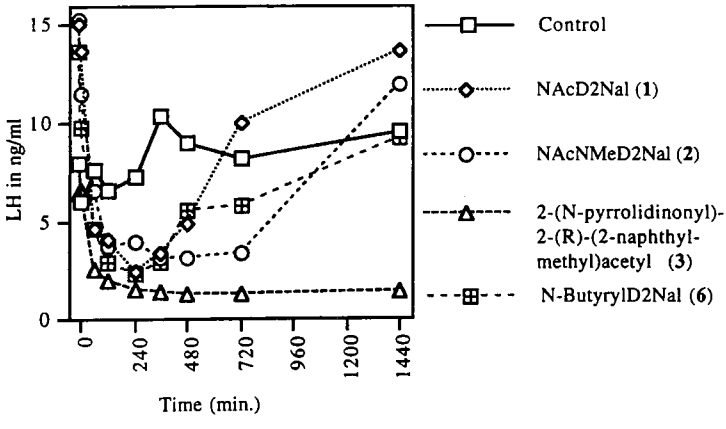

Figure 1. *Suppression of LH in the castrated rat following sc inlection of 30 μg/kg .*

Table 1. *In vitro activities of LHRH antagonists.*

X^1-D4C1Phe^2-D3Pal^3-Ser^4-NMeTyr^5-DCit^6-Leu^7-Arg^8-Pro^9-DAla^{10}-NH_2

Compound	X	pA_2[a]	ED_{50}[b]
1	NAcD2Nal	10.87±0.34	1.65±0.37
2	NAcNMeD2Nal	10.61±0.20	< 3.0
3	[c]PNA	11.09±0.25	7.98±3.9
4	N-FormylD2Nal	11.35±0.05	< 3.0
5	N-PropionylD2Nal	11.40±0.14	3.61±0.19
6	N-ButyrylD2Nal	11.25±0.05	2.98±1.09

[a]pA_2 = the negative logarithm of the concentration of antagonist that requires 2-fold higher concentration of agonist to release LH from rat pituitary cells. [b]ED_{50} = the effective dose of antagonist that gives 50% of maximal release of histamine from rat peritoneal mast cells. [c]PNA = 2-(N-pyrrolidinonyl)-2-(R)-(2-naphthylmethyl)acetyl.

antagonist **2** had an ED_{50} equivalent to the parent. As a next modification, we linked the N-α-methyl with the acetyl group of residue 1 to form a lactam. The antagonist 2-(N-pyrrolidinonyl)-2-(R)-(2-naphthyl-methyl)-acetyl-D4ClPhe-D3Pal-Ser-NMeTyr-D-Cit-Leu-Arg-Pro-DAla-NH_2 (**3**) was as potent as the parent *in vitro* and had a prolonged suppression of LH *in vivo* (Figure 1). Analog **3** had an ED_{50} for HR four-fold higher than the parent indicating an improved safety profile. To determine whether this effect was due to additional hydrophobicity at the N-terminus we also prepared the N-propionyl-D2Nal[1] analog (**5**) and N-butyryl-D2Nal[1] analog (**6**). These antagonists had improved HR ED_{50}'s, but did not have increased *in vivo* duration of LH suppression (Figure 1).

In summary, upon restriction of the N-terminus of (**1**), either by N-methylation or by linking the acetyl group to the α-N-methyl, we produced LHRH antagonists which *in vitro* were equally potent to the parent in inhibiting LH release, and in the castrate rat had longer duration of action. Antagonist **3** also had a better safety profile as determined by HR ED_{50}.

References

1. Haviv, F., Fitzpatrick, T.D., Nichols, C.J., Swenson, R.E., Bush, E.N., Diaz, G., Nguyen, A.T., Nellans, H.N., Hoffman, D.J., Ghanbari, H., Johnson, E.S., Love, S., Cybulski, V.A., Greer, J., *J. Med. Chem.*, 36 (1993) 928.
2. Bush, E.N., Nguyen, A.T., Diaz, G.J., Love, S.K., Mikusa, J.P., Cybulski, V.A., Carlson, R.P., Leal, J.A., Haviv, F., Fitzpatrick, T.D., Nichols, C.J., Swenson, R.E., Mort, N.A., Johnson, E.S., Dodge, P.W., Knittle, J., Greer, J., *Endocrin. Journal*, 1 (1993) 291.
3. Karten, M.J., Hook, W.A., Siraganian, R.P., Coy, D.H., Folkers, K., Rivier, J.E., Roeske, R.W., in Vickery, B.H. and Nestor, J.J., (Eds.), 'LHRH and Its Analogs, Contraceptive and Therapeutic Applications', Part 2, MTP Press, Ltd., Lancaster, Boston, the Hague 1987, p. 179.

Peptides: Chemistry, Structure and Biology
Pravin T.P. Kaumaya and Robert S. Hodges (Eds.)
Mayflower Scientific Ltd., 1996

279
Structure-Activity Studies of GnRH Antagonists Having Dipolar Residues

L. Guo, Z. Tian, P.J. Edwards, Y.L. Zhang, N. Shobana and R.W. Roeske

Department of Biochemistry and Molecular Biology, Indiana University School of Medicine, Indianapolis, IN 46202, USA

Introduction

During the past two decades, many efforts have been made to find GnRH antagonists with enhanced antiovulatory potency (AO) and low histamine releasing toxicity (HRT). It is well-established that antagonists having a negatively-charged residue such as D-Glu^6 have low HRT, as well as low AO activity [1]. Earlier we have also shown that GnRH antagonist D-Glu(taurine)^6, which has a negatively charged sulfonic acid moiety in position 6, has low HRT and low AO activity [2]. Here we report the synthesis of several GnRH antagonists having a residue (**1**), (**2**) or (**3**) (Figure 1) in position 6 or 3. These compounds represent an attempt to have both the AO benefit of a positively-charged residue and the low histamine releasing benefit of a negatively-charged residue.

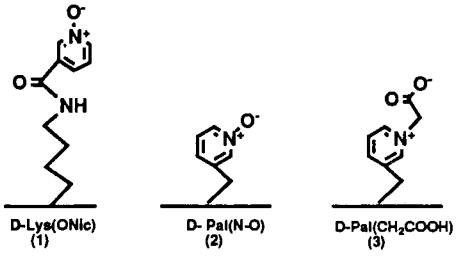

Figure 1. *The structures of dipolar residues.*

Results and discussion

The peptides having amino acid derivative D-Lys(ONic) (**1**) were made by a post-synthesis solid phase modification method in which Boc-D-Lys(Fmoc) was used. The Fmoc protecting group was removed with 50% piperidine in DMF and the free amino group was acylated with nicotinic acid-N-oxide. Boc-3-D-pyridylalanine-N-oxide was easily prepared from Boc-3-(3'-pyridyl)-D-alanine in 80% yield by oxidation with 3-chloroperoxybenzoic acid. Antagonists containing dipolar residue (**3**) were synthesized with Boc-3-D-Pal($CH_2COOBzl$) which was prepared by N-alkylation of Boc-3(3'-pyridyl)-D-alanine with benzyl 2-bromoacetate.

All the peptides with amino acid derivatives (**1**), (**2**) or (**3**) were synthesized using standard automated Boc/Benzyl solid phase protocol. After treatment with HF/10% anisole, peptides were purified by preparative HPLC and characterized by amino acid analysis and mass spectrometry.

As shown in Table 1, compared with the antagonist D-Glu(taurine)^6, GnRH D-Pal(N-O)^6 has almost same level of HRT, but much better AO activity, 50% inhibition of ovulation at a dose of 1μg in rats. GnRH D-Lys(Onic)^6 (entry 3) and D-Pal (CH_2COOH)^6 (entry 2) also have low HRT and good AOA of 1/8, 6/8 at 1.0 μg. Substitution of N-Me-Tyr^5 for Tyr^5 does not influence the AOA and HRT to any extent (entries 3 and 4). Replacement of D-Pal(N-O)^6 by D-Pal(N-O)^3 increases the HRT remarkably, from 145 to 25 μg/ml (entries 5 and 6).

Table 1. *Characteristics of GnRH Antagonists with or without dipolar residues.*

Entry	Other residues in a sequence of (Ac-D-Nal^1,4-Cl-D-Phe^2,..., Lys(ipr)^8, D-Ala^{10})GnRH	AOA[a]	HR ED50 μg/ml[b]
1	D-Pal^3, D-Glu(taurine)^6	1/8 (5.0 μg)	131
2	D-Pal^3, D-Pal(CH_2COOH)^6	6/8 (1.0 μg)	75
3	D-Pal^3, D-Lys(Onic)^6	1/8 (1.0 μg)	48
4	D-Pal^3,N-Me-Tyr^5,D-Lys(Onic)^6	4/8 (1.0 μg)	40
5	D-Pal^3, D-Pal(N-O)^6	4/8 (1.0 μg)	145
6	D-Pal(N-O)^3, D-Pal(ipr)^6	6/8 (1.0 μg)	25

[a]AOA is anti-ovulatory activity expressed by number of rats ovulated/number of rats tested at a dose given in micrograms per rat.
[b]HR assay is tested *in vitro* using rat mast cells.

Acknowledgments

This work was supported by the Contraceptive Development Branch of NICHD. We thank Ms. Haitao Li for technical assistance in preparing Boc-Pal(N-O) and Dr. Christopher Molineaux of Pharmaceutical Peptides Inc., for some of the HR assays.

References

1. Roeske, R.W., Chaturvedi, N.C., Hrinyo-Pavlina, T. and Kowalczuk, M., in Vickery, B.H. and Nestor Jr., J.J. (Eds.), 'LHRH and Its Analogs: Contraceptive and Therapeutic Applications, Part 2', MTP Press, Norwell, MA, U.S.A., 1987, p.17.
2. Roeske, R.W., Edwards, P.J., Tian, Z., Indiana University School of Medicine, Indianapolis, Indiana, unpublished data.

Peptides: Chemistry, Structure and Biology
Pravin T.P. Kaumaya and Robert S. Hodges (Eds.)
Mayflower Scientific Ltd., 1996

280
Biochemical Approaches to Mechanism of Delta Sleep Inducing Peptide (DSIP) Action

I.A. Prudchenko[1], I.I. Mikhaleva[1], E.M. Khvatova[2] and N.A. Rubanova[2]

[1]Shemyakin - Ovchinnikov Institute of Bioorganic Chemistry, Russian Academy of Sciences, Miklukho-Maklaya 16/10, 117871, Moscow, GSP-7, Russia
[2]Nizhnii Novgorod Medical Academy, Minina-Pozharskogo 10/1, 603005, Nizhnii Novgorod, Russia

Introduction

Isolated from cerebral venous blood of rabbits as a sleep factor, DSIP displays a number of other non-sleep effects [1]. According to our data, the most pronounced feature of its multifunctional physiological action is the highly expressed stress-protective and adaptogenic activity. A number of DSIP analogues was synthesized and their antiepileptic and antimetastatic potency was investigated in some test-models along with DSIP. Structure-activity dependencies were established for this series of compounds [2, 3]. The mechanism of action for DSIP is poorly understood although biochemical approaches have shed more light on this.

Results and Discussion

In the present study, the metabolic effects of DSIP were estimated under experimental hypoxical stress. The peptides were injected i.p. to rats at a dose of 120 μg/kg prior to stressful short-term housing in a reduced atmosphere. The functional state of brain mitochondria was analyzed.

Changes in enzyme activity are the key mechanism regulating metabolic processes providing alterations in the functional state of an organism. Translocation and changes in activity of mitochondrial enzymes localized on the membrane of these organelles play a major role. Mitochondrial creatine kinase being involved in regulation of ATP/ADP transport through mitochondrial membranes is one of the most important enzymes of energetic metabolism. Under DSIP injection in rats, the activity of this enzyme in brain mitochondria was increased about 30%, while under hypoxic conditions the effect was more pronounced with a 65% increase. Monoamine oxidase type A (MAO-A) is known as an important brain enzyme participating in metabolism of biogenic monoamines. MAO-A exhibited the activity only in mitochondrial fraction and this activity was practically not found in cytoplasmic fraction obtained from the brain of intact animals. Subjection of rats to hypoxic conditions led to a decrease in MAO-A activity in the mitochondria and its appearance in the cytoplasm. Preliminary injection of DSIP (i.p.,

120 μg/kg) to rats prior to stressful housing in a reduced atmosphere partially inhibited hypoxia induced changes. Mitochondrial MAO-A activity was increased about 46% in comparison with DSIP-untreated rats with hypoxia although it did not reach the values corresponding to intact animals. At the same time, the opposite effect of DSIP on MAO-A activity in the cytoplasm may be traced. In addition, DSIP has a tendency to normalize the serotonin content in the brain of rats with hypoxia. DSIP also completely normalized the ability of another enzyme, hexokinase (key enzyme in glucose utilization in brain), to absorb on mitochondrial membranes that deviated from the normal level under stress.

In order to evaluate the relationships between structure and activity we investigated the related effects of DSIP analogues in rats with hypoxia. Therefore, several DSIP analogues varying in positions 1, 2 and 6 were synthesized by solid-phase method on the 9500 Peptide Synthesizer (MilliGen/Biosearch) [3].

To compare efficiency of these analogues, we analyzed the changes in activity of mitochondrial MAO-A and also in the content of serotonin in rat brain after their injection prior to hypoxia manipulation. The data obtained were compared with corresponding values for rats subjected to hypoxia without preliminary injection of analogues. We found analogues ID-3 and ID-5 much more active than DSIP. They almost fully prevented stress-induced changes in the mitochondrial MAO-A activity and serotonin content in rat brain. It should be noted that the analogue ID-5 was found to be active also as antiepileptic agent [3]. Similar action on serotonin level was found for all other tested analogues. Analogues ID-1 and ID-8 were inactive in relation to MAO-A activity. It follows from the above results that activity of DSIP is sensitive to structural alterations of the molecule.

DSIP and some of its analogues can modulate changes in brain mitochondria MAO-A activity induced by hypoxia in rats. These peptides possess preventing action. This effect of DSIP might be attributed to the ability of this peptide to decrease the intensity of lipid membrane peroxidation [4] and thereby to retain the association of the enzyme with mitochondrial membranes.

Thus a number of DSIP analogues was tested and among them there were some compounds with an enhanced ability to counteract hypoxia induced changes in MAO-A activity and serotonin content in comparison with native neuropeptide.

References

1. Graf, M.V. and Kastin, A.J., *Peptides*, 7 (1986) 1165.
2. Prudchenko, I., Stashevskaya, L., Shepel, E., Mikhaleva, I., Ivanov, V., Shmalko, Y., Chaly, A., Umansky, V. and Grinzhevskaya, S., *Russian Journal of Bioorganic Chemistry*, 19 (1993) 707.
3. Prudchenko, I., Stashevskaya, L., Mikhaleva, I., Ivanov, V., Shandra, A., Godlevsky, L. and Mazarati, A., *Russian Journal of Bioorganic Chemistry,* 19 (1993) 23.
4. Rikhireva, G.T., Makletsova, M.G., Mendzheritskii, A.M., Vartanyan, L.S., Gurevich, S.M., Lozovskaya, E.L., Kopylovskii, S.A., Rylova, A.V., Prudchenko, I.A. and Mikhaleva, I.I., *Biology Bulletin of the Russian Academy of Sciences,* 20 (1993) 201.

Peptides: Chemistry, Structure and Biology
Pravin T.P. Kaumaya and Robert S. Hodges (Eds.)
Mayflower Scientific Ltd., 1996

281
Design and Synthesis of Novel Thyrotropin Releasing Hormone Analogues Containing Amide Bond Replacements

G.J. Anderson[1], Baljit Kaur[1] and Julie A Kelly[2]

[1]*Department of Chemistry, Manchester Metropolitan University, Chester Street, Manchester M1 5GD, United Kingdom*
[2]*Department of Biochemistry, Trinity College, Dublin 2, Ireland*

Introduction

Thyrotropin Releasing Hormone (TRH, *p*Glu-His-Pro-NH_2) stimulates the release of thyrotropin and a number of other hormones from the anterior pituitary [1]. In addition to these endocrine effects, TRH produces a wide range of stimulatory effects in the central nervous system (CNS). TRH and a number of analogues have thus been investigated for clinical use in diseased states such as motor neurone disease, Alzheimer's disease and in cases of spinal injury [2]. TRH and its analogues are rapidly degraded *in vivo,* however, and suffer from lack of discrimination between endocrine and central receptors, which may give rise to unwanted side-effects [3].

We report here our initial synthetic studies on TRH, where the labile amide bond between the first two residues is replaced by ether (-CH_2-O-) and thioether (-CH_2-S-) moieties, in an attempt to increase half-life and/or receptor specificity.

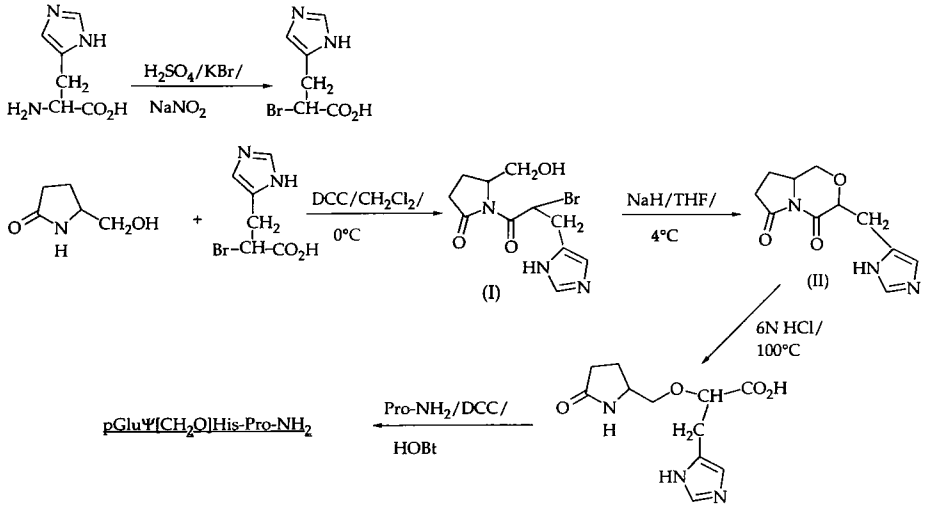

Figure 1. *Synthesis of TRH ether analogs.*

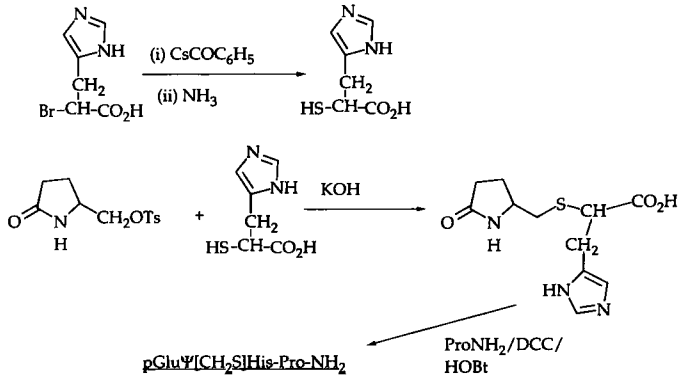

Figure 2. *Synthesis of TRH thioether analogs.*

Results and Discussion

The synthetic protocols adopted are outlined in Figures 1 and 2. Steric hindrance precluded the straightforward addition of the amino alcohol to the α-bromoacid (Figure 1) during synthesis of the ether pseudo-dipeptide and an alternative scheme was used during synthesis of this analogue.

The stability of these analogues to *in vivo* degradation and biological activity will be investigated.

Acknowledgments

GJA gratefully acknowledges receipt of travel grants from the Welcome Trust and the Biochemical Society (UK).

References

1. Morley, J.E., *Endocrine Rev.*, 2 (1981) 396-436.
2. Griffiths, E.C., *Clin. Sci.* 73 (1987) 449-457.
3. Griffiths, E.C., Kelly, J.A., Ashcroft, A., Ward, D.J. and Robson, B., *Ann. NY Acad. Sci.*, 553 (1989) 217-231

Session XIII
Peptide Mimetics

Chairs: Murray Goodman and Waleed Danho

Peptides: Chemistry, Structure and Biology
Pravin T.P. Kaumaya and Robert S. Hodges (Eds.)
Mayflower Scientific Ltd., 1996

282
A Novel Series of Non-peptide Endothelin Receptor Antagonists

J.D. Elliott, D.L. Bryan, P. Nambi and E.H. Ohlstein

SmithKline Beecham Pharmaceuticals, King of Prussia, PA 19406, USA

Introduction

The endothelins (ETs), discovered in 1988 [1], are a family of three isopeptides ET-1 1, ET-2 and ET-3. All three of these peptides are encoded in the human genome and each is composed of 21 amino acids, with disulfide linkages between cysteine residues at positions 1,15 and 3,11. The ETs elicit their effects through binding to receptors of the G-protein coupled seven-transmembrane spanning superfamily. Two receptor sub-types have been fully characterized from human tissues through molecular cloning and expression. The ET_A subtype binds ET-1 and ET-2 with higher affinity than ET-3 and is principally located on vascular smooth muscle cells where it mediates vasoconstriction and proliferation. The ET_B subtype which binds all three ETs with equal, high affinity is also linked to vasoconstriction in certain vascular beds, but in addition mediates the release of endothelium-derived nitric oxide.

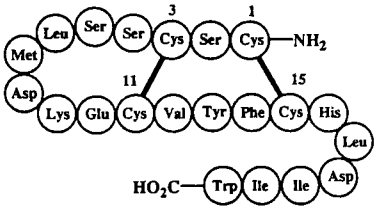

1 Endothelin-1

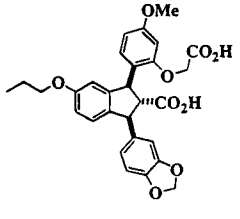

2 SB 209670

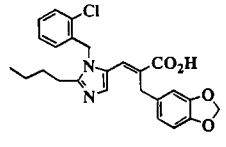

3 SK&F 107328

Evidence is mounting to support the existence of additional receptor subtypes and at present, despite extensive animal model studies, controversy surrounds the optimal antagonist selectivity considered necessary for the treatment of human disorders [2]. This critical question will only be resolved by clinical trials, which are now ongoing, and may depend upon the disease targetted. Our own involvement in the ET receptor antagonist area began with screening non-peptide compounds from our G-protein coupled receptor ligand collection. As a result of implementation of a peptidomimetic hypothesis involving mimicry of ET-1, the effort culminated in the preparation of SB 209670, 2, a potent mixed antagonist of ET_A and ET_B receptors (K_i's: 0.4nM and 15nM, respectively) [3].

Results and Discussion

From our investigations with the indane series of antagonists (*e.g.* 2) it was apparent that both the 2-carboxyl and the benzodioxole moieties of these molecules are important for high affinity binding. Further searching of our compound collection based upon these structural components led to the discovery of SK&F 107328, 3, which was shown to be a ligand for ET_A and ET_B receptors (K_i's: 420nM and 3400nM, respectively). SK&F 107328 was originally prepared for our angiotensin II receptor antagonist program (K_i = 170nM, AT-1) and its discovery in the present context adds it to the growing list of so called *permissive structures*, *i.e.* ligands which bind multiple G-protein coupled receptors.

While an overlay of the framework of 3 on the indane nucleus 2 (A, Figure 1) indicates a good fit between the corresponding benzodioxole rings and carboxylic acids, the 3-phenyl of the indane does not overlay well with the N-benzyl substituent of the imidazole. Further inspection of molecular models suggests that a superior overlay with

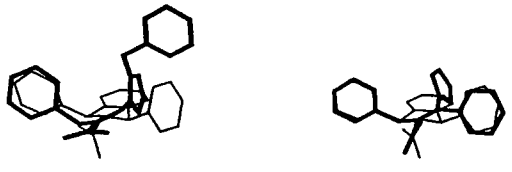

Figure 1. *Molecular modeling overlays of the nucleus of SB 209670 with the framework of SK&F 107328 (A) and the framework of SB 209834 (B).*

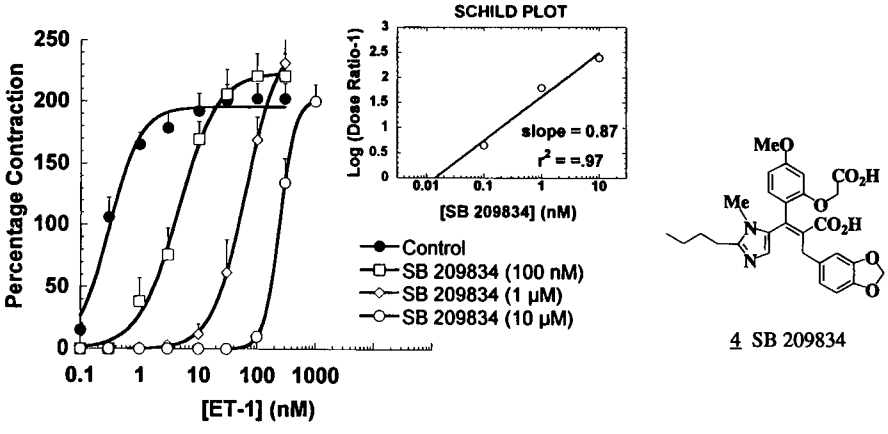

Figure 2. *Inhibition of ET_A-mediated vasoconstriction in isolated rat aorta by SB 209834. Schild analysis for the inhibition of ET-1 contraction in isolated rat aorta by SB 209834.*

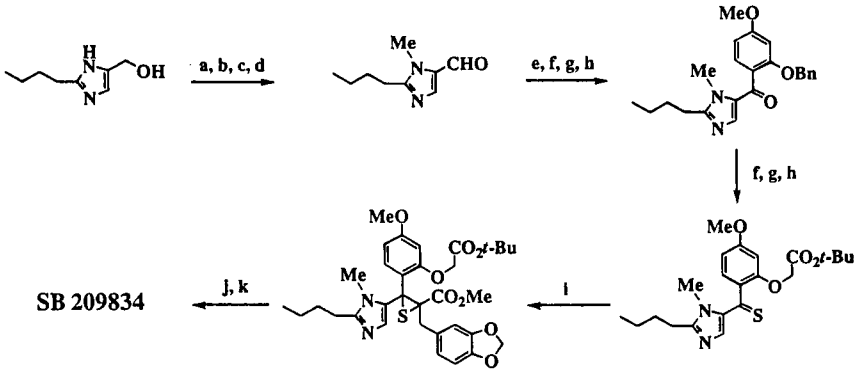

Scheme 1. *(a) NIS, EtOH, 45° (91%); (b) MnO_2, CH_2Cl_2 (54%); (c) $(CH_3)_2SO_4$, Bu_4NF, 5A sieves, THF (84%); (d) 10% Pd/C, KOAc, MeOH (99%); (e) (2-benzyloxymethoxy-4-methoxyphenyl magnesium bromide, then MnO_2, CH_2Cl_2, (79%); (f) 10% Pd/C, 1atm. H_2, EtOAc (91%); (g) NaH, t-butyl bromoacetate, DMF (93%); (h) Lawesson's Reagent, toluene (69%); (i) methyl-2-diazo-3-(5-benzodioxole)propionate, ether (92%), chromatography 60:40 mixture; (j) Treatment of major isomer with $P(OCH_3)_3$, N-methylimidazole (66%); (k) NaOH, iPrOH, then HCl aq., pH 3-3.5 (62%).*

the indane can be obtained by incorporation of an aryl moiety at the 3-position of the acrylic acid (B, Figure 1). Furthermore, removal of the N-benzyl substituent was anticipated, on the basis of previous SAR studies, to reduce AT-1 receptor affinity. As a result, SB 209834, 4, was prepared and found to have high affinity for ET_A receptors (K_i=2nM), measurable, albeit weaker, affinity for ET_B receptors (K_i=500nM) and no apparent affinity for AT-1 receptors. The potency of 4 at ET_A receptors was confirmed in a functional assay. Thus, in the isolated rat aorta, treatment with 4 produces parallel rightward shifts in the concentration-response curve to ET1, K_b=9nM (Figure 2). Compound 4 shows no agonist activity in this tissue and Schild analysis is consistent with competitive antagonism. Our synthesis of 4 is shown in Scheme 1.

In summary, we have designed a novel, achiral endothelin antagonist of high potency which is without measurable affinity to the AT-1 receptor.

References

1. Yanagisawa, M., Kurihara, H., Kimura, S., Tomobe, Y., Kobayashi, M., Mitsui, Y., Yazaki, Y., Goto, K., Masaki, T., *Nature*, 332 (1988) 411-415.
2. Ruffolo Jr., R.R. in Ruffolo, R.R., (ed.), 'Endothelin Receptors: From the Gene to the Human', CRC Press Inc., Boca Raton, FL, USA, 1995.
3. Elliott, J.D., Lago, M.A., Cousins, R.D., Gao, A., Leber, J.D., Erhard, K.F., Nambi, P., Elshourbagy, N.A., Kumar, C., Lee, J.A., Bean, J.W., DeBrosse, C.W., Eggleston, D.S., Brooks, D.P., Feuerstein, G., Ruffolo Jr., R.R., Weinstock, J., Gleason, J.G., Peishoff, C.E. and Ohlstein, E.H., *J. Med. Chem.*, 37 (1994) 1553-1557.

Peptides: Chemistry, Structure and Biology
Pravin T.P. Kaumaya and Robert S. Hodges (Eds.)
Mayflower Scientific Ltd., 1996

283
A New Template for Structure Based Design of Non-peptide HIV Protease Inhibitors

R.A. Chrusciel, L.L. Maggiora, J.M. Tustin, J.H. Kinner, W.J. Howe, K.D. Watenpaugh, B.C. Finzel, M.N. Janakiraman, P.K. Tomich, M.-M. Hornig, J.C. Lynn and C.W. Smith

Upjohn Laboratories, The Upjohn Co., Kalamazoo, MI, 49001, USA

Introduction

Inhibition of the aspartyl protease of the human immunodeficiency virus (HIV) remains an attractive target for the treatment of AIDS [1, 2]. Great progress has been made in the design of peptidomimetic inhibitors based on knowledge of peptide substrates of the enzyme [3]. In addition, broad based screening has identified the non-peptide template, 4-hydroxycoumarin, as an inhibitor of HIV-1 protease [4-6]. After a series of structure based design cycles it was discovered that appropriately branched substitution on a 4-hydroxypyrone template could replace the aromatic ring of the 4-hydroxycoumarin nucleus [4]. Chemical intuition suggested to us that the five-membered ring congener, tetronic acid, might also be a suitable template for potent HIV-1 protease inhibitors which might offer some advantageous physico-chemical properties. Molecular modelling using the x-ray crystal complexes of HIV protease and 4-hydroxypyrone inhibitors supported this contention and suggested that appropriately substituted tetronic acids could productively interact with the S_2 through S_2' binding pockets of the enzyme (Figure 1). In addition, microbial derived acyl-tetronic acids were reported to be weak HIV-1 protease inhibitors [7-9].

Results and Discussion

Initially, 3-cyclopropylphenylmethyl tetronic acids were prepared since this branched side chain had provided for potent 4-hydroxypyrone-based inhibitors [10]. Besides ring size, one of the most interesting structural design considerations between tetronic acid and 4-hydroxypyrone based inhibitors is the hybridization at the 5- (6-) position of the template. The 5-position in tetronic acid is a sp^3 hybridized carbon which allows for disubstitution. In addition, as an sp^3 carbon, the attached side chain(s) of the tetronic acid are oriented at angles different from that of the sp^2 hybridized carbon of the corresponding 6-position of the pyrone ring.

These structural differences provide unique opportunities to explore conformational space in the tetronic acid series unavailable in the pyrone based inhibitors. From a series of 5-monosubstituted alkyl and phenylalkyl tetronic acids the benzyl and phenylpropyl substituents were found to provide the most potent inhibitors, with the benzyl analogue

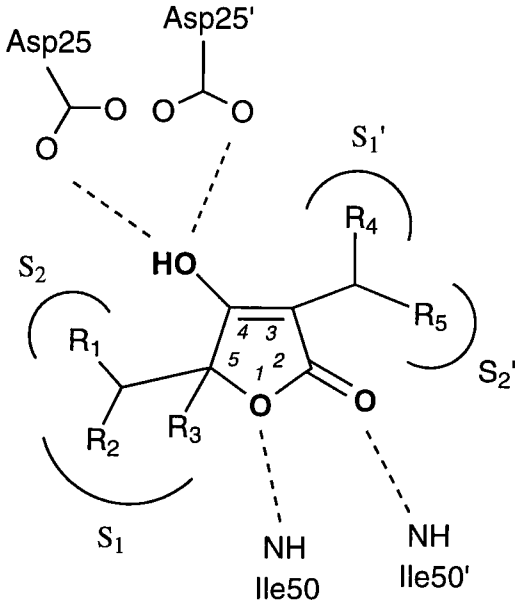

Figure 1. *Model of 3,5-substituted tetronic acid based HIV-1 protease inhibitors depicting key subsite and H-bonding interactions in the enzyme active site.*

(U-98807, Figure 1 where R_1 and R_5 are phenyl, R_2 and R_3 are proton and R_4 is cyclopropyl) possessing a K_i of 65 nM against HIV-1 protease. This potency was similar to U-96988, the 4-hydroxypyrone clinical candidate, but was achieved without introducing branching on the side chain at the 5-position.

With such a potent inhibitor in hand, it was possible to obtain an x-ray crystallographic structure of U-98807 while bound to HIV-2 protease and to update our modelling effort. As suggested by the initial modelling, the tetronic acid template successfully fulfilled the necessary binding interactions with the enzyme's catalytic Asp's and the flap Ile amides (in the absence of the ubiquitous water molecule). When overlaid by the bound structure of a similar 4-hydroxypyrone, the tetronic acid ring was found oriented in much the same way as the 4-hydroxypyrone ring, but shifted slightly relative to the catalytic Asp's. U-98807 was found to productively interact with the S_2, S_1' and S_2' subsites of the enzyme. However, the S_1 subsite remained essentially unoccupied. Subsequent modelling suggested that the S_1 subsite could be reached either by branching at the 5-α-position (a successful strategy in the 4-hydroxypyrone series) or by disubstitution at the 5-position with a relatively small alkyl group.

As predicted by the model, the analogue with 5-α-ethylbenzyl substitution (*i.e.*, Figure1 where R_1 is phenyl, R_2 is ethyl and R_3 is proton) was a potent inhibitor (K_i of 43 nM), but with only a modest increase over U-98807. The best inhibitor in the 5-α-substituted series was the 5-α-ethylbutyl analog (K_i of 27 nM). The ability to interact with the S_1 subsite was then explored *via* 5,5-disubstitution. Within this series as one substituent was held constant (*i.e.*, benzyl, phenylethyl or phenylpropyl) the most potent

inhibitors were obtained when the second side chain was propyl (K_i 4-6 nM) with decreased potency for smaller or larger groups. Again, this was not unexpected from the model based on the U-98807/enzyme complex.

The potent inhibitor 3-cyclopropylphenylmethyl-5-phenylpropyl-5-propyl tetronic acid (U-102377, K_i of 4 nM, Figure 1 where R_1 is phenylethyl, R_2 is proton, R_3 is propyl, R_4 is cyclopropyl and R_5 is phenyl) was co-crystallized with HIV-1 protease and the x-ray structure showed a surprising result. The ring of U-102377 was shifted significantly in the active site pocket allowing for less room in the S_2 subsite. Consequently, the 5-phenylpropyl side chain no longer occupied the S_2 subsite, as seen with U-98807, but reached instead through the S_1 subsite into the S_3 subsite. The smaller 5-propyl side chain was now in the S_2 subsite. Of interest, the activities of the 5-α-substituted and 5,5-disubstituted tetronic acids were consistent with the modelling predictions based on the initial x-ray structure, but possibly for the wrong reason. Nonetheless, the tetronic acid template provided very potent HIV-1 protease inhibitors.

References

1. Debouck, C. and Metcalf, B.W., *Drug Develop. Res.*, 21 (1990) 1.
2. Darke, P.L. and Huff, J.R., *Adv. Pharmacol.*, 25 (1994) 399.
3. Thaisrivongs, S., *Annu. Rep. Med. Chem.*, 29 (1994) 133.
4. Thaisrivongs, S., Tomich, P.K. Watenpaugh, K.D., Chong, K.-T., Howe, W.J., Yang, C.-P., Strohbach, J.W., Turner, S.R., McGrath, J.P., Bohanon, M.J., Lynn, J.C., Mulichak, A.M., Spinelli, P.A., Hinshaw, R.R., Pagano, P.J., Moon, J.B., Ruwart, M.J., Wilkinson, K.F., Rush, B.D., Zipp, G.L., Dalga, R.J., Schwende, F.J., Howard, G.M., Padbury, G.E., Toth, L.N., Zhao, A., Koeplinger, K.A., Kakuk, T.J., Cole, S.L., Zaya, R.M., Piper, R.C., and Jeffrey, P., *J. Med. Chem.*, 37 (1994) 3200.
5. Tummino, P.J., Ferguson, D., Hupe, D. and Hupe, D., *Biochem. Biophys. Res. Commun.*, 200 (1994) 1658.
6. Tummino, P.J., Ferguson, D. and Hupe, D., *Biochem. Biophys. Res. Commun.*, 201 (1994) 290.
7. Dolak, L.A., Seest, E.P., Ciadella, J.I. and Bohanon, M.J., *PCT Int. Appl.* 93/04055, Mar. 4, 1993.
8. Roggo, B.E., Petersen, F., Delmendo, R., Jenny, H., Peter, H.H., and Roesel, J., *J. Antibiotics*, 47 (1994) 136.
9. Roggo, B.E., Hug, P., Moss, S., Raschdor, F., and Peter, H.H., *J. Antibiotics*, 47 (1994) 143.
10. Romines, K.R., Watenpaugh, K.D., Tomich, P.K., Howe, W.J., Morris, J.K., Lovasz, K.D., Mulichak, A.M., Finzel, B.C., Lynn, J.C., Horng, M.-M., Schwende, F.J., Ruwart, M.J., Zipp, G.L., Chong, K.-T., Dolak, L.A., Toth, L.N., Howard, G.N., Rush, B.D., Wilkinson, K.F., Possert, P.L., Dalga, R.J., Hinshaw, R.R., *J. Med. Chem.*, 38 (1995) 1844.

Peptides: Chemistry, Structure and Biology
Pravin T.P. Kaumaya and Robert S. Hodges (Eds.)
Mayflower Scientific Ltd., 1996

284
GPIIb/IIIa Antagonists with Long Oral Duration Designed from Cyclic Peptides

J. Samanen, F.E. Ali, L. Barton, W. Bondinell, J. Burgess, J. Callahan, R. Calvo, W. Chen, L. Chen, K. Erhard, R. Heyes, S.-M. Hwang, D. Jakas, R. Keenan, T. Ku, C. Kwon, C.-P. Lee, W. Miller, K. Newlander, A. Nichols, C. Peishoff, G. Rhodes, S. Ross, A. Shu, R. Simpson, D. Takata, T.O. Yellin, I. Uzsinskas, J. Venslavsky, A. Wong, C.-K. Yuan and W. Huffman

SmithKline Beecham Pharmaceuticals, King of Prussia, PA 19406, USA

Introduction

We have described two series of 1,4-benzodiazepine GPIIb/IIIa antagonists. The first series [1], typified by compound 2 [2] bearing an amidinophenylamide in position eight, was designed from cyclic peptide antagonists, displaying a near atom-for-atom overlay with the RGD portion of peptide SK&F 107260 5 which displays a turn-extended-turn about RGD. The second series[3], typified by 4, bearing an amidinophenylamide in position seven, was found to readily overlay cyclo(Pro-Arg-Gly-Asp-Gly-Pro) 10 which displays a β turn about Gly-Asp. Although the spatial location of the 7-amidinophenyl

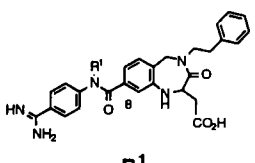

	R^1
1	H
2	CH_3

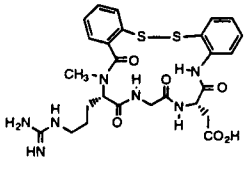

5, SK&F 107260

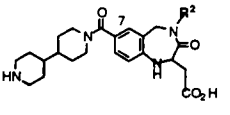

	R^1
6	CH_2CH_2Ph
7	CH_3
8, (2S)-SB 214857	CH_3
9, (2-R)	CH_3

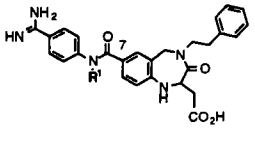

	R^1
3	H
4	CH_3

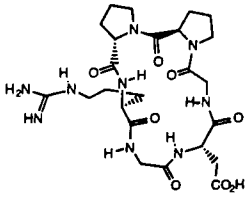

10, cyclo(Pro-Arg-Gly-Asp-Gly-D-Pro)

1- 4 , 6- 7 are racemic

Table 1. *In Vitro Activities of Peptide and Nonpeptide GPIIb/IIIa Antagonists.*

Compound	Configuration of Benzodiazepine at Position 2	Platelet Aggregation hPRP/ADP[a] IC_{50} (nM)	Binding Inhibition ^{3}H-5 / hGPIIb/IIIa[b] Ki (nM)
1	R,S	150	1.5
2	R,S	65	1.6
3	R,S	380	26
4	R,S	160	90
5	(S-Asp)	57.0	1.5
6	R,S	20	1.5
7	R,S	90	4.0
8	S	28	2.5
9	R	8167	1530
10	(S-Asp)	5260	1900

[a]Platelet aggregation in human platelet-rich plasma induced by ADP. [b]Binding of ^{3}H-SK&F 107260 to GPIIb/IIIa purified from human platelets, reconstituted in liposomes.

group in compounds 3 and 4, differs from the 8-amidinophenyl group in 1 and 2, the nonpeptides 3 and 4 display high affinity to human GPIIb/IIIa and high potency in a human platelet aggregation assay (Table 1) albeit lower than 1 and 2. Compounds 1 - 4 displayed potent *in vivo* activity after intravenous administration, but only 2 displayed activity *in vivo* after intraduodenal administration (Figure 1) [2]. The *in vivo* duration of 2, however, was insufficient for b.i.d. dosing. The hypothesis that superior activities in the 8-substituted series related to spatial location of the cation invoked a search for 7-substituents that could position a cationic group in the same region of space as the cation in 1 or 2.

Results and Discussion

That search led to the rigid bipiperidinyloxo group, which gave the 7-substituted compound 6, which was shown to be a potent GPIIb/IIIa antagonist (Table 1). Compound 6 was also potent *in vivo*, Figure 1, and superior to 2. Continued optimization of oral activity in the 7-series led to the discovery that replacement of the 4-phenethyl group with 4-Me, as in 7, resulted in a decrease in potency *in vitro* but a gain in activity *in vivo*, Figure 1. Both enantiomers of 7 were prepared by enantiospecfic synthesis from R and S aspartic acid [4]. The S-enantiomer 8 is considerably more potent *in vitro* than the R-enantiomer 9. SB 214857, 8, is a potent antiaggregatory agent after intravenous and intraduodenal administration and displays a long duration of action (Figure 1).

That 8 may be a nonpeptide mimetic of the peptide 5 comes from the fact that both compounds a) position cationic amine and anionic carboxylate groups in the same regions of space, and b) are derived from (S)-aspartic acid. ^{3}H-8, bearing tritium in the benzo-group, displays specific, saturable binding to human GPIIb/IIIa with a Kd of 2 nM, identical to the Ki of inhibition of ^{3}H-5 binding to GPIIb/IIIa by cold 8. ^{3}H-8 binding is completely reversed either by cold 8 or cold 5, even after preincubation for 1

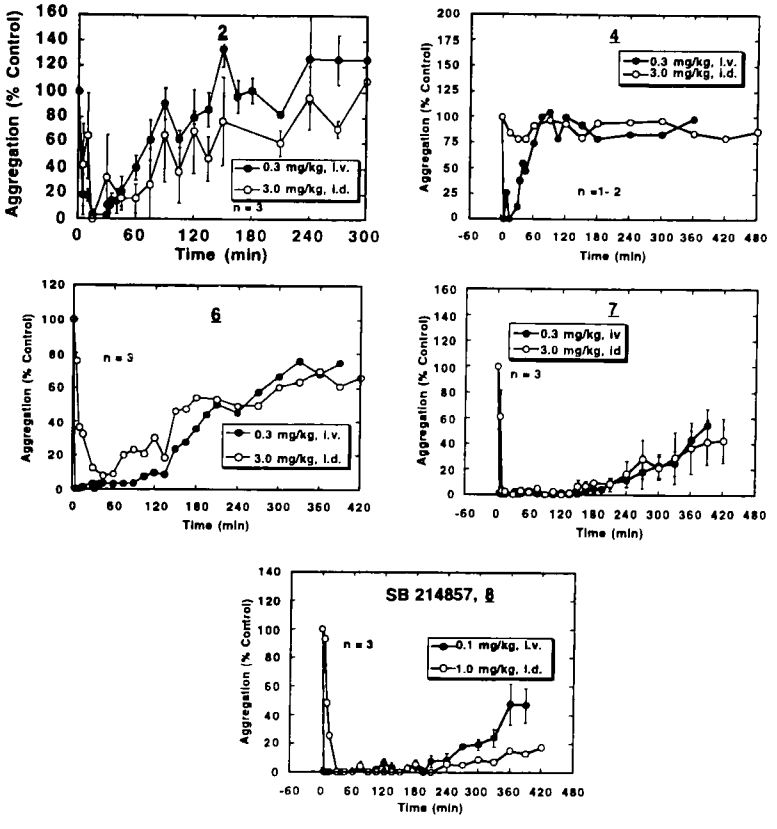

Figure 1. *Percent platelet aggregation (canine whole blood stimulated with collagen) ex vivo after intravenous administration, closed circles,or intraduodenal administration, open circles, to the conscious dog of compound 2, 4, 6, 7, and SB 214857, 8.*

hour. The Ki values for various compounds determined in either an ^{3}H-8 or ^{3}H-5 competition binding assay are similar [4]. Thus, we observe no appreciable difference between the binding of SB 214857 and SK&F 107260 to purified human GPIIb/IIIa. Thus, SB 214857 appears to be an example where the peptide and nonpeptide ligands may bind to the same receptor binding site.

References

1. Ku, T., Ali, F., Barton, L.S., *J. Amer. Chem. Soc.*, 115 (1993) 8861.
2. Bondinell, W., Keenan, R.M., Miller, W., *Biorg. Med. Chem.*, 2 (1994) 897.
3. Ku, T. , Miller, W., Bondinell, W., Keenan, R., *J. Med. Chem.*, 38 (1995) 9.
4. Miller, W. and Wong, A., unpublished data.

Peptides: Chemistry, Structure and Biology
Pravin T.P. Kaumaya and Robert S. Hodges (Eds.)
Mayflower Scientific Ltd., 1996

285
Sugar Amino Acids as Novel Peptidomimetics

E. Graf von Roedern[1], E. Lohof[2], M. Hoffmann[2], G. Hessler[2] and H. Kessler[2]

[1]Arbeitsgruppe für Bioorganische Chemie, Max Planck Institut für Biochemie, 82143 Martinsried, Germany
[2]Institut für Organische Chemie und Biochemie, Technische Universität München, 85747 Garching, Germany

Introduction

We have developed a new and uniform class of peptidomimetics by the incorporation of carbohydrates into the backbone of peptides [1, 2]. Carbohydrates are frequently found in natural products of therapeutic importance, but to our knowledge it is part of a peptidic structure only in the case of galantine I [3].

In order to use carbohydrates as peptide building blocks they have to be transformed into sugar amino acids (SAA). Here we present pyranoid ring structures that carry an amino and a carboxylic function in distinct substitution patterns. These SAA impart significant conformational restrictions when incorporated into peptides through the rigid six membered sugar ring.

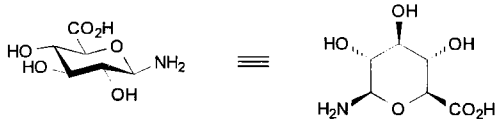

Figure 1. *Example for a sugar amino acid (SAA).*

A main advantage of the SAA is that they are more or less "natural" molecules in an "unnatural" combination. It is very unlikely that SAA-containing peptides are degraded enzymatically, but if processing occurs with the release of SAA they are most probably excreted by the phase II uronic acid pathway. Uronic acids are used as carrier molecules in the human body for an active decontamination [4]. Most of the other "unnatural" peptidomimetics have a totally unknown metabolism.

Results and Discussion

Figure 2 shows a series of SAA which can be used as a construction kit for peptide conformations; thereby the SAA offer the possibility to design mimetics from dipeptide isosteres to α-amino acids. The syntheses of all these SAA are straightforward and use cheap starting materials. SAA **3** and **5** are already known in the literature [5, 6].

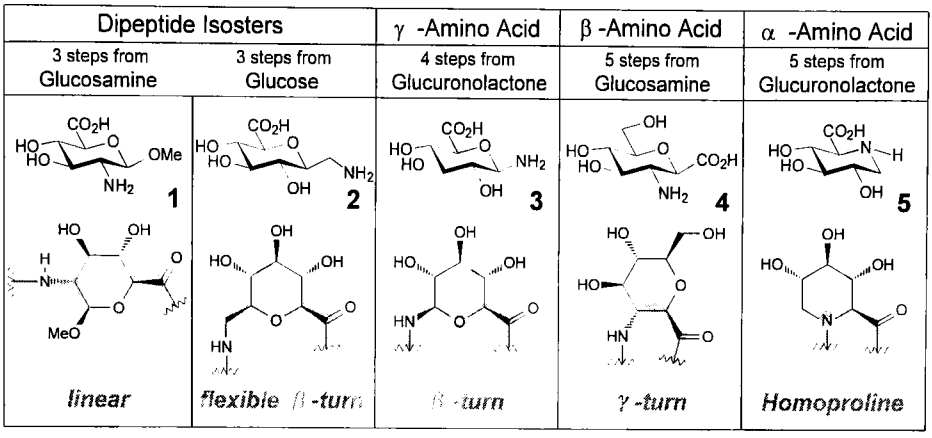

Figure 2. *SAA in a construction kit for peptide conformations.*

All SAA of Figure 2 contain a six membered ring with all substituents in equatorial positions. Therefore the chair conformation is very stable and rigid which allows the prediction of the conformational restrictions when incorporated in peptides. SAA **1** constrains a linear peptide conformation, whereas the others are turn mimetics. The diameter of the turn decreases from the left to the right. **2** and **3** serve as β-turn mimetics, **4** as a pseudo γ-turn mimetic and **5** is a homoproline or a tri-hydroxy pipecolic-acid.

Despite the different conformational restrictions introduced by these SAA, the physical, chemical and pharmaceutical properties should be more or less preserved because all SAA carry two or three hydroxy groups in a similar arrangement. On the other hand, the hydroxy groups can easily be modified, *e.g.*, by benzylation or by other hydroxy protecting groups. This will change the physical and chemical properties. The protecting groups could even serve as mimics for additional peptidic structure in a way which has been demonstrated by Hirschmann *et al.* [7].

In order to characterize the conformational behavior of the SAA, several cyclic SAA-peptides were synthesized (Figure 3). Their conformations were determined by

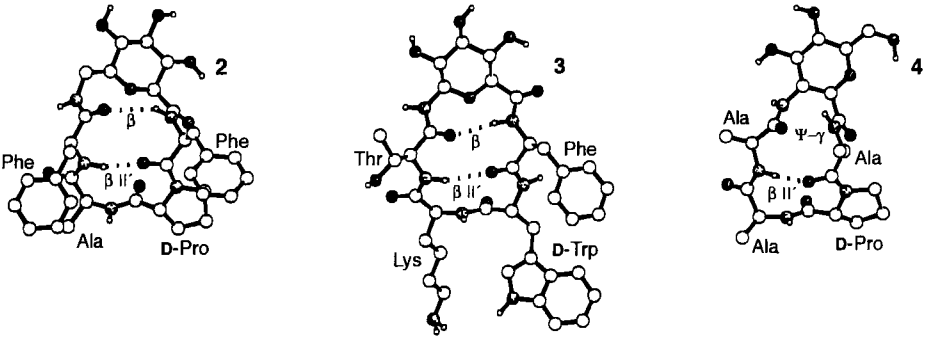

Figure 3. *Conformation of the SAA 2, 3 and 4 in cyclic peptides.*

NMR spectroscopy and molecular dynamics calculations. In these cyclic peptides, the SAA **2**, **3** and **4** are linked to tetrapeptides which contain one D-amino acid. The D-amino acid in *i+1* position of the lower loop stabilizes a βII'-turn. In case of the first two peptides, the SAA **2** and **3** occupy the *i+1* and *i+2* position of a pseudo upper β-turn. The peptide containing SAA **4** forms a narrow loop similar to a γ-turn.

The SAA have been employed in linear and cyclic peptides of biological importance. For example SAA **2** was used as a dipeptide isostere in the highly potent and $\alpha_v\beta_3$ selective cyclic RGD-peptide *cyclo*(-D-Phe-Val-Arg-Gly-Asp-) [8] where it replaces the D-Phe-Val moiety. A superposition of the SAA **2**-peptide with cyclo(-D-Phe-Val-Arg-Gly-Asp-) shows that the conformation of the active Arg-Gly-Asp motifs are very similar (Figure 4). So the SAA-peptide shows the same selectivity tendency although the activity is lower because the sugar peptide does not contain the important lipophilic side chains.

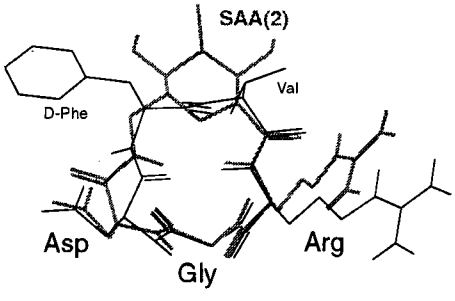

IC_{50}[nM]	D-Phe-Val - R G D	SAA(2) - R G D
Fibrinogen receptor	300	2200
Vitronectin receptor	3	275

Figure 4. *Superposition of cyclo(-D-Phe-Val-Arg-Gly-Asp-) with cyclo(-SAA(2)-Arg-Gly-Asp-) and their activity towards the fibrinogen and the vitronectin receptor.*

References

1. Graf von Roedern, E., Kessler, H., *Angew. Chem. Int. Ed. Engl.*, 33 (1994) 687.
2. Graf von Roedern, E., Kessler, H., Kutscher, B., Bernd, M., Klenner, T., (ASTA Medica), Ger. Pat. Appl. (8.11.1993) DE. 4338015; Eur. Pat. Appl. (17.10.1994), EP 94116355.2; US. Pat. Appl. (01.11.1994), US 08/332,071.
3. Sakai, N., Ohfune Y., *J. Am. Chem. Soc.*, 114 (1992) 998.
4. Keglevic, D., *Adv. Carbohydr. Chem.*, 36 (1979) 57.
5. Nitta, Y., Kuranari, M., Kondo, T., *Yakugaku Zasshi*, 81 (1961) 1166.
6. Bashyal, B.P., Chow, H.F., Fleet G.W.J., *Tetrahedron Lett.*, 27 (1986) 3205.
7. Hirschmann, R., Nicolaou, K.C., Pietranico, S., Leahy, E.M., Salvino, J., Arison, B., Cichy, M.A., Spoors, P.G., Skakespeare, W.C., Sprengler, P.A., Hamley, P., Smith, A.B.III, Reisine, T., Raynor, K., Maechler, L., Donaldson, C., Vale, W., Freidinger, R.M., Cascieri, M.R., Strader, C.D., *J. Am. Chem. Soc.*, 115 (1993) 12550.
8. Aumailley, M., Gurrath, M., Müller, G., Calvete, J., Timpl, R., Kessler, H., *FEBS Lett.* 291 (1991) 50.

Peptides: Chemistry, Structure and Biology
Pravin T.P. Kaumaya and Robert S. Hodges (Eds.)
Mayflower Scientific Ltd., 1996

286

Novel Enantioselective Syntheses of Methylated Amino Acids Based on Sharpless Asymmetric Dihydroxylation Reactions

H. Shao and M. Goodman

Department of Chemistry & Biochemistry University of California, San Diego
La Jolla, CA 92093, USA

Introduction

In recent years, the osmium-catalyzed asymmetric dihydroxylation (AD) introduced by Sharpless and coworkers has evolved into one of the most enantioselective processes known [1]. However, very little effort has been undertaken to explore the possible application of AD reactions in peptide chemistry. Herein we describe an efficient and enantioselective strategy using AD reactions to prepare multigram quantities of α,β-dimethylated amino acids and β-methylated amino acids.

Results and Discussion

In the AD reactions (Figure 1), we chose the commercially available α,β-unsaturated ester derivatives as the substrates, and the most versatile "dimeric" bis(dihydroquinidinyl) phthalazine as the catalytic ligands which are included in the reagent mixture of AD-mix-α and AD-mix-β.

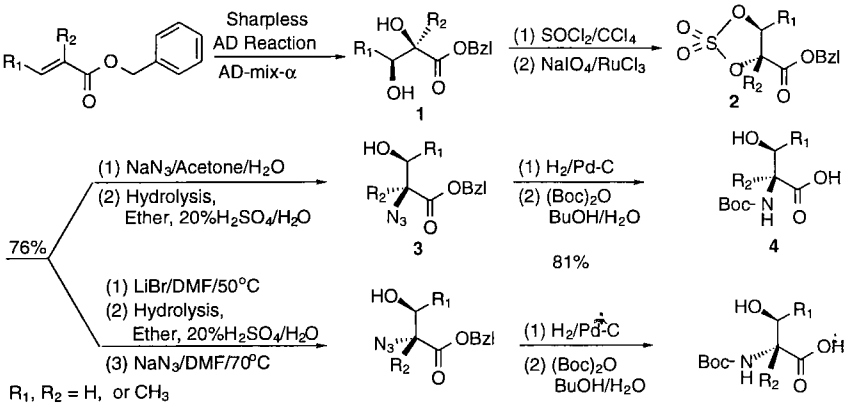

Figure 1. *Enantioselective syntheses of α-methylated amino acids.*

Starting with benzyl tiglate (60mmol, Figure 1: R_1, R_2=CH_3), the Sharpless AD reaction with AD-mix-α in the presence of $CH_3SO_2NH_2$ proceeds smoothly to give diol **1** with excellent optical purity (>96%ee). The diol **1** is converted to its 2,3-cyclic sulfite with $SOCl_2$ and oxidized to cyclic sulfate **2** in a one-pot fashion[2]. The subsequent nucleophilic substitution at the α-C of **2** with clean inversion of chirality and acidic hydrolysis provides the desired α-azido ester **3**. Compound **3** readily undergoes catalytic hydrogenation to produce the enantioisomerically pure (2S,3S) 2-methylthreonine. The X-ray diffraction analysis of (2S,3S) Boc-2-methylthreonine **4** proves the correct structure of the final product. In addition, the cyclic sulfate **3** can be converted to its diastereoisomer, (2R,3S) 2-methylthreonine by two sequential inversion steps with LiBr and NaN_3. The α-azido ester **3** can be stereospecifically transformed to the aziridine derivative. These aziridine compounds are very important intermediates for the synthesis of α,β-dimethylated cysteine[3] and tryptophan analogs (Figure 2).

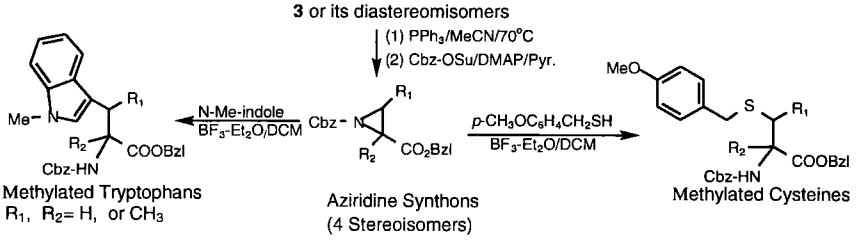

Figure 2. *Enantioselective synthesis of α,β-dimethylated cysteines and tryptophan.*

As an extension of the above strategy, we have synthesized the *allo*-threonine analogs and related cysteine and tryptophan derivatives starting with benzyl crotonate (Figure 1 and 2, R_1=CH_3, R_2=H). This efficient method can provide the *allo*-threonine in 30mmol scale and high optical purity (>99% ee) which we anticipate will provide large amounts of L- and D-*allo*-threonines in a facile manner.

In this report we demonstrate that the Sharpless asymmetric dihydroxylation reactions are very powerful routes to generate a variety of unusual amino acids. The reactions involved are clean, simple and readily scaled-up. This method is also a versatile strategy to synthesize more complex alkyl substituted amino acids. We are now actively examining such reactions.

References

1. Sharpless, K.B., *Chemical Reviews,* 94 (1994) 2483.
2. Machinaga N., Kibayashi, C., *J. Org. Chem.*, 56 (1991) 1386.
3. Shao, H., Zhu, Q., Goodman, M., *J. Org. Chem.* 60 (1995) 790.

Peptides: Chemistry, Structure and Biology
Pravin T.P. Kaumaya and Robert S. Hodges (Eds.)
Mayflower Scientific Ltd., 1996

287
1,2,4-Triazin-6-ones as Peptidomimetic Templates for Cholecystokinin-A Agonists

H.F. Schmitthenner, K.G. Doring, E.S. Downs, R.D. Simmons, J.A. Zongrone, R.P. Julien, F.C. Kaiser, T.D. Goodman and J.D. Rosamond

Departments of Chemistry and Biology, Astra Research Corporation, PO Box 20890, Rochester, NY 14602, USA

Introduction

Selective cholecystokinin-A (CCK-A) receptor agonists are of interest as appetite suppressants for treating obesity. All reported CCK-A agonists with potential therapeutic utility are reduced peptide analogs of CCK-8. Two examples are A-71623 (Boc-Trp-Lys(Tac)-Asp-MePhe-NH_2) [1] and ARL-15849 (Hpa(SO_3H)-Nle-Gly-Trp-Nle-MeAsp-Phe-NH_2) [2].

In an approach to increase *in-vivo* stability we designed a template to constrain residues of the tetrapeptide lead (Figure 1) [3]. We rationalized that the 1,2,4-triazin-6-one template could be readily synthesized from available chiral precursors and offer a robust, versatile scaffold for three of four residues of A-71623. This approach led to the discovery of CCK-A selective peptidomimetic agonists.

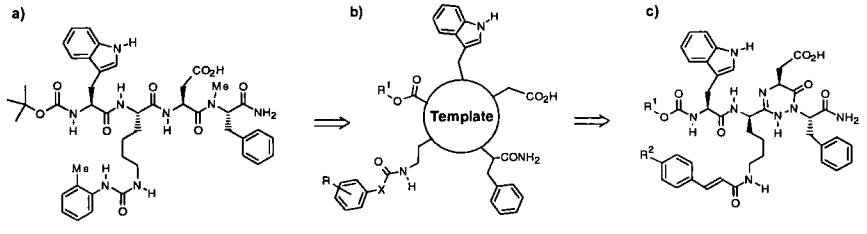

Figure 1. *a) tetrapeptide lead A-71623; b) template approach (R = CH_3, OH; R^1= tBu, iPr; X = NH, CH=CH); and c) 1,2,4-triazin-6-one leads (R^1 = tBu, iPr; R^2 = OH, OSO_3H).*

Results and Discussion

A synthesis for the 1,2,4-triazin-6-one peptidomimetics (Figure 2) was developed from thioamide containing dipeptide esters and hydrazino-acids available by Evans' chiral alkylation methods [4]. Useful synthetic features include regiospecific ring closure as shown, preservation of chirality at all centers, and stability of the 1,2,4-triazin-6-one to standard peptide elongation and side chain elaboration.

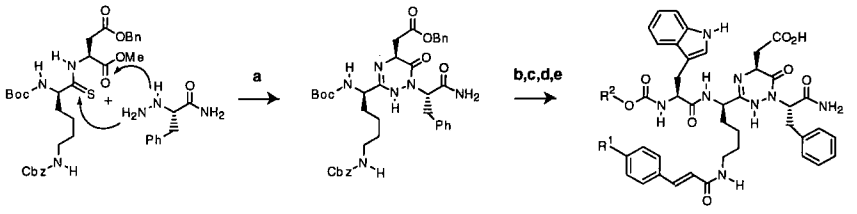

Figure 2. *Synthesis of 1,2,4-triazin-6-one ARL-16610 (R^1 = iPr, R^2 = OH). a) $Hg(OAc)_2$, b)HCl, c) iPrOCO-Trp-OH, TBTU, HOBt, d) H_2/Pd, e) p-hydroxycinnamoyl-OSu.*

A series of 1,2,4-triazin-6-ones analogous to A-71623 were synthesized with the template centered at each residue of the peptide. CCK-A affinity assays showed optimum activity in the triazinones centered at Asp with natural side chain length and chirality at each residue with the exception of Lys where D-Lys was preferred (Figure 2). Functional assays in phosphatidylinositol hydrolysis (PI) and guinea pig gallbladder contraction (GPGB) in the lead series showed that substitution on the ε-amino of Lys with *p*-hydroxycinnamic acid or its sulfated form led to full functional efficacy (Table 1).

In feeding inhibition (FI) experiments the lead compounds inhibited feeding in rats in a dose (ip) dependent manner (Table 1). This inhibition was reversed by the CCK-A antagonist MK-329 showing the mechanism was CCK-A receptor based. ARL-16610 was stable for over 8 hours in stomach acid and dog kidney homogenate models indicating excellent metabolic stability.

Table 1. *Affinity and functional assay results for 1,2,4-triazinone CCK -A peptidomimetics.*

ARL No.	R^1	R^2	CCK-A *vs* agonist[a] K_i(nM)	CCK-A *vs* antag[b] K_i(nM)	CCK-A *vs* antag[c] K_i(nM)	K_i Ratio *vs* antag[d]	PI Eff. (%)	GPGB EC_{50} (nM)	FI,ip ED_{50} (μg/kg)
15989	tBu	OH	30	200	820	4.2	70	80	3000
16446	tBu	OSO_3H	8.7	110	470	4.2	100	130	1200
16610	iPr	OH		180	1600	9.1	91	1400	300
16617	iPr	OSO_3H		100	570	5.5	90	55	70%[e]

[a][^{125}I]-BH-CCK-8, [b][^{3}H]-MK-329 with G-protein coupled, [c][^{3}H]-MK-329 with G-protein uncoupled, [d]G-protein uncoupled over coupled K_i, [e]Feeding inhibition at 1000 μg/kg.

References

1. Shiosaki, K., Lin, C.W., Kopecka, H., Tufano, M.D., Bianchi, B.R., Miller, T.R., Witte, D.G., Nadzan, A.M., *J. Med. Chem.*, 34 (1991) 2837.
2. Rosamond, J.D., Pierson, M.E., Kaiser, F.C., Zongrone, J.A., McCreedy, S.A., Comstock, J.M., Simmons, R.D., '1st Annual IBC International Symposium on Obesity', Washington, DC, February ,1995.
3. For reviews of peptide templates see, Gante, J., *Angew. Chem., Int. Ed.*, 33 (1994) 1699; Olsen, G., *J. Med. Chem.*, 36 (1993) 3039.
4. Evans, D., Britton, Dorow, R.L., Dellaria, J.F., *Tetrahedron*, 44 (1988) 17, 5525.

Peptides: Chemistry, Structure and Biology
Pravin T.P. Kaumaya and Robert S. Hodges (Eds.)
Mayflower Scientific Ltd., 1996

288

Design and Synthesis of Dermorphin Analogues Containing Heterocyclic Based Phe-Gly Mimetics

S. Borg[1], K. Luthman[1], L. Terenius[2], and U. Hacksell[1]

[1]*Department of Organic Pharmaceutical Chemistry, Uppsala University, BMC, S-751 23 Uppsala, Sweden*
[2]*Department of Clinical Neuroscience, Experimental Alcohol and Drug Addiction Research Section, Karolinska Hospital, S-171 76 Stockholm, Sweden*

Introduction

Modification of peptides to obtain chemically stable and/or conformationally restricted analogues can be done by replacement of amide bonds or peptide fragments with non peptidic moieties. Thus, five-membered heterocyclic ring systems, such as imidazole, oxazole, and thiazole, have been used as mimics to replace the peptide bond [1].

We have synthesized six different Phe-Gly analogues containing a 1,2,4-oxadiazole, a 1,3,4-oxadiazole, or a 1,2,4-triazole moiety. These ring systems are frequently used as ester and/or amide bioisosters in the synthesis of biologically active compounds [2]. The obtained dipeptidomimetics have been used as building blocks in solid phase peptide synthesis replacing Phe[3]-Gly[4] in dermorphin (Tyr-D-Ala-Phe-Gly-Tyr-Pro-Ser-NH_2) [3], which is a highly potent and selective μ-receptor ligand. The N-terminal tetrapeptide is the minimal sequence required for activity [4]. Examples of structural features suggested to be important for biological activity are the orientation of the aromatic side chains [5] and the Phe[3]-Gly[4] peptide bond [6]. We therefore consider dermorphin an interesting target for evaluation of the dipeptide analogues as mimics of Phe-Gly. The synthesized pseudopeptides **1-6** have been evaluated in a μ-receptor binding assay.

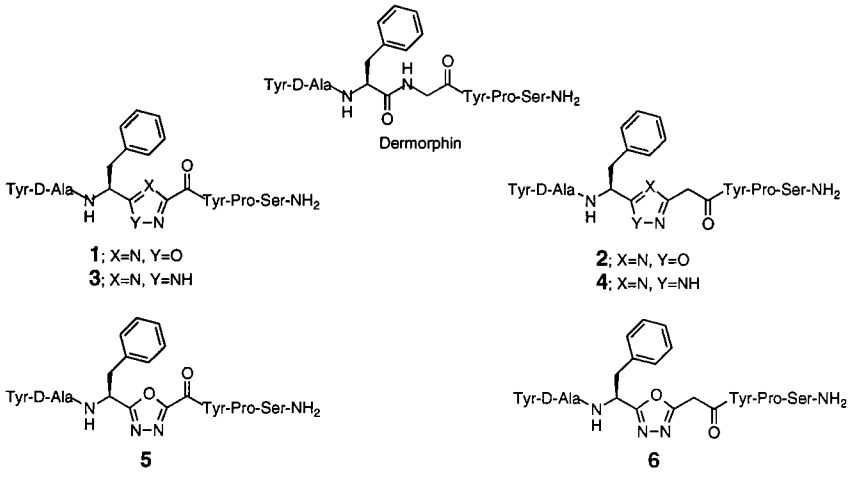

Results and Discussion

Phe-Gly analogues were synthesized by reported procedures for X-Gly mimetics [2]. Boc-L-Phe-OH was used as starting material. Enantiopurities were determined by HPLC on a chiral stationary phase. All compounds showed enantiopurities above 93% ee.

Manual solid phase peptide syntheses were performed on a MBHA-resin in a plastic syringe, using N^{α}Boc-protected amino acids. Benzyl was used as the side chain protecting group for Tyr and Ser, and HBTU/HOBt/DIEA were used as coupling reagents. The Boc-groups were removed with conc. TFA.

In the synthesis of the Phe-Gly fragments in **1**, **3**, **4**, **5**, and **6**, the carboxylic acid functions were protected as esters. These analogues were hydrolyzed prior to coupling to the resin. The derivatives having the carboxylic function attached directely to the heterocycle (the Phe-Gly residues in **1**, **3**, and **5**) cannot be isolated as acids after hydrolysis as they are readily decarboxylated. Therefore the couplings of these compounds were done using the carboxylates (**3** and **5**) or immediately after isolation of the acid (**1**). Couplings of the Phe-Gly analogues in **1**, **2**, and **5** were performed by formation of mixed anhydrides (EtOCOCl/NMM in DCM/DMF). Interestingly, the deprotection of N^{α} of the Phe-Gly residue with TFA resulted in racemization. To avoid this iodotrimethylsilane (TMSI) was used as deprotecting agent in that step. The peptide analogues **1-6** were purified by reversed phase HPLC and characterized by MS and amino acid analysis.

Receptor affinities for the μ-opioid receptor were determined by displacement of [^{3}H]DAMGO from rat brain (minus cerebellum) membrane preparations (Table I). Compounds **1**, **4**, **5**, and **6** showed high binding affinities for the μ-receptor, whereas **2** and **3** showed moderate and low affinities, respectively. Studies on the μ/∂ selectivity of **1-6** are ongoing.

Table 1. *μ-Receptor binding affinities of dermorphin analogues 1-6.*

Compound	DAMGO	1	2	3	4	5	6
[^{3}H]DAMGO K_i, nM	1.5	5	70	300	10	7	15

References

1. Gordon, T., Hansen, P., Morgan, B., Singh, J., Baizman, E. and Ward, S., *Bioorg. Med. Chem. Lett.*, 3 (1993) 915.
2. Borg, S., Estenne-Bouhtou, G., Luthman, K., Csöregh, I., Hesselink, W. and Hacksell, U., *J. Org. Chem.*, 60 (1995) 3112.
3. Montecucchi, P.C., de Castiglione, R., Piani, S., Gozzini, L. and Erspamer, V., *Int. J. Peptide Protein Res.*, 17 (1981) 275.
4. Broccardo, M., Erspamer, V., Falconieri Erspamer, G., Improta, G., Linari, G., Melchiorri, P. and Montecucchi, P.C., *Brit. J. Pharmacol.*, 73 (1981) 625.
5. Tourwé, D., Verschueren, K., Van Binst, G., Davis, P., Porreca, D. and Hruby, V.J., *Bioorg. Med. Chem. Lett.*, 2 (1992) 1305.

Peptides: Chemistry, Structure and Biology
Pravin T.P. Kaumaya and Robert S. Hodges (Eds.)
Mayflower Scientific Ltd., 1996

289
Solid-phase Synthesis of Peptides with Branched Side-chain Bridges and Their Conformational Effects

W. Zhang and J.W. Taylor

Department of Chemistry, Rutgers University, Piscataway, NJ 08855, USA

Introduction

Incorporation of conformational constraints into peptides or proteins is constructive for identifying the functional conformations of bioactive linear peptides, guiding the design of antagonists or agonists, and understanding protein folding processes. Various side-chain to side-chain bridges that stabilize secondary structures have been reported [1]. The aim of our present study is to develop the solid-phase synthesis and applications of a new type of cyclic peptide in which a non-native tri-functional amino acid (such as diaminobutyric acid - Dap) is used to link three side-chains of amino acids in one peptide chain simultaneously, forming a branched bridge. Such structures may serve as a peptidomimetic scaffold in stabilizing secondary structures, such as the α-helix, or even more complex structures. For α-helix stabilization, we have designed two such bicyclic peptides, 1 and 2 (Scheme 1), having three linked residues in positions i, i+3 and i+7 in the linear amino acid sequence. The sequences of our peptides were derived from early (i, i+4) lactam-bridged model peptides to allow comparisons [1a]. The conformational effects of these novel branched bridges have been studied by CD.

Results and Discussion

Previous studies have shown that solvent played an important role in solid-phase cyclization reactions. In the solvent mixture DMSO:NMP (1:4) the yield of the desired

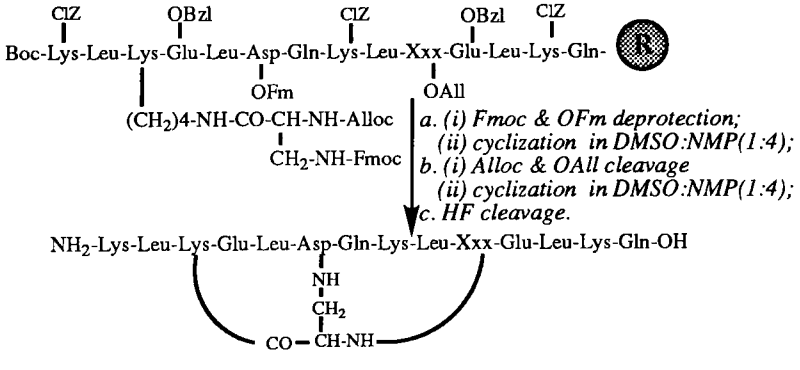

Scheme 1. *Synthetic route to Peptide 1 (Xxx=Asp) or Peptide 2 (Xxx=Glu).*

monomeric peptides was maximized [2]. As seen in Scheme 1, two consecutive solid-phase cyclizations, constructing branched-bridge cyclic peptides, have been achieved by combining standard Boc/Benzyl methods with the orthogonal Fmoc/OFm and Alloc/OAll [3] protecting groups. The use of an optimized solvent system (DMSO:NMP=1:4) for the cyclizations was essential for the successful synthesis of these peptides (Figure 1).

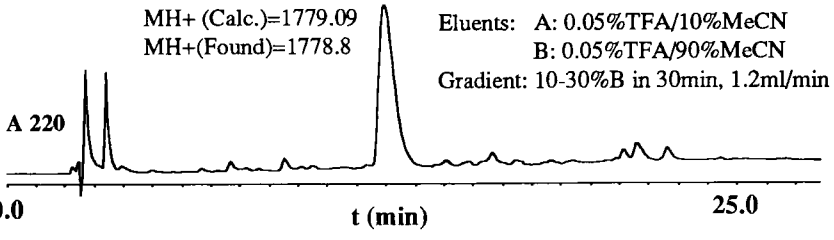

Figure 1. *HPLC profile of the crude Peptide 1 product after HF cleavage.*

Preliminary CD studies have been done in 10mM phosphate buffer, pH=7.0, or in 50% TFE at 25°C. As seen in Figure 2, Peptide 1 adopted a folded, nonhelical conformation in aqueous buffer or in 50% TFE, but Peptide 2 was substantially α-helical in 50% TFE. We hope to extend the application of branched side-chain bridges with multiple points of attachment to the stabilization of more complex structures.

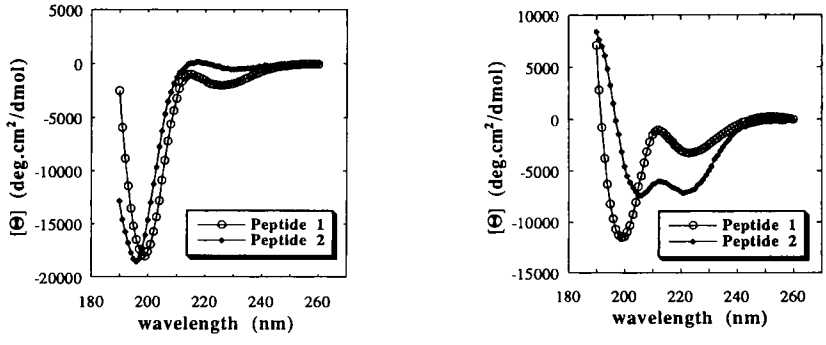

Figure 2. *CD Spectra of Peptide 1 and Peptide 2 in 10 mM phosephate buffer, pH=7.0 (left) and in 50% TFE (right).*

References

1. (a) Osapay, G., Taylor, J.W., *J. Am. Chem. Soc.*, 114 (1992) 6966. (b) Felix, A.M., Heimer, E.P., Wang, C.T., Lambros, T.J., Fournier, A., Mowles, T.F., Maines, S., Campbell, R.M., Wegrzynski, B.B., Toome, V., Fry, D., Madison, V.S., *Int. J. Pept. Protein Res.*, 32 (1982) 441, (c) Jackson, D.Y., King, D.S., Chmielewski, J., Singh, S., Schultz, P.G., *J. Am. Chem. Soc.*, 113 (1991) 9391; (d).Bracken, C., Gulyas, J., Taylor, J.W., Baum, J., *J. Am. Chem. Soc.*, 116 (1994) 6431.
2. Zhang, W., Taylor, J.W., *Tetrahedron Lett;* submitted.
3. Kates, S.A., Sole, N.A., Johnson, C.R., Hudson, D., Barany, G., Albericio, F., *Tetrahedron Lett.*, 34 (1993) 15491552.

Peptides: Chemistry, Structure and Biology
Pravin T.P. Kaumaya and Robert S. Hodges (Eds.)
Mayflower Scientific Ltd., 1996

290
Cyclization Tendency, Side Reactions and Racemization Examined with 400 Hexapeptides

S. Feiertag[1], K.-H. Wiesmüller[1], G.J. Nicholson[2] and G. Jung[1,2]

[1]NMI, Naturwissenschaftliches und Medizinisches Institut an der Universität Tübingen, D-72762 Reutlingen, Germany
[2]Institut für Organische Chemie, Universität Tübingen, D-72076 Tübingen, Germany

Introduction

Cyclic hexapeptides are extensively studied for structure activity relationships and one D-amino acid in the sequence is thought to favor the cyclization during synthesis due to its β-turn promoting properties [1]. To determine the prerequisites required for a successful cyclization we have synthesized 39 individually head-to-tail cyclized hexapeptides c[RGDSPO] and c[RGDSPo] including all usual L- (O) and D- (o) amino acids and Gly. The influence of the C-terminal residue on yield and racemization was examined. Since no difference in cyclization tendency has been observed when using L-amino acids in the C-terminal sequence position we have designed 400 cyclohexapeptides c[RO_1DSO_2Y] representing all possible combinations of the 20 L-amino acids in positions O_1 and O_2. The influence of Gly and Pro on cyclization tendency of linear all L-hexapeptides was investigated.

Results and Discussion

Linear hexapeptides were prepared by Fmoc/tBu strategy using Fmoc-amino acid-2-chlorotrityl resins on a multiple peptide synthesizer (Syro, MultiSynTech, Bochum, FRG). After cleavage from the resins with 20% acetic acid the fully side-chain protected peptides were individually and simultaneously cyclized in solution (0.001 M in DMF). Excess reagents were removed by washing steps, side chains were deprotected with TFA/scavenger and cyclic peptides were precipitated from ether.

For ring closure of RGDSPO and RGDSPo, three different reagents were used (TBTU, HATU, PPA) and crude cyclic peptides (purity > 80%) were obtained. Peptides containing amino acid residues with branched side chains in the C-terminal position (O = I, V, T; o = i, v, t) were only partially cyclized as shown by HPLC and electrospray ionization mass spectrometry (ESI-MS). Linear and modified linear (N_α-acetylated) peptides could be identified as side products. No difference was observed in the yield of cyclopeptides when TBTU, HATU or PPA were used for ring closure. L- and D- amino acids in the C-terminal position have no influence on cyclization of the hexapeptides RGDSPO and RGDSPo. Racemization of the C-terminal amino acids was determined by

Table 1. *Racemization of C-terminal amino acids in RGDSPO and RGDSPo (O = all L- and o = all D-amino acids) after cyclization with PPA determined by GC and HPLC (n.d. = not determined; ? = cyclopeptide was not identified due to side products in HPLC).*

	% Racemization			% Racemization	
c[RGDSPO]	GC	HPLC	c[RGDSPo]	GC	HPLC
A	n.d.	4.9	a	n.d.	3.1
C	n.d.	2.4	c	n.d.	3.7
D	n.d.	0.5	d	n.d.	0.8
E	9.1	1.2	e	3.1	0
F	5.2	1.4	f	6.2	1.8
H	14.2	4.4	h	6.4	0
I	31.8	?	i	16.2	?
K	n.d.	0.5	k	n.d.	3.0
L	21.0	1.3	l	10.3	2.3
M	7.0	1.6	m	2.3	0
N	n.d.	2.0	n	n.d.	1.0
P	n.d.	0	p	n.d.	1.0
Q	12.9	6.5	q	2.8	1.0
R	n.d.	4.0	r	n.d.	2.5
S	n.d.	0	s	n.d.	0
T	9.0	?	t	1.2	?
V	26.2	?	v	13.7	?
W	n.d.	0.5	w	n.d.	3.2
Y	6.0	1.2	y	3.6	3.2

GC on chiral phase (after hydrolysis in 6N HCl, 18 h, 110 °C) and HPLC (Table 1). Higher rates of racemization were observed using GC, since racemization occurs under the conditions of the hydrolysis and this amount of racemization adds up to the amount originally present in the peptide.

All 400 all-L-hexapeptides RO_1DSO_2Y were cyclized (≈ 80% yield) and were characterized by ESI-MS. Side reactions lead to products (< 25%) with higher molecular masses: +60 amu (N_α-acetylated linear peptides), +87 amu (N_α-acetylated linear peptide dimethylamides) [2] and +166 amu.

To conclude, L- and D- amino acids in the C-terminal position have no influence on the cyclization of the hexapeptides RGDSPO and RGDSPo. Ile, Val, Thr (D- or L-) in the C-terminal position reduced cyclization yields. We could not confirm investigations where Gly, Pro or D-configured residues in the sequence are reported as essential prerequisites for ring closure of linear hexapeptides [3].

References

1. Rose, G.D., Gierasch, L.M., Smith, J.A., *CRC Crit. Rev. Biochem.*, 18 (1985) 1.
2. Friedrich, A., Jäger, G., Radscheit, K., Uhmann, R., in Schneider, C.H. and Eberle, A.N. (Eds.), 'Peptides 1992', Escom, Leiden, The Netherlands, 1993, p. 47.
3. Kessler, H., Haase, B., *Int. J. Pept. Protein Res.*, 39 (1992) 36.

Peptides: Chemistry, Structure and Biology
Pravin T.P. Kaumaya and Robert S. Hodges (Eds.)
Mayflower Scientific Ltd., 1996

291

Use of Azabicycloalkane Amino Acids to Stabilize β-Turn Conformations in Model Peptides and Gramicidin S

H.-G. Lombart and W.D. Lubell

Département de chimie, Université de Montréal,
C.P. 6128, Succ. Centre Ville, Montréal, Québec, H3C 3J7, Canada

Introduction

We recently communicated methodology for synthesizing a new variety of conformationally rigid β-turn analogues *via* a Claisen condensation / reductive amination / lactam cyclization sequence [1]. Improvements in our procedure now provide gram quantities of enantiopure indolizidinone amino acids (IAAs). For example, (3*S*, 6*S*, 9*S*)-IAA-**1** is synthesized in 45% overall yield from L-N-(phenylfluorenyl)glutamate γ-methyl α-*t*-butyl diester. From L-glutamate, we have also synthesized diastereomeric indolizidinone amino acids (3*S*, 6*R*, 9*S*)- and (3*S*, 6*S*, 9*R*)-IAA-**1** [1]. In addition, we have synthesized (3*R*, 6*R*, 9*R*)- and (3*R*, 6*S*, 9*R*)-IAA-**1** *via* the same strategy from D-glutamate. Since our route gives easy access to these azabicycloalkane amino acid analogs, we have turned to study the stereochemical and structural factors governing the conformational preferences of IAAs in peptides. Here we report syntheses of N-acetyl N'-methylamide **2** as well as gramicidin S (GS) analog **3**.

(3*S*, 6*S*, 9*S*)-Indolizidinone Amino Acid (IAA)

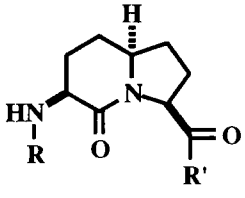

	R	R'
IAA:	H	OH
IAA-**1**:	Boc	OH
2:	$COCH_3$	$NHCH_3$

GS analog **3**: Cyclo[IAA-Val-Orn-Leu-IAA-Val-ORn-Leu]

Results and Discussion

The incorporation of IAA-**1** into peptides is readily accomplished using TBTU in acetonitrile [2]. N-Acetyl N'-methylamide (3*S*, 6*S*, 9*S*)-**2** was synthesized in 81% overall yield from IAA-**1** by coupling to $MeNH_2$, cleaving the Boc group with HCl in dioxane, and acetylating with acetic anhydride. Model studies on **2** as well as preliminary conformational analysis using NMR and FT-IR indicate that (3*S*, 6*S*, 9*S*)-**2** can adopt γ-turn as well as type II' β-turn conformations. The γ-turn structure is predicted to be the lower energy conformation for amide **2**. In addition, the IAA stereochemistry influences

the potential for β-turn formation which decreases in the order of (3*S*, 6*R*, 9*S*) → (3*S*, 6*S*, 9*S*) → (3*S*, 6*S*, 9*R*)-**2**.

Since the modification of GS with thiaindolizidinone amino acids was shown to give analogs possessing conformations and antibacterial activities similar to that of the native peptide [3, 4], the replacement of the D-Phe-Pro residues in GS by rigid dipeptide derivatives has become a standard method for measuring their capacity to serve as surrogates of the $i + 1$ and $i + 2$ residues in type II' β-turns [5-7]. Therefore, we have synthesized GS analog **3** using (3*S*, 6*S*, 9*S*)-IAA-**1** in order to examine the consequence of replacing the thiaindolizidinone sulfur by a methylene group as well as the effect of inverting the bridgehead stereochemistry.

A convergent approach and solution-phase techniques were used to synthesize GS analog **3**. IAA-**1** was coupled to H-Val-(Z)-Orn-Leu-allyl·TFA using TBTU and Et_3N in CH_3CN which provided Boc-IAA-Val-(Z)-Orn-Leu-allyl in 82% yield after chromatography on silica gel with 0-5 % MeOH in EtOAc as eluant. This material was then divided and independently deprotected at the C-terminal with $Pd(PPh_3)_4$ and morpholine in THF (94%) and at the N-terminal with TFA in CH_2Cl_2 (98%). The two tetrapeptides were then coupled with TBTU to furnish Boc-IAA-Val-(Z)-Orn-Leu-IAA-Val-(Z)-Orn-Leu-allyl in good yield. Deprotection of the allyl ester and Boc group as described above, followed by cyclization with TBTU furnished the protected GS analog (m/z = $[MH]^+$ 1282.3). No traces of dimeric nor polymeric products were observed by MS analysis of the cyclization reaction. Final hydrogenolysis of the Cbz protecting groups with Pd-black as catalyst in MeOH·HCl gave GS analog **3** (m/z = $[M]^+$ 1013.9).

In conclusion, we have used IAA-**1** to synthesize peptides **2** and **3**. Conformational analysis of **2** and **3** using NMR, FT-IR, and CD, as well as bioactivity studies of **3** are now in progress in order to further examine the use of IAAs to stabilize turn conformations in peptides.

Acknowledgments

This research was part supported by NSERC of Canada and FCAR of Québec. W.D.L. thanks Bio-Méga/Boehringer Ingelheim Recherche Inc. for a Young Investigator Award.

References

1. Lombart, H.-G. and Lubell, W.D., *J. Org. Chem.*, 59 (1994) 6147.
2. Lombart, H.-G. and Lubell, W.D.,in Maia H.L.S. (Ed.), 'Peptides 1994', ESCOM, Leiden, The Netherlands, 1995, p.696.
3. Sato, K. and Nagai, U., *J. Chem. Soc. Perkin Trans.* 1 (1986) 1231.
4. Bach, A.C., II, Markwalder, J.A. and Ripka, W.C., *Int. J. Pept. Protein Res.*, 38 (1991) 314.
5. De la Figuera, N., Jiménez, M.A., Biacs, M., García-López, M.T., Gonzaález-Muñiz, R. and Andreu, D., in Maia H.L.S. (Ed.), 'Peptides 1994', ESCOM, Leiden, The Netherlands, 1995, p.702.
6. Ripka, W.C., De Lucca, G.V., Bach, A.C., II, Pottorf, R.S. and Blaney, J.M., *Tetrahedron*, 49 (1993) 3609.
7. Graciani, N.R., Tsang, K.Y., McCutchen, S.L. and Kelly, J.W., *Bioorg. Med. Chem.* 2 (1994) 999.

Peptides: Chemistry, Structure and Biology
Pravin T.P. Kaumaya and Robert S. Hodges (Eds.)
Mayflower Scientific Ltd., 1996

292
Structure-Activity Relationship Studies of New Backbone-cyclic Substance P Analogs

G. Bitan[1], G. Byk[1], Y. Mashriki[2], M. Hanani[2] D. Halle[3], Z. Selinger[3] and C. Gilon[1]

Departments of Organic[1] and Biological[3] Chemistry, The Hebrew University of Jerusalem, Givat-Ram, Jerusalem 91904, Israel
Laboratory of Experimental Surgery[2], Hadassah University Hospital, Mount Scopus, Jerusalem 91240, Israel

Introduction

In 1992 it was claimed by Schwyzer that the activity of Substance P (SP) agonists and antagonists toward the NK-1 receptor is dependent upon the interaction between the phenyl rings of Phe^7 and Phe^8 and an electronegative atom (S,O) in an appropriate position [1] (position 11 in peptidic analogs). This theoretical hypothesis was supported by analogy of certain distances and angles in low-energy calculated conformations of SP and of the non-peptidic antagonist CP 96,345. According to Schwyzer, these conformational conditions enabling π interaction between the sulfur atom of Met^{11} and the phenyl rings, which appear also in the analogs Cycloseptide [2] and Spantide [3] are mandatory for both agonistic and antagonistic NK-1 activity.

At about the same time, we used backbone-cyclization [4] to prepare a new backbone to side-chain cyclic analog of WS-Septide [Ac-Arg^6, Pro^9]SP_{6-11} [5] in which Met^{11} was replaced by (D,L)-HCys, and the sulfhydryl group was linked to the backbone nitrogen of Gly in position 9 through a thioether and an amide bond yielding a 17 atom ring (Analog A, Figure 1). This peptide showed relatively high agonistic activity and selectivity for the NK-1 receptor [EC_{50}=2.0 x 10^{-8}M on NK-1 (guinea pig ileum, GPI) and >10^{-5} M on NK-2 (rat *vas deferens*) and NK-3 (rat portal vein)].

On the other hand, analogs in which Met^{11} was replaced by Glu γ-tert-butyl ester [6], Glu γ-benzyl ester [7] or Asp β-benzyl ester [8] were also found to be potent agonists of the NK-1 receptor, suggesting that a bulky lipophylic ester group at position 11 could substitute the thioether group.

Results and Discussion

We now present the preparation of new backbone to side-chain and backbone to backbone cyclic analogs, in which the $HCys^{11}$ residue was replaced by amino acids containing an ω-carboxyl moiety, such as (D and L) Asp, (D and L) Glu and N^{α}-(ω-carboxyalkylene)Gly. The ω-carboxyl was linked directly to the ω-amino group of N^{α}-(ω-aminoalkylene)Gly in position 9 forming a lactam ring (Analog B, Figure 1). Analogs containing rings between 13 and 20 atoms were prepared. The new analogs

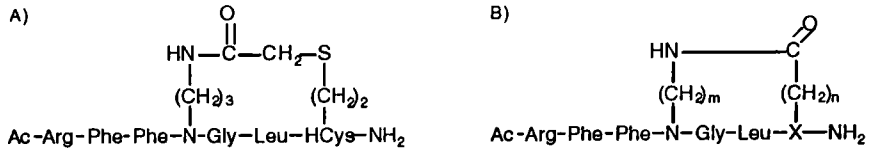

Figure 1. *A) Structure of the backbone to side-chain cyclic analog containing a thioether and amide bridge. B) General structure of the new analogs containing an amide bridge (m = 2,3,4,6; n =1,2,3,4,5; X = L-Asp, D-Asp, L-Glu-, D-Glu, N^{α}-(ω-carboxyalkylene)Gly).*

were detected *in vitro* for their agonistic activity by the guinea pig ileum assay with and without atropine, to distinguish between direct action on the NK-1 receptor of the smooth muscle and indirect action *via* the NK-3 neuronal receptor.

The results were not surprising. All Analogs showed EC_{50} values of 0.1-1 mM when tested on unblocked GPI. For some analogs, the activity was totally nullified in the presence of atropine.

There was no significant difference between cyclic and pre-cyclic analogs or when L or D amino acids or Gly building units were used in position 11.

In conclusion, replacing the thioether moiety of Analog A by an amide bond led to a stong decrease in the activity of the new $SP_{6\text{-}11}$ analogs. Apparently, a more lipophylic group in this position is required to compensate for the absence of the thioether group for NK-1 agonism. In accordance with the theory of Schwyzer, the activation of NK-1 is abolished upon exclusion of the sulfur atom, although the overall conformation is maintained.

Acknowledgments

This work was supported by Peptor Ltd., Rehovot, and the German-Israeli Foundation.

References

1. Schwyzer, R., *Brazilian J. med. Biol. Res.*, 25 (1992) 1077.
2. Saulitis, J. Mierke, D.F., Byk, G., Gilon, C. and Kessler, H., *J. Amer. Chem. Soc.*, 114 (1992) 4818.
3. Folkers, K. Rossel, S., Chu, J.-Y., Lue, L.-A., Tang, P.-Fl. and Ljungqvist, A., *Acta Chem. Scan.*, B40 (1986) 295.
4. Gilon, C., Halle, D., Chorev, M., Selinger, Z. and Byk, G., *Biopolymeres*, 31 (1991) 745.
5. Wörmser, U., Laufer, R., Hart, Y., Chorev, M., Gilon, C. and Selinger, Z., *EMBO J.*, 5 (1986) 2805.
6. Karagiannis, K., Manolopoulou, A., Stavropoulos, G., Poulos, C., Jordan, C.C. and Hagan, R.M., *Intl. J. Pept. Protein Res.*, 38 (1991) 350.
7. a) Poulos, C., Stavropoulos, G., Brown, J.R. and Jordan, C.C., *J. Med. Chem.*, 30 (1987) 1512. b) Stavropoulos, G., Karagiannis, K., Cordopatis, P., Halle, D., Gilon, C., Bar-Akiva, G., Selinger, Z. and Chorev, M., *Intl. J. Pept. Protein Res.*, 37 (1991) 180.
8. Karagiannis, K., Stavropoulos, G., Poulos, C., Jordan, C.C. and Hagan, R.M., *Intl. J. Pept. Protein Res.*, 42 (1993) 565.

Peptides: Chemistry, Structure and Biology
Pravin T.P. Kaumaya and Robert S. Hodges (Eds.)
Mayflower Scientific Ltd., 1996

293
Structure-Activity Relationships and Synthetic Study for Biphalin-1,1'-Stereochemical and Truncation Modifications

G. Li[1], W. Haq[1], L. Xiang[1], A. De Leon[2], P. Davis[2], R. Hughes[1], B. Lou[1], T.J. Gillespie[2], F. Porreca[2], T. Davis[2], M. Romanowski[1], X. Zhu[1], A. Misicka[1], A. Lipkowski[1], H.I. Yamamura[2], D.F. O'Brien[1] and V.J. Hruby[1]

Department of [1]Chemistry and [2]Pharmacology, University of Arizona, Tucson, AZ 85721, USA

Introduction

Biphalin, a dimeric enkephalin (Tyr-D-Ala-Gly-Phe-NH)$_2$, is a strong agonist for both δ and μ opioid receptors. Our previous study suggested that biphalin is a super antinociceptive peptide, 257- and 6.7-fold more potent than morphine and etorphine respectively, in eliciting antinociception [1]. Although biphalin has been known for more than a decade [2], very little progress has been made in this research area because of its unknown conformational structure and novel antinociceptive mechanism as well as its tedious multiplestep solution synthesis. Here we report a modified one-pot synthesis of the key precursor of biphalin, a NMR structural study and the role of unusual amino acids in biphalin molecular design from 1,1'-stereochemical and truncation modifications.

Results and Discussion

Four biphalin analogs were obtained by solution-phase synthesis using a convergent synthetic procedure. The optically pure 2', β-dimethyltyrosines were synthesized by an enantioselective method developed in this laboratory [3]. The key bridge precursor (Phe-NH-NH-Phe) was synthesized from a one-pot cross coupling reaction between Boc-Phe and hydrazine using BOP or HBTU reagents in DMF solution with great efficiency (95% yield). The further cross coupling reactions were conducted from the bridge dimer (1 equiv) and wing precursors (2 equiv).

The NMR structure study in DMSO solution showed that the two wings are symmetrically arranged on the two sides of the bridge dimer. There are two symmetric type II' β-turns in the biphalin structure. No hydrogen bonding was determined by dynamic NMR. However, a weak NOE between tyrosine and phenylalanine aromatic rings was observed. The aromatic interaction might be responsible for the two turns.

Opioid receptor binding affinities and selectivities in competition binding assays are listed in Table 1, and biological activities in the Guinea Pig Ileum (μ) and Mouse Vas

Table 1. *Binding affinities of biphalin analogs.*

Biphalin Analogs	IC_{50}(nM) δ[a]	μ[b]	μ/δ
$(Tyr\text{-}D\text{-}Ala\text{-}Gly\text{-}Phe\text{-}NH)_2$[c]	5.2	2.8	0.54
(2S,3S) ,2'-di-Me-Tyr-D-Ala-Gly-Phe-$NH)_2$	36	4.1	0.11
(2R,3R) ,2'-di-Me-Tyr-D-Ala-Gly-Phe-$NH)_2$	1800	130	0.07
$(Trp\text{-}D\text{-}Ala\text{-}Gly\text{-}Phe\text{-}NH)_2$	820	60	0.07
$(Tyr\text{-}D\text{-}Ala\text{-}Phe\text{-}NH)_2$	880	600	0.68

a, *versus* [^{3}H][*p*-Cl-Phe^4]DPDPE; b, *versus* [^{3}H]CTOP; c, estimated from K_i

Table 2. *Bioassay data of biphalin analogs.*

Biphalin Analogs	IC_{50}(nM) δ[a]	μ[b]	μ/δ
$(Tyr\text{-}D\text{-}Ala\text{-}Gly\text{-}Phe\text{-}NH)_2$	27	8.8	0.33
(2S,3S) ,2'-di-Me-Tyr-D-Ala-Gly-Phe-$NH)_2$	120	3.48	0.029
(2R,3R) ,2'-di-Me-Tyr-D-Ala-Gly-Phe-$NH)_2$	1750	611	0.35
$(Tyr\text{-}D\text{-}Ala\text{-}Phe\text{-}NH)_2$	57	830	14.7

Deferens (δ) assays are listed in Table 2. The data in Table 1 shows that substitution of Tyr[1] by (2S, 3S) 2',β-dimethyltyrosine provided improved binding selectivity for the μ opioid receptor, while the binding affinity for μ receptor remained almost the same as the native biphalin. The biological activity at μ receptor (Table 2) was enhanced more than 2 fold; however, the biological potency of δ receptor was decreased from 27 nM to 127 nM. Systematic replacements using 2',6',β-tri-Me-Tyr of (2S, 3S) stereoisomer will be conducted in the future. (2R, 3R) 2',β-di-Me-Tyr and Trp modifications resulted in poor binding or/and biological activities. These results further confirmed that a L-tyrosine is needed in biphalins. Another interesting observation is that the truncated biphalin $(Tyr\text{-}D\text{-}Ala\text{-}Gly\text{-}NH)_2$ resulted in δ selectivity rather than μ selectivity of the native biphalin. Membrane permeability studies of β-methyl modified biphalins is currently in progress. Supported by USPS, NIDA, University of Arizona Fellowship (G. Li) and Indian Govt. DBT (W. Haq).

References

1. Horan, P.J., Mattia, A., Bilsky, E.J., Weber, S., Davis, T.P., Yamamura, H.I., Malatynska, E., Appleyard, S.M., Slaninova, Misicka, A., Lipkowski, A.W., Hruby, V.J. Porreca, F. *J. Pharmacol. Exp. Ther.*, 265 (1993) 1446-1454.
2. (a) Lipkowski, A.W., Konecka, A.M., Sroczynska, I., *Peptides*, 3, (1982) 697-700; (b) Shimohigashi, Y., Costa, T., Chen, H.C., Rodbard, D., *Nature (London)*, 297 (1982) 333-335.
3. Li, G., Russell, K.C., Jarosinski, M.A., Hruby, V.J., *Tetrahedron Lett.*, 34 (1993) 2565-68.

Peptides: Chemistry, Structure and Biology
Pravin T.P. Kaumaya and Robert S. Hodges (Eds.)
Mayflower Scientific Ltd., 1996

294

Synthesis of 2(1*H*)-Pyrazinone Derivatives from Dipeptides and Their Application to the Preparation of Peptide Mimetics

H. Taguchi, T. Yokoi and Y. Okada

Faculty of Pharmaceutical Sciences, Kobe Gakuin University, Nishi-ku, Kobe 651-21, Japan

Introduction

Some naturally occurring 2(1*H*)-pyrazinone derivatives possess antibiotic and smooth muscle relaxation activity. Thus, great efforts have been directed towards the development of synthetic procedures for 2(1*H*)-pyrazinone derivatives. Of the various synthetic procedures evolved, each has some problems to be solved [1].

Previously, we reported a simple and convenient synthetic procedure for 2(1*H*)-pyrazinone derivatives starting from dipeptidyl chloromethyl ketones [2]. This novel method can afford 2(1*H*)-pyrazinone derivatives which contain desired substituents at positions 3 and 6. Here we report the synthesis of 2(1*H*)-pyrazinone derivatives which contain amino and/or carboxy function(s), as intermediates for the preparation of peptide mimetics.

Results and Discussion

As previously reported [3], each stereoisomeric dipeptidyl chloromethyl ketone gave similar cyclization yield. Therefore, an appropriate dipeptidyl chloromethyl ketone can afford the desired pyrazinone derivatives. For the introduction of the amino function, we selected lysine or ornithine and for the introduction of carboxy function, we selected aspartic acid or glutamic acid as the constituent amino acid of the dipeptide. As shown in Figure 1, synthesized dipeptidyl chloromethyl ketone was easily cyclized. The pyrazinone derivative obtained was hydrogenated over a Pd catalyst to give free amino and/or carboxy function(s)-containing pyrazinone.

In order to study the properties of the introduced amino group and carboxy group, various kinds of dipeptidyl chloromethyl ketones were prepared. During the cyclization reaction of H-Asp(OBzl)-Phe-CH_2Cl in MeOH, it was revealed that the benzyl ester group was partially substituted for a methyl group, and during hydrogenation of the formed pyrazinone derivative, decarboxylation easily occurred. These phenomena were due to the electron withdrawing property of the pyrazinone ring. However, such an ester interchange and decarboxylation described above did not occur in the case of cyclization of H-Phe-Asp(OBzl)-CH_2Cl in MeOH and catalytic hydrogenation of the formed pyrazinone derivative, respectively. From these results, it can be deduced that the

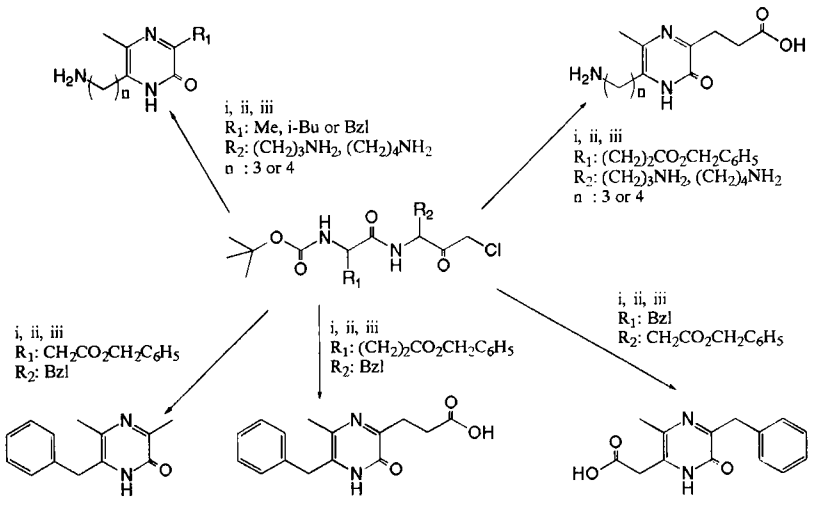

Figure 1. *Synthetic scheme for preparation of amino and/or carboxy group introduced 2(1H)-pyrazinone derivatives from dipeptidyl chlormethyl ketones. i) 4.9 N HCl/dioxane. ii) MeCN, 55°C, 1 h. iii) H_2/ Pd-black.*

methylene group attached to the position 3 but not position 6 of pyrazinone is the active one. The activity of the above mentioned methylene group was confirmed by the NMR measurement of exchange rate of hydrogen atoms of the methylene group with deuterium. The amino function was easily introduced by employing lysine or ornithine. Cyclization of H-Glu(OBzl)-Lys(Z)-CH_2Cl, followed by catalytic hydrogenation afforded an amino and carboxy function-containing pyrazinone derivative.

This synthetic strategy thus enabled us to obtain intermediates of peptide mimetics. These pyrazinone derivatives can be elongated N-terminally and/or C-terminally to prepare novel agonists, antagonists and enzyme inhibitors. Already, we have synthesized peptide mimetics which exhibited smooth muscle relaxation and enzyme inhibitory activities.

Acknowledgments

This work was supported in part by a grant from The Science Research Promotion Fund of the Japan Private School Promotion Foundation.

References

1. Jones, R.G. *J. Am. Chem. Soc.*, 71 (1949) 78.
2. Okada, Y., Taguchi, H., Nishiyama, Y. and Yokoi, T. *Tetrahedron Lett.*, 35 (1994) 1231.
3. Taguchi, H., Yokoi, T., Tsukatani, M. and Okada, Y., *Tetrahedron*, 51 (1995) 7361.

Peptides: Chemistry, Structure and Biology
Pravin T.P. Kaumaya and Robert S. Hodges (Eds.)
Mayflower Scientific Ltd., 1996

295
AzAsn-Pro-containing Azapeptides: Synthesis and Structure

F. André[1], C. Didierjean[2], G. Boussard[1], R. Vanderesse[1], A. Aubry[2] and M. Marraud[1]

[1]CNRS-URA-494, ENSIC-INPL, BP 451, 54001 Nancy, France
[2]CNRS-URA-809, UHP, BP 239, 54506 Vandoeuvre, France

Introduction

Azapeptides are peptide analogues where a nitrogen has been substituted for at least one $C^{\alpha}H$ group. They offer the advantage of modulating the conformational properties of the main chain with retention of the side chains which are eventually required for biological activity. The synthetic procedure using hydrazine condensation with an isocyanate, or by reacting an amine with an activated urethane is not efficient when proline must be coupled with an aza residue [1]. We have used triphosgene as a coupling agent for the synthesis of AzAsn-Pro-containing azapeptides. The Z-AzAsn-Pro-NHiPr azadipeptide and some analogues have been studied in solution (IR and NMR) and in the solid state (X-ray diffraction), and their conformational properties have been compared with those of the cognate peptide Boc-Asn-Pro-NHMe. We have also introduced by SPPS Z-Trp-AzAsn-Pro-OH in [$AzAsn^{68}$]MIR, an aza analogue of the immunogenic α67-76 AChR decapeptide (MIR = Trp-Asn-Pro-Ala-Asp-Tyr-Gly-Gly-Ile-Lys) [2]. The NMR data of both compounds have been compared in SDS aqueous solution where the MIR adopts a folded conformation resembling that in the MIR-antibody complex [3].

Results and Discussion

The synthesis of the azadi- and azatripeptides is illustrated in Figure 1. **3** was prepared by action of triphosgene on **2** which was obtained by regioselective Z-protection (85 % yield) of **1** using ZOSu. The *in situ* reaction of **3** with a C-protected Pro-derivative resulted in **4** or **6**. NH_3 treatment converted the AzAsp(OEt) residue into AzAsn, and the Z-protection was eliminated by catalytic hydrogenolysis. The tBu ester protection was necessary to prevent spontaneous cyclization of **6** during Z elimination. A threefold excess of **8** was coupled with the fully protected Ala-Asp(OBzl)-Tyr(2-BrZ)-Gly-Gly-Ile-Lys(2-ClZ) heptapeptide linked to a PAM-resin, using BOP as coupling agent. Resin and protecting group cleavage was achieved by TFA/TFMSA (10:1), after which the [$AzAsn^{68}$]MIR azadecapeptide was purified by HPLC using MeCN gradient in TFA 0.1 % water solution and on a C_{18} column.

The crystal structure of **4** and **5b** revealed a βI-like folded conformation (Figure 2) which was also observed for Boc-AzAla-Pro-NHiPr. The non-planarity of the AzAsn α-nitrogen (D-like chirality) results in a N^{α}-CO bond distance of 1.41 Å and its lone-pair

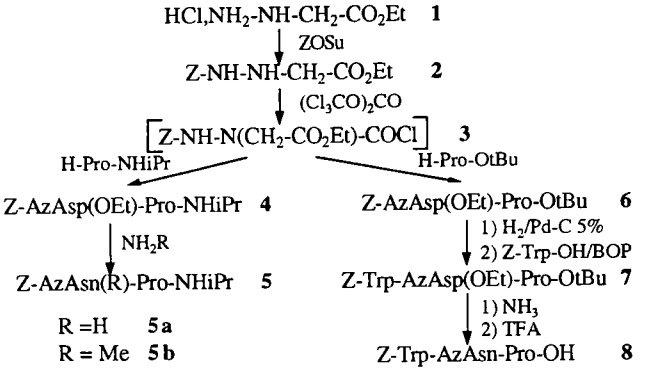

Figure 1. *Synthesis of AzAsn-Pro-containing azadi- and azatripeptides using triphosgene as a coupling agent.*

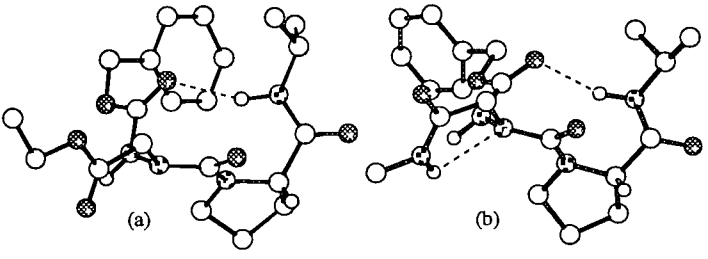

Figure 2. *βI-like folded crystal structure of the **4** and **5b** azadipeptides.*

becomes accessible to hydrogen bonding. This molecular structure is also largely preponderent in DCM solution, at variance with the cognate Boc-Asn-Pro-NHMe dipeptide which assumes an Asx-turn with a Me-NH to Asn-C$^{\gamma}$O hydrogen bond [4].

In SDS aqueous solution, the MIR decapeptide exhibits many short-range and medium-range Overhauser effects indicative of a rigid folded structure in which the Trp aromatic ring is close to the Pro, Tyr and Ile side-chains. In contrast, the [AzAsn^{68}]MIR, which proved to have no antibody affinity, exhibits fewer short-range NOESY correlations denoting a less tightly folded conformation.

Acknowledgments

The authors thank T. Tsouloufis and S. J. Tzartos for biological tests.

References

1. Gante, J., *Synthesis*, (1989) 405.
2. Papadouli, I., Potamianos, S., Hadjidakis, I., Bairaktari, E., Tsikaris, V., Sakarellos, C., Cung, M.T., Marraud, M. and Tzartos, S.J., *Biochem. J.*, 269 (1990) 239.
3. Orlewski, P. and Cung, M.T., ENSIC-INPL, France, Tsikaris, V. and Sakarellos, C., University of Ioannina, unpublished data.
4. Abbadi, A., Mcharfi, M., Aubry, A., Prémilat, S., Boussard, G. and Marraud, M., *J. Am. Chem. Soc.*, 113 (1991) 2729.

Peptides: Chemistry, Structure and Biology
Pravin T.P. Kaumaya and Robert S. Hodges (Eds.)
Mayflower Scientific Ltd., 1996

296
Differential Sensitivity of Cyclosporin A Amide Bonds for Inhibition of Cyclophilin

A.C. Bohnstedt[1], G.R. Flentke[2] and D.H. Rich[1,2]

[1]Department of Chemistry and [2]School of Pharmacy,
University of Wisconsin-Madison, Madison, WI 53706, USA

Introduction

The E-alkene replacement of the peptide bond first introduced by Sammes *et al.*,[1] has been incorporated into numerous biologically active peptides, *e.g.* enkephalin, substance P, cholecystokinin (CCK) analogs and renin inhibitors, with remarkably variable biological results. The complex between the potent immunosuppressant, Cyclosporin A (CsA, **1,**) (Figure 1), and its binding protein, Cyclophilin A (CyPA), contains 2 *trans* amide bonds that are involved in key hydrogen bonds to the protein [2]. Herein, we replace these critical 4,5- and 9,10-amide bonds with *E*-alkene bonds to assess the relative importance of peptide bonds for stabilization of the protein-peptide complexes.

Results and Discussion

Synthesis: The syntheses of [MeLeu^{9}ψ[*E*-CH=CH]Leu^{10}]CsA (**2**) and [MeLeu^4 ψ[*E*-CH=CH]Val^5]CsA (**3**) are shown in Schemes 1 and 2. For analog **2**, *E*-alkene isostere **4** [3] was esterified, deprotected and PyBrop-coupled to Fmoc-D-Ala in excellent yield (Scheme 1). Tetrahydrothiophene/$AlCl_3$-mediated hydrolysis of ester **5** gave acid **6** which was converted to the acid chloride and condensed with octapeptide **8**. Thus, linear undecapeptide **9** was obtained in 85% yield with no observable racemization because of the impossibility of azlactone formation during the fragment coupling. Boc-MeLeuψ[*E*-CH=CH]Val-OH (**10**) was coupled to MeLeu-Ala benzyl ester with BOP-Cl to give tetrapeptide **11** (Scheme 2). This intermediate was elaborated to analog **3** *via* standard protocol [4]. The poor yield obtained in the final cyclization step (**14** --→**3**) indicates the importance of the CsA 4,5-amide bond for facile cyclization. Presumably, intramolecular hydrogen bonds observed in the CsA $CHCl_3$ solution conformation promote ring closure by lowering the entropic barrier for this reaction [5].

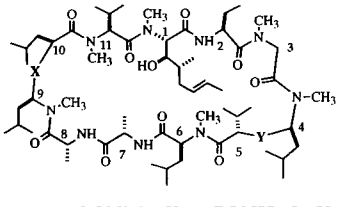

Figure 1. *CsA analogs. 1(CsA): X = CONMe, Y = CONH; 2: X = E-CH=CH, Y = CONH; 3: X = CONMe, Y = E-CH=CH.*

BocMeLeuψ[*E*-CH=CH]Leu-OH (**4**) ------- a,b,c (94%) -------→
FmocDAla-MeLeuψ[*E*-CH=CH]Leu-OMe (**5**) ------- d (90%) -------→
FmocDAla-MeLeuψ[*E*-CH=CH]Leu-OH (**6**)
←------ c,e (85%) ------ H-MeBmt-Abu-Sar-MeLeu-Val-MeLeu-AlaOBn (**7**)
←------ f (85%) ----- H-MeVal-MeBmt-Abu-Sar-MeLeu-Val-MeLeu-AlaOBn (**8**)
FmocDAla-MeLeuψ[*E*-CH=CH]Leu-MeVal-MeBmt-Abu-Sar-MeLeu-Val-MeLeu-AlaOBn (**9**)
----------g,h (62%) ----------→ **2**

Scheme 1. *Synthesis of CsA analog 2.*

←---------- i (76%) ---------- BocMeLeuψ[*E*-CH=CH]Val-OH (**10**)
←--------- j,i (73%) ---------- BocMeLeuψ[*E*-CH=CH]Val-MeLeu-AlaOBn (**11**)
←------- j,k (92%) ------- BocAbu-Sar-MeLeuψ[*E*-CH=CH]Val-MeLeu-AlaOBn (**12**)
←- l,m - N,O-isopropylidene-MeBmt-Abu-Sar-MeLeuψ[*E*-CH=CH]Val-MeLeu-AlaOBn (**13**)
FmocDAlaMeLeuMeLeuMeValMeBmtAbuSar-MeLeuψ[*E*-CH=CH]Val-MeLeu-AlaOBn (**14**)
----------g,h (25%) ----------→ **3**

Scheme 2. *Synthesis of CsA analog 3.*

Reagents: a) CH_2N_2, b) HCl, c) PyBrop/DIEA/Fmoc-aa, d) $AlCl_3/(CH_2CH_2)_2S$, e) Et_2NH, f) **6** (acid chloride)/DIEA, g) aq.NaOH/EtOH, h) $(Pr\text{-}PO_2)_3$/DMAP, i) BOP-Cl/DIEA/dipeptide j) TFA, k) DCC/HOBt/NMM/protected MeBmt, l) aq. HCl, m) BOP/NMM/tetrapeptide acid.

CyPA inhibition: Analog **2** binds >4000-fold less tightly to CyPA as compared to CsA (K_i (**2**) >25 μm, K_i(CsA) 6 nm) [6]. Thus, the hydrogen bond between Trp^{121} (CyPA) and the CsA $MeLeu^9$ carbonyl group observed from NMR and X-ray studies is exceedingly critical for CyPA inhibition. Still, this result is interesting since solvation factors are expected to favor CyPA inhibition by **2** [7]. Conversely, replacement of the 4,5-amide bond of CsA with an *E*-alkene moiety results in only an 8-fold loss of binding affinity (K_i (**3**) 47 nm). The observed intramolecular hydrogen bond between the CsA $MeBmt^1$ sidechain hydroxyl group and the $MeLeu^4$ carbonyl group, therefore, seems to have limited importance for CyPA inhibition.

Acknowledgments

Financial support from the NIH (AR-32007) is gratefully acknowledged.

References

1. Hann, M.M., Sammes, P.G., Kennewell, P.D. and Taylor, J.B., *J. Chem. Soc.*, 1 (1980) 234.
2. Thériault, Y., Logan, T.M., Meadows, R., Yu, L., Olejniczak, E.T., Holzman, T.F., Simmer, R.L. and Fesik, S.W., *Nature*, 361 (1993) 88.
3. Bohnstedt, A.C., Vara Prasad, J.V.N. and Rich, D.H., *Tetrahedron Lett.*, 34 (1993) 5217.
4. Colucci, W.J., Tung, R.D., Petri, J.A. and Rich, D.H., *J. Org. Chem.*, 55 (1990) 2895.
5. Wenger, R.M., *Helv. Chim. Acta,* 67 (1984) 502.
6. Kofron, J.L., Kuzmic, P., Kishore, V., Gemmecker, G., Fesik, S.W. and Rich, D.H., *J. Am. Chem. Soc.*, 114 (1992) 2670.
7. Morgan, B.P., Scholtz, J.M., Ballinger, M.D., Zipkin, I.D. and Bartlett, P.A., *J. Am. Chem. Soc.*, 113 (1991) 297.

Peptides: Chemistry, Structure and Biology
Pravin T.P. Kaumaya and Robert S. Hodges (Eds.)
Mayflower Scientific Ltd., 1996

297

Synthesis and Biological Evaluation of Substituted Benzimidazoles - Potential GPIIb/IIIa Receptor Antagonists

M. Rafalski, C. Xue and W.F DeGrado

The Du Pont Merck Pharmaceutical Co., Department of Chemical and Physical Sciences, Experimental Station, Wilmington, DE 19880, USA

Introduction

Glycoprotein GPIIb/IIIa is a surface platelet integrin which, *via* the plasma protein fibrinogen, links together activated platelets to form an aggregate. Platelet aggregation is involved in thrombotic disorders such as unstable angina, myocardial infraction and reocclusion after angiopasty. The RGD sequence is a key recognition domain for GPIIb/IIIa [1]. Inhibition of fibrinogen binding to GPIIb/IIIa is a good target for therapeutic prevention of platelet aggregation.

Results and Discussion

Our goal has been to design and synthesize a low-molecular weight centrally constrained fibrinogen receptor antagonist. We have previously shown that DMP 728, RGD containing cyclic peptide, is a potent inhibitor of platelet aggregation with an affinity of approximately 100 pM for binding to the receptor [2]. The analysis of the conformation of DMP728 by ^{1}H NMR [3] and computer modeling has led us to design nonpeptide antagonists with benzimidazole as a central constraint. These ligands contain a basic group to substitute for the guanidine of the Arg and an acidic moiety to mimic the carboxylate of the Asp. Benzimidazole containing inhibitors of platelet aggregation have fluorescence properties and could be readily employed as markers to follow the binding to GPIIb/IIIa. The chemistry leading to the benzimidazole is presented in Figure 1. The 6-carboxy-2-(4-cyano-phenyl)-benzimidazole, a starting material for further modification, was synthesized using two approaches, however, the condensation of 4-cyanobenzaldehyde with 3,4-diaminobenzioc acid *via* Schiff base gave a better purity of the crude product. During the condensation of 4-cyano-benzoyl chloride with 3,4-diaminobenzoic acid, 6-carboxy-2(methyl)-benzimidazole was also formed as a by-product. The antithrombotic effect of the synthesized nonpeptide analogs of DMP728 was assayed by the addition of the test compounds at various concentrations to platelet-rich plasma (PRP) prior to platelet activation by various agonists (ADP, collagen, arachidonate, thrombin, epinephrine). Table 1 presents selected examples of nonpeptide inhibitors of platelet aggregation and their $IC_{50}(\mu M)$. While this work was in progress, a related series of benzimidazole derivatives appeared in the patent literature.

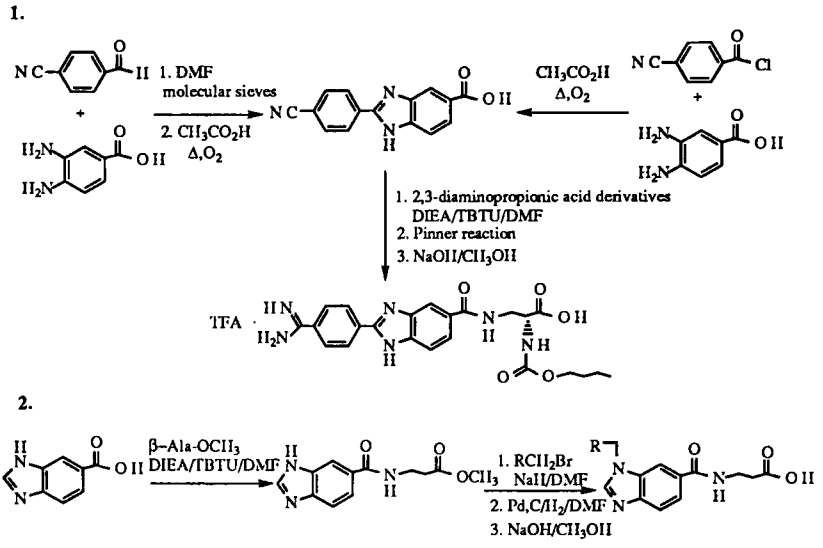

Figure 1. *Synthesis of benzimidazole derivatives.*

Table 1. *Structure - activity relationship of GPIIb/IIIa inhibitors.*

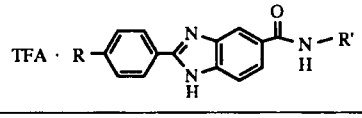

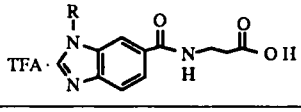

R	R'	$IC_{50}(\mu M)$	R	$IC_{50}(\mu M)$
	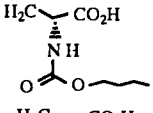	0.05	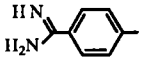	6.8
H_2NCH_2	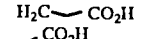	100	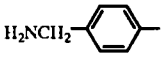	83
H_2NCH_2	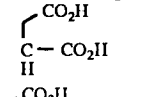	90		
H_2NCH_2	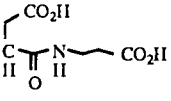	28	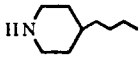	16

References

1. Ruoslahi, E., Pierschbacher, M.D., *Cell*, 44 (1986) 517.
2. Jackson, S., DeGrado, W.F., Dwivedi, A., Parthasarathy, A., Higley, A., Krywko, J., Rockwell, A., Markwalder, J., Wells, G., Wexler, R., Mousa, S., Harlow, R., *J. Am. Chem. Soc.*, 116 (1994) 3220.
3. Bach, A.C., Eyermann, C., Gross, J., Bower, M.J., Harlow, R., Weber, P.C., DeGrado, W.F., *J. Am. Chem. Soc.*, 116 (1994) 3207.

Peptides: Chemistry, Structure and Biology
Pravin T.P. Kaumaya and Robert S. Hodges (Eds.)
Mayflower Scientific Ltd., 1996

298

Competitve Inhibition of Proline Specific Enzymes by Amino Acid Thioxopyrrolidides and Thiazolidides

A. Stöckel[1], H.-U. Demuth[2] and K. Neubert[1]

[1]Department of Biochemistry/Biotechnology, Institute of Biochemistry, Martin-Luther-University Halle-Wittenberg, D-06099 Halle, Germany
[2]Department of Drug Biochemistry, Hans-Knöll-Institute e.V. Jena, D-06120 Halle, Germany

Introduction

Amino acid pyrrolidides (Pyr) and thiazolidides (Thia) are known as potent competitive inhibitors of dipeptidyl peptidase IV (DP IV) and prolyl endopeptidase (PEP) [1, 2]. Furthermore, it is known that a backbone modification such as the introduction of a thioxoamide bond, changes the binding properties and the hydrolytic stability of the protease substrates [3]. The influence of such a thioxoamide bond upon the inhibition of the following proteases was investigated using the serine enzymes PEP from *Flavobacterium meningosepticum* and human placenta, dipeptidyl peptidase II (DP II) from human placenta, DP IV from pig kidney and the metal-depending proteases aminopeptidase P (APP) from *Escherichia coli* and from rat intestine.

Table 1. *Competitive inhibition of PEP and DP IV.*

No 1 R-Ala-Pyr No 2 R-Phe-Pyr No 3 R-Val-Pyr No 4 R-Ile-Pyr
No 5 R-Ala-Thia No 6 R-Phe-Thia No 7 R-Val-Thia No 8 R-Ile-Thia

R= Boc for PEP R= H for APP, DP II, DP IV

No	bacterial PEP		human PEP		DP IV	
	amide K_i [μM]	thioxoamide K_i [μM]	amide K_i [μM]	thioxoamide K_i [μM]	amide K_i [μM]	thioxoamide K_i [μM]
1	34.6	134	0.0439	1.19	15.4[1]	47.6
2	54.6	122	1.6	77.3	2.26[1]	24.7
3	58.5	257	0.130	30.7	0.475[1]	1.07
4	40.9	301	0.184	11.1	0.243[1]	1.02
5	19.9	133	0.0193	0.414	3.39[2]	7.88
6	11.2	82.7	0.494	63.5	1.00	3.99
7	20.3	262	0.172	5.54	0.267[2]	0.208
8	23.3	190	0.183	11.7	0.126[2]	0.203

[1] Ref. 4 [2] Ref. 5

Results and Discussion

Amino acid amides were synthesized by use of conventional solution methods. The introduction of thioxoamide bond was obtained by use of Lawesson reagent. The inhibition was followed in continuous assays using chromogenic substrates with 4-nitroanilid residues (*p*NA). APP from rat was measured discontinuously by HPCE with Gly-Pro-Pro-*p*NA as substrate.

Generally, R-Xaa-Thia are better inhibitors than R-Xaa-Pyr for all investigated proteases. The results in Table 1 show that the amides of the general structure R-Xaa-Pyr and R-Xaa-Thia are better inhibitors of both PEP and DP IV than the corresponding thioxoamides. The difference of inhibition is up to two orders of magnitude. In contrast to the inhibition of PEP and DP IV, DP II is better inhibited by Xaa-ψ[CS-N]-Pyr and Xaa-ψ[CS-N]-Thia than by the corresponding amides (Table 2). This result displays the first selective inhibition of DP II and DP IV. A similar tendency was observed, inhibiting bacterial APP by compounds of both classes. APP from *E.coli* (and similarly APP from rat) is weakly inhibited by all tested compounds.

Table 2. *Competitive inhibition of DP II and APP.*

No	DP II		bacterial APP		rat APP
	amide K_i [μM]	thioxoamide K_i [μM]	amide K_i [mM]	thioxoamide K_i [mM]	thioxoamide K_i [mM]
1	21.8	3.32		17.6	
2	13.9	7.32		1.14	
3	26.7	8.23		24.8	21.4
4	30.2	4.75		2.43	
5	4.42	0.647	10.0	0.850	5.77
6	3.18	0.603	0.56	0.340	
7	7.66	0.920		2.92	
8	7.06	1.10	2.14	0.390	

Acknowledgments

This work was supported by a grant from DECHEMA. A.S. is grateful for a travel award from the American Peptide Society and from the Deutsche Forschungsgemeinschaft - Graduiertenkolleg [Ki 455/2-4].

References

1. Schön, E., Born, I., Demuth, H.-U., Faust, J., Neubert, K., Steinmetzer, T., Barth, A. and Ansorge, S., *Biol. Chem.*, 372 (1991) 305.
2. Tsuru, D., Yoshimoto, T., Koriyama, N. and Furukawa, S., *J. Biochem.*, 104 (1988) 580.
3. Schutkowski, M., Neubert, K. and Fischer, G., *Eur. J. Biochem.*, 221 (1994) 455.
4. Rahfeld, J.-U., Dissertation Martin-Luther-Universität Halle-Wittenberg (1989).
5. Steinmetzer, T., Dissertation Martin-Luther-Universität Halle-Wittenberg (1990).

Peptides: Chemistry, Structure and Biology
Pravin T.P. Kaumaya and Robert S. Hodges (Eds.)
Mayflower Scientific Ltd., 1996

299

Non-peptide Mimics of Neuropeptide Y: Analysis of Benextramine Structure-Activity Relationships at Y_1 and Y_2 Receptors

M.B. Doughty[1], P. Balse[1] and R. Tessel[2]

Departments of [1]Medicinal Chemistry and [2]Pharmacology and Toxicology, The University of Kansas, Lawrence, KS 66045, USA

Introduction

Our laboratories identified benextramine (dithiobis[N-(N-[2-methoxybenzyl]-6-amino-hexyl)-2-amino ethane]) as a competitive antagonist of neuropeptide Y (NPY) receptors in the rat brain and periphery based on comparison of its structural similarities with that of an NPY pharmacophore model [1, 2]. Subsequently, we designed two diguanidine analogs, the N,N'-dialkyl diguanidine SC3117 (**2**) and the N,N-dialkyl diguanidine CC2137 (**3**), which were characterized as potent non-peptide antagonists of NPY Y_2 receptors in the rat periphery [3, 4]; these analogs were also more active than benextramine in the rat brain cortex. In this study, analogs **3a-3f** (Figure 1) were synthesized to determine the importance of the benzylic amines and guanidinium groups of **3** for NPY receptor antagonist activity.

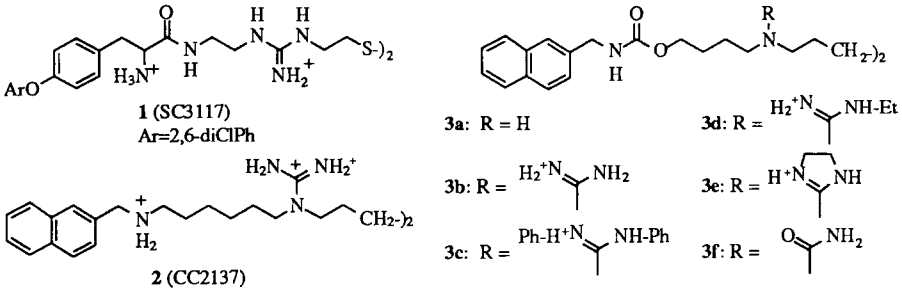

Figure 1. *Non-peptide mimics **1** and **2** and the analogs (**3a-3f**) synthesized in this study.*

Results and Discussion

Compound **3a** was synthesized by adapting a previous method [4]. Briefly, the diamide resulting from reaction of butyrolactone and hexanediamine was reduced with borane to the diamine, and after protection as its tBoc derivative, the dialcohol was treated with carbonyldiimidazole and 2-naphthylmethylamine. Deprotection of the tBoc groups gave **3a**. A convenient method to the guanidines and imidazolidines was developed; reaction of **3a** with methylthiopseudourea iodides gave the products in high yield and purity.

The NPY receptor systems were characterized as Y_1 or Y_2 based on the relative activities of NPY, PYY, [Leu^{31},Pro^{34}]NPY and NPY(13-36) (data not shown). Although diamine **3a** was inactive at the rat brain cortex Y_1 binding sites, the diguanidine **3b** and the diimidazolidine **3c** were two to three time more active than CC2137, evidence demonstrating that the secondary amines of CC2137 are not required for activity. Similarly, the poor activity of the diamine **3a** and the diurea analog **3f** demonstrates the importance of the charge on the guanidinium groups in this series. Additionally, the weak activity of these analogs at Y_2 binding sites in pig spleen as compared to the potent activity of SC3117 and CC2137 at the Y_2 postsynaptic receptors in the rat femoral artery is preliminary evidence for heterogeneity in NPY Y_2 receptors.

Table 1. *Summary of the activities of NPY non-peptide mimics at Y_1 receptors in rat brain, at Y_2 receptors in pig spleen, and at both Y_1 and Y_2 NPY receptors in the rat femoral artery.*

	IC_{50} (μM)		rat femoral artery IC_{50} (μM)[1]	
Compound	Rat Cortex[2]	Pig Spleen[2]	post Y_1	post Y_2
Benextramine	56 ± 8.0	110 ± 15	2.7 ± 0.2	2.7 ± 0.2
1 (SC3117)	19 ± 3.0	106 ± 23	>1000	0.043 ±0.004
2 (CC2137)	15 ± 2.6	nd[3]	>1000	0.0020 ± 4e-4
3a	>100	31 ± 9	nd	nd
3b	6.4 ± 1.6	30 ± 12	nd	nd
3c	>100	nd	nd	nd
3d	nd	nd	nd	nd
3e	4.1 ± 1.1	190 ± 28	nd	nd
3f	>100	460 ± 112	nd	nd

[1]IC_{50} (±SEM) in rat femoral artery is the concentration required to antagonize 50% of the vasoconstriction activity of either 1.0 μM [Leu^{31},Pro^{34}]NPY (for postsynaptic Y_1 receptors) or 1.0 μM NPY(13-36) (for postsynaptic Y_2 receptors). [2]IC_{50} (±SEM) in rat cortex (Y_1receptors) and pig spleen (Y_2 receptors) is the concentration of compound required to displace 50% of specifically bound 1.0 nM [^{3}H]NPY from membrane preparations (n=2 to 6). [3] not determined

Acknowledgments

Financial support for this research was provided by the National Institutes of Health and the Kansas Affiliate of the American Heart Association.

References

1. Doughty, M.B., Chu, S.S., Miller, D.W., Li, K. and Tessel, R.E., *Eur. J. Pharm.*, 185 (1990) 113.
2. Tessel, R.E., Miller, D.W., Misse, G.A., Dong, X. and Doughty, M.B., *J. Pharmacol. Exp. Ther.*, 265(1993), 1.
3. Doughty, M.B., Chu, S.S., Misse, G.A. and Tessel, R.E., *Bioorg. & Med. Chem. Lett.*, 2 (1992), 1497.
4. Chaurasia, C., Misse, G., Tessel, R. and Doughty, M.B., *J. Med. Chem.*, 37(1994), 2242.

Peptides: Chemistry, Structure and Biology
Pravin T.P. Kaumaya and Robert S. Hodges (Eds.)
Mayflower Scientific Ltd., 1996

300
Rational Design of Cycloalkyl Amino Acid Based Peptido-mimetics. Synthesis of Novel NK-1 Tachykinin Receptor Antagonists

A. Sisto[1], F. Arcamone[1], F. Centini[1], C.I. Fincham[1], P. Lombardi[1], E. Monteagudo[1], E. Potier[1], R. Terracciano[1], A. Giolitti[2] and K. Gröger[3]

[1]Chemistry Department, Menarini Ricerche Sud, 00040 Pomezia (Rome) Italy
[2]A. Menarini Farmaceutici, 50131 Firenze, Italy
[3]Berlin Chemie AG, Glieniger Weg 125, 12489 Berlin, Germany

Introduction

Substance P (SP) is an endogenous undecapeptide belonging to the tachykinin family, being the natural ligand for the NK-1 receptor. SP receptor antagonists have been investigated for their potential pharmacological application in inflammatory processes [1].

In a program aimed at synthesizing novel NK-1 receptor antagonists, we generated a bioactive model superimposing the low energy structures of peptide (FK-888) and non-peptide antagonists (SR-140333, CP-96345, CP-99994, CGP-47899). We replaced the Hyp in FK-888 with *(1R, 2S)*-2-amino cyclohexane carboxylic acid obtaining a series of NK-1 receptor antagonists with interesting biological activity [2]. By computational analysis, we noticed that, in our antagonists, the naphthyl and indolyl moieties were very close in space and we found the propensity to stacking between two aromatic rings was correlated with the biological activity. Therefore, we hypothesized that a π-π^* interaction was the key structural feature for the biological activity and that the 2-amino cycloalkyl-1-carboxylic acids (2 Ac^{n}c) act as "scaffolds" to bring the two aromatic rings in the right spatial position [3]. We decided to replace the 2 Ac^{n}c, with the aim of favouring the π-π^* interaction between two aromatic rings by decreasing the overall conformational flexibility with the 1-aminocycloalkyl-1-carboxylic acids (Ac^{n}c) [4].

Results and Discussion

We selected 1-aminocycloalkyl-1-carboxylic acids because of their known conformational rigidity which they impart when inserted in a peptide chain. We found by means of our computational studies a good reproduction of 3D placement of the three aromatic ring of FK-888 in the new analogues. As expected, the distribution of the low energy structures in our antagonists was strictly centered on those presenting a stacked assembly among the naphthyl and indolyl moieties. In order to verify this hypothesis, we have synthesized the Ac^{n}c analogues.

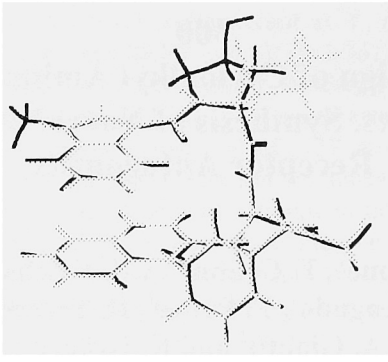

Figure 1. *Geometrical shape comparison of low energy structures of FK 888 (bold line) and MEN 10930 (dashed line).*

All the compounds synthesized have shown a higher binding affinity than their 2-aminocycloalkyl analogues, the most promising candidate being the Ac^6c derivative (MEN 10930).

Table 1. *Human lymphoblastoma IM9 cells binding data for FK-888 and new antagonists containing 1-aminocycloalkylcarboxylic acids analogues.*

Compounds		pK_i
FK 888	N-Me-13C-Hyp-L-2-Nal-NMeBzl	8,5
MEN 10725	13C-(1R,2S)cis 2-Ac^6c-L-2-Nal-NMeBzl	8,0
MEN 10930	13C-1-Ac^6c-L-2-Nal-NMeBzl	9,0
MEN 11084	13C-1-Ac^3c-L-2-Nal-NMeBzl	7,0
MEN 11118	13C-1-Ac^5c-L-2-Nal-NMeBzl	8,6

N-Me-I3C: [1(Me)indol-3-yl carbonyl]-; I3C: [1(H)indol-3-yl carbonyl]; 1-Ac^5c: 1-aminocyclopentane-1- carboxylic acid;

It is conceivable, and will be the object of further investigations, that the substitution of 2 Ac^nc with Ac^nc produces an increase in the stacking phenomenon.

References

1. Maggi, C.A., Patacchini, R., Rovero, P. and Giachetti, A., *J. Auton. Pharmacol.*, 13 (1993) 23.
2. Sisto, A., Centini, F., Fincham C.I., Potier, E.,Lombardi, P., Arcamone, F., Goso, C., Giolitti, A., Maggi, C.A., 'Proceeding of 4th Naples Workshop on Bioactive Peptides', Capri (Italy), 1994, p. 73
3. Sisto, A., Bonelli, F., Centini, F., Fincham, C.I., Potier, E., Monteagudo, E., Lombardi, P., Arcamone, F., Goso, C., Manzini, S., Giolitti, A., Maggi, C.A., Venanzi, M. and Pispisa, B., *Biopolymers,* 36 (1995) 511.
4. Paul, P.K.C., Sukumar, M., Bardi, R., Piazzesi , A.M., Valle, G., Toniolo, C., Balaram, P., *J. Am. Chem. Soc.*, 108 (1986) 6393.

Peptides: Chemistry, Structure and Biology
Pravin T.P. Kaumaya and Robert S. Hodges (Eds.)
Mayflower Scientific Ltd., 1996

301
Enzymatic Stability of Disulfide-Bridged Peptides and Their Lanthionine Analogs

S.H.H. Wang, S. Bahmanyar, J.P. Taulane and M. Goodman

Department of Chemistry and Biochemistry, University of California, San Diego La Jolla, CA 92093, USA

Introduction

Naturally-occurring peptide hormones such as opioid and neurohypophyseal hormones have exhibited potent biological activities *in vitro*, as well as *in vivo*. Many peptides are not good drug candidates because of their limited oral availability and their susceptibility to enzymatic degradation. It is essential in the design of novel peptidomimetic drugs to assess the effect of the structural modifications on *in vitro* metabolic stability. Modifications to the naturally-occurring peptide hormones include the incorporation of D-amino acid residues, retro-inverso peptide fragments, and cyclization through mainchain or sidechain couplings. In our laboratory, we have carried out modifications incorporating lanthionine (monosulfide bridged) diamino acids to form cyclic compounds, such as [D-Ala_L^2, L-Ala_L^5]enkephalinamide where Ala_L indicates the termini for a lanthionine residue. To assess the stability of both cystine-containing (disulfide-bridged) peptides and their corresponding lanthionine analogs to enzymatic degradation, we have modified existing assays [1]. Here, we report our results of stability studies on lanthionine-containing analogs of enkephalin, dermorphin and oxytocin.

Results and Discussion

Disulfide- and lanthionine-containing peptides were incubated with rat brain homogenates and initial rates of substrate disappearance determined *via* an HPLC method we have developed. The peptides were dissolved in 5mM Tris.HCl (pH 7.2) buffer and incubated with rat brain homogenates. Aliquots of the mixture were removed at intervals and enzymatic activity quenched with trifluoroacetic acid. Initial rate of substrate disappearance was followed *via* RP-HPLC. Many enzyme-catalyzed reactions follow pseudo-first order kinetics. Thus, plotting ln (% Remaining) *vs* time yields a line, the slope of which is the rate constant (k). Half-life values are calculated using the equation: $t_{1/2} = [(\ln 2)/k]$. These calculations were carried out using Cricket Graph III software.

Our results (Figure 1, Table 1) demonstrate that the lanthionine-containing peptides are less susceptible to degradation by the enzyme homogenates than the corresponding cystine-containing compounds. This relative increase in stability *in vitro* is an indication that they should be more stable *in vivo*, thus the lanthionine containing

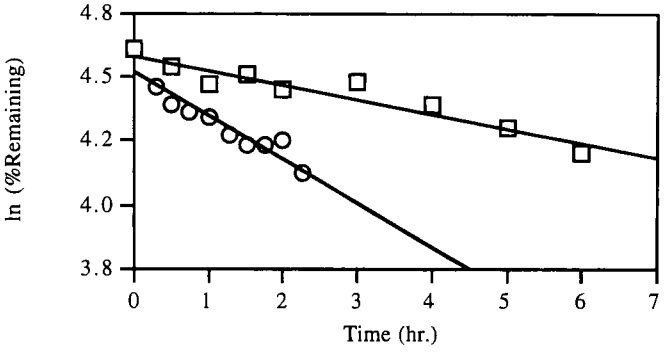

Figure 1. *Typical plot showing the enzymatic degradation of the cystine-containing enkephalin (-O-) and the lanthionine-containing enkephalin (-□-).*

Table 1. *Half-life ($t_{1/2}$) values.*

Compound / Peptide	Half-Life ($t_{1/2}$)
H-Tyr-D-Cys-Gly-Phe-L-Cys-NH_2 S— S	4.0 ± 0.1 hours
H-Tyr-D-Ala_L-Gly-Phe-L-Ala_L-NH_2 S	19.7 ± 0.5 hours
H-Tyr-D-Cys-Phe-L-Cys-OH S- S	1.5 ± 0.1 hours
H-Tyr-D-Ala_L-Phe-L-Ala_L-OH S	31.3 ± 0.8 hours
H-Cys-Tyr-Ile-Gln-Asn-Cys-Pro-Leu-Gly-NH_2 S S	1.9 ± 0.1 hours
H-Ala_L-Tyr-Ile-Gln-Asn-Ala_L-Pro-Leu-Gly-NH_2 S	5.0 ± 0.1 hours

peptides are expected to be better candidates for drug design. We are currently extending this study to other families of peptide hormones.

Acknowledgments

This work is supported by the National Institutes of Health (DK 15410 and DA 05539), the GAANN Fellowship, and fellowships provided by the Asahi Chemical Co., Ltd. and the CIBA Vision Corporation. The authors thank Dr. Tony Yaksh of the Anesthesiology Department of UCSD for the contribution of rat brains. We thank Dr. George Ösapay, Dr. Chang-Woo Lee and Hui Shao for the syntheses of these compounds.

Reference

1. Berman, J.M., Goodman, M., Nguyen, T.M.-D. and Schiller, P.W., *Biochem. Biophys. Res. Commun.*, 115 (1983) 864.

Peptides: Chemistry, Structure and Biology
Pravin T.P. Kaumaya and Robert S. Hodges (Eds.)
Mayflower Scientific Ltd., 1996

302
Nonpeptidic Bradykinin Antagonists from a Structurally Directed Non-peptide Combinatorial Library

S. Chakraverty, B.J. Mavunkel, R. Andy and D.J. Kyle

Scios Nova Inc., Sunnyvale, CA 94086, USA

Introduction

Much information has been generated which provides insights into the key structural features of bradykinin receptor binding sites and the residues which participate in ligand binding [1]. Moreover, there is evidence that agonist and antagonist ligands bind to different locations on the bradykinin B2 receptor. The design of non-peptide antagonists from this information requires the synthetic reassembly of the important structural moieties and functional groups onto non-peptide templates, each of which should ideally be consistent with the putative structure of these binding site models [2].

The three moieties required in this modular synthetic approach were, first, a positively charged N-terminal piece, second, a mid-section containing a bend or twist, and a mimetic of Phe^5 and third, a C-terminal piece of appropriate hydrophobicity and structurally simulating a type II' β-turn. The process of fragment re-assembly led ultimately to the synthesis of several general heterocyclic templates which were ideally suited for insertion either at module 2 or 3. In total, four completely unique non-peptide templates were designed and synthesized. These include 6,5-spirocycles, β- and γ-carbolenes, phenanthridinones, biphenylanilines and cinnamic acids. Each of these was designed within the framework of several criteria. First, a given scaffold must closely match the known SAR and be highly compatible with the putative ligand binding site structure. Second, each scaffold must be a relatively simple synthetic target, having readily available starting material, no chiral centers and having a total synthesis of not more that 4-5 steps. Finally, each template must have a "C-terminal" carboxylate and an "N-terminal" amino group with no interfering functionality such that it could be readily used in a solid phase synthetic strategy. To rapidly explore the receptor affinities of all possible combinations of these non-peptide templates at position X and Y of the sequence DArg-Arg-X-Y-Arg, a combinatorial synthetic approach was taken.

Results and Discussion

In this study, there were four different cinnamic acids, four different carbolines (β and γ), three different phenanthridinones, and five different spirocyclics. The variability of the phenanthridinione series was that the central ring could be opened or formed and the amino group could be meta or para substituted. In the carbolene series, the cyclic amino group was either at the β or γ position of the cyclohexenyl ring and the methylene chain

bearing the "C-terminal" carboxylate could be of variable length. The spirocyclic series was also varied in the carboxylate carbon linker length and also in the substitution on the 5-membered ring nitrogen. The cinnamic acids had two carbon chains which could be of varying length, one of which had the further possibility of containing a double bond. Rather than perform individual syntheses of all possible combinations of these templates, members of each ring type were pooled in equimolar amounts prior to incorporation into the sequence DArg-Arg-X-Y-Arg. Since each individual member of each pool was constructed on a similar carbocyclic scaffold, the chemical environment of the N-terminal amino group and C-terminal carboxylate groups were expected to follow similar kinetic and thermodynamic controls during solid phase synthesis.

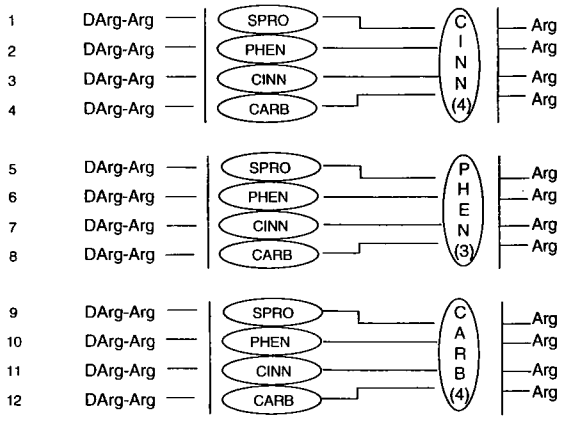

Figure 1. *Composition of twelve non-peptidic libraries of the sequence DArg-Arg-X-Y-Arg. Both X and Y were selected from the set of scaffolds described in the text.*

One of the twelve libraries synthesized (Figure 1) was of the series DArg-Arg-PHEN-CINN-Arg, and contained 12 different structures. Here, only the CINN position is randomized, and the PHEN moieties were specific. The first decoding breakdown sublibrary required the preparation of three new libraries of 4 compounds each. The final step in the process, required to elucidate the active component(s), was to synthesize and purify each of the 4 members of this library. Of the four novel non-peptidic structures only one, NPC 18884 (K_i 40 nM), had activity. This was shown to be an antagonist in a cellular assay measuring bradykinin-stimulated IP turnover (IC_{50} 1 μM). Overall, there were 285 possible structures to survey due to the number of structure-based scaffolds prepared. This was rapidly accomplished *via* 19 syntheses, 19 assays, and 4 purifications. This study demonstrates synergy between structure-based design and combinatorial methodology. Combinatorial assembly of structurally biased building blocks is a prudent synthetic compliment to inherently vague binding site models.

References

1. Kyle, D.J., Chakravarty, S., Sinsko, J.A., Stormann, T.M. *J. Med. Chem.*, 137 (1994) 1347.
2. Chakravarty, S., Mavunkel, B.J., Andy, R., Kyle, D.J. *Network Science*, 1 (1995) 1.

Session XIV
NMR

Chairs: Kenneth D. Kopple and
Arnold Satterthwait

Peptides: Chemistry, Structure and Biology
Pravin T.P. Kaumaya and Robert S. Hodges (Eds.)
Mayflower Scientific Ltd., 1996

303
Structure-function Relationship of Adenylate Kinase: Glu-101 in AMP Specificity

S. Beichner[1], I.-J. L. Byeon[3] and M.-D. Tsai[1,2,3]

Departments of [1]Chemistry and [2]Biochemistry and [3]Campus Chemical Instrument Center, The Ohio State University, Columbus, OH 43210, USA

Introduction

NMR has been used as an integral part of the analysis of the structure-function relationship of adenylate kinase (AK) from chicken muscle (overexpressed in *Escherichia coli*). The enzyme catalyzes the interconversion between MgATP+AMP and MgADP+ADP. In the earlier part of our studies, various site-specific mutants were constructed. One and two dimensional NMR were used to determine whether the global conformations of the mutants have been perturbed in comparison with the wild-type enzyme. Perturbation of the global conformation, if observed, suggests that the mutated residue is likely to play a structural role. If the global conformation has not been perturbed, then the mutant is subjected to detailed kinetic analysis to determine the functional role of the residue. This approach has allowed us to map out the substrate binding site and to understand the detailed mechanism of catalysis, as summarized in Tsai, *et al.*, 1991 [1].

As a complementary approach, NMR was used to identify the residues in proximity to substrates. The residues were then chosen for site-specific mutagenesis studies to determine their functional roles. To this end, we have performed total assignments of AK complexed to $MgAP_5A$ [2]. AP_5A has five phosphates between two adenosines and is a well established bisubstrate analog inhibitor of AK. Both ^{15}N and $^{15}N/^{13}C$ uniformly labeled enzymes have been used, and various two and three dimensional experiments have been performed. Although AK is a fairly large protein (21.6 kDa) in the NMR standard, we have been able to assign over 90% of the backbone ^{1}H, ^{13}C, and ^{15}N resonances, as well as a substantial amount of side chain resonances. The assignments were then used to determine the secondary structure of AK. Most importantly, the residues in proximity to the adenosine moieties of AP_5A have been identified. Gln-101 is one of the residues identified by NMR to be in proximity to the adenine ring of the AMP moiety. This residue was then further investigated by the first approach for its structural and functional roles. The results are described in this report.

Results and Discussion

The mutant Q101E, in which Gln-101 is replaced by Glu, has been constructed and purified as previously described [3]. As shown in Figure 1, the proton NMR spectrum of Q101E is very similar to that of the wildtype (WT) AK. This was further confirmed by

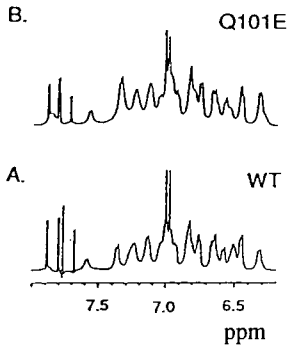

Figure 1. *Partial proton NMR spectra of WT AK (A) and Q101E (B).*

2D NOESY experiments for the enzymes in the free and the $MgAP_5A$ complexed forms (spectra not shown). Thus it can be concluded that the global conformation of the mutant has not been perturbed significantly, and that the functional data of the mutant can be interpreted with confidence.

The binding affinity toward $MgAP_5A$, however, is substantially lower for the mutant. The K_d value obtained from proton NMR titration experiments in Figure 2 is 0.04 mM, which amounts to a binding energy of *ca.* 5 kcal/mol. The corresponding value for WT AK is 11 kcal/mol [4]. Presumably because of the weakened binding affinity, the two adenosine moieties are in fast exchange on the NMR time scale as opposed to slow exchange for wildtype AK and many other mutants [2]. The weakened binding affinity could be caused by a perturbed interaction between the side chain of Glu-101 and the adenosine of the AMP moiety of $MgAP_5A$. This was confirmed by kinetic analysis.

Full kinetic analysis was performed by the procedure described previously [3, 4] and the results are summarized in Table 1. Comparison of the data between Q101E (column 3) and WT (column 2) indicates that k_{cat} decreases to 2% and AMP binding affinity decreases substantially. Furthermore, the specificity toward AMP is relaxed. While the activities of WT AK toward GMP and IMP were too low to be measured quantitatively, the activities of Q101E toward GMP and IMP became significant (columns 4 and 5). The results of NMR and kinetic analyses taken together suggest that the side chain of Gln-101 interacts with the adenine ring of AMP and controls the substrate specificity of AK toward AMP.

Table 1. *Comparison of kinetic data between WT and Q101E.*

Parameters[a]	WT/AMP[b]	Q101E/AMP	Q101E/GMP	Q101/IMP
k_{cat} (s-1)	650	14	1.7	0.094
K_{MgATP} (mM)	0.042	0.17	0.08	0.2
K_{NMP} (mM)	0.098	10.4	8.2	12.6
Ki_{MgATP} (mM)	0.16	0.097	0.094	0.082
Ki_{NMP} (mM)	0.37	5.9	10.9	5.2

[a]K and K_i values are Michaelis and dissociation constants, respectively.
[b]The data for WT are from [6]

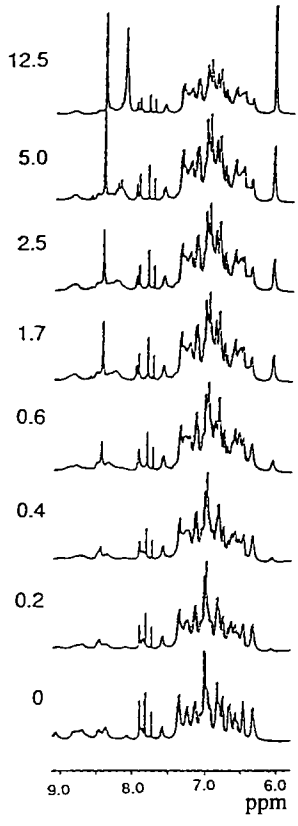

Figure 2. *Proton NMR titration of Q101E with $MgAP_5A$. The starting conc. of free enzyme is 1.8 mM. The ratios of [$MgAP_5A$]/[Q101E] are shown.*

Acknowledgments

This work was supported by NIH Grant GM43268. The paper is no.19 in the series. For paper no. 18, see [5].

References

1. Tsai, M.-D. and Yan, H., *Biochemistry*, 30 (1991) 6806.
2. Byeon, I.-J.L., Yan, H., Edison, A.S., Mooberry, E.S., Abildgaard, F., Markley, J.L. and Tsai, M.-D., *Biochemistry*, 32 (1993) 12508.
3. Tian, G., Sanders, C.R., II, Kishi, F., Nakazawa, A. and Tsai, M.-D., *Biochemistry*, 27 (1988) 5544.
4. Yan, H., Shi, Z. and Tsai, M.-D., *Biochemistry*, 29 (1990) 6385.
5. Byeon, I.-J.L., Shi, Z. and Tsai, M.-D., *Biochemistry*, 34 (1995) 3172.
6. Tian, G., Yan, H., Jiang, R.-T., Kishi, F., Nakazawa, A. and Tsai, M.-D., *Biochemistry*, 29 (1990) 4296.

Peptides: Chemistry, Structure and Biology
Pravin T.P. Kaumaya and Robert S. Hodges (Eds.)
Mayflower Scientific Ltd., 1996

304
Structure Refinement of Microcystin with Ensemble Calculations and NMR Data

D.F. Mierke[1], S. Rudolph-Böhner[2], G. Müller[3] and L. Moroder[2]

[1]Carlson School of Chemistry, Clark University, Worcester, MA 01610, USA
[2]Bioorganische Chemie, Max-Planck-Institut für Biochemie, D-82152 Martinsried, Germany
[3]Computational Chemistry, MD-IM-FA, Bayer AG, D-51368 Leverkusen, Germany

Introduction

A common problem with structure refinement utilizing NMR data is the presence of conformational averaging fast on the NMR time scale. In such cases, the NMR observables (*i.e.* NOEs, coupling constants) are averaged quantities and conformational restraints developed from the observables will be consistent with the averaged structure which may not be realistic or even physically possible. Therefore, the restraints used in computer simulations must be treated as averaged quantities. The inherent flexibility of peptides requires that great care be taken in the application of experimentally derived conformational restraints.

The method utilized in our laboratory to address this problem is to simulate a large number of structures (an ensemble) during the conformational refinement, a method we refer to as ensemble dynamics. Restraints developed from NOEs or coupling constants are applied as an average to the entire ensemble; each individual structure does not need to fulfill the conformational restraints, as long as the average (using the proper average R^{-6} or R^{-3} for NOEs and the cosine series, $\cos^2 \theta + \cos \theta$, for coupling constants) reproduces the NMR observables. Only if the ensemble average does not fulfill the experimental observation a penalty force is applied. One of the major advantages of ensemble averaging over other methods (*i.e.* time averaging of experimental restraints) is the fact that one need not to be concerned with multiple correlation times and the choice of the proper time-span over which to average. Of course, the answers from ensemble and time averaging must be the same if the system under investigation is ergodic. Results of the application of the ensemble method in the examination of model peptide systems are in the literature [1-3].

The ensemble calculation procedure was used in the conformational refinement of two microcystins: Leu[2],Arg[4] (LR) and Leu[2],Tyr[4] (LY). Both of these cyclic heptapeptides with the general formula, cyclo(-D-Ala[1]-X[2]-D-Me-isoAsp[3]-Y[4]-Adda[5]-D-isoGlu[6]-Mdha[7]-) where X and Y are variable L-amino acids, Adda is 3-amino-9-methoxy-2,6,8-trimethyl-10-phenyldeca-4,6-dienoic acid, Mdha is N-methyl dehydroalanine and D-Me-isoAsp is D-erythro-β-methyl aspartic acid, are potent inhibitors of type 1 and 2A protein phosphatases.

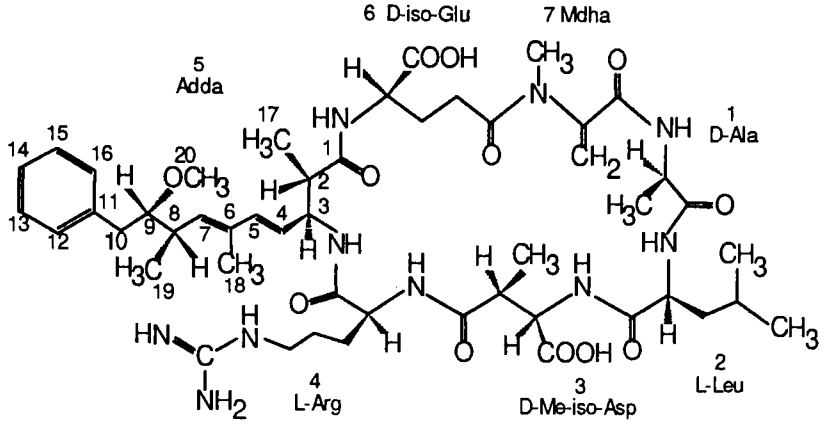

Figure 1. *Structural formula of LR microcystin.*

Classical refinement techniques, applying the experimental restraints to a single structure, failed to produce realistic conformations in agreement with the NMR data. Therefore, ensemble calculations were carried out for both the LR and LY microcystins using distances derived from NOEs.

Results and Discussion

The microcystins were examined by proton NMR in DMSO-d_6 at 500 MHz. All of the proton resonances were assigned using standard techniques as previously described [3, 4]. There were 64 (30 intraresidue, 21 sequential, 13 long range) and 79 (46 intraresidue, 15 sequential, 9 long range) NOEs observed for the LR and LY microcystins, respectively. Distance restraints were calculated using the standard two-spin approximation and the cross-peak from the β-methylene protons of glutamic acid as a reference (assuming a distance of 1.78 Å). The ensemble calculations were carried out with an ensemble of 500 structures using methods previously described [1].

The resulting structures from the ensemble calculation reproduce the NMR derived distances; there were no violations greater than 0.3 Å. For brevity, we concentrated on the results obtained for the LY microcystin. For one half of the molecule, -Leu[2]-D-isoAsp[3]-Tyr[4]-Adda[5]-, one conformation was observed. This indicates that the experimental data can be adequately described by one conformation (free simulations, using no restraints, show a complete random sampling of the ϕ,ψ space) [6]. For the other half of the molecule, centered about Mdha[7], two conformations were observed. This is illustrated in a Ramachandran plot (shown in Figure 2) for the dehydroalanine; two distinct populations with ϕ,ψ values of -30° ,+30° and +30° ,-30° are observed. Similar results are obtained for the residues adjacent to Mdha. The constraint from cyclization does not allow for a planar arrangement of the Mdha, although averaging over the ensemble, a planar conformation, with a ϕ,ψ of 0°,0° , would result.

The ensemble simulations presented here suggest that the LY microcystin is undergoing fast exchange between two conformations centered about Mdha. This

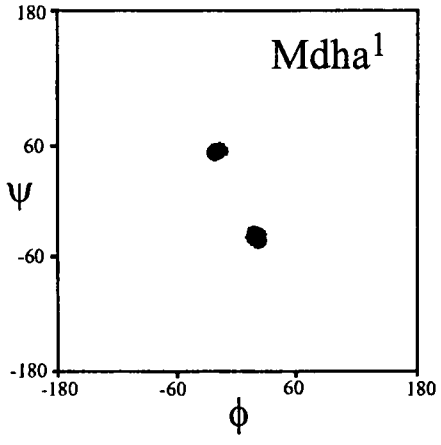

Figure 2. *A Ramachandran plot for N-methyl dehydroalanine illustrating the results obtained from the NOE-restrained ensemble simulations of the LY microcystin.*

finding would account for the inability of standard refinement procedures to reproduce the observations from NMR. The conclusions from the simulation of the LR microcystin are similar. These results indicate that, even for cyclic peptides, conformational averaging fast on the NMR time scale must be taken into account during computational structure refinement.

References

1. Mierke, D.F., Kurz, M. and Kessler, H., *J. Am. Chem. Soc.*, 116 (1994) 1042.
2. Mierke, D.F., Huber, T. and Kessler, H., *J. Comp. Aided Mol. Design*, 8 (1994) 29.
3. Mierke, D.F., Scheek, R.M. and Kessler, H., *Biopolymers*, 34 (1994) 559.
4. Rudolph-Böhner, S., Wu, J.T. and Moroder, L., *Biol. Chem.*, 374 (1993) 635.
5. Rudolph-Böhner, S., Mierke, D.F. and Moroder, L., *FEBS Lett.*, 349 (1994) 319.
6. Mierke, D.F., Rudolph-Böhner, S., Müller, G. and Moroder, L., *Biopolymers*, 36 (1995) 811.

Peptides: Chemistry, Structure and Biology
Pravin T.P. Kaumaya and Robert S. Hodges (Eds.)
Mayflower Scientific Ltd., 1996

305
Conformational Analysis of Single-chained Monelline

Y. Kobayashi[1], K. Miyazaki[1], T. Yoshida[1], H. Shimahara[1], Y. Kyogoku[1], S.J. Lee[1], H. Iijima[2] and P.A. Temmusi[3]

[1]Institute for Protein Research, Osaka University, Suita, Osaka 565, Japan
[2]Central Laboratories for Key Technology, Kirin Brewery Co. Ltd., Yokohama, Kanagawa 236, Japan
[3]Department of Chemistry, University of Naples, Naples, Italy

Introduction

Monelline is a sweet protein produced by an African plant, *Dioscoreophyllum cumminsii Diels*, which binds specifically on the human receptor of sweetness. It is sweeter than sucrose by the factor of 70,000 on a molar basis. The monelline molecule consists of two polypeptide chains, *i.e.* A chain with 45 amino acid residues and B chain with 50 residues. The X-ray analysis of native monelline by S.H. Kim revealed that the C-terminus of B-chain is located very close to the N-terminus of the A-chain in space. Gene cloning techniques were applied to fuse two chains at these termini and to produce a single-chained monelline. The resulting polypeptide was as sweet as natural monelline. It is interesting that the single-chained monelline had increased thermal stability and was renaturable after heat denaturation. In order to investigate the mechanism of how the molecule obtains this stability from the conformational aspect, we determined the solution conformation of the single-chained monelline by NMR and distance geometry calculations. Furthermore, the heteronuclear NMR relaxation measurements have been applied to study the system from the dynamic aspect. The single-chained monelline used in this experiment (hereafter called MNEI) was designed and characterized by Tancredi *et al.* [1], where a dipeptide unit, Gly-Phe, was inserted as a linker between A and B chains (Figure 1). After treatment at 80° C for 20 min, MNEI recovered almost complete activity. To prepare the isotope labeled MNEI, the synthetic fused monelline gene was expressed in M9 type culture medium which was labeled by ^{15}N and/or ^{13}C nuclei.

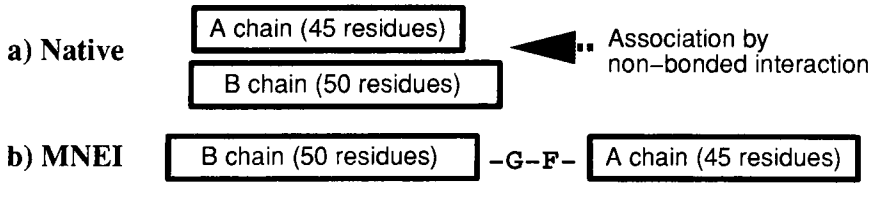

Figure 1. *Constructions of polypeptide chains for a) native monelline and b) MNEI.*

Results and Discussion

Using heteronuclear multi-dimensional NMR methods including HNCACB and H(CCO)NH, C(CO)NH methods, almost all signals coming from the backbone of the polypeptide chain except some of the signals relating to the N-terminal residue and the successive prolyl residues at the C terminal end were assigned. The chemical shift differences from the standard values expected for each amino acid residue existing in the random coil state are shown in Figure 2. It is well known that C_α carbon shows a down-field shift in an α-helical segment and an up-field shift in a peptide segment in a β-sheet conformation whereas C_β carbon has a tendency to show the reverse shifts in each case. Judging from these criteria, the secondary structure of MNEI was expected to have a distinct α-helical structure in the region of Phe11-Ile26 and at least four segments in β-sheet structure as shown in Figure 2. This secondary structure profile is consistent with those found in the crystal structures of native monelline and MNEI and in the solution structure of another single chained analog SCM where the two peptides were fused directly without spacing residues.

As distance information for the structure calculation, 458 distance constraints by the NOEs, 57 ϕ angle constraints and 70 distance constraints from hydrogen bonds, were obtained. Some fifty conformers were elucidated by simulated annealing calculations. Twenty-one structures among them were free from the violations of distance and angle constraints larger than 0.5 Å and 5°, respectively. These 21 structures, of which average value of rmsd from the averaged structure was 1.58 Å for backbone atoms are shown with superimposition in Figure 3. The structure profile of MNEI is characterized by an α-helix and five stranded anti-parallel β-sheet structure. This is very similar again to those found in crystal structures of native monelline and MNEI. The rmsd between the average structure of MNEI and its crystal structure was 1.84 Å. The respective peptide segments with ordered secondary structure elements of each resulting conformer showed

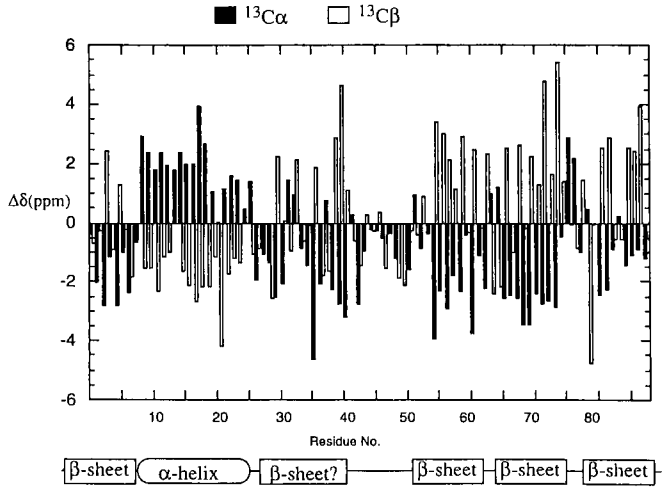

Figure 2. *Plot of secondary shift of Cα and Cβ resonances.*

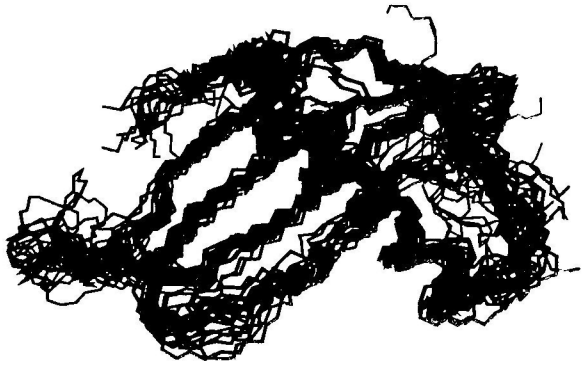

Figure 3. *Best fit superpositions of the backbone atoms of the 21 SA structures.*

good convergence. Thus, the rather poor convergence shown in Figure 3 might be attributed to the internal motion of the molecule.

The backbone dynamics of specific residues in NMEI was investigated by ^{15}N NMR relaxation measurements; T_1, T_2 and NOE of the amide ^{15}N, with interpretation in the term of motional parameters using the model free approach proposed by Lipari and Szabo [2]. First, the overall correlation time of the molecule was estimated with the average values of T_1 and T_2. Then the order parameters S^2 which describe the amplitudes of the internal motion were calculated for each residue. They are illustrated on the skeleton structure in Figure 4. The smaller values of S^2 found in the linker region indicates that poorly ordered structures with higher flexibility are localized around this peptide segment which has also rather large rmsd values and poor convergence as shown in Figure 3. Furthermore, the ^{13}C chemical shift differences in this region are very small. These facts reveal that the linker region takes a random coil structure in solution.

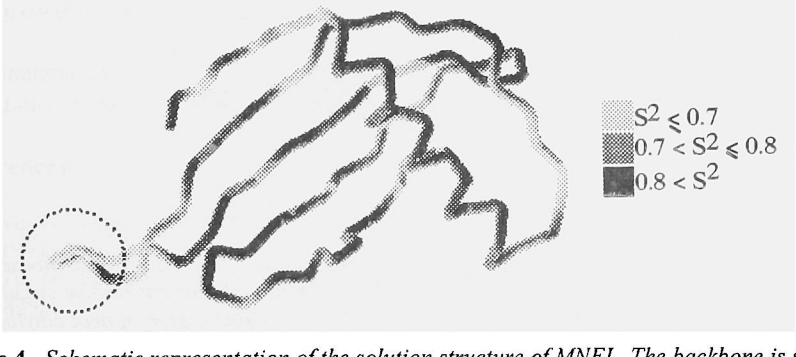

Figure 4. *Schematic representation of the solution structure of MNEI. The backbone is shaded according to the magnitude of the S^2.*

References

1. Tancredi, T., Iijima, H., Saviano, G., Amodeo, P. and Temussi, P., *FEBS Lett.*, 310 (1992) 27.
2. Lipari, G., and Szabo, A., *J. Am. Chem. Soc.*, 104 (1982) 4546.

Peptides: Chemistry, Structure and Biology
Pravin T.P. Kaumaya and Robert S. Hodges (Eds.)
Mayflower Scientific Ltd., 1996

306
On-line NMR Detection for Capillary Electrophoresis Applied to Peptide Analysis

D.L. Olson, T.L. Peck, A.G. Webb and J.V. Sweedler

Beckman Institute and Department of Chemistry
University of Illinois, 600 S. Mathews, Urbana, IL 61801, USA

Introduction

The ability to separate mass-limited mixtures of biological origin presents a problem of small-volume analysis. Most on-line detection schemes provide little information to elucidate the three-dimensional structure or chemical environment of separated components. To address this shortcoming, a method has been developed which employs on-line NMR analysis of compounds separated by capillary electrophoresis (CE) [1, 2]. The technique employs a microcoil fabricated of 50 μm wire wrapped around a capillary to form a 1-mm long, transmitter/receiver coil. A 75 μm i.d. capillary yields a sample chamber within the microcoil of just 5 nL, a 50,000-fold reduction in sample volume compared to conventional NMR. The layout of the apparatus and a typical spectrum is shown in Figure 1. Formerly, broad linewidths greater than 10 Hz prevented observation of proton scalar coupling. Now, resolution is similar to conventional 300 MHz NMR.

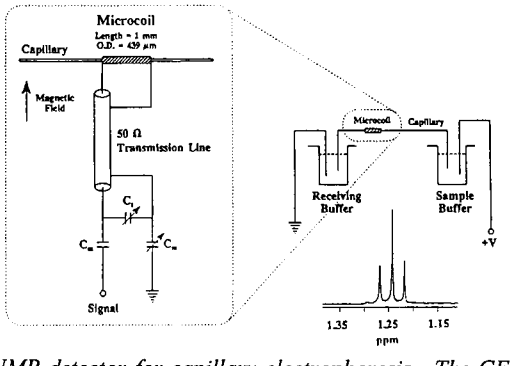

Figure 1. *Layout of NMR detector for capillary electrophoresis. The CE set-up is housed in a tube which fits in the magnet. The microcoil is wired to a traditional transmit/receive circuit. The inset shows a microcoil spectrum from a 300 MHz NMR of the triplet region of neat ethylbenzene with a linewidth of 0.6 Hz and good lineshape. The mass of sample enclosed within the 5 nL capillary detection cell is only 4.3 μg (41 nmol). The spectrum is from a single data acquisition.*

Results and Discussion

High resolution spectra with picomole detection limits of biochemicals have been achieved using microcoil NMR. Figure 2 shows a microcoil spectrum of *Aplysia*

californica α-bag cell peptide 1-7. The mass sensitivity (signal-to-noise ratio per μmol) of the microcoil is greatly enhanced compared to the traditional 5 mm spinning tube. The ratios of sensitivities of the microcoil to the 5 mm tube is over 130-fold [3]. For a given sample amount, this corresponds to a reduction in data acquisition time by a factor greater than 10,000.

Greatly improved spectroscopic methods, including 2-dimensional COSY spectra [3], now allow application of small-volume, on-line NMR analysis to a wide variety of biological problems, including single cell analysis.

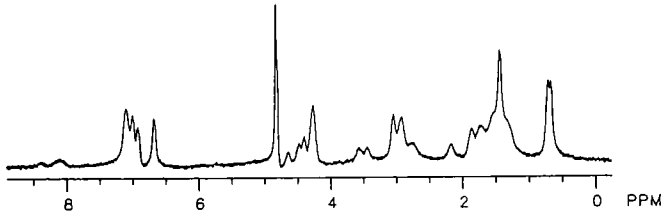

Figure 2. *300 MHz NMR spectrum of α-bag cell peptide (1-7). The 5 nL detection cell contains 3.0 μg (3.3 nmol) of sample. The detection limit (defined at S/N = 3) is 112 ng (124 pmol). The spectrum is from 256 acquisitions taken in 12 min.*

This work provides high resolution NMR spectra on nanoliter-volume samples containing microgram (nanomole) quantities of sample. This capability allows NMR to be used as a detector in CE [1, 2], microbore LC [4], small-scale stopped flow, and flow injection analyses. The microcoil method is particularly suited to mass-limited samples such as those of biological origin, those of synthetic or pharmaceutical interest, and when used as a detector for CE or other microseparations.

Acknowledgments

The financial support of a David and Lucille Packard Fellowship, and a National Science Foundation National Young Investigator Award (JVS) are appreciated.

References

1. Wu, N., Peck, T.L., Webb, A.G., Magin, R.L. and Sweedler, J.V. *J. Am. Chem. Soc.* 116 (1994) 7929.
2. Wu, N., Peck, T.L., Webb, A.G., Magin, R.L. and Sweedler, J.V., *Anal. Chem.* 66 (1994) 3849.
3. Olson, D.L., Peck, T.L., Webb, A.G. and Sweedler, J.V., *Science*, 270 (1995) 1967.
4. Wu, N., Peck, T.L., Webb, A.G., Magin, R.L. and Sweedler, J.V. *Anal. Chem.*, 67 (1995) 3101.

Peptides: Chemistry, Structure and Biology
Pravin T.P. Kaumaya and Robert S. Hodges (Eds.)
Mayflower Scientific Ltd., 1996

307

The Solution Structure of Tick Anticoagulant Peptide by ^{1}H-, ^{13}C-, and ^{15}N- NMR, and its Comparison with BPTI

M.S.L. Lim-Wilby[1], K. Hallenga[2] and T.K. Brunck[1]

[1]Corvas International, San Diego, CA 92121, USA
[2]Corvas NV, Gent, Belgium

Introduction

Tick anticoagulant peptide (TAP) is a 100-400 pM 60-residue inhibitor of the serine protease factor Xa (fXa) [1]. It is highly effective *in vivo* as an antithrombotic agent, indicating that fXa inhibition may be a viable means of preventing blood clots. Knowledge of TAP's tertiary structure, leading to the sites and mode of binding to fXa could be used to design novel orally-active small molecule inhibitors of fXa pro-coagulation activity.

TAP is exquisitely selective against fXa, having no inhibitory activity against a variety of proteases [1]. The molecule most structurally similar to TAP, basic pancreatic trypsin inhibitor, BPTI, inhibits also elastase, urokinase, plasmin, chymotrypsin, and kallikrein [2]. We will show that the mechanism of TAP binding to fXa is unique from the binding of BPTI/Kunitz inhibitors with their cognate serine proteases. Such differences may help to elucidate the nature of the binding of TAP to fXa.

Results and Discussion

Since TAP has a propensity to aggregate, complicating its structural assignments, studies using pulsed field gradient experiments and ^{13}C-double-filtered NOESY experiments of ^{13}C-labeled/unlabeled (1:1) TAP were performed to confirm that the sample under the final conditions (pH 2.5, 1.5 mM, 298 K, H_2O/D_2O (9:1) or D_2O) was monomeric. The assignment and nOe determination of the structure was achieved mostly with NOESYs performed with 60-240 ms mixing times, and checked with ^{13}C-^{1}H correlation, ^{15}N-^{1}H NOESY, and amide exchange experiments. Detailed discussion of the experimentally determined structure has been published [1].

We compared TAP with the crystal structure of BPTI by alignment of the β-sheets and α-helices of TAP and BPTI, which superimpose extremely well; the N-terminal 3_{10}-helices of TAP and BPTI have slightly different orientations in this alignment.

BPTI by NMR spectroscopy shows conformational flexibility at Cys^{14}-Cys^{38} and adjacent residues [1]. TAP has an insertion loop in this region, and its tertiary structure also shows structural and mobility differences at and near Cys^{15}-Cys^{39} for residues Asp^{13}-Asp^{16}, Ser^{35}, Trp^{37}, C^{39}, and Pro^{40}, *via* line-broadening effects in the NMR spectra [1].

In the BPTI/trypsin complex, the residues binding to trypsin are Thr^{11}, Pro^{13}-Ile^{19}, Val^{34}, and Gly^{36}-Arg^{39}. The positioning of TAP in the active site of fXa in a manner analogous to the BPTI/trypsin complex, aligning TAP with BPTI and the catalytic triad (Asp^{102}-His^{57}-Ser^{195}) of fXa with that of trypsin, produces many clashes that are not easily removed. Moreover, this model does not explain the results of other studies on TAP. TAP is not cleaved by fXa whereas BPTI is by trypsin. Therefore, TAP does not bind in a substrate-like mode. Mutation studies on TAP [1, 3] have shown that the residues critical to the activity of TAP, Tyr^{1}-Leu^{4}, Asp^{10}, and Asp^{47} are not those that would be predicted from a BPTI-trypsin binding mode [4]. Mao *et al.* have shown that the mutations $Asp^{10}\rightarrow Arg$ and $Tyr^{1}\rightarrow Trp$ produce mutants many times more potent [3]. We know from the TAP solution structure that the sidechains of the Arg^{3} and $Arg(Asp)^{10}$ are indeed separated by 10-20 Å, depending on their individual orientations.

The improvement in potency due to a second positive charge at Arg^{10} may indicate that there are two cation-binding sites in fXa for TAP. Indeed, fXa has two cationic binding sites (S_1 and S_3) which are about 10-17 Å apart. It is probable that these two sites are occupied by the chromogenic substrate S2765 (Z-DArg-Gly-Arg-PNA), the dibasic small molecule inhibitors such as diamidinoarylpropionic acid derivatives [5], and antistasin, a 30-60 pM inhibitor of fXa [6]. It is possible that the $Asp^{10}\rightarrow Arg$ mutant similarly binds Arg^{3} and Arg^{10} in both the S_1 and S_3 sites.

Therefore, in spite of the sequence and structural similarities of TAP to BPTI, the mutation studies show that the binding of TAP will present a unique mode of binding of an inhibitor to a serine protease. Modes of binding incorporating the above mentioned mutation result and the known cation binding sites of fXa are currently being modeled.

Acknowledgments

TAP samples were provided by Yves Laroche, Joris Messens, and Marc Lauwereys. We thank Ignace Lasters and Marc de Maeyer for valuable structural input. Factor Xa crystal coordinates were kindly provided by Professor Tulinsky. We appreciate the support and encouragement provided by Bill Ripka and George Vlasuk during this project. KH is currently in the Cummings Life Science Center, University of Chicago, IL 60637.

References

1. LimWilby, M.S.L., Hallenga, K., de Maeyer, M., Lasters, I., Vlasuk, G.P., and Brunck, T.K., *Protein Sci.*, 4 (1995) 178 and references cited therein.
2. Fritz, H. and Wunderer, G., *Drug Res.*, 33 (1983) 479.
3. Mao, S.S., Huang, J., Welebob, C., Neeper, M.P., Garsky, V.M., and Shafer, J.A., *Biochemistry,* 34 (1995) 5098.
4. Marquart, M., Walter, J., Diesenhofer, J., Bode, W., and Huber, R., *Acta Crystallogr.* B, 39 (1983) 480.
5. Nagahara, T., Yokohama, Y., Inamura, K., Katakura, S.I., Komoriya, S., Yamaguchi, H., Hara., T., and Iwamoto, M., *J. Med. Chem.*, 37 (1994) 1200.
6. Dunwiddie, C., Thornberry, N.A., Bull, H.G., Sardana, M., Friedman, P.A., Jacobs, J.W. and Simpson, E., *J. Biol. Chem.*, 264 (1989) 16694.

Peptides: Chemistry, Structure and Biology
Pravin T.P. Kaumaya and Robert S. Hodges (Eds.)
Mayflower Scientific Ltd., 1996

308
Identifying Determinants of Protein Structure with Loop Peptides

E. Cabezas, P.L. Wang and A.C. Satterthwait

Department of Molecular Biology, The Scripps Research Institute, La Jolla, CA 92037, USA

Introduction

Major advances in understanding determinants of protein structures have come from the systematic examination of peptides that adopt stable secondary structure in water [1, 2]. However, there are few studies on isolated loops from proteins [3]. It is important to identify determinants of loop structure since loops are well represented on protein surfaces, provide sites for receptor binding and can serve as bases for drugs and synthetic peptide vaccines. Here we report NMR structure determinations for dodecameric peptide loops selected for their enhanced affinities for an antiprotein monoclonal antibody [4]. Higher affinities are indicators of conformational constraint and identify potential mimetics for structural studies.

Results and Discussion

Linear Ac-GILDTSNPVKTGGG-NH_2, hydrazone loop [JILDTSNPVKTGZ]G-NH_2 and disulfide loop Ac[CILDTSNPVKTC]-NH_2 bind an antiprotein mouse monoclonal antibody, 4B7, with relative affinities of 1, 32 and 256 respectively [4]. The hydrazone loop was synthesized and cyclized on the solid support [4]. Each peptide was purified by HPLC and confirmed by FAB MS. NMR data for 20 mM solution of each peptide in 10% D_2O/H_2O, pH 5 at 24°C was collected from 1D and 2D DQF-COSY, P.E.COSY, TOCSY and ROESY spectra. Spectral data was processed with Biosym's Felix 2.3 software. Structure determinations were conducted using Biosym's NMRchitect and Discover software packages. Calculated structures were examined for disallowed geometries with Procheck [5].

NMR data for the two loops indicate that they adapt similar structures. More and stronger midrange NOE's for the disulfide loop show that it is better ordered than the hydrazone loop. Temperature coefficients for Ser (~3ppb/°C) and Asn (~1ppb/°C) mainchain amide protons are low providing evidence that the tips of both loops are well ordered. NOE's and the Asn temperature coefficient suggest that DTSN populates a Type I reverse turn. Distinct chemical shifts for geminal β protons, coupling constants and NOE's indicate that rotations of the side chains of DTSN are restricted. However, large αN(i, i+1) NOE's suggest that extended forms are in dynamic equilibrium with the ordered forms.

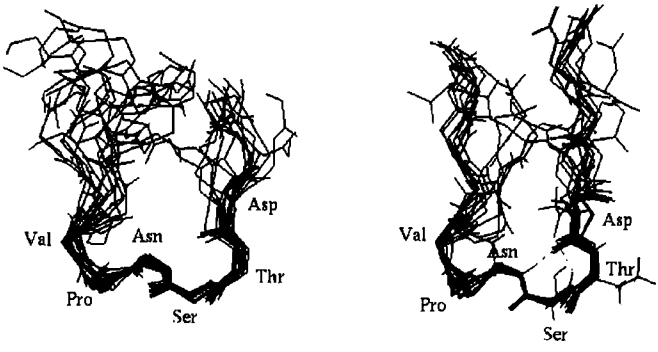

Figure 1. *Backbone traces of calculated structural families of hydrazone (left) and disulfide (right) loops. Hydrogen bonds are identified for a typical member of the disulfide family.*

Calculated structural families for both loops are well ordered at their tips, DTSNPV [Figure 1]. Hydrogen bonds form between Ser NH-Asp carboxylate sidechain and the Asn NH-Asp mainchain carbonyl oxygen. Disorder in the remainder of the peptide could reflect true disorder or an insufficient number of constraints. MAb 4B7 binds DTSNPV in conformations similar to the structural families [4]. These results suggest that the loops form significant populations of an ordered conformer in water that correspond to the native conformation.

The identification of a loop mimetic provides a starting point for investigating the role of individual amino acids in stabilizing the loop. The Asp side chain could play an important role as it does in initiating α-helix formation [6]. β-branched amino acids may restrict conformation in a loop context. Importantly, the enhanced affinity of MAb 4B7 for loops is accounted for by an improved conformation. Similar data for other loops and antibodies provides further targets for these studies.

Acknowledgments

This research was supported in part by the Agency for International Development DPE-5979-A-00-1035-00. This is publication 9486-MB from The Scripps Research Institute.

References

1. Dyson, H.J., Rance, M., Houghten, R.A., Lerner, R.A., Wright, P.E., *J. Mol. Biol.*, 201 (1988) 161.
2. Marqusee, S., Robbins, V.H., and Baldwin, R.L., *Proc. Natl. Acad. Sci. U.S.A.*, 86 (1989) 5286.
3. Blanco, F.J., Jimenez, M.A., Herranz, J., Rico M., Santoro J., Nieto, J.L., *J. Am. Chem. Soc.* 115 (1993) 5887.
4. Satterthwait, A.C., Cabezas, E., Calvo, J.C., Wu, J.X. Wang, P.L., Chen, S.Q., Kaslow, D.C., Livnah, O. and Stura, E.A., this volume.
5. Laskowski, R.A., MacArthur, M.W., Moss, D.S., Thornton, J.M., *J. Appl. Cryst.*, 26 (1993) 283.
6. Richardson, J.S., and Richardson, D.C., *Science*, 240 (1988) 1648.

Peptides: Chemistry, Structure and Biology
Pravin T.P. Kaumaya and Robert S. Hodges (Eds.)
Mayflower Scientific Ltd., 1996

309
Solution Structure of Ascidian Trypsin Inhibitor by NMR

H. Hemmi[1], T. Yoshida[2], T. Kumazaki[3], N. Nemoto[2], J. Hasegawa[2], Y. Kyogoku[2], H. Yokosawa[3] and Y. Kobayashi[2]

[1]Division of Marine Biochemistry, National Research Institute of Fisheries Science, Kanazawa, Yokohama 236, Japan
[2]Institute for Protein Research, Osaka University, Suita, Osaka 565, Japan
[3]Faculty of Pharmaceutical Sciences, Hokkaido University, Sapporo, Hokkaido 060, Japan

Introduction

Ascidian trypsin inhibitor (ATI) from hemolymph of a solitary ascidian, *Halocynthia roretzi,* is a single polypeptide chain with 55 amino acid residues that shows no extensive homology to other known protease inhibitors [1, 2]. It has four disulfide bridges in a molecule [3]. Two of these constitute CSH motif (cystine stabilized α-helical motif) that is characterized by an α-helical structure containing a Cys-X1-X2-X3-Cys sequence stabilized by two disulfide bridges with Cys-X-Cys, which is found in hormonal peptides (endothelin-1), honey bee toxins (apamin), scorpion toxins (charybdotoxin), *etc* [5-7]. The sequences Cys^{37}-Ala^{38}-Leu^{39}-Cys^{40}-Cys^{41} and Cys^{12}-Arg^{13}-Cys^{14} correspond to the above segment, where the disulfide bridges, Cys^{12}-Cys^{41} and Cys^{14}-Cys^{37}, are formed. There has been no report that Cys at the X3 position in the helix-forming segment forms the disulfide bridge with other Cys, as in ATI. In the present study, we analyzed the solution structure of ATI by means of 2D-NMR and simulated annealing calculations.

Results and Discussion

From the pattern of sequential and medium-range NOEs of ATI, together with the observed groupings of slow amide proton exchange, the secondary structure of ATI is characterized by an α-helical conformation in the sequence, Asn^{35}-His^{43}, and a three-stranded antiparallel β-sheet in the sequence, Leu^{21}-Ile^{26}, Ala^{29}-Arg^{34} and Glu^{48}-Asn^{51}. The 400 NOEs were converted into distance constraints, and structure calculation was carried out by simulated annealing (XPLOR version 3.1). The overall folding of the main chain of ATI is shown in Figure 1. The secondary structure and the overall folding of main chain of ATI were similar to those of typical Kazal-type inhibitors, such as the third domain of Japanese quail ovomucoid (OMJPQ3) and human pancreatic secretory trypsin inhibitor [8, 9]. Taken together, ATI can be classified as a member of the Kazal-type inhibitor family on the basis of the tertiary structure.

The present results also showed the Cys-X1-X2-X3-Cys segment of CSH motif in ATI forms α-helix conformation. This shows that the presence of Cys at the X3 position does not interfere with the formation of the helix of the CSH motif.

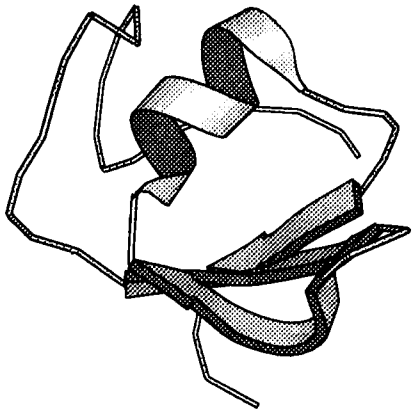

Figure 1. *Schematical representation of the solution structure of ATI. The picture was generated with program MOLSCRIPT.*

In the course of the studies on the structure of OMJPQ3, it appears that the situations of Asn^{33} and Asn^{39} in α-helix, as well as that of the half-cystines, were noteworthy. The side chain NH of Asn^{33} forms a hydrogen bond with the main chain carbonyl oxygens of Pro^{17} at P2 site and Asp^{19} at P'1 site of the scissile bond to act as a spacer between the reactive site loop (the primary contact region) and the secondary contact region (Tyr^{31}-Asn^{36}). The side chain of Asn^{39} forms a hydrogen bond with the main chain of Lys^{13} to participate in the stabilization of the reactive site conformation. Asn^{33} of OMJPQ3 corresponds to Asn^{35} of ATI, but Asn^{39} of the former is replaced by Cys^{41} in the latter. Cys^{41} forms a disulfide bridge with Cys^{12} and this is one of two disulfide bridges constituting the CSH motif. Therefore, the disulfide bridge seems to contribute to not only the stabilization of α-helical conformation but also that of the reactive site conformation. Furthermore, ATI is likely to have a more rigid structure than that of OMJPQ3 at the reactive site region.

References

1. Yokosawa, H., Odajima, R. and Ishii, S., *J. Biochem.*, 97 (1985) 1621.
2. Kumazaki, T., Hoshiba, N., Yokosawa, H. and Ishii, S., *J. Biochem.*, 107 (1990) 409.
3. Kumazaki, T. and Ishii, S., *J. Biochem.*, 107 (1990) 414.
4. Laskowski, M., Jr. and Kato, I., *Annu. Rev. Biochem.*, 49 (1980) 593.
5. Kobayashi,Y., Takashima, H., Tamaoki, H., Kyogoku, Y., Lambert, P., Kuroda, H., Chino, N., Watanabe, T. X., Kimura, T., Sakakibara, S. and Moroder, L., *Biopolymers.*, 31 (1991) 1213.
6. Tamaoki, H., Kobayashi, Y., Nishimura, S., Ohkubo, T., Kyogoku, Y., Nakajima, K., Kumagaye, S., Kimura, T. and Sakakibara, S., *Protein Eng.*, 4 (1991) 509.
7. Kobayashi, Y., Sato, A., Tamaoki, H., Nishimura, S., Kyogoku, Y., Ikenaka, K., Kondo, T., Mikoshiba, K., Hojo, H., Aimoto, S. and Moroder, L., *Neurochem. Int.*, 18 (1991) 525.
8. Papamokos, E., Weber, E., Bode, W., Huber, R., Empie, M. W., Kato, I. and Laskowski, M., Jr., *J. Mol. Biol.*, 158 (1982) 515.
9. Bolobnesi, M., Gatti, G., Menegatti, E., Guarneri, M., Marquart, M., Papamokos, E. and Huber, R., *J. Mol. Biol.*, 162 (1982) 839.

Peptides: Chemistry, Structure and Biology
Pravin T.P. Kaumaya and Robert S. Hodges (Eds.)
Mayflower Scientific Ltd., 1996

310
A Structural Study of Small, Polyhydroxymonoamide Renin Inhibitors

S. LaPlante[1], L. Tong[2], N. Aubry[1], S. Pav[2], G. Jung[1,3] and P. Anderson[1]

[1]Bio-Méga/Boehringer Ingelheim Research Inc., 2100 Cunard, Laval, Québec, H7S 2G5, Canada
[2]Boehringer Ingelheim Pharmaceuticals Inc., 900 Ridgebury Road, Ridgefield, CT 06877, USA
[3]Clinical Research Institute of Montreal, 110, avenue des Pins, Montréal, Québec, H2W 1R7, Canada

Introduction

Our laboratory has recently identified a series of potent polyhydroxymono-amide renin inhibitors (Figure 1a). A feature exhibited by these inhibitors is that a change in stereochemistry of carbinol C_3 as in **1** and **2**, and a change in hydroxyl position (C_4 to C_5) as in **1** and **3** results in small differences in binding potencies (IC_{50} values of 9, 7, and 12 nM, respectively). NMR spectroscopy was used to identify and compare the preferred solution conformations of these inhibitors. Comparisons were also made between the unbound structures determined by NMR and the renin-bound structures determined by X-ray crystallography.

Results and Discussion

A thorough analysis of ^{1}H J-coupling and ROESY NMR data suggested that inhibitor **1** has a predominant conformation in DMSO in the unbound state. By using NMR-derived restraints, the solution structure of **1** was modeled by a combination of distance geometry, energy minimization, and molecular dynamics. The twenty-five lowest-energy structures that satisfy the NMR data have a similar overall conformation. The lowest-energy structure that best satisfies the NMR data is shown as thick lines in Figure 1b. The solution structures of **2** and **3** were not subjected to the modeling protocol. However, it is likely that **2** and **3** have similar conformations as **1** in the unbound state as judged by the similarity of the J-coupling and ROESY data. The most noticeable difference was found along the torsion angle along the C_3-C_4 bond. Inhibitor **1** prefers one of three possible staggered rotamers, whereas this bond is conformationally averaged in **2** and **3**.

The crystal structures of inhibitors **1**, **2**, and **3** in complex with renin have been determined [1]. In each case, there are two distinct renin complexes per asymmetric unit. Figure 1b shows a superposition of the two inhibitor structures in the renin-bound state

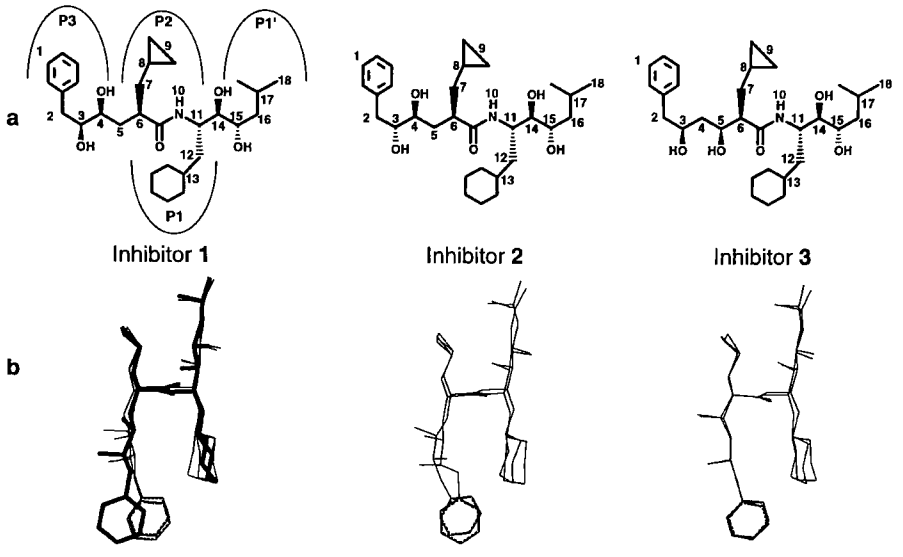

Figure 1. *(a) Inhibitors 1, 2, and 3 are shown. (b) The NMR solution structure of 1 in the unbound state is shown as thick lines. The crystal structures of inhibitors 1, 2, and 3 in the renin-bound state are shown as thin lines.*

(thin lines). All three inhibitors have similar overall conformations, although the P_3 position of **2** shows the greatest variability.

A comparison of the solution structure and the crystal structures show that the inhibitors assume similar conformations when unbound and renin-bound (with exceptions in the P_3 position). This similarity shows that gross conformational changes of the inhibitor are not prerequisite to binding renin. Figure 1b shows the unbound structure of **1** (thick lines) superimposed with the renin-bound structures (thin lines) of **1**. The left side of the NMR structure is slightly skewed or "propeller twisted" relative to the X-ray structures due to a small difference in the torsion angle along the carbonyl-C_6 bond which serves as a pivot for the right and left sides of the inhibitor. The extra conformational mobility observed at the P_3 position in the solution structures of **2** and **3** is evidently not detrimental to inhibitor potency. Interestingly, the crystal structures show that renin can accommodate different P_3 conformations of the inhibitor.

Reference

1. Tong, L., Pav, S., Lamarre, D., Pilote, L., LaPlante, S., Anderson, P. and Jung, G., *J. Mol. Biol.*, 250 (1995) 211.

Peptides: Chemistry, Structure and Biology
Pravin T.P. Kaumaya and Robert S. Hodges (Eds.)
Mayflower Scientific Ltd., 1996

311
Conformational Differences Between Ring Structures in a Series of Cyclic β-Casomorphin Analogs Determined by NMR Spectroscopy

K.A. Carpenter, R. Schmidt and P.W. Schiller

Laboratory of Chemical Biology and Peptide Research, Clinical Research Institute of Montreal, 110 Pine Avenue West, Montreal, Quebec, H2W 1R7, Canada

Introduction

Special effort is currently being directed towards the development of opioid peptide analogs that are mixed μ agonist/δ antagonists owing to the recent finding that pre-treatment of mice with the non-peptide δ antagonist naltrindole prevented the development of morphine tolerance and dependence [1]. The cyclic β-casomorphin analog H-Tyr-c[-D-Orn-2-Nal-D-Pro-Gly-] (**Gly5**) represents the first reported example of a cyclic peptide with mixed μ agonist/δ antagonist properties [2]. Here we report results of NMR conformational studies carried out on three analogs of **Gly5** in which Gly has been replaced by D-Ala (**D-Ala5**), Sar (**Sar5**) and NMe-Ala (**NMe-Ala5**) [3].

Results and Discussion

One-dimensional ^{1}H NMR spectra acquired for the three compounds in [$^2H_6$]DMSO at room temperature revealed larger than usual linewidths in the aliphatic region for **Sar5** which narrowed upon heating the sample from 25 to 50°C (Figure 1). This differential line broadening reflects conformational exchange that is most likely linked to *cis-trans* isomerization around the 2-Nal^3-D-Pro^4 and D-Pro^4-Sar^5 peptide bonds [4]. Observation of a significantly greater number of Nuclear Overhauser effects for **Sar5** compared to the other two compounds further supports the existence of **Sar5** structures with *cis* peptide bonds. Although N-alkylated amino acids are also contained in the ring structures of **D-Ala5** and **NMe-Ala5**, there was no experimental evidence of minor conformers with *cis* peptide bonds for either analog. Single component spectra were observed for all three compounds. This indicates that in the case of **Sar5** the fractional population of *cis* isomers was low.

Temperature coefficient data obtained for **D-Ala5**, **Sar5** and **NMe-Ala5** indicate that the amide protons are shielded from the solvent in a non-uniform manner (Table 1). A temperature coefficient between 3 and 4 ppb/K typical of a fully exposed proton was measured for the terminal exocyclic amine in all three cases. In contrast to **Sar5** and **NMe-Ala5**, the NH protons of residues 2, 3 and 5 of **D-Ala5** are all either shielded or engaged in intramolecular hydrogen bonding in a large proportion of the conformational ensemble.

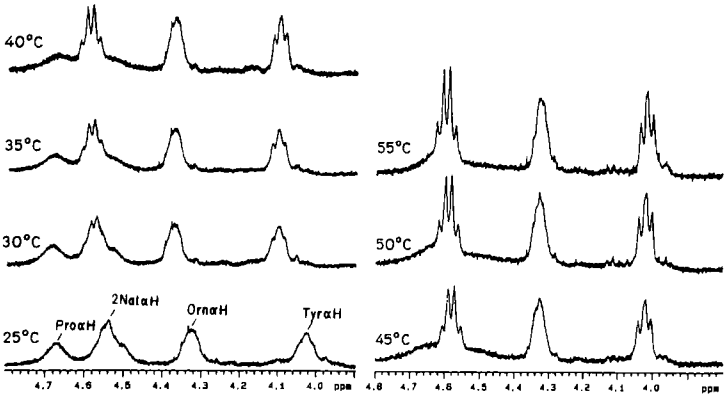

Figure 1. *^{1}H NMR spectra of **Sar5** in DMSO at the indicated temperatures.*

Table 1. *NH proton temperature coefficients for Tyr-c[D-Orn-2-Nal-D-Pro-Xaa-] (ppb/K).*

Proton	Xaa = D-Ala[5]	Xaa = Sar[5]	Xaa = NMe-Ala[5]
TyrNH	3.16	3.25	3.93
OrnNH	0.80	2.23	2.19
OrnεNH	0.67	2.74	2.72
2-NalNH	0.80	?	2.45
D-AlaNH	0.79	-	-

? indicates NH chemical shift could not be measured due to spectral overlap.

It can be concluded that all three cyclic β-casomorphin analogs studied exhibit distinctly different conformational properties in DMSO. The obtained structural information can be used for the design of more constrained, and more potent mixed μ agonist/δ antagonists.

Acknowledgments

Supported by grants from NSERCC and MRCC (UI-12356).

References

1. Abdelhamid, E.E., Sultana, M., Portoghese, P.S. and Takemori, A.E., *J. Pharmacol. Exp. Ther.*, 258 (1991) 299.
2. Schmidt, R., Vogel, D., Mrestani-Klaus, C., Brandt, W., Neubert, K., Chung, N.N., Lemieux, C. and Schiller, P.W., *J. Med. Chem.*, 37 (1994) 1136.
3. Schmidt, R., Chung, N.N., Lemieux, C. and Schiller, P.W., this volume.
4. Kopple, K.D., Baures, P.W., Bean, J.W., D Ambrosio, C.A., Hughes, J.L., Peishoff, C.E. and Eggleston, D.S., *J. Am. Chem. Soc.*, 114 (1992) 9615.

Peptides: Chemistry, Structure and Biology
Pravin T.P. Kaumaya and Robert S. Hodges (Eds.)
Mayflower Scientific Ltd., 1996

312
Effects of the Selective Reduction of Amide Carbonyl Groups on the Motilin 1-12 Structure

Y. Boulanger[1], A. Khiat[1], Y. Chen[1], P. Poitras[2] and S. St-Pierre[1]

[1]INRS-Santé, Université du Québec, Pointe-Claire, Quebec, H9R 1G6, Canada
[2]Centre de Recherche Clinique André-Viallet, Hôpital St-Luc,Montreal, Quebec, H2X 3J4, Canada

Introduction

Motilin is a 22-residue peptide hormone which stimulates the contractile activity of the stomach and upper small intestine [1]. The motilin 1-12 (M112) fragment displays biological effects similar to those of motilin *in vitro* [2]. Selective reduction of the amide groups of M112 to form CH_2NH isosteres resistant to enzymatic cleavage results in a decrease in contractile response for the analogs reduced in positions 1-2 (C12M112) and 2-3 (C23M112) and in a total loss of activity for all other positions [2]. In this study, the three-dimensional structures of M112 and its CH_2NH analogs were investigated by NMR and molecular modeling and correlated with biological activity.

Results and Discussion

The temperature dependences of the amide chemical shifts (temperature coefficients) for M112 and the CH_2NH analogs are presented in Table 1. The temperature coefficients of C12M112 and C23M112 are nearly identical to those of M112 for the amide protons of

Table 1. *Temperature coefficients (x 10^{-3} ppm/K) of amide protons of M112 and analogs*[a]

Residue	M112	C12	C23	C34	C45	C56	C67	C78	C89
F1	-1.71	-5.07	-5.99	-8.47	-2.54	-2.31	-1.74	-2.94	-4.94
V2	-6.96		-7.00	-7.09	-7.11	-7.43	-6.89	-7.44	-6.89
I4	-5.71	-7.18				-5.01	-5.44	-5.52	-6.04
F5	-5.29	-6.13					-6.04		
T6	-6.99	-7.14	-8.01	-4.79				-5.14	-5.66
Y7	-4.94	-4.99	-4.60	-4.39	-4.86	-9.62		-5.12	-5.36
G8	-6.98	-6.89	-6.94	-6.89	-6.98	-8.94			-2.22
E9	-5.29	-5.41	-5.81	-6.06	-5.93	-6.47	-6.19	-6.00	
L10	-5.72	-5.94	-5.73	-5.93	-5.96	-6.72	-8.42	-5.90	
Q11	-5.21	-5.94	-5.60	-5.49	-5.20	-6.31	-6.16	-6.40	
R12	-4.69	-4.77	-4.84				-4.92	-6.66	-5.81

[a] Cxy corresponds to M112 with a CH_2NH in position xy.

residues 6-12, suggesting an identical C-terminal structure. This is not the case for the other analogs. The N-terminal coefficients (residues 1-5) of all analogs are different from those of M112. Few hydrogen bonds are present.

Analysis of DQFCOSY, TOCSY and NOESY spectra lead to the assignment of all resonances of M112, C12M112 and C45M112. Between 38 and 55 intra-residue connectivities and between 27 and 54 inter-residue NOE connectivities were observed for the three molecules. Backbone dihedral angles derived from $^3J_{NH\alpha H}$ coupling constants were nearly identical for M112 and C12M112 but differed for C45M112.

Molecular modeling included conjugate gradients energy minimization, molecular dynamics, cluster analysis followed, for each cluster, by steepest descent energy minimization, introduction of the NMR constraints, molecular dynamics and conjugate gradients energy minimization. A total of 31, 30 and 27 of the 35 final structures of M112, C12M112 and C45M112, respectively, converged onto an identical folding pattern. None of these structures displayed NOE distance violations of more than 0.5 Å. The molecular models display H bonds consistent with the temperature coefficients: between the NH of Phe^1 and the CO of Ile^4 for M112, between the NH of Phe^1 and the CO of Val^2 in C45M112, and between the C-terminal NH_2 and the CO of Gln^{11} in C45M112. The overall structures of M112 and C12M112 are similar and present an analogous folding pattern in the C-terminal part but differ in the N-terminal part. However, the structure of C45M112 is different. For all three molecules, the Gly^8-Gln^{11} region is the best defined.

These conformational results based on different NMR parameters (NH exchange rates, chemical shifts, coupling constants, NOE distances) demonstrate that reduction of a single backbone carbonyl group leads to significant structural effects. Reduction in any position leads to structural perturbations in the N-terminal segment whereas reduction beyond position 3-4 causes changes in the whole molecule. This can be explained by an increase in flexibility resulting from the destruction of the planarity of the amide bond. Therefore, the desirable effects of protection against enzymatic cleavage provided by the methylene group produce structural disturbances affecting or destroying biological activity. Based on these results, conservation of the amide bond rigidity seems to be an essential element for the design of biologically active non-hydrolyzable peptide analogs.

Acknowledgments

The financial support of the Medical Research Council of Canada and of the Institut National de la Recherche Scientifique is gratefully acknowledged.

References

1. Itoh, Z., 'Motilin', Academic Press, San Diego, CA, 1990.
2. Miller, P., Gagnon, D., Dickner, M., Aubin, P., St-Pierre, S. and Poitras, P., *Peptides,* 16 (1995) 11.

Peptides: Chemistry, Structure and Biology
Pravin T.P. Kaumaya and Robert S. Hodges (Eds.)
Mayflower Scientific Ltd., 1996

313
Correlation Between the Structural Properties of Five Different FMDV Peptides and Their Serological Behaviour

M. Pegna[1], L. Ragona[2], G. Bravi[1], H. Molinari[3], L. Zetta[2], W.A. Gibbons[4], G. Siligardi[5], F. Brown[6], D. Rowlands[7] and P. Mascagni[1]

[1]Italfarmaco Research Centre, Cinisello B., 20092 Milan, Italy
[2]NMR Laboratory, CNR Centre, 20131 Milan, Italy
[3]Instituto Policattedra, University of Verona, 37100 Verona, Italy
[4]Department of Pharmaceutical Chemistry, School of Pharmacy London, WC1H OAJ, England, UK
[5]Department of Chemistry, Birkbeck College, London, WC1H OAJ, England, UK
[6]US Department of Agriculture, Greenport, NY 11944, USA
[7]Department of Molecular Sciences, Wellcome Foundation, Beckenham, BR3 3BS, England, UK

Introduction

FMDV is the cause of a disease afflicting domestic livestock. The disease can be prevented by vaccination but the preparation of appropriate vaccines is complicated by the occurrence of seven distinct serotypes and by the considerable antigenic variation within serotypes. The immunodominant site of the virus is contained within residues 141-160 of VP1. Several antigenic variants of serotype A12 have been isolated which differed only at positions 148 and 153 of VP1 (Figure 1) [1]. The 141-160 peptides corresponding to four of these variants (called peptides A,B,C and USA) have been compared by CD spectroscopy [2, 3]. The results were consistent with the classification of the peptides into two classes, A with C and USA with B, which had been derived from their serological behavior [1]. In this work, NMR and computer calculations were carried out on the four A12 peptides and on that from serotype O1K. A correlation between structure and serological behavior is provided.

Results and Discussion

NMR parameters, derived for peptides A, USA and O1K in TFE-OH solutions, were used for DG and RMD calculations. Those structures which were compatible with the NMR parameters were grouped into homogeneous sets based on Cα traces superimposition. The general characteristics common to most of the families thus identified were as follows.

Peptide O1K was largely helical. The C-terminal half region (residues 153 to 160) was also helical in A and USA while the conserved RGD triplet, used by the virus to bind

and to infect the host's cells, was part of a turn similar to that contained in the helix of peptide O1K. In peptide A the central residues formed a large loop stabilised by a H-bond between the NH of D147 and the CO of A152 (Figure 1). A similar loop was found in USA although restricted to fewer residues and stabilised, in the majority of cases, by interactions between D147 and S150 (Figure 1).

These results and those from additional NMR studies and calculations with and without NMR constraints carried out on A, USA, C and B permitted classification of the latter into the same two families deduced from CD and serological data. Furthermore, they offered a structural explanation for the antigenic variation within the A12 serotype and between serotypes. Thus, the major structural differences among the five peptides were found in the central region of the sequence where residues are less conserved (Figure 1). In the four A12 peptides, either G149 or S150 or both induce a bend with residue 148 defining the size of this bend\loop and hence the antibody specificity. Conversely in O1K the replacement of G and S with Q and V respectively (see Figure 1) changed the structure of this region of the peptide to that of a helix.

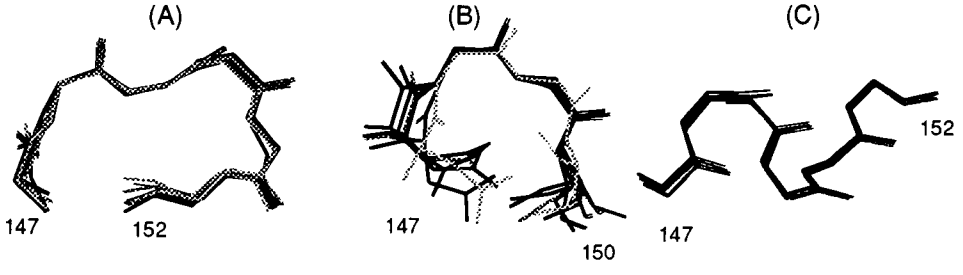


```
    141                  147 148          152 153                  160
A   Gly-Ser-Gly-Val-Arg-Gly-Asp-Ser-Gly-Ser-Leu-Ala-Leu-Arg-Val-Ala-Arg-Gln-Leu-Pro
B   ----------------------------------Leu-------------------Pro----------------------------------
C   ----------------------------------Ser-------------------Ser----------------------------------
USA ----------------------------------Phe-------------------Pro----------------------------------

O1K      -Asn-Leu-Arg-Gly-Asp-Leu-Gln-Val-Leu-Ala-Gln-Lys-Val-Ala-Arg-Thr-Leu-
```

Figure 1. *The central region of peptides A and C (A), USA and B (B) and O1K (C). The different structures could account for the antigenic variation induced by mutations at position 148 (A12 peptides) and positions 149 and 150 (O1K vs A12).*

References

1. Rowlands, D.J., Clark, B.E., Carrol, A.R., Brown, F., Nicholson, B.H., Bittle, J.L., Houghten, R.A. and Lerner, R.A., *Nature*, 306 (1983) 694.
2. Siligardi, G., Drake, A.F., Mascagni, P., Rowlands, D., Brown, F. and Gibbons W.A., *Int. J. Peptide Protein Res.*, 38 (1991) 519.
3. Siligardi, G., Drake, A.F., Mascagni, P., Rowlands, D., Brown, F. and Gibbons W.A., *Eur. J. Biochem.*, 199 (1991) 545.

Session XV
Peptides in Cancer

Chairs: John A. Smith and Michael D. Lairmore

&

Session XVI
Peptides in Immunology

Chairs: Conrad Schneider and Helene Grasse-Masse

Peptides: Chemistry, Structure and Biology
Pravin T.P. Kaumaya and Robert S. Hodges (Eds.)
Mayflower Scientific Ltd., 1996

314
Generation of Human Cytotoxic T Cells Specific for Human Carcinoembryonic Antigen (CEA) Peptides from Patients Immunized with Recombinant Vaccinia-CEA (rV-CEA) Vaccine

J. Schlom, S. Zaremba, C.A. Nieroda, M.Z. Zhu, J.M. Hamilton and K.Y. Tsang

National Cancer Institute, National Institutes of Health, Bethesda, MD 20892, USA

Introduction

Human CEA is extensively expressed on greater than 90% of human colorectal, gastric, and pancreatic carcinomas as well as approximately 50% of breast cancers and 70% of non-small cell lung cancers. CEA is also expressed to some extent on normal colon epithelium and in some fetal tissue. The CEA gene has been sequenced and shown to be part of the human immunoglobulin gene superfamily, and thus shares some homology with other molecules found on normal human tissues. At the amino acid level, CEA shares approximately 70% homology with NCA (non-specific cross reacting antigen) which is found on normal granulocytes. The immunogenicity of CEA in humans is at best controversial. Several papers claim antibodies to CEA in patients, while others report these observations are artifacts. No reports of the presence or absence of human T-cell responses to CEA exist.

Results and Discussion

One strategy that is being pursued to determine if one can induce T-cell responses to CEA in carcinoma patients is to place the CEA gene into vaccinia virus. Vaccinia was chosen as a vector for several reasons. Among these are: (a) its wide use in humans in the eradication of smallpox; (b) its ability to infect a wide range of cells, including professional antigen presenting cells (APCs), and express the inserted gene product in a manner that has the potential to be processed in the context of class I and/or class II MHC molecules; and (c) animal model studies have shown that the use of a recombinant human CEA vaccinia virus (designated rV-CEA) is superior to the use of soluble CEA in the induction of anti-tumor effects on established CEA expressing tumors. These findings correlated with the appearance of CEA specific cytotoxic T-lymphocytes (CTLs) in rV-CEA inoculated animals. rV-CEA has also been administered to rhesus monkeys and has been shown to induce CEA-specific T-cell responses with no toxicity.

It is important to emphasize, however, that experimental model results should have extremely limited extrapolation to potential human immune T-cell responses. For one, human CEA is a foreign gene in both mice and non-human primates. However, the more important point to consider is the question of whether human APCs, including tumors,

will process CEA in such a manner as to present specific CEA peptides in the context of human MHC, for human T-cell recognition. Since mouse and non-human primate MHC binding motifs are different from human motifs, studies in animal models cannot answer the question of T-cell immunogenicity in humans. Even the use of CEA transgenic mice could not answer these questions, because they would possess murine MHC motifs. Thus, while animal model studies were conducted to demonstrate that rV-CEA can indeed infect mammalian cells *in vivo* to a level as to induce immune responses, and to demonstrate lack of toxicity, only clinical trials can adequately answer the question as to the potential ability of rV-CEA to induce CEA specific human T-cell responses. A Phase I IRB approved clinical trial by the NCI/Navy Oncology Branch (M. Hamilton, P.I.) involving rV-CEA (Therion Biologics Corp.) in patients with metastatic carcinoma (gastrointestinal, lung, and breast) has been completed. No toxicity was observed other than usually seen with the smallpox vaccine. Even with the highest dose group receiving three monthly injections of 10^7 pfu rV-CEA, the maximum tolerated dose was not achieved.

Peripheral blood lymphocytes (PBLs) obtained from patients with metastatic carcinoma, both pre- and post-vaccination with rV-CEA, were analyzed for T-cell response to specific 9-11 mer CEA peptides selected to conform to human HLA class I-A2 motifs. While little or no T-cell growth was seen from pre-immunization PBLs of patients pulsed with CEA peptides and IL-2, T-cell lines were obtained from PBLs of patients post-vaccination, after 1 to 3 cycles of stimulation. Cytolytic T-cell lines from three A2 patients were established with one peptide (designated CAP-1) and the T-cell line (designated V24T) from one patient was chosen for detailed analysis. V24T was shown to be a CD8+/CD4+ double positive and to synthesize high levels of TNF-a when exposed to the 9 amino acid CAP-1 peptide. When autologous EBV-transformed B-cells were either incubated with CAP-1 peptide, or transduced with the CEA gene using a retroviral vector, they were lysed by the V24T cell lines. Allogeneic non-A2 EBV transformed B-cells were not lysed when incubated with CAP-1. A human colon carcinoma cell line which is CEA positive and A2 positive, was also lysed by the V24T cell line while two non-A2 CEA positive colon carcinoma cell lines were not. To further define the class I HLA-A2 restricted nature of the V24T cytotoxicity, the non-A2 CEA expressing colon carcinoma cell line was infected with a recombinant vaccinia virus expressing the HLA class I-A2 gene and was shown to become susceptible to V24T lysis. Cells infected with vector alone were not lysed.

These studies demonstrate for the first time, (a) the ability to generate a human cytolytic T-cell response to specific epitopes of CEA, (b) the class I HLA-A2 restricted nature of the T-cell mediated lysis, and (c) the ability of human tumor cells to endogenously synthesize CEA so as to present a specific CEA peptide in the context of MHC for T-cell lysis. These findings thus have implications in the development of specific second generation cancer immunotherapy protocols. Preclinical studies are currently underway to determine the efficacy of the use of other immunogens alone or in combination with rV-CEA. These include avian pox-CEA recombinants, baculovirus derived CEA, and peptides modeled to induce and/or enhance T-cell responses.

Activation of T-cells requires at least two signals: an antigen-specific signal delivered through the T-cell receptor and a costimulatory signal mediated through molecules designated B7-1 and B7-2. Previous studies have shown that introduction of

the B7 gene into tumors using retroviral vectors has led to enhanced antitumor effects. A limiting factor for potential clinical applications using this approach is the low efficiency of infection of retroviral vectors and consequent manipulations of infected cells. Vaccinia virus thus represents an alternative vector for B7 gene expression in tumor cells or antigen presenting cells. We have recently described the construction and characterization of recombinant vaccinia viruses containing the murine B7-1 and B7-2 genes (designated rV-B7-1 and rV-B7-2). Infection of cells with these constructs results in rapid and efficient cell surface expression of both B7-1 and B7-2 (>97% of cells express B7 at 4h).

In recent preclinical studies, we have demonstrated the an admixture of rV-B7 and rV-CEA (at proper ratios) greatly enhances CEA specific T-cell responses and anti-tumor activity. These studies also have implications for the admixture of rV-B7 with recombinant vaccinia viruses containing genes for other tumor associated antigens or genes for infectious agents in the activation of specific cytolytic T-cell population.

References

1. Kantor, J., Irvinem K., Abrams, S., Kaufman, H., DiPietro, J. and Schlom, J., *Natl Cancer Inst.*, 84 (1992) 1084.
2. H. Hand, P., Robbins, P.F., Salgaller, M.L., Poole, D.J. and Schlom, J., *Cancer Immunol. Immunother.*, 36 (1993) 65.
3. Kantor, J., Irvine, K., Abrams, S., Snoy, P., Olsen, R., Greiner, J., Eggensperger, D., Kaufman, H. and Schlom, J., *Cancer Res.*, 52 (1992) 6917.
4. Robbins, P.F., Eggensperger, D., Qi, C-F., Simpson, J. and Schlom, J., *Int. J. Cancer*, 53 (1993) 892.
5. Salgaller ,M.L., Bei, R., Schlom, J., Poole, D.J. and Robbins, P.F., *Cancer Res.*, 53 (1993) 2154.
6. Irvine, K., Kantor, J. and Schlom, J., *Vaccine Research*, 2 (1993) 79.
7. Kantor, J., Abrams, S., Irvine, K., Snoy, P., Kaufman, H. and Schlom, J., *Annals NY Acad. Sci.*, 690 (1993) 370.
8. Bei, R., Kantor, J., Kashmiri, S.V.S. and Schlom, J., *Mol. Immunol.*, 31 (1994) 771.
9. Conry, R.M., LoBuglio, A.F., Kantor, J., Schlom, J., Loechel, F., Moore, S.E., Sumerel, L.A., Barlow, D.L., Abrams, S. and Curiel, D.T., *Cancer Res.* , 54 (1994) 1164.
10. Bei ,R., Kantor, J., Kashmiri, S.V.S., Abrams, S. and Schlom, J., *J. Immunotherapy* , 16 (1994) 275.
11. Schlom, J., Kantor, J., Abrams, S., Tsang, K.Y., Panicali, D. and Hamilton, J.M., *Breast Cancer Res. Treat.*, in press.
12. Hodge, J.W., Abrams, S., Schlom, J. and Kantor, J., *Cancer Res.*, 54 (1994) 5552.
13. Tsang, K.Y., Nieroda, C.A., DeFilippi, R., Chung, Y.K., Yamaue, H., Greiner, J.W. and Schlom, J., *Vaccine Research* , 3 (1994) 183.
14. Bei, R., Paranavitana, C., Milenic, D., Kashmiri, S.V.S. and Schlom, J., *J. Clinical Lab. Analysis*, 16 (1995) 275.
15. Karr, J.F., Kantor, J.A., Horan Hand, P., Eggensperger, D.L. and Schlom, J., *Cancer Res.*, 55 (1995) 2455.
16. Hamilton, J.M., Chen, A.P., Nguyen, B., Gram, J., Abrams, S., Chung, Y., Kantor, J., Phares, J.C., Bastian, A., Brooks, C., Morrison, G., Allegra, C.J. and Schlom, *J. Am. Soc. Clin. Oncol. Proceedings*, Dallas, TX, 961 (1994) [abstr].
17. Tsang, K.Y., Zaremba, S., Nieroda, C.A., Zhu, M.Z., Hamilton, J.M. and Schlom, J. *J. Natl. Cancer Inst.*, 87 (1995) 982.

Peptides: Chemistry, Structure and Biology
Pravin T.P. Kaumaya and Robert S. Hodges (Eds.)
Mayflower Scientific Ltd., 1996

315
Peptide Vaccines For "Self" Tumor Antigens

M.L. Disis and M.A. Cheever

Department of Medicine, Division of Oncology, University of Washington, Seattle, WA 98195, USA

Introduction

In animal models, malignancy can be treated by vaccine and T cell therapy. In humans, one of the major obstacles in developing cancer vaccines has been the lack of defined target antigens. Recently, however, several groups have identified proteins in human malignancy that can be recognized by the patient immune system [1]. Identification of human tumor antigens is an important step towards extrapolating successful animal studies into immune therapies for human malignancy. One ploy to identify tumor antigens has been to characterize the antigens on autologous tumors that are recognized by autochthonous T cells [3]. Antigens identified by such studies have largely been "self" proteins expressed on normal as well as malignant cells [1-5]. These proteins may be expressed during fetal development, but present in adults in only a limited number of tissues, (*e.g.*, MAGE), or may be related to the normal function of the now malignant cell, (*e.g.* tyrosinase). In some circumstances, the proteins identified are involved in malignant transformation or the maintenance of the transformed state (*e.g.*, HER-2/neu or ras). Immune responses directed against each of these proteins have been detected in patients with a variety of cancers.

The realization that the immune systems of patients with cancer can generate responses against proteins expressed on their own malignancy, even self proteins, has intensified interest in the development of an effective cancer vaccine. However, methods to generate immune responses to "self" tumor antigens are not well defined. A key to inducing an immune response to self proteins may lie in the use of peptide based vaccines. In several model systems immunity to self or transgene encoded proteins has been elicited by immunization with peptides [7, 8]. T cells recognize antigen in the context of processed peptides that bind in the MHC molecule. Current theories of self recognition suggest that immunodominant epitopes of self proteins elicit tolerogemic responses [7]. Other potentially immunogenic epitopes, functionally defined as subdominant epitopes, are "ignored" by the immune system when in the protein, but are immunogenic as peptides. If subdominant epitopes could be identified for "self" tumor antigens, peptide vaccines might be most appropriate for generating responses.

Peptide vaccines have several advantages. Peptides are relatively easy to construct and produce and may retain chemical stability over time, decreasing lot to lot variation. Vectors with infectious or oncogenic potential are not necessary. Perhaps the most important advantage is the theoretical ability to manipulate the immune response with defined peptide epitopes. Protective immunity generated by vaccination depends on

elicitation of immune responses with appropriate function. Peptide vaccines will allow the generation of T cell populations specific for defined epitopes and with defined function thus allowing a directed and effective immune response.

Results and Discussion

The HER-2/neu oncogenic protein is a good model system in which to assess the efficacy of a peptide vaccine. The HER-2/neu oncogene (c-erbB-2) encodes a transmembrane protein with homology to epidermal growth factor receptor. HER-2/neu is amplified and overexpressed in 20-40% of invasive breast cancers, is associated with aggressive disease, and is an independent predictor of poor prognosis in subsets of patients [9]. HER-2/neu may also be related to cancer formation with overexpression being detectable in 50-60% of ductal carcinomas *in situ* [10].

Studies from our laboratory showed that some breast cancer patients with HER-2/neu overexpressing cancers have a preexistent immune response to the protein [5, 6]. Of 50 patients with HER-2/neu positive tumors, 42% had an antibody response to the protein. Only 4% of 145 normal blood donors had detectable antibody responses. CD4+ T cells specific for the HER-2/neu protein and peptides have also been detected in cancer patients [5, 6]. In 7 patients with HER-2/neu positive breast cancers, 3 had proliferative T cell responses directed against the protein and/or peptides. All three responded to peptide epitopes derived from both the intracellular (ICD) or extracellular (ECD) domains of the protein. One patient responded to the peptides, but not to the intact protein, indicating the intact protein may suppress an effective immune response. The 4 patients who did not have a response to the protein or peptides did not respond to tetanus toxoid used as a control.

The finding that some patients had an existent immune response to HER-2/neu was surprising in that others had previously attempted and failed to immunize rats to rat neu protein expressed by a recombinant vaccinia virus [11]. Although mice immunized with the same vectors developed vigorous immune responses to rat neu, when rats were immunized they did not develop detectable antibody or delayed type hypersensitivity responses to the protein. The conclusion was that mechanisms of tolerance prevented immunization in rats and would prevent immunization in humans. Presumably, immunization with intact HER-2/neu protein would be ineffective in generating immune responses.

To determine whether a peptide vaccine could elicit immunity to HER-2/neu, rats were immunized to peptides derived from the homologous rat protein, neu. The amino acid sequence of the rat neu protein was analyzed using a sequence motif searching program, "TSites", that incorporates several algorithms to distinguish peptide epitopes appropriate for class II MHC restricted T cell responses [12]. A panel of potential peptide epitopes was identified and constructed. Rat immunization studies validated that peptides identified in this manner can elicit both T cell and antibody immunity [13]. Rat neu and human HER-2/neu are 89% homologous. Rats were immunized with combinations of ECD and ICD peptides that are highly homologous or 100% homologous between rat and human neu proteins. Complete Freund's adjuvant was used. Immunization elicited IgG antibody responses that were specific for both rat and human

protein. Peptide immunizations also elicited CD4+ T cell proliferative responses specific for rat neu protein. Thus, the concept that HER-2/neu peptides can be used in vaccines to circumvent T cell and antibody tolerance is valid. Of note, there was no evidence of toxicity or autoimmunity through a five month observation period.

Immunogenic peptides identified in studies such as these may be directly applicable to the design of a vaccine for use in human cancers. Rat "self" peptides, rather than foreign peptides, were used to immunize rats so that the results might be extrapolated to the use of human peptides in humans. The peptides used were homologous to the human HER-2/neu sequence and the antibodies generated were specific for both rat and human protein. Thus, the results predict that immunization of humans with the same peptides is likely to generate similar immune responses. The induction of an immune response to rat neu in rats lays the foundation for testing peptide based vaccines in humans for generating immune responses to HER-2/neu protein in patients with HER-2/neu positive cancers.

Acknowledgments

This work was supported by a Berlex Oncology Foundation Fellowship to M.L.D. and by NIH Grants R37 CA30558 and R01 CA61912 to M.A.C. We wish to thank Faith Shiota for excellent technical assistance and Kent Slaven for animal technical support.

References

1. Pardoll, D.M., *Nature*, 369 (1994) 357.
2. van Der Bruggen, P., Traversari, C., Chomez, P., Lurquin, C. DePlaen, E., Van Den Eynde, B., Knuth, A. and Boon, T., *Science*, 254 (1991) 1643.
3. Jerome, K.R., Barnd, D.L., Bendt, K.M., Boyer, C.M., Taylor-Papadimitriou, J., McKenzie, I.F., Bast, R.C. Jr. and Finn, O.J., *Cancer Res.*, 51 (1991) 2908.
4. Houghton, A.N., *J. Exp. Med.*, 180 (1994) 1.
5 Disis, M.L., Calenoff, E., McLaughlin, G., Murphy, A.E., Chen, W., Groner, B., Jeschke, M., Lydon, N., McGlynn, E., Livingston, R.B., Moe, R. and Cheever, M.A., *Cancer Res.*, 54 (1994)16.
6. Cheever, M.A., Disis, M.L., Bernhard, H., Gralow, J.R., Hand, S.L., Huseby, E.S., Qin, H.L., Takahashi, M. and Chen, W., in G. Möller (Ed.) 'Immunological Reviews', Munksgaard Intl. Pub., (1995) 145 (1995) 33.
7. Sercarz, E.E., Lehmann, P.V., Ametani, A., Benichou, G., Miller, A. and Moudgil, K. *Ann. Rev. Immunol.*, 11 (1993) 729.
8. Cibotti, R., Kanellopoulos, J.M., Cabaniols, J.P., Halle-Panenko, O., Kosmatopoulos, K., Sercarz, E., and Kourilsky, P., *Proc. Natl. Acad. Sci. USA*, 89 (1992) 416.
9. Slamon, D., Clark, G., Wong, S., Levin, W., Ullrich, A. and McGuire, W., *Science*, 235 (1987) 177.
10. Allred, D., Clark, G., Molina, R., Tandon, A., Schnitt, S., Gilchrist, K., Osborne, C., Tormey, D. and McGuire, W., *Human Pathol.*, 23 (1992) 974.
11. Bernards, R., Destree, A., McKenzie, S., Gordon, E., Weinberg, R.A. and Panicali, D., *Proc. Natl. Acad. Sci. USA*, 84 (1987) 6854.
12. Feller, D. and de la Cruz, V.F., *Nature.*, 349 (1991) 720.
13. Disis, M.L., Gralow, J.R., Bernhard, H., Hand, S.L., Rubin, W.D., and Cheever, M.A., *J. Immunol.*, in press.

Peptides: Chemistry, Structure and Biology
Pravin T.P. Kaumaya and Robert S. Hodges (Eds.)
Mayflower Scientific Ltd., 1996

316

Enhanced Immunogenicity of Engineered Chimeric Oligopeptides Corresponding to Activating Mutations of the p21 *ras* Proto-oncogene

P.L. Triozzi[1], G.D. Stoner[2] and P.T.P. Kaumaya[3]

Departments of [1]Medicine, [2]Preventive Medicine and [3]Obstetrics and Gynecology, The Comprehensive Cancer Center and James Cancer Hospital and Research Institute, The Ohio State University, Columbus, OH 43210, USA

Introduction

Transforming proteins encoded by mutationally activated *ras* proto-oncogenes are potentially unique targets for cancer vaccines. The three *ras* proto-oncogenes, H-*ras*, K-*ras*, and N-*ras*, encode highly homologous, M_r 21,000, GTP-binding proteins [1]. Activating mutations are found in GTP-binding regions; virtually all relevant mutations are found in codons 12 (Gly), 13 (Gly), and 61 (Gln). The resultant oncoprotein remains in the constitutively activated, GTP-bound state. Activating *ras* mutations have been detected in a substantial proportion of many common malignancies, including lung, pancreatic, and colon. Experimental evidence *in vitro* and in transplantable tumor models supports the possibility that protection against tumors bearing activated *ras* can be achieved using vaccine approaches [2-4]. We have identified a rodent tumor model, A/J mouse lung, that is a very sensitive *in vivo* system for the detection of activating K-*ras* mutations [5, 6]. A/J mice are not only susceptible to lung tumor induction by chemical carcinogens but also have a high incidence of spontaneous tumors. The expression of activating *ras* mutations as well as the tumor progression in this model parallels that of human tumors. The patterns of chemically-induced *ras* mutations are specific for each chemical or class of chemicals. We examined the immunobiology of oligopeptides corresponding to activating mutations of p21 *ras* in this autochthonous tumor model system.

Results and Discussion

We first examined whether immune responses to *ras* oncopeptides could be elicited in A/J mice, as immune responses in the H-2^a background had not been previously reported. A/J mice were immunized using a mixture of three *ras* peptides corresponding to codons 5-17 and bearing activating substitutions at codon 12 [250 μg/0.2 ml of *ras*$(5\text{-}17)^{12G\rightarrow C}$, *ras*$(5\text{-}17)^{12G\rightarrow D}$, and *ras*$(5\text{-}17)^{12G\rightarrow V}$]. Codon 12 Asp is the most common spontaneous and chemically-induced mutation in A/J mice. Codon 12 Val substitutions occur spontaneously and in response to N-nitrosodiethylamine and benzo[*a*]pyrene. Codon 12 Cys rarely occurs spontaneously but does occur in response to benzo[*a*]pyrene. CGP-1 1637 (600 μg/0.6 ml)was used as the adjuvant in a squalene-based vehicle (1.2 ml). Each

mouse received 0.4 ml of the mixture (125 μg of peptide per mouse) s.q. and were boosted on day 14 with the same peptide mixture in vehicle without adjuvant. Spleens were harvested on day 24. Significant proliferative responses to *ras*(5-17)$^{12G\rightarrow C}$ and *ras*(5-17)$^{12G\rightarrow V}$ were induced. Proliferative responses to *ras*(5-17)$^{12G\rightarrow D}$ were very weak. Codon 12 Asp substitutions have also not been strongly immunogenic in H-2^{d} BALB/c and H-2^{b} C57BL/6 mice and in human studies [7, 8]. The role of "immune surveillance" in carcinogenesis is controversial. Interestingly, however, the most common activating spontaneous and carcinogen-induced substitution observed in A/J mice is only weakly immunogenic.

The immunogenicity of subunit peptide vaccines can be enhanced in a variety of ways. Covalent conjugation to large carrier molecules is undesirable, as this often results in hypersensitivity, loss or inappropriate presentation of epitopes, appearance of undefined structures, MHC restriction, and batch to batch conjugate variability. Antigenic peptides derived from, for example, tetanus toxin (TT) have been identified that appear to be "promiscuous" in their recognition in association with many MHC molecules. We have examined the effectiveness of engineered chimeric constructs incorporating promiscuous T-cell epitopes to enhance immunogenicity and to meet the challenge of MHC polymorphism. Our studies have indicated that certain haplotype-restricted immune responses can be bypassed by including promiscuous T-cell epitopes in the immunogen. Additional peptide length, although not predicted to bind in the peptide-binding groove of the MHC class II molecules, can enhance peptide capacity to stimulate T-cell responses; chimeric peptides containing promiscuous peptide can be more antigenic than native peptides and, significantly, do not require processing [9, 10].

We assembled a chimeric peptide consisting of *ras*(5-17)$^{12G\rightarrow D}$ (YKLVVVGAD GVGK) joined by a 4-residue linker sequence (LSPG) to TT3 (FNNFTVSFWLRVPK VSASHLE). We also engineered a chimeric consisting of the native *ras*(5-17) sequence similarly to TT3. TT3 was chosen because it poses few problems synthetically. A/J mice were immunized with 0.125 μg of the chimerics on day 1 and 14 using CGP-1 1637 as an adjuvant, splenocytes were collected on day 28, and lymphoproliferative responses to the chimeric peptide immunogens and to native peptide sequences assessed. Strong proliferative responses to the immunizing peptide were observed. Although there was cross-reactivity, likely an anti-TT3 response, enhanced lymphoproliferative responses to ras(5-17)$^{12G\rightarrow D}$ could be demonstrated in mice immunized with the *ras*(5-17)$^{12G\rightarrow D}$-TT3 chimeric in the presence of syngeneic antigen presenting cells (Figure 1).

The mechanism of the enhanced immunogenicity of the chimeric peptide incorporating a promiscuous T-cell epitope is not known. The additional peptide length may have improved the binding of native sequence to the H-2^{a} haplotype. It could be the result of a helper effect provided by the TT3 component of the chimeric peptide. The chimeric construct may also provide an entirely new set of peptides due to the new opportunities created by the fusion peptide sequence that can be better presented in the context of the formerly nonbinding/nonreactive MHC molecule. These studies in a relevant animal model do suggest the possibility that genetically restricted stimulatory activity of mutated *ras* peptides can, at least in one instance, be addressed. The safety and stability of these constructs may make them particularly useful in vaccine approaches targeting human oncogenes.

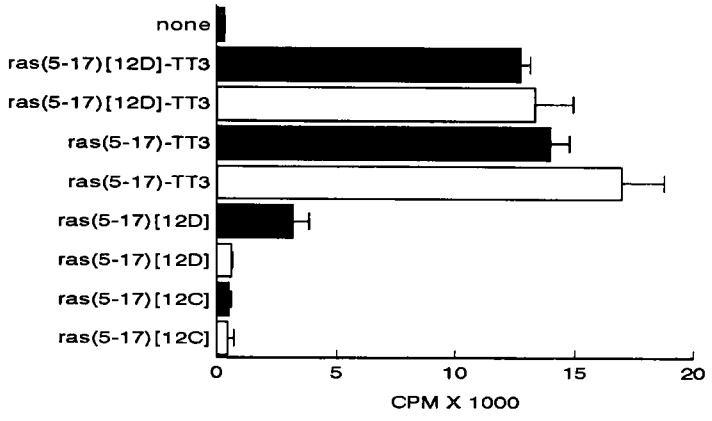

Figure 1. *Lymphoproliferative responses elicited by chimeric constructs. A/J mice were immunized in vivo with either ras(5-17)[12D]-TT3 (solid bars) or ras(5-17)-TT3 (open bars) chimeric constructs. Proliferative responses to the immunogen or oligopeptides corresponding to native sequences were assessed in vitro. Data represent mean ± SD for triplicate samples.*

Acknowledgments

Supported in part from by the Ohio State University Comprehensive Cancer Center Core Grant (2P30CA165058-16A1).

References

1. Barbacid, M., *Annu. Rev. Biochem* 56 (1987) 779.
2. Fenton, R.G., Taub, D.D., Kwak, L.W., Smith, M.R., and Longo, D.L., *J. Natl. Cancer Inst.* 85 (1993) 1294.
3. Peace, D.J., Smith, J.W., Chen, W., You, S-G, Cosand, W.L., Blake, J., and Cheever, M.A., *J. Exp. Med.* 179 (1994) 473.
4. Skipper, J. and Stauss, H.J., *J. Exp. Med.* 177 (1993) 1493.
5. You, M., Candrian, U., Maronpot, R.R., Stoner, G.D., and Anderson, M.W., *Proc. Natl. Acad. Sci. USA* 86 (1989) 3070.
6. Wang, Y., Wang, Y., Stoner, G., and You, M., *Cancer Res.* 53 (1993) 1620.
7. Peace, D.J., Chen, W., Nelson, H., and Cheever, M.A., *J. Immunol.* 146 (1991) 2059.
8. Gedde-Dahl, T., Eriksen, J.A., Thorsby, E., and Gaudernack, G., *Human Immunology* 33 (1992) 266.
9. Srinivasan, M., Domanico, S.Z., Kaumaya, P.T.P., and Pierce, S.K., *Eur. J. Immunol.* 23 (1993) 1011.
10. Kaumaya, P.T.P, Seo, Y.H., Kobs, S., Feng, N., Sheridan, J., and Stevens, V., *J. Molec. Recog.* 6 (1993) 81.
11. Valmori, D., Romero, J.F., Men, Y., Maryanski, J.L., Romero, P., and Corradin, G., *Eur. J. Immunol.* 24 (1994) 1458.

Peptides: Chemistry, Structure and Biology
Pravin T.P. Kaumaya and Robert S. Hodges (Eds.)
Mayflower Scientific Ltd., 1996

317
Peptide-loading of Class II Molecules in B Lymphocytes

X. Xu, J.M. Green, W. Song and S.K. Pierce

Department of Biochemistry, Molecular Biology and Cell Biology
Northwestern University, Evanston, IL 60208, USA

Introduction

Immune responses to foreign antigens, both antibody responses and cytolytic T cell responses, require the function of helper T lymphocytes. Antigen-dependent activation of helper T lymphocytes requires that the antigen be processed and presented by cells, such as B cells, which express the Major Histocompatibility Complex (MHC) class II molecules (reviewed in [1]). In B lymphocytes, processing involves the binding of antigen to surface Ig, internalization of antigen into acidic subcellular compartments where the antigen is proteolytically degraded and the resulting peptides bind to the class II molecules. The peptide-class II complexes are then displayed on the cell surface for recognition by T cells. Thus, protein antigens must be reduced to short peptide fragments bound to MHC class II molecules before immune responses can be initiated.

The class II molecule is a heterodimer of two 30kD proteins, α and β, which fold together to form two extracellular domains, one of which contains a peptide binding groove that accommodates peptides of 8 to 9 amino acids in length in an extended conformation (reviewed in [2]). Amino acid sequence analyses of the peptides isolated from class II molecules show that these range in length from 8 to over 25 residues. For the most part, these peptides are derived from exogenous proteins or cellular proteins present in the endocytic route. The class II α and β chains are synthesized in the endoplasmic reticulum where they bind to a third chain, the invariant chain (Ii). The Ii insures proper transport of the class II molecules to the subcellular site where peptides are loaded and blocks the binding of peptides to the class II molecules until the class II molecules reach the peptide-loading compartment. In the peptide-loading compartment, the Ii is proteolytically removed from class II. An intermediate in this process is a peptide of Ii called CLIP bound to the class II molecules. CLIP is removed from the class II molecules prior to binding of exogenous antigen. Because of the central role of antigen processing in immune responses, it important to elucidate the cellular and molecular mechanisms required for processed antigen class II complex assembly. Integral to such studies is the isolation and characterization of subcellular compartments in which key events in the assembly process occur. We have recently undertaken such studies in B lymphocytes which have processed antigen initially bound to the BCR.

Results and Discussion

Previous studies from this laboratory identified subcellular compartments in which class II molecules bind peptides [3]. Our particular focus was on the loading of class II

Table 1. *Subcellular compartments in the class II assembly pathway*[1].

Pooled Fractions:	1 - 4	5 - 10	11 - 12	13 - 15	16 - 19	20 - 22
EE	———					
LE	———	———				
PM		———				
ER		———				
GOLGI	———					
LYS						———
MITO		———				———
TGN TRANSPORT				———		
SDS-UNSTABLE	–	Θ	–	Θ	–	–
SDS-STABLE	–	Θ	–	–	–	Θ
Ii	–	Θ	–	Θ	–	–
HLA-DM	–	–	–	–	–	Θ
CLIP-Class II	–	–	–	–	–	Θ
PROCESSED Ag-CLASS II						
15 min	–	–	–	–	–	Θ
2 h	Θ		–	–	–	Θ
4 h	–	Θ	–	–	–	–
8 h	–	Θ	–	–	–	–
ANTIGEN-Ig						
0 min	–	Θ	–	–	–	–
30 min	Θ	Θ	–	–	–	Θ
1 h	–	Θ	–	–	–	Θ
2 h	–	–	–	–	–	Θ

[1] B cells were subjected to subcellular fractionation as described [3] and the subcellular fractions were assayed for a variety of enzymatic and serological markers which together define the early endosomes (EE), late endosomes (LE), plasma membrane (PM), endoplasmic reticulum (ER), Golgi apparatus (GOLGI), lysosomes (LYS), mitochondria (MITO), and trans Golgi network transport vesicles (TGN-transport). Fractions were assayed for SDS-stable class II molecules, invariant chain (Ii), HLA-DM, and CLIP-class II complexes. At various times after processing was initiated (15 min, 2 h, 4 h, 8 h), fractions were also assayed for the presence of functional processed antigen-class II complexes. The trafficking of antigen bound to the surface BCR, was followed in cells biotinylated to labeled surface Ig and incubated with ^{125}I-labeled Fab of anti-Ig, as an antigen. A - indicates no activity. A Θ indicates the activity was detected.

molecules with peptides derived from antigens initially bound to the BCR. B cells were incubated with antigen for various lengths of time and subjected to subcellular fractionation on Percoll density gradients. The gradient fractions were assayed for various enzymatic and serological markers identifying well characterized subcellular organelles. To identify peptide-loaded class II molecules, subcellular fractions were tested for the ability to stimulate an antigen-specific T cell hybrid *in vivo*. In addition, in separate experiments, class II molecules were immunoprecipitated from ^{35}S-labeled cells and assayed for the presence of SDS-stable class II heterodimers as an indication of

peptide-filled class II molecules. Alternatively, class II molecules were identified by Western blotting of subcellular fractions. The results are summarized in Table 1. We found that functional processed antigen-class II complexes capable of stimulating T cells were first formed in dense compartments which cosedimented with lysosomes and subsequently transported in endosomes to the plasma membrane. The presence of functional processed antigen-class II complexes correlated with the steady state levels of SDS-stable class II molecules, an indication of peptide-filled class II molecules. No Ii was detected in this compartment. HLA-DM, a molecule implicated in the loading of peptides onto class II [4] was present in this compartment, as were the CLIP-class II intermediates in the Ii-class II dissociation (Green, unpublished observation). Further experiments using inhibitors of Ii-class II dissociation showed that Ii-class II complexes were transported intact in vesicles which sediment in fractions 13-15 (Xu, unpublished observation). Upon entering the dense compartments, Ii is rapidly proteolytically removed from class II molecules and peptide is loaded.

We have also investigated the entry of antigen bound to the surface BCR into the peptide-loading compartment and found that the surface Ig normally trafficks to the dense compartments from the plasma membrane. The bivalent binding of antigen which cross-links the surface Ig increases the rate of transport of the Ig and antigen to the peptide loading compartment (Song, unpublished observations).

In summary, at present a reasonably detailed picture of the subcellular sites of antigen processing is emerging. The ability to isolate the compartments in which critical events in the pathway occur offers an important opportunity to explore the cellular machinery required for the degradation of antigen, the removal of Ii from class II molecules and the binding of the antigenic peptides to the class II molecules.

References

1. Germain, R.N., *Cell* 76 (1994) 287.
2. Cresswell, P., *Ann. Rev. Immunol.* 12 (1994) 259.
3. Qiu, Y., Xu, X., Wandinger-Ness, A., Dalke, D.P., and Pierce, S.K., *J. Cell Biol.* 125 (1994) 595.
4. DeMars, R. and Spies, T., *Trends in Cell Biol.* 2 (1992) 81.

Peptides: Chemistry, Structure and Biology
Pravin T.P. Kaumaya and Robert S. Hodges (Eds.)
Mayflower Scientific Ltd., 1996

318
Processing, Transport and MHC Restricted Presentation of Antigens Studied by Peptide Libraries

G. Jung[1,5], G. Niedermann[2], K. Eichmann[2], S. Uebel[1,3], R. Tampé[3], P. Walden[4], H.-G. Ihlenfeldt[1], W. Kraas[1], S. Kienle[5] and K.-H.Wiesmüller[5]

[1]Institute of Organic Chemistry, University of Tübingen, Germany
Max-Planck-Institutes for [2]Immunobiology, Freiburg, [3]Biochemistry, Martinsried, and [4]Biology, Tübingen, Germany
[5]Natural Science and Medicinal Institute at the University of Tübingen, D-72076 Tübingen, Germany

Introduction

The sequence motifs of peptide ligands binding to MHC class I and II molecules have been determined from isolated natural peptide libraries [1] for a large variety of HLA types using pool sequencing [2] and HPLC-MS. Independently from the analysis of natural peptide pools, the use of complex synthetic peptide libraries [3] in assays for MHC binding and for T cell recognition allows the exact determination of MHC restricted peptide motifs [4] and the construction of MHC blocker molecules. The self-nonself recognition mechanisms *via* MHC/peptide/T-cell receptors seem to be understood on the molecular level. Therefore the earlier steps in epitope selection, namely the processing of antigens [5] and the transport of peptide fragments [6] in the ER, is becoming a challenging field of research in immunochemistry. First, results concerning the immunodominance of epitopes and competition between peptides will be discussed. The contribution of proteasome mediated proteolysis to the hierarchy of epitopes and the involvement of the peptide transporters are selection principles prior to MHC binding as shown by our processing and binding studies using peptide libraries.

Results and Discussion

Self and foreign peptides presented at the surface of antigen presenting cells by MHC-class I molecules are distinguished by the receptor (TCR) of cytotoxic T-lymphocytes (CTL). These peptides originate from proteolytic cleavage of intracellular proteins and MHC I molecules are loaded with the peptides in the endoplasmatic reticulum (ER). Free peptides would be rapidly digested in the cytosol, therefore processed peptides are taken up by the heterodimeric, ATP-dependent peptide transporter protein (TAP 1 and 2) [6] immediately after proteasomal cleavage of a protein [5]. TAPs protect and transport peptides through the ER membrane to the nascent MHC I. After binding, the peptide-MHC I complex migrates to the outer

membrane. Thus, the selection and recognition processes *e.g.* for a viral CTL epitope include various contacts one after the other on proteasomes, TAP, MHC, and TCR. In addition, further events may take part such as ubiquitinylation of proteins prior to processing and binding of processed peptides to heat shock proteins (HSP 70) prior to transport and after TAP transport into the ER, they may bind to the glucose mediated chaperon gp 96 which is associated with MHC I.

It is not yet clear how all these proteins involved in processing, transport, and presentation of peptides act together in order to produce only very few highly defined CTL epitopes out of a very large number of potential epitopes within a viral protein. Little is known about the specificity of peptide selection especially for proteasomes and TAP.

Proteasome specificity. We have found experimental evidence for a major role of proteasomes in determining immunodominance of epitopes [5]. Two methods were used for localizing proteolytic cleavage sites of a dominant and a subdominant epitope within 22-peptides of ovalbumin. Firstly, controlled amounts of 22-peptides were introduced into the cytosol of target cells *via* pH-sensitive liposomes. The efficiency of MHC-restricted octapeptide presentation was determined by CTL assays specific for SIINFEKL (dominant CTL epitope) and KVVRFDKL (subdominant). Secondly, purified proteasomes were incubated with 22-peptides containing the minimized CTL epitopes and varied flanking regions. After 36h at 37 C, the digests were separated by HPLC and pool sequencing [2] was carried out. The parent substrates (*inter alia*) used for these experiments were the 22-peptides Ova Y51-71 (containing the subdominant K^b restricted epitope) and Ova Y249-269 (containing the dominant K^b restricted epitope). The latter was varied within the flanking regions by Gly and Pro replacements.

Ovalbumin Y51-71	YTQIN	KVVRFDKL	PGFGDSIEA
Ovalbumin Y249-269	YVSGLEQLE	SIINFEKL	TEWTS
Analogs	YGSGGGQGG	SIINFEKL	**PGGTG**
	YGSGGGQGG	SIINFEKL	TEWTS
	YVSGLEQLE	SIINFEKL	**P**EWTS

Consistent with the sequence motifs of naturally isolated self peptide pools of MHC I some specificity for cleavage after charged and hydrophobic residues was observed. 20S proteasomes cleave exactly the flanking regions at the N- and C-termini of the immunodominant Ova Y257-264 and destroy most of the subdominant Ova Y55-62 [5]. Thus, SIINFEKL is the major product of Ova Y257-264, whereas the predominant cleavage site of Ova Y51-71 is within the subdominant epitope. The introduction of proline or glycine at the flanking regions of the dominant CTL epitope results in inefficient processing of SIINFEKL, whereas introduction of the natural flanking regions from SIINFEKL into those of KVVRFDKL enhances processing of this subdominant epitope. Thus, inefficient processing may be one reason that subdominant epitopes although fitting to the allele-specific MHC binding motif are marginally generated and do not induce CTLs upon immunization with ovalbumin. However, subdominant epitopes may be excellent vaccine candidates. We have shown earlier that suitable lipopeptide immunogens carrying tripalmitoyl-S-glycerylcysteine induce long lasting memory CTLs against short peptides [7, 8].

Specificity of peptide transporters. Peptide libraries and a larger set of peptides of various lengths containing the core sequence RRYNASTEL (derived from the histone H3 CTL epitope RRYQKSTEL) were prepared as well as nonnatural substitution analogs. The peptides were used to investigate the binding specificity and transport capacity of the human TAP 1,2 complex reconstituted in insect cells [6]. As a reporter peptide in competition assays, we used iodine radiolabeled RRYNASTEL (affinity constant 310 ± 30 nM). Experimental evidence was found for stabilizing effects of N-terminal arginine and a hydrophobic C-terminus on peptide binding to TAP. However, no selectivity was observed within a range of 9-15 amino acids in length, the longest peptide decreased in affinity only 1,2-fold. Surprisingly the introduction of bulky β-[1-naphthyl]-L-alanine and ε-dansyl-lysine residues (originally designed for mapping label positions) strongly stabilize peptide binding in almost every position and ATP driven peptide translocation is still possible. Experiments with the random nonapeptide library X_9 compared to the sublibraries OX_8 clearly allowed the assignment of stabilizing and destabilizing residues in terms of Gibbs free enthalpy (ΔΔG).

References

1. Falk, K., Rötzschke, O., Stevanović, S., Jung, G. and Rammensee, H.-G., *Nature*, 351 (1991) 290.
2. Jung, G. and Stevanović, S., *Anal. Biochem.*, 212 (1993) 212.
3. Metzger, J.W., Kempter, C., Wiesmüller, K.-H. and Jung, G., *Anal. Biochem.*, 219 (1994) 261.
4. Udaka, K., Wiesmüller, K.-H., Kienle, S., Jung, G. and Walden P., *J. Exp. Med.*, 181 (1995) 2097.
5. Niedermann, G., Butz, S., Ihlenfeldt, H.-G., Grimm, R., Lucchiari, M., Hoschützky, H., Jung, G., Maier, B. and Eichmann, K., *Immunity*, 2 (1995) 289.
6. Uebel, S., Meyer, T., Kraas, W., Kienle, S., Wiesmüller, K.-H., Jung, G., and Tampé, R., *J. Biol. Chem.*, 31 (1995) 19512.
7. Deres, K., Schild, H.-J., Wiesmüller, K.-H., Jung, G., Rammensee, H.-G., *Nature*, 342 (1989) 561.
8. Schild, H., Norda, M., Deres, K., Falk, K., Rötzschke, O., Wiesmüller, K.-H., Jung, G., Rammensee, H.-G., *J. Exp. Med.*, 174 (1991) 1665.

Peptides: Chemistry, Structure and Biology
Pravin T.P. Kaumaya and Robert S. Hodges (Eds.)
Mayflower Scientific Ltd., 1996

319
Oral Tolerance as a Therapeutic Approach to Autoimmune Disease: Administration of Peptide Autoantigens

C.C. Whitacre, N.H. Javed, I.E. Gienapp and K.L. Cox

Department of Medical Microbiology and Immunology, College of Medicine, The Ohio State University, Columbus, OH 43210, USA

Introduction

Multiple sclerosis (MS) is a chronic demyelinating disease of the human central nervous system (CNS) which can be characterized clinically by a remitting-relapsing or a chronic progressive course. The perivascular infiltration of lymphoid and myeloid cells and concomitant demyelination has led to the theory that an autoimmune response against myelin antigens is involved in disease pathogenesis [1]. Perhaps the strongest evidence for an autoimmune reaction against myelin as a contributing factor in MS is the similarity between the clinical, histopathological and immunological features of MS and experimental autoimmune encephalomyelitis (EAE) in animals. Induced by a single injection of myelin basic protein (MBP) combined with complete Freund's adjuvant (CFA), EAE in the Lewis rat manifests clinically as a monophasic acute ascending paralysis, histopathologically by a quantifiable perivascular mononuclear cell infiltration in the CNS, and immunologically by the presence of cell-mediated and humoral antibody responses to MBP [2]. Recent interest in the treatment of EAE has focused on antigen-specific means of immunosuppression utilizing the oral administration of MBP [3, 4] and treatment with T cell receptor peptides [5,6].

We and others have reported that oral administration of MBP, derived from the guinea pig (GP), profoundly suppresses subsequently induced EAE in the Lewis rat by a mechanism of T cell anergy [7]. In contrast, the oral administration of the self antigen, rat MBP does not confer protection. In the present study, we have extended our investigation to determine the specificity of oral tolerance at the level of MBP synthetic peptides. We tested the tolerogenicity of the major encephalitogenic peptide 68-88 derived from guinea pig MBP and rat MBP, differing by a single amino acid, as well as the minor encephalitogenic MBP peptide 87-99. Our results indicate that the GP peptide 68-88 induced profound tolerance, whereas the rat peptide and peptide 87-99 did not.

Results and Discussion

We have previously reported that oral tolerance in EAE is specific for the fed antigen, extending to species specific determinants on the MBP molecule [3]. The encephalitogenic site on the MBP molecule responsible for causing EAE in the Lewis rat has been localized to the 68-88 region [8]. We examined the tolerogenicity and fine specificity of

synthetic peptide 68-88 derived from GP and rat MBP as well as the minor encephalitogenic peptide 87-99. The rat and GP 68-88 peptides differ by a single amino acid at position 80 (serine/threonine substitution) [9]. This particular residue has been proposed as a T cell receptor contact residue [10]. Our results show that animals fed 5 mg of GP 68-88, along with soybean trypsin inhibitor (STI) were protected from EAE induced with GP 68-88 or rat 68-88 compared with vehicle-fed control rats (Figure 1). The tolerance accompanying the oral administration of GP 68-88 was evidenced by suppression of clinical EAE, suppression of lymph node cell (LNC) proliferative responses, and marked reduction in IL-2 secretion in response to GP 68-88 and MBP antigens [11]. In contrast, feeding 5 mg of self peptide rat 68-88 or GP 87-99 with or without STI offered no protection (Figure 1). The LNC proliferative response to rat 68-88 was also suppressed in rats fed whole GP MBP or the rat peptide, irrespective of their clinical status [11]. Soybean trypsin inhibitor alone had no effect on EAE induction but peptides fed without STI were not protective, suggesting that STI presumably prevents the degradation of peptide in the gastrointestinal tract.

These findings of peptide specificity for oral tolerance confirm and extend our previous studies carried out at the whole MBP molecule level [3]. Such specificity suggests the contribution of a clonal anergy or deletional mechanism following oral administration of the major encephalitogenic epitope. The relative contribution of

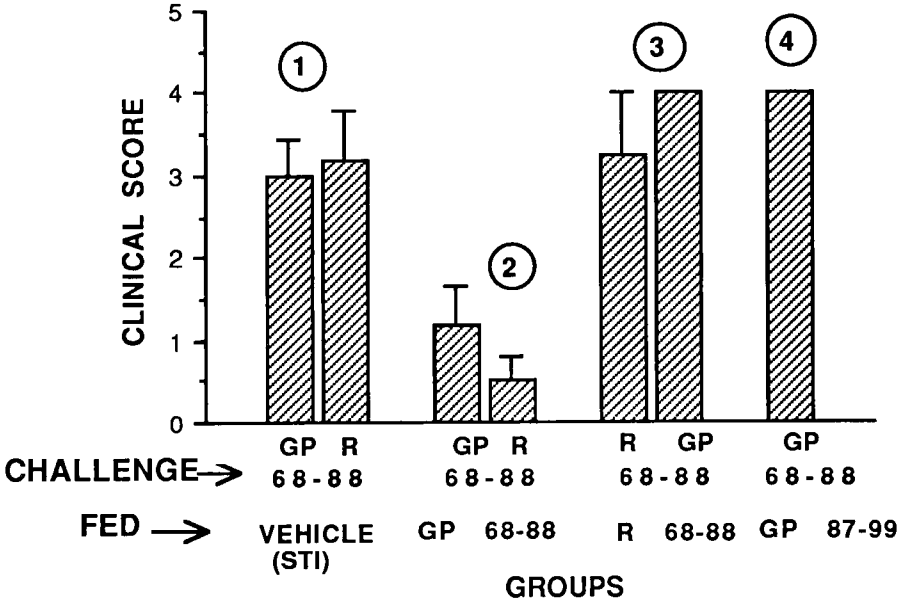

Figure 1. *Suppression of EAE clinical signs in female Lewis rats by the oral administration of guinea pig MBP 68-88 along with soybean trypsin inhibitor, but not rat 68-88 or GP 87-99. Values indicate mean maximum clinical score ± SEM. Numbers on each set of bars indicate the feeding groups. Results shown represent 5-6 rats per group from one experiment. This experiment was repeated 3 times with comparable results.*

anergy or other mechanisms to tolerance following oral administration of other peptide epitopes is not clear at present. The results of this study imply that: (1) tolerance to non-self MBP peptide GP 68-88 is occurring at the level of T-cell recognition; (2) GP 68-88 peptide which is encephalitogenic for the Lewis rat is able to confer profound tolerance when administered orally and that the tolerance achieved extends to the self peptide; (3) the presence of STI or an analogous protease inhibitor is essential for eliciting peptide induced oral tolerance. Thus, small structural differences at the single amino acid primary sequence level can produce dramatic differences in the clinical outcome following oral administration of peptides, with important implications for the design of human MS clinical trials.

Acknowledgments

The authors gratefully acknowledge the financial support provided by NIH grants NS23561, A135960, and National Multiple Sclerosis Society grants FG979 and RG2302.

References

1. McFarland, H.F., *Ann. N.Y. Acad. Sci.*, 540 (1988) 99.
2. Paterson, P.Y. and Swanborg, R.H., in Samter, M., Talmage, D.W., Frank, M.M., Austin, K.F. and Claman, H.N. (Eds.), 'Immunological Diseases', 4th ed, Little Brown & Co., Boston.
3. Bitar, D.M. and Whitacre, C.C., *Cell Immunol.* 112 (1988) 364.
4. Higgins, P.J. and Weiner, H.L., *J. Immunol,* 140 (1988) 440.
5. Vandenbark, A.A., Gill, T. and Offner, H.J., *J. Immunol,* 135 (1985) 223.
6. Howell, M.D., Winters, S.T., Olee, T., Powell, H.C., Carlo, D.J. and Brostoff, S.W., *Science*, 246 (1989) 668.
7. Whitacre, C.C., Bitar, D.M., Gienapp, I.E. and Orosz, C.G., *J. Immunol,* 147 (1991) 2155.
8. Chou, C.H.J., Chou, F.C.H., Kowalski, T.J., Shapira, R., Kibler, R.F., *J. NeuroChem.*, 28 (1977) 115.
9. Martensen, R.E., in Alvord, E.A., Kies, M.W. and Suckling, A.J. (Eds), 'Experimental Allergic Encephalomyelitis, A useful model for multiple sclerosis', Alan R. Liss, Inc., New York, NY, p. 511.
10. Mannie, M.D., Paterson, P.Y., U'Prichard, D.C. and Flouret, G., *J. Immunol,* 142 (1989) 2608.
11. Javed, N.H., Gienapp, I.E., Cox, K.L. and Whitacre, C.C., *J. Immunol,* 155 (1995) 1599.

Peptides: Chemistry, Structure and Biology
Pravin T.P. Kaumaya and Robert S. Hodges (Eds.)
Mayflower Scientific Ltd., 1996

320
Polyoxime Artificial Proteins as Vaccines

K. Rose[1], W. Zeng[1], M. Dragovic[1], L.E. Brown[2] and D.C. Jackson[2]

[1]*Medical Biochemistry, C.M.U., 1 rue Michel Servet, CH 1211, Geneva 4, Switzerland*
[2]*Dept. of Microbiology, University of Melbourne, Parkville 3052, Victoria, Australia*

Introduction

For vaccine and several other purposes (*e.g.* immunodiagnostics and therapy, gene therapy, enzyme engineering) it is desirable to construct macromolecular assemblies of high complexity yet of defined structure. In order to link the various components of such assemblies, it is necessary to use chemistry which is very mild and specific. Oxime chemistry [1] lends itself well to the assembly of constructions containing up to nine synthetic polypeptide chains. Native proteins may also be incorporated into these macromolecular assemblies of defined structure through appropriate site-specific chemical and enzymatic modification. We have already shown how, using oxime and thiol chemistry, it is possible to prepare a conjugate between an antibody fragment and the enzyme beta-lactamase [2], and we have described the synthesis of a $F(ab')_3$ trioxime of 152 kDa which shows much better tumor to non-tumor localization ratios than the clinical antibody from which it was derived [3]. In this communication, we show how oxime chemistry can be used to attach five copies of a synthetic peptide to a model native protein. A protein connected in this way could have a tissue targeting or particular immunostimulatory function, or simply be chosen to act as a source of T-helper epitopes.

Results and Discussion

The N-terminal Thr residue of a small model native protein was oxidized with periodate to a glyoxylyl function essentially according to Mikolajczyk *et al.*, [2] and reacted with a carrier molecule $NH_2OCH_2CO\text{-}Gly_3\text{-}[Lys(Ser)]_5\text{-}Gly\text{-}OH$ (Figure 1 steps 1 and 2) whose synthesis and properties have already been described [4]. The resulting mono-oxime protein-carrier conjugate was again oxidized with periodate to give the penta-aldehyde, which was reacted (Figure 1 steps 3 and 4) with an aminooxyacetylated synthetic influenza peptide $Ac\text{-}DC(SCH_2CH_2NHCOCH_2ONH_2)\text{-}TLIDALLGDPH\text{-}NH_2$ [5] leading to the formation of five further oxime bonds. The final hexa-oxime construction was characterized by reversed phase HPLC and electrospray ionization mass spectrometry (ESI-MS). It was found to be a single component as judged by reversed phase HPLC (Figure 2a) and to have the expected molecular weight as judged by ESI-MS (Figure 2b). About half of this weight is due to the native starting protein and about half is due to the five copies of synthetic peptide added to the structure. Techniques such as those described here permit the precision engineering of fairly complex macromolecular

NH_2-CHCO-rest-of-protein
HO-$CHCH_3$

Step 1 ↓ HIO_4

O=CHCO-rest-of-protein

Step 2 ↓ NH_2OCH_2CO-Gly$_3$-[Lys(Ser)]$_5$-Gly-OH

NOCH_2CO-Gly$_3$-[Lys(Ser)]$_5$-Gly-OH
‖
CHCO-rest-of-protein

Step 3 ↓ HIO_4

NOCH_2CO-Gly$_3$-[Lys(COCHO)]$_5$-Gly-OH
‖
CHCO-rest-of-protein

Step 4 ↓ NH_2OCH_2CO-peptide

NOCH_2CO-peptide
‖
NOCH_2CO-Gly$_3$-[Lys(COCH)]$_5$-Gly-OH
‖
CHCO-rest-of-protein

Figure 1. *Reaction scheme showing the four steps involved. Mild periodate treatment (Step 1) oxidizes the N-terminal aminoalcohol (Thr) to a glyoxylyl function, which forms an oxime bond with the carrier molecule (Step 2). Further periodate treatment (Step 3) oxidizes the aminoalcohol (Ser) residues of the carrier, which then react (Step 4) with the aminooxyacetylated peptide to give the final hexa-oxime construction.*

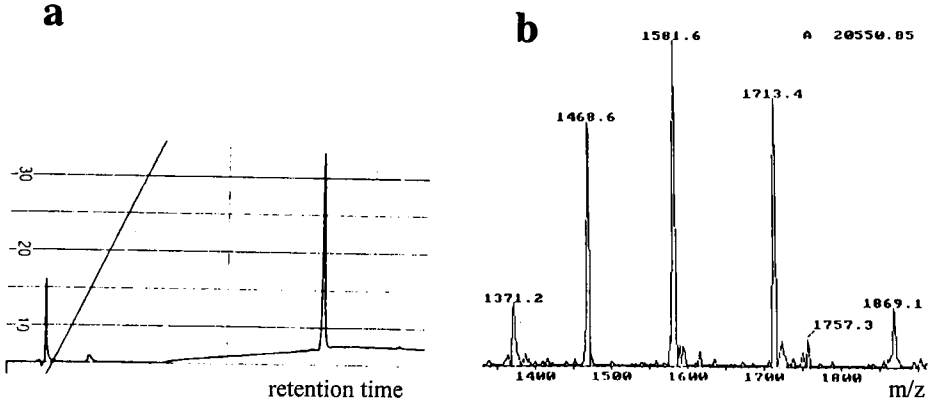

Figure 2. *(a) Analytical HPLC of purified hexa-oxime; (b) ESI-MS characterization: found 20550.85 +/- 5.54, calc. 20549.4.*

constructions for vaccine and other purposes. Synthetic polyoximes have recently been shown to elicit high titres of antibodies able to recognize native influenza virus and to stimulate, even at very low concentrations, proliferation of a peptide-specific T-cell clone [6].

Acknowledgments

We thank Mrs. Irène Rossitto-Borlat and Mr. Pierre-Olivier Regamey for expert technical assistance, and Gryphon Sciences Inc. for financial support.

References

1. Rose, K., *J. Am. Chem. Soc.* 116 (1994) 30-33.
2. Mikolajczyk, S.D., Meyer, D.L., Starling, J.S., Law, K.L., Rose, K., Dufour, B. and Offord, R.E., *Bioconj. Chem.* 5 (1994) 636-646.
3. Werlen, R.C., Lankinen, M., Offord, R.E., Schubiger, P.A., Smith, A. and Rose, K., *Cancer Res.*, 56 (1996) 809.
4. Vilaseca, L.-A., Rose, K., Werlen, R.C., Meunier, A., Offord, R.E., Nichols, C.L. and Scott, W.L., *Bioconj. Chem.* 4, (1993) 515-520.
5. Brown, L.E., White, D.O. and Jackson, D.C. (1993) *J. Virol.*, 67, 2887-2893.
6. Rose, K., Zeng, W., Brown, L.E. and Jackson, D.C., *Mol. Immunol.*, 32 (1995) 1031.

Peptides: Chemistry, Structure and Biology
Pravin T.P. Kaumaya and Robert S. Hodges (Eds.)
Mayflower Scientific Ltd., 1996

321

Positioning of Promiscuous T Cell Epitopes on a Single Matrix, Multicomponent Combination Vaccine In Elucidation of MHC-Unrestricted Responses

D. Woodbine[2,4], S. Conrad[2,4], A.M. DiGeorge[4] and P.T.P. Kaumaya[1,2,3,4,5]

[1]College of Medicine, [2]Comprehensive Cancer Center, [3]College of Biological Sciences, [4]Departments of Obstetrics and Gynecology, [5]Medical Biochemistry and Microbiology, The Ohio State University, Columbus, OH 43210, USA

Introduction

In our continuing work on the development of peptide models for vaccination, we have devised a single matrix, multicomponent strategy to incorporate fundamentally different B and T cell epitopes [1]. In such studies, we have demonstrated that template constructs containing different B and T epitopes were effective in eliciting enhanced immune responses [2], and able to bypass MHC restriction [3]. In the present study, we have designed and synthesized six additional peptides (see Table 1) with differential positioning to explore 1) the relationship between T and B epitopes within the single multicomponent matrix and 2) to further delineate the phemenon of MHC restriction in these constructs.

Results and Discussion

Peptide Synthesis and HPLC Purification. A combinatorial Fmoc/t-butyl, Fmoc/benzyl, Boc/benzyl approach as well as a fourth level of protecting group strategy (Npys) was used to synthesize the template constructs [3]. For synthesis of $(\alpha_N)1(TT)2$-X and $(\alpha_N)(TT)$-X, the C-terminal section of the template was synthesized using Boc protection of the α NH_2 of lysine and the amino terminal residue (Lys) bearing ε FMOC group. The first TT sequence was constructed using Fmoc/benzyl chemistry and the amino terminus of the TT sequence was capped by acetylation. After removal of the Boc group from the template strand, the next section of template was synthesized with Boc/-Lys(Fmoc) at the amino terminus. The second TT epitope was constructed using Fmoc/benzyl strategy. Peptides were cleaved by the low-high HF procedure and purified by semipreparative HPLC.

Immune Responses Groups of five mice each of three inbred strains (C3H/HeJ, BALB/c, C57BL/6) were immunized subcutaneously on the back and at the base of the tail as described previously [2]. The chimeric construct αNTT was immunogenic in all strains except BALB/c (Table 1). The $(\alpha N)_2$-$(TT)_2$-X which contained two copies of αN and

Table 1. *Antibody responses in mice to the various template constructs.*

Haplotypes Strains	H-2^b C57BL/6	H-2^k C3H/HeJ	H-2^d BALB/c	OUTBRED MICE
EPITOPE COMBINATION	TITERS vs NATIVE LDH-C_4 (No. Responders/No. Immunized)			
Chimeric				
αNTT	4000 (4/4)	12800 (5/5)	100 (0/5)	12800 (8/10)
dual B and T				
$(\alpha N)_2(TT)_2$-X	>51200 (5/5)	>51200 (5/5)	32000 (4/4)	>51200 (6/6)
one B & two T				
$(\alpha N)_1(TT)_2$-X	>12800 (4/4)	12800 (5/5)	12800 (5/5)	>12800 (9/9)
two B & one T				
$(\alpha N)_2(TT)_1$-X	12800 (4/5)	12800 (4/4)	12800 (5/5)	>12800 (8/8)
one B & one T				
$(\alpha N)_1(TT)_1$-X	1600 (5/5)	3200 (4/5)	3200 (2/5)	6400 (-)
one B & one T				
(αN)(TT)-X	400 (-)	400 (-)	800 (-)	(-) (-)
chimeric B and T				
αNTT Chimeric-X	>12800 (-)	1600 (-)	400 (-)	(-) (-)
one B no T				
αN-X	0 (-)	0 (-)	(-) (-)	(-) (-)

(-) not determined X Template

TT on a template was immunogenic in all strains. Thus, by assembling the B and T epitopes on a template, we were able to broaden the immune response in the strains tested. In order to further understand this phenomena, we synthesized as described above 6 additional template constructs. $(\alpha N)_1(TT)_2$-X containing only one copy of the B cell epitope was immuno- genic albeit with 4 fold lower titers. Similarly, $(\alpha N)_2$-$(TT)_1$-X with one T cell epitope was 4 fold less immunogenic suggesting that higher titers are obtained when 2 copies of either B or T are included. Interestingly, when the chimeric αNTT was assembled on the template, similar immunogenic profile compared to the chimeric αNTT was obtained. These results suggest that epitope orientation on the template construct is a unique phenomenon which may have important implication for vaccine design.

References

1. Kaumaya, P.T.P., Kobs-Conrad, S. and DiGeorge, A.M., in Epton, R. (Ed.), 'Innovation and Perspectives in Solid Phase Synthesis and Complementary Technologies', Mayflower Worldwide Ltd, Birmingham, 1994, p. 279.
2. Kobs-Conrad, S., Gerdau, A. and Kaumaya, P.T.P., in Smith, J.A. and Rivier, J. (Eds.), 'Peptides - Chemistry and Biology', 1992, p.886.
3. Lairmore, M.D., DiGeorge, A.M., Conrad, S.F., Trevino, A.V., Lal, R.B. and Kaumaya, P.T.P., *J. Virol.*, 69 (1995) 6077.

Peptides: Chemistry, Structure and Biology
Pravin T.P. Kaumaya and Robert S. Hodges (Eds.)
Mayflower Scientific Ltd., 1996

322
Constrained Synthetic Peptide Vaccines

A.C. Satterthwait[1], E. Cabezas[1], J.C. Calvo[1], J.X. Wu[1], P.L. Wang[1], S.Q. Chen[1], D.C. Kaslow[2], O. Livnah[1] and E.A. Stura[1]

[1]*Department of Molecular Biology, The Scripps Research Institute, La Jolla, CA 92037, USA*
[2]*N.I.A.I.D., N.I.H., Bethesda, MD 20892, USA*

Introduction

A critical issue involves the development of a strategy for identifying constrained synthetic peptide vaccines. We systematically vary the size and cadence of natural peptide sequences constrained with hydrogen bond mimics [1] while using neutralizing monoclonal antibodies to identify the best mimetic. Since every other amino acid in proteins engages in a hydrogen bond and most hydrogen bonds in proteins are localized, many potential conformations can be screened. Here we report on the use of this strategy for the identification of a constrained peptide corresponding to an epitope on Pfs25, a protein found on malaria sexual stages and recognized by a neutralizing monoclonal antibody, MAb 4B7 [2].

Results and Discussion

The epitope recognized by MAb 4B7, ILDTSNPVK, was initially mapped to a predicted β-hairpin loop on Pfs25 with overlapping peptides [3]. A series of loops varying in size (8-12 amino acids from the Pfs25 sequence) and cadence (overlap of one amino acid) was constrained with either a hydrazone covalent hydrogen bond mimic [1] or a disulfide link [4]. The hydrazone loops were synthesized and cyclized on the solid support using multiple cyclic peptide synthesis [1]. Each peptide was purified by HPLC and confirmed by FAB MS. Relative affinities for representative linear and loop peptides for MAb 4B7 were determined in ELISAs (Table 1). Hydrazone loop 1 and the disulfide loop bind MAb 4B7 with the highest affinities. Mouse polyclonal antisera raised against loop 1 but not the corresponding linear 1 bound and agglutinated *P. falciparum* malaria gametes [5]. Thus by constraining the peptide antigenicity and immunogenicity were significantly improved.

The high affinity loops, loop 1 and the disulfide loop, have been co- crystallized with MAb 4B7 [6]. X-ray crystal structures show that MAb 4B7 binds the tip of the loops, DTSNPVK, in similar conformations [7]. The NMR structure determinations of loop 1 and the disulfide loop in water show that the tips of both loops populate similar conformations to those bound by the antibody in the crystal structures [8].

Table 1. *Relative affinities of selected linear and loop peptides for MAb 4B7.*

Peptide	Sequence	Affinities
Linear 1	Ac-GILDTSNPVKTGGG-NH2	1
Hydrazone Loop 1	[JILDTSNPVKTGZ]G-NH2	32
Hydrazone Loop 2	[JILDTSNPVKTGGZ]G-NH2	4
Hydrazone Loop 3	[JCILDTSNPVKGZ]G-NH2	4
Hydrazone Loop 4	[JLDTSNPVKTGGZ]G-NH2	4
Hydrazone Loop 5	[JLDTSNPVKGZ]G-NH2	1
Disulfide Loop	Ac-[CILDTSNPVKC]-NH2	256

These results provide strong evidence that conformation plays an important role in antigenicity and immunogenicity. They underscore the subtle interplay of forces that lead to optimized mimetics. Link position in a natural sequence has a considerable effect on loop conformation. Both loop 5 and the disulfide loop include the recognized epitope but show a 256-fold difference in affinities for MAb 4B7. Addition of just one amino acid to Loop 1 yielding Loop 2 reduces affinity about 8-fold. Shifting the amino acid cadence within the optimal size class (Loops 1,3,4) reduces affinity 8-fold. NMR structure determinations for Loop 1 and the disulfide loop [8] show that the disulfide loop populates the MAb 4B7 bound conformer to a higher degree than the loop 1 as is reflected by the relative affinities. It would be difficult to predict these effects. MAbs provide important resources easily used to select optimized mimetics from series of loops that have been systematically varied in size and cadence. Importantly, Loop 1 displays enhanced immunogenicity [5]. A similar study on HIV peptides is reported [9].

Acknowledgments

This research was supported in part by Agency for International Development DPE-5979-A-00-1035-00. This is publication 9498-MB from The Scripps Research Institute.

References

1. Chiang, L.C., Cabezas, E., Calvo, J.C. and Satterthwait, A.C. in Hodges, R.S. and Smith, J.A.(Eds.) 'Peptides: Chemistry, Structure and Biology', ESCOM, Leiden, The Netherlands, 1994, p. 278.
2. Barr, P.J., Green, K.M., Gibson, H.I., Bathurst, I.C., Quakyi, I.A. and Kaslow, D.C., *J. Expt. Med.* 174 (1991) 1203.
3. Stura, E.A., Satterthwait, A.C., Calvo, J.C., Stefanko, R S., Langeveld, J.P. and Kaslow, D.C., *Acta Cryst.*, D50 (1994), 556.
4. Tam, J.P., Wu, C.R., Liu, W. and Zhang, J.W., *J. Am. Chem. Soc.*, 113 (1991), 6657.
5. Satterthwait, A.C., Cabezas, E., Calvo, J.C., Chen, S.Q., Wu J.X., Wang, P.L., Xie, Y.L., Stura, E.A. and Kaslow, D.C. in Lu, G.S., Tam, J.P and Du, Y.C. (Eds.) 'Peptides: Biology and Chemistry', ESCOM, Leiden, The Netherlands, 1995, p. 229.
6. Stura, E.A., Kang, A.S., Stefanko, R.S., Calvo, J.C., Kaslow, D.C. and Satterthwait, A.C., *Acta Cryst.*, D50 (1994), 535.
7. Livnah, O., Wang, P.L., Satterthwait, A.C. and Stura, E.A., unpublished work.
8. Cabezas, E., Wang, P.L. and Satterthwait, A.C., this volume.
9. Cabezas, E., Stanfield, R., Wilson, I. and Satterthwait, A.C., this volume.

Peptides: Chemistry, Structure and Biology
Pravin T.P. Kaumaya and Robert S. Hodges (Eds.)
Mayflower Scientific Ltd., 1996

323

Peptide Size and Affinity for MHC Determine the Selective Induction of TH1/TH2 Cells of Similar Antigen Specificity

P. Chaturvedi, Q. Yu, and B. Singh

Department of Microbiology and Immunology, University of Western Ontario, London, Ontario, N6A 5C1, Canada

Introduction

Based on the cytokine production T helper cells have been divided into two subsets: TH1 cells which secrete IL-2, IFN-γ and TNF-β while TH2 cells secrete IL-4, IL-5, IL-6 and IL-10 [1-4]. We show here that three strongly immunogenic peptides with overlapping sequences, K3, EYK$(EYA)_3$; K4, EYK$(EYA)_4$; and K1A2, EYKEYAAYA $(EYA)_2$, have different affinities for MHC. As determined by the cytokine profile, low affinity peptide K3 induced TH2 cells while the high affinity peptide K1A2 induced TH1 cells. K4 peptide with intermediate affinity induced both TH1 and TH2 cells. Therefore, we postulate that peptide size and its affinity for MHC control the induction of TH1 and/or TH2 cells of similar specificity *in vivo*.

Results and Discussion

We have reported earlier that K3, K4 and K1A2 peptides induce proliferative responses of different magnitude in BALB/c mice [5]. In direct binding assay to I-A^d , it was observed that K1A2 has relatively stronger affinity for I-A^d while K3 has weaker affinity. Peptide K4 has the affinity intermediate between K3 and K1A2 (Table1). K1A2 differs from K4 in having Ala at position 7 in place of Glu which seems to contribute to the I-A^d binding capacity of the K1A2 peptide. The small size of the K3 peptide seems to account for its lower affinity. The effect of affinity of the peptide on the activation of TH1 and TH2 cells was investigated. The lymph node cells from mice immunized with K3, K4 or K1A2 were cultured with either of the peptides and supernatants were assayed

Table 1. *Affinity of K3, K4 and K1A2 peptides for I-A^d.*

Peptide	Amino acid Sequence	[a]Inhibitory Concentration (IC50%, μM)
K3	E Y K E Y A E Y A E Y A	85.0
K4	E Y K E Y A E Y A E Y A E Y A	19.0
K1A2	E Y K E Y A A Y A E Y A E Y A	0.27

[a]Radiolabelled (^{125} I) ovalbumin peptide (323-339) and I-A^d was incubated as described before [6] with different concentrations of these peptides and the concentration of K3, K4 and K1A2 that was required for 50% inhibition of binding was measured.

for the presence of different cytokines. This showed that the peptide K1A2 with the highest affinity induces TH1 while K3 that has low affinity induces TH2 cells. K4 with intermediate affinity induces both TH1 and TH2 cells (Figure 1).

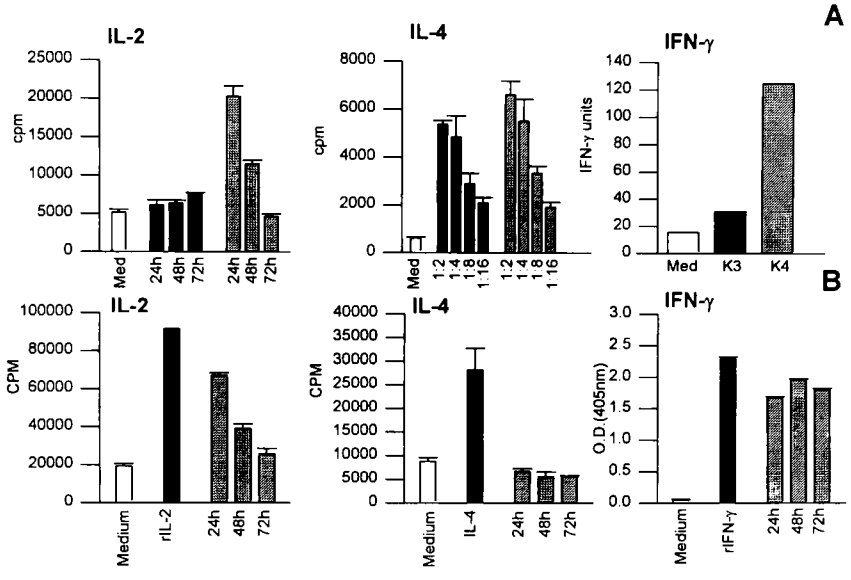

Figure 1. *Selective activation of TH1 and/or TH2 cells in response to K3, K4 and K1A2 peptides. BALB/c mice were immunized with 50μg of either of the peptide emulsified with CFA in hind foot pad. After ten days, lymph node cells were cultured with 50μg/ml of K3 (■) or K4 (▩) (1a) or K1A2 (1b). Supernatants were assayed for the presence of different cytokines as described [1].*

We postulate that affinity of the peptide is influenced by its size. Thus, a high affinity peptide forms more stable complex with MHC providing sufficient contact time for the activation of TH1 cells. On the other hand, low affinity peptides forming a less stable complex provide brief contact period sufficient for the activation of TH2 cells.

Acknowledgments

We thank Dr. A. Sette, Cytel, San Diego for the I-A^d binding studies.

References

1. Cherwinski, H.M., Schumacher, J.H., Brown, K.D. and Mosmann, T.R., *J. Exp. Med.*, 166 (1987) 1229.
2. Cher, D. and Mosmann, T., *J. Immunol.*, 138 (1987) 3688.
3. Killar, L., MacDonald, G., West, J., Woods, A. and Bottomly, K., *J. Immunol.*, 138 (1987) 1674.
4. Stevens, T.L., Bossie, A., Sanders, V.M., Fernandez-Botran, R., Coffman, R.L., Mosmann, T.R. and Vitetta, E.S., *Nature*, 334 (1988) 255.
5. Boyer, M., Novak, Z., Fotedar, A., Fraga, E. and Singh, B., *Eur. J. Immunol.*, 9 (1990) 2145.
6. Sette, A., Buus, S., Colon, S., Miles, C. and Grey, H.M., *J. Immunol.*, 142 (1989) 35.

Peptides: Chemistry, Structure and Biology
Pravin T.P. Kaumaya and Robert S. Hodges (Eds.)
Mayflower Scientific Ltd., 1996

324
T-Cell Interaction With Retro-Inverso Modified Peptides

J.P. Mayer[1], E. Sebzda[2], T. Zamborelli[1] and P.S. Ohashi[2]

[1]Amgen Boulder Inc., Boulder, CO 80301, USA
[2]The Ontario Cancer Institute, Toronto, Ontario, M5G 2M9, Canada

Introduction

The retro-inverso or retro-D modification involves the synthesis of a native sequence in reverse order using amino acids of opposite chirality. The surface presented by these analogs is topologically equivalent to the native surface while their backbone orientation is reversed [1]. In a therapeutic application, the enhanced proteolytic stability of these analogs may offer a significant advantage over native sequences [2]. The present study focuses on the ability of peptide specific T-cells to recognize a set of modified peptides. The model chosen for this study was the T-cell receptor transgenic mouse model (327 line) with specificity for the lymphocytic choriomeningitis virus glycoprotein peptide LCMV 33-41 presented by H-2D^b [3, 4]. We synthesized, in addition to the native 33-41 epitope (KAVYNFATM), the retro, the all-D, and retro-D versions of this peptide. These were tested at various concentrations in a T-cell proliferation assay.

Results and Discussion

The data from the T-cell study indicate only the retro-D analog as capable of inducing proliferation. Activity was observed in the micromolar range, which is several orders of magnitude higher than the concentration required for proliferation with the native sequence (Figure 1). Nevertheless, the ability of only the retro-D peptide to effect T-cell proliferation implies that overall topology or perhaps only several critical side chain contacts are essential for a proliferative response to occur. The lack of proliferation observed in the case of the all-D sequence indicates that a correct backbone configuration alone is insufficient to trigger a T-cell response even at high concentrations. An important consideration in interpreting these results is the role of the MHC and its ability to present modified peptides to a T-cell.

The negative results obtained with the retro and all-D analogs may reflect their inability to form a stable complex with the MHC molecule. The effect of retro, all-D, and retro-D modifications on MHC class II binding has been examined [5]. The resulting analogs had binding affinities in the low micromolar range but several orders of magnitude lower than the corresponding native peptides. In our study, the retro and all-D analogs failed to induce T-cell proliferation at similar concentrations. This data suggests that side chain topology is a key component of T-cell recognition.

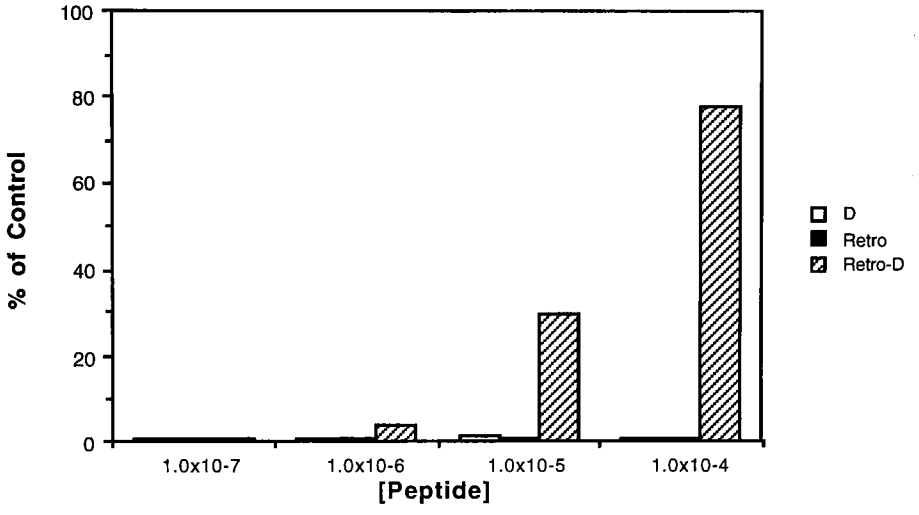

Figure 1. *T-cell proliferation assay.*

References

1. Chorev, M. and Goodman, M., *Acc. Chem. Res.*, 26 (1993) 266.
2. Jameson, B.A., McDonnell, J.M., Marini, J.C. and Korngold, R. *Nature,* 368 (1994) 744.
3. Pircher, H., Burki, K., Lang, R., Hengartner, Zinkernagel, R.M. *Nature,* 342, (1989), 559.
4. Sebzda, E., Wallace, V.A., Mayer, J.P., Yeung, R.S.M., Mak, T.W., Ohashi, P.S. *Science,* 263, (1994), 1615.
5. Hill, M.C., Liu, A., Marshall, K.W., Mayer, J.P., Jorgensen, B., Yuan, B., Cubbon, R., Nichols, E., Wicker, L. and Rothbard, J.B. *J. Immunol.*, 152, (1994) 2890.

Peptides: Chemistry, Structure and Biology
Pravin T.P. Kaumaya and Robert S. Hodges (Eds.)
Mayflower Scientific Ltd., 1996

325
An Investigation of the Relative Efficacy of Two Chimeric Synthetic Fimbrin Peptides as Immunogens Against Otitis Media in a Chinchilla Model

L.O. Bakaletz[1], P.T.P. Kaumaya[2], E. Leake[1], J. Billy[1] and D. Murwin[1]

College of Medicine, Departments of [1]Otolaryngology and [2]Obstetrics and Gynecology, The Ohio State University, Columbus, OH 43210, USA

Introduction

Fimbriae are one type of surface appendage expressed by nontypeable *Haemophilus influenzae* (NTHi) and are comprised of the subunit fimbrin [1, 2]. Fimbriae have been shown to be adhesins and a virulence factor for otitis media in chinchilla models of this major pediatric disease [2]. Toward the goal of developing a broadly protective vaccine against OM for use in an "outbred" pediatric population, we have identified and synthesized two peptides (LB1 and LB2) from areas of fimbrin protein predicted to be potentially immunoreactive domains based upon multiple algorithmic analyses. LB1 is a 19-mer representing Arg 117 to Gly 135 and LB2 is a 18-mer representing Tyr 163 to Thr 180 of fimbrin isolated from NTHi strain #1128 (Figure 1). Both have been co-linearly synthesized [3, 4] with a "promiscuous" T-cell epitope from the fusion protein of measles virus (MVF). In this study, we report the relative immunogenicity of LB1 and LB2 in rabbits and chinchillas; the ability of antisera directed against these chimeric peptides to recognize both denatured and native fimbrin protein as well as the ability of LB1 and LB2 to directly block bacterial adherence.

Results and Discussion

Synthetic chimeric fimbrin peptides LB1 and LB2 were found to be highly immunogenic in both rabbits and chinchillas (Table 1). Rabbit α-LB1 and α-LB2 and chinchilla α-LB2 also recognized denatured fimbrin of both a homologous and heterologous NTHi strain (#1128 and #86-028NP) *via* Western blot (not shown). Additionally, antisera generated against both LB1 and LB2 recognized native fimbriae expressed on the surface of whole bacterial cells *via* indirect immunogold labeling (not shown). LB1, but not LB2, directly inhibited adherence of NTHi to chinchilla tracheal mucosal epithelium in a dose-dependent manner (5% and 65% at 50 or 100 μg/ml, respectively).

In this study, we report the relative immunogenicity of two chimeric synthetic peptides of fimbrin, the subunit of one NTHi adhesin known as fimbriae. Their ability to induce high titered antibody in a chinchilla host which recognizes native protein,

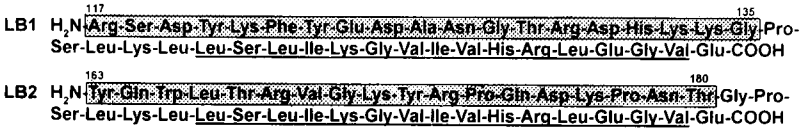

Figure 1. *Fimbrin peptides co-linearly synthesized with a "promiscuous" T-cell epitope. LB1 is a 19-mer representing fimbrin Arg117 to Gly135 and LB2 is an 18-mer representing fimbrin Tyr163 to Thr180 (shaded areas represent deduced fimbrin amino acid sequences). Both are linked via a 5 or 6 residue peptide to a "promiscuous" T-cell epitope from the fusion protein of measles virus (MVF seq 208-302, underlined).*

Table 1. *Titers induced in rabbits and chinchillas by chimeric synthetic fimbrin peptides versus synthetic peptides and fimbrial protein.*

Antigen	Host species	Reciprocal Titer* against		
		LB1	LB2	NTHi # 1128 fimbrial protein
LB1	Rabbit	200,000	10,000	10,000
LB2	Rabbit	50,000	100,000	10,000
LB1	Chinchilla	50,000	5,000	15,000
LB2	Chinchilla	1,000	50,000	10,000

* Pre-immune sera titers for all animals *versus* each of the three listed antigens was < 1:100.

indicates the potential for their use as immunogens against nasopharyngeal colonization by NTHi, the very first step in the disease course of otitis media. Efficacy studies using LB1 and LB2 as immunogens against nasopharyngeal colonization and otitis media in a chinchilla model are continuing.

Acknowledgments

This study is supported by funds from the Department of Otolaryngology and, in part, by a grant from NIDCD/NIH #DC00090.

References

1. Bakaletz, L.O., Tallan, B.M., Hoepf, T., DeMaria, T.F., Birck, H.G. and Lim, D.J., *Infect Immun.*, 56 (1988) 331.
2. Sirakova, T., Kolattukudy, P.E., Murwin, D., Billy, J., Leake, E., Lim, D.J., DeMaria, T.F., Bakaletz, L.O., *Infect Immun.*, 62 (1994) 2002.
3. Kaumaya, P.T.P., Berndt, K., Heindorn, D., Trewhella, J., Kezdy, F.J., and Goldberg, E., *Biochem.*, 29 (1990) 13.
4. Kaumaya, P.T.P., VanBuskirk, A.M., Goldberg, E. and Pierce, S.K., *J. Biol. Chem.*, 267 (1992) 6338.

Peptides: Chemistry, Structure and Biology
Pravin T.P. Kaumaya and Robert S. Hodges (Eds.)
Mayflower Scientific Ltd., 1996

326

SPC3, Synthetic Peptide Derived from the V3 Domain of HIV-1 gp120, Inhibits HIV-1 Entry into $CD4^+$ and $CD4^-$ Cells by Two Distinct Mechanisms

N. Yahi[1], J. Fantini[1], S. Baghdiguian[2], K. Mabrouk[1], C. Tamalet[3], H. Rochat[1], J. Van Rietschoten[1] and J-M. Sabatier[1]

[1]CNRS URA 1455, Laboratoire d'Ingéniérie des Protéines, Faculté de Médecine Nord, Bd Pierre Dramard, 13916 Marseille Cédex 20, France
[2]Laboratoire de Pathologie Comparée, CNRS-INRA URA 1184, Université Montpellier 2, 34095 Montpellier, France
[3]Laboratoire de Virologie, CHU la Timone, 13005 Marseille, France

Introduction

The third variable region of human immunodeficiency virus type 1 (HIV-1) surface envelope glycoprotein gp120 (V3 loop) plays a key role in HIV-1 infection and pathogenesis. This region contains the principal neutralization domain of HIV-1 gp120, and anti-V3 antibodies block HIV-1induced cell fusion. The V3 loop is involved in the post-binding events necessary for viral entry into $CD4^+$ cells. In addition, HIV-1 can infect some $CD4^-$ cells, suggesting the existence of alternative receptors. One such receptor, the glycosphingolipid galactosyl-ceramide (GalCer), has been identified in neural and intestinal epithelial cells. The infection of $CD4^-$/$GalCer^+$ colonic HT-29 cells can be blocked by anti-V3 antibodies which also inhibit binding of HIV-1 gp120 to GalCer. The V3 loop is directly involved in the binding of HIV-1 to the GalCer receptor.

Recently, we reported that a synthetic multibranched peptide (SPC3) containing eight V3 loop consensus motifs GPGRAF inhibited HIV-1 infection in both $CD4^+$ and $CD4^-$ cells [1]. This synthetic polymeric construction displays eight GPGRAF motifs radially branched on an uncharged poly-Lys core matrix. This peptide is a potent inhibitor of HIV-1 infection in human lymphocytes and macrophages [2] as well as in $CD4^-$ human colon epithelial cells. In the present communication, we show that SPC3 affects HIV-1 infection by two distinct mechanisms: i) prevention of GalCer-mediated HIV-1 attachment to the surface of $CD4^-$/$GalCer^+$ cells, and ii) postbinding inhibition of HIV-1 entry into $CD4^+$ lymphocytes.

Results and Discussion

Anti-HIV Activity of SPC3 in $CD4^+$ Lymphocytes. CEM cells exposed to HIV-1(LAI) for 1 hr were treated before, during and/or after viral exposure with 10 μM SPC3. Pretreatment of the cells with SPC3 did not result in an inhibition of infection.

Similar data were obtained when the peptide was present during the infection phase in competition with the virus. In contrast, a marked inhibition of HIV-1 production was observed when the cells were first exposed to HIV-1 for 1 hr and subsequently cultured in the presence of SPC3 during 7 days. This SPC3-induced antiviral effect could reflect an inhibition of infection and/or a blockade of HIV-1 expression. The latter is however unlikely since SPC3 did not affect the production of p24 by HIV-1 infected CEM-8E5 cells. Moreover, using an infectious center end point assay, we could estimate that less than 1 cell per 100,000 was infected by HIV-1 in SPC3-treated cultures versus 1 to 5 cells per 10 in untreated cultures. Thus, the antiviral activity of SPC3 corresponds to an inhibition of HIV-1 infection. Interestingly, it was not necessary to keep SPC3 in the culture medium throughout the experiment, since a minimal treatment of 2 hr after HIV-1 exposure was sufficient to inhibit infection. RIPA analysis of metabolically labelled CEM cells exposed to HIV-1 and treated or untreated with SPC3 indicated clearly that SPC3 does not affect the biosynthesis of the cellular proteins but only that of HIV-1 proteins. Ultrastructural analysis of CEM cells showed that SPC3 did not alter the morphology of these cells and that the antiviral activity of SPC3 could not be related to cellular toxicity. Binding test by the ELISA gp120-capture assay with CD4-coated plates showed that, at concentrations up to 100 μM, the peptide did not affect the interaction between gp120 and its binding site on the CDR2 domain of CD4.

AntiHIV Activity of SPC3 in $CD4^-/GalCer^+$ Cells. The mechanism of action of SPC3 was analyzed in $CD4^-/GalCer^+$ HT-29 cells. When SPC3 was added in competition with HIV-1(NDK), a marked inhibition of infection was observed. In remarkable contrast with the results obtained with $CD4^+$ lymphocytes, SPC3 had no effect on the infection of HT-29 cells when added after the initial contact with the virus: the presence of SPC3 during the whole phase of viral exposure was necessary to obtain an inhibition of infection. The binding of gp120 to GalCer on HPTLC plates was strongly inhibited by SPC3, but not by control peptides that do not inhibit HIV-1 infection of HT-29 cells.

Inasmuch as SPC3 mimicks a biologically active form of the V3 loop, the different facets of its antiviral activity could be related to: i) the involvement of the V3 loop in the interaction between gp120 and GalCer on the surface of $CD4^-/GalCer^+$ cells, and ii) the role of the V3 loop in the post-binding events which follow HIV-1 attachment to $CD4^+$ cells leading to virus fusion (3). In the latter case, it is likely that the V3 loop interacts with an accessory binding site necessary for the fusion to proceed. The nature of such a coreceptor has remained elusive. Due to the ability of the V3 loop to recognize GalCer, one should consider the possibility of a glycolipidic coreceptor allowing HIV-1 entry into $CD4^+$ lymphocytes.

References

1. Fantini, J., Yahi, N., Mabrouk, K., Van Rietschoten, J., Rochat, H. and Sabatier, J-M. *C. R. Acad. Sci. (Paris)*, 316 (1993) 1381.
2. Yahi, N., Fantini, J., Mabrouk, K., Tamalet, C., De Micco, P., Van Rietschoten, J., Rochat, H. & Sabatier, J-M., *J. Virol.*, 68 (1994) 5714.
3. Yahi, N., Fantini, J., Baghdiguian, S., Mabrouk, K., Tamalet, C., Rochat, H., Van Rietschoten, J., and Sabatier, J-M., *Proc. Natl. Acad. Sci., USA*, 92 (1995) 4867.

Peptides: Chemistry, Structure and Biology
Pravin T.P. Kaumaya and Robert S. Hodges (Eds.)
Mayflower Scientific Ltd., 1996

327

Cyclic Peptides Containing PEG in the Ring Structure Form Stable Complexes with Class I MHC Molecules

M. Bouvier[1] and D.C. Wiley[1,2]

[1]Department of Molecular and Cellular Biology and [2]Howard Hughes Medical Institute, Harvard University, Cambridge, MA 02138 USA

Introduction

Recognition of antigenic peptides bound in the groove of class I MHC molecules by receptors on $CD8^+$ T cells triggers cellular immune responses. This recognition event is critical to the process that leads to autoimmune diseases. Structural and functional studies have shown that several residues from the central portion of the peptide and from the α_1- and α_2-helices of MHC molecules were involved in this recognition. For the purpose of studying inhibition of T cell activation and the immunogenicity of class I MHC complexes, we have designed and synthesized *de novo* cyclic peptides that incorporate PEG in the ring structure.

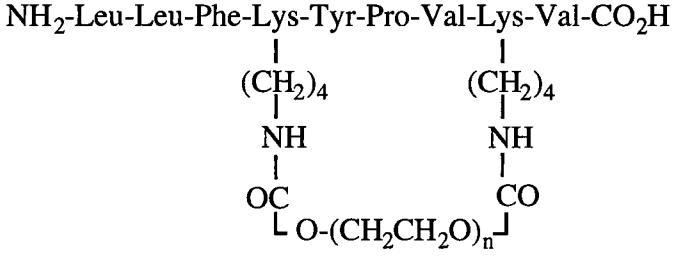

Results and Discussion

Design of cyclic peptides based on Tax peptide (LLFGYPVYV) was guided from knowledge of the conformation of several nonamers bound in the groove of HLA-A2 [1]. Peptide side chains at positions 4 and 8 are generally shown pointing up and therefore are ideal sites for the substitution of lysine residues. High molecular weight PEG dicarboxylic acids were used to link covalently the side chains of lysine residues resulting in large ring structures that include all residues predicted to contact the TCR. The excellent water solubility of the repeating oxyethylene group favors extension of PEG loops out of the binding site and toward TCRs. Functionalization of PEGs into PEG dicarboxylic acids was achieved as reported for monomethoxyPEG [2]. Starting materials of different average molecular weights were used; PEG 300, PEG 400, and PEG 600, which correspond to an average number of repeating oxyethylene unit (n

value) of 6.4, 8.7, and 13.2, respectively. Tax peptide was synthesized on HMP resin using Fmoc amino acids, Boc amino acid for the last residue, and 1-(4,4-dimethyl-2,6-dioxocyclohex-1-ylidene)ethyl (Dde) protecting groups for the side chains of lysine residues engaged in ring closure. Selective cleavage of Dde groups was achieved quantitatively with 1% hydrazine hydrate in NMP followed by cyclization of the liberated lysine side chains *via* PEG dicarboxylic acids. In this novel cyclization strategy, ring formation occurs on the support in a single step using a symmetrical homobifunctional spacer. The symmetrical nature of PEG molecules ensures that structurally homogeneous cyclic peptides are obtained. The cyclization reactions proceeded in DCM:DMF (1:9) using BOP and was complete after 24 hours. Final deprotection and cleavage of the peptide from the support was done with 95% TFA to afford desired cyclic peptides (Tax 300, Tax 400, and Tax 600) with ring size varying between about 44 and 65 atoms. Crude cyclic peptides were purified by RP-HPLC and eluted either as sharp (Tax 300 and Tax 400) or broad (Tax 600) peaks. In all cyclization reactions studied, the desired cyclomonomers were the major product with no evidence for formation of cyclodimers as analyzed by RP-HPLC. Peptide composition was confirmed by amino acid analysis and the presence of PEG was demonstrated by FABMS.

HLA-A2 complexes were reconstituted from *E. coli*-expressed human heavy chain and β_2m in the presence of excess cyclic peptides and purified by gel filtration chromatography [3]. All cyclic peptides promoted assembly of class I MHC complexes. FABMS analysis of purified complexes revealed the expected series of $[M + H]^+$ peptide ions confirming the association of cyclic peptides with HLA-A2. Thermal denaturation studies experiments were done to determine the effect of the peptide ring structure on the stability of complexes. Denaturation curves were obtained by monitoring the change in CD signal at 218 nm as a function of temperature [4]. Results showed that melting temperatures (T_m's) for HLA-A2 complexed with cyclic peptides are similar and range between 70.7°C (Tax 300) and 72.1°C (Tax 600), suggesting stabilization is essentially independent of the particular size of the peptide ring structure. Results also showed that the stability of these complexes is comparable with that of HLA-A2 complexed with Tax mutant peptide (LLFK (Ac)YPVK(Ac)V) (T_m = 68.9°C). Since measurement of melting temperatures by CD has been shown to correlate with peptide binding affinity for class I MHC complexes [4], these results suggest that cyclic peptides and Tax mutant peptide adopt similar bound conformations. These preliminary results show that PEG loops have no destabilizing effect on the structure of class I MHC complexes.

Acknowledgments

MB is supported by a Cancer Research Institute/F.M. Kirby Foundation Fellowship and DCW is an Investigator of the Howard Hughes Medical Institute.

References

1. Madden, D.R., Garboczi, D.N. and Wiley, D.C., *Cell,* 75 (1993) 693.
2. Gehrhardt, H. and Mutter, M., *Polym. Bull.,* 18 (1987) 487.
3. Garboczi, D.N., Hung, D.T. and Wiley D.C., *Proc. Natl. Acad. Sci. USA,* 89 (1992) 3429.

Peptides: Chemistry, Structure and Biology
Pravin T.P. Kaumaya and Robert S. Hodges (Eds.)
Mayflower Scientific Ltd., 1996

328
A Multi-dimensional Approach for the Isolation and Characterization of Antigenic Peptides

K.P. Williams[1], F. Hsieh[1], M. Petersson[2], D.M. Evans[1], F. Regnier[1], S. Martin[1], R. Kiessling[2] and S. Jindal[1]

[1]PerSeptive Biosystems Inc., Framingham, MA 01701, USA
[2]Microbiology and Tumorbiology Center, Karolinska Institute, Stockholm, S-171 77, Sweden

Introduction

The identification of the epitopes recognized by T lymphocytes in tumor development, infection, and autoimmune disease is of great interest for the development of immunotherapeutics, diagnostics, and vaccines [1]. Cytotoxic T lymphocytes (CTL) recognize the peptides presented by MHC class I on the cell surface. Recently it has become possible to analyze these naturally processed peptides directly [2, 3]. A typical strategy involves the elution of peptide material from MHC class I molecules isolated by immunoaffinity capture. The eluted material can be Edman sequenced directly - "pooled sequencing", or the peptides can be separated by a series of reversed-phase chromatographic steps, with subsequent sequencing by MS/MS [4]. At all stages of the peptide isolation procedure, peptides can be assessed for their ability to elicit a T cell response in a CTL assay. However, there are drawbacks to this approach. These multiple manual manipulations of small samples are slow, characteristically result in poor sample recovery, increased probability of contamination, and are poorly suited to analyze large numbers of samples.

In addition to MHC molecules, it has recently been postulated that heat shock proteins (Hsp) such as Hsp70 and Hsp90 by virtue of their ability to bind peptides may also play a role in antigen processing/presentation [5] possibly by chaperoning peptides to MHC or to the cell surface directly.

Results and Discussion

An objective of this research is to develop systems that can both isolate and characterize antigenic peptides in which manual transfer steps were eliminated. A multi-valved apparatus (Integral™ workstation) which allows automated, directed transfer of analyte between the various unit operations was used with an optional interface into an electrospray triple quadropole mass spectrometer.

We focused on characterizing peptides associated with MHC class I, and Hsp70 and Hsp60, after isolation from a tumor. Two mouse lymphoma tumors were used for these studies, RMA and MC57X. Lymphoma tissue was homogenized and lysates prepared as

previously described [6]. MHC class I and Hsp60 were isolated by immunoaffinity capture on specific MAb columns, and Hsc70 was isolated by a combination of IEC and HIC.

For these proteins, bound peptides were resolved after acid elution onto a series of RP columns. MHC class I peptides were assayed at each stage for T cell responses using anti-tumor CTL s. Peptide(s) present in each fraction off RP columns were collected and analyzed by mass spectrometry, either by ESI/MS/MS or by MALDI-TOF MS. A representative delayed extraction MALDI-TOF mass spectrum [7] of a tumor-derived RP peptide fraction positive in CTL assay is shown in Figure 1.

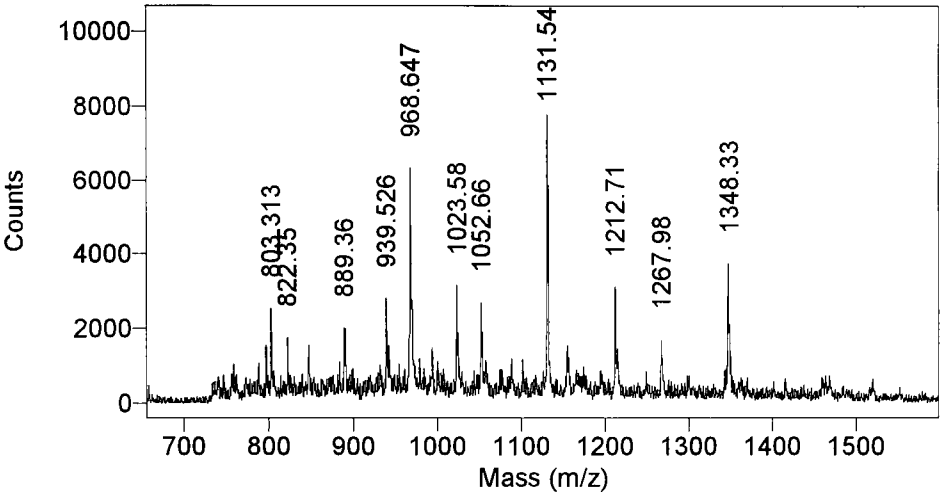

Figure 1. *Delayed extraction MALDI-TOF mass spectrum of tumor-derived peptides.*

References

1. Slinglhuff, C.L., Hunt, D.F. and Engelhard, V.H., *Curr. Opin. Immunol.*, 6 (1994) 733.
2. Englehard, V.H., *Curr. Opin. Immunol.*, 6 (1994) 13.
3. Cox, A.I., Skipper, J., Chen, Y., Henderson, R.A., Darrow T.L., Shabanowitz J., Engelhard, V.H., Hunt, D.F. and Slingluff, C.L., *Science*, 264 (1994) 716.
4. Engelhard, V.H., Appella, E., Benjamin, D.C., Bodnar, W.M., Cox, A.I.,., Chen, Y., Henderson, R.A., Huczko, E.L., Michel, H., Sakaguichi, K., Shabanowitz J., Sevilir, N., Slingluff, C.L and Hunt, D.F. in Sette, A. (Ed.) 'Chemical Immunology', Vol. 57, Karger, Basel, Switzerland, 1993. p.39.
5. Srivastava, P.K., Udono, H., Blachere, N.E. and Li, Z., *Immunogenetics,* 39 (1994) 93.
6. Franksson, L., Petersson, M., Kiessling R. and Karre K., *Eur. J. Immunol.*, 23 (1993) 2606.
7. Vestal, M., Juhasz, P. and Martin S., *Rapid. Commun. Mass Spectrom.*, 9 (1995) 1044.

Peptides: Chemistry, Structure and Biology
Pravin T.P. Kaumaya and Robert S. Hodges (Eds.)
Mayflower Scientific Ltd., 1996

329

Serum Amyloid A (SAA) and Corresponding Peptides Inhibit T-Cell Adhesion to Laminin and Bind to Human Neutrophils

L. Preciado-Patt and M. Fridkin

Department of Organic Chemistry, The Weizmann Institute of Science, Rehovot 7100, Israel

Introduction

Serum amyloid A (hSAA) is a normal human serum apolipoprotein component which exists in the body in complex with high density lipoprotein 3 (HDL_3) [1]. It is synthesized mainly in the liver in acute phase situations, chronic inflammation and neoplastic diseases [2]. Elevated amounts of hSAA are rapidly incorporated into HDL_3 while displacing Apo AI, suggesting that SAA might alter normal cholesterol metabolism [3]. Although acute phase roles for SAA have not been determined, several different functions have been suggested. SAA is proteolyzed by lysosomal enzymes originating from human polymorphonuclear leukocytes (PMN) [4, 5]. Peptides NYIGSDKYF (SAA 28-36) and GLPEKY (SAA 99-104), were identified among other proteolytic fragments. The former peptide is related to the cell binding domain (YIGSR) of laminin, an extracellular-matrix protein that plays an important role in immune-cell migration from blood vessels to inflammatory reaction sites [6]. SAA-related peptides corresponding to the 28-36 domain were capable of inhibiting the adhesion of human T-lymphocytes to laminin coated surfaces. These results suggest that SAA-derived peptides might play an important role in modulation of the inflammatory response. Adhesion of polymorphonuclear neutrophils to endothelial cells is a crucial step in the inflammatory reaction. It is conceivable that SAA and some of its fragments may effect this process.

Results and Discussion

The peptide SAA28-36 was isolated from digest of hSAA by lysosomal fraction of human neutrophils, and together with synthetic peptides related to the SAA28-40, was found capable to inhibit T-lymphocytes adhesion to laminin coated surfaces (Figure 1). In order to characterize quantitatively the binding of SAA to human PMNs, self-displacement experiments employing ^{125}I-rSAA were performed and a dissociation constant (Kd) of 7.11 x 10^{-8}M was determined. Competition assays with synthetic peptides related to SAA, revealed that the peptide SAA77-104 corresponding to the C-terminal domain inhibits the binding of ^{125}I-SAA to human PMNs. That peptide might exist in sera of patients who experienced amyloid deposition (*i.e.* AA 1-76) in various tissues. The C-terminal peptides SAA98-104 and SAA99-104 as well as the peptide

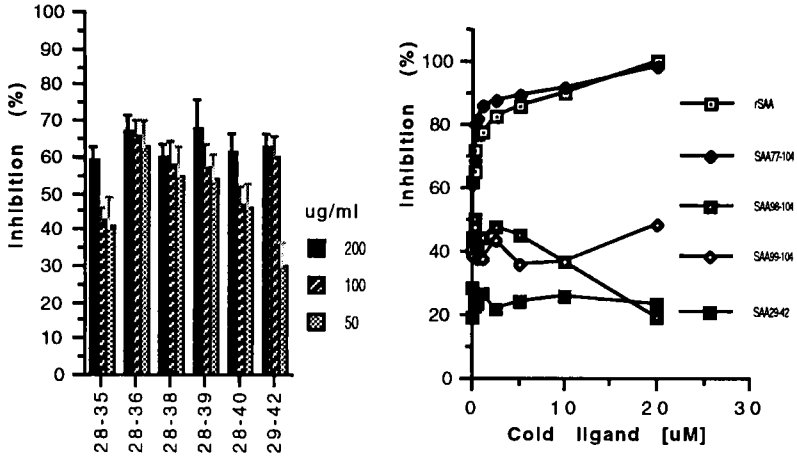

Figure 1. (left) *Adhesion of T-lymphocytes to laminin is inhibited in the presence of various concentrations of peptides related to the 28-40 sequence of rSAA. The peptide 29-42 was used as positive control [4].*

Figure 2. (right) *Inhibition of ^{125}I-rSAA binding to human PMNs by peptides from the C-terminal and the extra-cellular matrix domains of SAA. Mean values of five different experiments are shown.*

corresponding to the extracellular-matrix proteins domain SAA29-42, did not compete with ^{125}I-SAA binding (Figure 2).

The results of the present study reveal that SAA can specifically bind to human neutrophils. The binding constant is in the nM-range with about 10^5 binding sites/cell. SAA77-104 inhibited substantially the binding of ^{125}Ir-SAA. As mentioned, a massive proteolysis of SAA by neutrophilic enzymes yielded peptides capable of modulating adhesion of human T-lymphocytes to extracellular matrix proteins. Intact SAA may as well modulate adhesion. It is tempting to suggest that SAA is involved in mechanisms of adherance of neutrophils to endothelial cells. Thus, the migration of neutrophils through endothelial cells barriers from circulation to inflammatory loci is modulated by SAA.

References

1. Beneditt, E.P. and Eriksen, N., *Proc. Natl. Acad. Sci. USA*, 74 (1977) 4025.
2. Gorevic, P.D., Rosenthal, C.J. and Franklin, E.C., *Clin. Immunol. Immunopathol.*, 6 (1976) 83.
3. Whitehead, A.S., deBeer, M.C., Steel, D.M., *J. Biol. Chem.*, 267 (1992) 3862.
4. PreciadoPatt, L., Levartowski, D., Prass, M., Hershkovitz, R., Lider, O. and Fridkin, M., *Eur. J. Biochem.*, 223 (1994) 35.
5. Silverman, S.L., Cathcard, E.S., Skinner, M. and Cohen, A.S., *J. Immunol.*, 46 (1982) 737.
6. Iwamoto, Y., Robey, F.A., Graft, J., Susuki, F.A., Kleinman, H.K., Yamada, Y. and Martin, G.R., *Science*, 238 (1982) 1132.

Peptides: Chemistry, Structure and Biology
Pravin T.P. Kaumaya and Robert S. Hodges (Eds.)
Mayflower Scientific Ltd., 1996

330
A Synthetic Peptide-based Candidate Vaccine Against Rubella Virus

P. Chong[1], S. Gillam[2], S-P. Shi[1], A. Olivier[1] and M. Klein[1]

[1]Connaught Centre for Biotechnology Research, North York, Ontario, M2R 3T4, Canada
[2]The Childrens' Variety Research Centre, Univ. of British Columbia, Vancouver, British Columbia, V5Z 4H4, Canada

Introduction

Several live attenuated rubella vaccines have been introduced since 1969, but there are still medical concerns regarding routine immunization [1, 2]. These concerns include the risk of congenital infection of the fetus resulting in diabetes-related diseases and rubella-associated arthritis following rubella vaccination, as well as the possibility of re-infection of vaccinees by wild-type RV due to antigenic differences between wild-type and vaccine virus strains. In addition to these problems, rubella virus grows to a relatively low titer in tissue cultures and its structural proteins are difficult to purify. Therefore, there is a clear requirement for preparing a non-infectious rubella vaccine.

To design a synthetic peptide-based rubella vaccine, the RV-specific CTL determinants, the neutralization B-cell epitopes (BE) and the functional T-helper epitopes of individual viral proteins must be identified. Twenty-three, 15, and 11 overlapping peptides covering most of the E1, E2, and C protein sequences, respectively, were synthesized and used for human T-cell epitope mapping [3]. The objective of the present study was to determine whether a novel synthetic rubella vaccine candidate can be developed using a peptide corresponding to residues 190 to 243 of E1 which contains virus neutralization epitopes and three distinct human T-cell epitopes [3, 4].

Results and Discussion

To evaluate the immunogenicity of the synthetic RV vaccine candidates, a full length peptide (RV-EP27), containing residues 198-240 of the E1 protein, and several truncated peptides were designed (Table 1), synthesized, purified, and biochemically characterized. A hundred micrograms of individual linear peptides emulisifed in complete Fruend's adjuvant (CFA) were used to immunize guinea pigs intramuscularly. After two booster doses, IgG antibody responses were tested by peptide-specific ELISAs and immunoblotting against RV. All antisera reacted specifically with the immunizing peptide, and also recognized the E1 protein in immunoblots. The immunological properties of each antiserum were further characterized using haemagglutination inhibition (HAI) and virus neutralization (VN) assays. All antisera raised against linear

peptides failed to neutralize RV and had no HAI activity. To test whether the oxidized forms of both peptides RV-EP27 (residues 198-240) and RV-EP28 (residues 212-240), which contain two cysteines, could elicit neutralizing antibody responses, both RV-EP27 and -EP28 were oxidized in the presence of 15% DMSO, and purified by RP-HPLC. Guinea pig antisera raised against the oxidized form of either peptide were capable of neutralizing RV strain M33 in the absence of complement (Table 1), regardless of the adjuvant used (CFA or alum). The oxidized and linear RV-EP28 peptide in PBS were analysed by CD. The oxidized form was found to be more ordered and to exhibit a typical α-helical structure (two minimas at 205 and 222 nm, respectively). Therefore, the oxidized form of RV-EP28 represents a novel RV synthetic vaccine candidate since it contains human T helper cell epitopes and is capable of eliciting neutralizing antibody responses when formulated in alum.

Table 1. *Immunological properties of guinea pigs antisera raised against RV peptides.*

Immunogens	Peptide Sequences	VN[a]
RV-EP11/CFA	GQLEVQVPPDPGDLVEYIMN	0
RV-EP12/CFA	IMNYTGNQQSRWGLGSPNCH	0
RV-EP13/CFA	NCHGPDWASPVCQRHSPDCS	0
RV-EP25/CFA	PDPGDLVEYIMNYTGNQQSRWGLGSPNCHGPDWASP	0
RV-EP27/CFA	PDPGDLVEYIMNYTGNQQSRWGLGSPNCHGPDWASPVCQRHSP	0
$(RV\text{-}EP27)_{ox}$/CFA		160
$(RV\text{-}EP27)_{ox}$/alum		80
RV-EP28/CFA	GNQQSRWGLGSPNCHGPDWASPVCQRHSP	0
$(RV\text{-}EP28)_{ox}$/CFA		320
$(RV\text{-}EP28)_{ox}$/alum		80

[a]*Virus neutralization titers were determined by plaque assay in the absence of complement.*

References

1. Wolinsky, J.S. in Johnson, R.T. and Lyon, G. (Eds.) in 'Virus Infection and the Developing Nerous System', Kluwer Academic Publishers, Dordrecht. 1988, p125.
2. Tingle, A.J., Allen, M., Petty, R.E., Kettyls, G.D. and Chantler, J.K. *Ann. Rheum. Dis.* 45 (1986) 110.
3. Ou, D., Chong, P., Tingle, A.J. and Gillam, S., *J. Med. Virol.*, 40 (1993) 175.
4. Chaye, H., Chong, P., Tripet, B., Brush, B., and Gillam, S., *J. Clin. Virol.*, 13 (1993) 93.

Peptides: Chemistry, Structure and Biology
Pravin T.P. Kaumaya and Robert S. Hodges (Eds.)
Mayflower Scientific Ltd., 1996

331
Comparative Immunogenicity Studies of Different HIV-1 V3 Peptides

P. Chong, S-P. Shi, C. Sia, O. James, B. Tripet, T. Matthews and M. Klein

Connaught Centre for Biotechnology Research, North York, Ontario, M2R 3T4, Canada

Introduction

The third variable domain (V3) of the HIV-1 envelope protein gp120, has been shown to contain determinants responsible for cell tropism, infectivity and cytopathicity [1]. It is also the target for neutralizing antibodies and may harbor human cytotoxic T-lymphocytes (CTL) epitopes [1]. The present study was undertaken to investigate the immunochemical properties of V3 peptides that include linear or cyclized V3 loops, and linear T-B tandem peptides. Results from these studies should help us design and optimize peptide-based synthetic vaccines against HIV-1 infection.

Results and Discussion

V3 loop peptides corresponding to either BRU or MN clade B isolates were synthesized with and without terminal cysteine residues (Table 1), and purified for immunogenicity studies. In the presence of adjuvants (CFA or alum), all peptides were capable of eliciting IgG antibodies (titers range 1,600 to 12,500) recognizing both the immunizing peptides and rgp160. However, only the adjuvanted oxidized V3(MN) loop peptide induced antibodies which could inhibit syncytia formation mediated by the MN isolate (Table 1).

The yield for the oxidized V3(MN) loop peptide was low (~10%) and previous studies had indicated that core T-cell epitopes from hepatitis B and influenza viruses were more effective at presenting B epitopes than their envelope counterparts [2, 3]. We synthesized panels of linear T-B or B-T tandem peptides (Table 1) containing a T epitope from either the gp120 or p24 gag protein [4] linked to a V3 sequence from different isolates. These synthetic constructs were purified and used as immunogens in several animal models. Tandem peptides in T-B configuration elicited stronger anti-V3 IgG antibody responses than those obtained with the B-T tandem peptides (Table 1). These findings clearly demonstrate that the nature and magnitude of immune response markedly depend on the relative spatial orientation of the T- and B-cell epitopes. Furthermore, a limited N- or C-terminal truncation of the B epitope (CLTB-30 and -34) markedly reduced its ability to induce virus neutralizing antibodies.

A tetrameric multiple-antigenic peptide (MAP), (CLTB-36)4 was synthesized, purified and used to immunized guinea pigs 3 x 200 μg/dose. Antisera were tested

against theV3(MN) peptide and rgp160, as well as for virus neutralization activity. Results from these experiments indicated that the linear monomer and the MAP were immunogenically equipotent. Similar data were obtained in Balb/c mice. When cocktails of T-B tandem peptides were used as immunogens, the virus neutralization titers were significantly increased ranging from 5,000 to 25,000 (Table 1). Thus, selected peptide cocktails are potentially useful immunogens for inclusion in a synthetic HIV-1 vaccine.

Table 1. *Immunological properties of guinea pig antisera raised against HIV peptides*[a].

Immunogen	Peptide Sequences	rgp160	VN
V3(MN)	TRPNYNKRKRIHIGPGRAFYTTKNIIGTIRQAH	2,500	0
$V3(MN)_{ox}$	CTRPNYNKRKRIHIGPGRAFYTTKNIIGTIRQAHC	12,500	400
$V3(BRU)_{ox}$	CTRPNNNTRKSIRIQRGPGRAFVTIGKIGNMRQAHC	6,250	0
CLTB-30	GPKEPFRDYVDRFYKNKRKRIHIGPGRAF	2,500	0
CLTB-34	GPKEPFRDYVDRFYKRIHIGPGRAFYTTKN	6,250	200
CLTB-36	GPKEPFRDYVDRFYKNKRKRIHIGPGRAFYTTKN	12,500	1470
CLTB-37	NKRKRIHIGPGRAFYTTKNGPKEPFRDYVDRFYK	500	0
CLTB-84	GHKARVLAEAMSQVTNKRKRIHIGPGRAFYTTKN	6,250	385
CLTB-85	NKRKRIHIGPGRAFYTTKNGHKARVLAEAMSQVT	200	0
CLTB-91	KQIINMWQEVEKAMYANKRKRIHIGPGRAFYTTKN	12,500	800
CLTB-156	PIVQNIQGQMVHQAINTRKSIHIGPGRAFYTTG	6,250	385
CLTB-157	NTRKSIHIGPGRAFYTTGPIVQNIQGQMVHQAI	<50	NT
(CLTB-36)4	(GPKEPFRDYVDRFYKNKRKRIHIGPGRAFYTTKN)$4K_5$	62,500	1367
Cocktails	CLTB-36/-84/-91/-156	312,500	24825

[a]Three guinea pigs were immunized intramuscularly with 3 x 200 μg of each peptide absorbed onto alum. The antisera were tested against rgp160 by ELISAs and virus neutralization titers correspond to 90% reduction of RT activity in cell infected with the lymphocytotropic HIV-1 MN isolate. T-cell epitopes are underlined.

References

1. Rovinski, B. and Klein, M. in Kurstak, E. (Ed.), 'Modern Vaccinology', Plenum Medical, New York, 1994, p181.
2. Milich, D.R., McLachlan, A., Thornton, G.B. and Hughes, J.L., *Nature*, 329 (1987) 547.
3. Russell, S.M. and Liew, F.Y., *Nature*, 280 (1979) 147.
4. Chong, P., Sia, D.Y., Syndor, M. and Klein, M., *Feb. Letters*, 264 (1990) 231.

Peptides: Chemistry, Structure and Biology
Pravin T.P. Kaumaya and Robert S. Hodges (Eds.)
Mayflower Scientific Ltd., 1996

332
Counter Receptor Binding Domains That Block or Enhance Binding to LFA-1 or ICAM-1

T.J. Siahaan[1], S.A. Tibbetts[2], S.D.S. Jois[1], M.A. Chan[3] and S.H. Benedict[2]

Departments of [1]Pharmaceutical Chemistry, [2]Pharmacology and Toxicology, and [3]Microbiology, University of Kansas, Lawrence, KS 66045, USA

Introduction

Initiation of an immune response to antigen involves interaction of a small subset of T-cells with the antigen, followed by activation and proliferation of those T-cell clones. One important signal for T-cell activation is the binding between adhesion molecules (leukocyte function-associated antigen [LFA]-1, and intercellular adhesion molecule [ICAM]-1). This interaction can be blocked by MAbs [1] and peptide fragments from ICAM-1 [2, 3] and LFA-1 [4].

Results and Discussion

In this report, we evaluate the ability of peptide sequences from ICAM-1 and LFA-1 (α- and β-subunits) to: a) regulate binding of CD11a MAb to LFA-1 and CD54 MAb to ICAM-1 and b) inhibit homotypic adhesion of T cells such as Molt-3 (Table 1) [5]. Linear and cyclic peptides from the ICAM-1 sequence inhibited or enhanced binding of CD11a MAb to LFA-1. ICAM peptides, that inhibited or enhanced MAb binding, also inhibited homotypic adhesion of Molt-3 cells. This suggests that ICAM-1 derived peptides bound to LFA-1 on the cell surface and prevented CD11a MAb binding.

Peptides from the α- and β-subunits of LFA-1 can also regulate binding of CD54 MAb to ICAM-1 on Molt-3 cells and inhibit homotypic cell adhesion. Linear and cyclic peptides (*i.e.*, aLFA262-286), derived from the α-subunit insert region of LFA-1, enhanced binding of CD54 MAb to ICAM-1. Similarly, peptide aLFA466-491 from the divalent binding region of LFA-1 α-subunit inhibited the binding interaction of CD54 MAb to ICAM-1. Linear and cyclic peptides from the β-subunit of LFA-1 (*i.e.*, bLFA134-159) enhanced binding of CD54 MAb to ICAM-1. LFA-1 peptides, that inhibited or enhanced MAb binding, inhibited homotypic adhesion of Molt-3 cells.

To conclude, most peptides can enhance or block the MAb's (CD11a and CD54) binding to their respective target protein; peptides that blocked or enhanced MAb binding, blocked homotypic cell adhesion of Molt-3 cells. These results suggest that both ICAM-1 and LFA-1 may undergo conformational changes when they bind to peptides. Peptide cyclization can reduce or increase the peptide activity. Currently, we are completing the homotypic cell adhesion assay for all the peptides shown in Table 1.

Development of these peptides for *in vivo* use may result in a method of specifically eliminating T-cell clones that inappropriately recognize their self-antigen.

Table 1. *Activity of ICAM-1 and LFA-1 peptides to regulate MAb binding and homotypic cell adhesion.*

Peptide	Peptide Sequence	a	c
ICAM1-21	QTSVSPSKVILPRGGSVLVTG	-82%	+++
ICAM1-10	QTSVSPSKVI	-80%	++++
cICAM1-10	Cyclo(1,12)PenQTSVSPSKVIC	-2%	
ICAM6-15	PSKVILPRGG	-5%	
cICAM6-15	Cyclo(1,12)PenPSKVILPRGGC	-46%	
ICAM11-21	LPRGGSVLVTG	-26%	
cICAM11-21	Cyclo(1,12)CLPRGGSVLVTC	+122%	
ICAM26-50	DQPKLLGIETPLPKKELLLPGNNRK	+48%	++++
ICAM40-63	KELLLPGNNRKVYELSNVQEDSQP	-13%	
α-subunit		b	
aLFA262-286	ITDGEATDSGNIDAAKDII-YIIGI	+908%	++++
aLFA262-272	Linear-PenITDGEATDSGC	+56%	
caLFA262-272	Cyclo(1,12)PenITDGEATDSGC	+2%	
aLFA269-278	Linear-PenDSGNIDAAKDC	+96%	
caLFA269-278	Cyclo(1,12)PenDSGNIDAAKDC	+325%	
aLFA276-286	Linear-PenAKDIIYIIGIC	-10%	
aLFA466-491	GVDVDQDGET EL-IGAPLFYGEQRG	-25%	++++
β-subunit			
bLFA134-159	DLSYS-LDDLRNVKKLGGDLLRALNE	+233%	+++
bLFA134-144	Linear-PenDLSYSLDDLRC	+247%	
cbLFA134-144	Cyclo(1,12)PenDLSYSLDDLRC	+3%	
bLFA142-151	Linear-PenDLRNVKKLGGC	+4%	
cbLFA142-151	Cyclo(1,12)PenDLRNVKKLGGC	+5%	
bLFA150-159	Linear-PenGGDLLRALNEC	+25%	
cbLFA150-159	Cyclo(1,12)PenGGDLLRALNEC	+110%	

a) CD11a MAb binding to LFA-1; b) CD54 MAb binding to ICAM-1; (-) inhibition or (+) enhancement of MAb binding; c) (+++) inhibition of homotypic adhesion using 460 μM peptide.

Acknowledgments

Financial support was provided by the Higuchi Bioscience Center, University of Kansas.

References

1. Isobe, M., Yagita, H., Okumura, K., Ihara, A., *Science,* 255 (1992) 1125.
2. Ross, L., Hassman, F. and Molony, L., *J. Biol. Chem.*, 267 (1992) 8537.
3. Fecondo, J.V., Kent, S.B.H. and Boyd, A.W., *Proc. Natl. Acad. Sci., USA,* 88 (1991) 2879.
4. Stanley, P., Bates, P.A., Harvey, J., Bennett, R.I. and Hogg, N., *EMBO J.,* 13 (1994) 1790.
5. Benedict, S., Siahaan, T., Chan, M. and Tibbetts, S., US Patent, 229,531.

Peptides: Chemistry, Structure and Biology
Pravin T.P. Kaumaya and Robert S. Hodges (Eds.)
Mayflower Scientific Ltd., 1996

333
Mapping the Specificity of an Antibody Against an Oncogenic Sequence Using Peptide Combinatorial Libraries and Substitution Analogs: Implications for Breast Cancer Detection

J.R. Appel, J. Buencamino, R.A. Houghten and C. Pinilla

Torrey Pines Institute for Molecular Studies
3550 General Atomics Ct., San Diego, CA 92121, USA

Introduction

Proteins encoded by oncogenes, such as *c-erbB-2*, contain a consensus region that has homology with growth factor receptors and protein kinases. These proteins are known to be implicated in breast cancer by their presence in clinical samples of cancer patients. We are studying the specificities of a number of MAbs raised against this consensus region. A better understanding of the amino acid (aa) level specificity of these MAbs will aid in their use as selective probes for early breast cancer detection. Here we have characterized the specificity of a MAb raised against a synthetic peptide from this consensus region using individual substitution analogs and peptide combinatorial libraries.

Results and Discussion

A hexapeptide positional scanning combinatorial library was prepared using a pre-determined ratio of aa for each mixture coupling [1] in conjunction with simultaneous multiple peptide synthesis (SMPS) [2]. Hexapeptides derived from the library were synthesized on a COMPAS 242 multiple peptide synthesizer. Individual substitution analogs of the control peptide LGSGAFGTIYKG(C), corresponding to residues 138-149 of the oncogene *v-erbB*, were prepared by SMPS. Each residue of the antigenic determinant, which was identified as -AFGTIYKG- using omission analogs [3], was substituted with one of the other 19 L-aa. Competitive ELISA [4] was used to screen the hexapeptide library, subsequent hexapeptides, and the set of individual substitution analogs against MAb 172-12A4.

The concentration of each substitution analog necessary to inhibit 50% (IC_{50}) of MAb 172-12A4 binding to the control peptide adsorbed to the plate was determined. IC_{50} values for the 19 analogs at each position were averaged. This averaged IC_{50} value is termed the relative positional importance factor (RPIF) and represents the overall replaceability of a given position in the antigenic determinant [4]. It was found that mAb 172-12A4 recognized a discontinuous linear determinant, in which four residues were

specific and four residues were relatively redundant. The specific residues were phenylalanine (RPIF = 40.4), the next residue glycine (RPIF = 21.4), isoleucine (RPIF = 5.5), and lysine (RPIF = 20.3). Interestingly, glycine appears twice in the antigenic determinant, once as a specific residue and again as a redundant residue. This pattern of specificity was also found for the relatively conservative aa phenylalanine (specific residue) and tyrosine (redundant residue).

The positional scanning screening data yielded the most active aa residues at each position of the hexapeptide sequence (Table 1). This screening data was sufficient to locate the specific residues of the antigenic determinant, namely positions 2-7 since alanine and glycine at positions 1 and 8, respectively, were redundant. Tyrosine in position 1 of the library was nearly five-fold better than the expected phenylalanine and represents a conservative substitution. Sixteen individual peptides derived from the combinations of the most active aa at each position of the library were synthesized and assayed. Peptides having proline at the third position were at least 10-fold more active than those having glycine at the same position. Also, peptides having tyrosine at the second position were poorly recognized, indicating that the peptides responsible for the activity found for Ac-XYXXXX-NH_2 are not the same as those in Ac-YXXXXX-NH_2.

Peptide combinatorial libraries and individual substitutiuon analogs reveal similar patterns of specificity for peptide-antibody interactions. A complete set of substitution analogs yielded a "fingerprint" profile for this peptide-antibody interaction as well as the relative importance of each antigenic determinant residue. The screening data of the positional scanning library revealed a number of high affinity sequences. Finally, a single positional scanning combinatorial library can be used to study a number of different antigen-antibody interactions.

Table 1. *Library screening data and activities of peptides recognized by MAb 172-12A4.*

Library	Active residues	Peptide	IC_{50} (μM)
Ac-O_1XXXXX-NH_2	Y	Ac-YGPIDK-NH_2	1.2
Ac-XO_2XXXX-NH_2	G, Y	Ac-YGPIPK-NH_2	4.1
Ac-XXO_3XXX-NH_2	G, P	Ac-YGPIIK-NH_2	5.5
Ac-XXXO_4XX-NH_2	I	Ac-YGPIKK-NH_2	6.1
Ac-XXXXO_5X-NH_2	D, I, K, P	Ac-YGGIDK-NH_2	15
Ac-XXXXXO_6-NH_2	K	Ac-YGGIPK-NH_2	75
		all other peptides	>100

Acknowledgment

This work was funded by grant DAMD17-94-J-4110 from USAMRDC.

References

1. Pinilla, C., Appel, J.R., Blanc, P. and Houghten, R.A., *BioTechniques,* 13 (1992) 901.
2. Houghten, R.A., *Proc. Natl. Acad. Sci. USA,* 82 (1985) 5131.
3. Appel, J.R., Pinilla, C., Niman, H. and Houghten, R.A., *J. Immunol.,* 144 (1990) 976.
4. Pinilla, C., Appel, J.R. and Houghten, R.A., *Mol. Immunol.,* 30 (1993) 577.

Peptides: Chemistry, Structure and Biology
Pravin T.P. Kaumaya and Robert S. Hodges (Eds.)
Mayflower Scientific Ltd., 1996

334
Synthetic Peptide Vaccine For *Pseudomonas Aeruginosa*

D. Wade[1,2], P. Semchuk[2] and R.S. Hodges[2]

[1]*Waksman Institute of Microbiology, Rutgers University, Piscataway, NJ 08855, USA*
[2]*Protein Engineering Network of Centres of Excellence, 713 Heritage Medical Research Centre, University of Alberta, Edmonton, Alberta, T6G 2S2, Canada*

Introduction

Pseudomonas aeruginosa is a Gram-negative bacterium that is pathogenic for humans, and resistant to many antimicrobial agents. Infection with this organism begins when it attaches to a host epithelial cell *via* its pilus, a filamentous structure that is composed of a polymer of a single protein subunit, pilin [1]. We have been developing a synthetic peptide vaccine that is designed to stimulate the immune system to produce antibodies against pilin. Such antibodies would prevent infection by complexing with pilin and preventing the bacterium from binding to host cells.

Peptide vaccines were designed to contain either or both of the known T- and B-cell epitopes for *P. aeruginosa* strain K (PAK) pilin, and/or the promiscuous T-cell epitope of tetanus toxoid [2] to enhance immunogenicity, and/or coiled-coil sequences to promote dimerization and stability (Figure 1). Fourteen peptides were synthesized by solid phase methods [3], purified by RP-HPLC, and characterized by AAA and PDMS. Some of the peptides containing coiled-coil sequences were designed to be dimeric, with two identical chains linked by a single, C-terminal, disulfide bond. The peptides containing coiled-coil sequences were analyzed by CD to determine their stabilities to various concentrations of urea. All peptides were dissolved or suspended in a vehicle consisting of PBS and CFA (first injection), or PBS and incomplete FA (subsequent injections), and injected into mice or rabbits. Animal sera were collected periodically and analyzed by ELISA for the presence of antibodies to PAK pilin.

Results and Discussion

The arrangement of B- and T-cell epitopes in the peptide was important, with an amino terminal T-cell epitope and a carboxyl terminal B-cell epitope being most immunogenic. Peptides containing the promiscuous T-cell epitope of tetanus toxoid were more immunogenic than those with the pilin T-cell epitope, and those with the 17-residue, oxidized B-cell epitope of pilin were better than those with the 7-residue B-cell epitope. Coiled-coil dimerization domains enhanced the stabilities of peptides toward denaturation, and those containing the oxidized 21-residue domain were the most stable. However, the effects of these domains on immunogenicities were variable. The best

immunogen was a 34-residue peptide containing the promiscuous T-cell epitope of tetanus toxoid linked through a 2-residue spacer to the 17-residue, oxidized B-cell epitope of pilin (Figure 1, bottom).

(a) **D-E-Q-F-I-P-K** b) **K-C-T-S-D-Q-D-E-Q-F-I-P-K-G-C-S-K** (c) **S-A-N-G-A**

(d) **G-G** (e) **A-T-K-K-E-V-P-L-G-V-A-A-D-A-N-K-L-G** (f) **(E-I-E-A-L-K-A)$_2$**

(g) **Q-Y-I-K-A-N-S-K-F-I-G-I-T-E-L** (h) **(E-I-E-A-L-K-A-)$_2$-E-I-E-A-C-K-A**

Q-Y-I-K-A-N-S-K-F-I-G-I-T-E-L-G-G-K-C-T-S-D-Q-D-E-Q-F-I-P-K-G-C-S-K

Figure 1. *AA sequences of various components utilized to construct synthetic vaccines [(a)-(h)] and the entire AA sequence of the most immunogenic peptide tested (bottom). [(a) and (b)], B-cell epitopes of PAK pilin; [(c) and (d)], spacer sequences; (e) T-cell epitope of PAK pilin; [(f and (h)] 14- and 21-residue coiled-coil dimerization domains; (g) promiscuous T-cell epitope of tetanus toxoid.*

A synthetic peptide vaccine has been used to prevent infection by the malaria parasite [4], and our preliminary results indicate that the synthetic peptide vaccine approach may also be useful for the prevention of bacterial diseases.

Acknowledgments

D.W. gratefully acknowledges the Canadian Protein Engineering Network of Centres of Excellence (PENCE) for postdoctoral fellowship support from 1992-1994, and L. Daniels and I. Wilson for peptide synthesis and R. Luty for CD analysis.

References

1. Paranchych, W., Pasloske, B.L. and Sastry, P.A., in Chakrabarty, A.M., Gunsalus, I.C., Kaplan, S. and Silver, S. (Eds.), 'Pseudomonas: Biotransformations, Pathogenesis and Evolving Biotechnology', American Society of Microbiology, 1990, p. 343.
2. Seo, Y.H., Kobs-Conrad, S. and Kaumaya, P.T.P., in Schneider, C.H. and Eberle, A.N. (Eds.), 'Peptides 1992', ESCOM, Leiden, The Netherlands, 1993, p. 139.
3. Merrifield, R.B., *J. Am. Chem. Soc.*, 85 (1963) 2149.
4. Patarroyo, M.E., Amador, R., Clavijo, P., Moreno, A., Guzman, F., Romero, P., Tascon, R., Franco, A., Murillo, L.A., Ponton, G. and Trujillo, G., *Nature*, 332 (1988) 158.

Peptides: Chemistry, Structure and Biology
Pravin T.P. Kaumaya and Robert S. Hodges (Eds.)
Mayflower Scientific Ltd., 1996

335
Cross-reactivity of Antibodies to Retro-inverso Peptidomimetics with the Parent Protein Histone H3 and Chromatin Core Particle

N. Benkirane, G. Guichard, M.H.V. Van Regenmortel, J.P. Briand and S. Muller

Institut de Biologie Moléculaire et Cellulaire,
UPR 9021 CNRS, 15 rue Descartes, F-67084 Strasbourg Cédex, France

Introduction

Potential applications of pseudopeptides and peptidomimetics cover many aspects of basic immunology including synthetic vaccines, immuno-diagnostics, and the development of new generations of immunomodulators. Recently, we have analyzed the antigenic and immunogenic properties of an all D-, a retro-, and a retro-inverso- analogue of the model hexapeptide of sequence IRGERA corresponding to the COOH-terminal residues 130-135 of histone H3 [1, 2]. Both retro-analogues contained NH-CO bonds instead of the CO-NH peptide bonds, the chirality of each residue was maintained in the retro-peptide and inverted in the retro-inverso peptide. Regarding IgG1, IgG2a, and IgG2b antibodies, the retro-inverso-peptide was found to mimic the antigenic activity of the natural L-peptide but not of the all D- and retro-peptides. Conversely, the retro-peptide mimicked the all D-peptide but not the L- and retro-inverso-peptides.

In order to assess the potential use of retro-inverso-peptides as immunogens useful for vaccination or for eliciting antibody probes for immunotherapy, it was necessary to analyze in more detail the capacity of antibodies generated against these peptide analogues to react with the parent protein and particularly with assembled complex structures. The model peptide studied in the present investigation is particularly interesting to study crossreaction of anti-peptide antibodies since the region 130-135 of H3 is accessible at the surface of chromatin core particles, constituted by two copies of each core histone H2A, H2B, H3, H4, and 145 base pairs of DNA [3].

Results and Discussion

Four groups of two BALB/c mice were injected with the L, retro-inverso, D, and retro IRGERA analogues coupled to small unilamellar liposomes containing monophosphoryl lipid A as adjuvant and four fusion experiments were performed with the spleen cells of these mice. Nine positive clones secreting IgG1, IgG2a and IgG2b antibodies were amplified *in vitro* and purified. The capacity of mAbs to recognize the four peptide analogues and H3 was measured in the BIA core™ using antigens covalently linked to the dextran matrix through the free SH-group introduced in peptides for this purpose or

through amino-groups of histone H3. Equilibrium affinity constants of mAbs (anti-L and anti retro-inverso peptides) for the four peptide analogues and H3 are shown in Table 1.

The most important finding in this work was to show that three of the four mAbs to the retro-inverso IRGERA peptide bound equally well the retro-inverso and the natural peptide (with Ka values ranging from 0.6 to 1.9×10^9 M^{-1}) and that the four mAbs reacted with the cognate protein (Ka values, 0.3 to 2×10^9 M^{-1}).

Since several mAbs generated against IRGERA and the retro-inverso analogue recognized the parent histone H3, their capacity to recognize H3 in more complex structures such as core particles was further studied (Table 1). Three of the four mAbs reacted with chromatin core particles presented towards the liquid-phase by the N-terminal end of histone H2B (Ka values, 0.2 to 2.2×10^9 M^{-1}).

Table 1. *Equilibrium affinity constants measured in the BIAcore of mAbs induced against IRGERA (mAbs 4x8, 4x10, 4x11) and its retro-inverso (RI) analogue (mAbs 13x12, 13x14, 13x18).*

Antigens	Ka x 10^{-6} M^{-1}					
	Anti L-peptide mAbs			Anti RI-peptide mAbs		
	4x8	4x10	4x11	13x12	13x14	13x18
L-peptide	80	4486	3	1575	867	1637
RI-peptide	558	3640	225	1893	579	1596
Histone H3	4286	6571	2280	2003	263	2044
Core particle	1150	5928	1158	1707	187	2162

In the context of vaccine design, the demonstration that antibodies to a retro-inverso peptide can cross-react particularly well with the cognate nucleoprotein structure is very important and promising for further development. The antibodies described in this study [3] have been generated against the peptide analogue covalently bound to liposome containing the non-toxic adjuvant MPLA. Since the present study was performed with the C-terminal region of H3, which is known to be highly accessible and probably particularly mobile, the results should be confirmed with other exposed protein domains which correspond to internal sequences in the primary structure of the protein. However, collectively, the strategy is encouraging in respect to the potential use of retro-inverso peptides in the design of much more potent synthetic vaccines [4].

References

1. Benkirane, N., Friede, M., Guichard, G., Briand, J.P., Van Regenmortel, M.H.V. and Muller S., *J. Biol.Chem.*, 268 (1993) 26279.
2. Guichard, G., Benkirane, N., Zeder-Lutz, G., Van Regenmortel, M.H.V., Briand, J.P. and Muller,S., *Proc. Natl. Acad. Sci. USA*, 91 (1994) 9765.
3. Benkirane, N., Guichard, G., Van Regenmortel, M.H.V., Briand, J.P. and Muller S., *J. Biol. Chem.*, 270 (1995) 11921.
4. Muller, S., Guichard, G., Benkirane, N., Brown, F., Van Regenmortel, M.H.V. and Briand, J.P., *Pept. Res.*, 8 (1995) 138.

Peptides: Chemistry, Structure and Biology
Pravin T.P. Kaumaya and Robert S. Hodges (Eds.)
Mayflower Scientific Ltd., 1996

336
Defining Conformational Requirements for the Principle Neutralizing Determinant on HIV-1

E. Cabezas, R.L. Stanfield, I.A. Wilson and A.C. Satterthwait

Department of Molecular Biology, The Scripps Research Institute, La Jolla, CA 92037, USA

Introduction

Synthetic peptide vaccines provide a means for focusing the immune response on neutralizing epitopes. This could prove of importance in AIDS vaccine research. The "principal neutralizing determinant" (PND) on HIV-1 is an example. This epitope resides in the third variable region of the envelope glycoprotein gp120 and undergoes an extraordinary degree of mutation [1]. The "tip" of the V3 region, GPGRAF (MN strain), however, mutates to a lesser extent [1]. Monoclonal antibodies (MAbs) directed to the "tip" are among the few that neutralize primary isolates [2]. A cocktail vaccine based on "tip" amino acid sequences could prove effective.

Since the antigenicity and immunogenicity of linear peptides can be enhanced by folding them [3], we have initiated work to identify constrained peptides that mimic the conformation of the PND. Because this conformation is unknown, we rely on potent neutralizing MAbs to identify constrained peptides that bind better than corresponding linear peptides on the assumption that higher affinities reflect shape complementarity. This approach has led to the identification of a constrained PND peptide with a 256-fold increase in affinity for a potent HIV-1 neutralizing MAb.

Results and Discussion

The PND is predicted to form a β-hairpin loop with the critical GPGR sequence occupying a Type II turn at its apex [1]. β-hairpin loops are characterized by a ladder of hydrogen bonds spanning alternate pairs of amino acids. We systematically replaced predicted hydrogen bonds with the hydrazone covalent hydrogen bond mimic [4] to give a series of cyclic peptides varying in size (8-10 amino acids) and cadence (overlaps of one amino acid). Selected linear and disulfide peptide loops were also examined. Relative affinitites of loops were determined by ELISAs for MAb 58.2 [2]. This led to the identification of a loop 1, [JHIGPGRAFGGZ]G-NH_2, with a 64-fold improvement in affinity. MAb 58.2, provided by Repligen Corp., is well characterized and potently neutralizes primary isolates [2].

Both linear and loop peptides have been cocrystallized with MAb 58.2 and crystal structures determined [5]. The information provided by the structures led to the synthesis of a second series of loop peptides (Figure 1) with the goal of stabilizing the loop further with constrained amino acids, isoaminobutyric acid (Aib), and D-alanine.

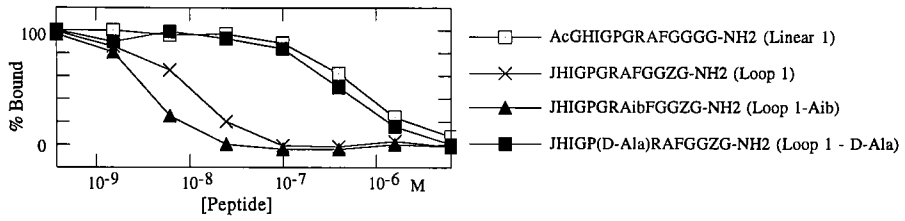

Figure 1. *Competition ELISAs of V3 Peptides for MAb 58.2.*

MAb 58.2 binds Loop 1 (Aib), [JHIGPGRAibFGGZ]G-NH_2, with a 256-fold higher affinity than the corresponding Linear 1 peptide. (D-Ala) reduced affinity for Loop 1 by 64-fold. Cyclization of the peptide accounts for most of the improvement in affinity while the substitution of Aib for Ala improves affinity by another 4-fold. Aib which stabilizes ϕ,ψ angles favorable to helices was anticipated to stabilize the bound conformation further and it did. D-Alanine was anticipated to stabilize a Type II turn and destabilize the bound conformation as observed.

The enhanced binding suggests that Loop 1 (Aib) adapts a conformation in water that mimics the conformation of the peptide as it is bound by the antibody. This possibility can be resolved by comparing NMR structure for the loop in water with an X-ray crystal structure bound by MAb 58.2. The identification of a bona fide mimetic would provide a vaccine candidate for testing whether the preference for a particular conformation plays a role in MAb 58.2 potency. Similar experiments with a constrained malaria peptide validate the approach [3].

Acknowledgments

This research was supported by NIH AI37512 (ACS) and GM46192 (IAW). RLS is a scholar of the American Foundation for AIDS Research. This is publication 9502-MB from The Scripps Research Institute.

References

1. LaRosa, G.J., Davide, J.P., Weinhold, K. Waterbury, J.A., Profy, A.T., Lewis, J.A., Langlois, A.J., Gordon, R.D., Boswell, R.N., Shadduck, P., Holley, L.H., Kaprlus, M., Bolognesi, D.P., Matthews, T.J., Emini, E.A. and Putney, S.D., *Science,* 249 (1990) 932.
2. White-Scharf, M.E., Potts, B.J., Smith,M., Sokolowski, K.A., Rusche, J.R. and Silver,S., *Virology,* 192 (1993) 197.
3. Satterthwait, A.C., Cabezas, E., Calvo, J.C., Wu, J.X., Chen, S.Q., Kaslow, D.C., Livnah, O., Stura, E.A., this volume.
4. Chiang, L-C., Cabezas, E., Calvo, J.C. and Satterthwait, A.C., in Hodges, R.S. and Smith, J.A. (Eds.) 'Peptides: Chemistry, Structure and Biology', ESCOM, Leiden, The Netherlands, 1994, p. 278.
5. Stanfield, R., Cabezas, E., Satterthwait, A.C., Stura, E.A. and Wilson, I.A., unpublished

Peptides: Chemistry, Structure and Biology
Pravin T.P. Kaumaya and Robert S. Hodges (Eds.)
Mayflower Scientific Ltd., 1996

337

Epitopes of Human Aggrecan Binding to Rheumatoid Arthritis Associated MHC Class II Molecules

C.B. Sigel, R.M. Campbell, N. Boulanger, C.J. Belunis, D.R. Bolin, Z. Nagy and A.M. Felix

Roche Research Center, Hoffmann-La Roche Inc., Nutley, NJ 07110, USA

Introduction

Rheumatoid arthritis (RA) is an autoimmune disease with unknown immunogen(s) which is characterized by progressive degradation of aggrecan and collagen II, the principal constituents of the joints. All autoimmune diseases proceed *via* a cell-mediated immune response involving the class II major histocombatibility complex (MHC) (also referred to as human leukocyte antigen, HLA), a bound peptide, and the receptor of a T-helper cell. Certain alleles of MHC class II are known to occur with increased frequency in patients with RA. These alleles are HLA-DRB1*0101 (DR1), DRB1*0401 (DR4Dw4), and DRB1*0404 (DR4Dw14). A recently solved crystal structure of HLA-DR1 [1, 2] shows that the peptide antigen is bound in an extended conformation to a groove on the protein surface. Pockets at the bottom of the cleft accomodate amino acid side chains.

Allele-specific sequence motifs of MHC-bound peptides have been found by analysis of naturally occuring antigens [3], chemical SAR, and by analysis of MHC-binding peptides identified by a phage display peptide library [4]. The strongest binding to the protein results from the interaction of a hydrophobic or aromatic amino acid with the pocket in position 1 of the binding groove. Other anchors are found in positions 4, 6, 7 and 9 of the bound peptides [5]. With the goal of finding possible autoimmunogens of RA, we used this information to search the protein sequence of human aggrecan for MHC epitopes.

Results and Discussion

Forty partial sequences which contained binding motifs for one or more of the RA-linked DR-molecules were selected for synthesis. The N-terminus of the sequences was chosen at position (i-3), relative to the hydrophobic anchor binding at position 1 of the MHC binding groove. The 14-mer peptides were synthesized by SPPS on BHA-polystyrene resin which had been derivatized with an Fmoc amide linker. Tea bag methodology [6] was used for standard Fmoc/tBu/Boc strategy with the following additional side chain protecting groups: Pmc for Arg, Trt for Asn, Gln and His. Coupling was performed by means of DIC/HOBt or by *in situ* neutralization/activation with DIEA/HBTU. After N-acetylation the peptides were cleaved from the resin with reagent K and subsequently purified by preparative RP-HPLC to >95%. All structures were established by amino acid analysis and FABMS.

The peptides were tested for binding to purified DR1, DR4Dw4 and DR4Dw14 molecules. Several sequences inhibited binding of an ^{125}I universal ligand to DR1 and DR4Dw4 in a scintillation proximity assay (SPA) with IC_{50} values in the low to intermediate nanomolar range (Table 1). The strong binding affinity of these peptides to the DR molecules can be explained by the presence of amino acids known to be good anchors in positions 1 (aromatic or hydrophobic), 4, 6, 7 and 9. Some of the sequences binding strongly to DR4Dw4 could also be predicted by a recently published algorithm [7]. Only intermediately good binding to DR4Dw14 could be observed. This may be attributed to the fact that the aromatic anchors in the selected peptides are too bulky for the smaller hydrophobic pocket at position 1 of DR4Dw14.

Table 1. *Binding of human aggrecan sequences to HLA-DR molecules measured by competitive SPA.*

human aggrecan peptide		MHC II molecule	IC_{50}[μM]
670-683	Ac-AFSFRGISAVPSPG-NH_2	DR1	0.01
36-49	Ac-PSPLRVLLGTSLTI-NH_2	DR1	0.04
193-206	Ac-EDGFHQSDAGWLAD-NH_2	DR1	0.29
417-413	Ac-PFTFAPEIGATAFA-NH_2	DR4Dw4	0.05
1804-1817	Ac-SGAYYGSGTPSSFP-NH_2	DR4Dw4	0.05
738-751	Ac-QTEWEPAYTPVGTS-NH_2	DR4Dw4	0.18
154-167	Ac-VFHYRAISTRYTLD-NH_2	DR4Dw4	0.35
298-311	Ac-SAGWLADRSVRYPI-NH_2	DR4Dw14	2.4
1776-1789	Ac-TPEFSGLPSGIAEV-NH_2	DR4Dw14	3.0

To conclude, we have synthesized, purified and fully characterized a set of 40 partial sequences of human aggrecan and identified several good binding sequences. To further establish their role as possible autoantigens, experiments studying the ability of these peptides to elicit a T-cell response are in progress.

References

1. Brown, J.H., Jardetzky, T.S., Gorga, J.C., Stern, L.J., Urban, R.G., Strominger, J.L. and Wiley, D.C., *Nature,* 364 (1993) 33.
2. Stern, L.J., Brown, J.H., Jardetzky, T.S., Gorga, J.C., Urban, R.G., Strominger, J.L. and Wiley, D.C., *Nature,* 368 (1994) 215.
3. Chicz, R.M., Urban, R.G., Gorga, J.C., Vignali, D.A.A., Lane, W.S. and Strominger, J.L., *J. Exp. Med.,* 178 (1993) 27.
4. Hammer, J., Valsasnini, P., Tolba, K. Bolin, D., Higelin, J., Takacs, B. and Sinagaglia, F., *Cell,* 74 (1993) 197.
5. Rammensee, H.-G., Friede, T.S. and Stevanovic, S., *Immunogenetics,* 41 (1995) 178.
6. Houghten, R.A., *Proc. Natl. Acad. Sci.,* 82 (1985) 5131.
7. Hammer, J., Bono, E., Belunis, C., Nagy, Z. and F. Sinagaglia, *J. Exp. Med.,* 180 (1994) 2353.

Peptides: Chemistry, Structure and Biology
Pravin T.P. Kaumaya and Robert S. Hodges (Eds.)
Mayflower Scientific Ltd., 1996

338
Use of Combinatorial Peptides, or "Mixotopes", for More Efficient Detection of Antibodies to a Non-variable Antigen

H. Gras-Masse[1], C. Rollin[1], J.M. Grzych[2], C. Rommens[1], C. Auriault[3] and A. Tartar[1]

[1]Faculté de Pharmacie, URA CNRS 1309, [2]INSERM U167-CNRS 624, [3]URA CNRS 1854, Institut Pasteur de Lille, 59000 Lille, France

Introduction

Enzyme-Linked-Immunosorbent-Assay or "ELISA" based on the use of synthetic peptides as solid-phase antigens has found useful serodiagnostic applications. However, this approach is often limited by the low intensity of the detectable signal. The mono-specific polyclonal antiboby population directed to a short peptide represents a variety of antibodies species. This leads to heterogeneous recognition of the immobilized antigen. Our idea was to use, as solid-phase antigen, a convergent combinatorial construct or "mixotope" [1] derived from the model sequence by degenerating each position by one to three amino-acids selected for their probable ability to mimic the original residue. Our hypothesis was that such a mixotope would contain, besides the original sequence, a population of closely related sequences able to detect more efficiently heteroclitic antibody populations. We have selected as a model the C-terminal peptide 190-211 derived from the Sm28-GST protein, a non-variable antigen expressed during infection by *Schistosoma mansoni,* and recognized by sera from infected individuals.

Results and discussion

We have defined 2 mixotopes in which the degeneracy was designed using mainly a replaceability matrix, proposed by Geysen [2], representing biological acceptability of amino acid substitution in antigenic peptides. (Table1).

These constructs, an irrelevant mixotope and the original 22-mer sequence were used as solid-phase antigens for the detection by ELISA of antibodies found in sera of rats

Table 1. *Two different mixotopes were synthesized, containing $13x10^6$ combinatorial, closely related peptides ("million-peptides mixotope") or $9x10^9$-peptides ("billion-peptides mixotope"). In each degenerate position, the different amino acids were introduced in an equivalent fraction.*

million-peptides mixotope	billion-peptides mixotope
ENLLASSPRLAKYLSNRPATPF	ENLLASSPRLAKYLSNRPATPF
DQIIGAA KIGRFIAQK GS L	DQIIGAAAKIGRFIAQKAGSAL
Q MMS MS M S	QDMMSTT AMSHLMTDH SA Y

experimentaly infected by *S. mansoni.* We have observed an equivalent reactivity of the million-peptides mixotope and the 22-mer peptide. The results clearly indicate an improvement of the detection when using the billion-peptides mixotope. No reactivity was found when using the irrelevant mixotope (not shown).

We then tested the reactivity of our mixotopes towards human sera from infected individuals. All sera reacted to the recombinant Sm28 GST protein. In this case also, the billion peptide mixotope was clearly a better antigen than million-peptides mixotope or the peptide itself (Figure 1, top). Most interestingly, a selection of 21 sera from infected individuals that were not reactive to the 190-211 peptide were positive with the billion-peptides mixotope, while no false positive reaction was observed among the 20 control sera (Figure 1, bottom).

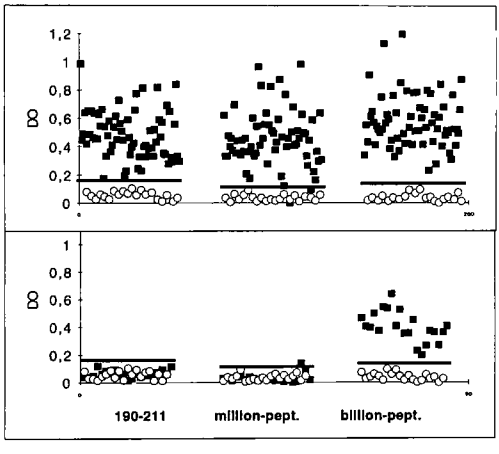

Figure 1. *Antibody response in a group of 20 healthy donors (open symbols), and a group of 66 (top) and 21 (bottom) human sera from S. mansoni infected individuals (closed symbols), against the 190-121 peptide, and its derived mixotopes.*

Antibody avidity to the different solid-phase antigens was examined in human sera by ELISA using thiocyanate elution [3]. No clear difference was observed when comparing the resistance to thiocyanate elution of the antibody binding to the univocal peptide or to the billion-peptide mixotope (not shown).

These results indicate that convergent combinatorial peptide constructs, or "mixotopes", designed from a replaceability matrix or physico-chemical data, can be used to significantly increase the sensitivity of serodiagnostic assays, even when they represent a non-variable part of a major antigen, without, at least in this case, a simultaneous increase of the background signal.

References

1. Gras-Masse, H., Ameisen, J.C., Boutillon, C., Bossus,M., Neyrinck, J.L., Deprez, B., Capron, A., Tartar, A., *Peptide Research,* 5 (1992) 211.
2. Geysen, H.M., Mason, T., Rodda, S., *J. Mol. Recognition,* 1 (1988) 32.
3. Pullen, G.R., Fitzgerald, M., Hosking, C., *J. Immun. Methods,* 86 (1986) 83.

Peptides: Chemistry, Structure and Biology
Pravin T.P. Kaumaya and Robert S. Hodges (Eds.)
Mayflower Scientific Ltd., 1996

339
Identification and Applications of Idiotype-specific Peptides for Two Murine B-Cell Lymphoma Cell Lines

K.S. Lam[1], Q. Lou[1], Z.-G. Zhao[1], M.L. Chen[1], S.E. Salmon[1], S. Wade[2] and M. Lebl[2]

[1]Arizona Cancer Center, and Department of Medicine, University of Arizona, Tucson, AZ 85724, USA
[2]Selectide Corporation, 1580 E. Hanley Blvd., Tucson, AZ 85737, USA

Introduction

Over 90% of human non-Hodgkin's lymphomas are B-cell type with specific cell surface immunoglobulins (or idiotypes). These surface idiotypes are potential therapeutic targets [1, 2]. Combinatorial peptide library methods based on the "one-bead one-chemical" concept (Selectide Process) were used to identify idiotype-specific peptide ligands of two murine lymphoma cell lines (WEHI-279 and WEHI-231) with surface IgMκ. The peptides were synthesized on solid-phase beads using a "split synthesis" method [3, 4] resulting in a huge library of peptide beads such that each solid-phase bead expressed only one peptide entity [4]. The peptide-bead library (10^6-10^7) was then screened with the purified surface idiotypes derived from two murine lymphoma cell lines. With an enzyme-linked assay system, the positive beads turned color. The colored beads were then physically isolated and the amino acid sequence of the peptide determined by an automatic protein microsequencer.

Results and Discussion

Table 1 shows the peptide motifs identified for the two murine lymphoma cell lines (WEHI-279 and WEHI-231). Both L- and D-amino acid peptide libraries were screened.

Table 1. *Idiotype-specific peptide motif.*

	Cell Lines	
Peptide Library	WEHI-231	WEHI-279
L-amino acid library (7-mer, 9-mer, and 11-mer)	WYTP WYDD WY(V/I)P	RWID RWFD
D-amino acid library (8-mer)	wGey(i/v)_v_ lw_ _pew(i/v) kw_Gp_w	_t_Gm_k_ _Gr_ _w_ _

The D-amino acid peptide ligands are particularly interesting as they are likely to be more resistant to proteolysis *in vivo* and therapeutically more useful.

Some of the ligands shown in Table 1 were resynthesized on beads and their ability to be stained by either the purified idiotypes or whole cell extract (extracted with 0.5% NP-40) coupled with a secondary antibody-enzyme conjugate system was confirmed. In addition, some of these peptide-beads (120 μm diameter) were able to bind strongly to intact cells (~8 μm diameter) resulting in a rosette. In addition to binding specifically to their corresponding idiotypes, these peptides (in a tetrameric form) upon binding to the intact lymphoma cells were able to induce signal transduction resulting in an elevated level of protein tyrosine phosphorylation.

We are currently working on the design and synthesis of oligomeric idiotype-specific peptides with the appropriate hydrophilic linkers. One of the bifunctional hydrophilic linkers that we have designed and synthesized is $FmocNHCH_2CH_2CH_2(OCH_2CH_2)_2$-$OCH_2CH_2CH_2NH$-$COCH_2CH_2COOH$. This was synthesized by mixing a readily available and inexpensive hydrophilic molecule 4,7,10-trioxo-1,13-tridecane diamine with equal molar amount of succinic anhydride followed by derivatizing the primary amino group with Fmoc-OSu. We have succeeded in using this linker in conjunction with lysine to synthesize tetrameric idiotype-specific peptides (analogous to the multiple antigen peptide system [5]). These oligomeric peptides are then conjugated with radio-nuclide or toxin for targeted-therapy of these lymphoma cells both *in vivo* and *in vitro*. In addition, we also plan to use these peptides as a model system to develop idiotype-specific peptide reconstituted liposomes for drug delivery studies.

References

1. Lam, K.S., *The West. J. Med.*, 158 (1993) 475.
2. Renschler, M.F., Bhatt, R.R., Dower, W.J., and Levy, R., *Proc. Natl. Acad. Sci. USA*, 91 (1994) 3623.
3. Furka, A., Sebestyen, F., Asgedom, M., and Dibo, G., *Int. J. Peptide Protein Res.*, 37 (1991) 487.
4. Lam, K.S., Salmon, S.E., Hersh, E.M., Hruby, V.J., Kazmierski, W.M. and Knapp, R.J., *Nature*, 354 (1991) 82.
5. Tam, J.P., *Proc. Natl. Acad. Sci. USA*, 85 (1988) 5409.

Peptides: Chemistry, Structure and Biology
Pravin T.P. Kaumaya and Robert S. Hodges (Eds.)
Mayflower Scientific Ltd., 1996

340
Tumour-imaging Peptides: Conformation-activity Relationship by CD Spectroscopy

R. Hussain[1,2], G. Siligardi[2], S. Adebakin[1,3], J.A. Cook[1], A.J.T. George[3], A.F. Drake[2] and N.S. Courtenay-Luck[1,3]

[1]*Antisoma Ltd., Samaritan Hospital, 153-173 Marylebone Rd, London, UK*
[2]*Department of Chemistry, Birkbeck College, 20 Gordon St, London, UK*
[3]*Department of Immunology, Royal Postgraduate Medical School, London, UK*

Introduction

In some epithelial cancer cells, mucin protein is abberantly glycosylated leaving regions of the mucin protein exposed to antibody binding [1-3]. The synthetic peptide YCAREP PTRTFAYWG (EPPT1) was found to have a significant affinity (Kd=20μM) for the deglycosylated mucin-derived peptide YVTSAPDTRPAPGST (PDTRP). The sequence of EPPT1 was based on the CDR3 V_H region of a monoclonal antibody (ASM2) raised against human epithelial cancer cells. The technetium-radiolabelled form of EPPT1 was found to be a good tumour-imaging candidate for diagnosis of breast carcinoma.

Here we present the binding properties, radiolabelling efficiency and conformational behaviours of several synthetic EPPT1 peptide analogues. The peptides were classified accordingly as active and non-active PDTRP-binding peptides. The conformational analysis of the free peptides as a function of solvent environment was carried out by CD spectroscopy. A structure-activity relationship was observed indicating a β-strand type of structure as the active binding feature.

Results and Discussion

The peptide binding study by resonant mirror biosensor showed different affinity as a function of peptide primary sequence (Table 1). The CD spectra of both active and non-active peptides showed the presence of irregular conformations in H_2O and SDS 20mM. In TFE, a significant degree of ordered conformations of α-helix or β-turn type were induced but did not correlate well with their binding properties (Table 1). In SDS 1mM, a conformational difference was observed between the active and non-active peptides. The active peptides exhibited CD spectra of aggregation of β-strand type whilst the non-active peptides showed CD spectra similar to those observed in H_2O and SDS 20mM. Extended conformation (β-strand, β-sheet, PII) has been observed as an important binding feature in several peptide/protein complexes and peptide inhibitors [4, 5]. A good correlation between the extended conformation of β-strand type and the binding affinity of the active peptides (Table 1) suggests this conformation as the binding feature of the EPPT tumour-imaging peptides. This information is vital for the

Table 1. *Structure-activity relationships and radiolabelling efficiencies of EPPT-containing peptides.*

Sequence	% Radio purity	Binding Affinity	Secondary structure by CD	
			TFE	SDS 1mM
YGGGSEPPTRTGGGGS	-	NA	β-turn/ α-helix	Irregular
EPPTRTFAY	-	NA	Irregular	Irregular
REPPTRTFAY	-	NA	Irregular	Irregular
YCAREPPTRTFAYWGQG	-	+++	β-turn/ α-helix	β-sheet
YCAREPPTRTFAYWG-NH_2	-	+++	β-turn/ α-helix	β-sheet
YECPAFRGTYRWAPT	97.0	NS	β-turn/ α-helix	Irregular
YCAREPPTRTFAYWG(EPPT1)	100.0	+++	β-turn/ α-helix	β-sheet
KYCAREPPTRTFAYWGQG	92.1	+++	β-turn/ α-helix	β-sheet
Ac-YCAREPPTRTFAYWG	-	+	β-turn/ α-helix	β-sheet (w)
YSAREPPTRTFAYWG	-	NA	β-turn/ α-helix	Irregular
YVAREPPTRTFAYWG	-	+	β-turn/ α-helix	β-sheet (w)
Ac-YCAREPPTRTFAYWG-NH_2	-	+	β-turn/ α-helix	β-sheet(vw)
YCAREPPTRTFAYWG | YCAREPPTRTFAYWG	-	++	β-turn/ α-helix	β-sheet
AREPPTRTFAY	-	NA	Irregular	Irregular
CAREPPTRTFAY	-	NA	Irregular	Irregular

NA: non-active, NS: non-specific, w: weak, vw: very weak, +: active, increase no. of (+), better the affinity to PDTRP.

design of novel EPPT analogues. Any modification to improve binding affinity must retain the ability of the peptides to adopt the extended conformation of β-strand type in solution.

Acknowledgments

We would like to thank the Mass Spectrometry Department (ULIRS), The School of Pharmacy, London, for MS facilities and RH would like to thank the American Peptide Society for the travel award.

References

1. Girling, A., Bartkova, J., Burchell, J., Gendler, S., Gillett, C. and Taylor- Papadimitriou, J., *Intl. J. Cancer,* 43 (1989) 1072.
2. Gendler, S., Taylor-Papadimitriou, J., Duhig, T., Rothbard, J. and Burchell, J., *J. Biol. Chem.*, 263 (1988), 12820.
3. Xing, P-X., Tjandra, J.J., Stacker, S.A., Teh, J.G., Thompson, T.H., McLaughlin, P.J. and McKenzie, I.F.C., 1989, *Immunol. Cell Biol.*, 67 (1989) 183.
4. Siligardi, G. and Drake, A.F., *Peptide Science*, 37 (1995) 281.
5. Hussain, R., Sergheraert, C., Drake, A.F. and Siligardi, G., *Biomedical Peptides, Proteins & Nucleic Acids,* 1 (1995) 69.

Peptides: Chemistry, Structure and Biology
Pravin T.P. Kaumaya and Robert S. Hodges (Eds.)
Mayflower Scientific Ltd., 1996

341
Immunological Evaluation of the Lipid-Core-Peptide (LCP) Adjuvant/Carrier System

I. Toth[1], N. Flinn[1], W.A. Gibbons[1] M. Good[2], W. Hayman[2] and F. Brown[3]

[1]*The School of Pharmacy, University of London, 29-39 Brunswick Sq., London, WC1N 1AX, UK*
[2]*Vaccine Technology, QIMR, The Bancroft Centre, 300 Herston Road, Brisbane, Qld. 4029, Australia*
[3]*Agricultural Research Service, Plum Island Animal Disease Center, Greenport, NY 11944, USA*

Introduction

We have developed a novel Lipid-Core-Peptide (LCP) system by incorporating lipidic amino acids into the polylysine system. We have obtained high antipeptide antibody titres in sera raised against an LCP-epitope of OMP of *Chlamydia trachomatis*, without using conventional adjuvants [1]. Here we report further work with the LCP system.

$[CH_3(CH_2)_nCH(\text{-}NH)CO\text{-}]_m\text{-}(Lys)_r\text{-}(peptide)_s$ **(LCP-peptide)**

Results and Discussion

Streptococci. Conserved T and B cell epitopes on the M protein of Streptococci group A (LRRDLDASREAKKQVEKALE = MG-145 and KLTEKEKALQAKLEAEAKA) were able to stimulate peptide specific antibodies in B10.BR and B10.D2 mice, respectively. Antisera to the former peptide, in bactericidal assay involving human neutrophils [2], could mediate killing of streptococci, evidence that conserved epitopes can be the targets of bactericidal antibodies, thus allowing development of immunologic memory and natural boosting of human immune response after natural exposure. Requirements that must be addressed for peptide MG-145 to become a successful streptococcal vaccine include the ability to induce antibodies to multiple local serotypes, the capacity for antigen presentation in the context of multiple HLA class II alleles, and the stimulation of high-titre IgG. A successful approach to induce a high titre antibody response was to incorporate peptide MG-145 into the LCP system [LCP1-MG-145, (n=11, m=3, r=7, s=8), LCP2-MG-145 (n=11, m=2, r=3, s=4), LCP3-MG-145 (n=11, m=3, r=3, s=8)]. Results from ELISA assay clearly showed that the LCP system dramatically increased the immunogenicity of this peptide in both the B10.BR and the B10.D2 mice (Figure 1).
Foot and mouth disease virus. Seven antigenic variants obtained from a single field isolate of FMDV serotype A12 differ only at residues 148 and 153 in the immuno-dominant loop of viral protein VP1. Synthetic peptides corresponding to the region 141-160 are highly immunogenic. We have synthesised and analyzed these seven

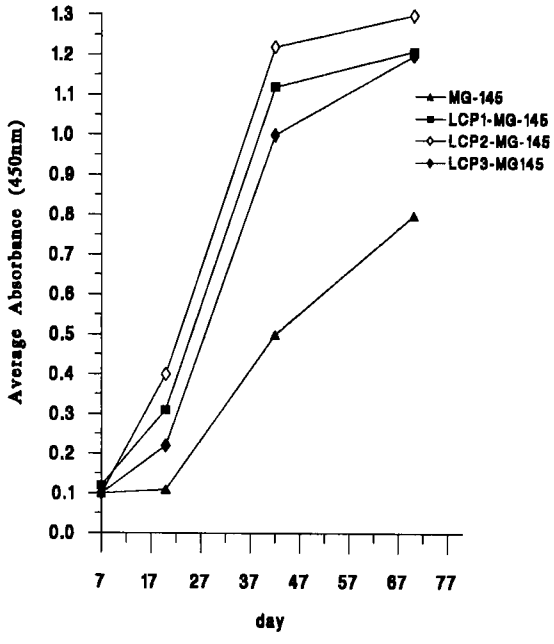

Figure 1. *Average absorbance (450nm) anti-MG-145, anti-LCP1-MG-145, anti-LC2P-MG-145 and anti-LCP3-MG-145 BR10.BR mouse serum at a dilution of 1:100.*

peptides corresponding to the immunodominant 141-160 sequence of VP1 to determine which substitutions are important with regard to antigenic specificity [3]. We have cyclized a peptide containing the 141-160 sequence *via* a disulphide bridge (cyclic-F5) and also incorporated F5 (^{141}GSGVRGDFGSLAPRVAR QL^{160}PC) to the LCP system (LCP-F5, n=11, m=3, r=7, s=8) and examined the immunogenicity of the compounds. LCP-F5 was administered without the use of any adjuvant, while the linear and cyclic forms of F5 were administered with Freund's adjuvants. LCP-F5 proved to be more immunogenic alone than the linear and cyclic peptides in Freund's adjuvants.

In summary. we have developed a novel vaccine adjuvant/carrier system which may be used to greatly enhance the immunogenicity of any potential peptide/vaccine epitope. Main advantages of the system are: (i) highly specific antibodies produced in high titres without the use of toxic adjuvants, (ii) vaccine and carrier are contained in a known molecular entity and can be synthesised easily in one complete step, using standard peptide synthetic protocols, (iii) compounds can be easily stored in a solid, stable form.

References

1. Zong, G., Toth, I., Reid, R., Brunham, R.C., *Journal of Immunology,* 151(7) (1993) 3728.
2. Pruksakom, S., Currie, B., Brandt, E., Martin, D., Galbraith, A., Phornphutkul, C., Hunsakunachai, S., Manmontri, A., Good, M.F., *Lancet,* 344 (1994) 639.
3. France, L.L., Piatti, P.G., Newman, J.F.E., Gibbons, W.A., Toth, I., Brown, F., *Proc. Nat. Acad. Sci. USA,* 91 (1994) 8442.

Peptides: Chemistry, Structure and Biology
Pravin T.P. Kaumaya and Robert S. Hodges (Eds.)
Mayflower Scientific Ltd., 1996

342
Cytolytic Processes Mediated by Biologically Active Peptides

E.Y. Blishchenko, O.A. Mernenko, I.I. Mirkina, D.K. Satpaev, N.M. Murashova, A.A. Karelin and V.T. Ivanov

Shemyakin-Ovchinnikov Institute of Bioorganic Chemistry, Russian Academy of Sciences, Moscow 117871, ul. Miklukho-Maklaya 16/10, Russia

Introduction

Tumor cell cytolysis has been associated with the action of the relatively small group of proteins, produced mainly by specialized killer cells. At the same time, a great number of substances, including the exogenous ligands of acetylcholine [1, 2], opiate [3] and tachikinine [4] receptors were demonstrated recently to induce cytolysis of tumor cells. To analyse the common pathways of cytolysis mediated by different substances we studied the cytolytic processes induced by a wide spectrum of peptides on different transformed cell lines.

Results and Discussion

Cytolytic activity of a large group of substances, including acetylcholine, opiate, and tachikinine receptor ligands was determined by Trypan blue inclusion method after 18 h of co-incubation with target cells . Cytolytic activity of each substance was examined in 10^{-7}-10^{-15} M concentration range. The mechanisms of DNA fragmentation were studied by agarose gel electrophoresis. The activity of these substances was compared with TNF, a well-characterized cytolytic protein. All cytolytic substances induced 1-4 discrete maxima of cytotoxicity, associated with different cytolytic processes, independently on cell line (Table 1).

Cytolytic processes induced by neurotoxin II from *Naja naja oxiana* cobra venom , substance P and TNF were studied within 1-8 hours of incubation and compared with valinomycin and its analogs. Distribution of cytolytic processes mediated by specific receptor-targeted substances differed significantly from the parameters of processes induced by peptides with non-receptoric action, valinomycin and its analogues. By use of the approach described we have obtained the following results:

1. Cytolysis of tumor cells can be induced by a wide spectrum of biologically active substances, acting through different receptor systems.
2. Comparative analysis of cytolytic processes induced by receptor-active and membrane-active (valinomycin and its analogs) peptides demonstrated significant differences in the mechanisms of cytolytic processes. At the same time cytolytic processes induced by receptor-active agents display a number of common characteristics for various cell lines.

Table 1. *Cytolytic processes induced at K562 (erythroid leukemia) and L929 (murine fibroblasts) tumor cells*[a].

Substance	Cell line	Concentration (M)											
		10^{-6}	10^{-7}	10^{-8}	10^{-9}	10^{-10}	10^{-11}	10^{-12}	10^{-13}	10^{-14}	10^{-15}	10^{-16}	10^{-17}
Neurotoxin II	K562	29A	11	2	8	10A	11	3	16A	23	22A	6	2
(Naja naja oxiana)	L929	0	15A	1	1	2	18	2	1	1	5	12A	1
Carbamylcholine	K562	18A	1	1	2	1	31A	2	1	18A	10	1	0
Tubocurarin	K562	4	18A	8	4	11	26A	12	1	10	21A	-	-
Atropine	K562	8	10	27A	13	11	24A	10	13A	11	12A	3	-
Neurotoxin II	K562	6	2	0	0	0	0	0	0	0	0	0	0
(carboxymethylated)	L929	4	0	0	0	0	-	-	-	-	-	-	-
Tumor Necrosis	K562	10A	6	4	14	16	22N	12	4	1	20N	18	1
Factor	L929	1	25A	13	2	24	33A	12	34	38A	30	50A	10
Met-Enkephalin	K562	-	4	4	4	7	4	6	9A	7	15A	2	0
Valorphin	K562	-	7	10N	7	1	2	12N	3	3	1	0	-
Neokyotorphin	K562	-	4	4	2	1	1	0	0	0	0	-	-
TSKY	K562	-	15	16	5	0	11	16	27	13	23	-	-
Substance P	K462	6	13	17A	1	3	6	11	26A	4	2	6A	0
	L929	3	2	1	2	1	4	6	12A	4	17A	11	1

[a] The reproducibility of results was tested in 10-15 experiments. The average deviation of results was < 3 %. Reliability of data obtained determined by Student's impaired t-test was $P < 0.05$. The maximal values of cytolytic activity are printed in bold. The mechanisms of DNA fragmentation are marked as A - apoptosis or N - necrosis.

The data obtained allowed us to develop screening criteria, which were used for further identification of biologically active peptides in lung extract. Low molecular weight fraction of acid extract of rat lung was separated by RP-HPLC and more than 140 components of this fraction were studied for cytotoxicity. About 12 % of isolated peptides induced specifically cytolysis of tumor cells. The amino acid sequences of nine peptides were determined. Seven cytolytic peptides were fragments of unknown proteins. The structure of one of the inactive components was identical to neo-kyotorphine (TSKYR), while its fragment (TSKY) was highly cytotoxic.

The results obtained show that cytotoxicity test can be used as a powerful tool for identification of biologically active substances.

References

1. Strizhkov, B.N., Blishchenko, E.Yu., Satpaev, D.K. and Karelin, A.A., *FEBS Lett.*, 37 (1994) 22.
2. Blishchenko, E. Yu. and Karelin, A.A., *Immunol. Lett.*, 42 (1994) 13.
3. Maneckjee, R. and Minna, J.D., *Cell Growth & Differentiation,* 5 (1994) 1033.
4. Reeve, J.G. and Bleehen, N.M., *Biochem. Biophys. Res. Commun.*, 199 (1994) 1313.

Peptides: Chemistry, Structure and Biology
Pravin T.P. Kaumaya and Robert S. Hodges (Eds.)
Mayflower Scientific Ltd., 1996

343
Biosensor Analysis of Antibody Binding to Branched Peptides Containing Two Antigenic Sequences

S. Fang[1], D.L. Jue[1], V. Udhayakumar[2], R.C. Reed[2], A.A. Lal[2] and R.M. Wohlhueter[1]

[1]Scientific Resources Program and [2]Division of Parasitic Dieases, National Center for Infectious Diseases, Centers for Disease Control and Prevention, Atlanta, GA 30333, USA

Introduction

In attempts to develop artificial malaria vaccines, we have synthesized various, four-branched peptides containing two different sequences. The immunogenicity of such large constructs is widely attested [1]. Our rationale for incorporating two sequences has been to enhance the immune response by providing T-cell epitopes or other targeting moieties along with a B-cell epitope. In this study, we focus on the antibody accessibility to epitopes of such constructs, using two B-cell epitopes, based on the circumsporozoite tandem repeat sequences of *Plasmodium falciparum* and a *Plasmodium vivax*-like variety of parasite [2]. The kinetics and equilibria of the binding of monoclonal antibodies to these epitopes were measured by means of a plasmon-resonance biosensor ("BIAcore", Pharmacia Biosensor) [3].

Results and Discussion

The branched peptide shown in the inset of Figure 1A, or linear peptides of the same sequences, were used as immobile ligands in the sensor cell. Mobile ligands were mAb "2A10" (specific for the NANP... branch) and mAb "VIV" (specific for the APGA... branch). Figure 1A shows detector traces for the association/dissociation of mAb VIV, at a series of concentrations. From the similarity of kinetic and equilibrium constants extracted from such data (K_D's $\approx$ 5 x 10^{-9}), we conclude that antibody binding is not influenced by epitope presentation in branched or linear form.

Figure 1B depicts an epitope mapping experiment, which tests the ability of the two mAb's to bind independently of one another. Prior binding of 2A10 does not affect subsequent (additive) binding of VIV. However, prior binding of VIV does block access of 2A10 to its specific site. Because neither mAb binds to the other's epitope in linear format (data not shown), the interference seems to be steric.

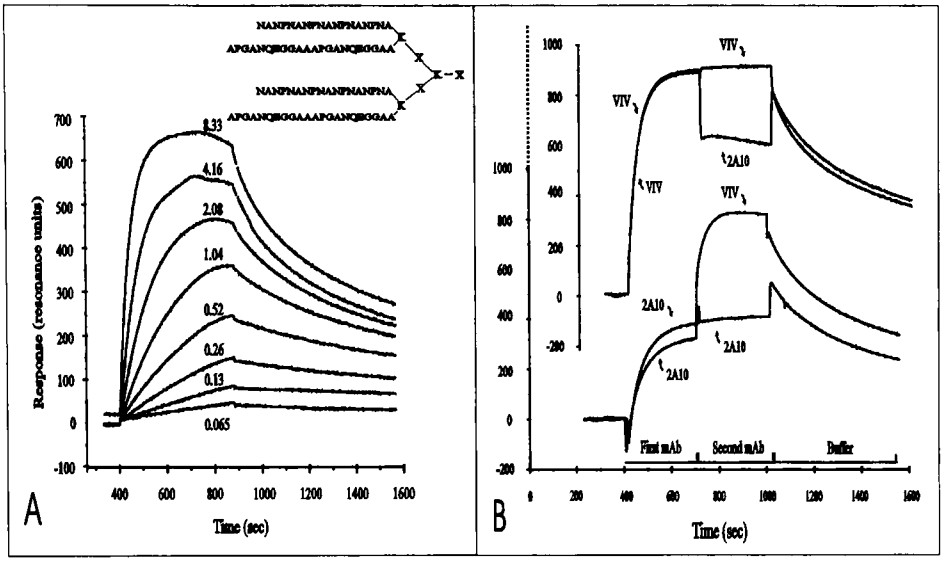

Figure 1. *A. Kinetics and equilibrium of VIV binding to a branched peptide (inset) in sensor cell. 30 µl of antibody solution was presented at 5 µl/min and 25°. The number on each curve gives the molar concentration of mAb. Kinetic constants were extracted by least square fitting. B. Tandem binding of the same or different mAbs. Conditions were similar to those in panel A, but a single saturating concentration of mAb was used.*

References

1. Tam, J., *Proc. Natl. Acad. Sci. USA,* 85 (1988) 5409.
2. Qari, S.H., Shi, Y.P., Goldman, I.F., Udhayajumar, V., Alpers, M., Collins, W.E. and Lal, A.A., *Lancet,* 341 (1993) 780.
3. Wohlhueter, R.M., Parekh, K., Udhayakumar, V., Fang, S. and Lal, A.A., *J. Immunol.* 153 (1994) 181.

Peptides: Chemistry, Structure and Biology
Pravin T.P. Kaumaya and Robert S. Hodges (Eds.)
Mayflower Scientific Ltd., 1996

344
A Conformationally Based Rational Design of Multiple Antigenic Peptide Carriers: The Potential for Disease Treatment

C. Sakarellos[1], V. Tsikaris[1], S. Kosma[1], M. Sakarellos-Daitsiotis[1], E. Vatzaki[2], S.J. Tzartos[2], M.T. Cung[3] and M. Marraud[3]

[1]Department of Chemistry, University of Ioannina, GR-45110, Ioannina, Greece
[2]Hellenic Pasteur Institute, 127 Vassilissis Sofias Avenue, GR-11521, Athens, Greece
[3]CNRS URA 494, ENSIC INPL, B.P. 451, F-54001, Nancy, France

Introduction

Conjugation of synthetic peptides to an artificial carrier has been applied to mimic protein-like globular structures for generating potent antigens or immunogens [1-3]. In this communication, we report on the design and synthesis of a new class of carriers in order to construct a novel Multiple Antigenic Peptide (MAP) system for potential disease treatment. To this end, the conformationally based (helical pattern) synthesis of a series of Sequential Oligopeptide Carriers (SOCs) formed by the Lys-Aib-Gly repeating unit has been successfully completed. Our goal is to provide carriers with a regular secondary structure, in which the antigens will not interact with each other, enhancing thus their original active conformation.

Results and Discussion

The sequential oligopeptide carriers (SOCs) have been synthesized step by step by solid phase on a Pam resin, followed by anchoring the antigenic peptides, also by solid phase (Figure1). The α67-76 fragment (MIR, Main Immunogenic Region) of the acetylcholine receptor (AChR) has been chosen as the antigenic peptide to treat Myasthenia Gravis. This design resulted in increased antibody recognition and optimization of the antigenic peptide concentration for a specific immunogenic response, for antibody depletion and for growing antibodies as potential vaccine candidates. Binding capacity of MAPs-SOCs was found to be ten times more enchanced compared to MIR and MIR analogues, suggesting that attachment of MIR on the SOCs can generate potent synthetic antigens. The conformational characteristics of the MAPs-SOCs were analyzed by ^{1}H NMR. The [Ala^{76}]-MIR decapeptides bound to the SOC_n showed a unique set of chemical shifts and NOE connectivities. This demonstrates that the [Ala^{76}]-MIR peptides, when bound to the SOC_n, are in the same magnetic environment, and probably do not interact with each other. Based on these preliminary biological immunoassays and conformational data we conclude that the helicoid pattern of our new class of SOCs favors the spatial orientation of the covalently bound antigenic peptides, so that potent antigens are efficiently recognized by the antibodies.

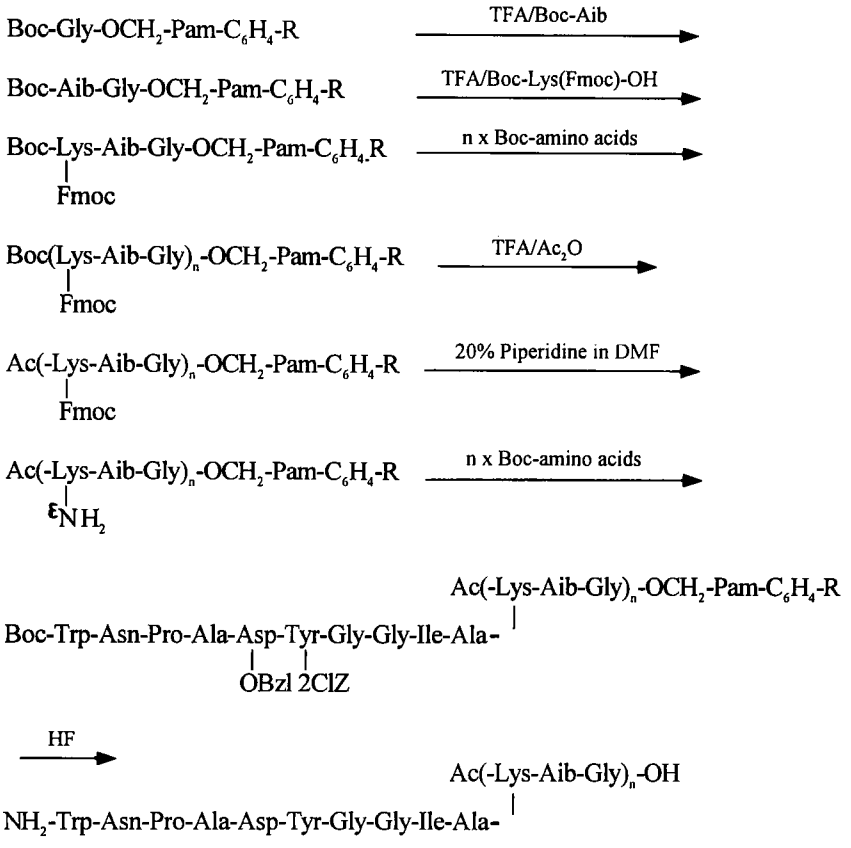

Figure 1. *Schematic representation of the synthesis of the [A[76]]MIR MAPs-SOCs.*

Acknowledgments

This work is dedicated to the memory of A.O. Mayomi and was supported by grants from EU, AFM and GSRT.

References

1. Tith, I., Hughes, R.A., Ward, P., Baldwin, M.A., Welham, K.J., McColm, A.M., Cox, D.M., Gibbons, W.A., *Intl. J. Pharm.*, 73 (1991) 259.
2. Tam, J.P., Lu, Y.A., *Proc. Natl. Acad. Sci. USA*, 86 (1989) 9084.
3. Metzger, J., Wiesmüller, KH., Schaude, R., Bessler, W.G., Jung, G., *Intl. J. Pept. Protein Res.*, 37 (1991) 46.

Peptides: Chemistry, Structure and Biology
Pravin T.P. Kaumaya and Robert S. Hodges (Eds.)
Mayflower Scientific Ltd., 1996

345
Development and Characterization of Antibodies Specific for Human Relaxin 2 (hRLX-2)

M. Meisenbach[1], F.P. Armbruster[1], S. Becker[1], H.J. Grön[2], G. Grübler[1], T.H. Lippert[1], G. Paulus[3] and W. Voelter[1]

[1]Abteilung für Physikalische Biochemie, Physiologisch-chemisches Institut der Universität Tübingen, Hoppe-Seylerstr.4, D-72076 Tübingen, Germany
[2]Immundiagnostik GmbH, Wiesenstr. 4, D-64625 Bensheim, Germany
[3] Shimadzu Europe GmbH, Albert-Hahn-Str. 6-10, D-47269 Duisburg, Germany

Introduction

The hormone relaxin, structurally related to insulin, is a polypeptide with a molecular weight of 6000 - 7000 dalton, depending on the species from which it has been isolated. There exists significant structural homology between different species (*e.g.* man, rat, pig) and also between the human relaxin, insulin, IGF-I and IGF-II. The main production site for relaxin is the corpus luteum graviditatis. However, it is also produced, in low concentrations, in the corpus luteum of non-pregnant woman. Also, relaxin or relaxin-like immunoreactive substances have been found in body fluids such as human milk and seminal plasma [1]. One of the main biological functions of relaxin is to facilitate delivery. The polypeptide inhibits the contractility of the myometrium and is responsible for the dilatation of the cervix. Besides these activities during pregnancy, the hormone seems to influence brain activity [2].

As a tool for the evaluation of the further biological relevance of hRLX-2, efficient specific antibodies are needed which are developed on the basis of prediction of antigenic sites [3] and experimental epitope mapping studies [4].

Results and Discussion

In the present study, two polyclonal antisera against human RLX-2 are characterized. The specificity of the antisera and the antigen-antibody interactions are determined by theoretical and experimental epitope mapping studies and both chains of relaxin were examined separately. According to the antigenic index calculations for the whole sequence of hRLX-2 only one single highly antigenic site is predicted, covering the amino acid residues 15-18 of the α-chain. However, results gained from experimental epitope mapping studies, using two polyclonal antisera gave evidence for at least two different epitopes in both chains. As the results show, the isolation of monospecific antibodies with hexapeptides located in an antigenic site region (fixed to Tentagel®) is more efficient, than sepharose bound peptides of the identical sequences, as probably in the latter case the active interacting sites for antibody binding become hidden as a result

of unspecific coupling reactions. The determination of the specificity of the isolated antibodies against the native hRLX-2 was carried out developing a radioimmunoassay with ^{125}J-labelled hRLX-2 as tracer. The described approach for gaining monospecific antibodies has several advantages compared to the production of monoclonal antibodies: i) polyclonal antibodies often have a higher affinity to the antigen compared to monoclonal ones, ii) the tedious development and production of monoclonal antibodies can be circumvented, and iii) several monospecific antibody populations might be isolated from one single antiserum. The highly specific antibodies, achievable with the described approach will be used as a new and valuable tool elucidating the recently discovered effects of relaxin on hypertension and tumor growth.

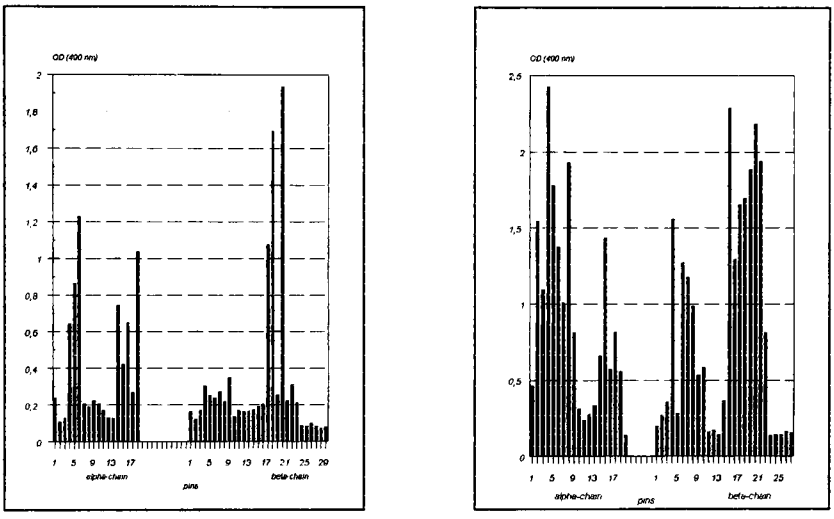

Figure 1. *Epitope mapping of relaxin, peformed with polyclonal antisera from rabbits against relaxin (on the left, rabbit 1); (on the right, rabbit 2); pins 1-18: hexapeptides of the α-chain; pins 1-29: hexapeptides of the β-chain.*

References

1. Lippert, T.H., Göd, B. and Voelter, W., *IRCS Medical Science*, 9 (1981) 295.
2. Osheroff, P.L. and Ho, W.H., *J. Biol. Chem.*, 268 (1993) 5193.
3. Voelter, W., Stoeva, S., Kaiser, T., Grübler, G., Mihelic, M., Echner, H., Haritos, A.A., Seeger, H. and Lippert T.H., *Pur. Applied Chem.*, 66 (1994) 2015.
4. Becker, S., Armbruster, F.P., Müller, B., Echner, H., Karpurniotu, A., Livaniou, E., Mihelic, M., Stoeva, S. and Voelter, W., *J. Immunol. Methods*, 177 (1994) 131-137.

Peptides: Chemistry, Structure and Biology
Pravin T.P. Kaumaya and Robert S. Hodges (Eds.)
Mayflower Scientific Ltd., 1996

346

Highly Efficient Multiple Peptide Synthesis and Characterization of Anchor and Non-anchor Residues on Peptide Binding to HLA Class I Molecules (HLA-B*3501)

K. Nokihara[1], M. Yamaguchi[1], C. Schönbach[2], M. Ibe[2], H. Shiga[2] and M. Takiguchi[2]

[1]Central Research Laboratory and Life Science Center of Shimadzu Corporation, Nakagyo-ku, 604 Kyoto, Japan
[2]Institute of Medical Science, University of Tokyo, Shirokanedai, Minato-ku, 108 Tokyo, Japan

Introduction

Human major histocompatibility complex class I molecules (HLA-I) bind endogenously processed self or viral peptides and present them to cytotoxic T cells. In the last decade, the direct association of peptides with the pocket-like structure of HLA-I has been demonstrated. The binding peptides generally consist of 8 to 10 amino acid residues [1] and two anchor residues are found within the peptide ligands [2, 3]. Previous studies showed that the anchors of self-peptides bound to HLA-B*3501 are at position 2 and the C-terminus [4]. We have recently developed an assay method suitable for screening large numbers of peptides by using flow cytometry with RMA-S cells transfected with HLA-genes [3]. The binding of peptides to HLA-I have been quantified by this assay system. The present paper will focus on highly efficient preparation of numerous peptides to refine anchor and non-anchor positions in the binding groove of HLA-B*3501.

Results and Discussion

Highly efficient preparation of *ca.* 200 peptides (8-12 AA) derived from virus proteins and their analogs was performed; *ca.* 120 peptides were binding peptides. Assembly of peptides was performed using a Shimadzu Model PSSM-8 [5]. C-terminal Pro-X peptides were easily obtained without special techniques and materials [6]. Fmoc amino acids were initially dissolved and pipetted into the amino acid station and pre-activated with HBTU. The rapid protocol with 10 min coupling times was employed. The peptides were obtained after simultaneous multiple cleavage followed by precipitation from ether. The crude peptides were characterized as good quality material by RP-HPLC and LSIMS or MALDI-TOF and used for the assay without further purification. The binding affinity was compared to that of self-peptide 37F (LPFDFTPGY) as described in [3]. A quantitative and statistic residue-pocket analysis at anchor and non-anchor positions was performed.

Amino acids were classified into four binding affinity classes and assigned ranks with a score of high (score 3), medium (score 2), low (score 1) and non-binders (score 0), respectively. Mean binding rank was calculated based on the score of each peptide. For these quantitative assays, the purity of the peptides is very important. We have also prepared peptide-mixtures (16 peptides with different sequences were contained in one synthesis column). However, this approach was not suitable for fine tuning of the binding characteristics. The binding of the octa-peptides was weaker than peptides with 9-12 amino acids, while these have similar affinity. Evaluation of binding affinity to HLA-B*3501 at position 9 of *ca.* 120 nona-peptides indicated that the side-chain aromatic ring (Tyr, Phe) at position 9 contributes more strongly to binding than aliphatic hydrophobic residues (Leu, Ile, Met), hence Tyr 9 showed the highest binding affinity, as previously found [7]. Position 2 renders another anchor for Pro. These residues were confirmed as a minimum requirement for binding. We have statistically analyzed binding characteristics in non-anchor positions (1 and 3~8) of nona-peptides to the HLA-B*3501. Positive and negative effects of non-anchor positions of nona-peptides was evaluated using *ca.* 120 peptides. The mean binding rank of each peptide was calculated using a Mann-Whitney U-test. Positive and negative effects on the binding between peptides and the above HLA molecules were determined and are summarized in Figure 1. Positive effects on the binding were found in amino acids with aliphatic side chain at positions 3 and 7, and in residues with side chain OH or SH groups at position 4. On the other hand, negative effects were observed in the non-bulky residues at the N-terminus and positively charged residues at positions 3, 5, and 7. Hence, each pocket fits, favors, or disfavors these residues. As the hydrogen-bond plays a crucial role for binding in the A-pocket of HLA-B*3501, non-bulky residues listed in Figure 1 do not form a suitable hydrogen-bond with Try of the A-pocket. Since position 4 is considered an auxiliary anchor [7], the present findings indicate that hydrophilic residues are favored at this position.

For the consideration of positive and negative effects, binding of nona-peptides to HLA-B*3501 was re-evaluated. Each residue was given a score of +1 for positive and -1

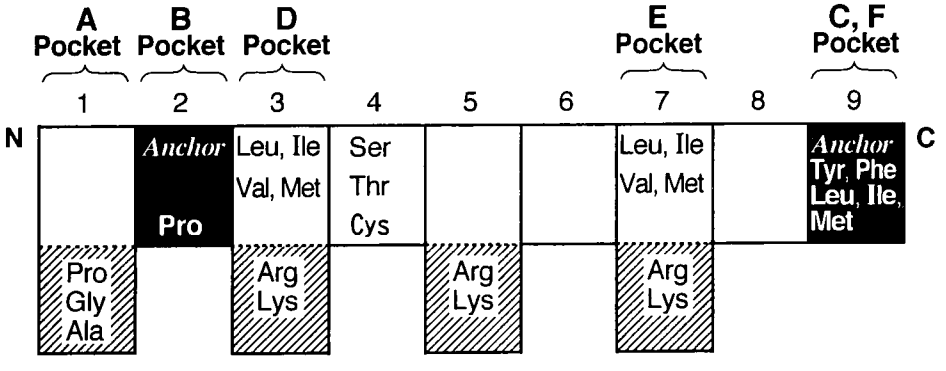

Figure 1. *Refined HLA-B*3501 binding motif for nona-peptides. Hatched residues in the lower panel are associated with low affinity to HLA-B*3501 and residues in the upper panel enhance binding to HLA-B*3501.*

for negative effects, so that the total score of each peptide indicated enhancement or reduction of binding. The ratio of HLA-B*3501 binding peptides was increased to more than 80% in peptides scoring more than 1, while that was decreased in peptides scoring less than -1. Thus, binding can be predicted by the positive and negative effects of non-anchor residues at positions 1, 3, 4, 5 and 7. In contrast with studies of peptide-binding to HLA-A2.1 by Ruppert *et al.* [8], the present studies with statistical analysis of the binding characteristics demonstrate that all residues corresponding to pockets play a prominent role in peptide binding to HLA-B*3501 and that a residue, which does not directly interact with pocket-residues, can play a dominant role in binding. Consequently, the refined binding motif of HLA-B35 will improve the efficiency of peptide epitope screening and provide new insight into interactions between HLA class I molecules and peptides.

References

1. Falk, K., Rötzschke, O., Stevanovic, S., Jung, G., Rammensee, H-G., *Nature*, 351 (1991) 290.
2. Elliot, T., Elvin, J., Cerundolo, V., Allen, H., Townsend, A., *Eur. Immunol.*, 22 (1992) 2085.
3. Takamiya, Y., Nokihara, K., Ferrone, S., Yamaguchi, M., Kano, K., Egawa, K. and Takiguchi, M., *Int. Immunol.*, 6, 255 (1994) 261.
4. Hill, A.V.S., Elvin, J., Willis, A.C., Aidoo, M., Allsopp, C.E.M., Gotch, F.M., Gao, M., Takiguchi, M., Greenwood, B.M., Townsend, A.R.M., McMichael, A.J. and Whittle, H.C., *Nature*, 360 (1992) 434.
5. Nokihara, K., Yamamoto, R., Hazama, M., Wakizawa, O. and Nakamura, S., in Epton, R. (Ed.), 'Innovation and Perspectives in Solid-Phase Synthesis 1992', Intercept Limited, Andover, 1992, p.445.
6. Nokihara, K., Kuriki, T., Yamada, H., Ando, E., Yokomizo, Y. and Yamaguchi, M., in Ohno, M.(Ed.), 'Peptide Chemistry 1994', Protein Research Foundation, Osaka, 1995, p.245.
7. Falk, K., Rötzschke, O., Grahovac, B., Schendel, D., Stevanovic, S., Jung, G. and Rammensee, H.G., *Immunogenetics*, 38 (1993) 161.
8. Ruppert, J., Sidney, J., Celis, E., Kubo, R.T., Gray, H.M. and Sette, A., *Cell*, 74 (1993) 929.

Mini Symposium I

Chairs: Teresa M. Kubiak and Tomi K. Sawyer

&

Mini Symposium II

Chairs: John W. Taylor and Susan Wang

Peptides: Chemistry, Structure and Biology
Pravin T.P. Kaumaya and Robert S. Hodges (Eds.)
Mayflower Scientific Ltd., 1996

347
Using Peptides to Dissect the Protein Folding Pathway of Lysozyme

J.J. Yang, M. Pitkeathly, L.J. Smith, T.A. Keiderling, K.A. Bolin, C. Redfield, C.M. Dobson and S.E. Radford

Oxford Centre for Molecular Sciences, New Chemistry Laboratory
University of Oxford, Oxford OX1 3QT, UK

Introduction

Hen lysozyme has been widely used as a model for studies of folding pathways and has been intensively studied using biophysical techniques such as mass spectrometry, hydrogen exchange pulse labelling and stopped-flow CD and fluorescence. A detailed folding pathway has been proposed [1] involving alternate folding routes and the presence of distinct folding domains of lysozyme (the α- and β- domains). The formation of a collapsed state within 5ms of refolding has been proposed based on the fact that deconvolution of the far UV CD suggests the presence of a native-like secondary structure content [2], that ANS fluorescence is enhanced most strongly at the earliest measurable time following initiation of folding and that the intrinsic Trp fluorescence of the states present at this time is resistant to quenching by iodide ions [1].

Peptide models have been used widely to study the folding pathways of proteins. The helical [3] and β-hairpin regions [4] of some proteins have been shown to have tendencies to form native-like structural elements even in isolation. The absence of the remainder of the protein in such peptides prevents acquisition of the native conformation in a co-operative manner and makes it possible to monitor the intrinsic conformational preferences of the sequence and to simplify the structural analysis of early folding intermediates. It has been proposed that the local conformational preferences of the peptides might play a very important role in the initiation of folding and in guiding the subsequent search of native-like conformational space. In this report, we describe studies by NMR and CD on several peptides from lysozyme to enable us to map possible folding initiation sites and model the early folding events in the lysozyme folding pathway.

Results and Discussion

Four peptides encompassing the entire amino acid sequence of hen lysozyme have been examined by far UV CD, and shown to have different conformational preferences in water [5-7]. In contrast to their similar helical contents in the native protein, two peptides from the α-domain in aqueous solution have very different structural

preferences. Thus, the peptide encompassing lysozyme residues 84-129 (Ac-LSSDITA SVNAAKKIVSDGNGMNAWVAWRNRC(Acm)KGTDVQAWIRGCRL-CO_2H), which contains the C (88-99), D (108-115) and the C-terminal 3^{10} (120-125) helices of the native structure, has been studied in detail using NMR and CD. Short peptides spanning each of the helices were also investigated. Within peptide 84-129 itself, regions which have remarkably different conformational preferences are observed. The first 21 residues appear predominantly unstructured, as judged by the small differences between observed CαH shifts and random coil values and the lack of medium range NOEs. Residues in the helix-D region of the peptide 84-129, however, display dramatically up field shifted CαH chemical shifts, a large number of medium range NOEs characteristic of helical structure, and three consecutive residues (Ala-110, Trp-111 and Arg-112) have $^3J_{HN\alpha}$ coupling constant values smaller than 6 Hz suggesting that they exist in a helical conformation. Finally, CαH chemical shifts and NOE patterns suggest that residues in the 3^{10} helix region also are helical in the long peptide.

Interestingly, the peptide 84-129 binds ANS with a concomitant large increase in fluorescence, suggesting that a significant hydrophobic surface exists in this peptide. This may arise from the interaction between the two structured regions revealed by the NMR studies, although there is no direct evidence that this is the case. We suggest, however, that a very early folding intermediate involving hydrophobic interactions within the D and 3^{10}-helices of lysozyme might serve as an initiation site in the folding of the intact protein.

References

1. Dobson, C.M., Evans, P.A. and Radford, S.E., *Phil. Trans. R. Soc. Lond. B* (1995) 17.
2. Chaffotte, A., Guillou, Y. and Goldberg, M.E., *Biochemistry*, 31 (1992) 9694.
3. Waltho, J.P., Feher, V.A., Merutka, G., Dyson, H.J. and Wright, P.E., *Biochemistry*, 32 (1993) 6337.
4. Cox, J.P.L., Evans, P.A., Packman, L.C., Williams, D.H. and Woolfson, D.N., *J. Mol. Biol.*, 234 (1993) 483.
5. Yang, J.J., Pitkeathly, M. and Radford, S.E., *Biochemistry*, 33 (1994), 7345.
6. Yang, J.J., Pitkeathly, M., Redfield, C., Dobson, C.M. and Radford, S.E., in Geisow, M. and Epton, R. (Eds), 'Perspectives on Protein Engineering & Complementary Technologies', Mayflower Worldwide Ltd., Birmingham, UK, 1994, p. 60.
7. Yang, J.J., Buck, M., Pitkeathly, M., Kotik, M., Haynie, D.T., Dobson, C.M. and Radford, S.E., *J. Mol. Biol.*, 252 (1995) 483.

Peptides: Chemistry, Structure and Biology
Pravin T.P. Kaumaya and Robert S. Hodges (Eds.)
Mayflower Scientific Ltd., 1996

348
Use of Retro-inverso Pseudopeptides for Mimicking Antigenic Sites and as Potential Synthetic Vaccines

G. Guichard

Institut de Biologie Moléculaire et Cellulaire, UPR 9021 CNRS,
15 rue Descartes, F-67084 Strasbourg Cédex, France

Introduction

Peptides have been shown to be particularly attractive in the design of potential synthetic vaccines. However, they are usually poorly immunogenic and the extent of cross- reactivity between the peptide and the epitopes of virus particles is often very limited. Another major problem limiting the use of peptides as vaccine is their instability. Pseudopeptides, because they are more stable to proteolysis could be a useful alternative to peptides as immunogens.

To study the usefulness of this approach, we have first characterized the antigenic and immunogenic properties of a retro-inverso analogue of a model hexapeptide of sequence IRGERA corresponding to the C-terminal residues 130-135 of histone H3 [1, 2]. The retro-inverso analogue which contains NH-CO bonds instead of natural peptide bonds was found to mimic the antigenic and immunogenic properties of the parent L-peptide [3]. This result prompted us to analyze the potential of retro-inverso peptides as possible candidate vaccines using as model the immunodominant epitope of foot and mouth disease virus (FMDV) located in residues 141-159 of the surface protein VP1.

Results and Discussion

We synthesized end group modified retro-inverso analogues of two synthetic peptides corresponding to two variants of serotype A, subtype 12 which differ only at position 153 (Table 1). A close mimicry of the COOH-terminus was achieved by using a malonate derivative which was incorporated into the peptide chain as a racemate, thereby generating a pair of diastereoisomers which could be separated by HPLC. The more rapidly eluted retro-inverso isomer was labelled RIa and the other one RIb.

Table 1. *Sequences of the parent peptides and retro-inverso analogs of two FMDV variants.*

	Name	Sequences (lower case letters indicate D-amino acids.)
FP	[Cys]^{140}FP(141-159)	C-G^{141}-S-G-V-R-G-D-**F**-G-S-L-A-**P**-R-V-A-R-Q-L^{159}
variant	RIa- and RIb-peptides	HO-m(R, S)Leu-q-r-a-v-r-**p**-a-l-s-G-**f**-d-G-r-v-G-s-G-c-NH_2
FL	[Cys]^{140}FL(141-159)	C-G-S-G-V-R-G-D-**F**-G-S-L-A-**L**-R-V-A-R-Q-L
variant	RIa- and RIb-peptides	HO-m(R, S)Leu-q-r-a-v-r-l-a-l-s-G-**f**-d-G-r-v-G-s-G-c-NH_2

The capacity of guinea pig antisera to intact FMDV particles, VP1 protein and parent peptide of variant FP and FL to recognize the corresponding RIa, RIb and L-peptide was also tested in ELISA. The retro-inverso peptides reacted as strongly as, or sometimes even better than, the L-peptides in these assays.

Antibodies to retro-inverso peptides were produced by injecting rabbits with pseudopeptides covalently coupled to small unilamellar liposomes containing mono-phosphoryl lipid A as adjuvant. A long-lasting antipeptide IgG response was obtained and antibodies were shown to strongly cross-react with the parent L-peptide [3].

Futhermore, the ability of the various anti-retro inverso analogues sera to recognize intact FMDV particles was tested. (Figure 1).

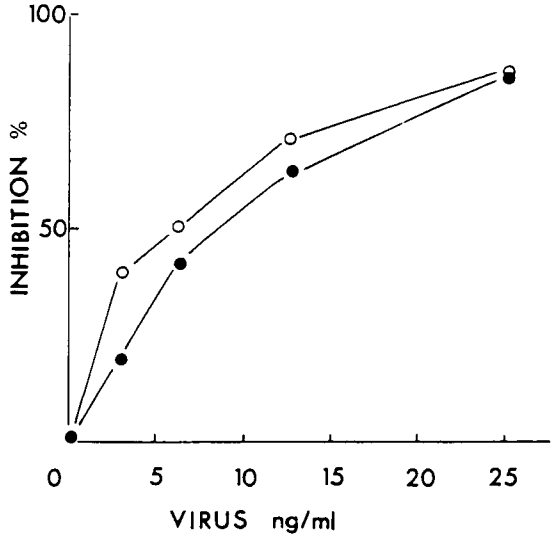

Figure 1. *Inhibition of the ELISA reaction between rabbit antisera to FMDV (variant FP) peptides and FP-RIb peptide BSA conjugate (2μM) by increasing concentration of FMDV (variant FP). (○): antiserum to L-peptide; (●): antiserum to RIb peptide. Antisera were diluted 1:32,000.*

As shown in Figure 1, antibodies to the RIb peptide recognized intact FMDV particles as well as did the L-peptide which suggests that retro-inverso peptides may be useful reagents for inducing a neutralizing anti-viral response.

References

1. Guichard, G.., Benkirane, N., Zeder-Lutz, G., Van Regenmortel, M.H.V., Briand, J.P. and Muller, S., *Proc. Natl. Acad. Sci. USA*, 91 (1994) 9765.
2. Benkirane, N., Guichard, G., Van Regenmortel, M.H.V. Briand, J.P. and Muller S., *J. Biol. Chem.*, 270 (1995) 11921.
3. Muller, S., Guichard, G., Benkirane, N., Brown, F., Van Regenmortel, M.H.V. and Briand, J.P., *Peptide Research*, 8 (1995) 138.

Peptides: Chemistry, Structure and Biology
Pravin T.P. Kaumaya and Robert S. Hodges (Eds.)
Mayflower Scientific Ltd., 1996

349

The Effects of Different Salts on the Role of Interhelical Electrostatic Repulsions in the Stability of Two-stranded α-Helical Coiled-coils

W.D. Kohn, O.D. Monera, C.M. Kay and R.S. Hodges

Department of Biochemistry and the Protein Engineering Network of Centres of Excellence, University of Alberta, Edmonton, Alberta, T6G 2H7, Canada

Introduction

Model two-stranded α-helical coiled-coils have proven useful for studying the principles of protein folding and stability involving both interchain and intrachain interactions [1]. The coiled-coil motif is characterized by a heptad repeat denoted as *abcdefg*, where positions *a* and *d* are occupied by hydrophobic residues and positions *e* and *g* by charged residues. Interchain electrostatic interactions between residues at the *e* and *g* positions have been shown to be important for determining coiled-coil dimerization specificity and stability [2, 3]. We have previously shown that an interchain i - i'+5 Glu-Glu repulsion between position *g* of one helix and *e'* of the other destabilizes the coiled-coil by 0.45 kcal/mol [4]. In this study we demonstrate the abilities of different salts to modulate the effects of these interchain electrostatic repulsions on coiled-coil formation and stability.

Results and Discussion

A native 35 residue peptide (denoted as Nx, Table 1), which contains no interchain or intrachain electrostatic interactions and contains neutral Gln residues at all the e and g

Table 1. *Sequences of the synthetic peptides used in this study*.*

Peptide Name	Interface Charge	Amino Acid Sequence
		1 5 10 15 20 25 30 35 g a b c d e f g a b c d e f g a b c d e f g a b c d e f g a b c d e f
Nx	**0**	Ac-Q-C-G-A-L-Q-K-Q-V-G-A-L-Q-K-Q-V-G-A-L-Q-K-Q-V-G-A-L-Q-K-Q-V-G-A-L-Q-K-amide
E4x	**-8**	Ac-E-C-G-A-L-E-K-E-V-G-A-L-E-K-Q-V-G-A-L-Q-K-Q-V-G-A-L-Q-K-Q-V-G-A-L-Q-K-amide
E6x	**-12**	Ac-E-C-G-A-L-E-K-E-V-G-A-L-E-K-E-V-G-A-L-E-K-Q-V-G-A-L-Q-K-Q-V-G-A-L-Q-K-amide
E8x	**-16**	Ac-E-C-G-A-L-E-K-E-V-G-A-L-E-K-E-V-G-A-L-E-K-E-V-G-A-L-E-K-Q-V-G-A-L-Q-K-amide
E10x	**-20**	Ac-E-C-G-A-L-E-K-E-V-G-A-L-E-K-E-V-G-A-L-E-K-E-V-G-A-L-E-K-E-V-G-A-L-E-K-amide

The mutants are named according to the number of Glu substitutions for Gln (shown in boxes) at the **e and **g** positions of the heptad repeat. All peptides contain a Cys residue at position 2, allowing formation of an interchain 2-2' disulfide bridge, designated by an x in the peptide name.*

positions, forms a stable two-stranded coiled-coil in benign 0.1M KCl, 50mM PO_4, pH 7 buffer with molar ellipticity at 220 nm $[\theta]_{220}$ = -32000 deg·cm^2/dmol. A series of analogs with varying numbers of substitutions of Glu for Gln were synthesized, leading to coiled-coils with a systematic increase in interchain repulsion. This correlated with a gradual loss of both helical content and stability as determined by urea denaturation studies.

The salts KCl and $LaCl_3$ both induced greater helical structure in the peptides. Thus, E10x, which displayed little helix in benign buffer $[\theta]_{220}$ = -1500, was induced to a maximum helical content of -28000 by addition of 2 M KCl while -33000 was obtained with only 50 mM $LaCl_3$. These salts also had dramatically different effects on the stability of the series of coiled-coils Nx - E8x as indicated by the urea denaturation profiles (Figure 1). While a high concentration of KCl was capable of overcoming the effects of interhelical charge repulsion on helical content, it could not overcome the effects of the repulsions on the apparent stability as indicated by the significant difference in the midpoints of the urea denaturation profiles ($[Urea]_{1/2}$, Figure 1A). In contrast, $LaCl_3$, present at only 50 mM fully suppressed the effects of interchain repulsions on coiled-coil stability as shown by the identical $[Urea]_{1/2}$ values (Figure 1B).

These results indicate that KCl cannot effectively mask interchain repulsions, but at high concentration can induce coiled-coil formation through the promotion of a greater hydrophobic effect. This greater hydrophobic effect is evident in the increase of the $[Urea]_{1/2}$ value of Nx from 6 M in low salt (0.1 M KCl) to 8.4 M in the high salt (3 M KCl) conditions of Figure 1A. $LaCl_3$ masks the effects of repulsions on both structure and stability at low concentrations. There appears to be direct interaction between La^{3+} ion and the charged Glu side-chains of the coiled-coils,which does not occur with K^+.

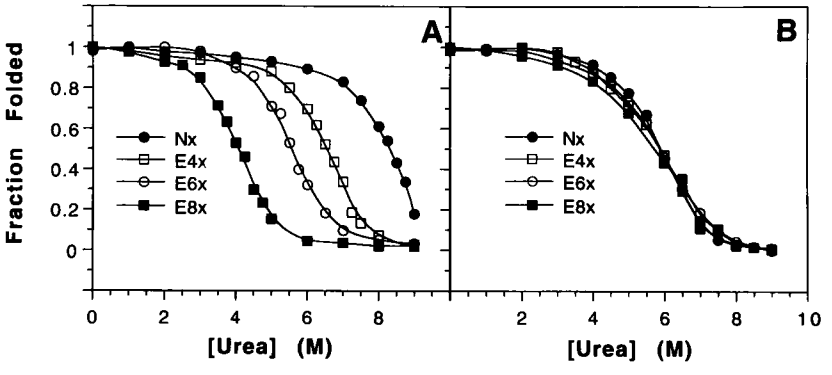

Figure 1. *Urea denaturation profiles at 20°C and pH 7. A, 50 mM PO_4, 3 M KCl buffer (ionic strength, μ = 3). B, 20 mM imidazole, 100 mM KCl, 50 mM $LaCl_3$ buffer (μ = 0.3). Fraction folded was determined from the molar ellipticity at 220 nm [4].*

References

1. Zhou, N.E., Zhu, B.Y., Kay, C.M. and Hodges, R.S., *Biopolymers*, 32 (1992) 419.
2. Zhou, N.E., Kay, C.M. and Hodges, R.S., *J. Mol. Biol.*, 237 (1994) 500.
3. Krylov, D., Mikhailenko, I. and Vinson, C., *EMBO J.*, 13 (1994) 2849.
4. Kohn, W.D., Kay, C.M. and Hodges, R.S., *Protein Science*, 4 (1995) 237.

Peptides: Chemistry, Structure and Biology
Pravin T.P. Kaumaya and Robert S. Hodges (Eds.)
Mayflower Scientific Ltd., 1996

350
Use of Topographical Modifications of Peptides to Examine Biological Mechanisms such as Prolongation

C. Haskell-Luevano[1], L.W. Boteju[1], H. Miwa[2], C. Job[1], F. Al-Obeidi[1], I. Gantz[2], M.E. Hadley[3] and V.J. Hruby[1]

Departments of [1]Chemistry and [3]Anatomy, University of Arizona, Tucson, AZ 85721, USA
[2]University of Michigan Medical Center, Ann Arbor, MI 48109, USA

Introduction

α-Melanotropin (Ac-Ser-Tyr-Ser-Met-Glu-His-Phe-Arg-Trp-Gly-Lys-Pro-Val-NH_2) is recognized for its role in skin darkening and has been the target of extensive structure-function studies for several decades. These analogues have been bioassayed to monitor relative potency and in some cases to examine a biological phenomena termed "prolongation," or residual activity. This phenomena of prolongation has been shown in our laboratories not to directly correlate with relative ligand efficacy, receptor specificity, ligand potency or enzyme stability. Therefore, peptides possessing this desired property could not be previously designed. We have designed and synthesized peptides incorporating the four isomers of β-MeTrp at position nine in a superpotent monocyclic peptide template [1, 2]. These peptides have exhibited differences in their topographical structure and ability to produce prolonged biological activity.

Results and Discussion

The peptides based on the template cyclo(Asp^5,Lys^{10})Ac-Nle^4-Asp^5-His^6-$DPhe^7$-Arg^8-β-$MeTrp^9$-Lys^{10}-NH_2 [1, 2] exhibited remarkable differences in their ability to maintain prolonged biological activity (Figure 1 next page). Table 1 (below) lists bioassay results. To further study the mechanism(s) that may be responsible for prolongation, dissociation properties from the melanocortin receptor, hMC1R [3, 4], were examined. These results

Table 1. *Biological results of the β-MeTrp-containing cyclic α-MSH(4-10) analogs.*

Isomer	Frog Skin EC_{50}(nM)	hMC1R Binding IC_{50}(nM)	hMC1R cAMP EC_{50}(nM)	hMC1R % Ligand Bound after 4 hours
(2R,3R) β-MeTrp	0.30	2.00	0.40	27
(2R,3S) β-MeTrp	0.06	3.00	1.00	16
(2S,3R) β-MeTrp	28.60	15.00	3.00	12
(2S,3S) β-MeTrp	0.44	0.50	0.30	72

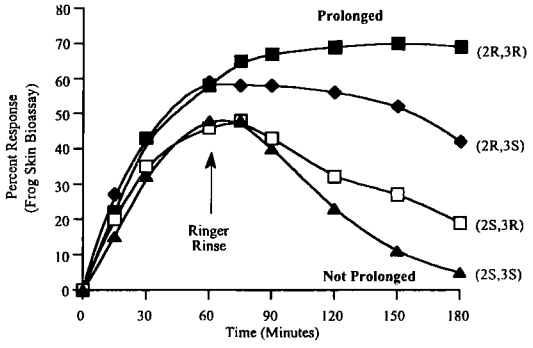

Figure 1. *Prolongation properties of cyclo(Asp,Lys)Ac-Nle-Asp-His-DPhe-Arg-β-MeTrp^9-Lys-NH_2 peptides.*

show that after the ligands have been removed from the assay medium for 4 hours, the (2S,3S) β-MeTrp-containing peptide remained 72% bound to the receptor. Remarkably, the relative dissociation rates (t½) observed for the peptides were of the order of hours. Conformational and topographical studies by ^{1}H NMR showed that the peptides possess similar peptide backbone conformations, with the primary structural differences occurring in the sidechain $\chi 1$ rotomer populations (Table 2).

Table 2. *Major sidechain rotomer population of the message residues in the β-MeTrp containing peptides.*

Isomer	DPhe	Arg	β-MeTrp
(2R,3R) β-MeTrp	trans	trans	gauche (+)
(2R,3S) β-MeTrp	gauche (+)	trans	gauche (+)
(2S,3R) β-MeTrp	trans	trans	trans
(2S,3S) β-MeTrp	trans	trans	gauche (-)

We conclude from these studies that the topography of the message residues DPhe-Arg-β-MeTrp, are responsible for the slow dissociation rates (hours) from the melanocortin receptor and that these topographical features can modulate prolonged biological activity. In addition, these results suggest that topographical modifications can be designed into compounds destined for clinical applications to also possess prolonged biological activities. This study was supported by a grant from the USPHS.

References

1. Al-Obeidi, F., Hadley, M.E., Pettitt, B.M. and Hruby, V.J., *J. Am. Chem. Soc.*, 111 (1989) 3413.
2. Haskell-Luevano, C., Miwa, H., Dickinson, C., Hruby, V.J., Yamada, T. and Gantz, I., *Biochem. Biophys. Res. Commun.*, 204 (1994) 1137.
3. Mountjoy, K.G., Robbins, L.S., Mortrud, M.T. and Cone, R.D., *Science*, 257 (1992) 1248.
4. Chhajlani, V. and Wikberg, J.E.S., *FEBS Lett.*, 309 (1992) 417.

Peptides: Chemistry, Structure and Biology
Pravin T.P. Kaumaya and Robert S. Hodges (Eds.)
Mayflower Scientific Ltd., 1996

351
Synthesis of 3- and 4-Mercaptoproline-containing Peptides Directed Toward Peptidomimetic Design

S.A. Kolodziej[1] and G.R. Marshall[2]

[1]*Monsanto Company, St. Louis, MO 63167, USA*
[2]*Center for Molecular Design, Washington University, St. Louis, MO 63130, USA*

Introduction

The synthesis of conformationally constrained analogs of biologically active peptides plays an important role in the study of peptide-receptor interactions. We have found that 3- and 4-mercaptoprolines are useful synthetic tools for introducing conformational constraints [1-4]. Replacement of a Cys or Hcy residue in a cyclic disulfide peptide by mercaptoproline results in a highly constrained bicyclic analog [1-3]. Alternatively, alkylation of mercaptoproline generates a constrained sidechain analog of an amino acid [4]. The introduction of a sulfur atom onto the pyrrolidine ring of proline generates an additional chiral center, thus *cis* and *trans* diastereomers are possible for both 3-mercaptoproline (3-MPc and 3-MPt) and 4-mercaptoproline (4-MPc and 4-MPt). Therefore, it is essential to have access to peptides containing all possible stereoisomers to completely assess the effect of substitution mercaptoproline at a given position.

Results and Discussion

We have previously reported synthetic routes to 4-MPt/c derivatives as pure enantiomers and 3-MPt/c as racemic mixtures [3, 4]. We now report a stereoselective route to the 3-MPt/c derivatives **1** and **2** based on the previously reported approach to 4-MPt/c (Scheme 1). The *cis*-3-hydroxyprolinol **3**, reported by Joullie and coworkers [5], was

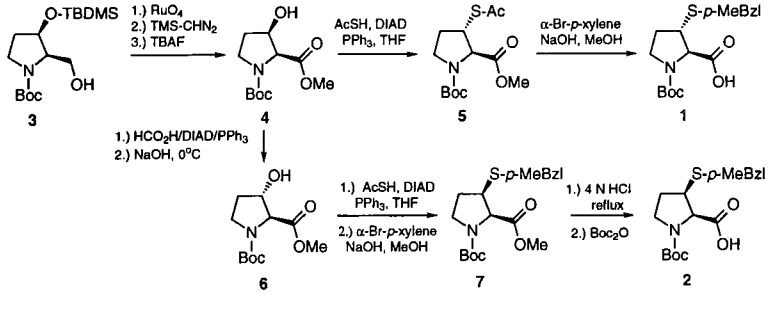

Scheme 1. *Stereoselective route to 3-MPt/c derivatives.*

readily converted to **4** in three steps with an overall yield of 68%. Reaction of **4** with thiolacetic acid under Mitsunobu conditions yielded thiolacetate **5**, which was converted to **1** in a one-pot transformation with an overall yield of 49%. Epimerization of **4** and further transformation as described for **1** yielded **7**. Cleavage of the methyl ester required an acidic hydrolysis, which also resulted in loss of the N-Boc group. Reprotection with Boc_2O afforded **2** in an overall yield of 19% from **3**.

We have previously reported the use of 3- and 4-MPt/c derivatives in the SPPS of analogs of bradykinin [1], ATII [2], and CCK [4]. Replacement of Met^2 in Ac-CCK_4 by 3- and 4-alkylthioprolines yielded several potent CCK-B selective analogs. In an effort to obtain a CCK-A selective analog, the four stereoisomers of Ac-CCK_4[3-mercaptoproline^2] were alkylated with a 2-ethyl *o*-toluyl urea (ETU) moiety, based on the CCK-A agonist Boc-CCK_4[Lys(Tac)^2] reported by Shiosaki *et al.* [6]. Only one stereoisomer, Ac-CCK_4 [L-3-MPc(ETU)^2], showed high affinity for the CCK-A receptors (IC_{50} = 16 nM). However, this analog proved to be an antagonist in functional assays. The implications of this analog for the CCK-A receptor-bound conformation will be published elsewhere. We have also used 3-MPt to design constrained analogs of CCK_7 that bind with high affinity at δ-opioid receptors using a model of the receptor-bound conformation of DPDPE-[7]. This study demonstrates the possibility of using three-dimensional models as templates for rational drug design. Also, an additional analog, DPDPE[L-3-MPt^5], was synthesized based on these results and shown to possess high affinity for the δ-opioid receptors (K_i=3.5 nM). Conformational analysis of this analog is reported in these proceedings [8].

Acknowledgments

The authors thank the National Institutes of Health for partial support of this work (GM48184) and for support of SAK in the form of a Postdoctoral Training Grant in Neuropharmacology (T32 NS07129). They also acknowledge the use of the facilities at the Washington University Mass Spectroscopy Resource (NIH grant RR00945). Thanks to J. Martinez and B. Nock for biological assays, and G. Nikiforovich for computer modeling studies and useful discussions.

References

1. Kaczmarek, K., Li, K.M., Skeean, R., Dooley, D., Humblet, C., Lunney, E., Marshall, G.R., in, Hodges, R.S. and Smith, J.A. (Eds.), 'Peptides: Chemistry, Structure and Biology', ESCOM, Leiden, The Netherlands, 1994, p. 687.
2. Plucinska, K., Kataoka, T., Yodo, M., Cody, W.L., He, J.X., Humblet, C., Lu, G.H., Lunney, E., Major, T.C., Panek, R.L., Schelkun, P., Skeean, R., Marshall, G.R., *J. Med. Chem,*. 36 (1993) 1902.
3. Kataoka, T., Beusen, D.D., Clark, J.D., Yodo, M., Marshall, G.R., *Biopolymers*, 32 (1992) 1519.
4. Kolodziej, S.A., Nikiforovich, G.V., Skeean, R., Lignon, M.F., Martinez, J., Marshall, G.R., *J. Med. Chem.*, 38 (1995) 137.
5. Ewing, W.R. and Joullie, M.M., *Heterocycles*, 27 (1988) 2843; Heffner, R.J. and Joullie, M.M., *Tetrahedron Lett.*, 30 (1989) 7021.

Peptides: Chemistry, Structure and Biology
Pravin T.P. Kaumaya and Robert S. Hodges (Eds.)
Mayflower Scientific Ltd., 1996

352

Intramolecular Acylation as a General Scheme for Chemical Ligation of Large, Unprotected Peptide Segments

C.F. Liu, C. Rao and J.P. Tam

Department of Microbiology and Immunology, Vanderbilt University, A5119 MCN, Nashville, TN 37232, USA

Introduction

For the past several years, an important advance in peptide chemistry has been the development of chemical ligation approaches using unprotected peptide segments as building blocks. Among these, particularly promising are those methods that utilize the proximity-driven intramolecular acylation as an alternative for the formation of peptide bonds [1-3], a principle first put into practice by Kemp *et al.* [1]. Using such approaches, the intrinsic entropic barrier of the intermolecular peptide bond-forming process is bypassed and the need of protection avoided due to the high chemoselectivity and regiospecificity of the reactions involved. We previously introduced a ligation method using an acyl glycolaldehyde ester for the capture with an N^{α}-Cys-peptide and O,N-acyl transfer to generate a proline-like structure at the ligation site [2]. This approach has been successfully applied to the syntheses of several active analogs of the HIV-1 protease through ligation at an Xxx-Pro bond. Recently, we designed a new method in which the key step is the specific capture of the C^{α}-thiol carboxylic acid of the first peptide by the activated side chain thiol of the Cys residue of the second peptide, bringing the two reacting groups engaged in peptide bond formation into close proximity to allow fast intramolecular acylation through a 6-member ring transition state. The resulting S-sulfhydryl (S-SH) is then removed by reduction to give the native Cys residue at the ligation site (Figure 1).

Results and Discussion

The first capture step involves a well-established and documented reaction which has been widely used for the formation of unsymmetrical disulfides in peptide synthesis. The subsequent intramolecular acylation involving a 6-member ring intermediate is an extremely fast reaction and has not been exploited so far for peptide bond formation. Model studies showed that reaction of Z-Gly-SH with Tfa·H-Cys(Npys)-Ala-OMe at pH 5-7 gave immediately Z-Gly-Cys(SH)-Ala-OMe. The intermediate acyl-disulfide was not detected because of the high rate of rearrangement. Z-Gly-Cys-Ala-OMe with a free SH was easily obtained by treating Z-Gly-Cys(SH)-Ala-OMe with DTT or trialkyl phosphine with release of H_2S. It is worthwhile to emphasize the high efficiency of this ligation scheme. In our syntheses of moderate to large peptides, we found that the

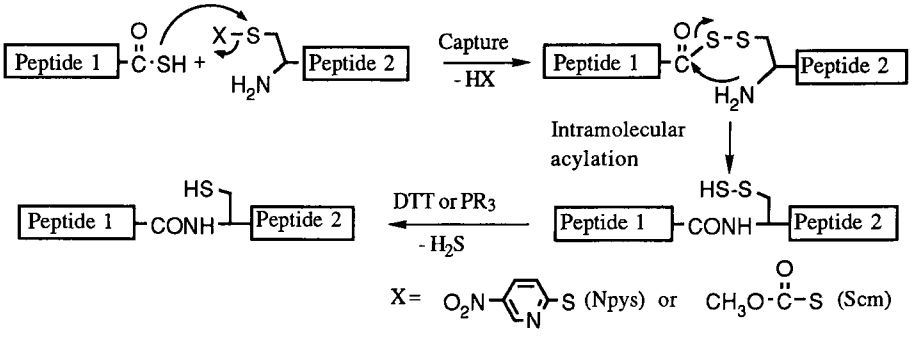

Figure 1. *A chemical ligation scheme involving intramolecular acylation.*

reaction of a thiol carboxylic acid with a Npys-or Scm-modified thiol was extremely fast and completed almost instantly upon mixture of two components even at pH as low as 1.5 - 2, while the molar concentrations of two components were in the micromolar range. This high reactivity is due both to the activated feature of a disulfide formed with the Scm or Npys group and to the low pKa value of the thiol carboxylic acid. For the intramolecular acylation, its efficiency is due to first, the close proximity of the α-acyl and α-amine and second, to the activation of the α-acyl carbonyl once the acyl disulfide was formed. The final reduction step was indispensible to afford the native Cys residue at the end of synthesis. Another interesting property of the S-SH product after rearrangement was its tendency to form tri- and tetrasulfides through disulfide exchange and oxidation. However, these side products had no effect on ligation yield since they were all converted to the desired Cys product upon reduction. The efficiency and specificity of this strategy makes it an attractive approach for the synthesis of proteins involving ligation of very large unprotected peptide segments of which relative low molar concentrations are expected. Although it is strategically close to the thiol-capture scheme developed by Kemp *et al.* who used a tricyclic dibenzofuran template to mediate the O,N-acyl transfer [1], our scheme does not use a template, and is therefore a thiol-capture strategy in the simplest form.

Acknowledgments

This work was in part supported by NIH grants CA35577 and CA36544.

References

1. Kemp, D.S. and Carey, R.I., *J. Org. Chem.*, 58 (1993) 2216.
2. (a) Liu, C-F. and Tam, J.P., *J. Am. Chem. Soc.*, 116 (1994) 4149. (b) Liu, C-F. and Tam, J.P., *Proc. Natl. Acad. Sci. USA*, 91 (1994) 6584.
3. Dawson, P.E., Muir, T.W., ClarkLewis, I. and Kent, S.B.H., *Science*, 266 (1994) 776.

Peptides: Chemistry, Structure and Biology
Pravin T.P. Kaumaya and Robert S. Hodges (Eds.)
Mayflower Scientific Ltd., 1996

353
Coupling of Ion Transport Processes and Signal Transduction Pathway to Trigger Colonic Paracellular Peptide Transport

W.C. Yen and V.H.L. Lee

University of Southern California, School of Pharmacy, Los Angeles, CA 90033, USA

Introduction

Directing peptide drug transport toward the paracellular pathway as a means to improve their oral absorption has recently gained interest due to the low enzymatic activity in the intercellular space. Previous studies have revealed that 4-phenylazobenzyloxycarbonyl-Pro-Leu-Gly-Pro-D-Arg (Pz-peptide), which was highly susceptible to intracellular collagenase action in the rabbit descending colon, penetrated exceedingly well there without the use of penetration enhancers and protease inhibitors [1]. It was hypothesized that this pentapeptide facilitates its own penetration by loosening the tight junctions between epithelial cells. The present study has three aims: (a) to demonstrate that Pz-peptide penetrates the colonic mucosa by a para- cellular mechanism, (b) to identify the cellular locus where Pz-peptide acts to facilitate paracellular transport, and (c) to elucidate the intracellular cascade of tight junctional opening elicited by Pz-peptide.

Results and Discussion

Pz-peptide at 3 mM induced 2 fold and 1-7-fold increase in the transport of paracellular marker mannitol (MW = 180, 3.6 Å) and FITC-dextran 4,000 (FD-4, MW = 4,000, 14 Å), respectively, in the rabbit descending colon. Furthermore, the effect of 3 mM Pz-peptide on junctional permeability was only observed from the mucosal to serosal direction as indicated by a 26% decrease in transepithelial electrical resistance (TEER), a measurement of paracellular permeability, in intestinal epithelial cell monolayers Caco-2.

Electrogenetic Na^+ absorption in the rabbit colon is known to be mediated by amiloride sensitive Na^+ channels on the apical membrane [2]. Expansion in the junctional dimension occurs when water flow across tight junctions is enhanced by increasing Na^+ influx into the cell [3]. It was hypothesized that Pz-peptide may activate Na^+ channels, resulting in solvent drag, thereby enhancing junctional permeability and transport of paracellular markers. This possibility was supported by reversal in enhancement in permeability of hydrophilic markers and decrease in Pz-peptide transport by an apical Na^+ channel blocker amiloride or removal of Na^+ ions from the mucosal solution in the descending colon (Table 1). We hypothesized that Pz-peptide enhanced paracellular permeability by activation of Na^+ transport followed by a rise of intracellular Ca^{2+}, $[Ca^{2+}]_i$, mediated by inositol 1,4,5-triphosphate (IP_3). This hypothesis was supported by 3 mM Pz-peptide-induced increase in IP_3 and $[Ca^{2+}]_i$ (Figure 1).

Table 1. *Modulation of Na^+ ions on Pz-peptide-induced increased in paracellular permeability (Mean ± s.d., n = 3. *: statistical significance at p < 0.05).*

	Papp (E-06, cm/sec)	
Condition	Mannitiol	FD-4
Control	2.16±0.14	0.19±0.05
3 mM Pz-peptide	4.42±0.27*	0.36±0.01*
3 mM Pz-peptide (+) 10 μM Amiloride	2.13±0.07	0.22±0.08
3 mM Pz-peptide (+) Na^+-free buffer	2.15±0.12	0.18±0.01

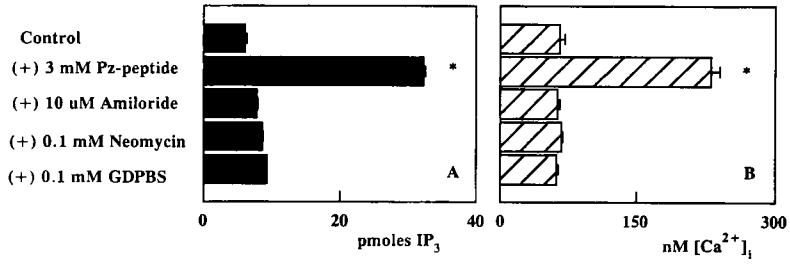

Figure 1. *Effect of Na^+ transport inhibitor amiloride, PLC inhibitor neomycin and G-protein inhibitor GDPβS on 3 mM Pz-peptide-induced release of peak IP_3 (Plot A) and $[Ca^{2+}]_i$ (Plot B) in the descending colon. Error bars represent S.E.M. for n = 3. Asterisks denote statistically significant difference from the control at p < 0.05.*

An increase in IP_3 followed by stimulation of Na^+ flux suggests a possible link between activation of Na^+ channels and phospholipase C (PLC), a key enzyme responsible for IP_3 turnover, by Pz-peptide. This possibility was further confirmed by reversal in enhancement in IP_3 and $[Ca^{2+}]_i$ when Na^+ channels, PLC and G-protein, guanine nucleotide-binding proteins known to modulate both PLC and Na^+ transport were inhibited by amiloride, neomycin and GDPβS, respectively (Figure 1).

In summary, investigation of intracellular changes of tight junctional opening elicited by Pz-peptide, for the first time, provides the link between Na^+ transport and signal transduction-induced release of second messengers relative to alteration of tight junctional permeability to facilitate paracellular drug transport.

Acknowledgments

This work was supported in part by NIH grant GM52812, by Astra-Hässle AB Department of Drug Delivery Research (Mölndal, Sweden), and Sandoz Research Institute Department of Drug Metabolism (East Hanover, NJ); and by the 1993 PMA Advanced Predoctoral Fellowship (WCY) and Gavin S. Herbert Professorship (VHLL).

References

1. Yen, W.C. and Lee, V.H.L., *J. Control Rel.*, 28 (1994) 97.
2. Schultz, S.G., Frizzell, R.A. and Nellans, H.N., *J. Membr. Biol.*, 33 (1976) 351.
3. Pappenheimer, J.R. and Reiss, K.Z., *J. Membr. Biol.*, 100 (1987) 123.

Peptides: Chemistry, Structure and Biology
Pravin T.P. Kaumaya and Robert S. Hodges (Eds.)
Mayflower Scientific Ltd., 1996

354
Conformational Homogeneity and Solvent Effects in Cyclic Peptides

R.K. Konat[1], D.F. Mierke[2], H. Kessler[1]

[1]*Institut für Organische Chemie und Biochemie, Technische Universität München, 85747 Garching, Germany*
[2]*Gustav H. Carlson School of Chemistry, Clark University, Worchester, MA 01610, USA*

Introduction

Homochiral cyclic tetrapeptides had been recently found in marine organisms [1]. The NMR data of cyclo(-Pro-Phe-Pro-Phe-) indicate that it exists in multiple conformations. Therefore, the cis-trans-cis-trans conformation of similar molecules found in crystals [2] was not the only structure in solution.

Results and Discussion

We have synthesized slightly modified analogues of this peptide (replacing Phe by Tyr, Trp and DPhe or introducing DPro instead of Pro) and studied their conformation by NMR spectroscopy. The homochiral cyclic tetrapeptides can assess a surprisingly large conformational space. For cyclo(-Pro-Trp-Pro-Phe-) and cyclo(-Pro-Tyr^{tBu}-Pro-Phe-) three conformations are observed in DMSO solution (Figure 1).

If a distinct structure is required, as in the case of quantitative structure activity relationships, the homochiral cyclic tetrapeptides should be avoided. Instead, we propose the use of modified derivatives with greater restrictions of conformational space, like cyclo(-DPro-Phe-Pro-Phe-) or cyclo(-Pro-DPhe-Pro-Phe-) [3]. Both peptides are excellent templates for the structural design of bioactive molecules. Peptides with two D-amino acids are not as useful, since the conformations of some of them are greatly effected by the solvent [*e.g.* 4].

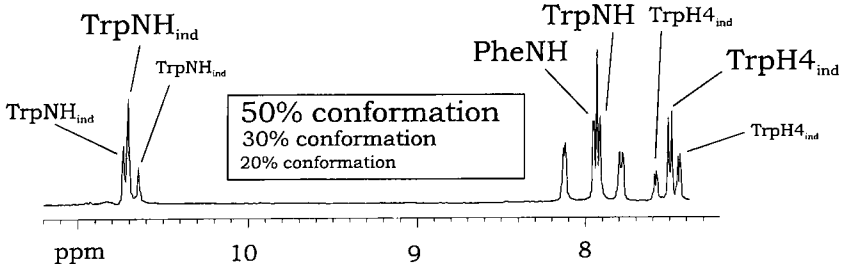

Figure 1. *Part of a 500 MHz ^{1}H NMR spectrum of cyclo(-Pro-Trp-Pro-Phe-) in d^6-DMSO at 300K. Chemical exchange of all conformers was proven by ROESY.*

We were also interested in evaluation of solvent effects. We studied these effects on a less constrained system, the homochiral cyclic octapeptide hymenistatin 1, cyclo(-Pro[1]-Pro[2]-Tyr[3]-Val[4]-Pro[5]-Leu[6]-Ile[7]-Ile[8]-) [5]. The NMR experiments in chloroform and DMSO indicate very strong solvent effects on the Leu[6]NH (Figure 2).

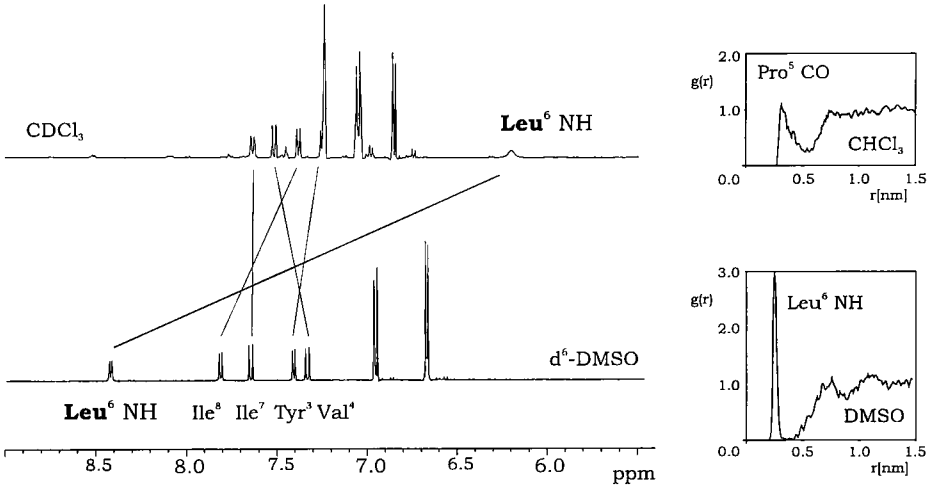

Figure 2. *NH regions of ^{1}H NMR spectra of hymenistatin 1 in $CDCl_3$ and d^6-DMSO (left side) and radial distribution function (rdf) of Pro[5] CO in chloroform and Leu[6] NH in DMSO (right). The distinct peak in the rdf indicates strong solvent interactions.*

The usual conformational studies with restrained molecular dynamics were followed by a "free" molecular dynamics trajectory in an explicit solvent environment and analysis of radial distribution functions. The role of the solvent was explained in both cases. In chloroform we found that Leu[6] NH is shielded by the neighbouring side chains, while the Pro[5] CO is exposed to the solvent. The Pro[5] CO-$HCCl_3$ interaction is confirmed by a distinct peak in the radial distribution function (Figure 2). In DMSO the Pro[5]-Leu[6] amide bond is flipped by about 180° and the Leu[6]NH is exposed towards the solvent. Here, the radial distribution function confirms a strong hydrogen bonding to DMSO, which is in full agreement with the NMR data.

References

1. Aracil, J.M., Badre, A., Fadli, M., Jeanty, G., Banaigs, B., Francisco, C., Lafargue, F., Heitz, A. and Aumelas, A., *Tetrahedron Lett.*, 32 (1991) 2609.
2. Chiang, C.C. and Karle, I.L., *Intl. J. Pept. Protein Res.*, 20 (1982) 133; Ueda, I., Ueda, T., Sada, I., Kato, T., Mikuruiya, M., Kida, S. and Izumiya, N., *Acta Cryst.* C40 (1984) 111.
3. Konat, R.K., Golic Grdadolnik, S., Schmitt, W. and Kessler, H., 'Peptides 1994', ESCOM, Leiden, The Netherlands, 1995, p. 521.
4. Rich, D.H.and Jasensky, R.D., *J. Am. Chem. Soc.*, 102 (1980) 1112.
5. Konat, R.K. Mierke, D.F., Kessler, H., Kutscher, B., Bernd, M. and Voegeli, R., *Helv. Chim. Acta,* 76 (1993) 1649.

Peptides: Chemistry, Structure and Biology
Pravin T.P. Kaumaya and Robert S. Hodges (Eds.)
Mayflower Scientific Ltd., 1996

355
Peptide Vaccine Strategy for Immunotherapy of Human Breast Cancer Using the Her-2/*neu* Oncogene

D. Woodbine[2,3], W. Aldrich[4], P. Triozzi[4,5], V. Stevens[1,3] and P.T.P. Kaumaya[1,2,3,6]

[1]College of Medicine, [2] Comprehensive Cancer Center, [3]Dept. of OB/GYN, [4]Division of Hematology and Oncology, [5]Dept. of Internal Medicine, [6]Medical Biochemistry and Microbiology, The Ohio State University, Columbus, OH 43210, USA

Introduction

Development of cancer vaccines has been hindered by the inability 1) to target vaccines to the appropriate arms of the immune system, 2) to define tumor antigens, 3) to utilize appropriate animal models and 4) to design and to perform appropriate clinical trials. A cancer vaccine that would be effective in an outbred human population must elicit specific B cell, helper T cell (T_h), and cytotoxic T cell (T_c) responses. Immunologically based strategies are probably the most effective ways to prevent and control disease. Antibodies to Her-2 have been identified in some breast carcinoma patients with Her-2 positive tumors but not in patients with Her-2 negative tumors or healthy donors suggesting that a humoral response may be invoked to Her-2 tumors in humans [1].

The proto-oncogene erbB2 or Her-2/*neu* encodes a 185kD transmembrane glycoprotein closely related to the epidermal growth factor (EGF) receptor tyrosine kinase [2]. Overexpression of Her-2 is believed to trigger the malignant phenotype in mammary epithelial cells. Overexpression of Her-2 has also been found in 20-30% of primary human breast cancers and correlates with a poor prognosis [3]. Extracellular accessibility of the protein makes it an ideal candidate for monoclonal antibody therapy.

Results and Discussion

Potential peptide candidates from Her-2/*neu* were predicted by computer-aided analysis using the algorithms of Hopp and Woods (hydrophilicity), Kyte and Doolittle (hydropathy), Rose (solvent exposure), Thornton (protrusion index) and Karplus and Shultz (mobility). The best ranked epitope, Her-2 sequence 376-395, was synthesized colinearly with a "promiscuous" T cell epitope MVF 288-302 and the *in vivo* and *in vitro* immune responses to the peptide were studied in outbred ICR mice and outbred New Zealand white rabbits.

Antibody (Ab) titers against the peptide immunogen increased steadily from the primary immunization through three weeks after the tertiary boost. Flow cytometric analysis revealed that antibodies raised to the peptide recognized the Her-2 receptor. As a negative control, sera from unimmunized animals were used while the positive control was a commercially available monoclonal antibody to HER-2/*neu*. A cell line which

overexpresses Her-2 (SKBR-3) was used. Pre-immune sera showed no binding while a significant increase in fluorescence intensity was seen with immune sera (Figure 1).

In addition to receptor binding, we determined whether the antibody can mediate changes in receptor conformation, inducing receptor dimerization and activating signalling pathways which affect cell growth, proliferation and differentiation. A [^{3}H] thymidine proliferation assay was conducted using the same serum sample as in the case of the flow cytometry assay. There was a 48% reduction in cell proliferation with serum from rabbit 1.

This study demonstrates that the Her-2/neu peptide generated high titers of antibody in outbred mice and rabbits. Antibodies raised against the peptide chimera were specific for the Her-2/*neu* oncoprotein as assessed by flow cytometry. The antibodies were effective as antiproliferative agents in the SKBR-3 cell line as shown by the [^{3}H] thymidine assay.

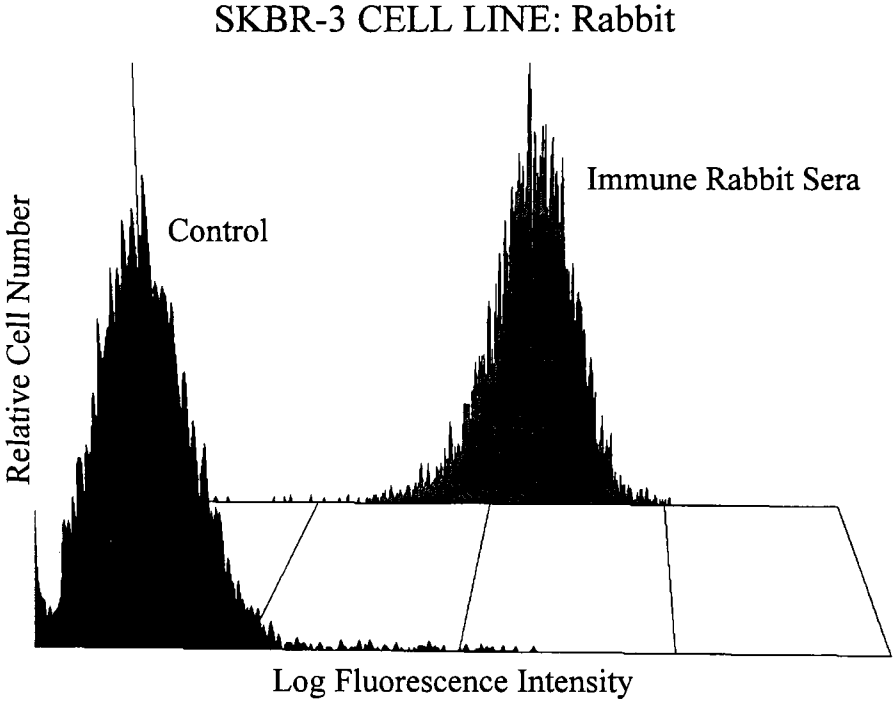

Figure 1. *Flow cytometric analysis determined that the antipeptide antibodies directly targeted the Her-2 receptor.*

References

1. Pupa, S.M., Menard, S., Andreola, S., Colnaghi, M.I., *Cancer Research*, 53 (1993) 5864.
2. Schechter, A.L., Stern, D.F. Vaidyanathan, L., Decker, S.J., Drebin, J.A., Greene, M.I. and Weinberg, R.A., *Nature*, 312 (1984) 513.
3. Slamon, D.J., Clark, G.M., Wong, S.G., Levin, W.J., Ullrich, A., McGuire, W.L., *Science*, 235 (1987) 177.

Peptides: Chemistry, Structure and Biology
Pravin T.P. Kaumaya and Robert S. Hodges (Eds.)
Mayflower Scientific Ltd., 1996

356
Synthesis of Cyclic Pseudopeptides Containing Both ψ[CH_2NH] and ψ[CH_2SO] Surrogates

J.J. Wen and A.F. Spatola

Department of Chemistry, University of Louisville, Louisville, KY 40292, USA

Introduction

Most bioactive peptides have certain structural motifs, such as turn and helical structures, where the hydrogen bonding patterns play a central role. Pseudopeptides could, in principle, stabilize bioactive peptides through new forms of intramolecular hydrogen bonding. We reasoned that this might be possible by incorporating both an optimized H-bond donor ψ[CH_2NH] and H-bond acceptor ψ[CH_2SO] as surrogates into a cyclic peptide host. To this end, we have succeeded for the first time in synthesizing a new type of cyclic pseudopeptide with both ψ[CH_2NH] and ψ[CH_2SO] amide bond surrogates.

Results and Discussion

Our ultimate objective was the synthesis of two diastereomeric cyclic pseudopeptides cyclo[Tyrψ[CH_2SO]Gly-β-Alaψ[CH_2NH]Ala-Phe-Leu](R) and (S) sulfoxide isomers). The initial target peptide was synthesized using a convergent strategy (Figure 1). Our attempts to synthesize the target peptide by employing a resin bound reductive amination [1] strategy with Boc-β-Ala-CHO failed due to the following disubstitution side reaction:

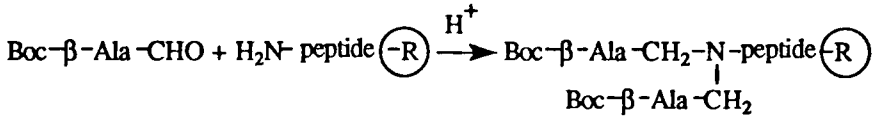

One possible way to overcome this disubstitution problem is to protect the primary amine with a reversible alkyl based protecting group -R introduced prior to the reductive amination step:

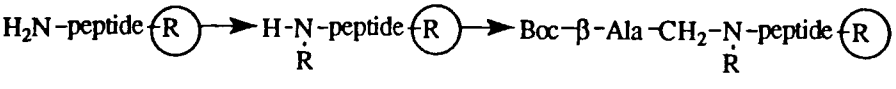

We found that a dimethoxydityl protecting group, where R = $CH(C_6H_4OCH_3)_2$, was too bulky to be useful here. On the other hand, the benzyl based 2-hydroxy-4-methoxy-benzyl protecting group, where R = $CH_2(C_6H_4OCH_3)$, [3] could be used but with

unacceptably low yields. Clearly, the main problem here is the incomplete coupling of Boc-β-Ala-CHO with the sterically hindered secondary amine. In order to circumvent this problem, we have developed a very effective resin bound nucleophilic displacement strategy which essentially eliminates the use of Boc-β-Ala-CHO during the synthesis (Figure 1).

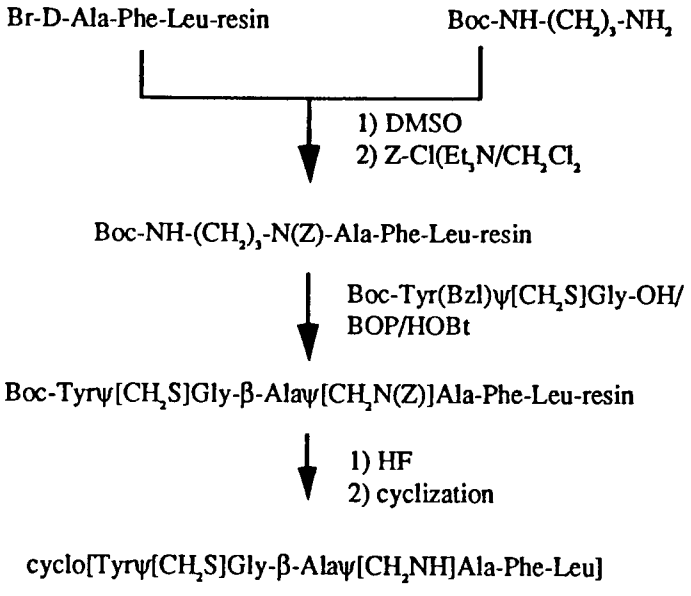

Figure 1. *A convergent synthetic scheme for the synthesis of the cyclic pseudopeptide.*

The displacement reaction proceeded with essentially quantitative yield. The resulting secondary amine was protected with a -Z- protecting group, followed by the coupling of Boc-Tyr(Bzl)ψ[CH_2S]-Gly-OH to the peptide resin. The crude linear pseudopeptide was obtained after HF cleavage and initially purified by an LH-20 column. The cyclization was effected by the DPPA/HOBt/$NaHCO_3$ strategy, and the resulting cyclic pseudopeptide was oxidized by hydrogen peroxide to afford one major isomer which was further separated and purified to homogeneity by a semi-preparative HPLC column. The identity of this isomer was thoroughly characterized by ES-MS, RP-HPLC and NMR.

Acknowledgments

This research was supported by NSF EPSCoR and NIH GM33376.

References

1. Sasaki, Y. and Coy, D.H., *Peptides,* 8 (1987) 119.
2. Kaljuste, K. and Unden, A., *Int. J. Peptide Protein Res.,* 42 (1993) 118.
3. Johnson, T., Quibell, M., Owen, D. and Sheppard, R.C., *J. Chem. Soc. Chem. Commun.,* (1993) 369.

Peptides: Chemistry, Structure and Biology
Pravin T.P. Kaumaya and Robert S. Hodges (Eds.)
Mayflower Scientific Ltd., 1996

357

Synthetic and Chemically Modified Models of Bovine Pancreatic Trypsin Inhibitor (BPTI) Folding Intermediates

E.J. Barbar[1], H. Pan[1], C.M. Gross[1,2], C. Woodward[1] and G. Barany[2]

[1]*Department of Biochemistry, University of Minnesota, St. Paul, MN 55108, USA*
[2]*Department of Chemistry, University of Minnesota, Minneapolis, MN 55455, USA*

Introduction

We are investigating chemically synthesized analogues of BPTI as models for partially folded intermediates in protein folding [1, 2]. All or some of the cysteine residues are replaced by α-amino-*n*-butyric acid (Abu), an isosteric, non-natural amino acid with a methyl group in place of sulfur, or by *S*-methylcysteine (Smc) derived by reduction/ alkylation of the native protein. The variant with only the 14-38 disulfide intact, $[14\text{-}38]_{Abu}$, has been analyzed by two-dimensional ^1H and ^1H-^{15}N NMR. Except for the central antiparallel β-sheet, all residues sample conformations that interconvert on a time scale of ms or longer. NOE analysis indicates that the main hydrophobic tertiary interactions involve tyrosine rings at residues 21, 23, and 35. Variants of $[14\text{-}38]_{Abu}$ with Tyr^{21} or Tyr^{23} replaced by alanine have the NMR and CD characteristics of disordered peptides. Variants of BPTI with all of the cysteines replaced by Abu or Smc, $[R]_{Abu}$ or $[R]_{Smc}$, show some non-random local structure.

Results and Discussion

NMR spectra were obtained at pH 4.6 and 1°C, conditions where $[14\text{-}38]_{Abu}$ is known to form a highly ordered β-sheet molten globule [2]. Site-specific ^{15}N-labeled samples were used to make assignments and identify chemical exchange cross-peaks. Analysis of chemical shifts, chemical exchange, hydrogen isotope exchange and NOEs indicates that $[14\text{-}38]_{Abu}$ is an ensemble of partially folded conformations [3]. The presence of 2 or 3 conformations, interconverting slowly on the NMR chemical shift time scale, is detected for all regions of the protein except the antiparallel β-sheet which remains intact and native-like. Figure 1 shows a model of the proposed structure of $[14\text{-}38]_{Abu}$.

The most prominent side-chain NOEs are those of Tyr^{21} and Tyr^{23} rings with turn residues, and Tyr^{35} with residues 11, 18 and 40. For Tyr^{23}, the interactions are local, with 25 (turn) and 29-30 (strand). For Tyr^{21}, the interactions are nonlocal, with 48 (C-terminal helix), 30, 32 (strand) and 46. The greater stabilization of the first turn of the 48-56 helix likely arises from interaction of Tyr^{21} with residues 46 and 48.

To verify the importance of the local and non-local interactions of Tyr^{21} and Tyr^{23}, variants of $[14\text{-}38]_{Abu}$ were synthesized with Ala replacing Tyr. These variants do not

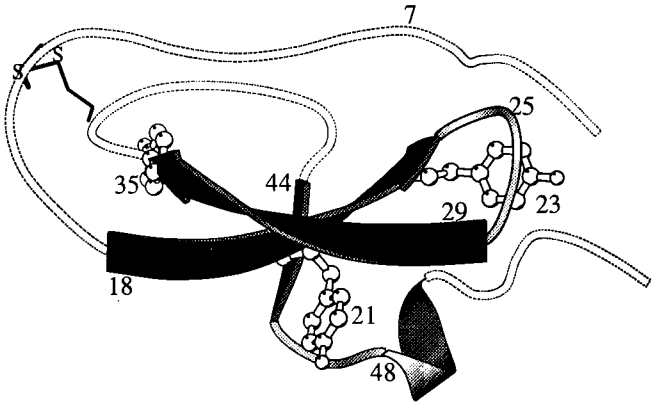

Figure 1. *Ribbon diagram of native BPTI. Side-chains of Tyr 21, 23 and 35 are shown with ball-and-stick. The dark regions are native-like in* $[14\text{-}38]_{Abu}$ *while those indicated with dotted lines fluctuate between 2 or 3 conformations.*

form ordered species, but rather have the NMR and CD characteristics of a disordered peptide with a disulfide cross-link.

We have used selective ^{13}C labeling of the *S*-methyl groups of the six cysteine residues of $[R]_{Smc}$ to check for the presence of ordered structure. Spectra showed that the dispersion of protons attached directly to ^{13}C in the *S*-methyl groups disappeared upon addition of 1.5 M GnHCl. The presence of a residual stable hydrophobic cluster detected in $[R]_{Abu}$ by ANS fluorescence [2] and in $[R]_{Smc}$ by ^{13}C NMR is consistent with the observation that hydrophobic interactions are important for the stability of intermediates which do not show stable secondary structure.

In summary, $[14\text{-}38]_{Abu}$ is an ensemble of partially folded fluctuating structures with a common stable core, corresponding to the slow exchange core [4]. Multiple local and non-local tertiary contacts of Tyr^{21}, $Tyr^{23}$and Tyr^{35} rings support the models of Dill *et al* [5] in which local hydrophobic interactions that are entropically more favorable in unfolded peptides are followed by non-local hydrophobic interactions (Tyr^{21}, Tyr^{35}) which are entropically less favorable.

Acknowledgments

We thank NIH GM 26242 (CW) and GM 51628 (GB and CW) for support of this work.

References

1. Ferrer, M., Woodward, C. and Barany, G., *Int. J. Peptide Protein Res.*, 40 (1992) 194.
2. Ferrer, M., Barany, G. and Woodward, C., *Nature Structural Biology*, 2 (1995) 211.
3. Barbar, E., Barany, G. and Woodward, C., *Biochemistry*, 34 (1995) 11423.
4. Woodward, C., *Trends Biochem. Sci.*, 18 (1993) 359.
5. Dill, K., Fiebig, K. and Chan, H., *Proc. Natl. Acad. Sci. USA*, 90 (1993) 1942.

Peptides: Chemistry, Structure and Biology
Pravin T.P. Kaumaya and Robert S. Hodges (Eds.)
Mayflower Scientific Ltd., 1996

358
Design, Synthesis and Characterization of a Peptide Inhibitor of the IgE-FcεRI Interaction

J.M. McDonnell[1], A.J. Beavil[1], R. Korngold[2], B.A. Jameson[2], H.J. Gould[1] and B.J. Sutton[1]

[1]The Randall Institute, King's College London, London, England, WC2B 5RL, UK
[2]The Jefferson Cancer Institute, Thomas Jefferson University, Philadelphia, PA 19125, USA

Introduction

The interaction between immunoglobulin E (IgE) and its high-affinity receptor FcεRI is central to allergic disease. IgE mediates allergy by binding through its Fc region to the cellular receptor, FcεRI, on mast cells and basophils, causing the release of chemical mediators. Studies from others groups [1, 2] and our own have mapped the binding site of FcεRI for IgE to the second domain of FcεRI α-chain. In particular, a region comprised of β-strands C and C' have been shown to be important in this interaction [3, 4]. In this study, we describe the development of a synthetic peptide inhibitor of the interaction between IgE and FcεRI. This peptide was constructed to mimic the shape and activity of the C-C' region and was designed from a model structure of the FcεRI α-chain.

Results and Discussion

A molecular model of the two extracellular immunoglobulin-like domains of FcεRI α-chain was constructed using the crystal structure of the second domain of CD2 [5] as a template as described previously [6]. Because the C-C' region had been identified as important in the interaction between FcεRI and IgE, we designed a number of peptides to mimic this region, which in the native molecule is predicted to adopt a β-hairpin structure. Peptides were modeled using molecular dynamics and Monte Carlo simulations. Candidate peptides which in simulations displayed the potential to mimic the structure of the C-C' region of the model protein structure were synthesized. The peptide cyclo(L-262) demonstrated biological activity. Cyclo(L-262) was synthesized using standard Fmoc chemistry on an ABI 430A automated peptide synthesizer with the following sequence: CIYYKDGEALKYC(D), all L-amino acids except the C-terminal cysteine. Peptides were assayed for their ability to inhibit the IgE-FcεRI interaction, using surface plasmon resonance to monitor binding (Figure 1). A binding constant of 2.6μM for cyclo(L-262) binding to IgE was calculated using the equilibrium equation, $[SL] = K_A [S]_t [L]/(1+K_A[L])$ where [SL] is the concentration of receptor ligand complex

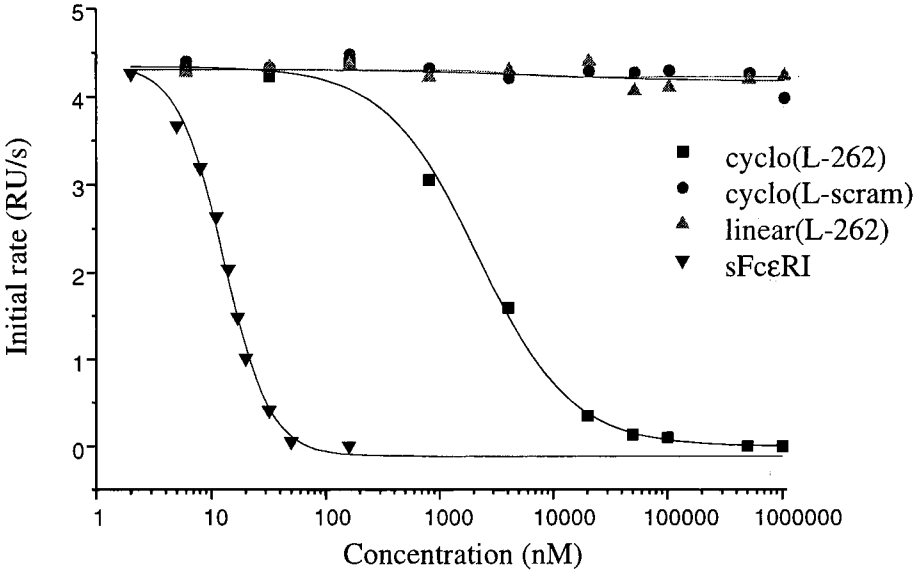

Figure 1. *Activity of the cyclo(L-262) peptide was measured by the ability to inhibit binding of IgE to an immobilized FcεRI α using surface plasmon resonance on a BIAcore (Pharmacia Biosensor, Uppsala, Sweden).*

at equilibrium, [L] is the concentration of free ligand and $[S]_t$ is the total concentration of receptor. Control peptides lacking the intramolecular disulfide and peptides with identical amino acid composition but scrambled sequence demonstrated no biological activity in this system. These data verify the importance of the C-C' region in the interaction between IgE and Fc εRI α-chain and identify the potential of this region for structure-based design of inhibitors of the IgE-FcεRI interaction.

Acknowledgments

Support from the National Asthma Campaign (UK) and the Medical Research Council (HJG and BJS) and a Hitchings-Elion Fellowship (JMM) are gratefully acknowledged.

References

1. Mallamaci, M.A., Chizzonite, R., Griffin, M., Nettleton, M., Hakimi, J., Tsien, W.H. and Kochan, J.P., *J. Biol. Chem.*, 268 (1993) 22076.
2. Robertson, M.W., *J. Biol. Chem.*, 268 (1993) 12736.
3. Hulett, M.D., Witort, E., Brinkworth, R.I., McKenzie, I.F.C. and Hogarth, P.M., *J. Biol. Chem.*, 269 (1994) 15287.
4. Riske, F., Hakimi, J., Mallamici, M., Griffin, M., Pilson, B., Tobkes, N., Lin, P., Danho, W., Kochan, J. and Chizzonite,R., *J. Biol. Chem.*, 266 (1991) 11245.
5. Jones, E.Y., Davis, S.J., Williams, A.F., Harlos, K. and Stuart, D.I., *Nature*, 360 (1992) 232.
6. Beavil, A.J., Beavil, R.L., Chan, C.M.W., Cook, J.P.D., Gould, H.J., Henry, A.J., Owens, R.J., Sutton, B.J. and Young, R.J., *Biochem. Soc. Trans.*, 21 (1993) 968.

Peptides: Chemistry, Structure and Biology
Pravin T.P. Kaumaya and Robert S. Hodges (Eds.)
Mayflower Scientific Ltd., 1996

359
Separation and Identification of Opioid Peptide Conformers

A. Kálmán[1], F. Thunecke[1], R. Schmidt[2], P.W. Schiller[2] and Cs. Horváth[1]

[1]*Department of Chemical Engineering, Yale University, New Haven, CT 06520, USA*
[2]*Laboratory of Chemical Biology and Peptide Research, Clinical Research Institute of Montreal, Montreal, Quebec, H2W 1R7, Canada*

Introduction

Peptides containing proline and/or another N-substituted amino acid are known to exist in both the *cis* and *trans* conformation due to the rotationally hindered peptide bond and they can be relatively stable at temperatures above 0°C [1, 2]. The isolation and identification of such peptide conformers is of growing interest to obtain authentic isomers and thus to facilitate the study of various biological processes such as protein folding/ refolding [3], immune response [4] and the opioid receptor recognition [5].

The goal of the present study was to examine the conditions for the separation of peptide conformers by RP-HPLC at low temperatures, followed by their isolation, as well as identification by NMR spectroscopy.

Results and Discussion

The scope of this investigation included the *cis-trans* conformers of the dipeptides Leu-Pro, Phe-Pro and Tyr-Pro as well as conformers of opioid peptides containing proline and/or the proline-like Tic (1,2,3,4-tetrahydro-isoquinoline-3-carboxylic acid) residues: Tyr-Pro-Phe, Tyr-Tic-Phe-Phe, Tyr-Pro-Phe-Pro-Gly, Tyr-Tic-Phe-Phe-Val-Val-Gly-NH_2 and Tyr-Tic-Phe-Gly-Tyr-Pro-Ser-NH_2.

The relatively slow *cis-trans* interconversion [6] permits the separation of the conformers by HPLC at subambient temperatures. It was shown earlier that on-column *cis-trans* isomerization interferes with the chromatographic separation, when the characteristic times of the interconversion and the separation process are commensurate [7]. By lowering the temperature, the interconversion which has a relatively high activation energy can be slowed down thereby diminishing this interference.

Chromatography with micropellicular and totally porous octadecylated silica stationary phases using aqueous methanol under isocratic elution conditions resulted in well separated peaks of the rotational isomers at sufficiently low temperatures (0°C to -25°C). In order to reach these separation temperatures, the jacketed columns were connected to a refrigerated circulating bath. Preparative RP-HPLC was carried out with eluents containing water and methanol, both deuterated, and the effluent fractions

containing each isomer were collected. The conformational states of the peptide isomers upon separation were conserved by storing the effluent fractions in liquid nitrogen.

In the past, conformer peaks of certain Xaa-Pro dipeptides were tentatively identified by using molecular models to estimate the hydrophobic contact area upon binding to the non-polar surface of the stationary phase, but NMR spectroscopy offers a more reliable means for the structural elucidation of species differing only in their stereochemical arrangement [8].

The Leu-Pro, Phe-Pro, Tyr-Pro and Tyr-Pro-Phe conformers were identified by ^{1}H-NMR spectroscopy at -15°C. The conformers were distinguished by using the well separated signals of $LeuH_\alpha$ and $PheH_\alpha$ for Leu-Pro and Phe-Pro, respectively, as well as $TyrH_{\phi ortho}$ in the case of peptides containing tyrosine. In all cases, the signals of the *cis* conformers are upfield shifted indicating a higher shielding. Upon comparing the NMR spectra of the isomers, for these peptides the retention order of the conformers was unambiguously established: in each case the *trans* conformer is eluted before the *cis* conformer and this suggests that the *cis* conformer binds stronger to nonpolar surfaces and therefore is more "hydrophobic" than the *trans* isomer. On the basis of NMR data obtained with β-casomorphin-5 (Tyr-Pro-Phe-Pro-Gly) the elution order of its four conformers was established as *trans-trans* (least retained), *trans-cis*, *cis-cis* and *cis-trans* (most retained).

Acknowledgments

A.K. is grateful to the Halasz Foundation and F.Th. to the Foundation of the German Chemical Industry for financial support. The work was supported by grants No. GM 20993 from National Institute of Health, US Public Health Service (to Cs.H.) and MT No. 5655 from the Medical Research Council of Canada (to P.W.S.).

References

1. Jacobson, J., Melander, W., Vaisnys, G. and Horváth, Cs., *J. Phys. Chem.*, 88 (1984) 4536.
2. Lin, L. and Brandts, J.F., *Biochemistry*, 22 (1983) 553.
3. Brandts, J.F., Halvorson, H.R. and Brennan, M., *Biochemistry*, 14 (1975) 4953.
4. Handschumacher, R.E., Harding, M.W., Rice, J., Drugge, R.J. and Speicher, D.W., *Science*, 226 (1984) 544.
5. Schmidt, R., Kálmán, A., Chung, N.N., Lemieux, C., Horváth, Cs. and Schiller, P.W., *Int. J. Pept. and Protein Res.*, 46 (1995) 47.
6. Grathwohl, C. and Wüthrich, K., *Biopolymers*, 20 (1981) 2632.
7. Melander, W.R., Jacobson, J. and Horváth, Cs., *J. Chromatogr.*, 234 (1982) 269.
8. Wüthrich, K., 'NMR of Proteins and Nucleic Acids', J. Wiley and Sons, New York, NY, USA, 1986, p.186.

Peptides: Chemistry, Structure and Biology
Pravin T.P. Kaumaya and Robert S. Hodges (Eds.)
Mayflower Scientific Ltd., 1996

360
New RGD Peptide Mimetics as Efficient Inhibitors of Platelet Aggregation

S. Chakravarty, Q. Dong and I. Ojima

Department of Chemistry, State University of New York at Stony Brook, Stony Brook, NY 11794, USA

Introduction

Platelet aggregation is essential in the maintenance of hemostasis, but its malfunction may cause serious cardiovascular and cerebrovascular diseases. Inhibition of such pathological platelet aggregation has been an attractive target for drug design efforts, which have mainly focused on mimicking the RGD recognition sequence in fibrinogen, whose interaction with the platelet surface receptor, GPIIb/IIIa, is the essential final step in platelet aggregation cascade [1]. We have rationally designed highly potent small molecule antagonists of GPIIb/IIIa conforming to a three-point pharmacophoric binding model shown below from our double-strand RGD peptide lead [2]. This report discusses salient features of the SAR of these inhibitors.

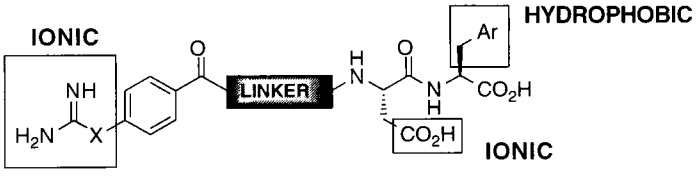

Results and Discussion

Starting from a basic RGDX pharmacophore, we recognized three major points of interaction and potential modification: the arginine side chain, the aspartyl side chain, and the hydrophobic X residue (Table 1). The amidinobenzoyl group was found to be the most effective arginine side chain surrogate, better than either the guanidinobenzoyl or the guanidinomethylbenzoyl moieties. In both the guanidinobenzoyl and amidinobenzoyl series, the most effective linker was β-alanine as in **2** (USB-IPA-1102, IC_{50} = 0.070 μM, PRP/ADP) and **14** (USB-IPA-1302, IC_{50} = 0.026 μM, PRP/ADP). Changing the C-terminal carboxylate to carboxamide (**21** and **22**) did not adversely affect activity. At the C-terminal position, (*S*)-Trp was found to impart highest activity in the guanidinobenzoyl series, while in the amidinobenzoyl series, the (*S*)-Tyr analog (**15**, USB-IPA-1305, IC_{50} = 0.020 μM, PRP/ADP) was most active. Interestingly, changing

Table 1. *Inhibition of Platelet Aggregation[a]: Effect of Linker Size, Arginine Side Chain Surrogates, and C-Terminal Amino Acid.*

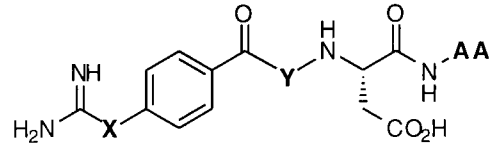

Compound	X	Y	AA	$IC_{50}(\mu M)^b$
1	NH	Gly	(S)-Trp	0.60
2	NH	β-Ala	(S)-Trp	0.070
3	NH	GABA[c]	(S)-Trp	>50
4	NH	Tyr	(S)-Trp	>50
5	NH	β-Ala	(S)-Phe	0.390
6	NH	β-Ala	(S)-Tyr	0.190
7	NH	β-Ala	(S)-(4-F)Phe[c]	1.7
8	NH	β-Ala	(S)-(6H)Phe[c]	0.088
9	NH	β-Ala	(S)-1-Nal[c]	0.77
10	NH	β-Ala	(S)-2-Nal[c]	0.32
11	NH	β-Ala	(R,S)-β-Phe[c]	6.1
12	NH	β-Ala	(S)-Phg[c]	2.9
13	$NHCH_2$	β-Ala	(S)-Trp	0.71
14	---	β-Ala	(S)-Trp	0.026
15	---	β-Ala	(S)-Tyr	0.020
16	---	β-Ala	(R)-Tyr	1.2
17	---	β-Ala	(S)-2-Nal[c]	0.044
18	---	β-Ala	(S)-(4-F)-Phe[c]	0.047
19	---	GABA[c]	(S)-Trp	>50
20	---	β-Ala	(S)-(6H)Phe	0.044
21	---	β-Ala	(S)-Trp-NH_2	0.031
22	---	β-Ala	(S)-Tyr-NH_2	0.050

[a]Human platelet aggregation was induced by ADP. [b]Normalized IC_{50} value based on the IC_{50} value of RGDF-NH_2 equal to 50 μM. Each value is the average of three runs and experimental error is within 15%. [c]GABA = γ-amino butanoic acid; (4-F)-Phe = 4-fluorophenylalanine; (6H)Phe = cyclohexylalanine; Nal = naphthylalanine; β-Phe = 3-phenyl-β-alanine; Phg = phenylglycine.

chirality of the Tyr residue to *R* (**16**) resulted in a drastic loss in activity. The postulated receptor site for the C-terminal residue otherwise appears to accommodate a variety of aromatic and non-aromatic hydrophobic groups.

References

1. Ojima, I., Chakravarty, S. and Dong, Q., *BioMed. Chem.*, 3 (1995) 337.
2. Ojima, I., Dong, Q., Eguchi, M., Oh, Y.I., Amann, C.M. and Coller, B.S., *BioMed. Chem. Lett.*, 4 (1994) 1749.

Peptides: Chemistry, Structure and Biology
Pravin T.P. Kaumaya and Robert S. Hodges (Eds.)
Mayflower Scientific Ltd., 1996

361
Vaccine Design: The Orthogonal Incorporation of Cyclic Peptides as Multiple Antigens Attached to Dendrimeric Cores

T.D. Pallin and J.P. Tam

Department of Microbiology and Immunology, Vanderbilt University, MCN A5119, Nashville, TN 37232, USA

Introduction

In order to develop a new and wide ranging strategy for the formation of constrained peptides, their subsequent use as building blocks for peptide dendrimers and unprotected proteins, we have investigated a general method for the synthesis of cyclic peptides. The method is based on the Domain Ligation Strategy [1, 2] where an intramolecular covalent bond is formed between a weak base and an aldehyde to give a cyclic oxime, oxazolidinone or thiazolidine. Such cyclizations would expand the conventional repetoire of disulphide or lactam formation. The reaction may be performed on a resin [3], or an unprotected linear peptide precursor may be cyclized in aqueous solution. Utilizing two weak bases, it is possible to cyclize the peptide and to assemble the constrained peptides onto branched templates to investigate modifications in vaccine design and delivery.

Results and Discussion

Linear precursors (Figure 1) were synthesized on a Wang resin using Fmoc chemistry and BOP activation. The lysine residue was introduced as Dde-Lys(Fmoc)-OH [4] and Boc-Ser(tBu)-OH coupled to the side chain.

For oxime cyclization, the peptide was cleaved from the resin to give the linear unprotected peptide precursor **1**. Using sodium periodate at pH 7, an aldehyde was obtained [5] as the α-oxoacyl moiety **2** which spontaneously cyclized in >90% yield to give the cyclic oxime **3**. The reaction, monitored by HPLC, was complete within 2 min.

Similar results were obtained for thiazolidine formation in which Z=Cys(StBu). Cys(StBu) was stable to the $NaIO_4$-mediated oxidation of serine (X=Ser, Figure 1) to form the α-oxoacyl derivative. The StBu was then removed by a water soluble phosphine derivative at pH5.5 and the resulting 1,2-aminothiol cyclized by thiazolidine formation. Cyclization was also accomplished on a resin where X= acetal [3]. Cys was deprotected with base and the acetal with mild acid. Following cyclization in DMF, the peptide was cleaved from the resin to give the desired constrained peptide in 20% yield.

Finally, a 1,2-aminothiol in the presence of a hydroxylamine **4** would allow orthogonal cyclizations. The peptide can be first cyclized by oxime formation and then

the thiol released by reduction of the S-*t*butylsulphenyl. Control of the pH conditions then allow the 1,2-aminothiol to displace the hydroxylamine from the oxime to give a cyclic thiazolidine. The resulting hydroxylamine is now available for further condensation reactions with other peptide fragments containing aldehyde moieties. In this way constrained "building blocks" can be assembled on various dendrimeric cores to form, multiple antigen peptides (MAPS).

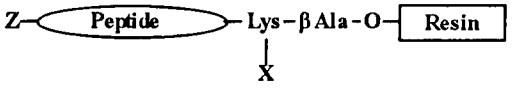

Aqueous cyclization: Z=H_2NOCH_2CO,Cys(StBu),X=Serine
Resin cyclization: Z=Cys(Fm),X=$(CH30)_2CH(CH_2)_nCO$
Peptide Sequence: GIGPGRAFG

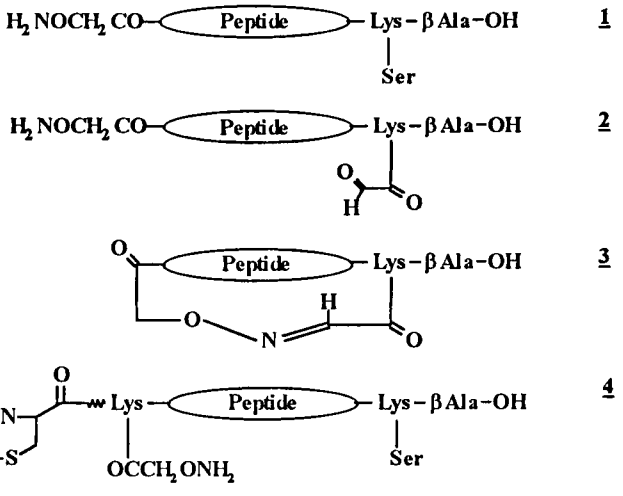

Figure 1. *The formation of cyclic oximes and thiazolidines.*

Acknowledgments

This work is supported in part by NIH grants AI28701, CA35577 and CA36544.

References

1. Liu, C-F and Tam, J.P., *J. Am. Chem. Soc.*, 116 (1994) 4149.
2. Shao, J. and Tam, J.P., *J. Am. Chem. Soc.*, 117 (1995) 3893.
3. Chiang, L.-C., Cabezas, E., Calvo, J. and Satterthwait, A.C., in Hodges, R.S and Smith, J.A, (Eds.), 'Peptides: Chemistry, Structure and Biology', Escom, Leiden, The Netherlands, 1994, p 278.
4. Bycroft, B.W., Chan, W.C., Chhadra, S.R., Hone, N.D., *J. Chem. Soc. Chem. Comm.*, (1993) 778.
5. Rose, K., *J. Am. Chem. Soc.*, 116 (1994) 30.

Peptides: Chemistry, Structure and Biology
Pravin T.P. Kaumaya and Robert S. Hodges (Eds.)
Mayflower Scientific Ltd., 1996

362
New Resins for Chemical Ligation and Cyclization of Unprotected Peptides

P. Botti, K.D. Eom and J.P. Tam

Department of Microbiology and Immunology, A5119 MCN, Vanderbilt University Nashville, TN 37232, USA

Introduction

Conformationally constrained peptides, particularly end-to-end cyclic peptides, are useful to enhance biological activity and proteolytic resistance. Although many methods for cyclizing peptides have been reported [1-3], none is known for end-to-end cyclization using unprotected peptides. Here we report such a strategy based on the domain ligation approach [4] for intramolecular amide cyclization and the development of a new resin support to attain its application.

Results and Discussion

A key functional group in our domain ligation strategy is the Cα-ester glycoaldehyde **5**. To provide such an ester aldehyde by solid phase synthesis we developed such a resin **3** by linking a Fmoc-Gly glyceric ester **1** to a benzaldehyde-polystyrene resin **2** [5] through an acetal handle (Figure 1). The synthesis of the desired peptide was then performed using Fmoc-tertbutyl chemistry with a N-terminal Cys containing S-tertbutyl protecting group. Cleavage by TFA released the peptide ester diol **4**. Oxidation with $NaIO_4$ generated the corresponding aldehyde **5**. Deprotection of the S-tertbutyl using Bu_3P at controlled pH gave the cyclized peptide **6** in excellent yield. The neutralizing determinant of the V3 loop of gp 120 of HIV-1 containing the sequence PGRAFG was used as a model. The linear peptide CGRAFG-Cα-ester-diol was obtained by solid phase synthesis on resin **3**. Cyclization at pH 4.5 as described in Figure 1 gave the cyclic thiazolidine peptide ester **6** as a diasteroisomer. The amide bond formation was effected through an intramolecular O,N acyl transfer reaction **7**, after adjusting the pH to 5.5. The reaction was completed in 4 days and afforded the cyclic peptide amide **8** in quantitative yield. Our strategy offers several advantages including convenient synthesis and purification of the linear peptide precursor, and allows the synthesis of large and complex cyclic peptides.

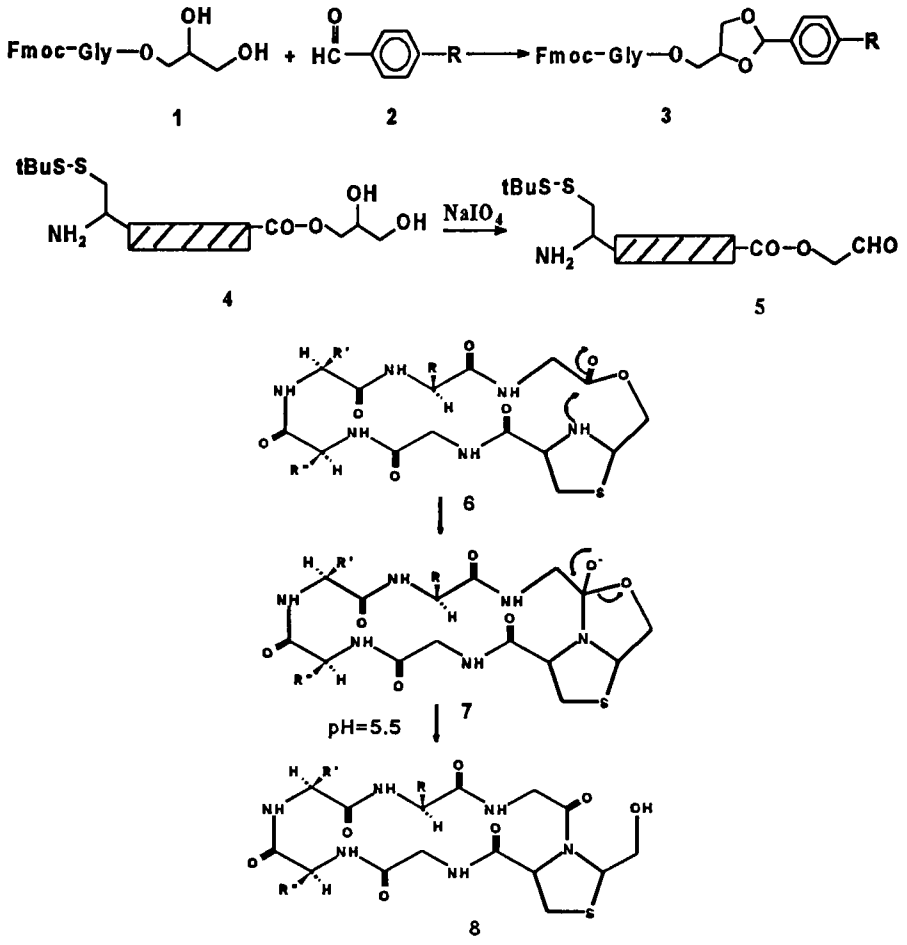

Figure 1. *Synthesis of linear peptide precursor containing Cα-glycolaldehyde and cyclization to obtain an end-to-end cyclic peptide.*

References

1. Byk. G. and Gilon C., *J. Org. Chem.*, 57 (1992) 5687.
2. Schiller, P.W., in Undenfriend, S. and Meienhofer, J. (Eds.), 'The Peptides', Academic Press, 1984, Vol. 6, p.254.
3. Kaljuste K. and Unden A., *Intl. J. Peptide Protein Res.*, 43 (1994) 505.
4. Liu C.F., and Tam J.P., *J. Am. Chem. Soc.*, 116 (1994) 4149.
5. Frechet J.M. and Schuerch C., *J. Am. Chem. Soc.*, 93 (1971) 492.

Peptides: Chemistry, Structure and Biology
Pravin T.P. Kaumaya and Robert S. Hodges (Eds.)
Mayflower Scientific Ltd., 1996

363
Chemical Ligation of Unprotected Peptides to Form X-Cys Bond by Nucleophilic Capture Using Thiocarboxylic Acid

J. Shao and J.P. Tam

Department of Microbiology and Immunology, School of Medicine, A5119- MCN, Vanderbilt University, Nashville, TN 37232, USA

Introduction

Chemical ligation using unprotected peptide segments and protein domains for synthesis of native and artificial proteins has attracted increasing attention. Unprotected peptide segments and protein domains as building blocks are conveniently produced by solid phase peptide synthesis and recombinant DNA technology. Thus such a strategy combines the benefits of both these techniques, and particularly the solution phase synthesis and purification methods. Our laboratory has developed a general approach of ligating peptide segments containing N-terminal cysteine [1-3]. In this approach, a covalent bond was first formed by a capture method, usually through the nucleophilic attack of the N-terminal cysteine on the electrophilic center of the other segment. The activation is effected by proximity leading to an intramolecular acyl transfer to link two segments through an amide bond. Here we describe a new approach of capture-ligation using C-terminal thiocarboxylic acid as a nucleophile to initiate a covalent thioester bond with the other segment bearing an electrophile at the N-terminus. After the S- to N-acyl transfer, the two segments are ligated together generating a native cysteinyl residue at the ligation site (Figure 1).

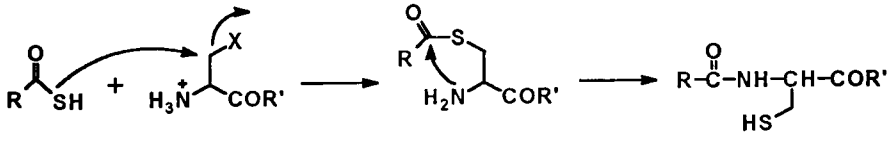

Figure 1. *Ligation of unprotected peptide segments through thioester capture-activation.*

Results and Discussion

We chose β-bromoalanine (BrAla) as the electrophile on the N-terminus of amine segments. Boc-BrAla was prepared from a one-step reaction of Boc-Ser-OH with PPh_3/CBr_4 [4] and then incorporated into amine segments. BrAla could be also obtained from the conversion of N-terminal serine in solid phase synthesis. The acyl segment with C-terminal thiocarboxylic acid was obtained using 4[(-Boc-Leu-S)benzyl]-phenoxyacetic amide resin [5]. Thioesterification of Leu-SH with BrAla at pH 5.2 to 6.2 was used as a

model reactionand two products with identical molecular weight were formed: the desired α-dipeptide **4** and isomeric β-dipeptide **5** derived from the ring opening at the α-position of aziridine (Figure 2). At pH 5.2, direct displacement (Figure 2, route i) was predominant and the desired α-peptide was obtained in 82% yield. At pH 6.2, aziridine formation became significant (Figure 2, route ii) and α-peptide yield decreased to 60%.

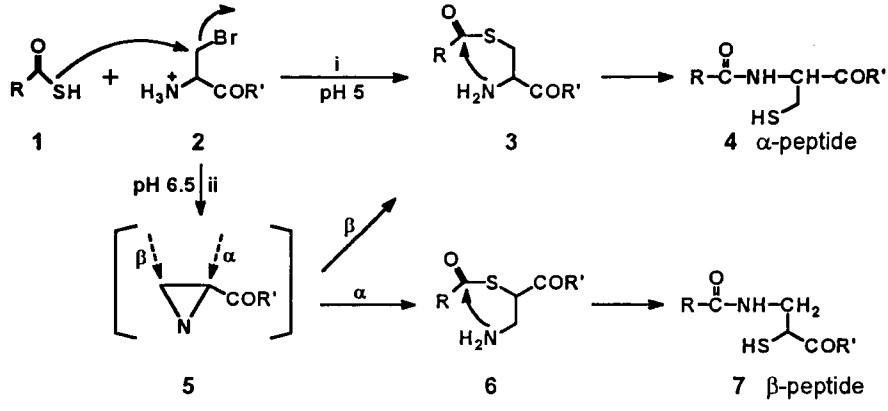

Figure 2. *Two pathways of forming thioester in model studies using Leu-SH and BrAla. i) direct SN2 displacement of bromo group leading to α-peptide; ii) formation of aziridine and subsequent ring opening leading to both α- and β-peptides.*

To illustrate the application of this thioester-capture approach, Sperm Activating Peptide (Cys^5-Cys^{10}, Ser-Ala-Lys-Leu-Cys-Pro-Gly-Gly-Asn-Cys-Val-OH) was synthesized by ligating Ser-Ala-Lys-Leu-SH with BrAla-Pro-Gly-Gly-Asn-Cys(Acm)-Val-OH. At pH 5.2, the reaction was complete in 12 h giving a single product with the expected molecular weight (Found: 1119.2, Calcd for $M+H^+$: 1119.3) having been obtained.

In conclusion, the thiocarboxylic acid capture approach offers advantages of fast ligation, direct, convenient preparation of acyl and amine segments, and avoiding the hydrolysis of thioester found in thiol-thioester exchange ligation.

Acknowledgments

This work is in part supported by NIH grant CA35577, AI28701, and CA36544.

References

1. Liu, C.F., Shao, J., Rao C. and Tam, J.P., in Hodges, R.S. and Smith, J.A. (Eds.), 'Peptides: Chemistry, Structure and Biology', Escom, Leiden, The Netherlands, 1994, p 218.
2. Liu, C.F. and Tam J.P., *J. Am. Chem. Soc.*, 116 (1994) 4149.
3. Shao, J. and Tam, J.P., *J. Am. Chem. Soc.*, 117 (1995) 3893.
4. Hayashi, H., Nakanishi, K., Brandon, C. and Marmur, J., *J. Am. Chem. Soc.*, 95 (1973) 8749.
5. Yamashiro, D. and Li, C.H., *Int. J. Pept. Prot. Res.*, 31 (1988) 322.

Peptides: Chemistry, Structure and Biology
Pravin T.P. Kaumaya and Robert S. Hodges (Eds.)
Mayflower Scientific Ltd., 1996

364

Protein Kinase C-α is Translocated to the Membrane by a Peptide Substrate in the Absence of Ca^{2+}

R.H. Bruins and R.M. Epand

Department of Biochemistry, McMaster University Health Sciences Centre, Hamilton, Ontario, Canada L8N 3Z5

Introduction

Protein Kinase C-alpha (PKC-α), a classical PKC isoform, is activated by a combination of agents including Ca^{2+}, diacylglycerol (DAG), and phosphatidylserine (PS). Upon binding a single Ca^{2+} ion, PKC-α translocates to membranes containing phosphatidyl serine [1]. Membrane components such as diacylglycerol can activate PKC-α, presumably by inducing the removal of the pseudosubstrate domain through a conformational change in the enzyme [2]. Activated PKC-α then phosphorylates S/T residues in proteins containing a consensus sequence with adjacent Arg and Lys residues [3]. Alternatively, Arg-rich substrates, such as protamine sulfate, can activate PKC-α catalyzed phosphorylation in the absence of these co-factors [4]. The mechanism of co-factor-independent phosphorylation of such substrates has not yet been elucidated. However, if Arg-rich substrates induced a conformational change in PKC-α similar to that of the Ca^{2+}-translocated form of the enzyme, it would provide an opportunity to study this process in the absence of membranes. In the present study, we demonstrate that an Arg-rich peptide (ARP) substrate of PKC-α can translocate the enzyme to a phospholipid bilayer in the absence of Ca^{2+}.

Results and Discussion

The translocation of PKC-α to a phospholipid bilayer was monitored by increased resonance energy transfer between Trp on the enzyme and dansyl-groups attached to lipid as well as by changes in the intrinsic tryptophan fluorescence. In the resonance energy transfer experiments, the presence of Ca^{2+} induced the translocation of PKC-α to the bilayer producing a 28% increase in fluorescence. No significant increase was observed when either EGTA or the MARCKS peptide (Ac-F-K-K-S-F-K-L-NH_2) was added to PKC-α in the presence of a bilayer. However, with the ARP (R_4-Y-G-S-R_5-Y) present along with PKC-α and a bilayer containing dansyl labelled lipid, a 25% increase of fluorescence was observed. Intrinsic tryptophan fluorescence studies confirmed the Ca^{2+} independent translocation of PKC-α to the membrane *via* the ARP, in that only Ca^{2+} or the ARP were able to produce a decrease in the intrinsic Trp fluorescence spectra of PKC-α in the presence of a membrane.

Upon translocation, hydrophobic sites of PKC-α insert into the membrane [5]. We have found, by three independent methods, that the binding of the ARP to PKC-α induces exposure of such hydrophobic sites. The fluorescent probes 1,1'-bis(4-anilino)-naphthalene-5,5'-disulfonic acid (bis-ANS) and PRODAN are responsive to the polarity of their environments [6, 7]. The ARP PKC-α complex produces a four fold greater increase in bis-ANS fluorescence than PKC-α alone. This is indicative of bis-ANS binding to hydrophobic sites on PKC-α. PRODAN, fluoresces around 520 nm in a polar environment while it shifts to 420 nm in more hydrophobic environments. When the ARP was added to a solution containing PKC-α and PRODAN an increase in emission at 420 nm is observed. However, if PRODAN is added after the ARP and PKC-α have mixed, an increase in emission at 520 nm is observed. This may indicate that the binding of ARP to PKC-α induces hydrophobic sites which then aggregate in the absence of phospholipid. Finally, the partitioning of the ARP PKC-α complex into Triton X-114 micelles was ascertained to further confirm the exposure of hydrophobic sites. In the absence of the ARP, a minimal amount of PKC-α sediments with the detergent phase. However, when the ARP is present, a four fold increase in enzyme activity is observed in the detergent phase. Thus, it is evident that the binding of the ARP to PKC-α induces the exposure of hydrophobic site(s) on the enzyme.

Lastly, the conformational changes that PKC-α undergoes upon membrane binding and activation (removal of the pseudosubstrate domain) can be monitored by the sensitivity to trypsin hydrolysis. With Ca^{2+} and phospholipid, PKC-α is cleaved at the hinge region producing fragments of 35 and 45 kDa and as well at the pseudosubstrate domain producing a nicked form of approximately 75 kDa [8, 9]. In the absence of phospholipid, with protamine sulfate and PKC-α, only the nicked form is produced [9]. The ARP inhibits trypsin to an extent but the inhibition does not differ in the presence and absence of phospholipid (as monitored by the hydrolysis of histones). However, the nicked form of PKC-α is partially evident in the absence of phospholipid with the ARP present, while in the presence of a bilayer, both the 35 and 45 kDa fragments are observed in the absence of Ca^{2+}. Therefore, the ARP·PKC-α translocated complex has similar susceptibility to trypsin at the hinge region. This indicates that ARP alone can partially induce the same conformational change in PKC-α that occurs with PS, DAG and Ca^{2+}.

References

1. Mosior, M. and Epand, R.M., *J. Biol. Chem.*, 269 (1994) 13798.
2. Mosior, M. and McLaughlin, S., *Biophys. J.* , 60 (1991) 149.
3. Kennelly, P.J and Krebs, E.G., *J. Biol. Chem.*, 266 (1991) 15555.
4. Bazzi, M.D. and Nelsestuen, G.L., *Biochemistry,* 26 (1987) 1974.
5. Lester, D.S., Collin, C., Etchenberrigaray, R., and Alkon, D.L., *Biochim. Biophys. Acta.*, 1039 (1990) 33.
6. Rosen, C.G. and Weber, G., *Biochemistry,* 8 (1969) 3915.
7. Weber, G. and Farris, F.J., *Biochemistry,* 18 (1979) 3075.
8. Orr, J.W., Keranen, L.M., and Newton, A.C., *J. Biol. Chem.*, 267 (1992) 15263.
9. Orr, J.W., and Newton, A.C., *J. Biol. Chem.*, 269 (1994) 8383.

Peptides: Chemistry, Structure and Biology
Pravin T.P. Kaumaya and Robert S. Hodges (Eds.)
Mayflower Scientific Ltd., 1996

365
Structures of Prion Proteins and Conformational Model of Prion Diseases

Z. Huang[1,2,3], S.B. Prusiner[1] and F.E. Cohen[2]

Departments of [1]Neurology and [2]Pharmaceutical Chemistry, University of California, San Francisco, CA 94143, USA
[3]Jefferson Cancer Institute, Thomas Jefferson University, Philadelphia, PA 19107, USA

Introduction

Prion proteins are responsible for a group of neurodegenerative diseases in humans and animals including scrapie, kuru, and Creutzfeldt Jakob disease (CJD). Prion proteins exist in two isoforms: the normal cellular form (PrP^C) and the abnormal disease causing form (PrP^{Sc}). PrP^C and PrP^{Sc} have identical amino acid sequences, but significantly differ from each other in their structures based on experimental studies using circular dichroism and infrared spectroscopy [1, 2]. This suggested that prion diseases could be a result of the conformational switch of PrP^C into PrP^{Sc} [3]. Therefore, understanding of the three-dimensional structure of PrP^C and PrP^{Sc} and the conformational transition between them is essential for the elucidation of the molecular mechanism of prion diseases. To date, efforts to obtain crystals for X-ray structure determinations have been unsuccessful because of the low level of expression of PrP^C and insolubility of PrP^{Sc}. Using a computational approach of combining molecular modeling techniques and spectroscopic and genetic data, we carried out computational studies to predict the three-dimensional structure of PrP^C and PrP^{Sc} based on a family of homologous amino acid sequences [4].

Results and Discussion

The computational procedures used for the prediction of the three-dimensional structures of PrP^C and PrP^{Sc} involved four major steps: (i) alignment of a family of homologous sequences, (ii) prediction of secondary structures, (iii) packing of secondary elements to generate all plausible tertiary structures and (iv) selection and refinement of final structural models.

In the study reported here, plausible three-dimensional structures of PrP^C and PrP^{Sc} were generated by applying computational approaches coupled with experimental data. PrP^C displays a four-helix bundle structure while PrP^{Sc} shows a β-sheet structure packed against two α-helices. In the absence of a threedimensional structure of PrP^C and PrP^{Sc} from either X-ray crystallography or NMR spectroscopy, these models provide a vehicle to rationalize much of the available biological and genetic data.

PrP^{Sc} seems to be able to multiply itself and cause disease in the absence of specific DNA or RNA. This raises a controversial question with respect to the unprecedented mechanism of prion replication. The predicted structures of PrP^{C} and PrP^{Sc} reveal a plausible mechanism for prion replication. As shown below, prion replication involves a process in which two α-helices of PrP^{C} are converted into a 4-strand β-sheet of PrP^{Sc}. Using the β-sheet as a template to direct this conformational change, infectious PrP^{Sc} could promote the conversion of non-infectious PrP^{C} to generate more PrP^{Sc} (Prion multiplication). These findings may provide a structural basis for prion diseases and the development of novel therapeutic strategies.

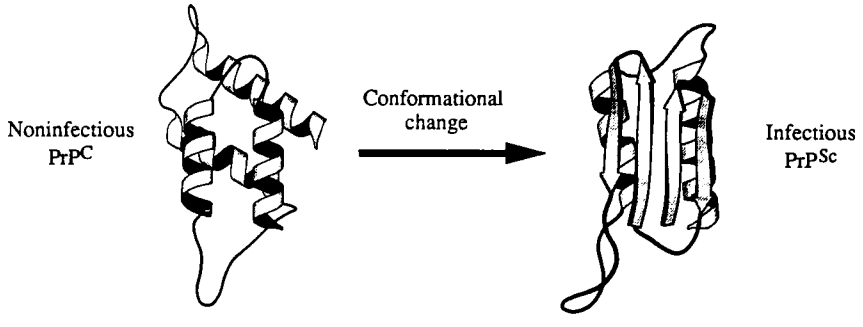

Figure 1. *Plausible three-dimensional structures of PrP^{C} and PrP^{Sc}. Prion replication involves a process of conformational change in which two α-helices of PrP^{C} are converted into a 4-strand β-sheet of PrP^{Sc}.*

Acknowledgments

We thank Professors Peter A. Kollman, Irwin D. Kuntz, Robert J. Fletterick, Thomas L. James, Michael A. Baldwin, and Gerald D. Fasman for insightful discussions. This work was supported by research grants from the National Institute of Health and a gift from the Sherman Fairchild Foundation.

References

1. Pan, K.M., Baldwin, M., Nguyen, J., Gasset, M., Serban, A., Groth, D., Mehlhorn, I., Huang, Z., Fletterick, R.J., Cohen, F.E. and Prusiner, S.B., *Proc. Natl. Acad. Sci. USA*, 90 (1993) 10962.
2. Safar, J., Roller, P.P., Gajdusek, D.C. and Gibbs, C.J., Jr., *J. Biol. Chem.*, 268 (1993) 20276.
3. Cohen, F.E., Pan, K.M., Huang, Z., Baldwin, M.A., Fletterick, R.J. and Prusiner, S.B., *Science*, 264 (1994) 530.
4. Huang, Z., Gabriel, J-M., Baldwin, M., Fletterick, R.J., Prusiner, S.B. and Cohen, F.E., *Proc. Natl. Acad. Sci. USA*, 91 (1994) 7139.

Peptides: Chemistry, Structure and Biology
Pravin T.P. Kaumaya and Robert S. Hodges (Eds.)
Mayflower Scientific Ltd., 1996

366
Synthetic Max and c-Myc Leucine Zippers Preferentially Form a Heterodimeric Parallel Coiled-coil

P. Lavigne, L.H. Kondejewski, M.E. Houston Jr., F.D. Sönnichsen, R.S. Hodges and C.M. Kay

Department of Biochemistry and the Protein Engineering Network of Centres of Excellence, University of Alberta, Edmonton, Alberta, T6G 2C6, Canada

Introduction

The oncoprotein c-Myc must heterodimerize with Max to bind DNA and perform its normal and oncogenic activity [1, 2]. c-Myc-Max heterodimer binds to DNA through a basic helix-loop-helix leucine zipper (b-HLH-zip) motif and it is proposed that leucine zipper domains could, in concert with the HLH regions, provide the specificity and stability of the b-HLH-zip motif [1, 2]. In this context, we have synthesized the peptides corresponding to the leucine zipper domains of Max and c-Myc with a N-terminal Cys-Gly-Gly linker and studied their dimerization behaviour using reversed-phase HPLC and CD spectroscopy.

Results and Discussion

Preferential c-Myc-Max disulfide-linked heterodimeric coiled-coil formation under air-oxidation (Figure 1B) and redox conditions (Figure 1D) at neutral pH has been observed. Based on the molar ellipticity at 222 nm (θ_{222}, -31,000 deg·cm^2·dmol^{-1}) and the $\theta_{222}/\theta_{208}$ ratio (1.07), the far UV CD spectrum of c-Myc-Max heterodimer indicates that it folds into a fully helical and parallel disulfide-linked two-stranded coiled-coil under benign conditions at room temperature [3]. According to their θ_{222} values (-22,000 and -15,000 deg·cm^2·dmol^{-1}) and $\theta_{222}/\theta_{208}$ ratios (0.95 and 0.77), oxidized Max homodimer (Max_2) partially folds and c-Myc homodimer ($c\text{-}Myc_2$) does not fold into a two-stranded parallel coiled-coil under benign conditions. Therefore, Max and c-Myc Leucine Zippers can fold into a heterodimeric coiled-coil independently of the HLH domain of the corresponding gene products [3]. The apparent instability of the corresponding homodimeric coiled-coils should favor heterodimer formation in a similar fashion to that described for the b-zip family [3-5]. We have described putative electrostatic interactions that are responsible for the specificity of the interaction; the salient feature being the potential formation of a His (position *d* in Max) - Glu (position *a* in c-Myc) buried salt-bridge [3]. We propose that in the b-HLH-zip family interhelical electrostatic interactions at positions *a* and *d* in the heptad repeat (rather than positions *e* and *g* in the b-zip family) play a key role in leucine zipper dimerization specificity.

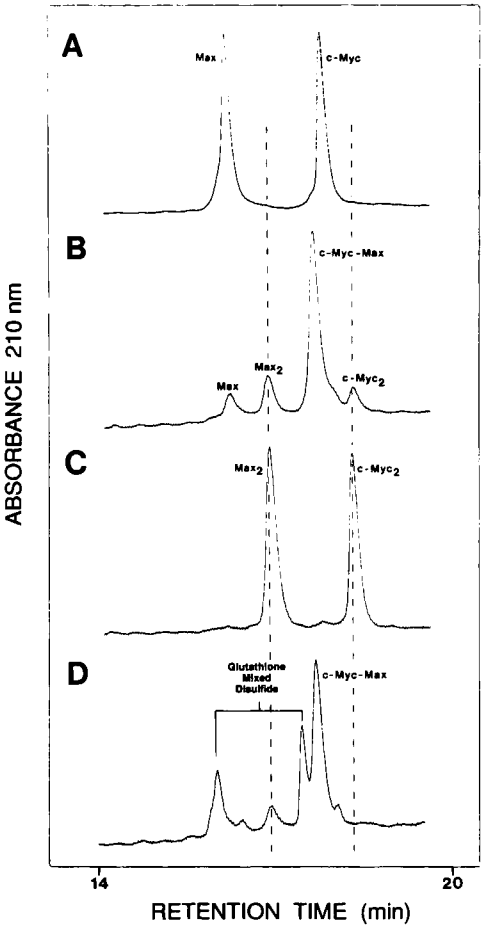

Figure 1. *RPC analysis of the dimerization behavior of N-terminal Cys-Gly- Gly c-Myc and Max leucine zippers at room temperature. (A) before and (B) after air-oxidation. (C) Redox experiment at time zero with Max and c-Myc disulfide-linked homodimers and (D) at equilibrium.*

References

1. Amanti, B., Brooks, M.W., Levy, N., Littlewood, T.D., Evan, G.I. and Land H., *Cell*, 72 (1993) 233.
2. Blackwood, E.M. and Eisenman, R.N., *Science*, 251 (1991) 1211.
3. Lavigne, P., Kondejewski, L.H., Houston, M.E. Jr., Sönnichsen, F.D., Lix, B., Sykes, B.D., Hodges, R.S. and Kay, C.M., *J. Mol. Biol.*, 254 (1995) 505.
4. O'Shea, E.K., Ruthkowski, R., Stafford, W.F. and Kim, P.S., *Science*, 241 (1989) 539.
5. Zhou, N.E., Kay, C.M. and Hodges, R.S., *J. Mol. Biol.*, 237 (1994) 500.

Peptides: Chemistry, Structure and Biology
Pravin T.P. Kaumaya and Robert S. Hodges (Eds.)
Mayflower Scientific Ltd., 1996

367
Novel Highly Cross-linked Supports for Solid Phase Peptide Synthesis

M. Kempe and G. Barany

Department of Chemistry, University of Minnesota, Minneapolis, MN 55455, USA

Introduction

Many organic chemical reactions traditionally carried out in homogeneous solution are now being adapted for solid-phase synthesis, thus creating a demand for suitable polymeric supports. For the solid-phase synthesis of peptides, most of the polymeric supports used have been low cross-linked, in order to assure good swelling properties. Earlier work from our laboratory has focused on supports that comprise polyethylene glycol (PEG) grafted onto low cross-linked polystyrene (PS). The resultant PEG-PS was shown to have several advantages with respect to PS [1].

The aim of the present work was to create novel highly cross-linked polymers still possessing good solvent swelling properties and which would be suitable as supports for various solid-phase synthesis applications. Branched PEG-containing cross-linkers were anticipated to be promising since (i) our earlier work on PEG-PS suggested the beneficial effect of PEG, and (ii) related cross-linkers lacking PEG have previously been reported to be useful for the preparation of supports for chromatography [2, 3].

Results and Discussion

The novel supports were prepared by copolymerization of the branched PEG-containing cross-linker **1** (trimethylolpropane ethoxylate (14/3 EO/OH) triacrylate) with (i) allylamine **2**, (ii) 2-aminoethyl methacrylate **3** and poly(ethylene glycol-400)-di-methacrylate **4**, (iii) 2-aminoethyl methacrylate **3** and poly(ethylene glycol) ethyl ether

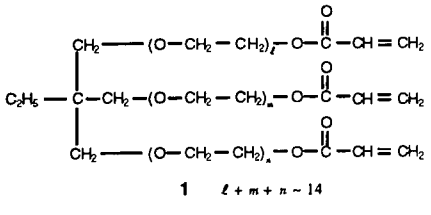

1 $\ell + m + n \sim 14$

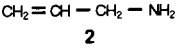

2

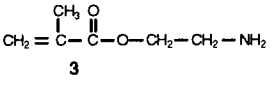

3

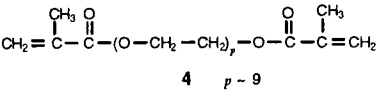

4 $p \sim 9$

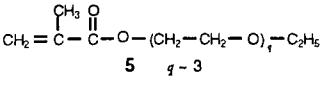

5 $q \sim 3$

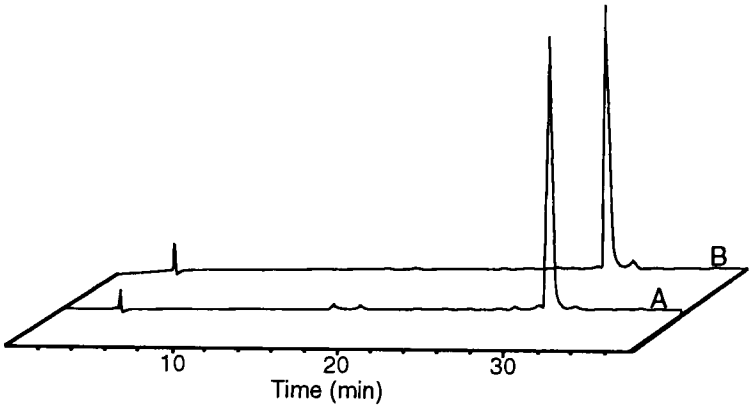

Figure 1. *HPLC chromatogram evaluating crude ACP (65-74) amide synthesized on a copolymer of* **1** *and* **2** *using (A) DIC and HOAt in DMF, or (B) DIC in MeCN, for couplings. A Vydac C_{18} reversed-phase column (4.6 x 250 mm) was eluted at a flow rate of 1 ml/min with a linear gradient over 30 min from 19:1 to 3:1 of 0.1% TFA in water and 0.1% TFA in MeCN. Peptides were detected spectrophotometrically at 220 nm.*

methacrylate **5**. The copolymers were prepared as bulk polymers, which were then ground and sieved (106-125 μm). An internal reference amino acid (Fmoc-Nle-OH) was coupled to the free amino groups on the resin particles, followed by deprotection and coupling of the handle Fmoc-5-(4-aminomethyl-3,5-dimethoxyphenoxy)valeric acid (PAL). These novel supports showed high swelling in various solvents (*e.g.*, DMF, MeCN, CH_2Cl_2, THF, H_2O). The challenging sequence 65-74 of acyl carrier protein (ACP) was synthesized successfully on the supports by Fmoc-chemistry, using both a conventional solvent (DMF) and a non-conventional solvent (acetonitrile) as the reaction as well as wash media (Figure 1). In addition, H-$(Ala)_{10}$-Val-NH_2 has been synthesized with results comparable to those obtained on commercial PEG-PS. Although these examples focus on solid-phase peptide synthesis, other experiments in progress are assessing the applicability of the described novel supports to the solid-phase synthesis of several other classes of organic molecules.

Acknowledgments

We thank the Royal Swedish Academy of Engineering Sciences' Hans Werthén Foundation for a postdoctoral fellowship (MK), and NIH (GM 42722 and 51628 to GB).

References

1. Zalipsky, S., Chang, J.L., Albericio, F. and Barany, G., *React. Polym.*, 22 (1994) 243, and references cited therein.
2. Reinholdsson, P., Hargitai, T., Isaksson, R. and Törnell, B., *Angew. Makromol. Chem.*, 192 (1991) 113.
3. Kempe, M. and Mosbach, K., *Tetrahedron Lett.*, 36 (1995) 3563.

Workshop I
Peptide Vaccines

Chairs: Fred Brown and Vernon Stevens

Workshop II
Peptides in Membranes

Chairs: Charles M. Deber and Gerald D. Fasman

Workshop III
Synthetic Peptide/Libraries

Chairs: Derek Hudson and Tom Lobl

Workshop IV
Peptide/Nonpeptide Mimetics

Chairs: Roger M. Freidinger and Arno F. Spatola

Peptides: Chemistry, Structure and Biology
Pravin T.P. Kaumaya and Robert S. Hodges (Eds.)
Mayflower Scientific Ltd., 1996

368
Peptide Vaccines: Dream or Reality?

F. Brown

Plum Island Animal Disease Center, Greenport, NY 11944, USA

Introduction

Protection against several infectious diseases of humans and animals has been achieved by vaccination. Tables 1 and 2 list the vaccines that are used currently in humans. Two classical methods are used to prepare virus vaccines and the vaccines against diphtheria and tetanus: (a) growth of the agents in large amounts followed by inactivation of their infectivity or toxicity without impairing their immunogenic activity and (b) weakening the pathogenic potential of the agents without impairing their ability to grow in the host and thus elicit appropriate immune responses.

Together, these two kinds of vaccine have made a great contribution to the health of humans and their domesticated animals. Nevertheless there are several reasons why we should not be satisfied with the current situation. For example, killed vaccines have several drawbacks:

- They present a hazard to personnel working with large amounts of human pathogens (*e.g.* rabies virus)
- They present a hazard to the environment such as that to livestock from foot-and-mouth disease virus
- The need to ensure complete inactivation of infectivity
- The presence of considerable amounts of cellular materials, leading to side effects
- More than one injection is usually required

Table 1. *Vaccines against viral diseases of humans.*

Disease	Type
Smallpox	Live
Measles	Live
Mumps	Live
Rubella	Live
Yellow fever	Live
Poliomyelitis	Live and killed
Acute respiratory disease (adenovirus)	Live
Rabies	Killed
Japanese Encephalitis	Killed
Influenza	Killed and subunit
Hepatitis A	Killed
Hepatitis B	Recombinant

Table 2. *Vaccines against bacterial diseases of humans.*

Disease	Type
Tuberculosis	Live
Whooping cough	Killed and subunit
Cholera	Killed
Typhoid	Killed and live
Typhus	Killed
Tetanus	Toxoid
Diphtheria	Toxoid
Meningitis	Subunit
-Haemophilus influenza type b	Polysaccharide-protein conjugate
-Meningococcal	Polysaccharide
Pneumonia	Polysaccharide

- Cold storage is required
- They have limited shelf life
- They fail to elicit protective immunity in all recipients

Attenuated vaccines also have drawbacks:

- The possible presence of adventitious agents in the cells and medium used for growth
- Occasional reversion to virulence
- Cold storage is essential
- They have limited shelf life.

More important, however, is the fact that there are several diseases for which the classical approaches are unlikely to be applicable because the causal agents cannot be grown in sufficient amounts (*e.g.* malaria, hepatitis C). Consequently, other ways of making vaccines have been investigated by studying the agents at the molecular level.

The New Technology. During the past three decades enormous advances have been made, not only in our knowledge of the composition of several micro-organisms but also in the way these elicit protective immune responses. Because of their relatively simple structures, compared with those of bacteria and parasites, more progress has been made with viruses. However, it is sobering to acknowledge that the first sub-unit vaccines were those prepared from the toxins excreted in cultures of the bacteria causing diphtheria and tetanus.

Dissection of the viruses causing influenza, rabies, and vesicular stomatitis by dissolving their lipid coats gives rise to sub-units which can be readily separated. From these studies, it emerged that protective immunity could be obtained by injection of only one or sometimes two proteins of a particular agent. An outstanding example is the high level of protection that can be elicited with the surface projections of rabies virus.

Detailed biochemical studies of virus replication provided maps of their genomes. These studies provided, in turn, the means of identifying the genes coding for those proteins of immunological interest. Consequently, as soon as methods for sequencing nucleic acids became available, the amino acid sequences of these immunologically important proteins could be derived. The pioneering experiments of Anderer and Sela's group with tobacco mosaic virus and MS_2 bacteriophage, in which they had shown that

short fragments of the viral proteins would elicit neutralizing antibody, could now be extended to viruses causing diseases in humans and animals.

Can peptides provide protection against disease? The early demonstrations by Anderer and Sela's group that short peptides could elicit neutralizing antibodies was soon confirmed for a variety of organisms. This led to considerable optimism that peptide vaccines would soon be available. The advantages of such vaccines are potentially enormous:

- The products are chemically defined
- They are stable indefinitely
- There is no infectious agent present
- Large scale production plant is not required
- They can be designed to stimulate appropriate immune responses
- They are ideal for incorporation into delayed release mechanisms

Considerable research allows the following conclusions to be drawn:

(a) In addition to the B cell epitope, a T cell epitope suitable for the recipient species is required. The T cell epitope can be part of the agent but a foreign epitope is also functional. The function of a carrier protein, once considered to be mandatory, was to provide a T-cell epitope.

(b) The sequential order of the B- and T-cell epitopes is important. There is some evidence that the less ordered structure of the T-B constructs may contribute to enhanced activity.

(c) Immunogenicity can be greatly enhanced by linking the B-cell epitope of hepatitis B virus with the immunostimulatory region of interleukin 1.

(d) Multiple copies of the B-cell epitope provide greatly enhanced responses, as demonstrated by the multiple antigenic peptide (MAP) system or by its presentation on the hepatitis B virus core or surface antigen.

(e) Good responses to B-cell epitopes can be obtained without using conventional adjuvants by presenting the sequence linked to a lipopeptide.

(f) Recent data indicate that the configuration of B-cell epitopes can be mimicked by retro inverso D-amino acid peptides. Astonishingly, preliminary evidence suggests that T-cell epitopes can also be mimicked by retro inverso D-amino acid peptides. These observations are important because D-amino acid peptides are much less vulnerable to proteolytic enzyme attack.

The practical advantages of peptide vaccines and the basic knowledge regarding the interaction of peptides with the major histo-compatibility complex provide convincing evidence that the dream of such vaccines may eventually become reality.

Peptides: Chemistry, Structure and Biology
Pravin T.P. Kaumaya and Robert S. Hodges (Eds.)
Mayflower Scientific Ltd., 1996

369

Transcending the Structuralist Paradigm in Immunology: Affinity and Biological Activity Rather than Purely Structural Considerations Should Guide the Design of Synthetic Peptide Epitopes

M.H.V. Van Regenmortel

Centre National de la Recherche Scientifique (CNRS), Institut de Biologie Moléculaire et Cellulaire, Strasbourg 67084, France

Introduction

The structuralist paradigm assumes that it is possible to understand complex biological recognition phenomena solely in terms of structural data. This paradigm corresponds to the prevailing research tradition among molecular biologists which is to reduce complex biological phenomena to simple physico-chemical interactions and to express all biological problems in structural terms. The structuralist paradigm emphasizes the key role played by structural analysis in explanatory models of biological specificity.

Current attempts to design the most effective synthetic B-cell epitopes are guided by this emphasis on structure, a concept which results from the selective attention to the visual experience of an object at a specific time. For proteins, structure refers to a visual time slice of what are essentially dynamic systems. Focusing only on protein spatial coordinates, as often done in structural analysis, is inadequate for understanding antigen-antibody recognition as it tends to minimize the contribution of induced fit and mutual adaptations to binding. Molecular dynamic simulations, NMR studies and kinetic measurements are needed to account for these facets of specific biological interactions.

In immunology, the structuralist paradigm has led to the expectation that it should be possible to design synthetic vaccines on the basis of X-ray structures of antibody-peptide complexes. It is widely assumed that success in rational ligand design will be achieved by the continued refinement of structural data to provide eventually full understanding of the steric and physico-chemical complementarity between epitopes and paratopes. However, literature review shows that our ability to predict the occurrence and affinity of antibody binding has hardly progressed in recent years. Attempts to use protein-protein docking for identifying antibody combining sites have been singularly ineffective.

In a recent study, it was shown that the frequency distribution of successfully docked, complementary antigen-antibody patches was the same whether the docking counterparts were able to bind or not [1]. Apparently, existing docking algorithms can only exclude partners that are sterically and chemically incompatible but they cannot identify among the many compatible shapes those which actually permit complex formation. The ineffectiveness of predictive docking and the impossibility to predict the binding energy of antibodies illustrates our limited understanding of what actually

accounts for the specificity of binding. Although the imprecision of existing docking algorithms may be partly responsible for this state of affairs, it seems likely that the neglect of bound water molecules and counterions and the unwarranted assumption that proteins are rigid bodies are the main reasons for the failure to predict potential binders. Since many of the charged groups and potential hydrogen bond partners are present on mobile surface side chains of the antigen and antibody, the complementarity observed in the complex may in fact not pre-exist in the free molecules before the occurrence of induced fit and mutual adaptation.

Results and Discussion

Since the earlier structural analyses of antigen-antibody complexes were done at medium resolution (about 3 to 2.5 Å), they did not allow the identification of bound water molecules within the crystals [2]. For many years, it was assumed that the interaction between epitope and paratope was very tight and that there were no water molecules at the interface. Subsequently, when the structures of the free and bound forms of the anti-lysozyme Fv D 1.3 antibody fragment were solved at 1.8 Å resolution, it was found that as many as 50 water molecules were located around the interface and were making hydrogen bonds with protein residues and with other water molecules [3]

As crystal structures of increased resolution become available for antigen-antibody complexes, it is likely that a general pattern will emerge with water as a constitutive part of X-ray derived molecular models of epitope-paratope interfaces. Although accurate positioning of solvent molecules in crystal structures is an essential requirement for understanding the structural and dynamic properties of proteins, the contribution of the water molecules to the measured binding affinity of the complexes is difficult to assess.

An epitope is not an intrinsic feature of a protein existing independently of its paratope partner. Both epitopes and paratopes are relational entities defined by their mutual complementarity and it makes no sense to analyze their properties outside of this relational nexus [4]. This means that the concept of epitope is derived from the process of binding to a complementary partner, and not from a structure that could be defined before the interaction has taken place. If it is accepted that epitopes and paratopes are relational entitites and that the binding process in the unique protein-solvent environment emerging from the close proximity of the two partners is also of a relational nature [1], it is conceivable that a purely structural analysis may never succeed in predicting which antibody molecules will be able to form stable complexes with a particular antigen. Science has been defined as the art of the soluble [5] and, if docking cannot be achieved using currently available methods, one may well question the validity of pursuing such attempts as a realistic scientific enterprise. If certain aims are not realizable, this is a rational ground for adopting different methods.

It seems that further understanding of immunological specificity requires another approach altogether, *i.e.* by analysis of binding activity instead of structure [4]. Functional analysis amounts to asking a different type of question about the nature of the interaction. The analysis of binding activity focuses on the time component of the interaction since it is based on the kinetic on and off rates of the reaction, and it does not consider the spatial or steric coordinates of the interacting molecules. By site-directed mutagenesis of antigen and antibody molecules and measurements of the binding affinity

of the mutated molecules, it is possible to attribute to various critical residues a certain amount of the free energy of complex formation. However, antigen-antibody binding should always be described and analyzed in terms of single atomic interactions and not in terms of whole residues. Speaking of contact residues is misleading since it is unlikely that all or even most of the atoms of a given residue participate in the interaction.

In many cases, substitutions of residues that are not in contact at the interface between epitope and paratope have been found to affect the binding affinity. It seems that exchanges of whole residues in a protein often produce small structural shifts that may propagate far beyond the mutated region. These small perturbations are not easily detected at the current resolution of structural data although they are able to significantly affect the binding activity. Such findings demonstrate the importance of binding measurements for achieving a complete description of the recognition site, both from a structural and functional point of view.

The recent introduction of biosensor instruments based on surface plasmon resonance [6] has greatly facilitated the quantitative measurement of binding interactions. Biosensor technology has been used widely to measure differences in antibody affinity arising from single substitutions or modifications in peptide antigens [7]. Such studies also make possible evaluation of the antigenic potential of peptide analogs such as retro-inverso peptides [8]. The measurement of binding affinity provides the most direct and relevant information for assessing functional activity of synthetic peptide epitopes.

In the so-called rational design of synthetic peptides able to mimic biologically relevant antigenic sites, it is customary to base the design mainly on structural parameters. However, it would seem equally important to use activity measurements for assessing the quality of mimicry achieved with synthetic constructs. Affinity and biological activity are direct measures of how well a peptide is likely to perform as antigen or immunogen. Structural information is necessary for suggesting which avenues should be explored for achieving antigen mimicry with synthetic peptides. However, it is essential to collect functional data as early as possible during the development of synthetic epitopes. Binding and affinity measurements are likely to be at least as useful as structural information for guiding the design of peptides endowed with improved biological or antigenic activity [9].

References

1. Carneiro, J. and Stewart, J., *J. Theor. Biol.*, 169 (1994) 391.
2. Davies, D.R., Padlan, E.A. and Sheriff, S., *Annu. Rev. Biochem.*, 59 (1990) 439.
3. Bhat, T.N., Bentley, G.A., Boulot, G., Greene, M.I., Tello, D., Dallacqua, W., Souchon, H., Schwarz, F.P., Mariuzza, R.A. and Poljak, R.J., *Proc. Natl. Acad. Sci. USA*, 91 (1994) 1089.
4. Van Regenmortel, M.H.V., *Immunol. Today*, 10 (1989) 266.
5. Medawar, P. in 'The Art of the Soluble', Methuen, London, 1967.
6. Malmqvist, M., *Nature*, 361 (1993) 186.
7. Rauffer, N., Zeder-Lutz, G., Wenger, R.M., Van Regenmortel, M.H.V. and Alschuh, D., *Molec. Immunol.*, 31 (1994) 913.
8. Guichard, G., Benkirane, N., Zeder-Lutz, G., Van Regenmortel, M.H.V., Briand, J.P. and Muller, S., *Proc. Natl. Acad. Sci. USA*, 91 (1994) 9765.
9. Van Regenmortel, M.V.H., *Biomed. Pept. Prot. Nucl. Acids*, 1 (1995) 109.

Peptides: Chemistry, Structure and Biology
Pravin T.P. Kaumaya and Robert S. Hodges (Eds.)
Mayflower Scientific Ltd., 1996

370
Synthetic, Structural and Immunochemical Approaches to Antigen-Antibody Interactions in Foot-and-Mouth Disease Virus

D. Andreu[1], J.A. Camarero[1], M.L. Valero[1], X. Roig[1], T. Haack[1], E. Giralt[1], N. Verdaguer[2], I. Fita[2], M.G. Mateu[3] and E. Domingo[3]

[1]*Department of Organic Chemistry, University of Barcelona, E-08028 Barcelona, Spain*
[2]*Department of Macromolecular Chemistry, Polytechnic University of Catalonia, E-08028 Barcelona, Spain*
[3]*Severo Ochoa Center for Molecular Biology, CSIC, E-28049 Madrid, Spain*

Introduction

Some of the problems underlying the use of peptide-based vaccines have to do with the difficulty inherent in reproducing complex (viral, protozoal, *etc.*) epitopes by means of relatively simple peptide constructions. The obvious challenges of this task are simplified when the immunodominant regions of an infective agent can be traced to a relatively small region (termed a continuous epitope) of a given protein antigen which can be appropriately reproduced by a linear peptide. Foot-and-mouth disease virus (FMDV) is a good candidate for this type of studies because its major antigenic site A, located at the G-H loop of VP1(residues 136-156 in serotype C-S8c1), contains several epitopes that can be faithfully reproduced by linear peptides.

Results and Discussion

We have carried out extensive immunochemical analysis of the antigenic structure of the GH loop of FMDV using MAbs reactive with YTASARGDLAHLTTTHARHLP (A21), a 21-residue peptide that reproduces antigenic site A, and analogs incorporating antigenically relevant mutations [1]. The effect of such changes at positions 146 and 147 on the conformation of the peptide has been examined by CD in the presence of the Fab fragment of SD6, a neutralizing MAb that recognizes site A of C-S8c1 [2]. Although A21 was shown to adopt an α-helical structure on binding to the antibody, globally the results did not support the notion of an α-helix as a critical feature in the interaction. The RGD sequence of site A, known to be involved in the infective process, was shown to be a target for most of the MAbs mapping at site A [3]. Obviously, mutations at nearby residues such as 146 or 147 are capable of generating enough structural diversity to deviate immune pressure from the highly conserved RGD motif without altering its functional conformation, thus ensuring viral propagation.

Even in those cases when a major part of the immune response can be related to a continuous epitope, the problem remains of stabilizing a mobile peptide sequence into a biologically significant conformation. For FMDV, the highly disordered nature of the G-H loop seriously limits the structural definition available from X-ray diffraction data [4, 5]. Our first attempts to model site A of FMDV C-S8c1 by conformational restriction of the linear sequence were done in the absence of any structural data on this serotype and were based on comparison with the homologous region of O_1BFS, for which a 3D structure was available [4]. Disulfide **1** and lactam **2** analogs of peptide A21 (Figure 1) were prepared by a variety of methods involving both solution and solid phase cyclizations [6, 7].

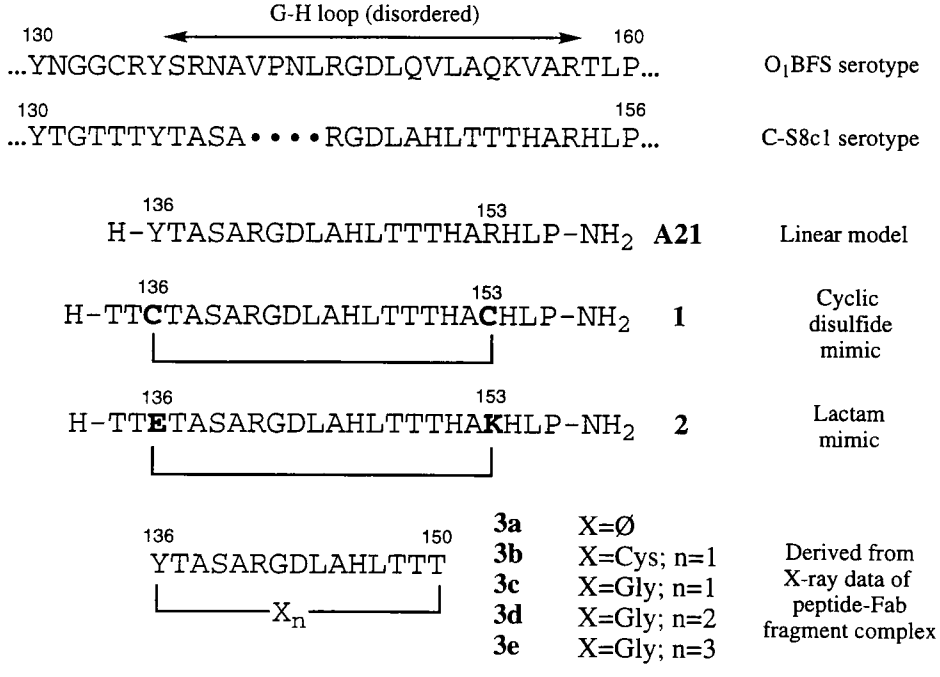

Figure 1. *Linear and cyclic models of the G-H loop (antigenic site A) of FMDV, serotype C-S8c1.*

The 3D structure of the C-8Sc1 serotype of FMDV, published a year ago [4], indicated that structural homologies between O and C serotypes, as it concerned antigenic site A, could be limited. At about the same time, more relevant information became available through crystallization and X ray diffraction analysis [8] of a Fab fragment of MAb SD6. Soon afterwards, the structure of a complex between this Fab fragment and the linear pentadecapeptide YTASARGDLAHLTTT (residues 136-150 of VP1) was resolved [9]. This provided decisive information about the interaction of site A with antibodies, particularly as related to the direct involvement of the RGD triplet in the specific interaction with an antigen receptor. The 3D structure also allowed an interpretation of viral neutralization by antibodies directed to site A, by direct blocking

of the interaction with the cell receptor. In addition, the data provided valuable insight for the design of structurally optimized mimics of site A. Interaction with the Fab fragment induces upon the peptide an almost cyclic conformation in which the C-terminal Thr^{150} is brought close to the N-terminal Tyr^{136}. An attempt to stabilize this arrangement was made by means of the head-to-tail series of analogs **3a-e**, which were prepared and cyclized by a variety of methods [10]. The antigenicity of peptides **1** and **2** towards a representative group of neutralizing MAbs was evaluated in competitive ELISA assays. In general, this type of cyclizations did not result in an improved recognition by any of the MAbs. In contrast, cyclization did have a clear enhancing effect on the immunogenicity of **1**. In guinea pigs, the cyclic disulfide peptide gave anti-FMDV and neutralization titers more than one order of magnitude higher than either the linear (A21) or the lactam analogs.

References

1. Carreño, C., Roig, X., Cairó, J.J., Camarero, J., Mateu, M.G., Domingo, E., Giralt, E. and Andreu, D., *Intl. J. Peptide Protein Res.*, 39 (1992) 41.
2. Roig, X., Novella, I.S., Giralt, E. and Andreu, D., *Lett. in Pept. Sci.*, 1 (1994) 39.
3. Novella, I.S., Borrego, B., Mateu, M.G., Domingo, E., Giralt, E. and Andreu, D., *FEBS Lett.*, 330 (1993) 253.
4. Acharya, R., Fry, E., Stuart, D., Fox, G., Rowlands, D. and Brown, F., *Nature*, 337 (1989) 709.
5. Lea, S., Hernández, J., Blakemore, W., Brocchi, E., Curry, S., Domingo, E., Fry, E., Abu-Ghazaleh, R., King, A., Newman, J., Stuart, D. and Mateu, M.G., *Structure*, 2 (1994) 123.
6. Camarero, J.A., Giralt, E. and Andreu, D., *Tetrahedron Lett.*, 36 (1995)1137.
7. Camarero, J.A., Cairó, J.J., Giralt, E. and Andreu, D., *J. Pept. Sci.*, 1 (1995) 245.
8. Verdaguer, N., Mateu, M.G., Bravo, J., Tormo, J., Giralt, E., Andreu, D., Domingo, E. and Fita, I., *Proteins*, 18 (1994) 201.
9. Verdaguer, N., Mateu, M.G., Andreu, D., Giralt, E., Domingo, E. and Fita, I., *EMBO J.*, 14 (1995) 1690.
10. Valero, M.L., Camarero, J.A., Adeva, A., Verdaguer, N., Fita, I., Mateu, M.G., Domingo, E., Giralt, E. and Andreu, D., *Biomed. Pept. Prot. Nucl. Acids*, 1 (1995) 133.

Peptides: Chemistry, Structure and Biology
Pravin T.P. Kaumaya and Robert S. Hodges (Eds.)
Mayflower Scientific Ltd., 1996

371
Peptide Conformation as a Function of the Molecular Environment

C.M. Deber and S.-C. Li

Biochemistry Research Division, Research Institute, Hospital for Sick Children, Toronto M5G 1X8, Canada
Department of Biochemistry, University of Toronto, Toronto M5S 1A8, Ontario, Canada

Introduction

Transmembrane helices of integral membrane proteins differ from helical segments in globular proteins in two aspects: amino acid composition and molecular environment. The impact of environment on the relative helical propensities and structural properties of peptide segments are now investigated using model peptides representing a condensed version of a single-spanning membrane protein [1]. The peptides have a prototypical sequence of H_2N-S-K-S-K-A-**X**-A-A-**X**-A-W-A-**X**-A-K-S-K-S-K-S-OH, where **X** = an uncharged amino acid (excluding Trp and Cys), and are designated AXA according to the corresponding repeating triads (underlined above) within the hydrophobic segment. Conformational studies on these peptides by circular dichroism (CD) spectroscopy revealed that the α-helical propensity of individual amino acids in the membrane environment is defined primarily by its side chain hydrophobicity rather than its side chain chemistry as in water [1].

Results and Discussion

Conformations of model peptides in aqueous buffer. The helical propensities of the guest residue "X" in aqueous environment were first examined by measuring the CD of the corresponding peptides. Results obtained from our system can then be compared with those measured using other reference peptides to assess the suitability of the present peptides for deriving helix propensity. In aqueous media, pH 7.0, we found that a few residues - notably Ala, Leu and Met - exhibited relatively higher helical propensity in their respective peptides AAA, ALA and AMA, consistent with the high P_α values predicted by Chou and Fasman [2] based on the frequency of occurrences of these residues in helical segments of globular proteins [1]. As well, there is a generally good correlation between the observed peptide ellipticities in aqueous buffer and those measured by Lyu et al [3] for a different reference peptide (Figure 1). These results indicate that the present peptides are suitable for the purpose of deriving helix propensities of amino acids.

Peptide conformation in membrane-mimetic environments. A variety of membrane-mimetic media, including detergent/lipid micelles, lipid vesicles, and organic solvents,

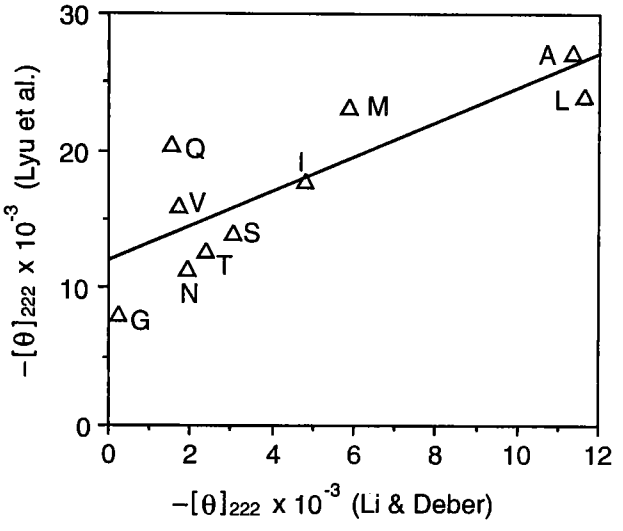

Figure 1. *Correlation of ellipticity data (θ_{222}, deg.cm^2/dmol) observed in aqueous buffer for the present peptides with those reported by Lyu et al. [3] for peptides $YSE_4K_4X_3E_4K_4$, where X = A, L, M, I, Q, S, V. T, N, or G (as labeled on the diagram). R = 0.84.*

have been employed in our laboratory to examine the conformation of the peptide as a function of molecular environment [1, 4]. In the present paper, data obtained in 10 mM SDS micelles (reported in Ref. 1) are used to derive the free energy of helix-coil transition according to the two state model [4]:

$$\Delta G = -RT\ln \frac{[\text{helix}]}{[\text{coil}]} = -RT\ln \frac{[\theta]_{\text{observed}} - [\theta]_{\text{coil}}}{[\theta]_{\text{helix}} - [\theta]_{\text{observed}}}$$

The ellipticity of a complete 20-residue α-helix, $[\theta]_{\text{helix}}$, is assumed to be -34,400 deg.cm^2/ dmol, while that of a random coil, $[\theta]_{\text{coil}}$, 0 [4]. The ΔΔG values - the free energy of helix-formation for the guest amino acids relative to Pro (in peptide APA) in SDS micelles can be calculated from the corresponding ΔG values of the peptides [4]. The magnitudes of the ΔΔG values are comparable to those determined for the corresponding amino acids in aqueous environments, suggesting that the same factors that stabilize the helical conformation in water, such as H-bonding of the peptide backbone, are likely the main contributors to helix-stability in membranes as well. Since intramolecular H-bonding is favored in the low dielectric environment of the membrane, we propose that discrepancies of free energy which do arise among individual guest amino acids result from differences in their side chain hydropathy; the latter factor dictates the inherent extent of association between the peptide hydrophobic core and the lipid. Consistent with this notion, helix-forming tendencies of the guest amino acids, as represented by the ΔΔG values, correlate closely with the corresponding residue hydropathy indices from the Kyte-Doolittle scale [correlation coefficient, 0.81 (Figure 3)]. It is also noticed that the current ΔΔG values span a much narrower range than those

determined in water, suggesting that the membrane environment is less discriminative than water. The negative nature of the free energy change indicates that all amino acids examined are good helix-formers relative to proline in the membrane environment of SDS. The ΔΔG values allow a ranking of the helical propensities for the guest amino acids in the membrane environment. In contrast with the situation in water, β-branched residues such as Val and Ile prove to be helix-promoting rather than helix-destabilizing.

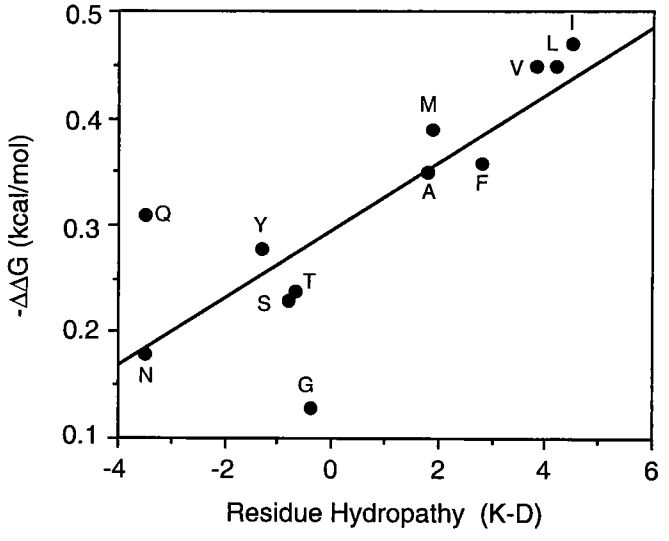

Figure 2. *Free energy of helix-formation for the guest amino acids in SDS micelles vs. their hydropathy indices. ΔΔG values are taken from ref. 4. Residue hydropathy values are as given in the Kyte-Doolittle scale [5]. R = 0.81.*

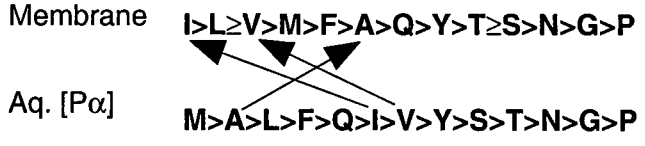

Figure 3. *Relative helix propensities of amino acids determined in the membrane-mimetic environment of SDS micelles vs. Chou-Fasman [P_α] for soluble proteins. Amino acids displaying the greatest alterations from one scale to the other are identified by arrows.*

References

1. Li, S-C. and Deber, C.M., *Nature Struct. Biol.*, 1 (1994) 368.
2. Chou, P.Y. and Fasman, G.D., *Annu. Rev. Biochem.*, 47 (1978) 251.
3. Lyu, P.C., Liff, M.I., Marky, L.A. and Kallenbach, N.R., *Science*, 250 (1990) 669.
4. Deber, C.M. and Li, S-C., *Biopolymers (Peptide Sci.)*, 37 (1995) 295.
5. Kyte, J. and Doolittle, R.F., *J. Mol. Biol.*, 157 (1982) 105.

Peptides: Chemistry, Structure and Biology
Pravin T.P. Kaumaya and Robert S. Hodges (Eds.)
Mayflower Scientific Ltd., 1996

372
Peptide Modulation of Membrane Stability

R.M. Epand

Department of Biochemistry, McMaster University Health Sciences Centre, Hamilton, Ontario, L8N 3Z5, Canada

Introduction

The amphipathic helix has been shown to play a role in the interaction of peptides and proteins with lipids [1]. Amphipathic helical peptides, as well as other peptides, can be either stabilizing to membrane bilayers or they can be lytic [2]. In the case of amphipathic helical peptides, the consequences of their incorporation into membranes depends, at least in part, on the size and charge distribution of the hydrophilic face of the amphipathic helix [3].

Bilayer Stabilizing Amphipathic Helical Peptides

One class of helix is the class A amphipathic helix which is characterized by having cationic residues near the hydrophobic/hydrophilic interface and anionic residues opposite to the hydrophobic face. Class A helices are found in the exchangeable plasma apolipoproteins. The class A amphipathic helices can stabilize membrane bilayers relative to inverted phases [4]. Membrane bilayers which are close to the bilayer to hexagonal phase transition temperature (T_H) possess negative curvature strain [5]. This physical property may have biological importance since microorganisms adjust the lipid composition of their membranes for them to be close to T_H [6-8]. Transbilayer diffusion of phospholipids also appears to be sensitive to curvature strain [9]. A biological process which requires the transbilayer diffusion of phospholipids is blood coagulation. Both the plasma apolipoprotein A-I (apo A-I) and a model peptide containing two class A amphipathic helices linked by a Pro can inhibit the generation of procoagulant activity in human erythrocytes [10]. This bilayer stabilization may contribute to the beneficial biological role of proteins containing class A helical segments, such as apo A-I.

Bilayer Destabilizing Amphipathic Helical Peptides

Many amphipathic helical peptides which are cytolytic contain class L peptides. Class L helices have a narrower hydrophilic domain of predominantly Lys residues. There are at least two distinct mechanisms by which these substances can perturb the integrity of membrane bilayers. One is by affecting curvature and the other is by forming pores through the membrane, composed of helical clusters. It is possible that any amphipathic helical peptide will form a pore at a high enough peptide to lipid ratio. However, certain

peptides form pores even at quite low mole fractions in the membrane. The pore-forming peptides can be lytic to cell membranes, not through a perturbation of the bulk physical properties of the membrane, but by promoting the leakage of ions through the membrane leading to osmotic lysis.

One of the interests in these peptides comes from the fact that a number of them have antibiotic activity. In order to be useful as antimicrobial agents in vertebrates, these peptides must be selectively lytic to microbes. Three of the factors that contribute to this selectivity have been identified [11] by comparing magainin, a class L antimicrobial peptide, with melittin, a cytolytic peptide. The factors include promotion of lysis by toxic peptides in the presence of anionic lipids on the outer surface of microorganisms but not animal cells. The requirement for anionic lipids has also been observed with the antimicrobial peptide, dermaseptin [12]. However, even peptides toxic to mammalian cells, such as δ-lysin [13], interact differently with anionic and zwitterionic lipids. Another difference that can lead to selectivity for microbial cells is the lack of cholesterol in their cell membrane [11, 14]. It has been suggested that class L peptides which are not toxic to animal cells have a Glu residue on the hydrophobic face of the amphipathic helix and that this Glu can form H-bonds with cholesterol to reduce the lytic activity of the peptide [14]. The third factor is the transmembrane potential which will increase the lytic action of magainin [11].

Viral Fusion Peptides

The fusion of enveloped viruses with target membranes is mediated by specific viral glycoproteins. For certain viruses there have been identified short segments of the these proteins which appear to be particularly important for membrane fusion. These viral fusion peptides have been used as a simple model to study some of the molecular details of processes involved in the initiation of membrane fusion. A property common to fusion peptides of both influenza virus [15] and Simian Immunodeficiency Virus (SIV) [16] is that they promote the formation of H_{II} phases. The wild type SIV fusion peptide has been shown to insert into membranes at an oblique angle to the bilayer normal and this property appears to be closely correlated with fusogenic activity [17]. We have recently studied the effect of these peptides on the morphology of several different lipids using x-ray diffraction [18].

Peptide Inhibitors of Viral Fusion

Viral fusion peptides increase the tendency of bilayers to convert to the H_{II} phase and peptides which raise T_H are often found to be inhibitors of viral fusion. Inhibitors include small peptides, such as Z-fFG [19, 20] as well as the class A amphipathic helix-containing apo A-I [21, 22]. Particularly potent in this regard are peptides which are anchored to the membrane by covalently attached lipid groups [23].

Acknowledgment

The support of the Medical Research Council of Canada is acknowledged.

References

1. Segrest, J.P., Jackson, R.L., Morrisett, J.D. and Gotto, A.M., Jr., *FEBS Lett.*, 38 (1974) 247.
2. Epand, R.M., Shai, Y., Segrest, J.P. and Anantharamaiah, G.M., *Biopolymers (Peptide Science)* 37 (1995) 319.
3. Segrest, J.P., de Loof, H., Dohlman, J.G., Brouillette, C.G. and Anantharamaiah, G.M., *Proteins,* 8 (1990) 103.
4. Tytler, E.M., Segrest, J.P., Epand, R.M., Nie, S.-Q., Epand, R.F., Mishra, V.K., Venkatachalapathi, Y.V. and Anantharamaiah, G.M., *J. Biol. Chem.*, 268 (1993) 22112.
5. Gruner, S.M., in Yeagle, P. (Ed.), 'The Structure of Biological Membranes', CRC Press, Boca Raton, FL, 1992, p.211.
6. Lindblom, G., Hauksson, J., Rilfors, L., Bergenstahl, B., Wieslander, A. and Erilsson, P.O., *J. Biol. Chem.*, 268 (1993) 16198.
7. Rilfors, L., Hauksson, J.B. and Lindblom, G., *Biochemistry*, 33 (1994) 6110.
8. Rietveld, A.G., Chupin, V.V., Koorengevel, M.J., Wienk, H.L.J., Dowhan,W. and de Kruijff, B., *J. Biol. Chem.*, 269 (1994) 28670.
9. Tournois, H., Henseleit, U., DeGier, J., DeKruijff, B. and Haest, C.W.M., *Biochim. Biophys. Acta,* 946 (1988) 173.
10. Epand, R.M., Stafford, A., Leon, B., Lock, P.E., Tytler, E.M., Segrest, J.P. and Anantharamaiah, G.M., *Arterioscler. Thromb.*, 14 (1994) 1775.
11. Matsuzaki, K., Sugishita, K.-I., Fujii, N. and Miyajima, K., *Biochemistry*, 34 (1995) 3423.
12. Pouny, Y., Rapaport, D., Mor, A., Nicolas, P. and Shai, Y., *Biochemistry,* 31 (1992) 12416.
13. Prenner, E., Hermetter, A., Paltauf, F., Laggner, P. and Lohner, K., ESF Workshop on "Principles and Applications of Liposomes" 1994, p. 166.
14. Tytler, E.M., Anantharamaiah, G.M., Walker, D.E., Mishra, V.K., Palgunachari, M.N. and Segrest, J.P., *Biochemistry,* 34 (1995) 4393.
15. Epand, R.M. and Epand, R.F., *Biochem. Biophys. Research Commun.,* 202 (1994) 1420.
16. Epand, R.F., Martin, I., Ruysschaert, J.-M. and Epand, R.M., *Biochem. Biophys. Research Commun.,* 205 (1994) 1938.
17. Martin, I., Dubois, M.-C., Defrise-Quertain, F., Saermark, T., Burny, A., Brasseur, R. and Ruysschaert, J.M., *J. Virology,* 68 (1994) 1139.
18. Colotto, A., Martin, I., Ruysschaert, J.-M. and Epand, R.M., (1996) this volume.
19. Epand, R.M., *Biosci. Rep.,* 6 (1986) 647.
20. Dentino, A.R., Westerman, P.W. and Yeagle, P.L., *Biochim. Biophys. Res. Commun.,* 1235 (1995) 213.
21. Owens, R.J., Anantharamaiah, G.M., Kahlon, J.B., Srinivas, R.V., Compans, R.W. and Segrest, J.P., *J. Clin. Invest.*, 86 (1990) 1142.
22. Srinivas, R.V., Birkedal, B., Owens, R.J., Anantharamaiah, G.M., Segrest, J.P. and Compans, R.W., *Virology,* 176 (1990) 48.
23. Epand, R.F., Moroder, L., Lutz, J., Flanagan, T.D., Nir, S. and Epand, R.M., (1995) this volume.

Peptides: Chemistry, Structure and Biology
Pravin T.P. Kaumaya and Robert S. Hodges (Eds.)
Mayflower Scientific Ltd., 1996

373
Synthetic Combinatorial Libraries Screened in Solution

C. Pinilla, J.R. Appel, S.E. Blondelle, C.T. Dooley, B. Dörner, J. Eichler, J.M. Ostresh and R.A. Houghten

Torrey Pines Institute for Molecular Studies, San Diego, CA 92121 USA

Introduction

Synthetic combinatorial libraries (SCLs) are composed of separate compound mixtures with one or more defined positions in the sequence. Since these mixtures are in solution, they have been used in a number of bioassays ranging from soluble receptors to whole cells. The initial SCL [1] was composed of 400 hexapeptide mixtures having the first two positions defined (O_1,O_2) and the remaining four positions consisted of approximately equimolar mixtures of 19 of the 20 natural amino acids. Thus, each of the 400 peptide mixtures is made up of 19^4= 130,321 individual hexamers, and the library represents a total of 52,321,400 individual peptides. This type of library is typically synthesized using the divide, couple and recombine method in combination with simultaneous multiple peptide synthesis. Individual active compounds are deconvoluted through an iterative process of the most active peptide mixtures in the library. The iterative process involves ranking, selecting and reducing the number of mixture positions while defining one more mixture position at each step. This SCL format has been utilized for the synthesis of various peptide and peptidomimetic libraries [2]. The screening of such libraries have led to the identification of potent antagonists [3] and agonists; an agonist with high selectivity for the μ receptor was identified from a hexapeptide library composed entirely of D- amino acids [4]. Also, highly active antimicrobial peptides have been identified from a library composed of L-, D- and unnatural amino acids [5].

An alternative approach, termed a positional scanning SCL (PS-SCL) [6], enables the identification of the most active residues at each position of a sequence in a single assay, thus avoiding the iterative process of synthesis and screening of the original SCL format. This approach has been used for the synthesis of a number of libraries varying in length and composition (Table 1). Other laboratories have used the positional scanning approach for the preparation and use of combinatorial libraries [7-9].

Results and Discussion

The broad applicability of combinatorial libraries is illustrated in Table 2, in which high affinity sequences for two different antigen-antibody interactions and two opioid receptors were identified from a nonacetylated hexapeptide PS-SCL. The versatility of SCLs is a consequence of the fact that they are composed of mixtures of compounds in

Table 1. *Positional scanning libraries.*

Length	Composition	Reference
Hexapeptide	L-amino acids	6, 10-13
Decapeptide	L-amino acids	14
Hexapeptide	D-amino acids	11
Tetrapeptide	L-, D- and unnatural amino acids	15
Cyclic tetramer template	L-amino acids and carboxylic acids	16
α-helical defined 18-mer	L-amino acids	17
Permethylated Hexamer	Modified L-amino acids	18
Reduced Hexamer	Reduced L-amino acids	19

Table 2. *Hexapeptide positional scanning library.*

Acceptor/ Assay	Positions/ Most Active Amino Acids	# of Individual Peptides Synthesized	3 Most Active Individual Sequences	IC_{50} (nM)	Ref.
	1 2 3 4 5 6				
mAb 3E7	Y G A F L D	16	YGGFNP-NH_2	1	11
Competitive ELISA	G MN		YGGFMQ-NH_2	1	
	P, Q		YGGFLP-NH_2	2	
mAb M1	D Y K AK A	16	DYKAKE-NH_2	3	13
Competitive ELISA	E E		DYKEKL-NH_2	5	
	L L		DYKQKE-NH_2	5	
	Q Q				
μ opioid receptor	Y G F F F F	16	YGGFMY-NH_2	17	10
RRA[a]	G L R		YGGFMR-NH_2	24	
	M		YGGFYY-NH_2	40	
	Y				

[a] Radioreceptor assay (^{3}H-DAMGO).

solution, which can be screened in virtually any bioassay of interest. The versatility is also reflected by the range of libraries with different formats and compositions. The concept of "libraries from libraries" [18], which is based on the post-synthetic modification of parent peptide or non-peptide libraries, opens the door to novel chemical diversities with great therapeutic potential.

Acknowledgments

This work was funded by Houghten Pharmaceuticals, Inc., San Diego, CA.

References

1. Houghten, R.A., Pinilla, C., Blondelle, S.E., Appel, J.R., Dooley, C.T. and Cuervo, J.H., *Nature,* 354 (1991) 84.
2. Pinilla, C., Appel, J., Blondelle, S., Dooley, C., Dörner, B, Eichler, J., Ostresh, J. and Houghten, R.A., *Biopolymers (Pept. Sci.),* 37 (1995) 221.
3. Dooley, C.T., Chung, N.N., Schiller, P.W. and Houghten, R.A., *Proc. Natl. Acad. Sci. USA,* 90 (1993) 10811.
4. Dooley, C.T., Chung, N.N., Wilkes, B.C., Schiller, P.W., Bidlack, J.M., Pasternak, G.W. and Houghten, R.A., *Science,* 266 (1994) 2019.
5. Blondelle, S.E., Takahashi, E., Weber, P.A., and Houghten, R.A., *Antimicrob. Agents & Chemother.,* 38 (1994) 2280.
6. Pinilla, C., Appel, J.R., Blanc, P. and R.A. Houghten, R.A., *BioTechniques,* 13 (1992) 901.
7. Wallace, A., Altamura, S., Toniatti, C., Vitelli, A., Bianchi, E., Delmastro, P., Ciliberto, G. and Pessi, A., *Peptide Research,* 7 (1994) 27.
8. Weismüller, K.-H., Udaka, K., Kienle, S., Walden, P. and Jung, G., in Maia, H.L.S. (Ed.), 'Peptides 1994', Escom, Leiden, The Netherlands, 1995, p.111.
9. Bianchi, E., Folgori, A., Wallace, A., Nicotra, M., Acali, S., Phalipon, A., Barbato, G., Bazzo, R., Cortese, R., Felici, F. and Pessi, A., *J. Mol. Biol.,* 247 (1995) 154.
10. Dooley, C.T. and Houghten, R.A., *Life Sci.*, 52 (1993) 1509.
11. Pinilla, C., Appel, J.R., Blondelle, S.E., Dooley, C.T., Eichler, J., Ostresh, J.M. and Houghten, R.A., *Drug Dev. Res.*, 33 (1994) 133.
12. Pinilla, C., Buencamino, J., Appel, J.R., Houghten, R.A., Brassard, J.A. and Ruggeri, Z.M., *Biomed. Pept., Prot. and Nucleic Acids,* 1 (1995) 199.
13. Pinilla, C., Buencamino, J., Appel, J.R., Hopp, T.P. and Houghten, R.A., *Molecular Diversity,* (1995) 1 (1995) 21.
14. Pinilla, C., Appel, J.R. and Houghten, R.A., *Biochemical J.,* 301 (1994) 847.
15. Dooley, C.T., Bower, A.N. and Houghten, R.A., this volume.
16. Eichler, J., Lucka, A.W. and Houghten, R.A., *Peptide Resarch,* 7 (1994) 300.
17. Blondelle, S.E., Takahashi, E., Houghten, R.A. and Pérez-Payá, E., in Maia, H.L.S. (Ed.), 'Peptides 1994', Escom, Leiden, The Netherlands, 1995, p.85.
18. Ostresh, J.M., Husar, G.M., Blondelle, S.E., Dörner, B., Weber, P.A. and Houghten, R.A., *Proc. Natl. Acad. Sci. USA*, 91 (1994) 11138.
19. Houghten, R.A., this volume.

Peptides: Chemistry, Structure and Biology
Pravin T.P. Kaumaya and Robert S. Hodges (Eds.)
Mayflower Scientific Ltd., 1996

374
Total Synthesis of Ribonuclease A Using Subtiligase

D.Y. Jackson[1], J. Burnier[1], C. Quan[1], M. Stanley[1], J. Tom[1] and J.A. Wells[2]

Departments of Bioorganic Chemistry[1] and Protein Engineering[2], Genentech Inc., South San Francisco, CA 94080, USA

Introduction

Protein engineering is usually limited to the application of mutagenesis and recombinant expression technologies utilizing the 20 naturally occuring amino acids. However, synthetic strategies have been developed recently which allow the incorporation of synthetic amino acids into proteins. These include total chemical synthesis [1] and blockwise chemical [2] or enzymatic [3] coupling of peptide fragments. Proteases can catalyze peptide bond formation from activated esters and amines [4], although in aqueous solution ester hydrolysis is favored over aminolysis. To solve this problem, Kaiser and co-workers [5] showed that a mutant of the serine protease subtilisin, in which the catalytic serine 221 was chemically converted to cysteine (Ser221Cys), catalyzed aminolysis over hydrolysis of peptide esters in aqueous solution. The activity of this mutant was significantly reduced making it an inefficient ligase. To improve the catalytic efficiency of thiol-subtilisin for ligation of peptide bonds in aqueous solution, Abrahmsen and co-workers [6] engineered a second mutation (Pro225Ala) which restored the activity of the ligase; we call this double mutant subtiligase. Here, we report the development of compatible peptide chemistry to allow the sequential block-wise ligation of peptides in aqueous solution using subtiligase. We have used this technology to synthesize ribonuclease A, a 124 residue enzyme [7]. We have also incorporated unnatural catalytic amino acids in order to alter the enzyme in a way not possible using conventional mutagenesis with natural amino acids. We believe this methodology may be useful for the synthesis or semisynthesis of a variety of proteins [8].

Results and Discussion

The strategy for protein synthesis using subtiligase (Figure 1) starts with preparation of a fully deprotected peptide (the acceptor) corresponding to the C-terminal fragment of the desired protein. The next most N-terminal fragment (the donor) is esterified with a glycolate-phenylalanyl amide group (glc-F-NH_2) on the C-terminus. This group affords efficient acylation of subtiligase based on the enzyme's preference for substrates containing glycine and phenylalanine at the P1' and P2' positions, respectively [6]. The donor fragment also contains an isonicotinyl protecting group (iNOC) on its N-terminus to prevent self ligation [9]. The iNOC group can be removed from the peptide after each ligation to afford a free N-terminus for subsequent ligations.

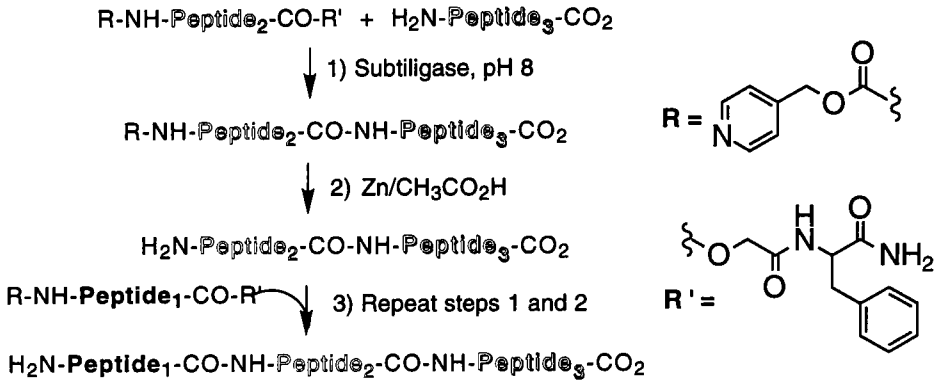

Figure 1. *Diagram showing the general strategy for synthesizing protein using subtiligase. Synthetic peptides are ligated together sequentially in a C N direction. After each ligation the N-terminus of the product is deprotected and the next peptide is ligated. The process is repeated until full length material is obtained. The structures of the N-terminal protecting group R (iNOC) and C-terminal ester R' (glc-F-NH_2) are shown at the bottom.*

RNase A was chosen as synthetic target because it has many unanswered interesting mechanistic questions (for review see [10]) and much is known about its crystalline [11] and solution structure [12]. Previous attempts to synthesize RNase A have yielded only trace amounts of impure protein [2, 13]. We divided RNase A into six peptide fragments (Table 1) based on subtilisin specificity [6].

The peptides were synthesized using BOC-chemistry [14] and ligated together in a sequential manner. The average yield per coupling step was 66% and per deprotection

Table 1. *Summary of yields for blockwise synthesis of wt RNase A*[a].

Step #	Fragment	Reaction	% Yield	mass (calculated: found)
1.	5 + 6	Ligation	63%	5370.7 : 5368.9
	iNOC-5-6	Deprotection	91%	5233.9 : 5234.4
2.	5-6 + 4	Ligation	76%	6832.0 : 6831.5
	iNOC-4-5-6	Deprotection	87%	6695.2 : 6695.0
3.	4-5-6 + 3	Ligation	68%	8075.4 : 8075.0
	iNOC-3-4-5-6	Deprotection	81%	7939.4 : 7938.5
4.	3-4-5-6 + 2	Ligation	55%	11675.6 : 11676
	iNOC-2-3-4-5-6	Deprotection	83%	11539.4 : 11538
5.	2-3-4-5-6 + 1	Ligation	67%	13824.0 : 13824
	iNOC-1-2-3-4-5-6	Deprotection	90%	13688.0 : 13687
6.	1-2-3-4-5-6	Refolding	54%	13679.8 : 13680

[a] Fragment peptides (**1-6**) were synthesized *via* standard methods and have amino acid sequences: **1** = iNOC-HN-KETAAAKFERQHMDSSTSAA-CO-R' (residues 1-20); **2** = iNOC-HN-SSSNY CNQMMKSRNLTKDRCKPVNTFVHESL-CO-R' (residues 21-51); **3** = iNOC-HN-ADVQA VCSQKNV-CO-R' (52-63); **4** = iNOC-HN-ACKNGQTNCYQSY-CO-R' (residues 64-76); **5** = iNOC-HN-STMSTETGSSKPNCAY-CO-R' (residues 77-97); **6** = H_2N-KTTQANKHIIVACE GNPYVPVHFDASV-CO_2H (residues 98-124) where iNOC = isonicotinyl and R' = glc - F-NH_2.

step was 86%. The product was purified by reverse phase HPLC in a yield of 54%. The synthetic RNase A was >98% pure as assessed by SDS-PAGE. The protein had a mass of 13,680 daltons as determined by electrospray ionization mass spectrometry that was identical to commercial RNase A (Sigma). The synthetic RNase A catalyzed the hydrolysis of 2',3'-cyclic CMP with a k_{cat} and K_m in agreement with literature values.

Clearly the incorporation of non-natural amino acids allows the electronic and steric properties of enzymes to be altered in ways not possible using conventional site-directed mutagenesis with naturally occurring amino acids. We have also shown the subtiligase technology is adaptable to semi-synthesis of proteins; peptides can be ligated onto the N-terminus of large natural or recombinant proteins or protein fragments [8]. Total protein synthesis using subtiligase may also provide access to proteins which are poorly expressed *in vivo*. Finally, the efficient incorporation of synthetic amino acids into proteins greatly enhances the ability of chemists and biologists to understand existing proteins and to create new proteins with altered and useful properties.

References

1. Kent, S.B.H., *Annu. Rev. Biochem.*, 57 (1988) 957.
2. Hirschmann, R., Nutt, R.F., Veber, D.F., Vitali, R.A., Varga, S.L., Jacob, T.A., Holly, F.W. and Denkewalter, R.G., *J. Am. Chem. Soc.*, 91 (1969) 502.
3. Wong, C., Schuster, M., Wang, P. and Sears, P., *J. Am. Chem. Soc.*, 115 (1993) 5893.
4. Kullman, W., 'Enzymatic Peptide Synthesis', CRC Press, Boca Raton, FL, USA, 1987.
5. Kaiser, E.T., *Acc. Chem. Res.*, 22 (1989) 47.
6. Abrahmsen, L., Tom, J., Burnier, J., Butcher, K.A., Kossiakoff, A. and Wells, J.A., *Biochem.*, 30 (1991) 4151.
7. Jackson, D.Y., Burnier, J., Quan, C., Stanley, M., Tom, J. and Wells, J.A., *Science*, 265 (1994) 247.
8. Chang, T.K., Jackson, D.Y., Burnier, J.P. and Wells, J.A., *Proc. Natl. Acad. Sci.*, 91 (1994) 12544.
9. Veber, D.F., Paleveda, W.J., Lee, Y.C. and Hirschmann, R., *J. Org. Chem.*,42 (1977) 3286.
10. Blackburn, P. and Moore, S., 'The Enzymes', Vol. 15, Academic Press, Inc., 1982.
11. Campbell, R.L. and Petsko, G.A., *Biochemistry*, 26 (1987) 8579.
12. Rico, M., J. Santoro, C. Gonzalez, M. Bruix, J. Neira, J. Nieto and J. Herranz , *J. Bio. NMR*, 1 (1991) 283.
13. Gutte, B. and Merrifield, R.B., *J. Biol. Chem.*, 246 (1971) 1922.
14. Bodanszky, M. and Bodanszky, A., 'The Practice of Peptide Synthesis', Springer-Verlag, New York, NY, USA, 1984.

Peptides: Chemistry, Structure and Biology
Pravin T.P. Kaumaya and Robert S. Hodges (Eds.)
Mayflower Scientific Ltd., 1996

375
Construction and Screening of Peptide and Nonpeptide Libraries Based on One-bead-One-compound Principle

M. Lebl[1], V. Krchňák[1], P. Štrop[1] and K.S. Lam[2]

[1]Selectide Corporation, Subsidiary of Marion Merrell Dow, Oro Valley, AZ 85737, USA
[2]Arizona Cancer Center and Department of Medicine, University of Arizona College of Medicine, Tucson, AZ 85724, USA

Introduction

The one-bead-one-compound library technique is composed of three main parts: (i) synthesizing of the library in which each solid phase particle carries a unique structure, (ii) identifying particles that interact with a given macromolecular target, and (iii) determining the structure responsible for the observed effect [1, 2]. There are several issues to be solved to successfully apply this technique. We will address only some of them: (i) manual and automated synthesis of peptide libraries and compounds identified in library screening; (ii) screening of solid phase libraries with both soluble and insoluble targets; (iii) synthesis of complete libraries; and (iv) synthesis of libraries with higher diversity than possible in peptide libraries. The one-bead-one-compound library technique was recently reviewed [2].

Results and Discussion

Synthesis of the library can be automated. A compound identified in library screening must be resynthesized for verification of its activity. The resynthesis of hits may become a bottleneck of the screening technology. It is necessary to use the capability of a multiple synthesizer, which can deliver the required number of compounds (peptides) for testing. However, all commercially available multiple synthesizers operate in a batch mode; *i.e.,* they cannot accept new sequences or prioritize syntheses once operation has commenced. The optimal reactor for solid phase peptide synthesis is a polypropylene syringe equipped with teflon frit [3], which we have used for synthesis of several thousand peptides. We have designed the MARS (multiple automatic robotic synthesizer) apparatus which synthesizes peptides in plastic syringes [4]. This machine can accept any number of synthetic requests and prioritize them immediately. The capacity is the simultaneous synthesis of twelve peptides. Overall throughput depends on the length of peptides to be synthesized and coupling time. For example, (considering two hours coupling time) it can synthesize approximately 12 octapeptides or 24 tetrapeptides a day. The robot operates continuously, and can synthesize peptides of any length or sequence in parallel. We have synthesized HIV protease (99 amino acids) together with a number of short peptides. Therefore, one hundred peptides per week is not an unusually high load.

Table 1. *Efficiency and success of on-bead-binding screening.*

Project	Time to first hit	No. libraries screened	No. compounds screened	No. hits identified	% hits confirmed
IIb/IIIa	2 wk	3	2,000,000	40	80
Thrombin	2 wk	20	20,000,000	>1000	95
Her-2	8 wk	18	43,000,000	47	27
Xa	8 wk	37	37,000,000	>800	75
VIIa	20 wk	36	36,000,000	200	3
RNase-H	4 wk	20	20,000,000	500	30
Oxidase	5 wk	9	2,800,000	84	3
Grb-2	4 wk	3	9,000,000	15	66
gp120/CD4	14 wk	5	16,000,000	17	43

Screening of a one-bead-one-compound library can be performed either by a solid phase binding assay, or by solution tests in a high-throughput mode. The practical performance of these tests has been described in detail [5, 6]. It is very important to include appropriate controls during the screening of a bead-bound library to eliminate nonspecific binding. The test is usually performed both in the presence and in the absence of a competitor several times, and only beads selected in repeated cycles of staining and decolorization are submitted for sequencing and resynthesis. An alternative to multiple rounds of screening is a technique using different colors in each step of bead staining [7]. Specificity of binding can be determined by the evaluation of bead color. Only compounds in which the biological activity has been verified in solution can be qualified as hits. Table 1 illustrates the time-lines and success rate in this type of screening. It ranges from more than 95% in the case of thrombin to 3% in the case of factor VIIa. On the other hand, structures identified in solution screening were found to be real hits in all cases. This advantage of solution screening is counterbalanced by its relatively low throughput; only several hundred thousand beads can be screened in one day, in comparison to millions screened by bead-binding assay.

Synthesis of libraries by the split and mix technique generates random mixtures of all possible structures. Therefore, there is always uncertainty about the completeness of the library [8]. This issue is especially important in the case of small libraries and in situations requiring the most economical use of reagents. We have designed a technique allowing the synthesis of all members of the particular library with only one representation of each structure. This technique is based on the principle of continually dividable carrier (membrane, thread), the synthetic "fate" of which can be easily traced based on its size or shape in the particular stage of the synthesis. Figure 1 illustrates the principle of this technique on the example of a library of eight compounds generated by three steps of randomization using two building blocks in each step. Each piece of solid carrier was cut in half in three consecutive steps and pieces were transferred to the next synthetic step, not randomly but in an organized way. We have prepared a peptide library of several thousand members and screened it both by binding and in a solution assay [9].

To increase the diversity achievable with linear peptides, we have synthesized cyclic as well as branched libraries in which not only alpha amino acids but also compounds

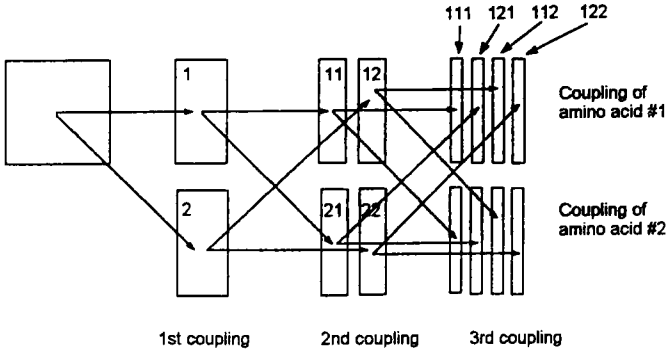

Figure 1. *General scheme for the synthesis of nonrandom libraries.*

with other combinations of amino and carboxy groups are part of the "backbone" [10]. Modifications of side chains of trifunctional amino acids in peptides is another way to increase diversity. We have also applied other reactions, such as Wittig or Mitsunobu reaction in library building (see elsewhere in this volume). In all these cases, as well as in the libraries based on a molecular "scaffold", we had to apply "coding" (see *e.g.* [11]) for elucidation of the structure, when structures in the library were not easily detectable by mass spectroscopy.

Acknowledgments

The hard work of all Tucson associates who made the realization of one-bead-one-compound technology possible is acknowledged.

References

1. Lam, K.S., Salmon, S.E., Hersch, E.M., Hruby, V.J., Kazmierski, W.M. and Knapp, R.J., *Nature,* 354 (1991) 82.
2. Lebl, M., Krchňák, V., Sepetov, N.F., Seligmann, B., Štrop, P., Felder, S. and Lam, K.S., *Biopolymers (Pept. Sci.),* 37 (1995) 177.
3. Krchňák, V. and Vágner, J., *Pept. Res.,* 3 (1990) 182.
4. Krchňák, V., Cabel, D., and Lebl, M., *Pept. Res.,* 9 (1996) 45.
5. Lebl, M., Krchňák, V., Salmon, S.E. and Lam, K.S., in 'Methods: A Companion to Meth. Enzymol.', 6 (1994) 381.
6. Lam, K.S. and Lebl, M., 'Methods: A Companion to Meth. Enzymol.', 6 (1994) 372.
7. Lam, K.S., Wade, S., Abdul-Latif, F. and Lebl, M., *J. Immunol. Methods,* 180 (1995) 219.
8. Burgess, K., Liaw, A. I. and Wang, N., *J. Med. Chem.* 37 (1994) 2985.
9. Stanková, M., Wade, S., Lam, K.S. and Lebl, M., *Pept. Res.,* 7 (1994) 292.
10. Krchňák, V., Weichsel, A.S., Cabel, D., and Lebl, M., *Pept. Res.,* 8 (1995) 198.
11. Nikolaiev, V., Stierandavá, A., Krchňák, V., Seligmann, B., Lam, K.S., Salmon, S.E. and Lebl,M., *Pept. Res.,* 6 (1993) 161.
12. Vágner, J., Krchňák, V., Sepetov, N.F., Štrop, P., Lam, K.S., Barany, G. and Lebl, M. in Epton, R. (Ed.), 'Innovation and Perspectives in Solid Phase Synthesis', Mayflower Worldwide, Birmingham, 1994, p. 347.

Peptides: Chemistry, Structure and Biology
Pravin T.P. Kaumaya and Robert S. Hodges (Eds.)
Mayflower Scientific Ltd., 1996

376
New Coupling Techniques for Solid Phase Peptide Synthesis

S.A. Kates[1], L.A. Carpino[2] and F. Albericio[3]

[1]*PerSeptive Biosystems Biosearch Products, Framingham, MA 01701, USA*
[2]*Department of Chemistry, University of Massachusetts, Amherst, MA 01003, USA*
[3]*Department of Organic Chemistry, University of Barcelona, 08028-Barcelona, Spain*

Introduction

The most common methods for peptide bond formation include the use of N,N-dicyclohexyl- and diisopropylcarbodiimides (DCC and DIPCDI, respectively), pentafluorophenyl esters (OPfp), and uronium or phosphonium salts built around N-hydroxybenzotriazole (HOBt). The carbodiimide and active ester techniques are also improved by the use of HOBt as an additive, a key step in each case being OBt ester formation.

A more efficient coupling additive, 1-hydroxy-7-azabenzotriazole (HOAt), a compound known since 1973 but only in other connections, was described in 1993 [1]. HOAt incorporates into the HOBt structure a pyridine nitrogen atom, strategically placed to enhance coupling rates and maintenance of chiral integrity. Both the uronium and phosphonium salts based on HOAt {N-[(dimethylamino)-1H-1,2,3-triazolo-[4,5-b]pyridin-1-ylmethylene]-N-methylmethanaminium hexafluorophosphate N-oxide (HATU), 7-azabenzotriazol-1-yloxytris(pyrrolidino)phosphonium hexafluorophosphate (PyAOP) and 1-(1-pyrrolidinyl-1H-1,2,3-triazolo[4,5-b]pyridin-1-yl methylene) pyrrolidinium hexafluorophosphate N-oxide (HAPyU)} were synthesized and compared with the common HOBt-derived reagents, BOP, PyBOP, HBTU, HBPyU, *etc.*, [2].

Results and Discussion

Early studies [1, 3] demonstrated that HOAt as an additive for carbodiimide and pentafluorophenyl ester coupling or built into stand-alone coupling reagents caused significant reductions in both coupling times and racemization or epimerization. For example, in the [3+3] coupling to give Z-Gly-Gly-Val-Ala-Gly-Gly-OMe, the use of HAPyU in the presence of collidine gave < 0.1% of the D,L-diastereomer whereas the corresponding HOBt analog gave 7.9% of this form.

Initial applications of HOAt-based additives as coupling reagents in solid phase synthesis involved the assembly of the common decapeptide model ACP (65-74) derived from the acyl carrier protein sequence (H-VQAAIDYING-NH_2) [4]. Using the Fmoc/*t*Bu strategy on PAL-PEG-PS resins with deliberately reduced coupling times and excesses of reagents, dramatic differences were observed relative to syntheses carried out *via* the HOBt-analogs. In the latter cases, the crude HPLC traces were essentially

catalogs of all the by-products expected for this well-known model (des-Asn[73], des-Ile[72], des-Ile[69], des-Val[75], and des-Ile[69], Ile[72]). For reasons still unclear, the coupling of Fmoc-Asn(Trt)-OH *via* HATU or PyAOP is improved by the addition of 1 equiv. of HOAt. No such improvement is noted for other amino acids.

Differences between HOAt- and HOBt-based syntheses are particularly significant in the case of peptides which incorporate hindered amino acids. The standard model, H-Tyr-Aib-Aib-Phe-Leu-NH_2, was assembled *via* HATU (4 equiv. amino acid/activator, 8 equiv. base, 2 h coupling for Tyr and Aib and 30 min for Phe and Leu) with an efficiency similar to that obtained *via* acid fluorides [5]. In a more demanding example, H-Tyr-Aib-Deg-Phe-Leu-NH_2 assembled under the same conditions gave a 1:1 mixture of the desired peptide and the des-Aib derivative. With HBTU activation, none of the pentapeptide was formed. Multiple extended-time couplings with HATU gave good conversion to the desired 5-mer. The highly challenging 20-mer, alamethicin acid, containing eight Aib residues and previously assembled by solid-phase methods only *via* acid fluorides could be obtained *via* HATU in excellent yield if the single Aib-Aib sequence is introduced *via* double coupling. HBTU gives none of the desired sequence.

Extreme steric effects are also observed with N-substituted amino acids. An appropriate model was a segment of cyclosporin (H-DAla-MeLeu-MeLeu-MeVal-Phe-Val-OH) which was assembled on a hyperacid-labile resin (HAL-PEG-PS) using 2x2 h couplings for the final three amino acids. The desired peptide was obtained in yields of 85% and 8% for HATU and HBTU, respectively [5, 6]. These results suggest that backbone protected amino acids (Hmb, Tmob) might be handled by the HOAt-based methodology.

Segment condensations onto resins are somewhat more demanding than analogous reactions carried out in solution in terms of configurational control. Preactivation times, identity of the base, and choice of solvent are all critical. For the coupling of Fmoc-Phe-Ser(*t*Bu)-OH onto H-Pro-PAL-PEG-PS and a number of related models, HATU/collidine/DMF-CH_2Cl_2 proved to be most effective, epimerization being at least 1/3 that of comparable HBTU couplings [7]. Differences among HOAt-based reagents may also be observed especially with regard to the retention of configuration during coupling processes [3]. A particularly striking example involves the cyclization of linear peptides in solution [8].

HOAt and the various HOAt-based coupling reagents are inert in solid form. HOAt itself is stable in DMF solution (0.3 M). The derived uronium salts are stable in DMF at 0.5 M concentration for up to 5 d whereas the corresponding phosphonium salt, *i.e.*, PyAOP is less stable, a possible indication of its greater reactivity.

References

1. Carpino, L.A., *J. Am. Chem. Soc.*, 115 (1993) 4397.
2. Abdelmoty, I., Albericio, F., Carpino, L.A., Foxman, B.M., and Kates, S.A., *Lett. Pept. Sci.*, 1 (1994) 57.
3. Carpino, L.A and El-Faham, A., *J. Org. Chem.*, 59 (1994) 695.
4. Carpino, L.A., El-Faham, A., Minor, C., and Albericio, F., *J. Chem. Soc., Chem. Commun.*, (1994) 201.

5. Carpino, L.A., El-Faham, E., Truran, G.A., Triolo, S.A., Shroff, H., Griffin, G.W., Minor, C.A., Kates, S.A., and Albericio, F., in Hodges, R.S. and Smith, J.A. (Eds.), 'Peptides: Chemistry, Structure and Biology', ESCOM, Leiden, The Netherlands 1994, pp. 124126.
6. Angell, Y.M., García-Echeverría, C., and Rich, D.H., *Tet. Lett.*, 35 (1994) 5981.
7. Carpino, L.A., El-Faham, A., and Albericio, F., *Tet. Lett.*, 35 (1994) 2279.
8. Ehrlich, A., Rothemund, S., Brudel, M., Beyermann, M., Carpino, L.A., and Bienert, M., *Tet. Lett.*, 34 (1993) 4781.

Peptides: Chemistry, Structure and Biology
Pravin T.P. Kaumaya and Robert S. Hodges (Eds.)
Mayflower Scientific Ltd., 1996

377
Nonpeptide Ligands for Peptide Receptors

R.M. Freidinger

Medicinal Chemistry Department, Merck Research Laboratories,
West Point, PA 19486, USA

Introduction

In the last ten years, rapid progress has been made in developing selective peptide receptor ligands with properties of orally administered drugs [1]. The majority of leads to these agents have been identified from natural product sources and synthetic chemical collections through directed screening. Medicinal chemistry efforts have optimized the properties of many of these leads. Here we highlight certain structures and observations that may facilitate identification of nonpeptide ligands for other peptide receptors.

Results and Discussion

Prior to 1985, nearly all examples of small molecule, nonpeptide ligands for peptide receptors were in the opioid field. The classic example is morphine. Many years of research have produced a structurally diverse group of selective opioid agonists and antagonists with several having significant utility in therapy. An important advance came with the discovery of asperlicin, a nonpeptide structure from *Aspergillus alliaceus*, which is a moderately potent cholecystokinin (CCK) receptor antagonist [2]. Directed screening using radioreceptor assays identified this lead and established that this approach has utility for finding novel peptide receptor ligands. Medicinal chemistry studies based on asperlicin led to highly potent and selective antagonists for the CCK-A receptor subtype exemplified by devazepide (MK-329). A key observation was the recognition of the utility of a 5-phenyl-1,4-benzodiazepine core structure in the design of these agents. Further elaboration of structure-activity relationships produced the potent, selective CCK-B antagonist L-365,260. Both of these agents exhibit good oral bioavailability and were chosen for human clinical trials. Subsequent research produced water soluble derivatives of MK-329 (*e.g.*, **1**) and water soluble CCK-B antagonists with enhanced potency and selectivity (*e.g.*, **2**). Recent studies in several laboratories have increased the structural diversity of nonpeptide CCK antagonists [3].

Receptor based screening has also identified novel oxytocin (OT) and vasopressin (AVP) receptor ligands [1]. Optimization of these leads produced the potent, selective, and orally bioavailable nonpeptide OT antagonist L-368,899, the AVP V1a antagonist OPC-21268, and the AVP V2 antagonist OPC-31260. All of these compounds were chosen for human clinical trials. Recently, using information from human receptor binding assays, the potent OT antagonist L-371,257 was designed from OPC-21268 [4]. Modeling studies have suggested potential relationships between binding elements in

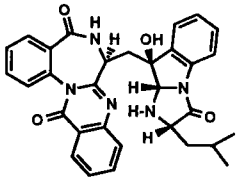

Asperlicin

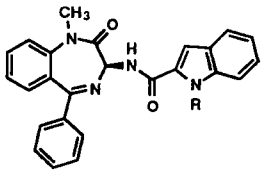

Devazepide, R = H
1, R = CH_2COOH

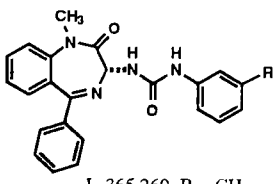

L-365,260, R = CH_3

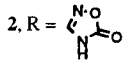

2, R =

several of the OT antagonist structural classes which may have utility for further design of improved ligands.

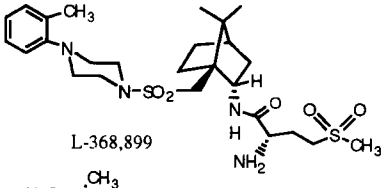

L-368,899

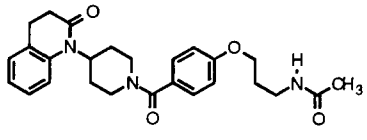

OPC-21268

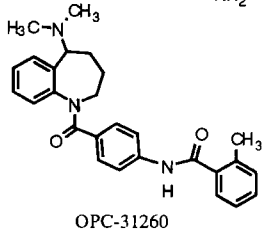

OPC-31260

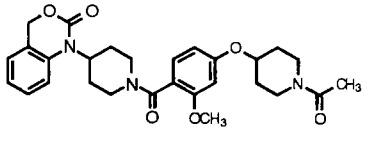

L-371,257

A weak affinity nonpeptide angiotensin II (AII) receptor ligand lead from a synthetic collection was optimized to the potent, orally bioavailable antihypertensive agent losartan [5]. This drug has been approved for marketing in the U.S.A. Until recently, all of the newly discovered nonpeptide ligands have been pure antagonists. It has proven possible, however, with simple structural modifications, to convert a potent AII antagonist **3** into a compound **4** with agonist properties [6]. This finding represents an important precedent showing that nonpeptide opioid ligands are not unique in their ability to have either agonist or antagonist properties.

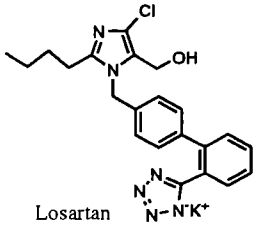

Losartan

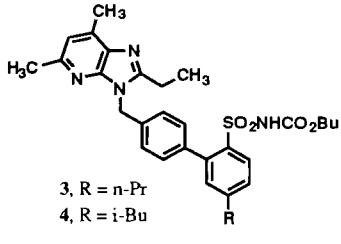

3, R = n-Pr
4, R = i-Bu

Many nonpeptide neurokinin (NK) antagonists have also been discovered, again primarily from screening leads [7]. Two pioneering examples (next page) are the NK1 antagonist CP-96,345 and the NK2 antagonist SR48968. Considerable structural diversity now exists in this area with several compounds in clinical trials.

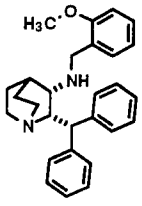

CP-96,345

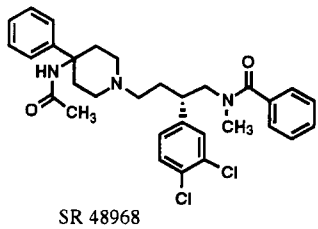

SR 48968

An important issue for design of nonpeptide ligands for peptide receptors is the relationship of receptor binding elements of peptide and nonpeptide ligands. Recent binding studies with selectively mutated CCK [8] and neurokinin [9] receptors and various ligands have indicated that antagonists can utilize different binding sites from those of native peptide agonists. These results emphasize that it is important that ligand design efforts not be restricted to structures of native peptide ligands.

From the research summarized herein, it is apparent that certain core "privileged structures" are found in ligands for multiple receptors within the G protein-coupled superfamily [10]. Examples are the 5-phenyl-1,4-benzodiazepine (opioid and CCK receptor ligands) and 4-arylpiperidines (opioid, oxytocin, and neurokinin receptor ligands). Such structures are being used for the generation of combinatorial libraries for screening in hopes of identifying novel leads for other receptors [11].

References

1. Freidinger, R.M., *Prog. Drug Res.*, 40 (1993) 33.
2. Chang, R.S.L., Lotti, V.J., Monaghan, R.L., Birnbaum, J., Stapley, EO., Goetz, M.A., Albers-Schonberg, G., Patchett, A.A., Liesch, J.M., Hensens, O.D., and Springer, J.P., *Science*, 230 (1985) 177.
3. Bock, M.G., Freidinger, R.M., Freedman, S.B., and Matassa, V.G., *Current Pharmaceutical Design*, 1 (1995) 279.
4. Williams, P.D., Clineschmidt, B.V., Erb, J.M., Freidinger, R.M., Guidotti, M.T., Lis, E.V., Pawluczyk, J.M., Pettibone, D.J., Reiss, D.R., Veber, D.F. and Woyden, C.J., *J. Med. Chem.*, 38 (1995) 4634.
5. Duncia, J.V., Carini, D.J., Chiu, A.T., Johnson, A.L., Price, W.A., Wong, P.C., Wexler, R.R., Timmermans, P.B.M.W.M.,. *Med. Res. Rev.*, 12 (1992) 149.
6. Kivlighn, S.D., Zingaro, G.J., Rivero, R.A., Huckle, W.R., Lotti, V.J., Chang, R.S.L., Schorn, T.W., Kevin, N., Johnson Jr., R.G., Greenlee, W.J., and Siegl, P.K.S., *Am. J. Physiol.*, 268 (1995) R820.
7. Lowe III, J.A. and Snider, R.M., *Ann. Rep. Med. Chem.*, 28 (1993) 99.
8. Kopin, A.S., McBride, E.W., Quinn, S.M., Kolakowski, L.F., and Beinborn, M., *J. Biol. Chem.*, 270 (1995) 5019.
9. Gether, U., Johansen, T.E., Snider, R.M., Lowe III, J.A., Nakanishi, S., and Schwartz, T.W., *Nature*, 362 (1993) 345.
10. Evans, B.E., Rittle, K.E., Bock, M.G., DiPardo, R.M., Freidinger, R.M., Whitter, W.L., Lundell, G.F., Veber, D.F., Anderson, P.S., Chang, R.S.L., Lotti, V.J., Cerino, D.J., Chen, T.B., Kling, P.J., Kunkel, K.A., Springer, J.P., and Hirschfield, J., *J. Med. Chem.*, 31 (1988) 2235.
11. Gordon, E.M., Barrett, R.W., Dower, W.J., Fodor, S.P.A., and Gallop, M.A., *J. Med. Chem.*, 37 (1994) 1385.

Peptides: Chemistry, Structure and Biology
Pravin T.P. Kaumaya and Robert S. Hodges (Eds.)
Mayflower Scientific Ltd., 1996

378
Amide Bond Surrogates as a Strategy for Peptide Limetic Design

A. F. Spatola

Department of Chemistry, University of Louisville, Louisville, KY 40292, USA

Introduction

The term "peptide limetic" has been used by Veber to refer to agonists or antagonists that bind to peptide receptors, in spite of their lack of similarity to traditional peptide structures or analogs [1]. We have previously suggested that the evolution between peptides and mimetics or limetics may be conveniently viewed as a continuum [2]. Using amide bond surrogates, conformational constraints, and other structural changes [3], a peptide lead structure can undergo a stepwise, systematic conversion to a nonpeptide replacement, when the latter is deemed advantageous.

Results and Discussion

It has been suggested by Hirschmann [4], Conradi [5], and others that bioavailability of peptides is compromised by the large desolvation energies accompanying multiple amide units. Table I contains a listing of various amide bond replacements (surrogates) and their general characteristics. Some of these (ψ[CHOH], ψ[CSNH], ψ[COO]) are found in naturally-occurring peptide analogs while others are primarily synthetic in origin. These units can be used to replace amide linkages susceptible to proteolytic degradation. Indeed, many of these structures have been incorporated within a variety of putative enzyme substrates at scissile linkages to provide effective enzyme inhibitors.

Certain residues are known to be quite lipophilic (*e.g.*, ψ[CH_2S], ψ[CH_2CH_2], or ψ[CH=CH]). Others, such as ψ[$CH_2NH_2^+$], introduce a new charge and thus enhance solubility in polar solvents. Table 2 shows a reversed phase-high performance liquid chromatography comparison of retention times for a series of closely related cyclic pseudopeptides. The relatively large spread in their elution behaviors correlates well with their structural characteristics.

Not all amide surrogates confer enzymic resistance. Thus ester bonds (ψ[COO]) and thioamides (ψ[CSNH]) can be cleaved by proteolytic enzymes. But these replacements often have other, useful properties that can be exploited. Thus, in a series of thionated analogs of thyrotropin releasing hormone (TRH), one analog, Top^1,Proψ[$CSNH_2$]^3-TRH (where Top = thiopyroglutamic acid) proved to show remarkable receptor selectivity between different classes of TRH receptors in the brain and hypothalamus [6]. Thionated enkephalin analogs similarly showed divergence in mu *vs.* delta opioid receptor binding, compared to their all-amide counterparts [7].

Incorporation of multiple amide bond surrogates may prove to be an effective method to prepare potent peptide analogs (limetics) that bear scant resemblance to their peptide precursors. Figure 1 shows the structure of a renin antagonist that has been shown to possess good oral bioavailability both in dogs and in humans [8]. By naming the structure as a peptide derivative using amide bond surrogate nomenclature [2], the concept of a continuum between peptides and limetics is perhaps more clear.

Table 1. *Relative RP-HPLC retention times for a series of cyclic opioid analogs containing single amide bond replacements.*

Surrogate	Comments
CH_2	Short, flexible
CH_2CH_2	Flexible
$CH_2CH_2CH_2$	Flexible spacer
CH=CH	Cis or trans; rigid
C≡C	Linear geometry
CH_2NH	Flexible, 2° amine
$COCH_2$	Flexible; H-bond acceptor
CH_2S	Flexible
CH_2SO	Flexible, chiral; H-bond acceptor
CH_2SO_2	More rigid
SCH_2	Synthetic challenge
CSNH	Rigid; hydrolyzable
NHCO	Rigid; enzyme resistant
CHOH	Statine; inhibitors
$CHOHCH_2$	Enzyme Inhibitor
CHOHCHOH	2 Chiral centers
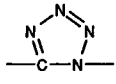	Cis configuration
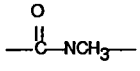	N-Me replacements

Table 2. *Amide bond surrogates and their characteristics.*

Structure	Retention Times (min)[a]
Tyr-c[D-Lys-Gly-Phe-Leu]	4
Tyr-c[D-Lys-Gly-Pheψ[CH_2S]Leu]	15.6
Tyr-c[D-Lys-Gly-Pheψ[CH_2SO]Leu]	11.2, 13.9
Tyr-c[D-Lys-Gly-Pheψ[CH_2NH]Leu]	~3[b]
Tyr-c[D-Lys-Glyψ[CSNH]Phe-Leu]	5.9

[a] 30-50%

[b] 18 min or 10-30% CH_3CN

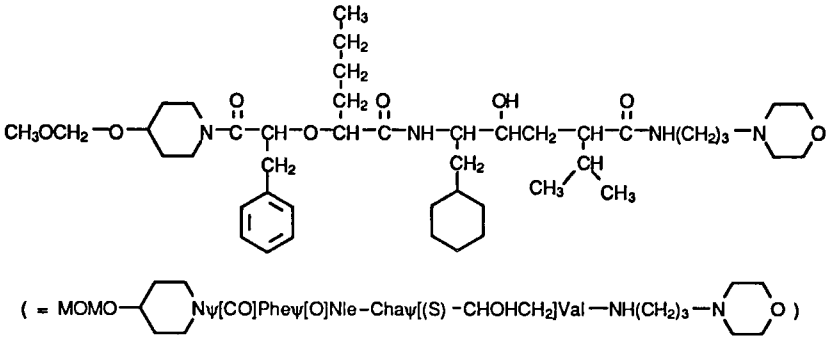

Figure 1. *Structure of a potent renin inhibitor with good oral activity.*

Amide bond surrogates can be synthetically challenging but provide medicinal chemists with a rich array of structural modifications possessing a wide variety of physical characteristics. It is likely that structures containing two or more amide surrogates, in both linear and cyclic forms, will be probed for new approaches for structure-function studies. Because many surrogates can be incorporated as protected pseudodipeptides *via* traditional solution or solid phase methods, the use of combinatorial methods may be especially well-suited to test their utility in a larger array of host candidates, thereby leveraging the synthetic effort.

References

1. Veber, D.F., in 'Peptides: Chemistry and Biology', Smith, J.A. and Rivier, J.E. (Eds.), ESCOM, Leiden, The Netherlands, 1992, p.3.
2. Spatola, A.F., in Weinstein, B. (Ed.), 'Chemistry and Biochemistry of Amino Acids, Peptides, and Proteins', Vol. 7, Marcel Dekker, New York, 1983, p. 267.
3. Goodman, M. and Ro, S. in Wolff, M.E. (ed.), 'Burger's Medicinal Chemistry and Drug Discovery, Fifth Edition', Vol. I, Principles and Practice, John Wiley, New York, 1994, p. 803.
4. Hirschmann, R., Smith, III, A.B., and Sprengeler, P.A., in Dean, P.M., Jolles, G, and Newton, C.G. (eds.) 'New Perspectives in Drug Design, Vol. 35', Academic Press, 1995, p.1.
5. Conradi, R.A., Hilgers, A.R., Ho, N.F.H., and Burton, P.S., *Pharmac. Res.*, 9 (1992) 435.
6. Lankiewicz, L., Bowers, C.Y., Reynolds, G.A., Labroo, V., Cohen, L.A., Vonhof, S., Siren, A.L., and Spatola, A.F., *Biochem. Biophys. Res. Commun.*, 184 (1992), 359.
7. Clausen, K., Spatola, A.F., Lemieux, C.; Schiller, P., and Lawesson, S.O., *Biochem. Biophys. Res. Commun.*, 120 (1984) 305.

Peptides: Chemistry, Structure and Biology
Pravin T.P. Kaumaya and Robert S. Hodges (Eds.)
Mayflower Scientific Ltd., 1996

379
Physicochemical and Biochemical Factors that Influence the Oral Bioavailability of Peptide Mimetics

R.T. Borchardt

Department of Pharmaceutical Chemistry, The University of Kansas, Lawrence, KS 66045, USA

Introduction

Recent advances in synthetic chemistry permit production of large quantities of various peptides and peptide mimetics possessing a diverse array of pharmacological effects. The clinical development of these peptide-based drugs, however, has been restricted due to their very low oral bioavailabilities and short *in vivo* half-lives [1]. Successful design of such molecules as orally available drugs is a major challenge for pharmaceutical scientists. Designing a suitable structure necessitates a balance between optimal pharmacological (*e.g.,* receptor binding) and optimal pharmaceutical properties (*e.g.,* membrane permeability, metabolic stability).

The epithelium lining of the gastrointestinal tract acts as a strategic interface between the external (*e.g.*, intestinal lumen) and internal milieu (*e.g.*, blood) of the body. This interface is both a physical and a biochemical barrier. Biochemically, the gastrointestinal tract is designed to break down dietary proteins into subunits (*e.g.*, peptides, amino acids) sufficiently small to be absorbed [2]. Digestive processes for peptides and proteins are catalyzed by a variety of proteases and peptidases. Due to the wide substrate specificity of these enzymes, it is not surprising that the metabolic barrier is considered to be important in limiting the absorption of peptide-based drugs. Another important aspect of the biochemical barrier is the existence of apically polarized efflux systems in the intestinal mucosa [3].

Physiologically, the intestinal epithelium also represents an important physical barrier. The organization and architecture of the intestinal mucosa, which have been extensively reviewed elsewhere [2], limit peptides to traversing the cell barrier *via* the paracellular and/or the transcellular route. The paracellular pathway is an aqueous, extracellular route across the epithelia that is followed by molecules according to their hydrophilicity, size, and charge. The main barrier to the paracellular diffusion of molecules is the region of the tight junctions or zonula occludens. Although the degree of permeability at the tight junctions varies significantly within different epithelia, tight junctions are generally reported to be impermeable to molecules with radii larger than 11-15Å [5].

The transcellular pathway involves movement of the solute across the apical cell membrane, through the cytoplasm and across the basolateral membrane by either active or passive processes. It is well known that di- and tripeptides are absorbed by both

active, carrier-mediated processes and simple passive diffusion. Generally, active processes are fairly substrate-specific, although exceptions have been found [5]. Although there is evidence that mucosal peptide/protein uptake is mediated by endocytic processes [2], in most cases this does not lead to transcytosis. Transcellular permeation by passive diffusion requires a solute to have optimal physicochemical properties, including size, lipophilicity (hydrophobicity and hydrogen bonding potential), and conformation [6]. For peptides and peptide mimetics, hydrogen bonding is a particularly important physicochemical characteristic [7-9].

Results and Discussion

The paracellular route has been of interest for the delivery of peptides and peptide mimetics because of the perception that it has limited proteolytic activity [1]. Recently, our laboratory has become interested in elucidating the structural features that influence the diffusion of peptides *via* the paracellular route. In one study, our laboratory determined the effect of conformation flexibility on the permeation of peptides through Caco-2 cell monolayers, an *in vitro* model for the intestinal mucosa [10]. We compared linear hexapeptides (H_2N-Trp-Ala-Gly-Gly-Asp-Ala-OH and Ac-Trp-Ala-Gly-Gly-Asp-Ala-NH_2) with a cyclic analog (cyclo[Trp-Ala-Gly-Gly-Asp-Ala]), which was covalently linked by the N-terminal and C-terminal ends. Solution structural analysis by means of 2-D NMR revealed that for the linear hexapeptides significant amounts of secondary structure (*e.g.,* βI turns) exist in a dynamic equilibrium with unfolded solution structures. In comparison, the cyclic analog existed in well-defined conformations containing βII turns. When the permeation of the Asp-containing peptides was determined across Caco-2 cell monolayers, the cyclic peptide was shown to be *ca.* 3 times more able to permeate than the linear, protected hexapeptide, and *ca.* 55 times more able to permeate than the linear, unprotected hexapeptide which was rapidly metabolized. This implies that cyclization has stabilized the peptide to metabolism, and it may have decreased the average molecular size, accounting for the observed increase in flux.

Proteins within the junctional complexes consist of polar amino acids with ionizable side chains. As a consequence, the junctional space exhibits an electrostatic field with a negative net charge that may affect the paracellular flux of molecules due to charge-charge interactions. Our laboratory recently demonstrated that the flux of several model peptides, Ac-Trp-Ala-Gly-Gly-X-Ala-NH_2 (X= Asp, Lys, Asn) and Ac-Tyr-ProX-Z-Val-NH_2 (X=Gly,Ile and Z=Asp,Asn), in Caco-2 cell monolayers did not show any discrimination based on the difference in charge [11, 12]. It was concluded that molecular radius and not charge predominantly limits the permeation of these penta- and hexapeptides through cell monolayers. However, with smaller peptides (*e.g.,* tripeptides), where size is not the predominant factor, charge could influence their flux *via* the paracellular pathway.

In an effort to alter the molecular radius of a peptide transiently and thus improve its permeation *via* the paracellular route, our laboratory has recently developed novel approaches for preparing cyclic prodrugs of the hexapeptide H_2N-Trp-Ala-Gly-Gly-Asp-Ala-OH [13, 14]. These prodrug systems utilize either a acyloxyalkoxycarbamate pro-moiety or a 3-(2'-hydroxy-4',6'-dimethylphenyl)-2,2-dimethyl propionic acid pro-

moiety. The conversion of both prodrugs to the peptide was significantly more rapid in rat or human blood than in buffer, suggesting esterase-mediated hydrolysis. In addition, when permeabilities were determined in Caco-2 cell monolayers, the permeation of the prodrugs was *ca.* 5 times greater than that of the metabolically stabilized, linear hexapeptide Ac-Trp-Ala-Gly-Gly-Asp-Ala-NH_2, and *ca.* 70 times greater than the linear, unprotected hexapeptide, which was rapidly metabolized and showed no transport.

The multiplicity of barrier mechanisms in the gastrointestinal tract represents a challenge for successful oral delivery of peptides. However, intestinal absorption of biologically active peptides may be possible through an understanding of the many different mechanisms that regulate the mucosal barrier. Hence, peptides can be modified to achieve enhanced chemical and enzymatic stability and improved permeation properties. Nevertheless, every biologically active peptide must be treated individually in order to improve its permeation through the intestinal mucosa.

Acknowledgments

The author's work in this area has been supported by grants from Glaxo, Inc. and The United States Public Health Service (GM-51633, GM-88539).

References

1. Amidon, G.L. and Lee, H.J., *Ann. Rev. Pharmacol. Toxicol.*, 34 (1994) 321.
2. Madara, J.L. and Trier, J.S., in Johnson, L.R. (Ed.), 'Physiology of the Gastrointestinal Tract', Raven Press, New York, 1994, p. 1577.
3. Collington, G.K., Hunter, J., Allen, C.N., Simmons, N.L. and Hirst, B.H., *Biochem. Pharmacol.*, 44 (1992) 417.
4. Ho, N.F.H., Day, J.S., Barsuhn, C.L., Burton, P.S. and Raub, T.J., *J. Controlled Release,* 11 (1990) 3.
5. Lowther, J., Hammond, S.M., Russel, K. and Fairclough, P.D., *J. Antimicrob. Chemother.,* 25 (1990) 183.
6. Burton, P.S., Conradi, R.A. and Hilgers, A.R., *Adv. Drug Delivery Rev.,* 7 (1991) 365.
7. Conradi, R.A., Hilgers, A.R., Ho, N.F.H., and Burton, P.S., *Pharm. Res.*, 9 (1992) 435.
8. Conradi, R.A., Hilgers, A.R., Ho, N.F.H., and Burton, P.S., *Pharm. Res.*, 8 (1991) 1453.
9. Kim, D.C., Burton, P.S., and Borchardt, R.T., *Pharm. Res.*, 10 (1993) 1710.
10. Okumu, F.W., Pauletti, G.M., Vander Velde, D.G., Siahaan, T.J. and Borchardt, R.T., *Pharm. Res.*, 12 (1995) 5-302 Abst. PDD 7438.
11. Okumu, F.W., Pauletti, G.M., Vander Velde, D.G., Siahaan, T.J. and Borchardt, R.T., *Pharm. Res.*, 12 (1995) 5-302 Abst. PDD 7437.
12. Knipp, G.K., Vander Velde, D.G., Siahaan,T.J., and Borchardt, R.T., *Pharm. Res.*, 12 (1995) 5-303 Abst. PDD 7441.
13. Pauletti, G.M., Gangwar, S. Wang, B., Siahaan, T.J., Vander Velde, D.G. and Borchardt, R.T., *Pharm. Res.*, 12 (1995) 5-208 Abst. PDD 7064.
14. Gangwar, S., Pauletti, G.M., Siahaan, T.J., Vander Velde, D.G., Stella, V.J. and Borchardt, R.T., *Pharm. Res.*, 12 (1995) 5-208 Abst. PDD 7063.

Author and Subject Indexes

Author Index

Subject Index

ISBN 0-9527011-0-3